INTERNATIONAL JOURNAL OF MODERN ENGINEERING RESEARCH (IJMER)

ISSN : 2249-6645

Volume 3 - Issue 3

Web : www.ijmer.com
Email : ijmer.editor@gmail.com

International Journal of Modern Engineering Research (IJMER)

Editorial Board

International Journal of Modern Engineering Research (IJMER)
www.ijmer.com Vol.3, Issue.3, May-June. 2013 pp-1263-1267 ISSN: 2249-6645

Experimental Study Using Different Tools/Electrodes E.G. Copper, Graphite on M.R.R of E.D.M Process and Selecting The Best One for Maximum M.R.R in Optimum Condition

Santanu Dey, [1] Dr. D.C.Roy[2]
[1]*Masters of Technology, Department of Mechanical Engineering Jalpaiguri Government Engineering College, Jalpaiguri–735102*
[2]*H.O.D & Professor of Mechanical Engineering, Jalpaiguri Government Engineering College, Jalpaiguri–735102, India*

Abstract: *EDM is the thermal erosion process in which metal is removed by a series of recurring electrical discharges between a cutting tool acting as an electrode and a conductive work piece, in the presence of a dielectric fluid. Electrical discharge machining (EDM) is a well-established machining option for manufacturing geometrically complex or hard material parts that are extremely difficult-to-machine by conventional machining processes. Its unique feature of using thermal energy to machine electrically conductive parts regardless of hardness has been its distinctive advantage in the manufacture of mould, die, automotive, aerospace and surgical components.*

Keywords: *M.R.R, Current, Impulse Duration, Spark Gap, Regression Analysis.*

I. Introduction

Electrical Discharge Machine (EDM) is now become the most important accepted technologies in manufacturing industries since many complex 3D shapes can be machined using a simple shaped tool electrode. Electrical discharge machine(EDM) is an important 'non-traditional manufacturing method', developed in the late1940s and has been accepted worldwide as a standard processing manufacture of forming tools to produce plastics moldings, die castings, forging dies and etc. New developments in the field of material science have led to new engineering metallic materials, composite materials, and high tech ceramics, having good mechanical properties and thermal characteristics as well as sufficient electrical conductivity so that they can readily be machined by spark erosion. At the present time, Electrical discharge machine (EDM) is a widespread technique used in industry for high precision machining of all types of conductive materials such as: metals, metallic alloys, graphite, or even some ceramic materials, of whatsoever hardness. Electrical discharge machine (EDM) technology is increasingly being used in tool, die and mould making industries, for machining of heat treated tool steels and advanced materials (super alloys, ceramics, and metal matrix composites) requiring high precision, complex shapes and high surface finish. Traditional machining technique is often based on the material removal using tool material harder than the work material and is unable to machine them economically. An electrical discharge machining (EDM) is based on the eroding effect of an electric spark on both the electrodes used. Electrical discharge machining (EDM) actually is a process of utilizing the removal phenomenon of electrical-discharge in dielectric. Therefore, the electrode plays an important role, which affects the material removal rate and the tool wear rate.

There are two main types of EDM-
- The ram type.
- The wire-cut type.

This project is based on the ram type EDM.
Ram type E.D.M
- The electrode/tool is attached to the ram that connected to the positive pole.
- The work piece is connected to the negative pole.
- The work is then positioned so that there is a gap between it and the electrode.
- The gap is then flooded with the dielectric fluid.
- The spark Temperatures generated can range from 7,760° to 11,650° Celsius.

II. Objective Of The Project

In this research work the main objective is to compare two electrodes e.g. (Copper & Graphite) using in EDM machining and selecting the best electrode on basis of highest Metal Removal Rate (MRR) and surface finish. Equipments used for EDM process:
- One mild steel metal piece (98.7*87.2*12).
- Copper & Graphite Electrode.
- Rustolic E.D.M. 20 Dielectric Fluid.
- EDM machine.

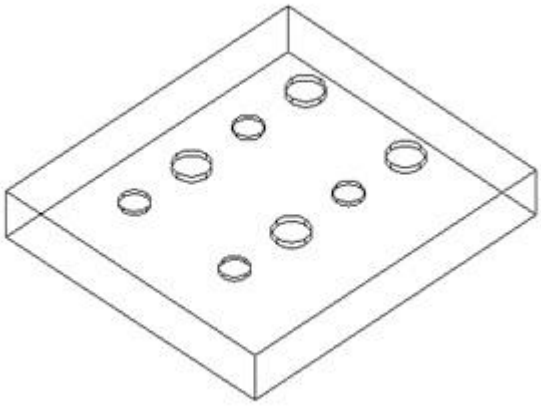

Figure: Top – view of work piece

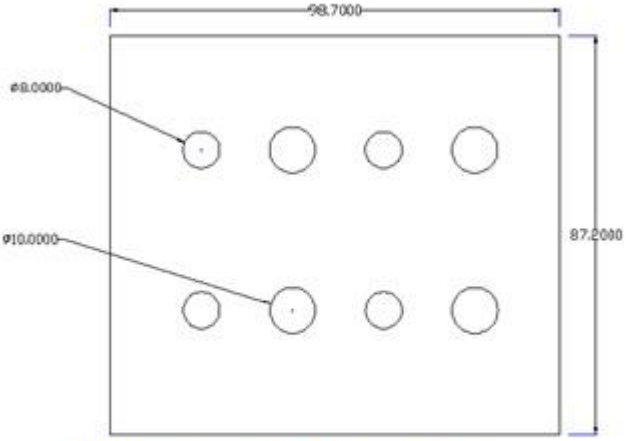

Figure: Isometric view of work piece

III. Observation Table

Copper electrode

Impulse	Spark Gap	I	U	T	Time		
					Idle	M/C	Total
1040	0.08	7	6	12	1.25	25.45	27.10
1050	0.14	8	6	15	1.14	6	7.14
1060	0.20	9	6	17	0.30	8.25	8.55
1070	0.26	10	6	18	0.36	6.40	7.26

Graphite electrode

Impulse	Spark Gap	I	U	T	Time		
					Idle	M/C	Total
1040	0.08	7	6	12	1.40	18.24	20.04
1050	0.14	8	6	15	0.23	6	6.23
1060	0.20	9	6	17	0.48	14.10	14.58
1070	0.26	10	6	18	0.58	11.58	12.16

Sample Calculation:-

M.R.R = $\frac{Volume}{Time}$

depth of hole (h) = 1mm

dia of the hole (d) = 8mm

Volume of the hole = $\frac{\pi}{4} * d^2 * h$

= $\frac{\pi}{4} * 8^2 * 1$

= 50.26 mm^3

M.R.R = $\frac{50.26}{25.45} mm^3/_{min}$ M/C Time=25.45min

= 1.975$mm^3/_{min}$

IV. Regression Analysis

Based on the experimental data gathered, statistical regression analysis enabled to study the correlation of process parameters with the MRR.

In this study, for three variables under consideration, a polynomial regression issued for modeling. The coefficients of regression model can be estimated from the experimental results. The effects of these variables and the interaction between them were included in this analyses and the developed model is expressed as interaction equation:

$Y=a+bX_1+cX_2+\ldots\ldots+nX_m$ (1)

Where a, b, c. Etc are co-efficient of their corresponding parameter.

The unknown coefficients are determined from the experimental data. Since, EDM process is non-linear in nature, a linear polynomial will be not able to predict the response accurately, and therefore the second-order model (quadratic model) is found to be adequately model the process.

Level of Observation:-

Control parameters	Level		Observed value
	Min. level	Max. level	
Current (Amp.)	7	10	M.R.R.(mm3/min)
Impulse Duration (µs.)	12	18	M.R.R. (mm3/min)
Spark Gap (mm.)	0.08	0.26	M.R.R.(mm^3/min)

Table -1: Result of experimental value

SL. NO.	Current (Amp.)	Impulse Duration (µs.)	Spark Gap (mm.)	A	B	C	Material Removal Rate {M.R.R.} (mm^3/min)
1	7	12	0.08	-1	-1	-1	1.975
2	7	12	0.26	-1	-1	1	2.76
3	7	18	0.08	-1	1	-1	8.38
4	7	18	0.26	-1	1	1	8.38
5	10	12	0.08	1	-1	-1	14.28
6	10	12	0.26	1	-1	1	8.36
7	10	18	0.08	1	1	-1	18.41
8	10	18	0.26	1	1	1	10.17

Here current, Impulse Duration and Spark Gap denoted as A, B and C. Equation (1) can be rewritten as in (2)

$$Y = C_o + C_a*A + C_b*B + C_c*C + C_d*A*B + C_e*A*C + C_f*B*C \quad (2)$$

Normal equations are:

$$\sum Y = nC_o + C_a\sum A + C_b\sum B + C_c\sum C + C_d\sum A*B + C_e*\sum A*C + C_f\sum B*C \quad (3)$$

$$\sum Y*A = C_o \sum A + C_a\sum A^2 + C_b\sum A*B + C_c\sum A*C + C_d\sum A^2*B + C_e*\sum A^2*C + C_f\sum A*B*C \quad (4)$$

$$\sum Y*B = C_o \sum B + C_a\sum A*B + C_b\sum B^2 + C_c\sum B*C + Cd\sum A.B^2 + C_e*\sum A*B*C + C_f\sum B^2*C \quad (5)$$

$$\sum Y*C = C_o \sum C + C_a\sum A*C + C_b\sum B*C + C_c\sum C^2 + Cd\sum A.B.C + C_e*\sum A*C^2 + C_f\sum B*C^2 \quad (6)$$

$$\sum Y.A.B = C_o\sum A.B + C_a\sum A^2\ B + C_b\ \sum AB^2 + C_c\sum A.B.C + Cd\sum A^2.B^2 + C_e*\sum A^2*B*C + C_f\ \sum A.B^2.C \quad (7)$$

$$Y\sum A*C = C_o\sum A*C + C_a\sum A^2*C + C_b\sum A*B*C + C_c\sum A*C^2 + C_d\sum A^2.B*C + C_e*\sum A^2*C^2 + C_f\sum A*B*C^2 \quad (8)$$

$$\sum Y*B*C = C_o\sum B*C + C_a\sum A*B*C + C_b\sum B^2*C + C_c\sum B*C^2 + C_d\sum A.B^2*C + C_e*\sum A*B^2*C + C_f\sum B^2*C^2 \quad (9)$$

Equation of the fitted model for MRR from solving above equations:

MRR = – 64.7089 + [(7.323 * current) + (2.402 * Impulse duration) + (119.229 * Spark gap) – {0.167 *(current * Impulse duration)} – {13.759 *(Current * Spark gap)} – {1.398 * (Impulse duration *Spark gap)}]

Table -2: Results showing the experimental and predicted value and error

SL. NO.	Current (amp.)	Impulse Duration (µs.)	Spark Gap (mm.)	Exp. MRR	Pred. MRR	Error	%Error
1	7	12	0.08	1.975	1.8393	0.1357	6.87
2	7	12	0.26	2.76	2.9945	0.1845	6.27
3	7	18	0.08	8.38	8.56626	0.18626	2.17
4	7	18	0.26	8.38	8.16162	0.21838	2.61
5	10	12	0.08	14.28	14.49414	0.21414	1.48
6	10	12	0.26	8.36	8.16948	0.195052	2.78
7	10	18	0.08	18.41	18.2151	0.1949	1.06
8	10	18	0.26	10.17	10.3806	0.2106	2.03

V. Graph & Table

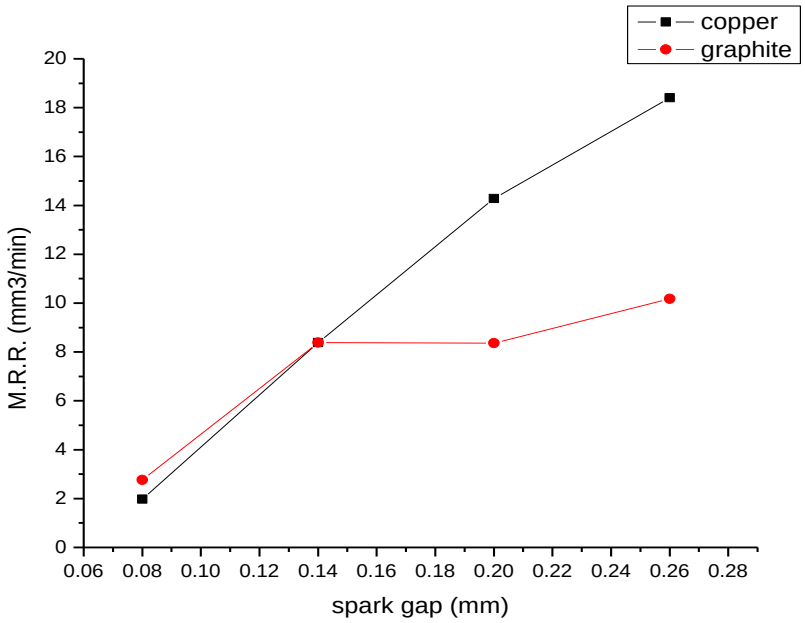

Table- 3: Spark gap v/s MRR

Spark gap (mm)	MRR (copper)	MRR (graphite)
0.08	1.9745	2.76
0.14	8.38	8.38
0.2	14.28	8.36
0.26	18.41	10.17

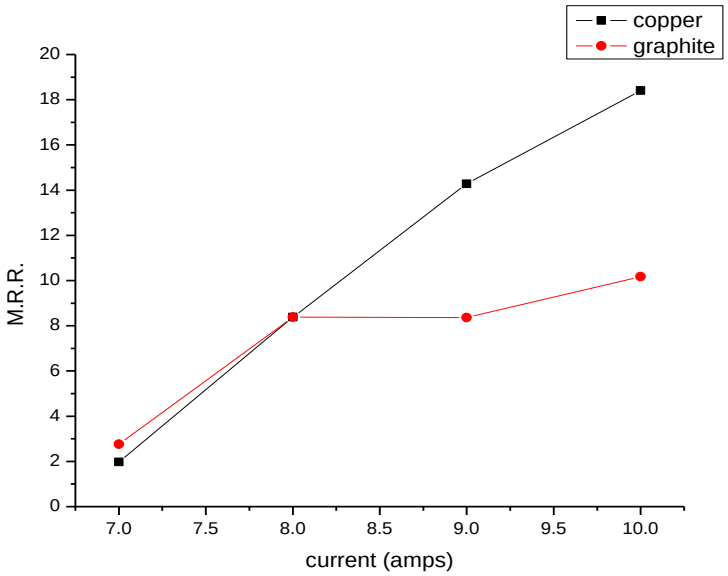

Table – 4: Current v/s MRR

Current (amps)	MRR (copper)	MRR (graphite)
7	1.9745	2.76
8	8.38	8.38
9	14.28	8.36
10	18.41	10.17

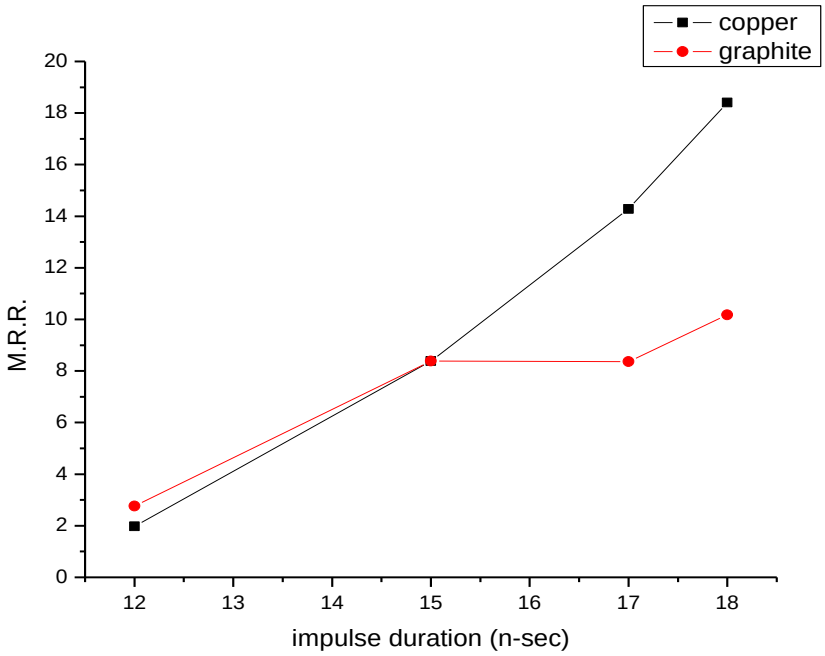

Table-5: Impulse duration v/s MRR

Impulse duration (n-sec)	MRR (copper)	MRR (graphite)
12	1.9745	2.76
15	8.38	8.38
17	14.28	8.36
18	18.41	10.17

VI. Conclusion

1. From the analysis of graph- it can be identified that at the initial stage MRR using graphite electrode is more as compare to copper electrode .Which implies that at low current, impulse duration and spark gap using graphite electrode is more economical. But as the value of the parameters increases, MRR with copper electrode increases more rapidly in respect of graphite electrode.
2. Finally, it can be concluded that graphite electrodes are best suitable for lower values of parameters and mainly for finishing work as graphite electrode produces better surface finish due to lower MRR and copper electrodes are suitable for high metal removal process where finish requirements are not significant.

References

Journal Paper:

[1]. Anand Pandey, Shankar Singh, Current research trends in variants of Electrical Discharge Machining: A review, International Journal of Engineering Science and Technology, Vol. 2(6), 2010, 2172-2191.

[2]. Mr. V. D. Patel, Prof. C. P. Patel, Mr. U.J. Patel, Analysis of Different Tool Material On MRR and Surface Roughness of Mild Steel In EDM, International Journal of Engineering Research and Applications (IJERA),Vol. 1, Issue 3, pp. 394-397.

[3]. J. Valentincic, D. Brissaud, M. Junkar, EDM process adaptation system in tool making industry ,Journal of Materials Processing Technology, Journal of Materials Processing Technology ,172 (2006) 291–298.

[4]. Qing GAO, Qin-he ZHANG, Shu-peng SU, Jian-hua ZHANG, Parameter optimization model in electrical discharge machining process,J Zhejiang Univ Sci A 2008 9(1):104-108.

Book:

[5]. P.K. Mishra, Nonconventional Machining, (Narosa Publishing House, 1997)

International Journal of Modern Engineering Research (IJMER)
www.ijmer.com Vol.3, Issue.3, May-June. 2013 pp-1268-1272 ISSN: 2249-6645

Job Shop Layout Design Using Group Technology

Gyan Tshering Lepcha, [1] Dr. D.C. Roy[2]
PG Student, Dept. of Mechanical Engineering, Jalpaiguri Govt. Engg.college, Jalpaiguri, India[1]
HOD & Professor, Dept. of Mechanical Engineering, Jalpaiguri Govt. Engg College, Jalpaiguri, India[2]

Abstract: *Every organization needs to remain competent to stay afloat in the sea of competitors with similar products and services. Smaller production companies, such as job shops, are often incapable of committing significant human or capital resources for the improvement of manufacturing flow times. However, there is considerable demand in these organizations for solutions that offer improvements without the risk involved in expending these resources. This paper presents a study that uses simulation to improve shop floor performance by means of certain operational parameters. In this study, an overview of the plant layout problem is covered for the particular company. The original motivation for redesigning the entire shop floor was the need to realize improvements in material flow and output level. Since the machines were scattered this made it very difficult to study the cost involving the flow of materials through these machines. So for the purpose of analyzing total material handling cost, 34 elements (jobs) were taken which are mainly processed through 6 machines, out of which 32 elements were divided into 4 part families using Direct Clustering Method (DCM) with group technology concept method and similar machines were arranged together to analyze the cost using Computerized Relative Allocation of Facilities Technique (CRAFT) with aide of computer graphics .Finally, a new job shop layout was designed, which yield minimum material handling cost.*

Keywords: *Job shop, Direct Clustering Method (DCM), Computerized Relative Allocation of Facilities Technique (CRAFT), Group Technology.*

I. Introduction

In the job shop environment, the need to improve manufacturing flow times has always been a critical factor to stay competitive. Simply adding human resources or capital equipment may improve flow times, but these alternatives can add tremendous fixed cost and risk to an organization. Most job shops cannot afford the investment needed to reduce their manufacturing flow time. Therefore, a more economical alternative would be of great value to smaller organizations.
In this study, a haphazard arrangements of machines in job shop was clubbed together to form separate machine cells and various layout was designed to investigate improvements in material flow and output level.34 elements were taken which are processed through six machines- lathe, milling, grinding, slotting, shaping and drilling. Other objectives of the study can be summarized as follows:

- To determine the inherent constraints and the bottlenecks in manufacturing process.
- To increase the percentage of annual production quantity completed on time without extra costs including subcontracting and overtime costs.
- To provide a solid base for supervision and face-to- face communication.

II. Design of the Study

To achieve the objectives of the study, the requirements of the following five steps were sequentially satisfied:

1. Part families were formed using Direct Clustering Method (DCM).
2. Similar machines were grouped together to form separate departments.
3. Physical layout of machines (intra-cell) and cells (inter-cell) were developed by means of powerful and well known CRAFT algorithm, which is the basis for many computer-aided layout programs.
4. New manufacturing system was modeled and analyzed to determine the system performance according to predetermined performance measures.
5. Final layout with optimum cost was developed.

III. Part Family Formation & Layout Design for Grout Technology Layout

According to Fraizer and Spriggs (1996), a GT layout is most appropriate for batch processing because parts are produced in small to medium batches and there is relative stability in the product mix. The GT cell creates a small, cost-effective assembly line within the production operation, but provides much more flexibility than traditional assembly lines. Because each cell is dedicated to producing a group or family of similar parts, switching between similar parts in the family is quick and easy. Only minimal setup time is required, compared with a changeover on an assembly line or with a traditional batch processing or job shop.

3.1. Part family Formation

For the part family formation Direct clustering Method was used

Step1. Calculate weight of each row,

Step2. Sort rows in descending order $w_j = \sum_i M_{ij}$

Step3. Calculate weight of each column,
Step4. Sort columns in ascending order
Step5. For I = 1 to n, move all columns j where Mij = 1, to the right while maintaining the order of the previous rows.
Step6. For j = m to 1, move all rows I, where Mij = 1, to the top, maintaining the order of the previous columns.
Step7. If current matrix = previous matrix, STOP; Else go to Step 5.

JOBS / MACHINES	11	19	28	29	14	16	26	27	30	17	18	20	12	15	24	1	2	3	4	6	7	9	21	22	23	25	5	8	10	13	31	32	33	34	RANK
Milling	0	0	0	0	1	1	1	1	0	0	0	0	1	1	1	1	1	1	1	1	1	1	0	0	0	0	1	1	1	1	0	0	0	0	1
Slotting	0	0	0	0	0	0	0	0	0	0	0	0	0	0	0	0	0	0	0	0	0	0	1	1	1	1	1	1	1	1	0	0	0	0	2
Lathe	1	1	1	1	1	1	1	1	1	1	1	1	1	1	1	1	1	1	1	1	1	1	1	1	1	1	1	1	1	1	0	0	0	0	3
Shaping	0	0	0	0	0	0	0	0	0	0	0	0	0	0	0	0	0	0	0	0	0	0	0	0	0	0	0	0	0	0	1	1	1	1	4
Grinding	0	0	0	0	0	0	0	0	0	0	0	0	0	0	0	1	1	1	1	1	1	1	0	0	0	0	0	0	0	0	1	1	1	1	5
Drilling	0	0	0	0	0	0	0	0	1	1	1	1	1	1	1	0	0	0	0	0	0	0	0	0	0	0	0	0	1	1	1	1	1	1	6

Therefore following Four part family is formed by using Direct Clustering method. Job 11,19 ,28 and 29 were omitted from part family, since there was no movement from one machine to other.

3.2. Layout Design

After the formation of Part families it has been seen that different members of part family consists six machining operations as a whole–Lathe , Milling, Grinding, Shaping, Slotting and Drilling.

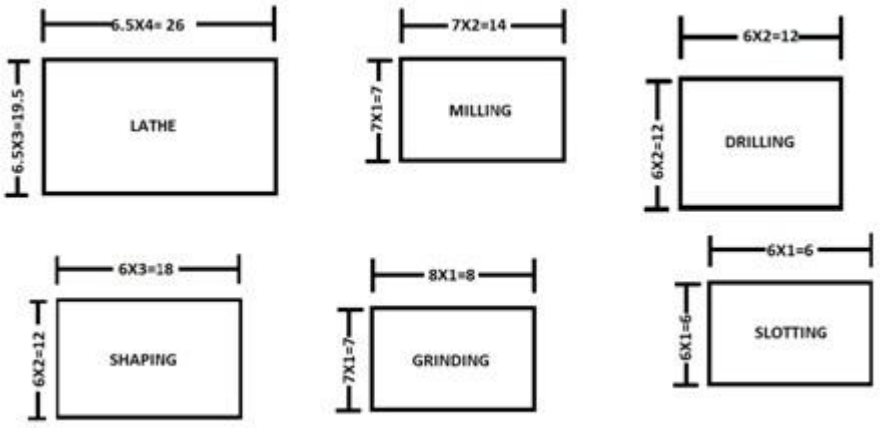

IV. Optimizing the Job Shop Layout

For the opmization of plant layout, Computer Relative Allocation of Facility Technique (CRAFT) with aide of computer graphics simulation was used.

CRAFT is one of the important computer programmes for the quantitative solution of process layout program. The program works in the following manner:

(a) An initial layout is given along with the problem.
(b) The load summary i.e. the to and fro movement frequencies between the various pairs of departments is also supplied.

The interdepartmental pair wise costs per unit distance are also given.
(c) With (a) and (b) as the inputs, CRAFT now interchanges a pair of departments which have
(i) either a common border, or
(ii) The same area requirement.

This is done by interchanging the centroid locations of the departments rather than an actual physical change. CRAFT considers centroid rectilinear distances for the cost computations.
(d) Having done this interchange of centroids it calculates the total costs for the modified layout.
(e) All possible pair wise interchanges are done and costs computed as in (c) and (d).
(f) The least cost interchange is then accepted.
(g) This interchange, i.e. the interchange in step (f) above is now done physically i.e. by physically interchanging the areas.

This may change actual centroid locations and intercentroid distances and therefore the total cost. This is the real cost.
(h) CRAFT now applies the pairwise interchange to the improved layout. That is step (c) through (h) are repeated until no further cost reduction is possible by the pairwise interchange of the centroids.
(i) The last layout is the solution obtained through CRAFT.

4.1. Criterion for Comparison

The flow multiplied by the distance and summed over all cells of the chart. We compute the cost for the flow from *i* to *j* as the product of the material handling cost, the flow and the distance between the departments. The cost of the layout is the sum of the flow cost.

$$\text{Min. } z = \sum_{i=1}^{n}\sum_{j=1}^{n} c_{ij} f_{ij} d_{ij}$$

Where c_{ij} = Material handling cost matrix per unit
f_{ij} = Load matrix
d_{ij} = distance matrix

4.2. Flow chart of CRAFT

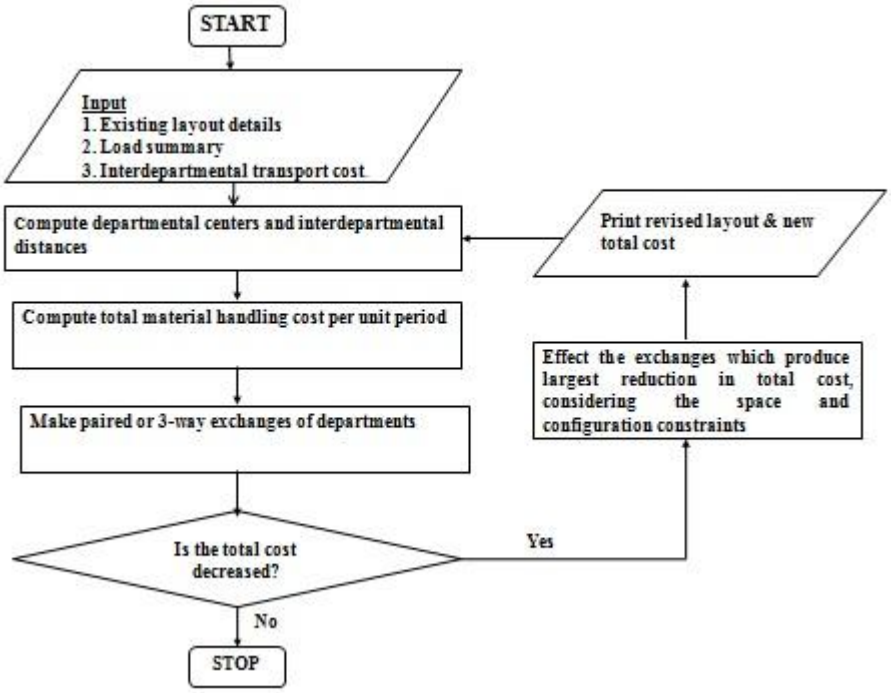

4.3. Input Data

To ascertain these results, actual data from a job shop was used to aid in developing a simulation of their shop layout

4.3.1. Initial layout

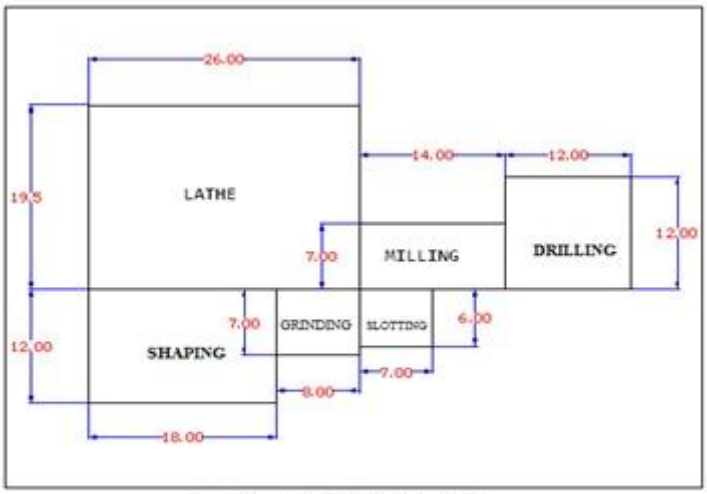

Fig1. Initial layout

Table I: Load matrix

	LATHE	SHAPING	MILLING	GRINDING	DRILLING	SLOTTING
LATHE	-	0	17	0	4	4
SHAPING	-	-	0	4	0	0
MILLING	-	-	-	6	3	4
GRINDING	-	-	-	-	4	0
DRILLING	-	-	-	-	-	0
SLOTTING	-	-	-	-	-	-

Table II: Cost matrix

	LATHE	SHAPING	MILLING	GRINDING	DRILLING	SLOTTING
LATHE	-	1	1	1	2	2
SHAPING	-	-	2	1	3	2
MILLING	-	-	-	2	1	1
GRINDING	-	-	-	-	3	1
DRILLING	-	-	-	-	-	2
SLOTTING	-	-	-	-	-	-

Table III: Distance Matrix (Initial Layout)

	LATHE	SHAPING	MILLING	GRINDING	DRILLING	SLOTTING
LATHE	-	19.75	26.25	22.25	36.75	28.75
SHAPING	-	-	33.5	15.5	49	23
MILLING	-	-	-	18	15.5	10.5
GRINDING	-	-	-	-	33.5	7.5
DRILLING	-	-	-	-	-	26
SLOTTING	-	-	-	-	-	-

V. Results

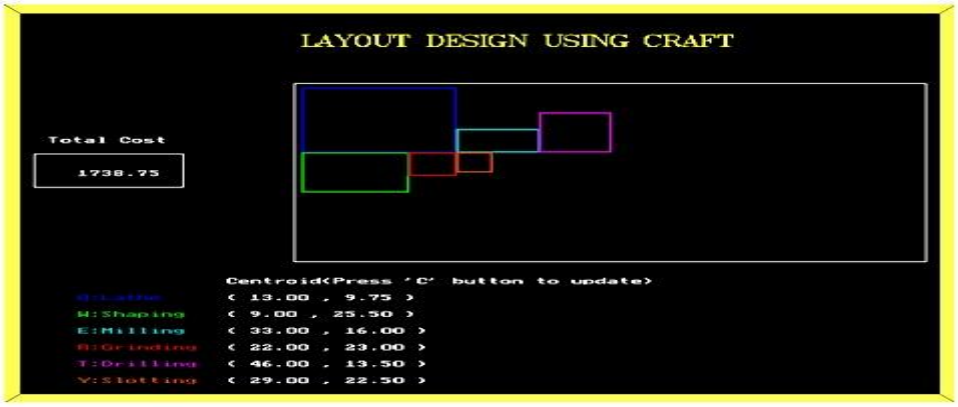

Fig.2. Simulation output for initial job shop layout

Total Cost (Initial Layout) = 1738.75 Units/Unit period

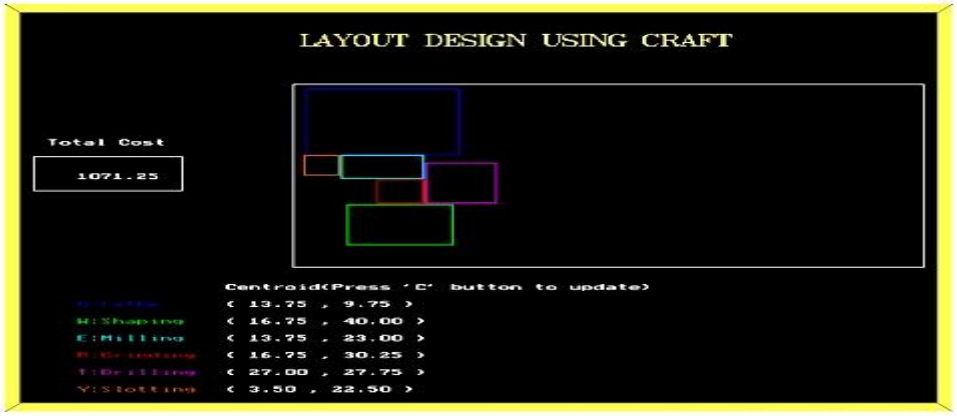

Fig.3. Simulation output of final layout (optimum layout)

Total Cost (Optimum Layout) = 1071.25 Units/Unit period

Table IV: Distance Matrix (Optimum Layout)

	LATHE	SHAPING	MILLING	GRINDING	DRILLING	SLOTTING
LATHE	-	33.25	13.25	23.5	31.25	23
SHAPING	-	-	20	9.75	22.5	30.75
MILLING	-	-	-	10.25	18	10.75
GRINDING	-	-	-	-	12.75	21
DRILLING	-	-	-	-	-	28.75
SLOTTING	-	-	-	-	-	-

VI. Discussion

By reconfiguring the machines of job shop by CRAFT method with incorporation of graphics simulation there was a huge reduction in total material handling cost i.e., from 1738.50 Units/Unit period (initial) to 1071.25 Units/ Unit period. The cost was calculated for the single unit of each item. So, this result will be more vital and profitable when the number of units of the items increases.

VII. Conclusion

This study was aimed at identifying alternative configurations of job shops without investing in additional capital or human resources, and by using layout design technique with incorporation of computer graphics programming. After collecting actual data of 32 jobs, a simulation model was developed to approximate the actual shop environment. Based on the results from this initial model, an optimum layout is developed. This final layout that incorporates group technology concept provides an optimum cost. This study shows that total material handling cost can be improved without investing in additional resources. The results are significant for job shops, especially smaller production firms that cannot afford to continually invest in new equipments and hire additional workers. The reconfiguration of floor shop into a group technology environment can reduce total material handling costs, thus improving the profit to the organization. This assist job shops in remaining competitive in the market.

VIII. Acknowledgements

On the submission of the paper report of "Job Shop Layout Design Using Group Technology Concept" I would like to extend my highest gratitude and sincere thanks to my supervisor Prof. D.C. Roy and for his constant motivation and support during the course of our paper. I truly appreciate and value his esteemed guidance and encouragement from the beginning to the end of this paper. I am indebted to him for having helped me to shape the problem and providing insights towards the solution.

References

Journal paper

[1] Barman, Samir and Joao Lisboa, „Cost Performance of Simple Priority Rule Combinations" , Journal of Manufacturing Technology Management, 21(5), 2010, 567-584.

[2] Flynn, BB and RF Jacobs, „A Simulation Comparison of Group Technology with Traditional Shop Manufacturing" , International Journal of Production Research, 24(5), 1986, 1171-1192.

[3] Flynn, BB and RF Jacobs, „An Experimental Comparison of Cellular (Group Technology) with Process Layout" Decision Sciences, 18(4), 1987, 562-581.

Book

[4] S.N. Chary, Production and Operations Management (Tata Mc Graw – Hill Company Limited, 1997)

International Journal of Modern Engineering Research (IJMER)
www.ijmer.com Vol.3, Issue.3, May-June. 2013 pp-1272-1278 ISSN: 2249-6645

Prospect of bioenergy substitution in tea industries of North East India

M. Saikia, [1] R. Bhowmik, [2] D. Baruah, [3] B. J. Dutta, [4] D.C.Baruah[5]
[1]*Dibrugarh University Institute of Engineering and Technology, Dibrugarh, Assam*
[2, 3] *Grijananda Choudhury Inst of Management and Technology, Guwahati, Assam*
[4]*Udipta Energy, Sibsagor, Assam*
[5]*Department of Energy, Tezpur University, Napaam, Assam-784028, India*

Abstract: *Tea industry plays a major part in the economy of the North Eastern region of India. About 54% of the tea produced in India comes from North East region. The energy requirement of the industry is high and is being provided by utilization of conventional fuel till now. But the increasing prices of fossil fuel have affected the economy of the industry and the production prices have gone up. This study is aimed at investigation of the prospect of switching over from conventional fuels to bioenergy in tea industry to a possible degree. The major areas of energy usage in a tea estate could be categorized as (i) thermal energy for process heat, (ii) electricity for machine operations, (iii) petroleum fuel for transportation and plantation and (iv) thermal and electrical energy for domestic purposes. Process heat and electricity are two major energy consuming areas in the industry. Biomass could be a possible alternative for supplementing and replacing the conventional fuel for these areas. Surplus agro-residues from nearby areas can be used for process heat. Biodiesel from locally produced non-farm and non-edible oil seeds could be alternative to petroleum fuel provided related issues are appropriately addressed. Densification of locally available loose biomass in conjunction with improved cook stove could reduce the consumption of wood. The economic feasibilities of these bioenergy technologies in the thrust areas are analyzed.*

Key words**:** *Tea industry, bioenergy, economics, North East India*

I. Introduction

The eight states comprising the North Eastern part of India, *i.e*. Assam, Arunachal Pradesh, Manipur, Meghalaya, Mizoram, Nagaland, Tripura and Sikkim, covers about 262000 Sqkm., accounting for about 7.9% of India's total geographical area. The region is rich in natural, mineral and material resources, but these resources have not been tapped to their full potential. The population is mainly agrarian in nature with more than 70% engaged in agriculture. Agriculture however is not quite productive for this region and characterized by lower level of inputs, resulting lack of self-sufficiency of food grain and poor economy. Tea is a dominant cash crop of northeastern region, Assam being the major contributor of tea of this region (Table 1). Northeastern states produce around 54% of India's total tea production with Assam alone contributing 51% of India's total and about one-sixth of the tea produced in the world. India is the second largest producer of tea after China, so it is notable that tea industry presents a sizeable chunk in the economy of the country.

Table 1State-wise production of tea in North east India, (*Source- Tea Board of India*)

State	2001	2002	2003	2004	2005	2006	2007
	(Figures in thousand kgs.)						
Assam	453587	433327	434759	435649	487487	502041	511885
Tripura	6506	6632	8577	7168	7515	7128	7856
Arunachal Pradesh	1047	950	1745	2219	2624	3748	5842
Nagaland	75	206	195	190	190	191	191
Manipur	101	100	119	110	108	110	110
Sikkim	110	81	107	150	157	167	82
Meghalaya	41	35	81	99	99	139	259
Mizoram	41	45	78	72	73	75	75

Apart from its direct contribution to the national economy, tea industry also employs a large section of population directly in production and processing sectors. Having several competitors in global as well as in domestic markets, reduction of production cost becomes a serious requirements for the tea producer. However, the rising prices of the energy involved in tea production have caused difficulties to combat price rise. The average tea auction prices in Guwahati Tea Auction centre in 2006 was about Rs 68 per kg, however, average price in 2010 becomes Rs 110, i.e. an increase of 61% in just 4 years[2] Major part of the price hike is attributed to the rise in fuel prices.

With the crisis of conventional energy systems, advocacy of bio-energy options like gasification, biofuels, agro-residue utilization and briquetting have become noticeable in recent times. There have also been some encouraging results, particularly in the fields of successful demonstrations of bioenergy in industries in India as well as abroad (Jorapur and Rajvanshi 1997, Tippayawong et al. 2010). Such attempts could not been seen for the tea industry, particularly in northeastern region. It is believed that in-depth analysis of the possibilities of bioenergy application in tea industry could

evolve some useful outcomes for the benefit of the tea industry.

The requirement of energy in tea processing industry is high with around 21% required as electrical energy and the remaining 79% supplied by conventional fuels (Baruah et al., 1996). It has been reported that the total specific thermal energy consumption in India varies between 4.45 to 6.84 kWh/kg of made tea while specific electrical energy consumption in India between 0.4 to 0.7kWh per kg of made tea (Sundaram et al.). The plantation and transportation sector in an estate also consumes a large amount of energy in the form of petro-fuels. And finally the working section of the industry also consumes energy for their household purpose in the form of firewood. Keeping in view of the above, the present investigation has been undertaken to analyze the feasibility of above-mentioned bioenergy options in tea industry both technologically and economically such that conventionally used fuels can be sustainably and economically be replaced.

II. Method and Materials

The present investigation aims to analyze the feasibility of bioenergy options in tea industry. This is done primarily through energy economic analyses as discussed below.

A. Biomass Gasification

Biomass gasification results fuel gas with prospect of utilization in process heating and electricity generation. The methods of estimating the economical feasibility for process heating and electricity generation are discussed below.

1) Process Heating: The details of the technology and other parameters considered for this option (Biomass gasification) of bioenergy are presented in Table 2.

Table 2: Parameters for analysis

Technology	Feed	Cost/kg (delivered at site as per 2010)	Thermal energy	Firing type
Coal-fired drier	Coal	Rs. 4.6	25 MJ/kg for North East coal	Indirect
Biomass gasifier based drier	Bamboo	Rs. 2	5 MJ/ m^3 of producer gas	Direct

Calculation is done considering the consumption of feed in both the routes to produce the same amount of thermal energy as per requirements of the mentioned tea estate. Bamboo is considered as feed for biomass gasification route as it is widely available in the North East region of India. Producer gas generation for woody biomass such as bamboo is about 2.5 m^3 per kg of feed. It may be added that the biomass consumption will be lower than as per above calculation as producer gas can be directly fired and flue gases can be used in the drier without contamination. Whereas in case of coal-firing, a heat exchanger becomes necessary as the flue gases from coal combustion cannot be directly used in the drier due to high degree of pollutants that would taint the tea.

2) Electricity Generation: Producer gas could be used for captive power generation. Two routes for power production are shown: one is by the use of dual fuel engines where producer gas can substitute up to more than 70% of the diesel, and the other is by utilization of producer gas to run 100% gas engines. In both cases, proper cleaning of gas is very necessary as the tar in producer gas tends to clog the inlets and valves of the engine. For the purpose of power generation by dual fuel engine mode, a 500 kW gasifier system with two units of 250 kW gensets is considered. Bamboo requirement for such a system is about 5 kg per litre of diesel replaced. Thus, bamboo and diesel consumption to meet the requirement are 350 kg per hour at the rate of Rs. 2 per kg and 30 liters at a rate of Rs 37 per litre respectively. Alternately, 100% gas engines can also be used to nullify the dependence on diesel but producer gas being a very low calorific value gas, there are a number of technical difficulties it its utilization. However, Cummins have recently made available commercial models of producer gas engines developed in conjunction with CGPL, IISc.

B. Process Heating in Tea Industry by Direct Firing of Agro Residue Route

Process heat can be produced via direct firing of paddy. Paddy available in nearby areas was assessed by multiplying area under rice cultivation and productivity per hectare. Using GIS technique the area under paddy crop cultivation in 14 development blocks of Sonitpur district was determined. Considering paddy straw yield of Sonitpur district to be 1487 kg per hectare [10], annual rice straw production was assessed. To compare cost effectiveness of direct paddy firing with coal fired systems, cost of production of thermal energy by both methods was determined.

Economic analysis of crop residue is done to determine the cost of rice straw. For the purpose, the costs of production, harvesting, collection, transportation and storage of the residue are taken into account.

1) Production Cost: A certain fraction of total cost of crop production is attributed to crop residue. Thus, crop residue production rate is the product of total cost of crop production and 5% residue fraction [10].
2) Harvesting Cost: Assuming harvesting is done manually, cost associated with harvesting can be determined by dividing daily wage rate (Rs per day) with harvesting capacity (Tonnes per day).
3) Collection Cost: The collection cost is estimated by dividing daily wage rate by carrying capacity (tonne per trip).
4) Transportation cost: Transportation cost can be determined by the method.

Fuel consumption per hour of operation ×cost of fuel +drivers wage per hour

Carrying capacity of transportive mode× transportation speed (km/h)

5) Storage cost: Storage cost includes handling and capital invested for storage facility. Storage cost could be rental cost of the space or the cost incurred to cover the residues to protect them from rain. Generally residues are dumped in open space and immediately fed to the system. Therefore, cost of storage is assumed to be negligible.
6) Total cost:Total cost is sum of production, harvesting, collection, transportation and storage cost.

C. Economics of Biodiesel in Transportation Section of Tea Estate

The diesel demand in the surveyed estate is about 40000 litres annually. Replacing 20% of diesel fuel requires 8000 litre of biodiesel. In this study, we propose to cultivate non edible oil bearing plants in fencing area. From the very first beginning of cultivation to blending, all the cost incurred is considered for checking feasibility of three different species such as nahor (Mesua ferrea Linn), ratanjyot*(*Jatropha curcas) and karanja (Pongamia glabra). A pilot biodiesel plant of 50 lt per day running for 8 hrs per day is assumed for biodiesel production. During economic analysis of biodiesel production, the residual value of the machine is taken as 5% of the purchase price of the machine; rate of interest rate on investment is taken as 11.5% of the average price of the machine; rate of insurance and taxes is taken as 2% of the average price of the machine; housing and shelter is taken as 1.5 % of the average price of the machine. The operational cost of biodiesel production involves the fixed cost and the variable cost. Fixed cost is the cost incurred by the ownership with or without the running the machine which can be calculated taking into account i) depreciation ii) interest on investment iii) insurance and taxes iv)investment on shelter for machinery whereas variable cost involves the i) cost of chemicals ii)electricity iii)repair and maintenance iv) wages.

D. Procedure of Economic Analysis to Determine feasibility of Wet Briquetting and Improved Cook Stove as an Energy Saving Combustion Device

1) Wet Briquetting: It is a simple procedure which involves decomposition of biomass, pressing of decomposed matter and drying of pressed briquettes which can be used as cooking fuel instead of wood. Unlike the screw press and extrusion type technology, it requires small investment that is why wet briquetting is proposed for the temporary works in the referred tea estate.
2) Economic analysis procedure/ simple cost benefit analysis: The parameters considered for analysis are based on village energy consumption survey. The aim is to estimate cost of production per day per family taking into consideration of following parameters

Table 3: Parameters of economic analysis

Parameters	Value
Daily wood requirement for a family of 4 members	7
Cost of wood per kg(Taking average), Rs	5
Daily fuel wood cost, Rs	35
Worker cost ,Rs	150
Requirement of worker for the project	6
Maintenance and equipment cost added to worker cost,%	15

Now comparing the cost per day per family to the cost of fuel wood usage per day per family we can determine whether briquette production is feasible or not for this group.

3) Conservation assessment improved cook stove: In rural households, generally earthen cook stoves are used. In this study, the saving one could do in monetary terms simply by using improved cook stoves is assessed in the households. Per capita consumption before and after use of improved cook stove is compared to assess the saving in energy in general. The parameters taken for consideration are

Table 4: Parameters used in conservation determination calculation

Parameters	Value
Fuel wood consumption for a family of 5 members, kg	7
Fuel wood cost, Rs	5
Fuel wood consumption reduction by improved cook stoves, %	40

III. Results and Discussion

A. Biomass Gasification for Process Heat and Electricity

By surveying in referred tea estate, coal consumed per hour was assessed to be 190 kg per hour. From the coal consumption rate, the thermal requirements is calculated is 1.3 MW and cost of coal per hour is Rs 874. If we wish to substitute coal with gasification of bamboo for producing same amount of thermal energy, cost of fuel becomes Rs 754 per

hour which shows clearly a saving of Rs120 per hour. The electrical consumption of the tea estate under study is about 894600 kWh monthly which includes the consumption in unit processes of manufacture and housing purposes. The monthly expenditure on electricity considering both grid charges and diesel consumption is around Rs.4.5 lakhs. The use of dual fuel engines, a 500kW gasifier system with two units of 250kW generator sets running with 70% substitution of diesel, shows a cost of Rs 4.35 Lakhs resulting in a saving of Rs15, 000. Calculation for 100% gas engines has not been done in this study due to unavailability of data.

B. Process Heating in Tea Industry by Direct Firing of Agro Residue Route

For the annual thermal energy need of 12592 GJ, total annual cost of coal for the factory reached Rs. 23 Lakhs for 2010 working year. Therefore, while thinking of using rice straw in place of coal, the cost of agro residue from field to factory should come at par with a price lesser than coal. The comparison of utilization of coal and rice straw for process heat in the tea industry is shown in table. The cost of coal and straw for process heating of tea is calculated by considering cost of coal and straw as Rs. 3.50 per kg and Rs. 1.37 per kg respectively. Thus, if coal is substituted by straw, the factory will make profit of approximately Rs. 11.6 lakhs annually.

Table 5: Comparison between utilization of coal and straw:

Parameters	Coal	Straw
Calorific value of fuel (MJ/kg)	25.00	14.50
Fuel requirement annually (MT)	504	869
Cost of fuel per kg (Rs.)	4.60	1.37
Fuel required per kg made tea (kg)	0.73	1.26
Cost of fuel annually approximately (Rs. in lakhs)	23.00	11.9
Approximately saving (Rs. in lakhs)		11.6

Though 132.26 million kg of straw is produced annually in this district, the straw available for energy purpose is estimated to be 116.19 million kg annually which is more than adequate. As rice straw has CV lower than that of coal, rice straw is required twice in amount that of coal and at a cost lower than coal.

Keeping in mind the above mentioned profits, Department of Energy of Tezpur University has developed a combustion device with heat exchanger which is compatible to tea dryer of the tea estate under study. Currently, the device is showing thermal efficiency of 61%. Further research on improvement is going on with additional insulation and modification to raise the thermal efficiency.

C. Use of Biodiesel Blended Fuel Transportation and Plantation

It is evident from the analysis that nahor (*Mesua ferrea linn*) and karanja (*Pongamia glabra*) among the three species taken for study have feasibility of meeting the demand of 20% substitution of petrodiesel.

Table 6: Brief analysis of biodiesel seed production with reference to Rupajuli tea estate:

Parameters	Nahor (**Mesua ferrea L**inn).	Ratanjyot(Jatropha curcas)	karanja (Pongamia glabra)
Tea plantation area, hectare	386.69	386.69	386.69
Tea plantation area, m^2	3866900	3866900	3866900
Length per side, m	1966	1966	1966
Plant spacing in meter, m	8	2.9	3
Total no of plants in fencing	976	2704	2616
Seed yield per plant per annum, kg	20	1.5	16
Percentage recovery,%	70	25	33
Total biodiesel available@ 85% sp.gr, litre	11614	861	11746

Table 7: Cost of biodiesel production economics

Parameters	Units	Values
Capacity	litre	50
Life of the machine	years	10
Cost of seed	Rs	10
Purchase price	Rs	500000
Total hourly fixed cost	Rs/l	7.57
Variable cost per litre of BD production	Rs/l	28.13
Total Cost per litre of BD production	Rs/l	35.70
Glycerol cost per litre of BD production	Rs/l	8.00
Cost per litre of BD production	Rs/l	27.70

As per Government of India, the price of biodiesel is Rs25 per litre [4] and if we go for biodiesel production taking a biodiesel plant capacity of 50litre per day running for 270 days taking seed cost as Rs10 per kg then also the production price comes to be around Rs 27.70 per litre (Table 7). Annual fuel cost saving after 20% replacement comes around Rs 74,400 in all types of species. But, considering the cultivation cost of non edible oil seed bearing plants nahor will be able to provide a feasible option of biodiesel cultivation and thereby production which could generate actual profit of around Rs 30,400 yearly taking into account the average cultivation cost.

D. Feasibility of Wet Briquette Technology and Fuel Saving by Use of Improved Cook Stove

1) Economic analysis of wet briquette technology: The low cost and guaranteed availability of densified biomass is the key motivation for fuel switch off. The economic analysis of wet briquetting project does satisfy the first criteria as briquettes could be provided at a much lower cost than wood. The fuel cost per day per family is estimated to be Rs 35. If briquette production cost is Rs 21 per family per day, than we can say the project is economically feasible. These projects engage a group of people. So, they have potential of being funded by Government under Swarnjayanti Gram Swarozgar Yojana [6].
2) Improved Cook Stoves for Fuel Economy and Betterment of Indoor Air Quality: Only fuel switching does not help in conservation of energy. Improved cook stoves with 40% reduction in wood consumption can lower fuel cost by 60% for a family. Moreover, it is seen that fuel consumption per head comes down from 2.8 kg to 0.56 kg. Government of India has taken steps in this direction and launched National Biomass Cook stoves Initiative (NCI) to develop next generation of cooking stoves having better feature of efficiency and fuel conservation. Apart from savings and fast operation, it helps to remove indoor air pollution by its exhaust removal features. This will surely relieve the women from frequent coughing and disease like asthma and other lung diseases.

IV. Conclusions

1. The possible substitution by gasification route showed a saving of Rs15, 000 by using bamboo as a feed material.
2. More than adequate availability of agro residue like rice straw in Sonitpur district has made direct firing of rice straw a lucrative option with a huge profit margin of Rs 11.6 Lakhs.
3. Similarly, in fuel use sector, by blending of diesel up to 20% saw a decrease in fuel cost by Rs 30,400.
4. Improved cook stoves with 40% reduction in wood consumption can lower fuel cost by 60% for a family.
5. Moreover, the above discussed thermal or power producing options are renewable and able to mitigate GHG and thereby making itself a good candidate for Clean Development Mechanism (CDM).

V. Acknowledgements

The authors sincerely acknowledge the staff of Rupajuli Tea Estate for their valuable suggestions and information on which this study is based. The authors would also like to thank Mr. Haradip Mahilary for providing the background for this work.

References

[1]. North Eastern Development Finance Corporation Limited, http://www.nedfi.com/
[2]. Tea Board of India, http:// www.teaboard.gov.in/
[3]. Ministry of Coal, Govt. of India. http://www.coal.nic.in.
[4]. Biodiesel purchase policy, Ministry of Petroleum and Natural Gas, Government of India, http://petroleum.nic.in/
[5]. National Rural Employment Guarantee Act 2005, http://www.nrega.nic.in/
[6]. Swarnajayanti Gram Swarozgar Yojana, Ministry of Rural Development, Government of India, http://rural.nic.in/
[7]. Sundaram E.G. & Kumar K.R.S., "Energy and Environmental Issues in Tea Industries: A Case Study", Department of Mechanical Engineering, Velammal Engineering College, Tamil Nadu, India.
[8]. Baruah D.C., Bhattacharya P.C. (1996), "Energy utilization pattern in the manufacture of black tea", Journal of Agricultural Mechanization in Asia, Africa and Latin America, Vol. 27 No.4, pp.65-70.

[9]. Das S; Jash T. (2009), "District-level biomass resource assessment: A case study of an Indian State West Bengal" Biomass & Bioenergy, 33, pp. 137–143.
[10]. Mahilary H. (2009), "Design and development of loose biomass fired furnace with an aim to substitute fossil fuel in tea industry", M.tech project thesis, Department of Energy, Tezpur University.
[11]. Singh J. & Gu S. (2010), "Biomass conversion to energy in India—A critique" Renewable and Sustainable Energy Reviews, vol 14, pp (1367–1378).
[12]. Grover P.D. (1996), "Biomass briquetting: Technology and practices", published by FAO Regional Wood Energy Development Programme in Asia, Bangkok, Thailand.
[13]. "Biomass Briquetting: An Overview", Bioenergy India, Issue 2, Dec 2009, pp. 21-27.
[14]. Venkataraman C., Sagar A.D., Habib G., Lam N., Smith K.R.(2010), " The Indian national initiative for advanced biomass cookstoves: The benefits of clean combustion", Energy for Susutainable Development, Vol 14, pp. 63-72
[15]. George Francis, Raphael Edinger and Klaus Becker, "A concept for simultaneous wasteland reclamation, fuel production, and socio-economic development in degraded areas in India: Need, potential and perspectives of Jatropha plantations", Natural Resources Forum, vol 29, pp. 12–24, 2005
[16]. Yogesh C. Sharma, Bhaskar Singh, John Korstad, "High Yield and Conversion of Biodiesel from a Nonedible Feedstock (Pongamia pinnata)". J.Agric. Food Chem., 2010 vol58, pp.242–247
[17]. Allen L. Robinson, Helle Junker, Larry L. Baxter "Pilot-Scale Investigation of the Influence of Coal-Biomass Cofiring on Ash Deposition" Energy & Fuels 2002, vol 16, pp 343-355, 2001
[18]. Thomas Nussbaumer "Combustion and Co-combustion of Biomass: Fundamentals, Technologies, and Primary Measures for Emission Reduction", Energy & Fuels, vol 17, pp 1510-1521, 2003.
[19]. N. Tippayawong , C . Chaichana, A. Promwangkwa, P. Rerkkriangkrai "Gasi fication of cashew nut shells for thermal application in local food processing factory" (in press) 2010
[20]. Ajeev jorapur, Anil K. Rajvanshi, "Sugarcane Leaf-Bagasse Gasifiers for Industrial Heating Applications" Biomass and Bioenergy, vol. 13, pp. 141-146. 1997

International Journal of Modern Engineering Research (IJMER)
www.ijmer.com Vol.3, Issue.3, May-June. 2013 pp-1279-1282 ISSN: 2249-6645

Structural Behaviour of Fibrous Concrete Using Polypropylene Fibres

Parveen,[1] Ankit Sharma[2]
[12]*Department of Civil Engineering DCRUST, Sonepat, Haryana, India*

Abstract: *The aim of the present study is to investigate the effect of variation of polypropylene fibres ranging from 0.1% to 0.4% along with 0.8% steel fibres on the behaviour of fibrous concrete. The mechanical properties of the concrete such as compressive and tensile strength have been investigated. The result shows that addition of polypropylene fibre has a little effect on the compressive strength, but there was significant increase in the tensile strength with increase in fibre volume fraction. The present investigation shows an increase of 47% of split tensile strength and 50% of flexural strength. The result shows that ultimate load mainly depended on percentage volume fraction of fibre.*

Keywords: *Ppf, Gfrp, Sfrc, Fbc, Pfrc*

I. INTRODUCTION

Concrete is known to be a brittle material when subjected to tensile stresses and impact loads; tensile strength of the concrete is approximately one tenth of its compressive strength. As a result of this, concrete members are unable to withstand such loads and stress that are usually encountered by concrete structural members. Usually, concrete members are reinforced with continuous reinforcing bars to withstand tensile stresses and to compensate for the lack of ductility and strength. The addition of steel reinforcement to concrete significantly increases its strength, but to produce a concrete with homogenous tensile properties and better micro cracking behaviour, fibres are advantageous. The introduction of fibres in concrete has brought a solution to develop a concrete having enhanced flexural and tensile strength, which are a new form of composite material. At the micro-level, fibres inhibit the initiation and growth of cracks, and after the micro-cracks coalesce into macro-cracks, fibres provide mechanisms that abate their unstable propagation, provide effective bridging, and impart sources of strength gain, toughness and ductility. Fibres are mostly discontinuous, randomly distributed throughout the cement matrices.

The randomly distributed short fibres are generally introduced into concrete to enhance its control crack system and mechanical properties such as toughness, impact resistance, ductility (post cracking), tensile strength etc. of basic matrix. There are many kinds of fibres, such as metallic, synthetic, natural etc which are being used in normal concrete as shown in Fig 1. The term fibre based concrete (FBC) is concrete containing fibrous material which increases its structural integrity. It contains short discrete fibres that are uniformly distributed and randomly oriented. Different type of fibres in concrete changes the character of fibre based concrete. Further properties of fibre based concrete changes with varying concrete, fibre materials geometries, distribution, orientation and densities. When fibre is added to a concrete mix, each and every individual fibre receives a coating of cement paste. Modification of synthetic fibre geometry includes monofilaments, fibrillated fibres, fibre mesh, wave cut fibre large end fibres etc. This increases bonding with cement matrices without increasing in its length and minimized chemical interaction between fibres and the cement matrices. Fibres also modifies and enhances the mechanical properties and behaviour of concrete during its application. Fibre can be used with admixture such as super plasticizer, air entraining, retarding, accelerating etc and all type of cement and concrete mixtures. These produce a special type of concrete with desired properties in fresh and hardened concrete. In present study polypropylene and steel fibres have been used. Polypropylene fibre having low modulus, light density, small monofilament diameter and not susceptible to corrosion and steel fibre increases its ductility, toughness, and impact resistance. Polypropylene and steel fibre is

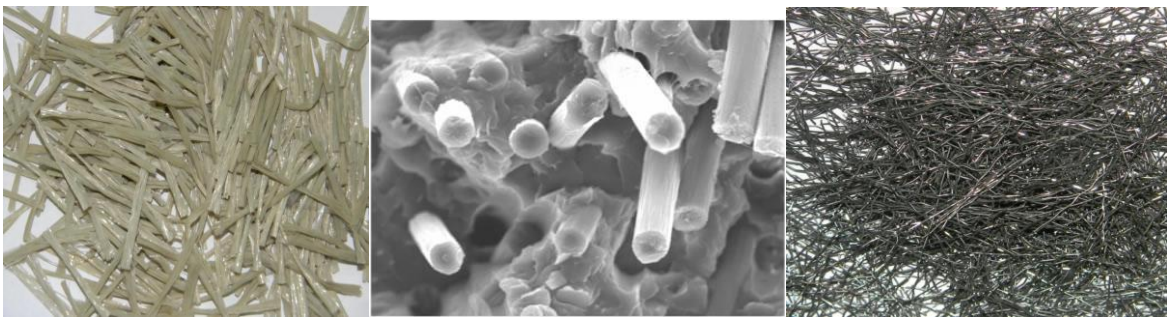

(a) (b) (c)

Figure 1. (a) polypropylene fiber (b) glass fiber (c) steel fiber

Considered to be an effective method for improving the shrinkage, cracking characteristics, toughness and impact resistance of concrete material Almost all FRCs used today commercially involve the use of a single fibre type. Clearly, a

given type of fibre can only be effective in a limited range of crack opening and deflection. The benefits of combining organic (polypropylene and nylon) and inorganic fibres (glass, asbestos and carbon) to achieve superior tensile strength and fracture toughness were recognized about 30 years back. Thereafter much research was not undertaken, recently again there is renewed interest in this field. In present study the structural behaviour of the fibre based concrete using hybrid fibres has been conducted.

II. EXPERIMENT AND RESULT

To achieve the objectives of research programme, an experimental investigation has been carried out on FBC. The cubes, cylinders & beams have been cast with varying percentages of fibre volume fraction. This chapter outlines the experimental program plan, properties of the constituent materials, concrete mix, casting of specimen and testing of specimen. The focus of experimental investigation is to assess the structural behaviour of fibre based concrete. To attain the aim of present study experimental investigation is carried out on 60 Nos. of fibre based reinforced concrete cubes, 60 nos. of fibre based reinforced concrete cylinder & 60 Nos. of fibre based reinforced concrete beams, having overall dimensions (L x B x D) as 150 x 150 x 150 mm for cubes, for cylinder (L x D) as (300 x 150 mm) & for beams (L x B x D) as 500 x 100 x 100 mm.

(a) (b) (c)

Figure 2. (a) Setup for compressive strength (b) Setup for Split Tensile strength (c) Setup for Flexural strength

A. Compressive Strength –

From the results it observed that the addition of the polypropylene fibre in the control mix has a little effect on the compressive strength. It is observed that the use of fibres increases the compressive strength of concrete when the polypropylene fibres were up to 0.2% and then reduction in compressive strength is observed. An increase in 7.5% in compressive strength occurs when the percentage of polypropylene fibre increases up to 0.2%. The decrease in compressive strength is observed when percentage of fibres increases beyond 0.2%. The increase in the compressive strength is due to the increase in bonding effect of fibre with matrix. With the increase in percentage volume of fibre beyond its optimum value (which is 0.2% in present case) compressive strength decreases, this is due to the increase in interference of fibre with each other. This will produce internal voids in concrete mix which leads to decrease the total density of mix and thereby decrease the compressive strength of the mix.

Table -1 Compressive Strength

Sr. No.	Percentage of polypropylene fibre along with 0.8% steel fibre	Compressive strength(N/mm2) After 7 Days	Compressive strength(N/mm2) After 28 Days
1	0%	27.86	39.84
2	0%+0.8%	28.40	40.50
3	0.1%+0.8%	28.54	40.90
4	0.2%+0.8%	29.92	42.82
5	0.3%+0.8%	27.90	40.02
6	0.4%+0.8%	27.08	39.58

B. Flexural Strength–

It is observed that with the increase in polypropylene fibre, the flexural strength increases. However, it is noticed that the rate of increase of flexural strength is more as compared to compressive strength. The results show that optimum dosage for flexure is 0.3% of polypropylene fibre along with 0.8% of steel fibre. The above results show that flexural strength increases with increase in fibre volume fraction; this is due to the additional load taken by the fibres present in the matrix. However, after increasing the volume percentage of polypropylene fibre beyond the optimum value (0.3%) improper mixing of fibres with the matrix takes place due to balling effect of fibre, this increases the amount of vibrations required to remove air voids from the mix which in turn causes the problem of bleeding and decreases flexural strength of the mix. The failure pattern of plain and hybrid fibrous concrete in flexural strength test shows that fibrous concrete are more ductile as compared to plain concrete. This is because when the matrix cracked, the load was transferred from the composite to the fibres at the crack surfaces, which prevents the brittle failure of the composite.

Table -2 Flexural Strength

Sr. No.	Percentage of polypropylene fibre along with 0.8% steel fibre	Flexural strength(N/mm2) After 7 Days	Flexural strength(N/mm2) After 28 Days
1	0%	3.63	4.67
2	0%+0.8%	3.73	4.80
3	0.1%+0.8%	3.92	5.57
4	0.2%+0.8%	4.40	6.19
5	0.3%+0.8%	5.01	7.20
6	0.4%+0.8%	4.15	5.92

C. Split Tensile Strength–

For studying the split tensile behaviour, cylinders of fibrous concrete were tested. The failure load was observed and the strength was calculated which is shown in Table 3. The figures show the effects of volume variation of polypropylene fibre and split tensile strength of concrete. It is noted that with the increase in the polypropylene fibres upto 0.3% the split tension strength increases. The above results shows that split tensile strength increases with increase in fibre volume fraction, because of the holding capacity of the fibres which helps in preventing the splitting of concrete. However, after increasing the volume percentage of polypropylene fibre beyond the optimum value (0.3%) improper mixing of fibres with the matrix takes place due to balling effect of fibre, this increases the amount of vibrations required to remove air voids from the mix which in turn causes the problem of bleeding and decreases split tensile strength of the mix.

Table -3 Split Tensile Strength

Sr. No.	Percentage of polypropylene fibre along with 0.8% steel fibre	Split tensile strength(N/mm2) After 7 Days	Split tensile strength(N/mm2) After 28 Days
1	0%	2.14	3.10
2	0%+0.8%	2.25	3.35
3	0.1%+0.8%	2.59	3.72
4	0.2%+0.8%	2.83	4.09
5	0.3%+0.8%	3.50	4.95
6	0.4%+0.8%	2.70	3.85

D. Stress Strain Response–

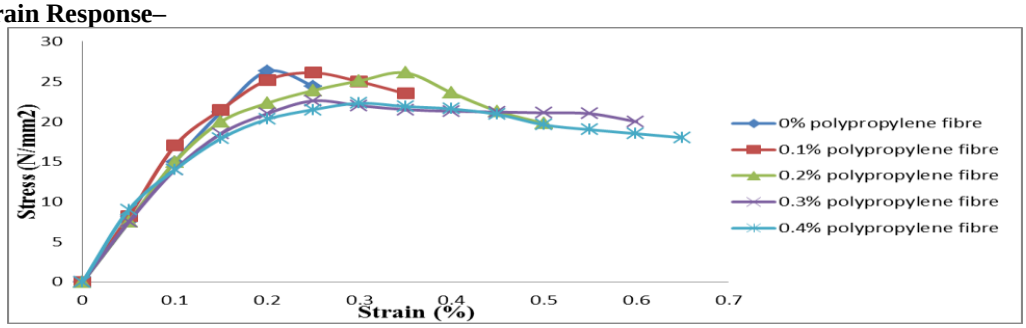

Figure 3. Stress strain response of FBC at different volume fraction of polypropylene fibre

Above figure shows there is significant change in strain of the concrete due to addition of fibres. Descending portion of the curve becomes more and more flatten as the fibre volume fraction increases. The relationship with different volume fraction of polypropylene fibre is shown in Fig. 3. Two different behaviour patterns are obtained as shown in stress strain curve. The stress-strain behaviour of the specimens containing polypropylene fibre upto 0.1% behaves in a similar trend to the control specimen. For these cases which contains 0% and 0.1% polypropylene fibre behaves like a brittle material of which the total energy is generated is elastic energy. However, non linear behaviour is seen for the other specimens which contains more than 0.1% of polypropylene fibre. Here, once the peak stress is reached the specimens continues to yield as shown in figure 3. Therefore it can be stated that concrete with higher percentage of polypropylene fibre possess higher toughness, since the generated energy is mainly plastic. Also it was found that as fibre volume increase failure strain also increases, which leads to more area under the curve, thus enhancing the toughness of the concrete.

III. CONCLUSION

Based on experimental investigation and analysis of results obtained, the following conclusions may be drawn broadly:

1. Steel-polypropylene mix shows a slight increase in the compressive strength as compared with the plain concrete. Hybrid (steel + polypropylene) fibre showed about 5.7% increase in compressive strength.
2. It is observed that polypropylene fibre have not contributed significantly towards compressive strength.
3. The maximum gain in compressive strength was achieved for 0.2% polypropylene fibre. Thereafter increase in fibre content has marginally reduced the compressive strength.
4. Hybrid FRC (steel + polypropylene) shows an increase in split tensile strength as compared to the plain concrete. Fibre reinforced concrete mix showed a considerable increase of about 47% in split tensile strength.

5. The maximum gain in split tensile strength was achieved for 0.3% polypropylene fibre. Thereafter increase in fibre content has marginally reduced the split tensile strength.
6. Steel-polypropylene fibre reinforced concrete showed increase in flexural strength when compared with steel fibre reinforced concrete.
7. The maximum gain in flexural strength was achieved for 0.3% polypropylene fibre. Thereafter increase in fibre content has marginally reduced the flexural strength.
8. From the present study it is observed that the optimum dosage of polypropylene fibre fraction is 0.3%.
9. Stress-Strain relationship showed that there was marginal increase in strain. Stress-Strain relationship shows that strain increases as the percentage of polypropylene fibre increases. As fibre volume increases failure strain also increases, which leads to more area under the curve, thus enhancing the toughness of concrete.

Reference

[1] A. Sivakumar, Manu Santhanam, "Mechanical properties of high strength concrete reinforced with metallic and non-metallic fibre", cement and concrete composite 29 (2007) 603-608.

[2] ASTM A820, "Steel fibre-reinforced concrete design consideration", (1997).

[3] Balaguru, P., and Ramakrishnan, V., Properties of Fiber Reinforced Concrete: Workability Behavior under Long Term Loading and Air-Void Characteristics", ACI Materials Journal, May-Jun, Vol. 85, No. 3, pp. 189-196,1988.

[4] Chote Soranakom, Bazin Mobasher, "flexure design of fibre reinforced concrete", ACI Material Journal (September 2009).

[5] C.D. Johnston, "Steel fibre reinforced mortar and concrete", A review of mechanical properties in fibre reinforced concrete ACI- SP 44- Detroit (1974).

[6] F.Puertas, T.Amat, Fernandez-Jimenez, T.Vazquez, "Mechanical and durable behavior of alkaline cement mortars reinforced with polypropylene fibres", Cement and Concrete Research 33 (2003) 2031-2036.

[7] Giuseppe Campione, Maria Letizia Mangiavillano, "fibrous reinforced concrete beam in flexure: experimental investigation, analytical modeling and design considerations" Engineering structures journal 30 (2008) 2970-2980.

[8] G.Ramakrishna, T.Sundararajan, " Impact strength of a few natural fibre reinforced cement mortar slabs: a comparative study", Cement and Concrete Composites 27 (2005) 547-553.

[9] G.R. Williamson, "The effect of steel fibres on compressive strength of the concrete," Fibre Reinforced Concrete, American Concrete Institude, Detroit, MI, (1974) pp. 195-207 (ACI).

[10] H. Krenchel, S.P. Shah, Restrained shrinkage tests with polypropylene fibre reinforced concrete, in: S.P. Shah, G.B. Baston (Eds.), Fibre Reinforced Concrete and Applications, American Concrete Institute SP-105, Detroit, 1987, pp. 141–158

[11] Indian Standard Code of practices for plain and reinforced concrete IS: 456:2000.

[12] Indian Standard methods of physical test for hydraulic cement. IS: 4031 (Part 6)-1988.

[13] Indian Standard methods of test for aggregates for concrete. IS: 2386 (Part-6)-2007.

[14] Indian Standard methods of chemical analysis of hydraulic cement. IS: 4032 (1985).

[15] Indian Standard recommended guidelines for concrete mix design. IS: 10262-1982.

[16] Indian Standard methods of tests for strength of concrete. IS: 516 (1991).

[17] LI Bei-xing, Chen Ming-xiang Cheng Fang Liu Lu-ping. " The mechanical properties of Fibre Reinforced concrete", Journal of Wuhan University of Technology (May 2004) vol. 19 No.3

[18] Lars Kutzign, Gert Konig, "Design Principals of steel fibre reinforced concrete- A Fracture Mechanics Approach", Leipzig Annual Civil Engineering Report LACER, vol.3 (1999).

[19] Machine Hsiea, Chijen Tua, P.S.Song, "Mechanical properties of polypropylene hybrid fibre-reinforced concrete", Material Science and Engineering A 494 (2008) 153-157.

[20] Menon and Pillai, "Reinforced concrete design", published by Tata McGraw-Hill Company (2007).

[21] Nguyen Van Chanh, "Steel fibre reinforced concrete", Advances in concrete technology volume 3- Gordon and Breach Science publishes.

[22] Naaman, A.E and Najm, "bond sleep mechanism of steel fibre in concrete", ACI material journal (1992), vol. 88 pp. 135-145.

[23] T. Budi Aulia, "Effect of polypropylene Fibres on the properties of high strength concretes", Institutes for Massivbau and Baustoffechnologi, University Leipzig, Lacer No. 7 (2002).

[24] T.S.Lok and J.R.Xiao, "Flexural strength assessment of steel fibre reinforced concrete," Journal of material in civil engineering, vol.11, No.3 (1999).

[25] Tantary, M.A.Ramajan, B.Upadhyay A and Prasad, J, "Mechanical properties of steel fibre based concrete", second national conference on recent Advances in Civil Engineering, Kochi, India (2006), pp.27-33.

[26] V M Malhortra, Carette, A Bilodeaue, "Mechanical properties and durability of Polypropylene fibre reinforced high-volume fly ash concrete for shotcrete applications", ACI Materials Journal,1994,91(5) 478-486.

[27] Waheeb Ahmed Al-Khaja. "Mechanical properties and time dependant deformation of polypropylene fibre concrete." J.King Univ, Vol. 7 Eng Sci. (1) pp 67-76.

[28] Yeol Choia, Robert L. Yuan, "Experimental relationship between splitting tensile strength and compressive strength of GFRC and PFRC", Cement and Concrete Research 35 (2005) 1587-1591.

[29] Youjiang Wang, "modeling of fibre pull-out from a cement matrix", International journal of cement composites and light weight concrete, Volume 10 No.3.

International Journal of Modern Engineering Research (IJMER)
www.ijmer.com Vol.3, Issue.3, May-June. 2013 pp-1283-1289 ISSN: 2249-6645

Review of Solar Chimney Power Technology and Its Potentials in Semi-Arid Region of Nigeria

G.M.Ngala, [1] A.T. Sulaiman, [2] I. Garba[3]
[13]*Department of Mechanical Engineering, University of Maiduguri*
[2]*Department of Mechanical Engineering, Bayero University, Kano, Nigeria*

Abstract: *Solar chimney (SC) is a natural draft device which uses solar radiation to provide upward momentum to the in-flowing air, thereby converting the thermal energy into kinetic energy. It uses a combination of three established technologies, namely, the greenhouse, the chimney, and the wind turbine. In this study the details of SC power technologies are described, and the status and development of this technology reviewed including the experimental and theoretical study status, as well as the economics for SC power technology. There are also potentials of citing this technology in Nigeria especially in the semi-arid region with solar sunshine hours of up to 9 hours, solar radiation of 7kW/m^2/day and enormous flat land.*

Keywords*;* Solar chimney (SC), Power plant (PP), Experimental model, Theoretical model, Green house, Wind turbine, Power conversion unit (PCU).

I. Introduction

Increasing in energy demand and large use of fossil fuels have generated great environmental concerns, solar chimney power plant (SCPP) offers interesting opportunities to use pollution free resources of energy. It is a natural power generator that uses solar radiation to increase the internal energy of flowing air. The air mechanical energy can be transformed into electric power through suitable wind turbine (Salah et al, 2010).A solar chimney is a combination of three established technologies, namely, the greenhouse, the chimney, and the wind turbine. The chimney, which is a long tubular structure, is placed in the centre of the circular greenhouse, while the wind turbine is mounted inside the chimney. This unique combination accomplishes the task of converting solar energy into electrical energy. Solar-to-electric conversion involves two intermediate stages; in the first stage, conversion of solar energy into thermal energy is accomplished in the greenhouse (also known as the collector) by means of the greenhouse effect, while in the second stage, the chimney converts the generated thermal energy into kinetic and ultimately into electric energy by using a combination of a wind turbine and generator (Pasumarthi and Sherif, 1998).

The SCPP has notable advantages in comparison with other power production technologies. These include the following: the collector in solar chimney power plant uses both direct and diffuse radiation;the ground provides a natural heat storage; the low number of rotating parts ensure its reliability; no cooling water is necessary for its operation; and simple materials and known technologies are used in its construction (Schlaich, 1995). The objective of this work is to review the concept development and recent advances in the field of solar chimney power technology and to assess its potentiality in semi-arid regions of Nigeria.

II. Solar chimney concept development

One of the earliest descriptions of a solar chimney power station was written in 1903 by Isidoro Cabanyes, a Spanish artillery colonel. He made public the proposition “Proyec to de motor solar” (solar engine project) introducing an apparatus consisting of an air heater attached to a house with a chimney. In the house interior, a kind of wind propeller was placed with the purpose of electricity production, (Cabanyes, 1903).In 1926 Prof. Bernard Dubos proposed to the French Academy of Sciences the construction of a Solar Aero-Electric Power Plant in North Africa with its solar chimney on the slope of the high height mountain,(Günther, 1931). The author claims that an ascending air speed of 50 m/s can be reached in the chimney, whose enormous amount of energy can be extracted by wind turbine.

In the face of the original concepts, the first outstanding action for the SCPP development was the prototype erection in 1982 in Manzanares, The 50 kW plant prototype built in Manzanares (Fig.1), is 194.6 m high, 0.00125 m-thickness metallic wall SC guyed and aPVC roof-covered collector 122 m in radius. Regardless of its dimensions, this prototype was considered as a small-scale experimental model. As the model was not intended for power generation, the peak power output was 50 kW. Haaf(1984) divulged preliminary test results including energy balances, collector efficiency values, pressure losses due to friction and losses in the turbine section,

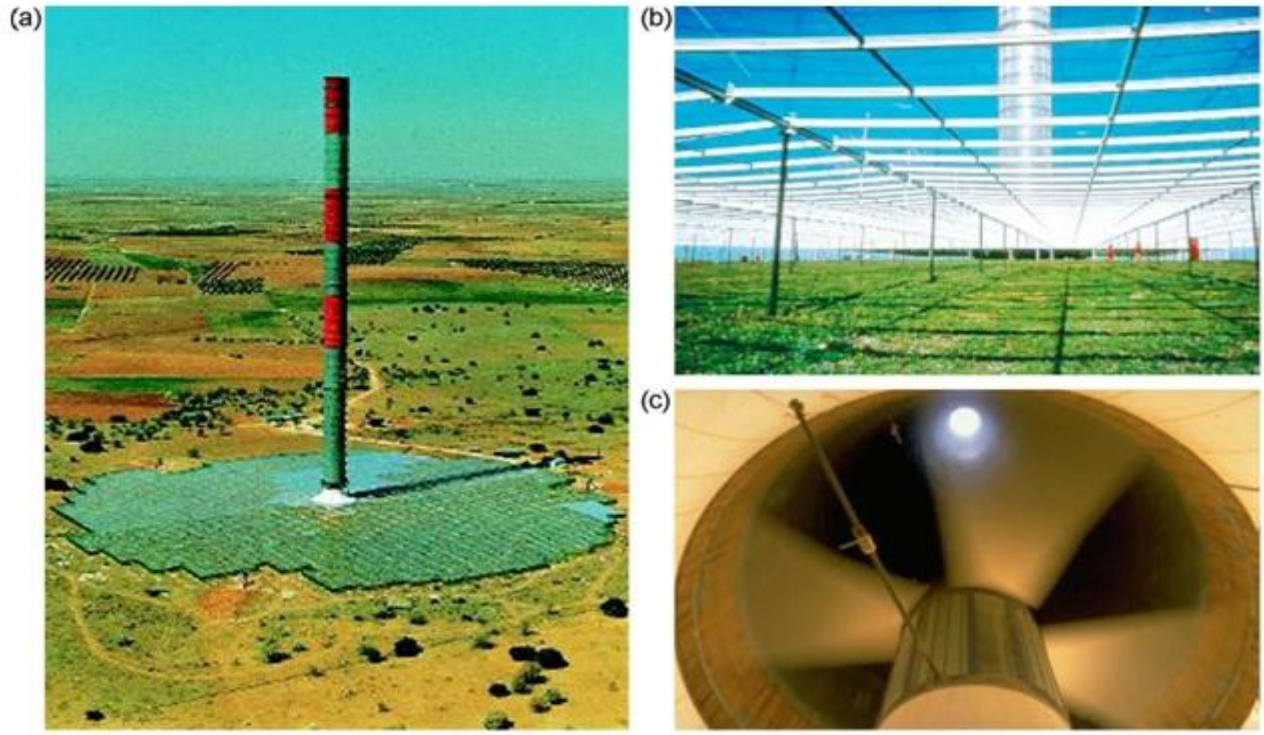

FIG: 1Pictures of Manzanares plant prototype: (a) whole plant; (b) collector; (c) turbine (Schlaich et al 2005)

Castillo (1984) suggested a new "soft" structure approach to the chimney building instead of the conventional "rigid" one. Several other studies were conducted after the construction and testing of the Manzanares prototype, these include transient and steady state fluid dynamic and thermal models, as well as, structural analysis for chimney, collector (including the ground natural heat storage capability) and turbine setups.

III. Study status and advances in solar chimney technology

1. Experiment studies

In the past decades, several experimental models of solar chimney were successively designed, built up, and tested. The Manzanaresplant has been operating for eight years from 1982 to 1989 (Schlaich, 1995). The power output profile correlates closely with solarinsolation profile during day time for this prototype plant without additional storage system, while, there is still an updraft during night time due to thermal storage capacity of natural soil which can be used to produce power during some hours of the night (Haaf, 1984).Krisst(1983), built a courtyard SC power setup with 10W power output. The collector base diameter and SC height were 6 m and 10 m respectively. In 1985, a micro-scale model with a SC 2 m high and 7 cmin diameter and a 9 m^2 collector was built by Kulunkin Turkey (Kulunk, 1985).

In 1997, a SC power setup was built by Pasurmarthi and Sherif in Florida, which had a Lexan roof covered collector of 9.15 m in diameter and a 7.92 m high SC with its diameter gradually decreasing from 2.44 m at the inlet to 0.61 m at the top (Pasurmarthi and Sherif,1998 and Sherif et al, 1995). Type I configuration has an aluminum plate absorber laid down on the ground under the collector roof. Two enhancements were tried on the Type I configuration collector to increase the power output. The Type I configuration collector base was extended18.3 m in diameter to form Type II configuration. Black visqueen and clear visqueen with transparency of about 60% were respectively used as the absorber and the roof for the extended parts of Type II configuration collector. An intermediate canvas absorber was introduced between the roof and the aluminum plate absorber inside the Type II configuration collector to improve the conversion efficiency of the collector and formType III configuration collector. The Type I configuration collector air temperature rise was about 15^oC, whereas the Type II and Type III collectors were able to raise the temperature by 25^oC and 28^oC, respectively. These showed the Type I configuration collector was not as effective, as type II and type III. In the Type II and Type III collectors the temperature variation in the extended section was almost the same, whereas in the Lexan roof covered collector section there was a marginal improvement in the Type III collector compared to the Type II collector. In the Type III collector, air flowed on either side of the extended canvas absorber, thus inducing an increase in mass flow rate, and hence power output (Pasurmarthi and Sherif, 1998).

A pilot SC setup consisting of an air collector 10 m in diameter and an 8 mhigh SC was built in Wuhan, China in 2002 and re-built several times (Zhou et al 2007a, 2007b and 2008). For up-to-date structure, collector roof and the SC were made of glass 4.8 mm in thickness and PVC, respectively. Temperature difference between the collector outlet and the ambient usually could reach 24.1^oC. An interesting phenomenon was found that air temperature inversion appeared in the latter SC after sunrise both on a cool day and on a warm day. The air temperature inversion was formed by the increasing

process of insolation from the minimum and cleared up some time later when the absorber bed was heated to a high enough temperature to let airflow break through the temperature inversion layer and normally flow out from the SC outlet.
Based on the need for plans for long-term energy strategies, Botswana's Ministry of Science and Technology designed and built a pilot SC power setup for research (Ketlogetswe, 2008). SC was manufactured from glass reinforced polyester material, which had an inner diameter of 2 m and a height of 22 m. The collector roof was made of a 5 mm thick clear glass supported by a steel framework. The collection area reached at approximately 160 m^2. The absorber under the roof was made of two layers of compacted soil approximately 10 mm thick and a layer of crushed stones. The layer of crushed stones was spread on the top surface of the compacted soil layer. A SC power setup was built with a SC 11 m high and 1 m in diameter on the campus of Universidade Federal de Minas Gerais, in Belo Horizonte, Brazil (Ferreira et al, 2008 and Maia et al, 2009a and 2009b). The SC structure was manufactured in five wood modules of 2.2 m high each, which was covered internally and externally with glass fiber. A SC power setup was also built up on the campus of Suleyman Demirel University, in Isparta, Turkey, which had 15 m high SC 1.2 m in diameter and a glass covered collector 16 m in diameter.

A small prototype demonstrating the combination of an experimental solar pond of approximately 4.2m diameter and 1.85m dept with a SC 8m high and 0.35m in diameter was constructed by Golder in the campus of RMIT University, in Bundoora, Australia in 2002 (Akbarzadeh,2009and Golder,2003). The water to air heat exchanger was equipped at the SC base. The SC was manufactured from flexible circular ducting which was insulated with60mmthick fiberglass and supported by the structure of a small experimental aero generator with in a fewmeters of the solar pond. Hot brine was extracted from the solar pond at a rate of 1.21 liter per minute through a diffuser placed at approximately 0.5mabove the bottom of the pond and was pumped through the heat exchanger. After delivering its heat to the air which passed through the heat exchanger and SC, the cooler brinewas returned to the bottom of the pond through a second diffuser. The measurements showed that for a solar pond temperature of 45^{o}C, the temperatures of the brine entering and exiting the heat exchanger could reach 37^{o}C and 25 ^{o}C, and the air entering through the heat exchanger was raised from the outside ambient temperature of 17^{o}C to an exit temperature of about 28 ^{o}C. An air flow velocity in the SC was measured at 1 m/s (Akbarzadeh, 2009and Golder, 2003).

2. Theoretical studies

Schlaich's pioneered the first work on the SC concept to harness solar energy, after that many researchers, such as;Haaf et al.(1983), Lautenschlaqer et al. (1985), Louis (1985), Mullett(1987), Padki and Sherif(1989a and b,1992 and 1999), Yan et al.(1991), Lodhi(1999), Bernardes et al.(1999), Schlaich et al. (2005,1995,2004), von Backstromet al, (2000,2002, 2003,2004 and 2006,), Bernardes et al. (2003), Dai et al. (2003), Zhou et al. (2006,2007b,2008,2009 and 2010), Ninic (2006),Nizetic and Klarin (2010), Pastohr et al. (2004), Ming et al. (2006,2007, 2008a and b), Danzomo (2008), Koonsrisuk and Chitsomboon (2007,2009a,b and c,2010), Roozbeh et al (2011), provided theoretical modeling investigations for large-scale SCPP. Pretorius (2004 and 2007), Guoliang et al (2011) performed the comprehensive studies on air flow and heat transfer in large-scale SCPP.

Two typical effective methods of controlling and enhancing power output from SCPP include introducing intermediate secondary roof under the first collector roof and additional closed water-filled thermal storage system on the ground. The results showed that intermediate secondary roof gave a much more uniform daily output profile compared to a plant with single roof. The incorporation of additional closed water-filled systemhas also proved to be a good mechanism for a power output controlling and enhancing, which gave a much more uniform daily output profile compared to a plant without such closed water-filled system (Schlaich et al, 2005).

3. Floating SC power technology

The conventional SC used for power generation is constructed by reinforced concrete. Although having a long service life, the reinforced concrete SC, whose height is required to be as high as possible in order to improve the efficiency of SCPP, has some disadvantages. The disadvantages include high construction cost and limited height because of the technological constraints and restrictions on the construction materials. There are also external limitations such as possible earthquakes, which can easily destroy super high SCs. Based on these facts, Papageorgiou (2004 and 2006) proposed a floating solar chimney (FSC) concept instead of reinforced concrete SC to be used for SCPP. FSC consists of three parts: main body, heavy base and folding lower part. The main body is composed of buoyant gases-filled cylindrical balloon rings tied up to each other with the help of supporting rings. The main body is fastened to the seat of the heavy base and the folding lower part is fastened to the lower part of the heavy base, which can withstand the exterior winds by letting the air enter and come out freely from its rings so that FSC can receive any suitable declination exposed to wind.

Papageorgiou (2004 and 2006) designed the FSC structure, and performed some work on FSC power plant, including investigation of external wind effect and optimum design of SCPP. Zhou et al. (2009c) performed economic analysis of FSC power plant using an economic model. Later, they proposed a novel solar thermal power plant with FSC stiffened onto a mountain-side, segment by segment and estimated the potential of the power generation of the system in China's deserts (Zhou and Yang, 2009).

IV. Potentials of solar chimney in semi arid region of Nigeria

Nigeria which is located between longitude 3^{o}and 14^{o}East of Greenwich and latitude 4^{o}and 14^{o}north of equator has about 160 million people and a total land area of 923,768 km^2.Nigeria lies within a high sunshine belt and thus has enormous solar energy potentials, according toBala et al (2000), Nigeria is endowed with an annual Average daily sunshine of 6.25 hours, ranging between about 3.5 hours at the coastal areas and 9.0 hours at the far northern boundary (semi-arid region).

Similarly, it has an annual average daily solar radiation of about 5.25 KW/m^2/day, varying between about 3.5 kW/m^2/day at the coastal Area and 7.0kW/m^2/dayat the northern boundary (semi-arid region). Nigeria receives about 4.851x 10^{12} KWh of energy per day from the sun. This is equivalent to about 1.082 million tonnes of oil Equivalent (mtoe) per day, and is about 4 thousand times the current daily crude oil production, and about 13 thousand times that of natural gas daily production based on energy unit. The country is also characterized with some cold and dusty atmosphere during the harmattan, in its northern part, for a period of about four months (November-February) annually. The dust has an attenuating effect on the solar radiation intensity, but this has little or no effect on SCPP since the collector uses both direct and diffuse radiation. The specific potentials of the semi-arid regions can be characterized by the availability of flat land in the northern Nigeria couple with the high intensity of solar radiation, such as 5.714kWh/m^2/day in Bauchi, 6.003kW/m^2/day in Kano,5.673kW/m^2/day in Kaduna,6.176kW/m^2/day in Maiduguri and 5.920kW/m^2/day in Sokoto. The average sunshine hour in the arid region is about 9 hours (UNIDO,2003).With this potentiality, the SC technology as an appropriate technology for power generation in semi-arid region of Nigeria cannot be overemphasized.

V. Economics

1. Economics for power generation

In order to assess the economics and competitiveness of SCPP, economic analyses were performed by several researchers (Schlaich (1995), Schlaich et al. (2004) and Bernardes (2004)). Schlaich (1995) estimated the costs for all plant components for various plant sizes.He also evaluated the levelised electricity cost (LEC) and performed the sensitivity analysis of LEC to the interest rate and the length of the depreciation period. Schlaich et al. (2004) presented the component costs and the LEC for various plants for fixed economic parameters. Bernardes (2004) also estimated the component costs and LEC of various-size SCPP, and performed the sensitivity analysis of LEC to the economic parameters. In addition to that, he derived a parametric cost model for the main plant components, i.e., collector, SC and PCU. Fluri et al. (2009) presented a more detailed cost model, including a first detailed cost model for the PCU, where the impact of carbon credits on LEC was also considered, and compared the results to Schlaich et al. (2004) and Bernardes (2004). For the purpose of comparison, two reference SCPPs with similar sizes as the 100MW plants respectively proposed by Schlaich et al. (2004) and Bernardes et al. (2004) were selected. In the detailed cost model, the SC cost includes the material cost, construction cost, hoisting cost, and transport cost, the collector cost includes the material cost, construction cost, and transport cost, and the PCU cost includes the cost of balance of station, generators, turbines, ducts, power electronics, central structure, controls, and supports. Fluri et al. (2009) estimated the power output of the reference SCPPs using Pretorius's thermodynamic model (Pretorius, 2007). The simulation results showed a lower peak power output of 66MW for Schlaich et al.'s reference plant, and 62MW for Bernardes's reference plant, instead of 100 MW. LEC for the Schlaich et al.'s 100MW plant therefore reached at a higher value of €0.270/kWh than Schlaich et al.'s at €0.1/kWh with the same economic parameters (i.e., interest rate = 6%, inflation rate = 3.5%, and depreciation period = 30 years). LEC for the Bernardes's 100MW plant at €0.43/kWh is far larger than the value at €0.125/kWh re-calculated using Bernardes's model with the same economic parameters (i.e., interest rate = 8%, inflation rate = 3.25%, depreciation period = 30 years, and construction period = 2 years). (Fluri et al. (2009) thought a very low LEC at€0.037/kWh actually quoted by Bernardes (2004) was caused by an error in calculation).

During operating period, the SCPP avoids the CO_2 emissions from coal-fired power plant, which typically emits 0.95 kg of CO_2 per kWh power output. Large amount of carbon credits was therefore obtained for SCPP. The fact that SCPP construction will need to consume fossil fuels is neglected because the coal-fired power plant construction also needs to consume fossil fuels, and long service life of reinforced concrete SC corresponds to the total of service life of two to three coal-fired power plant. When the potential impact of carbon credits on LEC is included in this model, the LEC decreases a little, for example, the LEC of Schlaich et al.'s 100MW plant decreases to €0.232/kWh. In usual, the reinforced concrete SC could use for more than 80 years, which would lead to further reduction in SCPP LEC.

2. Additional revenues

A great concern with all solar technologies is extensive use of lands because of low energy concentration of sunlight. The investment of large-scale SCPP is large, and the solar collector is the main cost factor of SCPP.

The best additional use of a solar collector would be for growing vegetables or fruits as a greenhouse for possible additional revenues. The ground under the collector roof requires to be irrigated with fresh water. However, fresh water could be scarce in the potential construction sites of SCPPs, which are often selected in deserts, where land is cheap and sunlight is abundant. In order to grow vegetables or fruit, some lands are selected for the locations of SCPP, which aren't yet deserts but are threatened to become a desert if the climate change goes on, or which has recently become a desert. With pleasure, a wet cultivated ground is often darker than a dry flat one, so that this albedo effect generates a synergy among agricultural and power productions. However, solar heating of an irrigated ground would generate much evaporation, i.e., convert parts of solar heat to latent heat, thus reducing power output largely. According to this principle, since 1998, South African researchers have designed and performed experimental and theoretical study on a mixed project of a SCPP and a large, possibly profitable greenhouse for additional agricultural use (http://www.greentower.net). In the greenhouse, some black 'shadowing nets' were used, whose purpose might be multiple. During day time, these black shadowing nets will absorb solar radiation, and provide the main source of sensible heat to the moving air, which will be hotter than the agricultural greenhouse air. So, quite no convection will drive both airs to switch their places. During night time, the ground is hotter than the black shadowing nets. This will drive air convection from the ground to the black shadowing nets. Black

shadowing nets can be the thermal contact point between cold collector operating air and the agricultural greenhouse mild warm air. When evaporated water coming from the ground is recondensed at the colder lower surface, the heat exchange would produce some dew, which will fall back to the humus. The 'shadowing nets' prevent steam from escaping into the SC, without wasting the fresh water and the latent heat.

Such a structure with 'shadowing nets' will give the whole system a very dark albedo. Of course, shadowing a greenhouse could slow down the photosynthesis, but, in very sunny regions, temperature and hygrometry regulations are an asset, especially if these shadowing nets can be adapted to the light conditions all the day.

In addition to use for heating collector operating air, at the same time, additional use of the outer 2/3 of solar collector area as greenhouse can increase production of a highly productive agricultural area from 100% to at least 270%, adding a virtual 170% to the existing land. Furthermore, vegetation in the collector also could increase heat and power production. These conclusions are mainly drawn based on Prof. Kroger's experimental and theoretical studies in 2000 (http://www.greentower.net.).

VI. Conclusion

Solar chimney (SC) power technology is a simple solar thermal power technology, which includes three familiar technologies: solar collector, SC, and PCU, e.g., turbine generators. The details of SC power technology are described, potentials of citing this power plant in Nigeria and the status and development of this technology reviewed, including, experimental and theoretical study status, and economics for this SC power technology. In addition the descriptions of other types of SC power technology are also done, however the average sunshine hour and solar radiation are 9 hours, and 7kW/m^2/day respectively. With this potentiality, the SC technology as an appropriate technology for power generation in semi-arid region of Nigeria cannot be overemphasized.

References

[1] Akbarzadeh A, Johnson P, Singh R.(2009), Examining potential benefits of combining a chimney with a salinity gradient solar pond for production of power in saltaffected areas. Solar Energy; 83:1345–59.
[2] Bala, E.J., Ojosu, J.O. and Umar, I. H. (2000). Government Policies and Programmes on the Development of Solar-PV Sub-sector in Nigeria. Nigerian Journal of Renewable Energy, Vol. 8, No. 1&2, pp. 1-6
[3] Bernardes MA dos S, Valle RM, Cortez MF.(1999), Numerical analysis of natural laminar convection in a radial solar heater. Int J ThermSci;38:42–50.
[4] Bernardes MA dos S, Voss A, Weinrebe G.(2003), Thermal and technical analyzes of solar chimneys. Solar Energy; 75:511–24.
[5] Bernardes MA dos S.(2004) Technische, okonomische und o kologischeAnalyse von Aufwindkraftwerken (Technical, economical and ecological analysis of SCPP). Ph.D. Thesis. Germany: Universitat Stuttgart.
[6] Cabanyes, I. (1903), Proyecto de Motor Solar, La EnergiaEléctrica - Revista General de Electricidad y susAplicaciones, 8, 61-65.
[7] Castillo, M. A. (1984), A New Solar Chimney Design to Harness Energy from the Atmosphere, in Spirit of Enterprise - The Rolex 1984 Rolex Awards, edited by M. Nagaiand A. e. J. Heiniger.
[8] Dai YJ, Huang HB, Wang RZ. (2003), Case study of solar chimney power plants in Northwestern regions of China. Renewable Energy; 28:1295–304.
[9] Danzomo, B. (2008), Performance studies on solar tower systems, an M.Eng. thesis, Bayero university Kano. Unpublished. Ferreira AG, Maia CB, Cortez MFB, Valle RM.(2008), Technical feasibility assessment of a solar chimney for food drying. Solar Energy; 82:198–205.
[10] Fluri TP, Pretorius JP, Van Dyk C, von Backstrom TW, Kroger DG, Van Zijl GPAG.(2009), Cost analysis of solar chimney power plants. Solar Energy, vol; 83:246–56.
[11] Gannon AJ.(2002) Solar chimney turbine performance. Ph.D. thesis. South Africa: University of Stellenbosch.
[12] Gannon AJ, von Backstrom TW.(2002), Solar chimney turbine part 1 of 2: design. In: International solar energy conference. p. 335–41.
[13] Guoliang X, Tingzhen M, Yuan P, Fanlong M, Cheng Z.(2011),Numerical analysis on the performance of solar chimney power plant system,Energy Conversion and Management, vol;52 ,876–883
[14] Golder K. (2003), Combined solar pond and solar chimney. Final year Mechanical Engineering Project. School of Aerospace, Mechanical and Manufacturing Engineering, Bundoora Campus, RMIT University, Melbourne, Australia.
[15] Günther, H. (1931), InhundertJahren, 78 pp., Kosmos - Gesellschaft der Naturfreunde, Stuttgart.
[16] Haaf W, Friedrich K, Mayr G, Schlaich J.(1983), Solar chimneys. Part I: Principle and construction of the pilot plant in Manzanares. Int J Solar Energy;2:3–20.
[17] Haaf, W. (1984), Solar Chimneys - Part II: Preliminary Test Results from the ManzanaresPilot Plant, edited, pp. 141 - 161, Taylor & Francis.
[18] http://www.greentower.net.Greentower
[19] Ketlogetswe C, Fiszdon JK, Seabe OO.(2008), Solar chimney power generation project—the case for Botswana. Renewable Sustain Energy Rev; 12: 2005–12.
[20] Koonsrisuk A, Chitsomboon T.(2007), Dynamic similarity in solar chimney modeling. Solar Energy vol; 81:1439–46.
[21] Koonsrisuk A, Chitsomboon T. (2009a), Partial geometric similarity for solar chimney power plant modeling. Solar Energy vol; 83:1611–8.
[22] Koonsrisuk A, Chitsomboon T. (2009b), Accuracy of theoretical models in the prediction of solar chimney performance. Solar Energy vol; 83:1764–71.
[23] Koonsrisuk A, Chitsomboon T. (2009c), a single dimensionless variable for solar chimney power plant modeling. Solar Energy vol; 83:2136–43.
[24] Koonsrisuk A, Lorente S, Bejan A.(2010),Constructal solar chimney configuration. International Journal of Heat and Mass Transfer vol; 53:327–33.

[25] Krisst RJK.(1983), Energy transfer system. Alternative Sources Energy 63:8–11.
[26] Kulunk H. (1985), A prototype solar convection chimney operated under Izmitconditions. In: Veiroglu TN, editor. Proceedings of the 7th Miami international conference on alternative energy sources.p. 162.
[27] Lautenschlaqer H, Haaf W, Schlaich J. (1985), New results from the solar chimney prototype and conclusions for large power plants. In: Commission of the European Communities, European. 231–5.
[28] Lodhi MAK.(1999), Application of helio-aero-gravity concept in producing energy and suppressing pollution. Energy Conversion Manage; 40: 407–21.
[29] Louis T. (1985), Optimizing collector efficiency of a solar chimney power plant. IEEE;219–22.
[30] Maia CB, Ferreira AG, Valle RM, Cortez MFB.(2009a), Theoretical evaluation of the influence of geometric parameters and materials on the behavior of theairflow in a solar chimney. Comput Fluids; 38:625–36.
[31] Maia CB, Ferreira AG, Valle RM, Cortez MFB.(2009b), Analysis of the airflow in a prototype of a solar chimney dryer. Heat Transfer Eng,vol;30:393–9.
[32] Ming TZ, Liu W, Xu GL, Xiong YB, Guan XH, Pan Y.(2008a) Analytical and numerical investigation of the solar chimney Numerical simulation of the solar chimney power plant systems coupled with turbine. Renewable Energy vol;33:897– 905.
[33] Ming TZ, Liu W, Xu GL.(2006), Analytical and numerical investigation of the solar chimney power plant systems. Int J Energy Res vol;30:861–73.
[34] Ming TZ, Liu W, Pan Y, Xu GL.(2008b) Numerical analysis of flow and heat transfer characteristics in solar chimney power plants with energy storage layer. Energy Convers Manage vol; 49:2872–9.
[35] Ming TZ, Liu W, Pan Y.(2007), Numerical analysis of the solar chimney power plant with energy storage layer. In: Proc. ISES 2007 solar world congress conference; 2007.p. 1800–5.
[36] Mullett LB.(1987), The solar chimney overall efficiency, design and performance. Int J of Ambient Energy,vol;8:35–40.
[37] Ninic N. (2006), Available energy of the air in solar chimneys and the possibility of its ground-level concentration. Solar Energy, vol; 80:804–11.
[38] Nizetic S, Klarin B.(2010), A simplified analytical approach for evaluation of the optimal ratio of pressure drop across the turbine in solar chimney power plants. Applied Energy vol;87:587–91.
[39] Padki MM, Sherif SA.(1989a), Solar chimney for medium-to large scale power generation. In: Proceedings of the Manila international symposium on the developmentand management of energy resources, vol. 1; p. 432–7.
[40] Padki MM, Sherif SA.(1989b)In: Solar chimney for power generation in rural areas. Seminar on energy conservation and generation through renewable resources, Ranchi, India. p. 91–6.
[41] Padki MM, Sherif SA.(1992), A mathematical model for solar chimneys. In: Proceedings of 1992 international renewable energy conference, vol. 1; p. 289–94.
[42] Padki MM, Sherif SA.(1999), On a simple analytical model for solar chimneys. Int J Energy Res;23:345–9.
[43] Papageorgiou CD.(2004), Floating solar chimney. WO2004/085846 A1/07-10-2004.
[44] Papageorgiou CD.(2006), Floating solar chimney. http://www.floatingsolarchimney.gr. April 28, 2006.
[45] Pastohr H, Kornadt O, GurlebeckK(2004), Numerical and analytical calculations of the temperature and flow field in the upwind power plant. Int J Energy Res vol;28:495–510.
[46] Pasumarthi N, Sherif SA.(1998), Experimental and theoretical performance of ademonstration solar chimney model. Part II: experimental and theoreticalresults and economic analysis. Int J Energy Res;vol;22:443–61.
[47] Pretorius JP.(2004), Solar tower power plant performance characteristics. Master thesis. South Africa: University of Stellenbosch.
[48] Pretorius JP.(2007), Optimization and control of a large-scale solar chimney power plant. Ph.D. thesis. South Africa: University of Stellenbosch.
[49] Roozbeh S, Majid A and Behzad H.(2011), Modeling and numerical simulation of solar chimney power plants, Solar energy vol 85, 829-38
[50] Salah L, Amor B, Toufik C(2010) Performance analysis of a solar chimney power plant in the southwestern region of Algeria,Renewable and Sustainable Energy Reviews, vol;14, 470–77
[51] Sherif SA, Pasumarthi N, Harker RA, Brinen GH.(1995), Performance of a demonstration solar chimney model for power generation. Final Technical Report No.UFME/SEECL-9507, Solar Energy and Energy Conversion Laboratory, Department of Mechanical Engineering, University of Florida, Gainesville
[52]Schlaich, J. (1995), The Solar Chimney: Electricity from the Sun, Edition Axel Menges, Stuttgart.
[53] Schlaich J, Bergermann R, Schiel W, Weinrebe G.(2005), Design of commercial solar updraft tower systems—utilization of solar induced convective flows forpower generation. J Solar Energy Eng;127:117–24.
[54] Schlaich J, Schiel W, Friedrich K, Schwarz G, WehowskyP, Meinecke W, et al.(1995), The solar chimney: transferability of results from the Manzanares solarchimney plant to larger scale-plants. Tech. Rep., SchlaichBergermann und Partner CEs, Stuttgart; 1995.
[55] Schlaich J, Bergermann R, Schiel W, Weinrebe G.(2004), Sustainable electricity generation with solar updraft towers. StructEngInt; 3.
[56] UNIDO, 2003, Renewable energy for rural industrialization and development in Nigeria, Energy commission of Nigeria.
[57] Von Backstrom TW, Gannon AJ.(2004), Solar chimney turbine characteristics. Solar Energy;76:235–41.
[58] von Backstrom TW, Bernhardt A,(2003) Gannon AJ. Pressure drop in solar power plant chimneys. J Solar Energy Eng;125:165–9.
[59] Von Backstrom TW, Fluri TP.(2006), Maximum fluid power condition in solar chimney power plants—an analytical approach. Solar Energy vol; 80:1417–23.
[60] Von BackstromTW, Gannon AJ (2000). Compressible flow through solar power plant chimneys. J Solar Energy Eng 2000;122:138–45.
[61] Yan MQ, Sherif SA, Kridli GT, Lee SS, Padki MM.(1991) Thermo-fluids analysis of solar chimneys. IndApplic Fluid Mech;ASME FED-2:125–30.
[62] Zhou XP, Yang JK, Xiao B, Hou GX.(2007a), Simulation of a pilot solar chimney power equipment. Renewable Energy;32:1637–44.
[63] Zhou XP, Yang JK.(2008), Temperature field of solar collector and application potential of solar chimney power systems in China. J Energy Inst; 81:25–30.

[64] Zhou XP, Yang JK, Xiao B, Hou GX.(2007b), Experimental study of the temperature field in a solar chimney power setup. ApplTherm Eng;27:2044–50.
[65] Zhou XP, Yang JK, Xiao B, Long F.(2008), Numerical study of a solar chimney thermal power setup using turbulent model. J Energy Inst;81:86–91.
[66] Zhou XP, Yang JK, Xiao B, Hou GX, Xing F.(2009a), Analysis of chimney height for solar chimney power plant. ApplThermEng;29:178–85.
[67] Zhou XP, Yang JK, Xiao B, Li J. (2009b) Night operation of solar chimney power system using solar ponds for heat storage. Int J Global Energy Issues 2009;31:193–207.
[68] Zhou XP, Wang F, Fan J, Ochieng RM.(2010), Performance of solar chimney power plant in Qinghai-Tibet Plateau. Renewable and Sustainable Energy Reviews.2010; corrected proofs,doi:10.1016/j.rser.04.017.
[69] Zhou XP, Yang JK, Xiao B.(2006), CFD Simulation study on flow field inside the solar power chimney. J Thermal Power ;35:23–6.
[70] Zhou XP, Yang JK, Wang F, Xiao B.(2009c), Economic analysis of floating solar chimneypower plant. Renewable and Sustainable Energy Review.vol;13:736–49.
[71] Zhou XP, Yang JK. (2009),A novel solar thermal power plant with floating chimneystiffened onto a mountain-side and potential of the power generation inChina's deserts. Heat Transfer Eng vol; 30: 400–7.

International Journal of Modern Engineering Research (IJMER)
www.ijmer.com Vol.3, Issue.3, May-June. 2013 pp-1290-1294 ISSN: 2249-6645

Comparative Analysis on Solar Cooking Using Box Type Solar Cooker with Finned Cooking Pot

Ismail Isa Rikoto, [1] Dr. Isa Garba
[12]*Department of Mechanical Engineering Bayero University, Kano*

Abstract: *A comparative investigation was conducted using a box type solar cooker with two different cooking pots at the testing area of so KO to Energy Research Centre, UsmanuDanfodiyo University. The two potsare identical in shape and volume with one of the pots external surface provided with fins. The result of two tests (water heating and boiling test) revealed that 75cl of water was raised to 95^{o}Cin 112 and 126 minutes for finned and unfinned cooking pot respectively. These figures represent 11% reduction in heating time. Similarly 0.3kg of rice was cooked in 120 and 150 minutes for the finned and unfinned cooking pots respectively. This clearly demonstrates that fins improved the heat transfer from the internal hot air of the cooker toward the interior of the pot where the water and rice to be heated and cooked were kept.*

Keywords: *solar heating, thermal insulation, concentrating solar cooker and thermal performance*

Significance of the Research

The solar cookers if available can offer a partial solution to multitude of cooking problems face by people of low income. A properly designed and improved cooker if introduce in to the market in mass scale can supplement the cooking energy requirement of several millions of people and reduce deforestation and environmental problems associated with the use of fossil fuels Solar cooker which is safe and simple to operate can satisfactorily be used for cooking in the presence of sunshine.

I. Introduction

Solar energy is the energy from the sun. The sun generates energy ina process called nuclear fusion. During this process four hydrogen nuclei combine to become helium atom with the release of energy. This energy is emitted to the space as solar radiation. A small fraction of this energy reaches the earth. Today solar energy is used in various applications such solar heating, distillation, drying, cooking etc. To cook food for nourishment is fundamental to any society and these require the use of energy in some form. The use of solar energy to cook food presents a viable alternative to the use of fuel wood, kerosene, and other fuels traditionally used in developing countries for the purpose of preparing food. Increased in the awareness of the global need for alternative energy source has led to proliferation of research and development in solar cooking. Solar cooking can be used as an effective mitigation tool with regards to global climate change, deforestation, and economic debasement of the world's poorest people. Solar Energy has tremendous advantages in tropical country like Nigeria because of it abundance and sustainable source of energy. The use of solar cookers will have a great potential of reducing the suffering of many people from the shortage and high cost of fossil and other sources fuels. It will also reduce the tedious task faces by rural women in search of fire wood for cooking. Several factors including access to materials, availability of traditional cooking fuels, climate, food preferences, and technical capabilities: affect people's perception of solar cooking. It is in the light of this that the author decided to investigate the effect of solar cooking using box type solar cooker with finned cooking pot. The purpose of the fins is to improve heat transfer from the cooker surface to the surrounding. Fins can be thought as an extension of the surface by adding additional surface area which enables additional heat flow to and from the medium it is in contact.

1.1.1 Description of Box type solar cooker and the cooking Pot

The solar cooker used in this investigation is the box type solar cooker developed at Sokoto Energy Research Centre, Usmanu Danfodiyo University. The cooker has a dimension of 0.5m by 0.5m by 18m, the sides and bottom of the tray are encased in wooden box. The clearance between the galvanized iron sheet and encasement is filled with 5cm foam to provide thermal insulation, the tray consist of movable doubled glass cover hinged to one side of the incasing at the top. The plate and the experimental set up of the cooker is shown in fig 1. The cooker was exposed to solar radiation. The absorber consist of a galvanized iron sheet painted black with thickness of 4mm. the photograph of the box solar cooker is shown in fig 1.For the purpose of this investigation, two cooking pots were used. They are made up aluminum painted black, are cylindrical in shape and have plat base. Both the cooking pots have identical lid, with a diameter of 14cm and height of 7cm.the lateral external surface of one of the cooking pot was provided with fins made of galvanize iron painted black. The fins used are rectangular in shape with a cross reaction. (5.5cm by .05cm) and have a length of 2.2cm, spaced at 1.5cm. (Arezki Harmin, 2008). The photograph of the finned and un finned pots were shown in figure 2. Arriving global solar radiation was focused on the solar cooker. For the purpose of this investigation boiling test and cooking test were conducted. Dasin et al 2011.

In Nigeria and many other developing countries commercial fuels like coal, kerosene, cooking gas and electricity are very expensive beyond the reach of common man. Majority of the people depend on fuel wood for cooking purposes. Cutting down of trees for fuel wood has led to fast and rapid depletion of our forest therefore increase fuel wood price which imposes

economic and social burden on the people as well as cause environmental and ecological problems. To date rural women in Nigerian and other developing countries use labor and waste considerable time of day in search of firewood to meet their cooking energy requirement. The necessity for the search for available and affordable alternative source of energy to supplement the use of firewood for food cooking cannot be over emphasized. Solar energy through solar cooking offers a possible solution to these problems.

II. Literature Review

Several research works was, conducted in different areas of solar cooking ranging from thermal testing and performance evaluation of different types of solar cooking devices. Such devices include concentrating solar cookers, Parabolic solar cookers, panel solar cookers, hot box solar cookers, square and rectangular box type of solar cookers, Double exposure solar cookers ,solar cookers with thermal storage and many others by various authors with the aim of improving the efficiencies of these cookers. Some of the authors that work in this area include:(Ali, 2000)**,** Design and carried out series of test in nine days in other to make comparison of the Sudanese box type solar cooker against the Indian designs. Sudanese solar cooker showed a better thermal performance. (Ibrahim, 2005), Conducted an experimental testing of box type solar cooker using the standard procedure of cooking power. The box type solar cooker was tested to accommodate four cooking pots in tatna (Egypt) under prevailing weather conditions. The experiment was performed in July 2002.the cooker was able to cook most kind of food with an overall utilization efficiency of 26.7%.(.Ammer, 2005)**,** carried out research on the title, theoretical and experimental assessment of double exposure solar cooker. The solar cooker is exposed to solar radiation from the top and bottom sides with a set of plane diffuse refection is used to direct radiation on to lower side of the absorber plate.

The performance of the cooker and the convectional box type solar cooker were investigated. Result under the same prevailing conditions show that the absorbers of the box type solar cooker and the double exposure solar cooker attain a stagnation temperatures of 140^{o}C and 165^{o}C respectively.(hussein, 1997). Work on the performance of the box type solar cooker with an auxiliary heating. The performance of the cooker was studied and analyzed. It was done with the help of a built in heating coil inside the cooker. It was found that the use of auxiliary source allow cooking on most cloudy days.(Nahar, 2003), work on performance and testing of hot box storage solar cooker. Hedesigned fabricated and tested a hot box solar cooker with used engine as storage materials so that cooking can be performed in late evening. The performance and testing of a storage solar cooker was investigated by measuring stagnation temperatures and conducting cooking trials. The efficiency of the hot box storage solar cooker was found to be 27.5%.(Ngwuoke, 2003)**,** Design constructed and measured performance of plane - reflector augmented box type solar cooker. The solar cooker consists of aluminum plate absorber painted with black matt and double glazed lid. They predicted water boiling times using the two figures of merit compared favorably with the measured values, the performance of the cooker with plane reflector in place was improved tremendously compare to that without the reflector.EssanAbdullahi*et al* 2010**,** work on cylindrical solar cooker with automatic two axes sun tracking system. He design, constructed and operated a cylindrical solar cooker with two axes sun tracking. He carried out series of test during different days in the year 2008 from 8:30am to 4:30pm.the test show that the solar cooker can increase water temperature up to 90^{o}C. (D.Y Dasin, 2011)Carried out a performance evaluation of parabolic concentrator solar energy cooker in tropical environment in AbubakarTafawaBalewa University Bauchi Nigeria there study revealed that the stagnation temperature of 120^{o}C, 116^{o}C, and 156oc were achieved respectively on three different days between the month of June and July. The boiling test of water indicated that 1kg of water on three different days was raised to 95^{o}C 96^{o}C in 60-75 minutes. Food cooking showed that 200g of of white rice was cooked in 75 minutes,200g of parboiled rice was cooked in 75 minutes,200g of beans was cooked in 90minute and 800g yam was cooked in 75 minutes.(Danmallam, 2011)Developed and carried a performance evaluation of rectangular and square box type cookers at So ko to Energy Research Centre, Usmanu Danfodiyo University under the same environmental conditions found that the rectangular box type cooker performs better than the square type. For a given type of solar cooker it is possible to reduce the cooking time by carrying out modification on the shape of the cooking vessel. These modifications can improve heat transfer to the food through the pot walls (Arezki Harmin et al 2008).Gaur et al (1999) proposed a cooking vessel provided with a concave lid. Their experimental study showed a reduction of 10-13% in cooking time compared to and ordinary cooking vessel under the same conditions.

III. Experimentation

The experimental testing of the solar cooker was conducted at the testing area of Sokoto Energy research centre.. During each test, both cooking pot were placed side by side on the absorber of the solar cooker and loaded with the same mass of water 75cl at the same temperature for water heating test. The temperatures of' the water in each pot as well as ambient temperature and global solar irradiation were recorded at 15 minute intervals using amulti-channel data logger system. Global components solar radiation was measured using CM11 typepyranometer. Both the two potwere filled with water was placed in the cooker, and was closed with double glazing cover until test end. The cooker was manually oriented according to azimuth at an interval of 15 mm in order to collect a maximum of solar radiation.

IV. Results

4.1 Water boiling test

Table1: Temperature distribution at various point of cooker for heating test

Time	Ambient temp (°C)	Water Finned pottemp (°C)	Water in Unfinned pot temp(°C)	Plate temp (°C)	Solar radiation W/m2	Wind speed(m/s)
11:15	40.1	39.6	39.6	75.1	864	0.4
11:30	41.5	55.2	53.9	83.9	897	0.5
11:45	41.7	68.4	64.2	88.4	951	0.4
12:00	44.6	77.4	73.5	93.5	965	0.9
12:15	41.6	80.9	76.1	97.4	953	0.8
12:30	43.3	87.6	81.5	114.3	961	0.1
12:45	42.8	91.7	87.2	117.6	968	0.2
13:00	45.1	94.2	92.7	120.9	944	0.6
13:15	44.4	96.4	94.6	124.7	915	0.9
13:30	44.3	97.8	95.2	129.5	905	0.8

Table 2: result of water heating test 0.75 liters

Mean ambient temperature (°C)	42.9
Initial water temperature (°C)	39.6
Time of boiling with finned pot (Min)	112
Time of boiling with un finned pot	126
Reduction in time (min)	14
% reduction in Boiling time (Min)	11

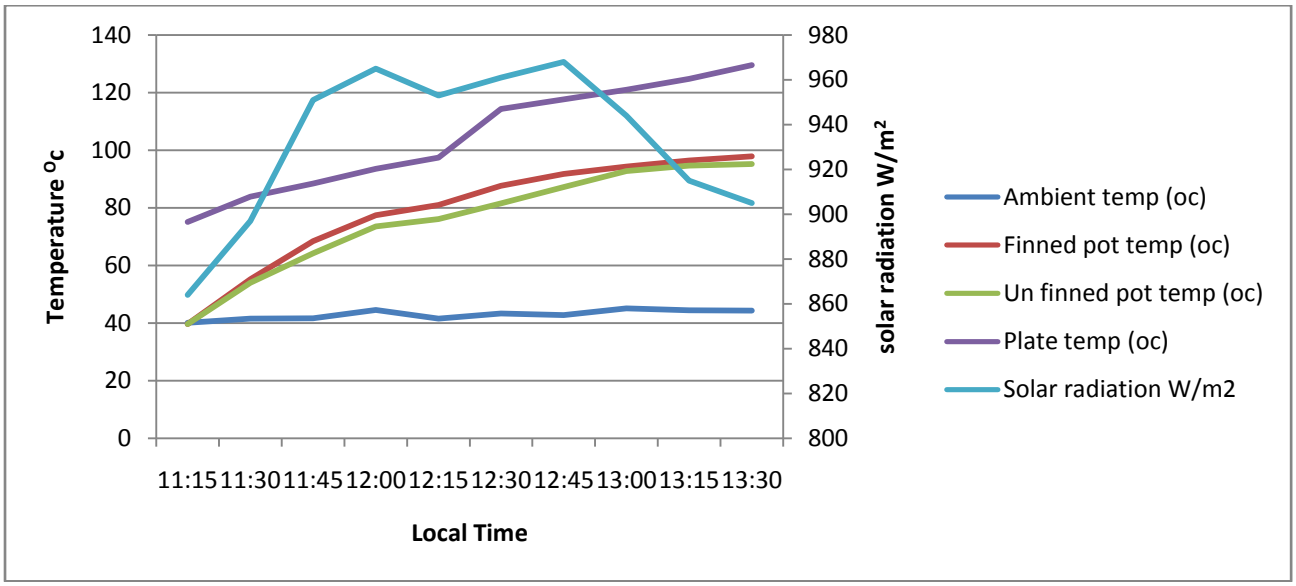

Fig 4: Water boiling test. Comparison between water temperature in the finned cooking pot and the water temperature in the UN finned cooking pot

Table 3: Temperature distribution at different times during the r rice cooking test on 28thFebruary, 2013

Time	Ambient temp (°C)	Finned pot temp (°C)	Unfinned pot temp (°C)	Solar radiation W/m2	Wind speed(m/s)
11:45	40.7	57.6	57.2	933	0.4
12:00	41.4	69.6	73.0	960	0.3
12:15	41.0	88.6	85.2	969	0,5
12:30	41.9	91.4	90.4	946	0.6
12:45	42.5	99.5	95.6	946	0.5
13:00	44.0	108.4	101.5	918	0.3
13:15	44.6	112.8	105.9	895	0.8
13:30	43.9	117.2	108.4	880	0.6
13:45	42:3	119.5	113.2	894	0.4
14:00	41:8	122.6	116.5	875	0.7
14:15	40.4	125.5	118.9	884	0.4

Table 4: Result of rice cooking test

Mass of the cooking pot	0.2kg
Volume of water	0.75l
Mass of rice	0.30kg
Mean ambient temperature(^{o}C)	42.2
Finned pot temperature at cooking time(^{o}C)	119.5
Un finned pot temperature at cooking time(^{o}C)	118.9
Time of cooking for finned pot (Min)	120
Time of cooking for un finned pot(Min)	150

V. Data Analysis and Discussion of Results

Fig. 4 shows the comparison between water temperature in the finned cooking pot and the water temperature in the unfinned cooking pot under the same test conditions on February 27th, 2013. It was found that the temperature of the water in the finned cooking pot was always higher than the temperature of water in the un finned cooking pot. The time taken for attaining boiling temperature (95 °C) by the two cooking vessels was 112 min for the finned, and 126 min for the un finned pot and finned cooking pot respectively.Table1: shows the various Temperature distributions at various point of cooker during the heating test. The ambient temperature fluctuates between 40.1^{o}C and 45.1^{o}C during the test period. The initial water temperature in the finned cooking pot and in the un finned cooking were the same 39.6^{o}C. The water in the finned cooking pot attained boiling temperature nearly 15 min earlier than time water in the unfinned cooking pot. The plate temperature for cooker under investigation was raised nearly 130^{o}C during the test period. For rice cooking test, table 3 shows the temperature distribution at different times during the rice cooking test on the 28th February, 2013. The ambient temperature fluctuate between 40.4^{o}C to 44.6^{o}C.it was also observed that the temperature on the finned pot is always higher than the temperature in the unfinned cooking pot throughout the period of the investigation.0.3kg of parboiled rice was cooked in 120min and 150 min for finned and unfinned pot respectively. The temperature of finned cooking pot at cooking time was 119.5^{o}C, while that of unfinned pot was 118.9^{o}C. The high cooking time could be attributed to observed openings around the glazing covers which lead to the heat lost in the cooker.

VI. Conclusion

The result of two tests (water heating and boiling test) revealed that 75cl of water was raised to 95^{o}C in 112 and 126 minutes for finned and unfinned cooking pot respectively. These figures represent an 11% reduction in heating time. Similarly 0.3kg of rice was cooked in 120 and 150 minutes for the finned and unfinned cooking pot respectively. The investigation has revealed that cooking time can be reduced by using a finned cooking pot. The reduction in cooking time is consistent with the increase of the heat transfer surface area by fins attached to the external surface of the cooking pot.

VII. Recommendations

Based on the investigation carried out the following recommendations are made:

i. Dimensions and geometry of the fins should be studied in more detail in order to optimize the performances of this kind of cooking pot.
ii. The investigation should be carried out at different season so as to understanding the cooking profile of various periods in the year.
iii. Manufacturers of cooking pot should produce cooking pot with fins to accommodate those who want to use them for solar cooking.
iv. Solar cooking should be encourage and popularize through mass production and distribution to students, rural dwellers and low income earners to supplement to high cost of convectional fuels such as kerosene, LPG ,Cooking gas and Fuel wood.

References

[1] Algiri A.H and Towale, H.A (2001): Efficient orientation impacts of box type solar cookers on the cooker performance. Solar Energy 70,165-170.
[2] Ammer E.H, (2003): Theoretical and experimental assessment of double exposure solar cooker, Energy Conservation and Management 44, 2034 – 2043.
[3] Arezki H. et al (2008).Experimental study of double exposure solar cooker with finned cooking Vessel. Solar Energy 82,287-289
[4] Dasin D.Y, Habou D, Rikoto II,(2011), Performance evaluation of parabolic solar [1]concentrator against international standard procedure in the tropical Environment. Nigerian Journal of Renewable Energy, 15, 20-28
[5] Funk P.A. (2000) Evaluating the International Standard Procedure for testing solar cookers and reporting performance. Solar Energy 68(1):1-7
[6] Garba M.M and Danmallam I.M, (2011): Performance evaluation of rectangular and square type box type cooker, Nigerian journal of Renewable Energy, 16. 120-126.
[7] Gaur.A, SinghO.P, Singh S.K, Pandey, G.N, (1999) Perfomance study of solar cooker with modified utensil. Renewable Energy, 28 1935 -1952

[8] Hussain M, Das K,and Huda A., (1997): The performance of the box type solar cooker with auxiliary heating. Renewable Energy, 12,151-155.
[9] Malik A.Q and Hussein bin Hamid (I996), Development of solar cooker in bruncas Darussalam, Renewable Energy, 7(4):419-425.
[10] Mohammad Ali, (2000): Design and testing of Sudanese solar box cooker. Renewable Energy, 21,573-581
[11] Mullick S.C, Kandpal T.C, and Saxena A.K. (1987), Thermal test procedure for box- type solar cookers, Solar Energy 39(4):353-360.
[12] Nahar N., (2003), Performance and testing of hot box storage solar cooker. Energy Conservation and Management, 44, 1323-1331
[13] Negi B.S and Purochit I. Experimental investigation of box type solar cooker employing a non – tracking concentrator, Energy conservation and management, 46:577 – 605.
[14] Okechukwu O., and Ugwuoke N, (2003), Design and measures performance of a plane reflector augmented box type solar cooker,28. 1935-1952
[15] Paul F.A 'ASAE standards: Drafted paper solar energy committee SE-414
[16] Sebaii E.I and Ibrahim A, (2005): Experimental testing of box type solar cooker using the standard procedure of cooking power, Renewable energy 30, 1861 -1871.

International Journal of Modern Engineering Research (IJMER)
www.ijmer.com Vol.3, Issue.3, May-June. 2013 pp-1295-1303 ISSN: 2249-6645

Study on the Effect of Stress Concentration on Cutout Orientation of Plates with Various Cutouts and Bluntness

M Mohan Kumar, [1] Rajesh S, [2] Yogesh H, [3] Yeshaswini B R[4]
[1]*Senior Scientist, STTD, CSIR-NAL, Karnataka, India*
[234]*Student, Department of Mechanical Engineering, SVCE, Karnataka, India*

Abstract: *Plates with variously shaped cut-out are often used in engineering structures. The understanding of the effect of cut-out on the load bearing capacity and stress concentration of panels is very important in designing of structures. Different cut-out shapes in structural elements are needed to reduce the weight of the structure or provide access to other parts of the structure. Extensive studies have been carried out on stress concentration in perforated panels which consider cut-out shapes, boundary conditions and bluntness of cut-outs. This study focuses on the stress concentration analysis of perforated panels with not only various cut-outs and bluntness but also different cut-out orientations. Therefore, at the design stage, once the direction of a major tensile force is known, the cut-outs can be aligned properly based on the findings of the work to reduce the stress concentration at the cut-outs thereby increasing the load bearing capacity of the panel.*

Keywords: *Bluntness, Cut-out, Load Bearing capacity, Orientation, Stress concentration factor, etc*

1. INTRODUCTION

Plates and shells of various constructions find wide uses as primary structural elements in aerospace, mechanical and civil engineering structures. In recent years, the increasing need for lightweight efficient structures has led to structural shape optimization. Different cut-out shapes in structural elements are needed to reduce the weight of the system and provide access to other parts of the structure. It is well known that the presence of a cut-out or hole in a stressed member creates highly localized stresses at the vicinity of the cut-out. The ratio of the maximum stress at the cut-out edge to the nominal stress is called the stress concentration factor (SCF). The understanding of the effects of cut-out on the load bearing capacity and stress concentration of such plates is very important in designing of structures.

The study of the importance of SCF in isotropic plates is well established. Previous works on stress concentration presented a series solution for stress field around circular holes in plates with arbitrary thickness [1]. A wide range of holes diameters to plate thickness was presented. Also Schwarz–Christoffel transformation was used to evaluate the stress concentration factor for an infinite plate with central triangular cut-out [2]. Stress and strain distributions along the boundary of rectangular cut-out in an infinite elastic plate were presented [2]. The relaxation element method was used to determine the stress fields in a plate with three circular cut-outs subjected to uni-axial tensile load [3]. And numerical results based on generalized work–energy method for rectangular plates with circular cut-out and circular plates with a rectangular cut-out was presented [4]. Ultimate strength of metallic plates with central circular cut-out under shear loading was also investigated [5]. The bluntness effects on stress concentration in perforated composite plates were also presented [6]. Optimum design of holes and notches by considering fatigue life were presented [7]. For a variety of materials, for various geometry of notches and fillets, stress concentration factor was presented [8].

However, it seems to be difficult to locate a work that quantifies the rotation effect of polygonal cut-outs on stress concentration. Therefore, this study mainly focuses on stress concentration analyses of aluminium plates according to cut-out orientation. Therefore, this study mainly focuses on stress concentration analyses of perforated aluminium plates with not only various cut outs (circle, triangle, and square) and bluntness (a counter measure of radius ratio, *r/R*) but also for different cut-out orientation (θ = 15, 30, 45). For the analyses, first, we select three different cut-outs: circle, triangle, and square; secondly, we identify a number of degrees of bluntness to describe the radius ratio; and finally, we consider the rotation of cut-outs. In the paper, stress concentration analyses are performed by, a general using MSC Patran & MSC Nastran, a general purpose finite element program. From the the analysis we estimate the stress concentration of plates with various cut-out shapes, bluntness and orientation.

2. Finite Element Model

Finite element analyses are conducted for the stress concentration analyses of perforated aluminium plates. The structural aluminium plates have dimensions 200 mm (x-direction), 200 mm (y-direction), and 5 mm (z-direction) as shown in Fig.1. Material properties are shown in Table 1 and the location of cut-out is the centre of the plates. To clearly observe the concentration effect, the plate size is modeled as rather large for the cut-out size. MSC NASTRAN, a general purpose finite element program, is used for the analysis. A 4-node shell element is used for modelling. To investigate stress concentration in an elastic range, the plates are modeled as a linear elastic material. The loading condition is a uni-axial tensile force at the left and right sides as shown in Fig.1. Based on Rezaeepazhand and Jafari (2005), stress concentration reaches up to eleven times, depending on cut-out shapes; hence, in the study, to limit the maximum stress to the elastic range, 20 MPa is loaded as the tensile loading condition. Since element size is critical for precise analysis, in the study, the size is 2 mm in most parts and 0.5 mm near the cut-out areas.

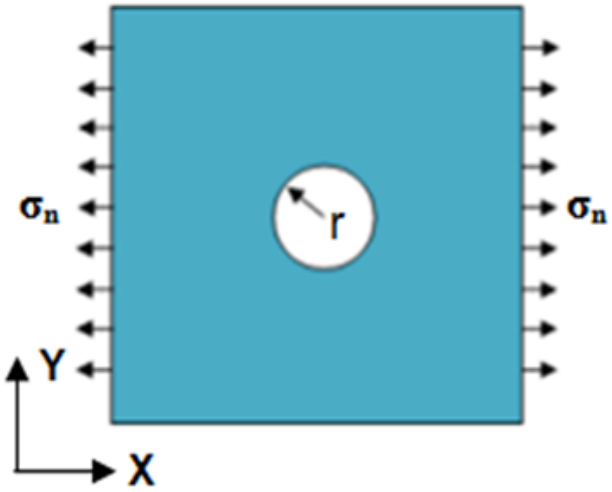

Figure 1: Loading condition: uni-axial tensile force

2.1 Material Properties

Table 2: Material properties of Aluminium 2024-T3

Material Properties	Values
Young's Modulus, (GPa)	73.1
Poisson ratio, μ	0.33
Tensile yield strength (MPa)	345
Tensile Ultimate strength (MPa)	483

3. Cut-Out Shapes, Bluntness and Rotation

We consider three cut-out shapes – circle, square, and regular triangle. For the square and triangle cut-outs the concept of inscribing circle is used, as shown in Figs.2 and 3, to compare with the corresponding circular cut-out. In the figures, the solid-lined circles are the inscribing circles in the polygons. The radius size of the circular cut-out is 10 mm. In general, to reduce the stress concentration at the edges of cut-outs, the edges are fabricated to be rounded. In the study, rather than 'roundness', we use 'bluntness' as a physical terminology to effectively describe stress concentration. As shown in Fig.4, a term 'radius ratio' is defined as the ratio of the edge radius (r) to the inscribing circle radius (R).

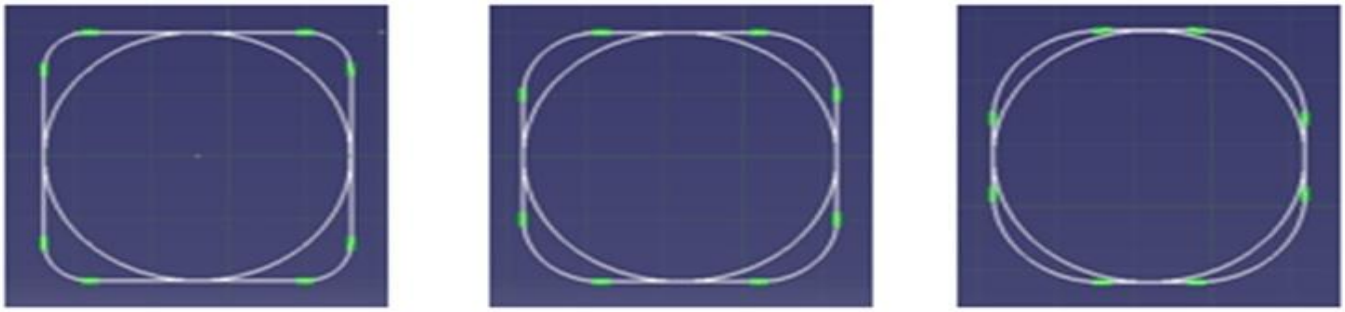

Figure 2: Square cut-out with *r/R* = 0.3(left), 0.5(centre), 0.7(right)

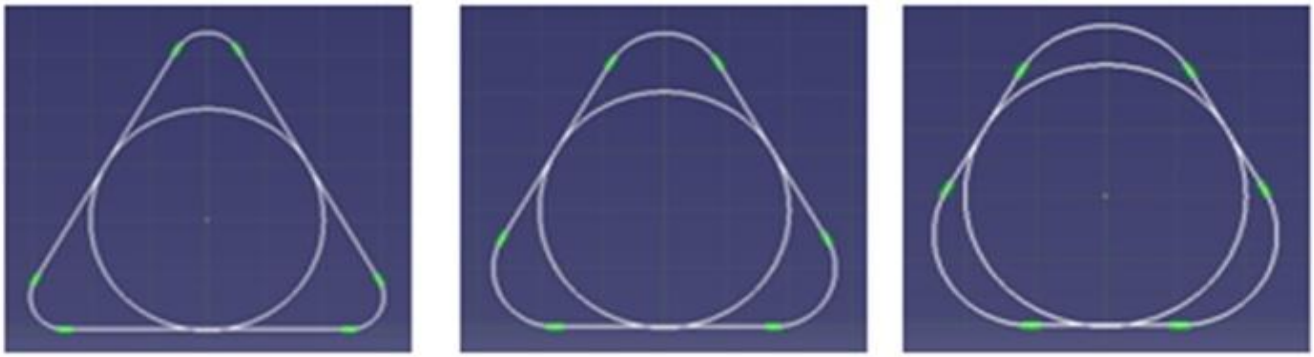

Figure 3: Triangle cut-out wit *r/R* = 0.3(left), 0.5(centre), 0.7(right)

Accordingly, bluntness is a counter measure to the radius ratio (r/R) because bluntness decreases as the radius ratio increases. For an extreme example, a circular cut-out has a unit radius ratio but it has zero bluntness. In other words, the degree of bluntness decreases as r/R increases. Here, again, we emphasize that the term 'bluntness' is used to describe that the edges of polygons are blunt. We consider a total of six different degrees of bluntness, including 0.1, 0.3, 0.5, 0.7, 0.9, and 1.0 for the polygon cut-outs. Figs.2 and 3 only show three of the six cases for the square and triangle cut-outs.

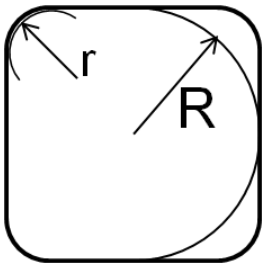

Figure 4: Radius ratio (r/R) defined by edge radius (r) and Inscribing circle radius (R)

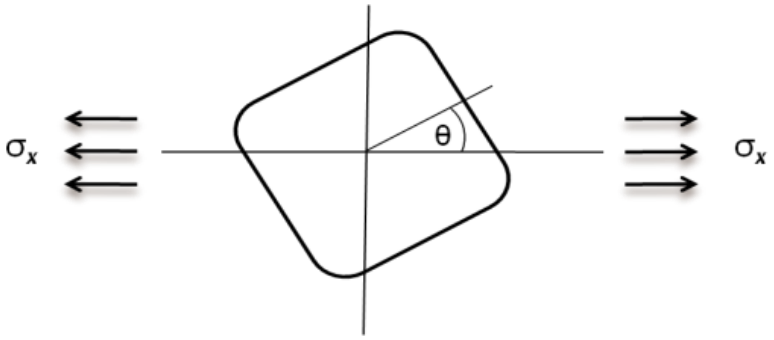

Figure 5: Rotation of cut-out

In addition to the shapes and bluntness, the last design consideration for cut-out patterns is orientation. Fig.5 shows the definition of orientation. The rotation angle θ represents how the cut-outs are oriented from the baseline (+x axis). As shown in the figure, the loading directions are fixed as they are. Fig.6 shows a number of parts of the rotated cut-outs for each case. By considering the symmetry of the polygonal cut-outs, the angle increment 15° is applied; hence, a total of three cases are considered (15°, 30° and 45°) for the square cut-outs and three cases (15°, 30° and 45°) for the triangular cut-outs.

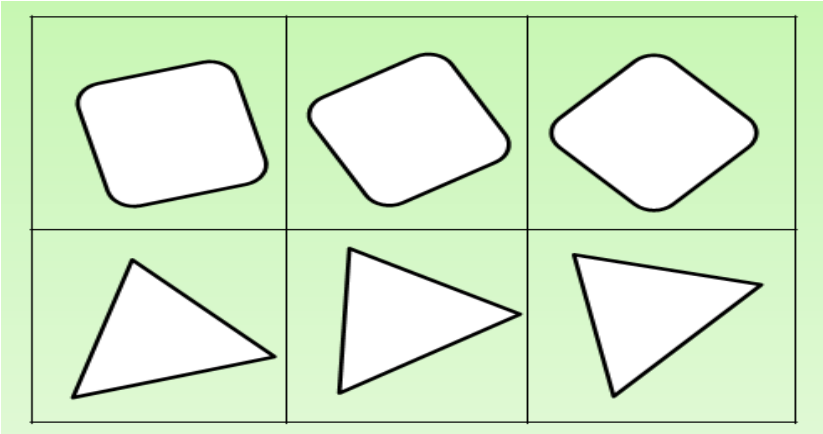

Figure 6: Square and Triangular cut-out with □ = 15° (left), 30° (centre), and □=45° (right

4. Results

By considering the design variables or factors – cut-out shape, the degree of bluntness, and cut-out rotation – the stress concentration pattern, the maximum von-Mises stress and the stress concentration factor are obtained. These results are as shown in the following sections.

4.1 Cut-Out Shapes and Bluntness

As mentioned previously, there are three different cut-out shapes – circle, square, and triangle. In addition, for considering bluntness (a counter measure of r/R), a total of six radius ratios are considered: r/R = 0.1, 0.3, 0.5, 0.7, 0.9 and 1.0 respectively. This section discusses the variation of stress concentration with respect to the cut-out shapes and bluntness. All of the other factors remain the same, for example the uni-axial tensile forces are fixed at 20 MPa.

Table 2: The maximum von-Mises stress and stress concentration factor

r/R	*Triangle*		*Square*	
	σ_{max}, MPa	SCF	σ_{max}, MPa	SCF
0.1	178	8.9	89.6	4.48
0.3	115	5.75	70	3.5
0.5	93.1	4.65	60.1	3
0.7	78.7	3.9	61	3.05
0.9	68	3.4	58.7	2.93
1	64.3	3.2	64.3	3.2

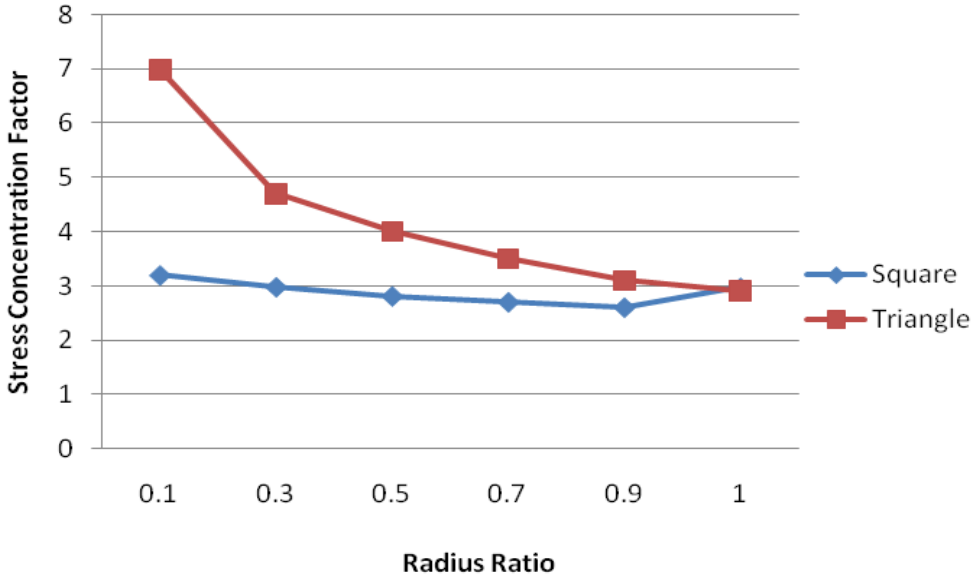

Figure 7: SCF with respect to radius ratio

It should be noted here that the zero bluntness (r/R = 1) actually means that the cut-out shape is a circle; hence, from the Table 2, we can see how the shapes and the degrees of bluntness vary the maximum von-mises stress and stress concentration factor. Fig.7 shows how the stress concentration factor (SCF) varies with respect to cut-out shapes and the radius ratio (a counter measure of degree of bluntness).

In the case of the circular cut-out, the maximum stress is 64.3 MPa and the stress concentration factor is 3.2. According to previous studies, the maximum stress is about three times the tensile force [8]. Since our tensile force is 20 MPa, the magnitude of 64.3 MPa exactly concurs with the previous observation. As shown in Table 2, the maximum von-Mises stresses and accordingly stress concentration factors change, depending on the cut-out shapes and bluntness.

In the case of the square cut-outs, although the quantities range between 89.6 and 64.3 MPa, they do not significantly differ from 60.26 MPa, which is the maximum von-Mises stress that occurred in the circularly-perforated aluminium plate. It is interesting to note that: (1) the stresses for r/R = 0.5, 0.7, and 0.9 are smaller than that of r/R = 1.0 which is the circular cut-out case, and (2) the maximum stress (89.6 MPa) occurs in the case of r/R = 0.1.

In the case of the triangular cut-outs, the results are quite consistent because: (1) all the stresses exceed that of the circular cut-out case, and (2) unlike the square cases, starting from the maximum stress (178 MPa) the stresses decrease as the degrees of radius ratio increases. In other words, the stresses increase as the degree of bluntness increases.

To visualize the stress patterns, two stress contours are shown in Figs.9 and 10. Fig.9 shows the stress contour in the case of the square cut-out with r/R = 0.1. The circle on the contour indicates the area having the maximum von-Mises stress. In addition, the left and right balloon shapes represent the areas under 11 MPa. Fig.10 shows the stress contour in the case of the triangle cut-out with r/R =0.1. The circle on the contour shows the area having the maximum von-Mises stress. Similarly, the left and right balloon shapes represent the area under 16 MPa. It is interesting to note that stress concentration occurs in the broad range of the top and bottom sides in the case of the square cut-out while stress concentration occurs in the narrow range of the top and bottom edges in the case of the triangle cut-out. From the observation, we can conclude that the bluntness effect on the stress concentration patterns is also dependent on cut-out shapes. However, in general, as bluntness increases, stress concentration increases.

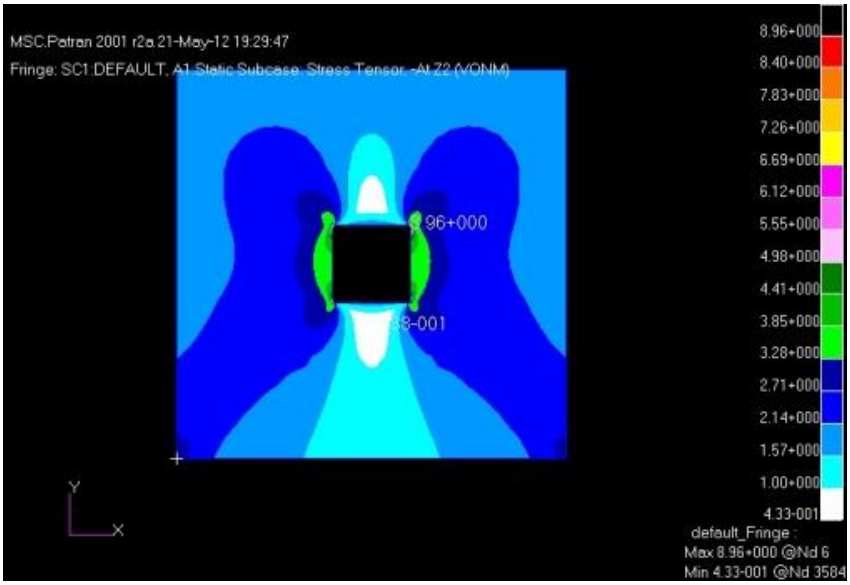

Figure 9: Stress contour of plate with square cut-out (r/R = 0.1)

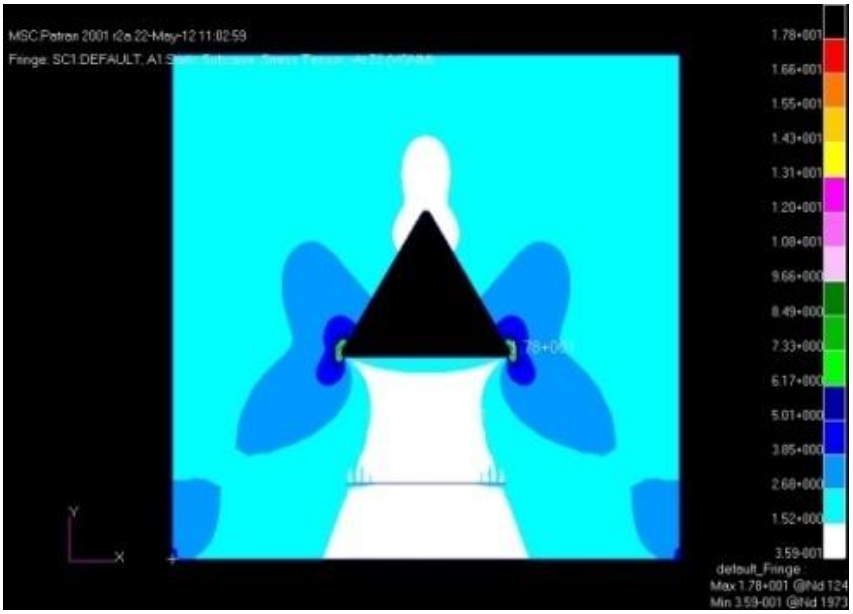

Figure 10: Stress contour of plate with triangle cut-out (r/R = 0.1)

4.2 Rotation of cut-outs

This section discusses the stress analysis results by considering the rotation of the cut-outs. In the cases of the square cut-out, three rotation angles are considered 15°, 30° and 45°, while three angles 15°, 30° and 45°, are considered in the case of the triangle cut-out. Table 3 shows the maximum von-Mises stresses and stress concentration factors for the aluminium plates with square cut-outs, which have the four rotations. As a result, we can see that many differences occur in the maximum stresses, depending on the rotation angle. However, for all of the cases consistently, the stresses increase as the rotation angles increase. By combining the rotation effect with the bluntness effect, the maximum stress (141 MPa) occurs in the case of the r/R = 0.1 (maximum bluntness) and the rotation of 45° (maximum rotation). In addition, we can see that with the exception of the zero rotation case, all the cases show that the maximum stress increases as the bluntness increases, as shown in Fig.11. Table 4 shows the maximum von-Mises stresses and stress concentration factors for the aluminium plates with triangle cut-outs, which have the three rotations. For all of the cases, the stresses increase as the rotation angles increase, as clearly shown in Fig.12. With both effects of the rotation angle and bluntness, the maximum stress (166 MPa) occurs in the case of the bluntness of r/R = 0.1 (maximum bluntness) and the rotation of 30°. Fig.13 shows the stress contour in the case of the square cut-out with r/R = 0.1 and rotation 45°, which gives the maximum stress. This figure represents different patterns from that of Fig. 9 showing the case of 0°. The maximum stress concentration occurs in the top and bottom edges. Fig.14 shows the stress contour in the case of the triangle cut-out with r/R = 0.1 and rotation 30°, which also gives the maximum stress. The maximum stress concentration occurs in the top edge.

Table 3: Maximum von-Mises stress and stress concentration factor (SCF) of square cut-outs with rotation angle

r/R	0° (MPa)	15° (MPa)	30° (MPa)	45° (MPa)
0.1	74	110	134	141
0.3	59.1	86.4	99.1	103
0.5	56.3	75	82.5	84.5
0.7	54	68	72	73.2
0.9	51.9	63.6	64.8	65.1
1	59.5	59.5	59.5	59.5

r/R	0° (SCF)	15° (SCF)	30° (SCF)	45° (SCF)
0.1	3.7	5.5	6.7	7
0.3	2.9	4.3	4.95	5.1
0.5	2.8	3.7	4.1	4.2
0.7	2.7	3.4	3.6	3.6
0.9	2.6	3.1	3.2	3.25
1	2.97	2.97	2.97	2.97

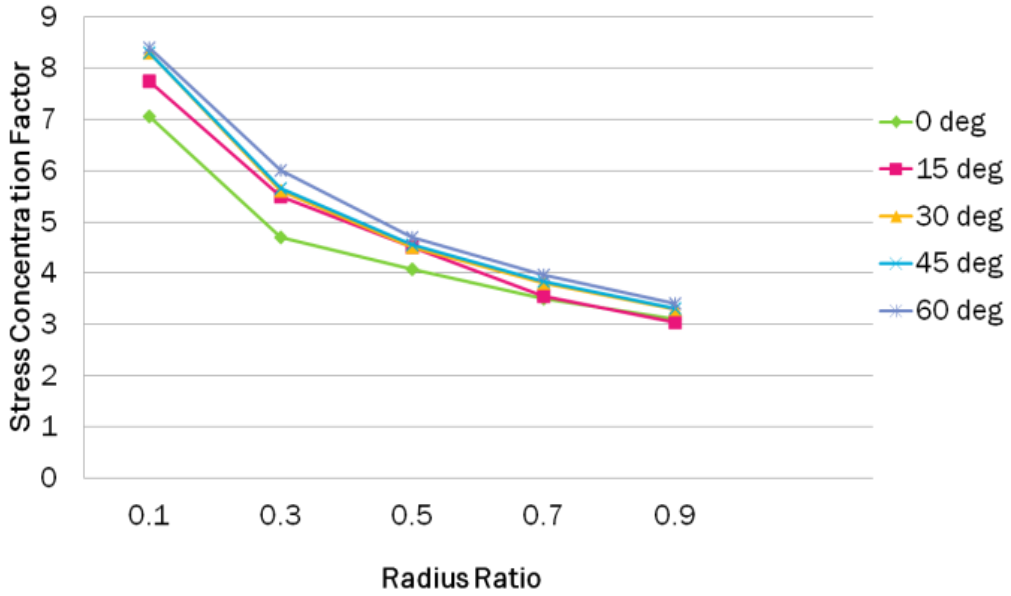

Figure 11: SCF with respect to rotation for square cut-outs

Table 4: Maximum von-Mises stress and stress concentration factor (SCF) of triangular cut-outs with rotation angle

r/R	0° (SCF)	15° (SCF)	30° (SCF)	45° (SCF)
0.1	141	155	166	166
0.3	95.5	110	112	113
0.5	81.5	89.7	90.5	91.1
0.7	69.8	71.1	76.5	76.8
0.9	62.1	60.8	66.3	66.3
1	59.5	59.5	59.5	59.5
r/R	0° (SCF)	15° (SCF)	30° (SCF)	45° (SCF)
0.1	7	7.7	8.3	8.3
0.3	4.7	5.5	5.6	5.65
0.5	4	4.5	4.5	4.55
0.7	3.5	3.5	3.8	3.84
0.9	3.1	3	3.3	3.31
1	2.9	2.9	2.9	2.9

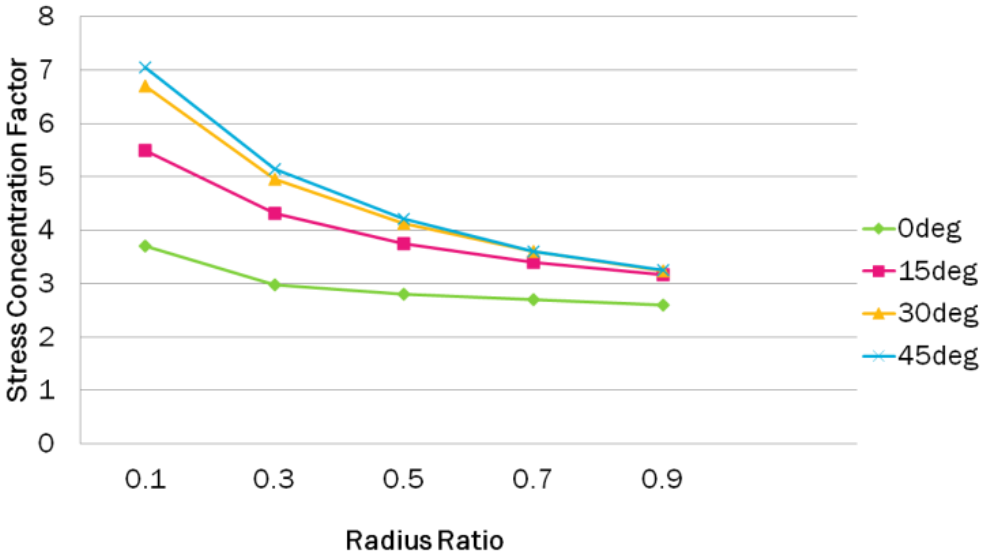

Figure 12: SCF with respect to rotation for triangle cut-outs

From the results (see Figs.9, 10, 13, and 14), in the case of the square cut-out, it is more advantageous to orient two sides of the square cut-out to be perpendicular to the applied tensile force because this reduces the maximum stress. For example, in the case of square cut-outs with r/R = 0.1, the maximum stress decreases from 141 (θ = 45°) to 74 MPa (θ = 0°), which is a 67 MPa or 47% decrease. Similarly, in the case of the triangle cut-out, it is also preferable to orient one side of the triangle cut-out to be perpendicular to the applied tensile forces because of stress reduction. For example, in the case of triangle cut-outs with r/R = 0.1, the maximum stress decreases from 166 (θ = 45°) to 141 MPa (θ = 0°), which is a 25 MPa or 15% decrease. Accordingly, at the design stage, determining the direction of a major tensile force is required. By aligning these polygon cut-outs as observed here, we can then reduce stress concentration.

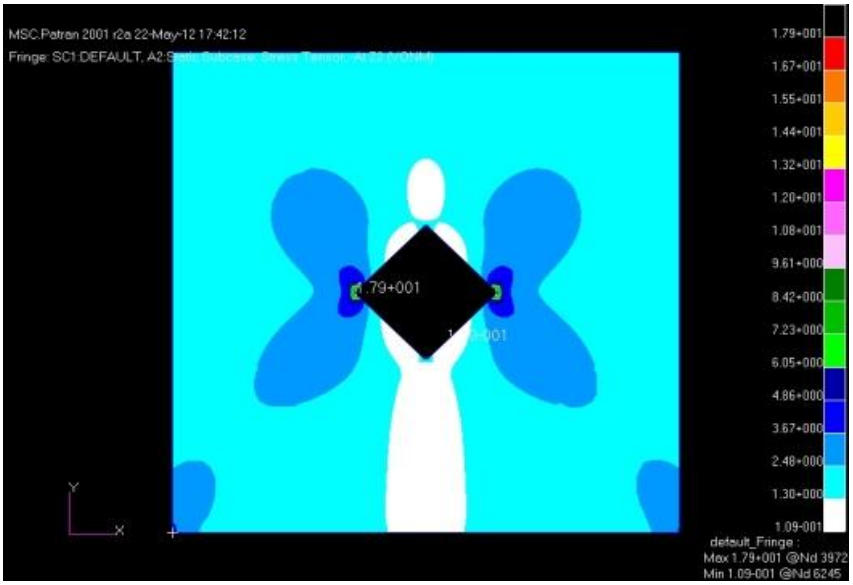

Figure 13: Stress contour for square cut-out (r/R = 0.1, □ = 45°)

In addition to rotation, similarly to the previous section, for all the degrees of orientation, it is also observed that the stress concentration decreases as the bluntness of the cut-outs decreases. For example, in the case of square cut-outs with 45° rotation, the maximum stress decreases from 141 (r/R = 0.1) to 65 MPa (r/R = 0.9), which is a 76 MPa or 54% decrease. Similarly, in the case of triangle cut-outs with 30° rotation, the maximum stress decreases from 166 (r/R = 0.1) to 66.3 MPa (r/R= 0.9) with a 100 MPa or 60% decrease.

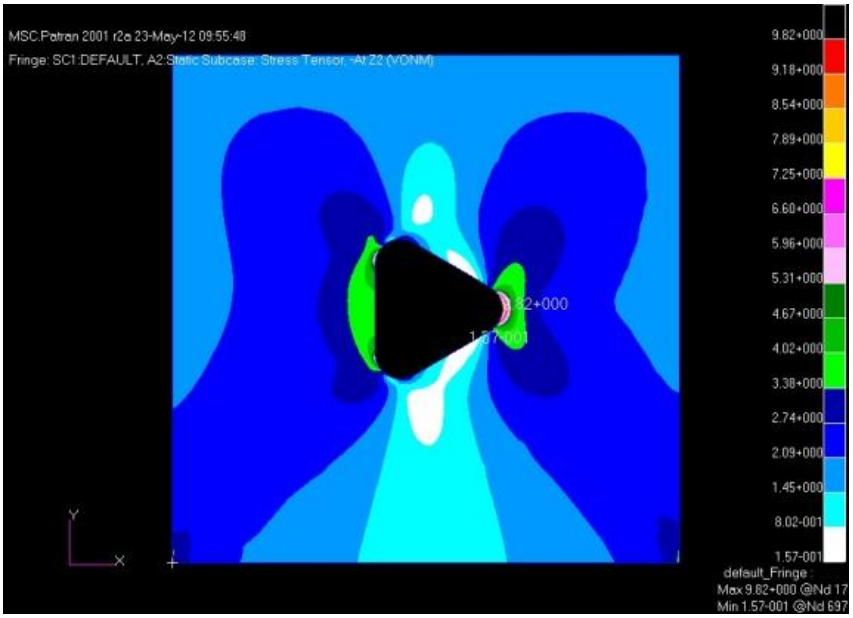

Figure 14: Stress contour for triangle cut-out (r/R = 0.1, □ = 30°)

Therefore, the next question among these two factors (rotation and bluntness) is which factor should preferably be controlled to minimize the stress concentration. Based on Tables 3 and 4 and Figs.11 and 12, we can clearly see that bluntness is a more effective factor. For example, as the bluntness approaches zero (r/R approached to unit), the maximum stresses tend to converge to 64.3 MPa (the maximum stress in the case of circular cut-out) and naturally the rotation effect vanishes. However, this does not reflect the manufacturing ease and cost. In a sense, it may be preferable to control orientation to reduce the manufacturing costs and cumbersome manufacturing. Therefore, at this analysis stage, the judgment should be handed over.

In summary, to minimize the stress concentration of the aluminium plates with polygon cut-outs, the cut-outs should have smooth edges and proper rotations. In other words, by controlling the smoothness (or bluntness) and rotation, we can minimize the stress concentration of the perforated aluminium plates. Among bluntness and rotation, controlling bluntness is analytically preferable to minimize the stress concentration.

5. Conclusions

This study presents stress concentration analyses of perforated aluminium plates with various shapes, bluntness, and rotation of polygonal cut-outs. For the analysis we intentionally limit resulting stresses in an elastic range by controlling the applied uniaxial tensile forces. We observed that the maximum stress in the perforated aluminium plate with the circular cut-out is about three times the applied force; hence, the previous observation performed by Pilkey et al. (2008) is verified. From the finite element analyses, the following findings are reported. Depending on cut-out shapes, bluntness and rotation effects on stress concentration vary. However, in general, as bluntness increases, the stress concentration increases, regardless of the shape and rotation. A more important finding is that the stress concentration increases as the cut-outs become more oriented from the baseline, which is the positive horizontal axis (+x) and one of the directions of the applied tensile forces. This fact demonstrates that the orientation is also a relatively significant design factor to reduce stress concentration. In general, in the case of the triangle cut-out, it is preferable to orient one side of the triangle cut-out to be perpendicular to the applied tensile forces. Similarly, in the case of the square cut-out, it is more advantageous to orient two sides of square cut-out to be perpendicular to the applied tensile force. Therefore, at the design stage, determining the direction of a major tensile force is required. By aligning these polygon cut-outs properly, we can then reduce stress concentration. This finding is mainly for uni-axial tensile forces in an elastic range. Other cases such as uni-axial compressive forces and bi-axial tensile and/or compressive forces should be considered for the future work. In addition, stress concentration analyses in a non-elastic range could be an interesting topic for future work.

Acknowledgement

The satisfaction and euphoria that accompany the successful completion of any task would be incomplete without the mention of the people whose constant guidance and encouragement aided in its completion. The authors would like to express the voice of gratitude and respect to all who had directly or indirectly supported for carrying out this study.

The authors would like to thank and acknowledge Mr. Shyam Chetty, Director, and Dr. Satish Chandra, Head, STTD, CSIR-National Aerospace Laboratories, Bangalore, India for their support and encouragement during this work. Also sincere thanks are acknowledged to The Principal, SVCE Bangalore for the support. Special thanks are acknowledged to The Head of the Department, Department of Mechanical Engineering, SVCE for his overwhelming support & encouragement.

References

Journal Papers:

[1] E.S. Folias, J.J. Wang: on the 3-dimensionl stress field around a circular holes in a plate of arbitrary thickness; Computational Mechanics, 6 (3) (1990), pp. 379–391.

[2] P.S. Theocaris, L. Petrou: Stress distributions and intensities at corners of equilateral triangular holes; International Journal of Fracture, 31 (1986), pp. 271–289.

[3] G.V. Lasko, Y.Y. Deryugin, S. Schmauder, D. Saraev: Determination of stresses near multiple pores and rigid inclusion by relaxation elements; Theoretical and Applied Fracture Mechanics, 34 (2000), pp. 93–100.

[4] A.V.Singh, U.K. Paul: Finite displacement static analysis of thin plate with an opening—a variational approach, International Journal of Solids and Structures, 40 (2003), pp. 4135–4151.

[5] Jeom Kee Paik: Ultimate strength of perforated aluminium plates under edge shear loading, Thin-Walled Structures, 45 (2007), pp. 301–306.

[6] J. Rezaeepazhand, M. Jafari: Stress analysis of perforated composite plates, Composite Structures, 71 (2005), pp. 463–468.

[7] H. Wu, B. Mu: On stress concentration for isotropic/orthotropic plates and cylinders with a circular holes Composites Part B: Engineering, 34 (2) (2003), pp. 127–134.

[8] J.H. Won, J.H. Choi, J.H. Gang, D.W. An, and G.J. Yoon: Local Shape Optimization of Notches in Airframe for Fatigue-Life Extension, J. of Korean Society of Mechanical Engineers, A32 (12) (2008), pp. 1132-1139.

Books:

[9] W.D. Pilkey, D.F. Pilkey, and R.E. Peterson: Peterson's Stress Concentration Factors, John Wiley and Sons, New York (2008).

[10] G.N. Savin: Stress Concentration around Holes Pergamon Press, New York (1961).

Proceedings Paper:

[11] D.Y. Kim, D.H. Shim, and M.J. Choi: A Stress Concentration Analysis Model for a Plate in the Aircraft Surface using Energy Method, Spring Conference of Korean Society for Precision Engineering, (2007), 553-554.

International Journal of Modern Engineering Research (IJMER)
www.ijmer.com Vol.3, Issue.3, May-June. 2013 pp-1304-1306 ISSN: 2249-6645

Conversion of Artificial Neural Networks (ANN) To Autonomous Neural Networks

H Bhargav,[1] Dr. Nataraj K. R,[2]
[1]*Assistant Professor, Department of Electrical and Electronics Engineering.Vidyavardhaka College of Engineering, Mysore, Karnataka, India.*
[2]*Professor, Department of Electronics and Communications Engineering.SJB Institute of Technology, Bangalore, Karnataka, India.*

Abstract: *This article points out some serious drawbacks of Artificial Neural Networks, when compared to human brain. According to this article definitely there is a need for implementing Artificial Neural Networks with a change in underlying concepts. To do this a clear picture of brain learning mechanism, which is free from all the possible misconceptions is essential. So this article makes an attempt to notify the aspects that need to be considered in order to make neural networks 'autonomous bodies', just like human brain.*

Keywords: *ANN, Autonomous Neural networks, brain-like learning and Subsystem control theory.*

I. INTRODUCTION

The greatest drawback of the current models of artificial neural networks is that they are human- intervention systems. Also their learning algorithms need constant attention. These learning algorithms cannot be used in future robots or any other systems which are supposed to be autonomous. It is therefore impossible to build autonomous systems without having autonomous learning algorithms.

This article points out the important differences from Artificial Neural Networks and human brain. Also this article points out the immediate need to improve the standards of current neural networks so that they can be rendered "Self-learning" and "completely autonomous.

Artificial neural networks should be developed in such a way that one who uses ANN should feel he has actually employed a human being for addressing the given real time problem. ANN can be approximated to human brain by improving its standards of learning. We know that ANNs are derivatives of human brain. But if ANN are developed such that they are capable of taking decisions independently under all the conditions without any human intervention, then ANNs can be nearly approximated to human brains.

II. Brain Learning Mechanism

The brain is a wonderful creation in the entire nature. While the animals use it only for basic needs, human brains can perform wonderful tasks. Human brain has inspired many scientists and researchers to construct artificial neural networks.

Brain is a vast network comprising of millions of neurons and connectivities to various organs. Brain is like a central processing unit,which governs the body functions effectively. Human brain is almost an autonomous system which does not require outside processes for controlling its learning phenomena. Also the brain recollects the previous experiences and its own interpretations to take decisions in a particular issue.

Sometimes the brain is also influenced by the modes of action and the decisions are made according to one of the modes of action. The other interesting feature of the brain is that it achieves a good co-ordination between the functioning of various organs.

Two of the main functions of the brain are memory and learning. There are of course many categories of memory (short term, medium term, long term, working memory, episodic memory and so on) and of learning (supervised, unsupervised, inductive, reinforcement and so on). In order to characterize the learning behavior of the brain, it is necessary to distinguish between these two functions. Learning generally implies learning of rules from examples. Memory, on the other hand, implies simple storing of facts and information for later recall (e.g. an image, a scene, a song, an instruction). Sometimes memory is often confused with learning. But the processes of memorization are different from that of learning. So memory and learning are not the same.

III. Misconceptions About Human Brain

There are several concoctions about human brain. Many researchers say that human brain is inferior to Artificial Neural Network. In fact Artificial Neural Networks are themselves derivatives of human brain. Human brain has got unlimited potential, with which it can explore the finest aspects of any concept and arrive at the proper conclusion. If human brain is properly understood then Artificial Neural Networks may be designed with a difference so that their degree of resemblance with human brain increases. Despite of numerous advancements in the field of Artificial Neural Networks, ANNs can't be still regarded as "duplicate" of human brain. Therefore it is of utmost importance to improve the features of ANN, so that it develops the brain like capacity to address the real time problems.

Some of the misconceptions of human brain are:

- **"A human's knowledge is volatile and may not become permanent. There are several factors that cause brain cells to die and if they do, the information that is stored in that part is lost and we start to forget".** - which is not very true because brain has distributed memory system and the memory loss is a very rare case. On the other hand if brain is utilized effectively then knowledge is never lost.
- **"Brain is always provided with the learning parameters to address a problem"**- In order to seek a solution for the given problem or to generalize well, human brain should be able to decide upon the network parameters like number of layers, number of neurons per layer, connection strengths and so on. So the learning parameters and networks themselves do not come "readymade". Since the natures of problems differ, brain has to decide on the different network designs and network parameters internally.
- **"Brain does not store any information prior to learning and learns instantaneously"-** one may think that if there is no memory requirement then the system is very efficient, but it consumes more time for processing. In this respect, human brain is superior to ANN because it has a memory. Human brain never learns instantaneously but it happens based on the information collected prior to learning. This conception violates the very basic behavioral facts. Remembering relative facts and examples is a part of human learning.
- **"Human brain's speed of processing is less compared to that of Artificial Neural Networks"-** In fact human brain can imagine anything at a greater speed compared to that of air. Artificial Neural Networks have to be first trained and after the learning phase is over, their speed can be measured. Sometimes speed also refers to a proper decision taking capability of a system. Before taking a task for processing, if a processing system can set priorities for the tasks or find effective ways to solve it then the system is to have speeded up the processing. On the other hand if the system simply processes the task without taking into account its pros & cons then it is actually wasting the precious time.
- **"Each Neuron in the brain is an autonomous body". –** The notion that each neuron adjusts its weights solely based on its inputs and outputs is not supported by any neurobiological evidence. In fact external agents can also influence the synaptic adjustments. If backpropagation learning algorithm is considered, then we can notice that each cell stores information about the input, output, error in processing the task by the network and also the contribution of individual cell to this error. This implies that no other entity external to cell or neuron is allowed to change its connection strengths. But this is logically inconsistent.

IV. How To Turn ANN To Autonomous Neural Network

The field of Artificial Neural Networks developed several learning algorithms over the years that work well only when there is human intervention. In order to make ANN to work properly their learning rates need to be reset and readjusted, and also different network designs have to be tried so that they can generalize well. Everything needs to be relearned from scratch when there is catastrophic forgetting in the network. There is a long list of such drawbacks that need to be seriously considered. One of the founder of this field and a past president of the International Neural Network Society (INNS) confided that "the neuro-boom *is over."*But many other scholars have kept on fighting the arguments against the current science on brain-like learning.

Minsky and Papert not only showed the limitations of the the perceptrons, the simple neural networks and also raised the deeper question of computational complexity of learning algorithms. Despite all the deeper and more disturbing questions raised by thoughtful critics, the neural network field is moving heedlessly with its research agenda. Now faced with fundamental challenges to the assumptions behind their brain like learning algorithms, prominent researchers in the field are finally calling for a "shake up of the field of neural networks" and for its "rebirth."

Artificial Neural Networks can become autonomous bodies if they are embodied with various capabilities as listed below:

- **ANN should be equipped with memory**, so that it operates at greater speed.
- **ANN should be capable of taking decisions about the task selection and processing**: this means that ANN should be capable of setting priorities to the tasks and also deciding the best possible way of processing, instead of merely operating on a given task**.**
- **ANN should be able to aim and fix target for processing tasks** without which the processing of tasks would take more time.
- **ANN should not be problem specific** but should be able to address any problem.
- **ANN should be capable of adjusting both the weights of synaptic connections as well the structure itself.**
- **ANN should also be able to sense the "situations" in the surrounding environment and address the given problem** without the aid of external teacher. Taking the situations (requirements, rules etc.) into consideration, ANN should act in order to get the desired output.
- **ANN should be having flexibility to switch over to different modes of action.** For instance if we desire ANN to work in the mode of passion then ANN should permit for the same.
- **ANN should have subsystems within itself that can control other subsystems** because of which any external source can control the behavior of neuron. This is quite different from "local learning concept" of current ANN technology [10].

Artificial Neural Networks can achieve "brain-like learning" if they are equipped with all these abilities. Artificial Neural Networks should be a combination of various activation functions and different topologies to become autonomous bodies.

V. Conclusions

The greatest drawback of the existing theories of artificial neural networks is the characterization of an autonomous learning system such as the brain. Despite of the clear definitions of the internal mechanisms of the brain [12], no one has characterized in a similar manner the external behavioral characteristics that they are supposed to produce.

Consequently, the ANN underwent algorithm development keeping in view local, autonomous learning, memory less learning, and instantaneous learning rather than from the point of view of "external behavioral characteristics" of human learning. If that set of external characteristics cannot be reproduced by a certain conjecture about the internal mechanisms, than that conjecture is not a valid one.

The current article essentially points to some of the current notions of human learning and showed their logical inconsistencies. So there is definitely a need for some new ideas about the internal mechanisms of the brain.

It would be better if the current ANN systems inadvertently acknowledge the ideas listed in the previous section and the most important among them is the last one, which asks us to use the concept of "master or controlling subsystem" that designs networks and sets learning parameters for them. Very recently has such non local means of learning has been used effectively to develop powerful learning algorithms that can design and train networks in polynomial time complexity [2, 9, 10].In addition, this "subsystem control" framework resolves many of the problems and dilemmas of current ANNs. Under such a framework, learning need not be necessarily instantaneous, but can wait until some information is collected about the problem. Learning can always be invoked by a controlling subsystem at a later point in time. This would also facilitate understanding the complexity of the problem before it has to be actually tackled, from the information that has been collected and stored already. Such a framework would also resolve the network design dilemma and the problems of algorithmic efficiency that have been negatively influencing this field for so long [2,9,10].So one can argue strongly for theories like "subsystem control" that are related to human brain and make use of such concepts in designing ANNs. If ANNs are designed with due considerations to actual behavior of human brain then undoubtedly ANNs become Autonomous Neural Networks.

References

[1] Church land, P. and Sejnowski, T. The Computational Brain. MIT Press, Cambridge, MA, 1992.
[2] Glover, F. Improved Linear Programming Models for Discriminant Analysis. Decision Sciences, 21 (1990), 4, 771-785.
[3] Grossberg, S. Nonlinear neural networks: principles, mechanisms, and architectures. Neural Networks, 1 (1988), 17-61.
[4] Hebb, D. O. The Organization of Behavior, a Neuropsychological Theory. New York: John Wiley, 1949.
[5] Levine, D. S. Introduction to Neural and Cognitive Modeling, Hillsdale, NJ: Lawrence Erlbaum, 1998.
[6] Minsky, M. and Papert, S. *Perceptrons*. The MIT Press, Cambridge, MA, 1988.
[7] Moody, J. & Darken, C. Fast Learning in Networks of Locally-Tuned Processing Units, Neural Computation. 1 (1989), 2, 281-294.
[8] Reilly, D.L., Cooper, L.N. and Elbaum, C. A Neural Model for Category Learning. Biological Cybernetics, 45 (1982), 35-41.
[9] Roy, A., Govil, S. & Miranda, R. An Algorithm to Generate Radial Basis Function (RBF)-like Nets for Classification Problems. Neural Networks, 8 (1995), 2, 179-202.
[10] Roy, A. Summary of panel discussion at ICNN'97 on connectionist learning. "Connectionist Learning: Is it Time to Reconsider the Foundations." INNS/ENNS/JNNS Newsletter, appearing with Neural Networks, 11 (1998), 2.
[11] Rumelhart, D.E., and McClelland, J.L.(eds.) Parallel Distributed Processing: Explorations in Microstructure of Cognition, Vol. 1: Foundations. MIT Press, Cambridge, MA., 1986, 318-362.
[12] Rumelhart, D.E. The Architecture of Mind: A Connectionist Approach. Chapter 8 in Haugeland, J. (ed), Mind Design II, 1997, MIT Press, 205-232.

International Journal of Modern Engineering Research (IJMER)
www.ijmer.com Vol.3, Issue.3, May-June. 2013 pp-1307-1308 ISSN: 2249-6645

File Replication to Access Files with Reasonable Response Time in Data Grid Environment… A Review Study

Dhananjay L. Joshi[1], Asst. Prof. S. A. Hasmi[2], Dr. Mrs. A. M. Rajurkar[3]
[123]*Department of CSE, M. G. M. College of Engineering, S. R. T. M. University Nanded, India*

Abstract: *Data Grid is an integrated architecture that connects multiple computers and its resources in distributed environment. The file replication is an effective functionality in Data Grid that not only minimizes total access time by replicating most accessed data file at appropriate location but also improve data files availability. This paper mainly deals with different file replication methodologies and enlists various effective strategies proposed by earlier authors to access data file with reasonable response time in Data Grid environment.*

Keywords: *Data Grid, Data File Replication, Replication Strategies, Simulation.*

I. Introduction

Data Grid is composed of set of sites and each site contains multiple computing, storage and networking resources. All sites are geographically connected to manage and store large data files of size Gigabytes and beyond in data repositories (sites) throughout the world. Data Grid provides an important service of data and/or data file replication in multiple locations, so that, it helps user not only to speed up data file access but also increases data file availability. A community of researchers distributed worldwide can access and share these replicated data files. In Data Grid, each data files are initially produced and stored in Grid sites. A Grid site may contain multiple data files and will be replicated in appropriate location in Data Grid to reduce access cost.

Many of the time Replication is confused with caching as they have multiple copies of file, and they have some differences. Replication is a server side phenomenon whereas caching is associated with a client. A server decides when and where to replicate files. A client request for a file and stores a copy of the file locally for use. Any other nearest client can also request for that cached copy.

Replication is that, it can enhance data availability and network performance. The replication of files in Data Grid follows the full or partial replication strategy. In full replication all files are replicated to all resources where as in partial replication files are replicated to some resources in the Data Grid. There are two replication schemes depending on the use access pattern: 1. Static Replication: in which replicas are kept until it is deleted. 2. Dynamic Replication: in which replicas are created and destroyed or replaced according to variation access of the pattern or environment behavior. In data replication there are three issues: 1. Replica Management- create, delete, move & modify replica. 2. Replica Selection-selecting appropriate replica across grid. 3. Replica Location-selecting physical locations of several replicas of desired data.

II. Literature Survey

1.1 Data Replication in Data Intensive Scientific Application with Performance Guarantee [1].

This paper deals with scientific data in the form of data files are produced, stored and replicated if necessary. The author proposed a centralized data replication algorithm (Greedy), it places one data file into the storage space of one site and algorithm terminates when all storage space of sites has been replicated with data files to minimize total access cost in the Data Grid. This algorithm that not only has a provable theoretical performance guarantee, but can be implemented in distributed and practical manner

Specifically, the author designed a polynomial time centralized replication algorithm that reduces total access cost by at least half of reduced by the optimal replication solution. Based on this centralized algorithm a localized distributed data caching algorithm is designed to make intelligent caching decisions. It is composed of Centralized Replica Catalogue (CRC): maintained at top level sites, which is essentially a list of replica sites list for each data file. Nearest Replica Catalogue (NRC): maintained at each sites which contains information of replica copy and nearest sites, and any changes made to NRC will be updated in CRC by sending message to top level site. Simulation results shows centralized greedy algorithm performs quite close to optimal algorithm.

1.2 Identifying Dynamic Replication Strategies for a High-Performance Data Grid [7].

This paper discusses about dynamic replication strategies for high performance; author presents data replication in hierarchical Data Grid model (as a tree topology) and six different replication strategies: (1)No Replication and Caching-where no replication takes place. (2)Best Client-The best client is one that has generated the most number of requests for that file, and then the node creates a replica of that file. (3)Cascading Replication- Once the threshold for a file is exceeded at the root replicas are created on next level but on the path of best client. (4)Plain Caching- The client request a file stores a copy locally. (5) Caching plus Cascading Replication- this combines strategy (3) & (4). The client caches file locally. The server identifies the popular files and propagates them down the hierarchy. (6) Fast Spread-replicas are created at each site along its path.

All of the above strategies are evaluated with three user access patterns: (1) Random Access- No locality in Access. (2) Temporal Locality- recently accessed files are likely to be accessed again. (3) Geographical plus Temporal locality- a recently accessed files are likely to be accessed again by a close site. Their simulation result shows Cascading (with geographical plus temporal locality) and Fast Spread (with random access) works better.

1.3 Analysis of Scheduling and Replica Optimization Strategies for Data Grids Using OptorSim [2].

In this paper, author discussed and concentrated on the effect of various job scheduling and data replication strategies with optimization as follows.

Scheduling Optimization Strategies: This algorithm decides when & where job should be executed by selecting the best job location. It calculates cost of running job on each site using following cost metrics. Access Cost: based on network status for obtaining required files. Queue Size & Queue Access Cost: gives total estimated access cost for all jobs in the queue.

Replica Optimization Strategies: is useful to minimize a single job's execution cost (as low a cost as possible) and to maximize the usefulness of locally stored files (by utilizing available data resources)by performing tasks *viz* replication decision, selection and file replacement. Author also considered three specific optimization strategies, one is LFU(Least Frequently Used) algorithm and two economic strategies are similar to each other, but uses different prediction functions, one is binomial based and other is Zipf-based, to calculate file values used in replication and file replacement decisions (sites can "buy" and "sell" files by using auction protocol mechanism).Their simulation result shows scheduling optimization reduces average times to execute jobs & economic based strategy have greatest effect.

1.4 Agent Based Replica Placement in a Data Grid Environment [3].

The author proposed an agent based replica placement algorithm for making a replica decision to select 'candidate site' for replica placement to reduce access cost, network traffic, and aggregated response time for the applications. To select a candidate site for a replica, an agent is deployed at each site that holds master copies of the files for which the replicas are to be created. The agent in this approach is autonomous, self-contained software capable of making independent decisions. Replica placement strategy considers two issues in choosing replica location: (1) placing a replica at proper site so that times taken for obtaining all files required by jobs are minimized. (2) Place a replica at sites that optimizes total execution time of the jobs executed in Data Grid.

The author extended the GridSim toolkit for decision making process for selection of candidate site by implementing Replica Catalogue and Replica Manager to maintain and control all replicas.

III. Conclusion

The data file replication performance depends on a variety of factors such as replica selection, placement, network traffic and bandwidth. This paper focuses on data file replication algorithms by following different file replication strategies using simulation environments. Well suited replication strategy can improve Data Grid performance depending on data file access situation.

References

Journal Papers:

[1] Dharma Teja Nukarapu,Bin Tang, Liqiang Wang and Shiyong Lu, "Data Replication in Data Intensive Scientific Applications with Performance Guarantee", IEEE Transaction on Parallel and Distributed Systems, Vol. 22, No 8, Aug 2011.

[2] D. G. Cameron, R. Carvavajal-Schiaffino, A. P. Millar, C. Nicholson, K. Stockinger and F. Zini, "Analysis of Scheduling and Replica Optimisation Strategies for Data Grids using OPtorSim ".

[3] Ms. Shaik Naseer and Dr. K. V. Madhu Murthy, "Agent Based Replica Placement in a Data Grid Environment", First Int'l Conference on Computational Intelligence, Communication Systems and Networks 2009.

[4] Mahesh Mayura and Ketan Shah,"A Review on File Replication Algorithms", journal of Sci. & Tech. Mgt. vol 3(2), july 2011.

Books:

[5] Pradip K Sinha, " Distributed Operating Systems-concepts and design", IEEE Computer Society Press, Prentice Hall of India 1998.

Thesis:

[6] Wong Yuk Key."Performance Analysis of Data Replication in Data Grid", University of Malaya, Kuala Lumpur, MALAYSIA, 2006/2007.

Proceedings Papers:

[7] Kavita Rananathan and Ian Foster, "Identifying Dynamic Replication Strategies for High Performance Data Grid", Proc. Second Int'l Workshop Grid Computing (Grid), 2001.

International Journal of Modern Engineering Research (IJMER)
www.ijmer.com Vol.3, Issue.3, May-June. 2013 pp-1309-1316 ISSN: 2249-6645

Design Development Experimental Approach of Industrial Product Enhancement Prior To Fabrication with Stereo Lithography

P.N.S. Srinivas, [1] A.Rahul kumar[2]
[12]*Asst Prof (Department of mechanical engineering), Sri Vasavi institute of engineering & technology, JNTUK, INDIA*

***Abstract*:** *As my research work is concerned with the optimization techniques by enhancing the rapid prototyping technique. In the manufacturing process of a particular product the in process parameters are going to qualitatively analyzed after the production process. This may lead to the various failures such as internal stresses, time dependent failures, cycling loading failures .to analyze these failures the losses incurred in the availability of skilled personals, inspection time , manufacturing& material cost. To overcome these failures one of the optimization technique is stereo lithography (Rapid prototyping) has been introduced.*

***Keywords*:** *Rapid protyping, cyclic loading factors, material cost, inspection.*

I. Introduction

Rapid prototyping automates the fabrication of a prototype part from a three- dimensional (3D) CAD drawing. This physical model conveys more complete information about the product earlier in the development cycle. The turnaround time for a typical rapid prototype part can take a few days. Conventional prototyping may take weeks or even months, depending on the method used. Rapid prototyping can be quicker more cost effective means of building prototypes as opposed to conventional methods. Fabrication process fall into 3 categories: Subtractive, Additive and compressive. In a subtractive process a block of material is carved out to produce the desired shape. An additive process builds materials by joining particles or layers or raw materials. A compressive process forces a semi solid or liquid into desired shape, in which it is induces to harden or solidify. Most conventional prototypes fall into subtractive category.

These would include machining processes such as milling, turning, and grinding. Machining methods are difficult to use on parts with very small internal cavities or complex geometries. Compressive processes, also conventional, include casting and molding .The new rapid prototyping technologies are additive processes. They can be categorized by material: photopolymer, thermoplastic, and adhesives. Photopolymer systems start with a liquid resin, which is then solidified by discriminating exposure to a specific wavelength of light, Thermoplastic systems begin with a solid material, which is then melted and fuses upon cooling. The adhesive systems use a binder to connect the primary construction material. Rapid prototyping systems are capable of creating parts with small internal cavities and complex geometries. Also, the integration of rapid prototyping and compressive processes has resulted in the quicker generation of patterns from which moulds are made.

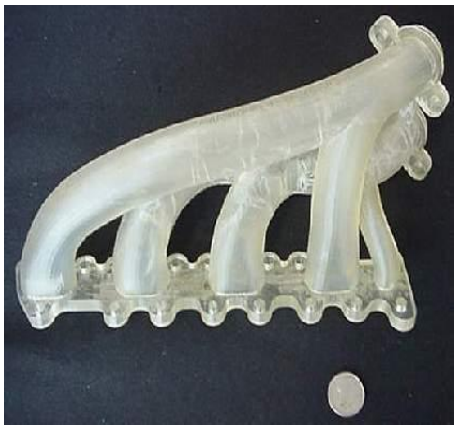

fig. Rapid Prototyped part

Rapid prototyping was commercially introduced in 1987 with the presentation of Stereo lithography. Several processes are now commercially available in the industry. They are as follows:

1. Stereo lithography
2. Selective Laser Sintering
3. Fused Deposition Modeling
4. Laminated Object Manufacturing
5. 3 D Inkjet Printing
6. Solid Ground Curing

Among these RP techniques Stereo lithography is most commonly and widely used.

II. The Basic Process

Although several rapid prototyping techniques exist, all employ the same basic five-step process. The steps are:

1. Create a CAD model of the design
2. Convert the CAD model to STL format
3. Slice the STL file into thin cross-sectional layers
4. Construct the model one layer atop another
5. Clean and finish the model

II.1.CAD Model Creation: First, the object to be built is modeled using a Computer-Aided Design (CAD) software package. Solid modelers, such as Pro/ENGINEER, tend to represent 3-D objects more accurately than wire-frame modelers such as AutoCAD, and will therefore yield better results. The designer can use a pre-existing CAD file or may wish to create one expressly for prototyping purposes. This process is identical for all of the RP build techniques.

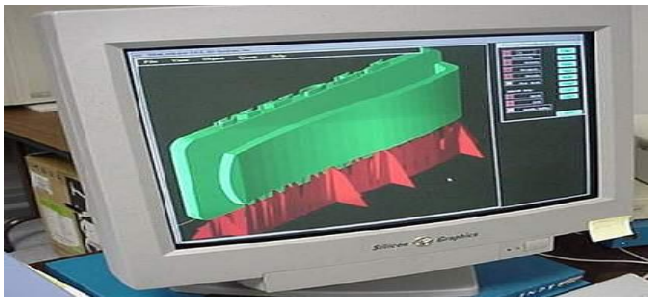

Fig.2 CAD Model

II.2.Conversion to STL Format: The various CAD packages use a number of different algorithms to represent solid objects. To establish consistency, the STL (stereo lithography, the first RP technique) format has been adopted as the standard of the rapid prototyping industry. The second step, therefore, is to convert the CAD file into STL format. This format represents a three-dimensional surface as an assembly of planar triangles, "like the facets of a cut jewel." [6] The file contains the coordinates of the vertices and the direction of the outward normal of each triangle. Because STL files use planar elements, they cannot represent curved surfaces exactly. Increasing the number of triangles improves the approximation, but at the cost of bigger file size. Large, complicated files require more time to pre-process and build, so the designer must balance accuracy with manageability to produce a useful STL file. Since the .stl format is universal, this process is identical for all of the RP build techniques.

II.3.Slice the STL File: In the third step, a pre-processing program prepares the STL file to be built. Several programs are available, and most allow the user to adjust the size, location and orientation of the model. Build orientation is important for several reasons. First, properties of rapid prototypes vary from one coordinate direction to another. For example, prototypes are usually weaker and less accurate in the z (vertical) direction than in the x-y plane. In addition, part orientation partially determines the amount of time required to build the model. Placing the shortest dimension in the z direction reduces the number of layers, thereby shortening build time. The pre-processing software slices the STL model into a number of layers from 0.01 mm to 0.7 mm thick, depending on the build technique. The program may also generate an auxiliary structure to support the model during the build. Supports are useful for delicate features such as overhangs, internal cavities, and thin-walled sections. Each PR machine manufacturer supplies their own proprietary pre-processing software.

II.4.Layer by Layer Construction: The fourth step is the actual construction of the part. Using one of several techniques (described in the next section) RP machines build one layer at a time from polymers, paper, or powdered metal. Most machines are fairly autonomous, needing little human intervention.

II.5.Clean and Finish: The final step is post-processing. This involves removing the prototype from the machine and detaching any supports. Some photosensitive materials need to be fully cured before use. Prototypes may also require minor cleaning and surface treatment. Sanding, sealing, and/or painting the model will improve its appearance and durability.

III. What Is Stereo Lithography?

SL is the most popular and widely is used rapid prototyping technology. It is a unique form of technology which allows for the translation of computer aided design drawing to3D solid objects within hours. In Stereo Lithography liquid plastic is solidified in precise patterns by laser beam resulting in solid epoxy realization of a 3D design. This ultraviolet laser beam is guided by CAD

Parts created using Stereo Lithography must be modeled through the use of CAD system, such as ANSYS, AUTOCAD, IDEAS; Pro.-Engineer etc. The CAD files are stored in STL format which defines the boundary surface of the object as mesh of interconnected triangle
Stereo Lithography process can be run in 3 modes:

1. Acces Mode.
2. Quick Cast
3. Solid Weave

The ACES mode produces crystal like transparency and exceptional strength at very high dimensional resolution. This mode of stereo lithography is perfect for parts that require exceptional visual quality such as lenses and optical components. Quick Cast is a SL mode creates quasi-hollow parts with a strong honey comb interior which is 80% hollow. From a quick cast prototype metal parts can be made 3-5 days. Solid weave boasts the quickest turnaround time of SLA modes without compromising on strength and precision. It is also most economical of three.

IV. Stereo Lithography Machine

Stereo lithography, also known as 3-D layering or 3-D printing, is accomplished using a special SLA machine containing a computer-controlled laser and a tank of light-curable plastic, or photopolymer

Stereo lithography machine

This machine has four important parts:

1. A tank filled with several gallons of liquid photopolymer. The photopolymer is a clear liquid plastic.
2. A perforated platform immersed in the tank. The platform moves up and down in the tank as the printing process proceeds
3. An ultraviolet laser
4. A computer that drives the laser and the platform

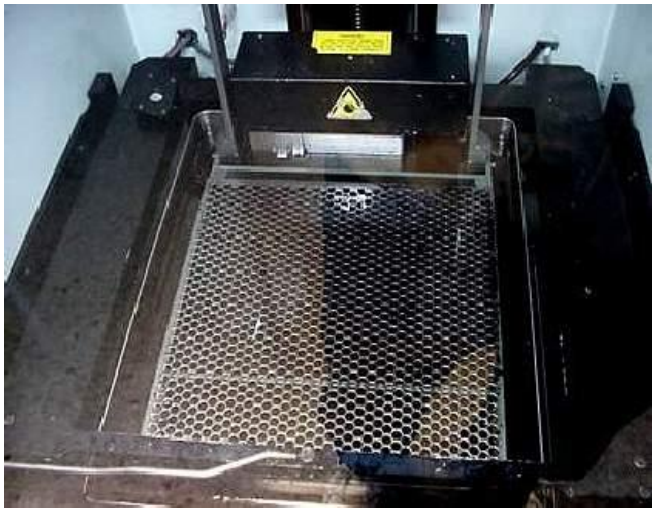

The platform in the tank of photopolymer at the beginning

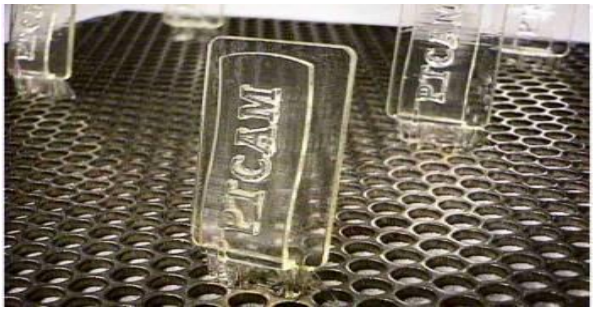

The platform at the end of a print run, shown here with several identical objects

INSIDE OF SLA MACHINE

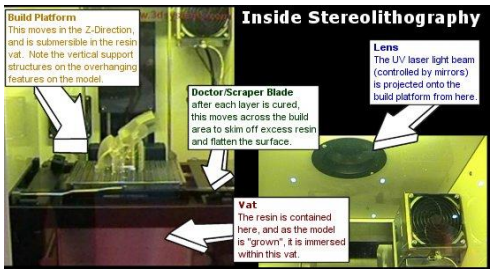

Object curing machines

V. The Stereo Lithography Process

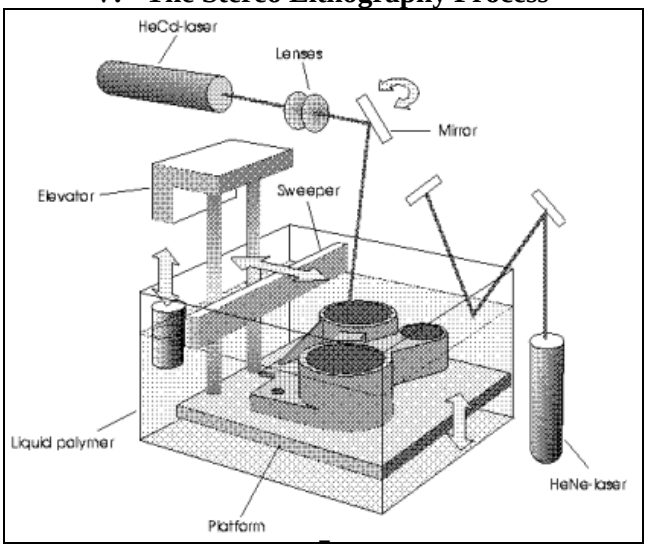

Fig 3: Schematic diagram of stereo lithography.

The basic Stereo lithography process consists of the following steps:

- A 3-D model of an object is created in a CAD program.
- Special computer software "cuts" the CAD model file into thin layers typically five to 10 layers per millimeter of part thickness.
- The 3-D printer's ultraviolet laser "paints" one of the layers, exposing the top surface of the liquid plastic in the tank and hardening it. The photopolymer is sensitive to ultraviolet light, so wherever the laser touches the photopolymer, the polymer hardens.
- The platform drops down into the tank a fraction of a millimeter, and then the laser "paints" the next layer on top of the previous layer.
- This process repeats, layer by layer, until the 3-dimensional plastic model is complete.
- Depending upon the size and number of objects being created, the laser might take a minute or two for each layer. A typical run might take six to 12 hours. Runs over several days are possible for large objects. The maximum size for the machine is an object 10 inches (25 cm) in each of three dimensions ... 10 x 10 x 10.
- When the process is complete, the SLA machine raises the platform with the completed 3-D object. If the finished object is small, several can be produced at the same time, sitting next to each other on the tray.
- Once the run is complete, the finished objects are rinsed with solvent to remove all uncured plastic and then "baked" in an ultraviolet oven that thoroughly cures the plastic

The sequence of steps for producing Stereo lithography layer is shown in the following figures;

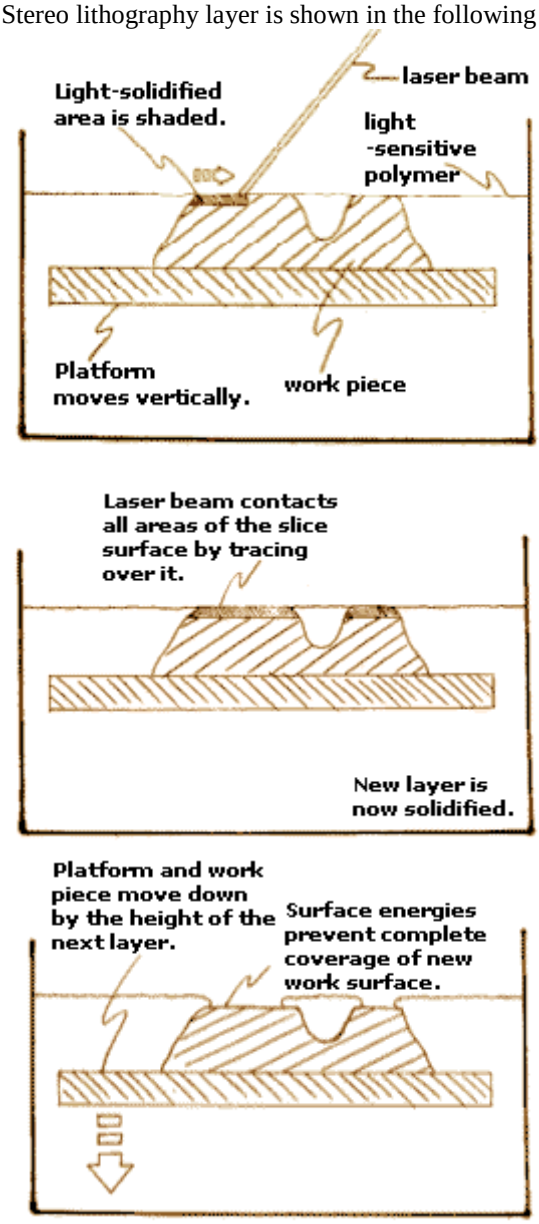

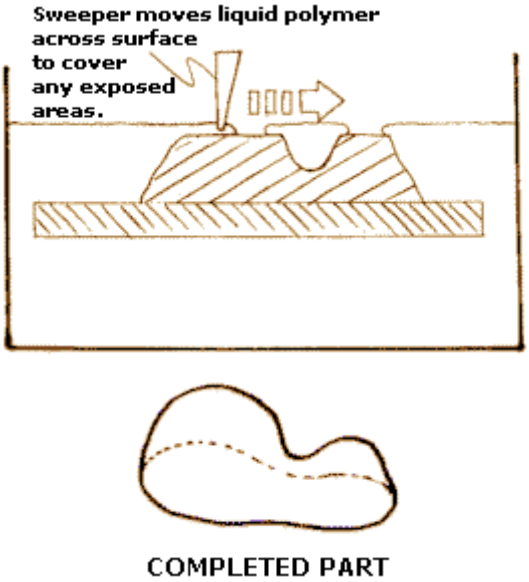

COMPLETED PART

Uncured resin is removed and the model is post-cured to fully cure the resin. Because of the layered process, the model has a surface composed of stair steps. Sanding can remove the stair steps for a cosmetic finish. Model build orientation is important for stair stepping and builds time. In general, orienting the long axis of the model vertically takes longer but has minimal stair steps. Orienting the long axis horizontally shortens build time but magnifies the stair steps. For aesthetic purposes, the model can be primed and painted.

During fabrication, if extremities of the part become too weak, it may be necessary to use supports to prop up the model. The supports can be generated by the program that creates the slices, and the supports are only used for fabrication. The following three figures show why supports are necessary:

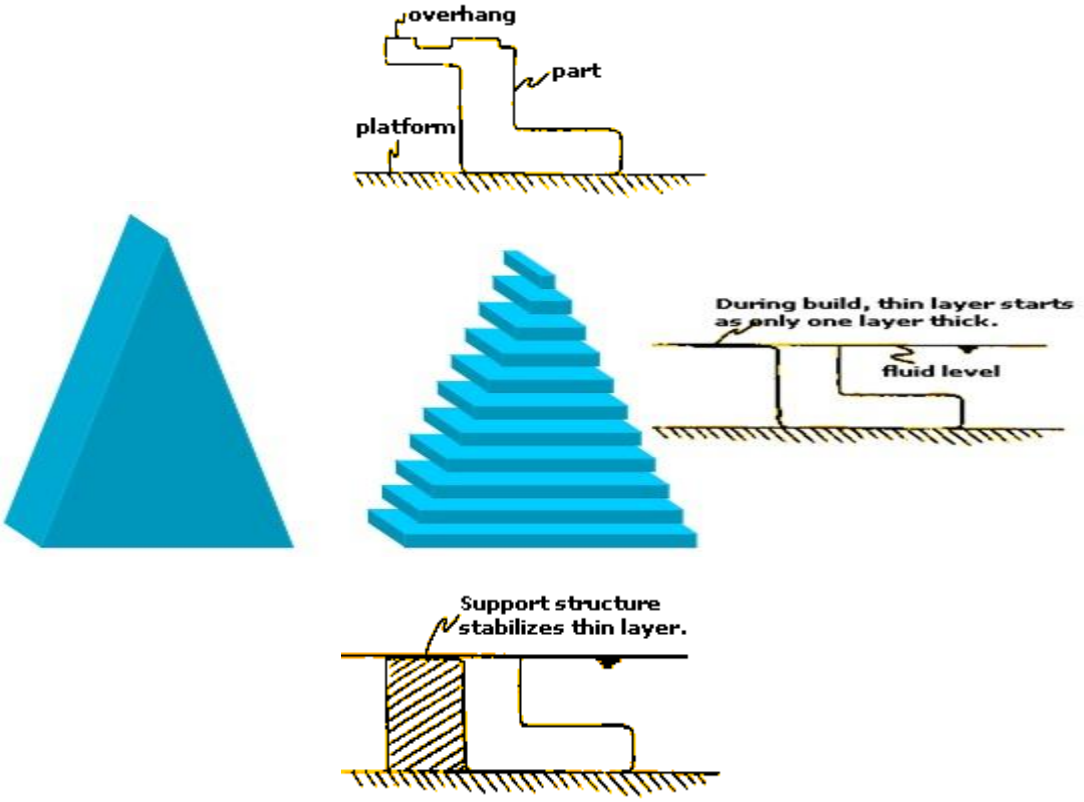

VI. Stl (Stereo Lithography) Files

The .STL file format has become SLA industry's standard CAD export format and is required to interact with stereo lithography machines. This format approximates the surfaces of a solid model with small triangles and was designed to give the proper amount of model detail required to operate the Stereo Lithography machines. Virtually all of today's modern CAD software programs are capable of producing an STL file. For the user, the process is often as simple as selecting File, Save As, STL.

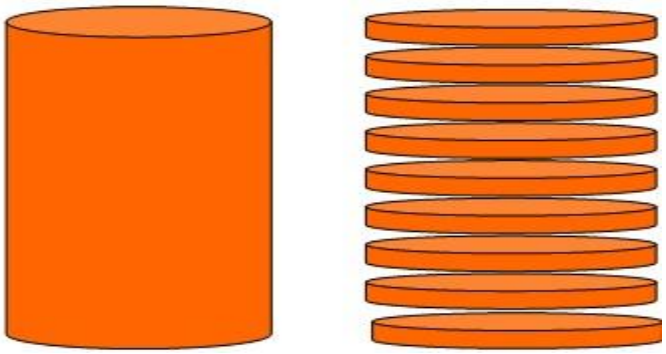

VII. Sla Accuracy

SLA**Y** parts may be built using normal or "high" resolution. Normal resolution is typically defined as SLA parts build using a .010" or larger laser beam diameter and .004" or greater layer thickness. Building parts in this manner results in the most cost-effective build, but may not catch all of the tiny features of small parts or tools. Normal resolution SLA can manufacture parts with tolerances of +/- .005 to .006 inches. This is the standard resolution available at most suppliers.

High resolution is defined as an SLA part builds using a .003" - .004" diameter laser beam and/or a layer thickness less than .004". Building parts with the smaller laser beam diameter results in parts with sharp corners and the thinnest possible walls. Thin layers reduce the cleanup required to smooth out contours or to polish tooling masters. High resolution SLA can manufacture parts with tolerances of +/- .002 to .003 inches. This build style results in the most accurate, highest quality parts available in the industry, but it is also slower and more expensive than normal resolution.

VIII. Sla Materials

A number of excellent photopolymer materials are now available for SLA rapid prototyping. Each material has unique properties which can be used to simulate more traditional metals or plastics for rapid prototypes. Some SLA resins mimic traditional engineering plastics such as PBT or ABS, with toughness and durability that make the resulting SLA parts suitable for mechanical testing and evaluation. Other SLA resins have properties similar to polypropylene, with fine features and details that can provide accurate test parts. If higher temperatures are needed, new SLA resins provide heat deflection resistance up to 220°F (105°C) as compared to traditional limits of 130°F (55°C). And, for near-metal performance, ceramic-filled SLA resins can be used to make parts with superior stiffness and high temperature resistance. The high stiffness also provides mechanical foundation for structural Nickel plating the resulting parts have a composite structure with mechanical and thermal performance approaching that of metal. New SLA resins are constantly being developed and refined to extend the mechanical and thermal performance of SLA parts.

Material	Appearance	Viscosity(cps)	Density(gm/cm^3)
DSM SOMOS R 1020	Optically clear	130 cps at 30^{0}c	1.12 gm/cm3 at 25^{0}c
DSM SOMOS R 9120	Transparent amber	450 cps at 30^0 c	1.13 gm/cm^3 at 25^{0}c
CIBATOOL R SL 5195	Clear	180 cps at 30^{0}c	1.16 g/cm^3 at 25^0 c

IX. Application of Sla Technology

- Aesthetical and conceptual models–It is used to produce models that are eye-catching and complex. This is because it can convert CAD exactly into 3-D coordinates.
- Parts requiring detail and accuracy–The resolution of laser used can be increased to sufficiently high levels. Also layer thickness can be varied. So we can make more accurate models.
- Master patterns for casting–Using this technology, master castings for processes like vacuum casting, investment casting, sand casting, injection molding.

X. Benefits of Sla

- Crisp and highly detailed pieces
- Speed of delivery(usually 2 to 3 days)
- Tolerance with .005 inch/inch
- Saves money
- Time saving
- Test product
- Locates error
- Improves design
- Sells product
- Rapid manufacturing

XI. Problems with Rapid Prototyping

The model is composed of several layers. When slant edges and curves are involved, no finishing is obtained. Instead a stair-case like appearance is the result. Also the parts involved are subjected to shrinkage and distortion.

Limited variety of materials in Rapid Prototyping Mechanical performance of the fabricated parts is limited by the materials used in the Rapid Prototyping process.

XII. Conclusion

Stereo Lithography saves time, money, allows speedy delivery and helps in improving design. Stereo Lithography can be applied to almost any industry including oil refining, petrochemical, power and marine industries. It is also the most effective and economical of all Rapid Prototyping techniques. It is still a technology in its growing stages and will prove to be a major technology in the future.

References

[1]. Advanced High Temperature Resins for Stereo Lithography" from proceedings of 7th International conference on Rapid Prototyping, University of Dayton, San Francisco
[2]. Pandey, P.M., Reddy, N.V., Dhande, S.G. (2004a) Part Deposition Orientation Studies in Layered Manufacturing, Proceeding of International Conference on Advanced Manufacturing Technology, pp. 907-912.
[3]. Pandey, P.M., Thrimurthullu, K., Reddy, N.V. (2004b) Optimal Part Deposition Orientation in FDM using Multi-Criteria GA, International Journal of Production Research, 42(19), pp. 4069-4089.
[4]. Pham, D.T., Dimov, S.S. (2001) Rapid Manufacturing, Springer-Verlag London Limited.
[5]. Singhal, S.K., Pandey, A.P., Pandey, P.M., Nagpal, A.K. (2005) Optimum Part Deposition Orientation in Stereo lithography, Computer Aided Design and Applications, 2(1-4)
[6]. Thrimurthullu, K., Pandey, P.M., Reddy, N.V. (2004) Part Deposition Orientation in Fused Deposition Modeling, International Journal of Machine Tools and Manufacture, 2004, 44, pp. 585-594

International Journal of Modern Engineering Research (IJMER)
www.ijmer.com Vol.3, Issue.3, May-June. 2013 pp-1317-1323 ISSN: 2249-6645

Experimental Analysis of Heat Transfer Augmentation by Using Twisted Tapes of Different Twist Ratio as Flow Arrangement inside the Tubes

A.Rahul kumar, [1] P.N.S Srinivas[2]
[12]*Asst Prof (Department of mechanical engineering), Sri Vasavi institute of engineering & technology, Jntuk, India*

Abstract: *The objective of this thesis is to investigate the swirl flow behavior and the laminar convective heat transfer in a circular tube with twisted-tape inserts. The fluid flow and thermal fields are simulated computationally in an effort to characterize their structure. Apart from this, issues like long term performance & detailed economic analysis of heat exchanger has to be studied. To achieve high heat transfer rate in an existing or new heat exchanger while taking care of the increased pumping power*.

Keywords**:** *Twisted tapes, pumping power, friction factor, enhancement techniques*

I. Introduction

Heat exchangers are used in different processes ranging from conversion, utilization & recovery of thermal energy in various industrial, commercial & domestic applications. Some common examples include steam generation & condensation in power & cogeneration plants; sensible heating & cooling in thermal processing of chemical, pharmaceutical & agricultural products; fluid heating in manufacturing & waste heat recovery etc. Increase in Heat exchanger's performance can lead to more economical design of heat exchanger which can help to make energy, material & cost savings related to a heat exchange process. The need to increase the thermal performance of heat exchangers, thereby effecting energy, material & cost savings have led to development & use of many techniques termed as—Heat transfer Augmentation. These techniques are also referred as—Heat transfer Enhancement or—Intensification. Augmentation techniques increase convective heat transfer by reducing the thermal resistance in a heat exchanger. Use of Heat transfer enhancement techniques lead to increase in heat transfer coefficient but at the cost of increase in pressure drop. So, while designing a heat exchanger using any of these techniques, analysis of heat transfer rate & pressure drop has to be done.

II. Twisted-Tape Flow and Heat Transfer

It is well known that energy transport is considerably improved if the flow is stirred and mixed well. This has been the underlying principle in the development of enhancement techniques that generate swirl flows. Among the techniques that promote secondary flows, twisted-tape inserts are perhaps the most convenient and effective (Manglik and Bergles, 2002).They are relatively easy to fabricate and fit in the tubes of shell-and-tube or tube-fin type heat exchangers. A typical usage in the multi-tube bundle of a shell-and-tube heat exchanger.

The geometrical features of a twisted tape, as depicted in Fig. 2.1, are described by its 180º twist pitch H, the thickness δ, and the width w. In most usage, where snug-to-tight-fitting tapes are used, $w \cong d$, and the severity of the tape twist is characterized by the dimensionless ratio $y = (H / d)$.

The helical twisting nature of the tape, besides providing the fluid a longer flow path or a greater residence time, imposes a helical force on the bulk flow that promotes the generation of secondary circulation. The consequent well-mixed helical swirl flow significantly enhances the convective heat transfer (Manglik and Bergles, 2002, 1993a, 1993b). In most cases, depending on how tightly the tape fits at the tube wall and what material it is made of, there may be some tape-fin effects as well. The enhanced heat transfer due to twisted-tape inserts, is also accompanied by an increase in pressure drop and suitable trade-offs must be considered by designers to optimize their thermal-hydraulic performance ratio $y = (H / d)$. The helical twisting nature of the tape, besides providing the fluid a longer flow path or a greater residence time, imposes a helical force on the bulk flow that promotes the generation of secondary circulation. The consequent well-mixed helical swirl flow significantly enhances the convective heat transfer (Manglik and Bergles, 2002, 1993a, 1993b). In most cases, depending on how tightly the tape fits at the tube wall and what material it is made of, there may be some tape-fin effects as well. The enhanced heat transfer due to twisted-tape inserts, is also accompanied by an increase in pressure drop and suitable trade-offs must be considered by designers to optimize their thermal-hydraulic performance.

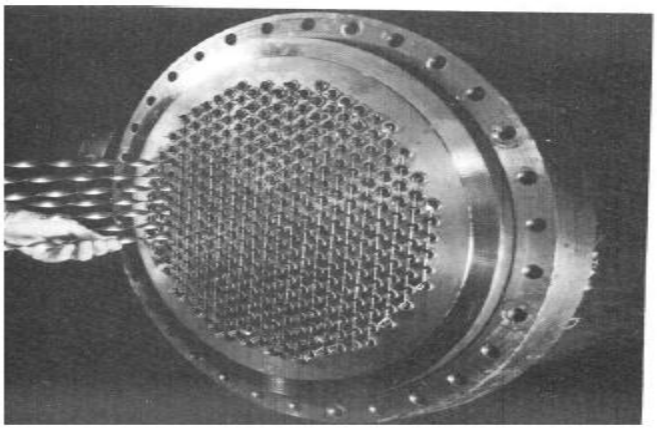

Shell-and-tube heat exchanges with twisted-tape inserts

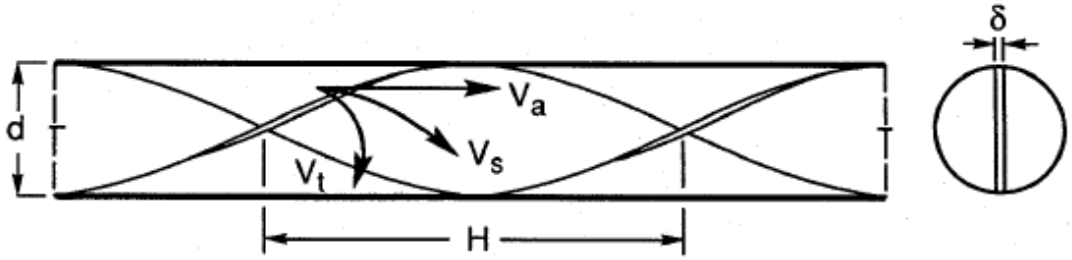

Fig.2.1 Twisted-tape geometry

III. Clasification Of Enhancement Techniques

Heat transfer enhancement or augmentation techniques refer to the improvement of thermo-hydraulic performance of heat exchangers. Existing enhancement techniques can be broadly classified into three different categories:

1. Passive Techniques
2. Active Techniques
3. Compound Techniques.

III.I.PASSIVE TECHNIQUES: These techniques generally use surface or geometrical modifications to the flow channel by incorporating inserts or additional devices. They promote higher heat transfer coefficients by disturbing or altering the existing flow behavior (except for extended surfaces) which also leads to increase in the pressure drop. In case of extended surfaces, effective heat transfer area on the side of the extended surface is increased. Passive techniques hold the advantage over the active techniques as they do not require any direct input of external power. Heat transfer augmentation by these techniques can be achieved by using:

1. Treated Surfaces
2. Rough surfaces
3. Extended surfaces
4. Swirl flow devices
5. Coiled tubes

III.II.ACTIVE TECHNIQUES: These techniques are more complex from the use and design point of view as the method requires some external power input to cause the desired flow modification and improvement in the rate of heat transfer. It finds limited application because of the need of external power in many practical applications. In comparison to the passive techniques, these techniques have not shown much potential as it is difficult to provide external power input in many cases. Various active techniques are as follows:

1. Mechanical Aids
2. Surface vibration
3. Fluid vibration.
4. Electrostatic fields.
5. Injection
6. Suction

III.III.COMPOUND TECHNIQUES: A compound augmentation technique is the one where more than one of the above mentioned techniques is used in combination with the purpose of further improving the thermo-hydraulic performance of a heat exchanger.

IV. Performance Evaluation Criteria

In most practical applications of enhancement techniques, the following performance objectives, along with a set of operating constraints and conditions, are usually considered for optimizing the use of a heat exchanger:

1. Increase the heat duty of an existing heat exchanger without altering the pumping power (or pressure drop) or flow rate requirements.
2. Reduce the approach temperature difference between the two heat-exchanging fluid streams for a specified heat load and size of exchanger.
3. Reduce the size or heat transfer surface area requirements for a specified heat duty and pressure drop or pumping power.
4. Reduce the process stream's pumping power requirements for a given heat load and exchanger surface area.

It may be noted that objective 1 accounts for increase in heat transfer rate, objective 2 and 4 yield savings in operating (or energy) costs, and objective 3 leads to material savings and reduced capital costs.

		Criterion number							
		R1	R2	R3	R4	R5	R6	R7	R8
Fixed	Basic Geometry	×	×	×	×				
	Flow Rate	×						×	×
	Pressure Drop		×				×		×
	Pumping Power			×					
	Heat Duty				×	×	×	×	×
Objective	Increase Heat Transfer	×	×	×					
	Reduce pumping power				×				
	Reduce Exchange Size					×	×	×	×

EXTENDED SURFACES: Extended or finned surfaces increase the heat transfer area which could be very effective in case of fluids with low heat transfer coefficients. This technique includes finned tube for shell & tube exchangers, plate fins for compact heat exchanger and finned heat sinks for electronic cooling.

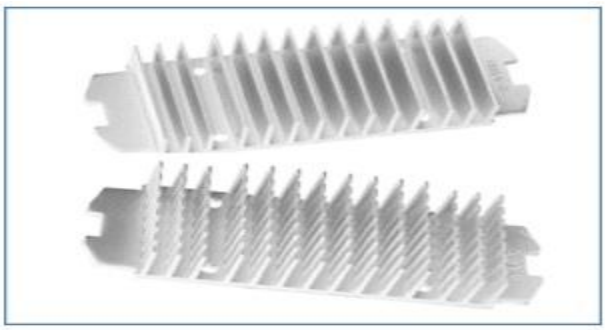

DISPLACED ENHANCEMENT DEVICES: Displaced enhancement devices displace the fluid elements from the core of the channel to heated or cooled surfaces and vice versa .Displaced enhancement devices include inserts like static mixer elements (e.g. Kenics, Sulzer), metallic mesh, and discs, wire matrix inserts, rings or balls.

Heatex wire matrix tube insert is one of the commercially available new displaced enhancement devices

SWIRL FLOW DEVICES: Swirl flow devices causes swirl flow or secondary flow in the fluid .A variety of devices can be employed to cause this effect which includes tube inserts, altered tube flow arrangements, and duct geometry modifications

TWISTED TAPE IN LAMINAR FLOW: Twisted tape increases the heat transfer coefficient with an increase in the pressure drop. Different configurations of twisted tapes, like full-length twisted tape, short length twisted tape, full length twisted tape with varying pitch, reduced width twisted tape and regularly spaced twisted tapes have been some impact on heat transfer process.

TWISTED TAPE IN TURBULENT FLOW: Unlike laminar flows where thermal resistance exist entirely over the cross section, it is limited to the thin viscous sub layer. So the main objective of the twisted tape in the turbulent region is to reduce that resistance near the wall to promote better heat transfer. Besides, a tube inserted with a twisted tape produces swirl and cause intermixing of the fluid which leads to better performance than a plain tube. Heat transfer rate is improved effectively with the increase in the frictional losses

FABRICATION OF TWISTED TAPES: The stainless steel strip of length 125cm, width 16mm and thickness 1.80mm were taken. Holes were drilled at both ends of every tape so that the two ends could be fixed to the metallic clamps. Desired twist was obtained using a Lathe machine. One end was kept fixed on the tool post of the lathe while the other end was given a slow rotatory motion by rotating the chuck side. During the whole operation the tape was kept under tension by applying a mild pressure on the tool post side to avoid its distortion. Three tapes with varying twist ratios were fabricated (y_w=5.25, y_w =4.39, y_w =3.69) as shown in fig

Twist ratio y=3.69

Twist ratio y=4.39

Twist ratio y=5.25

V. Specifications Of Heat Exchanger Used

The experimental study is done in a double pipe heat exchanger having the specifications as listed below:-
Specifications of Heat Exchanger: Inner pipe ID =
20mm
Inner pipe OD=24mm
Outer pipe ID =51mm
Outer pipe OD=58mm
Material of construction= Copper
Heat transfer length= 2.43m
Pressure tapping to pressure tapping length = 2.525m

Water at room temperature was allowed to flow through the inner pipe while hot water (set point 60°C) flowed through the annulus side in the counter current direction.

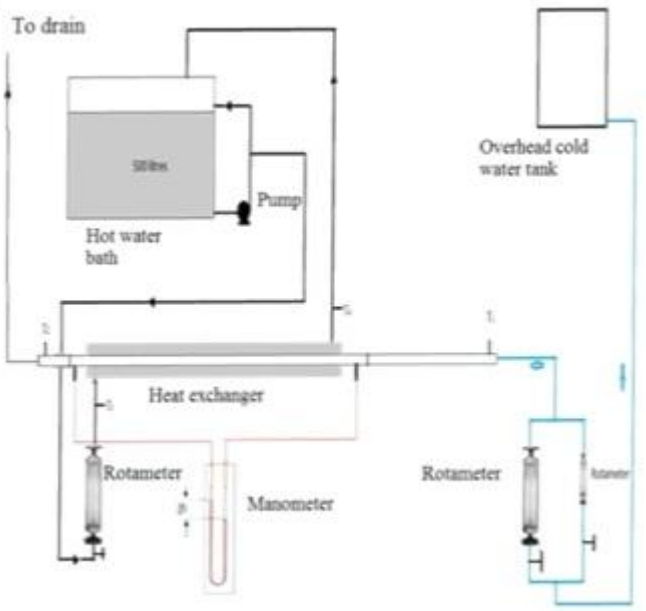

5.1 Block diagram for double pipe heat exchanger

Standard Equations Used:

I. Friction factor (f_0) calculations:

a. For Re< 2100

$f=16/R_e$

b. For Re>2100

Colburn's Equation:

$f=0.046/R_e^{0.2}$

II. Heat transfer calculations

i. Laminar Flow:

For Re<2100

Nu= f (Gz)

Where Gz= $1/(R_e x L_r x d_i)$

For Gz<100, Hausen Equation is used.

$$Nu = 3.66 + \frac{0\ 085Gz}{1+0.045Gz^{0.67}} \frac{}{\mu w} \ (\mu b)^{0.14}$$

b. For Gz>100, Seider Tate equation is used.

$$Nu = 1.86Gz^{1/3}(\frac{\mu_b}{\mu_w})^{0.14}$$

ii. Transition Zone:

For 2100<Re<10000, Hausen equation is used

$$Nu = 0.116\left(Re^{2/3} - 125\right) \times Pr^{1/3} \times (1 + (\frac{D}{l})^{2/3}(\frac{\mu_b}{\mu_w})^{0.14} \qquad (3.8)$$

iii. Turbulent Zone:

For Re>10000, Seider-Tate equation is used.

$$Nu = 0.023 \times Re^{0.8} \times Pr^{1/3} \times (\frac{\mu_b}{\mu_w})^{0.14} \qquad (3.9)$$

Viscosity correction Factor $(\frac{\mu_b}{\mu_w})^{0.14}$ is assumed to be equal to 1 for all Calculations as this value for water in present case will be very close to 1 & the data for wall temperatures is not measured.

VI. Results

The below table 5.2 gives correlations for variation of friction factor with Reynolds number for different twisted tapes along with the correlation coefficient, R^2 based on regression analysis. As we can see form the correlations it is quite clear that friction factor is increasing with decrease in twist ratio. As the R^2value is very close to 1, so we can easily make out that the correlation holds true for respective twisted tapes in the given range of Reynolds Number.

Table 5.2 Correlations for Friction Factor for different twisted tapes

SI No.	y_w	Correlation, f_a=	R^2
	TT		
1	3.69	$1.0386\times Re^{-0.380}$	0.9809
2	4.39	$0.5655\times Re^{-0.328}$	0.9916
3	5.25	$0.5226\times Re^{-0.326}$	0.9971

VII. Conclusion

The range of Performance evaluation criteria R_1 (based on constant mass flow rate) & R_3 (based on constant pumping power), & f_a/f_o for different tapes used is given below:

Table Range of R_1, R_3, f_a/f_o for different twisted tapes.

SI No.	Y	Range of R_1	Range of R_3	Range of f_a/f_o
	TT			
1	3.69	1.50-3.66	1.07-1.66	3.70-5.96
2	4.39	1.43-3.35	1.04-1.62	3.43-4.43
3	5.25	1.18-2.75	0.88-1.42	3.23-4.18

For same twist ratio, twisted tape shows higher heat transfer coefficient & friction factor increase because of higher degree of turbulence created.

On the basis of performance evaluation criteria R_1 & R_3, we can say that twisted tape shows better performance than smooth tube.

Twisted tape gives higher heat transfer coefficient than the smooth tube

References

[1]. Ames, F.E., Dvorak, L.A., and Morrow, M.J., 2004, "Turbulent Augmentation of Internal Convection Over Pins in Staggered Pin Fin Arrays," ASME Paper

[2]. Armstrong, J., and Winstanley, D., 1988, "A Review of Staggered Array Pin Fin Heat Transfer for Turbine Cooling Applications," ASME Journal of Turbomachinery, vol. 110, pp. 94-103.

[3]. Bejan, A., 2004, "Convection Heat Transfer," 3rd Edition. Hoboken, New Jersey: John Wiley and Sons, Inc.Brigham, B.A., and VanFossen, G.J., 1984, "Length-to-Diameter Ratio and Row Number Effects in Short Pin Fin Heat Transfer," ASME Journal of Engineering for Gas Turbines and Power, vol. 106, pp. 241-245.

[4]. Chyu, M.K., 1990, "Heat Transfer and Pressure Drop for Short Pin-Fin Arrays with Pin-Endwall Fillet," ASME Journal of Heat Transfer, vol. 112, pp. 926-932.

[5]. Chyu, M.K., Hsing, Y.C., Shih, T.I.-P., and Natarajan, V., 1998a, "Heat Transfer Contributions of Pins and End wall in Pin-Fin Arrays: Effects of Thermal Boundary Condition Modeling," ASME Paper 98-GT-175.

[6]. Chyu, M.K., Hsing, Y.C., and Natarajan, V., 1998b, "Convective Heat Transfer of Cubic Fin Arrays in a Narrow Channel," ASME Journal of Turbomachinery, vol. 120, pp. 362- 367.

International Journal of Modern Engineering Research (IJMER)
www.ijmer.com Vol.3, Issue.3, May-June. 2013 pp-1324-1329 ISSN: 2249-6645

Stress Intensification & Flexibility in Pipe Stress Analysis

Gaurav Bhende[1], Girish Tembhare[2]
[12]*Department of Mechanical Engineering, VJTI, Mumbai, India*

Abstract: *A typical piping system consists of combination of pipes and various fitting components like bends, Tees, O'lets etc. The plant piping systems are subjected to various types of loading due to weight, pressure, temperature, wind, water hammer etc. causing possible failure modes, based on type of loading, as plastic, rupture, fatigue, creep etc. In addition, pipe exhibits different geometric characteristics at fittings which have notable effect on the flexibility of the piping system. This in turn has influence on stress concentration at fittings and the loads produced due to it. This paper attempts to explain basic concepts of flexibility, stress intensification factors and their equations provided in ASME B31 codes. Authors have few observations on B31 SIF equations and hence attempted to compare the results of B31 SIF results against Finite Element Analysis providing the results at the end.*

Keywords: *Flexibility characteristics, Flexibility factor, Stress intensification factor.*

I. INTRODUCTION

In a typical piping system two pipes can be connected to each other directly as pipe to pipe joint or by means of various fittings viz. bends, Tee's, O'lets etc. Simple beam theories which can be applied to straight pipe may not be able to reflect true behavior of the piping fittings due to varying cross sections, thickness, curvatures etc. Hence it is essential to consider additional stresses at the fittings by introducing Stress Intensification Factor (SIF). This paper mainly discusses about the stress intensity calculations followed in Process Piping Plants referring to code ASME B31.3 [1] based on Markl's [2] great work in this domain.

II. FLEXIBILITY CHARACTERISTICS, FLEXIBILITY FACTOR & STRESS INTENSIFICATION FACTOR

To elaborate the concept of Stress Intensification factor (SIF), an example of bend has been considered.

Abbreviations:

$\frac{h}{T}$ =Flexibility characteristics
T =Nominal wall thickness of header pipe or bend, in
R_1 =Bend radius, in
r_2 =Mean radius of matching pipe, in
Sb =Bending stress, PSI
M =Bending moment, lb-in
Z =Section modulus of pipe, in^3
i =Stress intensification factor
N =Number of load cycles

2.1 Flexibility Characteristics, h

It is a geometric characteristics based on the nominal wall thickness and mean radius of the fitting. ASME B31.3 defines it as a unit less number calculated based on type of fitting.

Example: for a bend

$$h = \overline{T}\, R_1 / r_2^2 \qquad (1)$$

Flexibility characteristics is used to calculate Flexibility factor and SIF. It is in inverse proportion to Flexibility factor and SIFs.

2.2 Flexibility factor, k [3]

The most common fitting used in Piping system is 'Bend' due to its inherent flexibility characteristic which results due to its ability to ovalize under the action of bending moment. Consider a straight pipe (refer Figure 1) with length 'l' which will produce rotation 'Θ' under the action of bending moment 'M'. A bend having same diameter and thickness with same arc length 'l' under the action of same bending moment 'M' will exhibit 'k Θ' rotation. In nutshell, bend shows k times flexibility than the straight pipe, called as Flexibility factor.

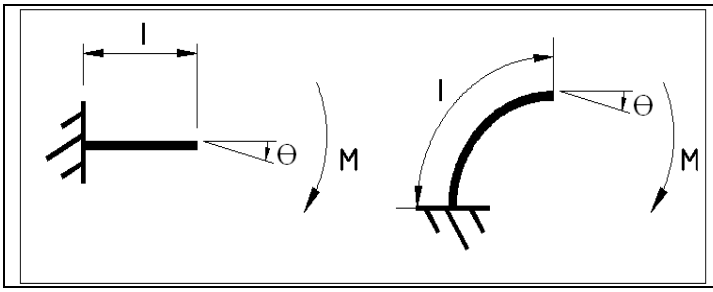

A flexibility factor is defined as the rotation of a pipe bends that of straight pipe of same diameter, wall thickness and length under the action of the same bending moment. [3]

Example: for a bend

$k = 1.65 / h$ (2)

Figure: 1

2.3 Stress Intensification Factor (SIF)

The behavior of a straight pipe and a bend under the externally applied bending moment is different. Straight pipe acts like a beam retaining the cross section as circular whereas, the bend takes oval shape (Figure 2). Due to ovalization of the bend the outer fiber comes closer to the neutral axis reducing moment of inertial and subsequently the section modulus of the bend which in turn enhances bending stress.

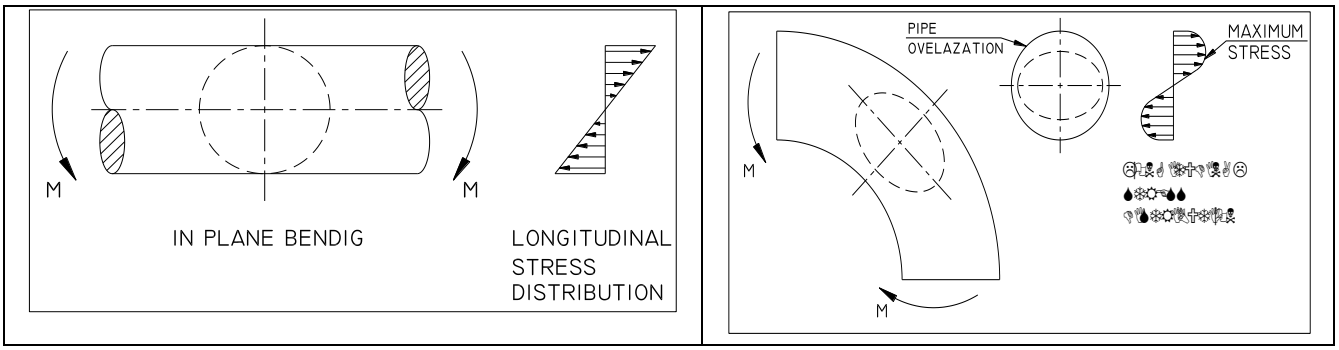

Figure 2

The bending stress in a straight pipe is calculated as

$Sb = M / Z$

The bending stress in a bend is calculated as
Sb' = M / Z' where Z' is reduced section modulus.
Thus the stresses in the bend are higher compared to straight pipe of same size due to the reduced cross section.
The SIF of Bend = Sb' / Sb.

To quote Markl, SIF can be defined *as 'the relation of rotation per unit length of the part in question produced by a moment, to the rotation per unit length of a straight pipe of the same nominal size and schedule or weight produced by the same moment'* [3] *or 'simply Actual Bending Stress to the Calculated Bending Stress'*

Example: for a bend

$i_{in\text{-}plane} = 0.9 / h^{2/3}$ (3)

$i_{out\text{-}plane} = 0.75 / h^{2/3}$ (4)

2.4 In-plane & Out-plane Bending moments

Simply, *'the bending moment which causes elbow to open or close in the plane formed by two limbs of elbow is called in-plane bending moment.' and 'the bending moment which causes one limb of elbow to displace out of the plane retaining other limb steady is called out-plane bending moment.'*

Figure 3 elaborates the said concepts of In-plane and Out-plane bending moments.

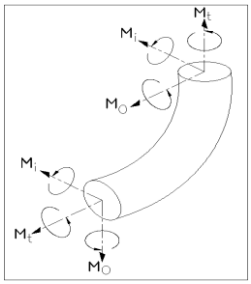

Figure 3

III. Experimental Evaluation & Theorotical Calculations Of SIF [4]

3.1 Markl's Experiment

Markl performed fatigue testing of various piping components in late 1940's. Most of the experiments were performed on 4 inch, SCH40, A106 Grade B pipes with Class 600 flanges. In one of the experiments two size on size un-

reinforced Tee's were tested and it was observed that they failed below ten thousand cycles of reversal displacement. Welds were tested in the as-welded condition. The experimental set up was as shown in the figure 4.

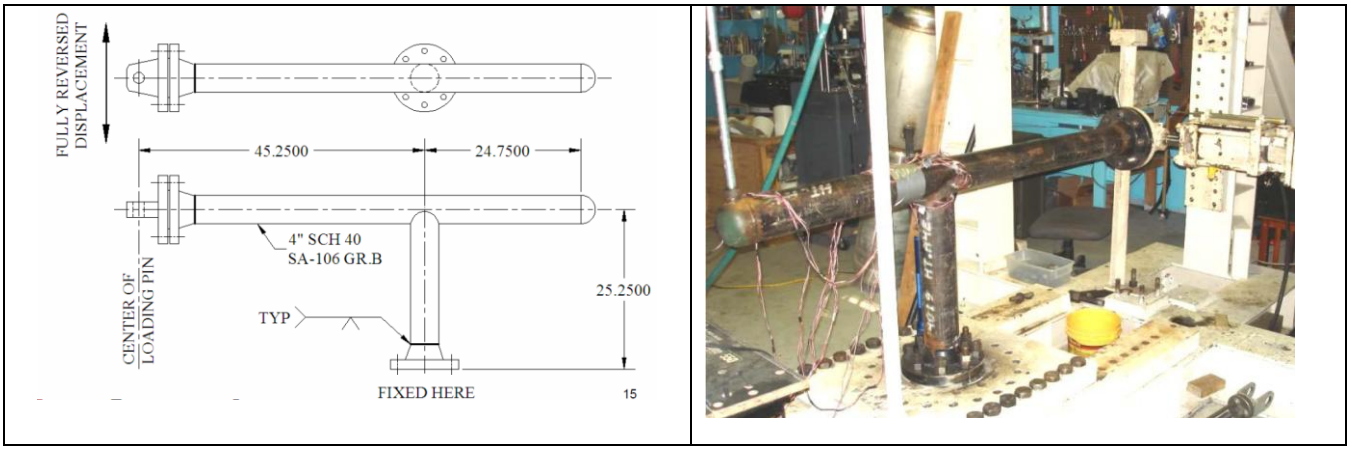

Figure 4

Markl's original work was based on the following equation (in PSI)

i. $S_f = 490000N^{(-0.2)}$ (5)

Where i = SIF, S_f = Stress range to failure, N = no. of cycles to failure

3.2 ASME B31 code equations for SIF [5][9]

Considering the example of bend under moment, the ovalization of pipe generates bending on the pipe wall which creates a high circumferential bending stress on the pipe wall. Since the pipe is oval at the bend and not circular, there cannot be direct comparison with non-ovalized bend. Hence the binding stress at bend is compared with the circular cross section of pipe.

The theoretical SIF's for circumferential stresses are [6]

$i_{ci} = 1.8 / h^{2/3}$ for in-plane bending (6)

$i_{co} = 1.5 / h^{2/3}$ for out-plane bending (7)

Markl and others observed that the theoretical SIF's are consistent with the test data. But the test performed on commercial pipe implied theoretical SIF of 2.0 against polished pipe which is mainly due to three factors – girth welds (welded or grinded), clamping - supporting effects and defects, surface roughness. Hence, in attempt of simplifying the analysis the SIF of commercial girth weld had been considered as unity modifying equations of SIFs in B31 codes as-

$i_i = 0.9 / h^{2/3}$ for in-plane bending (8)

$i_o = 0.75 / h^{2/3}$ for out-plane bending (9)

Table-1 below provides a part of Appendix D of ASME B31.3 indicating h, k and SIF values for different fittings.

Table-1

Description	Flexibility Factor, k	Stress Intensification Factor [Notes (2), (3)] Out-of-Plane, i_o	Stress Intensification Factor [Notes (2), (3)] In-Plane, i_i	Flexibility Characteristic, h	Sketch
Welding elbow or pipe bend [Notes (2), (4)-(7)]	$\frac{1.65}{h}$	$\frac{0.75}{h^{2/3}}$	$\frac{0.9}{h^{2/3}}$	$\frac{TR_1}{r_2^2}$	T, r_2, R_1 = bend radius

Description	Flexibility Factor, k	Stress Intensification Factor [Notes (2), (3)] Out-of-Plane, i_o	Stress Intensification Factor [Notes (2), (3)] In-Plane, i_i	Flexibility Characteristic, h	Sketch
Unreinforced fabricated tee [Notes (2), (4), (9), (11)]	1	$\frac{0.9}{h^{2/3}}$	$\frac{3}{4}i_o + \frac{1}{4}$	$\frac{T}{r_2}$	r_2, T

3.3 SIF calculation example

Based on different types of fittings ASME B31 code provides empirical formulae to calculate h, k and SIFs. Consider an Unreinforced fabricated Tee junction having following data-

Header outside diameter: Dh = 12.75”
Header nominal thickness: $\overline{T}$ = 0.375”
Branch outside diameter: Db = 10.625”
Branch nominal thickness: t = 0.365”
Mean radius of header: r_2 = 6.1875”

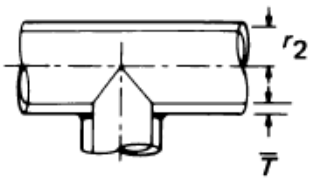

Figure 5

Flexibility characteristics: $h = \overline{T} / r_2 = 0.375 / 6.1875 = 0.06$
Flexibility factor: k = 1 (as per ASME B31, Appendix D)
Out-plane SIF: $i_o = 0.9 / h^{2/3} = 0.9 / 0.06^{2/3} = 0.9 / 0.154 = 5.83$ (as per ASME B31, Appendix D)
Out-plane SIF: $i_o = 0.9 / h^{2/3} = 0.9 / 0.06^{2/3} = 0.9 / 0.154 = 5.83$ (10

(10)
In-plane SIF: $i_i = 0.75 * i_o + 1/4 = 0.75 * 5.83 + 0.25 = 4.62$ (11)

The above results have compared with CAESAR II® [7] output and found consistent.

NODE	Axial Stress lb./sq.in.	Bending Stress lb./sq.in.	Torsion Stress lb./sq.in.	Hoop Stress lb./sq.in.	Max Stress Intensity lb./sq.in.	SIF In Plane	SIF Out Plane	Code Stress lb./sq.in.	Allowable Stress lb./sq.in.	Ratio %	Piping Code
20	-119.7	1005.1	0.0	0.0	1124.7	1.000	1.000	1005.1	49125.6	2.0	B31.3
30	-119.7	10716.9	0.0	0.0	10836.5	4.625	5.833	10716.9	45002.4	23.8	B31.3
30	0.0	0.0	0.0	0.0	0.0	4.625	5.833	0.0	42169.6	0.0	B31.3
40	0.0	0.0	0.0	0.0	0.0	1.000	1.000	0.0	49054.8	0.0	B31.3

IV. VALIDATING B31 SIF EQUATIONS AGAINST FEA ANALYSIS

Besides other observations on B31 SIF equation, authors have concentrated on one important observation that the SIF value of any fitting or elbow is irrespective of the branch properties i.e. branch diameter and branch thickness. Authors selected the unreinforced fabricated tee junction, similar to one of the Markl’s experiment as shown in Figure 4 to find out effect of various header and branch properties on SIF. Number of FEA models were analyzed changing one variable at a time out of four variables affecting SIF viz. Header outside diameter, header thickness, branch outside diameter and branch thickness

Table-2: Experiment summary

Factors	EXP-1	EXP-2	EXP-3	EXP-4
Header diameter	C	C	C	V
Header thickness	C	C	V	C
Branch diameter	C	V	C	C
Branch thickness	V	C	C	C

V = varying parameter, C = parameter kept constant

4.1 FEA Model

Ansys [8] software used to simulate experiment set up shown in Fig. 6. To achieve the surface geometry at the junction, a 2D element ‘shell 63’ with real constant as pipe thickness has been used. The boundary conditions are as shown in Figure 4. A force applied at flange end and the stresses were checked at the Unreinforced Tee junction. These stresses were compared against pipe with circular cross section to get SIF.

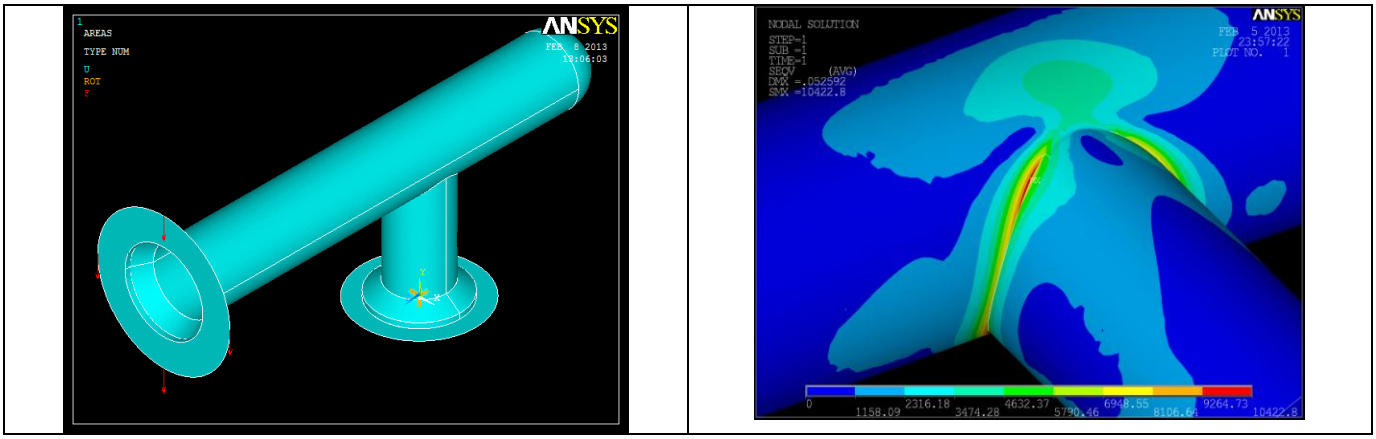

Figure 6

4.2 Results based on ASME B31 equations

The results based on B31 equations were obtained using CAESAR II analysis and that based on FEA analysis were obtained using ANSYS. Both the results have been graphically plotted in Fig.7 below.

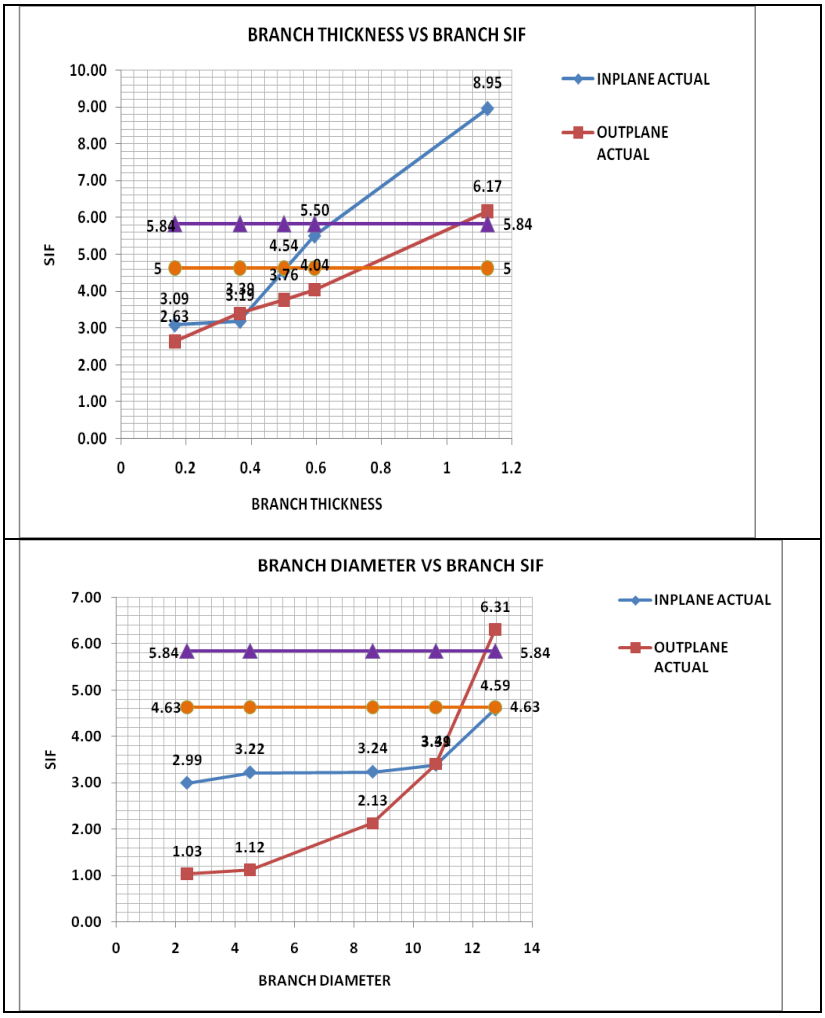

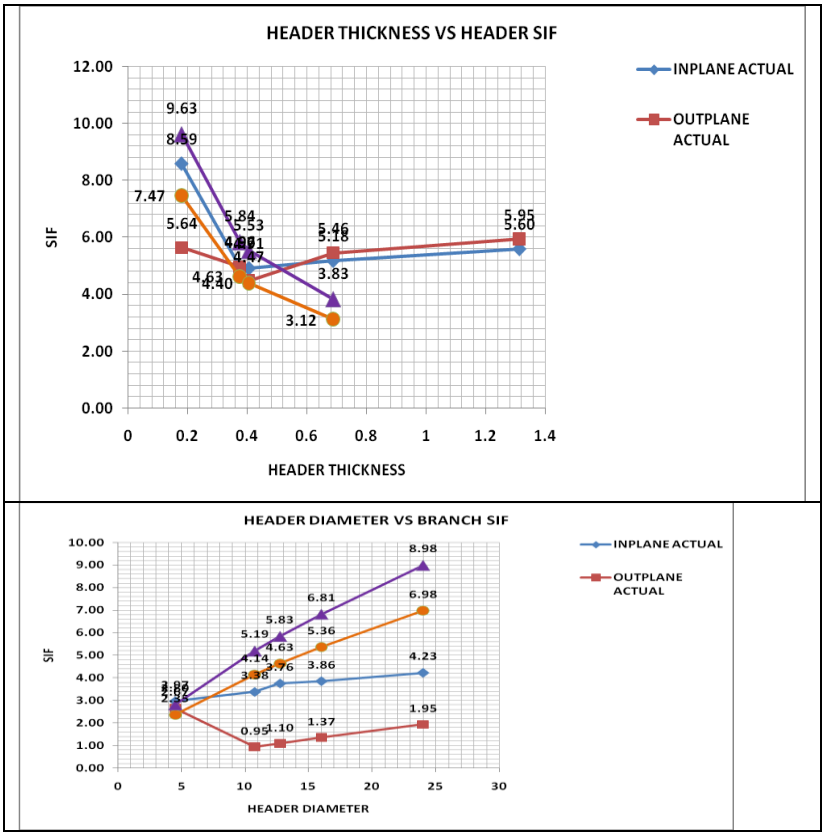

The observations based on B31 equations and that of FEA analysis are listed below-

1. B31 SIFs (In-plane & Out-plane) remain constant irrespective of branch thickness. FE analysis indicates branch In-plane and Out-plane SIF increases as branch thickness increases but the values are less compared to B31 equation. However, header SIFs decreases.
2. B31 SIFs remain constant irrespective of branch diameter. FE analysis indicates as branch diameter decreases header SIFs increase but branch SIFs decrease.
3. B31 SIF decreases as header thickness increases. FEA analysis indicates as header thickness increases the header in-plane SIF decreases, header out-plane SIF initially decreases and then increases, branch SIFs decreases.
4. B31 SIF decreases as header diameter decreases. FE analysis indicates that as header diameter decreases header SIFs decrease and branch in-plane SIF decreases, out-plane SIF initially decreases and then shows increasing trend.

These observations indicate that B31 code provides same SIF value for header and branch. However FE analysis provides different SIFs for branch and header. Even though in general B31 equations provide conservative values of SIF compared to FEA; at few occasion FE analysis provides higher SIF's. Hence, in case of critical systems in depth study is required before adapting any SIF value.

Additional points to be noted about SIF

a) The values of SIF for the same component can be different in different codes.
b) Different edition of same code can provide different value of SIF for the same component.
c) The multiplication fraction to be applied for SIF of same fitting can be different in different code.

References

[1] American Society of Mechanical Engineers, ASME B31.3 code for Pressure Piping. Edition 2010.
[2] Markl A.R.C. and George, H.H., 1950,"Fatigue Tests on Flanged assemblies," transactions of the ASME, 72(1), pp. 77-87.
[3] Diehl, David., "The Bend Flexibility Factor", COADE Mechanical Engineering News, October 2002.
[4] Hinnant, Chris., Paulin, Tony.,Paulin Research Group, "Experimental Evaluation of the Markl Fatigue Methods and ASME Piping Stress Intensification Factors", 2008 ASME PVP Conference, Chicago, IL, July 28, 2008
[5] Peng, L.C., Peng, T., Peng Engineering, Houston, Texas, USA, "Pipe Stress Engineering", ASME.
[6] M.W. Kellogs Company, 1956, "Design of Piping Systems, revised 2nd ed., John Wiley & Sons, New York.
[7] Intergraph CAESAR II® is a comprehensive and standard program for Pipe Stress Analysis used worldwide .
[8] ANSYS version 14, world recognized FEA based software.
[9] Bhattacharya, Anindya., Long, Daniel., "A Finite Element based Investigation of Stress Intensification and Flexibility Factors for Pipe Bends within and outside the Limitations of ASME B31 Piping Codes."

International Journal of Modern Engineering Research (IJMER)
www.ijmer.com Vol.3, Issue.3, May-June. 2013 pp-1330-1335 ISSN: 2249-6645

Optimisation of Weld Bead Parameters of Nickel Based Overlay Deposited By Plasma Transferred Arc Surfacing

Er. Bhaskarananda Dasgupta, [1] Dr. Sudip Mukherjee[2]
[1]Assistant Professor, Department Of Mechanical Engineering Siliguri Instiotute of Technology, Siliguri, West Bengal India
[2]Professor, Department Of Mechanical Engineering, Jalpaiguri Government Engineering College, Jalpaiguri, West Bengal, India

Abstract: *Plasma Transferred Arc surfacing is a kind of Plasma Transferred Arc Welding process..Plasma Transferred Arc surfacing (PTA) is increasingly used in applications where enhancement of wear, corrosion and heat resistance of materials surface is required. The shape of weld bead geometry affected by the PTA Welding process parameters is an indication of the quality of the weld. In this paper the analysis and optimization of weld bead parameters, during deposition of a Nickel based alloy Colmonoy on stainless steel plate by plasma transferred arc surfacing, are made and values of process parameters to produce optimal weld bead geometry are estimated. The experiments are conducted based on a five input process parameters and mathematical models are developed using multiple regression technique. The direct effects of input process parameters on weld bead geometry are discussed using graphs. Finally, optimization of the weld bead parameters, that is minimization of penetration and maximization of reinforcement and weld bead width, are made with a view to economize the input process parameters to achieve the desirable welding joint.*

Keywords: *PTA welding; Overlay; Stainless steel 316L; Colmonoy; Penetration; Reinforcement; Regression analysis; Mathematical model; Optimization*

I. Introduction

Weld deposition of hard facing alloys is commonly employed to enhance the tribological life of Engineering components subjected to hostile environments. There clamation of worn-out metal parts is demanded worldwide and for this demand PTA hard facing of hard, wear resistant thin surface layer of metals and alloys on suitable substrates is one of the proven surfacing techniques(7).In the recent years, PTA Surfacing is extensive used in applications such as valve industries, Hydraulic machineries, Mining industries, Earthmoving equipment, Chemical, Nuclear and Thermal power plants etc.PTA process can be considered as an advanced Gas Tungsten Arc welding process more widely used for overlay applications. The metal and alloy powder is carried from the powder feeder to the central electrode holder in the arc-gas stream. From the electrode holder the powder is directed to the constricted arc zone, where it is melted and fusion bonded to the base metal. Thus, smooth, thin deposits of overlays can be made through this way of precise control of feed stock by PTA welding process. Colmonoy5, a Nickel based alloy (Ni-Cr-B-Si-C) provides excellent resistance to abrasive and adhesive wear with resistance to corrosion and high temperature oxidation. It is widely applied in Thermal power plants, Chemical industries, Nuclear reactors, food processing industries etc. In nuclear reactors, use of Co based satellite alloys lead to induced activity which will harm the personnel involved in the maintenance of reactor components. Colmonoy5 is a good alternative to the Co based alloys used (9, 15) in nuclear applications, fabricated wearers instant bushes are made of hard facing alloys for high temperature applications. They report that there is a growing tendency to replace Co based alloys by Nickel based alloys, due to the high cost and scarcity of cobalt based alloys. The problem of cracking susceptibility of nickel based Colmonoy alloy hard faced deposits can be controlled by using preheating and slow cooling during deposition. Compared to other welding processes PTA surfacing requires less quantity of material to be deposited with improved mechanical and metallurgical properties.

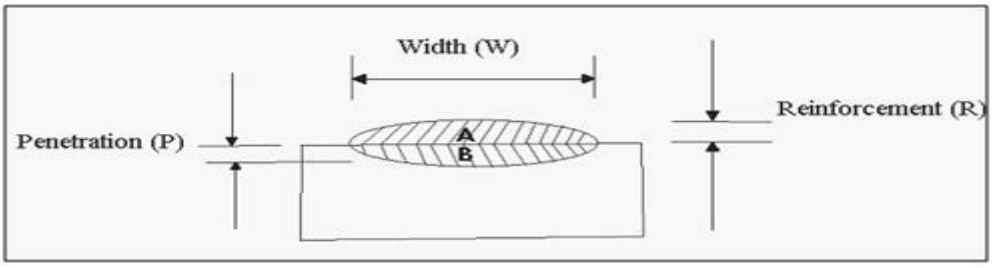

Figure 1: Weld bead geometry

The shape of the weld bead geometry is affected by the values of PTA process parameters used in deposition. These process parameters should be well established and categorized to enable automation and robotisation of PTA surfacing. Therefore it is imperative to develop mathematical models to predict the bead geometry and study the direct effects of various PTA process parameters on the weld bead shapes. The selection of welding procedure must be more specific to ensure that adequate bead quality is obtained(8).Further a complete control over the process parameters is essential to

produce quality welds with required bead geometry based on which the integrity of the weldment is known. It has been reported by researchers that in PTA surfacing, process quality can be represented by bead shape (11). Thus the weld pool geometry plays an important role in deter mining the mechanical and corrosion properties of the weld. Therefore, process parameters for obtaining optimal weldpool geometry. It is reported that five level factorial techniques can be employed for developing models to predict weld bead geometry(1,5,6,12,13).In this work, automatic PTA hard facing is carried out for depositing Colmonoy5 over Stainless steel 316L plates of size 150mmx90mmx30mm.The experiments are based on the central composite rotatable design matrix. Regression analysis was used to develop the model. Also, the main objective of this study is to optimize the weld bead parameters that is achieving minimum penetration, maximum reinforcement and maximum bead width which gives best weld joint and determining the corresponding process parameters. Penetration means the depth into substrate through which the filler metal penetrates. Reinforcement means height of filler metal on substrate. Weld width means the width of filler metal on substrate.

II. The Work To Be Carried Out Was Planned In The Following Order

1. Identification of important process parameters
2. Finding the upper and lower limits with different levels of the identified process parameters
3. Development of Design matrix.
4. Conducting experiments as per the design matrix
5. Recording the responses
6. Calculation of regression coefficients and development of mathematical model
7. Development of final mathematical model
8. Presenting the relation of process variables on bead geometry in graphical form.
9. Results and discussions.
10. Optimization of weld bead parameter.

Identification of Process parameters- The independently controllable process parameters identified based on their significant effect on weld bead geometry to carry out the experimental work are welding current(A),Oscillation width(O),Travel speed(S),Preheat temperature(T) and Powder feed rate(F) gas flow rate and Torch standoff distance. Welding current produce heat for fusion, Pre heat temperature and oscillation width (17) which may affect crack formation during hard facing, have to be properly controlled. Minimum torch travel speed gives better deposition of filler material on welding joints. In deposition of material the most effective process parameters are Welding current, Oscillation width, Travel speed, Preheat temperature and Powder feed rate, thus these process parameters are selected in the experiment and the Gas flow rate and Torch standoff distance are kept at constant levels.

Limits and Levels of Process Parameters- It has been observed from different experiments that best deposition of nickel on steel plate occurs when the process parameters vary between the levels given in table 1.The working ranges of all selected parameters are fixed by conducting trial runs. This are carried out by varying one parameter while keeping the rest of them at constant values. The working range of each process parameter is decided upon by inspecting the bead for a smooth appearance without any visible defects. The upper limit of a factor is coded as +2, in between levels is -1, 0,1and the lower limit is coded as-2. The chosen levels of the process parameters and notations are given in Table1.

Table 1: Levels of Process Variable

PARAMETER	UNITS	NOTATIONS	Factor Levels				
			-2	-1	0	1	2
Welding current	Amps	A	120	130	140	150	160
Oscillation width	mm	O	10	12	14	16	18
Travel speed	mm min^{-1}	S	79	86	93	100	107
Preheat Temp.	^{o}C	T	200	250	300	350	400
Powder Feed Rate	gm min^{-1}	F	36	38	40	42	44

Development of design matrix- The design matrix is developed according to the combinations normally taken in Genetic Algorithm process for five process parameters. The design matrix chosen to conduct the experiment is a central composite rotatable design. It consists of 32sets of coded conditions and comprising a half replication of 2^4=16 factorial design with 6centre points and 10 star points .All the welding parameters at the middle level (0) constitute centre points whereas the combination of each welding parameter at its lower value (-2) or higher value (2) with the other four parameters at the middle levels constitute the star points (2, 10, 14). Thus the 32 experimental runs allowed the estimation of linear, quadratic and two-way interactive effects of the process parameters on the weld bead geometry.

Experimental setup and procedure- The experiments are conducted by using a PTA welding machine, fabricated by National Automation Calcutta. Experiments are conducted by company and corresponding data are taken from their experiments. The PTA system has six modules namely traverse carriage unit, oscillator unit, powder feed unit, water-cooling unit, turntable unit and torch unit. All the units are supporting the effective functioning of the total PTA system. The experiments are conducted according to the design matrix at random to avoid systematic errors creeping into the system. Colmonoy 5 is deposited over stainless steel 316L plates 15cm x 9 cm.x3cm..Torch standoff distance, oscillating frequency, plasma/central gas flow rate, shielding gas flow rate and powder/carrier gas flow rate are kept constant respectively at10mm, 72cycles per minute, 3.5lpm, 12 lpm and 1.5 lpm while hard facing.

Experimental observation- The hard faced plates were cross sectioned at their midpoints to get the test samples. Those samples are prepared by the usual metallographic polishing methods and etched with aquaregia solution for carrying out weld bead geometry measurements. The profiles of the weld beads and the bead dimensions i.e. Penetration (**P)**, reinforcement (R) and weld width (**W)** are measured. The observed values of P, R and W are given in Table: 2.

Table 2: Design Matrix and Observed Values Of Weld Bead Dimensions

	Design matrix					weld bead dimensions		
S No	A	O	S	T	F	P mm	R mm	W mm
1	-1	-1	-1	-1	1	1.5	3.7	20
2	1	-1	-1	-1	-1	1.6	3.2	20.2
3	-1	1	-1	-1	-1	1.5	2.92	20.5
4	1	1	-1	-1	1	1.52	3.25	22.76
5	-1	-1	1	-1	-1	1.17	3.370	17.66
6	1	-1	1	-1	1	0.5	3.3	19
7	-1	1	1	-1	1	0.72	2.8	20.7
8	1	1	1	-1	-1	1.62	2.8	21.6
9	-1	-1	-1	1	-1	0.7	3.4	17.3
10	1	-1	-1	1	1	1.62	3.6	19.8
11	-1	1	-1	1	-1	0.52	3.1	19.9
12	1	1	-1	1	1	1	3.20	20.85
13	-1	-1	1	1	1	0.52	3.5	17
14	1	-1	1	1	-1	1.42	3.1	18
15	-1	1	1	1	-1	0.8	3.1	18.9
16	1	1	1	1	1	1.1	3.4	21.2
17	-2	0	0	0	0	0.275	3.475	18
18	2	0	0	0	0	1.65	3.3	21.3
19	0	-2	0	0	0	1.1	3.85	17.9
20	0	2	0	0	0	0.9	3.2	21.4
21	0	0	-2	0	0	0.75	3.65	20
22	0	0	2	0	0	0.75	3.15	19.5
23	0	0	0	-2	0	1.1	3.35	18.7
24	0	0	0	2	0	1.5	3.22	19.55
25	0	0	0	0	-2	0.87	3.52	19.5
26	0	0	0	0	2	0.7	3.55	19
27	0	0	0	0	0	0.95	3.55	19.4
28	0	0	0	0	0	0.95	3.5	18.5
29	0	0	0	0	0	1.2	3.55	19.2
30	0	0	0	0	0	0.9	3.4	18.6
31	0	0	0	0	0	0.9	3.6	19.4
32	0	0	0	0	0	1	3.35	18.6

III. Development Of Mathematical Models

The response function representing any of the weld bead dimensions like penetration ,reinforcement etc, can be expressed as Y=f(A,O,S,T,F),Where Y is the response or yield .The second order polynomial (regression equation) use to represent the response surface for k factors are given by:

$$Y= b_0+\sum_{i=1}^{k} b_i x_i+ \sum_{\substack{i=1 \\ i\neq j}}^{k} b_{ii} x_i^{\,2} + \sum_{ij=1}^{k} b_{ij}\, x_i x_j \quad \ldots\ldots\ldots\ldots\ldots\ldots\ldots\ldots (1)$$

The selected polynomial for five factors can be expressed:

$$Y=b_0+b_1A+b_2O+b_3S+b_4T+b_5F+b_{11}A^2+b_{22}O^2+b_{33}S^2+b_{44}T^2+b_{55}F^2+b_{12}AO+b_{13}AS+b_{14}AT+b_{15}AF+b_{23}OS+ b_{24}OT+b_{25}OF +b_{34}ST+b_{35}SF +b_{45}TF \quad \ldots(2)$$

Where b_0 is free term of the regression equation, the coefficients b_1, b_2, b_3, b_4, and b_5 are linear terms, the coefficients b_{11}, b_{22}, b_{33}, b_{44}, and b_{55} are quadratic terms, and the coefficients b_{12}, b_{13}, b_{14}, b_{15}, b_{23}, b_{24}, b_{25}, b_{34}, b_{35} and b_{45} are interaction terms.

Development of final mathematical model:

The co-efficient of the polynomials has been found by using MATLAB.Software.

The final mathematical models determined by the regression analysis are as follows:

$$P=0.95063+0.252A-0.038O-0.107S-0.063T-0.134F+0.027A^2+0.0368O^2-0.025S^2+0.111T^2-0.016F^2+0.072AO-0.028AS+0.159AT-0.027AF +0.110OS-0.091OT-0.064OF+0.122ST+0.092SF+0.023TF \quad \ldots. (3)$$

$$R=3.514-0.003A-0.179O-0.074S+0.020T+0.048F-0.049A^2-0.014O^2-0.045S^2-0.074T^2-0.012F^2+0.089AO-0.026AS+0.036AT+0.051AF+0.053OS+0.043OT-0.059OF+0.043ST-0.0029SF-0.037TF \ldots\ldots\ldots\ldots (4)$$

$$W=18.96+0.856A+1.11O-0.346S-0.220T+0.093F+0.164A^2+0.164O^2+0.189S^2+0.033T^2+0.064F^2+0.253AO-0.303AS+0.284AT-0.088AF+0.212OS-0.080OT-0.171OF+0.105ST+0.1714SF-0.165TF \ldots (5)$$

IV. Result And Discussion

The developed mathematical models can be used to predict the dimensions of the weld bead. Based on these models, the effects of process parameters on bead dimensions are computed and plotted by varying one parameter and keeping others at middle value. It is also possible to substitute the values for bead dimensions and get the corresponding values of PTA process parameters in coded form.

Discussion

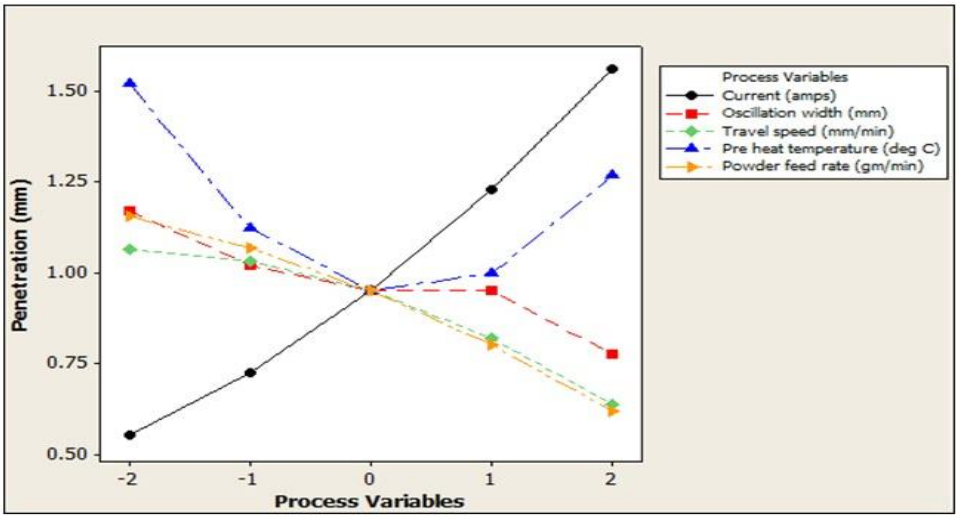

Figure 2: Direct effect of process variables on penetration

Direct effects of Process variables on Penetration

Figure2 shows that Penetration (P) increases significantly when welding current increases. This is attributed to the fact that heat input to the base metal increases when current is increased. Penetration decreases as Oscillation width increases. This is due to spreading of heat resulting from more melting of base metal. Penetration decreases steadily with the increase of Travel speed as less amount of powder is deposited per unit length of bead. Penetration decreases to a lower value when pre heat temperature increases but afterwards penetration increases with further increase of preheat temperature. This may be for the reasons that at lower preheat temperature the heat received from plasma arc will not spread in the stainless steel substrate due to lower thermal conductivity resulting in cushioning of arc. Penetration decreases with increase of Powder feed rate.

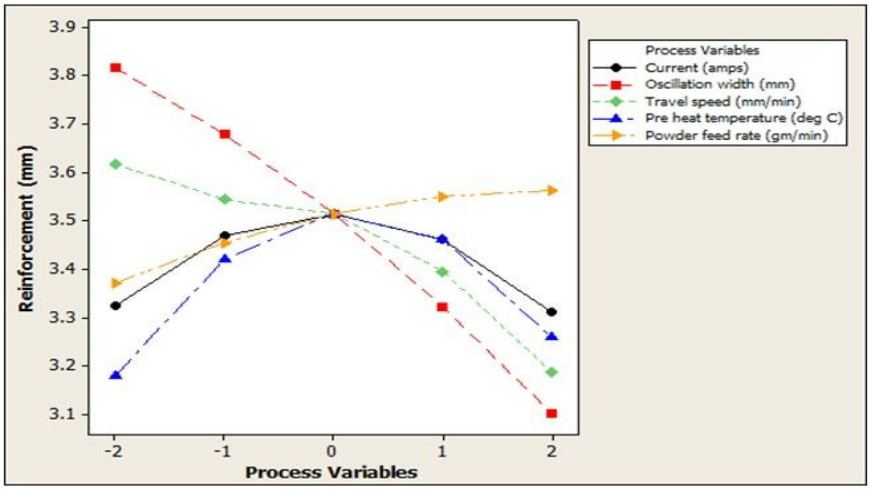

Figure 3: Direct effect of process variables on reinforcement

Direct effect of Process variables on Reinforcement

It is evident from Fig 3 that Reinforcement (R) increases initially and then decreases with increase of welding current. Reinforcement decreases with increase in oscillation width. This could possibly due to the fact that the deposited metal gets distributed along the width resulting in decreasing in reinforcement. Reinforcement decreases steadily from highest value with the increase of travel speed. This is due to reduce amount of powder deposit per unit length of bead. Reinforcement increases with increase of preheat temperature to its peak value then decreases with further increase of preheat temperature. Reinforcement increases steadily with increase of powder feed rate as more powder is deposited per unit length of weld bead.

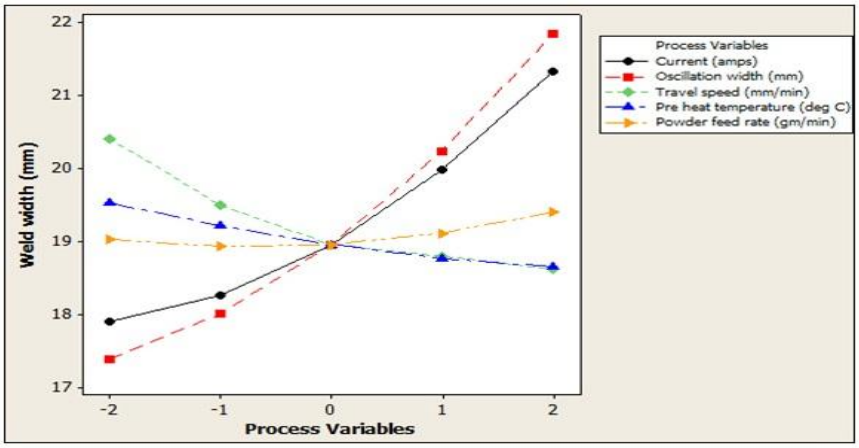

Figure 4: Direct effect of process variables on weld with

Direct effects of Process variables on Weld width

Figure 4 show that Weld width increases with increase of welding current .This is due to spreading of heat resulting of melting of more metal. Weld width increases steadily with increase in oscillation width due to decrease of Penetration. Weld bead decreases with increase of torch travel speed .This may be for reduced heat input per unit length of weld bead when travel speed is increased. Weld bead width reduces as the Preheat temperature increases. Weld width decreases initially but increases with increase of powder feed rate.

A better weld should have bead parameters as follows
1. Penetration should be minimum
2. Reinforcement should be maximum
3. Weld width should be maximum

The bead parameters are found independently considering their equations obtain from mathematical modeling as objective function. The best weld bead parameters are found by analyzing the graph between weld bead parameters and process parameters .The best weld bead parameters and the corresponding process parameters are as follow

a) Minimization of depth of penetration-

A(amps)	O(mm)	S(mm/min)	T(◦c)	F(gm./min)
120 (-2)	18 (2)	107(2)	300(0)	44(2)

Predicted minimum penetration = 0.463mm

b) **Maximization of height of reinforcement-**

A(amps)	O(mm)	S(mm/min)	T(◦c)	F(gm/min)
140 (0)	10 (-2)	79 (-2)	300(0)	44(2)

Predicted maximum reinforcement =4.29mm

c) Maximization of weld width-

A (amps)	O(mm)	S(mm/min)	T(◦c)	F (gm/min)
160 (2)	18 (2)	79 (-2)	250(-2)	44 (2)

Predicted maximum weld width =26.58mm

Hence the best of bead parameters for different sets of process variable is as follows
1. Penetration=0.463mm
2. Reinforcement = 4.29mm
3. Weld width = 26.58mm

V. Optimization

It is very difficult for an operator to perform the welding process to get best bead parameters using different sets of process variable. Hence it is necessary to find a single set of process variable which will provide the optimal bead parameters and are very close to the best bead parameters find with different sets of process variable.

Here optimization of the bead parameters is done by considering the three sets of process variable obtained for best bead parameters as mentioned above.

All possible combinations of process variables are carried by using MATLAB software and the corresponding bead parameters are recorded, neglecting negative ones.

It can be seen that there are 24 sets of valid process variables giving as many sets of bead parameters. It is found from results that optimum set of bead parameter is as follows

The process variables and corresponding optimum bead parameters are given below.

Table 3: Optimized values of bead parameters and corresponding process variables

A (amp)	O(mm)	S(mm/min)	T(°C)	F (gm./min)	P(mm)	R(mm)	W(mm)
160(2)	18(2)	79(-2)	300(0)	44(2)	0.640	3.1358	25.768

Condition for better welding joint

1. Higher amperage produces higher welding temperature which interns produces better fusion of metal. Better fusion produces better weld
2. More oscillation width produces more weld width.
3. Less travel speed of torch produces better reinforcement.
4. Medium pre heat temperature reduces the chance of cracking.
5. More powder feed rate produces more reinforcement.

According to the theory the best combination of process variables for optimum bead parameters should be as follows

Table 4: Combination of process variables for optimum bead parameters

A(amps)	O(mm)	S(mm/min)	T (◦c)	F(gm/min)
160(2)	18(2)	79(-2)	300(0)	44(2)

Accordingly the predicted bead parameters for this set are as follows
Penetration is 0.640 mm,
Reinforcement is 3.1358mm
Weld bead is25.768 mm

This is exactly the same set of bead parameters obtain by the optimization process. Hence it can be said that the optimization process is justifying the theory.

Comparison of the bead parameter received from different sets and single set of process variable.

Result obtain for best bead parameters for different sets of process variables			Result obtain for optimum bead parameters using single set of process variables		
Penetration	Reinforcement	Weld width	Penetration	Reinforcement	Weld width
0.463mm	4.29mm	26.58mm	0.640mm	3.135mm	25.768mm

Bibliography

[1] T.T.Allen, R.W.Richardson, D.P.Tagliable, G.P. Maul, Statistical processdesignforrobotic GMAweldingofsheet metal, Welding Journal 81/5(2002)69-172.
[2] W.G. Cochran, G.M. Cox, Experimental Designs, John Willy & sons Singapore 1957
[3] C.R. Das, S.K. Albert, A.K., Bhaduri, G. Kempulraj, A novel procedure for fabrication of wearresistantbushes for high temperature application, Journal of Materials Processing Technology141(2003)60-66.
[4] H. Eschnauer, Hard material powders and hard alloy powders for plasmas face coating, Thin Solid Films73 1980 pp 1-17.
[5] B. Howard, Surfacing for wear resistance, Stephen Helbaet al. (eds.), Modern Welding Technology, Prentice HallInc., New Jersey, 2022pp 721-726
[6] I.S.Kim, J.S.Son, Y.J.Jeung, Control and Optimisation of bead widthformulti-passwelding inroboticarcwelding processes, Australian Welding Journal 46 (2001)43-46
[7] R.Kaul,P.Ganesh,S.K.Albert,A.Jaishwal,N.P.Lalla,A. Gupta C.P.Pal ,A.K.NathLasercladdingof austenitic stainless steel with nickel base hard facing alloy, Surface Engineering19 (2003)pp269-273.
[8] K.Marimuthu, N.Murugan Prediction and optimization of weld bead geometry of Plasma transferred arc hard faced valve seat rings, Surface Engineering19/2(2003) 143-149.
[9] J.C.Mc.Glone, Weldbeadgeometryprediction –areview, Metal Construction14 (1982)378-384.
[10] D.C. Montgomery, Designand analysis of experiments, John Wiley&SonsInc., New York, 2001.
[11] P.K. Palani, N. Murugan, Optimizationofweld bead geometry of stainless steel cladding by flux Cored arc welding using Excel Solver, IWS Journal 2 (2005)15-19.
[12] A. Scotti, L.Alves, Albuquerque Rosa, Influence of oscillation parameter soncrack for mationin automaticFe-B hard facing, Journal of Materials Processing Technology 65 (1997)272-280.
[13] K.Y.Benyounis and A.G.OlbiOptimization of PTA welding process using Statistical and Numerical approach. (2005)
[14] Marimuthu and Murugan Effects of Plasma Transferred Arc Welding parameters on welding bead geometry, in computational materials science and surface engineering vol. 8 pp 51-88 (2006)
[15] Keung –Hueng Teseng et.al.Optimization of PTAW parameters. Journal of manufacturing science and production vol.10 pp 155-188 (2008)
[16] Siva, K.Murugan and Raghupathy Modelling, analysis and optimization of weld bead parameters of PTAW, computional materials science and surface engineering vol.1 pp 174-182 (2009)
[17] R .Logesh, K.Siva, N.Murugan, Optimization of weld bead geometry in PTAW hard faced on austenitic stainless steel plate using genetic algorithm. International journal of advanced manufacturing technology vol.41 pp 24-30

International Journal of Modern Engineering Research (IJMER)
www.ijmer.com Vol.3, Issue.3, May-June. 2013 pp-1336-1338 ISSN: 2249-6645

Common fixed point theorems in intuitionistic fuzzy metric space

Shams-ur-rahman, [1] Bhadra Man Tuladhar, [2] Ismat Beg[3]
[12]*Department of Natural Sciences, Kathmandu University, Nepal*
[3]*Department of Mathematics, Lahore University of Management Studies, Pakistan*

Abstract: *In this paper, we give the Mizoguchi-Takahashi's theorems into intuitionistic fuzzy metric space.*

Keywords: *Common fixed point, Fuzzy metric space, Intuitionistic fuzzy metric space.*

I. Introduction

The notion of fuzzy sets was introduced by A. Zadeh [11] in 1965. George and Veeramani [5] introduced the fuzzy metric space. Mihet [7] obtained some new results of modifying the notion of convergences in fuzzy metric space. Park [9] used the idea of intuitionistic fuzzy sets with the help of t-norm and t-conorm as a generalization of fuzzy metric space and introduced the notion of Cauchy sequences in an intuitionistic fuzzy metric space and also proved the Baire's theorem.

Alaca et al. [1] using the idea of intuitionistic fuzzy sets, defined the notion of intuitionistic fuzzy metric space similar to Park [9] with the help of continuous t-norms and continuous t-conorms as a generalization of fuzzy metric space due to Kramosil and Michalek [6]. Further, they introduced the notion of Cauchy sequences in intuitionistic fuzzy metric spaces and proved the well-known theorems of Banach [2] and Edelstein [3]. Many authors have studied the concept of intuitionistic fuzzy metric space and its applications [4, 10, 12, 13, 14].

The purpose of this paper, is to prove the Mizoguchi-Takahashi's [6] theorems in intuitionistic fuzzy metric space.

Definition 1.1: A binary operation $* : [0, 1] \times [0, 1] \to [0, 1]$ is continuous *t*-norm if * satisfy the following conditions:
(1) * is commutative and associative;
(2) * is continuous;
(3) $a * 1 = a$ for all $a \in [0, 1]$;
(4) $a * b \leq c * d$ whenever $a \leq c$ and $b \leq d$ for all $a, b, c, d \in [0, 1]$.

Definition 1.2: A binary operation $\lozenge : [0, 1] \times [0, 1] \to [0, 1]$ is continuous *t*-conorm if $\lozenge$ satisfy the following conditions:
(1) $\lozenge$ is commutative and associative;
(2) $\lozenge$ is continuous;
(3) $a \lozenge 0 = a$ for all $a \in [0, 1]$;
(4) $a \lozenge b \leq c \lozenge d$ whenever $a \leq c$ and $b \leq d$ for all $a, b, c, d \in [0, 1]$.

Definition 1.3: (Alaca et al.) [1] A 5-tuple $(X, M, N, *, \lozenge)$ is said to be an intuitionistic fuzzy metric space if X is an arbitrary set, * is a continuous *t*-norm, $\lozenge$ is a continuous *t*-conorm and M, N are fuzzy sets on $X^2 \times [0, \infty)$ satisfying the following conditions:
(1) $M(x, y, t) + N(x, y, t) \leq 1$ for all $x, y \in X$ and $t > 0$;
(2) $M(x, y, 0) = 0$ for all $x, y \in X$;
(3) $M(x, y, t) = 1$ for all $x, y \in X$ and $t > 0$ if and only if $x = y$;
(4) $M(x, y, t) = M(y, x, t)$ for all $x, y \in X$ and $t > 0$;
(5) $M(x, y, t) * M(y, z, s) \leq M(x, z, t + s)$ for all $x, y, z \in X$ and $s, t > 0$;
(6) for all $x, y \in X$ and $M(x, y, .) : [0, \infty) \to [0, 1]$ is left continuous;
(7) $\lim_{t\to\infty} M(x, y, t) = 1$ for all $x, y \in X$ and $t > 0$;
(8) $N(x, y, 0) = 1$ for all $x, y \in X$
(9) $N(x, y, t) = 0$ for all $x, y \in X$ and $t > 0$ if and only if $x = y$;
(10) $N(x, y, t) = N(y, x, t)$ for all $x, y \in X$ and $t > 0$;
(11) $N(x, y, t) \lozenge N(y, z, s) \geq N(x, z, t + s)$ for all $x, y, z \in X$ and $s, t > 0$;
(12) for all $x, y \in X$ and N(x, y, .) : $[0, \infty) \to [0, 1]$ is right continuous;
(13) $\lim_{t\to\infty} N(x, y, t) = 0$ for all $x, y \in X$

Then (M, N) is called an intuitionistic fuzzy metric space on X. The functions $M(x, y, t)$ and $N(x, y, t)$ denote the degree of nearness and the degree of non-nearness between x and y with respective to t, respectively.

Definition 1.4: Let $(X, M, N, *, \lozenge)$ be an intuitionistic fuzzy metric space, then

(a) a sequence $\{x_n\}$ in X is said to be Cauchy sequence if, for all $t > 0$ and $p > 0$ $\lim_{n\to\infty} M(x_{n+p}, x_n, t) = 1$ and $\lim_{n\to\infty} N(x_{n+p}, x_n, t) = 0$

(b) a sequence $\{x_n\}$ in X is said to be convergent sequence if, for all $t > 0$ and $p > 0$ $lim_{n\to\infty} M(x_n, x, t) = 1$ and $\lim_{n\to\infty} N(x_n, x, t) = 0$

(c) An intuitionistic fuzzy metric space $(X, M, N, *, \lozenge)$ is said to be complete if and only if every Cauchy sequence in X is convergent.

(d) An intuitionistic fuzzy metric space $(X, M, N, *, \lozenge)$ is said to be compact if every sequence in X contains a convergent subsequence.

Example 1.1: Let (X, d) be a metric space. Define t-norm $a * b = \min\{a, b\}$ and t-co-norm $a \lozenge b = \max\{a, b\}$ and for all $a, b \in X$ and $t > 0$.
Let us define $M(x, y, t) = t/(t + d(x, y))$ and $N(x, y, t) = d(x, y)/(t + d(x, y))$.
Then $(X, M, N, *, \lozenge)$ is an intuitionistic fuzzy metric space.

II. Main Results

In 1989, Mizoguchi and Takahashi [8] proved the following fixed point theorem.

Theorem2.1: **(Mizoguchi and Takahashi)** Let (X, d) be a complete metric space and T a map from X into $CB(X)$, where $CB(X)$ is the class of all nonempty closed bounded subsets of X. Assume that

$$H(Tx, Ty) \le \alpha(d(x, y))\, d(x, y)$$

For all $x, y \in X$, where α is a function from $[0,\infty)$ into $[0, 1)$ satisfying $\limsup_{s\to t+0} \alpha(s) < 1$ for all $t \in [0,\infty)$. Then there exists $z \in X$ such that $z \in Tz$.

In fact, Mizoguchi-Takahashi's fixed point theorem is a generalization of Nadler's fixed point theorem [13] which extended the Banach contraction principle to multivalued maps, but its primitive proof is different.

Then above theorem can be proved in an intuitionistic fuzzy metric space as follows.

Theorem 2.2: Let $(X, M, N, *, \lozenge)$ be a complete intuitionistic fuzzy metric space with continuous t-norm * and continuous t-conorm $\lozenge$ defined by $t * t \ge t$ and
$(1 - t) \lozenge (1 - t) \le (1 - t)$ for all $t \in [0, 1]$ and $T: X \to CB(X)$ is multivalued map and
$\varphi: [0, \infty) \to [0, 1)$ is continuous function. There exists $0 < k < 1$ such that for all $x, y \in X$
$M(Tx, Ty, kt) \ge M(x, y, t) * M(x, y, t)$ and $N(Tx, Ty, kt) \le N(x, y, t) \lozenge N(x, y, t)$, then T has fixed point in X.

Proof: Let $\{X_n\}$ be a sequence in X and $X_{m-1} = X_m$ for some m, T has a fixed point X_m. Suppose that $X_{n-1} \ne X_n$ then $M(x_n, \mathbf{x_{n+1}}, kt) = M(Tx_{n+1}, Tx_{n+2}, kt)$
$\ge M(x_{n+1}, x_{n+2}, t/k) * M(x_{n+1}, x_{n+2}, t/k) \ge M(x_{n+1}, x_{n+2}, t/k^2)$
and $N(x_{n+1}, x_{n+2}, kt) \le N(x_{n+1}, x_{n+2}, t/k^2)$
Hence for any positive integer p
$M(x_n, x_{n+p}, kt) \ge M(x_{n+1}, x_{n+2}, t/k) * \ldots$ p-times $\ldots * M(x_{p+1-n}, x_{p+2-n}, t/k^n)$
$N(x_n, x_{n+p}, kt) \le N(x_{n+1}, x_{n+2}, t/k) \lozenge \ldots$ p-times$\ldots \lozenge N(x_{p+1-n}, x_{p+2-n}, t/k^n)$
When $n \to \infty$ then $\lim_{n\to\infty} M(x_n, x_{n+1}, kt) \ge 1 * 1 * \ldots * 1 = 1$
and $\lim_{n\to\infty} N(x_n, x_{n+1}, kt) \le 0 \lozenge 0 \lozenge \ldots \lozenge 0 = 0$
It shows that $\{x_n\}$ is Cauchy sequence in X and so, by the completeness of X, $\{x_n\}$ converges to a point x, then $M(x_n, x, kt) \ge M(x_n, x, t/k^2)$
and $N(x_n, x, kt) \le N(x_n, x, t/k^2)$.
Let y be another fixed point in X and $x \ne y$ then
$M(x_n, y, kt) = M(Tx_n, Ty, kt) \ge M(x_n, y, t/k^2)$
and $N(x_n, y, kt) = N(Tx_n, Ty, kt) \le N(x_n, y, t/k^2)$ when $n \to \infty$ gives that $M(x_n, y, t/k^2) = 1$ and $N(x_n, y, t/k^2) = 0$ for all $t > 0$, therefore it shows that $x = y$ so x is the fixed point of T.

Theorem 2.3: Let $(X, M, N, *, \lozenge)$ be a compact intuitionistic fuzzy metric space with continuous t-norm * and continuous t-conorm $\lozenge$ defined by $t * t \ge t$ and
$(1 - t) \lozenge (1 - t) \le (1 - t)$ for all $t \in [0, 1]$ and $T: X \to CB(X)$ is multivalued map and
$\varphi: [0, \infty) \to [0, 1)$ is continuous function. There exists $0 < k < 1$ such that for all $x, y \in X$
$M(Tx, Ty, kt) \ge M(x, y, t) * M(x, y, t)$ and $N(Tx, Ty, kt) \le N(x, y, t) \lozenge N(x, y, t)$, then T has fixed point in X.

Proof: Let $\{X_n\}$ be a sequence in X and $X_{m-1} = X_m$ for some m, T has a fixed point X_m. Suppose that $X_{n-1} \ne X_n$ then $M(x_n, x_{n+1}, kt) = M(Tx_{n+1}, Tx_{n+2}, kt)$
$\ge M(x_{n+1}, x_{n+2}, t/k) * M(x_{n+1}, x_{n+2}, t/k) \ge M(x_{n+1}, x_{n+2}, t/k^2)$
and $N(x_{n+1}, x_{n+2}, kt) \le N(x_{n+1}, x_{n+2}, t/k^2)$
Hence for any positive integer p
$M(x_n, x_{n+p}, kt) \ge M(x_{n+1}, x_{n+2}, t/k) * \ldots$ p-times $\ldots * M(x_{p+1-n}, x_{p+2-n}, t/k^n)$

$N(x_n, x_{n+p}, kt) \leq N(x_{n+1}, x_{n+2}, t/k) \lozenge \ldots$ p-times $\ldots \lozenge N(x_{p+1-n}, x_{p+2-n}, t/k^n)$
When $n \to \infty$ then $\lim_{n\to\infty} M(x_n, x_{n+1}, kt) \geq 1 * 1 * \ldots * 1 = 1$
And $\lim_{n\to\infty} N(x_n, x_{n+1}, kt) \leq 0 \lozenge 0 \lozenge \ldots \lozenge 0 = 0$.
It shows that $\{x_n\}$ is Cauchy sequence in X, since X is compact so, $\{x_n\}$ has a convergent subsequence $\{x_{ni}\}$. Let $\lim_{i\to\infty} \{x_{ni}\} = y$. Now we assume that $y, Ty \notin \{x_n\}$. Since T is continuous for all x, y in X, then $\lim_{i\to\infty}(Tx_{ni}, Ty, t) \geq \lim_{i\to\infty} M(x_{ni}, y, t) = 1$ for each
$t > 0$, hence $\lim_{i\to\infty} Tx_{ni} = Ty$ similarly $\lim_{i\to\infty} T^2x_{ni} = T^2y$
(Now again assume that $Ty \neq Tx_{ni}$ for all i). Now we observe that
$M(x_{n1}, Tx_{n1}, t) < M(Tx_{n1}, T^2x_{n1}, t) < \ldots < M(Tx_{ni}, T^2x_{ni}, t) < \ldots < M(Tx_{ni+1}, T^2x_{ni+1}, t) < \ldots < 1$ for all $t > 0$. Thus $\{M(x_{ni}, Tx_{ni}, t)\}$ and $\{M(Tx_{ni}, T^2x_{ni}, t)\}$ are convergent sequences to a common limit, i.e. $M(y, Ty, t)$. It shows that $\{M(x_{ni}, Tx_{ni}, t)\} = \{M(Tx_{ni}, T^2x_{ni}, t)\}$ is contradiction. Hence $y = Ty$, is a common fixed point.

References:

[1] C. Alaca, D. Turkoglu, and C. Yildiz, Fixed points in intuitionistic fuzzy metric spaces, Chaos, Solitons and Fractals, 29 (2006), 1073–1078.
[2] S. Banach, Theorie les operations lineaires, Manograie Mathematyezne Warsaw Poland, 1932.
[3] M. Edelstein, On fixed and periodic points under contractive mappings, Journal of the London Mathematical Society, 37 (1962), 74–79
[4] V. Gregori, S. Romaguera, and P. Veeramani, A note on intuitionistic fuzzy metric spaces, Chaos, Solitons and Fractals 28 (2006), 902–905.
[5] A. George and P. Veeramani, on some results in fuzzy metric spaces, Fuzzy Sets and Systems, 64 (1994), no. 3, 395–399.
[6] I. Kramosil and J. Michálek, Fuzzy metric and Statistical metric spaces, Kybernetica (Prague), 11 (1975), no. 5, 336–344.
[7] D. Mihet¸, on fuzzy contractive mappings in fuzzy metric spaces, Fuzzy Sets and Systems, 158 (2007), 915–921.
[8] N. Mizoguchi and W. Takahashi, Fixed point theorems for multivalued mappings on complete metric spaces, J. Math. Anal. Appl. 141 (1989), 177–188.
[9] J. H. Park, Intuitionistic fuzzy metric spaces, Chaos, Solitons and Fractals, 22 (2004), no. 5, 1039–1046.
[10] R. Saadati and J. H. Park, on the intuitionistic fuzzy topological spaces, Chaos, Solitons and Fractals, 27 (2006), no. 2, 331–344.
[11] L. A. Zadeh, Fuzzy sets, Information and Control, 8 (1965), 338–353.
[12] T. K. Samanta and Sumit Mohinta, On Fixed-point theorems in Intuitionistic Fuzzy metric Space I, arXiv: 1103.2856v1 [math.GM]. 15 Mar 2011.
[13] Suziki, Tomonari, Mizoguchi-Takahashi's fixed point theorem is a real generalization of Nadler's, Journal of Mathematical Analysis and Applications, 340 (2008), 752-755.
[14] Wei-Shih Du, Some Generalizations of Mizoguchi-Takahashi's Fixed Point Theorem, Int. J. Contemp. Math Sciences, Vol 3, (2008), no 26, 1283-1288.

International Journal of Modern Engineering Research (IJMER)
www.ijmer.com Vol.3, Issue.3, May-June. 2013 pp-1339-1342 ISSN: 2249-6645

A Novel Method for Movie Character Identification and its Facial Expression Recognition

M. Dharmateja Purna, [1] N. Praveen[2]
[1]*M.Tech, Sri Sunflower College of Engineering & Technology, Lankapalli*
[2]*Asst. Professor, Dept. of ECE, Sri Sunflower College of Engineering & Technology, Lankapalli*

***Abstract*:** *Image processing is a method to convert an image into a digital form and perform some operations on it, in order to get an enhanced image or to extract some useful information from it. Face recognition is an important concept in image processing. The input of a face recognition system is always an image or video (movie). The output is an identification or verification of the subject or subjects that appear in the image or movie. Another important concept in image processing is facial expression recognition. Human facial expression recognition has attracted much attention in recent years because of its importance in realizing highly intelligent human machine interfaces. Facial expression plays important role in cognition of human emotions and facial expression recognition is the base of emotions understanding. In this paper, we propose a novel method for both face recognition and its facial expression. This is very helpful in situation when users want to identify human characters in movies and their facial expressions.*

***Keywords*:** *Face recognition, Facial expression, FCP, Template.*

I. INTRODUCTION

There are number of applications where face recognition [1] can play an important role including biometric authentication, high technology surveillance and security systems image retrieval and passive demographical data collections .it is observable that the behavior and social interaction are face recognition system could have great impact in improving human computer interaction systems in such a way as to make them be more user-friendly and acting more human-like. It is unarguable that the face is one the most important feature that characterizes human beings. By only looking ones faces, we are not only able to tell who they are but also perceive a lot of information such as their ages, emotions and names. This is why face recognition has received much interest in computer vision research community over past two decades. Figure 1 shows an example of movie character identification.

There are two main steps involved in recognizing names of humans presented in an image .These are- face detection and name classification [2], which are applied consecutively. In order to exploit uniqueness of faces in name recognition, the first step is to detect and localize those faces in the given images. This is the task achieved by face detection systems.

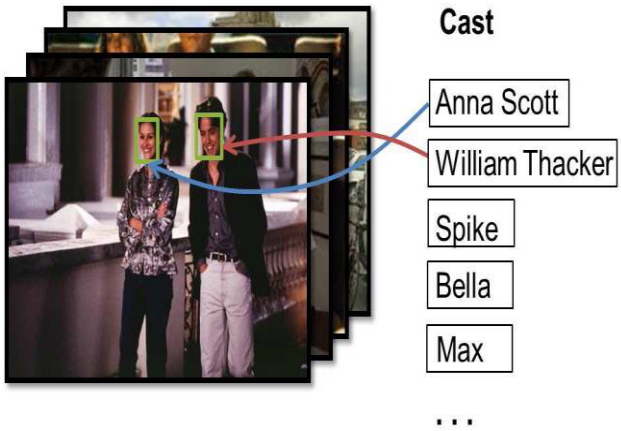

Figure 1: Example of movie character identification

Sometimes we want to know the facial expression (happy, sad, smiley, fear) of the recognized face. Facial expression recognition [3][4] is a process performed by humans or computers, which consists of(figure 2):

1. Locating faces in the scene (e.g., in an image- this step is also referred to as face detection),
2. Extracting facial features from the detected face region (e.g., detecting the shape of the facial components or describing the texture of the skin in a facial area; this step is referred to as facial feature extraction),
3. Analyzing the motion of facial features and the changes in the appearance of facial features and classifying this information into some facial expression- interpretative categories such as facial muscle activations like smile or frown, emotion (affect) categories like happiness or anger, attitude categories like (dis)liking or ambivalence, etc. (this step is also referred to as facial expression interpretation).

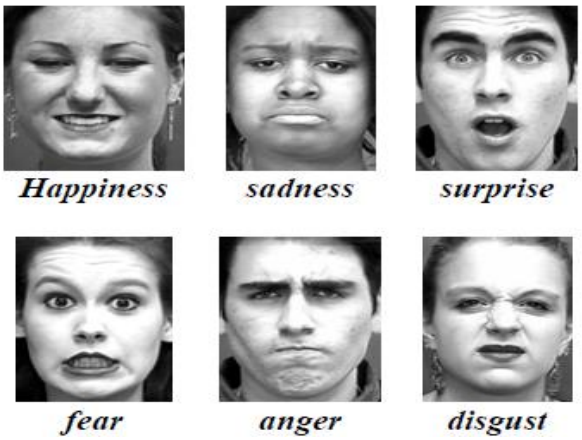

Figure 2: Different facial expressions

Monitoring and interpreting facial expressions can also provide important information to police, lawyers, security, and intelligence agents regarding person's identity (research in psychology suggests that facial expression recognition is much easier in familiar persons because it seems that people display the same, ''typical'' patterns of facial behavior in the same situations), deception (relevant studies in psychology suggest that visual features of facial expression function as cues to deception), and attitude (research in psychology indicates that social signals including accord and mirroring – mimicry of facial expressions, postures, etc., of one's interaction partner – are typical, usually unconscious gestures of wanting to get along with and be liked by the interaction partner). Automated facial reaction monitoring systems could form a valuable tool in law enforcement, as now only informal interpretations are typically used.

II. RELATED WORK

In [5], [6], the authors proposed, the faces are clustered by appearance and faces of a particular character are expected to be collected in a few pure clusters. Names for the identified clusters are then manually selected from the cast list. In [7], the authors proposed to manually label an initial set of face clusters and further cluster the rest face instances based on clothing within scenes. In [8], the authors have addressed the problem of finding particular characters by building a model/classifier of the character's appearance from user-provided training data. An interesting work combining character identification with web image retrieval is proposed in [9]. The character names in the cast are used as queries to search the face images and constitute gallery set. The probe face tracks in the movie are then identified as one of the characters by multi task joint sparse representation and classification.

In [10], the authors proposed to combine the film script with the subtitle for local face-name matching. Researchers from University of Pennsylvania utilized the readily available time-stamped resource, the closed captions, which is demonstrated more reliable than the OCR-based subtitles [11]. They investigated on the ambiguity issues in the local alignment between the video, screenplay and closed captions. A partially-supervised multi class classification problem is formulated. Recently, they attempted to address the character identification problem without the use of screenplay [12].

In [13], the authors proposed the facial action coding system (FACS) which represents the facial expression by a set of facial action units. In [14], the authors proposed an approach for analyzing and representing the dynamics of facial expression. Their system consists of locating of tracking the prominent facial features, optical flow analysis, and the classification. In [15], the authors extended the work of [14] by using connectionist architecture. Individual emotion networks were trained by viewing a set of sequences of one emotion for many of the objects. The trained neural network was then tested for the emotion recognition. In [16], the authors provided a facial expression representation by characterizing facial muscle activation. The facial motion estimation is operated by fitting the 3D deformable facial model to the face in an image for the muscle based representation. In [17], the authors developed a facial expression recognition method by using a synergetic pattern recognition approach. In [18], the authors proposed a facial expression recognition method to identify the shape of the mouth feature only. In[19], the authors used simple measurements (0 or 1) of the forehead wrinkle, eye opening, nostril furrow deepening, mouth opening, and eyebrow motion to recognize human facial expression.

III. PROPOSED WORK

The proposed work is shown in Figure 3. Our proposed work for the character recognition was motivated by the Bag-of-Features method [20]. The Bag-of-Features method extracts the feature points (i.e., image points that are described not necessarily by their color/intensity values, but by their local neighborhood based on, e.g., gradient information) from a set of training images. In the feature space, the feature points are grouped by a clustering algorithm. Based on the resulting clusters (all clusters together are referred to as code book and one cluster is referred to as visual word), occurrence histograms are then generated for each body part image. A classifier is then trained on the obtained histograms. Occurrence histograms reflect how many feature points are assigned to each of the visual word. Our approach is build on SIFT- [21] and CIE L*u*v* color-based code books that are obtained by clustering with k-means. A non-linear multi-class Support Vector Machine (SVM) is learned on the occurrence histograms.

The trained Support Vector Machines (or SVM models) are then used to predict the identity of the detected person. Probabilistic votes of connected body parts (i.e., body parts that belong to one and the same person) are combined for a more stable prediction. The training data is generated from an annotation data set in which the name of the corresponding character is noted for each of the body part. Based on the obtained annotation data, codebooks are generated and SVM models are learned. The codebooks and the SVM models are then applied subsequently on the entire video file. In this way, particular (human) characters are recognized at different points in time in a given video file. After obtaining a particular character, we need to identify the facial expression of that character.

To identify facial expression, template matching is being carried out by making use of convolution and correlation coefficients for the highest and perfect matching. The desired eyes, eyebrows and mouth templates are being excerpt from the image and the extracted results are shown in the form of bounded rectangles. The Facial characteristics points (FCP's) is being computed by knowing the top left coordinate of each template bounded by rectangles. Once we obtained the parameters from FCP's we set the threshold value and then proceed for creation of Decision tree. A decision tree is a classifier in the form of a tree structure. Information gain (IG) is used to select the most useful attributes for classification:

- The entropy of total data set is calculated
- The dataset is then split on the different attributes.
- The entropy of each branch is calculated then it is added proportionally to get the total entropy for the split.
- The resulting entropy is subtracted from the entropy before the split; with the result is the information gain.
- The attribute that have the largest information gain is chosen for the decision node.
- A branch set with a entropy of zero is the leaf node.
- Otherwise, further splitting to classify its data set.
- The ID3 algorithm is run recursively on the non leaf branches until all data is classified.

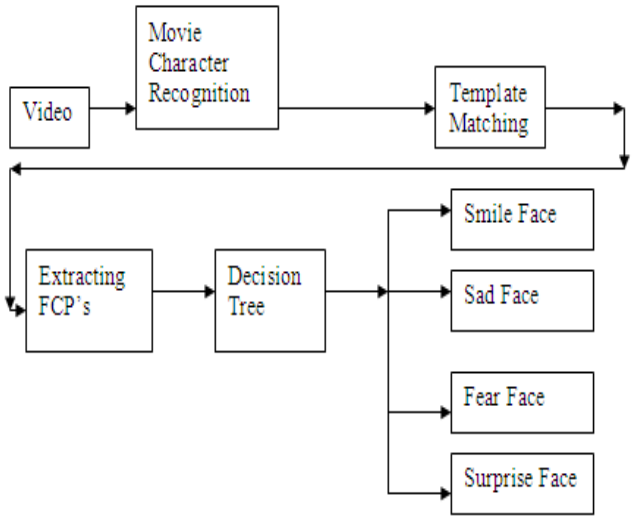

Figure 3: Proposed Method

IV. CONCLUSIONS

The proliferation of TV and movie provides large amount of digital video data. This has led to the requirement of efficient and effective techniques for movie or image content understanding and organization. Automatic image or video annotation is one of such key techniques. In this paper our focus is on annotating characters in the movies, which is called movie character identification and their facial expressions. The movie character identification is performed based on Bag-of-Features method extracts the feature points and SIFT and CIE L*u*v* color-based code books that are obtained by clustering with k-means. To identify facial expression, template matching is being carried out by making use of convolution and correlation coefficients for the highest and perfect matching. The Facial characteristics points (FCP's) is being computed by knowing the top left coordinate of each template bounded by rectangles. Once we obtained the parameters from FCP's we set the threshold value and then proceed for creation of Decision tree. After classification, we obtain the required facial expression of the identified character.

REFERENCES

[1] J. Stallkamp, H. K. Ekenel, and R. Stiefelhagen, "Video-based face recognition on real-world data," in Proc. Int. Conf. Comput. Vis., 2007, pp. 1–8.
[2] T. L. Berg, A. C. Berg, J. Edwards, M. Maire, R.White, Y. W. Teh, E. G. Learned-Miller, and D. A. Forsyth, "Names and faces in the news," in Proc. Comput. Vis. Pattern. Recognit., 2004.
[3] Tian, Y.L., Kanade, T., Cohn, J.F.: Facial expression analysis. In: Li, S.Z., Jain, A.K. (eds.) Handbook of Face Recognition, pp. 247–276. Springer, New York (2005)

[4] Pantic, M., Bartlett, M.S.: Machine analysis of facial expressions. In: Delac, K., Grgic, M. (eds.) Face Recognition, pp. 377–416. I-Tech Education and Publishing, Vienna, Austria (2007)
[5] A. W. Fitzgibbon and A. Zisserman, "On affine invariant clustering and automatic cast listing in movies," in ECCV (3), 2002, pp. 304–320.
[6] O. Arandjelovic and R. Cipolla, "Automatic cast listing in feature-length films with anisotropic manifold space," in CVPR (2), 2006, pp. 1513– 1520.
[7] D. Ramanan, S. Baker, and S. Kakade, "Leveraging archival video for building face datasets," in ICCV, 2007, pp. 1–8.
[8] M. Everingham and A. Zisserman, "Identifying individuals in video by combining"generative" and discriminative head models," in ICCV, 2005, pp. 1103–1110.
[9] M. Xu, X. Yuan, J. Shen, and S. Yan, "Cast2face: character identification in movie with actor-character correspondence," in ACM Multimedia, 2010, pp. 831–834.
[10] M. Everingham, J. Sivic, and A. Zissserman, "Hello! my name is... buffy automatic naming of characters in tv video," in Proceedings of BMVC, 2006, pp. 889–908.
[11] rT. Cour, C. Jordan, E. Miltsakaki, and B. Taskar, "Movie/script: Alignment and parsing of video and text transcription," in ECCV (4), 2008, pp. 158–171.
[12] T. Cour, B. Sapp, A. Nagle, and B. Taskar, "Talking pictures: Temporal grouping and dialog-supervised person recognition," in CVPR, 2010, pp. 1014–1021.
[13] P. Ekman and W. V. Friesen, Measuring facial movement with facial action coding system, in Emotion in Human Face (P. Ekman, Ed.), Cambridge Univ. Press, Cambridge, 1982.
[14] Y. Yacoob and L. Davis, Computing spatio-temporal representation of human face, in CVPR'94, June 21–23, 1994, Seattle, pp. 70–75. USA.
[15] M. Rosenblum, Y. Yacoob, and L. Davis,Human emotion recognition from motion using a radial basis function network architecture, in Proc. of IEEE Workshop on Motion of Non-Ridgid and Articulated Objects, Nov. 11–12, 1994, Austin, pp. 43–49, USA.
[16] I. A. Essa and A. Pentland, Facial expression recognition using virtually extracted facial action parameters, in Proc. of Int. Workshop on Auto. Face- and Gesture Recognition, pp. 35–40, Zurich, 1995.
[17] P. Vanger, R. Honlinger, and H. Haken, Applications of synergetics in decoding facial expression of emotion, in Proc. of Int. Workshop on Auto. Face- and Gesture Recognition, pp. 24–29, Zurich, 1995.
[18] Y. Moses, D. Reynard, and A. Blake, Determining facial expression in real-time, in Proc. of Int. Workshop on Automatic Face- and Gesture Recognition, pp. 332–337, Zurich, 1995.
[19] Y. Kitamura, J. Ohya, N. Ahuja, and F. Kishino, Computational taxonomy and recognition of facial expression, in Proc. of ACCV'93 Nov. 23–25, 1993, Osaka, Japan.
[20] Chris Dance, Jutta Willamowski, Lixin Fan, Cedric Bray, and Gabriela Csurka. Visual categorization with bags of keypoints. In ECCV International Workshop on Statistical Learning in Computer Vision, 2004.
[21] D. G. Lowe. Distinctive image features from scale-invariant keypoints. International Journal of Computer Vision, 60(2):91–110, 2004.

International Journal of Modern Engineering Research (IJMER)
www.ijmer.com Vol.3, Issue.3, May-June. 2013 pp-1343-1345 ISSN: 2249-6645

An Access Control Model for Online Social Networks

Sasikala Marla, [1] P.V.R. Raj Varma[2]
[1]*M.Tech, Sri Sunflower College of Engineering & Technology, Lankapalli*
[2]*Asst.Professor, Dept.of CSE, Sri Sunflower College of Engineering & Technology, Lankapalli*

Abstract: *Over the last decade online social networking sites have increased in popularity. This popularity has brought many users together, increasing their ability to share information. While the general information sharing is desirable, some users might be concerned with the privacy implications of disclosing so much personal information online. Currently users have two main options- They can either refuse to enter the information they are uncomfortable disclosing, or they may limit access to the information via privacy controls provided by the social networking site. It is important to note, however, that in the second case the information is stored remotely, and thus the control of the data is lost to the user. This paper presents an access control model for online social networks.*

Keywords: *Access control, OSN, Privacy.*

I. INTRODUCTION

Since its creation, the Internet has spawned many information sharing networks, the most well known of which is the World Wide Web. Recently, a new class of information networks called "Online Social Networks (OSN)" has exploded in popularity and now rival the traditional Web in terms of usage [1]. Social networking sites such as MySpace, Facebook, Orkut, and LinkedIn are the examples of wildly popular networks used to find and organize contacts. Other social networks such as Flickr, YouTube, and Google Video, are used to share the multimedia content, and others such as LiveJournal and BlogSpot are used to share blogs.

Unlike the traditional Web, which is largely organized by content, the online social networks embody users as first-class entities. Users join a network, publish their own content, and then create links to other users in the network called "friends". This basic user-to-user link structure facilitates online interaction by providing a mechanism for organizing both the real-world and virtual contacts, for finding other users with similar interests, and for locating content and knowledge that has been contributed or endorsed by "friends". The extreme popularity and the rapid growth of these online social networks represents a unique opportunity to study, understand, and leverage their properties. Not only can an in-depth understanding of online social network structure and growth aid in designing and evaluating current systems, it can lead to better designs of the future online social network based systems and to a deeper understanding of the impact of online social networks on the Internet. OSNs also offer many useful properties that can be leveraged to enhance information systems, such as enhancements to controlling information propagation, new directions for information search and retrieval, and new ways of reasoning about trust.

Users increasingly share content, recommendations, opinions, and ratings using the online social networks. However, the growing number of users and the increasing variety and volume of shared information on these sites aggravates two fundamental problems in information sharing- privacy and relevance. Since users are often sharing personal information, privacy and access control is critical. In particular, almost all privacy mechanisms available to users today are based on access control- users can specify which other users are able to view the content or information they upload.

II. NEED OF ACCESS CONTROL IN OSNS

OSNs have attracted a large amount of users to regularly connect, interact and share information with each other for different purposes. Users share a tremendous amount of content with other users in OSNs using various services available. The explosive growth of the sensitive or private user data that are readily available in OSNs has raised an urgent expectation for effective access control that can protect these data from unauthorized users in OSNs. Access control in the OSNs is typically based on the relationships among users in the social graph. That is, granting access to an accessing user is subject to the existence of either direct or indirect relationship of certain types between the accessing user and the controlling users of the target. Many existing OSN systems enforce a rudimentary and limited relationship-based access control mechanism, offering users the ability to choose from a pre-defined policy vocabulary, such as "private", "publlic", "friend" or "friend of friend". Google+[2] and Facebook [3] recently introduced customized relationships, namely "circle" and "friend list", providing users richer options to differentiate distinctly privileged user groups.

In OSNs, users are provided to create profiles, add content onto their pages (e.g., photos, videos, blogs, status updates and tweets), and share these resource objects with other peers. OSNs offer their users various types of user interaction services, including chatting, private messaging, poking and social games. As OSN systems mature, various types of resources need to be protected, such as user sessions, relationships among users and resources, access control policies and the events of users. As shown in Figure 1, users can launch access requests against both resources (e.g., view a photo or create an access control policy) and users (e.g., invite another user to a game or poke another user).

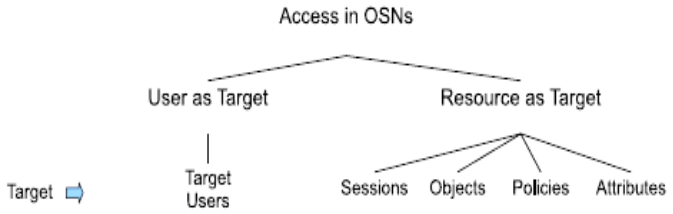

Figure 1: Taxonomy based on target

As shown in Figure 2, in OSN, a user can access other users (user as a target) or resources (resource as a target). By means of U2U(user to user), U2R(user to resource) and R2R(resource to resource) relationships, an accessing user and a target user can have a direct relationship or indirect relationships with user(s) in between, resource(s) in between or user(s) and resource(s) in between.

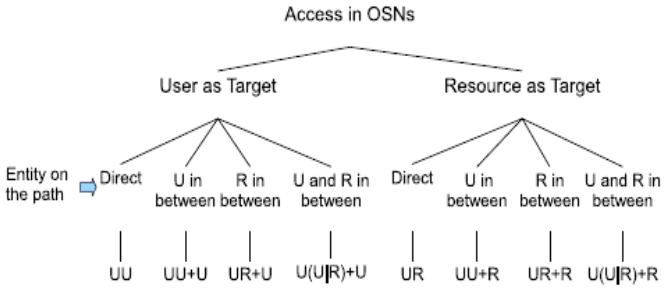

Figure 2: Access in OSNs

Likewise, an accessing user and the target resource can also be characterized in terms of the entities on the relating path. In the first two cases of accessing the target user, there is no resource involved. An accessing user should either have a particular direct U2U relationship (shown as UU) or a particular sequence of U2U relationships with the target user. Examples of such access to a target user are that Alice's direct friends can poke her, and Bob's friends of friends can request a friendship invitation to him. Similarly, a user may access a resource that directly relates to her (shown as UR), or may find a resource through one or more users in the network.

III. EXISTING WORK

Several access control models for OSNs have been introduced [4] [5]. Early access control solutions for OSNs introduced the trust-based access control inspired by the developments of trust and reputation computation in OSNs. The D-FOAF system [6] is primarily a Friend of a Friend (FOAF) ontology-based distributed identity management system for OSNs, where relationships are associated with a trust level, which indicates the level of friendship between the users participating in a given relationship. In [4], the authors introduced a conceptually-similar but more comprehensive trust-based access control model. This model allows the specification of access rules for the online resources, where authorized users are denoted in terms of the relationship type, depth, and trust level between users in OSNs.

In [7], the authors proposed an access control model that formalizes and generalizes the access control mechanism implemented in Facebook, admitting arbitrary policy vocabularies that are based on theoretical graph properties. In [12], the authors described relationship-based access control as one of new security paradigms that addresses unique requirements of Web 2.0. In [8], the authors proposed a semantic web based access control framework for social networks. The need of joint management for data sharing, especially photo sharing, in OSNs has been recognized by the recent work [9]. Other related work includes general conflict resolution mechanisms for access control [10] and learn-based generation of privacy policies for OSNs [11].

IV. PROPOSED WORK

In our proposed work, we present an application called MController for supporting collaborative management of shared data. It enables multiple associated users to specify their authorization policies and privacy preferences to co-control a shared data item. Consider the online social network "Facebook". Facebook server accepts inputs from the users, then forwards them to the application server. The application server is responsible for the input processing and collaborative management of the shared data. Information related to the user data such as user identifiers, friend lists, user groups, and user contents are stored in the MySQL database. Once the user installs MController in her/his Facebook space, MController can access user's basic information and contents. In particular, MController can retrieve and list all the photos, which are owned or uploaded by the user, or where the user was tagged. Then, the user can select any photo to specify the privacy preference. If the user is not the owner of the selected photo, he can only edit the privacy setting and sensitivity setting of the photo. Otherwise, if the user is an owner of the photo, then he can further configure the conflict resolution mechanism for the shared photo.

The core component of MController is the decision making module, which processes access requests and returns responses (either permit or deny) for the requests. Figure 3 depicts a system architecture of the decision making module in MController. To evaluate an access request, the policies of each controller of the targeted content are enforced first to generate a decision for the Mcontroller. Then, the decisions of all of the controllers are aggregated to yield a final decision as the response of the request. During the procedure of decision making, policy conflicts are resolved when evaluating the controllers' policies by adopting a strategy chain pre-defined by the controllers.

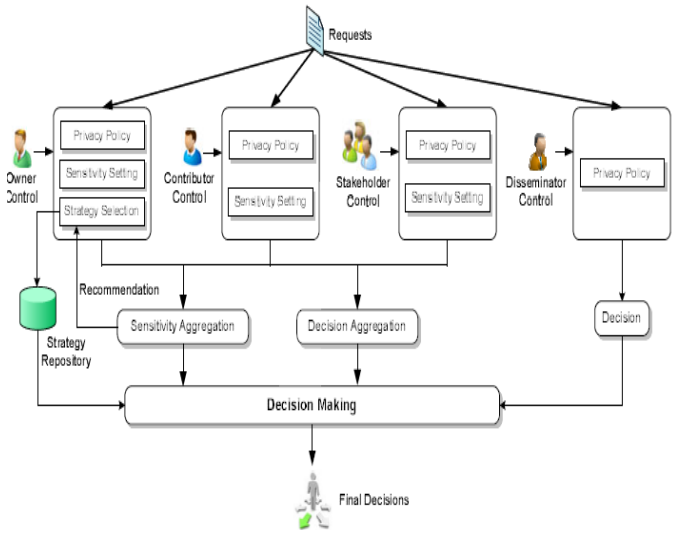

Figure 3: System Architecture of Decision Making in MController

In addition, multiparty privacy conflicts are also resolved based on the configured conflict resolution mechanism when aggregating the decisions of controllers. If the owner of the content chooses the automatic conflict resolution, the aggregated sensitivity value is utilized as a threshold for making a decision. Otherwise, multiparty privacy conflicts are resolved by applying the strategy selected by the owner, and the aggregated sensitivity score is considered as the recommendation for the strategy selection. Regarding access requests to the disseminated contents, the final decision is made by combining the disseminator's decision and the original controllers' decision through a deny-overrides combination strategy.

V. CONCLUSION

The explosive growth of the sensitive or private user data that are readily available in OSNs has raised an urgent expectation for effective access control that can protect these data from unauthorized users in OSNs. For access control, we use an application called "Mcontroller". It enables multiple associated users to specify their authorization policies and privacy preferences to co-control a shared data item. The core component of MController is the decision making module, which processes access requests and returns responses (either permit or deny) for the requests.

REFERENCES

[1] MySpace is the number one website in the U.S. according to Hitwise. Hit- Wise Press Release, July, 11, 2006. http://www.hitwise.com/press-center/ hitwiseHS2004/social-networking-june-2006.php.
[2] Google+ Privacy Policy. http://http://www.google.com/intl/en/+/ policy/.
[3] Facebook : http://www.facebook.com/.
[4] Carminati, B., Ferrari, E., Perego, A.: Rule-based access control for social networks. In: Meersman, R., Tari, Z., Herrero, P. (eds.) OTM2006Workshops. LNCS, vol. 4278, pp. 1734– 1744. Springer, Heidelberg, 2006.
[5] Fong, P.: Relationship-Based Access Control: Protection Model and Policy Language. In: Proceedings of the First ACM Conference on Data and Application Security and Privacy. ACM, New York, 2011.
[6] Kruk, S., Grzonkowski, S., Gzella, A., Woroniecki, T., Choi, H.: D-FOAF: Distributed identity management with access rights delegation. In: Mizoguchi, R., Shi, Z.-Z., Giunchiglia, F. (eds.) ASWC 2006. LNCS, vol. 4185, pp. 140–154. Springer, Heidelberg, 2006.
[7] Fong, P., Anwar, M., Zhao, Z.: A privacy preservation model for facebook-style social network systems. In: Backes, M., Ning, P. (eds.) ESORICS 2009. LNCS, vol. 5789, pp. 303– 320. Springer, Heidelberg, 2009.
[8] Brands, S.A.: Rethinking public key infrastructures and digital certificates: building in privacy. The MIT Press, Cambridge, 2000.
[9] Squicciarini, A., Shehab, M., Paci, F.: Collective privacy management in social networks. In: Proceedings of the 18th International Conference on World Wide Web, pp. 521–530. ACM, New York ,2009.
[10] Fisler, K., Krishnamurthi, S., Meyerovich, L.A., Tschantz, M.C.: Verification and changei mpact analysis of access-control policies. In: ICSE 2005: Proceedings of the 27th International Conference on Software Engineering, pp. 196–205. ACM, New York, 2005.
[11] Fang, L., LeFevre, K.: Privacy wizards for social networking sites. In: Proceedings of the 19th International Conference on World Wide Web, pp. 351–360. ACM, New York ,2010.
12] Carrie, E.: Access Control Requirements forWeb 2.0 Security and Privacy. In: Proc. ofWorkshop on Web 2.0 Security & Privacy (W2SP), Citeseer, 2007.

International Journal of Modern Engineering Research (IJMER)
www.ijmer.com Vol.3, Issue.3, May-June. 2013 pp-1346-1349 ISSN: 2249-6645

AONT- Based Packet Hiding Method for Preventing Jamming Attacks

M.prasanthi, [1] G. Bala Raju[2]
[1]*M.Tech, Sri Sunflower College of Engineering & Technology, Lankapalli*
[2]*Asst.Professor, Dept.of CSE, Sri Sunflower College of Engineering & Technology, Lankapalli*

Abstract: *Wireless networks now enjoy widespread commercial implementation because of their ease of use, low cost and setup. However, since accessing wireless media is much easier than tapping a wired network, then security becomes a serious concern when implementing any wireless network. We consider a particular class of Denial of Service (DoS) attacks called jamming attacks. In the simplest form of jamming, the attacker interferes with the reception of messages by transmitting a continuous jamming signal, or several short jamming pulses. Jamming results in the loss of link reliability, increased energy consumption, extended packet delays and disruption of end-to-end routes. The use of distinct, dedicated communication links to transmit data and control traffic introduces a single point of failure for a denial of service attack, in that an adversary may be able to jam control channel traffic and prevent relevant data traffic. To prevent such jamming attacks, in this paper we propose a packet hiding method based on all- or- nothing transforms (AONT).*

Keywords: *AONT, Cipher text, DOS, Jammer.*

I. INTRODUCTION

The broadcast nature of wireless networks makes them particularly vulnerable to the radio interference, which prevents the normal communications. This interference or jamming can destroy the wireless transmission and may occur either by means of unintentional interference or collision at the receiver side or intentional attacks. The jamming attack can be easily launched since it can be implemented by simply listening to the open medium and broadcasting in the same frequency band as sensor networks.

In order to cope with this kind of Denial-Of- Service (DOS) style attack, many strategies and techniques have been developed. The traditional method is to use the sophisticated physical layer technologies such as- DSSS (Direct Sequence Spread Spectrum) and FHSS (Frequency Hopping Spread Spectrum), which have been widely used in military communication. However, it can be too costly for the energy and frequency constrained networks. So many kinds of evasion strategies have been researched, such as wormhole-based anti-jamming techniques [1], channel surfing [2] and timing channel [3].

This paper presents a packet hiding method based on AONT to prevent jamming attacks. Jamming attack is a kind of Denial of Service (DOS) attack, which prevents other nodes from using the channel to communicate by occupying the channel that they are communicating on. We define the jammer in wireless sensor networks as an entity who is purposefully trying to interfere with the physical transmission and reception of wireless communications. A typical scenario of jamming attack is shown in the figure 1. The normal nodes C and D has been jammed by the malicious node "X", so the communications between the jammed nodes(C, D) and the normal nodes (A, B, E, H, I) are disrupted.

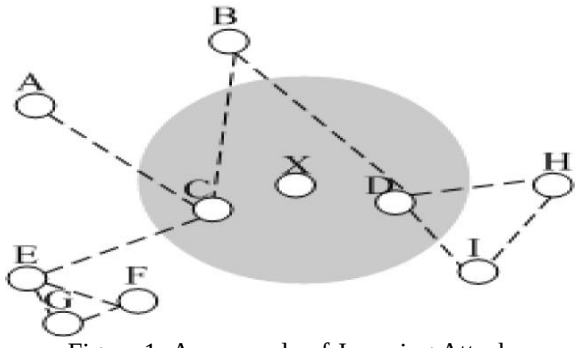

Figure 1: An example of Jamming Attack

II. TYPES OF JAMMERS

Jammers are of five types based on the time of their activity and the mode of attacks:

- Continuous Jammers
- Impersonate Jammers
- Unsystematic Jammers
- Systematic Jammers
- Exacting Jammers

A. Continuous Jammers

The continuous jammers [4] transmit the jamming or attack signal into the medium at a constant rate. Since the jamming signal uses the medium or channel, the other users will not sense the medium to be free for their legitimate service. The packets transmitted by these type of jammers are random meaningless messages. The jammers are small electronic devices powered by a battery with the limited power resources. Hence after a considerable time, the jammer dries its battery power and thus the medium is retrieved from the attack. Even an energy efficient jammer could not last for a considerable time but still for a limited span, the jammer completely blocks the services in a network. The packets could be identified from the content it stores and thus the attacker. The route could be blocked to prevent the network from the attack.

B. Impersonate Jammers

Impersonate jammers [5] sends the packets which resemble the original packets. The network administrator would not try to suspect these packets and thus allows the packets into the network. Yet these jammers are not energy efficient and thus dry out soon after. The only advantage is that it evades the detection mechanisms for a longer period of time.

C. Unsystematic Jammers

Unsystematic jammers [5] are the foundation of energy efficient jammers. These type of jammers extended their life span by limiting the time of activity. Packets are sent from these jammers at a random time rather than continuously thus serving for a longer period. The jammers would alternate their activity time that is they would be on for certain period of time and thus switched on for a certain time. Conserving the power at regular intervals increased their lifetime, causing a threat to the entire network.

D. Systematic Jammers

Systematic jammers [6] are the intelligent jammers of all other types. Unlike the unsystematic jammers, they follow a strict order to be switched- on and off. These are highly energy efficient and the most significant in attacking the resources in the netwrok. This type of jammers waits for the sender and the receiver nodes to start the communication process and then gets activated. The mode of attack is simplified and then the attack becomes more vulnerable to the network. If there is no communication between the nodes, then the jammers remains idle, and conserving the energy. Moreover the packets sent over the medium are similar to the legal data packets raising no different pattern to awaken the defense mechanisms.

E. Exacting Jammers

Exacting jammers are considered to be the critical jammers which have to be spotted immediately before irrecoverable changes occur in the network. The exacting jammers determine the nature of the packet sent in between the nodes of a network. Unless those packets are of high importance [7], they are free to move. Packets such as route request or route response or a packet of either important data or control flow would readily be subjected to the jamming attack. The source of the jamming attack, being a part of the original network, defines the longer time for suspicion.

III. RELATED WORK

Continuous jamming has been used as a denial-of-service (DoS) attack against voice communication since the 1940s [8]. Recently, several alternative jamming strategies have been demonstrated [9], [10]. Intelligent attacks which target the transmission of specific packets were presented in [11], [12]. In [12], the authors consider an attacker who infers eminent packet transmissions based on timing information at the MAC layer.

In both [11], [12], real-time packet classification was considered beyond the capabilities of the adversary. Selectivity was achieved through inference from the control messages already transmitted. Channel-selective jamming attacks were considered in [13]. It was shown that targeting the control channel reduces the required power for performing a denial- of- service attack by several orders of magnitude. In [14], the authors proposed a randomized frequency hopping algorithm, to protect the control channel inside jammers. Finally, in [10], the authors proposed a frequency hopping anti-jamming technique that does not require the sharing of a secret hopping sequence, between the communicating parties.

IV. ALL- OR- NOTHING TRANSFORM

The concept of an All-or-Nothing Transform (AONT) was introduced by Rivest [15] to increase the cost of brute force attacks on block ciphers without changing the key length. As defined in [15], an AONT is an efficiently computable transformation f, mapping sequences of blocks (i.e., fixed length strings) to sequences of blocks, which has the following properties:

1. Given all of f(x1,x2,…….xn)= (y1,y2,…..yn), it is easy to compute x1,x2,……xn.
2. Given all but one of the blocks of the output, it is infeasible to find out any information about any of the original blocks xi.

An AONT itself does not perform any encryption, since there is no secret key information involved in it.. However, if its output is encrypted, block- by- block, with a block cipher, the resulting scheme will have the following interesting property- An adversary cannot and out any information about any block of the message without decrypting all the blocks of the cipher text. Now if the adversary attempts to do an exhaustive search for the key, he will need to perform n' decryptions

before determining whether a given key is correct. Thus, the attack will be slowed down by a factor of n', without any change in the size of the secret key. This is particularly important in scenarios where the key length is of constrained to be insecure or marginally secure.

The use of AONT with encryption can be particularly useful for remotely keyed encryption i.e., applications where the part of the system that contains the keys is separate, and where bandwidth restrictions prevent us from sending the whole message from the insecure to the secure component [4]. An example of such a scenario would be the case where the keys are stored in the smartcard, and the user wishes to encrypt or decrypt large files. Through the use of AONT, we can completely eliminate any encryption components from the host system, and restrict such operations to the smartcard.

V. PROPOSED METHOD

In the proposed work, the packets are pre-processed by an AONT before transmission but remain unencrypted. The jammer cannot perform the packet classification until all pseudo-messages corresponding to the original packet have been received and the inverse transformation has been applied. Packet "m" is partitioned to a set of x input blocks m = {m1, m2, m3….}, which serve as an input to an The set of pseudo-messages m = {m1, m2, m3,…..} is transmitted over the wireless link. Recently Rivest motivated by different security concerns arising in the context of block ciphers, introduced an intriguing primitive called the All-Or-Nothing Transform (AONT). An AONT is an efficiently computable transformation "T" on strings such that

- For any string x, given *all* of T(x), one can efficiently recover "x"
- There exists some threshold such that any polynomial time adversery that learns all but bits of T(x) obtains no information about "X" (in a computational sense).

The AONT solves the problem of partial key exposure-rather than storing a secret key directly, we store the AONT applied to the secret key. If we can build an AONT, where the threshold value `is very small compared to the size of the output of the AONT, we obtain security against almost total exposure. Notice that this methodology applies to secret keys with arbitrary structure, and thus protects all the kinds of cryptographic systems. One can also consider AONT's that have a two-part output- a public output that doesn't need to be protected, and a secret output that has the exposure-resilience property stated above. Such a notion would also provide the kind of protection we try to achieve. The AONT has many other applications, as well, such as enhancing the security of block-ciphers and making the fixed-block size encryption schemes more efficient.

Figure 2 shows the proposed packet hiding method. The Sender transmits the message, which is divided into blocks of fixed size. These blocks are given as input to AONT. Then AONT encrypts these message blocks with a shared secret key and then sends to the receiver. Now the receiver decrypts these blocks with the same key, thus retrieves the original data.

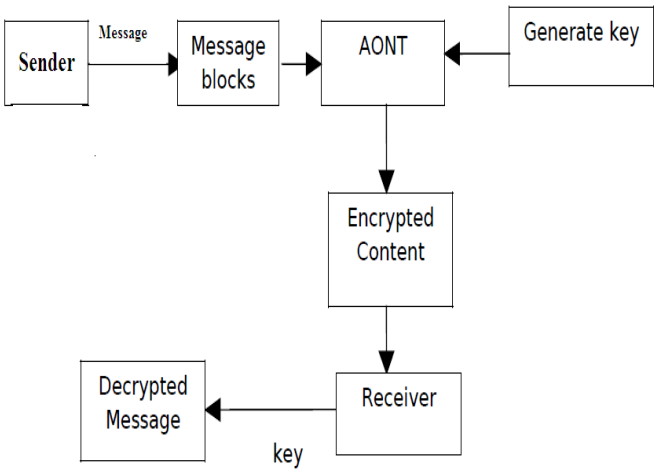

Figure 2: AONT- based packet hiding method

VI. CONCLUSION

Jamming attack is a kind of Denial of Service (DOS) attack, which prevents other nodes from using the channel to communicate by occupying the channel that they are communicating on. To prevent such attack, we propose a packet method based on All-or-Nothing Transform (AONT). An AONT itself does not perform any encryption, since there is no secret key information involved in it.. However, if its output is encrypted, block- by- block, with a block cipher, the resulting scheme will have the following interesting property- one must decrypt the entire cipher text before one can determine even one message block. This means that brute force searches against AONT encryption are slow down by a factor equal to the number of blocks in the cipher text.

REFERENCES

[1] Mario cagalj, srdjan capkun, jean hubaux, "Wormhole-Based Antijamming Techniques in Sensor Networks", IEEE TRANSACTIONS ON MOBILE COMPUTING, VOL. 6, NO. 1, JANUARY 2007.
[2] Wenyuan Xu , Wade Trappe, Yanyong Zhang, "Channel Surfing: Defending Wireless Sensor Networks from Interference", Cambridge, Massachusetts, USA, IPSN', 2007.
[3] Wenyuan Xu , Wade Trappe, Yanyong Zhang, "Anti-jamming Timing Channels for Wireless Networks", Alexandria, Virginia, USA, WiSec, 2008.
[4] G.Lin and G. Noubir."On link layer denial of service in data WirelessLANs".Wireless Communications and Mobile Computing, 5(3):273–284,May 2004.
[5] M. Wilhelm, I. Martinovic, J. Schmitt, and V. Lenders. "Reactivejamming in wireless networks: How realisticis the threat?" InProceedings of WiSec, 2011.
[6] W. Xu, T.Wood, W. Trappe, and Y. Zhang. "Channel surfing and spatial retreats: defenses against wireless denial of service". In Proceedings ofthe 3rd ACM workshop on Wireless security, pages 80–89, 2004.
[7] Alejandro Proano and Loukas Lazos. "Packet-Hiding Methods for Preventing Selective Jamming Attacks". IEEE Transactions on dependable and secure computing, Vol. 9, No. 1, January/February 2012.
[8] M. Simon, J. Omura, R. Scholtz, and B. Levitt. Spread spectrum communications handbook. McGraw-Hill Companies, 1994.
[9] G. Noubir and G. Lin. Low-power DoS attacks in data wireless LANs and countermeasures. ACM SIGMOBILE Mobile Computing and Communications Review, 7(3):29–30, 2003.
[10] C. Po¨pper, M. Strasser, and S. C˘ apkun. Jamming-resistant broadcast communication without shared keys. In Proceedings of the USENIX Security Symposium, 2009.
[11] Y. W. Law, M. Palaniswami, L. V. Hoesel, J. Doumen, P. Hartel, and P. Havinga. Energy-efficient link-layer jamming attacks against WSN MAC protocols. ACM Transactions on Sensor Networks, 5(1):1–38, 2009.
[12] D. Thuente and M. Acharya. Intelligent jamming in wireless networks with applications to 802.11b and other networks. In Proceedings of the IEEE MILCOM, 2006.
[13] A. Chan, X. Liu, G. Noubir, and B. Thapa. Control channel jamming: Resilience and identification of traitors. In Proceedings of the IEEE ISIT, 2007.
[14] L. Lazos, S. Liu, and M. Krunz. Mitigating control-channel jamming attacks in multi-channel ad hoc networks. In Proceedings of the second ACM conference on wireless network security, pages 169–180, 2009.
[15] Ronald Rivest, "All- or- nothing encryption and the package transform", 4th international workshop on fast software encryption, pages 210- 218, 1997.

Power Management in Multi- Relay MIMO- CNs

L.Suneel, [1] Y.Balasubramanyam[2]
[1]*M.Tech, Sri Sunflower College of Engineering & Technology, Lankapalli*
[2]*Asst.Professor, Dept.of ECE, Sri Sunflower College of Engineering & Technology, Lankapalli*

Abstract: *In recent years, co- operative networking has received substantial interest from the wireless networking and communications research communities. Many interesting problems for co- operative networks have been actively researched, such as throughput-optimal scheduling, network lifetime maximization, distributed routing, and MAC layer protocol design. Although there have been extensive studies concerning co- operative networks, most works on optimizing the performance of cooperative networks are limited by- three-node relay scheme and single-antenna systems. In co-operative networks, it is interesting to explore the idea of deploying multiple antennas at each node. With the multiple antennas, the source and the relays can multiplex independent data streams by exploiting the inherent independent spatial channels. In this paper, we consider the power allocation at the source and each relay to maximize the end-to-end achievable rate of multi relay MIMO-CN.*

Keywords: *AF, DF, Cooperative network, Relay.*

I. INTRODUCTION

Many Interesting problems for co-operative networks (CNs) have been actively researched such as throughput optimal scheduling [1]; network Maximization [2] distributed routing [3] and MAC layer protocol design [4]. Cooperation alleviates certain networking problems, such as collision resolution and routing, and allows for simpler networks of more complex links, rather than the complicated networks of simple links. Therefore, many upper layer aspects of the cooperative communications merit further research, e.g., the impacts on topology control and network capacity, especially in mobile ad hoc networks (MANETs), which can establish a dynamic network without a fixed infrastructure. Cooperative communications typically refers to a system where users share and coordinate their resources to enhance the information transmission quality. It is a generalization of the relay communication, in which multiple sources also serve as the relays for each other.

Early study of relaying problems appears in the information theory community to enhance the communication between the source and destination the basic three node relay scheme is shown in the Figure.1, where the message is retransmitted from source S to destination D is relayed by node R, which can overhear the message. A Common cooperative approach in this situation in relaying assignment i.e. we choose only one of the neighboring nodes as relay for which the three node relay scheme can be applied, now further improvement the system performance as shown in Figure 2.

In current scenario on cooperative networks with MIMO enabled nods remain limited. In cooperative networks, it is interesting to explore the idea of deploying multiple antennas at each node. Figure 2 indicates that all single antennas relay R1…., Rm as single virtual relay node with "M" antennas. Cooperative diversity is a cooperative multiple antenna technique for improving or maximizing the total network channel capacities for any given set of bandwidths which exploits user diversity by decoding the combined signal of the relayed signal and the direct signal in wireless multi hop networks.

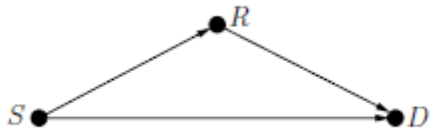

Figure 1: The basic three-node relay scheme

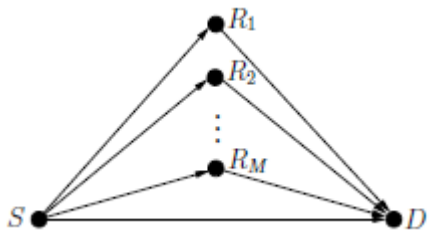

Figure 2: A cooperative network with multiple relays

Note that the user cooperation is another definition of cooperative diversity. User cooperation considers an additional fact that each user relays the other user's signal while the cooperative diversity can be also achieved by multi-hop relay networking systems. Actually we investigate that consideration the optimal power allocation at the source and each relay to maximize the end-to-end achievable rate of multi relay MIMO- CN. Now let us focus on the various relaying strategies like Amplify forward (AF) and Decode and forward (DF). In amplify forward, the relay nodes simply boost the energy of the signal received from the sender and retransmit it to the receiver. In decode and forward, the relay nodes will perform physical layer decoding and then forward the decoding result to the destinations.

II. RELATED WORK

In [5], the authors first considered the optimal relay amplification matrix for the basic three-node MIMO-CN under the assumption that the source-relay channel state information (CSI) is unknown. Their main conclusion is that when the direct link between the source and the destination is not present (i.e., pure relay), then the optimal amplification matrix adopts a "matching" structure. In [6], the authors independently arrived at the same conclusion via a different proof technique. Later in [7], the authors generalized the matching result to the three-node MIMO-CN network where the source has full CSI. In [8], the authors studied MIMO-CN with multiple AF relays, which is similar to our setting. However, their work differs from ours in that they assumed a sum power constraint across all the relay nodes, which is usually not realistic since each relay has its own power budget. Thus, a per node power constraint on each relay is more appropriate.

III. PROPOSED METHOD

In Proposed method we use Cooperative diversity. It is a cooperative multiple antenna technique for improving or maximizing the total network channel capacities for any given set of bandwidths which exploits user diversity by decoding the combined signal of the relayed signal and the direct signal in wireless multi hop networks. A conventional single hop system uses a direct transmission where a receiver decodes the information only based on the direct signal while regarding the relayed signal as interference, whereas the cooperative diversity considers the other signal as contribution. The modules in the proposed system are:

- Three-node relay transmission
- Network Constraints
- Relaying Strategies
- Cooperative Communications & Optimal Power allocation
- Multi-hop Transmission

A. Three-node relay transmission

With physical layer cooperative communications, there are three transmission manners- direct transmissions, multi-hop transmissions and cooperative transmissions. Direct transmissions and multi hop transmissions can be regarded as special types of cooperative transmissions. A direct transmission utilizes no relays while a multi hop transmission does not combine signals at the destination. The cooperative channel is a virtual multiple- input Multiple-output (MIMO) channel, where spatially distributed nodes are coordinated to form a virtual antenna to emulate multi-antenna transceivers.

B. Network Constraints

Two constraint conditions need to be taken into consideration in the network connectivity, which is the basic requirement in the topology control. The end-to-end network connectivity is guaranteed through a hop-by-hop manner in the objective function. Every node is in charge of the connections to all its neighbours. If all the neighbour connections are guaranteed, then the end-to-end connectivity in the whole network can be preserved. The other aspect that determines the network capacity is the path length. An end- to- end transmission that traverses more hops will import more data packets into the network. Although path length is mainly determined by the routing, MIMO – CN limits dividing a long link into too many hops locally. The limitation is two hops due to the fact that only two hop relaying are adopted.

C. Relaying Strategies

There are 2types of relaying strategies:

1. Amplify-and-forward (AF)
2. Decode-and-forward (DF)

In amplify-and-forward (AF), the relay nodes simply boost the energy of the signal received from the sender and retransmit it to the receiver. In decode-and-forward (DF), the relay nodes will perform physical-layer decoding and then forward the decoding result to the destinations. If multiple nodes are available for co- operation, their antennas can employ a space-time code in transmitting the relay signals. It is shown that co- operation at the physical layer can achieve full levels of diversity similar to a MIMO system, and hence can reduce the interference and increase the connectivity of wireless networks.

D. Cooperative Communications & Optimal Power allocation

Co- operative transmissions via a cooperative diversity occupying two consecutive slots. The destination node combines the two signals from the source and the relay to decode the information. Co- operative communications are due to the increased understanding of the benefits of multiple antenna systems. Although multiple-input multiple-output (MIMO) systems have been widely acknowledged, it is difficult for some wireless mobile devices to support the multiple antennas due to the size and cost constraints. Recent studies show that co- operative communications allow single antenna devices to work together to exploit the spatial diversity and reap the benefits of MIMO systems such as resistance to fading, high throughput, low transmitted power, and resilient networks.

E. Multi-hop Transmission

Multi-hop transmission can be illustrated using two hop transmission. When two- hop transmission is used, two time slots are consumed. In the first slot, messages are transmitted from the source to the relay, and the messages will be forwarded to the destination node in the second slot. The outage capacity of this two hop transmission can be derived considering the outage of each hop transmission.

IV. CONCLUSION

Co- operative communication has derived an interest for wireless network. Co- operative communication typically refers to a system where users share and coordinate their resources to enhance the information transmission quality. It is a generalization of the relay communication, in which the multiple sources also serve as relays for each other. In Proposed system we use Cooperative diversity. It is a co- operative multiple antenna technique for improving or maximizing total network channel capacities for any given set of bandwidths which exploits user diversity by decoding the combined signal of the relayed signal and the direct signal in wireless multi hop networks.

V. References

[1] Q. Guan et al., "Capacity-Optimized Topology Control for MANETs with Cooperative Communications," IEEE Trans. Wireless Commun.. vol. 10, July 2011, pp. 2162–70.
[2] P. Santi, "Topology Control in Wireless Ad Hoc and Sensor Networks," ACM Computing Surveys, vol. 37, no. 2, 2005, pp. 164–94.
[3] T. Cover and A. E. Gamal, "Capacity Theorems for the Relay Channel," IEEE Trans. Info. Theory, vol. 25, Sept. 1979, pp. 572–84.
[4] Q. Guan et al., "Impact of Topology Control on Capacity of Wireless Ad Hoc Networks," Proc. IEEE ICCS, Guangzhou, P. R. China, Nov. 2008.
[5] X. Tang and Y. Hua, "Optimal design of non-regenerative MIMO wireless relays," IEEE Trans. Wireless Commun., vol. 6, no. 4, pp. 1398– 1407, Apr. 2007.
[6] O. Mu˜noz-Medina, J. Vidal, and A. Agust´ın, "Linear transceiver design in nonregenerative relays with channel state information," IEEE Trans. Signal Process., vol. 55, no. 6, pp. 2593–2604, Jun. 2007.
[7] Z. Fang, Y. Hua, and J. D. Koshy, "Joint source and relay optimization for non-regenerative MIMO relay," in Proc. IEEE Workshop Sensor Array Multi-Channel Signal Processing, Waltham, WA, Jul. 12-14, 2006, pp. 239–243.
[8] Y. Fu, L. Yang, W.-P. Zhu, and Z. Yang, "A convex optimization design of relay precoder for two-hop MIMO relay networks," in Proc. IEEE ICC, Cape Town, South Africa, May 23-27, 2010.

International Journal of Modern Engineering Research (IJMER)
www.ijmer.com Vol.3, Issue.3, MayJune. 2013 pp13531356 ISSN: 22496645

Analysis of Rollback Recovery Techniques in Distributed Database Management System

Akanshika

Abstract: *As system continue to grow in size and complexity, they pose increasingly greater safety and risk management challenges. In this paper, we analyzed different methods of rollback recovery techniques and compare their performance. Idea that are used in the design, development, and performance of rollback recovery have been summarized. Independent check pointing, coordinate check pointing, communication induced checkpointing.*

Keywords: *Distributed database management system, rollback recovery, domino effect, checkpointing.*

I. Introduction

The database is a collection related data in an organized manner. This is the best way of storing the data .a distributed system can be visualised as a set of sites, each site consisting of a number of independent transactions. A distributed database is a database in which storage devices are not all attached to a common CPU. It may be stored in multiple computers located in the same physical location, or may be dispersed over a network of interconnected computers. A database state is represents the values of database objects that represent some real world entity. The database state is changed by the execution of a user transaction. Individual transaction running in isolation are assumed to be correct. When multiple user access multiple database objects residing on multiple site in distributed database system, the problem of recovery and keep the system in consistent state arises. This paper presents rollback recovery techniques to restore the system in most consistent state.

II. Recovery of Data

Recovery from transaction failures usually means that the database is restored to the most recent consistent state just before the time of failure. To do this the system must keep information about the changes that were applied to data items by various transactions.

2.1Issues in Recovery Protocol in ddbms

With distributed databases, guaranteeing atomicity and durability becomes more complicated. Transactions usually span more than one site, so if a transaction commits, then all the sites that are involved in the transaction have to commit. Also, if the transaction aborts, then all subtransactions have to abort. The problem is how to restore the data in most recent consistent state.

Rollback recovery is suitable where system availability requirement can tolerate the outage of computing system during recovery. It offers a resource efficient way of tolerating failures.

A [checkpoint] entry is recorded in the log periodically, when the system writes out to the database on disk all DBMS buffers that have been modified Consequence: all transactions whose [commit T] entry appears in the log before the [checkpoint], do not need to have their WRITE operations redone in case of a system crash (because all these updates have been recorded to disk during check pointing).

2.2consistency issue in distributed checkpoints

Local checkpoints: a local checkpoint is a snapshot of a process. A local state is not necessarily recorded as a local checkpoint, so the set of local checkpoints is only subset of the set of local state global checkpoint: a global checkpoint is a set of local checkpoints, one from each process. A local checkpoint can be part of global checkpoint if it does not contain any orphan message.

Definition for consistency criteria are provided by [3]:

"Given set of local checkpoints, can this set be extended to a global checkpoint that satisfies the consistency criterion P?" (Where P is traditional consistency, transitlessness, or storing consistency).

Traditional consistency : a global checkpoint is consistent if all its pairs of local checkpoints are consistent means does not exhibit any orphan message(a message m sent by a process Pi to a process Pj delivery of m is belong to Cj,y while its sending event not belong to Ci,x).

transitless global checkpoints: a global checkpoint is transitless if all its pairs of local checkpoints are transitless means a message m is intransit with respect to an ordered pair of local checkpoints (Ci,x, Cj,y) if send(m) belong to Ci,x and deliver(m) not belong to Cj,y.

Strong consistent global checkpoints: a global checkpoint is strongly consistent if all its pairs of local checkpoints are consistent and transitless.

Acceptability: let (Ci, Cj) be an ordered pair of checkpoints, Ci belonging to Pi and Cj belonging to Pj with i!= j. The ordered pair (Ci, Cj) is aceeptable if there is no cedge (e1, e2) with e1 issued by Pi, e2 issued by Pj, Cj> e1, and e2>Cj. A cedges(e1, e2) is such that e1 and e2 are two communication events that belong to different processes and concern the same message. We correspond to different message properties (orphan or intransit) and lead to different intentions of this generic graph.

Stable storage: rollback recovery uses stable storage to save checkpoints, event logs, and other recovery related information. Stable storage must ensure that the recovery data persist through the tolerated failures and their corresponding recoveries.

Garbage collection: checkpoints and event log consume storage resources. As the application progresses and more recovery information is collected, a subset of stored information may useless for recovery. Garbage collection is the deletion of such recovery information. A common approach to garbage collection is to identify the most recent consistent set of checkpoints which is called recovery line and discard all information related to events that occurred before line.

III. Checkpoint Based Rollback Recovery

Upon a failure, checkpoint based rollback recovery restores the system state to the most recent consistent state to the most recent consistent set of checkpoints, i.e. the recovery line. It does not rely on the PWD assumption, and so does not need to detect, log, or repaly non deterministic events. Checkpoint based protocols are therefore less restrictive and simpler to implement than log based rollback recovery. Checkpoint based rollback recovery techniques can be classified into three categories: uncoordinated checkpointing, coordinated checkpointing and communication induced check pointing.

3.1Uncoordinated Checkpointing

Uncoordinated checkpointing allows each process the maximum autonomy in deciding when to take checkpoints. The main advantage of this autonomy is that each process may take a checkpoint when it is most convenient. A process may reduce the overhead by taking checkpoints when the amount of state information to be saved is small. In uncoordinated check pointing possibility of the domino effect , which may cause the loss of large amount of useful work, possibly all the way back to the beginning of the computation uncoordinated check pointing forces each process to maintain multiple checkpoints, and to invoke periodically a garbage collection algorithm to reclaim the checkpoints that are no longer useful. It is not suitable for applications with frequent output commits because these require global coordination to compute recovery line, negating much of the advantage of autonomy.

If failure occurs, the recovering process initiates rollback by broadcasting a dependency request message to collect all the dependency in formation maintain by each process. The initiator then calculates the recovery line based on the global dependency information and broadcasts a rollback request message containing the recovery line. Upon receiving this message, a process whose current state belongs to the recovery line simply resumes execution otherwise its rolls back to an earlier checkpoint as indicated by the recovery line.

3.2 Coordinate check pointing

Coordinate checkpointing requires processes to orchestrate their checkpoints in order to form a consistent global state. Coordinate check pointing simplifies recovery and is not susceptible to domino effect, since every process restarts from its most recent checkpoint. Also, coordinated checkpointing requires each process to maintain only one permanent require each process to maintain only one permanent checkpoint on stable storage, reducing storage overhead and eliminating the need for garbage collection. Coordinate checkpointing is the large latency involved in committing output, since a global checkpoint is needed before message can be sent to OWP.

A straight forward approach to coordinated checkpointing is to block communication while the checkpointing executes. A coordinator takes a checkpoint and broadcasts a request message to all processes, asking them to take a checkpoint when process receive this message, it stop its execution flushes all communication channels, take a tentative checkpoint, and send an acknowledgement message back to the coordinator. After the coordinator receive the acknowledgements from all processes, it broadcasts a commit message that completes the two phase checkpointing protocol. After receiving the commit message, each process removes the old permanent checkpoint and atomically makes the tentative checkpoint permanent. The process is then free to resume exchange messages with other processes.

Minimal checkpoint coordination: coordinated check pointing requires all processes to participate in every checkpoint. This requirement generates valid concern about its scalability. It is desirable to reduce the number of processes involved in a coordinated checkpointing session. This can be done since the processes that need to communicated with the checkpoint initiator either or indirectly since the last checkpoint. Two phase protocol achieves minimal checkpoint coordination. During the first phase, the checkpoint initiator identifies all processes with it has communicated since the last checkpoint and send them a request, and so on, until no more processes can be identified. During the second phase, all processes identified in the first phase take a checkpoint. The result is a consistent checkpoint that involves only the participating processes.

3.3 communication induced checkpointing.

Communication induced check pointing (CIC) protocols avoid the domino effect without requiring all checkpoint to be coordinated. In this protocol processes take two kinds of checkpoints, loc al and forced. Local checkpoints can be taken independently, while forced checkpoints must be taken to guarantee the eventual progress of the recovery line. CIC protocols take forced checkpoint to prevent the creation of useless checkpoints, i.e. checkpoints that will never be part of a consistent global state. Useless checkpoints are not desirable because they do not contribute to the recovery of the system from failures, but they consume resources and caused performance overhead.

As opposed to coordinated checkpointing, CIC protocol s do not exchange any special coordination messages to determine when forced checkpoint should be taken: instead, they piggyback protocol specific information on each application message; the receiver than use this information to decide if it should take a forced checkpoint, this decision based on the receiver determining if past communication and checkpoint patterns can lead to the creation of useless checkpoint. CIC proto cols have been classified in one of two types. Model based check pointing and index based checkpointing

Model based protocol: model based check pointing relies on preventing pattern of communication and checkpoints that could result in Zcycle and useless checkpoints. A model is set up to detect the possibility that such patterns could be forming within in the system, according to some heuristic. A checkpoint is usually forced to prevent the undesirable pattern from occurring. The decision to force a checkpoint is done locally using the information piggybacked on the application messages. Therefore, under this style of check pointing it is possible that multiple processes detect the potential for inconsistent checkpoints and independently force local checkpoints to prevent the formation of undesirable patterns that may never actually materialize or that could be prevented by a single forced checkpoint. thus, model based check pointing always errs on the conservative side by taking more forced checkpoints than is probably necessary, because without explicit coordination, no process has complete information about the global state.

Index based protocol: index based CIC protocols guarantee, through forced checkpoints if necessary, that (1) if there are two checkpoints Ci,m and Cj,n such that Ci,m> Cj,n then timestamp of Cj,n >= timestamp of Ci,m, where ts(c) is the timestamp associated with checkpoint c; (2) consecutive local checkpoints of a process have increasing timestamps. The time stamps are piggybacked on application messages to help receivers decide when they should force a checkpoint. Protocol forces a processes to take a checkpoint upon receiving a message with piggy backed index greater than the local index, and guarantees that the checkpoints having same index at different processes from a consistent state.

IV. comparison

Different rollback recovery protocols offer different tradeoffs with respect to performance overhead latency of output commit, storage overhead ease of garbage collection, simplicity of recovery freedom from domino effect, freedom from orphan processes and extent of rollback. Table 1 summarize the different variation of rollback recovery protocols. Since garbage collection and recovery both involve calculating a recovery line, they can be performed by simple procedures under coordinate checkpoints. Coordinate check pointing can have unbounded rollbacks, and a process may need to retain up to N checkpoints if the optimal garbage collection algorithm is used.

	Uncoordinated check pointing	Coordinated check pointing	Communication induced Check pointing
checkpoint	Several	1	Several
Domino effect	Possible	No	No
Orphan process	Possible	No	No
Rollback Extent	unbounded	Last global checkpoint	Possibly several Checkpoint
Recovery Protocols	Distributed	Distributed	Distributed
Output Commit	Not possible	Global coordination required	Global coordination required

Table 1: A comparison between rollback recovery protocols

References

[1] R Guohong Cao and Mukesh Singhl" On Coordinated Checkpointing in Distributed Systems." vol. 9, no. 12, December 1998.
[2] Elmootazbellah N. Elnozahy and James S. Plank "Check pointing for PetaScale Systems: A Look into the Future of Practical Rollback Recovery." IEEE transactions on dependable and secure computing, vol. 1, no. 2, apriljune 2004.
[3] E.N.Elnozahy "A survey of rollback recovery protocols in message passing system" 2000.
[4] Bharat bhargava "Independent checkpoint and concurrent rollback for recovery in distributed system–an optimistic approach" 1997.
[5] Roberlo baldom "A communication induced check pointing protocol that insures rollback dependency traceability" 2004.
[6] David B. Johnson "Recovery in distributed system using optimistic message logging and checkpointing".1990

International Journal of Modern Engineering Research (IJMER)
www.ijmer.com Vol.3, Issue.3, May-June. 2013 pp-1357-1365 ISSN: 2249-6645

Energy Aware and Link Quality Based Routing in Wireless Sensor Networks under TinyOS-2.x

Dhaval Patel, [1] Bijal Chawla, [2] Chandresh Parekh[3]
[12]*PG Student, Department of Wireless Mobile Computing, Gujarat Technological University, India*
[3]*Head, Department of Electronics and Communication, Government Engineering College, Gujarat, India*

Abstract: *In WSN the size of sensor node is too small and in future it will become smaller and energy is one of the constraints in sensor node in WSN. In sensor node energy required to process data, transmitting data and receiving data. Communication requires more energy than processing data. Tiny OS is embedded operating system in sensor node. In Tiny OS 2.x there is routing protocol called collection tree protocol. Collection tree protocol finds the route according to link quality. But residual energy is key factor in sensor node. The proposed routing protocol improves routing mechanism in collection Tree protocol by energy based routing. The proposed algorithm (ELR) was compared with CTP protocol in terms of packet reception ratio (PRR) and number of nodes alive ratio of the network. This work was simulated in Castalia 3.2 and TOSSIM simulator. The results show that our algorithm performs better than CTP in terms of load distribution and increased lifetime.*

Keywords: *Collection Tree Protocol, Energy Aware Routing Protocol, Energy Measurement, Tinos, TOSSIM, Wireless Sensor Networks*

I. INTRODUCTION

Wireless sensor network is consisting of potentially large number of tiny sensor node communicating with each other for performing some task. The task is defined by some application like environmental monitoring, habitat monitoring, and health monitoring and home automation. The main purpose of sensor node is to sense data, process data and sends the data to sink node. Sink node is the node which is gathering information from sensor nodes. For doing this task sensor node requires energy. This energy is provided by battery. The battery has limited battery power. If the battery is gone down then sensor will not work longer. The nodes are mostly unattended hence the battery power is more precious [1].

WSN nodes require one operating system to work. Tiny OS is one of the operating system for WSN node. Tiny OS is a free and open source component-based event driven operating system, which addresses these issues of the WSN motes. Tiny OS is implemented using nes C (Network Embedded System C) language, which supports the event based concurrent model of Tiny OS [2][6]. Tiny OS provides components for packet communication, sensing, scheduling, routing and medium accessing etc. The routing protocols supported by this operating system is Collection Tree Protocol (CTP), it estimates the quality of the link based on either one of the link estimator protocols such as LEEP or four-bit link estimator.

In CTP protocol decides the parent node merely based on the link quality and thus a node with good link will always be selected as the parent node. It is apparent that a node with good wireless link will involve in more communication and be drained out quickly. These nodes will be exhausted soon and the network will be disconnected. Thus the balancing the traffic among the nodes is necessary and this can be archived by considering the residual energy of the node as one the metric in the routing strategy. In this paper we proposed a protocol (ELR), will choose the parent by considering link quality and residual energy of the node so, we can improve the lifetime of network.

The proposed algorithm (ELR) is implemented in TinyOS-2.X and tested with TOSSIM simulator, which can run the actual Tiny OS code without any real motes.

The rest of the paper is organized as follows: Section 2 gives introduction about Collection Tree protocol, Section 3 is survey of existing routing protocol, Section 4 describes proposed protocol and algorithm, Section 5 is performance analysis of proposed protocol (ELR), Section 6 gives the conclusion.

II. COLLECTION TREE PROTOCOL

CTP is routing protocol implemented in TinyOS-2.x. CTP uses routing messages (also called beacons) for tree construction and maintenance, and data messages to report application data to the sink. The standard implementation of CTP described in and evaluated in consists of three main logical software components: the Routing Engine (RE), the Forwarding Engine (FE), and the Link Estimator (LE). In the following, we will focus on the main role taken over by these three components.

Routing Engine [10]. The Routing Engine, an instance of which runs on each node, takes care of sending and receiving beacons as well as creating and updating the routing table. This table holds a list of neighbors from which the node can select its parent in the routing tree. The table is filled using the information extracted from the beacons. Along with the identifier of the neighboring nodes, the routing table holds further information, like a metric indicating the "quality" of a node as a potential parent.

In the case of CTP, this metric is the ETX (Expected Transmissions), which is communicated by a node to its neighbors through beacons exchange. A node having an ETX equal to n is expected to be able to deliver a data packet to the sink with a total of n transmissions, on average. The ETX of a node is defined as the "ETX of its parent plus the ETX of its link to its parent". More precisely, a node first computes, for each of its neighbors, the link quality of the current node-neighbor link. This metric, to which we refer to as the 1-hop ETX, or ETX1hop, is computed by the LE. For each of its neighbors the node then sums up the 1-hop ETX with the ETX the corresponding neighbors had declared in their routing beacons. The result of this sum is the metric which we call the multi-hop ETX, or ETXmhop. Since the ETXmhop of a neighbor quantifies the expected number of transmissions required to deliver a packet to a sink using that neighbor as a relay, the node clearly selects the neighbor corresponding to the lowest ETXmhop as its parent. The value of this ETXmhop is then included by the node in its own beacons so as to enable lower level nodes to compute their own ETXmhop. Clearly, the ETXmhop of a sink node is always 0.

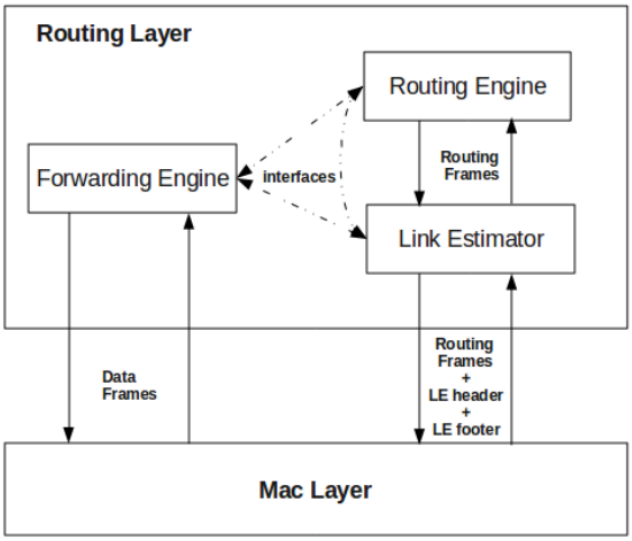

Fig. 1. Message flow and modules interaction [10]

Forwarding Engine [10]. The Forwarding Engine, as the name says, takes care of forwarding data packets which may either come from the application layer of the same node or from neighboring nodes. The FE is also responsible of detecting and repairing routing loops as well as suppressing duplicate packets.

Link Estimator [10]. The Link Estimator takes care of determining the inbound and outbound quality of 1-hop communication links. The LE computes the 1-hop ETX by collecting statistics over the number of beacons received and the number of successfully transmitted data packets. From these statistics, the LE computes the inbound metric as the ratio between the total number of beacons sent by the neighbor over the fraction of received beacons. Similarly, the outbound metric represents the expected number of transmission attempts required by the node to successfully deliver a data packet to its neighbor.

III. RELATED WORK

There are lots of researches done in improving collection tree protocol but only some of the protocols are addressing real life deployment of wireless sensor network. In literatures we found that routing decision is taken based on residual energy of only parent node.CTP is a pre-active routing protocol so energy value is not bound to only parent node but need to consider all the nodes in between sink node and source node. In our work we use min-max battery cost routing [8] to select route to sink node. And we used ELQR protocol as based paper for our research, ELQR protocol select parent based on 1-hop energy metric, we modify ELQR by multi-hop energy metric parameter because CTP is pre-active routing protocol so routing decision must be based on all hops in route.

3.1. RLQ: Resource Aware and Link Quality Based Routing Metric[3]

RLQ is routing protocol, for wireless sensor network. In RLQ routing decision is based on the link cost which is the sum of normalized energy cost for the transmitter and receiver. The energy cost depends on the energy consumption for transmission and reception, residual energy and the link quality. The weighing factors x and y are used to change the routing decision. If both are zero, the routing decision is based on the minimum hop count. If x=1 and y=0, the minimum total energy consumption path is the shortest path. If both x and y are 1, routing metric is based on both link quality and the residual energy of the node. This algorithm was tested in the test bed consisting of 21 Tmote sky nodes and the performance of RLQ is tested with shortest path algorithm, and LQI in terms of PRR, throughput and lifetime of the network.

3.2. LQER(Link Quality Estimation based Routing Protocol)[4]

The LQER protocol is a routing protocol with the objective of reliable data delivery in an energy efficient manner. LQER protocol makes the path selection based on the historical states of link quality after minimum hop field is established. In this paper, a dynamic window concept (m; k) is used to record the link historical information and which integrates the approach of minimum hop field. Here 'm' is the number of successful transmission over the link for the window size of 'k' previous transmissions.[6]

It uses Minimum Hop field establishment algorithm to find the minimum hop neighbors using flooding approach and each node will have the list of forwarding neighbors. Each node chooses its next hop candidate from this list, which are having best m/k value.

The LQER protocol is simulated in WSNSim for Mica2 platform and the performance parameters considered are energy efficiency and the packet success rate. The authors claim that the proposed algorithm performs better in terms of energy efficiency, packet loss rate and scalability.

3.3. Efficient and Multi-path protocol for Wireless Sensor Network [5]

[6]This protocol is designed for ensuring the QoS requirement of multimedia transmission such as throughput, delay etc. It is based on directed diffusion, which is scalable and uses single energy efficient path for data transmission. In multipath routing, disjoint multiple paths are chosen which are based on the link quality and the delay incurred in the path. The path cost for the selection of forwarding candidate is based on cumulative path_ETX and path_Delay. To get high throughput and low delay paths, the path cost is defined as

Path_Cost = Path_ETX ^{a} * Path_Dealy ^{b}

[6]The ETX based link quality is estimated from SNR value of the received packets and is calculated according to [12] and is given by ETX = 1/ (df * dr) where df and dr are the forward and reverse packet delivery ratio of the particular link. It is simulated in NS2 and provides high throughput and less delay, which are the requirement for the high quality video transmission

3.4. Energy And Link Quality Based Routing Tree (ELQR)[6]

In this paper, a protocol, takes the routing decision based on the link quality and the residual energy of the nodes. Each node will make one of its neighbours as its parent if the neighbor node has sufficient energy to forward the packet and the quality of the link to that node is good. A threshold is said for both parameters and the energy threshold is set well above 2V such that the lifetime of the node will be increased by reducing its load. The link quality increases with hop count and the node with less value will be chosen as the forwarding candidate. In this work, the threshold for the link quality is changed throughout the lifetime of the network to make the network alive by selecting the longer routes with more energy. Hence the routes with more energy and adequate wireless link quality will be chosen for the forwarding operation without exhausting the nodes in the optimal path. This algorithm is simulated on TOSSIM and it is tested on the test bed comprising of IRIS motes.

IV. ENERGY AWARE AND LINK QUALITY BASED ROUTING PROTOCOL (ELR)

This section outlines a routing protocol based on energy aware and link quality. ELR uses the link quality of wireless links and residual energy during the routing selection process to increase the system's reliability and assure QoS. It also provides mechanism to provide load balancing and avoid premature death of nodes/networks. We can improve current CTP by broadcasting new parameter called energy and maintaining this parameter to routing table for creation of tree.

The sink node is data gathering node and it broadcasts control packet periodically. It includes link quality parameter called ETX (Expected transmission) and residual energy.

ETX value is measured by link estimator engine. ETX of sink node is 0, because sink node does not have any parent node. Initially the energy of node is 100%. We take energy value in percentage because it is simple to carry percentage than joules value. Joule is unit of energy. To store and carry percentage value required only 2 bytes. This two parameter ETX and Residual energy is added in control packet. Sink node broadcast the control packet containing ETX value and energy value.

Figure 2 shows the procedure followed by the sink node for broadcasting a control packet. Sink node creates routing frame with ETX value, Energy value, etc. and broadcast control packet to its neighbor nodes.

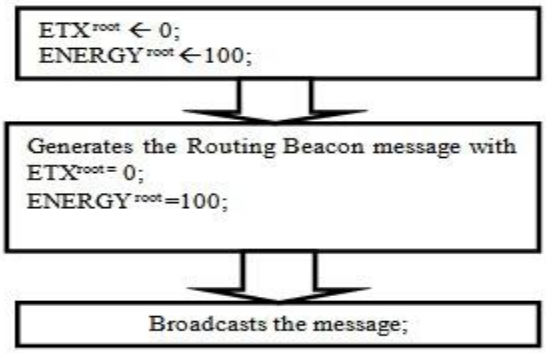

Fig2.Control Packer Broadcast

Figure 3 shows upon reception of control packet Sensor node (receiver) node extract control packet and get value of ETX and energy change their routing table entry to maintain tree. Sensor node(receiver) check the entry of sender node in routing table if node is present in routing table then only update the entry if node is not present in routing table then sensor node add entry to its routing table. Then after the sensor node will broadcast control packet to its neighbor nodes by obtaining new value of energy and ETX. Here energy is set to minimum energy of all nodes in route. This is similar to min-max battery cost routing [8]. Sensor node create control packet which contains information of ETX value and least energy value of all nodes in between to sink node.

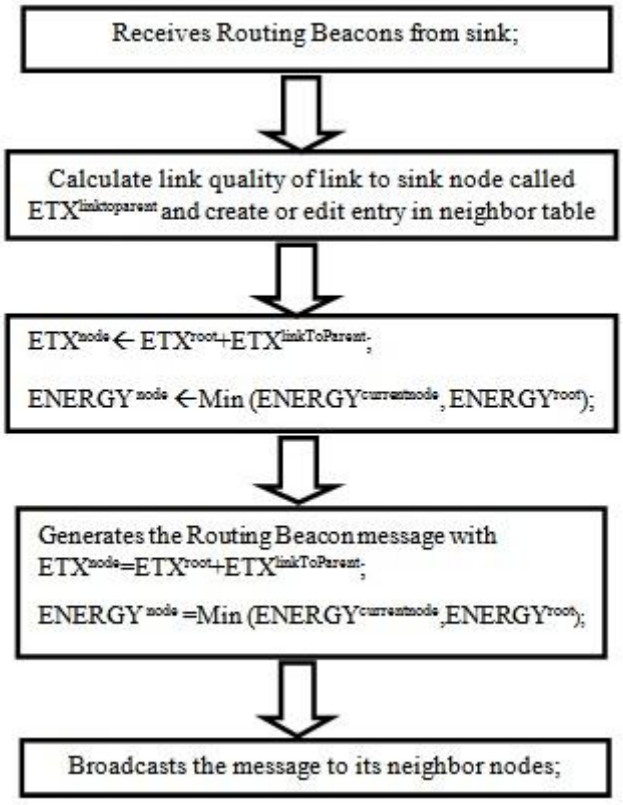

Fig.3. Control Packet Broadcast by sensor node

The limitations of node hardware and the quality variation of wireless links are great challenges to providing high service availability, especially in WSN applications, where it is necessary to create mechanisms that can identify and mitigate or solve the energy hole problem. Energy hole can be caused by congestion or overuse of route leading to the premature death of nodes. Routing solutions must be employed load balancing mechanisms that are able to divert traffic and thus increase QoS (less packet loss and delay rate) and reduce energy consumption. We create an algorithm to select parent based on two metric namely ETX and energy.

The best ETX route is selected by following algorithm:

Algorithm 1 Best ETX Route Selection Route Algorithm **bestETXRoute()**

```
1:  Let min ETX ←0xFFFF
2:  for RoutingTabel[i]
3:      if (min ETX > Routing Table[i].ETX)  & (Routing Table[i].valid)
4:          Min ETX ← Routing Table[i].ETX
5:          Ra← Routing Table[i].nodeid
6:      end if
7:  end for
8:  Return Ra
```

Fig.4. Algorithm for best ETX Route

In CTP route is selected based on only ETX value but we use ETX and residual energy of nodes to select best route. Algorithm 1 is used in CTP for finding best ETX path. We have used Algorithm 1, 2 and 3 for route selection.

The best Energy route is selected by following algorithm:

Algorithm 2 Best Energy Route Selection Route Algorithm **bestEnergyRoute()**

```
1:  Let maxEnergy ←0
2:  for RoutingTabel[i]
3:      if (maxenergy < Routing Table[i].energy)  & (Routing Table[i].valid)
4:          maxEnergy ← Routing Table[i].energy
5:          Rb← Routing Table[i].nodeid
6:      end if
7:  end for
8:  Return Rb
```

Fig.5. Algorithm for best Energy Route

The proposed algorithm (ELR) will select route based on link quality and residual energy of nodes. Algorithm 3 is proposed ELR protocol which select route to sink node.

In our algorithm, routing table has addition entry of energy which indicates least energy in route and control packet also carries this information. The algorithm searches for the node with the highest least energy node route among all the routes with minimum ETX, then that node will be taken as parent node. We used two threshold parameters E_{th} and $ETXdiff_{th}$. E_{th} is an energy threshold and $ETXdiff_{th}$ is ETX difference threshold. After selection of best ETX route and best energy route, algorithm find difference ETX. If difference ETX (ETX_{diff}) is less then $ETXdiff_{th}$ then best energy route will be selected. Otherwise further check for best ETX route has efficient energy to complete cycle of task. If best ETX route has energy greater then energy thresh hold, then best Energy route is selected otherwise best ETX route is set to invalid and it will be removed from selection of parent node and repeat cycle till algorithm does select a best route.

Algorithm 3 Selection Route Algorithm of ELR Protocol

```
1:  Let ETXdiff_th ← Expected Transmission Threshold
2:  Let E_th ←Energy Threshold
3:  Let Ra ←  bestETXRoute()
4:  Let Rb ← bestEnergyRoute()
5:  ETXdiff ← Rb.ETX – Ra.ETX
6:  if  Ra=Rb then
7:      SelectedRoute ← Ra
8:  else if ETXdiff ≤ ETXdiffth then
9:      SelectedRoute ← Rb
10: else
11:     if  Ra. energy ≤ Eth then
12:         Ra. valid ← False
13:         Repeat step 3
14:     end if
15: end if
```

Fig.6 Algorithm for ELR

V. IMPLEMENTATION OF ELR ALGORITHM

We implemented this algorithm in Tinyos-2.x in module ~\tos\lib\net\ctp. The energy consumption by sensor node is very challenging task because there is no tool to calculate energy consumption. We calculate remaining energy of nodes by software method. The energy used by sensor node is calculated runtime by tracking the time spent by components such as microcontroller, radio, sensor and memory. Each component consumes current. Energy consumption is calculated as
Energy=Current*Voltage*Time

Current and voltage depends on which mote we are using. In our implementation we take mote users manual [9] to calculate energy. In this manual we get value of current required by different modules (microcontroller, radio, sensor and memory). Figure 6[9] will show the system specification of all component of mote. Figure 7 shows the current required by components with duty cycle. Mote operates on 3V and radio in transmission mode take 12mA. If radio active for 1 ms then energy consumption is

Energy= $(12 * 10^{-3}) * (3) * (1 * 10^{*-3})$ joule
=36µjoule.

So like this we calculate energy spent by all components and deduct spent energy from initial energy to get remaining energy of node. For 2AA type battery capacity is 2000 joules initially.

SYSTEM SPECIFICATIONS		
Currents		**Example Duty Cycle**
Processor		
Current (full operation)	8 **mA**	1
Current sleep	8 µA	99
Radio		
Current in receive	8 mA	0.75
Current transmit	12 mA	0.25
Current sleep	2 µA	99
Logger Memory		
Write	15 mA	0
Read	4 mA	0
Sleep	2 µA	100
Sensor Board		
Current (full operation)	5 mA	1
Current sleep	5 µA	99

Fig. 7. System Specification.[9]

We add new parameter entry called energy in routing frame as well as in routing table. Figure 8 shows the routing frame with new parameter added energy.

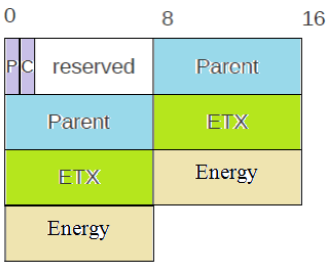

Fig. 8. Routing Frame.

The CtpRoutingEngine.nc is modified to implement ELR algorithm. We create new method Consumed Energy () to calculate consumed energy, which returns residual energy of mote and this is called periodically by the routing engine. The energy value is sent with the control packet and the nodes which receives control packet, will update their routing table with the updated energy value. The routing decision is modified according to ELR algorithm in the Update Route task.

The energy Threshold is set to 10%. When nodes have battery capacity less than 10% it will not work as intermediate node but it is able to send its own packet till death. The ETXdiffTh is set to 10.We can also change this threshold value because it is about link quality.

VI. PERFORMANCE ANALYSIS

We use TOSSIM simulator for test proposed protocol under Linux. TOSSIM is simulator for tiny OS developed by university of California at Berekely, USA, Which can run the actual tinyOS code without any motes[7][6].The hardware components are simulated using software at packet level and code developed for this simulator can be directly fused into the motes with minimum changes.

The simulation parameter used for creating the network topology is given below. The nodes are placed in uniform topology.

Parameter	**Value**
No. of Nodes	100
Topology	Uniform, Random
Size	500*500
Simulation Time in Seconds	1000,2000,4000,6000,8000,10000
Radio Model	Indoor
Initial Battery Capacity	100mA–hour

Table 1. Simulation Parameters

6.1. Simulation Results

The figure 9 shows the PRR value for two protocols with the simulation time from 1000 to 10000 seconds. X-axis shows the simulation time and Y-axis shows the packet reception ratio. The PRR value of proposed scheme is compared to the CTP protocol. The PRR value of the CTP protocol is almost same as ELR initially, but decreases as time advances. This is due to high link quality nodes are dead as time passed. But in ELR protocol load is distributed among all nodes, so we can get high packet reception ratio than CTP.

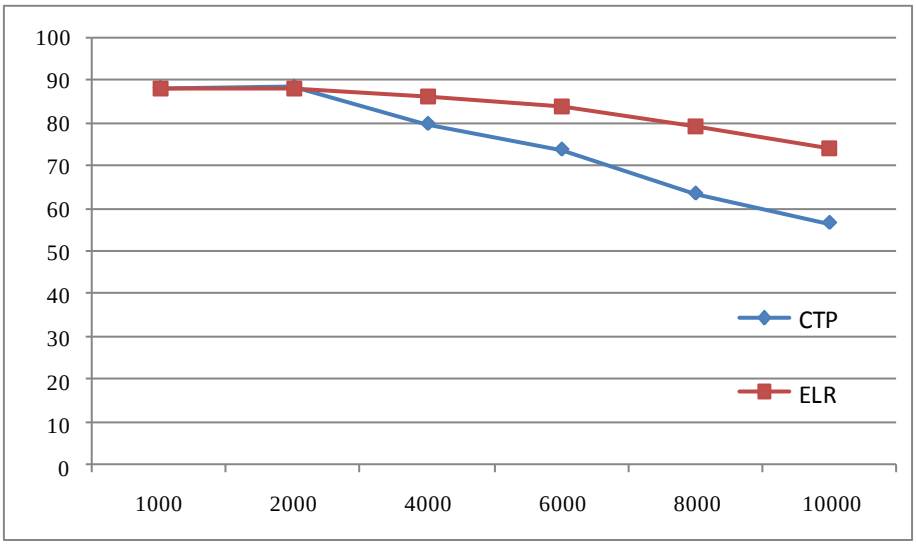

Fig. 9. Packet Reception Ratio

The Number of node alive over the simulation time is measured and shown in the figure 10. X-axis shows the simulation time and Y-axis shows the number of nodes alive. The time at which first node dies, is also calculated for CTP and ELR which are 2498 and 4596 seconds respectively. This result shows that network life is increased due to load balancing in ELR protocol.

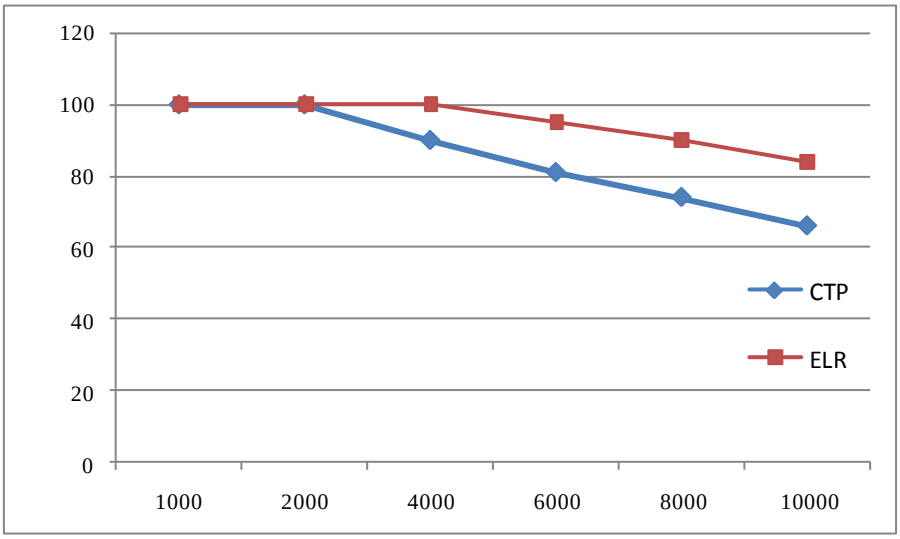

Fig. 10. Number of nodes alive

Figure 11 shows control packet overhead ratio value for two protocols for the simulation times from 1000 to 10000 seconds. X-axis shows the simulation time and Y-axis shows the control packet overhead ratio. In ELR control packet overhead is greater than CTP. This is due to receiving more recent updated energy value.

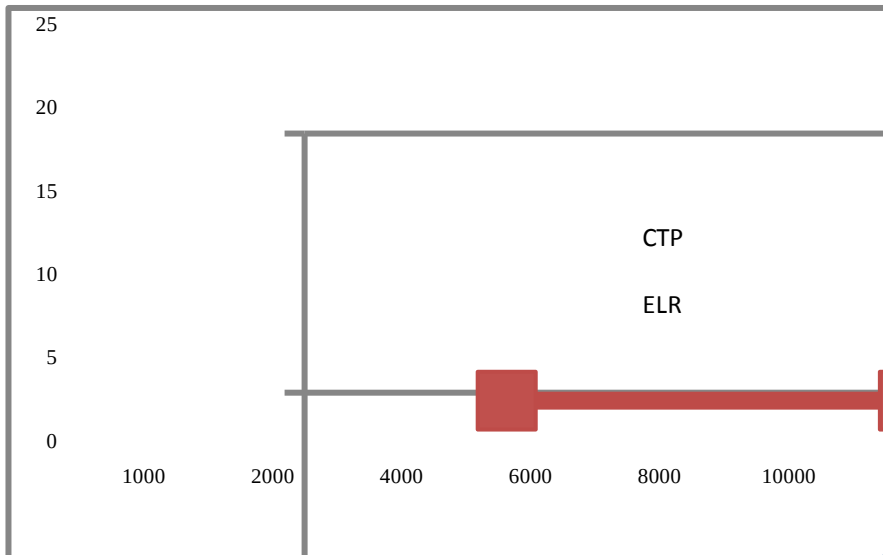

Fig. 11. Control Packet Overhead Ratio

Figure 12 shows the data packet retransmission ratio. X-axis shows the simulation time, Y-axis shows the retransmission ratio. The data packet retransmission increases as time is increased. The data packet retransmission ratio of CTP is almost same as ELR initially, but increases as time advances. This is because the node dies as time passes. Due to increased retransmission ratio delay increased in reception. Quality of service decreases if delay is increased.

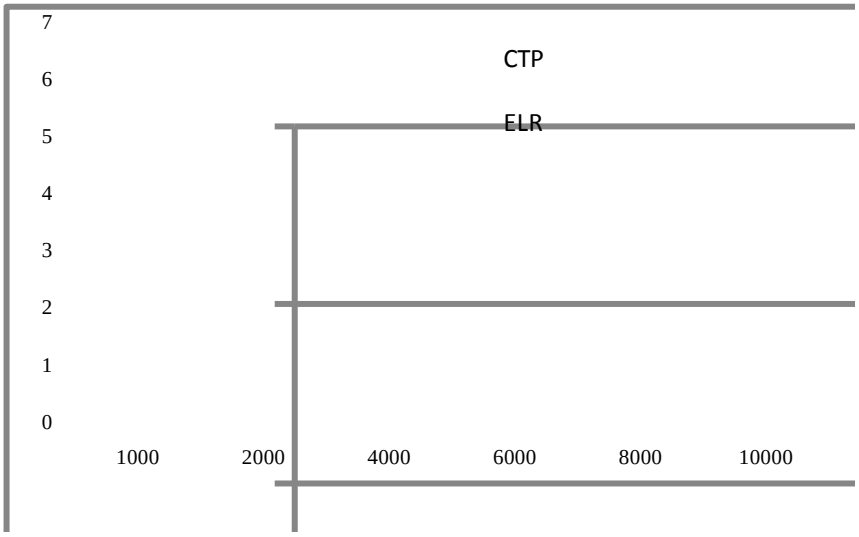

Fig. 12. Data Packet Retransmission Ratio

VII. CONCLUSION

Energy is an important resource in WSN. To increase network lifetime, the traffic load should be distributed among the forwarding nodes in such a way that they could be alive for a long time. In this paper, we proposed a protocol, which take the routing decision based on the link quality and the energy of nodes. Every node contains energy entry in routing table which indicates least energy node in route. We got this idea from min-max battery cost routing. Each node will make one of its neighbors as its parent if the parent has route to sink having efficient energy and good link. We found in our result that ELR protocol increases network lifetime by load balancing among forwarding nodes. The result shows that PRR is increased, Data packet retransmission is decreased and more number of nodes are alive than CTP with some overhead of control packet. The limitation of ELR and CTP is that PRR decreases if nodes are mobile.

REFERENCES

[1] I.Akyldiz, W. Su. Y.Sankarasubramanian and E. Cayirci(2000), "A Survey on Sensor Networks", IEEE Communication Magazine Vol. 40, No. 8, pp. 103 -114.
[2] P. Levis, S. Madden, D. Gay, J. Polastre, R. Szewczyk, K. Whitehouse, A. Woo, D. Gay, J. Hill, M. Welsh, E. Brewer and D. Culler (2005), "TinyOS: an operating system for sensor networks", Ambient Intelligence, Springer-verlag, pp. 115–148.
[3] V. Cagri Gungor, Chellury Sastry, Zhen Song and Ryan Integlia(2007), "Resource-Aware and Link Quality Based Routing Metric for Wireless Sensor and Actor Networks", IEEE International Conference on Communications, ICC '07, pp. 3364-3369.
[4] Chen J., Lin R., Li Y., Sun Y. (2008), "LQER: A Link Quality Estimation based Routing for Wireless Sensor Networks", Sensors. vol. 8, issue. 2, pp. 1025-1038.
[5] Shuang Li, Raghu Kisore Neelisetti, Cong Liu, and Alvin Lim (2010), "Efficient Multi-path protocol for Wireless Sensor Networks", Int. Jr. of Wireless & Mobile Networks, vol.2, No.1, pp. 110-130
[6] K. Pavai, D. Sridharan, S.A.V. Satya Murty A. Sivagami, "Energy and Link Quality Based Routing for Data Gathering Tree in Wireless Sensor Networks Under TINYOS -2.X," International Journal of Wireless & Mobile Networks, vol. 2, no. 2, pp. 47-60, 2010.
[7] Philip Levis, Nelson Lee, Matt Welsh, and David Culler (2003), "TOSSIM: Accurate and Scalable Simulation of Entire TinyOS Applications.' In Proceedings of the First ACM Conference on Embedded Networked Sensor Systems (SenSys 2003) pp. 126-137
[8] C-K. Toh, Hiroshi cob, and David A. Scott, "Performance Evaluation of Battery-life-Aware Routing Schemes for Wireless Ad Hoc Network" 2001 IEEE
[9] Mote Processor radio &Mote Interface boards user manual. Document part number: 7430-0021-09 Rev A [online:] http://www.cs.wmich.edu/gupta/teaching/cs5950/fall2011/mica%20pinouts%20from%20memsic%20mpr-mib_series_users_manual%207430-0021-09_a-t.pdf
[10] Collection Tree Protocol for Castalia for wireless sensor network simulator [Link:] https://ctp-castalia.googlecode.com/files/colesanti_santinis_2011_ctp-castalia.pdf

International Journal of Modern Engineering Research (IJMER)
www.ijmer.com Vol.3, Issue.3, May-June. 2013 pp-1366-1371 ISSN: 2249-6645

Strength of Blended Cement Sandcrete & Soilcrete Blocks Containing Afikpo Rice Husk Ash and Corn Cob Ash

L. O. Ettu, [1] K. C. Nwachukwu, [2] J. I. Arimanwa, [3] T. U. Anyanwu, [4]
S. O. Okpara[5]
[1,2,3,4]*Department of Civil Engineering, Federal University of Technology, Owerri, Nigeria*
[5]*Department of Building Technology, AkanuIbiam Federal Polytechnic, Unwana, Nigeria*

Abstract: *This work investigated the compressive strength of binary and ternary blended cementsandcrete and soilcreteblocks containing Afikpo rice husk ash (RHA) and corn cob ash (CCA). 135 solid sandcrete blocks and 135 solid soilcrete blocks of 450mm x 225mm x 125mm were produced with OPC-RHAbinary blended cement, 135with OPC-CCAbinary blended cement, and 135with OPC-RHA-CCAternary blended cement, each at percentage OPC replacement with pozzolan of 5%, 10%, 15%, 20%, and 25%.Three sandcrete blocks and three soilcreteblocks for each OPC-pozzolan mix and the control were crushed to obtain their compressive strengths at 3, 7, 14, 21, 28, 50, 90, 120, and 150 days of curing. Binary and ternary blended cement sandcrete and soilcrete block strength values were found to be higher than the control values beyond 50 days of hydration at 5-20% OPC replacement with pozzolan. The 150-day strength values for OPC-RHA-CCA ternary blended cement sandcreteand soilcrete blocks were respectively 6.10N/mm^{2}and 5.30N/mm^2 for 5% replacement, 6.00N/mm^{2}and 5.20N/mm^2 for 10% replacement, 5.85N/mm^{2}and 5.00N/mm^{2}for 15% replacement,5.70N/mm^{2}and 4.95N/mm^{2}for 20% replacement, and 5.35N/mm^{2}and 4.85N/mm^{2}for 25% replacement; while the control values were 5.20N/mm^2 and 4.80N/mm^2. Thus, OPC-RHA and OPC-CCA binary blended cements as well as OPC-RHA-CCA ternary blended cement could be used in producing sandcrete and soilcrete blocks with sufficient strength for use in building and minor civil engineering works where the need for high early strength is not a critical factor.*

KeyWords: *Binary blended cement, corn cob ash, pozzolan, rice husk ash, sandcrete block, soilcrete block, ternary blended cement.*

I. Introduction

Sandcrete and soilcrete blocks are cement composites commonly used as walling units in buildings all over South Eastern Nigeria and many other parts of Africa. The major constituents of sandcrete are water, cement, and sand while those of soilcrete are water, cement, and natural soil, especially laterite. These important construction materials have been greatly investigated by many researchers. Mama and Osadebe (2011) developed a mathematical model for optimizing the strength of laterizedsandcrete blocks. Joshua and Lawal (2011) successfully replaced sand with laterite in suitable optimal percentages to produce laterizedsandcrete blocks with adequate strength and more cost effectiveness than the traditional sandcrete blocks. Wenapereand Ephraim (2009) found that the compressive strength of sandcrete blocks increased with age of curing for all mixes tested at the water-cement ratio of 0.5. Their findings showed that the strength at ages 7, 14, and 21 days were 43%, 75%, and 92% of the 28-day strength respectively. Baiden and Tuuli (2004) confirmed that mix ratio, materials quality, and mixing of the constituent materials affect the quality of sandcrete blocks.

Within the past decade researchers in this field have focused largely on finding ways of reducing the cost of cement used in sandcrete and soilcrete block production so as to provide low-cost buildings in the suburbs and villages of South Eastern Nigeria and other places. For this reason agricultural by-products regarded as wastes in technologically underdeveloped societies are increasingly being investigated as partial replacement of Ordinary Portland Cement (OPC) in binary blended cement systems. Manasseh (2010) carried out an elaborate review of some of the commonest agro wastes that have been experimented as cement replacement in sandcrete making and found some of them such as rice husk ash (RHA) suitable. Apata and Alhassan (2012) recently evaluated locally available materials as partial replacement for cement and concluded that partial replacement of these local materials with 10% OPC can be adopted for low cost housing. Okpala (1993) had partially substituted cement with RHA in the percentage range of 30–60% at intervals of 10% while considering the effect on some properties of sandcrete blocks. His results revealed that up to 40% cement replacement would still be suitable for a sandcrete mix of 1:6 (cement/sand ratio) while up to 30%replacement would be suitable for a mix of 1:8. Aribisala and Bamisaye (2006) reported the successful use of bone powder as partial replacement for cement in concrete. Marthong (2012) used sawdust ash (SDA) as partial replacement of cement in sandcrete. Ganesan, Rajagopal, and Thangavel (2008) assessed the optimal level of replacement of OPC with RHA for strength and permeability properties of blended cement concrete. Nair, Jagadish, and Fraaij (2006) found that RHA could be a suitable alternative to OPC for rural housing.

Cisse and Laquerbe (2000) reported that sandcrete blocks obtained with unground Senegalese RHA as partial replacement of OPC had greater mechanical resistance than 100% OPC sandcrete blocks. Their study also revealed that the use of unground RHA enabled production of lightweight sandcrete block with insulating properties at a reduced cost. Agbede and Obam (2008) investigated the strength properties of OPC-RHA blended sandcrete blocks. They replaced various percentages of OPC with RHA and found that up to 17.5% of OPC can be replaced with RHA to produce good quality sandcrete blocks. Oyekan and Kamiyo (2011) reported thatsandcrete blocks made with RHA-blended cement had lower heat

storage capacity and lower thermal mass than 100% OPC sandcrete blocks. They explained that the increased thermal effusivity of the sandcrete block with RHA content is an advantage over 100% OPC sandcrete block as it enhances human thermal comfort. Wada et al. (2000) demonstrated that RHA mortar and concrete exhibited higher compressive strength than the control mortar and concrete. Mehta and Pirtz (2000) investigated the use of rice husk ash to reduce temperature in high strength mass concrete and concluded that RHA is very effective in reducing the temperature of mass concrete compared to OPC concrete. Sakr (2006) investigated the effects of silica fume and rice husk ash on the properties of heavy weight concrete and found that these pozzolans gave higher concrete strengths than OPC concrete at curing ages of 28 days and above. Malhotra and Mehta (2004) reported that ground RHA with finer particle size than OPC improves concrete properties as higher substitution amounts result in lower water absorption values and the addition of RHA causes an increment in the compressive strength. Cordeiro, Filho, and Fairbairn (2009) investigated Brazilian RHA and rice straw ash (RSA) and demonstrated that grinding increased the pozzolanicity of RHA and that high strength of RHA, RSA concrete makes production of blocks with good bearing strength in a rural setting possible. Their study showed that combination of RHA or RSA with lime produces a weak cementitious material which could however be used to stabilize laterite and improve the bearing strength of the material. Rukzon, Chindaprasirt, and Mahachai (2009) studied the effect of grinding on the chemical and physical properties of rice husk ash and the effects of RHA fineness on properties of mortar and found that pozzolans with finer particles had greater pozzolanic reaction. Habeeb and Fayyadh (2009) also investigated the influence of RHA average particle size on the properties of concrete and found that at early ages the strength was comparable, while at the age of 28 days finer RHA exhibited higher strength than the sample with coarser RHA. Cordeiro, Filho, and Fairbairn (2009) further investigated the influence of different grinding times on the particle size distribution and pozzolanic activity of RHA obtained by uncontrolled combustion in order to improve the performance of the RHA. The study revealed the possibility of using ultrafine residual RHA containing high-carbon content in high-performance concrete.

Some researchers have also investigated the possibility of ternary blended cement systems whereby OPC is blended with two different pozzolans. The ternary blended system has two additional environmental and economic advantages. First, it enables a further reduction of the quantity of OPC in blended cements. Second, it makes it possible for two pozzolans to be combined with OPC even if neither of them is available in very large quantity. Frı´as et al. (2005)studied the influence of calcining temperature as well as clay content in the pozzolanic activity of sugar cane straw-clay ashes-lime systems. All calcined samples showed very high pozzolanic activity and the fixation rate of lime varied with calcining temperature and clay content. Elinwa, Ejeh, and Akpabio (2005) investigated the use of sawdust ash in combination with metakaolin as a ternary blend with 3% added to act as an admixture in concrete. Tyagher, Utsev, and Adagba (2011) found that sawdust ash-lime mixture as partial replacement for OPC is suitable for the production of sandcrete hollow blocks. They reported that 10% replacement of OPC with SDA-lime gave the maximum strength at water-cement ratio of 0.55 for 1:8 mix ratio.Fadzil et al. (2008)studied the properties of ternary blended cementitious (TBC) systems containing OPC, ground Malaysian RHA, and fly ash (FA). They found that compressive strength of concrete containing TBC gave low strength at early ages, even lower than that of OPC, but higher than binary blended cementitious (BBC) concrete containing FA. Their results suggested the possibility of using TBC systems in the concrete construction industry and that TBC systems could be particularly useful in reducing the volume of OPC used. Rukzon and Chindaprasirt (2006) investigated the strength development of mortars made with ternary blends of OPC, ground RHA, and classified fly ash (FA). The results showed that the strength at the age of 28 and 90 days of the binary blended cement mortar containing 10 and 20% RHA were slightly higher than those of the control, but less than those of FA. Ternary blended cement mixes with 70% OPC and 30% of combined FA and RHA produced strengths similar to that of the control. The researchers concluded that 30% of OPC could be replaced with the combined FA and RHA pozzolans without significantly lowering the strength of the mixes.

Most of the previous researches on ternary blended cements were based on the ternary blending of OPC with an industrial by-product pozzolan such as FA or silica fume (SF) and an agricultural by-product pozzolan, especially RHA. Tons of agricultural wastes such as rice husk and corn cobare generated in Afikpo district and some othercommunities in South Eastern Nigeria due to intensified food production and local economic ventures. Not much has been reported on the possibility of binary combination of these Nigerian agricultural by-products with OPC in developing blended cements and no literature exists on the possibility of ternary blending of two of them with OPC. This work is part of a pioneer investigation of the suitability of using two Nigerian agricultural by-products in ternary blend with OPC for sandcrete and soilcreteblock making. The compressive strength of binary and ternary blended cementsandcrete and soilcreteblocks containing Afikpo rice husk ash and corn cob ash was specifically investigated. It is hoped that the successful utilization of Afikpo rice husk ash and corn cob ash in binary and ternary combination with OPC for making sandcrete and soilcreteblocks would help in reducing the cost of building and minor civil engineering projects that make much use of sandcrete and soilcrete blocks as well asadd economic value to these wastes.

II. Methodology

Rice husk was obtained from rice milling factories in Afikpo district ofEbonyi Stateand corn cob from Aba district in Abia State, both in South East Nigeria. These materials were air-dried, pulverized into smaller particles, and calcined into ashes in a locally fabricated furnace at temperatures generally below 650^{o}C. The rice husk ash (RHA) and corn cob ash (CCA) were sieved and large particles retained on the 600µm sieve were discarded while those passing the sieve were used for this work. No grinding or any special treatment to improve the quality of the ashes and enhance their pozzolanicity was applied.The RHA had a bulk density of 760 Kg/m^3, specific gravity of 1.81, and fineness modulus of 1.40. The CCA had a bulk density of 800 Kg/m^3, specific gravity of 1.90, and fineness modulus of 2.02. Other materials used for this work are

Ibeto brand of Ordinary Portland Cement (OPC) with a bulk density of 1650 Kg/m^3 and specific gravity of 3.13; river sand free from debris and organic materials with a bulk density of 1590 Kg/m^3, specific gravity of 2.68, and fineness modulus of 2.82;laterite also free from debris and organic materials with a bulk density of 1450 Kg/m^3, specific gravity of 2.30, and fineness modulus of 3.30; and water free from organic impurities.

A simple form of pozzolanicity test was carried out for each of the ashes. It consists of mixing a given mass of the ash with a given volume of Calcium hydroxide solution [$Ca(OH)_2$] of known concentration and titrating samples of the mixture against H_2SO_4 solution of known concentration at time intervals of 30, 60, 90, and 120 minutes using Methyl Orange as indicator at normal temperature. For each of the ashes the titre value was observed to reduce with time, confirming the ash as a pozzolan that fixed more and more of the calcium hydroxide, thereby reducing the alkalinity of the mixture.

A standard mix ratio of 1:6 (blended cement: sand (or laterite)) was used for both the sandcrete and the soilcrete blocks. Batching was by weight and a constant water/cement ratio of 0.6 was used. Mixing was done manually on a smooth concrete pavement. For binary blending with OPC, each of the ashes was first thoroughly blended with OPC at the required proportion and the homogenous blend was then mixed with the sand in the case of sandcrete blocks and with laterite in the case of soilcrete blocks, also at the required proportions. For ternary blending, the two ashes were first blended in equal proportions and subsequently blended with OPC at the required proportions before mixing with the sand or laterite, also at the required proportions. Water was then added gradually and the entire sandcreteor soilcreteheap was mixed thoroughly to ensure homogeneity.

One hundred and thirty-five (135) solid sandcrete blocks and one hundred and thirty-five (135) solid soilcrete blocks of 450mm x 225mm x 125mm were produced with OPC-RHAbinary blended cement, one hundred and thirty-five (135) with OPC-CCAbinary blended cement, and one hundred and thirty-five (135) with OPC-RHA-CCAternary blended cement, each at percentage OPC replacement with pozzolan of 5%, 10%, 15%, 20%, and 25%. Twenty seven (27) sandcreteblocks and twenty seven (27) soilcrete blocks were also produced with 100% OPC or 0% replacement with pozzolan to serve as control. This gives a total of 432 sandcrete blocks and 432 soilcrete blocks.All the blocks were cured by water sprinkling twice a day in a shed. Three sandcrete blocks and three soilcreteblocks for each OPC-pozzolan mix and the control were tested for saturated surface dry bulk density and crushed to obtain their compressive strengths at 3, 7, 14, 21, 28, 50, 90, 120, and 150 days of curing.

III. Results and Discussion

The pozzolanicity test confirmed both the RHA and the CCA as pozzolans since they fixed some quantities of lime over time. The particle size analysis showed that both ashes were much coarser than OPC, the reason being that they were not ground to finer particles. This implies that the compressive strength values obtained using them could still be improved upon if the ashes are ground to finer particles. The compressive strengths of the OPC-RHA and OPC-CCA binary blended cement sandcrete and soilcrete blocks as well as the OPC-RHA-CCA ternary blended cement sandcrete and soilcreteblocks are shown in tables 1, 2, and 3 for 3-14 days, 21-50 days, and 90-150 days of curing respectively.

Tables 1, 2, and 3 show that the strength values for OPC-RHA and OPC-CCA binary blended cement sandcrete and soilcrete blocks as well as those of OPC-RHA-CCA ternary blended cement sandcrete and soilcrete blocks were all less than the equivalent control values at 3-28 days of hydration for all percentage replacements of OPC with pozzolans. The strength values of the binary and ternary blended cement sandcrete and soilcrete blocks were the same with the equivalent control values at about 50 days of hydration and greater than the control values at curing ages beyond 50 days. The 150-day strength values for OPC-RHA-CCA ternary blended cement sandcreteand soilcrete blocks were respectively 6.10N/mm^{2}and 5.30N/mm^2 for 5% replacement, 6.00N/mm^{2}and 5.20N/mm^2 for 10% replacement, 5.85N/mm^{2}and 5.00N/mm^{2}for 15% replacement, 5.70N/mm^{2}and 4.95N/mm^{2}for 20% replacement, and 5.35N/mm^{2}and 4.85N/mm^{2}for 25% replacement; while the control values were 5.20N/mm^2 and 4.80N/mm^2. The lower strength values of blended cement sandcrete and soilcrete blocks at earlier days of hydration show that pozzolanic reaction was not yet much at those earlier periods; the pozzolanic reaction became higher at later curing ages and this accounts for the much increase in strength of blended cement sandcrete and soilcrete blocks compared to the control specimens.

Table 1. Compressive strength of blended OPC-RHA-CCA cement sandcrete and soilcreteblocks at 3-14 days of curing

OPC Plus	Compressive Strength of sandcrete blocks (N/mm^2)						Compressive Strength of soilcrete blocks (N/mm^2)					
	0% Poz.	5% Poz.	10% Poz.	15% Poz.	20% Poz.	25% Poz.	0% Poz.	5% Poz.	10% Poz.	15% Poz.	20% Poz.	25% Poz.
	Strength at 3 days											
RHA	0.90	0.70	0.60	0.55	0.50	0.45	0.80	0.60	0.50	0.45	0.35	0.30
CCA	0.90	0.65	0.60	0.50	0.45	0.40	0.80	0.55	0.50	0.40	0.35	0.30
RHA & CCA	0.90	0.65	0.60	0.50	0.50	0.40	0.80	0.60	0.55	0.45	0.35	0.30
	Strength at 7 days											
RHA	1.50	1.30	1.20	1.15	1.00	0.90	1.30	1.10	1.00	0.90	0.80	0.65

CCA	1.50	1.25	1.20	1.10	0.95	0.90	1.30	1.05	1.00	0.80	0.75	0.60
RHA & CCA	1.50	1.25	1.20	1.10	1.00	0.90	1.30	1.10	1.00	0.85	0.80	0.60
	Strength at 14 days											
RHA	2.70	2.40	2.30	2.20	2.05	1.90	2.30	2.00	1.90	1.80	1.65	1.50
CCA	2.70	2.35	2.25	2.10	2.00	1.90	2.30	1.90	1.80	1.75	1.60	1.50
RHA & CCA	2.70	2.35	2.25	2.15	2.00	1.90	2.30	1.95	1.90	1.75	1.60	1.55

Table 2. Compressive strength of blended OPC-RHA-CCA cement sandcrete and soilcreteblocks at 21-50 days of curing

OPC Plus	**Compressive Strength of sandcrete blocks (N/mm^2)**						**Compressive Strength of soilcrete blocks (N/mm^2)**					
	0% Poz.	**5% Poz.**	**10% Poz.**	**15% Poz.**	**20% Poz.**	**25% Poz.**	**0% Poz.**	**5% Poz.**	**10% Poz.**	**15% Poz.**	**20% Poz.**	**25% Poz.**
	Strength at 21 days											
RHA	3.50	3.25	3.15	3.10	3.00	2.80	3.10	2.80	2.70	2.60	2.55	2.40
CCA	3.50	3.15	3.05	3.00	2.90	2.70	3.10	2.70	2.65	2.50	2.40	2.30
RHA & CCA	3.50	3.20	3.10	3.00	2.90	2.75	3.10	2.70	2.65	2.50	2.45	2.30
	Strength at 28 days											
RHA	4.40	4.20	4.10	4.05	3.90	3.75	3.90	3.70	3.55	3.50	3.40	3.30
CCA	4.40	4.10	3.90	3.80	3.75	3.60	3.90	3.50	3.45	3.35	3.30	3.25
RHA & CCA	4.40	4.10	3.90	3.90	3.85	3.65	3.90	3.60	3.50	3.40	3.35	3.25
	Strength at 50 days											
RHA	4.70	4.70	4.60	4.55	4.50	4.30	4.30	4.50	4.45	4.30	4.10	4.00
CCA	4.70	4.60	4.50	4.40	4.35	4.20	4.30	4.40	4.30	4.25	4.05	3.95
RHA & CCA	4.70	4.60	4.55	4.40	4.40	4.30	4.30	4.40	4.30	4.25	4.10	4.00

Table 3. Compressive strength of blended OPC-RHA-CCA cement sandcrete and soilcreteblocks at 90-150 days of curing

OPC Plus	**Compressive Strength of sandcrete blocks (N/mm^2)**						**Compressive Strength of soilcrete blocks (N/mm^2)**					
	0% Poz.	**5% Poz.**	**10% Poz.**	**15% Poz.**	**20% Poz.**	**25% Poz.**	**0% Poz.**	**5% Poz.**	**10% Poz.**	**15% Poz.**	**20% Poz.**	**25% Poz.**
	Strength at 90 days											
RHA	4.90	5.25	5.10	5.00	4.90	4.80	4.50	4.90	4.80	4.65	4.60	4.45
CCA	4.90	5.10	5.00	4.90	4.80	4.65	4.50	4.85	4.75	4.60	4.55	4.30
RHA & CCA	4.90	5.20	5.10	4.90	4.85	4.70	4.50	4.90	4.75	4.60	4.55	4.30
	Strength at 120 days											
RHA	5.10	5.95	5.70	5.60	5.45	5.25	4.70	5.30	5.10	5.00	4.95	4.80
CCA	5.10	5.80	5.60	5.50	5.40	5.15	4.70	5.10	5.00	4.95	4.80	4.65
RHA & CCA	5.10	5.90	5.60	5.50	5.40	5.20	4.70	5.20	5.00	5.00	4.85	4.70
	Strength at 150 days											
RHA	5.20	6.25	6.10	5.90	5.75	5.45	4.80	5.50	5.30	5.10	5.00	4.90
CCA	5.20	6.00	5.90	5.80	5.70	5.30	4.80	5.25	5.15	5.00	4.90	4.85
RHA & CCA	5.20	6.10	6.00	5.85	5.70	5.35	4.80	5.30	5.20	5.00	4.95	4.85

It can also be seen from tables 1-3 that the strength values of OPC-RHA binary blended cement sandcrete and soilcreteblocks were consistently greater than those of OPC-CCA binary blended cementsandcrete and soilcreteblocks for all percentage replacements of OPC with pozzolans at all curing ages. This shows that RHA has a higher pozzolanic reactivity than CCA. The strength of the OPC-RHA-CCA ternary blended cement sandcrete and soilcreteblocks was consistently in-between the values of the OPC-RHA and OPC-CCA binary blended cement sandcrete and soilcrete blocks. Therefore, more RHA than CCA should be utilized if the two pozzolans are to be used in unequal proportions to optimize the strength of the OPC-RHA-CCA ternary blended cement sandcrete and soilcrete blocks. However, the closeness in strength values of OPC-RHA and OPC-CCA binary blended cement sandcrete and soilcrete blocks and the fact that the strength of the OPC-RHA-CCA ternary blended cement sandcrete and soilcreteblocks was in-between these values suggests that the two agricultural by-product pozzolans could be combined in any available proportions individually in binary blending or together in ternary blending with OPC in making blended cement sandcrete and soilcrete blocks.

The results in tables 1 to 3 further show that the values of soilcreteblock strength are consistently less than the corresponding values of sandcrete block strength for all percentages of OPC replacement with pozzolans and at all curing ages. This confirms that sand is better than laterite as fine aggregate material in making cement composites. However, a close examination of the results shows that the values of the soilcrete block strengths are not much different from those of sandcrete block strengths. For example, the 50-day strengths are 4.70N/mm^2 for sandcrete block and 4.30N/mm^2 for soilcrete block at 100% OPC and 4.55N/mm^2 for sandcrete block and 4.30N/mm^2 for soilcrete block at 10% replacement of OPC with RHA-CCA in ternary blending. This also confirms that laterite could be used as sole fine aggregate in making cement composites for low-cost houses in communities where sharp sand is difficult to obtain at affordable prices.

IV. Conclusions

OPC-RHA and OPC-CCA binary blended cement sandcrete and soilcreteblocks as well as OPC-RHA-CCA ternary blended cementsandcrete andsoilcreteblocks have compressive strength values less than those of 100% OPC sandcrete and soilcreteblocks for 5-25% replacement of OPC with pozzolans at 3-28 days of hydration. The blended cement sandcrete and soilcreteblock strength values become equal to the control values at about 50 days of curing and greater than the control values beyond 50 days of hydration. Thus, OPC-RHA and OPC-CCA binary blended cements as well as OPC-RHA-CCA ternary blended cement could be used in producing sandcrete and soilcreteblocks with sufficient strength for use in building and minor civil engineering works where the need for high early strength is not a critical factor.

The strength of OPC-RHA binary blended cement sandcrete and soilcreteblocks is consistently greater than that of OPC-CCA binary blended cement specimens for all percentage replacements of OPC with pozzolansand at all curing ages. The strength values of OPC-RHA-CCA ternary blended cement sandcrete and soilcreteblocks were consistently in-between the values of OPC-RHA and OPC-CCA binary blended cement sandcrete and soilcrete blocks. This suggests that more RHA should be used than CCA if the two pozzolans were to be used in unequal proportions to optimize the strength of the OPC-RHA-CCA ternary blended cementsandcrete and soilcrete blocks.

Moreover, the closeness in strength values of OPC-RHA and OPC-CCA binary blended cement sandcrete blocks (this closeness was also observed for soilcrete blocks) and the fact that the strength of the OPC-RHA-CCA ternary blended cement sandcrete blocks was in-between these values suggests that the two agricultural by-product pozzolans could be combined in any available proportions individually in binary blending or together in ternary blending with OPC in making blended cement sandcrete and soilcrete blocks for use in various Nigerian communities.

The strength values of soilcrete blocks were found to be less than those of sandcrete blocks for all percentages of OPC replacement with pozzolans and at all curing ages. Therefore, sand should be used in preference to laterite for making cement blocks. However, since the soilcrete block strengths were not much less than the equivalent sandcrete block strengths, good quality laterite could still be used for block making in the various communities where sand is scarce and unaffordable to the rural populace.

References

[1] Agbede, I. O., &Obam, S. O. (2008). Compressive Strength of Rice Husk Ash-Cement Sandcrete Blocks.Global Journal of Engineering Research, Vol. 7 (1), pp. 43-46.

[2] Apata.A.O. And Alhassan, A. Y. (2012).Evaluating Locally Available Materials as PartialReplacement for Cement.Journal of Emerging Trends in Engineering and Applied Sciences (JETEAS), 3 (4): 725-728.

[3] Aribisala, O.J. and Bamisaye, A. J. (2006).Viability of Bone Powder (BP) As PartialReplacement for Cement in Concrete.Botswana Journal of Technology, 15 (1): 22-26.

[4] Baiden, B. K. and Tuuli, M. M. (2004). Impact of quality control practices in sandcrete blocks production. Journal of Architectural Engineering, 10 (2): 53-60.

[5] Cisse, I. K., &Laquerbe, M. (2000).Mechanical characterization of sandcretes with rice huskash additions: study applied to Senegal. Cement and Concrete Research, 30 (1): 13– 18.

[6] Cordeiro, G. C., Filho, R. D. T., & Fairbairn, E. D. R. (2009). Use of ultrafine saw dust ash with high-carbon content as pozzolan in high performance concrete. Materials and Structures, 42: 983–992. DOI 10.1617/s11527-008-9437-z.

[7] Elinwa, A. U., Ejeh, S. P., &Akpabio, I. O. (2005). Using metakaolin to improve sawdust-ashconcrete. Concrete International, 27 (11), 49 - 52.

[8] Fadzil, A. M., Azmi, M. J. M., Hisyam, A. B. B., &Azizi, M. A. K. (2008). Engineering Properties of Ternary Blended Cement Containing Rice Husk Ash and Fly Ash as Partial Cement Replacement Materials.ICCBT, A (10): 125 – 134.

[9] Frı´as, M., Villar-Cocin˜a, E., Sa´nchez-de-Rojas, M. I., & Valencia-Morales, E. (2005). The effect that different pozzolanic activity methods has on the kinetic constants of the pozzolanic reaction in sugar cane straw-clay ash/lime systems: Application of a kinetic–diffusive model. Cement and Concrete Research, 35: 2137 – 2142.
[10] Ganesan, K., Rajagopal, K., and Thangavel, K. (2008). Rice husk ash blended cement: assessment of optimal level of replacement for strength and permeability properties of concrete. Constr. Build. Mater, 22 (8):1675-1683.
[11] Habeeb, G. A., &Fayyadh, M. M. (2009).Saw dust ash Concrete: the Effect of SDA Average Particle Size on Mechanical Properties and Drying Shrinkage.Australian Journal of Basic and Applied Sciences, 3(3): 1616-1622.
[12] Joshua, O. and Lawal, P. O. (2011). Cost Optimization of Sandcrete Blocks through Partial Replacement of Sandwith Lateritic Soil.Epistemics in Science, Engineering and Technology, 1 (3): 89-94.
[13] Mama, B.O. and Osadebe, N.N. (2011).Mathematical Model for the Optimization of Compressive Strength of LaterizedSandcrete Blocks. Nigerian Journal of Technology, 30(2): 80-86.
[14] Manasseh, J. (2010). A Review of Partial Replacement of Cement with Some Agro Wastes.Nigerian Journal of Technology, 29 (2): 12-20.
[15] Marthong, C. (2012). Sawdust Ash (SDA) as Partial Replacement of Cement. International Journal of Engineering Research and Applications(IJERA), 2(4): 1980-1985.
[16] Mehta, P. K. &Pirtz, D. (2000). Use of rice husk ash to reduce temperature in high strength mass concrete. ACI Journal Proceedings, 75:60-63.
[17] Nair, D. G., Jagadish, K. S., and Fraaij, A. (2006). Reactive pozzolanas from rice husk ash: An alternative to cement for rural housing. CemConcr. Res., 36 (6): 1062-1071.
[18] Okpala, D. C. (1993) Some Engineering Properties of Sandcrete Blocks Containing Rice Husk Ash.Journal of Building and Environment, 28 (3): 235-241.
[19] Oyekan, G. L. and Kamiyo, O. M. (2011).A study on the engineering properties of sandcreteblocks produced with rice husk ash blended cement. Journal of Engineering and Technology Research, 3(3): 88-98.
[20] Rukzon, S., &Chindaprasirt, P. (2006). Strength of ternary blended cement mortar containing Portland cement, rice husk ash and fly ash.J. Eng. Inst. Thailand, 17: 33-38 (547-551).
[21] Rukzon, S., Chindaprasirt, P., &Mahachai, R. (2009).Effect of grinding on chemical and physical properties of saw dust ash. International Journal of Minerals, Metallurgy and Materials, 16 (2): 242-247.
[22] Sakr, K. (2006). Effects of Silica Fume and Rice Husk Ash on the Properties of Heavy Weight Concrete.Journal of Materials in Civil Engineering, 18(3): 367-376.
[23] Tyagher, S. T., Utsev, J. T., and Adagba, T. (2011). Suitability of Sawdust Ash-Lime Mixture for Production of Sandcrete Hollow Blocks.Nigerian Journal of Technology, 30 (1): 79-84.
[24] Wada, I., Kawano, T., &Mokotomaeda, N. (2000).Strength properties of concrete incorporating highly reactive rice-husk ash. Transaction of Japan Concrete Institute, 21 (1): p. 57–62.
[25] Wenapere, D. A. and Ephraim, M. E. (2009).Physico-mechanical behaviour of sandcrete block masonry units. Journal of Building Appraisal 4: 301–309. doi:10.1057/jba.2009.8

International Journal of Modern Engineering Research (IJMER)
www.ijmer.com Vol.3, Issue.3, May-June. 2013 pp-1372-1376 ISSN: 2249-6645

Area and Power Efficient Modulo 2^n+1 Multiplier

K. Pitambar Patra, [1] Saket Shrivastava, [2] Snehlata Sahu, [3] Sujit Kumar Patel[4]
[1234]*Department of Electronics & Communication Engineering Jaypee University of Engineering & Technology, Guna*

Abstract: *In this paper area-power efficient modulo 2^n+1 multiplier is proposed. The result and one operand for the new modulo multipliers use weighted representation, while the other uses the diminished- 1. By using the radix-4 Booth recoding, the new multipliers reduce the number of the partial products to n/2 for even and (n+1)/2 for odd except for one correction term. According to our algorithm, the resulting partial products are added through inverted end around carry save adder into two operands, which are finally adder by a 2-stage n-bit adder containing 2:1 multiplexer. By using the purposed adder, the new multipliers reduce the area and power. The analytical and experimental result indicates that the new modulo 2^n+1 multipliers, offer reduced power and more compact area among all the existing structures.*

Keywords: *2-Stage n-Bit Adder, Modulo Multiplier, Residue Number System (RNS).*

I. INTRODUCTION

Residue number systems (RNS) reduce the delay of carries propagation, thus suitable for the implementation of high-speed digital signal processing devices. Some arithmetic operations, such as addition and multiplication, can be carried out more efficiently in RNS than in conventional two's complement systems. RNS has been adopted in the design of Digital Signal Processors (DSP), Finite Impulse Response (FIR) filters], image processing units, Discrete Cosine Transform (DCT) processors, communication components, cryptography, and other DSP applications . In recent years, efficient schemes for modulo multipliers have been studied intensively. Generally, modulo 2^n+1 multipliers can be divided into three categories, depending on the type of operands that they accept and output:

i. the result and both inputs use weighted representation;
ii. the result and both inputs use diminished-1 representation;
iii. The result and one input use weighted representation, while the other input uses diminished-1.

For the first category, Zimmermann et al. [1] used Booth encoding to realize, but depart from the diminished-1 arithmetic, which leads to a complex architecture with large area and delay requirements. For the second category, Wang *et al.* [2] proposed diminished-1 multipliers with -bit input operands. The multipliers use a non-Booth recoding and a zero partial-product counting circuit. The main drawback in this architecture was handling of zero inputs and results were not considered.

Curiger et al. [3] proposed new modulo multipliers by using the third category. This architecture use ROM based look-up methods are competitive. The main drawback in this architecture increasing n-bit, they become infeasible due to excessive memory requirements.

Jian et al. [4] also proposed for the third category architecture and reduce the memory requirement and speed up. The new architecture is based on n-bit addition and radix-4 booth algorithm, which is efficient and regular. We are replaced diminished-1 modulo 2^n+1 adder by 2-stage n-bit adder.

The remainder of the paper is organized as follows: mathematical formulation of Diminished-1 number representation computation of modulo multiplier is presented in Section II. The proposed structures are presented in Section III. Hardware and time complexity of the proposed structures are discussed and compared with the existing structures in Section IV. Conclusion is presented in Section V.

II. DIMINISHED -1 NUMBER REPRESENTATION

The modulo 2^n+1 arithmetic operations require (n+1) bit operands. To avoid (n+1)-bit circuits, the diminished-1 number system [15] has been adopted. Let d[A] be the diminished-1 representation of the normal binary number $A \in [0,2^n]$, namely

$$d[A] = |A-1|_{2^n+1} \qquad \text{(i)}$$

In (i), when $A \neq 0, d[A] \in [0,2^n-1]$,is an n -bit number, therefore (n+1) -bit circuits can be avoided in this case. However,

$$A = 0, d[A] = d[0] = |-1|_{2^n+1} = 2^n \qquad \text{(ii)}$$

Is an (n+1) -bit number. This leads to special treatment for d [0]. The diminished-1 arithmetic operations [15] are defined as

$$d[-A] = \overline{d[A]}, if d[A] \in [0,2^n-1] \qquad \text{(iii)}$$

$$d[A+B] = \left| d[A] + d[B] + 1 \right|_{2^n+1} \quad \text{(iv)}$$

$$d[A-B] = \left| d[A] + \overline{d[B]} + 1 \right|_{2^n+1} \quad \text{(v)}$$

$$d[AB] = \left| d[A] \times d[B] + d[A] + d[B] \right|_{2^n+1}$$

$$= \left| d[A] \times B + B - 1 \right|_{2^n+1} \quad \text{(vi)}$$

$$d[2^k, A] = iCLS(d[A], k) \quad \text{(vii)}$$

$$d[-2^k, A] = iCLS(\overline{d[A]}, k) \quad \text{(viii)}$$

Where $\overline{d[A]}$ represents the one's complement of d[A]. In (vii) and (viii) iCLS (d[a], k) is the k -bit left-circular shift of in which the bits circulated into the LSB are complemented.

III. PROPOSED ARCHITECTURE

In the new modulo 2^n+1 multiplication, the result and one input use weighted representations, while the other input uses diminished-1 representation. Let $d[A]=(a_n a_{n-1} \ldots a_1 a_0)_2$ be the diminished-1 representation of weighted A , $B=(b_n b_{n-1} \ldots b_1 b_0)_2$ and $P = \left| A \times B \right|_{2^n+1} = (p_{n-1} p_{n-2} \ldots . p_0)_2$ all be weighted one. According toradix-4 booth recording [15] the product can be written as

$$P = \left| A \times B \right|_{2^n+1} = \left| \sum_{i=0}^{K-1} PP_i + C + K \right|_{2^n+1} \quad \text{(ix)}$$

Where

$$C = \sum_{i=0}^{K-1} c_i$$

And $$K = \begin{cases} n/2, even \\ (n+1)/2, odd \end{cases}$$

From (ix) it is clear that the architecture consists of the partial products generator (PPG), the correction tern generator (CTG), the inverted end-around-carry carry save adder (EAC CSA) and 2-stage n-bit adder. Based on this architecture, a solution which is more effective is proposed.

The encoding scheme accordant with the radix-4 Booth recoding [4], the partial product generator (PPG) can be constructed with the well-known Booth encoder (BE) and Booth selector (BS). The different blocks used in PPG and EAC CSA are taken from [4].

In this paper, we modified BE block which take successive overlapping triplets ($b_{2i+1} b_{2i} b_{2i+1}$) and encodes each as an element of the set {-2,-1, 0, 1 2}. Each BE block produces 3 bits: 1x, 2x and Sign. The 3 bits along with the multiplicand are used to form partial products.

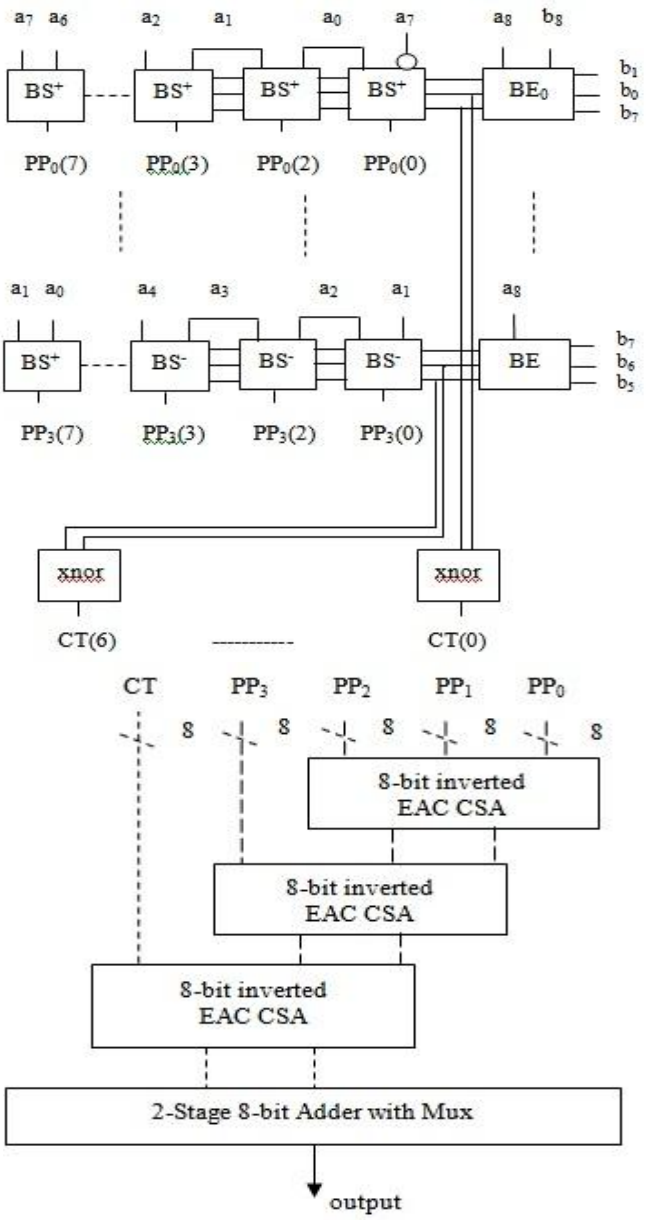

The CTG produces which has the form ($.....0x_{i+1}0x_i.....0x_10x_0$) with $x_i \in \{0,1\}$. Since the 2i-th bit x_i is 1 when the BE_i block encodes 0, otherwise x_i is 0, one XNOR gate accepting the 1x and 2x bits of the block can generate the 2i-th bit x_i.

The inverted EAC CSA tree can reduce the Partial Products to two numbers. The CSA tree is usually constructed with full adders (FA).Then the final two numbers from the tree is passed through the 2-stage n-bit adder. The 2-stage n-bit adder is consisting of two ripple carry adder with C_{in}=0 and C_{in}=1and one 2:1 multiplexer. The C_{out} of first n-bit ripple carry adder is act as control signal to the multiplexer. The two n-bit sum of the ripple carry adder is given to the multiplexer. If C_{out}=0 then the final sum is the sum where the C_{in} =1 as shown in fig.(3).

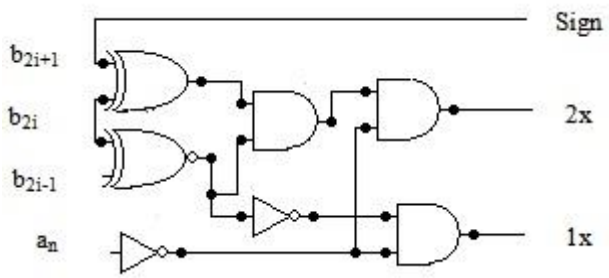

Figure 2(a): Booth encoder

Input			Output			Code
b_{2i+1}	b_{2i}	b_{2i-1}	Sign	2x	1x	
0	0	0	0	0	0	0
0	0	1	0	0	1	1
0	1	0	0	0	1	1
0	1	1	0	1	0	2
1	0	0	1	1	0	-2
1	0	1	1	0	1	-1
1	1	0	1	0	1	-1
1	1	1	1	0	0	-0

Figure 2(b): Truth table

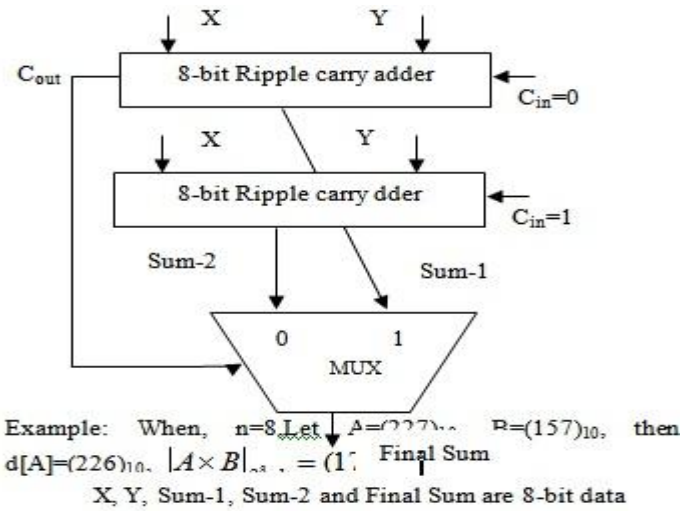

Figure 3: 2-Stage8-bit adder with Multiplexer

Example: When, n=8 ,Let A=$(227)_{10}$, B=$(157)_{10}$, then d[A]=$(226)_{10}$, $|A\times B|_{2^8+1}=(173)_{10}$.

Example

n=8,d[A]=$(11100010)_2$,B=$(10011101)_2$,$a_8=0$,$b_8=0$

Encode Partial Products

$(b_8 \vee (b_7 \oplus b_1))b_0(b_8 \vee b_7)$ --- 011---PP_0---11111111

b_3 b_2 $b_1 \cdot \overline{b_7}$ ---110---PP_1---01110111

b_5 b_4 b_3 ---011---PP_2---01000011

b_7 b_6 b_5 ---100---PP_3---11110001

CT=00000001

Calculation

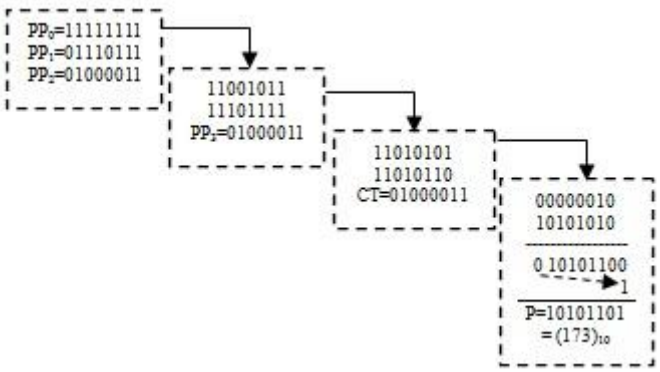

IV. RESULT AND SIMULATION

The proposed architecture has very low hardware complexity compared to [4], which consist of modulo 2^n+1 adder. In the proposed architecture, we use the 2-stage inverted n-bit adder. And calculate the output for 8, 12, 16-bit. To estimate the timing, area and power information for ASIC design, we have used Synopsys Design Compiler to synthesize the design into gate Level.

Comparison of Synopsys result in the proposed architecture and diminished-1 modulo 2^n+1 architecture is given in Table 1 and Table 2 respectively.

These improvements are reasonable. When compared with Diminished-1 modulo 2^n+1 multipliers for weighted representation; the blocks of the new multipliers are based on inverted n-bit adder architecture and use area-power efficient in n-bit adders.

Table 1: Synopsys Result for Area

Area(μm^2)			
Multiplier	8 bit	12 bit	16 bit
Proposed	4755.2651	8984.3446	15124.7143
Jian *et al*[4]	4901.5240	9127.5707	15370.098

Table 2: Synopsys Result for Power

Power at 50Hz(μW)			
Multiplier	8 bit	12 bit	16 bit
Proposed	13.6532	15.6768	29.0434
Jian *et al*[4]	14.2816	16.2569	30.0773

V. CONCLUSION

In this paper, we proposed the area-power efficient a modulo 2^n+1 multiplier. This architecture uses 2-stage n-bit adder, Booth recoding which reduces the number of the partial products to n/2 for even and (n+1)/2 for odd, this is the least number of the partial products among all modulo multipliers published. The reduction scheme uses the well-known inverted EAC CSA tree and the final 2-stage inverted n-bit adder generates the result. The circuit to handle the zero-input case is merged into the first Booth encoder and there is no extra delay to be added. The new multipliers, compared to existing implementations, offer better power while being more compact and their regular structure allows efficient VLSI implementations.

References

[1] R. Zimmermann," Efficient VLSI implementation of modulo $(2^n \pm 1)$ addition and multiplication," in Proc. 14th IEEE Symp. Comput. Arithm., Adelaide, Australia, Apr. 1999, pp. 158–167.

[2] Z.Wang, G. A. Jullien, andW. C.Miller, "An efficient tree architecture for modulo (2^n+1) multiplication," J. VLSI Signal Process. Syst., vol.14, no. 3, pp. 241–248, Dec. 1996.

[3] A. Curiger, H. Bonne berg, and H. Kaeslin, "Regular VLSI architectures for multiplication modulo (2^n+1) ," IEEE J. Solid-State Circuits,vol. 26, no. 7, pp. 990–994, Jul. 1991.

[4] J.W.Chen, R.H.Yao and W.J.Wu, Efficient "modulo (2^n+1) multipliers," IEEE Trans. VLSI systems, vol. 19, no 12, pp. 2149–2157, Dec. 2011.

International Journal of Modern Engineering Research (IJMER)
www.ijmer.com Vol.3, Issue.3, May-June. 2013 pp-1377-1381 ISSN: 2249-6645

Comparative Simulation studies on MacPherson Suspension System

A.Purushotham
Department of Mechanaical Engineering, SreeNidhi Institute of Science and Technolgy Ghatkesar, Hyderabad, A.P. India-501 301

Abstract: *Most of automobiles these days are using two suspension systems namely: double wishbone suspension system and McPherson suspension due to their good dynamic performance and higher passenger comfort. The MacPherson strut setup is still being used on high performance cars such as the Porsche 911, several Mercedes-Benz models and lower BMW models due to its light weight, design simplicity and low manufacturing cost. This paper proposes a systematic and comprehensive development of a two-dimensional mathematical model of a McPherson suspension. The model considers not only the vertical motion of the chassis (sprung mass) but also rotation and translation for unsprung mass (wheel assembly). Furthermore, this model includes wheel mass and its moment of inertia about the longitudinal axis. The paper offers an implementation of the model using Matlab- Simulink, whose dynamics have been validated against a realistic two dimensional model developed with the Ansys software.*

Keywords: *Simulink, ANSYS, suspension, active and passive system*

I. INTRODUCTION

Some common types of independent suspensions are: Swing axle, Sliding pair, McPhersonstrut, Upper and lower A-arm (double wishbone), Multi-link suspension, Semi-trailing arm suspension, Swinging arm, Leaf springs. The McPherson strut is a type of car suspension system which uses the axis of a telescopic damper as the upper steering pivot. It is widely used in modern vehicles and named after Earlie S. MacPherson, who developed the design. MacPherson struts consist of a wishbone or a substantial compression link stabilized by a secondary link which provides a bottom mounting point for the hub or axle of the wheel. This lower arm system provides both lateral and longitudinal location of the wheel. The upper part of the hub is rigidly fixed to the inner part of the strut proper, the outer part of which extends upwards directly to a mounting in the body shell of the vehicle.

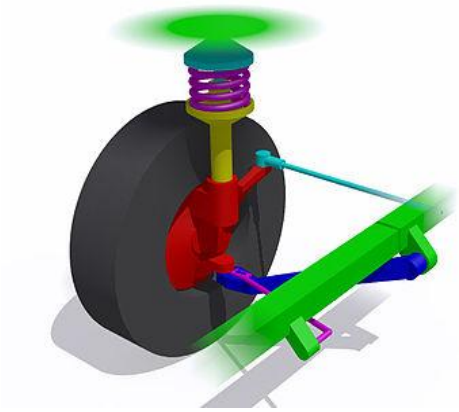

Fig. 1.1:Model of MacPherson

To be really successful, the MacPherson strut required the introduction of unibody (or monocogue) construction, because it needs a substantial vertical space and a strong top mount, which uni bodies can provide, while benefiting them by distributing stresses. The strut will usually carry both the coil spring on which the body is suspended and the shock absorber, which is usually in the form of a cartridge mounted within the strut. The strut also usually has a steering arm built into the lower inner portion. The whole assembly is very simple and can be preassembled into a unit; also by eliminating the upper control arm, it allows for more width in the engine compartment, which is useful for smaller cars, particularly with transverse -mounted engines such as most front wheel drive vehicles have. It can be further simplified, if needed, by substituting an anti-roll bar (torsion bar) for the radius arm. For those reasons, it has become almost ubiquitous with low cost manufacturers. Furthermore, it offers an easy method to set suspension geometry.

The McPherson suspension is widely used in small and medium size vehicles due to its light weight, compact size and low cost. Fig 1.1 shows a McPherson suspension system which consists of a suspension arm or control arm plus a spring-damper assembly (strut) firmly attached to the wheel assembly. Large and systematic changes in kinematic parameters, such as camber angle and track width are a major problem in modeling and controlling this type of suspension. The quarter-car linear model is commonly used to analyze the suspension dynamic behavior. However, this model does not

consider the suspension system structure, which affects significantly the system dynamic behavior. It has been shown in other research papers that two types of suspension geometries produce different responses in real systems and equivalent parameters have been proposed to improve the linear model. In the case of the McPherson suspension, its variable geometry provokes a nonlinear behavior, which can be analyzed with two dimensional linear models. This work proposes a systematic and comprehensive development of a linear two-dimensional ANSYS model of McPherson suspension. The model considers that sprung mass (chassis) moves vertically, and that the unsprungmass (wheel assembly) experiments a two-dimensional motion of rotation and translation. In addition, the model includes the wheel mass and its inertial moment about the longitudinal axis. Generalized coordinates Z_s and Z_u are used to see the transient response. The model also takes into account the geometric structure, as well as tyre damping and lateral stiffness, which have not been considered in other related works. Furthermore, the paper also describes the implementation of model using Matlab-Simulink. Simulation allows analyzing the system dynamic behavior versus road obstacles and depressions. Moreover, to validate the results, these have been compared with the realistic two-dimensional model of the McPherson suspension developed using Ansys software.

The rest of the paper is organized as follows. The brief literature review is given in section 2. In section 3 the results of simulation of Simulink model and ANSYS models are presented. Section 4 draws the conclusions.

II. Review of Literature

Survey of advanced suspension developments and related control applications can be seen [4]. The synthesis and analysis of suspension mechanisms various suspension systems are covered in [9]. All models of suspension systems are classified as active and passive systems. In passive systems are analyzed by many others with the spring and dampers [2, 6, 7]. All these studies are concentrated to see the effect of the suspension structure on equivalent suspension parameters like stiffness and damping ratios.[6].The modern Fuzzy control of semi active automotive suspensions is being studied by A. AbuKkhudair, R.muresan and S.Yang,[3].The dynamic models of MacPherson suspension are developed with all geometric parameters [1,3,7]; but all models involves non linear terms therefore the complicated mathamtical methods are required to obtain responses. In this paper two simulation models of Mac Pherson suspension developed in ANSYS and Simulink Softwares by eliminating no linearity. This will leads the solution easy with little compromise on the accuracy.

III. Simulation Results

The kinematic model of MacPherson suspension is developed in [1] and the same is shown in the Fig.3.1.

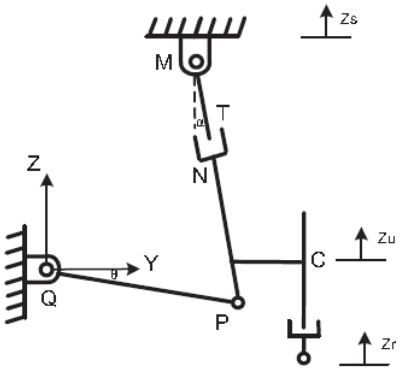

Fig.3.1:Kinematic model of MacPherson suspension

The key points are defined at Q, P, N, T, M, C as shown in Fig.3.1 and elements are generated in ANSYS software. The coordinates of these points are shown in Table.3.1. Model parameters are taken from earlier in the mathematical model [1] and shown in Table 3.2. Using the above parameters, the Ansys model is generated and transient analysis is carried out. The steps adopted for transient analysis are from the manual [10].The input considered is a square wave signal of 50mm amplitude,40s period with a phase shift of 15 sec. This disturbance is made as a road bump on which the wheel of automobile is passing over it. The response of the displacement sprung mass i.e the chasis of automobile and the response of acceleration of unsprung mass are extracted from the transient simulation studies in ANSYS. These responses are shown in Figures 3.2 and 3.3.

Table 3.1: Coordinates of key points

Key point	X coordinate(m)	Y Coordinate(m)
1	0	0
2	0.5791	-0.214
3	0.5588	0
4	0.5368	0.351
5	0.500	0.468
6	0.621	0
7	0.621	-0.351

Table 3.2: Model parameters

Particular	**Variable value**
Mass of the chassis(sprung mass) Kg	m_s=439.4
Mass of the tyre (unsprung mass)Kg	m_u=42.3
Suspension stiffness N/m	K_s=38404.0
Suspension damping Ns/m	B_s=3593.4
Tyre vertical stiffness N/m	K_t=310000.0
Tyre lateral stiffness	K_{tl}=190000.0
Tyre damping Ns/m	B_t=3100
Tyre effective radius m	R=0.3
Wheel inertia moment in x-axis Kg m^2	I_c=1.0

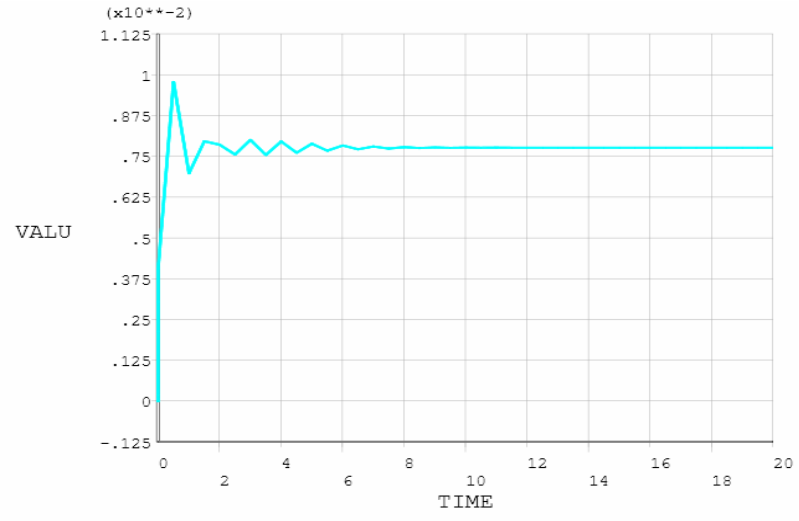

Fig.3.2: Response of displacement of chassis

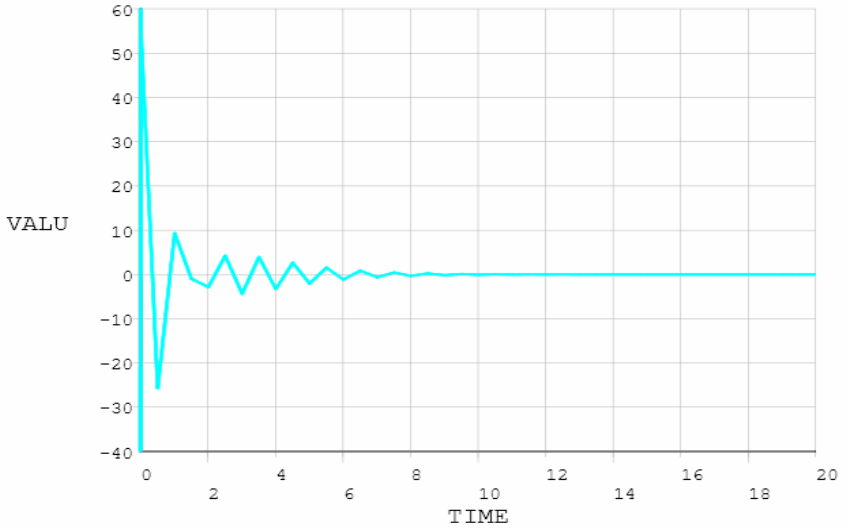

Fig.3.3 Response of Acceleration of the chassis

Now that the Simulink block diagram is completed [see Fig.3.4] based on the dynamics equations developed in the research worn in [1]. The dynamic response of the suspension system is carried out with similar disturbance generated by the road Z_r in the ANSYS Model The disturbance is modeled as a square wave signal of 50mm amplitude,40s period with a phase shift of 15 sec.

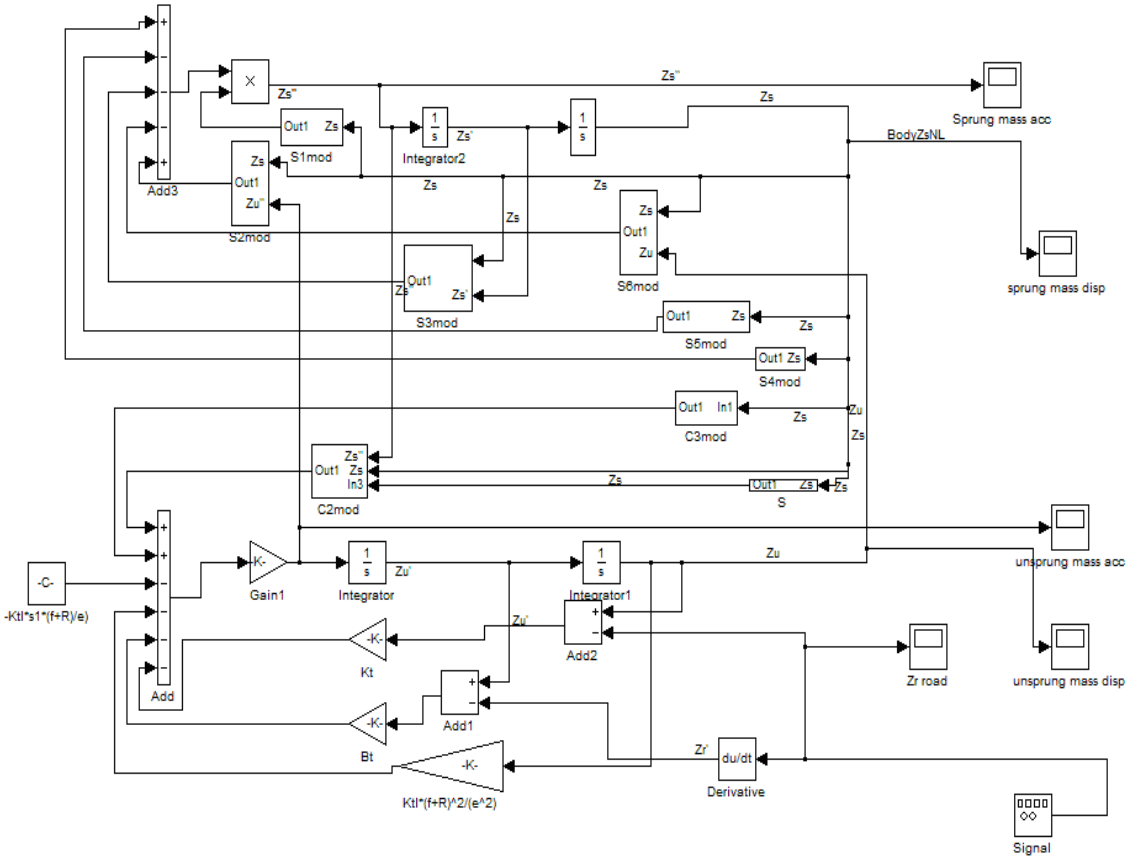

Fig.3.4: Simulink Block Diagram of Suspension System.

The response of displacement and acceleration of chassis obtained from block diagram are shown in Figures 3.5 and 3.6. The two simulation studies are showing almost same maximum values of displacement and acceleration of chassis. The acceleration experienced by the chassis is less than 10g m/s^2 .It indicates the designed MacPherson suspension giving satisfactory passenger comfortable acceleration**.**

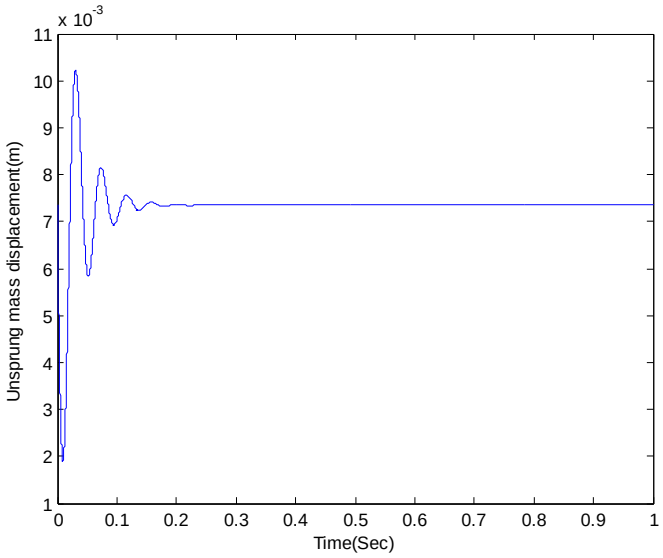

Fig.3.5: Displacement response of Chassis

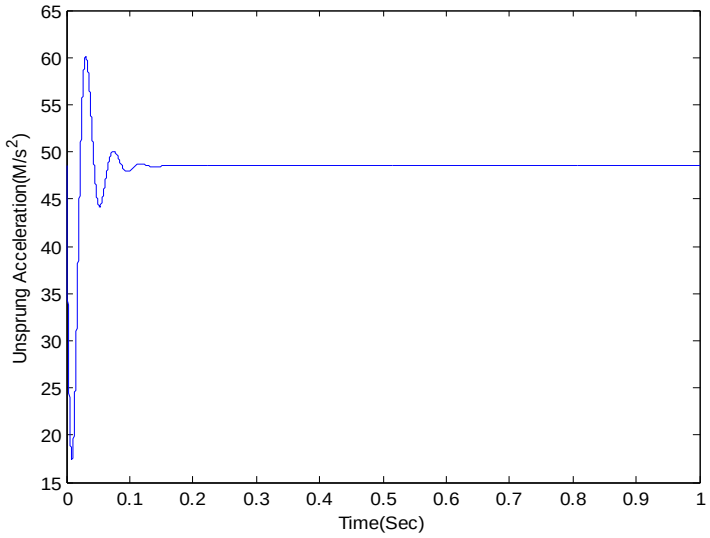

Fig.3.5: Acceleration response of Chassis

IV. CONCLUSIONS

In this paper, McPherson suspension system has been modeled after studying dynamic equations to study vibration characteristics of sprung mass of the automobile system with the inclusion of various design parameters such as stiffness, damping, masses, moment of inertia, etc. The commercial simulation software Simulink is used to implement dynamic equations to attain the acceleration and the displacement of the chassis of the automobile during the period in which the vehicle passes through various road conditions.

Due to the complexity involved in the mathematical expressions and executing them into the Simulink software, the model has been simplified with a two-dimensional approach. The Ansys software is used to implement a simplified two dimensional practical model of McPherson suspension.

The results obtained from Ansys model are compared with the mathematical model implemented on Simulink. It is observed that the displacement and acceleration of the chassis of the automobile obtained in Ansys are nearer to the values of mathematical model. With these developed models, the influence of suspension system parameters can be studied on the performance of passenger comfort.

V. ACKNOWLEDGEMENTS

The author thanks H.O.D.Mechanical Engineering AND Executive Director, Sree Nidhi Institute of Science and Technology: Hyderabad for their encouragement and help in bringing out this technical paper.

REFERENCES

Journal Papers:

[1] Jorge Hurel, Anthony Mandow "Dynamic modeling of Mc Pherson Suspension" IEEE Transaction on non linear dynamics, 2012, pp 414-1422.

[2] A.AbuKkhudair, R.muresan and S.Yang, "Fuzzy control of semi active automotive suspensions," in international conference on mechatronics and automation, 2009, pp 2118-2122.

[3] M.S Fallah, R.Bhat and W.F.Xie,"New model and simulation of MacPherson suspension system for ride control applications," Vehicle system Dynamics, vol. 47, p 195, 2009

[4] D Hrovat,"survey of advanced suspension developments and related optimal control applications," Automatica, vol.33, no.10, pp.1781-1817, 1997.

[5] C. Kim, P.I.Ro and H Kim,"Effect of the suspension structure on equivalent suspension parameters," automobile engineering. Proceedings of the institute of mechanical engineers, vol. 213, p. 457, 1999.

[6] C.Kim and P.I Ro,"reduced-order modeling and parameter estimation of suspension system" automobile engineering, proceedings of the institution of mechanical engineers.

[7] A.Stensson, C.Asplund and L. Karlsson "The nonlinear behavior of a MacPherson strut wheel suspension," vehicle system dynamics, vol.23, p 85, 1994.

[8] H Akcay and S. Turkay,"RMS performance limitations and contraints for quarter car active suspensions" in 16ht Mediterranean Confernce on Control and Automation, 2008, pp. 425-430.

[9] C.H Suh, "Synthesis and analysis of suspension mechanisms with use of displacement matrices" SAE transactions, vol 98, pp 171-182.

Text Book

[10] Dr. A.Purushotham: FEA BASICS WITH ANSYS" Manual, SNIST Internal College publication, 2010.

International Journal of Modern Engineering Research (IJMER)
www.ijmer.com Vol.3, Issue.3, May-June. 2013 pp-1382-1385 ISSN: 2249-6645

Design and BER Performance of MIMO-OFDM for Wireless Broadband Communications

M. Vani Divyatha, [1] B. Siva Reddy[2]
[12]*Dept. of Electronics & Communication G. Pulla Reddy Engineering College, Kurnool*

Abstract: *To achieve high data rates, speed and simultaneous increase in range and reliability without consuming extra radio frequency requires MIMO-OFDM for wireless broadband communication.*

This paper investigates the performance of MIMO-OFDM using different modulation schemes are used to encode and decode the data stream in wireless communication over AWGN channel for unknown transmitter and known receiver. In this paper first we integrate OFDM to MIMO. In particular; we apply MIMO detection methods based on VBLAST (Vertical Bells Lab Layered Space Time) architecture to improve spectral efficiency.

Keywords: *Orthogonal Frequency Division Multiplexing (OFDM); (Vertical Bells Lab Layered Space Time) VBLAST; Multiple Input Multiple Output (MIMO); Bit Error Rate (BER).*

I. Introduction

Now-a-days, wireless communication systems are playing crucial role. Initially, wireless systems were mainly designed to support voice. Later these are used to transfer the data, they gain popularity because of their ease of use and mobility .All wireless technology face the challenges of signal fading, multipath, increasing interference and limited spectrum. Orthogonal Frequency Division Multiplexing (OFDM) plays a crucial role and reduce receiver complexity in wireless broadband systems but in this case synchronization and channel estimation are very important, and it is replaced by Multiple Input Multiple output-Orthogonal Frequency Division Multiplexing (MIMO-OFDM) which is a multi-user OFDM that allows multiple accesses that scheme that combines TDM and FDM on the same channel, widely for the next generation wireless communication systems such as WLAN,WMAN, WiMAX and 3G-LTE standard in order to accommodate many users in the same channel at the same time. The use of MIMO technology in combination with OFDM, i.e., MIMO-OFDM is therefore seems to be an attractive solution for future broadband wireless systems. But this MIMO system having fast framing rate of the order of 1–2 μs will be polluted by ISI when operational in an environment having a typical time delay Spread of 200 μs. Thus an ISI value of 200/2 = 100 is an undesirable multi-path effect for the real MIMO system. Therefore MIMO cannot achieve zero ISI and hence cannot be utilized alone. OFDM based multi-carrier approach may be enabler for the MIMO broadband operation So the fast frames are slowed down first and converted to several slow sub frames and modulated to multiple carriers of OFDM. OFDM-MIMO is, therefore, useful technology which can be explored both for communication and remote sensing (radar).

MIMO concept was first introduced by Jack Winters in 1987 for two basic communication systems. The first was for communication between multiple mobiles and a base station with multiple antennas and the second for communication between two mobiles each with multiple antennas.MIMO systems in spatial multiplexing have two architectures namely Diagonal BLAST (D-BLAST) and Vertical BLAST (V-BLAST). D-BLAST uses diagonal approach which suffers from certain implementation complexities which make it inappropriate for initial implementation. Its main motivation is to increase diversity, and thus improve the robustness of the communication link. V-BLAST uses vector encoding process. Its main objective is to increase the capacity data rate in a constrained spectrum and spectral efficiency of the communication link.

Recently, IEEE 802.11n task group was formed with goal of increasing the application throughput by making changes in the PHY and MAC layer. The major challenge in the physical layer is the uses of multiple transmit and receive antennas and OFDM modulation, which comprises of OFDM modulation as well as subcarrier allocation. Therefore, it is significant to focus more attention on wireless communication technology. OFDM typically uses a higher FFT size, and divides the available sub-carriers into logical groups called sub-channels. Unlike OFDM that transmits the same amount of energy in each subcarrier, OFDM may transmit different amounts of energy in each sub-channel i.e., users may also occupy more than one sub channel depending upon their Quality of Service (QoS).

The rest of the paper is organized as follows: Section-II details V-BLAST Architecture. Section-III illustrates the overall design of OFDM-MIMO (V-BLAST). The implementation and simulation will be detailed in section-IV. Finally, section-V gives the main conclusions of the work.

II. V-Blast Architecture

The structure of the V-BLAST systems is described in fig.1Notation: Vector symbol a: (a_1, a2, a3, a4$_{\ldots\ldots}$ $a_{M)}$ ^{T}, No. of Tx = M_T, No. of Rx = M_R.

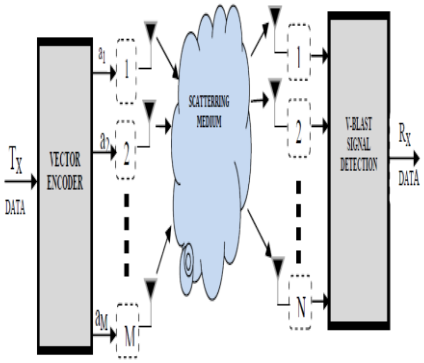

Fig.1. V-BLAST Architecture

A single data stream is demultiplexed into M sub streams, and each sub stream is then encoded into symbols and fed to its respective transmitter. Transmitters *1-*M_T operate co-channel at symbol rate *1/T* symbols/sec, with synchronized symbol timing. Each transmitter is itself an ordinary QAM transmitter. The collection of transmitters comprises, in effect, a vector –valued transmitter, where components of each transmitted M_T -vector are symbols drawn from a QAM constellation. We assume that same constellation is used for each sub stream, and that transmissions are organized into bursts of *L* symbols. The power launched by each transmitter is proportional to $1/M_{T\,so}$ that the total radiated power is constant and independent of M_T.

In V-BLAST, however, the vector encoding process is simply a demultiplex operation followed by independent bit-to-symbol mapping of each sub stream.

III. Exper Imental Setup for Ofdm- Mimo (V-Blast) Systems

The experiment is simulated as shown in fig.2. Assuming a AWGN channel with a maximum delay spread of 75ns, perfect channel knowledge at the receiver and perfect synchronization, no knowledge of the channel at the transmitter and employ interleaving. The modulation schemes employed are BPSK, QPSK and 16 QAM. The bandwidth of an IEEE 802.11a system is 20MHz.There are 256 sub-carriers in each OFDM symbol. These mark for an inter-carrier spacing Δf of $20X10^6$ /256 = 781.25 KHz.

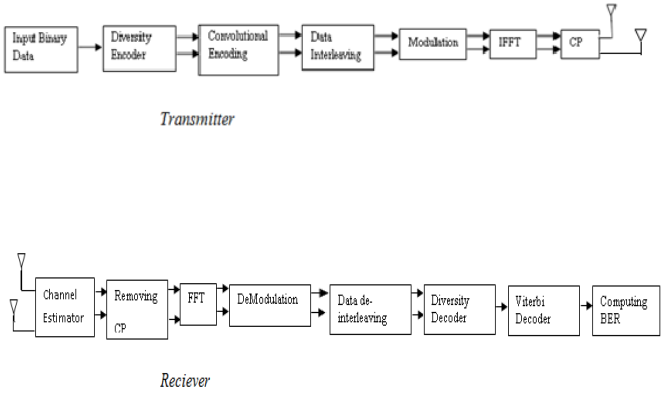

Fig.2. Block Diagram of OFDM-MIMO (V-Blast) System

The binary input data is initially sent to the diversity encoder. In diversity encoder spatial multiplexing is applied it prevents from long sequence of 0's and 1's .This splits the data into orthogonal streams. In the figure we are considering 2x2, 2x3, 2x4, 4x4 systems. The first stream is to the top, second stream to the second and it is continued to other streams likewise respectively. Here they are converted from serial to parallel. Thus the subcarriers are obtained. The subcarriers are then given to the convolution encoder. It is used for real time error correction. It is done by combining the fixed number of inputs. The input bits are stored in a fixed length shift registers and they are combined with the help of mod-2 adders. An input sequence and contents of shift registers perform modulo-two addition after information sequence is sent to shift registers, so that an output sequence is obtained. It is used to improve BER and to reduce high peak to average power ratio which is present in OFDM. . The de facto standard for this encoder is (2, 1, 7). The other rate ½ is achieved by puncturing the output if this encoder. Puncturing involves deleting coded bits from output data sequence, such that ratio of un-coded bits to coded bits is greater the mother code. The signal is then sent to the data interleaving. The idea of interleaving is to disperse a block of data in frequency so that the entire block does experience the deep fade in the channel. This prevents the burst errors at the receiver .Otherwise the convolution decoder will not perform very well in

presence of burst errors. The interleaved are grouped together to form symbols. The symbols are then modulated using BPSK, QPSK and 16QAM schemes. They are given to IFFT and append to the CP. Hence the information is transmitted in packets. The receiver is the exact inverse process after the incoming packets are received. Diversity decoder converts parallel sub streams to serial form. The serial form is given to Viterbi decoder and is mostly applied to convolution encoder and it uses maximum likelihood decoding technique. Noisy channels cause bit errors at the receiver. Viterbi algorithm estimates actual bit sequence using trellis diagram. Then the BER is computed.

IV. Simulation

The above system was simulated in the MATLAB.As we know that the system is known receiver and unknown transmitter the information from transmitter to receiver was received in the form of packet or frame. The received packets may be lost or include errors because of noisy channel. Performance analysis is done for different Modulation schemes and for different transmit and receive elements. We transmit our data by using OFDM technique in which large number of closely spaced orthogonal subcarriers is used to carry data. Each Carrier is modulated and demodulated with a modulation schemes. The encoded data is passed through Gaussian where Additive White Gaussian noise (AWGN) is added. There are some restrictions and disadvantages in digital wireless communication systems between transmitter and receiver where received signals arrive at receiver with different power and time delay due to reflection, diffraction and scattering effects. For this reasons Bit Error Rate (BER) value is relatively high. In this condition the digital wireless communication systems will not perform well.BER is the fundamental parameter to access the quality.BER is simply defined as: Number of error bits/Number of total bits. Noise in transmission medium disturbs the signal and causes data corruptions. Relation between signal and noise is described with SNR (signal-to-noise ratio).SNR is defined as: signal power/Noise power. SNR is inversely proportional with BER. The less the BER result is higher the SNR and the better communication quality. We note that as the diversity order increases the performance of V-Blast improves, which is to be expected. The diversity order at the receiver is more than $M_R–M_T+1$ and less than M_R. By using FFT approach as the number of subcarrier increases the better is accuracy due to high number of points. The data rate will also increase.

i) In comparison with three modulation schemes QPSK, BPSK and 16 QAM with keeping the transmitting elements fixed and varying receiving elements are shown in fig 3, 4, 5. BER is varied slightly due to its receiving diversity technique.
ii) Performance of BPSK can improve BER and data rate, at small value of SNR. It operates between 4 and 6dB.
iii) Performance of QPSK is better than BPSK for the same bandwidth but the data rate will be doubled. It operates between 8 and 10dB
iv) Performance of 16QAM has better SNR when compared with QPSK; BPSK .It operates between 10 and 14dB.

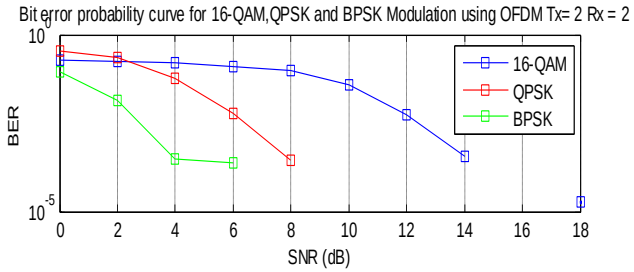

Fig.3. Performance of 2x2.Parameters: No. of FFT points=256; Channel=AWGN; Number of Data Carriers=256.

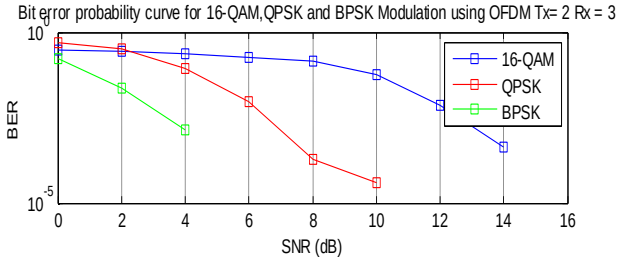

Fig.4. Performance of 2x3.Parameters: No. of FFT points=256; Channel=AWGN; Number of Data Carriers=256.

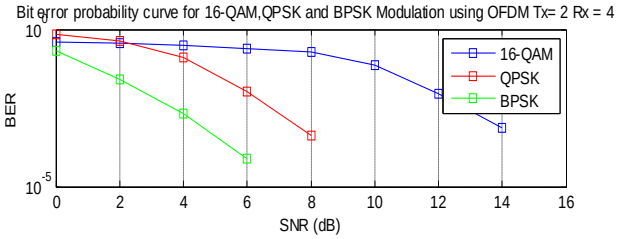

Fig.5. Performance of 2x4.Parameters: No. of FFT points=256; Channel=AWGN; Number of Data Carriers=256.

V) The 4x4 transmit and receiving elements as shown in fig 6 has better SNR in 16QAM when compared to other SNR.

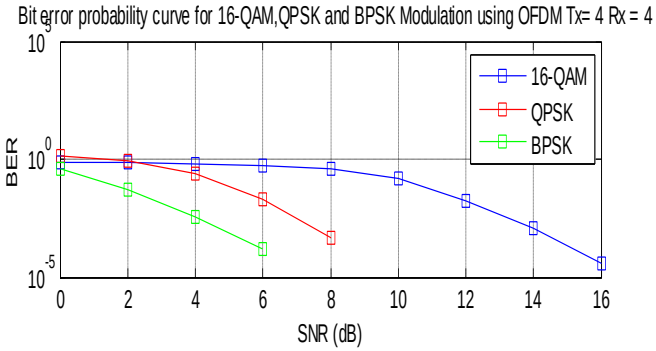

Fig.6. Performance of 4x4.Parameters: No. of FFTpoints=256; Channel=AWGN; Number of Data Carriers=256.

V. Conclusion

In this paper, we compare the performance of OFDM-MIMO (V-BLAST) in terms of BER using different modulation schemes by varying both transmitting and receiving elements on AWGN channel. It is found that by using VBLAST technique we can improve spectral efficiency.

References

[1] WiMAX Forum, Krishna Ramadas and Raj Jain, "WiMAX System Evaluation Methodology" version 2.1 July 2008
[2] Foschini, G . J., " Layered s p a c e -time a r c h i t e c t u r e for wireless communication in a fading environment when using multi-element antennas", Bell Labs Technical Journal, 1996.
[3] IEEE 2009 Nirmalendu Bikas Sinha "Hybrid Technology using OFDM for Next Generation Broad band Mobile Radio Communications".
[4] Zhangyong Ma and Young-il-Kim,"A Novel OFDM receiver in Flat Fading Channel", IEEE Confrence on advanced Communication technology, ICACT, Vol..2, pp.1052-54, 2005.
[5] H.B olcskei, D.Gesbert, and A.J.Paulraj,"On the capac ity of OFDM-based spatial multiplexing systems, IEEETrans.Commun" vol.50, no.2, pp.225-234, Feb.2002

International Journal of Modern Engineering Research (IJMER)
www.ijmer.com Vol.3, Issue.3, May-June. 2013 pp-1386-1388 ISSN: 2249-6645

A General Framework for Building Applications with Short and Sparse Documents

Syed Jani Basha, [1] Sayeed Yasin[2]
[1]*M.Tech, Nimra College of Engineering & Technology, Vijayawada, A.P., India*
[2]*Asst.Professor, Dept.of CSE, Nimra College of Engineering & Technology, Vijayawada, A.P., India*

Abstract: *with the explosion of e-commerce and online communication and publishing, texts become available in a variety of genres like Web search snippets, forum and chat messages, blogs, book and movie summaries, product descriptions, and customer reviews. Successfully processing them, therefore, becomes increasingly important in many Web applications. However, matching, classifying, and clustering these sorts of text and Web data pose new challenges. Unlike normal documents, these text and Web segments are usually noisier, less topic-focused, and much shorter, that is, they consist of from a dozen words to a few sentences. Because of the short length, they do not provide enough word co- occurrence or shared context for a good similarity measure. Therefore, normal machine learning methods usually fail to achieve the desire accuracy due to the data sparseness. To deal with these problems, we present a general framework that can discover the semantic relatedness between Web pages and ads by analyzing implicit or hidden topics for them.*

Keywords: *Classification, Clustering, Hidden topic, Sparse.*

I. INTRODUCTION

In contextual advertising, ad- messages are delivered based on the content of the Web pages that users are surfing. It can therefore provide Internet users with the information they are interested in and allow advertisers to reach their target customers in a non-intrusive way [1] [2]. In order to suggest the "right" ad- messages, contextual ad matching and ranking techniques are needed to be used. This has posed new challenges to the Web mining and IR researcher. Firstly, as words can have multiple meanings and some words in the target page are not important, they can lead to mismatch in the lexicon-based matching method. Moreover, a target page and an ad can still be a good match when they share no common terms or words but belong to the same topic.

To deal with these problems, we present a general framework that can discover the semantic relatedness between Web pages and ads by analyzing implicit or hidden topics for them. After that, both Web pages and the advertisements are expanded with their most relevant topics, which helps reduce the sparseness and make the data more topic-focused. The framework can therefore overcome the limitation of word choices, deal with a wide range of Web pages and ads, as well as processes future data, that is, previously unseen ads and Web pages, better. It is also easy to implement and general enough to be applied in different domains of advertising and in also different languages.

II. RELATED WORK

"Text categorization by boosting automatically extracted concepts" by Cai & Hoftmann in [3] is probably the study most related to our framework. This attempts to analyze topics from data using pLSA and uses both the original data and resulting topics to train two different weak classifiers for boosting. The difference is that they extracted topics only from the training and test data while we discover hidden topics from the external large-scale data collections. In addition, we aim at dealing with the short and sparse text and Web segments rather than normal text documents. Another related work is the use of topic features to improve the word sense disambiguation by Cai et al. [4].

In [5], the author Bollegala use search engines to get the semantic relatedness between words. Sahami & Heilman [8] also measure the relatedness between text snippets by using search engines and a similarity kernel function. Metzeler et al. [6] evaluated a wide range of similarity measures for short queries fromWeb search logs. Yih & Meek [7] considered this problem by improving Web-relevance similarity and the method in [8]. Gabrilovich & Markovitch [9] computing semantic relatedness for texts using Wikipedia concepts. Prior to recent topic analysis models, word clustering algorithms were introduced to improve text categorization in various different ways. Baker & McCallum [10] attempted to reduce dimensionality by class distribution-based clustering.

Bekkerman et al. [11] combined distributional clustering of words and SVMs. And Dhillon & Modha [12] introduced spherical *k*-means for clustering sparse text data. Clustering Web search has been becoming an active research topic during the past decade. Many clustering techniques were proposed to place search results into topic– oriented clusters [13].

III. PROPOSED FRAMEWORK

The proposed work consists of the document classification and the online contextual advertising. The first and foremost step is to analyze the hidden topics based on the semantic similarity. Once the topics are analyzed, then the classifier is built upon the hidden topics by integrating them with the available training data. For advertising, the web pages and the page ads will be matched and ranked based on their similarity.

A. Analysis with the Hidden Topics

Latent Dirichlet Allocation [14] [15] is a method to perform the latent (hidden) semantic analysis (LSA) to find the latent structure of topics and concepts in a text corpus. LSA is well known technique which partially addresses the synonymy and the polysemy issues. LDA is a probabilistic model for collection of discrete data and has been used in the text classification. The Latent Dirichlet Allocation (LDA) is similar to the Latent Semantic analysis (LSA) and Probabilistic LSA (pLSA), since they share some common assumptions such as, the documents having semantic structure, can infer topics from word-document and its co-occurences and the words related to the topic. In this classification of hidden topics process, the universal data set is collected and the topic analysis is done and then the training set data and the test set data are separated and then the training is performed on this set of data so that when the new data is inserted, then it could classify the given data under a specific domain or category.

B. Building Classifier with the Hidden Topics

Now- a- days, the continuous development of Internet has created a huge amount of documents which are difficult to manage, organize and navigate. As a result, the task of automatic classification, which is to categorize textual documents in to two or more predefined classes, has been received a lot of attentions. Several machine learning methods have been applied to text classification including decision trees, neural networks, support vector machines, etc. In the typical applications of machine learning methods, the training data is passed to a learning phrase. The result of the learning step is an appropriate classifier, which is capable of categorizing new documents. However, in the cases such as the training data is not as much as expected or the data to be classified is rare, learning with only training data can not provide us a satisfactory classifier. Inspired by this fact, we propose a general framework that enables us to enrich both training and new coming data with hidden topics from available large dataset so as to enhance the performance of text classification.

Classification with hidden topics is described in Figure 1. We first collect a very large external data collection called universal dataset. Next, a topic analysis technique such as pLSA, LDA, etc. is applied to the data set. The result of this step is an estimated topic model which consists of the hidden topics and the probability distributions of words over these topics. Upon this model, we can do topic inference for training dataset and the new data. For each document, the output of topic inference is a probability distribution of the hidden topics – the topics analyzed in the estimation phrase – given the document. The topic distributions of the training dataset are then combined with training dataset itself for learning classifier. In the similar way, the new documents, which need to be classified, are combined with their topic distributions to create the so called "new data with hidden topics" before passing to the learned classifier.

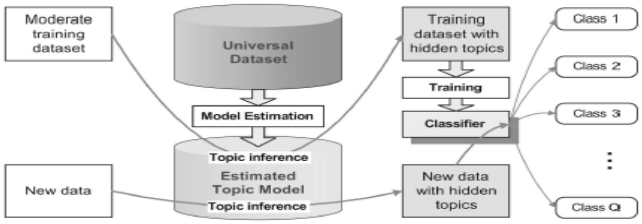

Figure 1: Classification with Hidden Topics

C. Building Clustering with the Hidden Topics

Text clustering is to automatically generate groups or clusters of documents based on the similarity or distance among documents. Unlike Classification, in clustering, the clusters are not known previously. Users can optionally give the requirement about the number of clusters. The documents will later be organized in to clusters, each of which contains "close" documents. Web clustering, which is a type of text clustering specific for the web pages, can be offline or online. Offline clustering means, it is to cluster the whole storage of available web documents and does not have the constraint of response time. In online clustering, the algorithms need to meet the real-time condition, i.e. the system need to perform clustering as fast as possible. For example, the algorithm should take the document snippets instead of the whole documents as input since the downloading of the original documents is time-consuming. The question here is how to enhance the quality of clustering for such document snippets in "online web clustering". Inspired by the fact those snippets are only small pieces of text (and thus poor in content) we propose the general framework to enrich them with hidden topics for clustering (Figure 2).

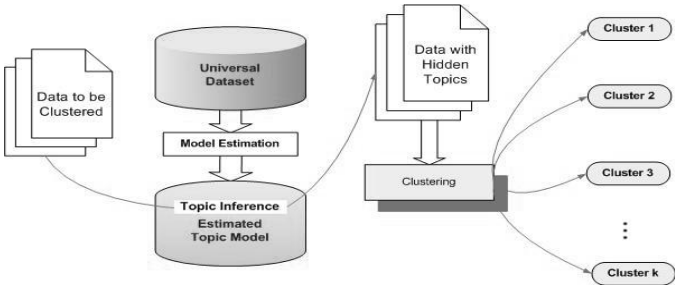

Figure 2: Clustering with Hidden Topics

D. Matching and Ranking of Contextual Advertisements

In matching and ranking of ads with the hidden topics, web pages ands the ads are matched based on their similarity. The similarities between those are measured using the cosine similarity. The ad- messages are arranged based on their similarity for each page. The keywords are also taken into consideration for ranking of the ads. The web pages and ad messages are considered and the topic inference is carried out for the both to identify under which category the web pages and the ad messages fall. The topic inference is very similar to the training process. Once the inference is done, then the new set of web pages and the ad messages are taken and then a contextual matching of those is done. The similarity is measured based on the context of the web pages and with ad messages. After identifying the contextual similarity, it is measured using the cosine similarity method, where the ranking process is done based on the similarity measure value. The web page related to the keyword that has the highest similarity value is ranked highest and given more preference while displaying the web search results. The similarity of the web page "*p"* and ads "*a"* is defined as follows:

sim_{AD} (p, a)=similarity (p, a) &

sim_{AD_kw} (p, a)=similarity (p, a U KWs)

Where KW is a set of keywords associated with the ad message "a".

IV. CONCLUSION

The proposed frame work presents a general framework for building classifiers that deal with short and sparse text & Web segments by making the most of hidden topics discovered from large scale data collections. The main motivation of this frame work is that many classification tasks working with short segments of text & Web, such as search snippets, forum & chat messages, blog & news feeds, product reviews, and book & movie summaries, fail to achieve high accuracy due to the data sparseness. We, therefore, come up with an idea of gaining external knowledge to make the data more related as well as expand the coverage of the classifiers to handle future data better. The underlying idea of the general framework is that for each classification task, we collect a large-scale external data collection called "universal dataset", and then build a classifier on both a (small) set of labeled training data and a rich set of hidden topics discovered from that data collection. The framework is general enough to be applied to different data domains and genres ranging from Web search results to the medical text. The advantages of the general framework are:

- The general framework is flexible and general enough to apply in any domain/language. Once we have trained a universal dataset, its hidden topics could be useful for several learning the tasks in the same domain.
- This is particularly useful in sparse data mining. Spare data like snippets returned from a search engine could be enriched with the hidden topics. Thus, enhanced performance can be achieved with this.
- Due to learning with the smaller data, the presented methods require less computational resources than semi-supervised learning.

REFERENCES

[1] P. Chatterjee, D. L. Hoffman, and T. P. Novak. Modeling the clickstream: Implications for web-based advertising efforts Marketing Science, 22(4):520–541, 2003
[2] R. Wang, P. Zhang, and M. Eredita. Understanding consumers attitude toward advertising. Proc. AMCIS, 2002.
[3] L. CAI and T. Hofmann. Text categorization by boosting automatically extracted concepts. Proc. ACM SIGIR, 2003.
[4] J. CAI, W. Lee, and Y. Teh. Improving WSD using topic features. Proc. EMNLP-CoNLL, 2007.
[5] D. Bollegala, Y. Matsuo, and M. Ishizuka. Measuring semantic similarity between words using Web search engines. Proc. WWW, 2007
[6] D. Metzler, S. Dumais, and C. Meek. Similarity measures for short segments of text. Proc. ECIR, 2007.
[7] W. Yih and C. Meek. Improving similarity measures for short segments of text. Proc. AAAI, 2007.
[8] M. Sahami and T. Heilman. A Webɲbased kernel function for measuring the similarity of short text snippets. Proc. WWW, 2006.
[9] E. Gabrilovich and S. Markovitch. Computing semantic relatedness using Wikipedia-based explicit semantic analysis Proc. IJCAI, 2007.
[10] L. Baker and A. McCallum. Distributional clustering of words for text classification Proc. ACM SIGIR, 1998
[11] R. Bekkerman, R. El-Yaniv, N. Tishby, and Y. Winter Distributional word clusters vs. words for text categorization. JMLR, 3:1183–1208, 2003.
[12] I. Dhillon and D. Modha. Concept decompositions for large sparse text data using clustering Machine Learning, 29(2–3):103–130, 2001.
[13] K. Kummamuru, R. Lotlikar, S. Roy, K. Singal, and R. Krishnapura A hierarchical monothetic document clustering algorithm for summarization and browsing search results Proc WWW, 2004
[14] Andrieu, C., Freitas, N.D., Doucet, A. and M.I. Jordan (2003), "An Introduction to MCMC for Machine Learning", Machine Learning Journal, pp. 5- 43.
[15] Bhattacharya, I. and Getoor, L. (2006), "A Latent Dirichlet Allocation Model for Entity Resolution", In Proceedings of 6th SIAM Conference on Data Mining, Maryland, USA.

International Journal of Modern Engineering Research (IJMER)
www.ijmer.com Vol.3, Issue.3, May-June. 2013 pp-1389-1392 ISSN: 2249-6645

Structural Monitoring Of Buildings Using Wireless Sensor Networks

M.Sri Ram Prasad, [1] Dr. Syed Khasim[2]
[1]*M.Tech (ES), Dept. of Electronics and Computer Engineering, KL University, Guntur Dist, A.P., India*
[2]*Assoc.Professor, Dept. of Electronics and Computer Engineering, KL University, Guntur Dist, A.P., India*

Abstract: *Present part of the structure of a buildings are found everywhere and is monitored using wireless sensor networks is one of the most emerging technologies for a risk mitigation. Buildings are subjected to natural risks such as earthquakes, strong winds and manmade risks such as fire and crimes. So we have to monitor different measurable factors such as aging of structural performance, fatigue, damage, gas leak, fire etc. To monitor these parameters by using different kinds of sensors which are placed in different parts of the building and provide risk control of the buildings from these hazards. In this paper a smart sensor based on the "Berkley Mote" platform is used for the monitoring of building and the "MICAz OEM Edition Mote" was proposed for the testing of building.*

Keywords: *Structural Performance, Fatigue, Damage, Gas leak, Fir.*

I. Introduction

Risk of buildings and civil engineering structures from natural hazards is large and growing. The 1995 Kobe earthquake in Japan killed over 6,400 people and the number of completely destroyed buildings and houses was over 100,000. The 2004 and 2007 Niigata earthquake in Japan, tsunami by the 2004 Indian Ocean earthquake, and the 2005 Hurricane Katrina in New Orleans caused heavy damage.Wireless sensor network (WSN) is key technology to realize the present computing and networking environment and it is expected that such an advanced technology will play an important role for natural hazard mitigation[3,8].A research on present part of the structure of buildings are monitored by using wireless sensor networks is discussed and actual application to high-risk buildings are described[4].

Role of sensor networks:

A wireless sensor network plays an important role in such strategies and can be connected to the internet so that this information can be used to monitoring future risks. Wireless sensors [2] are easy to install, remove, and replace at any location, and are expected to become increasingly smaller by using MEMS technology. They will provide a present, networked sensing environment in buildings.For example, the acceleration and strain at numerous locations on each beam and column, temperature and light in each room, images and sounds in desired regions can be obtained by the "smart dust" sensors [1, 3]. Additionally, a single type of sensor such as a condenser microphone can be used for multiple purposes, for example, to detect earthquake, fires and intrusions. Furthermore, a fiber optic network is not only utilized as infrastructure for information technology, but also as a "wired" sensor network.The following table shows the various kinds of hazards, and possible applications and combinations of sensors.

Sensor Application

Hazard	Application	Sensor
Earthqu-ake / Wind	observation	acceleration
	experiment	acceleration, strain
	structural control	acceleration
	health monitoring	acceleration, strain
	damage detection	acceleration, strain
Fire	fire detection	temperature, smoke,acoustic, olfactory
	gas leak detection	olfactory
	alarm, warning	sounder
	evacuation control	temperature, smoke, acoustic, olfactory
Crime	surveillance	acceleration, smoke, acoustic, light, camera
	Security alert	sounder

II. Berkeley Mote

The Berkeley motes are a family of embedded sensor nodes sharing roughly the same architecture.Let us take the MICA mote as an example. The MICA motes have a two-CPU design. The main microcontroller (MCU), an Atmel ATmega128L, takes care of regular processing. A separate and much less capable coprocessor is only active when the MCU is being reprogrammed.The ATmega103L MCU has integrated 512 KB flash memory and 4 KB of data memory. Given these small memory sizes, writing software for motes is challenging [5].

MICAz OEM **EDITION MOTE:**

MICAz OEM EDITION Mote

- OEM Module for Battery-Powered Mesh Network Sensor Nodes
- Postage Stamp Form Factor.
- It is a IEEE 802.15.4, 2.4 GHz Radio for up to 250 kbps Data Rate [6, 8].
- XMesh™ Mesh Networking Protocols.
- Analog and Digital I/O Interface for Easy Sensor Integration [6, 8].

Internal Architecture of MICAz OEM MOTE:

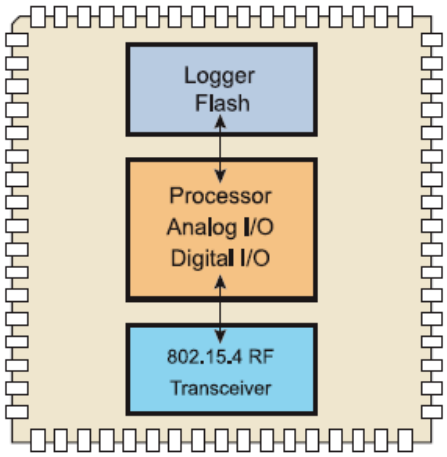

MICAz OEM Mote Powerful design features include:

- Optimized processor/radio module integration based on MEMSIC's extensive Mote development and deployment.
- Flexible onboard hardware interface for both standard and custom sensing devices.
- Comprehensive software support, including sensor board drivers and algorithms, via MEMSIC's industry leading XMesh™ software technology.

The MICAz OEM Edition is the functional equivalent of MEMSIC's popular MPR2400 MICAz Mote in a postage stamp form factor. This inherent design continuity makes the MICAz OEM Edition an ideal solution for next-generation mesh networking products and designs [7, 9, 12].

The MICAz OEM Edition is offered in a 68-pin LCC form factor for high-volume surface-mount integra-tion.By utilizing open platform, standards based interfaces the OEM Module offers users an attractive value proposition consisting of easily differentiated, low-power 2.4 GHz IEEE 802.15.4 compliant radio modules that can be rapidly designed and built[7,9,12].

Processor & Radio Platform:

- IEEE 802.15.4 compliant/ZigBee capable RF transceiver.
- 2.4 GHz globally compatible ISM band.
- Direct sequence spread spectrum radio for RF interference resistance and inherent data security.
- 250 kbps high data rate radio.
- 68-pin package designed for easy sensor integration including light, temperature, RH, barometric pressure, acoustic, magnetic, acceleration or seismic, etc.

Software support:

- Optimized, industry proven, XMesh™ networking stack for low-power, self forming, high reliability wireless networks.
- Open interfaces for integration and customization of sensor node applications and works with operating system called TinyOS.

Specifications

Processor/radio	**MICAz Mote**	**Remarks**
Processor Performance		
Program Flash Memory	128k bytes	
Measurement Flash	512k bytes	>100,000 Measurements
Configuration EEPROM	4k bytes	
RAM	4k bytes	
Serial Communications	UART	0-3v transmission levels
Analog to Digital Converter	10 bit ADC	8 channel, 0-3v input
Other Interfaces	Digital I/O,I2C,SPI	
Current draw	8 mA	Active mode
	<15uA	Sleep mode
RF Transceiver		
Frequency band	2400MHz to 2483.5MHz	ISM band
Transmit(TX) data rate	250 kbps	
RF Power	3 dbm (max), 0 dbm (typ)	
Receive Sensitivity	-90 dbm (min),-94 dbm(typ)	
Current Draw	19.7mA	Receive mode
	11mA TX, -10 dbm	
	14mA TX, -5 dbm	
	17.4mA TX, 0 dbm	
	1 uA	Sleep mode, voltage regulator OFF
Electromaechanical		
External Power	2.4V - 3.6V	
Size (in)	0.95 x 0.95	LCC68
(mm)	24.13 x 24.13	

OEM Design Kit:

For prototyping and development, MEMSIC provides Mote Works™, a fully integrated software platform and a complete OEM Design kit, consisting of pre-programmed OEM Edition Reference Designs, OEM Edition Modules, sensor or data acquisition boards and an Ethernet base station. The Mote Works™ software platform is optimized for low-power battery-operated networks providing an end-to-end platform across all tiers of wireless sensor networking applications [6].

TinyOS:

TinyOS is an open-source operating system designed for embedded systems with very limited resources, like the Mica series of motes. TinyOS uses the NesC language, an extension to C, with similar syntax, that attempts to embody the structuring concepts and execution model. As an embedded operating system, it responds to hardware events with handlers, while also allowing tasks, which are equivalent to functions in other programming languages.TinyOS does not implement object sharing[10,11].

III. Conclusion

The feasibility of structural monitoring of buildings using the smart sensors was discussed and the MICAz OEM EDITION Mote was proposed as a wireless sensor to check the performance of the building. Further research on more effective modes of communication is needed to achieve a wireless sensor network for building risk monitoring.

References

[1] A Survey on Sensor Networks-Ian F.Akyildiz, Weilian Su, Yogesh- Sankarasubramaniam, Erdal Cayirci Georgia Institute of Technology.
[2] Risk Monitoring of Buildings Using Wireless Sensor Network- N. Kurata, B.F. Spencer, Jr., M. Ruiz-Sandoval, 2008.
[3] Building Risk Monitoring Using Wireless Sensor Network- Narito Kurata, Billie F.Spencer Jr, Manuel Ruiz-Sandoval, 2004.
[4] Structural health monitoring: sensors and systems - Janousek, L Hudec.R.Electro., 2012.
[5] Berkeley Mote:-http://webs.cs.berkeley.edu/.
[6] Micaz Oem Edition Mote:- http://www.xbow.com/Products/Product_pdf_files/Wireless_pdf/MICA.pdfes/Wireless_pdf/MICAz OEM EDITION MOTE datasheets.pdf.
[7] Comparison Of Feasibility Of Risk Monitoring In Buildings In Two Wireless Sensor Network MICA MOTE AND MEMS-Vineeta Gupta & Komal Gupta,2012.
[8] Actual Application of Ubiquitous Structural Monitoring System using Wireless Sensor Networks - Narito Kurata, Makoto Suzuki, Shunsuke Saruwatari and Hiroyuki Morikawa,2008.
[9] Performance Measurements of Motes Sensor Networks:-G. Anastasi, A.Falchi, A.Passarella Dept. of Information Engineering University of Pisa Via Diotisalvi, 2 – 56122 Pisa, Italy, M. Conti, E. Gregori IIT Institute CNR, Via G. Moruzzi, 1 – 56124 Pisa, Italy.
[10] TinyOS tutorials:- http://www.tinyos.ney/tinyos-1.x/doc/tutorial/.
[11] Sensor Network Lab Exercises Using TinyOS and MicaZ Motes- Jens Mache, Chris Allick, John Charnas, Alex Hickman, Damon Tyman.
[12] Sensor Network Motes-Portability & Performance Ph.D. dissertation by Martin Leopold.

International Journal of Modern Engineering Research (IJMER)
www.ijmer.com Vol.3, Issue.3, May-June. 2013 pp-1393-1395 ISSN: 2249-6645

Managing Business Analysis for Agile Development

Rohit Prakash, [1] Neha Agarwal[2]
[1]*Student M.Tech CSE Final Year, Amity University, Noida, U.P., India*
[2]*Assistant Professor, Department of CSE, Amity University, Noida, U.P., India*

Abstract: *Agile development methodologies are helping software companies and development teams to align to the new evolving economy. Agile gainsay and hampers our notion of software engineering practices and project management techniques and methodology, and the way we lead our project teams. The Agile movement impacts each role on a project team in a different way and creates a lot of chances to learn new skills and develop new ways of working and gaining success together. Agile introduces a major shift in the way teams look at software requirements gathering and when they are defined in the process. Agile Business Analysts are an unified part of the team throughout the life of the software project development cycle and alleviate collaboration across a broader cross section of the project team and the business. Collaboration, management, facilitation, leadership, coaching and team building become significant new skills required for BA on Agile projects. Leadership and management are key components critical to their success.*

Keywords: *Conventional requirement, Agile management techniques, Collaborative requirement, New Business Analysis skills, Agile on conventional project*

I. INTRODUCTION

Moving from old project work to agile project work will impact all functional role on a project team separately:

- For Business Analysts (BA), successfully managing an agile project depends on defining requirements in smaller increments and working more collaboratively with the team through the life of the project.
- For Project Managers, success moving to Agile development methodologies depends on acquiring the skills necessary to progressively plan a project through its lifecycle rather than at the onset. Project Managers will also need to acquire new ways of intellect project control and risk.
- For Quality Testers, evolving to an agile framework will mean developing the skills necessary to write tests and validate code in parallel with development.

This paper will explore the impact agile development methodologies are having on the BA community, what new skills are required, and what BAs can do to ease the changeover.

II. CONVENTIONAL REQUIRMENT

The BA's are learned to believe that they can and should define detailed requirements at the starting of a project. Built in this philosophy there are several challenging assumptions. Conventional requirements analysis assumes that:

- Customer can definitively know, enounce, and functionally define what the system or software should do at the end of the project
- Once documented, the requirements will not change – at least not without potential project delays, budget overruns, or scrawny feature sets
- Requirements process is captive to a single product owner who sits apart from the development team picturing the product
- Does not acknowledge the inherited uncertainty in software development that agile methodologies seek to embrace

Experience shows us that these assumptions are wrong. As we learn more about the evolving system, our knowledge will impact the system we want to build. The process of creating the system helps the team learn more about what is possible. The act of creating the requirements will cause them to change. Agile methodologies boost us to embrace this kind of work to adopt in our projects. We start realizing that change really is nice, it helps us to deliver greater value to our customers and attempting to define everything up front results in continuous change management. To fully understanding the impact that Agile has on the BA role, it is helpful and required to understand how agile projects are running.

III. AGILE PROJECT MANAGEMENT

According to Agile Project Management the processes need to create good software in today's world are not predictable. Requirements with technologies change and as individual team member productivity is highly varying. When processes are not fixed and results cannot be predicted, we cannot use planning methods that based on only predictability. Instead of it, we need to adjust and change the processes and guide them to give our required outcomes. Agile project management does this by maintaining and keeping progress highly visible, inspecting project outcomes regularly, and maintaining an ability to adapt to changing circumstances as required.

Benefits of Agile Project Management are produced in incremental part by having an enormous amount of accountability and responsibility on team members. Great teams build great software and those should be trusted and

appointed and charge to deliver. The Agile Project Manager helps the team to always stay focused on the several business issues and help them to correct and removes obstacles that hinders the team's ability to deliver final product. The focus is on the team because they are who ultimately going to deliver.

As agile teams are self-organizing, agile project manager focuses much on leadership as compared to a conventional development environment. Several skills like coaching, facilitation and team building are important components for project success. The project manager is creating a trust and an environment where each individual are motivated to contribute to the team's success for project. Project Managers focus little on assigning tasks and managing plan and much on maintaining the solid structure and discipline of the agile team. By trusting that through visibility, regular inspection, and proper adaptation the team will deliver the noticeable and desired results. This philosophy change the role of the BA for how requirements are gathered, distilled, and managed [1].

IV. COLLABORATIVE REQUIRMENTS

1. Introduction

As opposed to conventional requirements gathering, where the BA major works with the client is only to gather requirements, here agile team members are involved in gathering and defining all product requirements. Domain specific technical team members and testing team or QA team collaborate with the product owner and the BA to develop and maintain the project specifications by bringing their all technical skills and experience into this collaborative and collective process. Increasing interaction enables and ensures team to develop requirement document and specifications that can be created and tested under the all project constraints.

To deal with scope on an agile project, specifications and requirements must be considered in two dimensions which are breadth first and then depth. It is necessary to understand the breadth of what we want to build early in the project cycle. Working with breadth of the solution helps team to understand scope and cost that will facilitate them estimating, release and planning. The breadth of a project starts to frame the boundaries of the product and helps to manage and cope the organization's expectations. Breadth of the requirements is a much little investment of time and resources as compared with dealing with the entire depth. The details are likely to evolve when we progress through the project so defining it early has little value. To have a good understanding of the breadth of project requirements early in the project lifecycle helps development team start to define the set of all possible solutions. The BA plays a major role in alleviate the conversation between the product owner, managers, the technical team with QA team. BA ensures that the full scope of requirements has been defined and balanced by technical and domain understanding of the solution.

Once the team has created the breadth of the solution, then they begin incrementally looking at depth of it. The BA take the lead in helping the team by bring requirements to this next level of detail. For this we have to abandon our conventional notions of the Marketing, Product Requirements Document and the list of the system specifications. Instead, we have to focus only on how the system will behave in future.

To manage requirements effectively in a conventional and traditional environment, Business Analysts sort through many-to-many (M-to-M) relationships [2] between business design, and specifications elements. Because of complex interactions among these M-to-M relationships, requirements management industry had created tools to trace their interdependence among them. BA will track the impact of any requirement change to its corresponding design element or from a change in design element back to requirement. This process can get even more complex when one traces into the software component and test results.

1.1. Agile Requirements

Based on the level of process required by an company, BAs will use either use cases or user stories. Agile methods basically tend to be light weight specifications and requirements are documented as user stories. User story is a high level description of system behavior and it is not a full specification of the requirement but a placeholder for conversation about the requirement of system. The user story will be fully documented and specified as it is brought into a development cycle. After delivered, a user story represents a fully functional slice of the overall system. Here are the suggested guidelines to determine what makes a good user story. Bill Wake defined the INVEST model for definition of requirements [3]:

Independent

- Avoid dependencies among stories
- Write to establish foundation
- Combine them if possible in a single iteration

Valuable

- Each story should show some value to the Users and Stakeholders

Estimable

- Enough detail should be provided to allow the team to estimate
- Team will only encounter problems estimating if the story is very big, or if insufficient information is given, or if there is lack of domain knowledge about it

Sized Appropriately

- Every story should be small enough so it should be completed in a single iteration
- Stories that needed to be worked on in near future should be smaller with more detailed and big stories are acceptable if planned further out

Testable

- Acceptance criteria should be written in customer terms
- Tests should be automated if possible
- Every team members should demand a clear acceptance criterion for it.

V. NEW ANALYSIS SKILLS FOR BA

Agile BA will basically depend on facilitation skills of people instead of on conventional projects. BA's role is to conduct a discussion between product owner and software development team. BA will bring a tremendous amount of system and domain knowledge to the discussion and is positioned to get functional requirements from product owner. BAs help to translate user requirements into more technical language for the development team. Apart from coaching, facilitation and team building, agile BA needs to think about the software development process in new and non conventional ways. Agile helps us to decouple breadth of the solution from the depth of the solution to deliver smaller increments of production-ready code. This can cause a difficulty for some analysts making the transition to Agile from traditional way and will create opportunities to learn about how to write feature (functional) driven requirements [4]. BA can be asked to work on an agile project as the project has a high need for written functional specifications and design documents. In both case, BA primary role is to conduct understanding and communication.

While it is ideal is to have a product owner or an on-site customer, for many teams this is not possible. For those teams, the BA may have to fill the role of a customer proxy. Having the role of the customer proxy puts a significant amount of additional responsibility on the role of the BA. In this scenario, the BA is asked to understand the needs of the customer and translate those needs to the development team. This model introduces risk because the true end customer is not directly involved with the people developing the product. The BA can mitigate this risk by encouraging the product owner to review the evolving system as frequently as possible.

VI. AGILE ON CONVENTIONAL PROJECT

Moving to agile is not usually the decision of the Business Analyst. However, given the BA's critical role on the project, there is often quite a bit they can do to help set the stage for an agile transition. The BA can encourage collaboration between the product owners and the technical teams. This will ensure that requirements are balanced and feasible[5]. This will tend toward managing expectations and helping the project owner to understand the cost of the solution they are spending. The BA can begin to demonstrate the value of loosely coupled functional specifications and begin introducing use cases or user stories to the team members. When the specifications are completed, the development team will derive value from a functionally-driven specification. System will be easy to develop and test and traceability will be a non-issue. If software team has dedicated QA members, agile requirements will enable functional testing process. Test plans should be derived from functional organized specifications.

VII. CONCLUSION

Success in present economy needs us to react quickly to always changing software market conditions. Traditional and conventional products delivery methodologies alone cannot deliver quick enough in such highly uncertain project domains. Software agile processes allow BA and development teams to meet changing demands of their customers while developing nice environments where all team members want to work.

BA can play a major role on an agile team success, by shift their traditional and conventional thinking about requirements. Secondly, Business Analyst's need to consider learning new skills for understanding and writing requirement documents and new techniques for managing them. Success for result will depend mainly on how well BAs learn and adapt to these new ways of working with all kinds of requirements, using group collaboration and setting up functional and technical teams.

REFERENCES

Journal Papers:
[1] Mike Cottmeyer, V. Lee Henson, Application The Agile Business Analyst, Version 1
Books:
[2] BABOK (Published by IIBA).
Online WebPages:
[3] http://www.bridging-the-gap.com/agile-project-business-analyst-case-study/
[4] http://www.agilemodeling.com/essays/businessAnalysts.htm
Theses:
[5] Avsharn Bachoo, A Business Analysis Methodology, University of Witwatersrand, 2006

International Journal of Modern Engineering Research (IJMER)
www.ijmer.com Vol.3, Issue.3, May-June. 2013 pp-1396-1399 ISSN: 2249-6645

Secure Outsourcing Mechanism for Linear Programming in Cloud Computing

Shaik Kalesha, [1] G.Sridevi[2]
[1]M.Tech, Nimra College of Engineering & Technology, Vijayawada, A.P., India
[2]Assoc.Professor, Dept.of CSE, Nimra College of Engineering & Technology, Vijayawada, A.P., India

Abstract: *Cloud Computing is a subscription based service where you can obtain the networked storage space and computer resources. In cloud computing model, the customers plug into the cloud to access IT resources which are priced and provided on demand services. This cloud computing model composed of five essential characteristics, three service models and four deployment models. Users can store their data in the cloud and there is a lot of personal information and potentially secure data that people store on their computers, and this information is now being transferred to the cloud. Here we must ensure the security of user's data, which is in stored in the cloud. This paper presents the secure outsourcing mechanism for linear programming in the cloud computing environment. Linear programming is an algorithmic and computational tool which captures the first order effects of various system parameters that should be optimized, and is essential to the engineering optimization. It has been widely used in various engineering disciplines that analyze and optimize real world systems, such as - packet routing, flow control, power management of data centers, etc.*

Keywords: *Cloud, Linear programming, Security.*

I. INTRODUCTION

The end of this decade is marked by a paradigm shift of the industrial information technology towards the subscription based or pay-per-use service business model known as cloud computing [1]. This paradigm provides users with a long list of advantages, such as- provision computing capabilities; broad, heterogeneous network access; resource pooling and rapid elasticity with measured services [2]. Huge amounts of data being retrieved from the geographically distributed data sources, and non-localized data-handling requirements, creates such a change in technological as well as business model. One of the prominent services offered in the cloud computing is the cloud data storage, in which subscribers do not have to store their data on their own servers, where instead their data will be stored on the cloud service provider's servers.

In cloud computing, the subscribers have to pay the service providers for this storage service. This service does not only provides flexibility and the scalability for the data storage, it also provide customers with the benefit of paying only for the amount of data they need to store for a particular period of time, without any concerns for efficient storage mechanisms and maintainability issues with large amounts of data storage. In addition to these benefits, the customers can easily access their data from any geographical region where the Cloud Service Provider's network or Internet can be accessed. An example of the cloud computing is shown in Figure 1.

Along with these unprecedented advantages, the cloud data storage also redefines the security issues targeted on customer's outsourced data (data that is not stored/retrieved from the costumers own servers). Since the cloud service providers (SP) are separate market entities, data integrity and privacy are the most critical issues that need to be addressed in cloud computing. Even though the cloud service providers have standard regulations and has powerful infrastructure to ensure customer's data privacy and provide a better availability, the reports of privacy breach and service outage have been apparent in last few years [3] [4] [5].

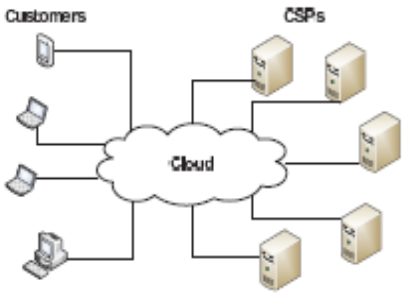

Figure 1: Cloud Computing Architecture Example

This paper presents the secure outsourcing mechanism for linear programming (LP) in the cloud computing environment. Linear programming is an algorithmic and computational tool which captures the first order effects of various system parameters that should be optimized, and is essential to the engineering optimization. It has been widely used in various engineering disciplines that analyze and optimize real world systems, such as - packet routing, flow control, power management of data centers, etc.

II. RELATED WORK

General secure computation outsourcing that fulfills all the aforementioned requirements, such as input/output privacy and correctness/soundness guarantee has been shown feasible in theory by Gennaro et al. [6]. However, it is currently not practical due to the huge computation complexity. Atallah et al. explore a list of work [7][8] for securely outsourcing specific applications. The customized solutions are expected to be very efficient than the general way of constructing the circuits. In [7], they give the first investigation of secure outsourcing of numerical and scientific computation. Later on in [8] and [9], Atallah et al. give two protocol designs for both secure sequence comparison outsourcing and the secure algebraic computation outsourcing. However, both protocols use heavy cryptographic primitive such as homomorphic encryptions [10] and/or oblivious transfer [11] and do not scale well for large problem set.

Hohenberger et al. [12] provide protocols for secure outsourcing of modular exponentiation, which is considered as prohibitively expensive in most public-key cryptography operations. Recently, Atallah [13] et al. give a provably secure protocol for secure outsourcing matrix multiplications based on secret sharing [14]. Another large existing list of work that relates to ours is Secure Multi-party Computation (SMC), first introduced by Yao [15] and later extended by Goldreich et al. [16] and many others. Very recently, Wang et al. [17] give the first study of secure outsourcing of linear programming in cloud computing. Their solution is based on the problem transformation, and has the advantage of bringing customer savings without introducing substantial overhead on cloud. However, those techniques involve cubic time computational burden matrix-matrix operations, which the weak customer in our case is not necessarily able to handle for large-scale problems.

III. PROPOSED WORK

Our proposed mechanism consists of three phases:

A. Problem Transformation

In this phase, the cloud customer would initialize a randomized key generation algorithm and prepare the LE problem into some encrypted form ϕ_K via key K. Transformation and encryption operations will be needed when necessary.

The customer who has coefficient vector "b" and seeks solution "x" satisfying Ax = b cannot directly starts the ProbSolve with cloud, since such interaction may expose the private information on final result x. Thus, we still need a transformation technique to allow the customer to properly hide such information first. The customer picks a random vector r $\in R^n$ as his secret keying material, the new LE problem is written as:

$$Ay = b' \quad \text{---------- (1)}$$

Where y = x + r and b' = b + Ar. Equation (1) can be rewritten as follows:

$$y^{K-1} = T.y^{(k)} + C' \quad \text{---------- (2)}$$

Where T= $D^{-1}.R$, $c' = D^{-1}.b'$, and A= D + R.

The whole procedure of "ProbTransform" is summarized in the following Algorithm 1.

Algorithm1:
Data: original problem Φ =(A,b)
Result: transformed problem as shown in Equation (2)

Step 1: Pick random r $\in R^n$
Step 2: Compute b^1 =b+Ar, and $c^1 = D^{-1}.b^1$
Step 3: Replace tuple (x,c) in Equation (2) with (y=x+r, c^1)
Return transformed problem as Equation (2).

B. Problem Solving

In this phase, the cloud customer would use the encrypted form ϕ_K of LE to start the computation outsourcing process. In case of using the iterative methods, the protocol ends when the solution within the required accuracy is found.

After the problem transformation step, now we are ready to describe the phase of "ProbSolve". The purpose of the protocol is to let the customer securely harness the cloud for the most expensive computation, i.e., the matrix-vector multiplication T. $y^{(K)}$ in Eq. (2) for each algorithm iteration, k = 1, 2,……L. assume without loss of generality that our main protocol of solving LE works over integers. All arithmetic is modular with respect to the modulus "N" of the homomorphic encryption, and the modulus is large enough to contain the answer. For the first iteration, the customer starts

the initial guess on the vector $y^{(0)} = (y1^{(0)}, y2^{(0)}, \ldots\ldots yn^{(0)})^T$, and then sends it to the cloud. The cloud server, in possession of the encrypted matrix Enc (T), computes the value Enc (T. $y^{(0)}$) by using the homomorphic property of the encryption:

$$\mathrm{Enc}(\mathbf{T} \cdot \mathbf{y}^{(0)})[i] = \mathrm{Enc}(\sum_{j=1}^{n} \mathbf{T}[i,j] \cdot y_j^{(0)})$$

$$= \prod_{j=1}^{n} \mathrm{Enc}(\mathbf{T}[i,j])^{y_j^{(0)}} \quad \text{------- (3)}$$

After receiving Enc (T. $y^{(0)}$) the customer decrypts and gets value T. $y^{(0)}$ Using his private key. He then updates the next approximation $y^{(1)}$ = T. $y^{(0)}$ + $c^{'}$ via Equ (2). The protocol execution continues until the result converges, as shown in the following Algorithm 2.

Algorithm 2:

Data: Transformed problem with input c^1 and Enc (T)
Result: Solution x to the original problem Φ = (A, b)
% L: Maximum number of iterations to be performed;
% $\in$: Measurement of convergence point;

Step 1: Customer picks $y^{(0)} \in (Z_N)^N$
For (k<-0 to L) do

Step 2: Customer sends $y^{(k)}$ to cloud

Step 3: Cloud computes Enc (T $y^{(k)}$) via Equation (3)

Step 4: Customer decrypts T $y^{(k)}$ via his private key
If $\| y^{(k)} - y^{(k+1)} \| <= \in$ then

Step 5: break with convergence point $y^{(k+1)}$

Step 6: return x= $y^{(k+1)}$ - r

C. Result Verification

In this phase, the cloud customer would verify the encrypted result produced from the cloud server, using the randomized secret key K. A correct output "x" to the problem is produced by decrypting the encrypted output. When the validation fails, the customer output $\perp$, indicating the cloud server was cheating.

IV. CONCLUSION

Cloud Computing provides convenient on demand network access to a shared pool of configurable computing resources that can be rapidly deployed with the great efficiency and minimal management overhead. Focusing on the engineering and scientific computing problems, this proposed work investigates secure outsourcing for widely applicable large-scale systems of linear equations (LE), which are among the most popular algorithmic and computational tools in various engineering disciplines that analyze and optimize real-world systems. Our proposed work has three phases- problem transformation, problem solving and result verification. In problem transformation, the cloud customer would initialize a randomized key generation algorithm and prepare the LE problem into some encrypted form ϕ_K via key K. Transformation and encryption operations will be needed when necessary. In problem solving, the cloud customer would use the encrypted form ϕ_K of LE to start the computation outsourcing process. In case of using the iterative methods, the protocol ends when the solution within the required accuracy is found. In result verification, the cloud customer would verify the encrypted result produced from the cloud server, using the randomized secret key K.

REFERENCES

[1] M. Armbrust, A. Fox, R. Grifth, A. D. Joseph, R. Katz, A. Konwinski, G. Lee, D. Patterson, A. Rabkin, I. Stoica, and M. Zaharia. Above the clouds: A berkeley view of cloud computing. Technical report, University of California at Berkeley, February 2009.
[2] P. Mell, T. Grance, "Draft NIST working definition of cloud computing", Referenced on June. 3rd, 2009, online at http://csrc.nist.gov/groups/SNS/cloud-computing/index.html, 2009.
[3] Amazon.com, "Amazon s3 availablity event: July 20, 2008", online at http://status.aws.amazon.com/s3-20080720.html, 2008.
[4] M. Arrington, "Gmail Disaster: Reports of mass email deletions", Online at http://www.techcrunch.com/2006/12/28/gmail-disasterreports-ofmass- email-deletions/, December 2006.
[5] J. Kincaid, "MediaMax/TheLinkup Closes Its Doors", Online at http://www.techcrunch.com/2008/-7/10/mediamaxthelinkup-closes-itsdorrs/, July 2008
[6] R. Gennaro, C. Gentry, and B. Parno, "Non-interactive verifiable computing: Outsourcing computation to untrusted workers," in Proc. Of CRYPTO'10, Aug. 2010.
[7] M. J. Atallah, K. N. Pantazopoulos, J. R. Rice, and E. H. Spafford, "Secure outsourcing of scientific computations," Advances in Computers, vol. 54, pp. 216–272, 2001.
[8] M. J. Atallah and J. Li, "Secure outsourcing of sequence comparisons," Int. J. Inf. Sec., vol. 4, no. 4, pp. 277–287, 2005
[9] D. Benjamin and M. J. Atallah, "Private and cheating-free outsourcing of algebraic computations," in Proc. of 6th Conf. on Privacy, Security, and Trust (PST), 2008, pp. 240–245.
[10] P. Paillier, "Public-key cryptosystems based on composite degree residuosity classes," in Proc. of EUROCRYPT'99, 1999, pp. 223–238.
[11] S. Even, O. Goldreich, and A. Lempel, "A randomized protocol for signing contracts," Commun ACM, vol. 28, no. 6, pp. 637–647, 1985.
[12] S. Hohenberger and A. Lysyanskaya, "How to securely outsource cryptographic computations" in Proc. of TCC, 2005 pp. 264–282.
[13] M. Atallah and K. Frikken, "Securely outsourcing linear algebra computations," in Proc. of ASIACCS, 2010, pp. 48–59
[14] A. Shamir, "How to share a secret," Commun. ACM, vol. 22, no. 11, pp. 612–613, 1979
[15] A. C.-C. Yao, "Protocols for secure computations (extended abstract)," in Proc. of FOCS'82, 1982, pp 160–164
[16] O. Goldreich, S. Micali, and A. Wigderson, "How to play any mental game or a completeness theorem for protocols with honest majority," in Proc. of STOC'87, 1987, pp 218–229
[17] C. Wang, K. Ren, and J. Wang, "Secure and practical outsourcing of linear programming in cloud computing," in Proc. of IEEE INFOCOM, 2011

International Journal of Modern Engineering Research (IJMER)
www.ijmer.com Vol.3, Issue.3, May-June. 2013 pp-1400-1402 ISSN: 2249-6645

Skyline Query Processing using Filtering in Distributed Environment

Shaik Shafi, [1] Sayeed Yasin[2]
[1]M.Tech, Nimra College of Engineering & Technology, Vijayawada, A.P., India
[2]Asst.Professor, Dept.of CSE, Nimra College of Engineering & Technology, Vijayawada, A.P., India

Abstract: *Skyline is used in a distributed database, because the database will not be in one system. It will be stored in multiple systems reside at different locations, if it is connected using internet. A Query is called as "Skyline", which query works or execute based on data points. "Skyline" query returns many multidimensional points. It extracts the information from different places of distributed database at different sites. Skyline query returns all the interesting points that are not dominated by any other points. Skyline queries play an important role in multi criteria decision making and the user preference applications. For example, a tourist can issue a skyline query on a hotel relation to get those hotels with high stars and cheap prices. This paper presents the skyline query processing in distributed environment using filtering.*

Keywords: *Data sites, Distributed environment, Filtering, Query.*

I. INTRODUCTION

Developments in the past couple of years have revealed a trend towards distributed data management and the storage systems. In the presence of the huge amounts of data that today's systems are providing access to, it is a tedious task for a user to find the most interesting available data without using the advanced query types, such as skyline queries. Whereas the problem is known as the skylines in database research, in other areas it was already known before as the maximum vector problem or the Pareto optimum [1] [2]. The popularity of the the skyline operator is mainly due to its applicability for decision making applications; skyline queries help users make intelligent decisions over complex data, where different and often conflicting criteria are considered.

Skyline queries have originally been proposed for centralized environments [3], i.e., single-database environments. As now- a- days data is increasingly stored and processed in a distributed way, skyline processing over distributed data has attracted much attention recently. Skyline query processing in the distributed environments poses inherent challenges and requires non-traditional techniques due to the distribution of content and the lack of global knowledge. There are various different distributed systems with a different requirements and unique characteristics that have to be exploited for efficient skyline processing. Peer-to-peer (P2P) systems can be considered as an example of the distributed system architecture for which several distributed skyline approaches have been proposed. Other architectures, such as the Web information systems, parallel shared-nothing architectures, distributed data streams, or wireless sensor networks have different requirements.

The variety of existing distributed systems leads to the variety of existing distributed skyline approaches. Moreover, the fact that several skyline variants, beyond the traditional skyline operator, have also been proposed in the past decade [4] [5] leads to various distributed approaches that support different skyline variants. The most important variants are- subspace skylines (only some attributes of a tuple are considered for evaluation), constrained skylines, and dynamic skyline queries (the skyline is not executed in the original data space but the data points are transformed into another data space before evaluating the skyline). The characteristic of the skyline variants requires sophisticated and specialized algorithms for efficient processing. Depending on the underlying network and the communication architecture, these variants allow for different optimizations.

II. RELATED WORK

A distributed skyline query can be processed by evaluating multiple constrained skyline queries on the different servers. A framework, called SkyPlan [6] has been proposed that maps the dependencies between the queries into a graph and generates cost-aware execution plans. The one of the possible ways to deal with geographically scattered data has been studied using a framework called PadDSkyline [7]. The theme of incomparability for skyline computation has also been explored. The authors have proposed and compared skyline computation based on dominance and incomparability through algorithms BSkyTree-S and BSkyTree-P [8]. The progressive skyline computations using DSL [9] and other algorithms [10] have also been proposed for query load balancing. The advent of the multi-core processors is making a profound impact on software development.

In [11] , the authors have modified the basic skyline computation algorithms SFS (Sort Filter Skyline), BBS (Branch and Bound Skyline) and SSkyline (Simple Skyline) to induce the possible parallelism in them and have proposed a new algorithm PSkyline (Parallel Skyline). In [12], the authors have proposed an algorithm called as SSP (Search Space Partitioning) which exploits features of BATON -Balanced Tree Overlay network for indexing the dataset so that in structured peer to peer network, the peers will be accessed to the minimum and exact data sub space to compute the skyline can be searched efficiently. Other aspects of the parallel skyline computation like rank-aware queries, constrained skyline queries and progressive skyline computation in P2P networks have been proposed in [13] respectively. Proper data sub space partitioning is another aspect of the parallel skyline computation. The related approaches have been discussed in [14].

III. PROPOSED WORK

In our proposed work, given a distributed environment without any overlay structures, our main objective is efficient query processing strategies that shorten the overall query response time. We first speed up the overall query processing by achieving parallelism of the distributed query execution. Given a skyline query with some constraints, all relevant sites are partitioned into incomparable groups among which the query can be executed in parallel. Within each group, specific plans are proposed to further improve the query processing involving all intra- group sites. On a processing site, multiple filtering points are deliberately picked based on their overall dominating potential from the "local skyline". They are then sent to the other sites with the query request, where they help identify more unqualified points that would otherwise be reported as false positives, and thus, reducing the communication cost between data sites.

Filtering points are selected from the local skyline result that initially obtained. Suppose that the initial skyline result is SKinit = {s1; s2; . . . ; sl}, we need to select K (<l) points from it as the "multiple" filtering points. We study two heuristics that guide the selection of K filtering points from l(>k) skyline points. The first heuristic for selecting the multiple filtering points maximizes the sum of the values of all possible choices. To accomplish this, we need to sort points in SKinit in a non- ascending order and then pick the top-K ones. We call this heuristic MaxSum. It actually simplifies the computation by ignoring the overlapping between different "skyline" points dominating regions. The smaller the "overlapping" regions are, the more accurate the method will be. In the second heuristic, we intend to take into account the topology between the filtering points, to reduce the overlapping faced by the first heuristic. "Distance" is a simple metric to help consider this. Intuitively, the farther two "skyline" points are apart, the less their dominating regions overlap. Hence, we propose a greedy heuristic, called "MaxDist", which maximizes the distance between filtering points. The algorithm of this heuristic is shown in Algorithm 1.

Algorithm 1:
Maxdist (SKinit, K)

Input: SK_{init} is the initial skyline;
K is the number of filtering points needed;
Output: a set of multiple filtering points.

Step 1: $F_{flt} = \Phi$

Step 2: Pick S_i and S_j from SK_{init} satisfying $|S_i, S_j| > |S_i^1, S_j^1|$
$\forall$ 1<= S_i^1, S_j^1 <=l;

Step 3: F_{flt} = { S_i, S_j }; $SK^1 = SK_{init}$ -{ S_i, S_j };

Step 4: While $|F_{flt}|$<K do

Step 5: Pick S_i from SK^1 satisfying

$$\sum_{sj \in F_{flt}} |S_i, S_j| >= \sum_{sj \in F_{flt}} |S_i^1, S_j|, \forall\ S_i^1 \in SK^1$$

Step 6: $F_{flt} = F_{flt} \cup \{ S_i \}$; $SK^1 = SK_{init}$ -{ S_i };

Step 7: return F_{flt}

Initially, it picks from "SKinit" two points between which the distance is the largest among all pairs (line 2). Then, it incrementally selects points from "SKinit" and adds them to the filtering set, until K filtering points are obtained. In every incremental step, the point with the maximal sum of the distances to all current filtering points is selected (line 5).

The idea behind "MaxDist" heuristic is good, but it is difficult to implement strictly due to its computational complexity. Therefore, we count the sum of distance between a point and all the current filtering points in MaxDist, and then pick the one with the maximum sum as a new filtering point. The improved version of the basic heuristic "MaxDist", called "MaxDist2", is shown in Algorithm 2.

Algorithm 2:
Maxdist2(SKinit, K, Δ)

Input: SK_{init} is the initial skyline;
K is the number of filtering points needed;
Δ is the distance threshold
Output: a set of multiple filtering points.

Step 1: $F_{flt} = \Phi$

Step 2: Pick S_i and S_j from SK_{init} satisfying $|S_i, S_j| > |S_i^1, S_j^1|$

$\forall$ 1<= S_i^1, S_j^1 <=l;

Step 3: $F_{flt} = \{S_i, S_j\}$; $SK^1 = SK_{init} - \{S_i, S_j\}$;

Step 4: While $|F_{flt}|$<K do

Step 5: Pick S_i from SK^1 satisfying

$$\sum_{sj \in F_{flt}} |S_i, S_j| >= \sum_{sj \in F_{flt}} |S_i^1, S_j|, \forall\ S_i^1 \in SK^1$$

Step 6: and dist(S_i, S_j) > Δ;

Step 7: $F_{flt} = F_{flt} \cup \{S_i\}$; $SK^1 = SK_{init} - \{S_i\}$;

Step 8: return F_{flt}

IV. CONCLUSION

In this paper, we have addressed the problem of constrained skyline query processing in distributed environment. Given a skyline query with some constraints, all relevant sites are partitioned into incomparable groups among which the query can be executed in parallel. Within each group, specific plans are proposed to further improve the query processing involving all intra- group sites. On a processing site, multiple filtering points are deliberately picked based on their overall dominating potential from the "local skyline". They are then sent to the other sites with the query request, where they help identify more unqualified points that would otherwise be reported as false positives, and thus, reducing the communication cost between data sites.

REFERENCES

[1] H. T. Kung, F. Luccio, and F. P. Preparata. On finding the maxima of a set of vectors Journal of the ACM, 22(4):469–476, 1975
[2] F. P. Preparata and M. I. Shamos. Computational Geometry - An Introduction Springer, 1985
[3] S. Börzsönyi, D. Kossmann, and K. Stocker. The skyline operator. In ICDE, pages 421–432, 2001.
[4] B. Cui, H. Lu, Q. Xu, L. Chen, Y. Dai, and Y. Zhou. Parallel Distributed Processing of Constrained Skyline Queries by Filtering. In ICDE, pages 546–555, 2008.
[5] D. Papadias, Y. Tao, G. Fu, and B. Seeger. An Optimal and Progressive Algorithm for Skyline Queries In SIGMOD, pages 467–478, 2003.
[6] João B. Rocha-Junior, Akrivi Vlachou, Christos Doulkeridis, and Kjetil Nørvåg, "Efficient Execution Plans for Distributed Skyline Query Processing", Conf on EDBT, March 2011.
[7] Lijiang Chen, Bin Cui, Hua Lu, "Constrained Skyline Query Processing against Distributed Data Sites" IEEE TKDE, Vol. No 23 no 2, February 2011, pp. 204-217.
[8] Jngwuk Lee, Seung-won Hwang. "BskyTree: Scalable Skyline Computation Using A Balanced Pivot Selection.", EDBT 2010, March 22-26, Lausann, Switzerland, 2010, pp. 195-206.
[9] Ping Wu, Caijie Zhang, Ying Feng, Ben Y. Zhao, Divyakant Agrawal,, and Amr El Abbadi "Parallelizing Skyline Queries for Scalable Distribution", EDBT 2006, LNCS 3896, pp. 112–130.
[10] Lin Zhu, Shuigeng Zhou, Jihong Guan, "Efficient Skyline Retrieval on Peer-to-Peer Networks", Future Generation Communication and Networking (FGCN), 2007, pp. 309-314.
[11] Hyeonseung Im, Jonghyun Park, Sungwoo Park, "Parallel skyline computation on multi-core architectures", IEEE Int‟ l Conf. on Data Engineering (ICDE), 2009, pp. 808-823.
[12] Shiyuan Wang, Beng chin Ooi, Anthony Tung, Lizhen Xu, "Efficient Skyline Processing on Peer to Peer Networks", IEEE Int‟ l Conf. Data Eng. (ICDE), 2007.
[13] K. Hose, M. Karnstedt, A. Koch, K. Sattler, and D. Zinn, "Processing rank-aware queries in P2P systems" In Proceedings of DBISP2P, 205, pp. 238–249
[14] Akrivi Vlachou, Christos Doulkeridis, Yannis Kotidis, Michalis Vazirgiannis, "SKYPEER: Efficient Subspace Skyline Computation over Distributed Data",. IEEE Int‟ l Conf. Data Engineering (ICDE) 2007, pp. 416-425.

International Journal of Modern Engineering Research (IJMER)
www.ijmer.com Vol.3, Issue.3, May-June. 2013 pp-1403-1409 ISSN: 2249-6645

Road User Attitudes towards Safety Initiatives in Kuwait

Jamal AlMatawah, [1] Khair Jadaan[2]
[1]*Civil Engineering Department, College of Technological Studies, Kuwait*
[2]*Civil Engineering Department, University of Jordan, Jordan*

Abstract: *Among the factors that are far important to improve traffic safety is knowing the degree of interaction of the road users with reducing these accidents and trying to share their opinions and persuasions about such issues as breaking the law and their perception of the effectiveness of various countermeasures. A survey was carried out on a sample of road users in Kuwait from various nationalities, ages and cultures. The study aims at investigating the road user's opinion of the effectiveness of selected countermeasures in reducing the number of hazardous accidents in Kuwait. The study also investigates the potential level of support the road users would give to these measures if implemented.*

Keywords: *Road safety, Attitude, perception, favorability, effectiveness*

I. INTRODUCTION

Effective safety remedial measures constitute a main concern for both road safety authorities and the public. Information gained from the public regarding their attitudes towards remedial measures can be an important tool for use by politicians and decision makers to decide where they consider an overall framework for effective remedial measures, as well as when and how they introduce these measures [1]. Reported that the likely response of the public will often be an important factor in assessing the road safety solutions.

Introducing efficient road safety solutions and, hence, expecting encouraging results depends on the level of support by the government and the positive interaction by the road users [2]. For instance, introducing seat-belt legislation was not received by road users with an equal degree when comparing between the different societies (i.e., countries) of the world. Different societies means different cultures and, hence, different attitudes towards any safety application. Safety culture can be assessed by observing what value and priority the society gives through its policies and action [3].

Earlier work [4] indicated that the introduction and eventual effectiveness of many road safety initiatives often depend on the level of support offered - and likely to be given-by the road using public. One of the main factors related to the attitudes of road users towards introducing new road safety initiatives and countermeasures is their perception of such solutions. The public perception is explained by their belief "of how successful or effective a countermeasure might be in terms of making roads safer for themselves and other road users [5]". Subsequently, this study was based on surveying the road users' attitudes towards specific road safety measures for Kuwait.

II. METHOD

The survey investigates what the road users in Kuwait think about potential accident-reducing solutions. The attitudes of road users in Kuwait towards specific measures were investigated through distributing a pre-designed questionnaire. The measures were selected at the discretion and using the experience of the researchers of the measures being the most adequate and acceptable to the road-using public in Kuwait. A list of these measures is given in the Appendix.

The survey questionnaire included in the Appendix was based on 'how effective any of the suggested solutions would be in reducing the number of accidents on the roads (effectiveness). Also, responders were asked to indicate the level of support that he/she offers and likely to give to each measure (favourability). A total of 26 potential countermeasures were selected which tackled different areas and issues, covering, for example, road monitoring techniques, police enforcement, driver education and training, increasing or reducing speed limits, punishment and retribution legislations, and engineering.

Perceived effectiveness of the different countermeasure was obtained using standard Likert scale technique with a five point rating scale having a verbal label as follows:

1. Increases accidents
2. Do not know
3. No effect
4. Reduces accidents little
5. Reduces accidents so much

The level of support likely to be given by the respondents was measured using a 2-point scale; either in favour (2) or not in favour (1).

III. THE SAMPLE

The questionnaire was distributed to a random sample of 748 road users covering the various areas of Kuwait (which is a small country with a population of about 3.6 millions). Table1 shows the characteristics of the sample. It can be seen that the highest group of respondents were male (65%), Kuwaiti (65.9%), 18-25 years of age (33%), residents of

Hawalli governorate (26.7%), university level (44%). Most of the respondents (53%) were owners of a private car. These percentages are expected as they match the general characteristics of the total population of Kuwait. Male drivers in Kuwait constitute about 70% of total drivers, Kuwaiti population is about 77% of total, population of age between 18 and 25 years constitute 34 % of total, about 20% of total population *reside in* Hawalli governorate and private cars are 51 % of total registered vehicles in the country These results indicate that the sample, besides being random is a representative sample.

Table 1: Sample Characteristics

Road User Category	Group (Class)	Total Respondents	Percent
Gender	Male	487	65.11
	Female	261	34.89
Age (years)	18-25	246	32.89
	26-35	212	28.34
	36-45	152	20.34
	46-55	82	10.96
	Over 55	56	7.49
Nationality	Kuwaiti	493	65.91
	Arabian	164	21.93
	Asian	50	6.68
	Western	41	5.48
Education Level	Less than high-school	27	3.61
	High-school	186	24.87
	Diploma	111	14.04
	Graduate (University)	330	44.17
	Post-graduate	94	12.57
Area (Governorate)	Capital	167	22.33
	Hawalli	201	26.87
	Farwania	153	20.45
	Mubarak Kabeer	69	9.22
	Ahmadi	105	14.04
	Jahra	53	7.09
Vehicle Type	Saloon	395	52.81
	Van	16	2.14
	Jeep	264	35.29
	Pickup	17	2.27
	Truck	22	2.94
	Bus	21	2.81
	Motorcycle	13	1.74

IV. RESULTS

Two indices were introduced to obtain the ranking scores for each of the studied countermeasures. The first is the ”influence index” defined in terms of how effective the respondents thought a measure would be in reducing the number and severity of accidents. The second index is the “approval index” which is defined in terms of how much the respondents would be in favour of the measure actually being introduced.

The two averages (i.e., the Influence Index, II and Approval Index, AI) of the total responses for each measure were considered to obtain the overall average-point for that measure indicated by the letter S. The results of the data analysis for all studied measures are shown in Table 2 and depicted in Figs 1 and 2. The higher point average for a measure means more of the surveyed respondents perceive that measure likely to be effective or that they are in favour of its implementation.

Table 2 Arithmetic Means of the Perceived Effectiveness and Favourability of the Countermeasures

Countermeasure	Influence Index (II)	Approval Index (AI)
S1	3.638	1.461
S2	4.283	1.900
S3	4.417	1.928
S4	4.172	1.785
S5	4.380	1.767
S6	3.541	1.452
S7	4.202	1.704
S8	2.092	1.275
S9	4.135	1.856

S10	3.175	1.512
S11	4.191	1.809
S12	4.179	1.885
S13	3.821	1.584
S14	4.396	1.929
S15	4.398	1.886
S16	4.531	1.921
S17	4.361	1.925
S18	3.683	1.545
S19	3.983	1.714
S20	4.529	1.918
S21	4.365	1.855
S22	4.360	1.876
S23	4.469	1.861
S24	4.266	1.870
S25	4.210	1.838
S26	4.285	1.800

It can be seen that 19 out of 26 readings of the II values were above 4 meaning that the majority of the respondents believe that these measures are likely to be effective in reducing accidents.

The level of support to the measures (i.e., in favour or not) was almost similar to that for the effectiveness perception. Referring to Table 2 and Fig. 2, it can be seen that most of the point averages (i.e., AI values) are closer to the value of 2. (20 out of 26) are above 1.7 with only one measure,(increase the maximum speed limit from 120 to 140 km/h) was found close to 1 point, indicating that the measure would not be supported by the public.

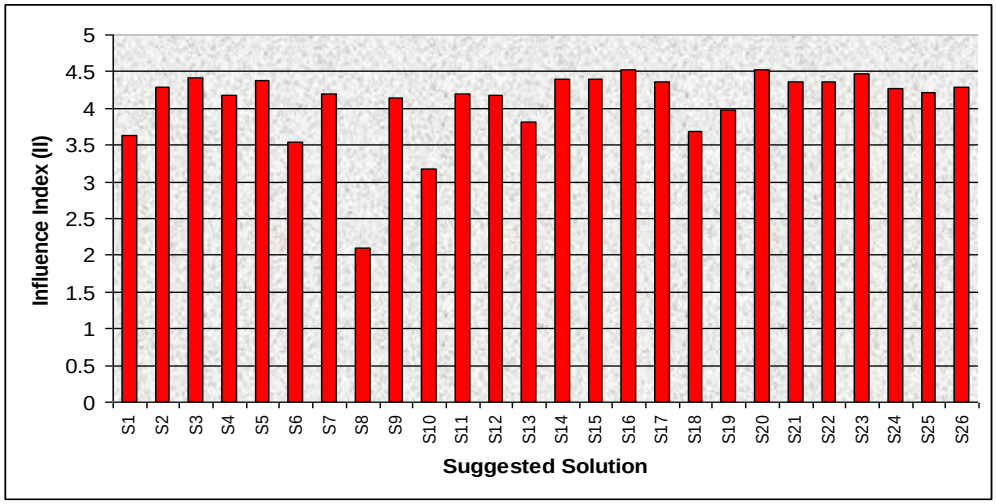

Figure 1: Influence Index Histogram

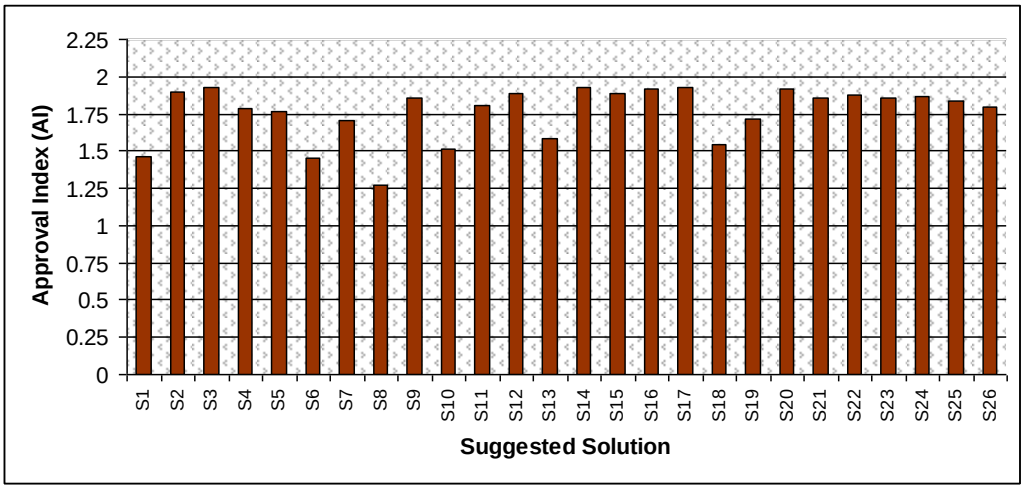

Figure 2: Approval Index Histogram

The two indices were used to obtain the ranking scores for each safety measure. As the indices represent the arithmetic mean of all the rating responses, then the higher indices are given a lower ranking indicating that the measure was perceived as being likely to result in a greater accident reduction or that its introduction would be more welcome. Table 3 shows the ranking of the studied measures in a descending order according to their effectiveness and according to their favourability. Hence, suggesting measure number S16 was seen to be the most likely to reduce accidents than the rest, and measure number S8 was the least effective.

Table 3 shows a reasonable agreement between public perception and support. If the top six measures in the table (S16, S20, S23, S3, S15 and S14) are taken into consideration, then they, with the exception of measure S23, represent the top-ranking measures for favourability as well. This parallel agreement is even more clear at the lower ranking programmes. The six least effective measures considered by the road users (S13, S18, S1, S6, S10 and S8) were also the least favoured by them, in almost similar ranking order. This agreement is illustrated in Fig.3.

Table 3: Ranking the Studied Measures According to Their Influence and Favourability Indices

Suggested Solution	Influence Index (II)	Rank II	Approval Index (AI)	Rank AI
S16	4.531	1	1.921	4
S20	4.529	2	1.918	5
S23	4.469	3	1.861	11
S3	4.417	4	1.928	2
S15	4.398	5	1.886	7
S14	4.396	6	1.929	1
S5	4.380	7	1.767	18
S21	4.365	8	1.855	13
S17	4.361	9	1.925	3
S22	4.360	10	1.876	9
S26	4.285	11	1.800	16
S2	4.283	12	1.900	6
S24	4.266	13	1.870	10
S25	4.210	14	1.838	14
S7	4.202	15	1.704	20
S11	4.191	16	1.809	15
S12	4.179	17	1.885	8
S4	4.172	18	1.785	17
S9	4.135	19	1.856	12
S19	3.983	20	1.714	19
S13	3.821	21	1.584	21
S18	3.683	22	1.545	22
S1	3.638	23	1.461	24
S6	3.541	24	1.452	25
S10	3.175	25	1.512	23
S8	2.092	26	1.275	26

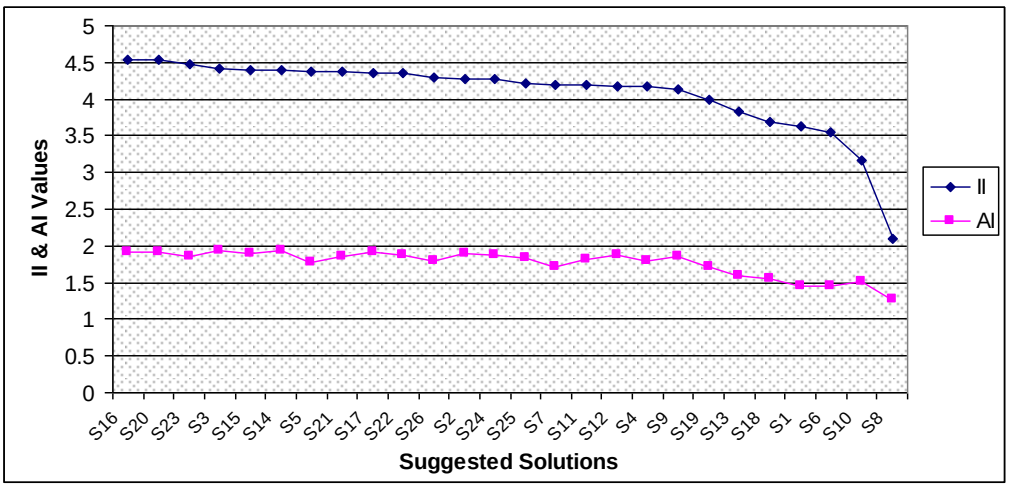

Figure 3: 2-lines Chart for the Influence and Approval Indices

Table 4 shows the top seven measures according to their favourability. It can be seen that five of those were also ranked among the top seven effective measures,

Table 4: The Top Seven Measures According to Approval Index

Suggested Solution	Influence Index (II)	Rank II	Approval Index (AI)	Rank AI
S14	4.396	6	1.929	1
S3	4.417	4	1.928	2
S17	4.361	9	1.925	3
S16	4.531	1	1.921	4
S20	4.529	2	1.918	5
S2	4.283	12	1.900	6
S15	4.398	5	1.886	7

V. DISCUSSION

The main findings of the survey can be grouped into two categories: the suggested countermeasures that received high priority in terms of effectiveness and approval by the road users; and those received the lowest interest and welcome by the road users. The top seven suggestions that produced higher index scores (II and AI) and the lowest four suggestions in terms of index scores (II and AI) are presented in Table 5.

Table 5: Highest and Lowest Measures Considering Both Indices

Suggested Solution	Measures	II-rank	AI-rank
	Highest		
Make sure that foreign chauffeurs for private homes are really eligible for driving license.	S16	1	4
Forbid truck and big-vehicle drivers from using middle lanes without necessity.	S20	2	5
Increase & improve road safety education in schools	S3	4	2
Put warning signs at usual accident sites.	S14	6	1
Improve driving test and be firm with it	S15	5	7
Increase the punishment against those who use mobile phones while driving.	S23	3	(11)
Improve traffic signs and put them in a reasonable distance before desired location	S17	(9)	3
	LOWEST		
Increase speed limit to 140km/hr instead of 120 km/hr on express-ways.	S8	26	26
Apply roundabouts more than traffic signals at intersections.	S10	25	23
Make legal age for having license 20 instead of 18.	S6	24	25
Reduce speed limit to 100km/hr on express-ways	S1	23	24

Three out of four measures that received lowest scores in Table 5 (S8, S10 and S1), whether in their effectiveness or in their approvals, are mainly linked with traffic engineering. The least of these (S8) was about increasing the speed limit, while S1 was the suggestion for reducing the speed limit. Both suggestions have been viewed by the public as irrelevant to reducing the number of accidents and were not supported. Also, switching the roundabout junctions into signal junctions did not interest the road users. S6, which suggests changing the legal age for having a driving license from 18 to 20, was not seen as a good solution and was not welcomed.

In contrast, the more welcomed solutions and thought to be effective in reducing the number of accidents were distributed between three main categories: Engineering, Education, and Legislation. More strict in licensing the Asian house drivers, prohibiting the big vehicles from using the middle lane (unless necessary), improve road safety education in schools, and Improve driving test are all related to driver behavior Issues. Whereas installing warning signs away in advance of the black-spot locations, and improving the design and the of traffic signals location, are related to traffic engineering.

The respondents' interest in educating the road users and improving their experience was obvious in the scores for suggestions S16, S3 and S15. Emphasizing upon the traffic administration in the Kuwaiti government to be much more strict in licensing the Asian house drivers exhibits the importance of education and experience. School education comes next indicating that the road users in Kuwait insist on establishing a good road-safety education in schools. S15, which calls for improving the vehicle driving test by the Kuwaiti authorities and strictly applying it also received a high score in terms of effectiveness and approval.

Legislations and punishment were also the concern of the public. Previous studies show that the drivers in Kuwait accept enforcement in terms of more strict and increase police presence on the road [6]. Suggestion coded S23 raise the issue of chastising or penalizing those who use the mobile phones while driving. This suggestion scored the 3rd highest value of

the II readings. For the approval by the respondents, it reached level 11 from 26 in the AI values. However, the AI reading for it (1.861) was very high and was towards a strong support by the public.

It should be noted that the majority of the studied measures have been welcomed by the road users and were viewed as effective which may dictate the need for an integrated programme that incorporate the most successful safety measures as perceived by the road users rather than prioritizing their implementation as separate measures.

VI. Conclusion

The study reveals that the road safety issue is of concern to road users in Kuwait and all respondents were keen to participate in finding appropriate solutions. The analysis of 748 responses regarding the road user perception towards the effectiveness and favourability of 26 carefully selected potential countermeasures produced a list of seven measures which are seen both effective and favourable. The majority of these measures are mainly linked with driver behavior issues. This may indicate that the road using public of Kuwait places the responsibility/blame on the concerned authorities.

It is recommended that a further and more comprehensive study be carried out to reach more definite conclusions regarding the identification of the most effective and favourable countermeasures which should then be implemented on a small scale to evaluate their performance before full scale application is launched.

REFERENCES

Journal Papers:

[1] Quimby, A. and Glendining, R, (1990). Perceived effectiveness and favorability towards some road accident countermeasures: A national survey, transport and roads research laboratory, contract report 234, Berkshire, U.K.

[2] Jadaan, K. S. (1996) Perceived Effectiveness towards Road Accident Countermeasures. Proceedings of the IPENZ Annual Conference, Dunedin, New Zealand, February 9-13, PP. 150-153

[3] Wiegmann, D. A, von Thaden, T. L., Mitchell Gibbons, A., (2007) A review of safety culture theory and its potential application to traffic safety, AAA foundation for Traffic Safety.

[4] Jadaan, K. S. and Alzahrani,A. H., (1993). Road Safety in GCC Countries, Proceedings of the 5th Organization of Islamic Capitals and Cities Symposium, Ankara, Turkey.

[5] Wilde, G.J.S. A psychometric investigation of driver's concerns for road safety and their opinion of various measures for accident prevention, Studies in transportation, Queens University, Ontario, Canada, 1975

[6] AL-Matawah, J. (2006) An Investigation of Drivers' Attitudes Towards Safety in Kuwait. Paper presented at the Annual Conference of UTSG, Leeds,U.K.

APPENDIX

COLLEGE OF TECHNOLOGICAL STUDIES

Dear Sir/Madam

This form of survey is a tool towards understanding some of road traffic activity and safety issues in Kuwait. This should lead to improving road safety. We are hoping that you participate in finding out solutions for reducing road accidents. Would you please, kindly and sincerely, fill this form so that the results would reflect the reality. The information here will only be used for research purposes.

In the **back of this paper** is a table of suggestions for improving road safety in Kuwait. We ask you kindly to give your opinion (what you think or believe) about each suggestion. All suggestions carry one main question: Do you think that the suggestion will reduce the number of accidents? The answer will be a choice of 5. You are requested to draw a circle around one of the five choices for each suggestion. In addition, for each suggestion, we need your opinion (content): Do you support it or not? Put √ under one of the 2 choices: In-favor or Not in-favor.

For example: If you think that *jail sentence for those who transgress traffic laws* will reduce the number of accidents significantly (so much) but you do not favor this suggestion of jail sentence then you should circle number 5 and put √ under Not in-favor.

Look at the examples:-

Suggestion	Reduces Accidents So Much	Reduces Accidents Little	No Effect	Do not Know	Increases Accidents	In-favor	Not In-favor
1- Jail penalty for who break the traffic law	(5)	4	3	2	1		√
2- Unlimited Speed on highways	5	4	3	2	(1)		√
3- Strict penalty for taxi drivers	5	(4)	3	2	1	√	

Needed information about you:

Age: --------years; *Gender: Male □ Female □;* *Profession: ----------*

Nationality: ---------- *Area of residence: ----------*

Education level: *Below secondary □* *Secondary □* *Diploma □*
University □ *Higher Degree □*

Marital status: *Married □* *Single □*

Type of vehicle you use: *Saloon □* *Van □* *Jeep □* *Pick-up □*

Truck □ *Bus* □ *Motorcycle* □ *Other:* ----------

Suggestion	Reduces Accidents So Much	Reduces Accidents Little	No Effect	Do not Know	Increases Accidents	In-favor	Not In-favor
1- Reduce speed limit to 100km/hr on express-ways.	5	4	3	2	1		
2- Increase pedestrian crossing facilities (pedestrian bridge, tunnel, signals).	5	4	3	2	1		
3- Increase & improve road safety education in schools.	5	4	3	2	1		
4- Increase traffic police patrol on roads.	5	4	3	2	1		
5- More seriousness in enforcing speed limit (such as hidden cameras, points against driver's license).	5	4	3	2	1		
6- Make legal age for having license 20 instead of 18.	5	4	3	2	1		
7- Increase punishments against law-breakers (increase fine, more points against driver's license, hold license for a time).	5	4	3	2	1		
8- Increase speed limit to 140km/hr instead of 120 km/hr on express-ways.	5	4	3	2	1		
9- Improve junction design (For instance, enlarge the intersection area to reduce conflict or confusion).	5	4	3	2	1		
10- Apply roundabouts more than traffic signals at intersections.	5	4	3	2	1		
11- Make it compulsory for driving learners to pass training courses before driving test.	5	4	3	2	1		
12- Increase traffic awareness programs (such as ads, flyers and, radio and TV).	5	4	3	2	1		
13- Increase road humps in residential areas.	5	4	3	2	1		
14- Put warning signs at usual accident sites.	5	4	3	2	1		
15- Improve driving test and be firm with it.	5	4	3	2	1		
16- Make sure that foreign chauffeurs for private homes are really eligible for driving license.	5	4	3	2	1		
17- Improve traffic signs and put them in a reasonable distance before desired location.	5	4	3	2	1		
18- Make traffic police-men wear civilian clothes and use ordinary cars to monitor.	5	4	3	2	1		
19- Intensify the punishment against those who drive very slow on middle lanes.	5	4	3	2	1		
20- Forbid truck and big-vehicle drivers from using middle lanes without necessity.	5	4	3	2	1		
21- Intensify the punishment against truck and goods-vehicle drivers who break the law.	5	4	3	2	1		
22- Intensify the punishment against those who use road shoulders without necessity.	5	4	3	2	1		
23- Increase the punishment against those who use mobile phones while driving.	5	4	3	2	1		
24- Be firm in approving the vehicle safety and eligibility before renewing the registration	5	4	3	2	1		
25- Making a traffic violation campaign against faulty vehicles (such as broken lights or bad tires).	5	4	3	2	1		
26- Increase monitoring-cameras on main roads and at traffic-signal intersections.	5	4	3	2	1		

Suggestions and Comments:

International Journal of Modern Engineering Research (IJMER)
www.ijmer.com Vol.3, Issue.3, May-June. 2013 pp-1410-1418 ISSN: 2249-6645

Lossy Transmission Lines Terminated by Parallel Connected RC-Loads and in Series Connected L-Load (I)

Vasil G. Angelov, [1] Andrey Zahariev[2]
[1]*Department of Mathematics, University of Mining and Geology" St. I. Rilski", 1700 Sofia, Bulgaria*
[2]*Faculty of Mathematics and Informatics, University of Plovdiv, Plovdiv, Bulgaria*

Abstract: *The present paper is the first part of investigations devoted to analysis of lossy transmission lines terminated by nonlinear parallel connected GC loads and in series connected L-load (cf. Fig. 1). First we formulate boundary conditions for lossy transmission line system on the base of Kirchhoff's law. Then we reduce the mixed problem for the hyperbolic system (Telegrapher equations) to an initial value problem for a neutral system on the boundary. We show that only oscillating solutions are characteristic for this case. Finally we analyze the arising nonlinearities.*

Keywords: *Fixed point theorem, Kirchhoff's law, Lossless transmission line, mixed problem for hyperbolic system, Neutral equation, Oscillatory solution*

I. INTRODUCTION

The transmission line theory is based on the Telegrapher equations, which from mathematical point of view presents a first order hyperbolic system of partial differential equations with unknown functions voltage and current. The subject of transmission lines has grown in importance because of the many applications (cf. [1]-[9]).

In the previous our papers we have considered lossless and lossy transmission lines terminated by various configuration of nonlinear (or linear) loads – in series connected, parallel connected and so on (cf. [10]-[16]). The main purpose of the present paper is to consider a lossless transmission line terminated by nonlinear *GCL*-loads placed in the following way: *GC*-loads are parallel connected and a *L*-load is in series connected (cf. Fig. 1).

The first difficulty is to derive the boundary conditions as a consequence of Kirchhoff's law (cf. Fig.1) and to formulate the mixed problem for the hyperbolic system. The second one is to reduce the mixed problem for the hyperbolic system to an initial value problem for neutral equations on the boundary. The third one is to introduce a suitable operator whose fixed point is an oscillatory solution of the problem stated. In the second part of the present paper by means of by fixed point method [17] we obtain an existence-uniqueness of an oscillatory solution.

The paper consists of four sections. In Section II on the base of Kirchhoff's law we derive boundary conditions and then formulate the mixed problem for the hyperbolic system or transmission line system. In Section III we reduce the mixed problem to an initial value problem on the boundary. In Section IV we analyse the arising nonlinearities and make some estimates which we use in the second part of the present paper.

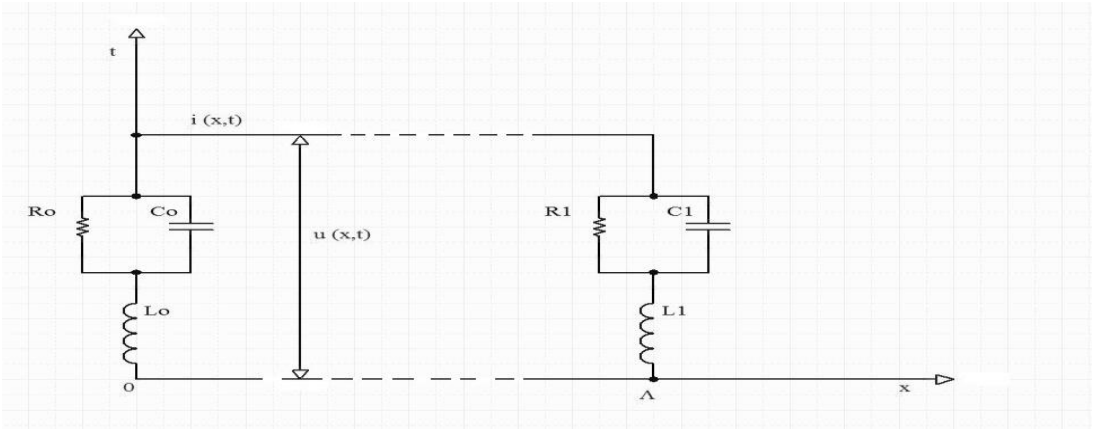

Fig. 1. Lossy transmission line terminated by circuits consisting of *RC*-elements in series connected to *L*-element

II. DERIVATION OF THE BOUNDARY CONDITIONS AND FORMULATION OF THE MIXED PROBLEM

In order to obtain the boundary conditions we have to take into account that if Λ is the length of the transmission line then, $T = \Lambda/(1/\sqrt{LC}) = \Lambda\sqrt{LC}$ where L is per unit length inductance and C – per unit-length capacitance

In accordance of Kirchhoff's *V*-law (cf. Fig. 1) we have to collect the currents of the elements G_p and C_p after that to collect the voltage of G_pC_p with the voltage of L_p $(p=0,1)$. But we deal with nonlinear elements, that is,

$$R_p(i)=\sum_{n=1}^{m} r_n^{(p)} i^n,\ (p=0,1) \text{ and } L_p(i)=\sum_{n=0}^{m} l_n^{(p)} i^n \ ,\ \widetilde{L}_p(i)=i\ .L_p(i)=i.\sum_{n=0}^{m} l_n^{(p)} i^n \ ,\quad \widetilde{C}_p(u)=u\,C_p(u)\ ;$$

$$\frac{d\widetilde{L}_p(i)}{dt}=\frac{d(i\,L_p(i))}{dt}=\frac{di}{dt}\left(L_p(i)+i\,\frac{dL_p(i)}{di}\right),\ (p=0,1);$$

$$\frac{d\widetilde{C}_p(u)}{dt}=\frac{d(u\,C_p(u))}{dt}=\frac{du}{dt}\left(C_p(u)+u\,\frac{dC_p(u)}{du}\right),\quad (p=0,1).$$

One can formulate boundary conditions corresponding to Fig. 1: for $x=0$ $(i_{G_0}+i_{C_0}=i_{G_0C_0}=i(0,t))$

$$\begin{aligned}&\left[u_{G_0C_0}\,\frac{dC_0(u_{G_0C_0})}{du_{G_0C_0}}+C_0(u_{G_0C_0})\right]\frac{du_{G_0C_0}}{dt}=-i(0,t)-G_0(u_{G_0C_0}),\\&\left[i(0,t)\,\frac{dL_0(i(0,t))}{di_{G_0C_0}}+L_0(i(0,t))\right]\frac{di(0,t)}{dt}=u(0,t)-u_{G_0C_0}(t)+E_0(t)\end{aligned}\tag{1}$$

And for $x=\Lambda$ $(i_{G_1}+i_{C_1}=i_{G_1C_1}=i(\Lambda,t))$:

$$\begin{aligned}&\left[u_{G_1C_1}\,\frac{dC_1(u_{G_1C_1})}{du_{G_1C_1}}+C_1(u_{G_1C_1})\right]\frac{du_{G_1C_1}}{dt}=i(\Lambda,t)-G_1(u_{G_1C_1})\\&\left[i(\Lambda,t)\,\frac{dL_1(i(\Lambda,t))}{di_{G_1C_1}}+L_1(i(\Lambda,t))\right]\frac{di(\Lambda,t)}{dt}=-u(\Lambda,t)+u_{G_1C_1}(t)-E_1(t).\end{aligned}\tag{2}$$

Here we consider the following lossy transmission line system:

$$\begin{aligned}&C\,\frac{\partial u(x,t)}{\partial t}+\frac{\partial i(x,t)}{\partial x}+Gu(x,t)=0\\&L\,\frac{\partial i(x,t)}{\partial t}+\frac{\partial u(x,t)}{\partial x}+Ri(x,t)=0\end{aligned}\tag{3}$$

$$(x,t)\in\Pi=\left\{(x,t)\in\Pi^2:(x,t)\in[0,\Lambda]\times[0,\infty)\right\}$$

Where $u(x,t)$ and $i(x,t)$ are the unknown voltage and current, while *L*, *C*, *R* and *G* are prescribed specific parameters of the line and $\Lambda > 0$ is its length.

For the above system (3) might be formulated the following mixed problem: to find $u(x,t)$ and $i(x,t)$ in Π such that the following initial conditions

$$u(x,0)=u_0(x),\ i(x,0)=i_0(x),\ x\in[0,\Lambda]\tag{4}$$

And boundary conditions (1) and (2) to be satisfied.

III. REDUCING THE MIXED PROBLEM TO AN INITIAL VALUE PROBLEM ON THE BOUNDARY

First we present (3) in the form:

$$\begin{aligned}&\frac{\partial u(x,t)}{\partial t}+\frac{1}{C}\,\frac{\partial i(x,t)}{\partial x}+\frac{G}{C}\,u(x,t)=0\\&\frac{\partial i(x,t)}{\partial t}+\frac{1}{L}\,\frac{\partial u(x,t)}{\partial x}+\frac{R}{L}\,i(x,t)=0\end{aligned}\tag{5}$$

And then write it in a matrix form

$$\frac{\partial U(x,t)}{\partial t} + A\frac{\partial U(x,t)}{\partial x} + BU(x,t) = 0 \tag{6}$$

Where

$$U(x,t) = \begin{bmatrix} u(x,t) \\ i(x,t) \end{bmatrix}, \quad \frac{\partial U(x,t)}{\partial t} = \begin{bmatrix} \frac{\partial u(x,t)}{\partial t} \\ \frac{\partial i(x,t)}{\partial t} \end{bmatrix}, \quad \frac{\partial U(x,t)}{\partial x} = \begin{bmatrix} \frac{\partial u(x,t)}{\partial x} \\ \frac{\partial i(x,t)}{\partial x} \end{bmatrix}, A = \begin{bmatrix} 0 & \frac{1}{C} \\ \frac{1}{L} & 0 \end{bmatrix}, \quad B = \begin{bmatrix} \frac{G}{C} & 0 \\ 0 & \frac{R}{L} \end{bmatrix}.$$

In order to transform the matrix A in a diagonal form we have to solve the characteristic equation: $\begin{vmatrix} -\lambda & 1/C \\ 1/L & -\lambda \end{vmatrix} = 0$ whose roots are $\lambda_1 = 1/\sqrt{LC}$, $\lambda_2 = -1/\sqrt{LC}$. For the eigen-vectors we obtain the following systems:

$$\begin{cases} -\frac{1}{\sqrt{LC}}\xi_1 + \frac{1}{L}\xi_2 = 0 \\ \frac{1}{C}\xi_1 - \frac{1}{\sqrt{LC}}\xi_2 = 0 \end{cases} \quad \text{And} \quad \begin{cases} \frac{1}{\sqrt{LC}}\xi_1 + \frac{1}{L}\xi_2 = 0 \\ \frac{1}{C}\xi_1 + \frac{1}{\sqrt{LC}}\xi_2 = 0 \end{cases}.$$

Hence $\left(\xi_1^{(1)}, \xi_2^{(1)}\right) = \left(\sqrt{C}, \sqrt{L}\right)$, $\left(\xi_1^{(2)}, \xi_2^{(2)}\right) = \left(-\sqrt{C}, \sqrt{L}\right)$

Denote by H the matrix formed by eigen-vectors $H = \begin{bmatrix} \sqrt{C} & \sqrt{L} \\ -\sqrt{C} & \sqrt{L} \end{bmatrix}$ and its inverse one $H^{-1} = \begin{bmatrix} \frac{1}{2\sqrt{C}} & -\frac{1}{2\sqrt{C}} \\ \frac{1}{2\sqrt{L}} & \frac{1}{2\sqrt{L}} \end{bmatrix}$. It is known that $A^{\text{can}} = HAH^{-1}$, where $A^{\text{can}} = \begin{bmatrix} 1/\sqrt{LC} & 0 \\ 0 & -1/\sqrt{LC} \end{bmatrix}$.

Introduce new variables $Z = HU$, (or $U = H^{-1}Z$)

$$Z = \begin{bmatrix} V(x,t) \\ I(x,t) \end{bmatrix}, \quad H = \begin{bmatrix} \sqrt{C} & \sqrt{L} \\ -\sqrt{C} & \sqrt{L} \end{bmatrix}, \quad U = \begin{bmatrix} u(x,t) \\ i(x,t) \end{bmatrix}.$$

Then

$$\begin{cases} V(x,t) = \sqrt{C}\,u(x,t) + \sqrt{L}\,i(x,t) \\ I(x,t) = -\sqrt{C}\,u(x,t) + \sqrt{L}\,i(x,t) \end{cases} \tag{7}$$

or

$$\begin{cases} u(x,t) = \frac{1}{2\sqrt{C}}V(x,t) - \frac{1}{2\sqrt{C}}I(x,t) \\ i(x,t) = \frac{1}{2\sqrt{L}}V(x,t) + \frac{1}{2\sqrt{L}}I(x,t). \end{cases} \tag{8}$$

Replacing $U(x,t) = H^{-1}Z(x,t)$ in (6) we obtain

$$\frac{\partial\left(H^{-1}Z\right)}{\partial t} + A\frac{\partial\left(H^{-1}Z\right)}{\partial x} + B\left(H^{-1}Z\right) = 0\,.$$

Since H^{-1} is a constant matrix we have

$$H^{-1}\frac{\partial Z(x,t)}{\partial t}+\left(AH^{-1}\right)\frac{\partial Z(x,t)}{\partial x}+\left(BH^{-1}\right)Z(x,t)=0\,.$$

After multiplication from the left by H we obtain $\frac{\partial Z}{\partial t}+H\left(AH^{-1}\right)\frac{\partial Z}{\partial x}+H\left(BH^{-1}\right)Z=0$, i.e.

$$\frac{\partial Z}{\partial t}+A^{can}\frac{\partial Z}{\partial x}+\left(HBH^{-1}\right)Z=0\,. \tag{9}$$

But

$$HBH^{-1}=\begin{bmatrix}\sqrt{C} & \sqrt{L}\\ -\sqrt{C} & \sqrt{L}\end{bmatrix}\begin{bmatrix}\frac{G}{C} & 0\\ 0 & \frac{R}{L}\end{bmatrix}\begin{bmatrix}\frac{1}{2\sqrt{C}} & -\frac{1}{2\sqrt{C}}\\ \frac{1}{2\sqrt{L}} & \frac{1}{2\sqrt{L}}\end{bmatrix}=\begin{bmatrix}\frac{1}{2}\left(\frac{G}{C}+\frac{R}{L}\right) & \frac{1}{2}\left(-\frac{G}{C}+\frac{R}{L}\right)\\ \frac{1}{2}\left(-\frac{G}{C}+\frac{R}{L}\right) & \frac{1}{2}\left(\frac{G}{C}+\frac{R}{L}\right)\end{bmatrix}.$$

Applying Heaviside condition $\frac{R}{L}=\frac{G}{C}$ we obtain

$$\begin{bmatrix}\frac{\partial V(x,t)}{\partial t}\\ \frac{\partial I(x,t)}{\partial t}\end{bmatrix}+\begin{bmatrix}\frac{1}{\sqrt{LC}} & 0\\ 0 & -\frac{1}{\sqrt{LC}}\end{bmatrix}\begin{bmatrix}\frac{\partial V(x,t)}{\partial x}\\ \frac{\partial I(x,t)}{\partial x}\end{bmatrix}+\begin{bmatrix}\frac{R}{L} & 0\\ 0 & \frac{R}{L}\end{bmatrix}\begin{bmatrix}V(x,t)\\ I(x,t)\end{bmatrix}=\begin{bmatrix}0\\ 0\end{bmatrix}. \tag{10}$$

The new initial conditions we obtain from (4):

$$V(x,0)=\sqrt{C}\,u(x,0)+\sqrt{L}\,i(x,0)=\sqrt{C}\,u_0(x)+\sqrt{L}\,i_0(x)\equiv V_0(x)\,,\ x\in[0,\Lambda] \tag{11}$$

$$I(x,0)=-\sqrt{C}\,u(x,0)+\sqrt{L}\,i(x,0)=-\sqrt{C}\,u_0(x)+\sqrt{L}\,i_0(x)\equiv I_0(x)\,,\ x\in[0,\Lambda]. \tag{12}$$

One can simplify (10) by the substitution:

$$W(x,t)=e^{\frac{R}{L}t}V(x,t)$$
$$J(x,t)=e^{\frac{R}{L}t}I(x,t)$$

Or

$$\begin{aligned}V(x,t)&=e^{-\frac{R}{L}t}W(x,t)\\ I(x,t)&=e^{-\frac{R}{L}t}J(x,t)\end{aligned}\,. \tag{13}$$

Substituting in (8) we obtain

$$\begin{cases}u(x,t)=\frac{1}{2\sqrt{C}}e^{-\frac{R}{L}t}W(x,t)-\frac{1}{2\sqrt{C}}e^{-\frac{R}{L}t}J(x,t)\\ i(x,t)=\frac{1}{2\sqrt{L}}e^{-\frac{R}{L}t}W(x,t)+\frac{1}{2\sqrt{L}}e^{-\frac{R}{L}t}J(x,t).\end{cases} \tag{14}$$

Then with respect to the variables $W(x,t)$ and $J(x,t)$ (10) looks like:

$$\begin{aligned}\frac{\partial W(x,t)}{\partial t}+\frac{1}{\sqrt{LC}}\frac{\partial W(x,t)}{\partial x}&=0,\\ \frac{\partial J(x,t)}{\partial t}-\frac{1}{\sqrt{LC}}\frac{\partial J(x,t)}{\partial x}&=0.\end{aligned} \tag{15}$$

The mixed problem for (1) - (4) can be reduced to an initial value problem for a neutral system. The neutral system is a nonlinear one in view of the nonlinear characteristics of the *RGLC*-elements.
From now on we propose two manners to obtain a neutral system for unknown voltage and current functions.

First manner: The solution of (15) is a pair of functions $W(x,t)=\Phi_W(x-vt)$ and $J(x,t)=\Phi_J(x+vt)$, where Φ_W and Φ_J are arbitrary smooth functions. From (14) we obtain

$$u(x,t)=\frac{e^{-\frac{R}{L}t}}{2\sqrt{C}}\left[\Phi_W(x-vt)-\Phi_J(x+vt)\right]$$
$$i(x,t)=\frac{e^{-\frac{R}{L}t}}{2\sqrt{L}}\left[\Phi_W(x-vt)+\Phi_J(x+vt)\right]. \tag{16}$$

Hence

$$\Phi_W(x-vt)=e^{\frac{R}{L}t}\left(\sqrt{C}\,u(x,t)+\sqrt{L}\,i(x,t)\right)$$
$$\Phi_J(x+vt)=e^{\frac{R}{L}t}\left(\sqrt{L}\,i(x,t)-\sqrt{C}\,u(x,t)\right). \tag{17}$$

For $x=\Lambda$ we obtain

$$\Phi_W(\Lambda-vt)=e^{\frac{R}{L}t}\left[\sqrt{C}\,u(\Lambda,t)+\sqrt{L}\,i(\Lambda,t)\right]$$
$$\Phi_J(\Lambda+vt)=e^{\frac{R}{L}t}\left[\sqrt{L}\,i(\Lambda,t)-\sqrt{C}\,u(\Lambda,t)\right] \tag{18}$$

Let us put $\Lambda-vt=-vt'\Rightarrow t=t'+\Lambda/v\equiv t'+T \quad (T=\Lambda/v)$ and then replacing t by $t'+T$ in the first equation of (18) we get

$$\Phi_W(-vt')=e^{\frac{R}{L}(t'+T)}\left[\sqrt{C}\,u(\Lambda,t'+T)+\sqrt{L}\,i(\Lambda,t'+T)\right].$$

For the second equation of (18) we put
$\Lambda+vt=vt''\Rightarrow t=t''-\Lambda/v\equiv t''-T \quad (T=\Lambda/v)$ And then we have

$$\Phi_J(vt'')=e^{\frac{R}{L}(t''-T)}[\sqrt{L}i(\Lambda,t''-T)-\sqrt{C}u(\Lambda,t''-T)].$$

So we obtain

$$\Phi_W(-vt)=e^{\frac{R}{L}(t+T)}\left[\sqrt{C}\,u(\Lambda,t+T)+\sqrt{L}\,i(\Lambda,t+T)\right] \tag{19}$$
$$\Phi_J(vt)=e^{\frac{R}{L}(t-T)}\left[\sqrt{L}\,i(\Lambda,t-T)-\sqrt{C}\,u(\Lambda,t-T)\right]. \tag{20}$$

From (16) by $x = 0$ we have

$$u(0,t)=\frac{e^{-\frac{R}{L}t}}{2\sqrt{C}}\left[\Phi_W(-vt)-\Phi_J(vt)\right]$$
$$i(0,t)=\frac{e^{-\frac{R}{L}t}}{2\sqrt{L}}\left[\Phi_W(-vt)+\Phi_J(vt)\right] \tag{21}$$

Substituting $\Phi_W(-vt)$ and $\Phi_J(vt)$ from (19) and (20) into (21) we obtain:

$$u(0,t)=\frac{1}{2\sqrt{C}}\left[e^{\frac{R(t+T)}{L}}\left(\sqrt{C}\,u(\Lambda,t+T)+\sqrt{L}\,i(\Lambda,t+T)\right)-e^{\frac{R(t-T)}{L}}\left(\sqrt{L}\,i(\Lambda,t-T)-\sqrt{C}\,u(\Lambda,t-T)\right)\right]$$
$$i(0,t)=\frac{1}{2\sqrt{C}}\left[e^{\frac{R(t+T)}{L}}\left(\sqrt{C}\,u(\Lambda,t+T)+\sqrt{L}\,i(\Lambda,t+T)\right)+e^{\frac{R(t-T)}{L}}\left(\sqrt{L}\,i(\Lambda,t-T)-\sqrt{C}\,u(\Lambda,t-T)\right)\right].$$

Substitute the above expressions into the boundary conditions (1), (2) we have

$$\frac{du_{G_0C_0}(t)}{dt}=\frac{e^{\frac{R(t+T)}{L}}\left(u(\Lambda,t+T)+Z_0\,i(\Lambda,t+T)\right)+e^{\frac{R(t-T)}{L}}\left(Z_0\,i(\Lambda,t-T)-u(\Lambda,t-T)\right)}{2Z_0\dfrac{d\widetilde{C}_0(u_{G_0C_0})}{du_{G_0C_0}}}-\frac{G_0(u_{G_0C_0})}{\dfrac{d\widetilde{C}_0(u_{G_0C_0})}{du_{G_0C_0}}},$$

$$\frac{1}{2Z_0}\frac{d}{dt}\left[e^{\frac{R(t+T)}{L}}\left(u(\Lambda,t+T)+Z_0\,i(\Lambda,t+T)\right)+e^{\frac{R(t-T)}{L}}\left(Z_0\,i(\Lambda,t-T)-u(\Lambda,t-T)\right)\right]=$$

$$=\frac{\left[e^{\frac{R(t+T)}{L}}\left(u(\Lambda,t+T)+Z_0\,i(\Lambda,t+T)\right)-e^{\frac{R(t-T)}{L}}\left(Z_0\,i(\Lambda,t-T)-u(\Lambda,t-T)\right)\right]-2u_{G_0C_0}(t)+2E_0(t)}{2d\widetilde{L}_0(i(0,t))/di_{G_0C_0}},$$

$$\frac{du_{G_1C_1}(t)}{dt}=\frac{i(\Lambda,t)-G_1(u_{G_1C_1})}{d\widetilde{C}_1(u_{G_1C_1})/du_{G_1C_1}},$$

$$\frac{di(\Lambda,t)}{dt}=\frac{-u(\Lambda,t)+u_{G_1C_1}(t)-E_1(t)}{d\widetilde{L}_1(i(\Lambda,t))/di_{G_1C_1}}.$$

Let us put $\tau\equiv t+T$ .Then we arrive at a system that we cannot formulate an initial value problem.

Second manner

We proceed from (14) and obtain

$$\begin{vmatrix}u(0,t)=\frac{1}{2\sqrt{C}}e^{-\frac{R}{L}t}W(0,t)-\frac{1}{2\sqrt{C}}e^{-\frac{R}{L}t}J(0,t)\\ i(0,t)=\frac{1}{2\sqrt{L}}e^{-\frac{R}{L}t}W(0,t)+\frac{1}{2\sqrt{L}}e^{-\frac{R}{L}t}J(0,t)\end{vmatrix}\ \text{And}\ \begin{vmatrix}u(\Lambda,t)=\frac{1}{2\sqrt{C}}e^{-\frac{R}{L}t}W(\Lambda,t)-\frac{1}{2\sqrt{C}}e^{-\frac{R}{L}t}J(\Lambda,t)\\ i(\Lambda,t)=\frac{1}{2\sqrt{L}}e^{-\frac{R}{L}t}W(\Lambda,t)+\frac{1}{2\sqrt{L}}e^{-\frac{R}{L}t}J(\Lambda,t).\end{vmatrix}$$

Substituting in (2.1) and (2.2) we obtain

$$\frac{du_{G_0C_0}(t)}{dt}=\frac{e^{-\frac{R}{L}t}W(0,t)+e^{-\frac{R}{L}t}J(0,t)-2\sqrt{L}G_0(u_{G_0C_0}(t))}{2\sqrt{L}\;d\widetilde{C}_0(u_{G_0C_0})/du_{G_0C_0}};$$

$$\frac{d}{dt}\left(e^{-\frac{R}{L}t}W(0,t)+e^{-\frac{R}{L}t}J(0,t)\right)=\frac{Z_0\,e^{-\frac{R}{L}t}W(0,t)-Z_0e^{-\frac{R}{L}t}J(0,t)-2\sqrt{L}u_{G_0C_0}(t)+2\sqrt{L}E_0(t)}{d\widetilde{L}_0(i(0,t))/di_{G_0C_0}};$$

$$\frac{du_{G_1C_1}(t)}{dt}=\frac{e^{-\frac{R}{L}t}W(\Lambda,t)+e^{-\frac{R}{L}t}J(\Lambda,t)-2\sqrt{L}G_1(u_{G_1C_1}(t))}{2\sqrt{L}\,dC_1(u_{G_1C_1})/du_{G_1C_1}};$$

$$\frac{d}{dt}\left(e^{-\frac{R}{L}t}W(\Lambda,t)+e^{-\frac{R}{L}t}J(\Lambda,t)\right)=\frac{-Z_0\,e^{-\frac{R}{L}t}W(\Lambda,t)+Z_0e^{-\frac{R}{L}t}J(\Lambda,t)+2\sqrt{L}u_{G_1C_1}(t)-2\sqrt{L}E_1(t)}{d\widetilde{L}_1(i(\Lambda,t))/di_{G_1C_1}}.$$

But

$$W(0,t)=W(\Lambda,t+T),\ J(0,t+T)=J(\Lambda,t)\ \Rightarrow\ W(0,t-T)=W(\Lambda,t),\ J(0,t)=J(\Lambda,t-T).$$

We choose $W(0,t)=W(t),\ J(t)=J(\Lambda,t)$ to be unknown functions and then the above system becomes

$$\frac{du_{G_0C_0}(t)}{dt}=\frac{e^{-\frac{R}{L}t}W(t)+e^{-\frac{R}{L}(t-T)}J(t-T)-2\sqrt{L}G_0(u_{G_0C_0}(t))}{2\sqrt{L}\ d\tilde{C}_0(u_{G_0C_0})/du_{G_0C_0}};$$

$$\frac{d}{dt}\left(e^{-\frac{R}{L}t}W(t)+e^{-\frac{R}{L}(t-T)}J(t-T)\right)=\frac{Z_0\,e^{-\frac{R}{L}t}W(t)-Z_0e^{-\frac{R}{L}(t-T)}J(t-T)-2\sqrt{L}\,u_{G_0C_0}(t)+2\sqrt{L}E_0(t)}{d\tilde{L}_0(i(0,t))/di_{G_0C_0}};$$

$$\frac{du_{G_1C_1}(t)}{dt}=\frac{e^{-\frac{R}{L}(t-T)}W(t-T)+e^{-\frac{R}{L}t}J(t)-2\sqrt{L}G_1(u_{G_1C_1}(t))}{2\sqrt{L}\ dC_1(u_{G_1C_1})/du_{G_1C_1}};\qquad(22)$$

$$\frac{d}{dt}\left(e^{-\frac{R}{L}(t-T)}W(t-T)+e^{-\frac{R}{L}t}J(t)\right)=\frac{-Z_0\,e^{-\frac{R}{L}(t-T)}W(t-T)+Z_0e^{-\frac{R}{L}t}J(t)+2\sqrt{L}u_{G_1C_1}(t)-2\sqrt{L}E_1(t)}{d\tilde{L}_1(i(\Lambda,t))/di_{G_1C_1}}.$$

We notice that if (22) has a periodic solution

$$\left(u_{G_0C_0}(t),W(t),u_{G_1C_1}(t),J(t)\right)$$

Then functions $e^{-\frac{R}{L}t}W(t)$, $e^{-\frac{R}{L}t}J(t)$ are oscillatory ones and vanishing exponentially at infinity. Therefore we put $\hat{W}(t)=e^{-\frac{R}{L}t}W(t)$, $\hat{J}(t)=e^{-\frac{R}{L}t}J(t)$ and then we can state the problem for existence-uniqueness of an oscillatory solution vanishing at infinity of the following system (we denote by $\hat{W}(t),\hat{J}(t)$ again by $W(t),J(t)$) and obtain:

$$\frac{du_{G_0C_0}(t)}{dt}=\frac{W(t)+J(t-T)-2\sqrt{L}G_0(u_{G_0C_0}(t))}{2\sqrt{L}\ d\tilde{C}_0(u_{G_0C_0})/du_{G_0C_0}},\ t\in[T;\infty);$$

$$\frac{dW(t)}{dt}=-\frac{dJ(t-T)}{dt}+\frac{Z_0\,W(t)-Z_0J(t-T)-2\sqrt{L}\,u_{G_0C_0}(t)+2\sqrt{L}E_0(t)}{d\tilde{L}_0(i(0,t))/di_{G_0C_0}},\ t\in[T;\infty);$$

$$\frac{du_{G_1C_1}(t)}{dt}=\frac{W(t-T)+J(t)-2\sqrt{L}G_1(u_{G_1C_1}(t))}{2\sqrt{L}\ dC_1(u_{G_1C_1})/du_{G_1C_1}},\ t\in[T;\infty);\qquad(23)$$

$$\frac{dJ(t)}{dt}=-\frac{dW(t-T)}{dt}+\frac{-Z_0\,W(t-T)+Z_0J(t)+2\sqrt{L}u_{G_1C_1}(t)-2\sqrt{L}E_1(t)}{d\tilde{L}_1(i(\Lambda,t))/di_{G_1C_1}},\ t\in[T;\infty);$$

$$u_{G_0C_0}(T)=u^T_{G_0C_0},\ u_{G_1C_1}(T)=u^T_{G_1C_1},\ W(t)=W_0(t),J(t)=J_0(t),\ \frac{dW(t)}{dt}=\frac{dW_0(t)}{dt},\ \frac{dJ(t)}{dt}=\frac{dJ_0(t)}{dt},t\in[0,T].$$

IV. Analysis Of The Arising Nonlinearities

First we precise the definition domains of the functions:

$$\frac{d\tilde{C}_p(u)}{dt}=\frac{d(C_p(u).u)}{dt},(p=0,1)$$

Where $C_p(u)=\frac{c_p}{\sqrt[h]{(1-u/\Phi_p)}}=\frac{c_p\sqrt[h]{\Phi_p}}{\sqrt[h]{\Phi_p-u}}$, $c_p>0,\Phi_p>0,h\in[2,3]$ are constants and $|u|\le\phi_0<\min\{\Phi_0,\Phi_1\}$. We have to show an interval for u where

$$\tilde{C}_p(u)=u.C_p(u)=c_p\sqrt[h]{\Phi_p}\ \frac{u}{\sqrt[h]{\Phi_p-u}}$$

Has a strictly positive lower bound.
First we calculate the derivatives

$$\frac{dC_p(u)}{du}=\frac{c_p\sqrt[h]{\Phi_p}}{h}\left(\Phi_p-u\right)^{-\frac{1+h}{h}}\ ;\quad \frac{d^2C_p(u)}{du^2}=\frac{c_p\sqrt[h]{\Phi_p}}{h}\frac{1+h}{h}\left(\Phi_p-u\right)^{-\frac{1+2h}{h}};$$

$$\frac{d\widetilde{C}_p(u)}{du}=C_p(u)+u\frac{dC_p(u)}{du}=c_p\sqrt[h]{\Phi_p}\left(\Phi_p-u\right)^{-\frac{1}{h}}+c_p\sqrt[h]{\Phi_p}\frac{u}{h}\left(\Phi_p-u\right)^{-\frac{1}{h}-1}=c_p\sqrt[h]{\Phi_p}\left[\Phi_p-\left(\frac{h-1}{h}\right)u\right]\left(\Phi_p-u\right)^{-1-\frac{1}{h}};$$

$$\frac{d^2\widetilde{C}_p(u)}{du^2}=c_p\sqrt[h]{\Phi_p}\left[-\left(\frac{h-1}{h}\right)\left(\Phi_p-u\right)^{-1-\frac{1}{h}}-\left(\Phi_p-\left(\frac{h-1}{h}\right)u\right)\left(1+\frac{1}{h}\right)\left(\Phi_p-u\right)^{-2-\frac{1}{h}}\right]=\frac{c_p\sqrt[h]{\Phi_p}}{h^2}\frac{-2h^2\Phi_p+\left(2h^2+h+1\right)u}{\left(\Phi_p-u\right)^{2+\frac{1}{h}}}.$$

Since $|u|\le\phi_0<\min\{\Phi_0,\Phi_1\}<\min\left\{\frac{h}{h-1}\Phi_0,\frac{h}{h-1}\Phi_1\right\}$ the derivative $\frac{d\widetilde{C}_p(u)}{du}>0$.

Then $\min\left\{\widetilde{C}_p(u):u\in[-\phi_0.\phi_0]\right\}=\min\left\{c_p\sqrt[h]{\Phi_p}\frac{\phi_0}{\sqrt[h]{\Phi_p-\phi_0}},c_p\sqrt[h]{\Phi_p}\left|\frac{-\phi_0}{\sqrt[h]{\Phi_p+\phi_0}}\right|\right\}=\frac{c_p\sqrt[h]{\Phi_p}\,\phi_0}{\sqrt[h]{\Phi_p+\phi_0}}=\hat{C}_p>0.$

Further on we have

$$\left|\frac{d\widetilde{C}_p(u)}{du}\right|\le\frac{2c_p\sqrt[h]{\Phi_p}}{h\left(\Phi_p-\phi_0\right)^{\frac{1}{h}+1}}+|u|\frac{(1+h)2c_p\sqrt[h]{\Phi_p}}{h^2\left(\Phi_p-\phi_0\right)^{\frac{1}{h}+2}}=\frac{2c_p\sqrt[h]{\Phi_p}\left[h\left(\Phi_p-\phi_0\right)+|u|(1+h)\right]}{h^2\ \sqrt[h]{\left(\Phi_p-\phi_0\right)^{1+2h}}}\le\ .$$

$$\le\frac{2c_p\sqrt[h]{\Phi_p}\left[h\left(\Phi_p-\phi_0\right)+\phi_0(1+h)\right]}{h^2\ \sqrt[h]{\left(\Phi_p-\phi_0\right)^{1+2h}}}=\frac{2c_p\sqrt[h]{\Phi_p}\left(h\Phi_p+\phi_0\right)}{h^2\ \sqrt[h]{\left(\Phi_p-\phi_0\right)^{1+2h}}}\equiv\breve{C}_p^{(1)}.$$

For $-\phi_0\le u\le\phi_0<\min\left\{\frac{h}{h+1},\Phi_0,\Phi_1\right\}$ it follows

$$\frac{d\widetilde{C}_p(u)}{du}=\frac{c_p\sqrt[h]{\Phi_p}}{\left(\Phi_p-u\right)^{\frac{1+h}{h}}}\left(\Phi_p-\frac{h-1}{h}u\right)\ge\frac{c_p\sqrt[h]{\Phi_p}}{\left(\Phi_p+\phi_0\right)^{\frac{1+h}{h}}}\left(\Phi_p-\frac{h-1}{h}\phi_0\right)\equiv\hat{C}_p^{(1)}.$$

Therefore

$$\min\left\{\widetilde{C}_p(u):\ u\in[-\phi_0,\phi_0]\right\}=\widetilde{C}_p(-\phi_0)=\frac{c_p\sqrt[h]{\Phi_p}}{h}\frac{h\Phi_p+(h-1)\phi_0}{\left(\Phi_p+\phi_0\right)^{1+\frac{1}{h}}}=\hat{C}_p,$$

$$\left|\frac{d^2\widetilde{C}_p(u)}{du^2}\right|\le\frac{c_p\sqrt[h]{\Phi_p}}{h^2}\left|\frac{-2h^2\Phi_p+\left(2h^2+h+1\right)u}{\left(\Phi_p-u\right)^{2+\frac{1}{h}}}\right|\le\frac{c_p\sqrt[h]{\Phi_p}}{h^2}\frac{2h^2\Phi_p+\left(2h^2+h+1\right)\phi_0}{\left(\Phi_p-\phi_0\right)^{2+\frac{1}{h}}}\equiv\breve{C}_p^{(2)}.$$

For the *I-V* characteristics we assume $R_p(i)=\sum_{n=1}^{m}r_n^{(p)}i^n,(p=0,1)$ and $L_p(i)=\sum_{n=0}^{m}l_n^{(p)}i^n$ then

$$\widetilde{L}_p(i)=i\ .L_p(i)=i.\sum_{n=0}^{m}l_n^{(p)}i^n.$$

For $\widetilde{L}_p(i)$ we get $\frac{d\widetilde{L}_p(i)}{di}=i\frac{dL_p(i)}{di}+L_p(i)=i\sum_{n=1}^{m}nl_n^{(p)}i^{n-1}+\sum_{n=1}^{m}l_n^{(p)}i^n=\sum_{n=1}^{m}(n+1)l_n^{(p)}i^n$.

Assumptions (C):

$|u(0,t)|\le\frac{e^{\mu T_0}\left(W_0+J_0\right)}{2}\le\phi_0;\ |u(\Lambda,t)|\le\frac{e^{\mu T_0}\left(W_0+J_0\right)}{2}\le\phi_0;\ |i(0,t)|\le\frac{e^{\mu T_0}\left(W_0+J_0\right)}{2Z_0}\le\mathrm{I}_0,\ |i(\Lambda,t)|\le\frac{e^{\mu T_0}\left(W_0+J_0\right)}{2Z_0}\le\mathrm{I}_0.$

Assumptions (L): $|i|\le\mathrm{I}_0<\infty\ \Rightarrow\ \frac{d\widetilde{L}_p(i)}{di}=\sum_{n=1}^{m}(n+1)l_n^{(p)}i^n\ge\hat{L}_p^{(1)}>0,$

$$\left|\frac{d\tilde{L}_p(i)}{di}\right| \le \sum_{n=1}^{m}(n+1)l_n^{(p)}\mathrm{I}_0{}^n = \breve{L}_p^{(1)},\ \left|\frac{d\tilde{L}_p^2(i)}{di^2}\right| \le \sum_{n=1}^{m-1} n(n+1)l_n^{(p)}\mathrm{I}_0{}^{n-1} = \breve{L}_p^{(2)}\ .$$

Assumptions (G): $G_0(i_{R_0L_0}) = \sum_{n=1}^{m} g_n^{(0)}(i_{R_0L_0})^n,\ G_1(i_{R_1L_1}) = \sum_{n=1}^{m} g_n^{(1)}(i_{R_1L_1})^n.$

V. CONCLUSION

Here we have investigated lossy transmission lines terminated by circuits different from parallel or in series connected *RGLC*-elements. It turned out that in this case one obtains more number of equations which leads to more complicated boundary conditions at both ends of the line. First difficulty is to find independent unknown functions − voltages and currents and to obtain a system of neutral differential equations. We show that just oscillatory solutions are specific for the lossy transmission lines and in the second part of the paper we formulate conditions for existence-uniqueness of an oscillatory solution. They can be easily applied to concrete problem because they are explicit type conditions − just inequalities between specific parameters of the line and characteristics of the circuit.

REFERENCES

[1] G. Miano, and A. Maffucci, Transmission lines and lumped circuits (Academic Press, NY, 2-nd ed., 2010)
[2] D. Pozar, Microwave engineering (J. Wiley & Sons, NY, 1998).
[3] C.R. Paul, Analysis of multi-conductor transmission lines (A Wiley-Inter science Publication, J. Wiley &Sons, NY, 1994).
[4] S. Ramom, J.R. Whinnery, and T.van Duzer, Fields and waves in communication electronics (J. Wiley & Sons, Inc. NY, 1994).
[5] S. Rosenstark, Transmission lines in computer engineering (Mc Grow-Hill, NY, 1994).
[6] P. Vizmuller, RF design guide systems, circuits and equations (Artech House, Inc., Boston - London, 1995).
[7] P.C. Magnusson, G.C. Alexander, and V.K. Tripathi, Transmission lines and wave propagation (CRC Press. Boka Raton, 3rd ed., 1992).
[8] J. Dunlop, and D.G. Smith, Telecommunications engineering (Chapman & Hall, London, 1994).
[9] V. Damgov, Nonlinear and parametric phenomena: Theory and applications in radio physical and mechanical systems (World Scientific: New Jersey, London, Singapore, 2004).
[10] V.G. Angelov, and M. Hristov, Distortion less lossy transmission lines terminated by in series connected RCL-loads. Circuits and Systems, 2(4), 2011, 297-310.
[11] V.G. Angelov, and D.Tz. Angelova, Oscillatory solutions of neutral equations with polynomial nonlinearities, in Recent Advances in Oscillation Theory − special issue published in International Journal of Differential Equations, Volume 2011, Article ID 949547, 2011, 12 pages.
[12] V.G. Angelov, Periodic regimes for distortion less lossy transmission lines terminated by parallel connected RCL-loads, in Transmission Lines: Theory, Types and Applications, (Nova Science Publishers, Inc., 2011) 259-293.
[13] V.G. Angelov, Oscillations in lossy transmission lines terminated by in series connected nonlinear RCL-loads, International Journal of Theoretical and Mathematical Physics, 2(5), (2012).
[14] V.G. Angelov, Various applications of fixed point theorems in uniform spaces. 10Th International Conference on Fixed Point Theory and its Applications. Cluj-Napoca, 2012.
[15] V.G. Angelov, Lossless transmission lines terminated by in series connected RL-loads parallel to C-load. International Journal of Theoretical and Mathematical Physics, 3(1), 2013.
[16] V.G. Angelov, A method for analysis of transmission lines terminated by nonlinear loads (submitted for publication).
[17] V.G. Angelov, Fixed points in uniform spaces and applications (Cluj University Press "Babes-Bolyia", Romania, 2009).

International Journal of Modern Engineering Research (IJMER)
www.ijmer.com Vol.3, Issue.3, May-June. 2013 pp-1419-1423 ISSN: 2249-6645

Modified Chattering Free Sliding Mode Control of DC Motor

Arun Prasad K.M, [1] Bindu M. Krishna, [2] Usha Nair[3]
[13]*Division of Electrical Engg, School of Engineering, Cochin University of science & Technology, Kochi, India*
[2]*Sophisticated Test and Instrumentation centre, Cochin University of Science and Technology, Kochi, India*

Abstract: *This paper is concerned with the design of a Modified Sliding Mode Controller for the position control of DC Motor. The DC motor can be modeled as a linear time invariant single input single output (SISO) system. In this paper synthesis and analysis of position control of a DC motor using chattering free sliding mode controller and conventional PID controllers are carried out and their performance is evaluated. The performance of modified sliding mode controller is superior to conventional PID controllers even in the presence of disturbances.*

Keyword: *chattering free Sliding mode controller; DC Motor; PID Controller*

I. INTRODUCTION

The proportional-integral-derivative (PID) controller is extensively used in many industrial control applications [1] due to is simplicity and effectiveness in implementation. The three controller parameters, proportional gain Kp, Integral gain Ki, and derivative gain Kd, are usually fixed. The disadvantage of PID controller is poor capability of dealing with system uncertainty, i.e., parameter variations and external disturbance. In recent years, there has been extensive research interest in robust control systems, where the fuzzy logic, neural network and sliding-mode based controllers [1] [2].

Sliding mode control (SMC) is one of the popular strategies to deal with uncertain control systems [3]. The main feature of SMC is the robustness against parameter variations and external disturbances and is widely used to obtain good dynamic performance of control systems. Various applications of SMC have been conducted, such as robotic manipulators, aircrafts, DC motors, chaotic systems etc. [4] [5] [6].

The finite speed of switching devices involved in SMC cause the phenomenon of chattering and it affects the performance of the system adversely. Chattering is a phenomenon of high frequency switching of the control action which causes high frequency oscillations in the output, heating up of electrical circuits and premature wear in actuators. A modified sliding mode control technique can reduce the chattering without sacrificing the robustness of the system.

DC motor are generally controlled by conventional Proportional – Integral – Derivative (PID) controllers. For effective implementation of PID controller it is necessary to know system's mathematical model for tuning PID parameters. However, it has been known that conventional PID controllers generally do not work well for non-linear systems, particularly complex and vague systems that have no precise mathematical models. To overcome these difficulties, various types of modified conventional PID controllers such as auto-tuning and adaptive PID controllers were developed lately [7].

This paper is focused on the performance comparison of the of the modified sliding mode controller with PID controller for the position control of a DC motor

II. MATHEMATICAL MODELING OF A DC MOTOR

DC motors are widely used in various industrial and electronic equipment where the position control with high accuracy is required. The electric circuit of the armature and the free body diagram of the rotor are shown in fig. 1. The desired speed is tracked according to the shaft position of the motor. A single controller is required to control the position as well as the speed of the motor. The controller is selected so that the error between the system output and reference signal eventually tends to its minimum value, ideally zero. The reference signal determines the desired position and/or speed. Depending on type, a DC motor may be controlled by varying the input voltage or field current.

Here the variation of input voltage is used as the control parameter for the position control. A constant dc voltage is selected as a reference signal to obtain the desired position of the motor. However, the method works successfully for any reference signal, particularly for any stepwise time-continuous function. This signal may be a periodic signal or any signal to get a desired shaft position, i.e. a desired angle between 0 and 360 degrees from a virtual horizontal line.

The dynamics of a DC motor is given in eqn (1)-eqn (5)

$$V_t = R_a I_a + L_a \frac{dI_a}{dt} + E_b \quad (1) \qquad T = J\frac{d\omega}{dt} B\omega - T_L \quad (2)$$

$$T = K_t I_a \quad (3) \qquad E_b = K_b \omega \quad (4)$$

$$\omega = \frac{d\theta}{dt} \quad (5)$$

Where

V	Input terminal voltage (v)	E_b	Back emf (v)
Ra	The armature resistance (ohm)	*La*	the armature inductance (H)
J	The moment of inertia of the rotor and load (Kg-m^2/s^2)	*Kt*	the torque constant (N-m/A)
B	The damping ratio of mechanical system (N/m/s)	*Kb*	the motor constant (v-s/rad)
θ	The angular displacement (rad)		

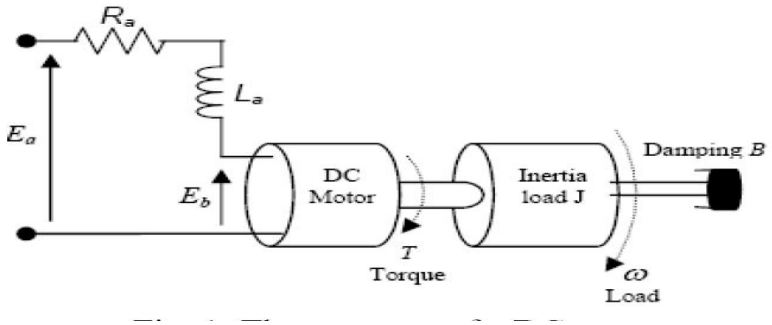

Fig.1. Structure of a DC Motor

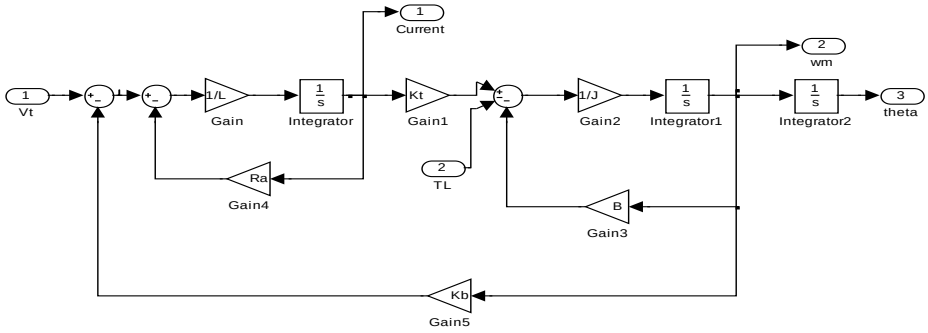

Fig.2. Simulink Block diagram of a DC Motor

III. Sliding Mode Control

Sliding mode control has long proved its interests. They are relative simplicity of design, control of independent motion (as long as sliding conditions are maintained) and invariance to process dynamics characteristics and external perturbations.

A Sliding Mode Controller is a Variable Structure Controller (VSC). Basically, a VSC includes several different continuous functions that can map plant state to a control. Surface and the switching among different functions are determined by plant state that is represented by a switching function. The basic control law of SMC is given by:

$$u = -ksign(s) \qquad (6)$$

Where k is a constant parameter, sign (·) is the sign function and s is the switching function. Chattering is a phenomenon present in the sliding mode control which affects the performance of the system significantly. In order to reduce the effect of chattering, the control law in the sliding mode controller is modified as $u = -ksat(s/\phi)$ and constant factor ϕ defines the thickness of the boundary layer. $sat(s/\phi)$ is a saturation function that is defined as:

$$sat(s/\phi) = \begin{cases} \dfrac{s}{\phi} & if \left|\dfrac{s}{\phi}\right| \le 1 \\ \text{sgn}(s/\phi) & if \left|\dfrac{s}{\phi}\right| > 1 \end{cases} \qquad (7)$$

The control strategy adopted here will guarantee the system trajectories move toward and stay on the sliding surface s=0 from any initial condition if the following condition meets:

$$s\dot{s} \le -\eta|s| \qquad (8)$$

Where η is a positive constant that guarantees the system trajectories hit the sliding surface in finite time .Using a sign function often causes chattering in practice. One solution is to introduce a boundary layer around the switch surface.

This controller is actually a continuous approximation of the ideal relay control. The consequence of this control scheme is that invariance of sliding mode control is lost. The system robustness is a function of the width of the boundary layer. The principle of designing sliding mode control law for arbitrary-order plants is to make the error and derivative of error of a variable is forced to zero. In the DC motor system the position error and its derivative are the selected coordinate variables those are forced to zero. Switching surface design consists of the construction of the switching function. The transient response of the system is determined by this switching surface if the sliding mode exists. First, the position error is introduced:

$$e(k) = \theta_{ref}(k) - \theta(k) \qquad (9)$$

Where θ_{ref} (k) and θ (k) are the respective responses of the desired reference track and actual rotor position, at the k the sampling interval and e(k) is the position error. The sliding surface (s) is defined with the tracking error (e) and its integral $\int edt$ and rate of change of e. The sliding surface is given by eqn (10)

$$s = \dot{e} + \lambda_1 e + \lambda_2 \int edt \qquad (10)$$

Where $\lambda_1, \lambda_2 > 0$ are a strictly positive real constant. Also the value of ϕ is taken as unity.

IV. PID CONTROLLER

The time domain representation of PID controller is given in eqn (11)

$$u(t) = K_p \left[e(t) + T_d \frac{de(t)}{dt} + \frac{1}{T_i} \int e(t)dt \right] \qquad (11)$$

Where e (t) is the error (difference between reference input and output), u(t) is the control variable, Kp is the proportional gain Td is the derivative time constant and Ti is the integral time constant. The above equation can also be written as eqn (12)

$$u(t) = K_p e(t) + K_d \frac{de(t)}{dt} + K_i \int e(t)dt \qquad (12)$$

Where Kd= Kp Td and Ki= Kp/ Ti. Each of these coefficients makes change in the characteristics of the response of the system. In order to get the desired performance characteristics of the system these parameters are to be accurately tuned. The tuning Process of the PID controller can be complex due to its iterative nature. First it is necessary to tune the proportional mode, then the integral and then the derivative mode to stabilize the overshoot. The tuning process is to be continued iteratively.

Ziegler-Nichols tuning method of PID controllers

The tuning of PID controller involves the selection of the best values of the gains of K_p, K_i and K_d of the control law. A number of methods are available for the tuning of PID controllers.

The tuning of a PID controller generally aims to match some predetermined ideal response profile for the closed loop system. Many algorithms are available to guarantee the best performance of the PID controller. The Ziegler-Nichols tuning method of PID controllers is presented here.

The Ziegler-Nichols tuning method is described in the following steps

- Set the controller to Proportional mode only
- Set the gain K_p to a small value
- Apply a step input to the system and observe the response
- Increase the K_p in steps and observe the step response in each step
- Keep increasing K_p until the response show constant amplitude oscillations
- Note the value of K_p and the time period of the sustained oscillations. This gain is the ultimate gain Ku and the time period is P_u
- Apply the criteria of the Table for the determination of the parameters of the PID controller

The PID controller parameters are selected for the Quarter Decay Response (QDR) according to the table.I

Table I. Zeigler-Nichols parameters for QDR

Control Action	K_p	K_i	K_d
P	$K_u/2$		
PI	$K_u/2.2$	$1.2\ K_p/P_u$	
PID	$K_u/1.7$	$2\ K_p/P_u$	$K_p\ P_u/8$

For the DC motor system the ultimate gain Ku and the time period is P_u are obtained as K_u=3.8, Pu=0.28sec. From these the PID controller parameters are obtained as K_p= 2.23 , K_i= 27.14 , K_d=1.33

V. SIMULATION RESULTS & DISCUSSIONS

In this section, the overall model of DC motor with PID controller and sliding mode controller is implemented in MATLAB/Simulink.

The simulink model of the PID controller is shown in fig. 3 and that of the modified chatter free SMC is shown in fig. 4. The fig.5 shows the response of the system with conventional sliding mode controller for a step input in presence of cyclic disturbance. Here the overshoot is considerably reduced as compared to PID controller. But the output is oscillating at high frequency due to chattering. The fig.6 shows the response of the system with modified chatter free SMC for a step input at no-load. The performance comparison is given in table II. From table it is clear that the performance of the sliding mode controller is far better than that of the PID controller

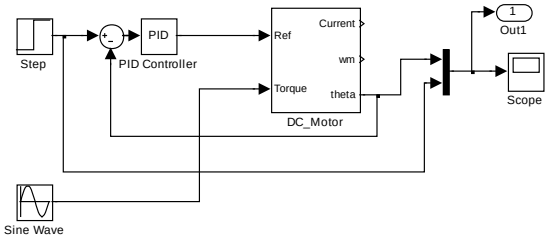

Fig.3. Simulink Block diagram of PID control

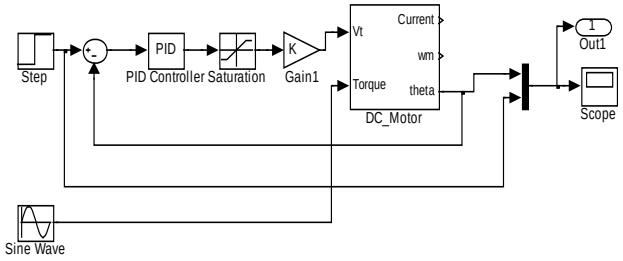

Fig.4. Simulink Block diagram of SMC

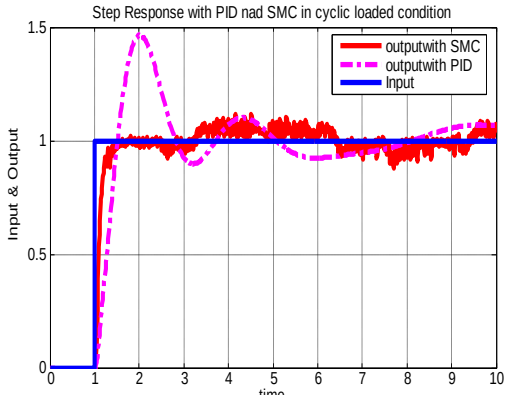

Fig.5. Step response with PID and conventional SMC in cyclic loaded condition

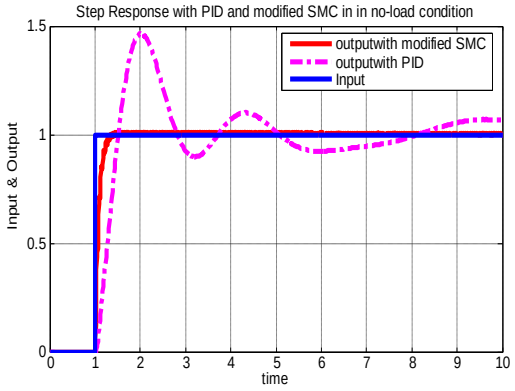

Fig.6. Step response with PID and modified SMC at no-load

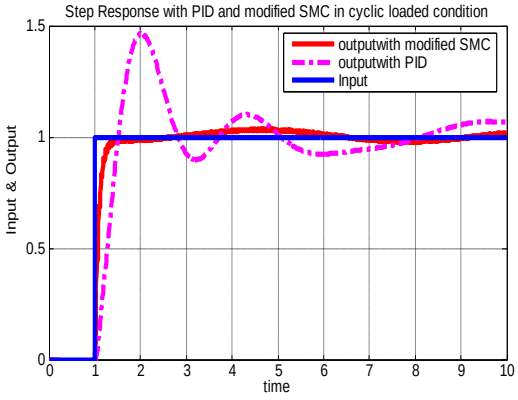

Fig.7. Step response with PID and modified SMC in cyclic loaded condition

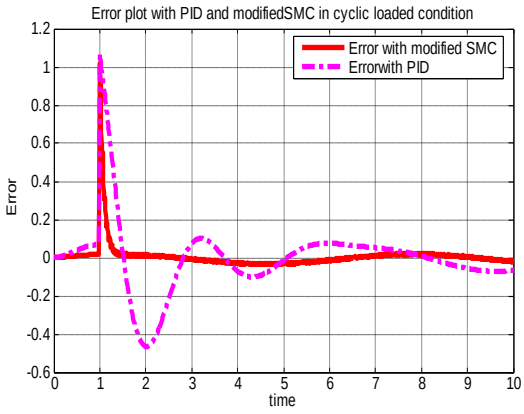

Fig.8. Error with PID and modified SMC in cvclic loaded condition

Fig.7 shows the step response of the system under disturbance by cyclic load. Under this condition also the sliding mode controller still shows better performance than the PID controller. Fig 8 shows the plot of error in this condition. So it is clear that the sliding mode controller is superior to PID controller even in the presence of disturbances like cyclic load or disturbance.

Table II. Performance comparison

	PID	Modified SMC
Rise time	0.6sce	0.4sec
Peak overshoot	40%	0%
Settling time	4 sec	0.4 sec

VI. CONCLUSION

This paper emphasizes on the effectiveness of position control of a DC motor with a Modified chattering free Sliding mode Controller and its merit over conventional PID controllers.

The PID controller and modified Sliding mode controller for the control of an armature controlled DC Motor is designed and is simulated using MATLAB and SIMULINK. From the obtained results it is clear that the performance of modified sliding mode controller is superior to that of PID controller.

The PID controller is very simple to design and very easy to implement and also give moderate performance under undisturbed conditions. But their performance deteriorates under disturbed condition like cyclic load. The sliding mode controller gives a better performance than that of PID controllers. The main problem associated with sliding mode controller is chattering. Reduced chattering may be achieved without sacrificing robust performance by modifying the control law of the sliding mode controller. The performance of the system with modified chattering free sliding mode controller is far better even in the presence of disturbances like cyclic load.

REFERENCES

[1] Oscar Montiel et.al. "Performance of a Simple Tuned Fuzzy Controller and a PID Controller on a DC Motor," Proceedings of the 2007 IEEE Symposium on Foundations of Computational Intelligence (FOCI 2007), pp 531-537, 2007

[2] Jan Vittek, Peter Bris and Mark Stulrajter, "Chattering Free Sliding Mode Control Law for Position Control of the Drive employing Induction Motor," 2008 Australasian Universities Power Engineering Conference AUPEC'08), P-038 pp1-6, 2008

[3] Vadim I. Utkin, "Variable structure systems with sliding modes", IEEE Transactions on Automatic Control, vol. AC-22, pp. 212–222, April 1977

[4] John Y. Hung, Weibing Gao and James C. Hung, "Variable structure control: A survey," IEEE Transactions on Industrial Electronics, vol.40, no.1, pp.2-22, February 1993.

[5] Raymond A. Decarlo, Stanislaw H.Zak and Gregory P. Matthews, "Variable structrure control of non-linear multivariable system," Proceedings of IEEE, vol. 76, No.3, pp. 212–232, March 1988.

[6] K.D. young, V.I. Utkin and U. Ozguner, "A control Engineer's guide to sliding mode control," IEEE Transactions on Control System Technology, vol.7, pp.328-342, 1999

[7] Q. G. Wang, B. Zou, T. H. Lee, and Q. Bi, "Auto-tuning of multivariable PID controller from decentralized relay feedback," Automatica, vol. 33, 1997, pp. 319-330.

International Journal of Modern Engineering Research (IJMER)
www.ijmer.com Vol.3, Issue.3, May-June. 2013 pp-1424-1427 ISSN: 2249-6645

Integral solution of the non-homogeneous heptic equation in terms of the generalised Fibonacci and Lucas sequences

$$x^5+y^5-(x^3+y^3)xy-4z^2w=3(p^2-T^2)^2w^3$$

S.Vidhyalakshmi, [1] K.Lakshmi, [2] M.A.Gopalan[3]
[123]*Department of Mathematics, Shrimati Indira Gandhi College, Trichy-620002*

Abstract: *We obtain infinitely many non-zero integer sextuples* (x,y,z,w,p,T) *satisfying the Non-homogeneous equation of degree seven with six unknowns given by* $x^5+y^5-(x^3+y^3)xy-4z^2w=3(p^2-T^2)^2w^3$. *The solutions are obtained in terms of the generalised Fibonacci and Lucas sequences. Recurrence relations for the variables are given. Various interesting relations between the solutions and special numbers, namely polygonal numbers, Pyramidal numbers, centered hexagonal pyramidal numbers and Four Dimensional Figurative numbers are presented.*

Keywords: *Fibonacci and Lucas sequences, heptic equation, integral solutions, Non-homogeneous equation, special numbers.*

MSC 2000 Mathematics subject classification: 11D41.

NOTATIONS:

$GF_n(k,s)=\dfrac{\alpha^n-\beta^n}{\alpha-\beta}\left(\alpha=\dfrac{k+\sqrt{k^2+4s}}{2},\beta=\dfrac{k-\sqrt{k^2+4s}}{2}\right)$ -Generalised Fibonacci sequence

$GL_n(k,s)=\alpha^n+\beta^n\left(\alpha=\dfrac{k+\sqrt{k^2+4s}}{2},\beta=\dfrac{k-\sqrt{k^2+4s}}{2}\right)$ -Generalised Lucas sequence

$T_{m,n}$ -Polygonal number of rank n with size m

P_n^m - Pyramidal number of rank n with size m

$CP_{n,6}$ - Centered hexagonal pyramidal number of rank n

$F_{4,n,3}$ -Four Dimensional Figurative number of rank n whose generating polygon is a triangle

I. Introduction

The theory of diophantine equations offers a rich variety of fascinating problems. In particular, homogeneous and non-homogeneous equations of higher degree have aroused the interest of numerous Mathematicians since antiquity [1-3].Particularly in [4, 5] special equations of sixth degree with four and five unknowns are studied. In [6-8] heptic equations with three and five unknowns are analysed. This paper concerns with the problem of determining non-trivial integral solution of the non- homogeneous equation of seventh degree with six unknowns given by $x^5+y^5-(x^3+y^3)xy-4z^2w=3(p^2-T^2)^2w^3$, in terms of the generalised fibonacci and lucas sequences. Recurrence relations for the variables are also given.Various interesting properties between the solutions and special numbers are presented.

II. Method of Analysis

The Diophantine equation representing the non- homogeneous equation of degree seven is given by

$$x^5+y^5-(x^3+y^3)xy-4z^2w=3(p^2-T^2)^2w^3 \quad (1)$$

Introduction of the transformations

$$x=u+v,\ y=u-v,\ z=2v,\ w=u,\ p=v+1,\ T=v-1,\ v>1 \quad (2)$$

In (1) leads to $v^2-2u^2=1$ (3)

The above equation (3) is a pellian equation, whose general solution is given by

$$\left.\begin{aligned} v_n &= \frac{1}{2}\left[\left(3+2\sqrt{2}\right)^{n+1}+\left(3-2\sqrt{2}\right)^{n+1}\right] \\ u_n &= \frac{1}{2\sqrt{2}}\left[\left(3+2\sqrt{2}\right)^{n+1}-\left(3-2\sqrt{2}\right)^{n+1}\right] n=0,1,2,..... \end{aligned}\right\} \quad (4)$$

The values of u_n and v_n can be written in terms of the generalised Fibonacci and Lucas sequences.

$$\left.\begin{aligned} v_n &= \frac{1}{2}GL_{n+1}(6,-1) \\ u_n &= 2GF_{n+1}(6,-1) \end{aligned}\right\} \quad (5)$$

In view of (2) and (5) the non-zero distinct integral solutions of (1) in terms of the generalised Fibonacci and Lucas sequences are obtained as

$$\left.\begin{aligned} x_n &= 2GF_{n+1}(6,-1)+\frac{1}{2}GL_{n+1}(6,-1) \\ y_n &= 2GF_{n+1}(6,-1)-\frac{1}{2}GL_{n+1}(6,-1) \\ z_n &= GL_{n+1}(6,-1) \\ w_n &= 2GF_{n+1}(6,-1) \\ p_n &= \frac{1}{2}GL_{n+1}(6,-1)+1 \\ T_n &= \frac{1}{2}GL_{n+1}(6,-1)-1, \quad n=0,1,2,3.... \end{aligned}\right\} \quad (6)$$

A few numerical examples are tabulated below:

n	x_n	y_n	z_n	w_n	p_n	T_n
0	5	-1	6	2	4	2
1	29	-5	34	12	18	16
2	169	-29	198	70	100	98
3	985	-169	1154	408	578	576
4	5741	-985	6726	2378	3364	3362
5	33461	-5741	39202	13860	19602	19600
6	195025	-33461	228486	80782	114244	114242

The above values of x_n, y_n, z_n, w_n, p_n, T_n, satisfy the following recurrence relations respectively.

$$x_{n+2}-6x_{n+1}+x_n=0$$
$$y_{n+2}-6y_{n+1}+y_n=0$$
$$z_{n+2}-6z_{n+1}+z_n=0$$
$$w_{n+2}-6w_{n+1}+w_n=0$$
$$p_{n+2}-6p_{n+1}+p_n=-4$$
$$T_{n+2}-6T_{n+1}+T_n=4$$

2.1 Properties:

1. $2GF_{n+1}(6,-1)+\frac{1}{2}GL_{n+1}(6,-1)+2GF_{n+2}(6,-1)-\frac{1}{2}GL_{n+2}(6,-1)=0$
2. $x_n+y_n+2w_n+z_n+p_n+T_n=8GF_{n+1}(6,-1)+2GL_{n+1}(6,-1)$
3. $x_n-y_n=p_n+T_n$
4. $T_{2n+1}-\frac{1}{2}GL_{2n+2}(6,-1)+1=0$

5. $x_{3n+2} - y_{3n+2} = GL_{3n+3}(6,-1)$
6. $w_{2n+1} = 2GL_{n+1}(6,-1).GF_{n+1}(6,-1)$
7. $GL_{3n+3}(6,-1) - 2T_{3n+2} = 0(\mathrm{mod}\,2)$
8. $x_n + y_n = 2w_n$
9. Each of the following is a nasty number:

a) $6(z_{2n+1} + 4)$

b) $3(2p_{2n+1} - GL_{n+1}(6,-1))$

c) $6(x_{2n+1} - y_{2n+1}) + 2p_2^5$

d) $48w_n^2 + 24F_{4,1,3}$

10. Each of the following is a cubical integer:

a) $4(z_n^2 + 2z_n w_n - 2x_{2n+1})$

b) $2p_{3n+2} + 3z_n - 2$

c) $x_{3n+2} - y_{3n+2} + 3z_n$

d) $x_{3n+2} - y_{3n+2} - 6p_n - 6$

e) $2T_{3n+2} + 3(x_n - y_n) + 2$

f) $2T_{3n+2} + 3z_n + 2$

g) $2T_{3n+2} + 6p_n - 4$

11. Each of the following is a biquadratic integer:

a) $2p_{4n+3} + 8T_{2n+1} + 2p_2^5$

b) $x_{4n+3} - y_{4n+3} + 4z_{2n+1} + 2T_{3,2}$

c) $2T_{4n+3} + 4(x_{2n+1} - y_{2n+1}) + CP_{2,6}$

d) $2T_{4n+3} + 8T_{2n+1} + T_{4,4}$

e) $8(z_{2n+1} - 8w_n^2)$

g) $2p_{4n+3} + 4(x_{2n+1} - y_{2n+1} + 2)$

h) $x_{4n+3} - y_{4n+3} + 4(x_{2n+1} - y_{2n+1}) + 6$

12. $2z_n w_n - z_{2n+1} - 2y_{2n+1} = 0$
13. $w_{2n+1} - z_n w_n = 0$
14. $x_{2n+1} + y_{2n+1} - 2z_n w_n = 0$
15. $x_{2n+1} + y_{2n+1} - 4p_n w_n + 4w_n = 0$
16. $z_n^2 - x_{2n+1} + y_{2n+1} \equiv 0(\mathrm{mod}\,2)$
17. $x_{3n+2} + y_{3n+2} = 2w_n(z_{2n+1} + 1)$
18. $w_{2n+1} - 2w_n p_n + 2w_n = 0$

19. Define:

$X = z_n$, Y=2($\mathrm{p_n} - 1$), $Z = z_{2n+1} + 2$

It is to be noted that the triple (X, Y, Z) satisfies the Elliptic Paraboloid $X^2 + Y^2 = 2Z$

20. Define:

$X = z_n$, Y=2$\mathrm{T_n} + 2$, w = $\mathrm{x}_{2n+1} - y_{2n+1} + 2$

It is to be noted that the triple (X, Y, W) satisfies the Hyperbolic Paraboloid $2X^2 - Y^2 = W$

21. Define:

$X = z_{2n+1} + 2,\ \mathrm{Y}=2\mathrm{T}_{2n+1} + 4,\ \mathrm{Z} = \mathrm{x}_{2n+1} - y_{2n+1} + 2$

It is to be noted that the triple (X, Y, Z) satisfies the Cone $X^2 + Y^2 = 2Z^2$

22. Define:

$X = 2T_n + 2,\ \mathrm{Y}= \mathrm{x}_{2n+1} - y_{2n+1} + 2$

It is to be noted that the pair (X, Y) satisfies the parabola $X^2 = Y$

III. Conclusion

One may be able to get the solutions to (1) in terms of other choices of number sequences. For example, the solution to (1) is also written in terms of Pell and Pell-Lucas sequence as follows:

$$\left.\begin{aligned} x_n &= 2P_{2n+2}(2,1) + \frac{1}{2}PL_{2n+2}(2,1) \\ y_n &= 2P_{2n+2}(2,1) - \frac{1}{2}PL_{2n+2}(2,1) \\ z_n &= PL_{2n+2}(2,1) \\ w_n &= 2P_{2n+2}(2,1) \\ p_n &= \frac{1}{2}PL_{2n+2}(2,1) + 1 \\ T_n &= \frac{1}{2}PL_{2n+2}(2,1) - 1,\ n = 0,1,2,3.... \end{aligned}\right\} \qquad (7)$$

The corresponding properties can also be obtained in terms of number sequences.

References

[1] L.E.Dickson, History of Theory of Numbers Vol.11, Chelsea Publishing company,New York 1952.
[2] L.J.Mordell, Diophantine equation Academic Press, London1969
[3] Carmichael, R.D.,The theory of numbers and Diophantine Analysis Dover Publications, New York 1959
[4] M.A.Gopalan, S.Vidhyalakshmi and K.Lakshmi, on the non- homogeneous sextic equation $x^4 + 2(x^2 + w)x^2y^2 + y^4 = z^4$, International Journal of Applied Mathematics and Applications, 4(2), 2012, 171-173
[5] M.A.Gopalan, S.Vidhyalakshmi and K.Lakshmi, Integral Solutions of the sextic equation with five Unknowns $x^3 + y^3 = z^3 + w^3 + 3(x + y)T^5$ International Journal of Engineering Sciences & Research Technology, 1(10,) 2012, 562-564
[6] M.A.Gopalan and sangeetha.G, parametric integral solutions of the heptic equation with 5unknown $x^4 - y^4 + 2(x^3 + y^3)(x - y) = 2(X^2 - Y^2)z^5$, Bessel Journal of Mathematics 1(1), 2011, 17-22
[7] M.A.Gopalan and sangeetha.G, on the heptic diophantine equations with 5 unknowns $x^4 - y^4 = (X^2 - Y^2)z^5$, Antarctica Journal of Mathematics, 9(5), 2012, 371-375
[8] Manjusomnath, G.sangeetha and M.A.Gopalan, on the non-homogeneous heptic equations with 3 unknowns $x^3 + (2^p - 1)y^5 = z^7$, Diophantine journal of Mathematics, 1 (2), 2012, 17-121

International Journal of Modern Engineering Research (IJMER)
www.ijmer.com Vol.3, Issue.3, May-June. 2013 pp-1428-1434 ISSN: 2249-6645

Lateral Load Analysis of R.C.C. Building

M.D. KEVADKAR, [1] P.B. KODAG[2]
[1]*M.E. [Structure] student, Department of Civil Engineering, Sinhgad College of Engineering, Pune*
[2]*Assistant Professor, Department of Civil Engineering, Sinhgad College of Engineering, Pune*

Abstract: *The structure in high seismic areas may be susceptible to the severe damage. Along with gravity load structure has to withstand to lateral load which can develop high stresses. Now a day, shear wall in R.C.structure and steel bracings in steel structure are most popular system to resist lateral load due to earthquake, wind, blast etc. The shear wall is one of the best lateral load resisting systems which is widely used in construction world but use of steel bracing will be the viable solution for enhancing earthquake resistance. In this study R.C.C. building is modeled and analyzed in three Parts I) Model without bracing and shear wall II) Model with different shear wall system III) Model with Different bracing system The computer aided analysis is done by using E-TABS to find out the effective lateral load system during earthquake in high seismic areas. The performance of the building is evaluated in terms of Lateral Displacement, Storey Shear and Storey Drifts, Base shear and Demand Capacity (Performance point). It is found that the X type of steel bracing system significantly contributes to the structural stiffness and reduces the maximum inter story drift, lateral displacement and demand capacity (Performance Point) of R.C.C building than the shear wall system.*

Keywords: *R.C. frame, Lateral displacement, storey shear, storey drift, Base shears, etc.*

I. Introduction

1.1 General

The primary purpose of all kinds of structural systems used in the building type of structures is to transfer gravity loads effectively. The most common loads resulting from the effect of gravity are dead load, live load and snow load. Besides these vertical loads, buildings are also subjected to lateral loads caused by wind, blasting or earthquake. Lateral loads can develop high stresses, produce sway movement or cause vibration. Therefore, it is very important for the structure to have sufficient strength against vertical loads together with adequate stiffness to resist lateral forces.

1.2 Strengthening of RCC building with shear wall

Reinforced concrete (RC) buildings often have vertical plate-like RC walls called Shear Walls in addition to slabs, beams and columns. These walls generally start at foundation level and are continuous throughout the building height. Their thickness can be as low as 200mm, or as high as 400mm in high rise buildings [50]. Shear walls are usually provided along both length and width of buildings, Shear walls are like vertically-oriented wide beams that carry earthquake loads downwards to the foundation. Properly designed and detailed buildings with shear walls have shown very good performance in past earthquakes [10]. Shear walls in high seismic regions require special detailing. However, in past earthquakes, even buildings with sufficient amount of walls that were not specially detailed for seismic performance (but had enough well-distributed reinforcement) were saved from collapse [16]. Shear wall buildings are a popular choice in many earthquake prone countries, like Chile, New Zealand and USA [10]. Shear walls are easy to construct, because reinforcement detailing of walls is relatively straight-forward and therefore easily implemented at site. Shear walls are efficient, both in terms of construction cost and effectiveness in minimizing earthquake damage in structural and non-structural elements[12][50]

Most RC buildings with shear walls also have columns; these columns primarily carry gravity loads (i.e., those due to self-weight and contents of building). Shear walls provide large strength and stiffness to buildings in the direction of their orientation [14], which significantly reduces lateral sway of the building and thereby reduces damage to structure and its contents. Since shear walls carry large horizontal earthquake forces, the overturning effects on them are large. Thus, design of their foundations requires special attention. Shear walls should be provided along preferably both length and width. However, if they are provided along only one direction, a proper grid of beams and columns in the vertical plane (called a moment-resistant frame) must be provided along the other direction to resist strong earthquake effects[13][14].

1.3Strengthening of RCC building with Steel Bracing

Steel bracing is a highly efficient and economical method of resisting horizontal forces in a frame structure [6]. Bracing has been used to stabilize laterally for the majority of the world's tallest building structures as well as one of the major retrofit measures [1]. Bracing is efficient because the diagonals work in axial stress and therefore call for minimum member sizes in providing stiffness and strength against horizontal shear [42]. A number of researchers have investigated various techniques such as infilling walls, adding walls to existing columns, encasing columns, and adding steel bracing to improve the strength and/or ductility of existing buildings[27][28]. A bracing system improves the seismic performance of the frame by increasing its lateral stiffness and capacity [26]. Through the addition of the bracing system, load could be transferred out of the frame and into the braces, bypassing the weak columns while increasing strength [29]. Steel braced frames are efficient structural systems for buildings subjected to seismic or wind lateral loadings. Therefore, the use of steel bracing systems for retrofitting reinforced concrete is a frame with inadequate lateral resistance is attractive. Existing RC

framed buildings designed without seismic criteria and ductile detailing can represent a considerable hazard during earthquake ground motions [7]. The non-ductile behaviour of these frames derives from the inadequate transverse reinforcement in columns, beams and joints, from bond slip of beam bottom reinforcement at the joint, from the poor confinement of the columns [5].

In the presence of these deficiencies the upgrading of seismic performance may be realized with the introduction of new structural members such as steel bracing systems or RC shear walls. The introduction of steel braces in steel structures and of RC shear walls in RC structures. However, the use of steel bracing systems for RC buildings may have both practical and economical advantages [1]. In particular, this system offers advantages such as the ability to accommodate openings and the minimal added weight of the structure. Furthermore, if it is realized with external steel systems (External Bracing) the minimum disruption to the full operationally of the building is obtained [18]. There are two types of bracing systems, Concentric Bracing System and Eccentric Bracing System [2]. The steel braces are usually placed in vertically aligned spans. This system allows obtaining a great increase of stiffness with a minimal added weight, and so it is very effective for existing structure for which the poor lateral stiffness is the main problem [9]. The concentric bracings increase the lateral stiffness of the frame, thus increasing the natural frequency and also usually decreasing the lateral drift. However, increase in the stiffness may attract a larger inertia force due to earthquake. Further, while the bracings decrease the bending moments and shear forces in columns, they increase the axial compression in the columns to which they are connected. Since reinforced concrete columns are strong in compression, it may not pose a problem to retrofit in RC frame using concentric steel bracings [43].

Eccentric Bracings reduce the lateral stiffness of the system and improve the energy dissipation capacity [9]. Due to eccentric connection of the braces to beams, the lateral stiffness of the system depends upon the flexural stiffness of the beams and columns, thus reducing the lateral stiffness of the frame. The vertical component of the bracing forces due to earthquake cause lateral concentrated load on the beams at the point of connection of the eccentric bracings.[18]

II. Modelling

The E-TABS software is used to develop 3D model and to carry out the analysis. The lateral loads to be applied on the buildings are based on the Indian standards. The study is performed for seismic zone III as per IS 456 (Dead load, Live Load) IS 1893:2002 (Earthquake load), IS875: 1987(Wind Load). The building consists of reinforced concrete and brick masonry elements.

G+12 storied building analyzed for seismic and gravity forces.
G+12 storied building analyzed with different types Shear wall system
G+12 storied building analyzed with different types of bracing systems.
The different type Bracings placed for peripheral columns only.

To find out effectiveness of steel bracing and shear wall to RCC building there is need o study parameters as Lateral displacement, Story shear, Story drift, Pushover curve, capacity and demand of structure for that there is need to do linear and nonlinear analysis of structure.

2.1 Model Data:-

Structure	SMRF
No. Of stories	G+12
Storey Height	3.00 m
Material property	
Grade of concrete	M25
Grade of Steel	Fe 415
Member Properties	
Thickness of slab	0.125 m
Beam Size	0.30 x 0.45 m
Column Size	0.30 x 0.60 m
Load Intensities	
Seismic Zone	III

Table 2.1

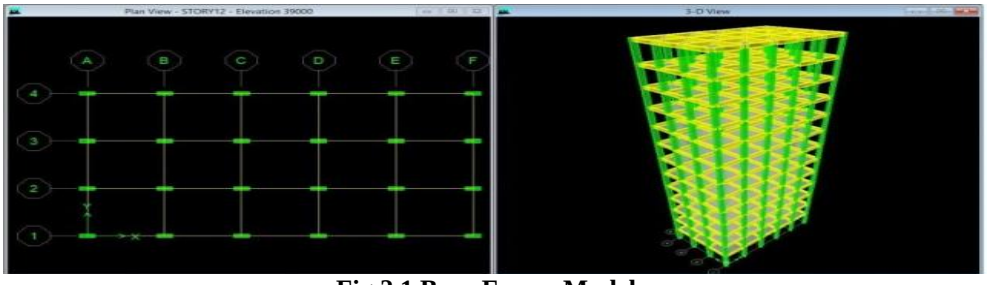

Fig.2.1 Bare Frame Model

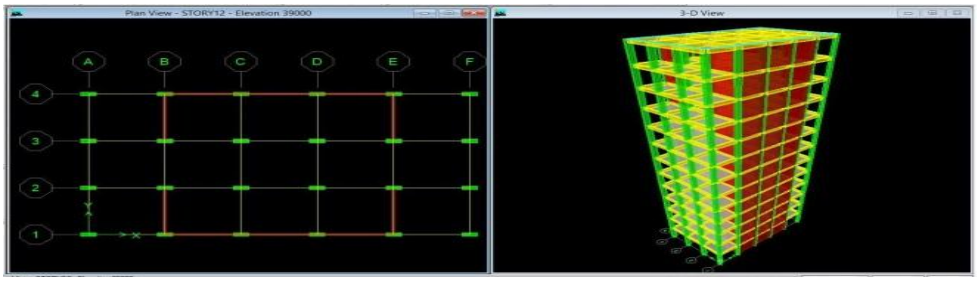

Fig. 2.2 SW Type-III

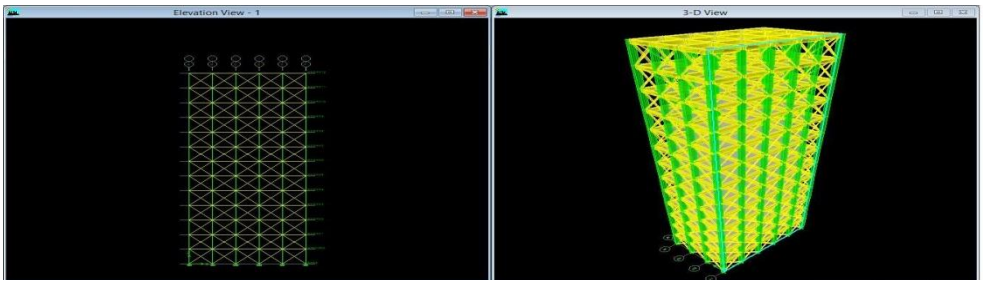

Fig.2.3 SB Type-I

III. Result and Discussion

Analysis of G+12 storied bare frame model, Shear wall model and steel bracing model is done using standard software, from the analysis results obtained, bare frame model ,SW Type-III and G+12 SB Type-I are compared. The comparison of these results to find effective lateral load resisting system is as below.

3.1 Linear Analysis

3.1.1 Lateral Displacement

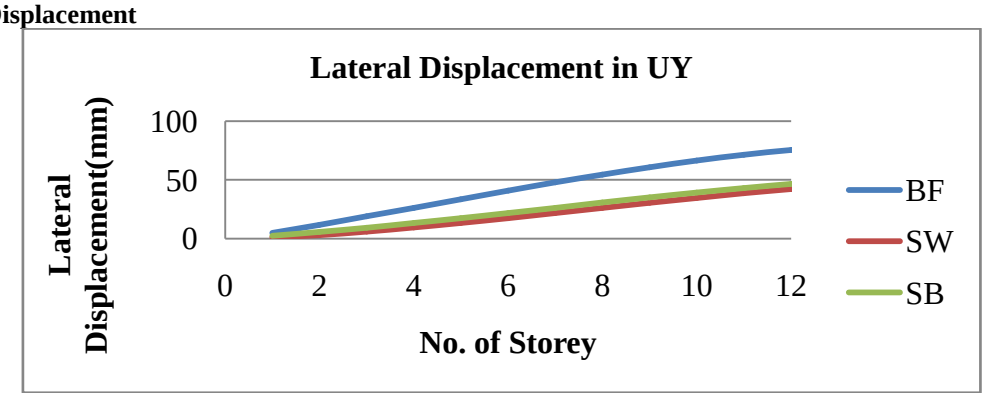

Fig.3.1

Lateral displacement of bare frame model is controlled by Shear wall and steel bracing as a lateral load resisting system. The lateral displacement of the bare frame model is 56.38 mm in X direction and 78.28 mm, in Y direction. The lateral displacement of bare frame models is reduced by 70 to 80 % in X Direction and 50 to 55 % in Y direction as compare with shear wall model. The lateral displacement of bare frame models is reduced by 40 to 50 % in X & Y direction as compare with Steel bracing model.

3.1.2 Storey Drift

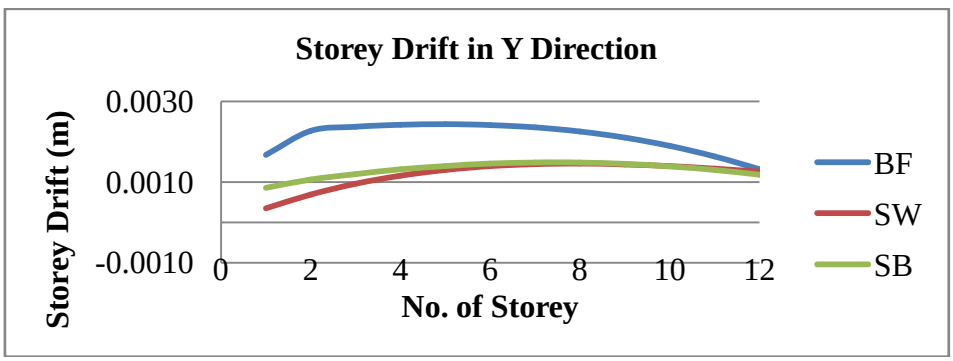

Fig.3.2

Shear wall and steel bracing significantly decrease in the story drift compared with bare frame model which is within limitas per clause no 7.11.1 of IS-1893 (Part-1):2002.

3.1.3 Storey Shear

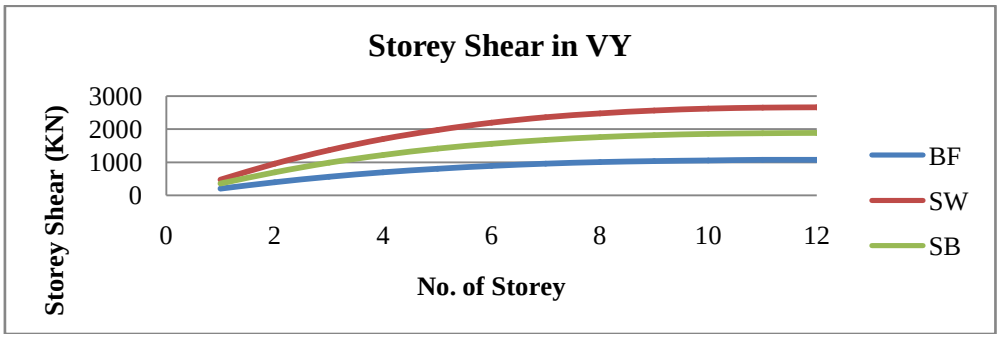

Fig.3.3

The maximum storey shear of the bare frame model is 1505.24 KN in X direction and 1078.16 KN in Y direction. The Storey shear of shear wall model is 80 to 100 % more than bare frame. The storey shear steel braced model in X direction is 60 to 70 % and 50 to 60 % in Y direction more than bare frame model.

3.2 Non Linear Analysis

3.2.2 Demand Spectrum

It can be observed that demand spectrum of bare frame model intersect away from D which means that the structure will behave poorly during imposed seismic excitation and need remedial measures. The demand spectrum of model with shear wall intersect near even point B and IO, which means that an elastic response and good security. It can observe demand of model with steel bracing intersect the capacity curve near the even point between B and IO, which means that an elastic response and good security margin.

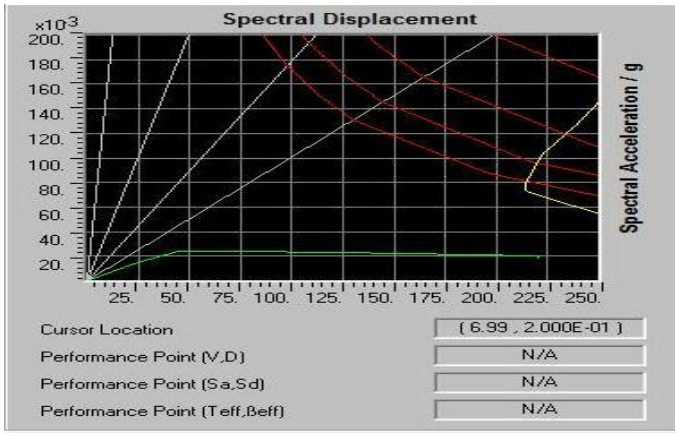

Figure.3.4 Performance Point of Bare frame model (Push Y)

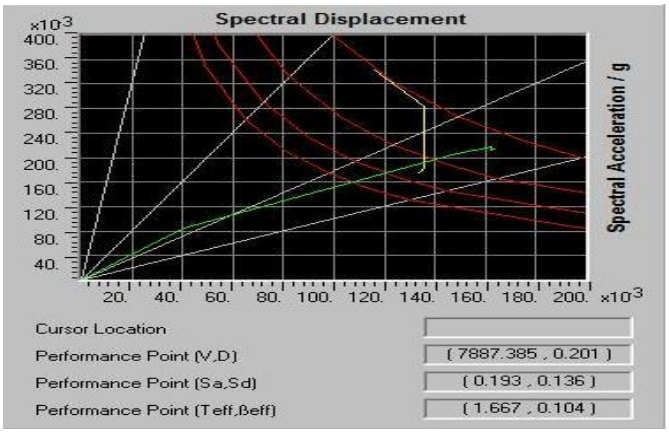

Figure.3.5 Performance Point of shear wall (Push Y)

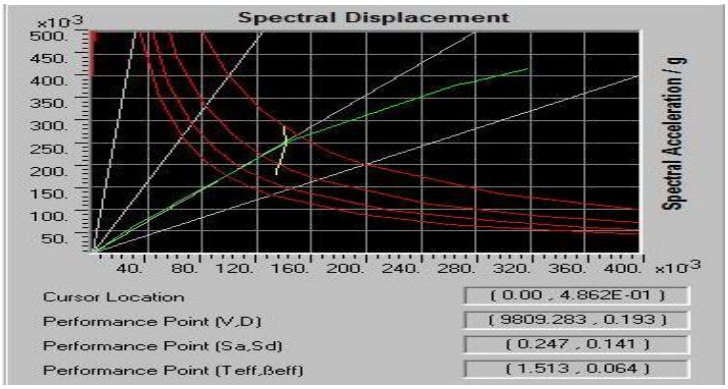

Figure.3.6 Performance Point of Steel Bracing (Push Y)

3.2.3 Plastic Hinge Mechanism

Model with shear wall shows better performance than bare frame model. The yielding of model with shear wall occurs at events C-D at step-2 and D-E at step 5-10. Model with steel bracing shows better performance. The yielding of the model with steel bracing occurs at event B-IO and IO-LS and LS-CP the amount of damage in this structure will be limited.

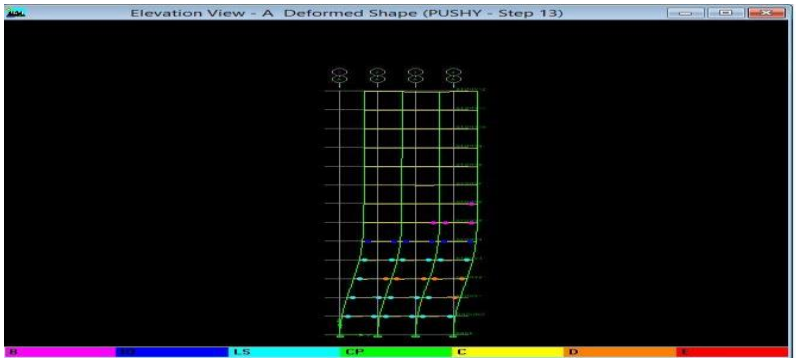

Figure.3.7 Plastic Hinge Mechanism of Bare frame model in (Push Y)

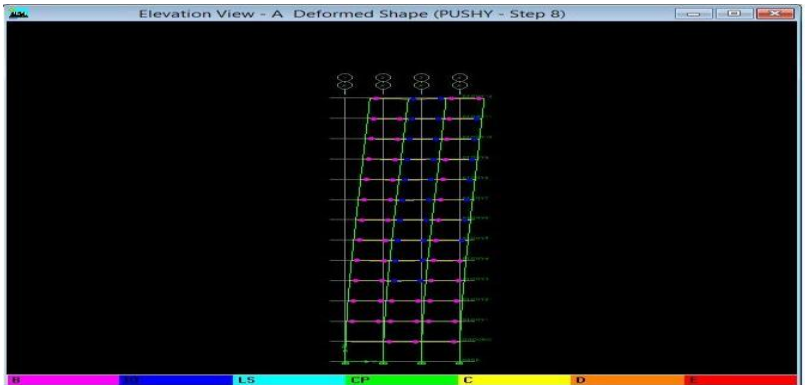

Figure.3.8 Plastic Hinge Mechanism of SW (Push Y)

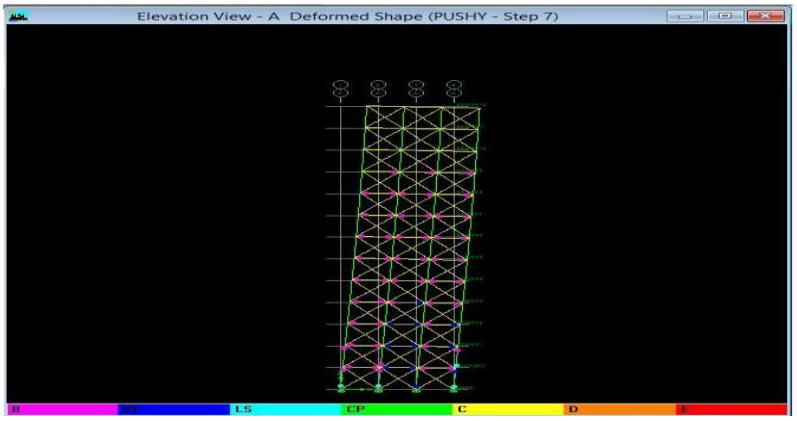

Figure.3.9 Plastic Hinge Mechanism of SB (Push Y)

IV. Conclusion

G+ 12 bare frame model, shear wall model and Steel bracing model is analyzed using standard software. The following conclusions are drawn based on present study.

1) The concept of using steel bracing is one of the advantageous concepts which can be used to strengthen structure
2) Steel bracings reduce flexure and shear demands on beams and columns and transfer the lateral load through axial load mechanism.
3) The lateral displacement of the building is reduced by 40 to 60 % by the use of shear wall Type-III and X Type steel bracing system.
4) Storey drift of the Shear wall and steel braced model is within the limit as clause no 7.11.1 of IS-1893 (Part-1):2002.
5) Steel bracings can be used as an alternative to the other strengthening techniques available as the total weight of structure changes significantly.
6) Shear wall has more storey shear as compare to steel bracing but there is 10 to15% difference in lateral displacement between shear wall and steel bracing.
7) Shear wall and steel bracing increases the level of safety since the demand curve intersect near the elastic domain.
8) Capacity of the steel braced structure is more as compare to the shear wall structure.
9) Steel bracing has more margin of safety against collapse as compare with shear wall.

References

[1] Bush T. D., Jones "Behavior of RC frame strengthened using structural steel bracing", Journal of Structural Engineering, Vol. 117, No.4, April, 1991
[2] Desai J.P., Jain A.K. and AryaA.S, "Seismic response of R. C. braced frames", Computers and Structures Volume 29 No.4, pp 557-568, 1988.
[3] Ghaffarzadeh H. and Maheri M.R., "Cyclic tests on the internally braced RC frames", Dept. of Civil Engineering, Shiraz University, Shiraz, Iran, 2006.
[4] IS 1893(part 1) 2002, "Criteria for earthquake resistant design of structures, part 1-general provisions and buildings", 5th revision, Bureau of Indian Standards, New Delhi, India.
[5] Marc Badoux and James O. Jirsa, "Steel bracing of RC frames for seismic retrofitting Journal of Structural Engineering, Vol. 116, No. 1, January, 1990.
[6] Maheri M.R. and SahebiA, "Use of steel bracings in reinforced concrete frame Engineering Structures, Vol. 19, No.12, pp 1018-1024, 1997.
[7] Mahmoud R. Maheri, "Recent advances in seismic retrofit of RC frames", Asian Journal of Civil Engineering (Building and Housing) Vol. 6, No. 5 pp 373-391, 2005.
[8] RavikumarG.andKalyanaraman, "Seismic design and retrofit of RC multistoried buildings with steel bracing", National Program on Earthquake Engineering Education, 2005.
[9] Ferraioli, M., Avossa, "Performance based assessment of R.C. buildings strengthened with steel braces", Proceedings of the 2 nd International Congress Naples, Italy, 2006.
[10] Prof. Mark fintel"Shear wall – an answer for the seismic resistant? "Proc Concrete International, July 1992
[11] Romy Mohan et. al. "Dynamic Analysis of RCC Buildings with Shear Wall" International Journal of Earth Sciences and Engineering ISSN 0974-5904, Volume 04, No 06 SPL, October 2011, pp 659-662
[12] A. M. Pande, 'Displacement Control of High Rise Structures with the Provision of Shear Wall,' International Journal of Engineering Research and Applications (IJERA) ISSN: 2248-9622 Vol. 1, Issue 4, pp. 1515-1521
[13] Rahul RANA, Limin JIN and AtilaZEKIOGLU, Pushover analysis of 19 story concrete shear wall building'13th World Conference on Earthquake Engineering Vancouver, B.C., Canada August 1-6, 2004 Paper No. 133
[14] P. S. Kumbhare, A. C. Saoji ,Effectiveness of Changing Reinforced Concrete Shear Wall Location on Multi-storeyed Building, International Journal of Engineering Research and Applications (IJERA)ISSN: 2248-9622 www.ijera.com Vol. 2, Issue 3, May-Jun 2012, pp.1786-1793
[15] Xiao-Kang ZOU and Chun-Man CHAN ,Seismic drift performance based design optimization of reinforced concrete buildings.13th World Conference on Earthquake Engineering Vancouver, B.C., Canada August 1-6, 2004 Paper No. 223
[16] RS Malik, SK Madan, VK Sehgal, Effect of Height on Seismic Response of Reinforced Cement Concrete Framed Buildings with Curtailed Shear Wall-
[17] Ricardo A. Medina, Story shear strength pattern for performance based seismic of regular frame.-ISET Journal of Earthquake Technology, Paper No. 442, Vol. 41, No. 1, March 2004, pp. 101-125
[18] A. Ghobarah, H. AbouElfath, Rehabilitation of a reinforced concrete frame using eccentric steel bracing, Engineering Structures 23 (2001) 745–755
[19] M.A. Youssefa, _H. Ghaffarzadehb, M. Nehdia, Seismic performance of RC frames with concentric internal steel bracing-Engineering Structures 29 (2007) 1561–1568
[20] M.R. Maheri and H. Ghaffarzadeh, Seismic design basis for internally braced frame, The 14 Th World Conference on Earthquake Engineering October 12-17, 2008, Beijing, China
[21] A Kadid, D.Yahiaoui, Seismic Assessment of Braced RC FramesProcedia Engineering 00 (2011) 000–0
[22] Shan-HuaXu and Di-Tao NiuSeismic Behavior of Reinforced Concrete Braced Frame Aci Structural Journal, Title no. 100-S14
[23] A. Vijay Kumaret. al. Pushover analysis of Existing RC structure, European Journal of Scientific Research ISSN 1450-216X Vol.71 No.2 (2012), pp. 195-202
[24] -Abhishek R, BijuV, Effect of Lateral load pattern in Pushover analysis,10th National Conference on Technological Trends (NCTT09) 6-7 Nov 200
[25] Federic M. Mazzolani, Gaetano dellacorte, Experimental analysis of steel dissipative bracing system for seismic upgrading-Journal of Civil Engineering and Management 2009 15(1): 7–19
[26] S.C. Goel and H.S. Lee, Strengthening RC structure with ductile steel bracing-

[27] T.EI Amoury, A.Ghobarah, Retrofit of RC Frames using FRP Jacketing or steel bracing-JSEE: Summer 2005, Vol. 7, No. 2
[28] M.R. Maheri, Recent advances in seismic retrofit of RC Frames-Asian Journal Of Civil Engineering (Building And Housing) VOL. 6, NO. 5 (2005) PAGES 373-391
[29] -S.C. Goel and A.C. MasriSeismic strengthening of an RC Slab-Column frames with ductile steel bracing Eleventh conference on earthquake engineering ISBN 0080428223
[30] H. Gaffarazadeh and M.R. Maheri, Cyclic test on the internally braced RC frames-SEE: Fall 2006, Vol. 8, No. 3 /
[31] M.R. Maheri, A.Hadjipour, Experimental investigation and design of steel bracing and concrete frame –Engineering Structures 25 (2003) 1707–1714
[32] H. Gaffarazadeh and M.R. Maheri, Capacity interaction between the steel bracing and concrete frames, 7 th international congress on civil engineering
[33] RafaelSabelli, ChunhoChang, Seismic demands on steel braced frame building with buckling restrained braces
[34] Alfaonso volcano, Fabio Mazza, Comparative study of the seismic performance of frames using different dissipative braces-12 WCEE2000 (Italian Ministry of the University and Scientific and Technological Research)
[35] S.T. Cheng, Van jeng, Seismic assessment and strengthening method of existing RC building in response to code revision-Earthquake engineering and engineering seismology Volume 3, Number 1, March 2001, pp. 67–77
[36] H. Gaffarazadeh and M.R. MaheriConnectionoverstrength in steel braced RC Frames Engineering Structures 30 (2008) 1938–1948
[37] D.R. Sahoo, D.C. Rai, Seismic strengthening of non ductile reinforces concrete frames using aluminium shear link as energy dissipation devices Engineering structures 32(2010)3548 3557
[38] M.R. Maheri, M.Razazan, Pushover tests on X- braced and Knee braces RC frames-Engineering Structures 25 (2003) 1697–1705
[39] A Valcano and F. Mazza, Seismic analysis and design of RC frames with dissipative braces-Engineering Structures 32 (2010) 2995–3010
[40] E.A. Godliner-D, A. Tena, Behaviour of Moment Resisting RC frames-The 14thWorld Conference on Earthquake Engineering October 12-17, 2008, Beijing, China
[41] Cengizhan D, Murat Diclei, Analytical study on seismic retrofitting of RC Building using steel braces
[42] T.D. Bush, EA Jones,J.O. Jirsa, Behaviour of RC frames strengthening using steel bracing Downloaded 18 Aug 2010 to 121.242.76.214. Redistribution subject to ASCE license or copyright.
[43] Viswanath K.G. Prakash K.B. and Anant Desai, Seismic analysis of steel braced RC frame International Journal of Civil and Structural Engineering Volume 1, No 1, and 2010 ISSN 0976 – 4399
[44] FEMA.NEHRP guidelines for the seismic rehabilitation of buildings (FEMA 273). Washington (DC): Building Seismic Safety Council; 1997.
[45] ATC. Seismic evaluation and retrofit of concrete buildings—volume 1(ATC-40). Report No. SSC 96-01. Redwood City (CA): Applied Technology Council; 1996.
[46] ATC 55. Evaluation and improvement of inelastic seismic analysis procedures. (2001).
[47] ATC, NEHRP Guidelines for the Seismic Rehabilitation of Buildings, FEMA 273 Report, prepared by the Applied Technology Council for the Building Seismic Safety Council, published by the Federal Emergency Management Agency, Washington, D.C. 1997a.
[48] ATC, Next-Generation Performance-Based Seismic Design Guidelines: Program Plan for New and Existing Buildings, FEMA 445, Federal Emergency Management Agency, Washington, D.C. 2006.
[49] M.Y.Kaltakci, M.H.Arslan, and G.Yavuz, Effect of Internal and External Shear Wall Location on Strengthening Weak RC Frames, Transaction A: Civil Engineering Vol. 17, No. 4, pp. 312{323 cSharif University of Technology, August 2010
[50] AshishS.Agrawal, S.D.Charkha,' Effect of change in shear wall location on story drift of multistory building subjected to lateral loads' International Journal of Engineering Research and Applications (IJERA) ISSN: 2248-9622 www.ijera.com Vol. 2, Issue 3, May-Jun 2012, pp.1786-1793
[51] Mahmoud R. Maheri, R. Akbari, Seismicbehaviour factor, R, for steel X-braced and knee-braced RC buildings, Engineering Structures 25 (2003) 1505–1513
[52] Anshuman., DipenduBhunia, BhavinRamjiyani,Solution of Shear Wall Location in Multi-Storey Building, International Journal Of Civil And Structural Engineering Volume 2, No 2, 2011, ISSN 0976 – 4399
[53] IS 1893 (Part 1) 2002
[54] IITK Earthquake tips
[55] www.asce.org
[56] www.sciencedirect.com
[57] www.springerlink.com
[58] www.scholar.google.com

International Journal of Modern Engineering Research (IJMER)
www.ijmer.com Vol.3, Issue.3, May-June. 2013 pp-1435-1441 ISSN: 2249-6645

Thermal barrier Analysis in Diesel

K. Sridhar, [1] R. Reji Kumar, [2] M. Narasimha[3]
[123]*Lecturer, School of Mechanical and Industrial Engineering Bahirdar University, Bahirdar, Ethiopia*

Abstract: *The specific outputs of some diesel engine applications have produced thermal loadings in excess of the strength of typical aluminium piston alloys. Functionally graded coatings are used to increase performances of high temperature components in diesel engines. Thermal barrier coating are being evaluated to return the components durability to acceptable levels as well as providing a means of lowering heat rejection. This paper discusses the use of a finite element model to analyze these thermal barrier coating systems, including the impact of material properties, coating thickness, residual stress and boundary conditions.*

These coatings consist of a transition from the metallic bond layer to cermet and from cermet to the ceramic layer. Thermal analyses were employed to deposit metallic, cermet and ceramic powders such as NiCrAl, NiCrAl+MgZrO3 and MgZrO3 on the substrate. The numerical results of AlSi and steel pistons are compared with each other. It was shown that the maximum surface temperature of the functional graded coating AlSi alloy and steel pistons was increased by 28% and 17%, respectively. In this study, thermal behavior of functional graded coatings on AlSi and steel piston materials was investigated by means of using a commercial code, namely ANSYS

Key Words: *Zirconia, Mullite, Alumina, Thermal efficiency, Electron Beam Physical Vapour Deposition*

List of Symbols

Symbol	Description	Unit
Nomenclature		
H	Heat transfer coefficient	W/m2/K
ρ	density	Kg/m3
A	Area	mm^2
P_m	Indicated Mean Effective Pressure,	N/mm^2
D	Diameter of bore	m
P	Thermal expansion	$° C^{-1}$
N	Speed	rpm
N	Number of strokes	Strokes/min
Cp	Specific heat capacity	J/Kg/K
Tc	Temperature at center of the piston	° C
Te	Temperature at edge of the piston	° C
K	Thermal conductivity	W/m/K
Abbreviation		
HCV	Higher calorific value	KJ/Kg
BP	Brake power	KW
TBC	Thermal barrier coating	
EBPVD	Electron beam physical vapor deposition	

I. Introduction

The demand for energy is increasing day by day. The world is depending mostly on fossil fuels to face this energy needs. The increase in standard of living demands better mode of transport, hence a large number of automobile companies has been introduced. Automobiles provide better transport but the combustion of fuel in automobile engine creates harmful effluents, which has an adverse effect on water and air.Combustion generated pollution is by far the largest man made contribution to atmospheric pollution. The principal pollutants emitted by the automobile engines are CO, NO_X, HC and particulates. The modern day automobiles is a result of several technological improvements that have happened over the years and would continue to do so to meet the performance demands of Exhaust-Gas Emissions, Fuel Consumption, Power Output, Convenience and Safety.In order to reduce emissions and increasing engine performance, modern car engines carefully designed to control the amount of fuel they burn. An effective way for reducing automotive emission and increase engine's performance is accomplished by coating automobile piston head with low thermal conductivity material such as ceramic. This process is known as Thermal Barrier Coating (TBC).

ANSYS is general-purpose finite element analysis (FEA) software package. Finite Element Analysis is a numerical method of deconstructing a complex system into very small pieces (of user-designated size) called elements. The software implements equations that govern the behaviour of these elements and solves them all; creating a comprehensive explanation of how the system acts as a whole. These results then can be presented in tabulated or graphical forms. This type of analysis is typically used for the design and optimization of a system far too complex to analyze by hand. Systems that may fit into

this category are too complex due to their geometry, scale, or governing equations.ANSYS is the standard FEA teaching tool within the Mechanical Engineering Department at many colleges. ANSYS is also used in Civil and Electrical Engineering, as well as the Physics and Chemistry departments. ANSYS provides a cost-effective way to explore the performance of products or processes in a virtual environment. This type of product development is termed virtual prototyping.

With virtual prototyping techniques, users can iterate various scenarios to optimize the product long before the manufacturing is started. This enables a reduction in the level of risk, and in the cost of ineffective designs. The multifaceted nature of ANSYS also provides a means to ensure that users are able to see the effect of a design on the whole behavior of the product, be it electromagnetic, thermal, mechanical etc.ANSYS is capable of both steady state and transient analysis of any solid with thermal boundary conditions. Steady-state thermal analyses calculate the effects of steady thermal loads on a system or component. Users often perform a steady-state analysis before doing a transient thermal analysis, to help establish initial conditions. A steady-state analysis also can be the last step of a transient thermal analysis; performed after all transient effects have diminished.

A steady-state thermal analysis may be either linear, with constant material properties; or nonlinear, with material properties that depend on temperature. The thermal properties of most material vary with temperature. This temperature dependency being appreciable, the analysis becomes nonlinear. Radiation boundary conditions also make the analysis nonlinear. Transient calculations are time dependent and ANSYS can both solve distributions as well as create video for time incremental displays of models. The ANSYS/Multiphysics, ANSYS/Mechanical, ANSYS/FLOTRAN, and ANSYS/Thermal products support steady-state thermal analysis. A steady-state thermal analysis calculates the effects of steady thermal loads on a system or component. Engineer/analysts often perform a steady-state analysis before doing a transient thermal analysis, to help establish initial conditions. A steady-state analysis also can be the last step of a transient thermal analysis, performed after all transient effects have diminished. You can use steady-state thermal analysis to determine temperatures, thermal gradients, heat flow rates, and heat fluxes in an object that are caused by thermal loads that do not vary over time. A steady-state thermal analysis may be either linear, with constant material properties; or nonlinear, with material properties that depend on temperature. The thermal properties of most material do vary with temperature, so the analysis usually is nonlinear. Including radiation effects also makes the analysis nonlinear.

II. Literature Review

Ekrem Buyukkaya and Muhammed Cerit investigated the effects of ceramic coating over diesel engine piston using 3D finite element method; they found that maximum surface temperature of the coated piston with material which has low thermal conductivity is improved approximately 48% for the AlSi alloy and 35% for the steel.[1]. EkremBuyukkaya, Department of Mechanical Engineering, Esentepe Campus, Turkey.. Thermal analysis of functionally graded coating AlSi alloy and steel pistons... Thermal analyses were employed to deposit metallic, cermet and ceramic powders such as NiCrAl, NiCrAl+MgZrO3 and MgZrO3 on the substrate. The numerical results of AlSi and steel pistons are compared with each other. It was shown that the maximum surface temperature of the functional graded coating AlSi alloy and steel pistons was increased by 28% and 17%, respectively. [2]. Imdat Taymazinvestigated the effect of thermal barrier coatings on diesel engine performance his results indicate a reduction in fuel consumption and an improvement in the efficiency of the diesel engine.[3]. P. M. Pierz investigated the thermal barrier coating development for diesel engine aluminum piston he found that the resulting predicted temperatures and stresses on the piston, together with material strength information, the primary cause of coating failure is proposed to be low cycle fatigue resulting from localized yielding when the coating is hot and in compression.[4]. O. Altun ,Mechanical Engineering Department , Turkey., Investigated in Problems for determining the thermal conductivity of TBCs by laser-flash method., Laser-flash method is the most widely used experimental technique to determine the thermal conductivity of APS TBCs at high temperatures. The research contributes to better understanding and recognition the importance of sample preparation in laser-flash method.[5]

S. C. Mishra., Laser and Plasma Technology Department, Mumbai, India. Investigated in Microstructure, Adhesion, and Erosion Wear of Plasma Sprayed Alumina–Titanium Composite Coatings.. Adhesion strength value of the coating varies with operating power. The trend of erosion of the coatings seems to follow the mechanism predicted for brittle materials. Coating deposited at 18kW power level shows a higher erosion rate than that of the sample deposited at 11kW power level [6]. H.W. Grunling and W. Mannsmann, ABB Kraftwerrke AG, KallstadterStz 1, 6800 Mannheim 31, Germany., investigated in Plasma sprayed thermal barrier coatings for industrial gas turbines: morphology, processing and properties. The properties of thermal barrier coating systems depend strongly on the structure and phase composition of the coating layers and the morphology of and the adhesion at the ceramic-metal interface. They have to be controlled by the process itself, the process parameters and the characteristics of the applied materials. [7]. A. J. Slifka, National Institute of Standards and Technology, Boulder. Thermal-Conductivity Apparatus for Steady-State, Comparative Measurement of Ceramic Coatings, and an apparatus has been developed to measure the thermal conductivity of ceramic coatings. Since the method uses an infrared microscope for temperature measurement, coatings as thin as 20 _m can, in principle, be measured using this technique. This steady-state, comparative measurement method uses the known thermal conductivity of the substrate material as the reference material for heat-flow measurement.[8]. Dongming Zhu Ohio Aerospace Institute, Cleveland, Ohio. Effect of Layer-Graded Bond Coats on Edge Stress Concentration and Oxidation Behavior of Thermal Barrier Coatings.. A low thermal expansion and layer-graded bond coat system, that consists of plasma-sprayed FeCoNiCrAI and FeCrA1Y coatings and a high velocity oxy fuel (HVOF) sprayed FeCrAIY coating, was developed for minimizing the thermal stresses and providing excellent oxidation resistance.[9]. S. Alphine', M. Derrien, Thermal Barrier Coatings: the Thermal Conductivity challenge. In this paper, the importance of the challenge associated with the control of the thermal

conduct why of thermal barrier coatings for turbine engines hot stages is being reviewed. It is firstly illustrated by the description of a practical aeronautic coated and uncoated turbine blade design exercise. The various contributions to TBC thermal conductivity are then reviewed. [10].

III. Thermal Barrier Coating

Thermal barrier coatings are highly advanced material systems applied to metallic surfaces, such as gas turbine aero-engine and diesel engine parts, operating at elevated temperatures. These coatings serve to insulate metallic components from large and prolonged heat loads by utilizing thermally insulating materials which can sustain an appreciable temperature difference between the load bearing alloys and the coating surface. In doing so, these coatings can allow for higher operating temperatures while limiting the thermal exposure of structural components, extending part life by reducing oxidation and thermal fatigue. In fact, in conjunction with active film cooling, Thermal barrier coatings permit flame temperatures higher than the melting point of the metal airfoil in some turbine applications.Modern Thermal barrier coatings are required to not only limit heat transfer through the coating but to also protect engine components from oxidation and hot corrosion. No single coating composition appears able to satisfy these multifunctional requirements. As a result, a "coating system" has evolved. Research in the last 20 years has led to a preferred coating system consisting of three separate layers such as metal substrate, bond coat and ceramic coating to achieve long term effectiveness in the high temperature, oxidative and corrosive use environment for which they are intended to function.

The application of Thermal barrier coatings on the diesel engine piston head reduces the heat loss to the engine cooling-jacket through the surfaces exposed to the heat transfer such as cylinder head, liner, piston crown and piston rings. It is important to calculate the piston temperature distribution in order to control the thermal stresses and deformations within acceptable levels. The temperature distribution enables the designer to optimize the thermal aspects of the piston design at lower cost, before the first prototype is constructed. As much as 60% of the total engine mechanical power lost is generated by piston ring assembly. Most of the internal combustion (IC) engine pistons are made of aluminum alloy which has a thermal expansion coefficient 80% higher than the cylinder bore material made of cast iron. This leads to some differences between running and the design clearances. Therefore, analysis of the piston thermal behavior is extremely crucial in designing more efficient engines. The thermal analysis of piston is important from different point of views. First, the highest temperature of any point on piston should not exceed 66% of the melting point temperature of the alloy. This limiting temperature for the current engine piston alloy is about 370°C. This temperature level can be increased in ceramic coating diesel engines.

Thermal barrier coatings consist of three layers. They are the metal substrate, metallic bond coat and ceramic topcoat. The metal substrate and metallic bond coat are metal layers and the topcoat is the ceramic layer. The metal substrate is typically a high temperature aluminium alloy that is either in single crystal or polycrystalline form. The metallic bond coat is an alloy typically with the composition of Nickel, Cobalt, Chromium, Aluminium. The bond coat creates a bond between the ceramic coat and substrate. The third coat is the ceramic topcoat, Zirconia (ZrO_3), Mullite($3Al_2O_3$-$2SiO_2$), Alumina (Al_2O_3) which is desirable for having very low conductivity while remaining stable at nominal operating temperatures typically seen in applications. This layer creates the largest thermal gradient of the thermal barrier coating. In industry, thermal barrier coatings are produced in a number of ways.

- Electron Beam Physical Vapor Deposition (EBPVD)
- Air Plasma Spray (APS)
- Electrostatic Spray Assisted Vapour Deposition (ESAVD)
- Direct Vapor Deposition

Diesel engine piston made of Aluminium Alloy is taken for this study and ceramic material having low thermal conductivity is preferred as the coating material on the piston head or crown.

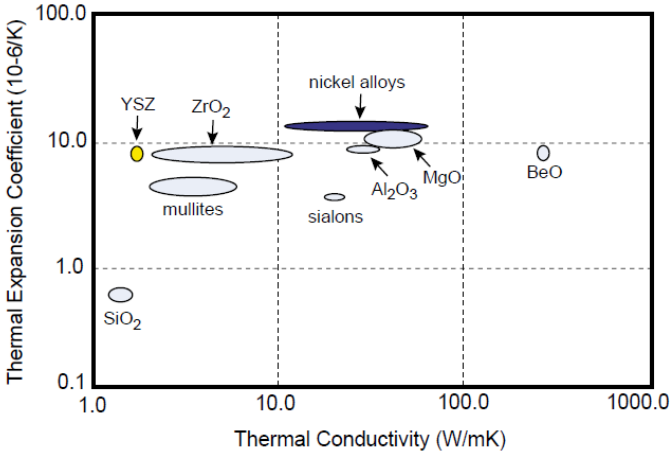

Fig.1. Materials for thermal barrier coating

The ceramic material choosen for this study should have low thermal conductivity and thermal expansion as shown in the above graph. The selected materials are as follows,

- Zirconia (ZrO_2)
- Mullite ($3Al_2O_3$-$2SiO_2$)
- Alumina (Al_2O_3)

IV. Electron Beam Physical Vapor Deposition

EB-PVD is an evaporation process for applying ceramic thermal barrier coatings to gas turbine engine parts .It has been the favored deposition process technique for TBCs because of the increased durability of coating that is produced when compared to other deposition processes. EB-PVD TB exhibits a columnar microstructure that provides outstanding resistance against thermal shocks and mechanical strains. Figure presents a diagram of the coating chamber where the EB-PVD process takes place.The EB-PVD process takes place in a vacuum chamber consisting of a vacuum-pumping system, horizontal manipulator, a water-cooled crucible containing a ceramic ingot to be evaporated, an electron-beam gun, and the work piece being coated. The electron beam gun produces electrons, which directly impinge on the top surface on the ceramic coating, located in the crucible, and bring the surface to a temperature high enough that vapor steam is produced. The vapor steam produces a vapor cloud, which condenses on the substrate and thus forms a coating. The substrate is held in the middle of vapor cloud by a horizontal manipulator that allows for height variation in the chamber. During the coating process, oxygen or other gases may be bled into the vapor cloud in order to promote a stoichiometric reaction of ceramic material. An .over source.heater or an electron beam gun may be used for substrate heating, which keeps the substrate at a desired temperature.

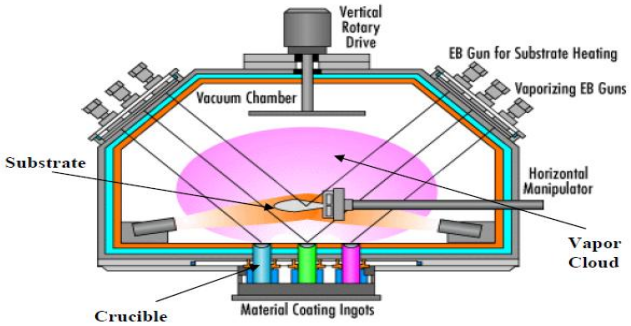

Figure 2. EB-PVD Coating Chamber

In our six stroke engine we are placing thermal barrier component in between the cylinder block and cylinder liner. The heat is transferred from the combustion chamber to the cylinder block through the cylinder liner and thermal barrier. The heat flow rate through the thermal barrier is low. Materials of thermal barrier are discussed in the forthcoming chapters.

V. Simulation

In this project work, ANSYS workbench 10 software has been used to investigate the temperature distribution in the ceramic coated Aluminium alloy piston and to compare the maximum surface temperature of the uncoated Aluminium alloy piston with ceramic coated Aluminium alloy piston, ceramic materials such as Zirconia stabilized with magnesium oxide, Mullite and Alumina were used for this study

In the numerical simulation performed, a diesel engine piston, made of Al alloy is analyzed. 3-D finite element thermal analyses are carried out on both uncoated and ceramic coated pistons. In the model, surface-to-surface contact elements are defined between piston ring and ring grove. Piston thermal boundary conditions consist of the ring land and skirt thermal boundary condition, underside thermal boundary condition, combustion side thermal boundary condition. Convective heat transfer coefficients and ambience temperatures were specified as the thermal boundary conditions.

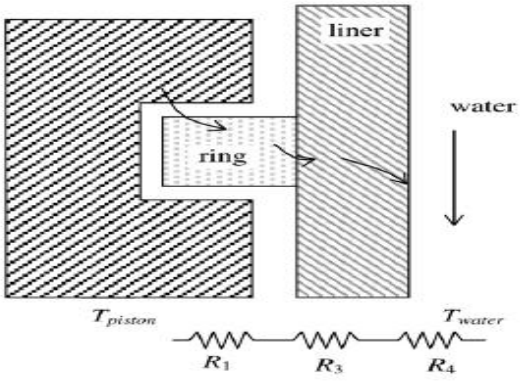

Fig 3. Thermal circuit of heat transfer resistances in the region of the rings.

R_1: Conductive resistance of the ring,
R_2: Conductive resistance of the oil film is negligible,
R_3: Conductive resistance of the liner,
R_4: Convective resistance between the liner and the cooling water.

Thermal circuit of heat transfer resistances in the ring land is to be set with the following assumptions.
1) The effect of piston motion on the heat transfer is neglected.
2) The rings and skirt are fully engulfed in oil and there are no cavitations.
3) The rings do not twist.
4) The heat transfer mode in the oil film is neglected.

Table .1.Thermal properties of parts

Material	Thermal conductivityW/m^0C
Piston (Al-Si)	155
Oil Ring	33
Compression Ring	52
Liner	55

The resistances are:
Conductive resistance of the ring, $R_1=(\ln(r_1/r_2)/2\pi L_1K_{ring})$ = 0.085048 m^2k/kw
Conductive resistance of the film, $R_2=(\ln(r_3/r_2)/2\pi L_2K_{oil})$ = $8x10^{-5}$ m^2k/kw
Conductive resistance of the liner, $R_3=(\ln(r_4/r_3)/2\pi L_3K_{block})$ = 0.06417 m^2k/kw
Conductive resistance between the liner and cooling water, R_4 = $1/(h_{water}A_s)$ =0.171 m^2k/kw
Total resistance R_{tot}=0.32 m^2k/kw
The effective heat transfer is obtained from, $h_{eff}=1/R_{tot}xA_{eff}$ = 617.68 w/m^2k
The value of convective heat transfer coefficient of crown underside is, $h_{un1}=900(N/4600)^{0.35}$ =672.415 w/m^2k
The value of convective heat transfer coefficient of piston skirt underside, $hun2=240(N/4600)^{0.35}$ =179.31 w/m^2k
The Crevice heat transfer coefficient, h=k/S =230 w/m^2k

Table 2.Coating Materials

Properties	Aluminium-Silicon Alloy	Zirconia stabilized with Magnesium oxide ($ZrMgO_3$)	Mullite ($3Al_2O_3•2SiO_2$)	Alumina (Al_2O_3)
Density kg/m³	2.68 x10³	5.6 x10³	2.8 x10³	3.69 x10³
Thermal expansion (20 ºC) ºC⁻¹	$19.4x10^{-6}$	$10x10^{-6}$	$5.4x10^{-6}$	$7.3x10^{-6}$
Specific heat capacity J/(kg*K)	850	400	950	880
Thermal conductivity W/(m*K)	154	2.5	6	18

Initial Conditions
Piston top surface temperature : 400^0C
Piston skirt temperature : 110^0C
Boundary Conditions
The Crevice convective heat transfer coefficient, h = 230 w/m^2k
The piston crown or head underside convective heat transfer coefficient, h_{un1} = 672.415 w/m^2k
The piston skirt underside convective heat transfer coefficient, h_{un2} = 179.31 w/m^2k

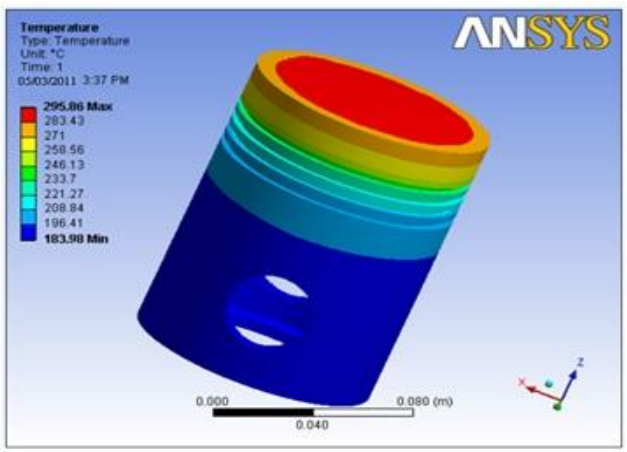

Fig .4 Uncoated Aluminium alloy piston

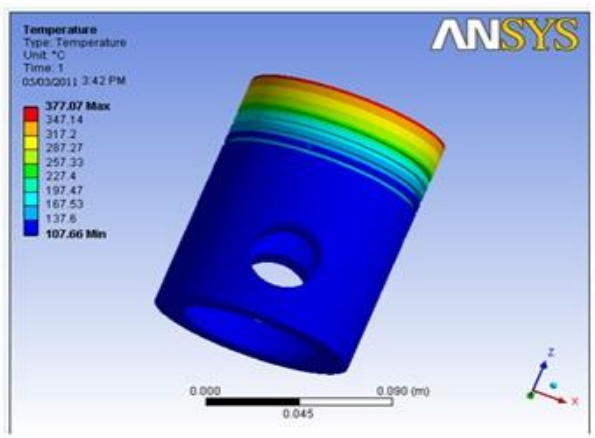

Fig 5.Ceramic material Zirconia coated piston

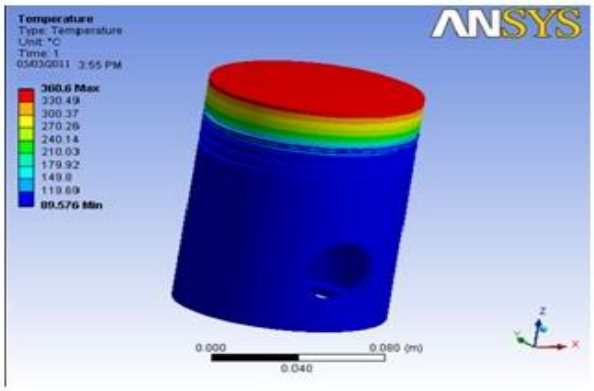

Fig .6 Ceramic materialMullite coated piston

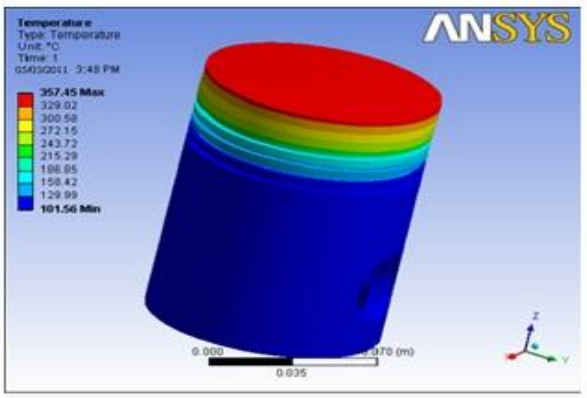

Fig 7. Ceramic material Alumina coated piston

VI. Results and Discussion

Finite element analysis were performed to evaluate temperature gradients of the uncoated Aluminium alloy piston and ceramic materials such as partially stabilised zirconia with magnesium oxide ($ZrMgO_3$), Mullite and Alumina (Al_2O_3) coated Aluminium alloy piston. The temperature distributions of an uncoated aluminium alloy piston are shown in the figure 4. The maximum surface temperature on the piston crown of the Aluminium alloy piston is determined as 295.86^{0}C.The temperature distributions of the ceramic materials such as partially stabilised zirconia with magnesium oxide ($ZrMgO_3$), Mullite and Alumina (Al_2O_3) coated Aluminium alloy piston is shown in the figure 5, figure 6, figure7, respectively.The maximum surface temperature on the piston crown for Ziconia coated Aluminium alloy piston is determined as 377.07^{0}C, For Mullite Coating it is 360.6^{0}C and for Alumina coating it is 357.45^{0}C.

Fig.8 represents the temperature distribution comparison curve of uncoated Aluminium alloy piston with zirconia, Mullite and Alumina coated piston. It is clear that the maximum surface temperature of Zirconia coated piston (377.07^{0}C) is more than the conventional Aluminium alloy piston (295.86^{0}C).and the maximum surface temperature of Mullite coated piston (360.6^{0}C) is more than the conventional Aluminium alloy piston (295.86^{0}C) and the maximum surface temperature of Alumina coated piston (377.07^{0}C) is more than the conventional Aluminium alloy piston (295.86^{0}C).From the graphical representation the ceramic material partially stabilized Zirconia gives more performance to the diesel engine taken for this study.

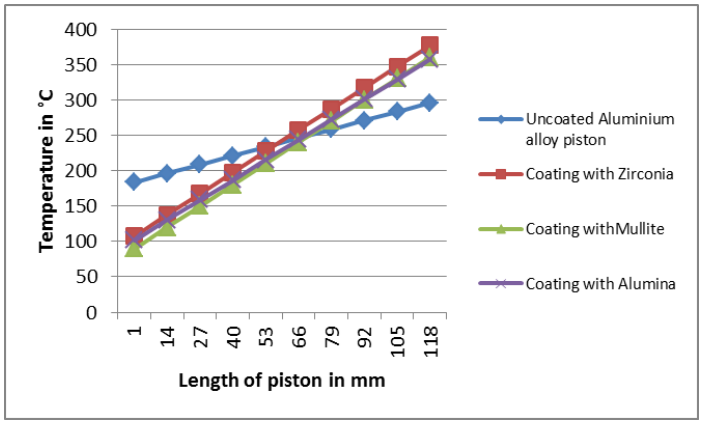

Fig. 8.Comparisons of coated Aluminium alloy piston with uncoated Aluminium alloy piston

VII. Conclusion

A comparative evaluation was made between the temperature distributions of the uncoated aluminium alloy piston and the ceramic coated piston. The maximum surface temperature of the ceramic coated piston is improved approximately 28% for Zirconia stabilised with magnesium oxide ($ZrMgO_3$) coating, 22% for Mullite coating ($3Al_2O_3$-$2SiO_2$) and 21% for Alumina (Al_2O_3) than the uncoated piston by means of ceramic coating. According to the software simulations conducted in this project, it has been concluded that the using of ceramic coating for Aluminium alloy piston increases the temperature of the combustion chamber of the engine and the thermal strength of the base metal.Finally the combustion chamber temperature increases the thermal efficiency of the engine also increases.

References

[1]. EkremBuyukkaya, (2008) Thermal analysis of functionally graded coating AlSi alloy and steel pistons.
[2]. EkremBuyukkaya, MuhammetCerit, (2008) Thermal analysis of a ceramic coating diesel engine piston using 3-D finite element method.
[3]. Imdat Taymaz, (2006) the effect of thermal barrier coatings on diesel engine performance.
[4]. P.M. Pierz, (1993) Thermal barrier coating development for diesel engine aluminium pistons.
[5]. O. ALTUN, Investicated in Problems for determining the thermal conductivity of TBCs by laser-flash method
[6]. S. C. MISHRA., investigated in Microstructure, Adhesion, and Erosion Wear of Plasma Sprayed Alumina–Titanium Composite Coatings
[7]. H.W. GRUNLING and W. MANNSMANN, ABB Kraftwerrke AG, KallstadterStz 1, 6800 Mannheim 31, Germany., Investigated in Plasma sprayed thermal barrier coatings for industrial gas turbines: morphology, processing and properties
[8]. A. J. SLIFKA, National Institute of Standards and Technology, Boulder. Thermal-Conductivity Apparatus for Steady-State, Comparative Measurement of Ceramic Coatings
[9]. DONGMING ZHU Ohio Aerospace Institute, Cleveland, Ohio. Effect of Layer-Graded Bond Coats on Edge Stress Concentration and Oxidation Behavior of Thermal Barrier Coatings.
[10]. S. Alphine', M. Derrien*, A review of Thermal Barrier Coatings for turbine.

Authors Bibliography:

K. Sridhar-received his B.E., Degree in Mechanical Engineering from Anna University, Chennai. He received M.E. Degree from ANNA University, Coimbatore. Currently working as a teaching faculty in the School of Mechanical and Industrial Engineering, Institute of Technology, Bahir Dar, University, Bahir Dar, Ethiopia.

R.Rejikumar received his B.E., Degree in Mechanical Engineering from Anna University, Chennai. He received M.E. Degree from ANNA University, Thiruchirapalli. Currently working as a teaching faculty in the School of Mechanical and Industrial Engineering, Institute of Technology, Bahir Dar, University, Bahir Dar, Ethiopia

Mr. M. Narasimha received his B.Tech. Degree in Mechanical Engineering from JNTU, Hyderabad, India. He received M.E. Degree from VMU, TAMILNADU; currently working as a teaching Faculty in the School of Mechanical and Industrial Engineering, Institute of Technology, Bahir Dar University, Bahir Dar, Ethiopia.

International Journal of Modern Engineering Research (IJMER)
www.ijmer.com Vol.3, Issue.3, May-June. 2013 pp-1442-1446 ISSN: 2249-6645

Need For Strengthening Automobile Industry in Ethiopia

M. Narasimha, [1] R. Rejikumar, [2] K. Sridhar[3]
[123]*Lecturer, School of Mechanical and Industrial Engineering, Bahir Dar University, Bahir Dar, Ethiopia,*

Abstract: *The main purpose of this paper is to analyze automotive industry and its trend in strengthening the industry in Ethiopia. In recent years, the condition of the automotive sector is increasing and it is playing a vital role in the national economy. Although the automotive sector is playing significant role, it is still at low level and many factors contributed for that, including*

- Government regulations
- Road conditions
- Purchasing power of people
- Lack of skilled manpower and capacity
- Shortage of capital

To address those issues, the research conducted for both primary and secondary data. The collected data were analyzed and the result of the analysis was summarized into positive and negative aspects. It was revealed that the positive aspects, contribution to the national economy, future growth prospects, employment opportunity and profitability of the operation. Outweigh the negative aspects. As the research had scope and limitations, it was recommended to the government authorities to undertake further studies to make an informed decision on how to strengthen automobile industry for the growth and development in Ethiopia.

Key Words**:** *Automobile Industry, Automobile vehicles, Spare parts & Government Policies.*

I. Introduction

Ethiopia, being one of the African countries, requires continuous improvement in agriculture, manufacturing and automobile sectors. In accomplishing the development on these sectors, the role of infrastructure is vital. The developments of the infrastructure in turn highly depend on the availability of various types of vehicles (cars, pickups, trucks etc...) construction machineries and agricultural equipment's. In addition, Ethiopia is one of the land – locked countries in Africa. It uses mainly Djibouti port, which is located about 1000 KM. from Addis Ababa for import and export of goods. The transportation of goods from Djibouti port to parts of Ethiopia and from various parts of the country to port is done using trucks.

Since Ethiopia doesn't manufacture automotive, construction machinery and agricultural equipment's locally at present, it imports those from various countries of the world. Automotive importing companies are importing vehicles to the market. The marketing trends of automotive is necessary to clearly see the demand supply gap and for the growth. This paper mainly prepared to reveal the truck market trend in Ethiopia and to indicate ways of increasing the contribution of the automotive sector to the economy. The over view of investment opportunity in relation to the automotive industry.

It is observed that the present status of automobile industry in Ethiopia, the potential of the industry and the demand of automobile vehicles including their spare parts. In Ethiopia many imported vehicles from different parts of the world are in daily use. Maximum numbers of vehicles are of Toyota. Also the spare parts are imported spending lot of money and time. The main source of transport is for all the classes of people are taxis and busses in the country. There are some private taxies playing in almost all the cities like vans, three wheelers Bajaj and TVS from India which is the cheapest mode of transport for the poor people.

Buses, mini buses are operated linking inter states or regions by fleet of transport agencies to transport the public. Also many trucks and Lorries are being used to transport the goods of different categories. There is no train facility in the country and no railway links to connect the cities of the country. People are using flight connections of airlines to travel long distance in order to meet emergency needs. Ethiopia land consist of high lands most of the part hills and uneven surface. The Ethiopian Highlands cover most of the country.

Buses, trucks with trolleys and minibuses including earth moving equipment, Luxury cars and light duty vehicles all are imported as used vehicles from other countries. Now trend is picking up to run motor bikes on the roads of all most all cities by some citizens. All these motor bikes are getting imported from India (TVS& Bajaj) & China (Lifan). The export and import agencies, Djibouti port authorities and Government duty all are added to the value of the products and the traders demand more profits from all this products, all these are taxed to the customers and the customers have to pay more money for the product.

1.1. Ethiopian Industrial Policy

The Government's broad economic and industry specific policies are designed to increase the growth potential and international competitiveness. [1]In addition, Ethiopia's extensive minerals and energy resources ensure that Ethiopia has relatively low utility charges for industrial users. Ethiopia's levels of educational attainment are a source of competitive

advantage and underpin the skills base of the workforce. [2]The Ethiopian Government is undertaking initiatives across the education spectrum to produce employees who will better meet the changing needs of future employers.[3] Ethiopia's welcoming attitude to foreign investment, today, *Invest Ethiopia*, the Government's inward investment agency, provides foreign firms with information in regard to potential investment opportunities in Ethiopia.[5],[6] *Invest Ethiopia* can provide information on location, joint venture partners, establishment costs and skills and taxation information. .

All of the motor vehicles operating in the country are imported. [2]As a result, the following statistics of import of motor vehicles will provide a clear picture of the growth of the automotive.

1.2. Import And Export In Ethiopia

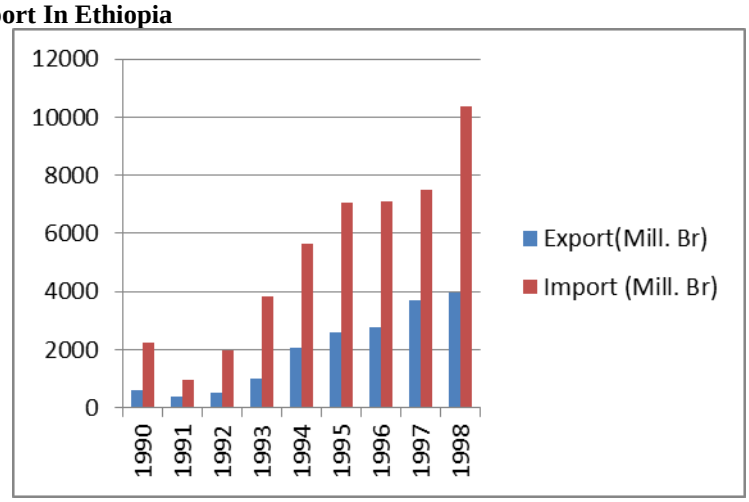

Fig.1. Import and export in Ethiopia

1.3. Factors Affecting The Automotive Market

- Fluctuating demand (seasonality of the demand)
- Tough terrain (road condition)
- Lack of capacity in repair and maintenance
- Lack of foreign currency for importation
- Lack of adequate bank finance

There are good numbers of industries in operation throughout the country in various sectors and are in different fields. Mostly the sugar and cement industry is doing well in the country. Agricultural industry, textile industry and spare parts manufacturing units including floricultural industry are some of the additional activities.

1.4. Auto Spare Parts Production

The spare parts manufacturing company Akaki industry is well established company in the country apart from the other industries like Mesfin Industrial Engineering, Maru metal and automotive company, are operating for manufacturing the trolleys and for tankers production.[7][BISHOFTU automotive industry, FDRE metals & Engineering Corporation, Metals and Engineering Corporation Adama, Agricultural Machinery Industry, Bus body units and auto garages/works shops are in operation for the full capacities. There are some steel manufacturing units producing nails and zinc sheet manufacturing. As mentioned earlier the spare parts and vehicle manufacturing industry is not in operation. [8]Main focus of the above mentioned industries is assembling, upgrading and localizing city and cross country buses, mid and mini-buses, construction, military and agricultural vehicles. So emphasis is to be made to establish this industry in the country to have their own products.

1.5. Value Of Import Of Motor Vehicles

Table.1. Import motor vehicles

Period	Motor vehicles (in thousand	Increase from previous year	Increase during five years
1979 -	135789	-	
1980 -	165328	22%	
1981 -	259372	57%	
1982 -	164765	-36%	
1983 -	210621	28%	
1984 -	179589	-15%	32%

1985 -	287134	60%	
1986 -	339324	18%	
1987 -	369944	9%	
1988 -	379220	-25%	
1989 –	189288	-32%	5%
1990 –	249844	32%	
1991 –	177203	-29%	
1992 –	402403	127%	
1993 –	825890	105%	
1994 –	1015951	23%	43%
1995 –	1393422	37%	
1996 –	1117480	-20%	
1997 –	795978	-29%	
1998 –	1390946	75%	
1999 –	1548459	11%	52%
2000 -	1456285	-6%	
2001 –	1437245	-1%	
2002 –	1817630	26%	
2003 -	2124501	17%	37%

The growth of the automotive sector can also be analyzed from the employment creation perspective. As the following table indicates, the employment creation of the sector has been gradually increasing though with fluctuation for some years. [9]As it's discussed above, the manufacture of motor vehicles in Ethiopia is limited to assembly, manufacture of bodies of vehicles and small scale manufacture of parts and accessories.

1.6. Number Of Employees

Table.2. Employees list

INDUSTRIAL GROUP	NUMBER OF EMPLOYEES				
	2000/01	2001/02	2002/03	2003/04	2004/05
Manufacture of motor vehicles	1,060	1,082	1,019	1,130	1,232
Manufacture of bodies for motor vehicles	987	1,009	946	1,029	1,148
Manufacture of parts and accessories for	73	73	73	101	84

The above table indicates that the number of employees engaged in the manufacture of motor vehicles bodies and accessories increased from 1,060 in year 2000/ 2001 to 1,232 in year 2004/05. [2]This overall increase in number of employees engaged in the sector by more than 16% implies the growing trend in the manufacturing section of the automotive industry

II. An Over View Of Asian Countries Automobile Industry

2.1. Export Market of China from 1990 to 2000

Table.3. Export Market of China

Year	Total (in unit)	Trucks (in unit)	Passenger cars (in unit)	Auto parts (ten thousands of US$)	Total auto products (ten thousands of US$)
1990	4 431	3 254	73	8 170	12 784
1991	4 108	2 253	789	10 138	15 284
1992	6 375	2 243	914	12 395	30 615
1993	11 116	4 534	2 866	17 165	42 422
1994	18 648	10 234	784	24 580	51 520
1995	17 747	9 070	1 413	37 609	72 138
1996	15 112	6 525	635	38 208	81 650
1997	14 868	8 297	1 073	44 718	98 784
1998	13 627	8 176	653	48 960	88 343
1999	22 717	3 868	326	70 599	118 727
2000	39 327	7 093	523	152 400	247 900

2.2. Automobile Industry in India

In India, as in many other countries, the auto industry is one of the largest industries. It is one of the key sectors of the economy. [10]The industry comprises of automobile and the auto component sectors and encompasses commercial vehicles, multi utility vehicles, passenger cars, two-wheelers, three-wheelers, tractors and related auto components. [11], [12]There are at present 13 manufacturers of passenger cars and multi utility vehicles, 7 manufacturers of commercial vehicles, 11 of 2- or 3-wheelers and 10 of tractors besides 4 manufacturers of engines.

2.2.1. Indian car exports, 1996-2001 (number)

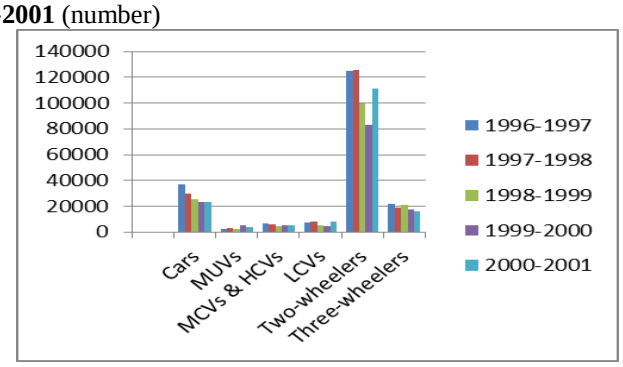

Fig.2. Car exports in India

2.2.2. Main export destinations

Table 4. Main export destinations

Cars	Egypt, Kenya, Nigeria, Somalia, Tanzania, Afghanistan, Nepal, Turkey, Hungary, Greece, Italy, Netherlands, Spain, Austria, Malta
CVs	Egypt, African countries, Nepal, Sri Lanka, Jordan, Kuwait, Hungary, Russian Federation, France, Brazil
Two-wheelers	African countries; Bangladesh; Sri Lanka; Turkey; United Arab Emirates; Paraguay; United Kingdom; Germany; Argentina; Mexico; Australia; Hong Kong, China

2.2.3. Projected export turnover (millions of USD)

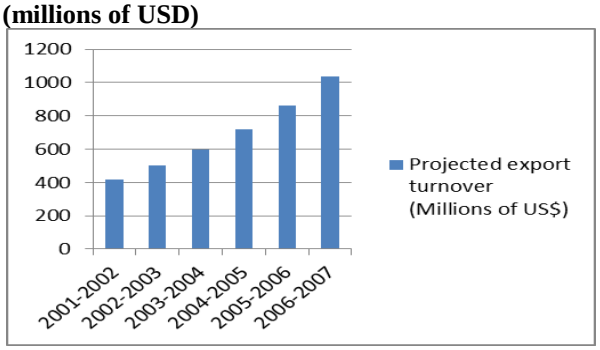

Fig.3. Projects export turnover

2.2.4. Export market size (in USD bln)

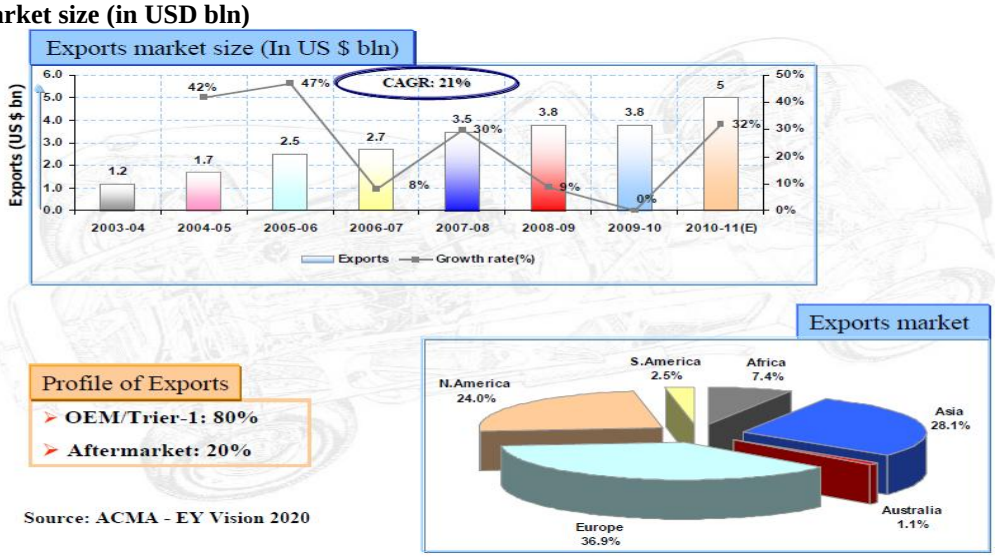

Fig. 4. Export market

III. Conclusion

The development level of automobile industry in the country is low in comparison to other developing countries. ETHIOPIA, being a trucking country, the potential is high but not being exploited properly. There are various factors which contribute for hindrance of the sectors development. The main points are Government regulation, tax inconsistent, production output, shortage of road access, lack of foreign currency and finance for the purchase of trucks.

The contribution of the automobile industry for the economy and employment creation is big compared with the investment outlay to the industry. Therefore attention to be paid in strengthening the Automobile industry is must. Upgrading the capacity in maintenance and servicing of auto motives is important.

Major decision to improve and enhance the operation of the automotive industry lies in the hands of Transport authority, which is believed to be staffed with under qualified personnel. Strengthening automotive industry is one of the ways to increase the growth of the national economy.

References

[1]. Business review of Ethiopian herald
[2]. Capital weekly magazine of Ethiopia
[3]. Central statistical agency, Report on Large and medium scale manufacturing and Electricity Industries Survey
[4]. Fortuna. Weekly magazine of Ethiopia
[5]. Commerce & industry Bureau master plan of Amhara region
[6]. Mnst & Young. (2004). Due Diligence Report on Bekelcha Transport Enterprise
[7]. BISHOFTU automotive industry business brochure
[8]. Strategy Report, Shebelle Transport Enterprise, Ernst &Young
[9]. National Bank of Ethiopia, Quarterly Bulletin, Fiscal Year Series, Volume 20.No.4, Fourth Quarter, 2004/2005
[10]. Asian countries automobile industry conferences, journals and broachers.
[11]. Indian auto component Industry over view
[12]. ACMA – EY Vision 2020

Authors Bibliography:

M. Narasimha- received his B.Tech. Degree in Mechanical Engineering from JNTU, HYDERABAD. He received M.E. Degree from VMU, TAMILNADU. Currently working as teaching faculty in the School of Mechanical and Industrial Engineering, Institute of Technology, Bahir Dar University, Bahir Dar, Ethiopia.

R. Rejikumar- received his B.E., Degree in Mechanical Engineering from Anna University, Chennai. He received M.E. Degree from ANNA University, Thiruchirapalli. Currently working as Teaching Faculty in the School of Mechanical and Industrial Engineering, Institute of Technology, Bahir Dar, University, Bahir Dar, Ethiopia

K.Sridhar- received his B.E., Degree in Mechanical Engineering from Anna University, Chennai. He received M.E. Degree from ANNA University, Coimbatore. Currently working as Teaching Faculty in the School of Mechanical and Industrial Engineering, Institute of Technology, Bahir Dar, University, Bahir Dar, Ethiopia

International Journal of Modern Engineering Research (IJMER)
www.ijmer.com Vol.3, Issue.3, May-June. 2013 pp-1447-1453 ISSN: 2249-6645

FPGA implementation of high speed PI like Fuzzy control system for industrial automation applications

G. Kamalesh,[1] T. Thammi Redddy[2]
[1]*ECE Department, GPR College of Engineering, Kurnool, India*
[2]*ECE Department, Associate Professor of GPR College of Engineering, Kurnool, India*

***Abstract*:** *The modern digital control systems demand faster and robust calculation components for robotic and industrial automation applications. This type of elements are becoming more essential with the utilization of some new control algorithms, like the fuzzy control, the adaptive control, the sliding mode control, etc. The PID controllers are most widely used controllers in the industrial control systems. Fuzzy logic control presents a computationally efficient and robust alternative to conventional controllers for many systems. Although the traditional control methods which use mathematical models of systems to design an adequate controller, the fuzzy logic controllers use fuzzy deductions or inferences for the synthesis of controllers are powerful and robust.*

Digital controllers are implemented two styles; hardware based and software based. The software based implementation can be carried out on PC or any DSP processor. Such implementations will be inherently slower due to serial nature of the processor's execution style. The FPGA platform carrying advantages of both ASIC and processor is more suitable option. On FPGA one can easily achieve higher speeds occupying only less area. In this project PI like fuzzy logic controller (PIFLC) will be implemented in VHDL for FPGA platform. This is a general purpose controller that can be used for different applications. This controller has three stages: the fuzzification, the inference and the defuzzification. The first component in the PIFLC is the fuzzifier that transforms crisp inputs into a set of membership values in the interval [0, 1] in the corresponding fuzzy sets. The knowledge base of the fuzzy controller consists of a database of linguistics statements (rules), which states the relationship between the input domain fuzzy sets and output domain fuzzy sets. Inference block implements this logic. The last step is the defuzzification and the final output is determined by weighted average of all contributions of the output sets.

Keyword: *PI Like Fuzzy Control System, Industrial Application, FPGA, Fuzzy logic.*

I. Introduction

Fuzzy Logic is a problem-solving control system methodology that lends itself to implementation in systems ranging from simple, small, embedded micro-controllers to large, networked, multi-channel PC or workstation-based data acquisition and control systems. It can be implemented in hardware, software, or a combination of both. Fuzzy Logic provides a simple way to arrive at a definite conclusion based upon ambiguous, imprecise, noisy, or missing input information. Fuzzy Logic's approach to control problems mimics how a person would make decisions, only much faster. Fuzzy Logic incorporates a simple, rule-based IF X AND Y THEN Z approach to a solving control problem rather than attempting to model a system mathematically. The Fuzzy Logic model is empirically-based, relying on an operator's experience rather than their technical understanding of the system. For example consider what you do in the shower if the temperature is too cold: you will make the water comfortable very quickly with little trouble. Fuzzy Logic is capable of mimicking this type of behavior but at very high rate. Fuzzy Logic requires some numerical parameters in order to operate such as what is considered significant error and significant rate-of-change-of-error, but exact values of these numbers are usually not critical unless very responsive performance is required in which case empirical tuning would determine them. For example, a simple temperature control system could use a single temperature feedback sensor whose data is subtracted from the command signal to compute "error" and then time-differentiated to yield the error slope or rate-of-change-of-error, hereafter called "error-dot". Error might have units of degs F and a small error considered to be 2F while a large error is 5F. The "error-dot" might then have units of degs/min with a small error-dot being 5F/min and a large one being 15F/min. These values don't have to be symmetrical and can be "tweaked" once the system is operating in order to optimize performance. Generally, Fuzzy Logic is so forgiving that the system will probably work the first time without any tweaking.

Fuzzy Logic Used:

- Define the control objectives and criteria: What am I trying to control? What do I have to do to control the system? What kind of response do I need? What are the possible (probable) system failure modes?
- Determine the input and output relationships and choose a minimum number of variables for input to the Fuzzy Logic engine (typically error and rate-of-change-of-error).
- Using the rule-based structure of Fuzzy Logic, break the control problem down into a series of IF X AND Y THEN Z rules that define the desired system output response for given system input conditions. The number and complexity of rules depends on the number of input parameters that are to be processed and the number fuzzy variables associated with each parameter. If possible, use at least one variable and its time derivative. Although it is possible to use a single, instantaneous error parameter without knowing its rate of change, this cripples the system's ability to minimize overshoot for a step inputs.

- Create Fuzzy Logic membership functions that define the meaning (values) of Input/Output terms used in the rules.
- Create the necessary pre- and post-processing Fuzzy Logic routines if implementing in S/W, otherwise program the rules into the Fuzzy Logic H/W engine.
- Test the system, evaluate the results, tune the rules and membership functions, and retest until satisfactory results are obtained.

II. Block Diagram Of Pi-Like Fuzzy Controller Modification

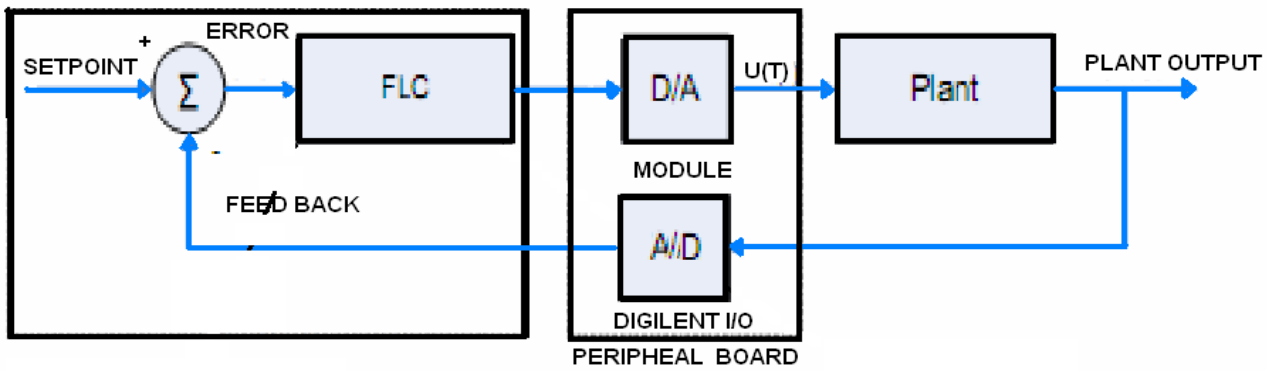

Fig .1Layout of the proposed controller in a unity feedback control system

Pi-Like Fuzzy Controller Modification is the general layout of the controller chip in a unity feedback control system is shown in Fig.1

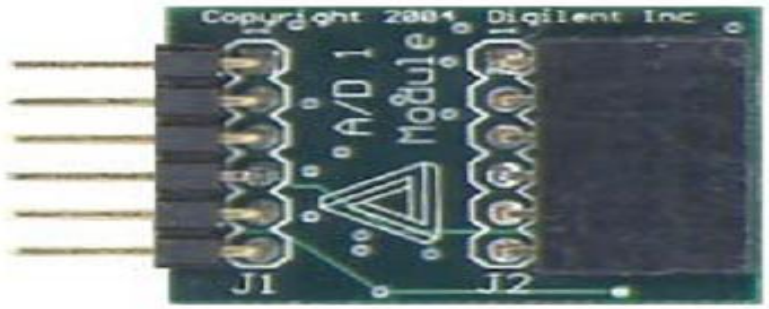

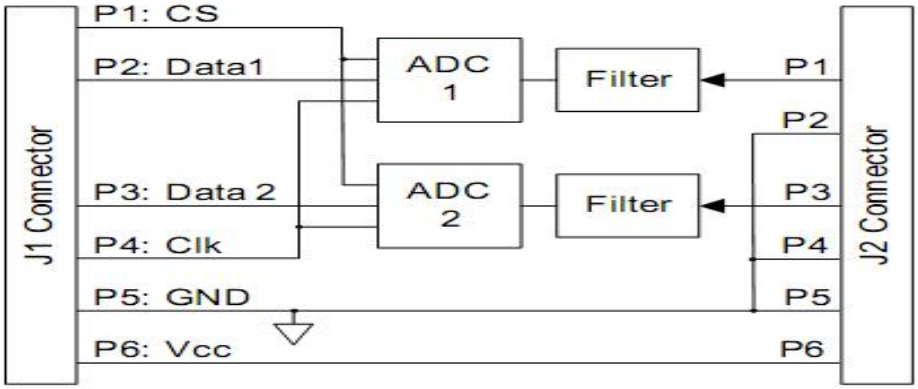

2.1analog Input Interface (Adc):

FPGAs are well suited for serial Analog to Digital (A/D) converters. This is mainly because serial interface consumes less communication lines while the FPGA is fast enough to accommodate the high speed serial data. The ADCS7476MSPS is a high speed, low power, 12-bit A/D converter. Consumes 80 ns time for one cycle. A/D converter is a high speed serial interface that interfaces easily to FPGAs. The A/D interface adapter (AD1_PMOD) is implemented within the FPGA. (Fig.2). Inside the FPGA, this adapter facilitates parallel data acquisition. Sampling is initiated at the rising edge of a clock applied at the line sample. The timing diagram of the communication protocol obtained with Modelsim is illustrated in Fig. The whole conversion and acquisition period is 1.2 µs allowing sampling up to a rate of 20 MHz Sample per second.

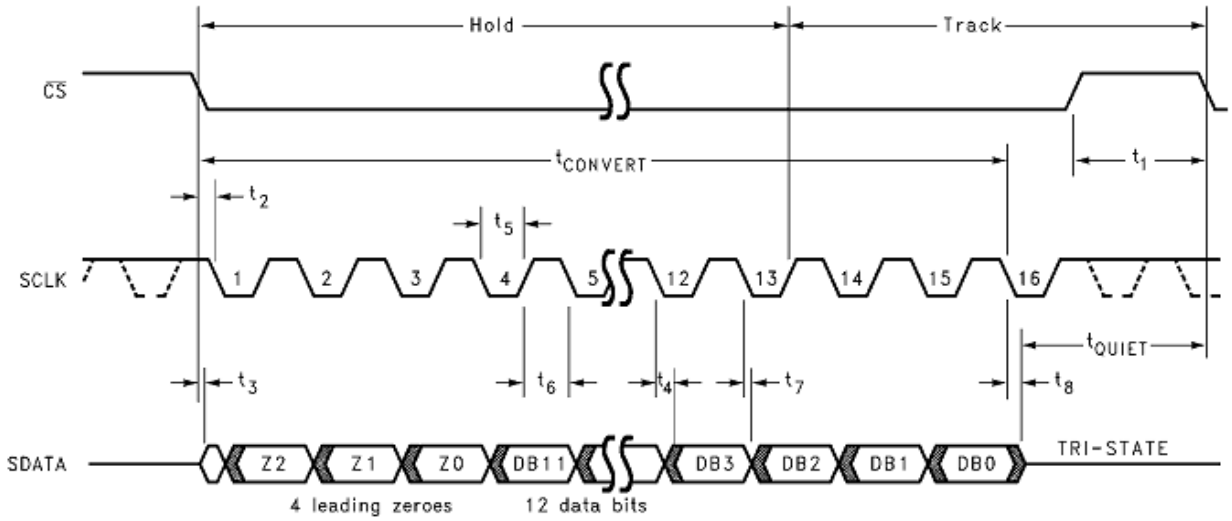

Fig 2. ADCS7476 Serial Interface Timing Diagram Timing diagram

2.2analog Output Interface (Dac):

The DAC121S101 is a dual, 12-bit voltage out Digital to Analog (D/A) converter. This device uses a versatile 6-wire serial interface that operates at a clock up to 20 MHz. The serial input register is 16 bits wide; 12 bits act as data bits for the D/A converter, It is interfaced to an FPGA as illustrated in Fig. 3. The D/A interface adapter (DAC_toplevel), which is implemented within the FPGA, facilitates parallel data input for the dual D/A converters. The timing diagram of the communication protocol is illustrated in Fig. 5. The transmission period of a sample is 80 ns allowing D/A conversion at an excellent rate of 12.5MHz.

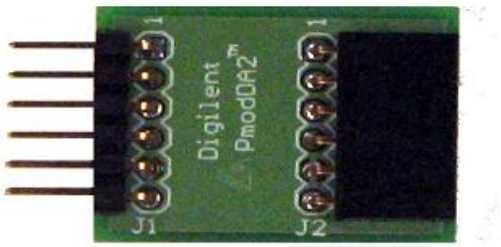

Figure 1
Digilent PmodDA2

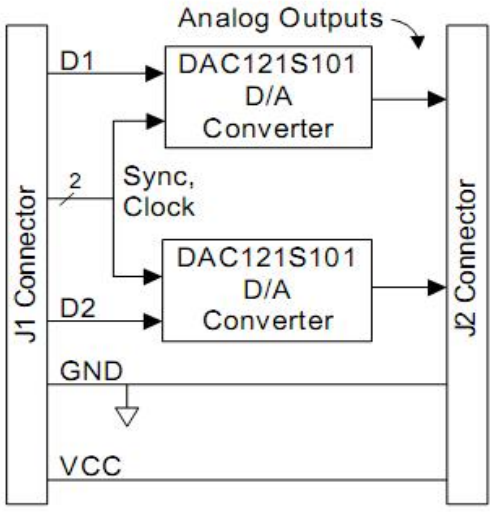

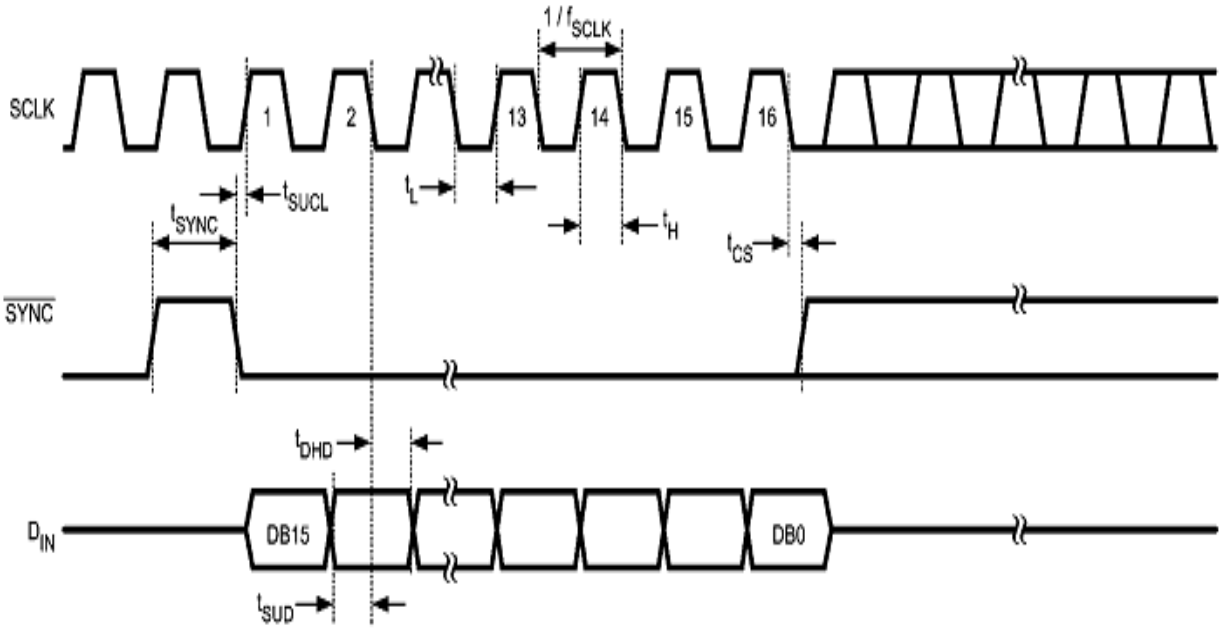

Fig.3. DAC121S101 Timing

2.3fuzzy Controller:

The PI-like Fuzzy Logic Controller (PIFLC) has two inputs the error (e) and its change (Δe) and one output the change of control (Δu). This controller follows in its logic the three stages:

1) fuzzification,
2) inference and
3) defuzzification.

We do remark that scaling factors can be introduced for input variables and the output one denoted respectively ke, kde and kdu (Fig. 4).

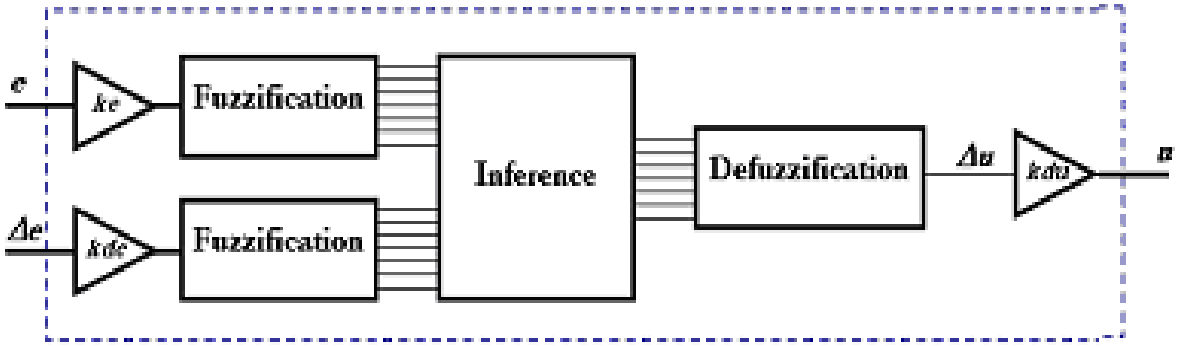

Fig.4.Block diagram of PIFLC

1.3.1fuzzification:

The first component in the PIFLC is the fuzzifier that transforms crisp inputs into a set of membership values in the interval [0, 1] in the corresponding fuzzy sets. The membership function shapes are typically triangular, trapezoidal or exponential. In this, the membership functions are triangular-shaped and the maximum value is scaled to 40 instead of 1 which is found in other documents describing fuzzy theory. This way the calculation complexity is greatly reduced because the multiplying operation becomes only one addition or subtraction. With a setpoint and a measure coded on 8 bits, the intervals of the fuzzy sets are selected in order to cover all the range between -127 and 127. Fig. 7 shows triangular membership functions for error (e) and its change (Δe) with fuzzy labels NB (negative big), NM (negative medium), NS (negative small), ZO (zero), PS (positive small), PM (positive medium) and PB (positive big). For the output, the membership functions are given in Fig. 8 and correspond to singletons in order to simplify the defuzzification process.

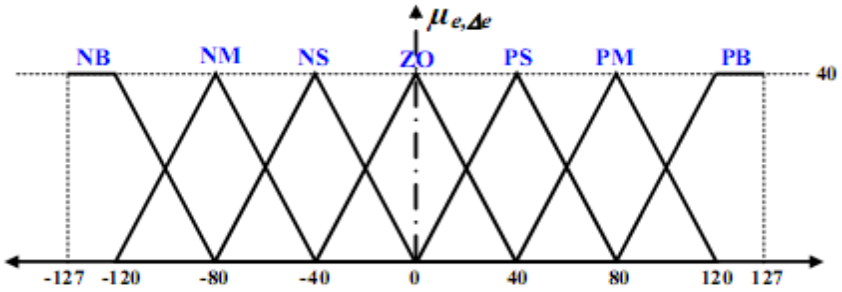

Fig.5. Triangular membership functions of inputs

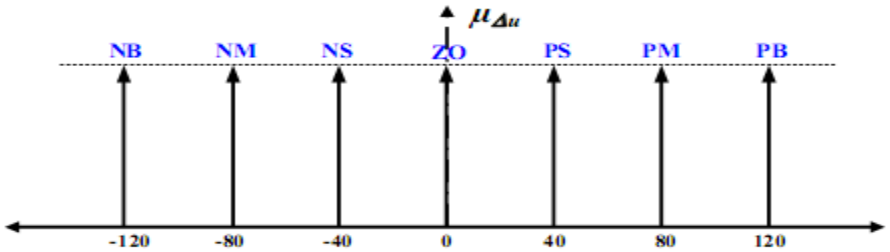

Fig. 6. Singleton membership functions of output

The representation of this is
-127 to -120 is represented as (NB) i.e 000
-120 to -80 is represented as (NM) i.e 001
-80 to -40 is represented as (NS) i.e 010
-40 to 40 is represented as ZERO i.e 011
40 to 80 is represented as (PS) i.e 101
80 to 120 is represented as (PM) i.e 110
120 to 127 is represented as (PB) i.e 111

2.3.2 Inference:

The knowledge base of the fuzzy controller consists of a database of linguistics statements (rules), which states the relationship between the input domain fuzzy sets and output domain fuzzy sets. For a system with two inputs, the error (e) and change of error (Δe), and single output, each having seven fizzy sets, the rules can be represented in tabular form as shown in Table I. A maximum of 4 rules can be active at any time with triangular membership functions. The min-max inference method uses the min operator to find the minimum membership degree between the two inputs resulting from rule conditions and the rules are finally combined by using the OR operator and interpreted as the max operation for each possible value of the output variable.

Δe \ e	NB	NM	NS	Z	PS	PM	PB
NB	NB	NB	NB	NB	NM	NS	ZO
NM	NB	NB	NB	NM	NS	ZO	PS
NS	NB	NB	NM	NS	ZO	PS	PM
Z	NB	NM	NS	ZO	PS	PM	PB
PS	NM	NS	ZO	PS	PM	PB	PB
PM	NS	ZO	PS	PM	PB	PB	PB
PB	ZO	PS	PM	PB	PB	PB	PB

Table I. Mac Vicar-Whelan Rules Base

2.3.3 Defuzzification:

The last step is the defuzzification and the final output is determined by weighted average of all contributions of the output sets. It is obtained by finding the centroid point of the function which is the result of the multiplication of the output membership function and the Inference output vector Y. The general mathematical formula which is used to obtain the centroid point is:

$$\Delta u = \frac{\sum_{i=1}^{5} Y[i] \times S[i]}{\sum_{i=1}^{5} Y[i]}$$

Y (i) are the i-th members of the output vector, S (i) are the multiplying coefficients of the output membership function.

III. FPGA Implementation Of High Speed PI Like Fuzzy Control System Final Outputs

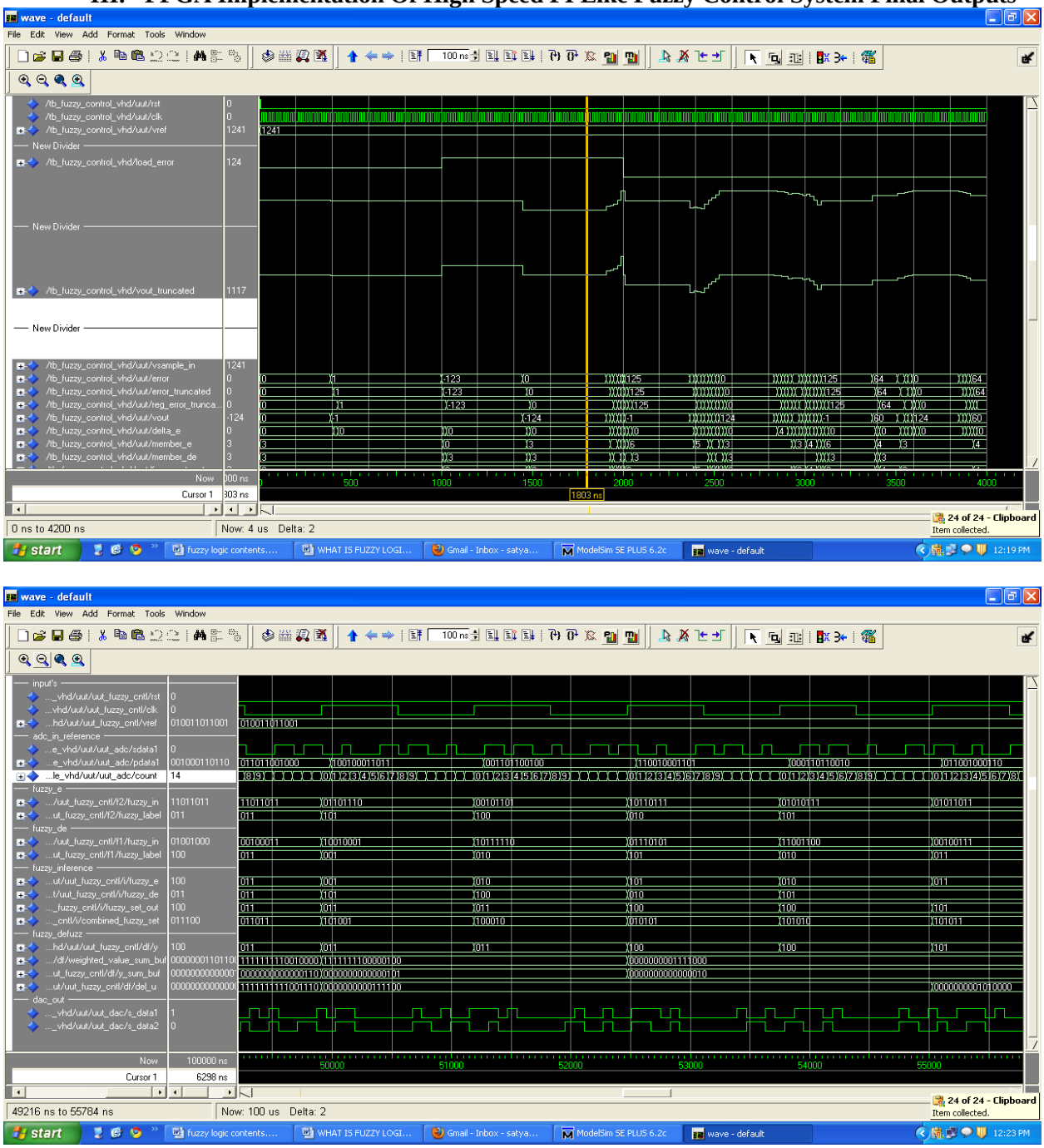

Fig.7. PI like Fuzzy control system Final output simulation wave forms

IV. Applications

Fuzzy logic is an innovative technology that enhances conventional system design with engineering expertise. The use of fuzzy logic can help to circumvent the need for rigorous mathematical modeling. Fuzzy logic is a true extension of conventional logic, and fuzzy logic controllers are a true extension of linear control models. Hence anything that was built using conventional design techniques can be built with fuzzy logic, and vice-versa. However, in a number of cases, conventional design methods would have been overly complex and, in many cases, might prove simpler, faster and more efficient. The key to successful use of fuzzy logic is clever combination with conventional techniques. Also, a fuzzy system is time-invariant and deterministic. Therefore any verification and stability analysis method can be used with fuzzy logic, too.

- Pattern recognition and classification
- Fuzzy clustering
- Image and speech processing
- Fuzzy systems for prediction
- Fuzzy control
- Monitoring
- Diagnosis
- Optimization and decision making

V. Advantages

One can circumvent the need for rigorous mathematical modeling with the use of fuzzy logic. Unlike the reasoning based on classical logic, fuzzy reasoning aims at the modeling of reasoning schemes based on uncertain or imprecise information. The past several years have witnessed a rapid growth in the number and variety of applications of fuzzy logic. The most visible applications are in the realms of consumer products, intelligent control and industrial systems. Less visible, but of growing importance, are applications relating to data processing, fault diagnosis, man-machine interfaces, quality control and decision support systems. Although fuzzy logic has been and still is controversial to some extent, its successes are now too obvious to be denied.

VI. Tools and Hard Ware

- Simulation software -Modelsim Xilinx Edition (MXE)
- Synthesis, P&R - Xilinx ISE
- On chip verification - Xilinx Chip scope
- Hardware– Xilinx Spartan 3 Family FPGA board

VII. Conclusion

This paper presents an approach for the implementation of a fuzzy logic controller on an FPGA using VHDL. A fuzzy logic controller with 2-inputs and 1-output is simulated and each block's verification is carried out using logic simulator. The FLC is implemented on a Xilinx Spartan-3 FPGA and used to control first order system to demonstrate its validity. The controller with the analog to digital and digital to analog interfaces was found to be fully functional. The FLC can also be used for control purposes in other applications. Also the length of input and output of the FLC can be increased to achieve better results.

References

[1] Hassan M.Y.and Sharif W.F. "Design of FPGA based PID-like Fuzzy Controller for Industrial applications".
[2] Maheshappa H. D., Samuel R. D., Prakashan A., "Digital PID Controller for Speed Control of DC Motors", IETETechnical Review Journal, V6, N3, PP171-176, India 1989.
[3] Masmoudi N., Hachicha M. and Kamoun L., "Hardware Design of Programmable Fuzzy Controller on FPGA".IEEE International Fuzzy Systems Conference Proceedings, Seoul, Korea, 22-25 August, 1999.
[4] Masmoudi N., Samet L., Kharrat M.W., Kamoun L. "Implementation of a PID Controller on FPGA", Forth ICECS'97, IEEE International Conference on Electronics, Circuits and Systems, Volume 2, pp 550-554, Caire Egypte15-18, December 1997.
[5] Montiel O., Maldonado Y., Sepulveda R. and Castillo O., "Simple Tuned Fuzzy Controller Embedded into an FPGA". Fuzzy Information Processing Society, NAFIPS. Annual Meeting of the North American, New York, USA, Mai 19-22, 2008.
[6] Singh S. and Rattan K. S., "Implementation of a Fuzzy Logic Controller on an FPGA using VHDL". Fuzzy Information Processing Society. 22nd International Conference of the North American NAFIPS, Chicago, Illinois, USA, Jully 24-26, 2003.
[7] Tang J., "PID Controller using the TMS320C31 DSK with On-line Parameter Adjustment for Real-Time DC Motor Speed and Position Control", IEEE International Symposium on Industrial Electronics, V2, PP 86-791, Pusan 2001.

International Journal of Modern Engineering Research (IJMER)
www.ijmer.com Vol. 3, Issue. 3, May.-June. 2013 pp-1454-1457 ISSN: 2249-6645

Morphological characterization of Brazilian organ clays using AFM and SEM studies

A. Tejedor De León[1], G. Navarro[2], J. Rubio[2]

[1]*Depto de Materiales y Metalurgia, Centro Regional de Veraguas – Universidad Tecnológica de Panamá*
[2] *Laboratorio de Processamento Mineral – Depto. de Metalurgia – Universidade Federal do Rio Grande do Sul - Brasil*
[3] *Laboratorio de Tecnologia Mineral e Ambiental – Escola de Engeharia – Universidade Federal do Rio Grande do Sul - Brasil*

ABSTRACT: *A combination of SEM (Scanning Electron Microscopy) and AFM (Atomic Force Microscopy) techniques was used to characterise the morphology of Brazilian montmorillonites before and after intercalation of some organic compounds. AFM revealed that the layers are staked over above the others. The surface of the particles consisted of layers bounded with smooth flat basal planes and larger edges ending in some cascade-like steps 184 µm wide. Some micro and macro valleys (0.6 µm deep) are distributed throughout the whole area and irregularities on basal planes may be attributed to the crystallographic conditions of the genesis of these Brazilian montmorillonites. The mapping performed over 20 x 40 areas showed adhesion forces of 11 nN magnitude on bare clay mineral in the Na+ form and 40 nN for the calcium form. Forces between 10 and 6 nN were found after organic intercalation. In general, the intercalation caused significant changes in the surface properties of clay mineral. The combination of AFM and SEM studies provided evidence about the poorl crystallinity of the Brazilian montmorillonites.*

Keywords: *Atomic Force Microscopy, organoclays, montmorillonites, Scanning Electron Microscopý Volume 3, Issue 2, Mar. – Apr. 2013.*

I. INTRODUCTION

Although the production of modified montmorillonites by the intercalation of organic compounds has been recognised in many areas [1-4], little is known about the influence on its morphology.
The morphology of clay mineral was studied by electron microscopy [5] [6] and these studies revealed a multiplicity of microsteps on the clay mineral surfaces.

Atomic Force Microscopy [7] has rapidly spread throughout many fields of science [8-10] [5] due to its high versatility. While height images provided quantitative topographic information, deflection images often revealed finer surface details. The AFM can also record the force felt by the cantilever as the probe tip is brought close to - and even into - a surface and then pulled away [10]. This technique can be used to measure long range attractive or repulsive forces between the probe tip and the surface, elucidating local chemical and mechanical properties and even the thickness of adsorbed molecular layers or bond rupture lengths [7].

The aim of this work was to characterise the surface morphology of a Brazilian motmorillonite in the calcium and sodium form and after intercalation of two organic compounds using a combination of SEM and AFM techniques.

II. MATERIALS AND METHODS

2.1 Materials

BRASGEL, an industrial Brazilian montmorillonite in Na^{1+} form Campina Grande – Paraiba, Brazil, BENTOCAL, a montmorillonite saturated with calcium cations. The organoclays used in these studies (FENAN and ETIL) was obtained by the intercalation of two organic compounds, 1.1 ortho phenantroline and Ethylenediamine respectively.

2.2 Atomic force microscopy studies

The morphological structure of different montmorillonites samples and its contact force curve were determined by AFM by the contact mode (Digital Nanoscope IIIa, 3000 system, Si_3N_4 micro cantilever). The force curve obtained for each bentonite sample was utilised to calculate the nominal contact force of the tip on the surface samples, defined by the equations:

$F = k\Delta z$ (1)

$\Delta z = ADP$ (2)

where: F = Contact force in nN; k = spring constant of the micro cantilever, 0.6 Nm^{-1}; Δz = distance from de control point, nm; A = number of divisions of the cantilever deflection; D = potential applied, V/divisions; P = piezo sensitivity constant, 2 nmV^{-1}.

2.3 Scanning electron microscopy studies

SEM studies were performed with a Phillips XL-30 ESEM scanning microscope operating normally with up to 30 kV acceleration voltage field emission gun. The samples were attached to a metal mount by carbon tape. Due to the insulating nature of the materials, the samples were coated with a 20 nm thick layer of gold (Balzer Union SCD 040 Sputter Coater system under argon vacuum.)

III. RESULTS AND DISCUSION

3.1 Topographical analysis

The nanotopography of BRASGEL sample is shown in Figure 1.

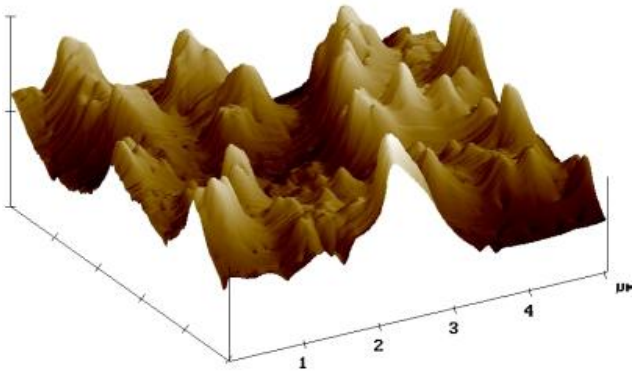

Figure 1: Contac Mode Atomic Force Microscopy (CM-AFM) images of sodium Brazilian montmorillonite (BRAGEL)

The 3D images of the sample, obtained by AFM studies, show different topography at various levels. The surface of BRASGEL shows complex morphological features with irregular and elongated edges, well-defined "hills" and several depressions, suggesting a surface with great roughness; the edges of the flakes, not clearly defined, are ragged and irregular. It also shows a successive "mountain range" with intermittent micro and macrovalleys (~ 0.6 µm deep). This observation may be linked to a poorly crystallisation conditions [5] whereby the Brazilian bentonites were formed [11].

Figure 2 for the Ca-montmorillonite (BENTOCAL) shows the presence of a large jagged and an irregular edge and an isolated volcano (~184 nm height)in the surface.

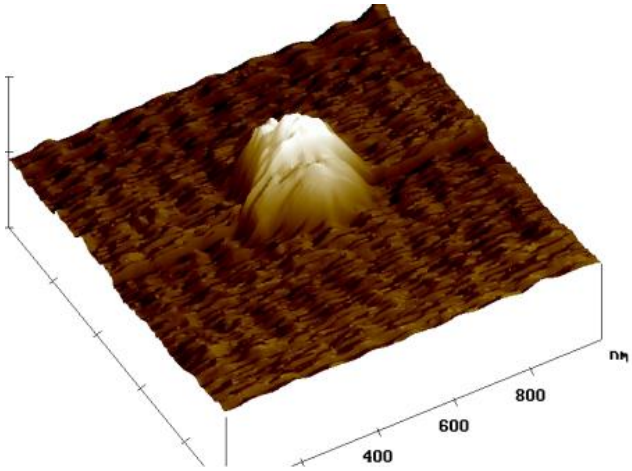

Figure 2: AFM micrographs from the surface of BENTOCAL

In the middle of the figure appears a defect caused by the tip – tip artefacts during image acquisition. Nevertheless microvalleys and grooves are seen (arrow marks). The surface is continuous and appears smooth. Also seen are the cascade.-like step structures, 280-345 nm wide as described by [5] who studied the nanomorphology of well and poorly crystallized kaolinites.

Figure 3 obtained after Phenanthroline intercalation shows an apparently smooth surface unlike the non-treated montmorillonite.

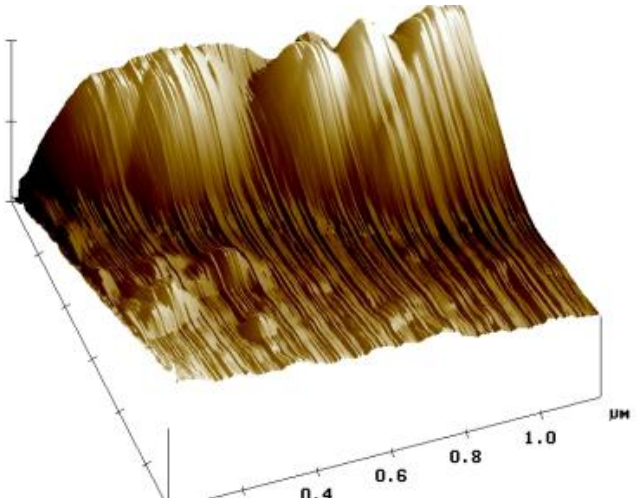

Figure 3: AFM micrographs on well-ordered montmorillonite after phenanthroline intercalation (FENAN)

The overall topography is relatively regular and the basal planes are staked one above the other. The surface topography of the organoclay became smoother and presented a massive cascade-like structure at the layer edges.

Figure 4 shows a typical F-E (force vs. extension) curve obtained on the BRASGEL surface. The the slope of the curve suggests that the tip moved on a hard surface, and a typical large adhesion interaction curve was represented [10].

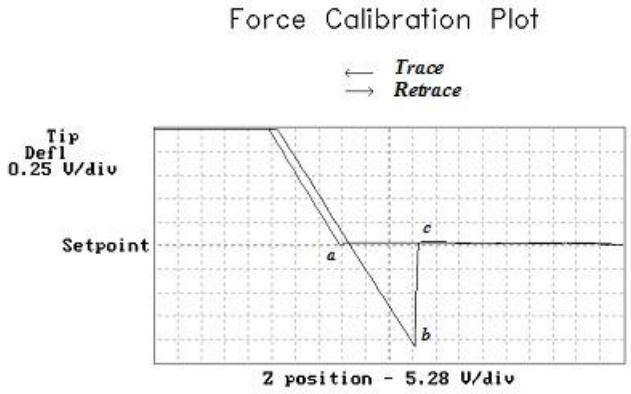

Figure 4: Computing contact force obtainen by AFM to the BRASGEL montmorillonite.

The force curve represents the deflection signal for each complete trace-retrace cycle of the piezo. At point *a*, the cantilever is not deflected but due to attractive forces between the tip and the bentonite surface, the tip sticks to the sample, and the cantilever is pulled down as the piezo continues to retract. Eventually, the spring force of the bent cantilever overcomes the attractive forces, and the cantilever quickly returns to its non-deflected, non-contact position. This is represented by point *c.* At point **b**, the spring force of the cantilever equals the attractive forces between the tip and the surface. The indentation in the surface was extremely "rough" (677.32 nm) and the extension of the sample was in the range of 5 x 5 µm. The contact forces for the other samples were calculated by employing equations 1 and 2 (Table 1).

Table 1: Contact forces onto Brazilian motmorillonites.

Samples	*Resulting conctac force, nN*
BRASGEL	11
BENTOCAL	40
FENAN	10
ETIL	6

The BRASGEL sample presents an attactive contact force of 11 nN, between the sodium motmorillonite surface and the silicon nitride tip. In the case of alcium montmorillonite (BENTOCAL) the force increased to 40 nN. After the intercalation of Orthophenanthroline and Ethylenediamine the significantly reduced.

3.2. Micro structural analysis

The SEM image of BRASGEL bentonite shows a continuous surface, even though it contains small particles and the edges of the lamellar are jagged and irregular (Fig. 5). The presence of a greater number of smaller size particles between the lamellar make the sample less compact and less rigid (Frost et al., 2002). The form presented by the Brazilian bentonites, is a typical "terraces landform" [11]

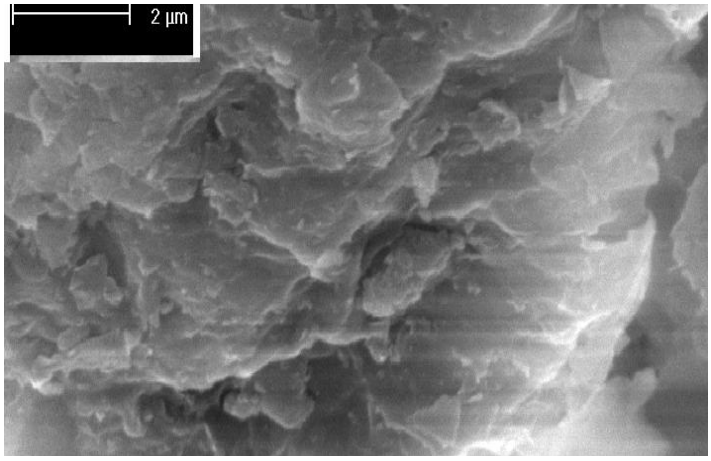

Figure 5: SEM micrographs of the motmorillonite (sodium form) - BRASGEL

IV. CONCLUSIONS

The results of these studies reveal that AFM and SEM are important complementary tools while investigating clay mineral surfaces.

Intercalation of EP and OP molecules caused a significant change in the surface properties of the Brazilian montmorillonite.

The correlation between the AFM and SEM studies provided information about the poor crystalline of the Brazilian bentonite particles which, despite the poor crystallinity, the bentonites were very easy to grafted with OP.

The resulting OP organoclays shown more stability in terms of the resulting contact force performed in the sequence works: intercalation, copper ions adsorption and desorption experiments than the bentonites grafted with ET.

ACKNOWLEDGEMENTS

The authors are grateful to UTP (Panama), UFRGS (Brazil) and to the University of Nevada, Reno, Nevada, (USA) for technical support. Bentonit União Nordeste S.A. is also thanked for the supply of the bentonite clay samples.

REFERENCES

[1] De León, A.T.; Nunes, D.G. and Rubio, J. Adsorption of Cu ions onto a 1.10 phenanthroline-grafted Brazilian bentonite. *Clays and Clay Minerlas*. 1, 2003, 58 -64.
[2] Krishna, B.S.; Murty, D.S.R.; Jai Prakash, B.S. Surfactant-modified clay as adsorbent for chromate. Applied *Clay Science*. 20, 2001, 65-71.
[3] Mortland, M.M.; Berkheiser, V. Triethylene diamine-clay complexes as matrices for adsorption and catalytic reactions. *Clays and Clay Minerals*. 24, 1976, 60-63.
[4] Cox, M.; Rus-Romero, J.R.; Sheriff, T.S. The application of montmorillonite clays impregnated with organic extractants for the removal of metals from aqueous solution Part I. The preparation of clays impregnated with di-(2-ethylhexyl) phosphoric acid and their use for the removal of copper (II). *Chemical Engineering Journal*. 84, 2001. 107-113.
[5] Zbik, M.; Smart, R.St.C. Nanomorphology of kaolinites: comparative SEM and AFM studies. *Clays and Clay Minerals*. 46, 1998, 153-160.
[6] Thompson, D.W.; Macmillan, J.J.; Wyatt, D.A. Electron microscope studies of the surface microstructures of layer-lattice silicates. *Journal of Colloid and Interface Science*. 82, 1981, 362-372.
[7] Binnig, G.; Quate, C.F.; Gerber, Ch. Atomic force microscope. *Physical Review Letters*. 56, 1986, 930-933.
[8] Senna, L.F.; Achete, C.A.; Simão, R.A.; Hirsch, T. Comparative study between the electrochemical behavior of TiN, TiCxNy and CrN hard coatings by using microscopy and electrochemical techniques. *Materials Research*. 4, 2001, 137-141.
[9] Oréfice, R.L.; Brennan, A. Evaluation of the interactions between polymeric chains and surfaces with different structures performed by an atomic force microscope. *Materials Research*. 1, 1998, 19-28.
[10] Ikai, A.; Afrin R.; Itoh, A.; Thogersen, H.C.; Hayashi, Y.; Osada, T. Force measurements for membrane protein manipulation. Colloids and Surfaces B*: Biointerfaces*. 23, 2002, 165-171.
[11] Gopinath, T.R.; Schuster, H-D.; Schuckmann, W.K. (1981). Modelo de ocorrência e gênese da argila bentonítica de Boa Vista, Campina Grande, Paraíba. *Revista Brasileira de Geociências*. 11, 1981, 185-192.

International Journal of Modern Engineering Research (IJMER)
www.ijmer.com Vol. 3, Issue. 3, May.-June. 2013 pp-1458-1461 ISSN: 2249-6645

An Innovative Approach for Humidity Control by Using Deliquescent Materials in Test Chambers

Prof. L. B. Diwakar, Prof. A. M. Patil
Dept. of Mechanical Engg. PVPIT, Sangli. Maharashtra, India.

***Abstract*:** Humidity plays a vital role in the industrial spheres where there is an imminent needs to control the humidity to appraise the product quality. Among the industries are pulp and paper, sugar, textiles, pharma, air conditioner, food processing and formation of photonic band gap films. Essentially control of humidity in the above areas in the associated manufacturing industries attracts the researchers in recent days to develop latest techniques to implement control techniques effectively. Use of effective methods and to promote scopes for research oriented program for further developments in the field of computer based control of humidity to archive the goal of product quality. This is an honest attempt to review some papers published in various international journals which address the critical influences of humidity and its control strategy. To that account a brief survey on the papers titled on humidity control in various journals is also done.

***Key Words*:** Humidity, Controller, Product quality, Human comfort.

I. Introduction

The necessity to control temperature and humidity for sample testing or any such application is increasing day by day. The test chambers find wide applications in electronic, agriculture, component testing, textile and pharmaceutical industries.

The conventional approach to design such a system is to build a cooling/ heating system in conjunction with humidity control system. The humidity control system presently requires a series of complex instrumentation and controls namely a humidity transmitter, a Programmable Logic Controller, power contactors, a pan humidifier, a set of solenoid valves and a heater. All these components are high valued items and total cost of the equipment becomes prohibitive for average users who need these type of equipments.

This innovative approach would be a cost effective solution to control and maintain the above mentioned parameters namely temperature and humidity by using "Deliquescence" property of the material that is ability to absorb and release the moisture from the surroundings

II. Literature Review

Traditionally, deliquescent compounds, usually salts, are used to reduce relative humidity in a closed environment. It is well known that different compounds have varying affinity for moisture. For example, each deliquescent compound has a characteristic capacity for moisture adsorption and a characteristic equilibrium relative humidity (ERH) when hydrated.

Cerolinini et.al.[1]Desiccants can be considered humidity controllers in that they have been used to completely (or almost completely) remove all water vapor from the air from a closed system. An effective desiccant in sufficient quantity will adsorb water vapor from the air in a package, lowering the equilibrium relative humidity (ERH) to the point where condensation will no longer occur, or to a point where the threshold ERH within a sealed package or system is never exceeded under the conditions to which the package or system will be exposed.

Prowse and Wilkinson M. [3] described the specific humectant in such cases is chosen based on the desired equilibrium relative humidity (ERH). The salt may be single in nature, such as lithium chloride. A mixture of two salts may also be used. As an example, a solution of potassium carbonate has a relative humidity of about 43%. Therefore, a solution of potassium carbonate with excess undissolved crystals of potassium carbonate will maintain a constant relative humidity of approximately 43%. If the relative humidity begins to rise above 43%, the salt solution would pick up moisture from the environment thus lowering the relative humidity closer to 43%. Conversely, if the relative humidity begins to fall below 43%, the solution would release moisture until the surrounding environment reaches approximately 43%. The ERH values for different saturated aqueous salt solutions can vary from 11% to 98%.

Deschenes and Stone [4] described inventions for humidity control devices describe a viscous solution contained within a fabric or non-woven polymeric pouch. The viscous solution in such cases has included water, salt, and may have had a thickening material (such as alginate or xanthan gum). In practice, these salt solutions were difficult to handle because they are liquids which can spill or soak through the package or vessel containing them. Even a stabilized salt solution can weep or wick out of a package which must of necessity be porous to water vapor in order to function.

ASHRAE [6]Fundamental volume explained a method of determining the absolute humidity and relative humidity.Compounding this problem is the fact that the tendency to weep becomes greater as the humectants attracts moisture from its environment and becomes more fluid. With a fluid, even a thickened fluid, seepage may occur through a package if the moisture permeation rate of the film or pouch is too great, or if the surface energy or "wettability" is too high. This would obviously be counterproductive to the desired goal of protecting a product. nding on the temperature.

III. Proposed Work

A) Theoretical

The proposed work includes the manufacturing and testing of a 100 liters capacity test chamber. It will have a set temperature facility from + 4 deg C to + 60 deg C with a digital temperature indicator cum controller. It will have refrigeration and heating system. For humidity control a certain amount of deliquescent material will be kept inside the chamber. Deliquescence is a property of the material to absorb moisture from the surrounding space. These substances have strong affinity for water and absorb large amount of water. This amount of water absorbed depends on the surrounding temperature. The higher the temperature, the lower the capacity to absorb the moisture. Consequently, at higher temperatures, it will 'release' the moisture to the surroundings and at lower temperatures it will absorb more moisture, thereby, maintaining a fairly constant relative humidity of the surroundings. The process being reversible and no chemical change taking place, no frequent replenishment of the material is required.

B) Experimental Setup

1. A test chamber
2. A refrigeration system with temperature control
3. Hygrometer for measuring humidity

IV. Objectives

9.1) To design and manufacture a test chamber with provision of heating and cooling (refrigeration) system having a temperature controller with facility to set the desired temperature.

9.2) To use deliquescent materials such as zinc chloride, potassium hydroxide sodium hydroxide, magnesium chloride (any two of the above) to control humidity.

9.3) To test the chamber and monitor inside conditions.

9.4) To optimize the deliquescent material quantity for the particular volume of test chamber.

Action Plan (Methodology)

a) To design and manufacture a test chamber of about 40 liters net volume having adequate insulation.

b) To provide the equipment for the chamber in order to achieve the processes of cooling, heating, humidification, and de-humidification. It will require a fractional hp capacity compressor, air cooled condenser, an expansion device, forced convection air cooled evaporator, a re-heater and a steam type humidifier.

c) To incorporate necessary instrumentation including temperature indicator & controller, humidity indicator & controller to observe, record and control the required parameters such as chamber temperature and humidity.

d) To control the chamber conditions by conventional methods and by other methods as described earlier.

e) To evaluate the effectiveness of the non-conventional methods.

f) To optimize the quantity of deliquescent material for the particular range temperature and humidity control.

Symbol	Description
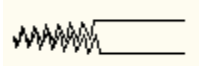	Temp.Sensor, Thermocouple
	Direction of refrigerant flow

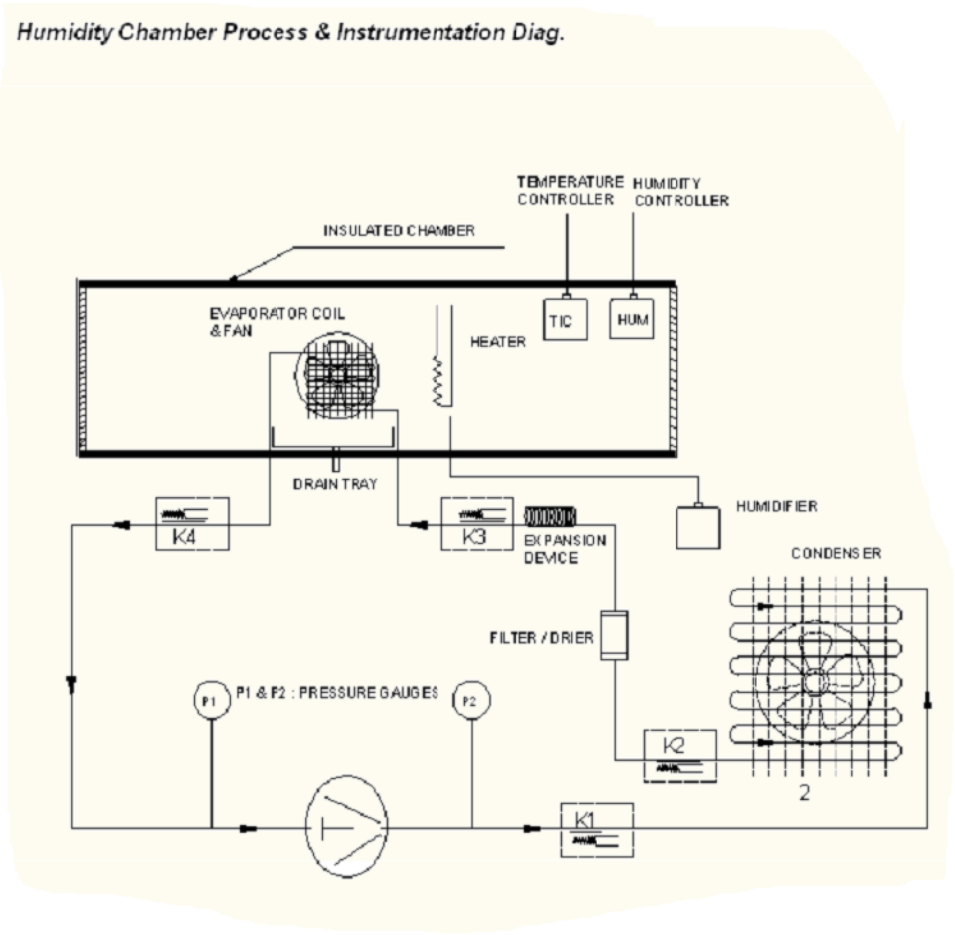

K_1-Temp. after compression
K_2 - Temp. after Condensation

TECHNICAL SPECIFICATIONS OF THE TEST CHAMBER

• *Test chamber capacity*	*:*	*40 liters*
• *MOC of test chamber*	*:*	*CRCA Powder coated.*
• *Insulation*		*65 mm PUF or equivalent.*
• *Compressor*		*Hermetically sealed, Copeland or equivalent make*
• *Refrigerant*		*R-134a- Eco friendly.*
• *Condenser*		*Natural/forced convection air cooled*
• *Drier/filter*		*Molecular sieve type provided*
• *Expansion device*		*Capillary tube*
• *Evaporator*		*Forced convection air cooled*
• *Temperature control*		*Digital temperature controller provided. Sub-zero or equivalent make.*
• *Humidity control*		*Digital type subzero make*
• *De-humidifier*		*Re-heater: 125 Watts provided.*
• *Humidifier*		*Immersion heater type provided.*
• *Pressure indication*		*Dial type pressure gauges, 2 nos provided.*
• *Energymeter*		*Provided to record total power consumption of equipment..*
• *Size of the equipment*		*600 x 1200 x 600 (LxHxD) mm*
• *Supply*		*230 Volts; 50Hz; 1 Ph.*

V. Concluding Remark

On review of various literatures on humidity control, it can be concluded that the humidity can be controlled by using specific property of various deliquescent materials. These substances have strong affinity for water & absorb large amount of water. The amount of water absorbed depends on surrounding temp. Higher the temp lower is the capacity to absorb the moisture. Hence while controlling the humidity the temp must be maintained correctly.

References

[1] S. Cerolininin M D orazio,Moisture buffering capacity of highly absorbing materials, int. jou. of Energy and Buliding,Elsevier 2009.
[2] Marnix van Belleghem, Hendric Jansteeman Design of Test chamber for investigation of Moisture
[3] Effects of humidity on mechanical properties Prowse M S, Wilkinson M.
[4] Climate change mortality and adaption Olive Descheles and Michel greenstone.

International Journal of Modern Engineering Research (IJMER)
www.ijmer.com Vol. 3, Issue. 3, May.-June. 2013 pp-1462-1466 ISSN: 2249-6645

Determinants in the Use of Mobile Communication Technology for Content and Pedagogical Skills Development of Technical Teachers in Anambra State of Nigeria

Onwusuru I. M[1], Uka C.S[2], Ogungbenro A.O[3]
[13]*Electronics Development Institute, Awka, National Agency for Science and Infrastructure, Federal Ministry of Science and Technology, (Nigeria)*
[2]*Federal College of Education (Technical) Umunze, Orumba South LGA Anambra State, (Nigeria)*

Abstract: *Most mobile phones possess features and applications that perform many digital functions. Unfortunately, Nigerian teachers who possess these phones do not know and utilize these capabilities. Hence there is need to train them on how to make efficient use of the phone features especially for professional development purposes. The major purpose of this study was to identify the determinants in using mobile communication technology for subject matter knowledge update and pedagogical skills improvement of technology teachers in Anambra state. Five research questions and five hypotheses, guided this study. The major findings of the study, among others include: browsing with phone provides net service to rural teachers and this helps in updating their knowledge; mobile phone enhances short message data collection for teacher projects and this supports immediate knowledge update; using phone, teachers can download materials which could be used for classroom explanation thereby concretizing and supporting pedagogy. The study concluded that mobile communication technology which is affordable, cheap, accessible, etc, now posses some enhanced feature which can be used to fill some professional development needs for teachers. It was however recommended among others that workshops and seminars should be organized regularly to create awareness and train teachers on the capabilities of mobile phones and how to use the features for educational purposes.*

I. Introduction

Background of the study

Mobile communication technologies (MCT) are modified computers with the features to simplify their usability, accessibility and portability. These are one of the fastest and on-going growing telecommunication technologies in the world. These devices have the capability of transmitting, processing and receiving date, voice and video signals through wireless link. According to Darby, (2005), mobile communication technologies can be defined as those technologies which depend upon the broader phenomenon of internet protocol (IP) convergence when data, voice and video travel over a single channel. There are numerous mobile communication technologies which include laptop and notebook computers, palmtop computers or personal digital assistants, mobile phones (GSM) and 'smart phones', global positioning system (GPS) devices, wireless debit/credit card payment terminals, etc. One of these technologies which is by far the best and most widely used in mobile communication is mobile phone.

Mobile phone is a type of mobile communication technology with the capacity of sending and receiving data at rates up to 9600 bps, to users on POTs (Plain Old Telephone Service), Packet Switched Public Data Networks, and Circuit Switched Public Data Networks using a variety of access methods and protocols, Scourias (2007). It is a digital network which does not require a modem between the user and the network, rather an inbuilt audio modem interworks with POTs. Mobile phone system exists in every continent thus the acronym GSM which aptly stands for Global System for Mobile communication (Scourias, 2007).

There are different versions of mobile phone. Some are more sophisticated than others. Specifically, third generation (3G) phones are embedded with enhanced features that enable its wide range of usability. Among others, some features of 3G mobile phone include wireless fidelity (Wi-Fi, a type of wireless local area network technology for internet browsing), MP3 playback, memo recording, personal organizer functions, E-mail, instant messaging, built-in cameras and camcorders, Push-to-Talk (PTT), Infrared and Bluetooth Connectivity, ability to watch streaming video or download video for later viewing, general packet radio service (GPRS) data services, i.e data networking services for mobile phones , radio frequency identification (RFID), video calling, dial-up services i.e data networking services using GSM as modems, virtual private networks i.e secure access to a private network, even connectivity to television stations. It is therefore possible to network the mobile device to a home office or the internet even while on transit.

The total value of mobile data services exceeds the value of paid services on the Internet, and was worth 31 billion dollars in 2006 (Netsize Guide 2008). Some of these features of mobile phone have been explored by many people from different parts of the world. Apart from the telephony services, the features have been utilized and found relevant in educational system. Bridget (2007), made a trial in initiating the use of mobile phone in his training with some teachers in developing countries. This program was launched in 2003 in the Philippines under the name text2teach. The situation was such that teachers in remote areas received training and used mobile phone to access the state-of-the art learning materials. These teachers accessed an extensive library of science, math, and language videos simply by sending SMS message via a mobile phone. This they achieved by sending SMS which signals a satellite that then delivers digital files to a video recorder connected to a television in the classroom. The technology has thus, allowed high quality content to be delivered in remote areas at the cost of a cell phone SMS.

Nevertheless, the hints above have highlighted the fact that mobile phones (GSM) can be manipulated as education enhancing devices. These efficiencies and capabilities of mobile phone have been identified and utilized by advanced countries. In Nigeria, there are over 1.3 million subscribers of GSM including technology teachers. To majority of these teachers, GSM is a device meant for just making and receiving calls. Some view the acquisition of highly enhanced phones as an avenue for showing off. The thought of utilizing GSM for teachers' professional development purpose has rarely been envisaged in Nigeria. Characteristics of GSM such as independence to main power source, portability and small size, affordability, battery operated and rechargeable, less power requiring liquid crystal display (LCD), downloadable for upgrade and file transfer, memory expansion and its wireless connectivity to network and internet has offered it the advantage of being useful anywhere and anytime within the IP convergence area. This paper therefore identifies the determinant issues in using mobile communication technology to improve teacher's expertise for enhanced student's achievement through subject matter knowledge update and pedagogical skill improvement.

Purpose of the Study

The main purpose of this study is to identify the determinants affecting the use of mobile communication technology (MCT) for subject matter update and pedagogical skill improvement for professional development purpose of technology teachers. Specifically, the study identified the:

1. Issues on the use of MCT for updating subject matter knowledge of practicing technology teachers.
2. Ways in which MCT can be used to improve pedagogical skills for technology teachers.

Research Questions

The study will find answers to the following questions:

1. What are the issues pertaining to the use of MCT in updating subject matter knowledge of practicing technology teachers?
2. How can MCT support pedagogical skills improvement of technology teachers?

Research Hypotheses

H_{O1}: There is no statistical difference in the mean of the responses of teachers with NCE and B.SC/B.ED qualification on the use of MCT in updating subject matter knowledge of practicing technology teachers.

H_{O2}: There is no statistical difference in the mean of the responses of male and female teachers on the use of MCT in improving pedagogical skills for technology teachers.

Research Design

The study adopted survey research design. The population of the study comprised all the 137 technology teachers in 10 technical schools in Anambra state of Nigeria. According to the data collected on 3rd March 2008 from the State Education Commission headquarters Awka, there are 10 technical schools in Anambra state which include GTC Umunze (12 technology teachers), GTC Umuchu (12 technology teachers), GTC Umuleri (18 technology teachers), GTC Enugwuagidi (16 technology teachers), GTC UTU (16 technology teachers), GTC Nnewi (14 technology teachers), GTC Nkpor (12 technology teachers), GTC Alor (8 technology teachers), GTC Osamala (3 technology teachers), and GTC Onitsha (26 technology teachers). Since the population of this study is not very large, the study did not make use of sample, rather, the entire population was studied. A researcher designed questionnaire was used for the data collection. The questionnaire was made of three sections; section A, B and C. Section A consisted of items on the background information of the respondents. Section B was made of items eliciting information on MCT as an instrument for update of subject matter knowledge of teachers. Section C consisted of items on improvement of pedagogical skills for technology teachers through MCT. The questionnaire was validated by three experts from Industrial Technical Department, University of Nigeria Nsukka, and two experts in information communication (ICT) from Management Information System, (MIS), University of Nigeria Nsukka. A 5-points Likert rating scale of strongly agree (SA), Agree (A), Undecided (U), Disagree (D), and Strongly disagree (SD) was used with values of 5,4,3,2 and 1 respectively. Mean and standard deviation was used to answer the two research questions. In analyzing the hypotheses, t-Test was used.

II. Results

Research Question one

What are the issues pertaining to the use of MCT in updating subject matter knowledge of practicing technology teachers?

Table 1

Mean and Standard Deviation of Respondents on MCT and subject matter knowledge update of practicing technology teachers.

S/N	ITEM STATEMENT	Mean	Std. Deviation	Decision
1.	Downloading many materials on phone memory card saves the problem of carrying text-books around and this supports knowledge update at any time.	4.04	1.10	Agree
2.	Browsing with phone provides net service to rural teachers and this helps in updating their knowledge.	4.20	0.87	Agree

3.	Downloading and reading materials with phone necessitate subject matter knowledge update for teachers anytime, anywhere.	4.02	0.96	Agree
4.	Sourcing information using mobile phones provides quick personal subject matter knowledge up-date.	4.07	0.97	Agree
5.	Learning to use the features in mobile phone will enhance teachers' proficiency in the use of other ICT for subject matter knowledge update.	4.16	0.83	Agree
6.	Mobile phone enhances short message data collection for teacher projects and this supports immediate knowledge update.	4.17	0.83	Agree
7.	Storing course content and other reading materials in phone enables the teacher to read at anywhere and anytime thereby supporting their knowledge update.	4.09	1.05	Agree

Research Question two
How can MCT support pedagogical skills improvement of technology teachers?

Table 2
Mean and Standard Deviation of respondents on MCT and improvement of pedagogical skills of technology teachers.

S/N	ITEM STATEMENT	Mean	Std. Deviation	ecision
1	Using mobile phone in teaching will motivate learning thereby supporting teachers' pedagogy skills.	3.58	1.28	Agree
2	Using phone, teachers can download materials which could be used for classroom explanation thereby concretizing and supporting pedagogy.	4.23	3.75	Agree
3	Asking students to answer certain questions through SMS will enable the teacher to give immediate feedback and this enhances learning.	3.72	1.11	Agree
4	Answering questions through SMS will give the teacher avenue for instant monitoring of the level of students' understanding thereby necessitating proper pedagogy adjustment.	3.88	1.02	Agree
5	Teachers can create online library on the net and allow students access it via mobile phone for further reading and this supports pedagogy.	3.98	0.98	Agree
6	Using mobile phone-enabled video projector, mobile phone can be used to deliver the contents to a classroom and this will act as motivating factor to students thereby enhancing pedagogy.	3.94	1.09	Agree
7	Mobile phone can be programmed to allow students to access curriculum and course content on the net easily and this encourages reading ahead, thereby supporting pedagogy.	4.12	1.03	Agree
8	Through mobile phone teachers can easily get linked with students for scheduling of lecture time and this aids teacher in fixing convenient time for teaching.	4.05	0.96	Agree
9	Contents of lessons can be programmed in phone as games and simulations and teachers can use this to increase interest in learning thereby supporting their pedagogy.	3.90	0.98	Agree
10	Teachers can use mobile phone to give multiple-choice quizzes via the net with immediate feedback and this will supports their teaching skills.	3.82	1.15	Agree

Table 1 shows that the teachers are in agreement that all the items listed were issues pertaining to the use of MCT in updating subject matter knowledge of practicing technology teachers in technical schools in Anambra state.
In table 2, it was also agreed that all the researcher's items were ways in which MCT can support pedagogical skills improvement of technology teachers.

III. Hypothesis one

H_{O1}: There is no statistical difference in the mean responses of teachers with B.SC/equivalent and NCE/Equivalent qualification on the use of MCT in updating subject matter knowledge of practicing technology teachers.

Among other respondents, there were seventy four (74) technology teachers with B.SC/Equivalent and thirty six (36) teachers with NCE/Equivalent. The responses of each of the groups were recorded and the mean and standard deviation of each of the group were calculated.

Table 3
T-test Analysis of Mean and Standard deviation of Reponses of Technology Teachers with B.SC/equivalent and NCE/Equivalent

S/N	NCE/Equivalent		B.Sc/Equivalent		t-cal	Sig (2-tailed)
	X_1	$S.D_1$	X_2	$S.D_2$		
1.	3.78	1.29	4.09	1.02	-1.40	0.17
2.	3.94	0.92	4.24	0.82	-1.71	0.09
3.	3.64	1.10	4.12	0.89	-2.47	0.02*
4	3.83	1.16	4.22	0.82	-2.00	0.05*
5.	3.89	1.01	4.26	0.76	-2.14	0.04*
6.	3.78	1.01	4.32	0.69	-3.33	0.00*
7.	3.64	1.20	4.24	0.93	-2.90	0.01*

df = 108, level of Significant = 0 .05

Hypothesis two

H_{O2}: There is no statistical difference in the mean responses of male and female teachers on the use of MCT in improving pedagogical skills for technology teachers.

Table 4:
T-test Analysis of Mean and Standard deviation of Reponses of male and female Technology Teachers

S/N	MALE TEACHERS		FEMALE TEACHERS		t-cal	Sig(2-tailled)
	X_1	$S.D_1$	X_2	$S.D_2$		
1	3.57	1.23	3.58	1.34	-0.04	0.97
2	3.91	1.02	4.67	5.63	-1.15	0.25
3	3.76	1.051	3.67	1.20	0.44	0.66
4	3.93	1.08	3.82	0.95	0.63	0.53
5	4.00	0.92	3.95	1.08	0.31	0.76
6	4.08	1.11	3.75	1.19	1.74	0.08
7	4.09	0.96	4.16	1.14	-0.38	0.70
8	4.09	0.90	3.98	1.05	0.65	0.52
9	4.00	0.90	3.76	1.07	1.36	0.18
10	3.79	1.13	3.85	1.19	-0.33	0.74

DF = 128, level of significance = 0.05

In the analysis, "sig (2-tailled)" are the figures showing the probability/significance level in which the calculated t-value were significant. From table 3 above, the significance levels of items 3, 4, 5, 6, and 7 are less than or equal to the stated 0.05 level of significance therefore the null hypothesis is rejected. On the other hand, the significance level of items 1, and 2 are greater than 0.05 therefore the null hypothesis is accepted. From table 4, the analysis revealed that the significance level for all the items are greater than the stated 0.05 level of significance, therefore the null hypothesis were accepted.

IV. Summary of Findings

Based on the outcome of the study, the following are the listed major findings of the study.

1. Browsing with phone provides net service to rural teachers and this helps in updating their knowledge.
2. Mobile phone enhances short message data collection for teacher projects and this supports immediate knowledge update.
3. Using phone, teachers can download materials which could be used for classroom explanation thereby concretizing and supporting pedagogy.
4. Mobile phone can be programmed to allow students to access curriculum and course content on the net easily and this encourages reading ahead, thereby supporting pedagogy.

Through mobile phone teachers can easily get linked with students for scheduling of lecture time and this aids teacher in fixing convenient time for teaching.

V. Discussion

Mobile phone technology is the handiest and simple technology which can be utilized any where anytime. Previous studies have shown that advanced countries have identified the advantages obtainable in mobile phone if utilized for educational purpose. As it was discovered in the literature that the thought of using mobile phone for academics purpose has not been raised in Nigeria, the findings of this study revealed the determinant issues in integrating mobile phone into academics in Nigeria, especially for subject matter knowledge update and pedagogical skill improvement for teachers professional development purpose.

The findings as regards the issues pertaining to the use of MCT in updating subject matter knowledge of practicing technology teachers revealed that; Browsing with phone provides net service to rural teachers and this helps in updating their

knowledge; Downloading and reading materials with phone necessitate subject matter knowledge update for teachers anytime, anywhere; Using phone, teachers can download materials which could be used for classroom explanation thereby concretizing and supporting pedagogy. These findings corroborate the view of Thomas (2005) as he described mobile phone as device that has the potential of enabling knowledge update through a network of devices, people, and situations that allow complex learning experiences to play out. Presenting knowledge update as anywhere and anytime learning, simple mobile phone technology which a teacher has at hand can be used to create relevant and meaningful knowledge update situations that a teacher authors himself, in a location that the teacher finds meaningful and relevant.

This fact that mobile phone can support knowledge update at anytime and anywhere has however earlier been disclosed by Lonsdale, Baber, Sharples, Byrne, Arvanitis, Brundell and Beale (2004) when they noted in their study that Mobile devices are especially well situated to context-aware applications simply because they are available in different contexts, and so can draw on those contexts, to enhance knowledge update activity. On this premise still, Shih, Chang, Chen, and Wang (2005) had also hinted that the self-regulated system of mobile phone thus provides those engaging in education with a portable and personalized learning environment, thereby cultivating a self-motivated, self-directed, and self-regulated subject matter knowledge update for teachers.

Furthermore, pertaining how MCT can support pedagogical skills improvement of technology teachers, it was found that Mobile phone can be programmed to allow students to access curriculum and course content on the net and this encourages reading ahead, thereby supporting pedagogy. Roschelle (2003) supported the above findings when he remarked that the use of mobile phone and even other mobile devices for pedagogy gives rise to a change in the nature of the teaching, as a catalyst for motivated and richer discussion of the pertinent topics. Equally, the study found that through mobile phone teachers can easily get linked with students for scheduling of lecture time and this aids teacher in fixing convenient time for teaching. This goes in line with the view of Naismith (2006) that using mobile phone, content and feedback can be tailored to suit particular curriculum areas. Further on this finding, Naismith (2006) had also earlier discovered in his study that in higher education, mobile phones can provide course materials to students including due dates for assignments and information about timetable changes or lecture venue changes.

VI. Conclusion

Teachers need to be away of the possibilities and the way of utilizing there most handy technology to update their subject matter knowledge and improve their pedagogical skills for their professional development purpose. The findings of this study revealed that some teachers in Nigeria do not really know the possibility of utilizing mobile phones for educational purpose. Mobile phone, a mobile communication technology which is affordable, cheap, accessible, etc, now posses some enhance feature which can be used to bring some professional development needs to the door step of some teachers. This study found that this simple device has been integrated into educational programmes in some other countries like Philippine and was confirmed very helpful and useful. Most teachers in Nigeria especially those in the rural areas have these devices and use it for just calling and receiving calls without knowing all its other capabilities. Should the capacities of these devices be explored and be made known to the teachers, their benefit in other professional development programmes will be maximized. In line with the findings of this study, the following recommendations were made: Findings of this study should be made available to teachers so as to let them know that their mobile phones can do more than just calls and can be utilized for professional development; Workshops and seminars should be organized regularly to enable teacher know the capabilities of mobile phones and be trained on how to use the features for educational purposes; The teacher trainers, in their teachings to meet the demands of the society, should stress the importance of exploring the features of mobile phones and utilize them for educational purpose.

Refrences

[1] Darby, G (2005). Opportunities and issues of M-learning in Asia-pacific development. Report on International workshop on Mobile learning for Expanding Educational Opportunities 16-20 May 2005, Tokyo, Japan. ICT in Education Unit, UNESCO Bankok, 2005. UNESCO Asia and pacific Regional Bureau for Education 920 Sukhumvit Rd, Prakanong Bankok 10110, Thailand.

[2] Lonsdale, P, Baber, C, Sharples, M, Byrne, W, Arvanitis, T, Brundell, P and Beale, H (2004). Context awareness for MOBIlearn: creating an engaging learning experience in an art museum. Proceeding of MLEARN 2004. Bracciano, Rome: LSDA.

[3] Naismith, L, Lonsdale, P, Vavoula, G, & Sharples, M. (2004). Literature review of mobile technology and learning . A report or NESTA Futurelab. University of Birmingham. Retrieved on 3rd February 2008 from http/www.nestafuturelab.org/research/review.

[4] Netsize Guide (2008). Mobile phone. Retrieved on 23rd February 2008 from"http:// en.wikipedia. org/wiki/Mobile_phone features" \o "Mobile phone features.

[5] Roschelle, J. (2003). Unlocking the learning value of wireless mobile devices. Journal of Computer Assisted Learning. 19 (3): 260-272.

[6] Scourias, J (2007). Overview of the Global System for Mobile Communication. Retrieved on 23rd February 2008 from jscouria@www.shoshin.uwaterloo.com.

[7] Thomas, M. (2005). *E-learning on the move.* Guardian.co.uk. (Retrieved <22/02/2008>) http://education.guardian.co.uk/elearning/comment/0,10577,1490476,00.html

International Journal of Modern Engineering Research (IJMER)
www.ijmer.com Vol. 3, Issue. 3, May.-June. 2013 pp-1467-1469 ISSN: 2249-6645

Analysis of wings using Airfoil NACA 4412 at different angle of attack

Mahendra Agrawal, [1] Gaurav Saxena[2]
[1]*Department of mechanical engineering, Assistant professor, SRCEM banmore, RGPV University, India*
[2]*Department of mechanical engineering SRCEM banmore, RGPV University, India*

Abstract: *The purpose of this paper is to analysis the basic aerodynamic theory of wings and the provide an introduction to wind tunnel testing. This is followed by the result from the wind tunnel testing of a NACA4412 and the analysis of the data.*

Lift increase at the angle of attack increase at certain point and at this point it become maximum. After that if the angle of attack is increased by further, drag become the dominant factor and the wind enters the stall mode.

Keywords: *Air Foil, Angle of attack, Drag Force, Lift Force*

I. INTRODUCTION

The purpose of this report is to present an Introduction to structure and theory of wings. Also, it includes some background information on wind tunnels and wind tunnel testing. Lastly, this report describes the procedure for testing the NACA 4412 airfoil and presents a number of graphs and tables evaluating the data obtained through these tests. The objective is to find the angle of attack at which the lift is maximized in order to get the best performance of this wing when in flight.

This report is based on the research on basic aerodynamics of wings and fundamentals of wind tunnel testing. In addition, it will present the results from testing the NACA 4412. This data is then presented through tables and graphs using Microsoft Excel.

II. AIM OF EXPERIMENT

The present research describes the application of different turbulence models for flow around NACA 4412 aerofoil at angle of attack 15 degree, 20 degree, 22.5 degree. It is designed to investigate the change in the structure of the flow as a function of using different turbulence models, to investigate the performance of these turbulence models and to compare them with the available accurate experimental data. An improved understanding of the physical characteristics of separation on the aerofoil sections and in the region of the trailing edge is of direct value for the improvement of high life wings for aircraft. The configuration were planned with the knowledge that a small intermittent separated region will be formed at angle of attack □a = 15º, that corresponds to the position of maximum lift of a NACA 4412 aerofoil section

III. WIND TUNNEL TESTING OF THE AIRFOIL

Wind tunnel testing is a crucial step in the design of an aircraft. It can give quite accurate information on the performance of an aircraft or a section of an aircraft by taking data on a scale model. This can save enormous amounts of money by testing models instead of prototypes. It is also much safer to test in a wind tunnel than out in the open. The following section covers the theory of the wind tunnels and procedures for testing the NACA 4412 airfoil.

IV. THEORY OF WIND TUNNELS

All wind tunnels can be divided into one of two types: open circuit (also called “straight through”) or closed circuit (also called “return flow”) 6. Open circuit wind tunnels pull the air from the environment into the tunnel and release the air back into the environment, whereas the closed circuit continually circulates the same air throughout the tunnel. The wind tunnel we used is a single return flow wind tunnel, shown in Figure.

Figure: The wind tunnel we used to test our airfoil.

Closed circuit wind tunnels are advantageous over open circuit wind tunnels for the following reasons: the quality of the flow can be easily controlled with screens and corner turning vanes; less energy is required to create an airflow of a given size and velocity; the wind tunnel runs more quietly. The disadvantages are the initial expense of building and need to change the air if it is significantly heated or polluted with smoke from smoke testing or engines7. Fortunately, neither of the disadvantages affected us.

V. TURBULENCE MODELS

The inlet boundary velocity U□was set to 18.4 m/sec for all turbulence models for direct comparison with the flying hot-wires measurements. The corresponding Reynolds number is 0.36 x 106 based on the chord *c* of the airfoil (250 mm). A computational grid of 150 ×150 was fixed for all models. Three different turbulence models were used, two equation models such as Realizable and RNG k-Reynolds and Reynolds Stress Model (RSM). These models selected because they are most widely used in aerodynamic industry, and they have well documented strength. Also these models proved to have a superior performance for flows involving strong streamline curvature. All computations have been performed on the same grid to ensure that the presented solution for each model will be compared with each other. Flow conditions around the airfoil were built up by finite element analysis using FLUENT 5 software by Fluent Inc.

VI. FIGURES AND TABLES

Figure 1 Pressure coefficient (for angle of attack 15)

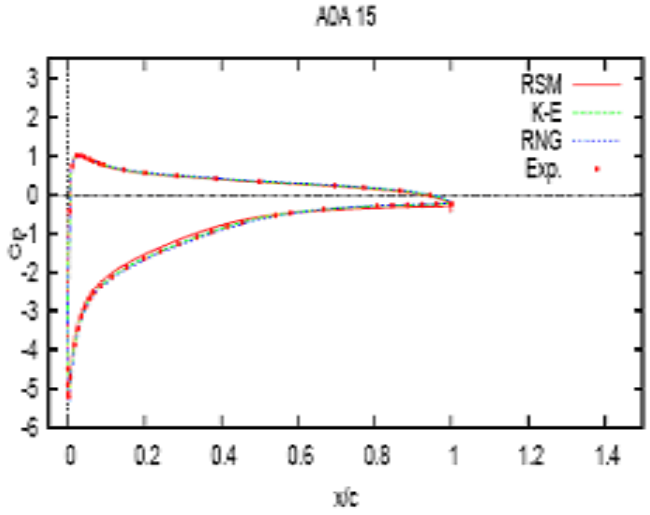

Figure 2 Friction coefficient (for angle of attack 15)

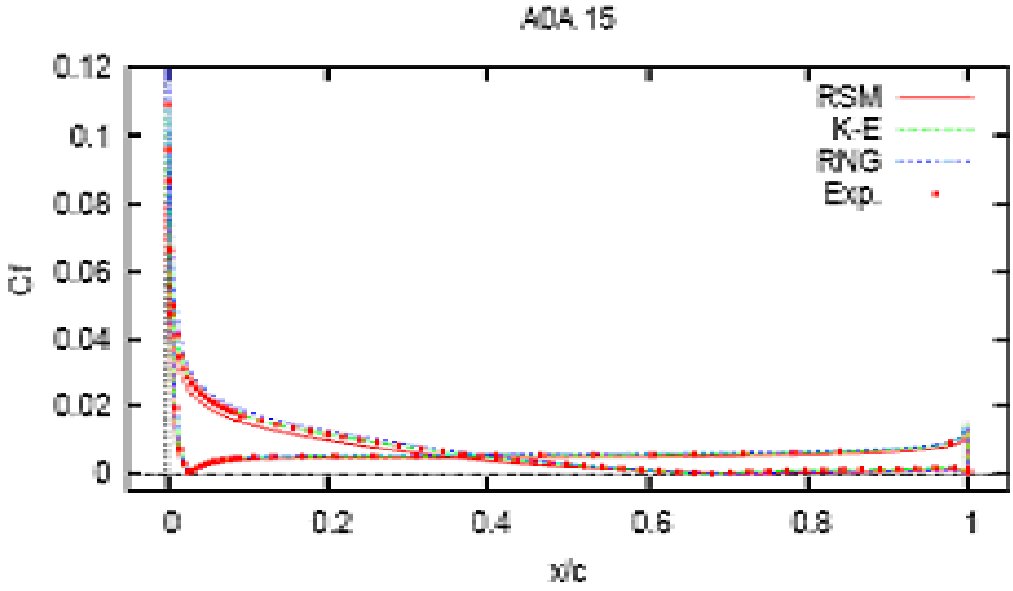

VII. CONCLUSION

One of the most important aspects of a turbulence model for aerodynamic applications is its ability to accurately predict adverse pressure gradient boundary-layer flows. It is especially important that a model be able to predict the location of flow separation and the wake behavior associated with it.

This study found that the turbulence models had captured the physics of unsteady separated flow. The resulting surface pressure coefficients, skin friction, velocity vectors, and Reynolds stresses are compared with flying hot wire experimental data, and the models produce very similar results. Also excellent agreements between computational and experimental surface pressures and skin friction were observed.

REFERENCES

[1] Badran O.O. 1993. A flying hot-wire study of separated flows. Ph.D thesis. University of Bradford, UK.
[2] Rumsey, C. L., Gatski, T. B. 2001. Recent turbulence model advances applied to multielement airfoil computations. Journal of aircraft, vol. 38, no. 5.
[3] O.O.Badran. O.O. and Bruun, H.H. 2003. Turbulent flow over a NACA 4412 airfoil at angle of attack 15 degree**.** Proceedings of FEDSM'03, 4th ASME_JSME Joint Fluids Engineering Conference, Honolulu, Hawaii, USA, July 6-11, 2003.
[4] Adair D.1987. Characteristics of a trailing flap flow with small separation. Experiments in Fluids 5, 114-128.
[5] Adair D. and Horne W.C. 1989. Turbulent separated flow over and downstream of a two-element airfoil. Experiments in Fluids 7, 531-541.
[6] Al-Kayiem H.H and Bruun H.H. 1991. Evaluation of a flying x hot-wire probe system. Meas. Sci. Technol. 2, 374-380.
[7] Coles D. and Wadcock A. (1979). Flying-hot-wire study of flow past an NACA 4412 airfoil at maximum lift. AIAA 17:4, 321-329.
[8] Nakayama A. 1985. Characteristics of the flow around conventional and supercritical airfoils. J. Fluid Mech 160, 155-179.
[9] Seetharam H.C. and Wentz W.H. 1977. Experimental investigation of subsonic turbulent separated boundary layers on an airfoil. J. Aircraft 14:1, 51-55.
[10] Simpson R.L, Chew Y.T. and Shivaprasad B.G. (1981). The structure of a separating turbulent boundary layer. Part 1: Mean flow and Reynolds stresses. J. Fluid Mech 113, 23-53.
[11] Thompson B.E and Whitelaw J.H. (1984). Flying hot-wire anemometry. Experiments in fluids 2, 47-55.
[12] Wadcock A.J. (1978). Flying hot-wire study of two-dimensional turbulent separation on an NACA 4412 airfoil at maximum lift. Ph.D. Thesis, C.I.T, USA.
[13] Maddah, S. R. Gough, T. Pierscionek, B. Bruun, H.H.. 2002. Investigation of slat heel effect on the flow field over multi-element aerofoils. Experimental Thermal and Fluid Science**,** Volume 25, Issue 8, February 2002, Pages 651-658
[14] Burns, T.F., and Mueller, T.J. (1982). "Experimental Studies of the Eppler 61 airfoil at low Reynolds numbers". AIAA 20th Aerospace Science Meeting, Orland, Florida.
[15] Hastings, R. C., and William, B.R. (1984). "Studies of the flow field near an NACA 4412 aerofoil at nearly maximum lift. Royal Aircraft Establishment, Hants., Tech. Memo, AERO 2026, pp.1-11.

International Journal of Modern Engineering Research (IJMER)
www.ijmer.com Vol. 3, Issue. 3, May.-June. 2013 pp-1470-1474 ISSN: 2249-6645

Comparative Study, Design and Performance Analysis of Wide Slot Antenna with Patch-Feed for Bandwidth Enhancement

Pragya Jain, [1] Prof. Sunil Kumar Singh[2]
[1, 2] *EC Department, Jabalpur Engg. College, Jabalpur*

Abstract: *This paper presents a design of triangular wide slot antenna with same shaped patch which is fed by CPW. Patch is working as a radiating element and wide slot working as a ground. Detail simulation is conducted to understand its behaviour and optimize for broad band operation. The results are analysed and discussed in terms of return loss, VSWR, Gain, current distribution etc. The result shows that the Impedance bandwidth is greatly enhanced 116 %(2.1 Ghz-7.9 Ghz). This large operating bandwidth is optained by choosing suitable combination of Feed- Slot shapes, Feed gap width and Waveguide width. To understand the effects of various dimentional parameters numerical sensitivity analysis is also done*
Keywords: *Band width, Co planar waveguide, Patch-feed, Feed-gap, wide slot antennas.*

I. Introduction

In recent years, there have been a growing research activities on CPW feed wide slot antennas [1]-[5], because of there favourable impedance characteristics. These antennas have several appealing advantages over common patch antennas like wide band width, good impedance matching and bidirectional as well as unidirectional radiation patterns. The CPW feeding line also has advantages over microstrip feed lines such as low dispersion, low radiation leakage, their easy integration with active devices or MMICs and ability to control their characteristics impedance.

Although many CPW feed wide slot antennas are proposed for wide band applications but studies on the effect of the interaction between feed and slot on impedance bandwidth are rare. In this paper attention is paid on the effects on the interaction between slot and small patch, feed gap width (h) and waveguide width (g). It was found that properly choosing suitable combination of the antennas (slot as well as feed) and by tuning their dimensions significant enhanced bandwidth can be obtained.

II. Antenna Design

"Fig 1" shows the geometry of proposed antenna fabricated on the FR4 substrate with thickness of 0.8 mm and dielectric constant 4.4. Antenna has a triangular-shape slot and an equilateral triangular-patch feed with an edge length of 15 mm. Patch is working as a radiating element fed by CPW and wide slot working as a ground. By study of various papers [1]-[10] three design rules are followed:

A. Feed and slot shape should be similar
B. The widths and lengths for both feeds are about one third of the slot size
C. Lengths are close to but less than the quarter wavelength measured at the lower frequency edge. The lengths are shorter than a printed monopole at the same frequency, because the slot edge acts as a capacitive load to the monopole.

Theoretical formulas

The resonance frequency corresponding to the various modes can be given by

$$f_r = \frac{ck_{mn}}{2\Pi\sqrt{\varepsilon_r}} = \frac{2c\sqrt{m^2+mn+n^2}}{3a\sqrt{\varepsilon_r}}$$

$$k_{mn} = \frac{4\Pi\sqrt{m^2+mn+n^2}}{3a}$$

Where, c = free velocity of light and **…..** is the wave number For lowest order the resonance frequency is given by

$$f_r = \frac{2c}{3a\sqrt{\varepsilon_r}} \quad \text{--------} \quad (1)$$

In these formulas the effects of fringing fields are not considered. The resonant frequency can be determined more accurately, if dielectric constant and length of the patch **a** is replaced by effective dielectric constant "ε_{reff}" and effective length "a_{eff}", Effective Dielectric constant of substrate determined by "Resonant line method" is given by**:**

$$\varepsilon_{reff} = \frac{\varepsilon_r+1}{2} + \frac{\varepsilon_r-1}{2}\left[1+12\frac{h}{W}\right]^{-\frac{1}{2}}$$

And $a_{eff} = a + \frac{h}{\sqrt{\varepsilon_r}}$.

Hence, the resonant frequency is

$$f_r = \frac{2c}{3a_{eff}\sqrt{\varepsilon_{eff}}} \quad \text{--------} \quad (2)$$

As we know that the wide slot antennas should have very low aspact ratio (close to 1), so the length of the patch is calculated from equation (2) is further modified and taking round figure. Length and width of the patch is 15mm and Length and width of the slot is 52.7mm.

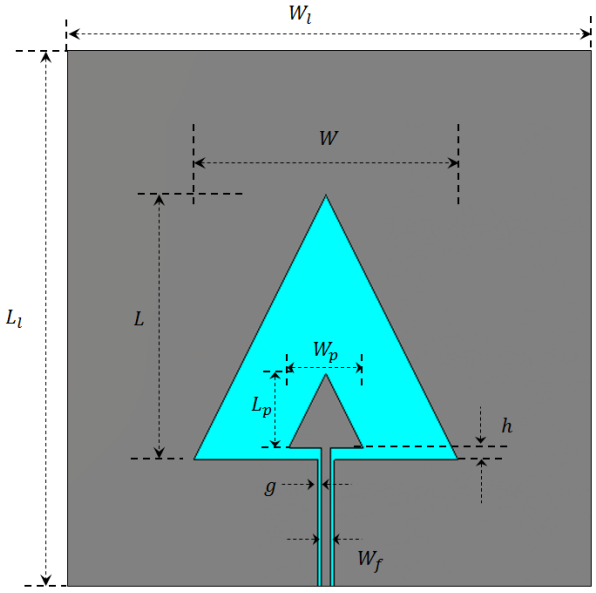

Figure 1: Geometry of proposed antenna

All dimensions in **mm**

L_l	W_l	L_p	W_p	L	W	W_f	h	g
110	110	15	15	52.7	52.7	2	2.5	0.7

III. Smulated Results and Discussion

A. Return loss and antenna bandwidth

The center frequency is selected as the one at which the return loss is minimum. The bandwidth of the antenna is said to be those range of frequencies over which the return loss is greater than 7.3 dB, Thus we measure required band at return loss -10dB. From return loss plot given in "fig 2" it is found that impedance band width is 116% and center frequency is 5 GHzs

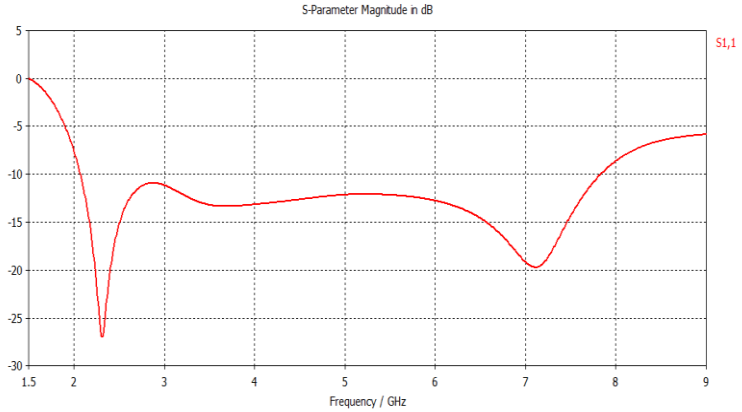

Figure 2: Return Loss Characteristics (S_{11} < -10 dB)

B. VSWR Plot

Voltage standing wave ratio (VSWR) of wide slot antenna shown in "fig 3" shows most of the frequency band VSWR lies between 1.5 – 2 which is excellent. At f = 5 GHz the value of VSWR is 1.6

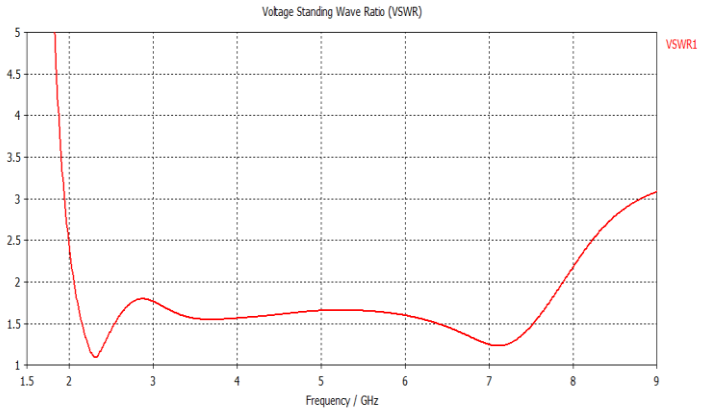

Figure 3: VSWR Characteristics (VSWR < 2)

C. Gain Vs Frequency Plot

"Fig 4" shows that simulated results at the desired frequency band. At frequency 6 GHz the gain is maximum 7.6 dbi.

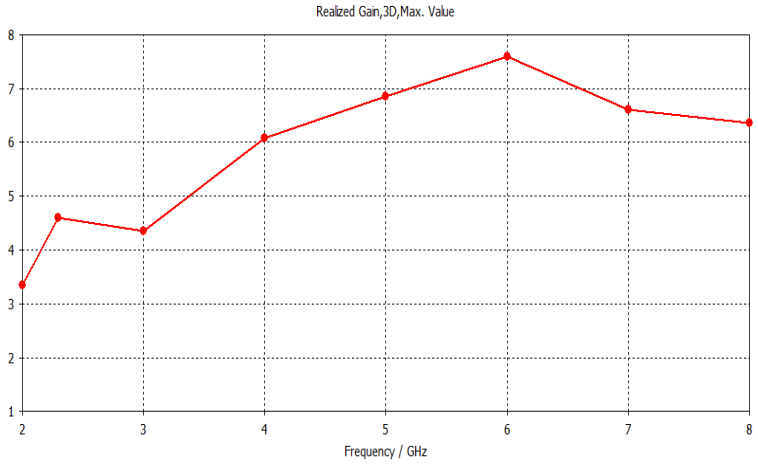

Figure 4: Gain Characteristics

D. Radiation pattern

E-field and H-field plots are given in "fig 5" at frequencies 2.3 GHz, 5 GHZ and 7 GHz. Antenna radiates in nearly omni direction to its surface

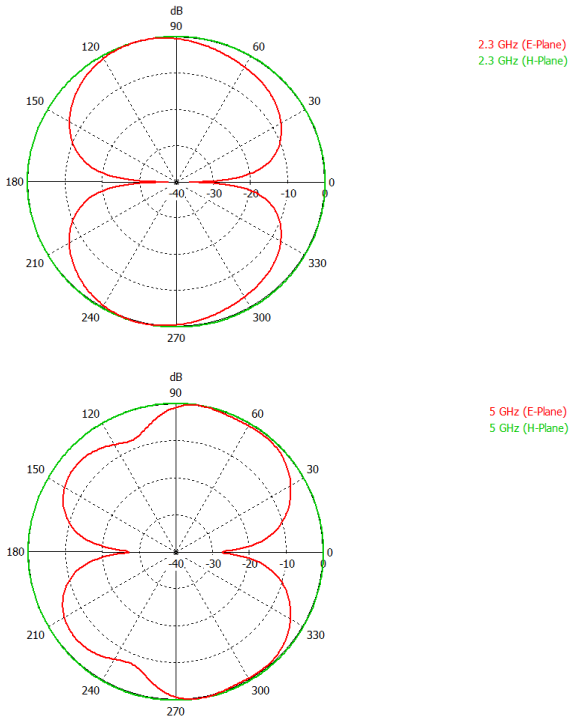

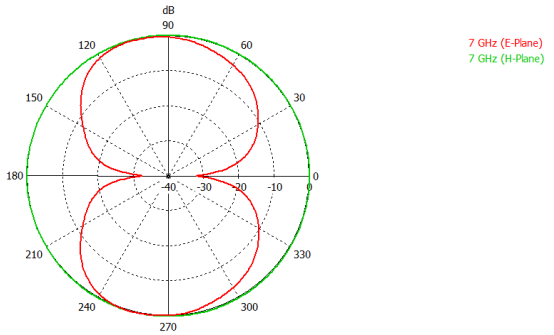

Figure 5: Radiation Pattern Characteristics for 2.3GHz, 5GHz and 7 GHz(E and H plane)

E. Current Distribution

Through the study on different slot shapes, it is found that currents flowing on the edge of the slot will increase the cross-polarization component in the H-plane and cause the main beam to tilt away from the broadside direction in the E-plane. From the simulation, "fig 6" shows the surface current distribution for resonant frequencies 2.3 GHz and 7 GHz and at center frequency 5 GHz. The patterns of the antenna generated by triangular slots, among the different slot shapes, are the most stable across the operating band and the antenna is linearly polarized.

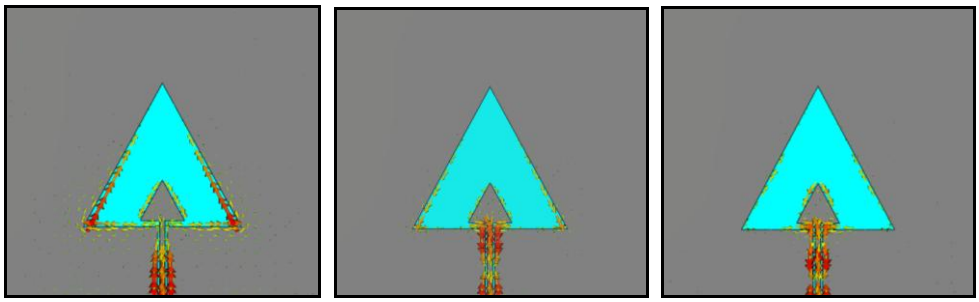

Figure 6: Surface Current Distribution for 2.3GHz, 5 GHz and 7 GHz

IV. Numerical Sensitivity Analysis

A. Patch length Lp and Wp

As the patch length increased upto 17 mm, the resonating frequency decreases and as the length decreases to 13 mm the band width reduces. "Fig 7" shows the graph for Length and Width. At Lp = Wp= 15 mm, there is an optimized performance.

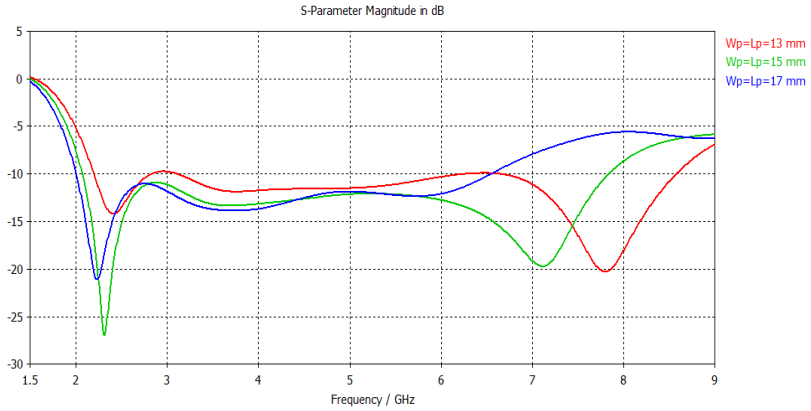

Figure 7: Return loss characteristics for different Wp and Lp of antenna

B. Feed Graph 'h' (coupling between feed and slot)

The feed gap effect on the impedance matching is investigated in [1] and it is found that good impedance matching can be obtained by enhancing the coupling between the feed and slot. When the coupling is increased to a certain value, an optimum impedance bandwidth can be obtained. However, if the coupling is further increased beyond this value, the impedance matching will deteriorate; showing that over coupling can also degrade the impedance matching as under coupling. "Fig. 8" shows the simulated return losses of Antenna with feed gaps of 1.5, 2 and 2.5 mm. It can be observed that the frequency corresponding to the lower edge of the bandwidth is fairly independent of the feed gap 'h', but the frequency corresponding to the upper edge is heavily dependent on it. Moreover, tapering the feed gap will further increase the impedance bandwidth.

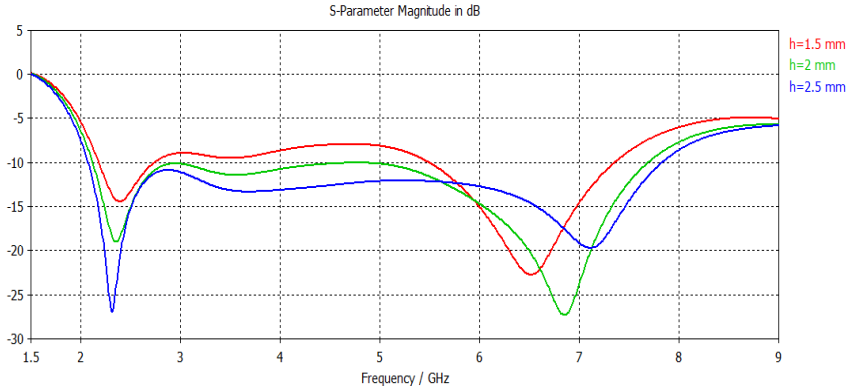

Figure 8: Return loss characteristics for different h of antenna

C. Width of the waveguide 'g'

Width of waveguide 'g' also has major influence to the Return loss characteristics. "Fig 9" shows that g = 0.7 mm gives constant pattern and wide frequency range. For g = 0.5 mm pattern crosses the -10 dbi reference line.

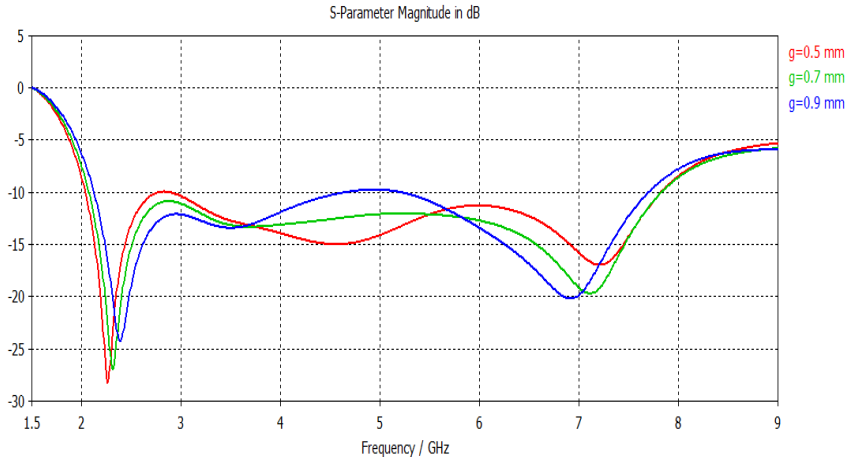

Figure 9: Return loss characteristics for different g of antenna

V. Conclusion

A CPW feed wide slot antenna has been developed and 116% bandwidth is achieved with stable radiation patterns across the whole band. It is found that the antenna feed and slot shapes should be similar for optimum impedance matching, but for better radiation patterns, a triangular shape slot should be used. In addition, the proposed antenna has small size, exhibit stable and almost omni directional radiation patterns in entire operating frequency band, relatively high gain and low cross polarization. Based on these findings the proposed antenna can be further improved for commercial purpose like WLAN, Wi-Fi, Wi- MAX, WTM.

References

[1] H.-D. Chen, "Broadband CPW-fed square slot antennas with a widened tuning stub," IEEE Trans. Antennas Propagat., vol. 51, pp. 1982–1986, 2003.
[2] M. K. Kim, K. Kim, Y. H. Suh, and I. Park, "A T-shaped microstrip-line-fed wide-slot antenna," in IEEE AP-S Int. Symp., 2000, pp. 1500–1503.
[3] Y.W. Jang, "Broadband cross-shaped microstrip-fed slot antenna," Electron. Lett., vol. 36, pp. 2056–2057, 2000.
[4] J.-Y. Sze and K. L. Wong, "Bandwidth enhancement of a microstripline-fed printed wide-slot antenna," IEEE Trans. Antennas Propagat., vol. 49, pp. 1020–1024, 2001.
[5] P. H. Rao, "Feed effects on the dimensions of wide-band slot antennas," Microwave Opt. Tech. Lett., vol. 40, pp. 77–79, 2004.
[6] P. H. Rao, V. F. Fusco, and R. Cahill, "Linearly polarized radial stub fed high performance wide-band slot antenna," Electron. Lett, vol. 37, pp. 335–337, 2001.
[7] Y. W. Jang, "Experimental study of large bandwidth three-offset microstripline-fed slot antenna," IEEE Microwave Wireless Comp. Lett., vol. 11, pp. 425–426, 2001.
[8] "Large-bandwidth double-T-shaped microstrip-fed single-layer single-slot antenna," Microwave Opt. Tech. Lett., vol. 30, pp. 185–187, 2001.
[9] "A circular microstrip-fed single-layer single-slot antenna for multi-band mobile communications," Microwave Opt. Tech. Lett., vol. 37, pp. 59–62, 2003.
[10] "Experimental study of a large bandwidth rectangular microstrip-fed circular slot antenna," Microwave Opt. Tech. Lett., vol. 33, pp. 316–318, 2002.

International Journal of Modern Engineering Research (IJMER)
www.ijmer.com Vol. 3, Issue. 3, May.-June. 2013 pp-1475-1481 ISSN: 2249-6645

Design and Simulation of Low Power 6TSRAM and Control its Leakage Current Using Sleepy Keeper Approach in different Topology

Bikash Khandal, [1] Bikash Roy[2]
[12]*Btech Student, Department of Electronics and Communication Engineering, North Eastern Regional Institute of Science and Technology, India*

Abstract : *Today, low power memory is given most priority in VLSI design. The power is most important aspect for today's technology. So the power reduction for one cell is the vital role in memory design techniques. As the technology growing portable device (e.g. Cell phone, PDA) increases, the Static Power Consumption (Leakage Power) became a significant issue. Leakage current in standby mode is the major part of power loss. We concentrate on the technique that to reduce the leakage current in standby mode. The one CMOS transistor leakage current due to various parameters is the essentiel role of power consumption. The CMOS leakage current to the process level can be decreased by using sleepy keeper technique. The advantages in this technique are ultra-low leakage with dual Vth, state-saving, less area penalty and faster than other techniques like sleepy stack approach, sleep, Zig Zag.*

This project's focus is to reduce leakage power consumption of an 6TSRAM by employing Sleepy Keeper technique in different topology.

Keywords: *CMOS, Leakage current, sleep, Sleepy Stack, Sleepy Keeper, SRAM, Threshold Voltage*

I. INTRODUCTION

Semiconductor memory technology is an essential element of today's electronics. Normally based around semiconductor technology, memory is used in any equipment that uses a processor of one form or another. Indeed as processors have become more popular and the number of microprocessor controlled items has increased so has the requirement for semiconductor memory. An additional driver has been the fact that the software associated with the processors and computers has become more sophisticated and much larger, and this too has greatly increased the requirement for semiconductor memory. In view of the pressure on memory, new and improved semiconductor memory technologies are being researched and development can be very rapid. Nevertheless, the more mature semiconductor memory technologies are still in widespread use and will remain so for many years to come. In addition to these new applications such as digital cameras, PDAs and many more applications have given rise to the need to memories. Accordingly it is not uncommon to see semiconductor memories of 8 Gigabyte and much more required for various applications. With the rapid growth in the requirement for semiconductor memories there have been a number of technologies and types of memory that have emerged. Names such as ROM, RAM, EPROM, EEPROM, Flash memory, DRAM, SRAM, SDRAM, and the very new MRAM can now be seen in the electronics literature. Each one has its own advantages and area in which it may be used.[1][2]

Previously many works had been done in the field of Leakage Current reduction using different techniques like Sleep, Sleep, Zigzag, Stack, Sleepy-Stack, Leakage feedback in different circuits.

Here we present a new VLSI technique to reduce leakage power, the Sleepy Keeper Technique provides an efficient way to reduce leakage power, but disadvantage of this technique increase the delay as the transistor are increased. In this paper 6TSRAM cell was designed with Sleepy Keeper technique and analyze the Leakage, Dynamic power consumption and Static power consumption in different topology.

II. LEAKAGE CURRENT

With the rapid progress in semiconductor technology, chip density and operation frequency have increased, making the power consumption in battery-operated portable devices a major concern. High power consumption reduces the battery service life. IC power dissipation consists of different components depending on the circuit operating mode. First, the switching or dynamic power component dominates during the active mode of operation. Second, there are two primary leakage sources, the *active* component and the *standby* leakage component. The standby leakage may be made significantly smaller than the active leakage by changing the body bias conditions or by power-gating.

There are four main sources of leakage current in a CMOS transistor (Fig 1): Reverse-biased junction leakage current (IREV), Gate induced drain leakage (IGIDL), Gate direct-tunneling leakage (IG), Sub threshold (weak inversion) leakage (ISUB). [3]

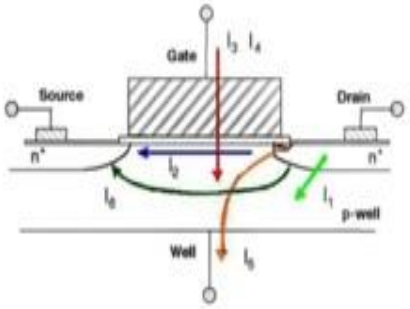

Fig.1Source of Leakage Current in CMOS Transistor

III. Method of Controlling Leakage Power

Dynamic power has been a predominant source of power dissipation recently. However, static power dissipation is becoming a significant fraction of the total power. Leakage power has become a top concern to the field of VLSI. The leakage problem is worse than generally thought because the simple, traditional leakage power estimation of multiplying the average transistor leakage. Leakage power has become a top concern for IC designers in deep submicron process technology nodes 65nm and below. Leakage power is primarily the result of unwanted sub threshold current through the transistor channel when the transistor is turned off. Here some methods that are already used to control the leakage power are Sleep, Zigzag, Stack, Sleepy-Stack, Leakage feedback.

The most well-known traditional approach is the sleep approach [2][3]. In the sleep approach, both (i) an additional "sleep" PMOS transistor is placed between VDD and the pull-up network of a circuit and (ii) an additional "sleep" NMOS transistor is placed between the pull-down network and GND. These sleep transistors turn off the circuit by cutting off the power rails. Fig 3 shows its structure. The sleep transistors are turned on when the circuit is active and turned off when the circuit is idle. By cutting off the power source, this technique can reduce leakage power effectively.

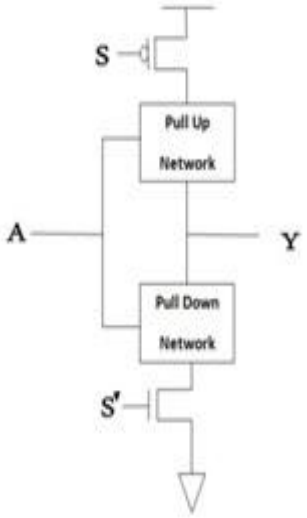

Fig. 2 Sleepy Approach

Another technique for leakage power reduction is the stack approach, which forces a stack effect by breaking down an existing transistor into two half size transistors [5]. Fig 4 shows its structure. When the two transistors are turned off together, induced reverse bias between the two transistors results in sub-threshold leakage current reduction.

The sleepy stack approach combines the sleep and stack approaches. The sleepy stack technique divides existing transistors into two half size transistors like the stack approach [6][7]. Then sleep transistors are added in parallel to one of the divided transistors. Fig 3 shows its structure. During sleep mode, sleep transistors are turned off and stacked transistors suppress leakage current while saving state. Each sleep transistor, placed in parallel to the one of the stacked transistors, reduces resistance of the path, so delay is decreased during active mode.

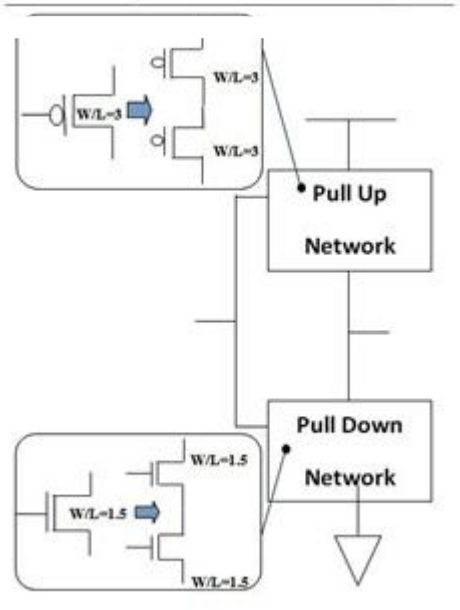

Fig.3 Stack Approach

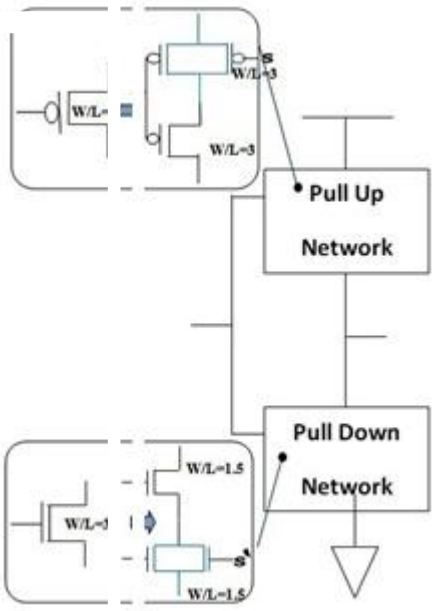

Fig.. Sleepy Stack Approach

The leakage feedback approach is based on the sleep approach. However, the leakage feedback approach uses two additional transistors to maintain logic state during sleep mode, and the two transistors are driven by the output of an inverter which is driven by output of the circuit implemented utilizing leakage feedback [7]. As shown in Fig.6, a PMOS transistor is placed in parallel to the sleep transistor (S) and a NMOS transistor is placed in parallel to the sleep transistor (S'). The two transistors are driven by the output of the inverter which is driven by the output of the circuit. During sleep mode, sleep transistors are turned off and one of the transistors in parallel to the sleep transistors keep the connection with the appropriate power rail.[4][5][6][7]

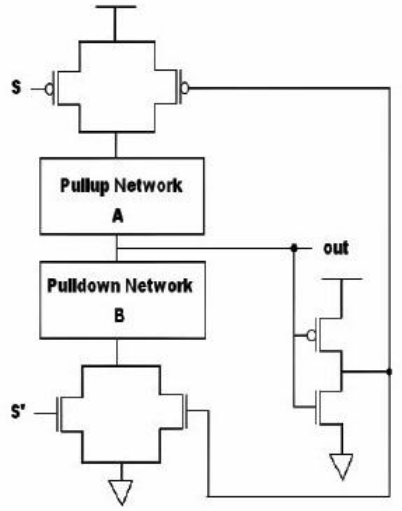

Fig. 5 Leakage Feedback Approach

IV. PROPOSED APPROACH: SLEEPY KEEPER

In this section, we describe our new leakage reduction technique, which we call the "sleepy keeper" approach. This section explains the structure of the sleepy keeper approach as well as how it operates. The basic problem with traditional CMOS is that the transistor are used only in their most efficient, and naturally inverting way namely, PMOS transistor connected to V_{dd} and NMOS transistors connected to is GND. It is well known that pMOS transistors are not efficient at passing GND; similarly it is well known that NMOS transistors are not efficient at passing V_{dd}. However to maintain '1' in sleep mode, given that the value '1' valued has already been calculated, the sleepy keeper approaches uses this output value '1' and an NMOS transistor connected to V_{dd} to maintain output value equal to '1' when in sleep mode. For example, when the output is '1' for an inverter design utilizing the sleepy keeper approach, the current path is shown in the figure, similarly to maintain a value of '0' in sleep mode, given that the '0' value has already be calculated, the sleepy keeper uses this output value of '0' and the p MOS transistor connected to ground to maintain output value equal to '0' when in sleep mode. For example when the output is '0' for an inverter implemented using the sleepy keeper approach, the current path is shown in Fig.6 [7][8][9].

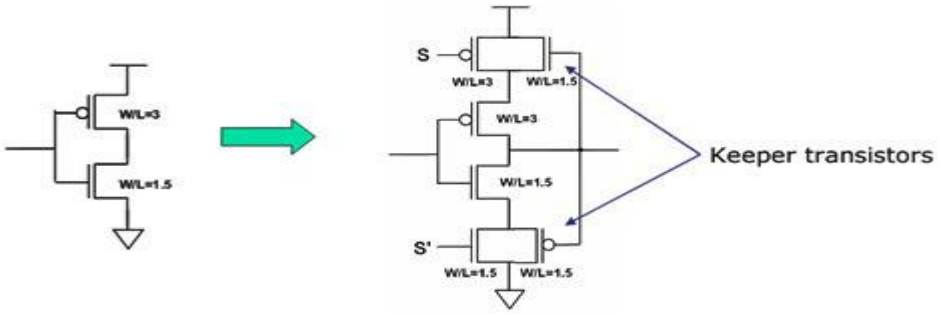

Fig.6 CMOS Inverter to Sleepy Keeper Inverter

V. SRAM

SRAM or Static random Access memory is a form of semiconductor memory widely used in electronics, microprocessor and general computing applications. This form of semiconductor memory gains its name from the fact that data is held in there in a static fashion, and does not need to be dynamically updated. While the data in the SRAM memory does not need to be refreshed dynamically. Static random access memory (SRAM) is a type of volatile semiconductor memory to store binary logic '1' and '0' bits. SRAM uses bi stable latching circuitry made of Transistors MOSFETS to store each bit. When the cell is chosen, the value to be written is stored in the cross-coupled flip-flops. A basic SRAM cell consists of two cross coupled inverters forming a simple latch as storage elements and two switches connecting these two inverters to complementary bit lines to communicate with the outside of the cell.

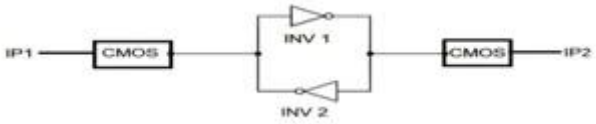

Fig.7 Cross Coupled inverter SRAM cell

VI. 6TSRAM

The schematic of SRAM cell is shown in the Fig.8. It has 2 pull up PMOS and 2 NMOS pull down transistors as two cross coupled inverters and two 2 NMOS access transistors to access the SRAM cell during Read and Write operations. Both the bit lines (BL and BLB) are used to transfer the data during the read and write operations in a differential manner. Bit 0 or 1 in a SRAM cell is stored using two cross coupled inverters. This storage cell has two stable states **0** and **1** which is reinforced because of cross coupling. Two additional *access* transistors serve to control the access to the storage cell during read and write operations. So a typical SRAM cell is a six transistor structure. A 6T SRAM cell requires a careful device sizing to ensure read stability, write margin and data retention in standby modes. Access to the cell is enabled by the word line which controls the two access transistors M5 and M6. They in turn control whether the cell should be connected to the bit lines. Bit lines are used for both read and write operations. Two bit lines are not necessary but they are provided to improve noise margins. In read stability, M1 transistor is required to be much larger than M5 transistor to make sure that the node between M1 and M5 does not flip. In write mode, bit lines overpower cell with a new value. High bit lines must not overpower inverters during read operation.

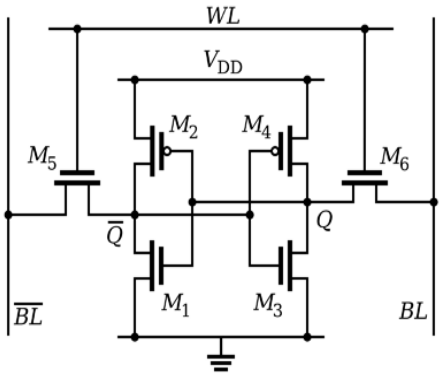

Fig.8 6T SRAM

Read Operation:

The read cycle starts by pre-charging both the bit lines to a logical 1 and then asserting the word line, enabling both the access transistors. If a 1 is stored in the cell, this value is transferred to the bit lines by leaving BL (bit line) at its pre-charged value and discharging BLB to a logical 0 through M1 and M5. The transistors M4 and M6 pull the bit line to a logical 1. If the content of the memory is a 0, then BL is pulled to a logical 0 and BLB to a logical 1.

Write Operation:

If a 0 is to be written, BL and BLB are set to 0 and 1 respectively. A 1 is written by inverting the values of the bit lines. WL (word line) is then asserted and the value that is to be stored is latched in.

VII. DESIGN AND SIMULATION

We have design simple 6TSRAM and 6TSRAM with Sleepy Keeper approach in different technology, the schematic and layouts are designed using Microwind.

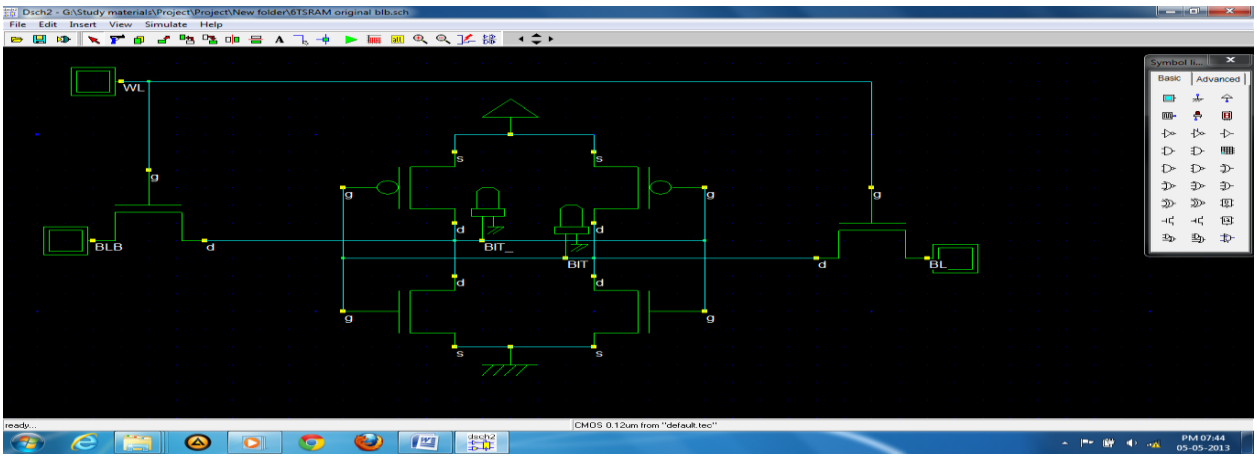

Fig.9 Basic 6TSRAM Cell

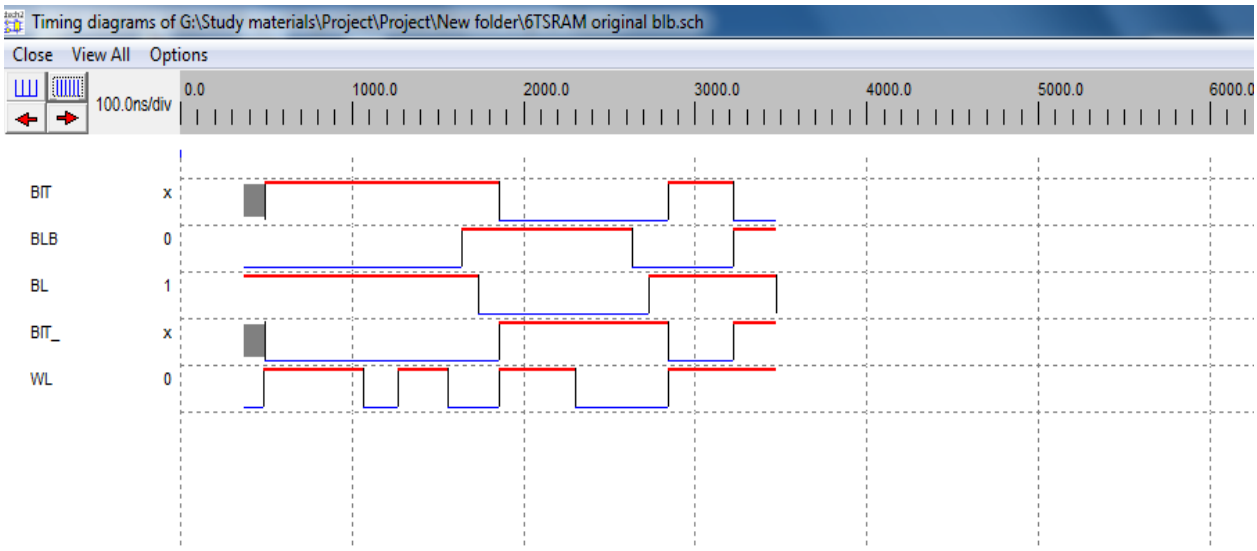

Fig.10 Simulation Result of Basic 6T SRAM cell

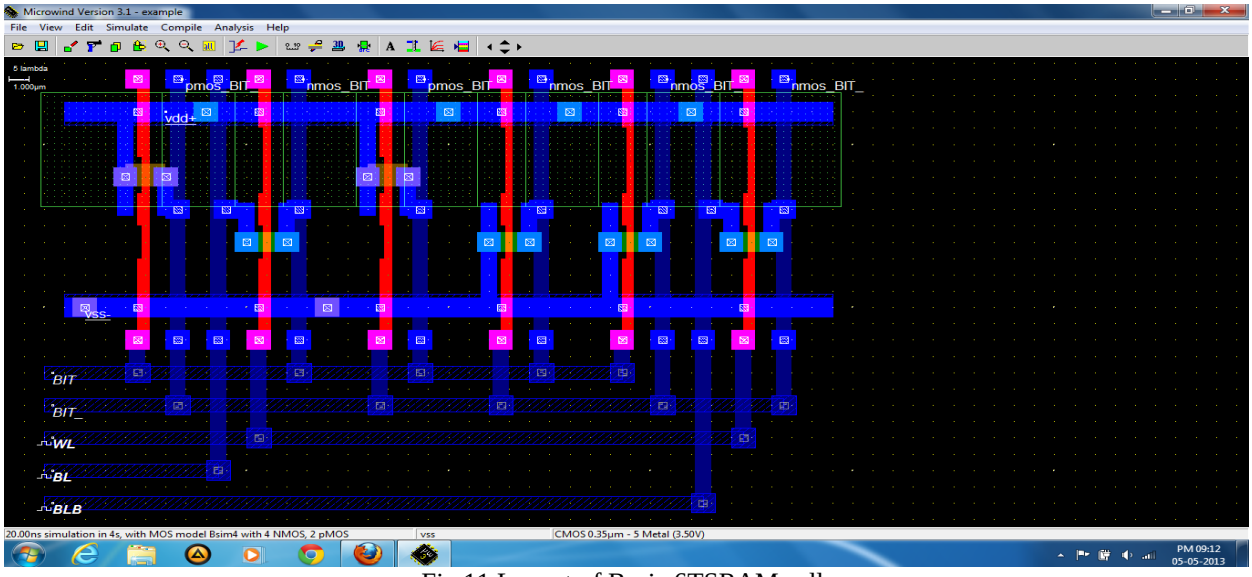

Fig.11 Layout of Basic 6TSRAM cell

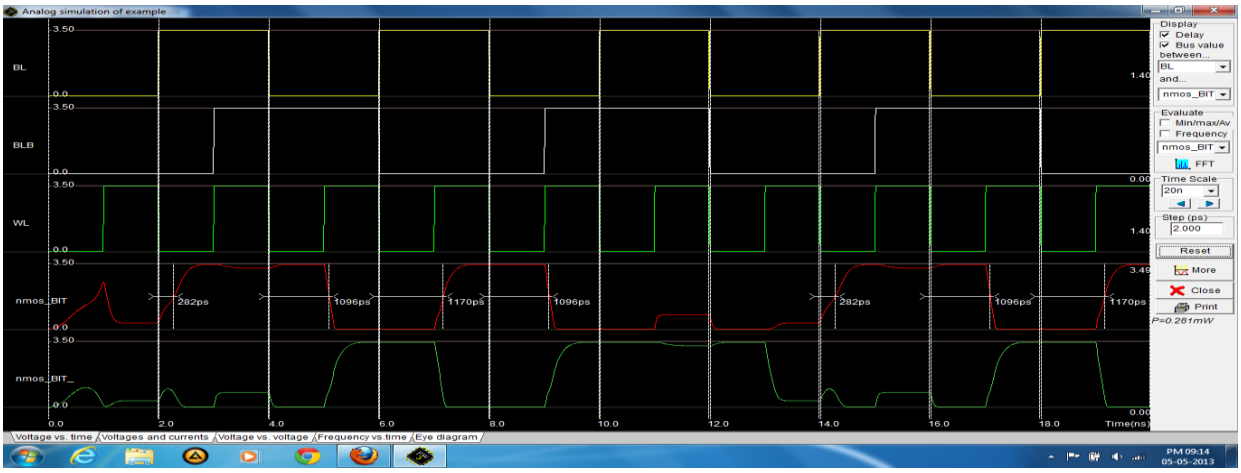

Fig.12 Output of basic 6TSRAM

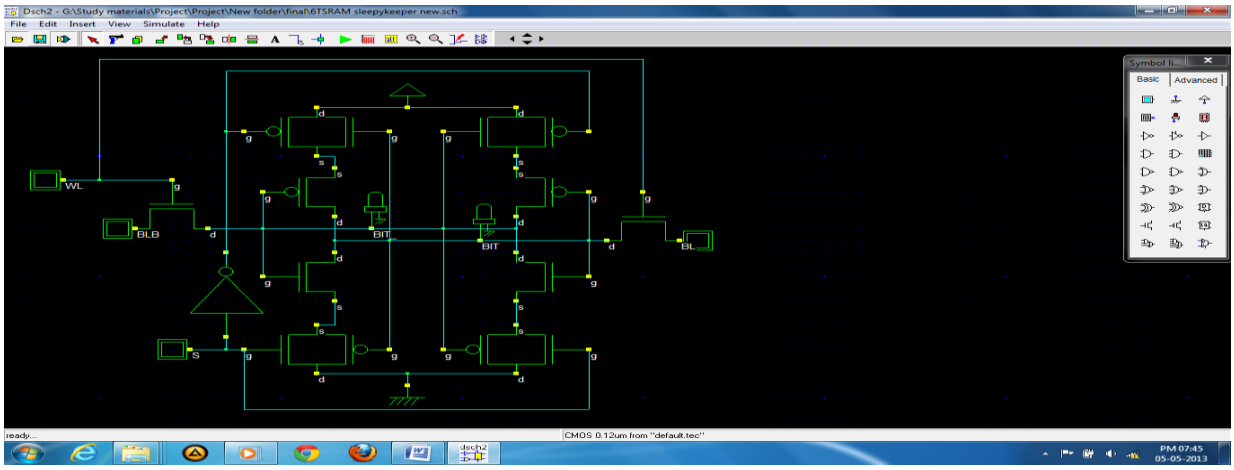

Fig.13 6TSRAm cell using Sleepy Keeper Approach

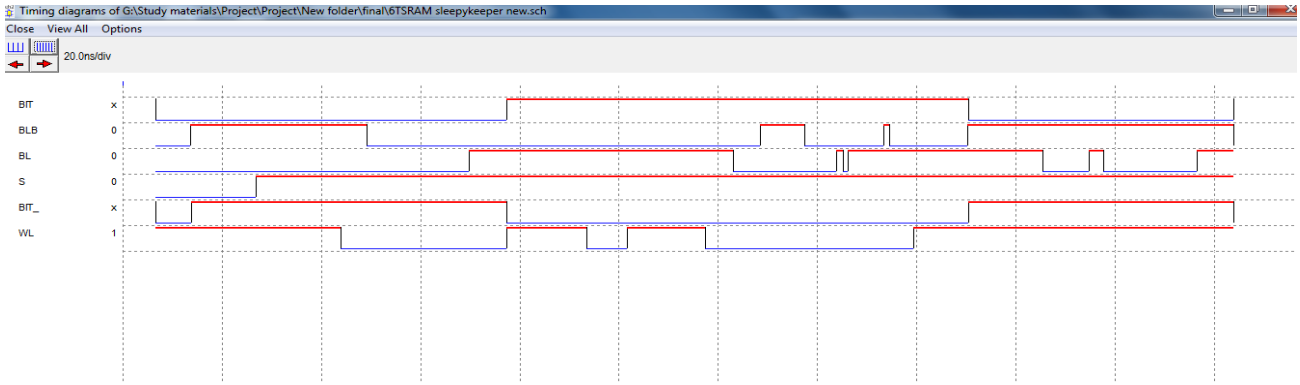

Fig.14 Simulation result of 6TSRAM with Sleepy Keeper Approach

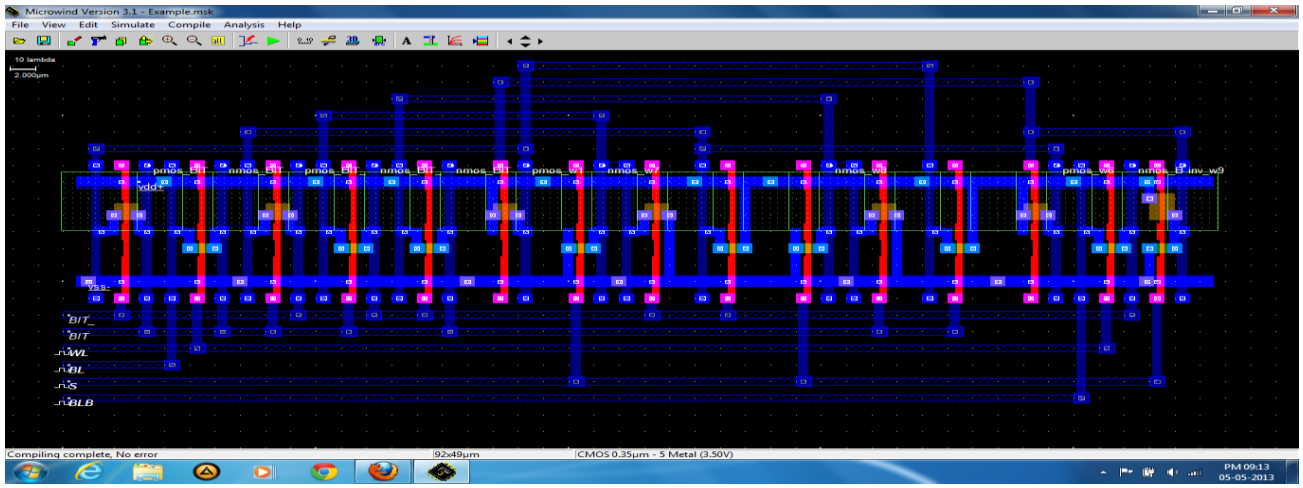

Fig.14 Layout of 6TSRAM using Sleepy Keeper Approach

Comparison between Basic 6TSRAM and 6TSRAM using sleepy Keeper Approach

Topology	Basic SRAM (W)	SRAM using Sleepy Keeper approach (W)
350 nm	270 E-06	90 E-06
250 nm	178 E-06	62 E-06
180 nm	108 E-06	43 E-06
120 nm	96 E-06	37 E-06
65 nm	36 E-06	13 E-06

Table 1. Power consumption of basic 6TSRAM and SRAM using Sleepy Keeper Technique

VIII. CONCLUSION

In this paper we design 6TSRAM by using the "Sleepy Keeper" leakage current reduction technique. The proposed circuits were designed in 65, 120, 180, 250, 350 nanometer CMOS/VLSI technology. In this paper we observed that the proposed technique "Sleepy Keeper" have low power consumption when compared to the other low power techniques and

having delay and area overhead. Based on simulations result with a SRAM Architecture circuit, we find that "Sleepy Keeper approach" achieves up to 65 % less power consumption. Hence it is concluded that the proposed 6TSRAM is used for low power designs and these designed techniques are used for high performance and low power applications.

IX. ACKNOWLEDGEMENTS

We are very thankful to our institute North Eastern Regional Institute of Science and Technology, Arunachal Pradesh, for providing us lab facility, and also to our guide Mr**. Manish Kumar, Assistant Professor, Electronics and Communication Department, NERIST.** We had design and simulate the result in Micro-wind 3.1 software.

REFERENCES

[1] Z. Chen, M. Johnson, L. Wei and K. Roy, "Estimation of Standby Leakage Power in CMOS Circuits Considering Accurate Modeling of Transistor Stacks," International Symposium on Low Power Electronics and Design, pp. 239-244, August 1998.
[2] International Technology Roadmap for Semiconductors by Semiconductor Industry Association, http://public.itrs.net, 2007.
[3] S. Mutoh et al., "1-V Power Supply High-speed Digital Circuit Technology with Multi-threshold- Voltage CMOS," IEEE Journal of Solis-State Circuits, Vol. 30, No. 8, pp. 847-854, August 1995.
[4] Design Of Low Power 8 Bit Sram Architecture Using Leakage Feed Back With Stack & Sleep Stack With Keeper, International Journal of Engineering Research and Applications (IJERA) ISSN: 2248-9622 www.ijera.com Vol. 2, Issue 2,Mar-Apr 2012, pp.192-201
[5] Low-Power Cache Design Using 7t Sram Cell, Ieee Transactions On Circuits And Systems— Ii: Express Briefs, Vol. 54, No. 4, April 2007, pp.318-322
[6] J. Park, "Sleepy Stack: a New Approach to Low Power VLSI and Memory, " Ph.D. Dissertation, School of Electrical and Computer Engineering, Georgia Institute of Technology, 2005.
[7] J.C. Park, V. J. Mooney III and P. Pfeiffenberger, "Sleepy Stack Reduction of Leakage Power," Proceeding of the International Workshop on Power and Timing Modeling, Optimization and Simulation, pp. 148-158, September 2004.
[8] S. Mutoh et al., "1-V Power Supply High-speed Digital Circuit Technology with Multithreshold-Voltage CMOS," IEEE Journal of Solis-State Circuits, Vol. 30, No. 8, pp. 847-854, August 1995.
[9] M. Powell, S.-H. Yang, B. Falsafi, K. Roy and T. N. Vijaykumar,"Gated-Vdd: A Circuit Technique to Reduce Leakage in Deepsubmicron Cache Memories," International Symposium on Low Power Electronics and Design, pp. 90-95, July 2000.

Author's Profile:

Bikash Khandal

Born on 26 January 1991, doing Btech (Final Year) in Electronics and Communication Engineering, from North Eastern Regional Institute of Technology.

Bikash Roy:

Born on 12 May 1989, doing Btech (Final Year) in Electronics and Communication Engineering, from North Eastern Regional Institute of Technology

International Journal of Modern Engineering Research (IJMER)
www.ijmer.com Vol. 3, Issue. 3, May.-June. 2013 pp-1482-1486 ISSN: 2249-6645

Performance and Analysis of Video Compression Using Block Based Singular Value Decomposition Algorithm

M. Anto Bennet[1], R. Nithyadevi[2], Dr. I. Jacob Reglend[3], Dr. C. Nagarajan[4]
[1]*Associate Professor in Department of ECE, Nandha Engineering College, Erode (TN), India*
[2]*PG Student,(Applied Electronics), Nandha Engineering College ,Erode(TN),India.*
[3]*Professor in Department of EEE, Noorul Islam University, Nagercoil (TN), India*
[4]*Professor in Department of EEE, Muthayammal Engineering College, Erode (TN), India.*

Abstract: *This paper presents analysis of video compression based on block SVD Algorithm. Video compression is a process of efficiently coding digital video to reduce the number of bits required in representing video frames. Its purpose is to reduce the storage space and transmission cost while maintaining good quality. Current video compression standards like MPEG, H.26x series are highly computationally expensive and hence they are not suitable for real time applications. Current applications like video calling, video conferencing require low complexity video compression algorithms. The block SVD algorithms are used to provide higher PSNR at the same bit rate. Further we can analysis to reduce the time complexity of the video compression process based on block SVD Algorithm.*

Index Terms: *Block SVD, Low-Complexity video Compression.*

I. Introduction

Video compression is one of the most important blocks of an image acquisition system. With the growth of multimedia and internet, compressions Techniques have become the thrust area in the fields of computers. Many different video compression techniques currently exist for the compression of different types of video frames. Video compression is fundamental to the efficient and cost-effective use of digital imaging technology and applications. In video compression the images are called as frames. Due to the rapid developments in internet technology and computers, popularity of video streaming applications is rapidly growing. Therefore today, storing and transmitting uncompressed raw video requires large storage space and network bandwidth. Special algorithms which take these characteristics of the video into account can compress the video with high compression ratios. In a video, the images called as frames are streamed at the rate of 25-30 frames per second (fps). Video is characterized by huge amount of data. An uncompressed CIF video at a resolution of 288 X 352 at 25 fps has a data rate of30.41Mbits/s. As a result, transmission of raw video requires huge bandwidth. Also, the memory required to store this uncompressed video is enormous. These two drawbacks make it impractical to use raw video. To reduce the transmission bandwidth and the storage requirements, video compression is done. During compression, the redundant information is removed.

Video is a sequence of images which are displayed in order. Each of these images is called a frame. This technology (video compression) reduces redundancies in spatial and temporal directions. Spatial reduction physically reduces the size of the video data by selectively discarding up to a fourth or more of unneeded parts of the original data in a frame. Temporal reduction, Inter-frame delta compression or motion compression, significantly reduces the amount of data needed to store a video frame by encoding only the pixels that change between consecutive frames in a sequence. Compression algorithms typically exploit spatial, temporal and psycho-visual redundancies. Present in a video. Some of the widely used video compression algorithms are MJPEG, MPEG series and H.26x series. In MJPEG (Motion JPEG), each frame is individually coded using the JPEG algorithm. MJPEG does not exploit the temporal redundancies in the video and therefore it results in lower compression. A compression ratio of around 10:1 to 15:1 can be achieved using MJPEG without introducing any visual artifacts. MPEG (Moving Pictures Experts Group) is an experts group set by ISO and IEC. They have come up with standards like MPEG-1, MPEG-2, MPEG-4 etc. which have been widely used for video compression.

The heart of MPEG or H.26x algorithm is the motion estimation and motion compensation block. Motion estimation and compensation is responsible for exploiting the temporal redundancies in the video. Here, rather than coding each block independently, a block in the current frame is used to find the same block in the previous frame. Rather than sending the entire block, only the error and the motion vectors are encoded and sent to the decoder. Therefore the block can be represented with lower number of bits. Motion estimation and compensation is an efficient algorithm and a compression anywhere between 30:1 to 100:1 can be achieved. However, it is highly computationally complex. Due to the high computationally complexity, the power consumption is increased thereby reducing the battery life. Also, hardware implementation becomes difficult. We proposed Block SVD algorithm low computational complexity so greatly reduced time complexity.

The Comparison of the proposed block SVD coding scheme existing relevant non-ME-based low complexity code shows its advantage, which provides higher PSNR at the same bit rate [1]. In SVD algorithm when singular value increases size of compressed image also increases, the quality of compressed image also improve. In BTC with increase in size of block visual quality of image degrades and there is no much reduce in compression size with increase of block size. In DCT when coefficient value is increase Image quality improve of compressed image remains same [2].The latest video compression standard MPEG-4, AVC/H.264 gives 50% improvement in compression efficiency compared to previous standard. Increased computational complexity at the encoder [3].A video surveillance compression system the main problem

is to increase in computational complexity, high energy consumptions, short batter life [4].The main problem for this hybrid coding system also causes interframe dependence in decompression ,the error occur frequently in the error- prone channel, so losses occurred in the channel [5] . Error resilient pre/post-filtering for DCT-based block coding systems coding efficiency heavily suffers from ignoring correlation between blocks. So blocking artifacts present at low bit rate [6]. DCT-SVD video compression technique cannot provide good compression and also energy loss is high [7]. The 2D SVD is the deals with only smaller matrices [8]. H.264/AVC is the higher compression efficiency .It is high computational complexity at the encoder due to the ME process. It is estimated that for the h.264 code, the computational complexity of inter frame coding 5-10 times higher than that of inter frame [9]. The adaptive algorithm which reduces the average memory bandwidth and power consumption is high [10]. Fast three step algorithms cannot be used in low power real time application resource scarce system [11].The high complexity process for encoder side because of two stage adaptive vector quantization is used to implement coding technique [12]. Optimum bit rate pyramid coding method the quality of the reconstructed image is ranged from lossless image compression. It's used for low bit requirement application like visual telephone and telebrowsing only [13].The PIT algorithm is encoding this sequence by transmitting from smallest to the largest size .so it's take longer time for the encoding process [14]. The main drawback of JPEG is blackness appears in the images when the compression ratio is pushed too high [15].

II. Singular Value Decomposition

In Linear Algebra, Singular Value decomposition is nothing but factorization of a matrix in the form

$$A = U \Sigma V \qquad (1)$$

Where U and V are orthogonal matrices and Σ is a diagonal matrix.
A= (Orthogonal) (Diagonal) (Orthogonal)

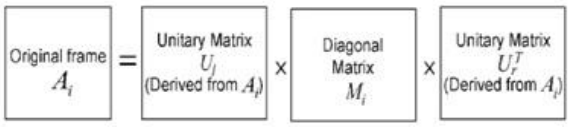

Fig .1.SVD decomposition

Fig .1.shows the SVD decomposition process. The columns of U are composed of the eigenvectors of A^T , the columns of V are composed of the eigenvectors of A^TA. The diagonal values of Σ are nothing but the square roots of the non-zero eigenvalues of both AA^T and A^TA.2D-SVD is an extension of the above mentioned 1DSVD.2D-SVD has been extensively studied for computer vision. The main drawback of 1D-SVD for image compression applications is that, even though it provides the most energy compaction (the coefficients are present only along the diagonal), it requires the transmission of the two eigenvector matrices for each block. This incurs very high overhead thereby reducing the compression efficiency. In 2D-SVD, the eigenvector matrices are extracted from a group of blocks. Therefore, the two matrices have to be transmitted only for a group of blocks. This results in higher compression. The block SVD algorithms are used to achieve higher PSNR at the same bit rate.

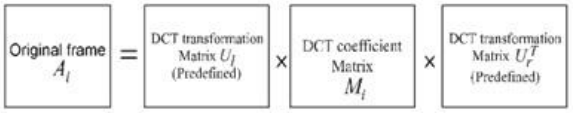

Fig. 2.DCT decomposition

For the DCT one fixed matrix is used, thus U_l=Ur. The DCT decomposition is shown in Fig.2. Since the transformation matrix is fixed, we can simply represent Ai with Mi.

The main problem for block-based 1-D SVD coding is that, although its coefficient matrix contains the fewest nonzero coefficients compared with other transforms, its and transformation matrices are not fixed and, hence, need to be sent to the decoder for each frame. As a result, the overall coding efficiency for the block-based 1-D SVD coding is not very promising.

III. 2d SVD Process

An image or a video frame can be divided into m x m non overlapping blocks. The 2D SVD decomposition is shown in Fig. 3.

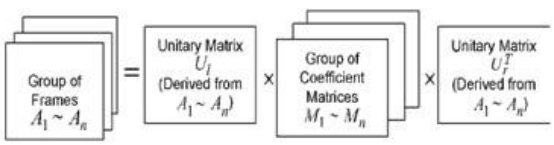

Fig. 3.Two-dimensional SVD decomposition

The basic algorithm to find the coefficient matrix is given below:

1) Given a group of frames $A_1 \ldots\ldots A_n$, find the mean frame Amean. Obtain the mean subtracted frames .i.e. $A_i^1 = A_i - A_{mean}$

2) For any GOB (Group of Blocks), B in the mean-subtracted frames, we denote as each block in B as $b_1 \ldots\ldots b_n$. For each GOB, find the row-row and column-column covariance matrices F and G

$$F=\sum_{i=0}^{n} bib\,T \quad (2)$$

$$G=\sum_{i=0}^{n} bT\,bi \quad (3)$$

U_l and Ur are made up of the k principal eigenvectors of F and s principal eigenvectors of respectively. It has been reported in that the lowest mean squared error is obtained when k=s=1.

3) The coefficient matrix M is obtained using the formula

$$M= U_l^T b_i U_r \quad (4)$$

it is to be noted that Miis not a diagonal
Matrix. However, most of the non-zero coefficients willbe located close to the principal diagonal.

4) To get back the original frame, the mean subtracted block is first obtained using the Formula

$$bi=U_l Mi U_r^T \quad (5)$$

The near optimal approximation of each block is obtained using

$$b_i^{\text{“}}=b_i^{\text{’}}+b_{mean} \quad (6)$$

Where bmean is the corresponding block in the mean frame

IV. Proposed Technique

The application of the algorithm proposed in yielded the following observation. The Fig. 4 shows the video compression based on block SVD algorithm. The various steps are involved in the process of Block SVD video compression techniques. The sequence of process is input video sequence, pre-processing frames, block SVD, decoding and finally will get the reconstructed video sequence.

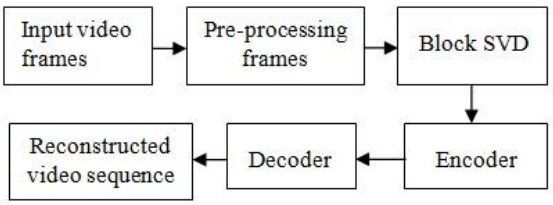

Fig.4. Video compression based on Block SVD method

In video compression the images are called as the frames. Input video frames are given the input to the pre-processing frames. Pre-processing algorithms improve on the performance of a video compression system. Its increases compression efficiency and attenuates coding artifacts. The size of the video frames is high means it's not display for some applications. So the frames are reconstructed to the standard size. Block SVD algorithm used for data reduction technique. The purpose of an encoder is to reduce the number of bits in the original image. Each frame is divided into several blocks. The block sizes are m x m non –over lapping group of blocks (GOB). The group of co-efficient matrices is optimized for block SVD. According to the experiment minimum mean square error is achieved. The decoder is the reverse steps of encoder process. The group of information is decoded in the function of decoder. Here the group of information size is small, successfully received. The Each frame are decode independently, just like an intra frame video codec. The sampling and quantization techniques are used to remove the error in decoder process. Finally get the quality of the reconstructed video frames and also sizes of frames are reduced. It's the purpose of reducing storage space in the memory.

Proposed Algorithm:

1) For videos with low motion, increase in GOP increased the compression ratio while maintaining the PSNR almost constant. This is because the percentage of GI to the coefficients is reduced, while maintaining the energy compaction property of SVD.
2) For videos with high motion, increase in GOP decreased the compression ratio and the PSNR also reduced. This is because the energy is distributed over a large number of coefficients thereby reducing the coding efficiency.

From the above observation it is clear that, for videos with low motion, a large GOP can be used and for videos with high motion a very low value of GOP must be used to maintain the compression ratio and the PSNR. The proposed algorithm is based on this inference:

1) First, the incoming images are divided into 8X8 non-overlapping blocks, Bj where j=0…$\frac{heightxwidth}{64}$
2) For each block Bj, the difference between the current block and the corresponding block in the 10th next frame is computed. The sum of these differences is computed.
3) If this sum is less than the threshold *th*, then the GOP value is set to GOPhigh. If it is greater than the threshold, then it is set to GOPlow. For each block, a group related information is first sent to the decoder. In this GI, the first bit set to 1 if GOP = GOPhigh and it is set to 0 if GOP = GOPlow.
4) The mean block b mean, is calculated using the formula

$$b_{mean} = \frac{1}{GOP}\sum_{i=1}^{GOP} bi \qquad (7)$$

The mean block is then encoded using the JPEG algorithm. It is to be noted that, GOPhigh is chosen to be an integral multiple of GOPlow. If the GOP is GOPlow then GOPhigh GOPlow number of mean blocks are sent.

5) Block SVD mentioned above is used to obtain the corresponding eigenvector matrices U_l^j and U_r^j the group of 8 X 8 coefficient matrices M_1^j…..M_n^j
6) The eigenvectors U_l^j =(U_1^j…..U_8^j) and U_r^j = (U_r^j…..U_r^j) are encoded using the Vector Quantization strategy. Code books of length 256, 256, 128, 128, 128, 64, 64, and 32 are used to quantize the eigenvectors respectively. Eigenvectors derived by applying the Block SVD algorithm to some standard sequences are used to learn the codebooks. The LBG algorithm is used to learn these codebooks. These codebooks are stored in both encoder and decoder, therefore the coding of the eigenvectors is achieved using the least amount of bits possible.
7) There is no need to transmit all the obtained eigenvectors. Let =M_i^j(x,y)denote the coefficient value at frame i of block j at position (x,y). If Xmax denotes the maximum x position of the non-zero coefficients for block j and frames i...N and Ymax denotes the maximum y position of the non-zero coefficients, then we need to transmit only the eigenvectors (U_1^j…..$U_{X\,max}^j$) and (V_1^j…..U_{Ymax}^j) . Six bits are included in GI, to denote the number of eigenvectors sent per GOB.
8) The coefficient matrices M_1^j….M_n^j are then quantized, zigzag read and entropy encoded using the JPEG algorithm.

V. Results

The proposed Block SVD algorithm the GOP was set as 16, as it was found that this provided the highest PSNR for a given bit rate for the specified sequences (Akiyo, Claire).Figure 5 shows the plot of PSNR vs. Bit rate for varying GOP, when the proposed algorithm is applied to the first 192 frames of Claire. From this plot it is clear that the highest PSNR is obtained when GOPhigh = 48 and GOPlow = 4.

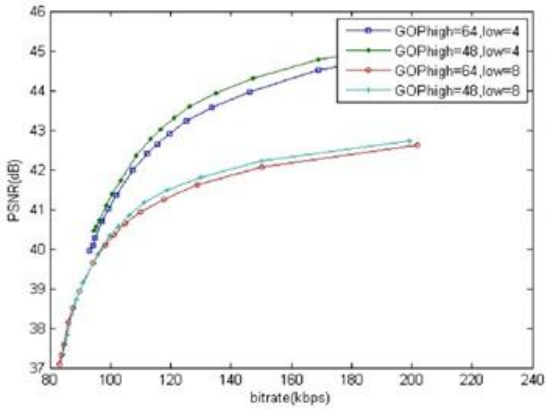

Fig.5. PSNR vs. Bit rate for varying GOP (first 192 frames of Claire).

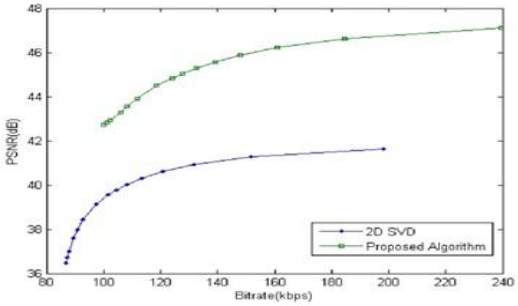

Fig. 6. PSNR vs. Bit rate for Akiyo

Fig.6. gives the plot of PSNR vs. Bit rate for the first 192frames of the Akiyo test sequence.To obtain these results, the GOP of Block SVD algorithm was set as 16 and for the proposed algorithm, GOP_{high} was chosen as 48 and GOP_{low} was chosen as 4. It can be seen clearly from these figures that, our proposed algorithm gives almost 2dB higher PSNR at the same bit rate.

VI. Conclusion

The video compression based on block SVD algorithm was implemented in MATLAB. Video compression is gaining popularity since storage and network bandwidth requirements are able to be reduced with compression. Many algorithms for video compression which are designed with a different target in mind have been proposed. Video compression such as H.261, 263 and 263+, MPEG-1, 2, 4, 7 and H.264. Most recent efforts on video compression for video have focused on scalable video coding. The primary objectives of on-going research on scalable video coding are to achieve high compression efficiency high flexibility (bandwidth scalability) and/or low complexity. Due to the conflicting nature of efficiency, flexibility and complexity, each scalable video coding scheme seeks tradeoffs on the three factors. Designers of video services need to choose an appropriate scalable video coding scheme, which meets the target efficiency and flexibility at an affordable cost and complexity. The biggest advantage of hybrid video coding technique is that it is designed for real time transmission. The low complexity video coding based on Block SVD algorithm used to get reconstructed video frames. The higher PSNR are present at the same bit rate Further we can analysis to reduce the time complexity of the video compression process based on block SVD Algorithm.

References

[1] ZhouyeGu, WeisiLin,Bu-sung Lee, ChiewTong Lau(2012) , " Low - Complexity Video Coding based On Two-Dimensional Singular Value Decomposition", IEEE Transactions on Image Processing, vol. 21, no. 2 , pp 674-687.
[2] Gupta.D ,Pradeep Singh (2012), " A Comparative study of Image Compression between Singular value decomposition, Block truncating coding, Discrete cosine transform and Wavelet ", IJCSNS International journal of computer science and network security", vol.12 No.2
[3] Bahari. A, Arslan.T, and Erdogan .A.T (2009), "Low-Power H.264 Video Compression architectures for Mobile Communication ," IEEE Trans . CircuitSyst. Video Technol., vol. 19, no. 9, pp. 1251–1261.
[4] Liu .L. -M, Li .Z and Delp .E.J (2009) , " Efficien and Low - Complexity Surveillance Video compression using backward - channel aware Wyner-Ziv Video Coding," IEEE Trans. Circuits Syst. Video Technol., vol. 19, no. 4, pp. 453– 465.
[5] Vo . D. T, and Nguyen .T. Q (2008), " Quality enhancement for motion JPEG using Temporal redundancies , " IEEE Trans.Circuits Syst. Video Technol., vol. 18, no.5 , pp. 609–619.
[6] Tu .C.-J, Tran.T. D, andLiang.J (2006), " Error resilient pre / post - filtering for DCT - based block coding systems ," IEEE Trans. Image Process.,vol. 15, no. 1, pp.30–39.
[7] Tong , Lin; Rao, K.R. (2006) , "A Hybrid DCT - SVD Video Compression Technique (HDCTSVD)," Electrical Engineering Department , University of Texas at Arlington, U.S.,
[8] Ding .C and Ye.J (2005) , "Two - Dimensional singular value decomposition (2DSVD) for 2 – D maps and images ," in Proc. SIAM Int. Conf. Data Mining , 2005, pp. 32–43.
[9] Wiegand .T, Sullivan G. J (2003), Bjontegaard .G, and Luthra A. , "Overview of The H.264/AVC video coding standard," IEEE Trans. Circuits Syst. Video Technol., vol. 13, no. 7, pp. 560–576.
[10] DeVleeschouwer.C, Nilsson. T (2002), Denolf.K ,and ormans.J ,"Algorithmicand architectural co - design of a motion - estimation engine for low-power video devices ," IEEE Trans . Circuits Syst.Video Technol., vol. 12, no. 12, pp. 1093–1105.
[11] Jong – Nam kim and Tae-sun choi (1998) " A Fast three – step search algorithm with minimum checking points using unimodal error surface assumption ", IEEE Trans.Consumer electronics,, vol.44,No.3.
[12] Awad Al - Asmari. Kh and AbobakarAhmed.S(1998),"Low Bit Rate Hybrid Coding Scheme For Progressive Image Transmission , " IEEE Trans . Consumer electronics, vol.44, No.1.
[13] Al -Asmari. Kh (1995)," Optimum bit rate pyramid coding withlow computational and memory requirements," IEEE Trans. Circuit and Syst. For video Tech., Vol.5, No.3.
[14] Hwang .W and Derin. H (1995)," Multi resolution multiresourceprogressiveimage transmission," IEEE Trans.Image Processing, Vol.4, No.3.pp .1128-1140.
[15] Pennebaker .W. B and Mitchel .J .L (1993)," JPEG still image data compression standard," Van Nostrand Reinhold, New York.

International Journal of Modern Engineering Research (IJMER)
www.ijmer.com Vol. 3, Issue. 3, May.-June. 2013 pp-1487-1492 ISSN: 2249-6645

Observations on Homogeneous Cubic Equation with Four Unknowns

$$X^3+Y^3=7^{2n}ZW^2$$

S. Vidhyalakshmi[1], M. A. Gopalan[2], A. Kavitha[3]
[123]*Professor, PG and Research Department of Mathematics, Shrimati Indira Gandhi college, Trichy-620 002, Tamil nadu, India*

Abstract: *The non-homogeneous cubic equation with three unknowns represented by the diophantine equation* $X^3+Y^3=7^{2n}ZW^2$ *is analyzed for its patterns of non-zero distinct integral solutions. A few interesting relations between the solutions and special numbers are exhibited.*

Keywords: *Integral solutions, non-homogeneous cubic equation with three unknowns.*

M. Sc 2000 mathematics subject classification: 11D25

Notations:

$t_{m,n}$: Polygonal number of rank n with size m

S_n : Star number of rank n

$\Pr_n$: Pronic number of rank n

j_n : Jacobsthal lucas number of rank n

J_n : Jacobsthal number of rank n

$CP_{m,n}$: Centered Polygonal number of rank n with size m.

G_n : Gnomonic number of rank n

Ky_n : Kynea number of rank n

I. Introduction

The Diophantine equations offer an unlimited field for research due to their variety [1-3]. In particular, one may refer [4-14] for cubic equations with four unknowns. This communication concerns with yet another interesting equation $X^3+Y^3=7^{2n}ZW^2$ representing non-homogeneous cubic with four unknowns for determining its infinitely many non-zero integral points. Various relations between the solutions and special polygonal numbers, centered polygonal numbers, Jacobsthal numbers and kynea numbers are exhibited.

II. Method of Analysis

The cubic equation with four unknowns to be solved for its distinct non-zero integral solution is

$$x^3+y^3=7^{2n}zw^2 \quad (1)$$

Introduction of the transformations,

$$x=u+v,\ y=u-v,\ z=2u \quad (2)$$

in (1) leads to

$$u^2+3v^2=7^{2n}w^2 \quad (3)$$

We present below different methods of solving (3) and thus, in view of (2), different patterns of solutions to (1) are obtained

Pattern: 1.1

Let $w=a^2+3b^2$ (4)

write 7 as

$$7=(2+i\sqrt{3})(2-i\sqrt{3}) \quad (5)$$

Using (4) and (5) in (3) and applying the method of factorization, define

$$(u+i\sqrt{3}v)=(2+i\sqrt{3})^{2n}(a+i\sqrt{3}b)^2 \quad (6)$$

Since the complex number raised to any integer power is also a complex number, we write

$$(2+i\sqrt{3})^{2n} = A_1 + i\sqrt{3}B_1 \quad (7)$$

Where $A_1 = \frac{1}{2}[(2+i\sqrt{3})^{2n} + (2-i\sqrt{3})^{2n}]$

$$B_1 = \frac{1}{2i\sqrt{3}}[(2+i\sqrt{3})^{2n} - (2-i\sqrt{3})^{2n}]$$

Using (7) in (6) and equating the real and imaginary parts, we have

$$\left.\begin{aligned} u &= A_1(a^2-3b^2) - B_1(6ab) \\ v &= A_1(2ab) + B_1(a^2-3b^2) \end{aligned}\right\} \quad (8)$$

Using (8) in (2), we get

$$\left.\begin{aligned} x(a,b) &= A_1(a^2-3b^2+2ab) + B_1(a^2-3b^2-6ab) \\ y(a,b) &= A_1(a^2-3b^2-2ab) - B_1(6ab+a^2-3b^2) \\ z(a,b) &= A_1(2a^2-6b^2) - B_1(12ab) \end{aligned}\right\} \quad (9)$$

Thus, (4) and (9) represent the non-trivial integral solutions of (1)

Properties: 1.2

(i) $x(2^n,1) = A_1(ky_n - 2) + B_1(3J_{2n} - 6j_n + 6(-1)^n - 2)$

(ii) $w(2^n,1) = j_{2n} + 2$

(iii) $z(n,n+1) = -A_1(CP_{8,n} + 16t_{3,n} - 8t_{4,5} + 5) - B_1(24t_{3,n})$

Pattern: 2.1

Write 7 as $7 = \frac{(5+i\sqrt{3})(5-i\sqrt{3})}{4}$ (10)

And $(5+i\sqrt{3})^{2n} = A_2 + i\sqrt{3}B_2$ (11)

Where, $A_2 = \frac{1}{2}[(5+i\sqrt{3})^{2n} + (5-i\sqrt{3})^{2n}]$

$$B_2 = \frac{1}{2i\sqrt{3}}[(5+i\sqrt{3})^{2n} - (5-i\sqrt{3})^{2n}]$$

Using (4), (10), (11) in (3) and employing the method of factorization, we have

$$u + i\sqrt{3}v = \frac{1}{2^{2n}}(A_2 + i\sqrt{3}B_2)(a^2 - 3b^2 + 2i\sqrt{3}ab)$$

Equating real and imaginary parts, we get

$$\left.\begin{aligned} u &= \frac{1}{2^{2n}}[A_2(a^2-3b^2) - B_2(6ab)] \\ v &= \frac{1}{2^{2n}}[A_2(2ab) + B_2(a^2-3b^2)] \end{aligned}\right\} \quad (12)$$

Thus, taking $a = 2^n A$ and $b = 2^n B$ the non-zero distinct integral solutions to (1) are given by

$$x(A,B) = A_2(A^2 - 3B^2 + 2AB) + B_2(A^2 - 3B^2 - 6AB)$$

$$Y(A,B) = A_2(A^2 - 3B^2 - 2AB) - B_2(A^2 - 3B^2 + 6AB)$$

$$Z(A,B) = A_2(2A^2 - 6B^2) - B_2(12AB)$$

$$W(A,B) = 2^{2n}(A^2 + 3B^2)$$

Properties:2.2

$$(i)w(2^n,1) = [3J_{2n} + 1][j_{2n} + 2]$$

$(ii)y(1,n) = A_2[-2t_{5,n} - 3\mathrm{Pr}_n + 3t_{4,n} + 1] - B_2[-S_n + 3t_{4,n} + 2]$

$(iii)x(n+1,n) = A_2[4\mathrm{Pr}_n - 4t_{4,n} + 1] - B_2[4t_{4,n} + 4\mathrm{Pr}_n - 1]$

Pattern:3.1

Introduce the linear transformations

$u = \alpha + 3T, v = \alpha - T$ (13)

Let $w = a^2 + 12b^2$ (14)

Write 7 as

$$7 = \frac{(4 + i\sqrt{12})(4 - i\sqrt{12})}{4} \quad (15)$$

and $(4 + i\sqrt{12})^{2n} = (A_3 + i\sqrt{12}B_3)$ (16)

Where $A_3 = \frac{1}{2}\left[(4 + i\sqrt{12}))^{2n} + (4 - i\sqrt{12})^{2n}\right]$

$$B_3 = \frac{1}{2i\sqrt{12}}\left[(4 + i\sqrt{12}))^{2n} - (4 - i\sqrt{12})^{2n}\right]$$

Using (14), (15) and (16) and employing the method of factorization, define

$$2\alpha + i\sqrt{12}T = \frac{1}{2^{2n}}[A_3 + i\sqrt{12}B_3)(a^2 - 12b^2 + i2\sqrt{12}ab)$$

Equating real and imaginary parts, we have

$$\left.\begin{aligned}\alpha &= \frac{1}{2^{2n+1}}[A_3(a^2 - 12b^2) - B_3(24ab)]\\ T &= \frac{1}{2^{2n}}[A_3(2ab) + B_3(a^2 - 12b^2)\end{aligned}\right\} \quad (17)$$

Substituting (17) in (13), we get

$$\left.\begin{aligned}u &= \frac{1}{2^{2n+1}}[A_3(a^2 - 12b^2 + 12ab) - B_3(24ab - 6a^2 + 72b^2)\\ v &= \frac{1}{2^{2n+1}}[A_3(a^2 - 12b^2 - 4ab) - B_3(24ab + 2a^2 - 24b^2)]\end{aligned}\right\} \quad (18)$$

Replacing a by $A2^{n+1}$ and b $B2^{n+1}$, the corresponding integral solutions are given by

$x(A,B) = 2[A_3(2A^2 - 24B^2 + 8AB) - B_3(48AB - 4A^2 + 48B^2)]$

$y(A,B) = 2[A_3(16AB) - B_3(-8A^2 + 96B^2)]$

$z(A,B) = 4[A_3(A^2 - 12B^2 + 12AB) - B_3(24AB - 6A^2 + 72B^2)]$

$w(A,B) = 2^{2n+2}(A^2 + 12B^2)$

Properties: 3.2

$(i)x(n,1) = 2[A_3(CP_{4,n} + 6\mathrm{Pr}_n - 6t_{4,n} - 25) - B_3(-t_{10,n} + 45\mathrm{Pr}_n - 45t_{4,n} + 48)]$

$(ii)y(n+1,n) = A_3(32\mathrm{Pr}_n) - 16B_3(t_{24,n} + 8\mathrm{Pr}_n - 8t_{4,n} + 1)$

$(iii)w(2^n,1) = j_{4n+1} + 9J_{2n+3} - 2$

Note: .3.3

Replacing (13) by $u = \alpha - 3T$ and $v = \alpha + T$ (19)

And repeating the process as in pattern.3 the corresponding non-zero distinct integral solutions to (1) are obtain as

$x(A,B) = 2[A_3(2A^2 - 24B^2 - 8AB) + B_3(-48AB + A^2 - 12B^2)]$

$y(A,B) = 2[A_3(-16AB) - B_3(3A^2 - 36B^2)]$

$z(A,B) = 4[A_3(A^2 - 12B^2 - 12AB) - B_3(24AB + A^2 - 12B^2)]$

$$w(A,B) = 2^{2n+2}(A^2 + 12B^2)$$

Properties: 3.4

$$(i)x(n,1) = A_3(t_{10,n} - 13\,\mathrm{Pr}_n + 13t_{4,n} - 48) + B_3(t_{6,n} - 95\,\mathrm{Pr}_n + 95t_{4,n} - 24)$$
$$(ii)y(n,1) = A_3(-32\,\mathrm{Pr}_n + 32t_{4,n}) + 6B_3(12t_{4,n} - 1)$$
$$(iii)z(n,1) = A_3(t_{10,n} - 45\,\mathrm{Pr}_n + 45t_{4,n} - 48) - B_3(CP_{8,n} + 95\,\mathrm{Pr}_n - 95t_{4,n} - 49)$$

Pattern:4.1

Instead of (15) we write 7 as

$$7 = \frac{(10 + i\sqrt{12})(10 - i\sqrt{12})}{16} \tag{20}$$

And $(10 + i\sqrt{12})^{2n} = (A_4 + i\sqrt{12}B_4)$ (21)

Where $A_4 = \frac{1}{2}[(10 + i\sqrt{12})^{2n} + (10 - i\sqrt{12})^{2n}$

$$B_4 = \frac{1}{2i\sqrt{12}}[(10 + i\sqrt{12})^{2n} - (10 - i\sqrt{12})^{2n}$$

Using (14), (20) and (21) and equating real and imaginary parts, we have

$$\left.\begin{aligned}\alpha &= \frac{1}{2^{4n+1}}[A_4(a^2 - 12b^2) - B_4(24ab)] \\ T &= \frac{1}{2^{4n}}[A_4(2ab) + B_4(a^2 - 12b^2)]\end{aligned}\right\} \tag{22}$$

Substituting (22) in (13), we get

$$u = \frac{1}{2^{4n+1}}[A_4(a^2 - 12b^2 + 12ab) - B_4(24ab - 6a^2 + 72b^2)]$$
$$v = \frac{1}{2^{4n+1}}[A_4(a^2 - 12b^2 - 4ab) - B_4(24ab + 2a^2 - 24b^2)]$$

To get a integer solution replacing a by $2^{n+1}A$ and b by $2^{n+1}B$

$$x(A,B) = 2[A_4(2A^2 - 24B^2 + 8AB) - B_4(48AB - 4A^2 + 48B^2)]$$
$$y(A,B) = 2[A_4(16AB) - B_4(-8A^2 + 96B^2)]$$
$$z(A,B) = 4[A_4(A^2 - 12B^2 + 12AB) - B_4(24AB - 6A^2 + 72B^2)]$$
$$w(A,B) = 2^{4n+2}(A^2 + 12B^2)$$

Properties: 4.2

(i) $x(2^n,1) = 4A_4(ky_n + 2j_n - 11 - 2(-1)^n) + 8B_4(ky_n - 14j_n - 11 + 14(-1)^n)$

(ii) $y(n,1) = A_4(32t_{3,n} - 32t_{4,n}) - B_4(-16t_{4,n} + 192)$

(iii) $z(n+1,n) = 4[A_4(t_{4,n} + 7G_n + 8) - B_4(CP_{16,n} + CP_{20,n} + 78t_{4,n} - 8)]$

Note: 4.3

Using (19) and repeating the process as in pattern.4, the non-zero distinct integral solutions to (1) are given by

$$x(A,B) = 2[A_4(2A^2 - 24B^2 - 8AB) - B_4(48AB + 4A^2 - 48B^2)]$$
$$y(A,B) = 2[A_4(-16AB) - B_4(8A^2 - 96B^2)]$$
$$z(A,B) = 4[A_4(A^2 - 12B^2 - 12AB) - B_4(24AB + 6A^2 - 72B^2)]$$
$$w(A,B) = 2^{4n+2}(A^2 + 12B^2)$$

Properties:4.4

$(i)x(n,1) = A_4[4(t_{6,n} - 3\Pr_n + 2t_{4,n} - 12)] - 8B_4[CP_{4,n} + 10\Pr_n - 11t_{4,n} - 13]$

$(ii)y(n+1,n) = -64A_4t_{3,n} + 16B_4(t_{8,n} + 8t_{4,n} - 1)$

$(iii)z(n+1,n) = -4A(CP_{20,n} + 13t_{4,n} - 1) + 24B_4(t_{12,n} + 2t_{4,n})$

Pattern: 5.1

(3) can be written as

$$\frac{3v}{7^n w - u} = \frac{7^n w + u}{v} = \frac{p}{q}, q \neq 0 \quad (23)$$

Which is equivalent to the system of equations

$$pu + 3vq - 7^n wp = 0 \quad (24)$$

$$qu - pv + 7^n qw = 0 \quad (25)$$

Applying the cross-multiplication method, we get

$u = 7^n(3q^2 - p^2)$

$v = -2 * 7^n pq$

$w = -p^2 - 3q^2$

Thus, the corresponding non zero distinct integral solutions to (1) are given by

$x = 7^n(3q^2 - p^2 - 2pq)$

$y = 7^n(3q^2 - p^2 + 2pq)$

$z = 2 * 7^n(3q^2 - p^2)$

$w = -p^2 - 3q^2$

Properties: 5.2

$(i)7^n[x(7^n,1)]$ is a difference of two square

$(ii)x(7^n,1) + y(7^n,1) \equiv 0 (\mathrm{mod}\, 7)$

$(iii)6 * 7^n[x(7^n,7^n) - y(7^n,7^n)]$ is a nasty number

$(iv)z(7^n,7^n)$ is a perfect square

$(v)w(2^n,1) = -(j_{2n} + 2)$

Pattern: 5.3

(23) can be written as

$$\frac{v}{7^n w - u} = \frac{7^n w + u}{3v} = \frac{p}{q} \quad (26)$$

Repeating the process as in pattern.5, the non-zero distinct integral solutions to (1) are obtain as

$x = 7^n(q^2 - 3p^2 - 2pq)$, $y = 7^n(q^2 - 3p^2 + 2pq)$

$z = 2 * 7^n(q^2 - 3p^2)$, $w = -(3p^2 + q^2)$

Properties: 5.4

$(i)x(n,1) = -7^n(CP_{6,n} - \Pr_n + t_{4,n} - 2)$

$(ii)y(1,n) = 7(CP_{4,n} - t_{4,n} - 4)$

$(iii)z(n,n+1) = 2 * 7(-2t_{4,n} + G_n + 2)$

III. Conclusion

To conclude, one may search for other pattern of solutions and their corresponding properties

References

[1] Dickson. I. E. ‘”History of the Theory of Numbers’’ (Vol 2. Diophantine analysis, New York, Dover, 2005).
[2] Mordell .L J., “Diophantine Equations’’ (Academic Press, New York, 1969)
[3] Carmichael. R.D. “The Theory of numbers and Diophantine Analysis’’, (New York, Dover, 1959).
[4] M.AGopalan and K.Geetha, Observations on cubic equation with four unknowns $x^3+y^3+xy(x+y)=z^3+2(x+y)w^2$, International journal of pure and Applied Mathematical sciences, Vol.6, No: 1, 2013, 25-30
[5] M.A.Gopalan and S.Premalatha, Integral solutions of $(x+y)(xy+w^2)=2(k^2+1)z^3$, Bulletin of Pure and Applied sciences, vol.29E,No:2 2009,197-202.
[6] M.A.Gopalan and V.Pandichelvi, Remarkable solutions on the cubic equations with four unknowns $x^3+y^3+z^3=28(x+y+z)w^2$, Antarctica J.Math., Vol.7, No.4, 2010, 393-401,
[7] M.A.Gopalan and S.Premalatha, On the cubic Diophantine equation with 4 unknowns $(x-y)(xy-w^2)=2(n^2=2n)z^3$, Integral journal of Mathematical sciences, Vol.9, No.12, Jan-June 2010, 171-175
[8] M.A.Gopalan and J.Kaligarani, Integral solutions of $x^3+y^3+(x+y)xy=z^3+w^3+zw(z+w)$, Bulletin of Pure and Applied sciences, Vol.29E, No.1, 2010, 169-173
[9] M.A.Gopalan and S.Premalatha, Integral solutions of $(x+y)(xy+w^2)=2(k+1)z^3$, the global journal of Applied Mathematics and mathematical sciences, Vol.3, N0:1-2, Jan-Dec.2010, 51-55
[10] M.A.Gopalan, S.Vidhyalakshmi and S.Mallika, Observation on the Cubic equations with 4 unknowns $xy+2z^2=w^3$, The Global journal of Mathematics and Mathematical Sciences, Vol.2, No.1, 2012,69-74
[11] M.A.Gopalan V.Sangeetha and Manju Somanath, Lattice points on the homogeneous cubic equation with 4 unknowns $(x+y)(xy+w^2)=(k^2-1)z^3, k>1$, Indian journal of sciences, vol.2, No.4, 2013, 97-99.
[12] M.A.Gopalan, S.Vidhyalakshmi and G.Sumathi On the homogeneous cubic equation with 4 unknowns $x^3+y^3=14z^3-3w^2(x+y)$, Discovery, Vol.2, No.4, Oct.2012, 17-19
[13] M.AGopalan, S. Vidhyalakshmi and S.Mallika,, Observation on the Cubic equations with 4 unknowns $2(x^3+y^3)=z^3+w^2(x+y)$, IJAMP, Vol.4,No.2, July-Dec. 2012, 103-107,
[14] M.A.Gopalan and V.Pandichelvi, on the cubic equations with four unknowns $x^2-xy+y^2+k^2+2kw=(k^2+3)z^3$, Impact J.Sci.Tech., Vol.1, No.1 2012, 81-86

International Journal of Modern Engineering Research (IJMER)
www.ijmer.com Vol. 3, Issue. 3, May.-June. 2013 pp-1493-1500 ISSN: 2249-6645

Study on Effect of Manual Metal Arc Welding Process Parameters on Width of Heat Affected Zone (Haz) For Ms 1005 Steel

Ajay N.Boob, [1] Prof.G. K.Gattani[2]
[1]*P.G. Student, M.E (CAD/CAM) B.N.College of Engineering. Pusad Dist. Yavatmal*
[2]*Associate, Professor B.N.College of Engineering. Pusad Dist. Yavatmal*

Abstract: *Heat flow in welding is mainly due to heat input by welding source in a limited zone and it subsequent flow into body of work piece by conduction. A limited amount of heat loss is by a way of convection and radiation. Local Heating and cooling of metal shrinkage on solidification and structural change on solidification cause temperature distribution. In the present work, authors have investigated the width of HAZ with various process parameters like heat input & welding speed. In manual metal arc welding (MMAW), selecting appropriate values for process variables is essential in order to control heat-affected zone (HAZ) dimensions and get the required bead size and quality.*
In this study, the effect of various welding parameters on the weldability of Mild Steel specimens having dimensions 125mm× 75mm× 5 mm welded by manual metal arc welding (MMAW) for single V-Butt joint were investigated. The welding current, arc voltage, welding speed, heat input rate are chosen as welding parameters. The effect of these parameters on the size of Heat affected zone is investigated.
Key Words: *MMAW, welding speed, heat input, heat affected zone (HAZ).*

I. Introduction

Manual metal arc welding was first invented in Russia in 1888. It involved a bare metal rod with no flux coating to give a protective gas shield. The development of coated electrodes did not occur until the early 1900s when the Kjellberg process was invented in Sweden and the Quasi-arc method was introduced in the UK [1]. It is worth noting that coated electrodes were slow to be adopted because of their high cost.

However, it was inevitable that as the demand for sound welds grew, manual metal arc became synonymous with coated electrodes. When an arc is struck between the metal rod (electrode) and the work piece, both the rod and work piece surface melt to form a weld pool. Simultaneous melting of the flux coating on the rod will form gas and slag which protects the weld pool from the surrounding atmosphere. The slag will solidify and cool and must be chipped off the weld bead once the weld run is complete (or before the next weld pass is deposited).[2]

Welding is an efficient and economical method for joining of metals. Welding has made significant impact on the large number of industry by raising their operational efficiency, productivity & service life the plant and relevant equipment. Welding is one of the most common fabrication techniques which is extensively used to obtained good quality weld joints for various structural components. The present trend in the fabrication industries is to automate welding processes to obtained high production rate.

Arc welding, which is heat-type welding, is one of the most important manufacturing operations for the joining of structural elements for a wide range of applications, including guide way for trains, ships, bridges, building structures, automobiles, and nuclear reactors, to name a few. It requires a continuous supply of either direct or alternating electric current, which create an electric arc to generate enough heat to melt the metal and form a weld.

The arc welding process is a remarkably complex operation involving extremely high temperatures, which produces severe distortions and high levels of residual stresses. These extreme phenomena tend to reduce the strength of a structure, which becomes vulnerable to fracture, buckling, corrosion and other type of failures.

Hardness is very important mechanical property of material but during welding high heating and rapid cooling influence the hardness of the weld as well as the Heat affected zone (HAZ). Also the optimum hardness of weld and heat affected zone (HAZ) at minimal heat input rate for 60˚ and 70˚ bevel angle weldments have been investigated.[3]

A mathematical models was developed to Study the effects of process variables and heat input on the heat affected zone (HAZ) of submerged arc welds in structural steel pipes.[4]

High deposition rate welding process which can produced a smooth bead with deep penetration at a faster travel speed also welding input parameters plays a very significant role in determining the quality of the weld joint have been investigated.[5] .

A numerical model of fluid flow and temperature field in GMAW was established according to the new mode of arc heat flux distribution. By using a numerical simulation technique, the effects of welding heat input on microstructure and hardness in HAZ of HQ130 steel were studied[6].

The effect of welding parameters on the size of the heat affected zone (HAZ) and its relative size as compared to the weld bead of submerged arc welding. It is discovered that the welding parameters influences the size of weld bead and HAZ differently which can be relate to the effect of welding parameters on the various melting efficiencies. This difference in behavior of HAZ and weld bead can be explored to minimize the harmful effect of HAZ in future welds.[7]

In this study, the effect of various welding parameters on the weld ability of Mild Steel specimens having dimensions 125mm× 75mm× 5 mm welded by manual metal arc welding (MMAW) for single V-Butt joint were investigated. The welding current, arc voltage, welding speed, heat input rate are chosen as welding parameters.
The effect of these parameters on the size of heat affected zone is investigated.

II. Experimental Procedure

2.1 Material

The material used for manual metal arc welding (MMAW) is SAE 1005 mild steel.
The entire specimens were machined into the dimensions of 125mm long x 75mm x 04mm thick.
The details composition (weight %) of specimens is shown in Table 1. This metal had very good welding characteristics and could be welded by all of the common welding techniques.
The typical Thermal and Mechanical properties of carbon steels at room temperature (25°C) are shown in Table 2

Table 1 The Chemical Composition of the used steel (SAE 1005) (weight %) of specimens [9,10]

Sample Identity	C	Si	Mn	P	S	Cr	Mo	Ni	Al	C	Ti
Wt%	0.035	0.024	0.104	0.0062	0.0033	0.007	0.0047	0.0102	0.039	0.004	0.0026

Table 2 Thermal and Mechanical properties of Steel SAE1005 [9, 10]

Property	**Value**	**Unit**
Conductivity	42	W/mk
Specific Heat	481	J/Kg-K
Density	7872	Kg/m
Poisson's Ratio	0.27-0.30	
Elastic Modulus	190 to 210	GPa

2.2 Welding Tools

This sections provides the important specifications of the tool used in the welding process

2.2.1 Welding Machine

Welding machine used for welding is a general purpose welding machine (Usha Welding Machine ® C/O). The Technical Specifications of Welding Machine are as stated in Table 3

Fig. 1 Welding Machine

Table: 3 Technical specification of welding machine

Welding Machine Model	Welding Range (mA)	Striking voltage (V)	Duty range	Welding voltage(kVA)	Primary voltage(V)	Primary current (Amp)
EAD 25	50 to 250	65	60%	32	220-440	30 to 20

2.2.2 Welding rod

Welding rod is an electrode used to weld the metal. The Technical Specifications of Welding rods are as stated in Table 4

Fig. 2 Welding electrode/rod

Table: 4 Technical specification of welding rod/electrode

Material	Diameter	Length	AWS/SFA	IS
MS	3.15mm	350 mm	5.1m, E6013	8142004-ER4211X

2.3 Sample Preparation

The Choice of sample for a microscopic study is very important. In the manual welding process the speed of welding varies along the length. Therefore a sample is taken from the middle section of the welded plate where the welder's speed of welding is assumed to be constant. In the present experimentation SAE1005 M.S sheet was selected. Six sample plates of dimensions (12.5x7.5x0.5) cm3 were cut from the sheet. All the six plates of mild steel were welded on their surfaces lengthwise by varying the parameters. Each sample is tested for varying welding speed, current & voltage which is shown in table 5. Heat input has been calculatd & shown before each sample in table no.5. The photographic views of the welded plates are shown in Fig.4.

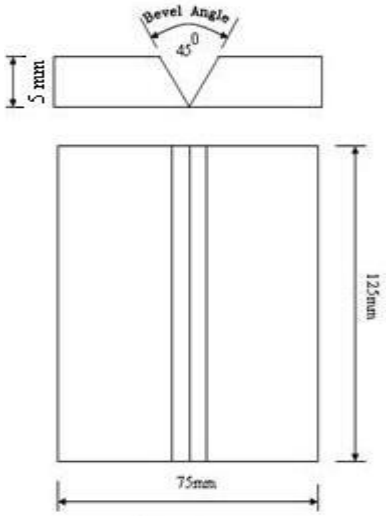

Fig. 3


Front side of welded material Back side of welded material
Fig. 4 Welded Specimens

Table 5 Process parameters used in the experimentation.

S. No.	Welding voltage(V)	Welding current(A)	Arc time(sec)	Welding speed (mm/min)	Heat Input** (J/mm)
1	30	**150**	**43**	**174.42**	**1547.98**
2	30	**150**	**36.9**	**203.25**	**1328.41**
3	30	**150**	**27.15**	**276.24**	**977.37**
4	30	**200**	**47.8**	**156.90**	**2294.34**
5	30	**200**	**41.2**	**182.03**	**1977.69**
6	30	**200**	**36.2**	**207.18**	**1737.61**

Welding speed (v): Welding Speed is defined as the rate of travel of the electrode along the seam or the rate of travel of the work under the electrode along the seam. Weld travel Speed = Travel of electrode/arc time, mm/min.[1]

****Heat input rate (Q):** Heat input is a relative measure of the energy transferred per unit length of weld. Heat input is typically calculated as the ratio of the power (i.e., voltagex current) to the velocity of the heat source (i.e., the arc) as follows -

Heat input rate or arc energy = V×I×60 /v joules per mm

Where, V= arc voltage in volts, I = welding current in ampere,v = speed of welding in mm/min.[1]

III. 3. Result & Discussion

3.1microstructure of Weld Metal:-

To study the metallurgical structure of the base metal, weld zone as well as heat affected zone (HAZ) with different heat inputs of all the samples have been cleaned by zero grade emery paper. All the samples were dipped in 2% nital agent & finally dried by using air blower. The microstructure of base metal, weld zone as well as heat affected zone(HAZ) of all the samples have been carried out by optical microscope having 400X zoom. The metallurgical structure of base metal, weld & HAZ of all the samples are shown in figure. 5,6,7,8,9,10

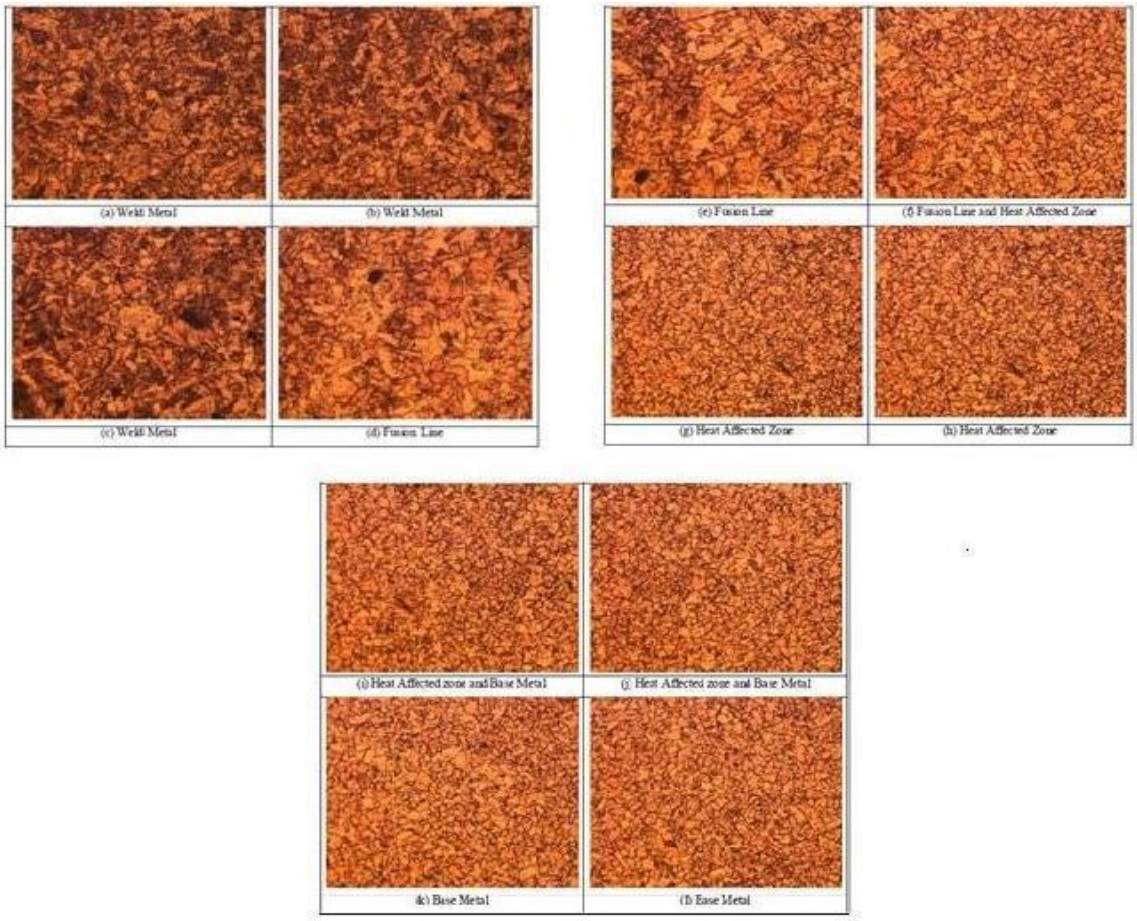

Figure : 5 Microstructure with heat input = 1547.98J/mm

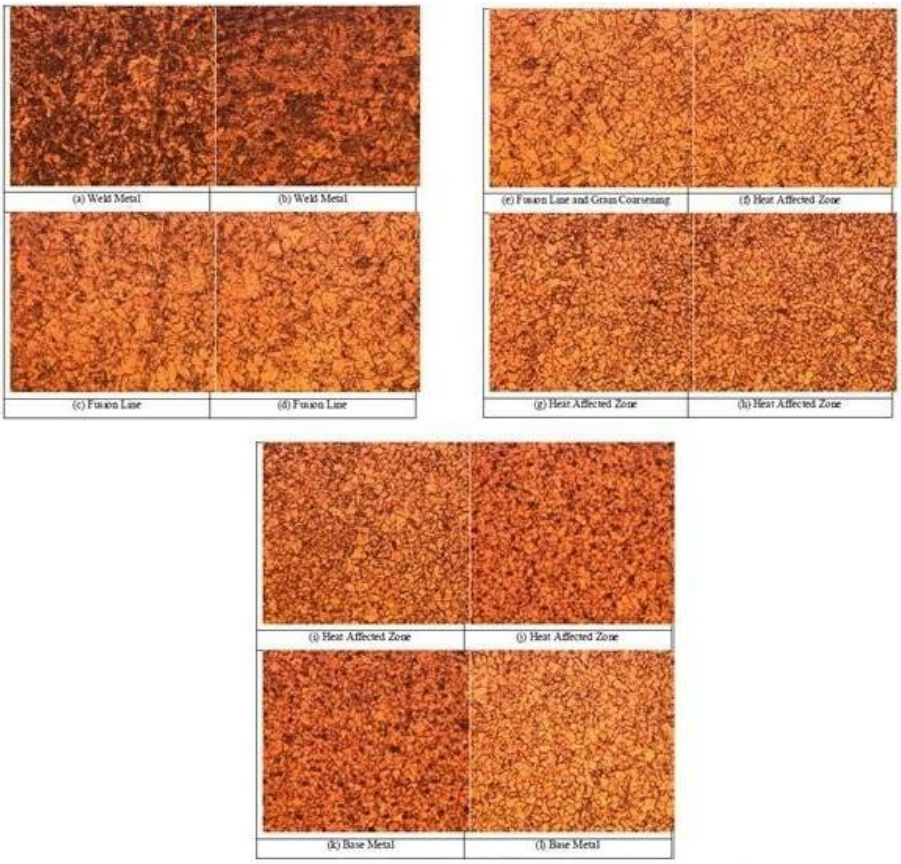

Figure : 6 Microstructure with heat input = 1547.98J/mm

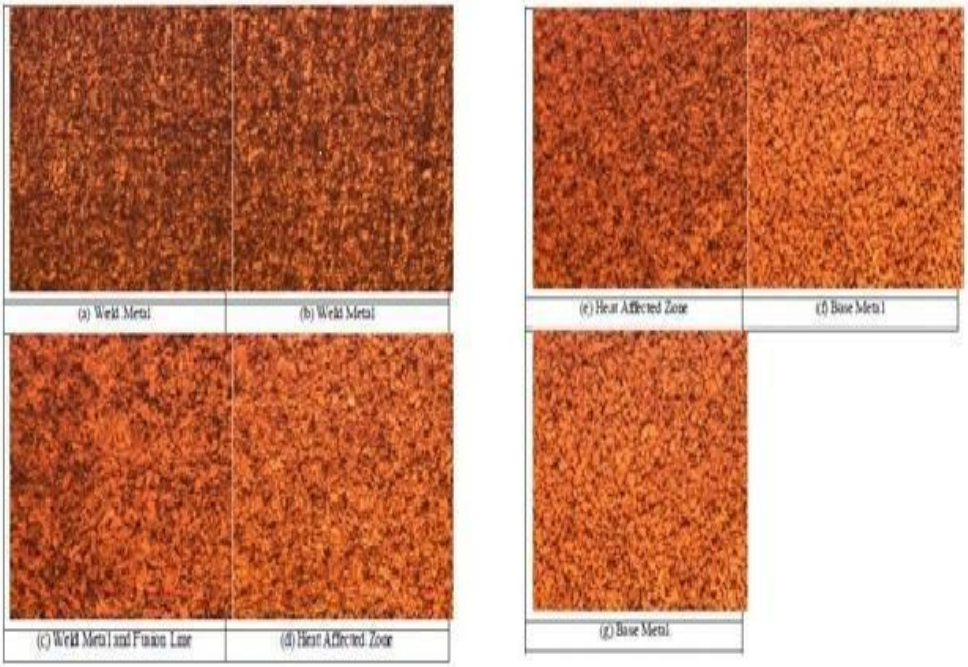

Figure : 7 Microstructure with heat input = 977.37 J/mm

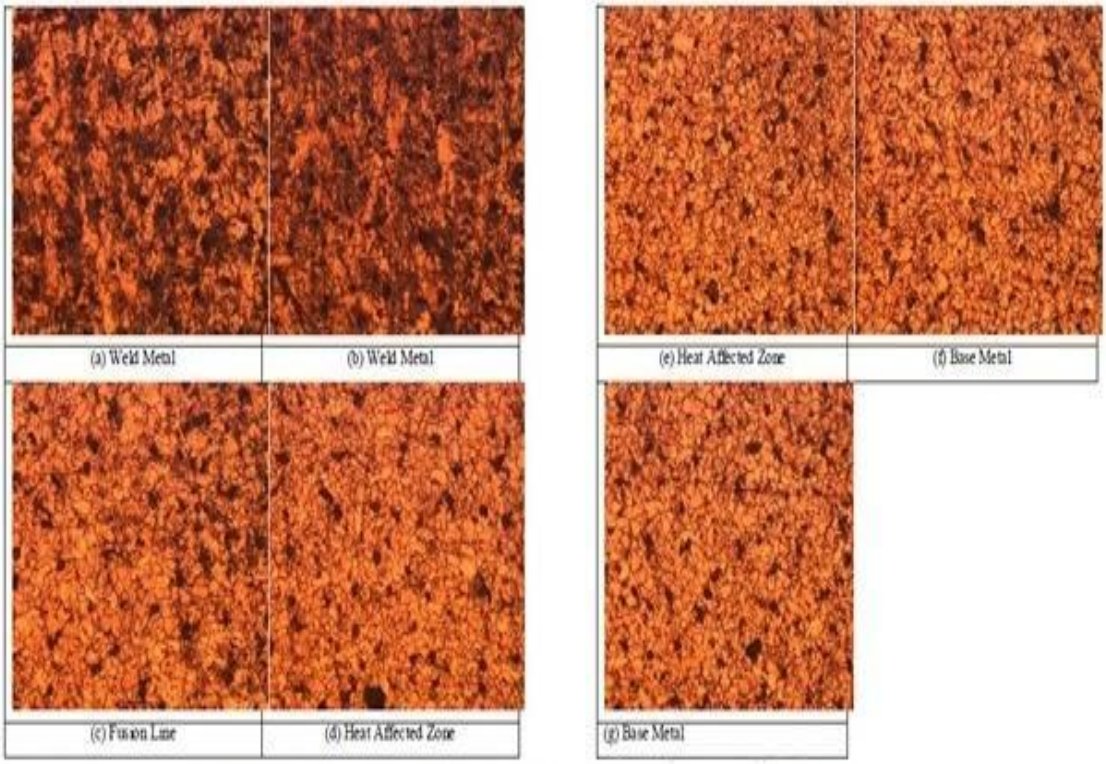

Figure : 8 Microstructure with heat input =2294.37 J/mm

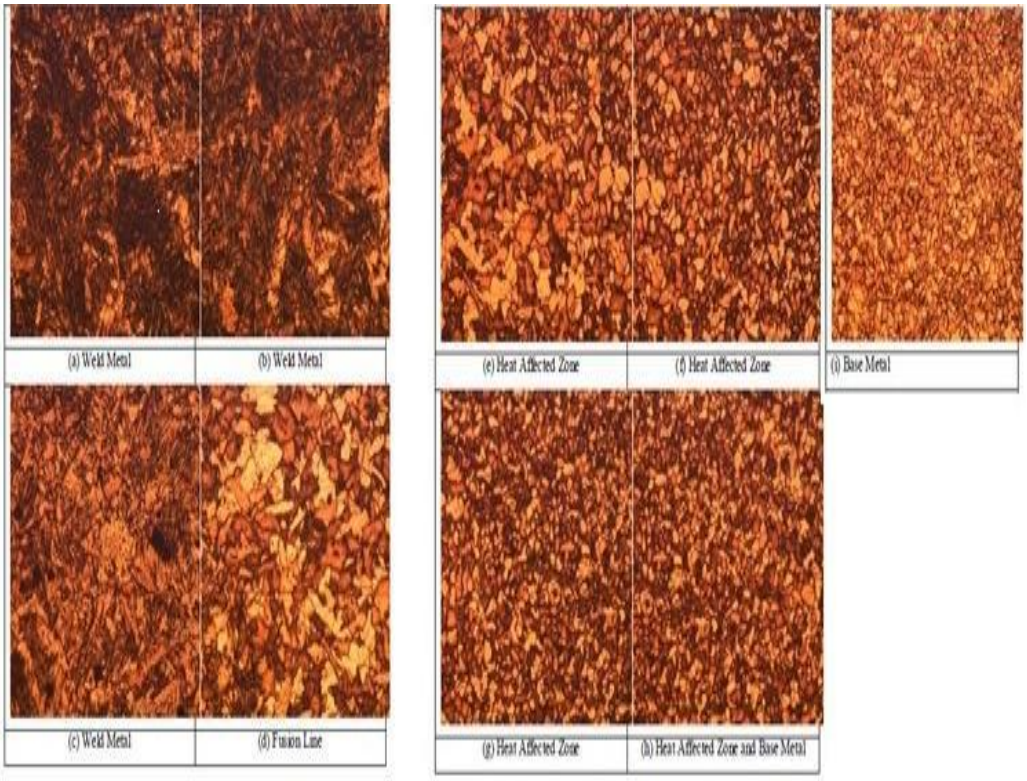

Figure : 9 Microstructure with heat input =1977.41 J/mm

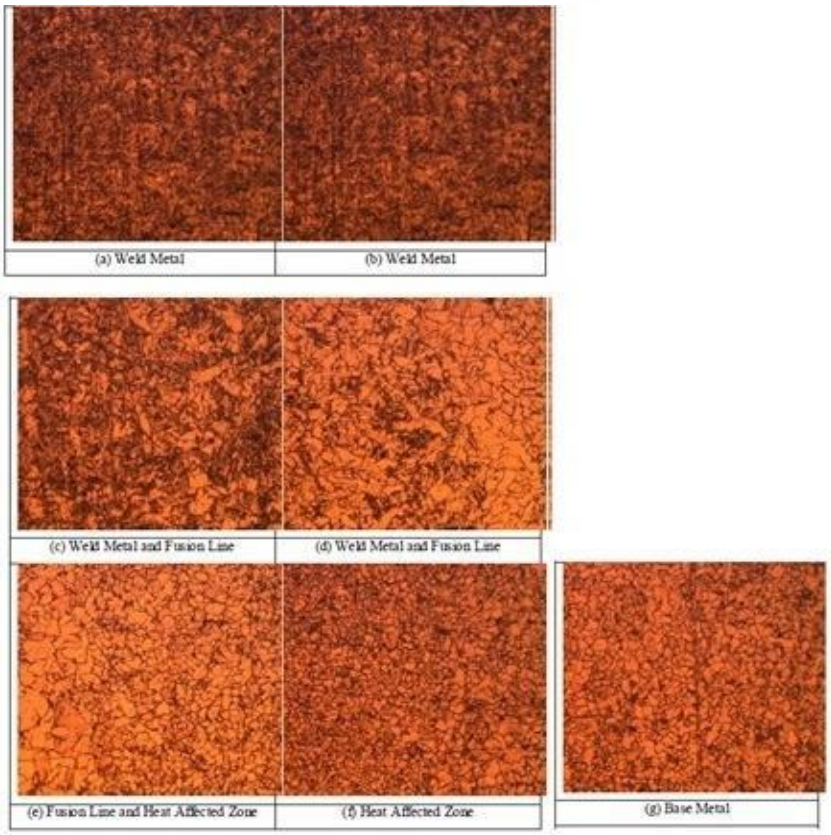

Figure : 10 Microstructure with heat input =1737.61 J/mm

The microstructure of base metal is shown in Fig. 5 (k) (l), 6 (k) (l), 7 (f) (g), 8 (f) (g), 9 (i), 10 (g). The observation results show that the base metal is consistent with a bainite microstructure and the grain size also indicate that the grain size of the bainite bind is also very small. Because of the small ferrite plate where the original austenite microstructure is refined, a refined bainite microstructure is gained and then the strength and impact toughness of base metal are improved.

The microstructure of the weld zone under different heat inputs are shown in Fig.5 (a) (b) (c), 6 (a) (b), 7 (a) (b) (c), 8 (a) (b), 9(a) (b) (c), 10 (a) (b) (c). The microstructure of the welds under different heat inputs is consistent with acicular ferrite and the plate proeutectoid ferrite along the grain boundary. The impact toughness of the weld depends on the proportion of acicular ferrite and the plate proeutectoid ferrite. The crack is easy to initiate and propagate in proeutectoid ferrite, so when the proportion of proeutectoid ferrite is very high, the toughness of the weld will be deteriorated. The fined acicular ferrite is useful to improve the impact toughness of welds because the crossing distribution grain boundaries can impede the propagation of cracks.

Fig. 6 (e) shows the effect of heat input on the microstructure of coarsened grain zone. The coarsening of original austenite grain and the formation of brittle microstructure are the main cause for the decrease of toughness in coarsened grain zone. It can be seen from Fig. 6 (e) that the original austenite grain size increases with the Increase of heat input. In addition, the size of lath bainite and the proportion of granular bainite in coarse grain zone also increase with the increase of heat input, which results in the decrease of toughness in coarsened grain zone under high heat input.

3.2 Effect of Process Parameters on HAZ

The portion of the parent material which has been heated above the critical temperature but has not melted. It is understood that several process control parameters in MAW influence bead geometry, microstructure as well as weld chemistry. Their combined effect is reflected on the mechanical properties of the weld in terms of weld quality as well as joint performance. The study of the various works, review that, the selection of the suitable process parameters are the primary means by which acceptable heat affected zone properties, optimized bead geometry. The increase in amount of heat input increases the width of HAZ. Figure 11 shows the variation of width of HAZ with the change in Heat Input. Figure 12 shows the variation of width of HAZ with the change in Speed of welding

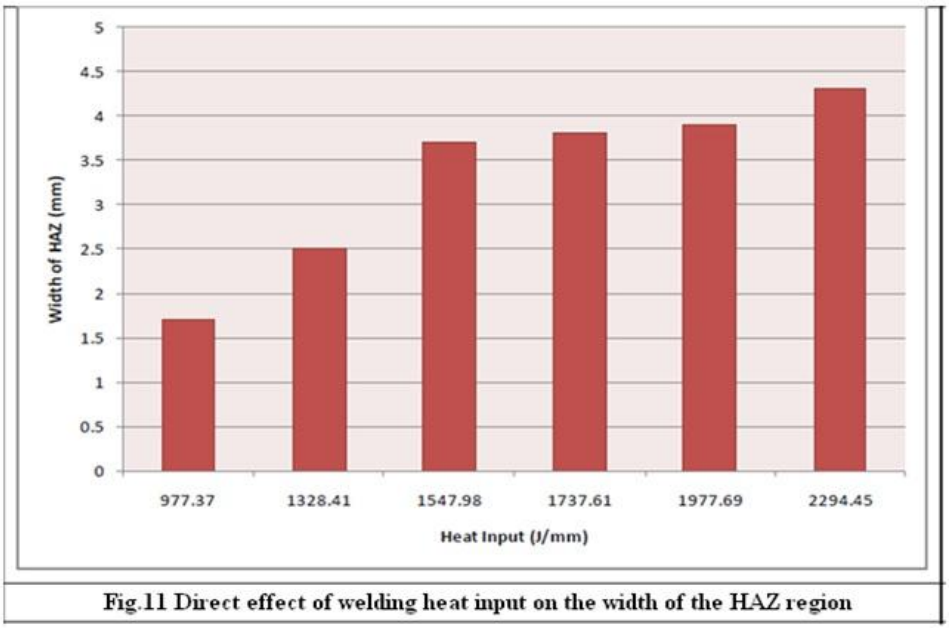

Fig.11 Direct effect of welding heat input on the width of the HAZ region

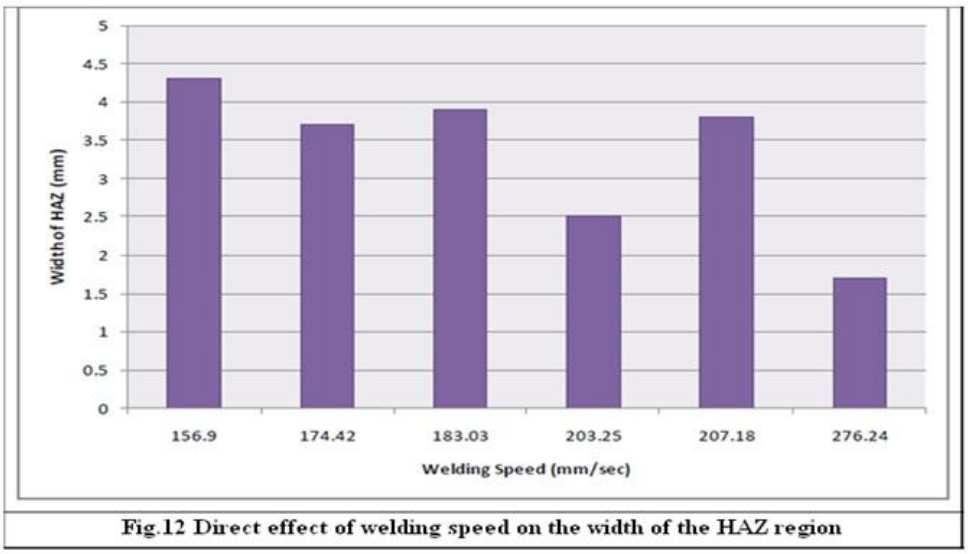

Fig.12 Direct effect of welding speed on the width of the HAZ region

In manual metal arc welding (MMAW), selecting appropriate values for process variables is essential in order to control heat-affected zone (HAZ) dimensions and get the required bead size and quality. Effects of process variables on HAZ parameters are shown in Fig 11 and 12.The dimensions of the different HAZ layers increases with the increases in, heat input but decreases with increases in welding speed. Increasing the speed of travel and maintaining constant arc voltage and current will reduce the width of bead and also increase penetration until an optimum speed is reached at which penetration will be maximum. Increasing the speed beyond this optimum will result in decreasing enetration. In the arc welding process increase in welding speed causes: Decrease in the heat input per unit length of the weld. Decrease in the electrode burn off rate. Decrease in the weld reinforcement.
If the welding speed decreases beyond a certain point, the penetration also will decrease due to the pressure of the large amount of weld pool beneath the electrode, which will cushion the arc penetrating force.

IV. Conclusion

Due to different heat input the microstructure of base metal as shown in Fig. 5 (k) (l), 6 (k) (l), 7 (f) (g), 8 (f) (g), 9 (i), 10 (g). And because of the small ferrite plate where the original austenite microstructure is refined, a refined bainite microstructure is gained and then the strength and impact toughness of base metal are improved.

The coarsening of original austenite grain and the formation of brittle microstructure are the main cause for the decrease of toughness in coarsened grain zone. It can be seen from Fig. 6 (e) that the original austenite grain size increases with the increase of heat input. In addition, the size of lath bainite and the proportion of granular bainite in coarse grain zone also increase with the increase of heat input, which results in the decrease of toughness in coarsened grain zone under high heat input.

Trend of Direct effect of welding heat input and welding speed on width of HAZ as shown in graphs no 11 ,12-

1. Heat input is the most significant factor for controlling width of Heat affected zone (HAZ).and since welding speed increase the width of HAZ decreases, proper control on welding speed is become the important parameter for controlling the HAZ..
2. In manual metal arc welding (MMAW), selecting appropriate values for process variables is essential in order to control heat-affected zone (HAZ) dimensions and get the required bead size and quality.

V. Scope for Further Work

In the present study authors have consider voltage, current& speed parameter to test HAZ and thereby metals property like microstructure, weld bead & weld quality. The study can be extended by considering other parameters like arc time , weld angle & welding types as a future scope over HAZ & there by effect on metal properties like compressive & tensile strength.

References

[1] "Advances in Welding Science and Technology," edited by *S.* A. David, ASM International, Materials Park, Ohio, 1986.
[2] "Recent Trends in Welding Science and Technology," edited by *S.* A. David and J. M.Vitek, ASM International, Materials Park, Ohio, 1990.
[3] A.Mujumdar of NIT Agartala, Tripura (west) , 'Study of the effect of Bevel angle & welding heat input on Mchanical properties of Mild Steel wldments'. A international journal of Mechanical & Material Engineering, Volume 6, No.2 (June 2011) , pg 280-290
[4] V. Gunarajandn and Murugan, "Prediction of Heat-Affected Zone Characteristics in Submerged Arc Welding of Structural Steel Pipes", Welding Journal, January 2002
[5] Ravindra pal singh, R.K.Garg & D.K.Shukla of NIT, Jalandhar, Panjab, "Parametric effect on mechanical properties in Submerge arc welding process', in international journal of Engg.science & Technology (IJEST) volume 4, No.02, feb.2012. "
[6] S Sun and C S Wu , "Effects of welding heat input on microstructure and hardness in heat-affected zone of HQ130 steel". Institute of Materials Joining, Shandong University of Technology, Jinan 250061, China.
[7] Lee et al, "Effect of Welding Parameters on the Size of Heat Affected Zone of Submerged Arc Welding", Division of Material Engineering, School of Applied Science Nanyang Technological University, Singapore.
[8] Lee, C. S., Chandel, R. S. and Seow, H. P. (2000) 'Effect of Welding Parameters on the Size of Heat Affected Zone of Submerged Arc Welding', Materials and Manufacturing Processes, 15: 5, 649 — 666.
[9] Weisman C, American Welding Society, Welding Handbook: Fundamentals of Welding, Seventh Ed. vol. 1. 1976.
[10] Easterling, K. Introduction to physical Metallurgy of Welding, 2 edition, 1992(Butterworth-Heinemann Limited, Oxford).

International Journal of Modern Engineering Research (IJMER)
www.ijmer.com Vol. 3, Issue. 3, May.-June. 2013 pp-1501-1503 ISSN: 2249-6645

On The Transcendental Equation

$$\sqrt[3]{X^2+Y^2}+\sqrt[3]{Z^2+W^2}=2(k^2+s^2)R^5$$

M. A. Gopalan[1], S. Vidhyalakshmi[2], S. Mallika[3]
[123]*Department of mathematics, Srimathi Indira Gandhi College, Trichy. 620002.*

Abstract: *The transcendental equation with five unknowns given by,* $\sqrt[3]{X^2+Y^2}+\sqrt[3]{Z^2+W^2}=2(k^2+s^2)R^5$ *is analyzed for its infinitely many non-zero integral solutions.*

Keywords: *Transcendental equations, Integral solutions.*

Mathematics Subject classification Number: *11D99*

I. Introduction

Diophantine equations have an unlimited field of research by reason of their variety. Most of the Diophantine problems are algebraic equations [1-3].It seems that much work has not been done to obtain integral solutions of transcendental equations. In this context, one may refer [4-10].This communication analyzes a transcendental equation given by $\sqrt[3]{x^2+y^2}+\sqrt[3]{z^2+w^2}=2(k^2+s^2)R^5$ for its infinitely many non-zero integer quintuples (x,y,z,w,R).

II. Method Of Analysis

The transcendental equation to be solved is

$$\sqrt[3]{x^2+y^2}+\sqrt[3]{z^2+w^2}=2(k^2+s^2)R^5 \quad (1)$$

Where k and s are non-zero integer constants.
To start with, the substitution

$$\left.\begin{aligned} x&=m(m^2+n^2)\\ y&=n(m^2+n^2)\\ z&=m^3-3mn^2\\ w&=3m^2n-n^3 \end{aligned}\right\rangle \quad (2)$$

In (1) ,lead to

$$m^2+n^2=(k^2+s^2)R^5 \quad (3)$$

Which is analyzed for its distinct integral solutions when

i) k^2+s^2 is not perfect square

ii) k^2+s^2 is a perfect square.

Case:1 k^2+s^2 is not a perfect square.
Assume

$$R=a^2+b^2 \quad (4)$$

Using (4) in (3) and employing the method of factorization, define,

$$(m+in)=(k+is)(a+ib)^5$$

Equating real and imaginary parts, we get,

$$\left.\begin{aligned} m&=kf(a,b)-sg(a,b)\\ n&=sf(a,b)+kg(a,b) \end{aligned}\right| \quad (5)$$

Where $f(a,b)=a^5-10a^3b^2+5ab^4$

$$g(a,b) = 5a^4b - 10a^2b^3 + b^5$$

Using (5) in (2), the non-zero distinct integer values of x,y,z,w are,

$$\left.\begin{aligned} x &= [kf(a,b) - sg(a,b)](k^2+s^2)[f^2(a,b)+g^2(a,b)] \\ y &= [sf(a,b) + kg(a,b)](k^2+s^2)[f^2(a,b)+g^2(a,b)] \\ z &= [kf(a,b) - sg(a,b)][(k^2-3s^2)f^2(a,b) + (s^2-3k^2)g^2(a,b) - 8ksf(a,b)g(a,b)] \\ w &= [sf(a,b) + kg(a,b)][(3k^2-s^2)f^2(a,b) + (3s^2-k^2)g^2(a,b) - 8ksf(a,b)g(a,b)] \end{aligned}\right\} \quad (6)$$

Thus (4) and (6) represents the non-zero integral solutions of (1).
A few numerical examples are given in the table I below.

Table I Numerical examples:

x	y	Z	w	R
640	-1920	-1664	1152	2
493750	18750	490906	56142	5
-1875000	-546875	-1287000	-1469125	5
-1828125	687500	-922077	1721764	5

Case II: $k^2 + s^2$ **ia a perfect square**

Let $k^2 + s^2 = d^2$ (7)

Using (4) and (7) in (3) and employing the method of factorization define

$$(m+in)(m-in) = (id)(-id)(a+ib)^5$$

Equating real and imaginary parts, we get,

$$\left.\begin{aligned} m &= -dg(a,b) \\ n &= df(a,b) \end{aligned}\right\} \quad (8)$$

Using (8) in (2), non-zero integral solutions of x,y,z,w are given by,

$$\left.\begin{aligned} x &= (-d^3)[g^3(a,b) + f^2(a,b)g(a,b)] \\ y &= d^3[f(a,b)g^2(a,b) + f^3(a,b)] \\ z &= d^3[3f^2(a,b)g(a,b) - g^3(a,b)] \\ w &= d^3[3f(a,b)g^2(a,b) - f^3(a,b)] \end{aligned}\right\} \quad (9)$$

Thus (4) and (9) represents the non-zero integral solutions of (1)
Numerical examples are given in the Table 2 below

Table II Numerical examples:

x	y	z	W	R
16000	-16000	-16000	-16000	2
281216	-281216	-281216	-281216	2
-281490625	-260893750	238794127	-300466114	5
-124417736704	249036300000	227941548032	-246810701824	8

From the above table, we see that each of the expressions $\pm 2(3x+z)$ and $\pm 2(3y-w)$ is a cubical integer.

III. Conclusion

One may search for other patterns of solutions.

References

[1] L.E.Dickson,History of Theory of numbers,Vol.2,Chelsea publishing company,Newyork,1952.
[2] L.J.Mordel, Diophantine Equations, Academic press, Newyork, 1969.
[3] hantia.B.L and Supriya Mohanty [1985], '' *Nasty numbers and thei characterizations''* Mathematical Education,Vol-II,No.1 Pg.34-37
[4] M.A Gopalan, and S.Devibala, ''*A remarkable Transcendental Equation''* Antartica.J.Math.3 (2),(2006),209-215.
[5] M.A.Gopalan, V.Pandichelvi ''*On transcendental equation* $z = \sqrt[3]{x+\sqrt{B}y} + \sqrt[3]{x-\sqrt{B}y}$ ''Antartica . J.Math, 6(1),(2009),55-58.
[6] M.A.Gopalan and J Kaliga Rani, ''*On the Transcendental equation* $x + g\sqrt{x} + y + h\sqrt{y} = z + g\sqrt{z}$'' International Journal of mathematical sciences, Vol.9, No.1-2, (2010), 177-182,
[7] M.A.Gopalan and V.Pandichelvi, ''*Observations on the transcendental equation* $z = \sqrt[2]{x} + \sqrt[3]{kx+y^2}$'' Diophantus J.Math., 1(2), (2012), 59-68.
[8] M.A.Gopalan and J.Kaliga Rani, ''*On the Transcendental equation* $x + \sqrt{x} + y + \sqrt{y} = z + \sqrt{z}$ '' Diophantus.J.Math.1 (1) (2012), 9-14.
[9] M.A.Gopalan, Manju Somanath and N.Vanitha, ''*On Special Transcendental Equations''*Reflections des ERA-JMS, Vol.7, issue 2(2012), 187-192.
[10] V.Pandichelvi, ''*An Exclusive Transcendental equations* $\sqrt[3]{x^2+y^2} + \sqrt[3]{z^2+w^2} = (k^2+1)R^2$'' International Journal of Engineering Sciences and Research Technology, Vol.2, No.2 (2013), 939-944.

International Journal of Modern Engineering Research (IJMER)
www.ijmer.com Vol. 3, Issue. 3, May.-June. 2013 pp-1504-1511 ISSN: 2249-6645

Abrasive Jet Machining

Shripad Chopade[1], Sagar Kauthalkar[2], Dr. Pushpendra Kumar Sharma[3]
1 (shripad shashikant chopade, scholar student of Mechanical Department, Nri-ist Bhopal, India)
2 (sagar pradip kauthalkar, scholar student of Mechanical Department, Nri-ist Bhopal, India)
3(Dr. Pushpendra kumar sharma, Head & Guide of Mechanical Department, Nri-ist Bhopal, India)

ABSTACT: Abrasive water jet machine tools are suddenly being a hit in the market since they are quick to program and could make money on short runs. They are quick to set up, and offer quick turn-around on the machine. They complement existing tools used for either primary or secondary operations and could make parts quickly out of virtually out of any material. One of the major advantages is that they do not heat the material. All sorts of intricate shapes are easy to make. They turns to be a money making machine.

Keywords Abrasive Delivery System, Control System, Mixing tubes, Pump, Nozzle, Motion System

I. Introduction

A machine shop without a water jet is like a carpenter without a hammer ultimately. Sure the carpenter can use the back of his crow bar to hammer in nails, but there is a better way. It is important to understand that abrasive jets are not the same thing as the water jet although they are nearly the same. Water Jet technology has been around since the early 1970s or so, and abrasive jets extended the concept about ten years later. Both technologies use the principle of pressuring water to extremely high pressure, and allowing the water to escape through opening typically called the orifice or jewel. Water jets use the beam of water exiting the orifice to cut soft stuffs like candy bars, but are not effective for cutting harder materials. The inlet water is typically pressurized between 20000 and 60000 Pounds per Square Inch (PSI). This is forced through a tiny wall in the jewel which is typically .007" to .015" diameter (0.18 to0.4 mm).This creates a very high velocity beam of water. Abrasive jets use the same beam of water to accelerate abrasive particles to speeds fast enough to cut through much faster material.

II. Abrasive Delivery System

A simple fixed abrasive flow rate is all that's needed for smooth, accurate cutting. Modern abrasive feed systems are eliminating the trouble-prone vibratory feeders and solids metering valves of earlier systems and using a simple fixed-diameter orifice to meter the abrasive flow from the bottom of a small feed hopper located immediately adjacent to the nozzle on the Y-axis carriage. An orifice metering system is extremely reliable and extremely repeatable. Once the flow of abrasive through the orifice is measured during machine set-up, the value can be entered into the control computer program and no adjustment or fine-tuning of abrasive flow will ever be needed. The small abrasive hopper located on the Y-axis carriage typically holds about a 45-minute supply of abrasive and can be refilled with a hand scoop while cutting is underway.

2.1 Control System Fundamental limitation of traditional CNC control systems.

Historically, water jet and abrasive jet cutting tables have used traditional CNC control systems employing the familiar machine tool "G-code." However, there is a rapid movement away from this technology for abrasive jet systems, particularly those for short-run and limited-production machine shop applications. G-code controllers were developed to move a rigid cutting tool, such as an end mill or mechanical cutter. The feed rate for these tools is generally held constant or varied only in discrete increments for corners and curves. Each time a change in the feed rate is desired programming entry must be made. A water jet or abrasive jet definitely is not a rigid cutting tool; using a constant feed rate will result in severe undercutting or taper on corners and around curves. Moreover, making discrete step changes in feed rate will also result in an uneven cut where the transition occurs. Changes in the feed rate for corners and curves must be made smoothly and gradually, with the rate of change determined by the type of material being cut, the thickness, the part geometry and a host of nozzle parameters.

The control algorithm that computes exactly how the feed rate should vary for a given geometry in a given material to make a precise part. The algorithm actually determines desired variations in the feed rate every 0.0005" (0.012 mm) along the tool path to provide an extremely smooth feed rate profile and a very accurate part. Using G-Code to convert this desired feed rate profile into actual control instructions for the servo motors would require a tremendous amount of programming and controller memory. Instead, the power and memory of the modern PC can be used to compute and store the entire tool path and feed rate profile and then directly drive the servomotors that control the X-Y motion. These results in a more precise part that is considerably easier to create than if G-code programming were used.

2.2 Pump: Intensifier pump Early ultra-high pressure cutting systems used hydraulic intensifier pumps exclusively. At the time, the intensifier pump was the only pump capable of reliably creating pressures high enough for water jet machining. An engine or electric motor drives a hydraulic pump which pumps hydraulic fluid at pressures from 1,000 to 4,000 psi (6,900 to 27,600 kpa) into the intensifier cylinder. The hydraulic fluid then pushes on a large piston to generate a high force on a

small-diameter plunger. This plunger pressurizes water to a level that is proportional to the relative cross-sectional areas of the large piston and the small plunger.

Crankshaft Pump The centuries-old technology behind crankshaft pumps is based on the use of a mechanical crankshaft to move any number of individual pistons or plungers back and forth in a cylinder. Check valves in each cylinder allow water to enter the cylinder as the plunger retracts and then exit the cylinder into the outlet manifold as the plunger advances into the cylinder. Crankshaft pumps are inherently more efficient than intensifier pumps because they do not require a power-robbing hydraulic system. In addition, crankshaft pumps with three or more cylinders can be designed to provide a very uniform pressure output without needing to use an attenuator system.

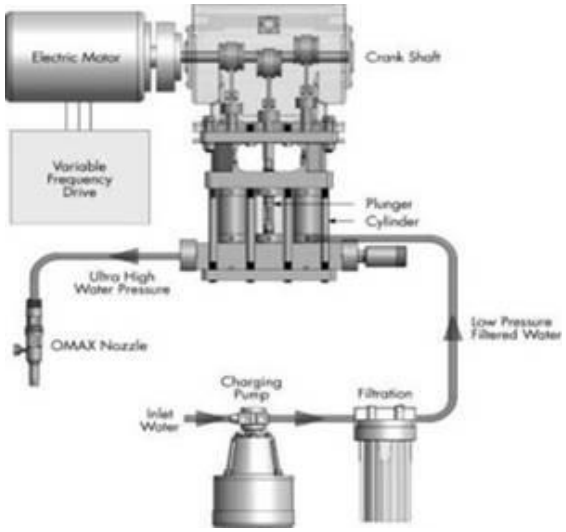

FIG: 1 Crankshaft pump

Crankshaft pumps were not generally used in ultra-high pressure applications until fairly recently. This was because the typical crankshaft pump operated at more strokes per minute than an intensifier pump and caused unacceptably short life of seals and check valves. Improvements in seal designs and materials, combined with the wide availability and reduced cost of ceramic valve components, made it possible to operate a crankshaft pump in the 40,000 to 50,000 psi (280,000 to 345,000 kpa) range with excellent reliability. This represented a major breakthrough in the use of such pumps for abrasive jet cutting. Experience has shown that an abrasive jet does not really need the full 60,000 psi (414,000 kpa) capability of an intensifier pump. In an abrasive jet, the abrasive material does the actual cutting while the water merely acts as a medium to carry it past the material being cut.

FIG: 2 Typical 20/30 horsepower crankshafts driven triplex pump.

This greatly diminishes the benefits of using ultra-high pressure. Indeed many abrasive jet operators with 60,000 psi (414,000 kPa) intensifier pumps have learned that they get smoother cuts and more reliability if they operate their abrasive jets in the 40,000 to 50,000 psi (276,000 to 345,000 kpa) range. Now that crankshaft pumps produce pressures in that range, an increasing number of abrasive jet systems are being sold with the more efficient and easily maintained crankshaft-type pumps.

2.3Nozzles

All types of abrasive jet systems use the same basic two-stage nozzle as shown in the FIG. First, water passes through a small-diameter jewel orifice to form a narrow jet. The water jet then passes through a small chamber where a Venturi effect creates a slight vacuum that pulls abrasive material and air into this area through a feed tube. The abrasive particles are accelerated by the moving stream of water and together they pass into a long, hollow cylindrical ceramic mixing tube. The resulting mix of abrasive and water exits the mixing tube as a coherent stream and cuts the material. It's critical

that the jewel orifice and the mixing tube be precisely aligned to ensure that the water jet passes directly down the center of the mixing tube. Otherwise the quality of the abrasive jet will be diffused, the quality of the cuts it produces will be poor, and the life of the mixing tube will be short.

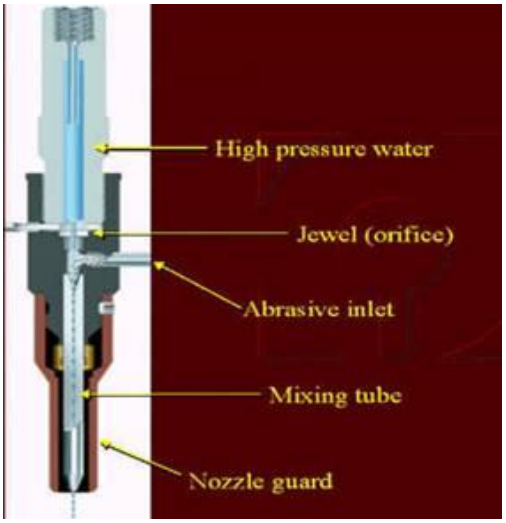

FIG: 3. Typical abrasive jet nozzle

The typical orifice diameter for an abrasive jet nozzle is 0.010" to 0.014" (0.25 mm to 0.35 mm). The orifice jewel may be ruby, sapphire or diamond, with sapphire being the most common.

The venturi chamber between the jewel orifice and the top of the mixing tube is an area that is subject to wear. This wear is caused by the erosive action of the abrasive stream as it enters the side of the chamber and is entrained by the water jet. Some nozzles provide a carbide liner to minimize this wear. Precise alignment of the jewel orifice and the mixing tube is critical to mixing tube life. This is particularly true for the relatively small diameter 0.030" (0.75 mm).

Mixing Tube

The mixing tube is where the abrasive mixes with the high-pressure water.

The mixing tube should be replaced when tolerances drop below acceptable levels. For maximum accuracy, replace the mixing tube more frequently. The size of the kerf and cutting performance are the best indicators of mixing tube wear.

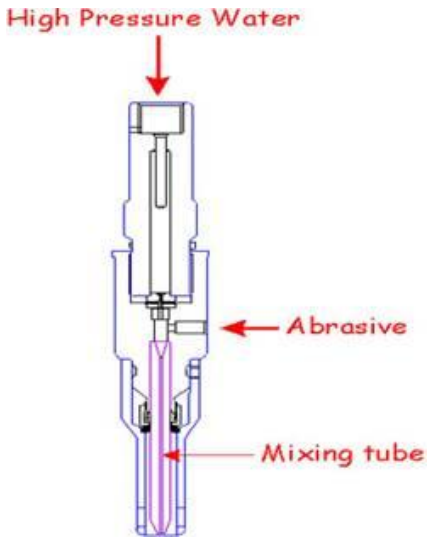

FIG: 4 Mixing Tube

2.4 Motion System:

X-Y Tables

In order to make precision parts, an abrasive jet system must have a precision X-Y table and motion control system. Tables fall into three general categories:

i) Floor-mounted gantry systems with separate cutting tables

ii) Integrated table/gantry systems

iii) Floor-mounted cantilever systems with separate cutting tables
Each type of system has its benefits and drawbacks.

1. Floor-mounted gantry with separate cutting table

A floor-mounted gantry with a separate cutting table is the most common approach used by water jet system manufacturers. A framework that supports the X-Y motion system is secured directly to the floor and straddles a separate cutting table and catcher tank. The nozzle(s) is mounted to a carriage which moves along a gantry beam that straddles the table. The gantry beam is supported on each end by a guide system and is moved by ball screws, rack and pinion assemblies or drive belts located at each end. The parallel drive mechanisms are either operated by two electronically-coupled drive motors or by a single motor driving a mechanically-coupled drive system.

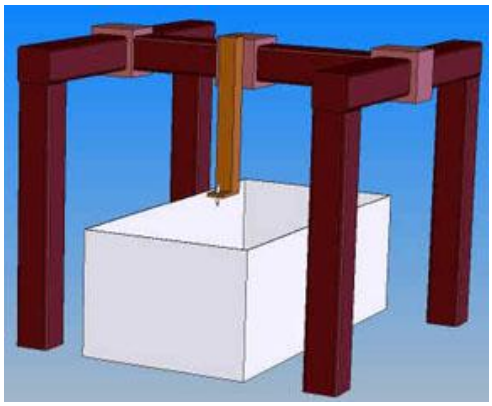

2. Integrated table/gantry system

The integrated table/gantry system is very similar to the traditional gantry system previously described, except that the guides for the gantry beam are integrated into the cutting table. Because of this the X-Y motion system and the material support table are part of the same overall structure and unwanted relative motion between them is eliminated. In this type of system, the floor is not a vital part of the system structure. This system is typically more accurate than the more traditional separate gantry and table.

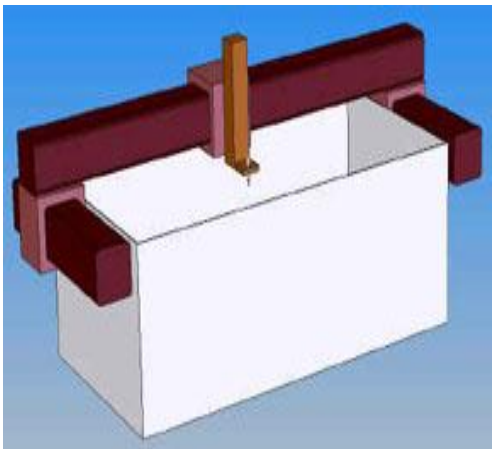

3. Floor-mounted cantilever system with separate cutting table

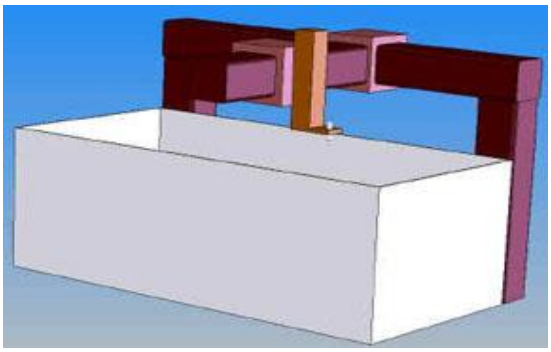

This type of system uses a floor-mounted X-axis and a cantilevered Y-axis mounted to the X-axis carriage. The nozzle mounts to a carriage on the Y-axis. The cutting table is totally separate from the X-Y motion structure.

III. Working

A typical abrasive jet machining center is made up of the following components:

High pressure water starts at the pump, and is delivered through special high pressure plumbing to the nozzle. At the nozzle, abrasive is (typically) introduced, and as the abrasive/water mixture exits, cutting is performed.

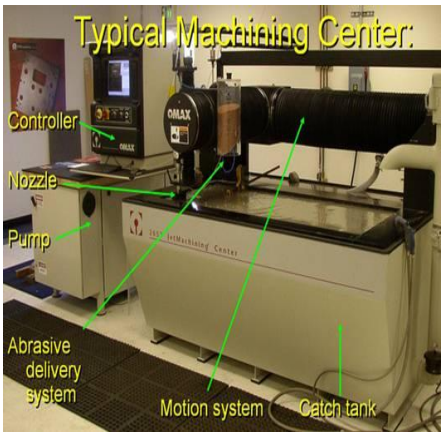

FIG: 5 Typical Machining Centre

once the jet has exited the nozzle; the energy is dissipated into the catch tank, which is usually full of water and debris from previous cuts. The motion of the cutting head is typically handled by an X / Y-axis structure. Control of the motion is typically done via a computer following the lines and arcs from a CAD drawing.

IV. AJM FEATURES

(A)Obtainable tolerances:

You need a machine with good precision to get precision parts, but there are many other factors that are just as important. A precise machine starts with a precise table, but it is the control of the jet that brings the precision to the part.

A key factor in precision is software - not hardware. This is also true for cutting speed. Good software can increase cutting speeds dramatically. This is because it is only through sophisticated software that the machine can compensate for a "floppy tool" made from a stream of water, air, and abrasive. Obtainable tolerances vary greatly from manufacturer to manufacturer. Most of this variation comes from differences in controller technology, and some of the variation comes from machine construction. Significant advances are made in the control of the process allowing for higher tolerances.

(B)Material to machine - Harder materials typically exhibit less taper, and taper is a big factor in determining what kind of tolerances you can hold. It is possible to compensate for taper by adjusting the cutting speed, and/or tilting the cutting head opposite of the taper direction.

(C)Material thickness - As the material gets thicker, it becomes more difficult to control the behavior of the jet as it exits out the bottom. This will cause blow-out in the corners, and taper around curves. Materials thinner than 1/4" (6mm) tend to exhibit the most taper (which is perhaps the opposite of what you might expect.), and with thicker materials, the controller must be quite sophisticated in order to get decent cuts around complex geometry.

(D)Accuracy of table - Obviously, the more precise is the positioning the jet, the more precise will be the machine part.

(E)Stability of table - Vibrations between the motion system and the material, poor velocity control, and other sudden variances in conditions can cause blemishes in the part ("witness marks"), the hardware that is out there varies greatly in stability and susceptibility to vibrations. If the cutting head vibrates relative to the part, the part will be ugly.

(F)Control of the abrasive jet - Because your cutting tool is basically a beam of water, it acts like a "floppy tool". The jet lags between where it first enters your material and where it exits.

V. Machining Aspects

1. Around curves: As the jet makes its way around a radius, the jet down, and let the tail catch up with the head. (And / or tilt the cutting head to compensate)

2. Inside corners: As the jet enters the corner, the traverse speed must slow down to allow the jets tail to catch up. Otherwise the tail lag will cause the corner to "blow out" a little. As the jet exits the corner, the feed rate must not be increased too quickly, otherwise the jet will kick back and damage the part.

3. Feed rate: When the jet slows down, its kerf width grows slightly.

4. Acceleration: Any sudden movement (like a change in feed rate) will cause a slight blemish as well. Thus for highest precision it is necessary to control the acceleration as well as feed rate.

5. Nozzle Focus: Some nozzles produce more taper than others. Longer nozzles usually produce less taper. Smaller diameter nozzles also produce less taper. Holding the nozzle close to the work piece produces less taper as well.

6. Speed of cutting: Typically, the slower the cutting, the higher the tolerance. This is because as the cutting is slowed down, the surface finish improves, and the taper begins to disappear. However in some cases it is possible to slow the cutting down so much that tolerances begin to get worse due to reverse taper.

7. Active taper compensation: Some newer machines now have the option of tilting the cutting head against the taper. This can be used to virtually eliminate the taper, or to purposely add taper into a part. The big advantage to active taper compensation is that taper can be reduced without having to slow the cutting down. ("Taper" is when the edge of the part is not 100% perpendicular.) I have an entire page dedicated to this topic elsewhere in this web site. If you want to go there now.

8. Kerf width: Kerf width, which is the width of the cutting beam, determines how sharp of an inside corner you can make. About the smallest practical abrasive jet nozzle will give you a kerf width of .020" (0.5mm) in diameter. Higher horsepower machines require larger nozzles, due to the amount of water and abrasive that they flow through. Some water jet (water only) nozzles have very fine kerf widths (like .003" / 0.076mm). Likewise, it is possible to make ultra-small abrasive jet nozzles, but they are problematic.

9. Consistency of Pump Pressure: Variations in water jet pump pressure can cause marks on the final part. It is important that the pump pressure vary as little as possible while machining is in progress to prevent these. (This becomes an issue only when looking for better than +-.005" (0.125mm) tolerances, however). Typically it is older Intensifier type pumps that exhibit this problem. Some newer intensifiers, and as far as I know all crankshaft driven pumps have smoother pressure delivery, and this is not an issue.

10. Cutting speeds: Ideally, you want to make the most precise part possible in the least amount of time, and for the least amount of money. Cutting speeds are a function of the material to cut, the geometry of the part, the software and controller doing the motion, the power and efficiency of the pump making the pressure, and a few other factors such as the abrasive used. The primary factors that determine cutting speed Material being cut (And how thick it is)

Hardness: Generally speaking, harder materials cut slower than soft materials. However, there are a lot of exceptions to this. For example, granite, which is quite hard, cuts significantly faster than Copper, which is quite soft. This is because the granite easily breaks up because it is brittle. It is also interesting to note that hardened tool steel cuts almost as quickly as mild steel. (Though "absolute black" granite, which is tough as nails, actually cuts a bit slower than copper)

Thickness: The thicker the material, the slower the cut. For example, a part that might take 1 minute in 1/8" (3mm) steel, might take a half hour in 2" (50mm) thick steel, and maybe 20 hours in 10 inch (250mm) thick steel.

Geometry of the part: It is necessary to slow the cutting down in order to navigate sharp corners and curves. It also takes additional time to pierce the material. Therefore, parts with lots of holes and sharp corners will cut much slower than simpler shapes.

Desired Result: If you want a high tolerance part and / or a smooth surface finish, then the part will take longer to make. Note that you can make some areas of a part high tolerance and other areas fast, so you can mix and match to get the optimal balance between cutting speed and final part quality.

Software controlling the motion: This is probably one of the most overlooked aspects of abrasive jet machining by novice users. You would not think that software would have much to do with the speed of cutting. In fact, this is true if all you are doing is cutting in a straight line. However, as soon as you introduce any complexity to the part, such as a corner, there is great opportunity for software to optimize the cutting speed. The difference, as it turns out, is all through software that automatically optimizes the tool path to provide the desired precision in the least amount of time. Basically, what the software does, is looks at the geometry of the part, and then modify the feed rates and add "tweaks" to the cutting in order to squeeze the maximum amount of speed. It does this by finding the optimal speeds and accelerations for all curves and corners, setting the optimal length and feed rate for all pierce points, adding special "corner pass" elements at corners to allow the cutting to go right past the corners where it can, etc. It was found that by simply optimizing the corners that we could get about a factor of two in cutting speed over a hand-optimized part. Then, over the next 10 years or so, we added a lot more optimizations in terms of faster piercing, corner passing, improved cutting models and such, and were able to get another factor of 2 in cutting speed for some parts, while at the same time increasing the precision. So, software matters! And one of the most beautiful things about optimizing in software is that it does not cost any money. In fact, it saves money, because if you cut faster through software, you use less abrasive and put less wear and tear on all the high-pressure components!

Power at the nozzle (pressure and water flow rate): The more horsepower at the nozzle, the faster you can cut. How much horsepower makes it to the nozzle is a function of the pressure and the orifice that it's being squeezed through. (Note: do not confuse "horsepower" with "horsepower at the nozzle". It is the power that actually makes it to the nozzle that is most important. Having a big motor makes no difference, if the power all goes into wasted heat!) Simply put, the higher the pressure, the faster the cut. The more water you flow, the faster the cut. Unfortunately, as the pressure increases, so does the cost and maintenance, so this is not as simple as it seems. A good way to learn more about how pressure and jewel size effect-cutting rates, and to calculate "nozzle horsepower" is to run the Abrasive jet Feed Rate Calculator, which you can download from this web site.

Type of abrasive: In the industry, pretty much everyone uses 80 mesh garnets for their abrasive. However, it is possible to cut slightly faster with harder abrasives. However, the harder abrasives also cause the mixing tube on the nozzle to wear rapidly. So, pretty much everyone uses garnet. It is worth mentioning that not all garnet is the same. There are big

variations between purity, hardness, sharpness, etc, that can also affect the cutting speed and operating cost. **Quality of abrasive:** Typically, abrasive jets consume between 0.5 and 1 Lb (0.25 and 0.5Kg) of abrasive per minute. There is a sweet spot for every nozzle size and pressure as to what amount of abrasive flow rate will cut the fastest, and what amount will cut the cheapest.

VI. Comparison to Other Machining Processes

1. Comparison with EDM Key Wire EDM strengths
i) Extremely precise parts are possible [±0.0001" (±0.025mm)]
ii) Very thick parts [over 12" (30 cm)] can be made
iii) Intentional taper can be put into a part for die clearance and other uses
Key Precision Abrasive jet strengths
iv) Five to ten times faster in parts less than 1" (2.5 cm) thick [but, at ±0.003" (±0.1 mm), less precise as well
vi) No Heat Affected Zone (HAZ), so no need for secondary operations to remove the HAZ or additional heat-treating to compensate for it
vii) Works well in non-conductive materials (such as glass, stone, plastic) as well as conductive materials
viii) Can pierce material directly without the need for a pre-drilled starter hole
ix) Can produce large parts at reasonable costs
x) Simple and rapid programming and set-up with minimal fixturing

2. Comparing abrasive jet to laser
Key laser strengths
i) Very fast production in thin, non-reflective materials such as sheet steel.
ii) Accuracy to ±0.001" (±0.025 mm) or better in thin material.

Key precision abrasive jet strengths
iii) Can produce parts up to 2" (5.1 cm) thick in virtually any material while holding tolerances on the order of ±0.003" to ±0.005" (±0.08 to ±0.1 mm).
iv) Can machine reflective, conductive and thicker materials such as stainless steel and aluminum, copper and brass.
v) Cuts without melting, providing a smooth uniform surface with very little burr or dross.
vi) No heat-affected zone (HAZ), which may eliminate the need for a secondary operation to remove HAZ and makes conventional secondary operations, such as reaming or tapping, easier to perform.
vii) No noxious gas or vapors produced during cutting.
viii) Simple and rapid programming and set-up for short-run parts.

3. Comparison of precision abrasive jet to milling
Key mill or machining center strengths
i) A well-understood familiar technology.
ii) Able to make three-dimensional parts.
iii) Rapid production if set up and programmed for long-run parts.
Key precision abrasive jet strengths
iv) Very rapid programming and set-up does not require a highly trained operator.
v) Very low cutting loads mean that fixturing is easier and also means that intricate and delicate parts can be machined.
vi) One cutting tool performs all machining functions in all materials, so there is no need to purchase and calibrate multiple cutting tools.
vii) Large cutting envelope compared to a machining center of comparable price.
viii) Minimal burr compared to conventional machining. Environmentally friendly; no oil-soaked chips and minimal scrap.
xi) The key reasons traditional job shops buy a precision abrasive jet is to get new projects, become more competitive, and make more money.

4. Comparison of precision abrasive jet to milling
Key mill or machining center strengths
i) A well-understood familiar technology.
ii) Able to make three-dimensional parts.
iii) Rapid production if set up and programmed for long-run parts.
Key precision abrasive jet strengths
iv) Very rapid programming and set-up does not require a highly trained operator.
v) Very low cutting loads mean that fixturing is easier and also means that intricate and delicate parts can be machined.
vii) One cutting tool performs all machining functions in all materials, so there is no need to purchase and calibrate multiple cutting tools.br>
viii) Large cutting envelope compared to a machining center of comparable price.
ix) Minimal burr compared to conventional machining. Environmentally friendly; no oil-soaked chips and minimal scrap.

x) The key reasons traditional job shops buy a precision abrasive jet is to get new projects, become more competitive, and make more money.

VII. Machinable Materials

Virtually any material can be cut by using AJM method i.e. harder materials like titanium to steel Aluminum, Steel, Titanium Laminates Flammable materials Cut thin stuff, or thick stuff Brittle materials like glass, ceramic, quartz, stone. Laminates Flammable materials Cut thin stuff, or thick stuff.

VIII. Conclusion

The better performance, and the applications presented above statements confirm that **ABRASIVE JET MACHINING (**AJM) will continue to expand. Industry is convinced that the large aerospace segment will take off in near the future, together with other segments that are currently showing interest in AJM method. From operator experiences the abrasive jets are capable of anywhere from 0.5mm-0.025mm precision. High precision manufacturing needs can be met by using AJM method. Newer machines are capable of 3D machining thus making it an important in specialty manufacturing. The new software's used will minimize time and investments, thereby making it possible for more manufacturers of precision part to install AJM centers.

Acknowledgment

The author wishes to acknowledge the Project Guide Dr. Pushpendra Kumar Sharma, Head of Department Nri-ist Bhopal, India, for their continual guidance.

References

[1] Processes and Materials of Manufacture by R.A. LINDBERG
[2] www.edufive.com/seminartopics.html
[3] www.pcmag.com/encyclopedia

International Journal of Modern Engineering Research (IJMER)
www.ijmer.com Vol. 3, Issue. 3, May.-June. 2013 pp-1512-1519 ISSN: 2249-6645

Studies on effect of various operating parameters & foaming agents- Drying of fruits and vegetables

S. Sharada
Assistant Professor
Department of Chemical Engineering, JNTUACEA, ANANTAPUR

Abstract: *The foam mat drying is a good way of dehydrating liquids foods in short times. Due to the porous structure of the foamed materials, mass transfer is enhanced leading to shorter dehydration times. This technique can be successfully employed for drying a variety of fruit juice concentration and pulps. The dried powders have good reconstitution characteristics. These studies are particularly applicable for drying of fruit and vegetable pulps drying such as guava, bananas and tomato etc. with some of the commonly used foaming agents like egg albumin and soya protein.*

The drying studies are carried out in a tray drier. The drying curves are drawn with different operating parameters and foaming agents. Falling rate is observed for the foam at different timings. Drying rates are compared and the drying time is evaluated by drying the foam at 55^{o}C to 80^{o}C. These studies are helpful for evaluating best drying to get good quality dried powders.

Keywords: *mass transfer, foaming agents, falling rate, reconstitution characteristics*

I. INTRODUCTION

Drying is a process of moisture removal due to simultaneous heat and mass transfer from the surrounding environment .the transfer of energy depends on the air temperature, air humidity, air flow rate and pressure. Rate of moisture transfer is governed by some of factors such as physical nature of the food, temperature, composition and initial moisture content. Foam mat is drying is one the very effective methods employed for the removal of moisture from the fruit pulps to obtain a free flowing powder that have good reconstitutions characteristic. it is the simplest method of drying in which a liquid food concentrate along with a suitable foaming agent is whipped to form a stable foam and is subjected to dehydration in the form of a mat of foam [1,2].rate of drying in this process comparatively very high because of enormous increase in liquid-gas interface, in spite of the fact that the heat transfer is impeded by a large volume of gas present in the foamed mass [3].

NanjunaSwamy et al [4] reported on the drying of fruit juice and pulps. Glycerol monostearate , egg albumin, ground nut protein isolate, gur gum and carboxy methyl cellulose (CMC) were employed in the preliminary trials as foaming agents.. Anjaria and chivate [5] reported that foam mat drying of certain model system multiple constant rate periods and falling rate periods foam mat drying was ideally suitable for drying of sticky and viscous slurries. Bolin and salunke [6] reported the physicochemical and volatile flavor changes occurring in fruit juices during concentration and foam mat drying.over the years, the foam-mat drying have been applied to many fruits including banana, guava, apple [7], tomato juice[8]. Lewicki and Konopacka [9] reported the mass transfer and volatile retention during the foam mat drying.
Drying occurs in multiple constant rate periods due to periodic bursting of successive layers of foam bubbles, thus exposing new surfaces for heat and mass transfer as the drying progresses [10, 11]. The foam-mat dried products have better reconstitution properties because of their honeycomb structure and are superior to drum and spray dried products [12]

II. Materials and methods

2.1. Materials

The fruits and vegetables Viz., guava, banana and tomato were procured from the local market.

2.2. Foaming agents:

1. Egg albumin
2. Soya protein isolate

2.3. Methods

Studies were conducted with different concentrations of foaming agents at temperature ranging from 55^{o}C to 75^{o}C.they are as follows:

a. Guava pulp foamed with egg albumin
b. Guava pulp foamed with soya protein isolate
c. Guava pulp foamed with egg albumin and water
d. Banana pulp foamed with egg albumin
e. Banana pulp foamed with soya protein isolate
f. Banana pulp foamed with egg albumin and water.
g. Tomato pulp foamed with egg albumin.
h. Tomato pulp foamed with soya protein isolate
i. Tomato pulp foamed with egg albumin and water.

2.3.1. Preparation of pulps: Guava pulp was prepared by scooping out the pulp along with seeds from fruits. Then these seeds were separated from pulp by rubbing the mixture on 14mesh sieve where the most of the pulp is passed through the mesh leaving seeds. This pulp was then smoothly blended in a mixer. Creamy white pulp was obtained which was ready for analysis. In the same way banana pulp and tomato pulp were prepared.

2.3.2. Preparation of foam:

1. Preaparation of guava foam

Guava pulp was foamed by dispersing initially 0.25% to 1% of the foaming agent in a known quantity of water of 50%.the mixture was then stirred at 300rpm using magnetic stirrer for about 15minutes.stable foam was thus prepared in a stable form previously weighed amount of guava pulp was slowly added . Homogeneous foam slurry was thus prepared and the foam slurry was ready for carrying out the foam mat drying process. In the first case of foaming agent used was egg albumin followed by soya protein isolate. Along with egg albumin and soya protein isolate sometimes water was also added which acted as a stabilizer of the foam for different cases. Stability of the foam played an important role while foam was subjected to drying. During drying they should not be any damage to the foam structure. The same process was done for the preparation of Banana and tomato pulp.

2.3.3. Determination of initial moisture content of the foam: The moisture content was determined by AOAC method [6]. A small amount of this sample (approx. 2 gm) was taken in a pre-weighed petri dish. A sample in the petri dish was dried in an oven for overnight or until the constant weight is reached at 1000^{o}C. The difference in the weight of the sample gave the amount of moisture content and percentage of moisture content was calculated.

% moisture = (Wt of moisture) / (Wt of sample – Wt of moisture) * 100

2.3.4. Preparation of soya protein isolate: Soya bean isolate can be defined as major proteineous fraction of soya bean prepared from superior quality, clean soya bean by removing preponderance of non protein components by physical and chemical process. Food grade, defatted soya bean flour was the basic raw material for the preparation of soya protein isolate. Soya protein isolate was prepared by mixing soya flour and water in the ratio of 1:20. The pH of this mixture adjusted to 9 to 10 by adding 0.1 N NaOH drop by drop. The mixture was centrifuged for 20 min at 5000rpm. Supernatant was adjusted to the pH 4.5 by slowly adding 1N Hcl drop by drop. This was again centrifuged to separate the precipitate to get the soya protein isolate. It was then stored in cool and dry place preferable below 28^{o}C at a relative humidity of 65% or less. The flow sheet for the process of preparing soya protein isolate is shown in the figure1.

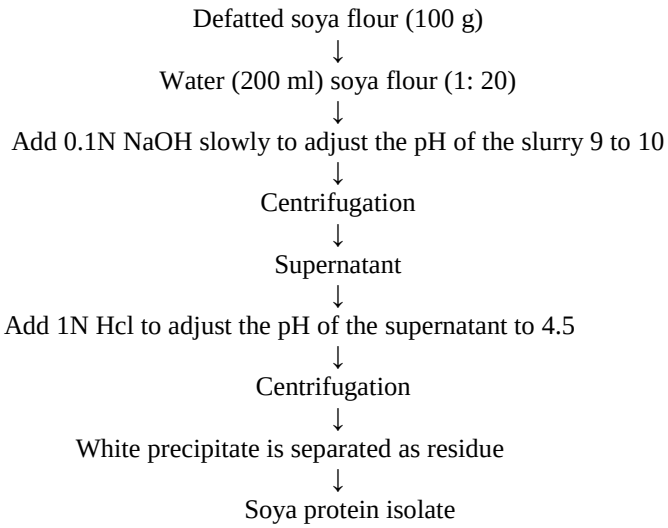

Figure 1: Flow sheet for the preparation of soya protein isolate

2.4. Drying studies: known quantity of the foam was taken into a tray kept in a tray drier. The tray was kept in tray drier until the foam gets dried. This process was carried at different temperatures ranging from 550^{o}C to 800^{o}C. The weights of the sample were taken for every 5minutes, till the foam gets dried. Initial moisture content was determined by AOAC method [13]. Final moisture content of the dried foam in sample in tray drier was also determined. A fine crispy powder was obtained and flakes were observed after some samples which were due to the foaming agent. Considering the experimental samples the good and the best suited foaming agent for these fruits were observed. The same procedure was followed for tomato, banana and guava pulp.

2.5. Rate Curves: A free flowing powder was obtained after drying. However for some samples, the powders were not free flowing. This is due to the foaming agent. The powder is then stored in poly ethylene covers and thus can be used for flavor.

From the data obtained after foam mat drying, curves of moisture content as a function of time were plotted. This was useful directly in determining the time required for drying. Much information were obtained if the data were converted into rates of drying expressed as –dX/ dt and plotted against moisture content **X.** for this purpose the smooth curves for moisture content versus drying time data tangents were drawn for different point to obtain the values for drying rates and drying rate curves were drawn.

III. Results and Discussions

Dried powders were made from tomato, banana and guava by using foam mat drying technique. The tangents were drawn for drying curves and –dx/dt was determined and converted into rate of drying for which the values are shown in the tables 4.1.a to 4.3.b.Maximum moisture (X) for guava, banana and tomato foamed with soya protein isolate and egg albumin against time was determined. From the data available from experiments conducted, it can be observes that the moisture content was decreasing with time. Similarly data was also collected for banana and tomato.

Rate of drying was evaluated from drying curves. The drying curves were drowning with the data on rate of drying versus moisture content at any time. Multiple constant rate periods was observed for different fruits foamed agents because of periodic bursting of successive layers of foam bubbles giving rise to new layer each time.

Data for moisture content of foam dried of guava, banana and tomato samples with time from initial moisture constant to final moisture content are shown in the table 4.1.a. variation of moisture content were shown and the drying curves in figure 4.7, 4.8, 4.9 for guava , banana and tomato with soya protein isolate as a foaming agent for which values are shown in table 4.3a. In the case of foam mat drying of fruit and vegetables pulps constant rate periods falling the rate periods were obtained. The pulp of fruit and vegetables does not change the behavior of the foam mat drying.

Drying was fast in all the above model systems considered. Higher drying resulted in less drying times of the pulp of any fruit and vegetables. The foam mat dried guava powder was in cream color where as a pleasant red color was observed. These powders were highly reconstitutable in water.

Multiple constant rate periods were not observed in control process unlike in the case of foam mat drying. Drying rates were not higher in these cases. Consequently more time was required when compared to the foam mat drying method. As can be seen figures 4.1, 4.2, 4.3, which were drawn from table 4.1a shows the drying data and observed that the initial moisture content decreases with time at 65^{o}C.The drying data for foam mat drying of guava, tomato and banana samples were done under 12mesh size with egg albumin as a foaming agent and water is converted into drying rate vs moisture content are shown in table 4.1.b.

As can be seen figures 4.4, 4.5, 4.6, which are drawn from table 4.2.a shows the drying data and observed the initial moisture content decreases with time at 65^{o}C. Here guava, tomato and banana samples were done under 14 mesh size with egg albumin as a foaming agent dried. The drying data for foam mat drying of guava, tomato and banana samples under 14 mesh with egg albumin as a foaming agent is converted into drying rate vs moisture content are shown in table 4.2.b. From the figures 4.10, 4.11 and 4.12 we can observe the particles of smaller diameters have more drying rates than that of larger particles for the guava, tomato and banana samples with foaming agent as 1 weight percent egg albumin and water because the drying depends on the particle size and specific surface of drying material. The larger particles and uneven surface of drying material takes more time to drying. From the figure 4.13, 4.14 and 4.15 we can observe the particles of samples with egg albumin gives larger drying rates than the samples with 1 weight percent of foaming agent. The drying of material depends on the density of the particles. The less dense particles gives larger drying rates. The foam with egg albumin as a foaming agent ha less density than the foam with soya protein isolate as a foaming agent.

IV. Conclusion

Studies on foam mat drying of the guava, tomato and banana were carried out. The creation of foam has resulted increased surface area for drying with the increase in surface area exposed for drying, increased the rate of drying. Where the low density foams dried at relatively low temperature in an ordinary forced circulation drier. Foam mat drying has results in fruit leathers or powders which otherwise would not have been possible by normal drying. The mat dried powders were good quality and were highly reconstitubel in water.

The foaming agent has effect on rate of drying. Of the various foaming agents dried. Egg albumin was found to be the best. Hence the foam mat drying method is highly feasible in producing fruit and vegetable powders of acceptable quality at reasonable cost under the experimental conditions employed.

References

[1] Morgan, A.I., R.P. Graham, L.F.Ginnette and G.Williams (1961). Recent developments in foam-mat drying. Food technology, 15:37-39.
[2] Berry, R.E., O.W. Bissett and J.C.Lastinger (1965). Method for evaluating foams from citrus concentrations. Food technology, 19(7):144-147.
[3] Chandak .A.j and Chivate M.R, " Recent developments in foam mat drying . " Indian Food packers, 26-31,1972.
[4] Nanjundaswamy.A.M,siddappa.G.S, Gowramma.R.V. and StyanarayanaRao.B.A" Drying of fruits juices and pulps by the foaming technique.", Journal of food science and technology,2(2),63-65.(1965).
[5] Anjari.B.V and Chivate.M.RK, " studies in foam mat drying." Indian chemical engineers,8(3), T64-T68.(1966).
[6] Bolin.H.R, salunkhe.D.K, "Physicochemical and volatile flavor changes occurring in fruit juices during concentration and foam mat drying." Journal of food sciences, 36, 665-668.(1971).

[7] Jayaram, K.S., Goverdhan, T., Sankaran, R., Bhatia, B.S.& Nath, H.(1974). Compressed ready to eat fruited cereals.Journal of food science and Technology, 11(3), 181-185.
[8] Kadam, D.M.& Balasubramanian, S. (2011). Foam mat drying of tomato juice. Jornal of Food Processing and preservation, 35(4), 488-495.
[9] Mass Transfer and Volatiles Retention During Foam-Mat Drying of Food Models P.P. Lewicki, D. Konopacka, Warsaw Agri. Univ., Warsaw, Poland
[10] Hart, M.R., R.P. Graham L.F. Ginnette and A.I.Morgan (1963). Foams for foam-mat drying. Food Technology, 17:1302-1304.
[11] Martin,R.O.,G.Narasimhan, R.K.Singh and A.C.Weitnaner (1992). Food dehydration.In:D.R.Heldman and D.B.Lund (Ed) handbook of food Engineering, Academic press, London.pp.530-531.
[12] Chandak, A.J and M.R.Chivate (1974). Studies in foam-mat drying of coffee extract.Indian food packer, 28(2):17-27.
[13] AOAC official's methods of analysis of the association of official analytical chemist.14th edition.Association of official's chemist, Washington DC (1984).

S.No	Time, t (min)	Moisuture content , X (g moisture/g dry solid)		
		Guava	Tomato	banana
1	0	10.08	30	8.7
2	5	9.76	22	7.8
3	10	8.16	17.66013.33	7
4	15	6.9	9.33	6.8
5	20	6.25	7	6.6
6	25	5.25	3.66	6.4
7	30	4.5	3.66	5.7
8	35	3.83	3.66	5.5
9	40	3.5	2.33	5.4
10	45	3.3	0.33	4.8
11	50	1.8	0	4.4
12	55	1.5	0	3.4
13	60	1.08	0	3.0
14	65	0.75	0	2.2
15	70	0.416	0	2.1
16	75	0.33	0	1.9
17	80	0	0	0
18	85	0	0	0

Table 4.1.a: drying data for the samples under 12 mesh size

S.No	Guava		tomato		Banana	
	Moisture content, X (g moisture/g dry solids)	Drying rate N (g/ cm^2min)	Moisture content, X (g moisture/g dry solids)	Drying rate N (g/ cm^2min)	Moisture content, X (g moisture/g dry solids)	Drying rate N (g/ cm^2min)
1	6.9	0.0367	26	0.13565	7.5	0.031
2	5.3	0.0366	19.5	0.111	5.5	0.024
3	3.8	0.0354	12	0.0827	4.8	0.016
4	2.3	0.0278	5	0.056	3.4	0.014
5	0.7	0.0240	3	0.034	2.2	0.006

Table4.1.b: drying data for the samples under 12 mesh size

S.No	Time, t (Minutes)	Moisture content , X (g moisture / g dry solid)		
		guava	Tomato	Banana
1	0	4	24.5	1.8
2	5	3.8	20.5	1.68
3	10	3.46	18.5	1.54
4	15	2.93	17	1.45
5	20	2.3	9	1.18
6	25	1.93	5	0.9
7	30	1.26	1	0.54
8	35	0.93	1	0.5
9	40	0.8	1	0.4
10	45	0.46	0.5	0.318

11	50	0.2	0	0.045
12	55	0.13	0	0
13	60	0.13	0	0
14	65	0	0	0
15	70	0	0	0

Table 4.2.a: drying data for foam- mat drying of samples using egg albumin as a foaming agent under 14 mesh sizes.

S.No	Guava		tomato		Banana	
	Moisture content, X (g moisture/g dry solids)	Drying rate N (g/ cm^2min)	Moisture content, X (g moisture/g dry solids)	Drying rate N (g/ cm^2min)	Moisture content, X (g moisture/g dry solids)	Drying rate N (g/ cm^2min)
1	6.9	0.01236	26	0.06656	7.5	0.04168
2	5.3	0.00957	19.5	0.05112	5.5	0.0361
3	3.8	0.00697	12	0.03329	4.8	0.0342
4	2.3	0.00434	5	0.01656	3.4	0.0303
5	0.7	0.015	3	0.00002	2.2	0.02704

Table 4.2.b: drying rate data for the samples under 18 Mesh size

S.No	Time, t (Minutes)	Moisture content , X (g moisture / g dry solid)		
		guava	Tomato	Banana
1	0	5.25	8.6	20.5
2	5	4.75	8.4	15
3	10	3.125	8.0	13.5
4	15	3.02	7.4	12
5	20	2.875	6.6	11.5
6	25	1.965	6	11
7	30	0.625	3.4	10.5
8	35	0.52	2.4	9.5
9	40	0.25	1.4	8.5
10	45	0	0.4	8
11	50	0	0	7
12	55	0	0	6
13	60	0	0	5
14	65	0	0	3
15	70	0	0	1.5
16	75	0	0	0
17	80	0	0	0

Table 4.3.a. Drying rate for foam-mat drying of samples using soya protein isolate a foaming agent under 18 Mesh

S.No	Guava		tomato		Banana	
	Moisture content, X (g moisture/g dry solids)	Drying rate N (g/ cm^2min)	Moisture content, X (g moisture/g dry solids)	Drying rate N (g/ cm^2min)	Moisture content, X (g moisture/g dry solids)	Drying rate N (g/ cm^2min)
1	6.9	0.01236	26	0.06656	7.5	0.04168
2	5.3	0.00957	19.5	0.05112	5.5	0.0361
3	3.8	0.00697	12	0.03329	4.8	0.0342
4	2.3	0.00434	5	0.01656	3.4	0.0303
5	0.7	0.0015	3	0.00002	2.2	0.02704

Table 4.3.b: drying data for the samples under 14 Mesh size.

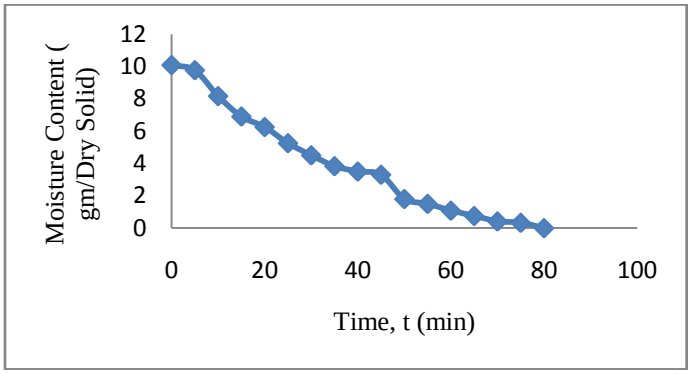

Fig: 4.1. Drying curve for guava (12 meshes) with Egg albumin as a foaming agent at 65°C

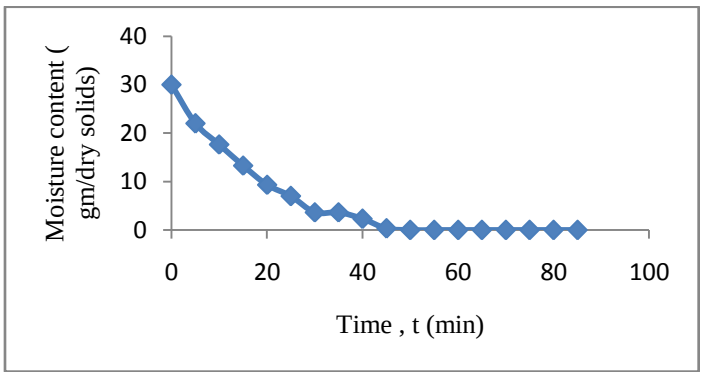

Fig: 4.2. Drying curve for Tomato (12 mesh) with Egg albumin as a foaming agent at 65°C

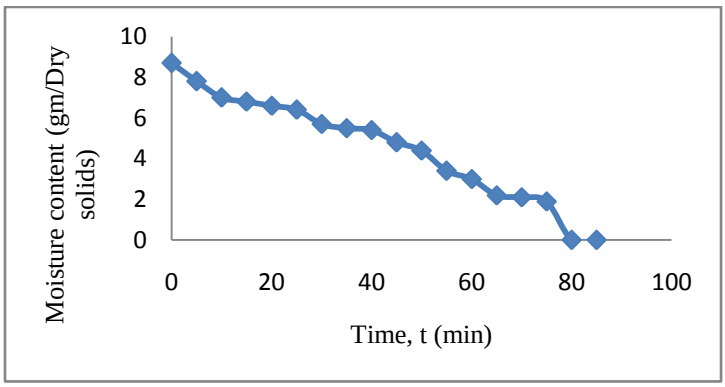

Fig: 4.3. Drying curve for Banana (12 mesh) with Egg albumin as a foaming agent at 65°C

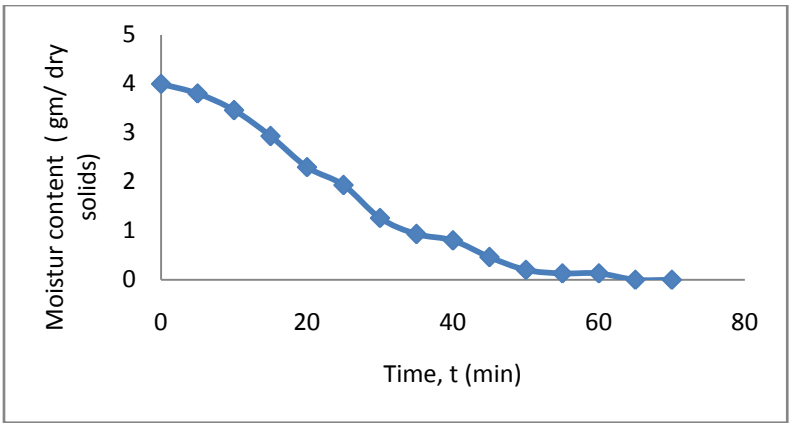

Fig: 4.4. Drying curve for Guava (18 mesh) with Egg albumin as a foaming agent at 65°C

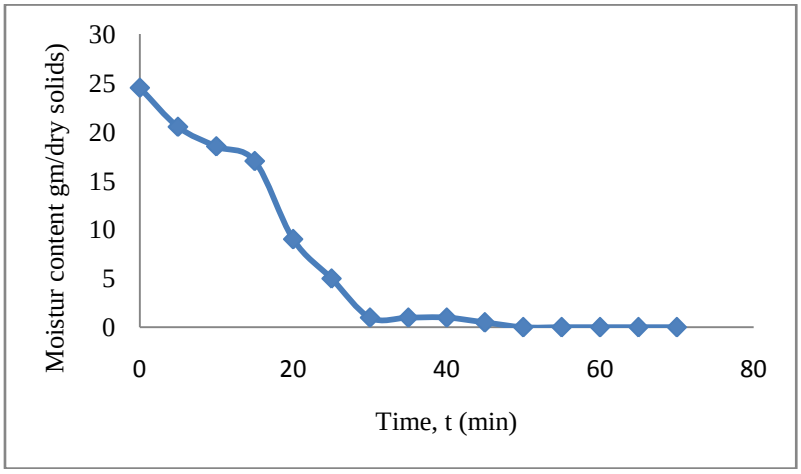

Fig: 4.5. Drying curve for Tomato (18 mesh) with Egg albumin as a foaming agent at 65°C

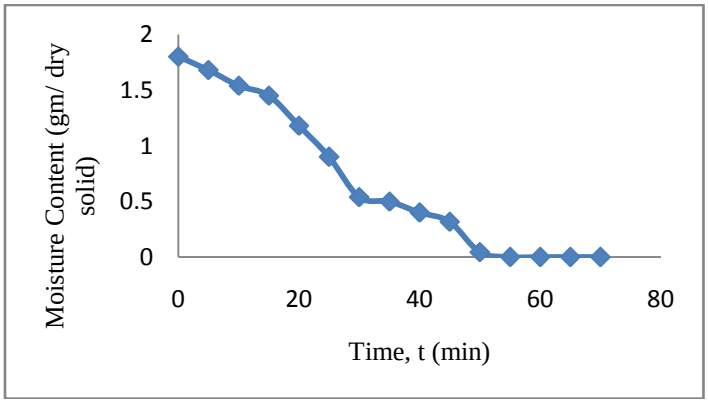

Fig: 4.6. Drying curve for Banana (18 mesh) with Egg albumin as a foaming agent at 65°C

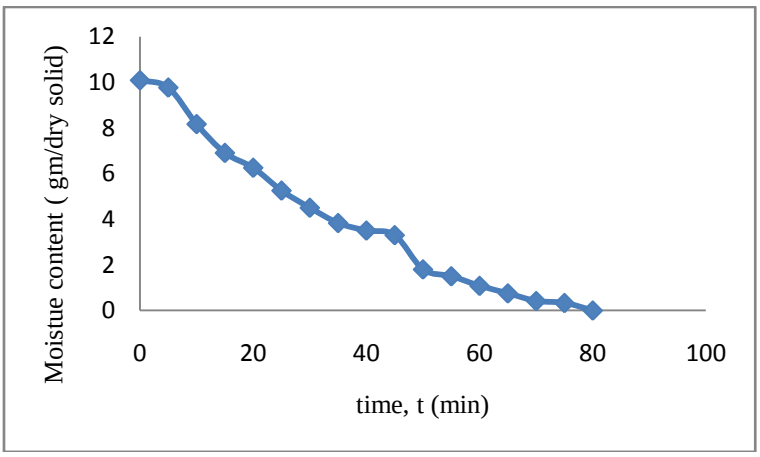

Fig: 4.7. Drying curve for banana (18 mesh) with Soya protein as a foaming agent at 65°C

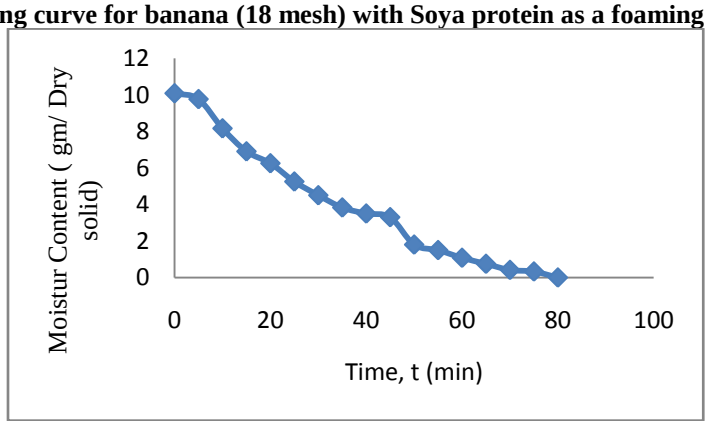

Fig: 4.8. Drying curve for Tomato (18 mesh) with Soya protein as a foaming agent at 65°C

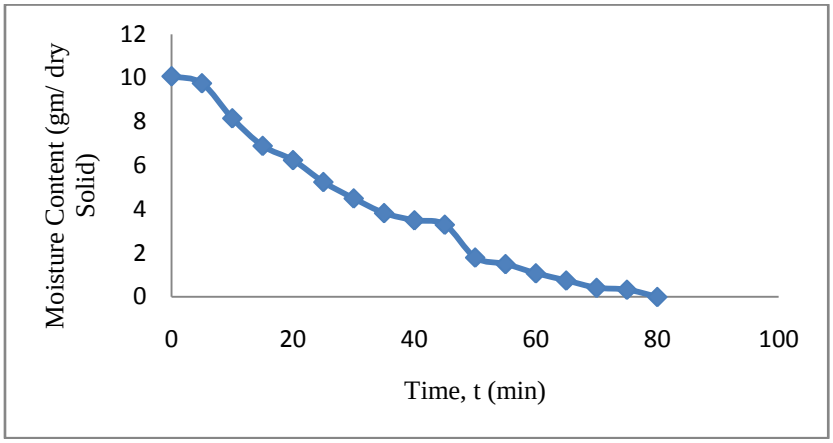

Fig: 4.9. Drying curve for Banana (18 mesh) with Soya protein as a foaming agent at 65^{o}C

Nomenclature:
Moisture content, X (g moisture/g dry solids)
Drying rate N (g/ cm^{2}min)
Time t (min)
Temperature ^{o}C
Carboxy methyl cellulose (CMC)

International Journal of Modern Engineering Research (IJMER)
www.ijmer.com Vol. 3, Issue. 3, May.-June. 2013 pp-1520-1522 ISSN: 2249-6645

On pairs of Special Polygonal numbers with Unit difference

M. A. Gopalan[1], Manju Somanath[2], K.Geetha[3]
[1]*Department of Mathematics, Shrimati Indira Gandhi college, Trichirapalli*
[2]*Department of Mathematics, National College, Trichirapalli*
[3]*Department of Mathematics, Cauvery College for Women, Trichirapalli*

Abstract: *We obtain the ranks of m-gonal numbers such that the difference between any two special m-gonal numbers is unity. The recurrence relations satisfied by the ranks of each m-gonal numbers are also presented.*
Keyword: *Special polygonal numbers*
MSC classification code: *11D99*

I. INTRODUCTION

Number is the essence of mathematical calculation. Variety of numbers has variety of range and richness. Many numbers exhibit fascinating properties, they form sequences, they form patterns and also and so on [1, 2, 3]. In [4] explicit formulas for the ranks of Triangular number which simultaneously equal to Pentagonal, Octagonal, Decagonal and Dodecagonal numbers in turn are presented. Denoting the ranks of Triangular, Pentagonal, Hexagonal, Octagonal, and Heptagonal, decagonal and Dodecagonal number by the symbols N, P, Q, M, H, D and T respectively. In [5], the following relations are studied:

1. N- P = 1 2. N – M = 1 3. N – H = 1 4. N – D = 1
1. N – T = 1 6. P – M =1 7. P – Q = 1 8. P – H = 1

In [6], the ranks of m-gonal numbers such that the difference between any two m-gonal numbers is unity. The recurrence relations satisfied by the ranks of each m-gonal number in turn are presented. In this communication, we make an attempt to obtain the ranks of other special pairs of m-gonal numbers such that the difference between any two m-gonal numbers is unity. The recurrence relations satisfied by the ranks of m-gonal numbers are also presented.

II. Method of Analysis

1) Centered hexagonal number – Triangular number =1

Denoting the ranks of the centered hexagonal number and Triangular number to be A and M respectively, the identify is given by

Centered hexagonal number – Triangular number = 1 (1)

is written as $$y^2 = 6x^2 - 5 \quad (2)$$

where $$x = 2A+1,\ y = 2M+1 \quad (3)$$

whose initial solution is $x_0 = 3, y_0 = 7$

Let (x_s, y_s) be the general solution of the pellian

$$y^2 = 6x^2 + 1$$

where $$\tilde{x}_s = \frac{1}{2\sqrt{6}}\left(\left(5+2\sqrt{6}\right)^{s+1} - \left(5-2\sqrt{6}\right)^{s+1}\right)$$

$$\tilde{y}_s = \frac{1}{2}\left(\left(5+2\sqrt{6}\right)^{s+1} + \left(5-2\sqrt{6}\right)^{s+1}\right),\ s = 0,1,2...$$

Applying Brahmagupta's lemma between the solutions (x_0, y_0) and $(\tilde{x}_0, \tilde{y}_0)$ the sequence of values of x and y satisfying equation (2) is given by

$$x_s = \frac{1}{2\sqrt{6}}\left(\left(5+2\sqrt{6}\right)^{s+1}\left(7+3\sqrt{6}\right) - \left(5-2\sqrt{6}\right)^{s+1}\left(7-3\sqrt{6}\right)\right)$$

$$y_s = \frac{1}{2}\left(\left(5+2\sqrt{6}\right)^{s+1}\left(7+3\sqrt{6}\right) + \left(5-2\sqrt{6}\right)^{s+1}\left(7-3\sqrt{6}\right)\right),\ s = 0,1,2...$$

Inview of (3), the ranks of centered hexagonal number and Triangular number are respectively given by

$$A_s = \frac{1}{4\sqrt{6}}\left(\left(5+2\sqrt{6}\right)^{s+1}\left(7+3\sqrt{6}\right) - \left(5-2\sqrt{6}\right)^{s+1}\left(7-3\sqrt{6}\right) - 2\sqrt{6}\right)$$

$$M_s = \frac{1}{4}\left(\left(5+2\sqrt{6}\right)^{s+1}\left(7+3\sqrt{6}\right)+\left(5-2\sqrt{6}\right)^{s+1}\left(7-3\sqrt{6}\right)-2\right),\ s=0,1,2...$$

and their corresponding recurrence relations are found to be

$$A_{s+2}-10A_{s+1}+A_s-4=0$$

$$M_{s+2}-10M_{s+1}+M_s-4=0,\ s=0,1,2...$$

In similar manner, we present below the ranks of other special Polygonal numbers with unit difference in a tabular form

S. No	M-Gonal number	General forms of ranks
1	Centered heptagonal number(B) Triangular number(M)	$B_s = \frac{1}{4\sqrt{7}}\left(\left(8+3\sqrt{7}\right)^{s+1}\left(13+5\sqrt{7}\right)-\left(8-3\sqrt{7}\right)^{s+1}\left(13-5\sqrt{7}\right)-2\sqrt{7}\right)$ $M_s = \frac{1}{4}\left(\left(8+3\sqrt{7}\right)^{s+1}\left(13+5\sqrt{7}\right)+\left(8-3\sqrt{7}\right)^{s+1}\left(13-5\sqrt{7}\right)-2\right),\ s=0,1,2...$
2	Centered decagonal number(C) Triangular number(M)	$C_s = \frac{1}{4\sqrt{20}}\left(\left(9+2\sqrt{20}\right)^{s+1}\left(31+7\sqrt{20}\right)-\left(9-2\sqrt{20}\right)^{s+1}\left(31-7\sqrt{20}\right)-2\sqrt{20}\right)$ $M_s = \frac{1}{4}\left(\left(9+2\sqrt{20}\right)^{s+1}\left(31+7\sqrt{20}\right)+\left(9-2\sqrt{20}\right)^{s+1}\left(31-7\sqrt{20}\right)-2\right),$ $s=0,1,2...$
3	Centered hendecagonal number(D) Triangular number(M)	$D_s = \frac{1}{4\sqrt{11}}\left(\left(10+3\sqrt{11}\right)^{s+1}\left(23+7\sqrt{11}\right)-\left(10-3\sqrt{11}\right)^{s+1}\left(23-7\sqrt{11}\right)-2\sqrt{11}\right)$ $M_s = \frac{1}{4}\left(\left(10+3\sqrt{11}\right)^{s+1}\left(23+7\sqrt{11}\right)+\left(10-3\sqrt{11}\right)^{s+1}\left(23-7\sqrt{11}\right)-2\right),$ $s=0,1,2...$
4	Centered Tetradecagonal number(E) Triangular number(M)	$E_s = \frac{1}{4\sqrt{14}}\left(\left(15+4\sqrt{14}\right)^{s+1}\left(41+11\sqrt{14}\right)-\left(15-4\sqrt{14}\right)^{s+1}\left(41-11\sqrt{14}\right)-2\sqrt{14}\right.$ $M_s = \frac{1}{4}\left(\left(15+4\sqrt{14}\right)^{s+1}\left(41+11\sqrt{14}\right)+\left(15-4\sqrt{14}\right)^{s+1}\left(41-11\sqrt{14}\right)-2\right),$ $s=0,1,2...$
5	Centered Pentadecagonal number(F) Triangular number(M)	$F_s = \frac{1}{4\sqrt{15}}\left(\left(4+\sqrt{15}\right)^{s+1}\left(11+3\sqrt{15}\right)-\left(4-\sqrt{15}\right)^{s+1}\left(11-3\sqrt{15}\right)-2\sqrt{15}\right)$ $M_s = \frac{1}{4}\left(\left(4+\sqrt{15}\right)^{s+1}\left(11+3\sqrt{15}\right)+\left(4-\sqrt{15}\right)^{s+1}\left(11-3\sqrt{15}\right)-2\right),$ $s=0,1,2...$
6	Centered Icosagonal number(G) Triangular number(M)	$G_s = \frac{1}{4\sqrt{20}}\left(\left(9+2\sqrt{20}\right)^{s+1}\left(49+11\sqrt{20}\right)-\left(9-2\sqrt{20}\right)^{s+1}\left(49-11\sqrt{20}\right)-2\sqrt{20}\right.$ $M_s = \frac{1}{4}\left(\left(9+2\sqrt{20}\right)^{s+1}\left(49+11\sqrt{20}\right)+\left(9-2\sqrt{20}\right)^{s+1}\left(49-11\sqrt{20}\right)+2\right),$ $s=0,1,2...$

The recurrence relations satisfied by the ranks of each of the special polygonal numbers with unit difference presented in the table above are as follows

S. No	Recurrence relations
1	$B_{s+2} = 16B_{s+1} - B_s + 7;\ B_0 = 39, B_1 = 629$ $M_{s+2} = 16M_{s+1} - M_s + 7;\ M_0 = 104, M_1 = 1665$
2	$C_{s+2} = 18C_{s+1} - C_s + 8;\ C_0 = 62, C_1 = 1121$ $M_{s+2} = 18M_{s+1} - M_s + 8;\ M_0 = 279, M_1 = 5015$
3	$D_{s+2} = 20D_{s+1} - D_s + 9;\ D_0 = 69, D_1 = 1386$ $M_{s+2} = 20M_{s+1} - M_s + 9;\ M_0 = 230, M_1 = 4598$
4	$E_{s+2} = 30E_{s+1} - E_s + 14;\ E_0 = 164, E_1 = 4929$ $M_{s+2} = 30M_{s+1} - M_s + 14;\ M_0 = 615, M_1 = 18444$
5	$F_{s+2} = 8F_{s+1} - F_s + 3;\ F_0 = 44, F_1 = 90$ $M_{s+2} = 8M_{s+1} - M_s + 3;\ M_0 = 11, M_1 = 350$
6	$G_{s+2} = 18G_{s+1} - G_s + 8;\ G_0 = 98, G_1 = 1767$ $M_{s+2} = 18M_{s+1} - M_s + 8;\ M_0 = 440, M_1 = 7904$

III. Conclusion

To conclude, one may search for the other M-gonal numbers satisfying the relation under consideration.

References

[1] T.S.Bhanumathy, Ancient Indian Mathematics, New Age Publishers Ltd, New Delhi, 1995.
[2] L.E.Dikson, "History of Theory of Numbers", Chelsa Publishing Company, New York, Vol.2, 1952.
[3] Shailesh Shirali, "Mathematical Marvels", A Primer on number sequences, Universities Press, 2001.
[4] M.A.Gopalan and S.Devibala, "Equality of Triangular Numbers with Special m-gonal numbers", Bulletin of Allahabad Mathematical Society, Vol.21, Pp.25-29, 2006.
[5] M.A.Gopalan, Manju Somanath, N.Vanitha, " On pairs of m-gonal numbers with unit difference", Advances in Theorectial and Applied Mathematics, Vol.1, No.3, Pp.197-200, 2006.
[6] M.A.Gopalan, Manju Somanath, N.Vanitha, "On pairs of m-gonal numbers with unit difference", Reflections des ERA-JMS, Vol.4, Issue4, Pp.365-376, 2009.

International Journal of Modern Engineering Research (IJMER)
www.ijmer.com Vol. 3, Issue. 3, May.-June. 2013 pp-1523-1528 ISSN: 2249-6645

Power Optimization of Linear Feedback Shift Register (LFSR) for Low Power BIST implemented in HDL

R. Vara PrasadaRao[1], N. Anjaneya Varaprasad[2], G. Sudhakar Babu[3], C. Murali Mohan[4]
Assistant professor, SVIT, Hampapuram, Anantapuram (Dt), Andhra Pradesh

ABSTRACT: *LFSR based Pseudo random test pattern generator is used in the testing of ASIC chips which generates random sequences of test patterns. This project deals with the design of LFSR and also how to multiplex the Test inputs with the ASIC inputs to reduce the additional test input pins required for the ASIC.*
This project presents a novel low-transition Linear Feedback Shift Register (LFSR) that is based on some new observations about the output sequence of a conventional LFSR. The proposed design, called bit-swapping LFSR (BS-LFSR), is composed of an LFSR and a 2 × 1 multiplexer. When used to generate test patterns for scan-based built-in self-tests, it reduces the number of transitions that occur at the scan-chain input during scan shift operation by 50% when compared to those patterns produced by a conventional LFSR.
Hence, it reduces the overall switching activity in the circuit under test during test applications. The BS-LFSR is combined with a scan-chain-ordering algorithm that orders the cells in a way that reduces the average and peak power (scan and capture) in the test cycle or while scanning out a response to a signature analyzer. These techniques have a substantial effect on average- and peak power reductions with negligible effect on fault coverage or test application time. Experimental results on ISCAS'89 benchmark circuits show up to 65% and 55% reductions in average and peak power, respectively. Index Terms Built-in self-test (BIST), linear feedback shift register (LFSR), low-power test, pseudorandom pattern generator, scan-chain ordering, weighted switching activity (WSA).
Keywords: *LFSR, Optimization, Low Power, Test Patterns*

I. Introduction

The main challenging areas in VLSI are performance, cost, testing, area, reliability and power. The demand for portable computing devices and communications system are increasing rapidly. These applications require low power dissipation for VLSI circuits. The power dissipation during test mode is 200% more than in normal mode [1]. Hence it is important aspect to optimize power during testing. Power optimization is one of the main challenges.
There are various factors that affect the cost of chip like packaging, application, testing etc. In VLSI, according to thumb rule 5000 of the total integrated circuits cost is due to testing. During testing two key challenges are:

- Cost of testing that can't be scaled.
- Engineering effort for generating test vectors increases as complexity of circuit increases.

Based on 1997 SIA data, the upper curve shows the fabrication cost of transistor and lower curve shows the testing cost of transistor. Figure 1 shows that the fabrication cost transistor decreases over the decades according to Moore's law but the testing cost as constant.

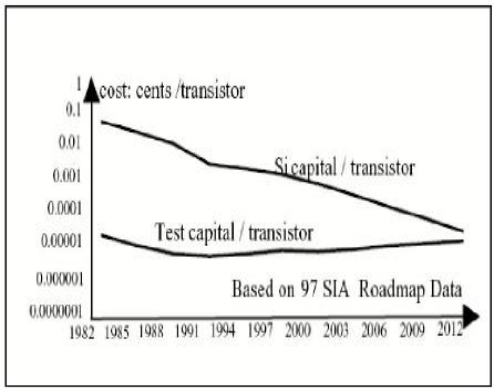

Figure 1: Fabrication cost versus testing cost

There are main two sources of power dissipation in digital circuits; these are static and dynamic power dissipation. Static power dissipation is mainly due to leakage current and its contribution to total power dissipation is very small. Dynamic power dissipation is due to switching i.e. the power consumed due to short circuit current flow and charging of load capacitances is given by equation:

$$P = 0.5\, VDD^2\, E(SW)\, CL\, Fclk$$

Where VDD is supply voltage, E (SW) is the average number of output transitions per 1/fclk, fclk is the clock frequency and CL is the physical capacitance at the output of the gate. Dynamic power dissipation contributed to total power dissipation. From the above equation the dynamic power depends on three parameters: Supply voltage, Clock frequency,

switching activity. To reduce the dynamic power dissipation by using first two parameter only at the expense of circuit performance. But power reduction using the switching activity doesn't degrade the performance of the circuit. Power dissipation during the testing is one of most important issue [12]. There are several reasons for this power increased in test mode.

- To test large circuit, circuits are partitioned to save the test time but this parallel testing result in excessive energy and power dissipation.
- Due to the lack of at-speed equipment availability, delay is introduced in the circuit during testing. This cause power dissipation.
- In the successive functional input vectors applied to a given circuits in normal mode have a significant correlation. While the correlation between consecutive test patterns can be very low. This can cause large switching activity in the circuit during test than that during its normal operation. Power dissipation in CMOS circuits is proportional to switching activity, this excessive switching during test may be responsible for cost, reliability, performance verification, autonomy and technology related problems.

During testing large power is dissipated than in the normal mode. This is due to lack of correlation between the successive test patterns generated by ATPG (for external testing) or LFSR (for BIST) and this large power dissipation causes following effects:

- The increased power may be responsible for cost, reliability, performance verification, autonomy and technology related problems. Low power dissipation during test application is thus becoming an equally important figure of merit in today's VLSI circuits design and is expected to become one of the major objectives in the near future.
- High power and ground noise caused by high switching during testing are serious problem where the supply connects are poor. Thus excessive noise can change the logic state of the circuit lines leading good dies to fail the test and hence loss of yields.
- As the circuit is designed in the deep sub micron (DSM) technology, this uses small supply voltages and hence this reduces the use of special cooling equipment to remove the excessive heat during test.
- Low power testing is done at speed. But in other testing techniques, circuits are added to lower the frequency of circuit during test.

For complex circuits, hierarchical approach is used. The advantage of hierarchical approach is that every block is tested separately. Test input is given to each block and output is observed and verified. DFT (Design For Testability) is the action of placing features in a chip design process to enhance the ability to generate vectors, achieve a measured quality level or reduce cost of testing. The conventional DFT approaches use scan and BIST.

In this paper a modified low power LFSR are used in which the number of transitions of test pattern are reduced testing. The remainder paper is organized as follows: Section 2 describes the previous work while section 3 presents the proposed work. Section 4 describes the simulation results and conclusions.

II. Prior work

There has been various low power approaches proposed to solve the problem of power dissipation during the testing. Some of the earliest work that has been proposed for optimizing the power during testing are discussed in this section of paper. One method is to use Random Single Input Change (RISC) test generation, which is used to generate low power test pattern. In this method, power consumption is reduced but at the additional cost is between 19% to 13%. Another technique was proposed in [5]. This approach proposed a low transition LFSR for BIST applications. This reduces the average and peak power of circuit during testing. In [6] approach, a fault model and ATPG algorithm is chosen first and then test pattern are generated to obtain the desired fault coverage. There are various advantages of test pattern generation at a higher level than the gate level. While *F. Corno et al* has proposed for the low power test pattern generation for sequential circuit [7]. In this paper, redundancy is introduced during testing and this reduces the power consumption without affecting the fault coverage. In [8], it is shown that different LFSR architecture affects the power consumed and the hardware used. *Jinkyu Lee et al* [9] developed a LFSR reseeding scheme. In this approach, there are two goals, first is to reduce the number of transition in scan chain. Second is to reduce the number of specified bits generated by LFSR reseeding.

III. BIST Architecture

It is very important to choose the proper LFSR architecture for achieving the appropriate fault coverage. Every architecture consumes different power even for same polynomial. Another problem associated with choosing LFSR is LFSR design issue, which includes LFSR partitioning, in this the LFSR are differentiated on the basis of hardware cost and testing time cost.

A typical BIST architecture consists of a test pattern generator (TPG), usually implemented as a linear feedback shift register (LFSR), a test response analyzer (TRA), implemented as a multiple input shift register (MISR), and a BIST control unit (BCU), all implemented on the chip (Figure 1). This approach allows applying at-speed tests and eliminates the need for an external tester. The BIST architecture components are given below.

Circuit Under Test (CUT): It is the portion of the circuit tested in BIST mode. It can be sequential, combinational or a memory. Their Primary Input (PI) and Primary output (PO) delimit it.

Test pattern generator (TPG): It generates the test patterns for the CUT. It is a dedicated circuit or a microprocessor. The patterns may be generated in pseudorandom or deterministically.

Multiple input signatures register (MISR): It is designed for signature analysis, which is a technique for data compression. MISR are frequently implemented in portability of alias. MISR are frequently implemented in BIST designs, in which output response are compressed by MISR

Test Response Analysis (TRA): It analyses the value sequence on PO and compares it with the expected output.

BIST controller Unit (BCU): It controls the test execution; it manages the TPG, TRA and reconfigures the CUT and the multiplexer. It is activated by the Normal/Test signal and generates Go/No go.

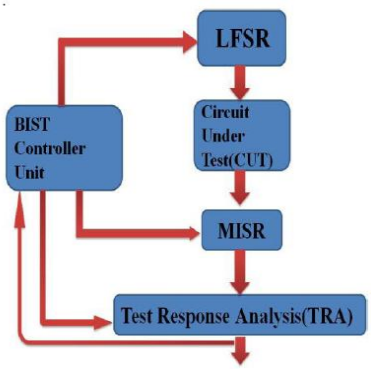

Figure 2 BIST Architecture

IV. Algorithm for Low Power LFSR

As discussed in the previous section LFSR is used to generate test patterns for BIST. In this, test patterns are generated externally by LFSR, which is inexpensive and high speed. LFSR is a circuit consists of flip-flops in series. LFSR is a shift register where output bit is an XOR function of some input bits. The initial value of LFSR is called seed value. LFSR's seed value has a significant effect on energy consumption [3].

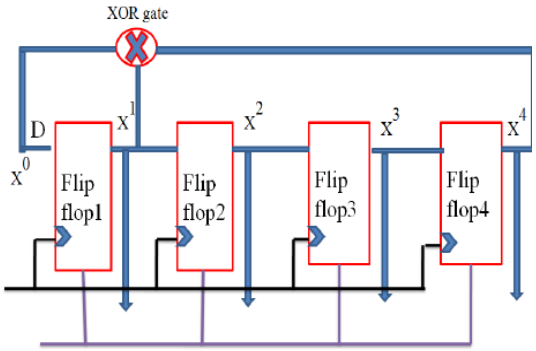

Figure 3: LFSR in which input of first flip-flop is xored with last flip-flop.

The output that influence the input are called tap. A LFSR is represented by as polynomial, which is also known as characteristic polynomial used to determine the feedback taps, which determine the length of random pattern generation. The output of LFSR is combination of 1's and 0's. A common clock signal is applied to all flip-flops, which enable the propagation of logical values from input to output of flip-flops. Increasing the correlation between bits reduces the power dissipation. This can be achieved by adding more number of test vectors, which decreases the switching activity [4].

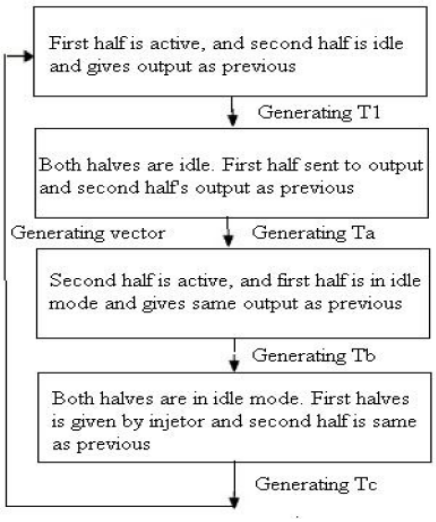

Figure 4: Proposed algorithm for low power LFSR

LFSR is characterized by the polynomial by its characteristics polynomial and inverse of characteristics polynomial is generated polynomial. In this approach the 3 intermediate test vectors are generated between every two successive vectors (say TI, T2). The total number of signal transition occurs between these 5 vectors are equivalent to the number of transition occurs between the 2 vectors. Hence the power consumption is reduced. Additional circuit is used for few logic gates in order to generate 3 intermediate vectors. The 3 intermediate vectors (Ta, Tb, Tc) are achieved by modifying conventional flip-flops outputs and low power outputs. The first level of hierarchy from top to down includes logic circuit design for propagation either the present or next state of flip-flop to second level of hierarchy. Second level of hierarchy is implementing Multiplexed (MUX) function i.e. selecting two states to propagate to output as shown in flow. Second level of hierarchy is implementing Multiplexed (MUX) function i.e. selecting two states to propagate to output as shown in flow:

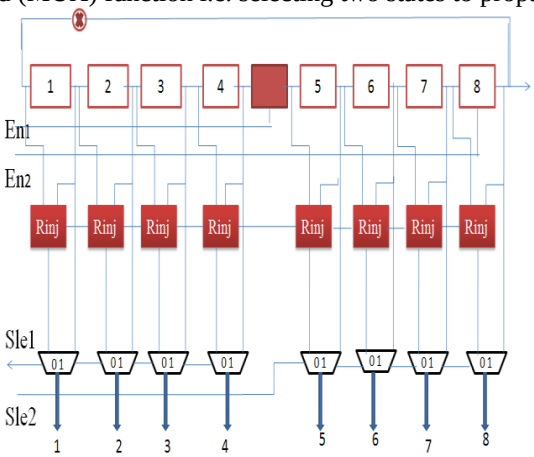

Figure 5: Low power linear feedback shift register

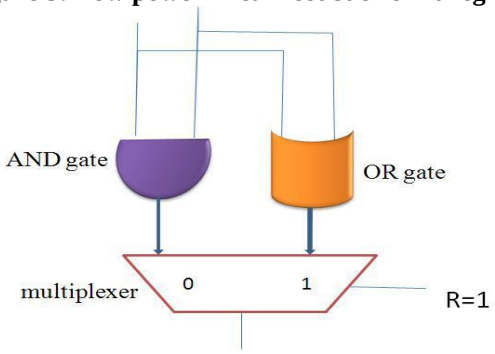

Figure 6: Injector Circuit

The EDA tool is used in which conventional and low power LFSR is coded in VHDL hardware descriptive language and a seed value is given (0100101001011010110100l0O100101101011) to the polynomial and primitive value polynomial in LFSR block. The outputs of the 36-bit LFSR are used as the inputs to the c432 ISCAS-85 a benchmark circuit of interrupt controller. In this c432 is used as CUT; the generated code is synthesized in Xilinx Web Pack 10.1 for Spartan 3e device. The hardware summary is obtained for each method implementation log file of Xilinx 10.1 project navigator.

V. Results And Conclusion

The results obtained from the Xilinx 10.1 implementation with the device xc3s200-4pq208 in which, we have generated VCD file after the post simulation. X power is used to calculate the with the simulation files. Results are obtained for each case and comparison of power dissipation is made on the basis of reports is shown in figure. It is observed that the total power consumed in modified LFSR is 46% less than the power consumed with normal LFSR and output dynamic power is decreased by 44.6 %.

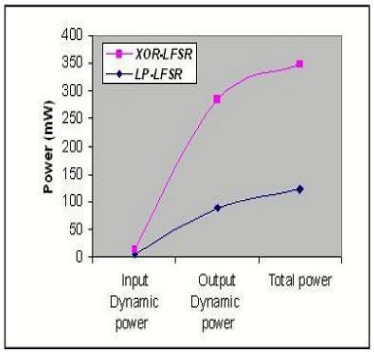

Figure 7: Comparison of Power dissipation in testing with conventional and low power LFSR

It is concluded that low power LFSR is very useful for BIST implementation in which the CUT may be Combinational, sequential and memory circuits. Using low power LFSR technique we can further decrease the power in BIST implementation.

Simulation results:

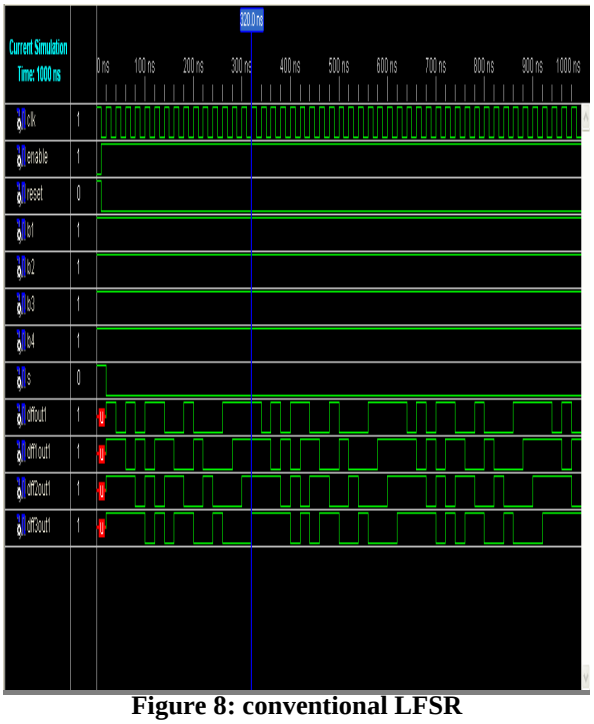

Figure 8: conventional LFSR

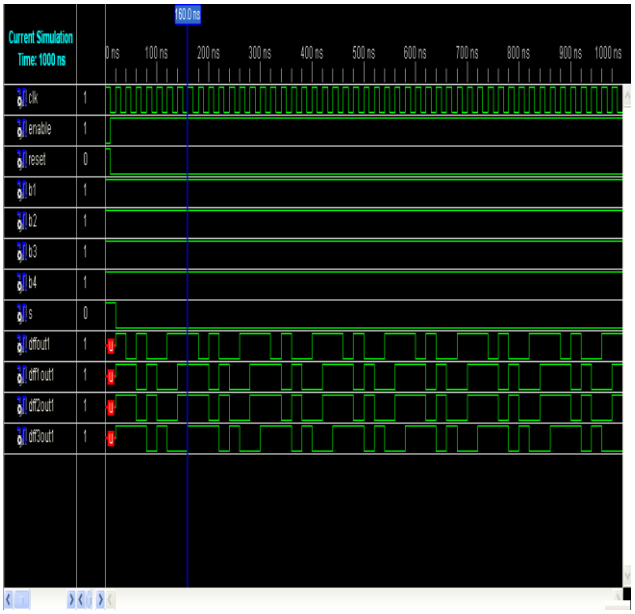

Figure 9: low power LFSR

References

[1] N. Ahmed, M. H. Tehranipour, M. Nourani" Low Power Pattern Generation for BIST Architecture"
[2] Balwinder Singh, Arun Khosla, Sukhleen Bindra" Power Optimization of Linear Feedback Shift Register (LFSR) for Low Power BIST"
[3] E. Atoofian, S. Hatami, Z. Navabi, M. Alisaface and A. Afzali-Kusha," A New Low-Power Scan-Path Architecture," IEEE International Symposium, Vol.5, pp.5278 - 5281, 23-26 May 2005
[4] Dr.K.Gunavathi,Mr.K.ParamasivaM,Ms.P.Subashini Lavanya, M.Umamageswaran," A novel BIST TPG for testing of VLSI circuits", IEEE International Conference on Industrial and Information Systems, pp.8 - 11, August 2006.
[5] Mohammad Tehranipoor, Mehrdad Nourani, Nisar Ahmed," Low-Transition LFSR for BIST-Based Applications," 14th Asian Test Symposium, pp. 138- 143, 18-21 Dec. 2005.

[6] F. Corno, P. Prinetto, M. Rebaudengo, M. Sonza Reorda," A Test Pattern Generation methodology for low power consumption," pp.1-5, 2008.
[7] Jinkyu Lee and Nur A. Touba," LFSR-Reseeding Scheme Achieving Low-Power dissipation during Test," IEEE transactions on computer- aided design of integrated circuits and systems, 26(2), February 2007

Authors Biography

R. Varaprasadarao Assistant Professor, Dept of ECE SVIT, Hampapuram, Anantapur, Andhra Pradesh, India He has 3 years of teaching experience He received his M.Tech (VLSI) from JNTUA, Anantapuram, B.Tech (ECE) from JNTUA, Anantapuram. He is interested in VLSI Design, Embedded systems and communication.

N. Anjaneya Varaprasad Associate Professor, HOD- Dept of ECE SVIT, hampapuram, Anantapur He has 17 years of teaching experience He received his M.Tech(VLSI) from Sathyabhama University, Chennai, B.Tech (ECE) from Gulbarga University, Karnataka. He is interested in VLSI Design, Embedded systems and communication.

G. Sudhakar Babu, Assistant Professor Dept of Science, SVIT, Hampapuram, Anantapur He has 11 years of teaching experience He received his M.Phil from Allagappa University, Tamilnadu, He is interested in Embedded systems and Semiconductos.

C. Murali Mohan, Associate Prof Dept of ECE SVIT, Hampapuram, Anantapur He has 18 years of teaching experience He received his M.tech from sathyabhama University, Chennai, He is interested in VLSI Design, Embedded systems and communication.

International Journal of Modern Engineering Research (IJMER)
www.ijmer.com Vol. 3, Issue. 3, May.-June. 2013 pp-1529-1533 ISSN: 2249-6645

Fatigue and Corrosion Fatigue Behavior of Nickel Alloys in Saline Solutions

Aezeden Mohamed
Faculty of Engineering and Applied Science, Memorial University, St. John's, NF, Canada, A1B 2X3

ABSTRACT : *Nickel based alloys have been developed as materials offering superior corrosion fatigue. The fatigue performance of IN600, IN601 and C22 was examined in increasing saline solution severity of 3.5% sodium chloride at pH = 6.8. Results of fatigue and corrosion fatigue tests indicate that the fatigue lives of IN600, IN601 and C22 tested in 3.5 % sodium chloride solution (NaCl) are essentially the same as for specimens tested in air. Fatigue fractures presented a ductile appearance in specimens tested in both air and in a saline solution, thus providing additional evidence of there being no effect of the 3.5% sodium solutions on fatigue strength.*
Keywords: *Air, C22, fatigue, IN600, IN601, solution.*

I. INTRODUCTION

Fatigue is the time-dependent growth of subcritical cracks under cyclic loading [1]. Fatigue cracking is one of the most common causes of failure of engineering structures, can go undetected, be unexpected, and can result in catastrophic failures.

Fatigue and fatigue damage in the presence of various corrosive media have been the subjects of sustained research in materials engineering technology for more than a century [2]. Metals and their alloys, when they are exposed to aggressive environments and cyclic stresses, can suffer a degradation of fatigue resistance. Even laboratory air containing some moisture has been shown to influence crack propagation rates of materials when compared with those obtained from tests in vacuum or in dehumidified inert gases. Measures to avoid such corrosion cracking include careful materials selection, heat treatment, and modifications of material/environment interactions through coating, controlled solution chemistry, inhibition, and applied potentials. Find better solutions are of extreme importance in several industries, including and especially in aerospace and power generation and offshore service.

Nnumerous studies have been carried out on the mechanical and chemical properties of nickel alloys [3-5]. Nickel alloys containing chromium and molybdenum are used in a wide variety of environments involving corrosive media because these elements significantly improve corrosion properties [6-8].

Understanding the processes of fatigue cracking of these nickel alloys in corrosive environments is key to developing processes for the addition of alloying elements and for materials and manufacturing process selection. For example, fatigue crack initiation in materials used in environments containing corrosive media has been attributed to various factors such as the presence of pitting corrosion sites. Increased corrosion fatigue enhanced deformation was proposed to explain the apparent intensification of intrusions and extrusions in materials [6-10].

The current study was conducted to determine and to compare the effect of alloying elements on the fatigue and corrosion fatigue behavior of the nickel-based alloys, IN600, IN601 and C22.

II. EXPERIMENTAL PROGRAM

2.1 Material

The IN600, IN601 and C22 alloys were chosen because of the possibility that chloride ions (Cl), could severely disorder passive film and then damage the oxide film. In addition, chloride ions can be found in dry and wet atmospheric conditions. The chemical composition (wt. %) of these alloys is reported in [11]. For the tests reported in this study, standard fatigue specimens with dimensions shown in Figure 1 were machined from the as-received material.

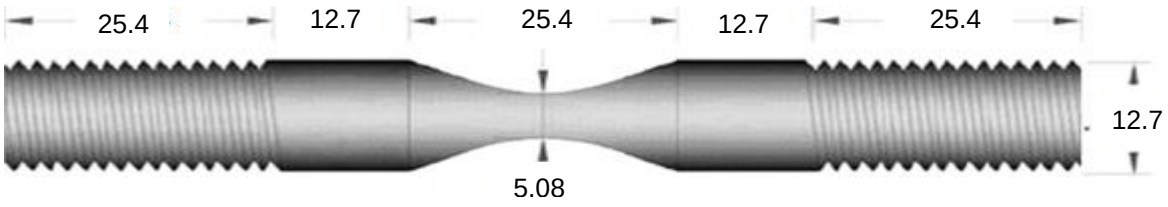

Figure 1Dimensions of fatigue specimen in (mm)

2.2 Fatigue Test Equipment

Fatigue tests were conducted on annealed specimens of the three alloys at a constant frequency of 10 Hz under axial tension-tension load in two environments - air and 3.5 % sodium chloride (NaCl) solution and were conducted on an Instron 1337 testing machine, connected to an Instron 8500 programmable control unit. The Instron 1337 unit has a load cell with a full load scale of 1000 kg/1V. The servo-hydraulic test unit applies a load through a hydraulic actuator, while a computer-controlled servomechanism controls the oil flow to the actuator. The specimen is mounted on the test unit between the actuator and the load cell by screwing it into the test fixture as shown in Figure 2. The Instron 8500 programmable control unit was used to set up all the testing parameters. Furthermore, the control unit also received data from the displacement

gauge and the load cell throughout each test. The data were processed in real time by the computer and, based on the programmed test parameters, feedback sent to the servo valve to control the hydraulic actuator.

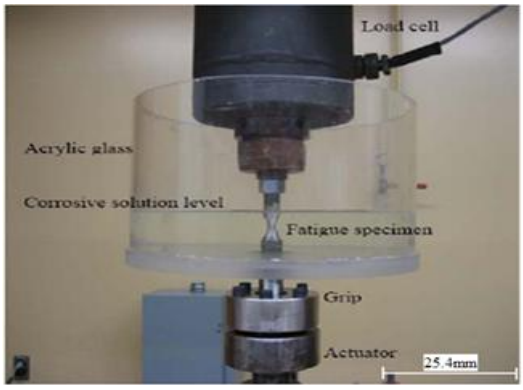

Figure 2 Photograph of Instron testing machine and corrosion cell

Fatigue tests in corrosive solutions were performed by enclosing the specimen within an "O" ring sealed, acrylic glass cylinder, as shown in Figure 3. An O-ring was installed at the bottom of the cell to permit the transfer of load to the specimen while preventing leakage of the saline solution (Figure 3).

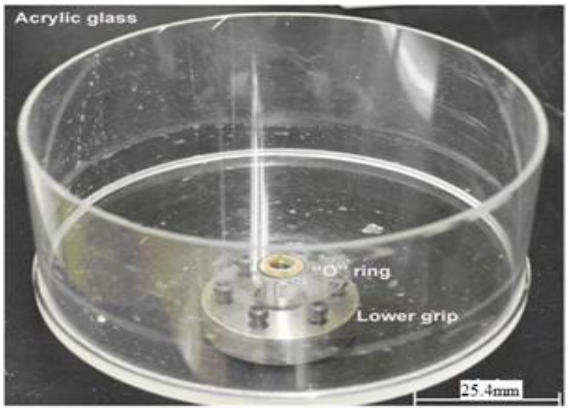

Figure 3 Micrograph showing corrosion cell connected to the grip from the bottom

III. RESULTS AND DISCUSSION

Fatigue tests were first conducted in air to provide a baseline for comparing with results in aqueous solutions of 3.5 % NaCl solution at pH = 6.8. The results of the fatigue testing are presented in the form of stress to cycle to failure curves (Figures 4-6).

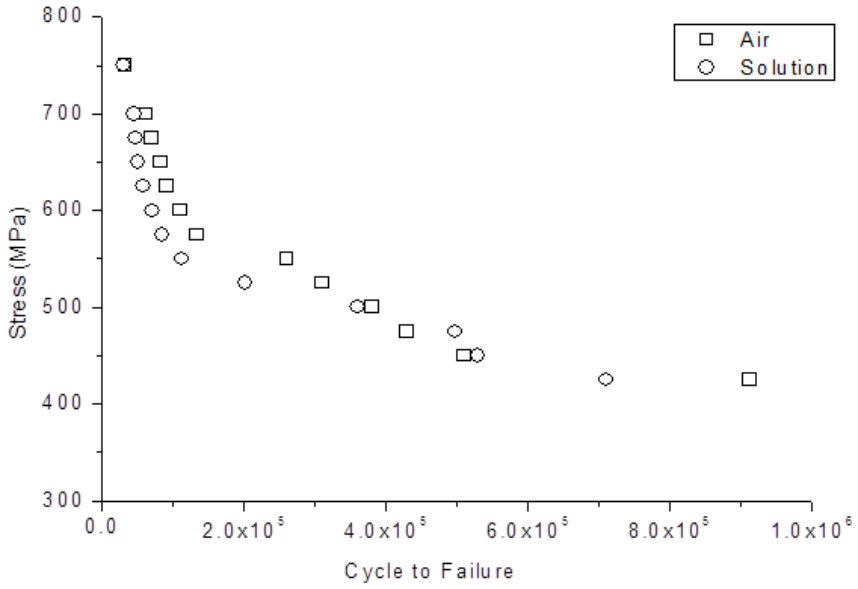

Figure 4 Fatigue test curves of IN600 in air and in 3.5%NaCl at pH = 6.8

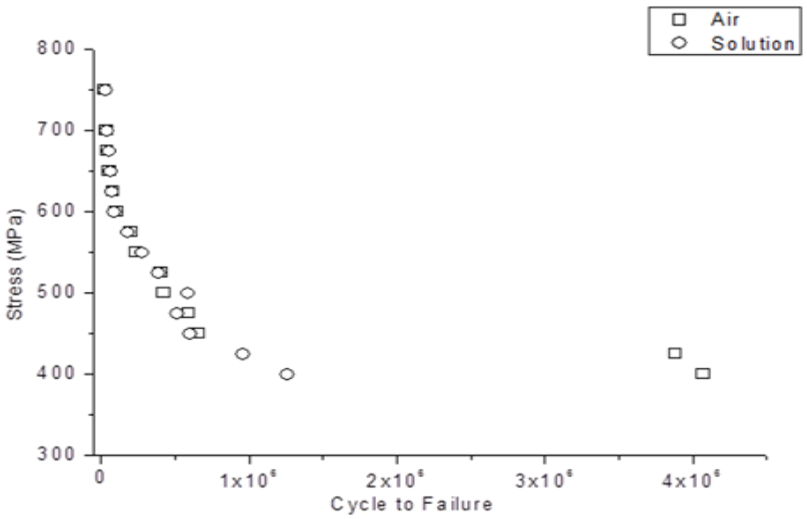

Figure 5 Fatigue test curves of IN601in air and in 3.5%NaCl at pH = 6.8

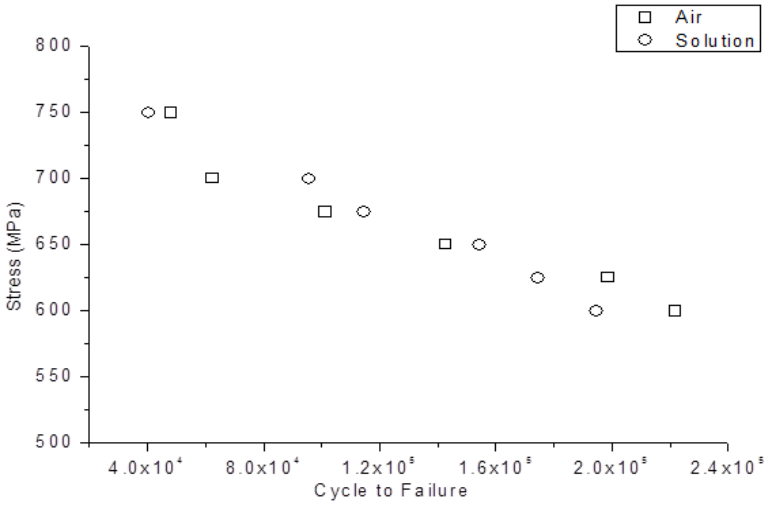

Figure 6 Fatigue test curves of C22 in air and in 3.5%NaCl at pH = 6.8

Test data show that fatigue in 3.5 %. NaCl solution had little effect and difference not statistically significant and hence, essentially the same on the fatigue strength of any of the alloys as the fatigue test curves are similar to those for specimens tested in air (Figs 4-6).

The test data are supported by scanning electron microscopy (SEM) which shows similar fracture surfaces for specimens tested in air and those tested in 3.5% NaCl solution (Figs. 7-9). In both cases, the fracture surfaces have a ductile character with fatigue striations. There is no evidence for corrosion or cleavage fracture. It was therefore concluded that all three alloys had excellent corrosion resistance in 3.5 % NaCl solution.

Appearance of striations is evidence that the fracture was definitely caused by fatigue. However, if striations do not appear, this does not necessarily mean the fracture is not due to fatigue. Typical striations were observed in a number of specimens of C22 alloy as shown in Figure 10.

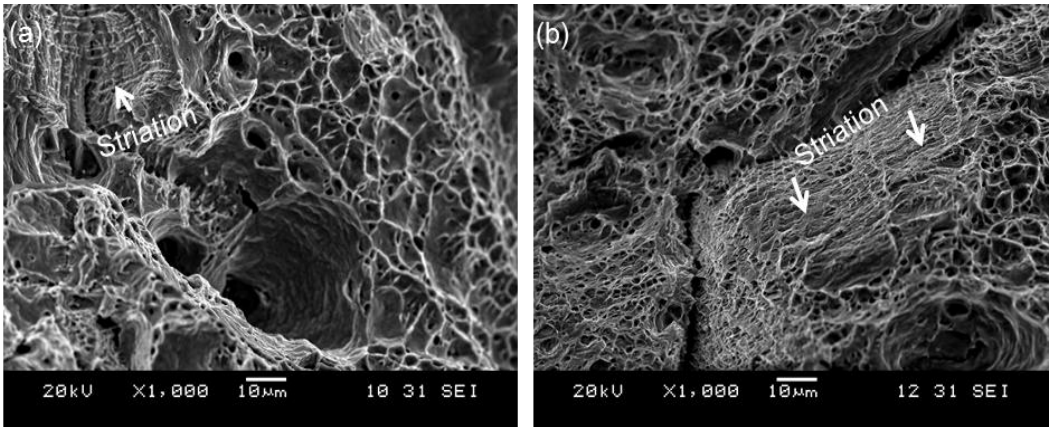

Figure 7 Fatigue fracture surface of IN600 (a) in air, and (b) in 3.5%NaCl solution at pH 6.8

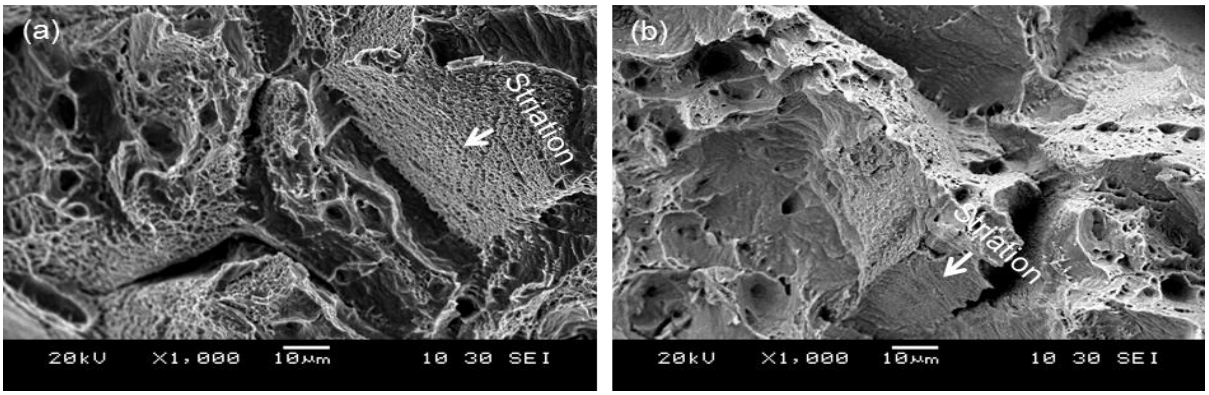

Figure 8 Fatigue fracture surface of IN601 (a) in air, and (b) in 3.5%NaCl solution at pH = 6.8

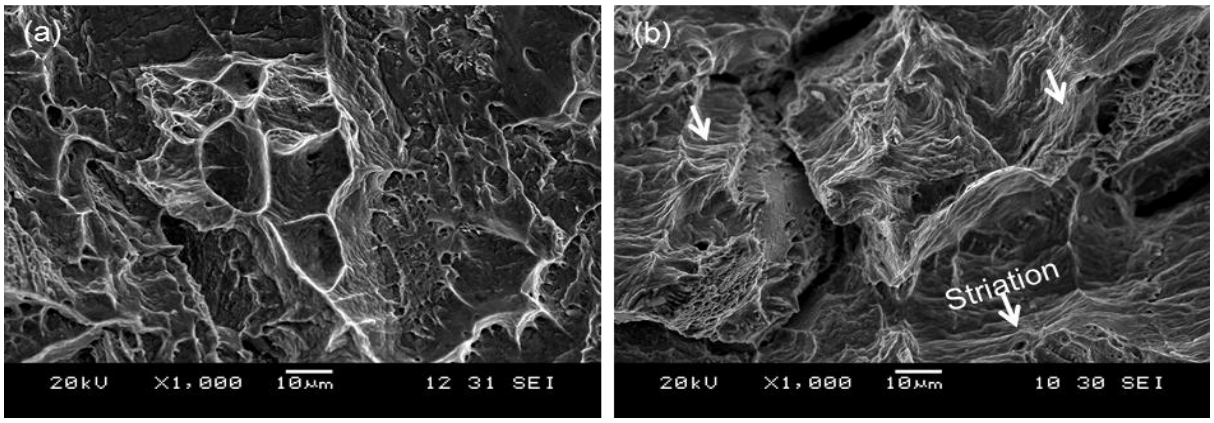

Figure 9 Fatigue fracture surfaces of C22 (a) in air, and (b) in 3.5%NaCl solution at pH = 6.8

A similar study of corrosion fatigue on annealed type 316 stainless steel showed the maximum stress level for failure in 0.5 M sodium chloride aqueous solution at pH = 4.2 was one-third lower than in air after a similar number of cycles [12].

Microscopic examination showed crack initiation resulting from pit formation, and crack coalescence was suggested as an explanation for the decrease in the maximum stress level for corrosion fatigue. The nickel alloys used in the study reported here has a greater resistance to corrosion pitting than type 316 stainless steel and therefore a comparatively greater resistance to crevice corrosion and degradation of fatigue strength [12].

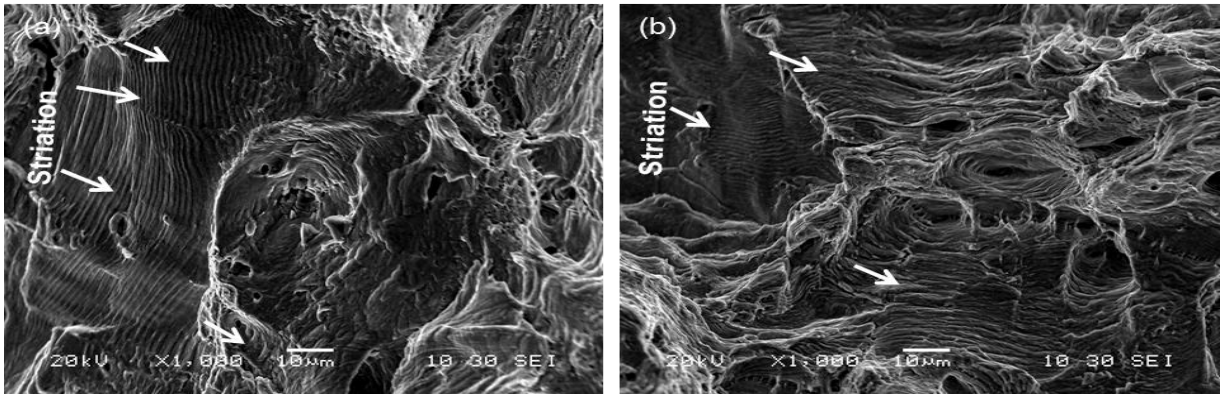

Figure 10 Typical striations observed on fatigue fracture surface of alloy C22 (a) and (b)

IV. CONCLUSION

The 3.5% NaCl solution at pH 6.8 had no effect on the fatigue life of any of the three alloys tested. Fracture surfaces for specimens tested in air showed no differences to those in specimens tested in 3.5% NaCl solution. Hence, all three alloys had excellent corrosion resistance in 3.5 % NaCl solution.

REFERENCES

[1] A. C., Lloyd, J. J. Noël, N. S. McIntyre, and D. W. Shoesmith. The open-circuit ennoblement of alloy C-22 and other Ni-Cr-Mo Alloys. *Journal of the Minerals, Metals and Materials Society, 57(1),* 2005, 31-35.

[2] H. O., Fuchs, and R. S., Stephens. *Metal fatigue in engineering*, (New York, John Wiley and Sons, 1980) 26-74.

[3] H. Akio, S. Kentaro, and K. F. Koboyashi. Microstructure and mechanical properties of laser beam welded Inconel 718. *International Journal of Material Process Technology, 13(1-2),* 1998, 28-44.

[4] J. G. Gonzalez, I. Rodriguiez, and L. Fionova, Effect of structural evolution in Inconel 601 on intergranular corrosion, *Material Chemistry. Physics, 56 (1),* 1998, 70-73.

[5] X. Lin, and X. Chen. Laser ablation rates of Inconel and aluminum with femo and nanosecond pulses. *In Proceedings of CLEO*, San Francisco, 1998.

[6] R.B Rebak, and J.C.A, Estil. Study of corrosion behavior of Ni-22Cr-13Mo-3W alloy under hygroscopic salt deposits on hot surface, *MRS Fall Meeting, Boston, MA, Report # UCRL*-JC-148826, 2002, 1-20.

[7] B. A. Kehler. Crevice corrosion stabilization and repassivation behavior of alloys 625.*Corrosion Journal, 57*, 2001, 1042-1065.

[8] D. D. Gorhe. Development of an electrochemical reactivation test procedure for detecting microstructural hetrogeneity in Ni-Cr-Mo-W alloy weld. *Journal of Materials Science, 39*, 2004, 2257-2261.

[9] D. D. Gorhe. Electrochemical methods to detect susceptibility of Ni-Cr-Mo-W Alloy 22 to intergranular corrosion. *Metallurgical and Materials Transactions A, 36*, 2005, 1153-1167.

[10] G. O. Ilevbare. The effect of welding on the crevice breakdown and repassivation potentials of alloy 22 in 5M CaCl2 between 45 and 120^{o}C.*The Electrochemical Society*, Inc, ABS. 464, 204th Meeting, 2003, 464-465.

[11] A. Mohamed. Cyclic deformation of Hastelloy and Inconel alloys and slip bands formation. *International Journal of Modern Engineering Research, 3(2),* 2013, 1253-1255.

[12] Y. Qian, and J. R. Cahoon. Crack Initiation mechanisms for corrosion fatigue of austenitic stainless steel. *Corrosion Science, 53*, 1997, 129-135.

International Journal of Modern Engineering Research (IJMER)
www.ijmer.com Vol.3, Issue.3, May-June. 2013 pp-1534-1547 ISSN: 2249-6645

Area Model Mediating Learning of Area Measurement: A Case Study of African American Students

Nosisi N Feza
Human Sciences Research Council Education and Skills Department Pretoria South Africa

Abstract: *The over-arching gap in research is regarding the instructional needs and the cultural capital that African American students bring to the mathematics classroom. Given the reality that most African American students in the United States will learn mathematics from a white, middle-class teacher. Using models of learning in teaching of mathematics for diverse students might bridge the cultural differences between teachers and students. The case study of 5 fifth grade African American students illustrate that using gradual release model with area model in mediating learning of area measurement, allowed these students to achieve the higher levels of abstraction in their thinking.*

Keywords: *area model, cognitive variability, learning trajectories, internalization, context-based problems*

I. Introduction

Measurement is an indispensable everyday mathematical activity worldwide. The idea of measurement is too broad and attempting to define it will do disservice to the topic itself [1]. However, Russell (1900) cited by [1] give a broader description that encompasses aspects of measurements related to this study. They describe measurement of magnitude as a method used to define some properties of a particular object by using mathematical concepts like number, relations and functions. Therefore, measurement is the activity of determining the magnitude of a quantity by comparison with a standard for that quantity. In this paper measurement of magnitude refers to measuring the surface area that uses the properties of the shape measured, using number, rows and columns as vehicle to expose students to the relations between length and area and conceptualize the formula of *l X b = area*. Area measurement integrates mathematical concepts as [2] state, "it can develop other areas of mathematics including reasoning and logic" (p.163). These other areas are patterns leading to algebraic thought, geometric reasoning leading to logic, and number operations as tools for generalizing etc.

Measurement concept performance of fourth grade US students is lower than number and probability [3], [4], [5]. Black students' average performance on math content in [5] was 217 for measurement, 220 for number, 227 for probability, 229 for algebra and 226 for geometry. According to these results measurement has the lowest average performance for Black students. Few studies [6]; [7] and [8] have investigated fifth grade students' processes in understanding 3D arrays and 2D arrays. Their results showed that students demonstrated complicated structures in working with these arrays. [9] suggested an inquiry-based approach in studying these complicated mental structures. [10] used a cognition-based assessment in understanding these structures. This paper is contributing towards extending their work focusing on area measurement and using area model as a mediation tool. This paper aims to use an area model as a tool in mediating and eliciting processes of conceptual development of area to 5 fifth grade African American students. To describe these thought processes the following question will be addressed:

What role can area model play in mediating learning of area to African American fifth grade students?

This paper is structured into four parts: the *first part* present and describe the theoretical framework employed as lenses for discussing the findings. This is followed by discussion of the area concept this study employs in eliciting African American students' thought processes. The *second part* focuses on the methodology of the reported study. The *third part* presents findings. These findings are presented using themes with measurement learning trajectories hypothesized by [2]. The *fourth part* engages with the current literature in discussing the findings of the study and then draws and presents the final conclusions on the reported study.

II. Theoretical Framework

The theoretical framework used in this paper is influenced by Vygotskian theory of internalization of ideas, and Ernest's philosophy of connectionist approach to teaching of mathematics.

II.1 Vygotskian theory of internalization

Internalization refers to the psychological process of transforming intermental to intramental through mediation of student's cultural tools [11]. The mental structures that form when conceptualization of a concept takes place [2]. [12], [13] asserts that ideas/concepts are tools. When these tools are not personalized they are external however, when they become personalized meaning they become internal tools [14]. This psychological process of personalizing meaning is internalization/interiorization in Vygotskian language.

[15] defines internalization as a five phases process. The phases are "(1) the phase in which the given phenomenon does not manifest itself yet; (2) the phase in which its initial traces seem to appear for the first time, always with corresponding analysis of the psychological tools and social forces that bring this phenomenon to life; (3) the phase in which the phenomenon reaches its climax, always linked to social interaction and usage of tools; (4) the phase of its gradual interiorization; (5) and finally the phase in which it appears that the phenomenon has been there, quite naturally in our heads, resembling inherited individual property that was just waiting its time to be actualized". Ageyev's phases give a clear

developmental path for internalization of ideas using cultural mediation tools. Activities with peers or with an educator encourage social engagement that brings the phenomenon to reach the climax. Clearly for this internalization to occur educator's role is to create activities that connects with students' mediation tools pushing for intermental ideas to be intramental [14]. Social interaction with peers and educator plays an integral part for moving a student towards mental climax. The educator fulfills the purpose of philosophy of mathematics education in assisting students' mental structures to reach actualization of mathematical concepts [15].

II.2 Ernest's philosophy of connectionism

[15] claims that educators have distinct philosophies of mathematics that influence their perspective of philosophy of mathematics education. Absolutist philosophy of mathematics is demonstrated in practice by instruction that is transmissionist. This instruction is characterized by memorization of rules and formulas, [17] while fallibilist philosophy of mathematics is transferred towards creation of ideas that acquire broader instruction [18]. Fallibilist philosopher believes that mathematical knowledge is created instead of being discovered or a set of rules that already exist. This study is influenced by the fallibilist philosophy that if mathematics is created, the creator has to connect new ideas with existing mental structures of students recognizing the influence of their environment as well as their culture that determines their way of knowing. This instructional approach in Ernest' term is a connectionist instructional approach. The teaching experiments employed by this reported study are influenced by connectionism and internalization of concepts or ideas in teaching area measurement.

II.3 Area measurement conceptualization

Research that demonstrates how young children learn reveals that mediation and use of technology lead to internalized measurement concepts [19]; [20]; [21]; [22]; [23]. Nonetheless, research on older children's processes of conceptualizing measurement concepts is still limited.

[24] Described area as a concept that connects a number of mathematical concepts. Understanding of area measurement demands coordination of all the concepts involved, i.e., structuring, adding, and multiplication that leads to functions. [2] Divide the area foundational concepts into six sub-concepts of area that follows:

Attribute of area: Quantitative meaning of space
Equal partitioning: Using congruency is dividing two-dimensional space into equal parts.
Units and unit iteration: Covering space with the same units without gaps or overlaps.
Accumulation and additivity: Adding rows and column repeatedly.
Structuring space*: The concept is* realizing multiplicative structures of the rows and columns.
Conservation: Composing and decomposing of shapes exposing students to the idea of area staying the same even if it is rearranged. [2] argue that these foundational concepts form basis of building students' conceptual understanding of area measurement.

III. Methodology

III.1 Context

The study was conducted in a public school in Western New York. The sampled school comprised of 30 % black population, 10 % of Hispanic students, and the majority (60%) was white students. About 31% of the students qualified for free lunch.

III.2 Participants

There were fourteen 5th grade African American students in the whole school. Seven of them were in a math special class and the other seven in a mainstream math class. Only students in the mainstream math class participated in this study. Out of the seven students, six brought back their parents' consent forms. The math teacher was requested to share students' performance results for the previous year. From the six students with consent, a selection of five who represented varying performance was conducted. Two of these students attended both mainstream and special math classes, two others were high performers while the other one was on average.

III.3 Data Collection

The reported study employed clinical individual pre-interviews and post-interviews with students and teaching experiments. The pre-interviews were conducted to inform the designing of teaching experiments and to instruct at the thinking level of students. Whereas the post-interviews were used as a measuring stick of the area concept gains student made during teaching experiments and to study the role of the area model.

III.3.1 Interviews

The pre and post clinical interviews were conducted prior and after teaching experiments. Each interview was between 10 to 15 minutes. Video and audio recorders were used to collect data. Field notes were taken during interviews for the purpose of triangulating data.

II.3.2 teaching experiments

The teaching experiments focused on mediation of new area measurement concepts, after establishing students' zone of proximal development. [12] zone of proximal development has two linked perspectives that are psychological

perspective on student's development and pedagogical development on instruction. He argues that these two perspectives are connected. The student's zone of proximal development (ZPD) is the level the student demonstrates when solving a task independently. Then mediation of new ideas is connected to the student's ZPD for student intellectual development to occur.

The individual teaching experiments were used in order to describe and engage with students personalized ideas that they use in solving problems that involve measurement concepts. One main teaching experiment was designed with follow up episodes intended to address students' needs in understanding the area concept. Each lesson lasted 20 minutes with each student. The follow up episodes varied in time depending on students' level and pace. The teaching experiments were both audio and video taped for audibility and capturing of all different kinds of communication the student undertook during a lesson. The field notes were taken with students' written work to triangulate for credibility in describing students' thinking.

Figure 1 represents the triangulation of the data sources, techniques and tools used in this study.

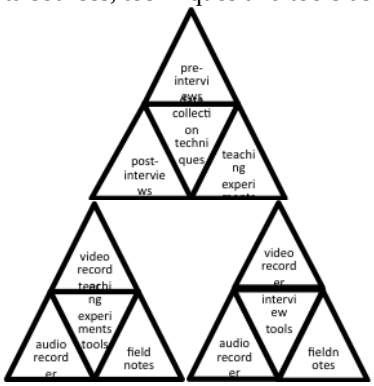

Figure 1: Triangulation of data sources, techniques and tools

II.4 Data analysis

In this study data collection and analysis were inseparable. The analysis continuously informed data collection and also assisted in engaging with the data [25]. Analysis of the pre-interviews of area concepts was conducted using a table. Each student's responses were put in the table and grouped by color-coding similar levels of thinking using [2] learning trajectories for area.

Each color represented a specific level for the area attribute. Below is a summarized description of the learning trajectories used to analyze the interviews reported in this study [14].

II.4.1 Hierarchical Area Measurement learning trajectories

Pre-Area Quantity Recognizer: Students show little specific concepts of area. For example, when students have a task to cover any surface they cover by packing tiles on top of each other without a plan of covering the space at all.

Area Simple Comparer: Students may compare areas using one side. In this case it is possible for students to compare only lengths of the areas without considering the width of the area.

Side-to-Side Area Measure: Students cover a rectangular space with physical tiles but cannot organize, co-ordinate the 2D space. Mostly they cover sides and fiddle with the space in the middle.

Primitive coverer: When counting squares covering the area students skip count, loose track, sometimes count some squares repeatedly. Covering of spacing might have gaps or overlapping.

Area Unit Relater and Repeater: Students count one row at a time. Student has not developed the structure of rows and columns. S/he counts one unit at a time keeping track.

Partial Row Structurer: Counts rows but sometimes does not count all rows. The column existence is not yet realized. The relationship between the rows and the columns has not been recognized yet.

Row and Column Structurer: Students count rows and draw rows of squares to determine area.

Area Conserver: Conserve area by determining different looking surfaces as equal.

Array Structurer: Use multiplicative structures in filling up and counting area [10].

Conceptualization of area measurement is an integral part towards mastering calculating skills of area. The area formula is not the same for different shapes, therefore knowing formulas without understanding creates barriers for further development in understanding the Pick's theorem that allows students to calculate area of any polygon. This might sound

abstract but with the understanding or the six sub-concepts of area suggested by [2] give this fundamental understanding. Internalization of these concepts has its own developmental path for each student. The learning trajectories hypothesized by [2] became the relevant tool for analyzing the developmental path of these five African American students.

The analysis of the post-interviews was simply analytical using the learning trajectories. The results of this analysis supported the teaching experiment themes that respond to the question of the study reported. The teaching experiments data was transcribed from the video tapes, and audio tapes. Each transcription was typed with numbered rows to assist analysis. The field notes taken from the interviews were also typed and numbered in rows too. Data from each of the three data sources were analyzed separately. Each typed data was annotated with low inference phrases. Those annotations were put into tables. Each table was color coded to group similar phrases and single out odd ones. Once those annotations were in colors analytical memos were written for each annotated data to make sense of the patterns and odd annotations. Descriptive codes emerged from the three groups of data. The codes were triangulated and area measurement themes emerged. Those themes were context-based instruction, area model, and responsibility.

The three themes responded on "the role of area model in mediating leaning of area and the processes these students went through in conceptualizing area" Each student is reported under the themes that emerged. Figure 2 illustrates how themes were divided in response to the study's question.

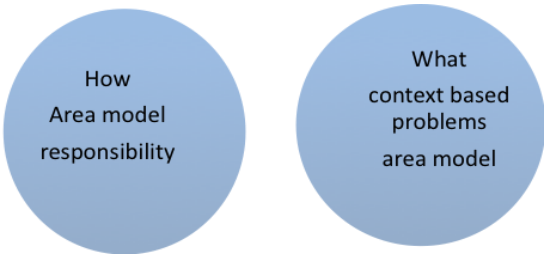

Figure 2: Division of area measurement themes

IV. Findings

The findings are presented firstly by describing the area measurement understanding of the fifth grade African American students' prior teaching experiments. Then, emerged themes from the area teaching experiments will be presented and discussed. The findings from the pre and post interviews are presented graphically in order to demonstrate the trajectory levels of the African American students' prior and post teaching experiments.

IV.1 Students' Developmental Progression Levels

The learning trajectories used in this study were designed for young children's developmental progression in measurement concepts [2]. The research conducted to develop these learning trajectories was undertaken from pre-school to 8 yr olds. However, the pre-interviews of this study revealed that these fifth grade students' developmental levels were still missing some developmental progression levels in the early childhood standards. The pre-interview data present the levels of development of the five African American students' prior teaching experiments.

Out of the five students, Portia and Jerome (pseudonyms) were able to cover the shape with the correct number of squares without touching them. They were both able to see the relationship between the square and the triangle, that two triangles cover the square and use their square covering response to get the correct answer for covering surface area with triangles. The other three students could not cover the shape correctly physically, they had overlaps and gaps. They were also unable to neither cover the shape with the triangle nor see any of the relationships between the two shapes. Four of them were primitive coverers only one of them was an Area Unit Relater and Repeater. Below is the graphical presentation of their developmental trajectory levels prior teaching experiments.

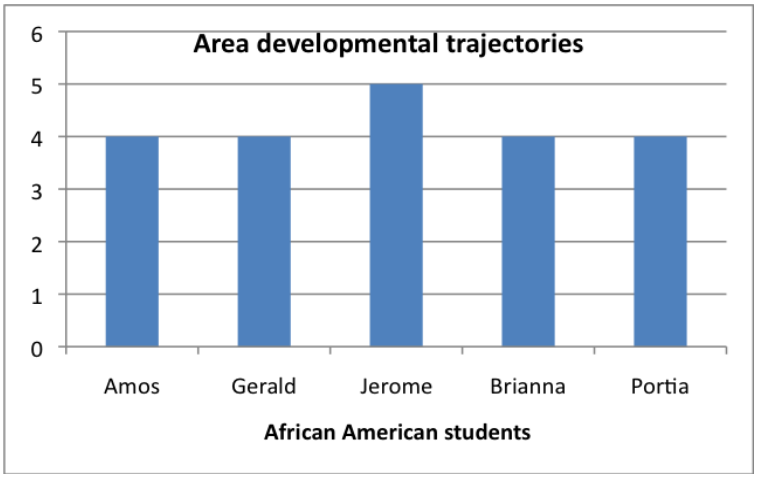

V1.2 teaching experiments themes

The first teaching experiments theme, context based instruction addresses the instructional support that meets African American needs regardless of their challenges. Then two themes, responsibility and area model responded to the African American students' ways of learning area measurement.

IV.2.1 Context based instruction

The shape used to find area had two challenges for the students, first the shape had missing lengths, and secondly it was an L shape. The rationale behind these challenges is to diagnose student's ZPD so as to give the instruction at their actual level and establish their potential. Students' knowledge of a rectangle was the connecting concept as all students knew the properties of a rectangle and could easily use them to learn the area model. For example, Jerome and Amos had a similar approach in attempting to find the missing lengths of the shape of the land. The following was my dialogue with Amos:

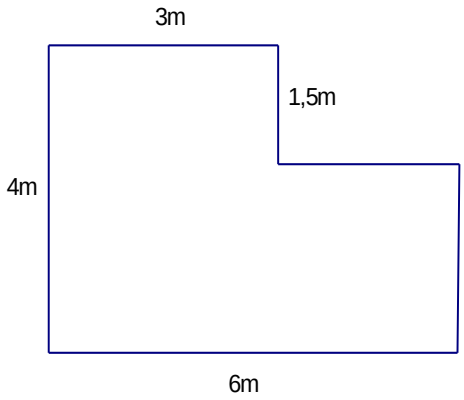

R: This diagram represents the gardening land my uncle has. He wants to calculate the amount of space he has but need fence to protect the land from animals first. He has some missing lengths on it. Help him calculate the missing lengths of his land?

Amos: His length is 14.5 meters.

This step showed that the context of the story made it simple to do perimeter informally. An opportunity presented itself for learning and teaching and the following was my approach in connecting all that Amos brought with him, completing the perimeter problem that was emerging was vital for in-depth understanding of area.

R: Does that mean this side is not going to be fenced and this other side. He does not want any animals in his land. How are we going to get the missing lengths?

Amos: This side is

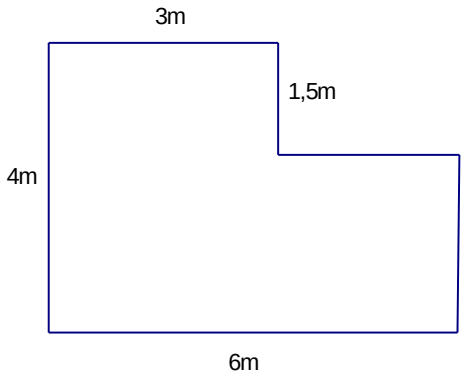

R: Oh you think this side (the 3m side) and this side are the same? (The side he labeled 3m)

Amos: Yes

R: Ok what if we do this. We try and make this shape a familiar one by using some dotted lines as follows:

R: What will be this side if you have to give us the whole side (side marked with arrows)?

Amos: 4m

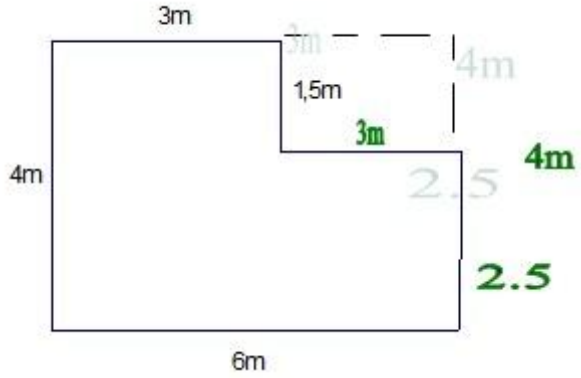

R: Why is it 4 now?
Amos: Because it's the same as the other one on the other side (pointing opposite side). The side on that side of 6m will also be 6 because they are the same.
R: So what will be the length from this corner to here? (The one below 1.5m)
Amos: 3m
R: Oh, why?
Amos: Because this one is 6m and that one has 3m and the missing one is 3m.
R: Write it then where it belongs. What about the other missing length on that side opposite to 4?
Amos: wrote the following on the paper

1.5
+3.5
5.0

He then wrote again the following:

1.5
+2.5
4.0

The missing length is 2.5m.

Finding these missing lengths with these five students informed the researcher of their internalized ideas and ideas that have not been internalized yet. The two boys Amos and Jerome were able to transfer their understanding of properties of a rectangle to the L shape in finding lengths. While the other three students, Gerald, Brianna and Portia could not find the missing lengths on their own. They demonstrated that they have not yet internalized the knowledge of properties of a rectangle. It was still external knowledge to them, as they could not transfer it to another context. The researcher had to work with them using rectangles. These teaching episodes are not reported, as they are not the focus of this paper. Area measurement mediation is the focus of this paper.

Area model

The actual problem students have to solve was to calculate the area of the land. Each student experience and approach is reported in learning area using area model. Each student was given the L shape to start with. The Area model pushed individual students differently. The results show that it assisted others to connect ideas that were already there easily.

Jerome's journey
R: Divide the garden and calculate the area of each portion.
Jerome: (divides the land this way)

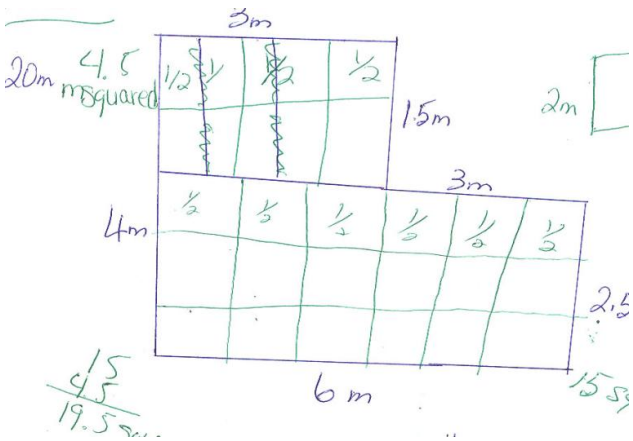

R: Now that you have divided the land, tell me which portion of it you want me to work with you on? Choose the one you want me to help you with? We have a 3 by 1.5 land and a 6 by 2.5 land.
Jerome: This one (pointing a 6 by 2.5 land)
R: If I want to get squares that cover this land. I am going to make columns that are 6 because of the 6m. (Making the 6 columns). Does that make sense? Still I do not have squares I have only columns.
Jerome: I know.
R: What do you know?
Jerome: You need to make rows now that will help you make the squares.
R: Yes. But how many?
Jerome: You need 2
R: Only 2
Jerome: And then you need half way.
R: This is half. So you think we have squares now?
Jerome: Mh mh
R: So how many squares is this portion? Can you count them?
Jerome: 1,2,3,4,5,6,7,8,9,10,11,12,13,14,15,16,17,18. 18 squares.
R: I do not agree with you. These (pointing the row of halves) are not squares they are half squares.
Jerome: Oh---.1, 2, 3, 4, 5, 6, 7, 8, 9, 10, 11, 12, 13, 14, 15. 15 squares.
R: You have 15 square meters. Remember Uncle wants to know the Area of the whole land. So you need to do the other portion too.
Jerome: I need 3 columns. I need one and a half across. I have three.
R: What about these? (The row of halves)
Jerome: 4 ½ square meters?
R: You can even write square meters as m^2. What is the area of the whole land then?
Jerome: writes

15
+4.5
19.5 square meters.

R: Can you try and find Area of this one?

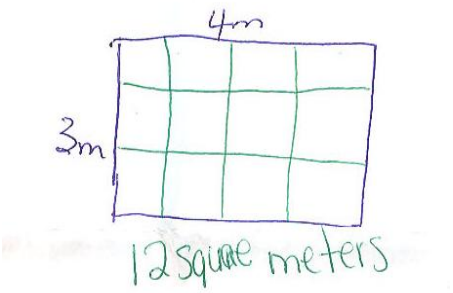

Jerome: (divide the land independently as shown in the diagram above and wrote.) 12 square meters (without counting them).

Jerome started at the second phase of internalization the phenomenon of columns and rows. Before this teaching experiment he could not count all the rows but now a connection took place in his mind that made him see that he needs to draw rows on those columns to get the squares he needed. Seeing the columns the researcher drew caused connection of some mental structures. His pace of internalizing the area model required only 25% of the researcher's demonstration and he took over and ran with it. His challenge was dealing with halves and conceptualizing square as units. This caused climax as he kept on counting half squares as full squares and could not see the relationship between rows and columns before. His area measurement learning path started from partial row structurer straight to an Array Structurer jumping three learning trajectories.

Gerald's journey

This episode demonstrates Gerald's pace and approach in internalizing the area model.

R: Now that the garden is fenced uncle wants to divide it into two portions. Divide the garden and calculate the area of each portion. Do you know the area?

Gerald: Yes
R: Divide the land into two portions.

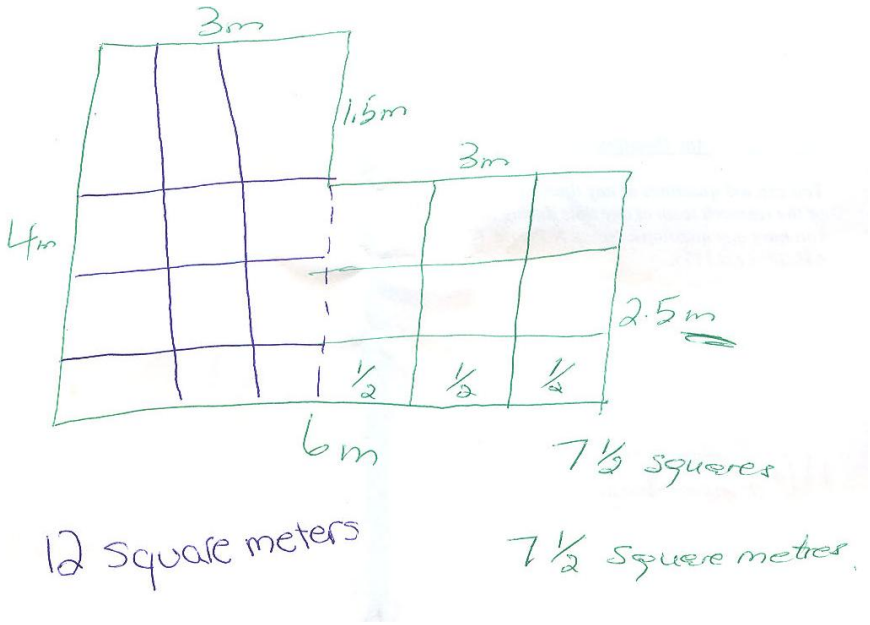

Gerald: (divide the land as above.)
R: By Area he wants to know how many square meters cover his land. Do you know how many squares?
Gerald: No

R: I will make squares with you. For the side with 3m I will make 3 columns. (working on the small portion). Then on the 2.5m I will make two and a half rows. (I wrote a ½ inside each half square). Now see I have squares can you count them for me.
Gerald: 9
R: Wow I don't see 9 show me.
Gerald: Counts them one by one. 7 ½ squares.
R: These squares have names. What is the name?
Gerald: Square meters.
R: Now I want you to do the big one. How many rows are you going to make?
Gerald: Four rows.
R: Ok make them.
Gerald: Draw columns and rows in the 3 by 4 side as shown in the diagram above. (4 rows and 3 columns)
R: How many squares is that portion?
Gerald: It's 12 squares.
R: Is it only 12 squares?
Gerald: It's 12 square meters.
R: What is the total area now? Can you add it up for him?
Gerald: writes

$$\begin{array}{r} 12 \\ +\ 7\ ½ \\ \hline 19\ ½ \text{ square meters} \end{array}$$

R: Do you know that you have just done Area? Let's see if we can find area of simple shapes now that one was complicated. Work out this one. Find the sides that are not labeled first.

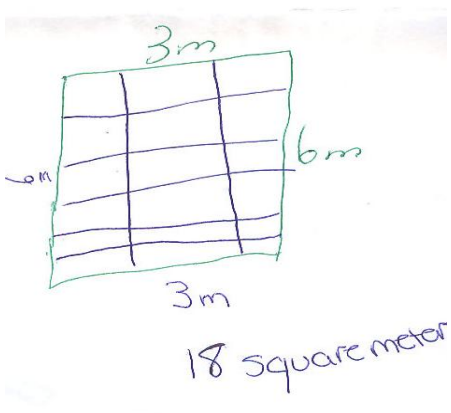

Gerald: (first labeled the missing length).
That is good. Calculate the area now.
Jerome: (draw rows and columns as shown in the drawing and writes) 18 square meters.

R: Let's do the last one:

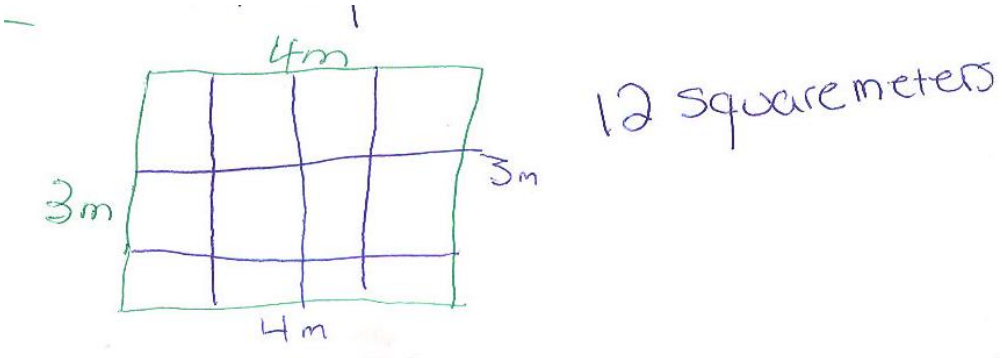

Gerald: (label missing lengths and writes) 12 square meters.

Gerald showed that he needed the area model to make sense of area. He needed full demonstration before he used it. He was challenged by fractional parts but through mediation he progressed. The model assisted his actualization of area and pushed him to an Array structurer. He had to master the area unit relater and repeater first and jumped to Array structurer from there.

Amos's journey
R: Now that the garden is fenced let us divide it into two portions. Divide the garden and calculate the area of each portion.
R: Do you know how we can find square meters?
Amos: I will try and draw squares.
R: Great. To make it easy for us divide this into two lands. So that it can be easy to work with. Where would you divide it?
Amos divided the diagram as follows:

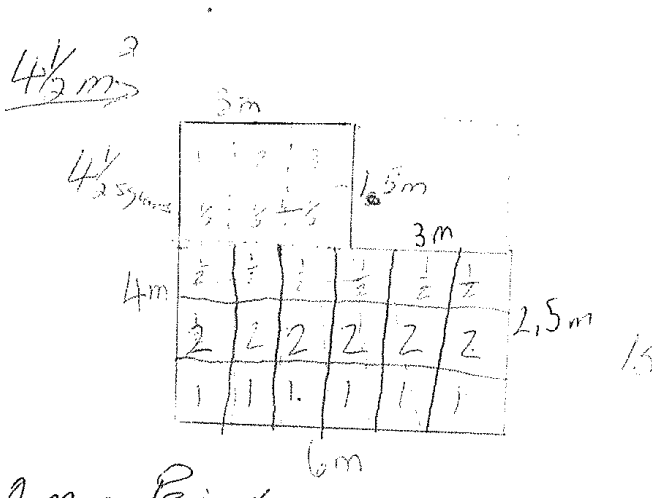

R: So you have the land cut into two portions one with 3m by 1.5m and 6m by 2.5 m. Let's work with one portion at a time. Do you know how we are going to make these squares? We have three meters and then I think we can divide it into three equal portions. Then we divide it again into 1 1/2. How many square meters is that portion?
Amos: 5 ½
R: How come?
Amos: I counted them.
R: Remember we have half squares there. Can you show me?
Adam: Yes
R: How many are they?
Amos: 3
R: So how many squares do you get then?
Amos: I get 4 ½ squares
R: How did you get that?
Amos: I counted the three full squares then combine two half squares to one and have four then added the other half.
R: What kind of squares are they? Let's look back on our division what were we dividing?

Amos: Meters
R: So our squares are square meters. Now I want you to do the other portion by your self.
Amos: (quietly divide the bottom part as follows: Check the diagram above to see his work. He labeled his first row of squares 1 each square then the second row he labeled 2 each square then the third row he labels a ½ each square then he started counting them.) 1, 2, 3,4,5,6 (then when he gets to the second row he counts) 8, 10, 12, 14
R: Ok tell me what is it that you are counting why you are adding two's now, show me.
Amos: I am adding what is in the squares.
R: Oh why do you have two in those squares?
Amos: They are in the second row.
R: Why do you have halves in the third row then?
Amos: Because I did not want to forget that they were halves.
R: What makes the second row two's then?
Amos: I don't know.
R: What must you do?
Amos: Count the squares as one each.
R: How many square meters is this portion?
Amos: 15 square meters.
R: Ok I think we need to do more. You said the first portion is 4 ½ square meters and this one is 15 meters. What is the total area of uncle's land?
Amos: 19 ½ square meters.
R: I would like you to try working the area of this one.
Amos first labeled the sides that were not labeled. He drew the columns like this twice. Check below. I had to draw a diagram teaching him columns and rows.

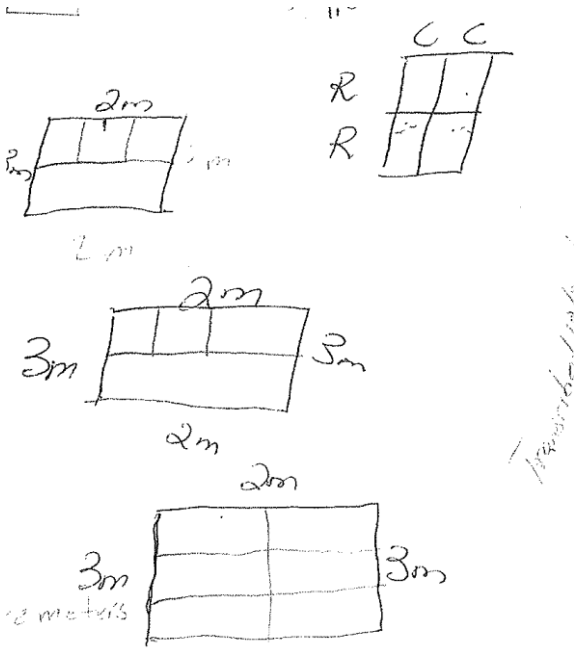

R: How are you dividing this land?
Amos: Three rows and two columns.
R: Can you show me columns first?
Amos: Point the rows.
R: Ok me too I used to call those columns. But the line you made across forms rows and then the lines that go down for columns. Ok how many meters are on the side on top?
Amos: Two
R: So how many columns are you suppose to have then?
Amos: Two
R: What about the other side?
Amos: I must make 3 rows
Can you draw then now? Amos: draws the fourth diagram above.
This is six square meters.
R: That is good Amos can you try and find Area for this one too.

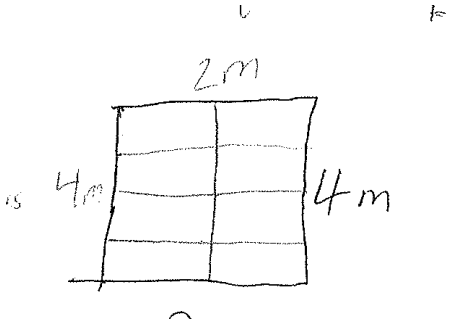

Amos: (label it first) then draw columns and rows as shown above. The Area is 8 square meters.

Amos' journey was unique compared to his peers. He did not grasp the area model after the researcher demonstration. When he started he was challenged by the rows and columns he had to master them first then move to the area unit relater and repeater before he moved to array structurer.

Portia's journey

R: Now that the garden is fenced. How many square meters cover his land?

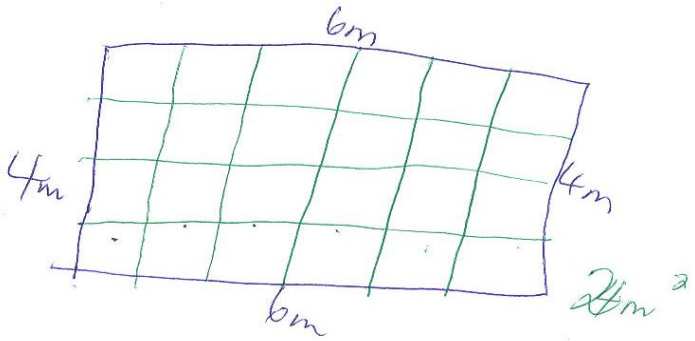

Portia: It has two square meters.

R: Let's see it has 6m long and then I will make 6 columns. (Making 6 columns). Then it is 4m wide then I make 4 rows. Whu, I have squares. How many squares is this land?

Portia: (count squares one by one) 24 squares.

R: Can you try and find area with this little land I give you now.

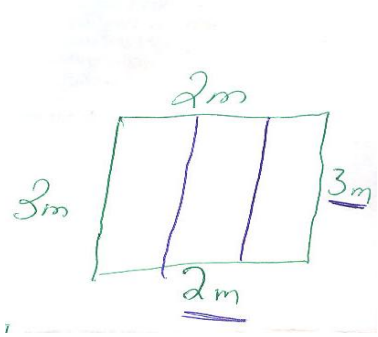

Portia: (label the sides first with bold labeling) She then makes three columns.

R: Why are you making 3 columns?

Portia: I am making the columns that are oh, I am suppose to make two.

R: I like it when you say oh, ok let's work with another diagram.

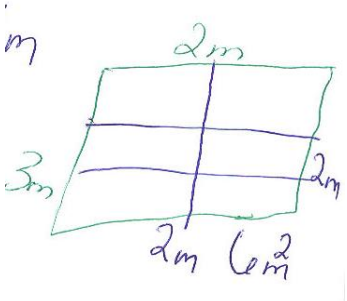

Portia: makes two columns as above and three rows.
R: How many square meters do you have?
Portia: 6 squares
R: Write $6m^2$ this is how we write them in mathematics.
Portia: writes $6m^2$

Briana's journery
R: Now that the garden is fenced uncle wants to divide it into two portions. Divide the garden and calculate the area of each portion.
Briana: (divides the land like this using dotted lines for dividing)

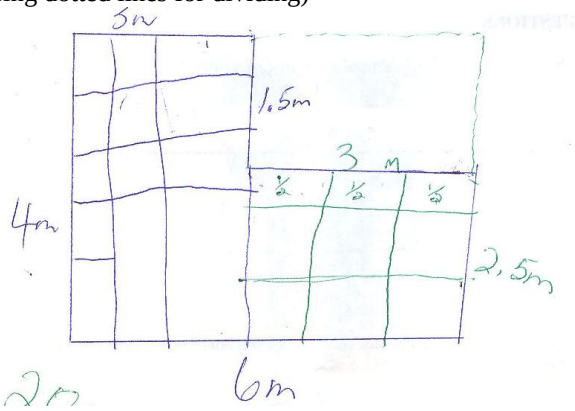

R: Now we have two lands. Which one do you want me to help you with?
Briana: The small one.
R: This is 3m long and 2.5m wide. Let's make squares. Because this is 3 I will make 3 columns (refer to figure). And because this is 2 ½ meters I will make 2 ½ rows.(refer to figure) Now I have squares. How many squares are they? Can you tell me?
Briana: 9 squares
R: I can't see 9. Show me how you got 9.
Briana: 1, 2, 3,4,5,6, ½ and ½ is 1 and there is a 1/2 and it's 7 ½ squares.
R: Now make your own squares in the other portion it is 4m long and 3m wide.
Briana: (makes three columns then struggle to make the rows)
R: Let me make another drawing for you.

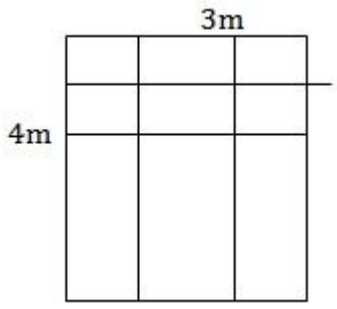

Briana: (continues to struggle in drawing)

Briana did not move further that row structurer during teaching experiments. Her development was not evident except that moved back to Side-to- Side Area measure showing regression at the end of her teaching experiments.

IV.2.2 Release of Responsibility

The area model was an attempt used in addressing the abstract conception of area. With the language challenge the study employed a gradual release of responsibility approach in mediating use of area model. A model in mathematics teaching and learning is used to introduce an abstract idea. Mathematical ideas are not tangible or visible, and because of that nature cannot be easily mediated. It is important to note that a model is not a concept but a model used to make the concept accessible. Thus, a model represents the concept. In this case releasing responsibility of doing area model gradually assisted instruction and comprehension of the problem. The researcher took 100% responsibility introducing the model except with Jerome who grasped it immediately. However, other students needed more time to grasp with Portia regressing. Below is a line graph presenting each student developmental path using the learning trajectories.

Each student's path is unique. Jerome and Gerald's path during teaching experiments was linear, while Amos and Portia needed to go back to area unit relater and repeater to have a solid understanding. Briana moved one level up and moved back two levels showing regression at the end of the teaching experiments.

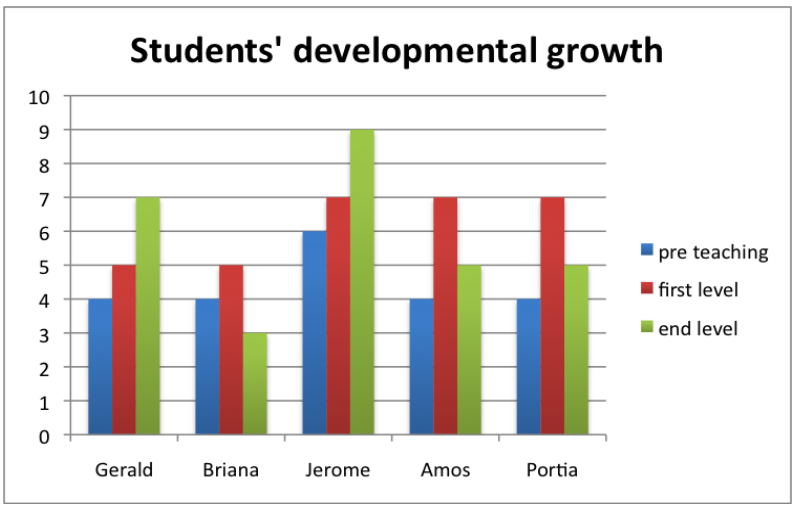

The following graphical representations below present the difference between pre-interviews and post-interviews these students took before and after teaching experiments for the area measurement.

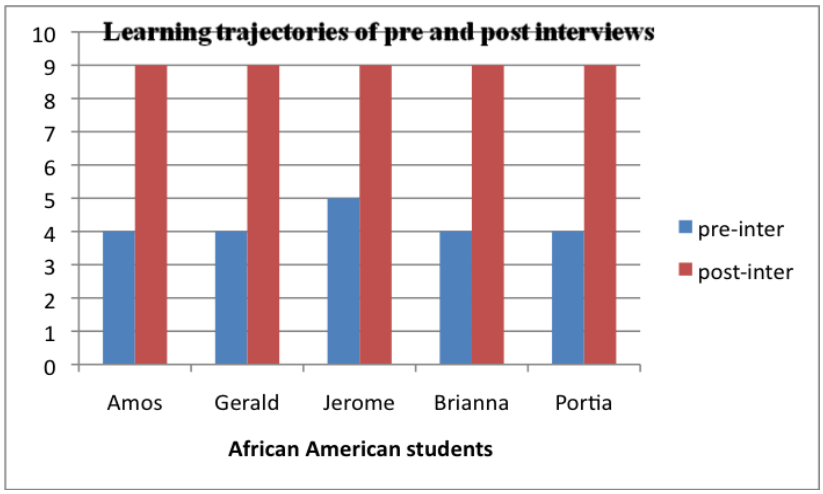

From this graph it is clear that Briana was not regressing but touch basing internalizing the concepts. Her route support the statement made by [2] about these learning trajectories that they are hierarchical but students develop through them differently. Some students develop linear but some mental structures are formed through intertwined progress.

V. Discussion and Conclusion

This study's results reveal four important components of learning area measurement concept by 5 fifth grade African American students of different performance levels. (1) Integrating a language model and a mathematics model gave access to abstract ideas of area measurement. (2) The learning trajectories can be used as assessment tools to inform practice. (3) Students cognitive structures are complicated and varied [26]. (4) African American students have potential for learning and are diverse in their learning. Area model became a powerful teaching tool that students were able to internalize and transfer to other area problems in unique ways [27]; [28]. However, on its own it could not assist students in conceptualizing area without the language model [29]. This paper supports the Vygotskian perspective of directing instruction to the student level of development. It also supports [26] argument of prevalence of variability in students' cognition at all levels. In this paper Briana demonstrated a unique way of learning by moving from a lower level of development to a higher level and then goes back two levels down. During assessment interviews Briana demonstrated an enormous growth that moved her from a third level to the highest level of abstraction, level 9. Briana's case demonstrated variability within [26]. Reflecting on the other four students in the study two students, Gerald and Jerome development was linear following the learning trajectories hierarchically. However, Amos and Portia showed some similarities in their development that moved to higher development first then regressed two levels down. Looking closely at their development they both developed uniquely up. Amos moved from Primitive cover to partial row structurer and took time to see relationships between rows and columns. When he did, understanding unit relater and repeater was easy for him. On the other hand Portia was still thinking in terms of length and focusing on length before she noticed rows, then columns. These two cases demonstrate variability between that could be explored further in research.

References

[1] Blakers. A. L, Studies in Mathematics Volume XVII. Mathematical concept of Elementary measurement. School Mathematics Study Group 1967.
[2] Clements, D., & Sarama, J, Learning and Teaching Early Math: The Learning Trajectories Approach. New York: Routledge, 2009.
[3] NAEP, the Nation's Report Card. National Assessment of Educational Progress, 2007. Retrieved February 24, 2008, from http://nces.ed.gov/nationsreportcard/mathematics/
[4] NAEP, the Nation's Report Card. National Assessment of Educational Progress, 2008. Retrieved September 14, 2009 from http://nces.ed.gov/nationsreportcard/mathematics/
[5] NAEP, the Nation's Report Card. National Assessment of Educational Progress, 2009. Retrieved July 22, 2010, from http://nationsreportcard.gov/math_2009/gr4_national.asp
[6] Battista, M. T., Clements, D. H., Arnoff, J., Battista, K., & Van Auken Borrow, C., Students' spatial structuring of 2D arrays of squares. Journal for the Research in Mathematics Education, 29(5), 1998, 503–532.
[7] Clements, D., Teaching length measurement: Research challenges. School science and Mathematics, 99(1), 1999, 5–11.
[8] Battista, M. T., Fifth graders' enumeration of cubes in 3D arrays: Conceptual progress in an inquiry-based classroom. Journal for Research in Mathematics Education, 30(4), 1999, 417–448.
[9] Battista, M. T., & Clements, D. H., Student understands of three-dimensional rectangular arrays of cubes. Journal for Research in Mathematics Education, 27, 1996, 258–292.
[10] Battista, M. T., Applying Cognition-based Assessment to Elementary School Students' Development of Understanding of Area and Volume Measurement. Mathematical Thinking and Learning an International Journal, 6(2), 2004, 185-204.
[11] Lantolf, J. P., Intrapersonal Communication and Internalization in the Second Language Classroom. In A. Kozulin, B. Gindis, S. A. Ageyev, & S. M. Miller (Eds.), Vygotsky's Education Theory in Cultural Context. (New York, Cambridge Press, 2003).
[12] Vygotsky, L. S., Mind in society: The development of higher psychological process. (Cambridge, MA: Harvard University Press, 1978).
[13] Vygotsky, L. S., The history of development of higher mental functions. (New York: Plenum Press, 1997).
[14] Feza, N., My culture my learning capital my tool for thought. N Tutelea (Ed). LAP LAMBERT Academic Publishing, Germany, 2012.
[15] Ageyev, V. S. (2003). Vygotsy in the Mirror of Cultural Interpretations. In A. Kozulin, B. Gindis, S. A. Ageyev, & S. M. Miller (Eds.), Vygotsky's Education Theory in Cultural Context. (New York, Cambridge Press, 2003).
[16] Ernest, P. (1991). The Philosophy of Mathematics Education, London: Falmer Press.
[17] Ernest, P. (2006). A Semiotic Perspective of Mathematical Activity: The Case Number. Educational Studies in Mathematics.
[18] Ernest, P. (1993). The Philosophy of Mathematics Education. Studies in Mathematics Education Series: 1 Bristol, PA: Falmer Press.
[19] Clements, D. Battista, M. T., & Sarama, J. (1998). Development of Concepts of Geometric Figures in a Specially Designed Logo Computer Environment. Focus on Learning Problems in Mathematics, 20(2), 47-64.
[20] Greeno, J. G., & Hall, R. (1997). Practicing representation: Learning with and about representational forms. Phi Delta Kappan, 78, 1–24.
[21] Lehrer, R., Jenkins, M., & Osana, H. (1999a). Longitudinal study of children's reasoning about space and geometry. In R. Lehrer & D. Chazan (Eds.), Designing learning environments for developing understanding of geometry and space (pp. 137–167).Mahwah, NJ: Lawrence Erlbaum.
[22] Lehrer, R., Jacobson, C., Kemeny, V., & Strom, D. (1999b). Building on children's intuitions to develop mathematical understanding of space. In E. Fennema & T. A. Romberg (Eds.), Mathematics classrooms that promote understanding (pp. 63-87). Mahwah, NJ: Lawrence Erlbaum Associates.
[23] McClain, K., Cobb, P., Gravemeijer, K., & Estes. (1999). Developing mathematical reasoning within the context of measurement. In X. Stiff, V. Lee, R. Curcio, & R. Frances (Eds.), Developing mathematical reasoning in grades K-12, 93-106.Reston, VA: NCTM.
[24] Outhred, L., & Mitchelmore, M. C. (2000). Young children are intuitive understanding of rectangular area measurement. Journal for Research in Mathematics Education, 31(2), 144–167.
[25] Ely, M., Anzul, M., Friedman, T., Garner, D. & Steinmetz, A. M. (1991). Doing Qualitative Research Circles within Circles. Bristol, PA: The Falmer Press, Taylor & Francis Inc.
[26] Siegler, R. S. (2007). Cognitive variability. Developmental science, 10(1), 104-109.
[27] Schultz, J. E. (2001). Area Models- Spanning the Mathematics of Grades 3-9. Arithmetic teacher, 39(2), 42-46.
[28] Ball, D. L., Lubienski, S., & Mewborn, D. (2001). Research on teaching mathematics: The unsolved problem of teacher mathematical knowledge. In V. Richardson (Ed.), Handbook of research on teaching 4th Ed. New York: Mcmillan.
[29] Pearson, P. D. & Gallagher, M. C. (1983). The Instruction of Reading Comprehension. Contemporary Educational Psychology, 8, 317-344.

International Journal of Modern Engineering Research (IJMER)
www.ijmer.com Vol. 3, Issue. 3, May.-June. 2013 pp-1548-1553 ISSN: 2249-6645

Topology Optimization of Aluminium Alloy Wheel

Ch. P. V. Ravi Kumar[1], Prof. R. Satya Meher
[1] *M.Tech Student, QIS College of Engineering & Technology, Ongole – 523272, Andhra Pradesh*
[2] *Professors, Department Of Mechanical Engineering, QIS College of Engineering & Technology, Ongole – 523272, Andhra Pradesh*

Abstract: *A great number of wheel tests are required in designing and manufacturing of wheels to meet satisfactory requirements. The impact performance of a wheel is the major concern. Numerical implementation of impact test is essential to shorten the design time, improve the mechanical performance and lower development cost.*

Project includes the "Topology Optimization of Cast Aluminium Alloy wheel" using impact analysis. Since the fail value of plastic strain for standard Cast Aluminium Alloy Wheel is 4.0%, cracks will appear if the Plastic Strain value is greater than 4%. This analysis will predict the plastic strain0s induced during impact testing. Topology Optimization is carried out by increasing the thickness of the rim until the plastic strain value is below 4%.

The main objective of the project is to generate a Finite element model (Hexa & Penta elements) using Hypermesh V10.0 with all the properties, materials, loads and Boundary conditions as specified by the client. Impact analysis is carried out using LS-Dyna software to predict the plastic strains during impact test.

Topology Optimization is carried out by changing the thickness of the rim of the Cast Aluminium Alloy Wheel until the value of the plastic strain is less than 4.0%.

Keywords: *Topology Optimization, Impact test, Finite element analysis, Plastic Strain.*

I. Introduction

Road wheel is an important structural member of the vehicular suspension system that supports the static and dynamic loads encountered during vehicle operation. Since the rims, on which cars move, are the most vital elements in a vehicle, they must be designed carefully. Safety and economy are particularly of major concerns when designing a mechanical structure so that the people could use them safely and economically. Style, weight, manufacturability and performance are the four major technical issues related to the design of a new wheel and/or its optimization. The wheels are made of either steel or cast/forge aluminium alloys. Aluminium is the metal with features of excellent lightness, corrosion resistance, etc. In particular, the rims, which are made of aluminium casting alloys, are more preferable because of their weight and cost.

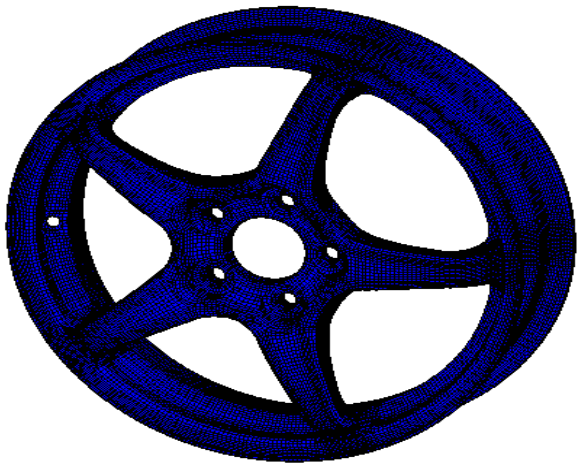

Figure 1. The Finite element model of Aluminium Alloy Wheel

Automotive manufacturers have been developing safe, fuel efficient and lightweight vehicular components to meet governmental regulations and industry standards. In the real service conditions, the determination of mechanical behaviour of the wheel is important, but the testing and inspection of the wheels during their development process is time consuming and costly. For economic reasons, it is important to reduce the time spent during the development and testing phase of a new wheel. A 3–D stress analysis of aluminium car road wheels involves complicated geometry. Therefore, it is difficult to estimate the stresses by using elementary mechanical approximations. For this purpose, Finite Element Analysis (FEA) is generally used in the design stage of product development to investigate the mechanical performance of prototype designs. FEA simulation of the wheel tests can significantly reduce the time and cost required to finalise the wheel design. Thus, the design modifications could be conducted on a component to examine how the change would influence its performance, without making costly alteration to tooling and equipment in real production. Therefore, in order to replace the physical test, the FEA simulation of the impact test should supply reliable results and sufficient information. In this regard, it is important to evaluate the effect of wheel impact performance during the impact test.

In this study, finite element analysis was conducted to simulate a cast aluminium wheel, shown in Figure 1 for the impact test according to the standard ISO 7141, using commercial LS-Dyna. The numerical model of an aluminium alloy wheel and striker were generated taking into account, the large deformable and highly non–linear material properties. In the case of strike that changes its magnitude and direction within a very short time, explicit coded software that considers dynamic forces as well as static forces is employed rather than implicit method used for static problems. The model includes elasto–plastic material for aluminium.

II. Impact Test Equipment And Procedure

Mechanical performance of road wheels under normal or severe driving conditions is evaluated by using three standard methods, such as impact, radial fatigue and rotary fatigue tests. The rotating bending test simulates cornering induced loads by applying a constant rotating bending moment to the wheel. In the radial fatigue test, the wheel and tire assembly are loaded radially against a constantly rotating drum to simulate the radial loading on the wheel. The wheel impact test is used to evaluate the impact performance, in which the striker is dropped from a specified height above the tire–wheel assembly. It is considered to be the case where the wheel collides with the curb of the road or a large obstacle. The test is designed to evaluate the frontal impact resistance of wheel and tire assemblies used in all cars and multi–purpose vehicles. The test is specifically related to vehicle pothole tests that are undertaken by most vehicle manufacturers. The scope has been expanded to allow the use of a striker that can be angled to preferentially impact the inboard and outboard wheel flange. Before the test, a wheel undergoes complete visual inspection to ensure that no cracks exist in the body. In order to pass the impact test, the wheel must meet the following minimum performance standards: There will no visible fracture of the central member of the wheel assembly, no separation of the central member from the rim, no sudden loss of tire air pressure and deformation of the wheel assembly, or fracture in the area of the rim section contracted by the faceplate weight system do not constitute a failure (International standard, 1995).

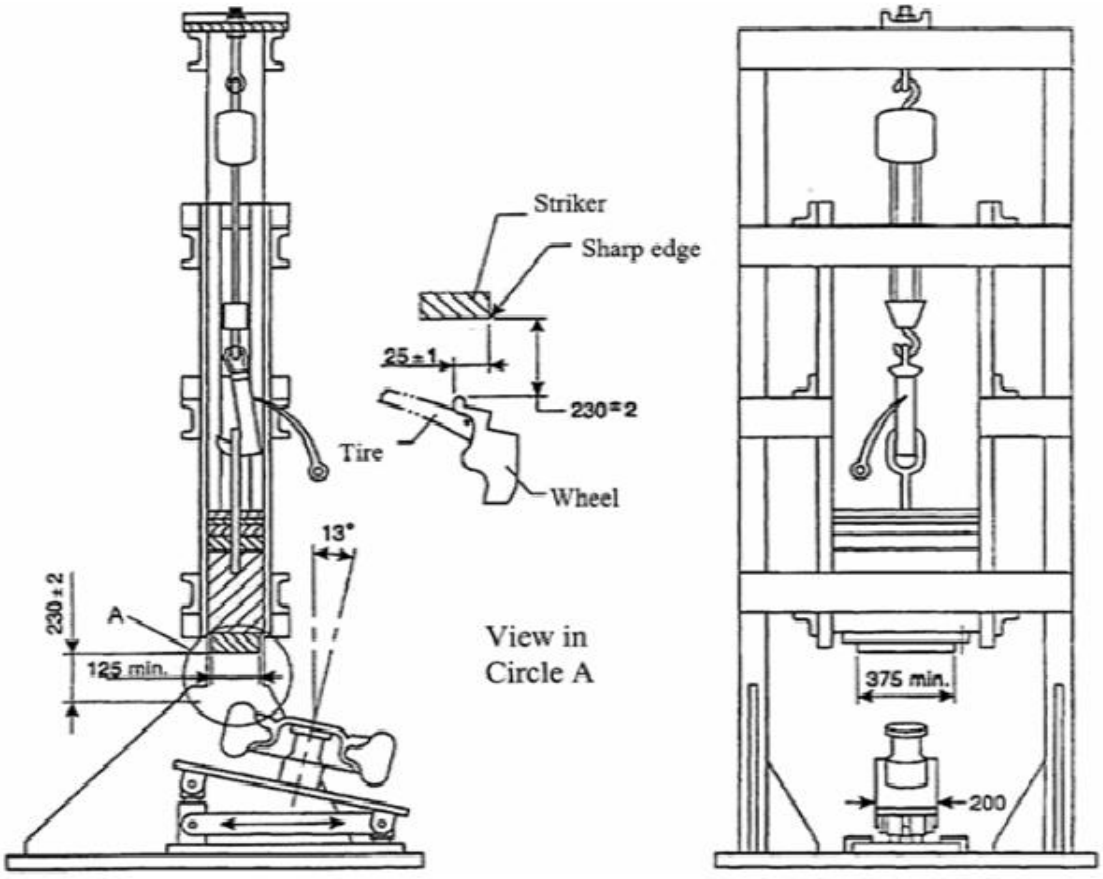

Figure 2. Schematic diagram of Wheel Impact test machine

The impact test standard provides detailed test procedures and equipment description for the impact test. A test machine is shown schematically in Figure 2. The test set up, in which a striker applies an impact to the rim flange of a wheel. The wheels are mounted with its axis at an angle of 13 degrees (± 1 degree) to the vertical, so that its highest point is presented to the vertically acting striker. The impacting face of the striker is at least 125 mm wide and 375 mm long. The freely dropping height of the striker is 230 mm (± 2 mm) above the highest point of the rim flange. The striker is placed over the tire and its edge overlaps the rim flange by 25 mm. The inflation pressure of the tire can be specified by manufacturer taking into account, the serves conditions. An inflation pressure of 200 kPa, which in real service condition, was applied on the inner surface of tire and portion rim (International Standard, 1995).

III. Material Properties

The material properties of A356 Cast Aluminium Alloy that is widely used in automotive engineering industry was considered in the FE simulation. Mechanical properties of aluminium alloy are given in Table 1.

Table 1. Mechanical Properties of Aluminium Alloy

Elasticity Modulus	Poisson's ratio	Density	Yield stress	Ultimate stress
72.4 GPa	0.33	2.67E-09 tonne/mm^3	218 MPa	283 MPa

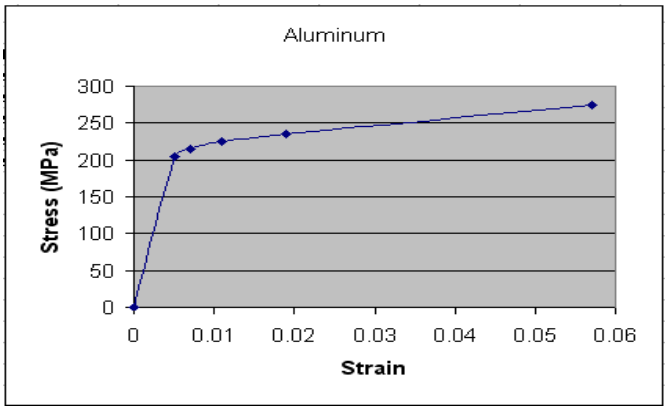

Figure 3. Engineering Stress-Strain diagram of Aluminium Alloy

A nonlinear elasto–plastic material model was used to describe the material behaviour of aluminium wheel in the analysis. The engineering stress–strain curve of the aluminium alloy is plotted in Figure 3. The striker used in this analysis was modelled as an elastic material using steel material properties.

Table 2. Mechanical Properties of Steel

Elasticity Modulus	Poisson's ratio	Density	Yield stress	Ultimate stress
210 GPa	0.3	7.85E-09 tonne/mm^3	250 MPa	400 MPa

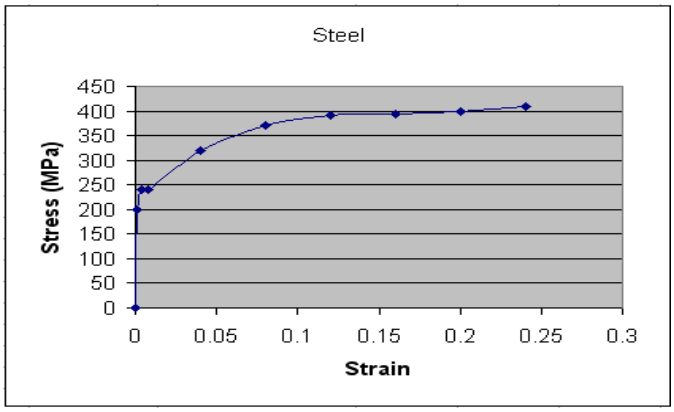

Figure 3. Engineering Stress-Strain diagram of Steel

IV. Finite Element Analysis

The purpose of this analysis is to predict the plastic strains induced during Impact testing. Modelling the mechanical response of impact test rim is extremely complex. Commercial finite element software LS-Dyna is utilized to perform 3–D impact analysis of wheel impact test. The numerical modelling of wheel impact test obeys the experimental procedure, which was described in the ISO 7141. The whole numerical model is an assembly consisting of three portions, namely a wheel, fixture and striker shown in Figure 4.

Uniform shapes and forms of elements play important role in the sensitivity of the results when using the finite element method. Therefore, the meshing of the wheel, fixture and impact striker models is mainly constructed by 3–D structural solid having 8– node finite element. It can tolerate irregular shapes without much loss of accuracy. The fixture model was generated based on the assumption. However, including every detail, it makes the model too complicated to be solved within a reasonable time limit. In order to simplify and reduce the overall size of the model, some of the features which are not essential in cornering, are either simplified. All degrees of freedom of the nodes on the mounting surface of the hub and bolt holes were fully constrained. The nodes at the surface between the wheel and striker are constrained to move together. The full model including rim, fixture and striker compose of **159757** elements. The mass of the striker is a variable

related to the maximum static wheel load as presented in Equation 1. The unit of mass is kilogram:

$$m = 0.6\, m_w + 180 \quad \text{----------} \quad (1)$$

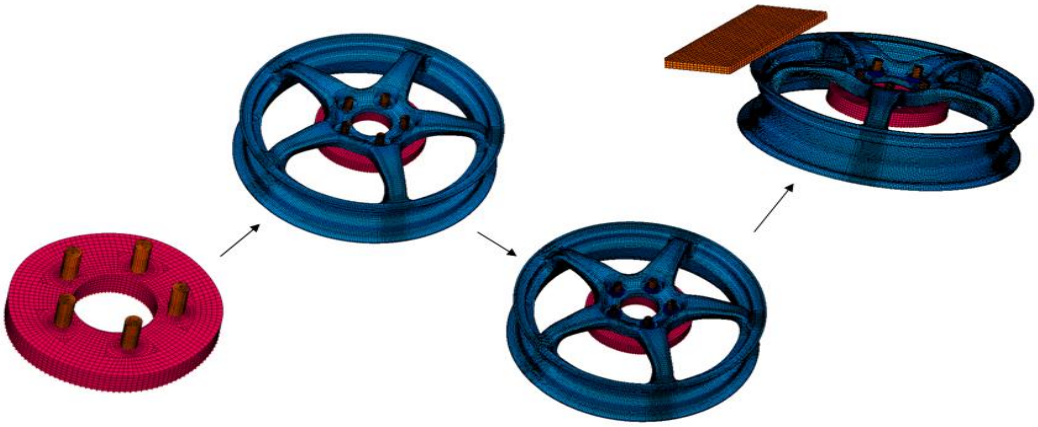

Figure 4. Finite element model of the Wheel Assembly with Striker

Where m is the mass of striker, and m_w is the maximum static wheel loading as specified by the wheel and/or vehicle manufacturer. Mass of the striker for the wheel–tire was determined to be -570 kg. The volume of the striker was adjusted so that the total mass of the striker is the same as that of the striker used in a real impact test. Striker dimensions are 15 mm in height, 125 mm in width and 375 mm in length. The striker was constrained in the horizontal direction to ensure that the striker could only be displaced vertically as in the impact test. For the purpose of reducing computational time, the initial dropping height, which represents the distance between the lower surface of the striker and the impact point on the rim flange, was modified from the prescribed value of 230 mm to 0, but with similar impact energy. The magnitude of the initial velocity of the striker prior to impact was calculated using the following equation and applying the energy conservation principle.

$$V = \sqrt{2gh} \quad \text{----------} \quad (2)$$

Where V is the initial impact velocity of the striker, g is the acceleration of gravity and h = 0.23 m is the initial height of the striker. The Boundary Conditions of the Alloy wheel for impact analysis is shown in figure 5.

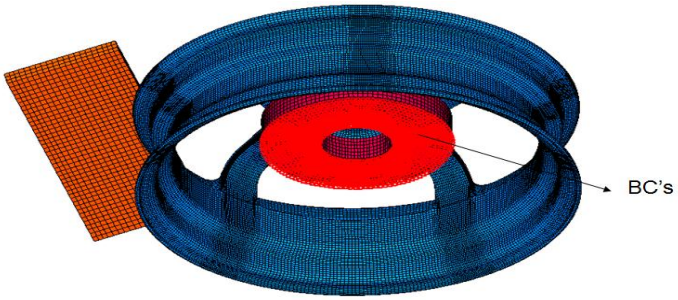

Figure 5. *Boundary Conditions of* Finite element model of the Wheel Assembly with Striker

Topology optimization is carried out by changing the rim thickness of the alloy wheel as shown in figure 6, until the value of the plastic strain is less than 4.0%.

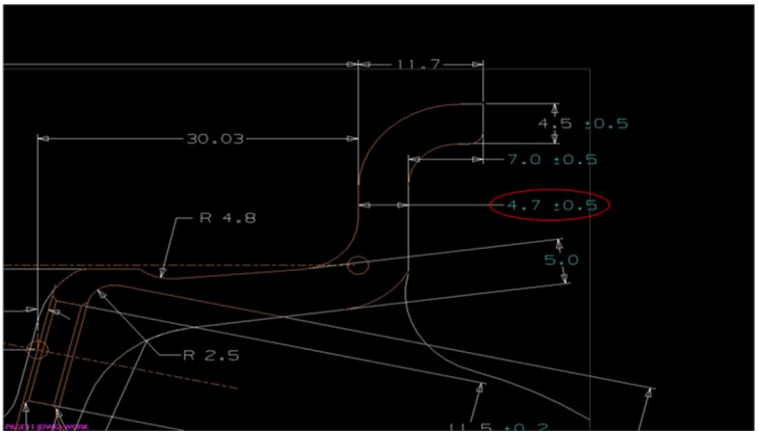

Figure 5. *Thickness of the rim indicated in circled area*

Several load cases have been performed by changing the thickness of the rim. Out of which, the following are the three load case studies where a change of plastic strain noticed drastically while post-processing.

Case-1: The thickness of the rim is 3.5 mm

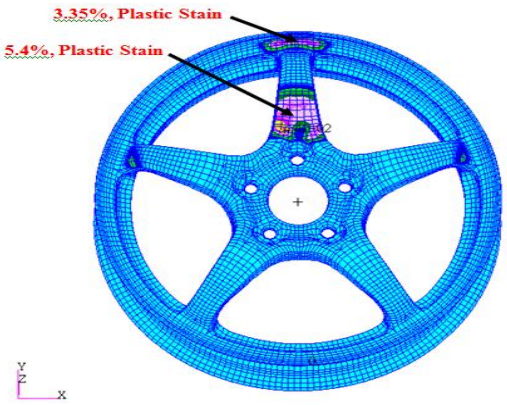

Case-2: The thickness of the rim is 4.7 mm

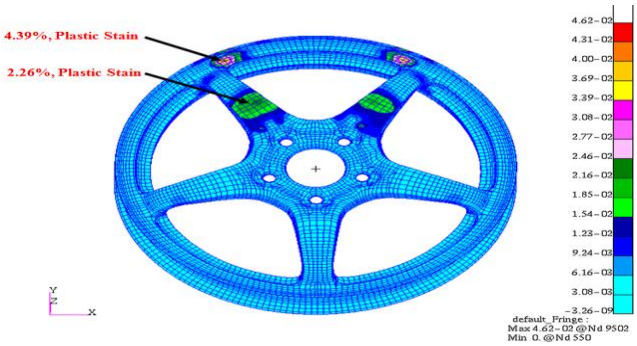

Case-3: The thickness of the rim is 5.9 mm

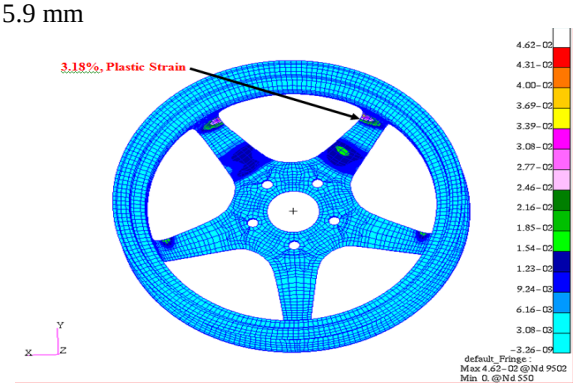

Failure Criteria: Cracks will appear if the plastic strains are higher than 4%

V. Summary

The Effective Plastic Strain for the three load cases are as following:

Load case with rim thickness of 5.9mm	Load case with rim thickness of 4.7mm	Load case with rim thickness of 3.5mm
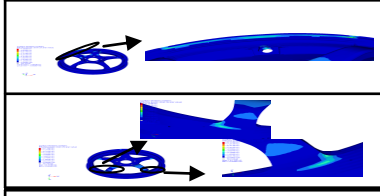		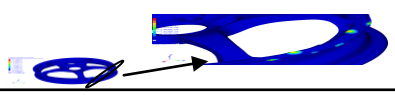
	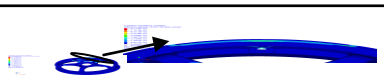	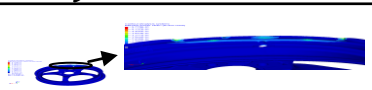
Effective Plastic Strain for rim thickness of 5.9mm	**Effective Plastic Strain for rim thickness of 4.7mm**	**Effective Plastic Strain for rim thickness of 3.5mm**
3.2 %	**4.4%**	**5.4%**

VI. Conclusion

The response of wheel assembly during the impact test is a critical phenomenon. In this paper, a numerical study of impact test of the wheel assembly was performed using explicit finite element code. 3–D finite element analysis with a reasonable mesh size can reliably estimate the response. Such results will help to predict the locations, in which the failure may take place during impact test and improve the design of a wheel with required mechanical performance. Topology optimization is carried out using impact test on Aluminium alloy wheels by varying thickness of the rim and the results obtained are shown above. Since the standard fail value of plastic strain for standard wheel is 4.0%, the thickness of Cast Aluminium Alloy Wheel should be 5.9mm from the results obtained above which will perform satisfactorily.

References

[1] Muhammet Cerit. Numerical simulation of dynamic side impact test for an Aluminium alloy wheel, Department of Mechanical Engineering, Sakarya University, Turkey. August-2010

[2] Si-Young Kwak, Jie Cheng and Jeong-Kil Choi. Impact analysis of casting parts considering shrinkage cavity defect, Department of Virtual Engineering, School of Engineering, Korea University of Science & Technology, Daejeon, Korea. August-2010.

[3] C. Bosi, G.L. Garagnani, R.Tovo. Fatigue Properties of a Aluminium Alloy for Rims of Car Wheels, Department of Ingegneria, University of Degli Studi Di Ferrara, Italy.

[4] Mi Guoga, Liu Xiangyu, Wang Kuangfei, Fu Hengzhi. Numerical simulation of low pressure die-casting aluminium wheel, Department of Mechanical Engineering, Chengde Petroleum College, Chengde 067000, P. R. China. August-2008.

[5] Mohd Izzat Faliqfarhan Bin Baharom. Simulation test of Automotive Alloy Wheel Using CAE Software, Department of Mechanical Engineering, University of Malaysia Pahang. October-2008

[6] Cleginaldo Pereira de Carvalho, Herman Jacobus Cornelis Voorwald. Automotive Wheels – An Approach for Structural Analysis and Fatigue Life Prediction, Department of Materials Tecnology, Brasil. November-2001.

International Journal of Modern Engineering Research (IJMER)
www.ijmer.com Vol. 3, Issue. 3, May.-June. 2013 pp-1554-1560 ISSN: 2249-6645

Displacement and Protest Movements-The Indian Experience

Dr. J. Uma Rao
Lecturer, Damodaram Sanjivayya National Law University

Abstract: *Large scale river projects involve construction of dams at several places, construction of reservoirs and canals and this would invariably result in large scale upheaval of communities and necessitate their rehabilitation. Displacement has important dimensions, economic, sociological and legal. All the facets are inherent parts of human life and are interwoven, with overlapping boundaries. From the sociological point of view, the various hardships suffered by the affected people and the different protest movements, and the methods to suppress them are examined. This paper focuses on protest movements against large scale projects like the Silent Valley Project, the Tehri dam, the Koel Karo project. The use of the law by the state for suppressing these movements by use of the Official Secrets Act, 1923, The Criminal Procedure Code 1973, The Terrorist and Disruptive Activities (Prevention) Act (TADA) , Prevention of Terrorist Activities Act (POTA) and some Irrigation Acts is highlighted in suppressing the protest movements.*

Key Words*- development, protest movements, Acts*

After Independence, India aimed at achieving rapid economic growth and at attaining self-sufficiency in all areas. Industrialism and large-scale development projects were thought to be symbols of progress. India's socialist philosophy also played an important role. The most influential development model of the twentieth century has been industrial development. Development was inseparably linked with major and mega projects including dams, ostensibly to augment water resources.

Large scale construction, which involves acquisition of land and which leads to displacement, was seen as a necessary extension of development and critics of the projects have been called not just anti-project and anti-development, but also anti-national and democratic activities like protest marches were often treated as public order problems. Politicians, policy makers and engineers may claim that the attendant results were not anticipated and that displacement was an unintended consequence, but historical records say something quite different.

The figures of displacement of people vary from a conservative estimate of 110 lakhs to a figure of 185 lakhs during the period 1951-1990. Since Independence over 1600 major dams and tens of thousands of medium and similar irrigation projects have been built with canal systems, and the invariable consequences of water logging and soil salination. Another estimate places the number closer to 210 lakhs by these dams till 1985.[1] These figures do not include the sizeable number of people who are not acknowledged as being 'Project Affected' (i.e., by loss of livelihood caused by natural resource extraction or degradation), those displaced in urban areas and those victimised by the processes of secondary displacement (those whose livelihoods are adversely affected either as a direct or indirect or as a short term or long term consequence of the developmental intervention, but who are not acknowledged as 'project affected people or PAPs). In several cases their numbers exceed officially recognised PAPs. If these are tallied the number of those displaced since independence would be as high as 4 crores. Another way to view the magnitude of the displacement process by considering the financial resources spent on big projects. An estimate says that from 1947 to 1980 India spent 15% of its total national expenditure on building dams.[2]

Due to large-scale displacement that has occurred worldwide, it would be no exaggeration to call the 20th century the 'Century of displacement'.

I. Bureacratic Attitude

In our celebration of nation building, the sacrifices demanded by rulers were thought to be justified. Pandit Nehru was one of the first who legitimised this attitude. At the foundation laying ceremony of India's first major river-valley project, the Hirakud in Orissa, he said "if you have to suffer you should suffer in the interests of the country"[3] Smt. Indira Gandhi the then Prime Minister of India in a letter to Baba Amte on August 30, 1984 said "I am most unhappy that development projects displace tribal people from their habitat, especially as project authorities do not always take care to properly rehabilitate the affected population. But sometimes there is no alternative and we have to go ahead in the larger interest"[4] A veil behind which the State, the politicians and the bureaucracy have taken refuge is the utilisation principle, which says that there should be maximum benefit to the maximum people and minimum harm/pain to the minimum, but the figures paint an altogether different picture. This principle is invoked to provide legitimacy to the displacement and to show that it is in the greater public interest and that the individual interest has to make way to greater public good.

1. Vijay Paranjpye- "High Dams on the Narmada, A Holistic Analysis of the River Valley Projects" (INTACH) 1990,as quoted by Smithu Kothari , in "Whose Nation? The Displaced as Victims of Development" EPW Vol 31 (24) p 1476 at p.1477.
2. Dilip D'Souza, "Narmada Dammed-An enquiry into the politics of development," 2002,p 01.
3. The Bombay Chronicle April 12, 1948, as quoted by Smithu Kothari , in "Whose Nation? The Displaced as Victims of Development" EPW Vol 31 (24) p 1476 at p.1478.
4. Edward Goldsmith and Nicholas Hildyard Ceds, "The Social and Environment effects of large Dams Vol-II p.245", as quoted by Smithu Kothari , in "Whose Nation? The Displaced as Victims of Development" EPW Vol 31 (24) p 1476 at p.1477.

II. Effect On Tribals

Tribals comprise 7.5% of the country's population. Over 40% of those displaced till 1990 come from these communities, underscoring the fact that tribals are disproportionably affected by developmental displacement.[5] A large mass of humanity has had to leave their homes, farms, neighborhoods, and entire communities have had to start their lives from scratch due to displacement. Most of the Dams are in predominantly tribal areas and tribal cultures are distinct from those groups belonging to modern economy. They are marginalised from the mainstream political system and are vulnerable to exploitation. The special needs of tribals have not been taken into account in past resettlement plans and policies and their encounter with the modern economy through displacement mostly resulted in material impoverishment and social disintegration.

There are, of course exceptions to this attitude as with the Apa Tanis Project in Subansiri district of Arunachal Pradesh, where outsiders were not allowed to enter the valley. It was ensured that there was cash flow into the valley. Village Panchayats and local bodies consisted of tribal leaders and members. Disputes were settled by tribal courts and local bodies were also the law enforcers. Schools were established where children were educated irrespective of parental means.[6] But instances like the Apa Tanis project are very few. Displacement brings about drastic changes in people's lives as they permanently alter the ways in which the land, water and other natural resources were being used. For Example, the Barh Mukti Andolan has documented how entire villages have switched from farming to fishing and how all able bodied persons have migrated in the dismal search for any work.[7]

III. Effect on Women

Women's trauma is particularly compounded by the loss of access to fuel, fodder and food collection, which inevitably requires greater time and effort. Few resettlement sites have made provisions for this. Such women experience greater indigence and are forced into the labour market. There is a disruption in established relationships. Children are adversely affected since schooling is less accessible.

Developmental projects have brought in suffering in all countries generally and developing poor countries particularly. The law in India is not equipped, at best ill equipped, to counter this attitude.

The close of the 20th century will be remembered for the large numbers of people evicted from their houses, farms and communities and forced to find a living elsewhere. Resettlement has consequently gained importance in development literature due to (i) A worldwide concern over the adverse environmental and social costs of large infrastructure projects (ii) The well organised and well publicised resistance movements against involuntary resettlement in many countries of the world for[8].

Anthropologists have identified two different types of displacements. (a) Voluntary, (b) Involuntary. Two factors, "Push" and "Pull" have been identified. The "Pull" factor is identified with voluntary relocation. It consists of mostly young families who still manifest their social and economic ties with their villages. Such families have the luxury of coming back to their native places. Ties are maintained with people/relatives back in the villages which serve as cushioning and are great stress relievers in cases people come across harsh conditions in their new surroundings.

The ouster by large-scale projects comes under involuntary relocation, which is identified with the "Push" factor. It forces people out of their traditional localities. Levels of anxiety and insecurity are much higher for example oustees of the Narmada and Tehri projects. Entire villages were forced to move out. It consists of two closely related yet distinct processes, displacing people and rebuilding their livelihoods. The complexity of involuntary resettlement and the diversity of project situation make good resettlement a difficult task. When people are displaced, production systems get dismantled, kinship grouping gets disrupted and long established residential settlements disorganised. Jobs and assets are lost, links between producers and customers are often severed and local markets get disrupted. People's lives are affected in painful ways. Such resettlement is usually the outcome of a planned political decision and is deemed to fit into the nation's ideology and the larger social good. People displaced by wars/famines can return to their homes once the cause has subsided and therefore support in the interim is an adequate measure, while development induced displacement is permanent in nature. Interim sustenance and support is therefore not enough for income generating and living conditions. Short term programmes like provision of relief payments and refugee camps are not enough.

IV. The Scudder-Colson Theory of Relocation

This theory has greatly affected resettlement theory and policy across many countries. This theory says that relocation, whether voluntary or compulsory is a stressful experience. Members of communities undergoing relocation react in predictable and broadly similar ways.

It is also said that initially, in the time up to relocation and few years of adjustment thereof, people's behaviour is conservative. They avoid risks and stick to familiar practices and groups of people. Once they establish themselves economically and socially, they are less stressful and insecure and there is a change in people's attitude. They take risks, are innovative, are more flexible and individualistic when compared to people who have not been resettled. A community is said to be successfully resettled when it has integrated itself into wider regional setting in such a way that it has attained

5. The 29th report of the Commissioner of S.C. & S.T
6. Sangeeta Goyal,, "Economic Perspectives on Resettlement and Rehabilitation" EPW,Vol 31(24) p 1461 at p 1464.
7. Dunu Roy 'Large Dams for whose benefit?' EPW, Vol. 29(50) p. 3129.
8. Roli Asthana "Involuntry Resettlement, Survey of International Experience" – EPW Vol 31(24) p. 1468.

economic and administrative ability.[9]Since there are no rigorous global statistics available about development induced displacement, the magnitude of the problem cannot be fully appreciated. It is a reality that large scale building of dams along with canals, reservoirs etc. would bring in more and more people in the category of involuntary displacement. Added to this, the infrastructure to sustain such projects like building of roads, housing colonies, industrial estates and power houses would force many more people into the displaced category.

A Risk Model shows how impoverishment can occur as a result of displacement. It points out that when displacement or relocation leave people worse off, empirical evidence reveals a set of 8 recurrent characteristics that need to be closely monitored. They all contribute to a process of impoverishment. The risks thus to be avoided are:

- Lawlessness
- Joblessness,
- Homelessness,
- Marginalisation,
- Morbidity,
- Food insecurity,
- Loss of access to common property and
- Social disarticulation.

If a person, who has relocated, successfully comes out without falling into any of the above-mentioned categories, he can be said to have been successfully relocated and resettled. [10] One way to measure the success or failure of the rehabilitation measures adopted by a country is to study the opposition by affected and supportive groups to their displacement and the method and spirit in which such opposition is handled by the state and the concerned authorities.

V. Protest Movements

Protest indicates demonstration or expression of disapproval / dissent / discontent on some issue. In a democracy, the expectation is that the Government's decisions reflect the majority will. However, in view of the division of ideology or political party system, there is probability of disagreement on the Government's decision. Article 19 (1) (a) guarantees the right to express dissent. Article 19(1)(b) says that all citizens shall have the right to assemble peaceably and without arms. Infact an important component of democracy is the right to protest and having the Government to listen to the people's grievances. "To treat all protest as a nuisance, a violation of public order, the most common attitude of the administration and the Courts, is to misunderstand democracy fundamentally."[11] The question is when the state plans meticulously every minute detail of the construction of the project, why can't the same concern and foresight be extended towards the displacement misery it would cause and the costs and methods of rehabilitation?

The resistance to development projects is not new. By the mid 19th century itself, communities had mobilised to oppose colonial policies of resource extraction, like the Epidemic Commission of 1864, followed by the Canal Commissions of 1885 and 1888. The spirited protests of Raja Digambar Mitter and L. Ghosh prior to 1890 were noteworthy. Be it the Drainage Committee of 1907 or the Flood committee of 1928, report after report lays down clear evidence of the devastating impact of projects on population. From 1947 Kapil Bhattacharaya warned repeatedly how the proposed dams, roads and bridges would impoverish both nature and society. Nobody listened, because they said there was not 'sufficient evidence'.[12] There were protests against the Forest Act of 1876. Most of these protests were from tribal areas which were most affected. The beginnings of the anti-dam movement can be traced back to the issues raised by the affected farmers of the Mulshi dam, 1921-24. The environmental and social costs of constructing large dams were raised by prominent social reformers like Senapati Bapat and Vinayak Bhuskute.[13]

The voices of contentious engineers like Kapil Bhattacharya, who pointed out the mistakes in Damodar Valley Corporation, inspired leaders like Ram Manohar Lohia to take up the struggle. Ram Manohar Lohia, in the late 1950s and 1960s organised one of the earliest post-independence protests against developmental displacement. It was one of the most remarkable struggles for justice for 3 lakh people who were to be displaced by the Rihand Dam (U.P.). A day before submergence, 100 political activists and community leaders were picked up and imprisoned. There was no effort to rehabilitate those displaced and the fate of over 70% is not known while the remaining have faced the repeated trauma of multiple displacement.[14]

A. The Silent Valley Project:

The Silent Valley Project (SVP) was perhaps the 1st instance where the development vs. environment debate gained prominence. In the late 1970s the Kuntipuzha River in Kerala's Palaghat district flowing through a valley was considered an ideal place for constructing a dam. The envisaged benefits were irrigational potential of 10,000 hectares, generation of 240 megawatts of power in addition to job creation. On the other hand, construction of the dam would lead to destruction of one of the world's richest biological heritages. The controversy started with a report of the task force, which recommended that

9. Ibid at p.1469.
10. Ibid pp.1469-1470, Developed by Michael .M. Cernea (1990).
11. K.Balagopal "Right to Protest" ,The New Indian Express, Vskp.Ed., 15-8-07 p.5.
12. Supra note 7.
13. See generally Sanjay Sangvi, "The New Politics of Environmental Socialism in India" in the book titled "Globalisation and Social Movements" Ed. P.G. Jogdand and S.M. Michael, 2003 p.219 at p 220.
14. Smithu Kothari , in "Whose Nation? The Displaced as Victims of Development" EPW Vol 31 (24) p 1476 at,p. 1485., End note 42.

the project be abandoned and the area be declared a biosphere reserve However, if the Government would not abandon the project for any reason, the report laid down several safeguards, which resulted in the controversy. The project was opposed by Kerala Sastra Sahitya Parishat (KSSP), an effective grassroots environmental body, and an organisation called the Friends of the Trees, both of these being supported by a Save Silent Valley Committee in Bombay supported by World Wild Life Fund (WWF) etc. The project was supported by the Government of Kerala and the Kerala State Electricity Board. Soon several international organisations also joined in support of the environmentalists. The Government of Kerala then approached the Prime Minister of the day and asked that the project be given the green signal. This gave rise to a furore and the Kerala Government was asked to stop further work in late 1979. Later two committees were appointed to study the feasibility of the project. The first one was headed by the famous agricultural scientist, Dr. M.S. Swaminathan who asked for the project to be stopped. The second committee headed by Prof. M.G.K. Menon also submitted a report. The personal note of Mr. Menon was that the project be stopped and it was stopped in 1983. It is to be noted that the movement was successful inspite of the Governments' determined efforts to carry out the project and the non-interventionist stand adopted by the Kerala High Court which had the following to say "we were taken through copious, extracts from various works, reports and other materials regarding the technical feasibility of the project. But in this region we cannot substitute our judgment for that of the Government, on the question as to whether a national asset is to be more conveniently utilised as a hydro-electric project with prospects of greater power generation, or retained in its pristine glory for preservation of forests and wildlife, prevention of soil erosion.[15]

The success of the Silent Valley Movement is considered a golden chapter in the history of the conservation movement, but there seems to be a renewed interest in the project. Though the proposal is not exactly in the same area which was constituted a global heritage site in 1984, it seems to be close enough to be near it to pose a threat, as the Pathrakkadavu Hydro Electric Project proposed on the Kunti river proposed just outside the boundary of the park could pose a threat to the silent valley eco system. The Kerala Sastra Sahitya Parishat which was instrumental in the silent valley movement advises further studies to be taken up before any further project is taken up. Rapid EIA done by the KSEB (Kerala State Electricity Board) also acknowledged the threat to the flora and fauna. The fundamentals of the project regarding rainfall data on which the feasibility of the project depends are also questioned. It is lamented that such arguments continue to fall on ears deafened by the vociferous ideology of development. Like dams, ideologies too have time and cost overruns.[16]The sustained campaigns and protests seem not to have been in vain as borne out by the fact the Kerala Cabinet approved a proposal to create a buffer zone for the Silent Valley National Park, which would have the status of a reserve forest.[17]

B. The Tehri Dam:

The Tehri dam was always perceived as a threat by the local population who consider the river Bhagirathi not only as a means of livelihood, but have religious, cultural and emotional ties with it for generations. As early as in 1965, when Sri K.L.Rao, the noted engineer and Minister visited the area, the people expressed their apprehensions about and the opposition to the project to him. Nevertheless, the Planning Commission approved the project in 1972. In 1973, the Communist Party of India organised an agitation against the project. However the Government of Uttar Pradesh obtained administrative approval in 1976. In retaliation 35 gram sakhas in Tehri district passed a joint resolution opposing the project. The Zilla parishad also opposed the project but the Government decided to go ahead with it. To oppose the Government's action the Tehri Band Virodh Sangharsh Samiti(TBVSS) was formed, which passed a unanimous resolution opposing construction of the dam. Turning a deaf ear to this, the Government awarded construction contracts which led to severe protests from all sections of the Society.[18] The opposition strategies included press campaigns, reports, seminars and litigation.

The points of contention were, in this case not only the usual Government apathy towards R & R but also a threat of catastrophic proportions posed by the project. The Tehri Hydro Electric Development Corporation (THEDC) was formed to implement the project. Though the environment clearance was not obtained, initial funds were released and later the Finance Ministry insisted that the clearance be obtained for further release of funds. The Environment Ministry comprising of experts recommended that the project wouldn't be cleared as not only was it unsafe but also data regarding vital aspects such as rehabilitation, disaster planning, watershed management etc. was not available. Instead of accepting this report, the Government set up an expert committee to study the feasibility.

This committee had one expert seismologist, the internationally well known Vinod Gaur, who insisted that the committee should take into account the likelihood of an earthquake beyond 8 points on the Richter scale. Though the committee agreed initially, the committee considered the likelihood of an earthquake of 7 on Richter scale as adequate.[19] The approximate energy released by an earthquake of 7 magnitude is equivalent to the explosive power of 90,700 tonnes of(TriNitroToluene) TNT, and that of 8.5 magnitude is 2,86,15,850 tonnes of TNT. Even a lay man can see that a structure designed for 7 magnitude can hardly withstand the pressure of an earthquake of 8.5 magnitude.[20] The Government, to overcome the recommendation of Dr. Gaur, assigned the tasks to the Ministry of Mines, which is known as an aggressive pro-development agency, with an unenviable environment track record. The Department of Mines chose as their expert Prof. Jaikrishna, who was an earthquake engineer, and not a seismologist and he opined that the design of the dam was quite safe

15. See generally OP 2949 of 1979 Society for Protection of Silent Valley and others Vs Union of India (from unreported decision of Kerala H.C) Armin Rosencranz *et al*, "Environmental Law and Policy in India" , 1995, p. 285.
16. "New Whispers in Silent Valley", The Hindu Magazine, Vskp.Ed.,1-08-2004, p.1.
17. "Buffer zone proposal for Silent Valley approved", The Hindu Vskp.Ed.,7-6-2007 p.7.
18. Armin Rosencranz *et al*, "Environmental Law and Policy in India" , 1995,, at p. 290.
19. Sundarlal Bahuguna.-"Investment in disaster?" The Hindu Survey of Environment, 1991,p 28 at p. 28.
20. *Ibid.*

against the strongest expected earthquake.[21] The dam was also a point of controversy between The Ministry of Power and the Ministry of Environment. Even between the Government and the environmentalists, the safety aspect assumed more importance than the rehabilitation aspect, unlike the Narmada, where R & R is the focal point.[22]

The TBVSS filed a petition under Article 32.[23] It contended *inter-alia* that:

- The dam was seismologically risky posing severe threat to downstream settlements like Haridwar and Rishikesh.
- The State had no right to sanction such projects for temporary benefits, which would permanently alter land use.
- The dam life would not be more than 20 years due to silting up.
- The risks far outweigh the benefits.

The Supreme Court, relying on the statements of Prof. Jai Krishna, discussed earlier, held that the Government of India could not be said not to have applied its mind nor has it failed to consider the relevant aspects of safety and dismissed the petition.[24]

In the year 1991, when the region shook on an earthquake of 6.1 on the Richter scale, destroying 2000 settlements and killing 800 people, the safety aspects of the dam were questioned again by the TBVSS but the Tehri Hydro Electric Development Corporation (THEDC) insisted that the dam was not affected by the earthquake. The dam was constructed and people began to move out from 2001 onwards and different regions were submerged from 2001. Though the land acquisition began from 1979 onwards, the people still unrehabilitated are estimated at 13000 – 18000 families. Some families who were rehabilitated were asked to move again for some other projects- an airport.[25]On fourth August 2004 a tunnel in the project caved in resulting in loss of life, evoking anguish from several environmentalists. "Environment activist Vandana Shiva urged the Government to reassess the costs involved in the construction of the Tehri dam in the wake of the tunnel collapse. The large scale dam and road building in the Himalayas was playing havoc with the region's eco-system."[26] It was reported that the accident at the Tehri Hydro Electric Project at Uttaranchal had led to fresh demands by environmentalists and non-governmental organisations (NGOs) to stop the filling up of the dam's reservoir and review all on going hydel projects in the Himalayan region. It was the second such incident at Tehri in three years after 60 workers were buried alive during a landslip in 2001. Also questioned was the functioning of the committee constituted by the Supreme Court to monitor rehabilitation and environmental compliance.[27] On 29/10/2005, the Uttarakhand High Court ordered the closure of Tunnel 2. In October 2005 the last of the Tehri dam gates was closed and the old town of Tehri disappeared under water.

Though the builders and engineers of the dam call it a marvel, the environmentalists and the affected people call it a dam built on their tears, one of them being Sundarlal Bahuguna.[28] The judgment in the Tehri dam case and the one in Narmada case are perceived as retrogressive and as encouraging other similar projects. "With no NBA to deal with, bolstered by the Supreme Court's hostile judgments on the Sardar and Tehri dams, the Madhya Pradesh Government and its partner the NHPC have rampaged through the region with a callousness that would shock even a seasoned cynic." [29]

C. Koel Karo:

In erstwhile Bihar, before its division into Jharkhand, Chhattisgarh and present day Bihar, two dams were proposed to be built on the northern and southern banks of Koel Karo River. The benefits from the dams were generation of 710 MW of power only, as no irrigation was envisaged. It was estimated at that time that the villages and people affected would be 130 and two lakhs respectively. The background for the project was that the drought of 1967 in Palamau, followed by a famine necessitated a solution. The then prime minister came up with the idea of a dam to be built on the North Koel River. In 1970, the Koel Karo Jan Sanghatana was formed. The proposed construction sites of Koel Karo dam were tribal dominant. In 1994, the opposition movement gained momentum, and around 70,000 tribal oustees gathered at the submergence zone and organised strong protests. An appeal was filed on their behalf in the Supreme Court, which stayed land acquisition proceedings by the Government for five years. As soon as the five years expired, the Government again announced that it would again build the dam, but with the Jharkhand Mukthi Morcha (JMM) active in those parts, the resistance built up rapidly and the fight against the dam is still continuing. After formation of Jharkhand State, the Government of the day again wanted to take up construction of the dams, this again led to protests.[30]

In February 2001 Adivasis protested against the Koel Karo dam, at the police outpost at Tapkura, Jharkhand. A large contingent of police opened fire from rifles and sten guns on about 5000 people gathered, which resulted in 9 people

21. *Supra note* 20 p. 301.
22. See generally, Kalpana Sharma "Involving a new philosophy", The Hindu Survey of Environment 1992, p. 47.
23. Remedies for enforcement of rights conferred by this part :-
    1) The right to move the Supreme Court by appropriate proceedings for the enforcement of the rights conferred by this Part is guaranteed.
    2) The Supreme Court shall have power to issue directions or orders or writs, including writs in the nature of *habeas corpus*, *mandamus*, prohibition, *quo warranto* and *certiorari*, which ever may be appropriate, for the enforcement of any of the rights conferred by this Part.
    3) Without prejudice to the powers conferred on the Supreme Court by clauses (1) & (2), Parliament may by law empower any other court to exercise within the local limits of its jurisdiction all or any of the powers exercisable by the Supreme Court under clause (2).
    4) The right guaranteed by this article shall not be suspended except as otherwise provided for by this Constitution
24. *TBVSS Vs State of UP* 1992 (Supp) 1 SCC 44.
25. See generally "Ravi Chopra and Rajendra Bansal, Tehri Engineers Pride, Peoples sorrow", The Hindu Survey of Environment 2006, p 87 at pp. 87-90.
26. "Tehri Accident Toll 27;Hopes of Finding Survivors Fade",The Hindu, Vskp Ed., 5-8- 2004, p.1.
27. "Review On-Going Hydel Projects",The Hindu Vskp Ed., 4-08-2004, p.11.
28. *Supra note* 25, pp. 87-90.
29. Arundhati Roy, "An Ordinary Person's Guide to Empire.", 2005, p. 256.
30. *Supra note* 24 p.49 and Meghnath, "Palamau from 'no' to 'yes' on dams."- The Hindu Survey of the Environment 2001, p,165 pp.165-172.

being killed and 22 injured. The Adivasis were protesting against the construction of the dam, as it would submerge the forest area on which they were dependant.

Interestingly, though the adivasis form about 8% of the country's population they form 47% of the people displaced due to large projects.[31] Irrespective of the political party in power, large dams and multipurpose projects occupy prominent mind space and the struggle of the affected goes on.

It can be observed that large scale displacement has been and continues to take place affecting millions of people adversely, particularly the poor, the downtrodden and the tribals. The government's and the bureaucrat's attitude towards this continues to be callous .There have been protest movements against this, but with the exception of very few they cannot be termed successful. The State's use of draconian laws like the Official Secret's Act 1923,the Criminal Procedure Code, TADA , POTA and also some Irrigation Acts has been the reason for suppressing the protest movements.

III. Protest Movements and The State's Response

Having seen in some detail the reaction of the affected people to some developmental projects, a look at the manner and method adopted by the state in dealing with these reactions would be in order. It is said that law has both liberation and repression potential. An attempt is made to see which laws are used and how they are used in dealing with people's movements. Broadly speaking, the laws used are the Official Secrets Act 1923, The Code of Criminal Procedure 1973,and State Irrigation Acts.

A. Official Secrets Act, 1923:

It is a vestige of the Colonial Government. It is a draconian law that has drawn harsh criticism. Under this Act, information from any Government is considered official information, and hence it can be used to override freedom of information requests. The colonial administration remained deliberately alienated from the people at large, with provisions such as the Official Secrets Act shielding it from any public scrutiny. This all-powerful state apparatus bore down heavily on the impoverished peasantry, with the once well-organised village-level systems of management and self-governance largely destroyed.[32] Independent democratic India has not been able to shake off this colonial legacy and the usage of the Official Secrets Act is viewed skeptically, particularly with reference to developmental projects as shown by these lines, "In cases of inter-state or international disputes, river flows are classified as secret, making constructive work on conflict-resolution very difficult. When certain projects face opposition and controversy on environmental or human (displacement) grounds, the Act is sometimes invoked to deny information (or even physical access to place) to the people. This is a widely recognised evil."[33] The Government is authorised under this Act to declare certain places as prohibited. These places are to be such that information about, destruction of or interference with these places would benefit an enemy. One wonders how the Act can be put to use against peaceful protest movements against dams. A protest may give rise to a suspicion that sabotage may occur at a protest site, but imposition of the Act contravenes Article 19(2) of notification to bring a police station, a bus station, a hospital, a school, and markets under Official Secrets Act reasonable? … What is so strategic about the bus stand in Kevadia colony that entering it and raising slogans in it are offences punishable with three years imprisonment or are considered acts of spying, punishable with imprisonment of 14 years?"[34]

B. The Code of Criminal Procedure [Section 144]:

Section 144 is used where speedy or immediate remedy is needed, if a duly authorised District Magistrate opines so. The magistrate may direct a person to abstain from doing certain acts or with regard to any property under the person's possession or management, if the magistrate opines that his direction will prevent obstruction, annoyance or injury to lawfully employed persons, or prevents danger to human life or safety or prevents disturbance to public tranquility, riot or affray. Where it is not possible to serve notice, ex-parte order can be passed and the order under the section can be against an individual or persons of a particular area or general public visiting a particular area .The order under this section shall be in force for two months extendable by a period of 6 months by the State Government. Order issued under this section may be rescinded by the magistrate or State Government either on own motion or application. This Section is used to prevent assembly of activists at project sites. The objective of the section is to prevent obstruction, annoyance or injury to any person who is lawfully employed and the prevention of danger to human life, health or safety, as well as to prevent disturbance of public tranquility or a riot. Though the Section speaks of Public Peace, the moot question is whether the activities of those opposing the state's lopsided policies can be prevented under this guise. This section continues to be used against those who take up the cause of the Project displaced. "In a democracy like India, almost the entire Delhi is under section 144. How can the aam admi (common man) seek redress?" [35]

The other Acts used against movements were The Terrorist and Disruptive Activities Act (TADA) and Prevention of Terrorist Activities Act (POTA), both of which stand repealed as on date. These Acts principally aimed at preventing terrorist activities by agents of foreign powers like ISI and their cells etc. in India as well as acts of terrorism perpetrated by Indians. It is ridiculous to use these Acts against tribals who oppose big dams, which threaten the tribals' livelihood. The

31. Rajani Iyer, "Water Privatization and people's Organizations"- in the book titled "Globalisation and Social Movements - Struggle for Humane Society" Ed. P.G.Jogdand and S.Michael, p 239,at pp.246-247.
32. Madhav Gadgil and Ramachandra Guha, "The Use and Abuse of Nature", 2004 p.12.
33. Ramaswamy R. Iyer, "Water- Perspective, Issues, Concerns", 2003, p.149.
34. See generally Furquan Ahmed"Popular Movement In Water Resources Management and the Role of Law"-in the book titled "Water Laws in India Ed.Chhatrapathi Singh,"*I1992 p.243 at* ,p.250.
35. "Medha Patkar, Others Detained", The Hindu, 20-6-2006, Vskp. Ed. p.12.

TADA has been used in Bhoopalpatnam and Inchampalli Projects. The Gujarat government, in connection with the Narmada Project, has also used it .It is lamentable that statutes enacted for prevention of terrorists and unlawful activities are invoked against protesters whose very livelihood is affected by the large projects. Though both these Acts have been abolished, The Unlawful Activities (Prevention) Amendment Act,is still in force. Section 15[36] of the said Act can be invoked to prevent and repress any dissatisfaction expressed through agitation in connection with construction of large dams. The section is very wide in its scope and there is every likelihood of it being invoked in connection with protests regarding construction of dams and the resultant agitations, if any that may arise. The section is very widely worded thus making it easy to be misutilised.

C. Irrigation Acts:

Various States have different irrigation Acts under which, wide powers are bestowed on the land officers. Most of the provisions are penal in nature and go against people's initiative to tackle the water problem faced by them. The powers range from withholding information about projects to seeking police help under the pretext that the protesters are interfering with irrigation.

The harassment faced by the Tarun Bharat Sangh (TBS) in Alwar district in Rajasthan best shows this aspect. TBS was a voluntary organistion, which had enlisted local co-operation and brought water to the dry and arid regions of Rajasthan. The work was funded and carried on by the communities themselves. Though permission was obtained beforehand from Block Development Officer and the District Magistrate, the State Machinery did a U turn and contemplated action against the communities including demolition of the tanks put up by them, as they were, in the Government's eyes, not properly constructed and thus could endanger the people living close by. But much to the chagrin of the Government, some of the legally sanctioned and technically sound tanks constructed by the Government were washed away, those constructed by TBS, continue to function.[37]

Another cause taken up by TBS was against mining. All the rainwater disappeared into these mines. The mines also deprived cattle of grazing land and posed danger to human and animal life. TBS approached Supreme Court and was given a favorable verdict, in the form of an order by the Supreme Court that no mining could be carried on in the protected area.[38] The State Government, inspite of this, wanted to continue mining activities and false affidavits were filed, protesting TBS activists were attacked and even attempts were made on Rajender Singh's life. In fact the mine owners attacked Rajender Singh's car, which was duly noted by Justice M.C. Jain who was on a fact finding mission. The Supreme Court ordered that one of the mine owners, who carried on the assault be imprisoned for one week for contempt of court.[39] The Supreme Court made the Centre declare the Aravali a fragile Eco-system and banned mining. This notification was got watered down by the mine owners. In response to these, the TBS organized a 3-month Satyagraha in 1993. After some years, the State Government started responding positively and acknowledged that the work done by TBS had regenerated forests. The State Irrigation department, which declared dams built by TBS illegal and threatened demolition, started co-operation.[40]

It can be observed that large scale displacement has been and continues to take place affecting millions of people adversely, particularly the poor, the downtrodden and the tribals. The government's and the bureaucrat's attitude towards this continues to be callous.There have been protest movements against this, but with the exception of very few they cannot be termed successful. The State's use of draconian laws like the Official Secret's Act 1923,the Criminal Procedure Code, TADA , POTA and also some Irrigation Acts has been the reason for suppressing the protest movements.

Lastly one would like to conclude that economic progress of the country is very important ,but it cannot and should not be at the cost of the people.

36. Section 15 is very broadly worded and can take in any agitation it says "…or detains any person and threatens to kill injure such person in order to compel the Government in India or the Government of a foreign country or any other person to do or abstain from doing any act,commits a terrorists act".
37. *Supra note*34, p.253.
38. *Tarun Bharat Sangh,Alwar Vs Union of India* AIR 1992 SC514 atp518.
39. *Tarun Bhatat Sangh ,Alwar Vs Union of India* AIR 1993 SC 293 at p 295.
40. See generally "Kiss of Life for Mother Earth", from the book titled "Prophets of New India", 2004, p. 203 at pp. 210- 213.

International Journal of Modern Engineering Research (IJMER)
www.ijmer.com Vol. 3, Issue. 3, May.-June. 2013 pp-1561-1565 ISSN: 2249-6645

Role of Job Satisfaction on Job Performance of Teachers from Government and Private Polytechnics

Datta B. Pawase
M. S, M. B. A, [PhD] Research Scholar, JJT University, Jhunjhunu, Rajasthan

Abstract: *An individual's general attitude towards his or her job is called as job satisfaction. It is the difference between the amount of rewards one receives and the amount he or she believes should receive. Job satisfaction has the direct relation with the job performance of an employee. Lower job satisfaction tends to lead to both turnover and absenteeism, whereas high job satisfaction results in increased job performance. Public sector and private sector differ in nature of work, rewards and pay*

Key Words*: Job Satisfaction, Job Performance, Job Involvement, Public Sector, Private Sector*

I. Introduction

Executives tend to prefer mentally challenging jobs i.e. which give opportunity to use their skills and abilities, and offer a variety of tasks, Public Sector and Private Sector differ in the nature of work, working conditions, job environment, job challenges, authorities and responsibilities, rewards and pay structures, promotion policies, and growth opportunities. All these factors tend to the job satisfaction of the employees.[3] Globalization has given wide spread effect on the stated factors both in public sector and private sector. Hon. Minister Shri. Yashavantrao Chavan made a decision to allow private organizations to open and run *structures etc., which tend to job satisfaction of the employees. The paper highlights the role of job satisfaction on job performance of teachers from government and private polytechnic colleges. The factors of the job satisfaction have a different nature in government and private polytechnics. The author has done statistical analysis of the factors to achieve the results of the job satisfaction over job performance of teachers from government and private polytechnics.* freedom and feedback on how well they are doing. Under conditions of moderate challenges, they experience pleasure and satisfaction. High level of complexities and challenges in job brings frustration while, low level or repetitive jobs bring boredom to the executives.[1]technical, medical and other institutionsoffering professional education on unaided basis. Now after more than 25 years to this decision, we find these institutions achieving markable growth and development. These unaided institutions are contributing at high level in meeting the demand of professionals in the country. On the other hand the Government aided institutions are also changing their strategies and policies to cope with and tosupport the changes in corporate sector. Job security and pension schemes are no more Developments in Information Technology have created challenging and interesting environment in performing the jobs. One who is accepting these challenges and keeping himself or herself in pace is getting more and more opportunities with higher and higher returns.[2] Hence, it has become significant to study the level of the job satisfaction of the teachers in government aided institutions and unaided private colleges, and study the role of job satisfaction on their job performance. In this paper we have made a study of job satisfaction of teachers from government and private polytechnics, and the role of job satisfaction on their job performance.

II. Objectives

1. To study the role of total job satisfaction of the teachers from government and private polytechnics.
2. To study the role of payments on job satisfaction of the teachers from government and private polytechnics.
3. To find out the role of promotion on job satisfaction of the teachers from government and private polytechnics.
4. To determine the role of supervision on job satisfaction of the teachers from government and private polytechnics.
5. To study the role of fringe benefits on job satisfaction of the teachers from government and private polytechnics. effective to stop the turnover of the teachers in both the sectors
6. To determine the role of contingent rewards on job satisfaction of the teachers from government and private polytechnics.
7. To study the role of operating conditions on job satisfaction of the teachers from government and private polytechnics.
8. To determine the role of coworkers on job satisfaction of the teachers from government and private polytechnics.
9. To determine the role of nature of work on job satisfaction of the teachers from government and private polytechnics.
10. To study the role of communication on job satisfaction of the teachers from government and private polytechnics.
11. To study the role of job satisfaction on job performance of the teachers from government and private polytechnics.
12. To study the role of job satisfaction on turnover of the teachers from government and private polytechnics.

III. Hypothesis

1. Job satisfaction plays an important role on the performance of the teachers from government and private polytechnics.
2. Job performance is associated with job satisfaction of the teachers from government and private polytechnics.
3. There is no difference between the teachers from government and private polytechnics.
4. There is no difference between the teachers from government and private polytechnics.

IV. Review of Literature

Kaplan R A, Bosh off A B, Keller man A M.(2000) studied the job involvement and job satisfaction of south Africa nurses and expressed fear that wide spread dissatisfaction may lead to fewer people entering the profession.[4] Singh Mira(1990) studied job satisfaction and performance of bank officers and bank clerical staff.[7] Robbins(1993) studied employee attitudes toward involvement in and satisfaction with the job and commitment to the employing organization have become of compelling interest to industrial psychologists because of their impact on behavior at work. Thomas K. Bauer (2004) made survey on working conditions over workers job satisfaction. David Zatz (1996) analyzed that job involvement and inter role conflict do not seem to be directly related.[8] Susan J. Linz, Anastasia Semykina (2005) found that individuals who exhibit internal locus of control perform better, but this result is not always statistically significant.[9]

V. Methodology

The samples were selected from teachers from government and private polytechnics of Dhule city. The researcher collected data of 15 teachers from government polytechnics and15 teachers from private polytechnics. Job Satisfaction Scale by Paul E. Spector (1994), and Job Performance Scale by A.P.Singh and D.N.Pestonjee,1981 were used to collect the data. Mean, S.D. *t* technique is used for study the mean difference of both the groups.

VI. Results

Table I: shows the mean difference for job performance and job satisfaction among the teachers of government aided polytechnic and private unaided polytechnic.

Table 1. Mean difference for job performance and job satisfaction

Sr. No.	Factor	Govt. Polytechnic (N=15)		Private Polytechnic (N=15)		*t*
		Mean ($\bar{X}$)	S.D. ($\bar{\sigma}$)	Mean ($\bar{X}$)	S. D. ($\bar{\sigma}$)	
1	Job Performance	46.667	4.44	46.6	3.05	0.048
2	Total Job Satisfaction	140.067	16.23	135.933	21.59	0.5944
3	Pay Factor	14.33	4.011	14.13	3.879	0.1388
4	Promotion Factor	12.066	4.959	15.8	2.879	2.521
5	Supervision Factor	16.6	2.471	15.4	3.895	1.007
6	Fringe benefits	13.4	4.127	13.8	3.798	0.276
7	Contingent Rewards	14.66	3.238	14.53	2.499	0.1262
8	Operating Conditions	11.6	2.602	11.8	2.712	0.206
9	Co-workers	19.8	2.481	16.266	3.623	3.11
10	Nature of work	18.33	3.091	18.86	3.30	0.456
11	Communication on	19.266	4.218	15.33	4.205	2.557

VII. Analysis

1. Job Performance: The mean for job performance of government polytechnic teachers is 46.667 and S.D. is 4.44; the mean for private polytechnic teachers is 46.6 and
S.D. is 3.05. The obtained 't' is 0.048.hence the hypothesis is accepted and there is no difference between teachers of government and private polytechnic for their job performance. Though the overall impressions of all the 14 factors regarding the job performance among both the groups are interrelated with each other, there is no difference between both the groups. Through the statistical analysis, the quality of work performance, efforts expended on the job, ability to work without supervision and dependability is at higher level among the government polytechnic teachers. The initiative on the job is showing higher level in private polytechnic teachers. This analysis represents that the job performance depends upon the different aspects of the job.

2. Job Satisfaction: The mean for total job satisfaction of government polytechnic teachers is 140.067 and S.D. is 16.23; the mean for private sector employees is 135.933 and S.D. is 21.49. The obtained 't' is 0.5944 which is accepted at 0.05 level. Hence the hypothesis is accepted and there is no significant difference between government and private polytechnic teachers for their total job satisfaction. Through the overall impression, the government polytechnic teachers' mean is higher than the mean of teachers from private polytechnic. There are various factors which are responsible for the job satisfaction of government polytechnic teachers. The mean difference between both the groups is 4.133, which is representing that there is mean difference for job satisfaction, though the obtained 't' is less than the tabulated value. Hence the hypothesis is accepted. Both the groups are showing the level of job satisfaction which is illustrated in factor wise analysis.

3. Pay Factor: The mean for the pay factor of job satisfaction of government polytechnic teachers is 14.33 and S.D. is 4.011; the mean for private polytechnic teachers is 14.13 and S.D. is 3.879. The obtained 't' is 0.1388, which is accepted at 0.05 level. Hence the hypothesis is accepted and there is no significant difference between government and private polytechnic teachers for the pay factor of job satisfaction. Through the overall impression of the government polytechnic teachers, the satisfaction about the stability and chances of salary increment are more in comparison with the private polytechnic teachers. While there is no difference regarding the fair payment and appreciation between the teachers from government and private polytechnics. The obtained 't' is less than the tabulated value, hence the hypothesis is accepted.

4. Promotion: The mean for the promotion factor of job satisfaction of government polytechnic teachers is 12.066 and S.D. is 4.959; the mean for private polytechnic teachers is 15.8 and S.D. is 2.879. The obtained 't' is 2.521, which is not significant at 0.05 level. Hence the hypothesis is rejected and there is significant difference between both the groups on the promotion factor. The teachers from the government polytechnic are not satisfied for this factor, because they are always in the conflict of promotion because of various social, political and government policies regarding caste, religion wise priority than the seniority and knowledge. Therefore they are not having satisfaction because of the promotion opportunity. While in private polytechnics, there is opportunity to the person with quality. The promotion with the quality is main criteria in private sector and efficient persons always prove their quality. Hence they are having large job satisfaction regarding promotion.

5. Supervision: The mean for the supervision factor of job satisfaction of government polytechnic teachers is 16.6 and S.D. is 2.471; the mean for private polytechnic teachers is
15.4 and S.D. is 3.895 The obtained 't' is 1.007, which is accepted at 0.05 level. Hence the hypothesis is accepted and there is no significant difference between government polytechnic and private polytechnic teachers for the supervision factor of job satisfaction. Through the overall impression of all the four sub-factors of supervision regarding the job satisfaction among both the groups, they are interrelated with each other and there is no difference between both the groups. Through the statistical analysis, competency level of supervision and interest in feeling of the teachers is at higher level among the government polytechnic teachers, while there is more fairness for supervision among private polytechnic teachers. However, both the groups like their supervisor and are satisfied for the factor of supervision. The obtained't' is less than the tabulated value, hence the hypothesis is accepted.

6. Fringe Benefits: The mean for the fringe benefits factor of job satisfaction of government polytechnic teachers is 13.4 and S.D. is 4.127; the mean of private polytechnic teachers is 13.8 and S.D. is 3.798 The obtained 't' is 0.276, which is accepted at 0.05 level. Hence the hypothesis is accepted and there is no significant difference between government and private polytechnic teachers for the fringe benefit factor of job satisfaction. Through the overall impression of all the four sub-factors of fringe benefits regarding the job satisfaction among both the groups, they are interrelated with each other and there is no difference between both the groups. Through the statistical analysis, both the groups are satisfied with the benefits they receive and feel as compatible with the other organization. The level of satisfaction for the benefits received is at higher level among the government polytechnic teachers. While the private polytechnic teachers feel the benefit package more equitable than the government polytechnic teachers. The obtained 't' is less than tabulated value, hence the hypothesis is accepted.

7. Contingent Rewards: The mean for the contingent rewards factor of job satisfaction of government polytechnic teachers is 14.66 and
S.D. is 3.238; the mean of private polytechnic teachers is 14.53 and S.D. is 2.499 The obtained 't' is 0.1262, which is accepted at0.05 level. Hence the hypothesis is acceptedand there is no significant difference between government and private polytechnic teachers for the contingent rewards factor of job satisfaction. Through the overall impression of all the four sub-factors of contingent rewards regarding the job satisfaction among both the groups, they are interrelated with each other and there is no difference between both the groups. Through the statistical analysis, the level of recognition, appreciation and rewards is higher among government polytechnic teachers, while the private polytechnic teachers are more satisfied with the way they are rewarded. The obtained 't' is less than tabulated value, hence the hypothesis is accepted.

8. Operating Conditions: The mean for the operating conditions factor of job satisfaction of government polytechnic teachers is 11.6 and S.D. is 2.602; the mean of private polytechnic teachers is 11.8 and S.D. is 2.712 The obtained 't' is 0.206, which is accepted at 0.05 level. Hence the hypothesis is accepted and there is no significant difference between government and private polytechnic teachers for the operating conditions factor of job satisfaction. Through the overall impression of all the four sub-factors of operating conditions regarding the job satisfaction among both the groups, they are interrelated with each other and there is no difference between both the groups. Through the statistical analysis, both the groups are satisfied about the operating conditions. The level of satisfaction is higher among the government polytechnic teachers for the rules and procedures, while the private polytechnic teachers are more satisfiedregarding paper work required because there is excessive paper work in the public sector organization. The obtained 't' is less than tabulated value, hence the hypothesis is accepted.

9. O-workers: The mean for the co-workers factor of job satisfaction of government polytechnic teachers is 19.8 and S.D. is 2.481. The mean of private polytechnic teachers is 16.266 and S.D. is 3.623. The obtained 't' is 3.11, which is not significant at 0.05 level. Hence the hypothesis is rejected and there is significant difference between government and private polytechnic teachers for the coworker factor of job satisfaction. Through the statistical analysis, the teachers from private polytechnics are not satisfied for this factor because of the competition involved at work. The more efficient teachers get more opportunities, hence the relationships among the teachers are found tense. The government polytechnic teachers are more satisfied as no such competition upon quality is involved. The public sector employees have their unions, hence the relationships among employees are found more satisfactory. While in most of the private sector organizations, either unions are not formed or they are not strong. Hence the government polytechnic teachers have large job satisfaction regarding co-workers.

10. Nature of Work: The mean for the nature of work factor of job satisfaction of government polytechnic teachers is 18.33 and S.D. is 3.091; the mean for private polytechnic teachers is 18.86 and S.D. is 3.30. The obtained 't' is 0.456, which is accepted at 0.05level. Hence the hypothesis is accepted and there is no significant difference between government and private polytechnic teachers for the nature of work factor of job satisfaction. Through the overall impression of all the four sub-factors of nature of work regarding the job satisfaction among both the groups, they are interrelated with each other and there is no difference between both the groups. Through the statistical analysis, both the groups are satisfied about the nature of work. The level of satisfaction is higher among the government polytechnic teachers as they like the work, feel a sense of pride and enjoy the job, while the level of satisfaction about the challenges in job is higher among the private polytechnic teachers. The nature of job in public sector organization is a routine one and bound to the rules, regulations and procedures. Hence the employees in public sector feel their job as meaningless. There are everyday new challenges in the private sector job, hence the employee in private sector are found more satisfied for the nature of the work. The obtained 't' is less than the tabulated value, hence the hypothesis is accepted.

Communication Factor: The mean for the communication factor of job satisfaction of government polytechnic teachers is 19.266 and S.D. is 4.218; the mean for private polytechnic teachers is 15.33 and S.D. is The obtained 't' is 2.557, which is not significant at 0.05 level. Hence the hypothesis is rejected and there is significant difference between government and private polytechnic teachers for the communication factor of job satisfaction. Through the statistical analysis, the teachers from private polytechnic are not satisfied because of the hierarchy levels at the work place, and because of competitions the goal are not clearly explained. They do not know the complete nature of the job and it is not clear to them what is going on in the organization. Hence the communication is poor in private polytechnics. While in government polytechnic, no such competition is involved, the paper work is strong and information is available in the form of circulars to each and every employee. Hence government polytechnic teachers are more satisfied for communication factor of job satisfaction.

With respect to the interpretation and statistical analysis, the job performance is associated with the job satisfaction because in three factors i.e. promotion, coworkers, and communication, hypothesis is rejected. It indicates that these three factors are negatively representing the job performance according to the job satisfaction. Therefore the role of job satisfaction is very dominant for the job performance according to the environmental situation in public and private sector.

VIII. Conclusion

1. There is no difference for job performance among teachers from government and private polytechnics.
2. There is no difference for job satisfaction among teachers from government and private polytechnics.
3. There is no difference between teachers from government and private polytechnics for their jobsatisfaction with respect to pay factor.
4. There is significant difference between teachers from government and private polytechnics for their job satisfaction with respect to promotion factor.
5. There is no difference between teachers from government and private polytechnics for their job satisfaction with respect to supervision factor.
6. There is no difference between teachers from government and private polytechnics for their job satisfaction with respect to fringe benefits factor.
7. There is no difference between teachers from government and private polytechnics for their job satisfaction with respect to contingent rewards factor.
8. There is no difference between teachers from government and private polytechnics for their job satisfaction with respect to operating conditions factor.
9. There is significant difference between teachers from government and private polytechnics for their job satisfaction with respect to coworker's factor.
10. There is no difference between teachers from government and private polytechnics for their job satisfaction with respect to nature of work factor.
11. There is significant difference between teachers from government and private polytechnics for their job satisfaction with respect to communication factor.

Limitations

1. The sample size is very small.
2. No other variables are included in the study for analysis e.g. age, sex, education, experience etc.

Recommendations

1. This study is useful for the differentiation of the government and private colleges and education field.
2. This study is representative of pilot study and useful to the policy makers, students and parents to understand the merits and demerits in the education field.

References

[1]. Fred Luthans (2008), *Organizational Behavior*, McGraw Hill Ltd.
[2]. Gary Dessler (2007), *Human Resource Management*, Pearson Education Incorporation.
[3]. John W. Newstrom (2007), *Organizational Behavior – Human Behavior at Work*, Tata McGraw Hill Publishing Co. Ltd.
[4]. Kalpan R A, Boshoff A B, Kellerman A M (2005), *Job involvement and job satisfaction of South African Nurses*, MEDLINE, PMID: 1845612
[5]. Paul Hersey, Kenneth H. Blanchard, Dewey E. Johnson (2005), *Management of Organisational Behavior – Leading Human Resources*, Pearson Education
[6]. Robert Knoop (1995) *Relationships among the job involvement, job satisfaction, and Organizational commitment of thenurses*, The Journal of Psychology, Vol. 129, Issue: 6, page 643.
[7]. Singh Mira (1990), *Job Satisfaction, Job Involvement and Participation Amongst Different Categories of Bank Employees*, Indian Institute of Management, Ahmedabad working Papers, 891.
[8]. Susan J. Linz, Anastasia Semykina (2005), *Attitudes and Performance: An analysis of Russian Workers*, William Davidson Institute Working Paper No. 758.

International Journal of Modern Engineering Research (IJMER)
www.ijmer.com Vol. 3, Issue. 3, May.-June. 2013 pp-1566-1570 ISSN: 2249-6645

A New Proposed Software Engineering Methodologyfor Healthcare Applications Development

Abdullah Al-Dahmash, Samir El-Masri
Department of Information Systems, College of Computers and Information Sciences
King Saud University, Riyadh, KSA

Abstract: *The health Information system is widely expected to increase patient safety and reduce medical errors. Design and implementation of a healthcare system need to consider the software engineering principles and methodologies. In this paper, a literature review has been carried out for healthcare systems implementation. The paper also discusses three common software methodologies and their uses in the healthcare domain. A Software Engineering Methodology for Healthcare Applications development (SEMHTA) will be proposed. SEMHTA has been introduced in this paper to solve the healthcare software development challenges. This paper also provides a comparison between the most common software engineering methodologies and the new proposed one.*

Keywords:*Healthcare system, Software Engineering Methodology, Healthcare software implementation.*

I. Introduction

The aim of the healthcare systems is to achieve the best possible support for patient care and to provide the optimal medical care. The healthcare systems should support good health, fair financial contribution, and excellent services. Healthcare industry has rapidly grown in the last decade, especially in developing countries. Medical software implementation represents one of the major future challenges in healthcare industry. Using healthcare information systems will increase the number of health services, improve the quality of care and reduce the medical errors. The use of information systems in the healthcare industry is dramatically increasing. A successfully implementation of healthcare software in healthcare organization appears to be a difficult task. Software engineering for healthcare systems is an emerging field for software developers and IT specialists. Software engineering methodologies are being used in healthcare the same way used in other industries. The nature of systems and industry such as healthcare systems should be considered in the software-development methodology. A healthcare system has properties and features that need to be addressed, as they are different from other systems. For these reasons, we are proposing a new software engineering methodology for healthcare applications SEMHTA. This methodology is supposed to solve the software-development issues and challenges in the healthcare domain. The main reason for developing a new software engineering methodology for healthcare such as SEMHTA is the need for building a reliable and secure healthcare system with a high performance.

II. Literature Review

In general, software engineering involves the analysis, design, implementation, testing, maintenance and documentation of software systems. Since the concept of software engineering as a discipline was known more than three decades ago, there have been different definitions of software engineering. The Software Engineering Institute at Carnegie Mellon University gives the following definition: software engineering is that form of engineering that applies the principles of computer science to achieving cost-effective solutions to software problems [1]. The IEEE Computer Society in a joint effort with the ACM agreed on the following definition: The application of a systematic, disciplined, quantifiable approach to the development, operation, and maintenance of software [2]. Software engineering methodology can be defined as a group of techniques and tools used in the development of software. Methodology should describe each phase of the software-development life cycle. Software methodology normally does not specify the details. These details usually left to the organization's needs and requirements. The major difference between a methodology and a framework is that a framework should be used at a more abstract level [3]. In the last two decades healthcare applications and the use of information systems in health industry have grown rapidly. The idea of healthcare today is much different from what it was 10 years ago. Healthcare is now more than simply medical care and treatment. The goal of healthcare is to provide more efficient services to enjoy a healthy society. Therefore, healthcare information system is a comprehensive, integrated and designed to manage the medical and administrative aspects of a medical organization [4]. The principal goal of IT application in healthcare is the quality improvement of medical care. Therefore, the healthcare system has to be characterized by a high reliable system [5]. Electronic medical information systems have been identified as an enable to keep healthcare systems sustainable, reliable and safety. A 2005 RAND study estimates that the U.S.A. could save $81 billion annually and help to improve the healthcare industry through the adoption of high quality electronic medical information systems [6]. The definition of "medical software" must consider the new aspects of management and maintenance of the software engineering. Moreover, the technological development in the healthcare field has made medical software more invasive and more maintainable [7]. Healthcare software systems should be designed under several aspects that may not be realized by the software engineers. Successful implementation requires a partnership between healthcare professionals and software engineers. Healthcare professionals and software engineers can have different expectations and understanding of the system. Healthcare professionals have a little understanding of software and may not be motivated to use it. Software engineers need to be aware of the nature and requirements of the medical software [8].

III. RESEARCH QUESTION

In order to develop a new healthcare application, there should be a software engineering methodology followed to produce the system. There are a lot of software engineering methodologies available. What are the advantages and disadvantages of each methodology? Do those methodologies support non-functional requirements for healthcare projects such as reliability, performance, security and availability? What is the new proposed methodology? These are the questions that will be discussed in this paper.

IV. Most Common Software Engineering Methodologies

In this section, the most common software engineering methodologies and their use in healthcare projects will be discussed:

Waterfall Model: The waterfall model is a sequential design in which deployment seen as a waterfall through the stages of planning, analysis, design, implementation and testing. Issues such as time-consuming and unclear requirements at the early stages are seen as obstacles for the waterfall model. In response to these issues and other's issues of the waterfall model many modified waterfall models have been introduced [9].

Iterative Model: In this model, the overall life cycle is composed from several iterations. The iteration is consisted from a couple of activities: planning, analysis, design, implementation and testing. At the end of the iteration there should be an iteration delivery which is in most cases the iteration release. Most iteration releases are internal. The final iteration is the completed product [10]. Figure [1] describes the iterative model.

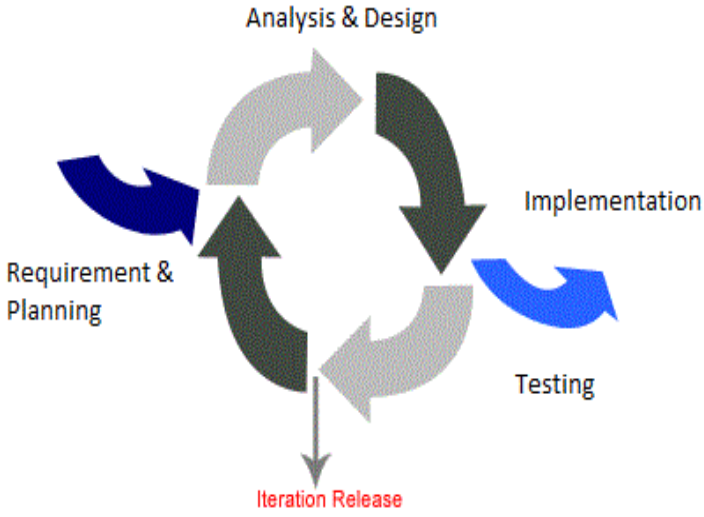

Figure1: The Iterative Model

Agile Model: The agile model defines a set of principles and practices, which aims to minimize the documentation activities. The main goal of an agile model is to do the development activities with high professionalism and less efforts and documents. The major advantage of using an agile model is the development time factor. The disadvantage of this approach is its needs of high knowledge and experienced team [11].

V. Healthcare Software Issues

Health care is a complex socio-technical system. There is an opinion that information technology can induce errors, instead of correcting them [12]. There are several issues need to be considered in dealing with healthcare systems. Issues such as reliability, security and performance are the main issues in this field.

Performance: performance is a non-functional requirement which is a very important requirement for any software. From a healthcare software perspective, the performance issue can be seen in form of [13]:

Performance issue related to the data: there are two important issues with the data in health-care projects, which are data accuracy and data availability. Performance issue related to healthcare staff: performance issues from health-care staff's viewpoints: appropriateness of information, the communication via the healthcare system and integrity of the system.

Performance issue related to patients: at the end, there is a relationship between the healthcare system and the patients. The healthcare system provides services to the patient. Performance issues from patient's perspective: reduce the waiting time, privacy and increase of satisfaction.

Security: Security's requirements describe which security mechanisms to use. Security's requirements focus on what it should be achieved – not how [14]. Health care system is not like other IT systems, it deals with patient's data and other confident data. So security requirement is one of the most challenges that facing software engineers when they try to develop

a healthcare software. Security's requirement of healthcare software should be focused on areas such as patient's data and medical record data protection.

Reliability*:* reliability analysis of a healthcare system is similar with reliability engineering in other projects. There are a lot of methodologies to analyze the project reliability such as software reliability analysis, hardware reliability analysis and human reliability analysis (HRA). In [15] the healthcare system includes four components hardware, software, human factor and organization factor. To analyze the reliability of a healthcare system should throw a measure of performance of each one from these components.

Availability: the availability of a hardware/software is the percentage of time when the system is up and running [16]. In healthcare software, availability is a critical characteristic. In healthcare, all medical systems should be 24/7 for an emergency event and for a surgery. So the software methodology for a healthcare project needs to consider the availability of the system as a demand and as a challenge too.

VI. Software Engineering Methodology For Healthcare Applications (Semhta)

The new proposed methodology should solve issues faced by software engineers and healthcare specialists whendealing with developing a new system. SEMHTA will focus on the healthcare system properties and nature. The new methodology considers the healthcare background of the end user and the impact on the development activities. SEMHTA is built on four main phases: Planning and Analysis, Design and Build, Implementation, Validation and delivery. Each phase contains several activities, and each phase is interconnected with other phases. SEMHTA actually try to merge the software engineering life cycle with the project management activities. SEMHTA framework is described in figure [2].

Planning and Analysis Phase

The Planning Phase is often the most challenging phase to build healthcare applications. Planning phase involves the creationof a set of plans to help guide technical and healthcare teams through the execution of the system. The purpose of the Planning Phase is to plan all project processes and activities. In addition, to build channels between the healthcare specialists and the software-development team in order to improve the communication between them.

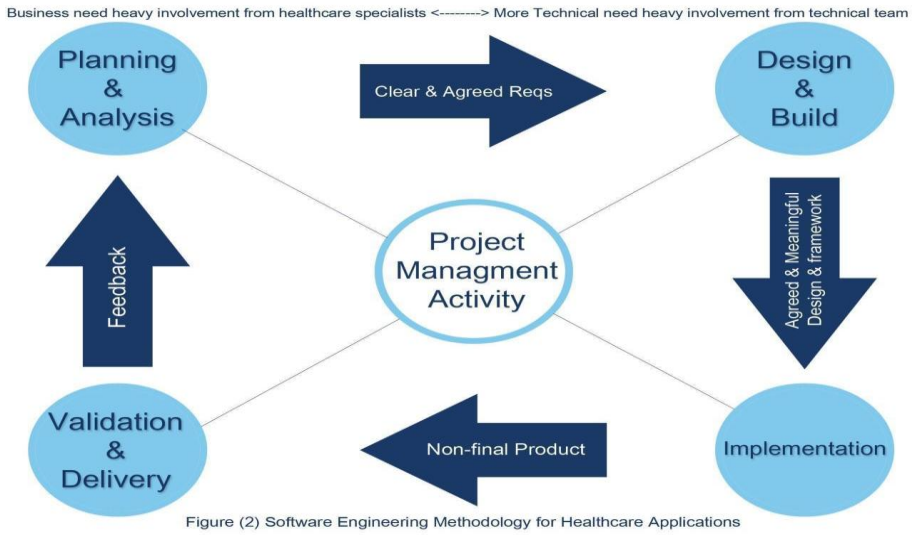

Figure (2) Software Engineering Methodology for Healthcare Applications

There must be a common understanding of the system among all healthcare staff and project development team. The deliverable result at the end of the planning phase is a complete project plan document. During the analysis phase, the main activity is to gather hospital's requirements and environmental considerations. The analysis phase defines the requirements of the system, independent of how these requirements will be implemented. Many techniques are used to gather and manage system requirements. In SEMHTA, the workshops' technique is the one used for manage the requirements. The requirements workshop involves the users from different background such as physicians, informaticists, top management and even some hospital's patients. The deliverable result at the end of this phase is a detailed and analysed requirements document. The requirement document does not specify the architectural or implementation details, but specifies information at the higher level of description. Requirements document should be written in simple words understandable by all healthcare and business users. Involvement of the healthcare specialist is a key factor to build a requirements document that reflects the essentially demand of the system. Involvement of the end user in all requirements identification activities will guarantee a high reliable system and perfect operational solution. Planning and analysis activities are described in figure [3].

Figure[3] Planning and Analysis phase in SEMHTA

Design and Build Phase

In the design phase, the architecture of the healthcare system is established. This phase starts with the requirements document delivered by the planning and analysis phase. The architecture defines components, interfaces and behaviors of the healthcare system. The deliverable result at the end of the design phase is the design document. The design document describes a technical plan to implement the requirements. Details on computer programming languages and environments, machines, packages, memory size, platform and many other technical details are established and agreed on at the end of the design phase in SEMHTA. The requirements document must guide all processes and activities in the design phase. SEMHTA suggests that there should be a significant participation from the healthcare specialists in defining the design document.

Implementation phase

In the implementation phase, the development team builds the components that identified in the design phase. In SEMHTA, with a given design document from the design and build phase and the requirements document from the planning and analysis phase, the development team should implement correctly what it has been requested. The implementation phase of SEMHTA deals with issues of quality, performance, libraries and debugging. The deliverable result at the end of the implementation phase is the product itself.

Validation and Delivery phase

In many software engineering methodologies, the validation phase is a separate phase which is performed by a different team after the completion of the implementation. Unfortunately delegating validation and testing to another team leads to many errors and mistakes undiscovered “No one knows the system more than the development team". SEMHTA suggests that the testing and validating activities should be performed by a joint team. The joint team members are development team, testers, healthcare specialists and end users. This will lead to a secure and available healthcare system. Again, SEMHTA suggests that all validation activities should be driven by the requirements document. In case of any problem in the product, more clarifications, and feedbacks should go back to the analysis phase.

SEMHTA and Project Management Activities

It is very clear that SEMHTA makes a bridge between software engineering and project management activities. In the planning and analysis phase, the concept of building the project plan is a good example of this relationship. In SEMHTA, in order to develop software, there should be a heavy involvement from healthcare specialists. Furthermore, an important factor that will lead this development to a success is to apply all project management concepts and practices into the software engineering methodology.

VII. Comparisons Of Software Engineering Methodologies

In table 1, there is a comparison between the software engineering methodologies that have been described early with our new proposed SEMHTA. The comparison is based on the healthcare system issues such as reliability, performance, security and availability. This comparison is only valid for healthcare applications.

Table 1. Comparisons of Software Engineering Methodologies

Methodology Issue	Waterfall	Incremental	Agile	SEMHTA
Reliability	Low	High	Low	High
Performance	Moderate	High	High	High
Security	High	Low	Low	High
Availability	Moderate	Moderate	Moderate	Moderate

VIII. Conclusion And Future Work

In this paper, a new software engineering methodology SEMHTA has been proposed. SEMHTA methodology is composed from four main phases; planning and analysis, design and build, implementation and validation and delivery. The new proposed methodology specially built for healthcare applications and systems. A brief review has been done on the common software engineering methodologies. The paper has discussed some software-development issues when dealing with healthcare industry. The paper provides a comparison across the common software methodologies with SEMHTA showing the strengths of the new proposed methodology over others. The comparison between the methodologies focuses on the healthcare's software-development issues. Future research activities may deal with areas to improve SEMHTA efficiency, build SEMHTA architecture model and study the impact of SEMHTA on a healthcare project. Future research in this area can be on fields such as study nature and characteristics of healthcare systems, the relationship between healthcare specialists and software engineers within a healthcare project life cycle and many other areas.

References

[1] Ford, G., 1990 SEI Report on Undergraduate Software Engineering Education, CMU Technical Report no. CMUlSEI-90-TR-003, 1990.
[2] IEEE. IEEE Standard Glossary of Software Engineering Terminology, IEEE Std 610.12, 1990.
[3] Mnkandla, E., About Software Engineering Frameworks and Methodologies, IEEE, 2009.
[4] Key, W. and Liu, Z., Software Engineering in Public Health: Opportunities and Challenges, International Conference on Computer Distributed Control and Intelligent Environmental Monitoring, 2010.
[5] Zaitseva, E. and Levashenko, V., Reliability Analysis of Healthcare System, the Federated Conference on Computer Science and Information Systems, 2011, pp. 169–175.
[6] Weber-Jahnke, J. and Price, M., Engineering Medical Information Systems: Architecture, Data and Usability & Security, 29th International Conference on Software Engineering, 2007.
[7] R. Miniati, F. Dori, E. Iadanza and M. F. Medici, Medical Software Management:A failure analysis approach for maintenance and safety plan, 32nd Annual International Conference of the IEEE EMBS Buenos Aires, Argentina, 2010.
[8] Ried, L. and et.all, Design and Implementation of a Hospital Quality Assurance Program (H-QAP), IEEE, 2011.
[9] Birrell, N., Ould, M., A Practical Handbook for Software Development, Cambridge University Press, USA, 2003, pp.16-21.
[10] Larman, C., Agile and Iterative Development: A Manger 'sGuide,Addison-Wesley, USA, 2004, pp. 9-12.
[11] Ambler, W., Agile Model Driven Development (AMDD), XOOTIC MAGAZINE, 2007.
[12] Aarts, J., Towards safe electronic health records: A socio-technical perspective and the need for incident reporting, Health PolicyandTechnology, 2010, pp.8-15.
[13] Ozdemir, D. and Gozlu, S., *Investigation of Performance Criteria for Health Information Systems*, *PICMET 2008 Proceedings*, 2008.
[14] *Jensen, J., Tondel, I. and Anderson, H., Reusable Security Requirements for Healthcare Applications*, *International Conference on Availability, Reliability and Security*, 2009.
[15] Zaitseva, E., Reliability Analysis Methods for Healthcare system, *3rd IntConf on Human System Interaction*, Poland, 2010, pp.211-216.
[16] Candea, G. and FOX, A., Designing for High Availability and Measurability, *1st Workshop on Evaluating and Architecting System Dependability (EASY)*, 2001.

International Journal of Modern Engineering Research (IJMER)
www.ijmer.com Vol. 3, Issue. 3, May.-June. 2013 pp-1571-1576 ISSN: 2249-6645

Performance Evaluation of Breera Using Net Logo Simulator

Prof. Dr. Saad Talib Hasson, Alyaa. Abdul-Moneim Al-Najar
College of Sciences, University of Babylon, IRAQ,

Abstract: Recently increased the attention of researchers wireless sensor Networks (WSNs) because of their active role in tracking and monitoring. In traditional WSNs the sensory information is collected and sent to the base station during specific periods of time, continuously and this method can be expensive because they reduce the life of the network because a lot of energy consumption and need high bandwidth. In this paper the sensory information will be collected and send to the base station only by the sensors which physical changes occur in their reigns. This paper shows the use of under development protocol named Base Energy-Efficient Routing Algorithm (BREERA), in the process of collecting sensory information and studies the most important factors that affect performance under terms (average PDF, average total energy, average throughput, average LBF and average dead nodes.

Keywords*: WSNs, LBF, throughput, BREERA, PDF.*

I. INTRODUCTION

Wireless Sensor Networks (WSNs) are a hundred or thousand sensors, distributed randomly or manually in specific area. There are many applications of WSNs such as environmental monitoring, facility monitoring, and target detection[1]. The simulation language used for the construction of the idea of protocol BREERA on WSN is the language NetLogo. NetLogo is a multi agent programming language distinguished by being easy language understanding and application, the possibility of speed control implementation, did not need high specification for computer which will be such as the simulation language NS2, supported many graphical interfaces and the programmer can design the graphical interface its won and support his application , free recourse and other feathers that can be recognized by the programmer through the use of them [2].

II. Sensor Node

Sensor node is a device that have ability to sensing physical changes within a specific environment and communicat it. The sensor node consists of five main components: controller, transceiver , external memory and power source and sensor

III. CLUSTERING

Clustering is an organizing process of unordered objects in groups called clusters. Each cluster consist of two components: the cluster-head and members. In some applications of heterogeneous networks clustering is working to compilation of the same nodes together [4]. The Load Balancing Factor (LBF**)** is measures how well balanced in the cluster head nodes of the network [5].

IV. Throughput

Throughput defined as the total number of massages which received by the destination per time unit delivered from one sensor node[6] .

V. RELATED WORKS

M.Chatterjee at 2001 designed clustering algorithm based on the weight of the node in the cluster formation. Node with the lowest weight became the head-cluster and its neighbouring nodes members. This algorithm called Weighted clustering Algorithm(WCA). Calculating the weight of the node depends on four factors: the difference degree, distance summation to all its neighbours, mobility and the accumulative time. The coefficient used in weights calculation are w1=0.7, w2= 0.2, w3= 0.05, w4 = 0.05 ,The sum of these co-efficient is equal 1 [7].

Sucec.J at 2002 designed clustering algorithm makes the node that has largest number of neighbouring nodes as a cluster-head. The number of degree of the node means the number of neighbouring nodes. This algorithm called Highest-degree Algorithm (HD) [8].

Toh.c.k at 2002 designed clustering algorithm make the node with lowest ID to become a cluster-head and neighbouring nodes become its members [9]. This algorithm called Lowest Identifier Algorithm (LID).

Tzung-Pei Hong at 2010 noted WSNs consume power more than MANETs, so he suggested to add fifth weight to the WCA to make it more suitable to implement with WSNs. This algorithm called Improved Weighted Clustering Algorithm (IWCA) [10].

Mohamed at 2011 designed clustering algorithm called based Random Energy-Efficient (BREERA). This algorithm makes the effective nodes become cluster-head and the other of its neighbouring nodes become members. Nodes that are close to the base station doesn't need to the clustering process but rather send its sensing information directly to the base station. Nodes away from the base station form clusters and send its sensing information with each other towards the base station. The cluster head node sends messages to the next cluster-head, which is farther member. The next cluster-head looking into its members if one of them is the target node , were not it send a messages to one of the cluster-heads of

neighbouring clusters with maximum energy and so on forward the target nod (the base station). Each node in the network just need to know who its cluster head without knowing any information about their neighbours nodes like the previous algorithms that mentioned above previously. Hops number means the Number of Cluster-heads between the sink and the node from where new message is generated. Each massage in this routing algorithm have upper limit number of hops called threshold, if any message have number of hops larger than threshold value is died[2].Algorithm (1) illustrates steps of BREERA clustering as below.

Algorithm (1) : Clustering Procedure:

Action1

Input: Nodes number, messages number, broadcast range.

Output: Forming clusters.

Process :

1. Start.
2. Ask nodes if node has messages and far from the sink and not member for any cluster then
3. Make it as a cluster-head.
4. If the neighbouring nodes are not connected to any cluster then
5. Make them as members.
6. Decrement the energy of each member node.
7. End if .
8. Decrement the energy of the cluster-head node.
14. End if.

Action 2

Process :

1. Ask nodes member of clusters to make the farthest one of them from its cluster-head to be the next cluster-head.
2. Ask nodes in its broadcast range if they not connected with any cluster then
3. Make them as members.
4. Decrement the energy of each member node.
5. End if .
6. Decrement the energy of the cluster-head node.
7. End if.
8. End.

VI. PROPOSED WORK

The major drawbacks of the protocol BREERA is losing the more effective nodes from the network rapidly. We suggest using a counter with cluster-heads to avoid focuses on some nodes to play the role cluster-head for a long time. Using counter with the cluster-heads saving the energy for more effective nodes, make them work along time as possible and then saving the energy for all the network

a. Network Size Simulations

The suggested environment was designed in different scenarios, each scenario contains 25 nodes and increased by 25 in each step up to 500 nodes. Each scenario was runes and simulated in an operation manner (30) times in order to get near real results from simulation programs. The resulted information was listed in NetLogo table form contains about 600 rows. The table (1) indicates the built environment to be simulated under varying different parameters.

Table (1): WSN environment

Parameter	Value
The simulator	NetLogo 4.3.1 version (2011)
Nodes type	Genoese
Nodes number	Changeable (25,50,75,100,.....500)
Routing algorithm	BREERA
Pause time type	Uniform , 1s
Speed type	Uniform , 5m/s

We suggest all parameters are fixed except nodes numbers are variable. The simulation program with each scenario of specific nodes number repeated 30 times, to become the total simulation results 600 organized in a large data table in 600 rows.

Table (2) is the first part of the final results from the large data table that contains 600 rows. Each row in the table (2) illustrates the average of each 30 rows of the data table with specific nodes number of the network as follows.

Table (2): First part simulation results

Nodes Number	Average LBF	Average PDF
25	3.63650637	0.835
50	0.95031624	0.792333333
75	0.42116597	0.788333333
100	0.2661274	0.816666667
125	0.16096985	0.798333333
150	0.0969477	0.830666667
175	0.06251914	0.707
200	0.0863828	0.807
225	0.03889089	0.848
250	0.04610051	0.813333333
275	0.02866468	0.801333333
300	0.03032888	0.808666667
325	0.0324322	0.776
350	0.03319148	0.743
375	0.02613955	0.789333333
400	0.0156899	0.774666667
425	0.01839744	0.824
450	0.02013971	0.813333333
475	0.01336914	0.821
500	0.01716935	0.762333333

Table (3) is the second part of the final results from the large data table that contains 600 rows. Each row in the table (3) illustrates the average of each 30 rows of the data table with specific nodes number of the network as below.

Table (3): Second part simulation results

Nodes Number	Average Throughput	Average Dead Nodes
25	3.20491255	1.266666667
50	4.306367515	1.033333333
75	4.196641102	0.933333333
100	9.689316468	0.966666667
125	2.727711056	1.4
150	6.435626892	1.1
175	10.83104068	1.233333333
200	10.43457186	1.233333333
225	11.14498324	1.1
250	2.806787514	1.233333333
275	9.163704467	1.366666667
300	2.919376564	1.366666667
325	9.408042136	0.866666667
350	5.861975855	1.666666667
375	9.026012648	1.166666667
400	7.331723401	1.2
425	9.977181198	1.366666667
450	2.639134462	1.133333333
475	6.617376538	1.033333333
500	6.466969617	1.566666667

The results in the table (2) and table (3) are graphed in figures follow to show the relationship between the network metrics and their effects it behavior. Fig. 1 shows the relationship between the average dead nodes and a different numbers of nodes.

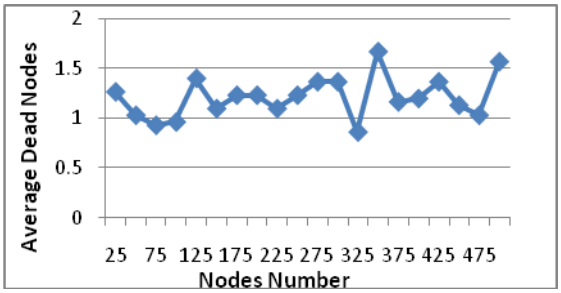

Fig. 1: Average dead nodes with a different numbers of nodes.

Fig. 2 shows the relationship between average throughput and a different numbers of nodes as follow.

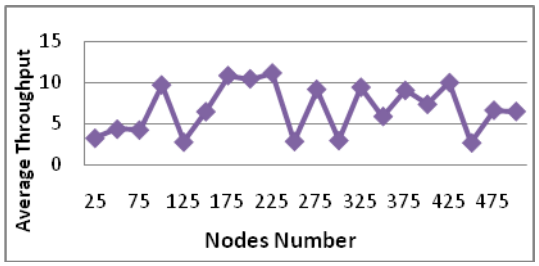

Fig. 2: Average throughput with a different numbers of nodes.

Fig. 3 shows the relationship between average LBF and a different numbers of nodes as below.

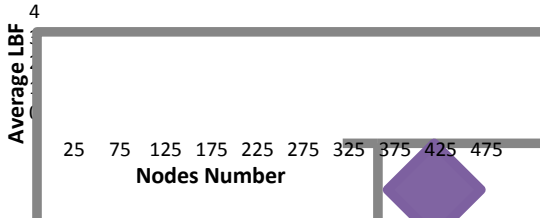

Fig. 3: Average LBF with a different numbers of nodes.

Fig. 4 shows the relationship between average PDF with a different numbers of nodes.

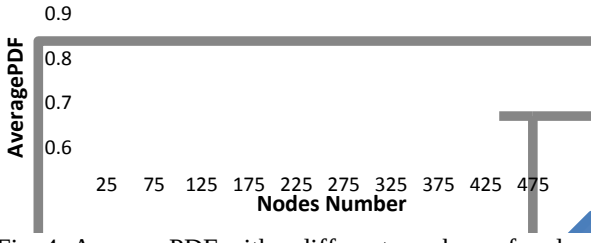

Fig. 4: Average PDF with a different numbers of nodes.

B Nodes speeds Simulations

The effectiveness of nodes speeds on the performance of BREERA was studied. We suggest apply the simulation program of WSN with three values of nodes speeds (5m/s ,10m/s and random speeds). Table (4) shows suggested WSNs environment as follow.

Table (4): WSN environment

Parameter	Value
The simulator	NetLogo 4.3.1 version (2011)
Nodes type	Genoese
Nodes number	500
Routing algorithm	BREERA
Pause time type	Uniform , 1 s
Nodes speeds type	Uniform 5m/s, 10 m/s and random speeds
Broadcast range	15 m
Hops' number	3

Parameters in the table (4) applied with the simulation program of BREERA 30 times with each nodes speed. Table (5) is the first part of the final results from the large data table that contains 90 rows. Each row in the table (2) illustrates the average of each 30 rows of the data table with specific nodes number of the network as below.

Table (5): First part simulation results

Nodes speeds	Average Dead nodes	Average Total Energy	Average PDF
5 m/s	1.0333333	48235.92667	0.5791
10 m/s	1.1	47706.38	0.906
random	0.9333333	48454.61667	0.907666667

Table (6) is the second part of the final results from the large data table that contains 90 rows. Each row in the table (6) illustrates the average of each 30 rows of the data table with specific nodes number of the network as below.

Table (6): Second part simulation results

Average LBF	Average Throughput
0.168457351	4.304558732
0.003327787	17.48638874
0.003039119	23.89773697

The results in the table (5) and in the table (6) are graphed in figures follow to show the relationship between the network metrics and their effects it behavior. Fig. 5 shows the relationship between the average dead nodes and nodes speeds .

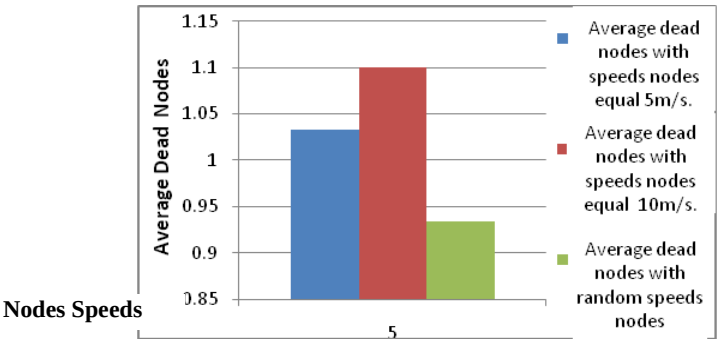

Fig. 5: Average dead nodes with a different value of nodes speeds.

Fig. 6 shows the relationship between average total energy of network and nodes speeds.

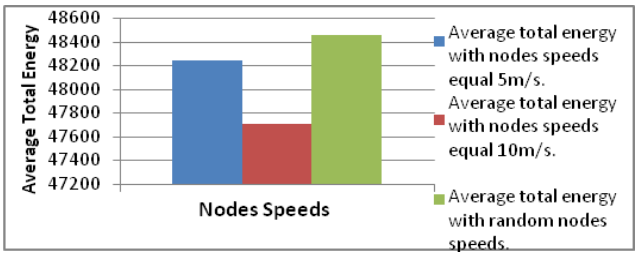

Fig. 6: Average total energy with a different value of nodes speeds.

Fig. 7 shows the relationship between average PDF and the nodes speeds.

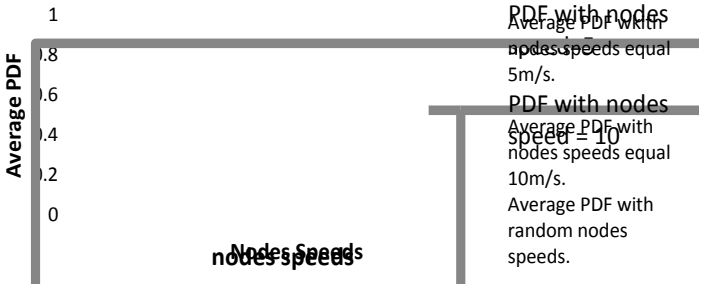

Fig. 7: Average PDF with a different value of nodes speeds.

Fig. 8 shows the relationship between average LBF and nodes speeds.

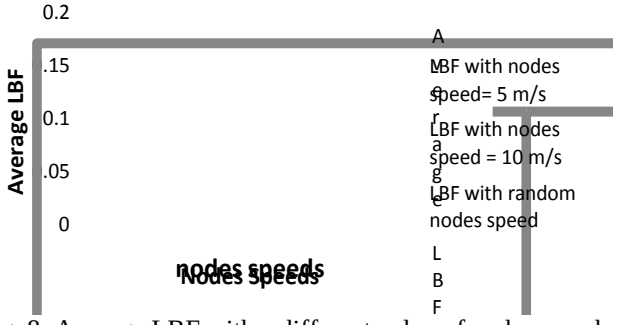

Fig. 8: Average LBF with a different value of nodes speeds.

Fig. 9 shows the relationship between average throughput nodes speeds.

Fig. 9: Average throughput with a different value of nodes speeds.

VII. Conclusion

Network size factor has an effect on the performance of the BREERA, when network size increased the performance of BREERA dropped under terms (average dead nodes, average LBF and average PDF) and rises under term average throughput. Average dead nodes increased when network size increased because the cluster-head node became responsible for the largest number of members and it will depletes their energy. Average LBF decreased when network size increased because the number of cluster-heads become very small and suitable the network size especially the number of cluster-heads according to BREERA not determined by any equation or law. Average LBF depends on the random effectiveness nodes. Average PDF decreased when the network size decreased because the hops 'number become not suitable the size of the network. Average throughput increased when the nodes size increased because of the increased number of nodes sent the sensing data (messages) to the sink. Nodes Speeds factor has an effect on the performance of BREERA , when nodes speeds increased the performance of BREERA dropped under terms (average dead nodes , average total energy and average LBF) and rises under terms (average throughput and y a average PDF). Average dead nodes increased when nodes speeds increased because of the rapid change to form clusters. Average total energy decrease when nodes speeds increased because of the increased number of lost nodes. Average throughput increased when nodes speeds increased because of the high probability of approach the sink. Average PDF increased when nodes speeds increased because the messages will shorten long distances toward the sink with a few hops' number and so messages may be able to access the sink before they reach the value of threshold.

References

[1] Yashpal Singh, Kamal Deep and S Niranjan, "Multiple Criteria Clustering of Mobile Agents inWSN ",International Journal of Wireless & Mobile Networks (IJWMN) Vol. 4, No. 3, June 2012.
[2] Muhammad Tabassum Tahir, " Performance Evaluation of Biased Clustering Technique and Random Algorithm For Wireless Sensor Networks ", A dissertation submitted to the school of Engineering -Liverpool John Moore s University in fulfilment of the requirements of MSC Project, 2011.
[3] I.F. Akyildiz, W. Su, Y. Sankarasubramaniam and E.Cayirci, "Wireless Sensor Network : a survey", Broadband and Wireless Networking Laboratory " ,School of Electrical and computer Engineering ,Georgia Institute of Technology Atlanta, GA 30332, USA, 2001.
[4] Vivek Katiyar, Narottam Chand, Surender Soni, "Clustering Algorithms for Heterogeneous Wireless Sensor Network: A Survey ", International Journal of Applied Engineering Research, DINDIGUL,Volume 1, No 2, 2010.
[5] Suryadeep Biswal and Dimol Soren, "Study of Different Mobility Models and Clustering Algorithms like Weighted Clustering Algorithm (WCA) and Dynamic Mobility Adaptive Clustering Algorithm(DMAC) ", BSC. thesis submitted to the department of Computer and Engineering National Institute of Technology, 2007.
[6] Vikas Singla and Parveen Kakkar, "Traffic Pattern based performance comparison of Reactive and Proactive protocols of Mobile Ad-hoc Networks", International Journal of Computer Applications (0975 – 8887), August 2010.
[7] M.Chatterjee ,S.K. Das, and D. Tugut, WCA : " A Weighted Clustering Algorithm for mobile ad hoc networks, Cluster Computing, vol.5, no. 2, pp.193-204, 2002 .
[8] Sucec.J. and Marsic.I, "Clustering overhead for hierarchical routing in mobile ad hoc networks ",IEEE proceeding, 002.
[9] Toh.c.k, and Chai K Toh ," Ad hoc Mobile Wireless Networks protocols and Systems ", New Jersey :Prentice Hall PTR, 2002.
[10] Tzung-Pei Hong and Cheng-His Wu ," An Improved Weighted Clustering Algorithm for Detection of Application Nodes in Hetrogeneous Sensor Networks ", Journal of International Hiding and Multimedia Signal Processing, 2011 .

International Journal of Modern Engineering Research (IJMER)
www.ijmer.com Vol. 3, Issue. 3, May - June 2013 pp-1577-1581 ISSN: 2249-6645

Easier Management Strategy for Small and Large Enterprise Networks with Enhanced Security

Sreelakshmi Ganesh[1], Binu A[2]
Post Graduate Student, Department of Information Technology, Rajagiri School of Engineering & Technology, Kerala, India
Assistant Professor, Department of Information Technology, Rajagiri School of Engineering & Technology, Kerala, India

ABSTRACT: *The goal of this paper is to make Enterprise Network more manageable, secure and thereby reducing complexities without adding a new layer of protocols, applications and scripts to the existing network. This goal is achieved by proposing new network architecture for Enterprise known as Ethane. Ethane is built on the principle that, the only way to manage and secure networks is to identify the origin of all packets, and hold the user (or machine) accountable for it. So first, using Ethane all users, hosts and switches used in the network are well authenticated and tracking is performed in intervals. All packets are identified with their sender or origin. Secondly, Ethane implements a network-wide policy language in terms of users, machines and services. That is, before a packet flows into the network, it is verified against certain access-deny policies, whether to access or deny the flow of data into the network depending upon the behavior and type of flow. Ethane uses simple flow-based switches called Ethane Switches that will permit or deny flows under the control of a centralized controller. Each network contains a centralized controller that decides if a flow is to be allowed into the network. It makes its decisions based on a set of rules that make up a policy. This architecture has been found backwards-compatible with many existing switches and hosts. Ethane can be deployed in both hardware and software supporting both wired and wireless hosts. To avoid broadcast traffic for service and resource discovery, Ethane proposes a new device, the EtherProxy that can be inserted into an existing Ethernet to suppress broadcast traffic.*

Keywords: *ACL, Central controller, Ethane, FSL, NAT*

I. INTRODUCTION

Security and management can be considered as a remarkable part of all our present–day enterprise networks. Each member of the enterprise network is responsible for the security, protection and management of the electronic information resources over which he or she has control. If we consider the Enterprise network, security has become a big problem, as most commonly everyday critical data has to be received and transferred. Enterprise networks are indeed huge networks that can run many applications and protocols mostly working under high security and reliability constraints. It has become a risky task for many network engineers to manage the network as the business productivity is more affected by network misconfigurations and disruptions. The current solutions are weak making the enterprise network more expensive and error prone. Also, most of present day networks require skilled network engineers for the manual configurations of network to attain better security, which is again not a better solution. Different approaches are developed to make an enterprise network highly secure and manageable. The first method is to make use of dedicated network appliance hardware's like middleboxes that can transform, inspect, filter or otherwise manipulates traffic. These middleboxes can exert their control effectively only if placed at network choke-points.

Second method is adding network functionalities which includes providing network diagnosis tools , adding VLANS , for broadcast segmentation, NAT, Access control list (ACLs) to access and deny type of flow , and filters to isolate users, to instrument the routing and spanning tree algorithms to support better connectivity management, and then to collect packet traces to allow auditing. All this will add complexity to the existing network as new layer of protocols, scripts and applications are added. Increasing complexity will make the network less scalable and difficult to manage, less reliable and ultimately less secure. Instead, we believe the answer lies in removing complexity from the switches and routers, reducing them to the very simplest forwarding devices. We believe that the decision of who can communicate with whom should be managed by a network-wide policy running in software in a centralized location.

To make our network more manageable and secure we change the existing network architecture by suggesting ETHANE framework which is based on Ethernet. We need to rethink the enterprise network to make it more manageable without adding new layer of complexity on the top of existing network. Ethane has been built successfully in Stanford University Computer Science Department supporting 300 hosts and it is found that Ethane can be used in campus and university network supporting wired and wireless hosts.

Ethane works based on three principals. First, design a network where connectivity is governed by central policy over high-level names enforced robustly. It is convenient to declare which services a user is allowed to use and to which machine they can connect. Secondly, allowing the network manager to determine the route of packets via policy. These include packets to pass through some intermediate middleboxes like intrusion detection system, firewall and so on. The third principle is that, there must be a strong and secure binding between the packets and their origin. Most of today's bindings have problems.

An Attacker can always interpose between any of the bindings and perform IP or MAC spoofing. Also there arise problems when the bindings change dynamically or when the physical network changes. Since the ARP and DHCP are unauthenticated we go for strong and secure bindings between packets and the source.

To achieve these principles in enterprise network, centralized control architecture was adopted. Centralized solutions are a suitable method for the management of enterprise networks.

The paper is organized as follows. Section I is the introduction to the paper. Section II describes overview of ETHANE design. Section III elaborates the working of ETHANE. The controller components are described in Section IV. Section V, describes a policy language FSL that is used to manage the Ethane implementation. Related Work is elaborated in Section VI followed by proposal for improvement in Section VII. The rest of Section deals with Conclusion.

II. ETHANE DESIGN OUTLINE

The two components involved in the ETHANE design are (i) Controller and (ii) Ethane switches. The controller acts as the main leader in the enterprise networks and has control of the entire network topology. A central policy is declared at this controller and helps to decide which user can communicate with whom after explicit permission. The policy can be access policies, deny policies and waypoints. When a new packet flow arrives, Controller verifies the flow against the network wide security policy. If the flow is allowed, the Controller chooses a route for the flow and installs the accepted flow-entry to entire switches along the path. But, If the flow is denied, no flow-entry will be added and the packets are not forwarded further.The controller keep track of all the bindings (mainly handling IP address, DNS lookups, authentication of user, switches and end-hosts) providing more security and authentication in the network.

The second component Ethane Switch plays a very important role in managing the Ethane design. Ethane design can know the origin of packet,by keeping track of all the users, hosts and authenticating namespace and addresses. The Ethane switch can replace the normal Ethernet switches and are basically simple switches. These switches include a managed flow table and establish a secure connection with the controller. The flow table consists of flow entries that contain a header, an action and per-flow authorised data. Header is needed to decide the type of flow (TCP, UDP, and IP), Ethernet headers and physical port information of the switch. Action helps the switch to decide what to do with the packet. Action can be forwarding packet, updating packet-byte information, setting the number of inactive entries. Controller will remove the inactive entries due to timeout. Per-flow authorised flow has per-flow entries mainly for application data flow and per-host entries for the hosts that are misbehaving.

Instead of adding functionalities like ACL, NAT, MAC or IP address look up , Spanning tree etc. to entire switches along the path , a method to reduce the cost, power consumption and complexity can be achieved in the network by adding more functionalities in a single location like a controller by enforcing some global security policies.

The Ethane switch requires a local switch manager to establish and maintain a secure connection to the controller for monitoring link status, providing an interface for any additional switch-specific administration and diagnostics.

2.1 Name space, Bindings , Policy language

A Controller evaluates the incoming packets against set of rules like guest visitor accessing the http using proxy server. Today's namespace stores lot of names (hosts, users, services, protocols).These names are bound to network realities (like DNS names mapping to IP, MAC to IP and so on). If the mappings between these names, IP, MAC are unauthenticated, attackers can easily attack the network and it becomes a well-known weakness in the current network.

A controller running in the Software or hardware PC can make the namespace consistent as components join, leave and move around the network. Any network state changes require updating the bindings at the controller. Ethane provides strong and secure bindings between the packet and the origin. Ethane takes over all the bindings of addresses. When host uses DHCP to request an IP, Ethane assigns it knowing to which switch port the machine is connected, enabling ethane to attribute an arriving packet to a physical port.Secondly, the packet has to come from a machine that is registetred on the network.The controller can record all the packet flow entries and bindings in a log, that can be used later to regenerate the network events.

For a controller to enforce network fine grained policy, it is essential to write a policy language. The policies are specified using a simple declarative policy language. These policy language runs on high level names supporting large enterprise networks. Ethane uses a policy language known as *FSL* (Flow-based Security language). FSL includes set of rules pertaining to a flow consisting of a condition and corresponding action. These rules or policies can be allow, deny and waypoint policies.

III. WORKING OF ETHANE

The working of a simple Ethane Network consists of the following steps which is demonstrated using figure 1.

a) **Registration:** The switches, hosts and users in the network must be registered at the controller along with the credentials or authorizations for the purpose of authentication. Every host can be authenticated using MAC address, users with username and password, and switches using secure certificates.

b) **Bootstrapping:** The connectivity is maintained by bootstrapping switches by creating a spanning tree with the root as the controller. Spanning tree creation helps to avoid network loops and broadcast storms. Each switch in the spanning tree authenticates with the controller and establishes a secure channel to it. After maintaining a secure connection, the switches send link state information to the controller, using which it can reconstruct the network topology.

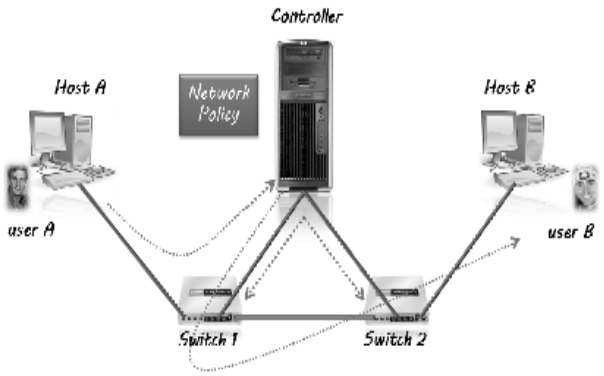

Figure 1: Communication in Ethane Network

c) **Authentication:** From the above figure 1, the user A will come into connection with Host A. Since there are no flow entries for the new user or new host existing in Switch 1, it will initially forward all the Host A packets to the controller. Host A request a DHCP to the controller. After checking host A's MAC address , the controller will allocate an IP address (Ip A) for it, binding host A to IpA., IpA to Mac A , and Mac A to a physical port on switch 1.UserA opens a web browser where the traffic is first directed to Controller, authenticating using a Web form . Once authenticated , User A is bound to Host A.

d) **Flow Setup:** A connection is initiated by User A to User B. The packet is forwarded to the Controller by Switch 1 after determining that the packet does not match any active entries in its flow table. On receiving the packet, the Controller decides whether to allow or deny the flow, or require it to traverse a set of waypoints based on the type of flow and using policy language. If the flow is allowed, the Controller computes the route of flow. The Controller then adds a new entry to the flow tables of all the Switches along the path.

e) **Forwarding:** If the Controller allowed the path, it sends the packet back to switch 1, which forwards it based on the new flow entry. Subsequent packets from the flow are forwarded directly by the Switch and are not sent to the Controller. The flow-entry is kept in the switch until it times out

IV. CONTROLLER COMPONENTS

Controller who is the root of Enterprise Networks consists of several components. These includes:

a) **Authentication:** It authenticates users and hosts using credentials stored in the registration database.The credentials for the user include username, password and are authenticated via Web interface.Switches can authenticate using their MAC address, registered in the database.

b) **Policy File:** When a new flow arrives, it is verified against certain policies or rules so as to accept deny or route through a waypoint.

c) **Route Computation:** It uses the network topology to pick the flow's route. Route can be calculated using shortest path algorithm.

d) **Switch Manager:** The topology contains a switch manager, which receives link updates from the Switches so that it becomes easier to reconstruct the network topology for route computation.

e) **Registration Database:** All entities like hosts, protocols , switches ,users etc. are registered via a Web interface to the controller in the database. Example: Authentication of switches are done by seeing if they are registered.

f) **Bindings:** can easily track all the bindings between names, addresses, and physical ports on the network, even as Switches, hosts, and users join, leave, and move around the network. Controller can even record or log the bindings so that each log can be queried to know the bind state at any timestamp.

g) **Permission Check and Access Granting:** Upon receiving a packet, the Controller checks the policy to see what actions apply to it.

h) **Policy Compiler:** This is required to compile the policy file in the controller.

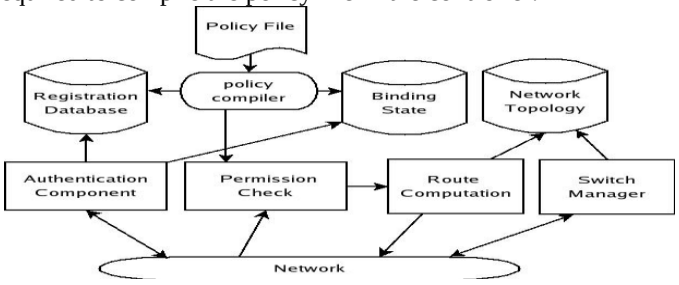

Figure 2: Controller Components

Fig 2 illustrates the high-level view of controller components. In many cases when the centralized controller fails, there are techniques and approaches to replicate the controller and improve the fault tolerance and scalability.

V. POLICY LANGUAGE

Policy Language is a declarative language to define policies or set of rules in the controller and Ethane Network.These policy languages are used for expressing and enforcing Flow-based Network security policies and for the easy administratition of the controller.To control the Ethane network, a DATALOG-based language with negation called FSL has been developed. FSL policies are set of rules used to bind unidirectional flows to constraints that should be placed on the flows. The policy language includes a condition and an Action. For example, the rule to specify that user *bob* is allowed to communicate with the Web server using HTTP is:

$$[\mathbf{allow}() <= \mathbf{usrc}(\text{“bob"}) \wedge \mathbf{tpdst}(\text{“http"}) \wedge \mathbf{hdst}(\text{“websrv"})].$$

A condition is a conjunction of zero or more literals describing the set of flows an action should applied to. Example : If the user initiating the flow is “bob” **and** the flow destination transport protocol is “HTTP” **and** the flow destination is host “websrv,” then the flow is *allowed*.

The Actions include allow, deny and waypoint. The language or policy can be developed in C++ or python. Sample policy file developed using python is shown below:

```
allow() <= tpdst(8888) ∧ hdst(“emerson”)
fn_action(“http_redirect”) <= in(‘laptops’,HSRC) ∧ usrc(“unauthenticated”)
# allow ARP and DHCP
allow() <= protocol(‘arp’)
allow() <= protocol(‘dhcps’) ∧ hdst(“gateway”)
allow() <= protocol(‘dhcpc’) ∧ hsrc(“gateway”)
# allow computers to ssh into anyone
allow() <= protocol(‘ssh’) ∧ in(‘computers’, HSRC)
# dissallow testing machines from communicating externally
deny() <= in(‘testing’, HSRC) | in(‘testing’, HDST)
# servers should be inbound-only
deny() <= isConnRequest() ∧ (in(‘servers’, HSRC) | in(‘printers’, HSRC))
# printers should be inbound-only
deny() <= isConnRequest() ∧ (in(‘printers’, HSRC) | in(‘printers’, HSRC))
# laptops and mobile devices should be outbound-only
deny() <= isConnRequest() ∧ (in(‘mobile’, HDST) | in(‘laptops’, HDST))
# allow workstations unfettered access
allow() <= in(‘workstations’, HSRC) | in(‘workstations’, HDST)
# allow known devices to communicate as long as they abide by the
# previous rules.
allow() <= in(‘all’, HSRC)
# default deny
deny() <= True
```

Figure 3: Sample Policy file format

VI. RELATED WORK

The network goals of any enterprise can be achieved by enforcing global network policies in a centralized controller. Better security and management can be achieved by use of Ethane design thereby reducing the overall complexities .These policies are maintained on the flow of packets. By simply updating the controller at central location adding of functionalities and features, for achieving security and management becomes easy. Ipsilon Networks work for providing a switched, multiservice fast and simple path to traditional IP routers by caching routing decisions.Using FSL ,apart from allow –deny policies , waypoints can also be configured. FSL was evolved from Pol-Eth, the old Ethane policy language, and supports dynamic group memberships, negation, conflict resolution, and distributed authorship.FSL policy language can be applied to all types of packet flow thereby setting priorities for different type of users. For a large enterprise networks, setting VLAN (logical broadcast domain) becomes a hectic task as it requires much hand-holding and manual configuration each time. Rather than configuring VLAN on all switches, Ethane controller can provide simpler control over isolation, connectivity and diagnostics. Also many identity-based networking custom switches provides less control over the network data-path. This control can be achieved using ETHANE.

VII. PROPOSAL FOR IMPROVEMENT

To avoid broadcast traffic for service and resource discovery, paper proposes a new device, the EtherProxy that can be inserted into an existing Ethernet to suppress broadcast traffic. For protocols that use broadcast, an EtherProxy caches protocol information carried by protocol messages passing through it. Then for each of those protocols, the EtherProxy employs an algorithm that may suppress subsequent broadcast protocol messages with the aid of the cached protocol information. For example, an EtherProxy can cache the ARP response to an ARP request. Subsequent ARP requests for the same IP address can be served directly from the EtherProxy’s cache rather than broadcasting the request over the network. EtherProxy is backward compatible and requires no changes to existing hardware, software, or protocols. Moreover, it requires no configuration. This allows a single Ethernet network, with a single broadcast domain, to scale to much larger sizes than before. The EtherProxy intercepts broadcast packets it recognizes then it either (1) responds to a host’s query, sent via a broadcast packet, itself using its cached information and without forwarding the request packet to the network, (2)

replaces the broadcast destination address in the packet with the appropriate unicast destination address, cached at the EtherProxy, and then sends the packet over the network, or (3) passes on the broadcast packet as is, if it contains information that needs to be disseminated to all hosts in the network. If the broadcast packet's protocol is not recognized and there is no rule for handling it, then the packet is just passed through. Every protocol using broadcast packets can be handled by one of the approaches mentioned above.

VIII. CONCLUSION

Using ETHANE, it becomes much easier to manage the Enterprise network than expected. Ethane Network is highly Scalable and enables adding new hosts, switches, new users, new protocols. It provides fast and easy method to set new policy rules in a single Central location. In case of failure of central location, the Controller can be replicated. It allows extending the policy language, adding new routing algorithms. Controller can scale to support quite large networks. Ethane Switch will be significantly simpler, smaller, and lower power than current Ethernet switches and routers that are very costly.

To avoid broadcast traffic for service and resource discovery, paper proposes a new device, the EtherProxy that can be inserted into an existing Ethernet to suppress broadcast traffic. For protocols that use broadcast, an EtherProxy caches protocol information carried by protocol messages passing through it. Then for each of those protocols, the EtherProxy employs an algorithm that may suppress subsequent broadcast protocol messages with the aid of the cached protocol information. For example, an EtherProxy can cache the ARP response to an ARP request. Subsequent ARP requests for the same IP address can be served directly from the EtherProxy's cache rather than broadcasting the request over the network. EtherProxy is backward compatible and requires no changes to existing hardware, software, or protocols. Moreover, it requires no configuration. This allows a single Ethernet network, with a single broadcast domain, to scale to much larger sizes than before. The EtherProxy intercepts broadcast packets it recognizes then it either (1) responds to a host's query, sent via a broadcast packet, itself using its cached information and without forwarding the request packet to the network, (2) replaces the broadcast destination address in the packet with the appropriate unicast destination address, cached at the EtherProxy, and then sends the packet over the network, or (3) passes on the broadcast packet as is, if it contains information that needs to be disseminated to all hosts in the network. If the broadcast packet's protocol is not recognized and there is no rule for handling it, then the packet is just passed through. Every protocol using broadcast packets can be handled by one of the approaches mentioned above.

REFERENCES

[1] Casado,M. Stanford Univ., Stanford, CA, USA Freedman, M.J, Pettit,JianyingLuo,Gude,N.,McKeown,N., Shenker, S "*Rethinking Enterprise Network Control*" ,Networking, IEEE/ACM Transactions on Aug. 2009 Volume: 17 , Page(s): 1270 – 1283" .
[2] Roscoe, S. Hand, R. Isaacs, R. Mortier, and P. Jardetzky,"Predicate routing: Enabling controlled networking," *Comput. Commun. Rev.*, vol.33, no. 1, 2009.
[3] M. Casado, M. J. Freedman, J. Pettit, J. Luo, N. McKeown, and S.Shenker, "*Ethane: Taking control of the enterprise*," in *Proc. SIGCOMM*, Kyoto, Japan, Aug. 2008, pp. 1–12.
[4] A. Myers, E. Ng, and H. Zhang, "*Rethinking the service model: Scaling Ethernet to a million nodes*," presented at the HotNets, Nov. 2008
[5] *"Cisco Network Admission Control,"* [Online]. Available: http://www.cisco.com/
[6] *"Microsoft Network Access Protection,"* http://www.microsoft.com/technet/network/nap/default.mspx
[7] *"Alterpoint,"* [Online]. Available: http://www.alterpoint.com/
[8] G. Xie, J. Zhan, D. A. Maltz, H. Zhang, A. Greenberg, and G. Hjalmtysson, "*Routing design in operational networks: A look from the inside*," in *Proc. SIGCOMM*, Sep. 2004, pp. 27–40.
[9] D. Caldwell, A. Gilbert, J. Gottlieb, A. Greenberg, G. Hjalmtysson, and J. Rexford, "*The cutting edge of IP router configuration*," *Comput. Commun. Rev.*, vol. 34, no. 1, pp. 21–26, 2004.
[10] A. Greenberg, G. Hjalmtysson, D. A. Maltz, A. Myers, J. Rexford, G. Xie, H. Yan, J. Zhan, and H. Zhang, "*A clean slate 4D approach to network control and management*," *Comput. Commun. Rev.*, vol. 35, no. 5, pp. 41–54, Oct. 2005.
[11] M. Casado, T. Garfinkel, A. Akella, M. J. Freedman, D. Boneh, N. McKeown, and S. Shenker, "*SANE: A protection architecture for enterprise networks*," in *Proc. USENIX Security Symp.*, Aug. 2006, vol. 15, Article No. 10.
[12] T. Hinrichs, N. Gude, M. Casado, J. Mitchell, and S. Shenker, "*Practical declarative network management*," presented at the ACM Workshop: Res. Enterprise Netw., 2009.
[13] C. Demetrescu and G. Italiano, "*A new approach to dynamic all pairs shortest paths,"* in *Proc. STOC*, 2003, pp. 159–166.

International Journal of Modern Engineering Research (IJMER)
www.ijmer.com Vol. 3, Issue. 3, May - June 2013 pp-1582-1586 ISSN: 2249-6645

Jit: Various Aspects of Its Implementation

D. K. Singh[1], Dr. Satyendra Singh[2]
[1]*Division of MPA Engineering, Netaji Subhas Institute of Technology, New Delhi – 110078*
[2]*Deptt. of Mechanical Engineering, B. T. Kumaon Institute of Technology, Dwarahat-263653 (Almora) Uttarakhand*

Abstract: *Many factors affect JIT implementation directly or indirectly. Factors such as product quality and lead time directly affect the implementation of JIT. On the other hand, factors such as work environment, working conditions, motivation, flexibility whether manufacturing or organizational affect JIT implementation indirectly, although their impact is no less important than those affecting directly. The present paper thoroughly explores these factors and discusses the extent to which they affect JIT and its implementation.*

Keywords*: JIT, Kaizen, TQM, Quality Circle, Lead Time, FMS, Information Technology, Supply chain, SCM.*

I. Quality Management Approach and JIT

Quality is a powerful tool for productivity improvement. It can be measured using many parameters. It should comply design specifications, which is measured in terms of percentage of defects, incidence of reworking times and frequency of replacement. Quality ensures reliability and maintainability of product, defined as the ability of the product to perform its intended functions without failure over time, and in case of failure, the facility to restore it. Quality has a key role in inventory management. It ensures defect-free products and reduces work-in-process (WIP) inventory drastically. It reduces inspection costs, which has a direct impact on production cost. It reduces lead time and ensures speedy delivery of products to a customer. A customer is more easily attracted towards quality products because of their ability to satisfy him to the maximum level [1]. Customer satisfaction through quality has become the necessity for a company to survive in the market. Quality is being used as a competitive weapon to excel. At the same time, the company registers increase in sales and profits due to increased level of quality driven customer satisfaction. Quality products have short stay and waiting time before being sold in the market and offer increased rate of consumption and hence increased circulation of material flow, which in turn, reduces the level of in-process inventory. On the other hand, poor quality products are more likely to be rejected and may affect the brandability of a company and thus loosing the customer's goodwill. Also, poor quality products render the production system less productive as they increase machine down time and involve longer processing time.

JIT particularly influences the quality dimension more directly connected to a production system. The principle of quality at source should be used where errors or defects in a product or service is detected and rectified at the source and not passed on to the customer. Quality at source starts with the quality of raw material. It will result in saving in inspection cost and the cost associated with replacing the defective items. Issues considered vital today may not be relevant tomorrow. So adapting to the change becomes more relevant at a particular point of time. Predicting the impending changes, keeping in mind customer's requirements, and proacting accordingly can produce miraculous results for the organization. This requires dynamics from within and quickness to respond. It applies to quality also. Attaining one time improvement in quality is not enough. Quality needs to be continuously improved upon to make it always relevant and in demand [2]. And doing so will make the task of JIT implementation always easier. Kaizen is useful in improving the existing features or adding features in the product. Improved quality has many positive implications for a company wishing to stay longer in the market. Kaizen encompasses incremental improvement everywhere. Total quality management (TQM) is an integrated management concept directed at continuous improvement of product or service quality [3, 4]. It immensely helps in improving manufacturing environment. JIT and TQM have played key role in improving organizational effectiveness in today's competitive and ever-changing world market. While JIT philosophy concentrates more on improving manufacturing efficiency by eliminating non-value added activities and minimizing inventory, TQM, on the other hand, thrusts upon improving the overall effectiveness of a company through a focus on quality improvement [5]. JIT eliminates waste through simplification of manufacturing processes [6, 7], eliminates excess inventory in order to reduce related production cost and emphasizes on the use of small lot size so as to meet quick customer requirements.

II. Geographical Considerations And JIT

Proximity of suppliers to their manufacturers has immense impact on JIT implementation. If suppliers are near to the site of manufacturing, uncertainty relating to transportation of materials can be managed without much problem, hence continuity in the production system can be ensured as usual. At the same time, transportation costs are drastically cut short. It leads to reduction in overall costs of production, and timely delivery of goods to customers with highest level of customer satisfaction. That is, it accelerates JIT implementation. In case, when suppliers are scattered apart, the coordination activities of supply chain network are relatively complex, raising uncertainty in timely supply of raw materials. This condition forces the unit to keep surplus stock to meet the fluctuating demand level. It may increase inventory holding cost. Japan is the most suitable example for JIT implementation. Because of Japan's geography and the long-term relationships between suppliers and manufacturers, Japanese suppliers tended to be located much closer physically to their customers, making daily delivery possible. As a result, the costs of transportation and storage got reduced significantly; and secondly it also reduced the manufacturing lead times. Wilson [8] has pointed out that one of the principal reasons why Toyota became successful in implementing JIT lies in the fact that its suppliers were located in the same area as the company itself existed. He further

states that, in the United States components often have to be shipped through hundreds of miles of distance and may be getting delayed by adverse weather conditions, particularly in winter. O'Neal [9], while addressing geographical considerations between manufacturers and suppliers has found that geographical dispersal impedes JIT implementation.

III. Organizational Components: Structure, Culture And Openness And JIT

Organizational structure is the formal system of task and authority relationships that control how people coordinate their actions and use resources to achieve organizational goal [10, 11]. For any organization, an appropriate structure is one that facilitates effective responses to problems of coordination and motivation. Choosing the right number of managers and hierarchical levels is important, as it affects decision making, which influences organizational effectiveness. The choice affects communication and motivation. Having too many hierarchical levels may hinder communication. As the chain of command lengthens, communication between managers at the top and bottom of the hierarchy takes longer. Decision making slows, and the slowdown hurts the performance of organizations that need to respond quickly to customer's needs or the actions of competitors. Also, as the number of levels in the hierarchy increases, the authority and responsibly of managers decrease and this affects the motivation in the organization. Motivation provides conducive atmosphere for JIT implementation. In fact, it accelerates JIT implementation. In order to implement fast decision, number of levels should be carefully decided and to be kept at minimum. Quality circle, an important component of JIT, is the best example of limited number of persons acting in a group and delivering best for the organization. JIT requires fast decision making so as to accelerate the processes.

Organizational culture is the shared values, principles, traditions and ways of doing things that influence the way organizational members interact with each other and with suppliers, customers and other people outside the organization. In most organizations, these important shared values and practices have evolved over time and determine, in large degree, what employees perceive about their organizational experiences and how they behave in the organization [12,13,14]. The important role of human resource management practices in JIT implementation has been stressed upon by many researchers [15, 16]. For successful implementation of either JIT or TQM, a change in corporate culture or a conducive organizational climate has been regarded as one of the major common infrastructural supports [17, 18, 19, and 20]. Organizational climate represents the enduring characteristics of a company that is reflected in the attitudes employees show towards the policies, practices and conditions in the work environment. Many researchers have emphasized on the critical role of Japanese culture in the successful implementation of JIT [21, 22, and 23]. Japanese culture inspires and encourages the individual to achieve a goal which is within reach, but requires a great deal of discipline and development of a higher level of commitment to achieve. Japanese workers are totally committed to their work and the company. They are loyal, co-operative, and flexible and willing to work long hours when needed. Workers are offered life-time employment, decisions are taken collectively involving people from top to bottom, and the management keeps a paternalistic approach towards workers and has respect for their workers. This kind of relationship between workers and managers help to build a platform of trust and belief, where one can rely upon another, and may contribute in a supportive way. As workers develop a better sense of ownership of the process, they tend to suggest more for improvement. Employee motivation and cooperation are critical in JIT implementation. Koufteros [24] has found that employee involvement is an essential element for pull production system, which is a major characteristics of a JIT system. Toyota did not stop working on JIT after originating it and continue to improve its implementation. Some of the US companies have adopted the Japanese culture approach to implement JIT and have reported success [25, 26]. More and more companies are changing their work atmosphere and getting inspired by the Japanese culture.

Management systems and processes are gradually becoming more participative in nature. The reliance of JIT on a participative management style implies a higher level of employee involvement and empowerment than would have been seen in traditional organization [5]. Flexibility in management is the essential element for survival amidst the turbulence of the changing environment especially, in the global changing international trade scenario and competitiveness in the world market. More transparency and a greater sense of participative decision making at different levels of management are vital. JIT works most effectively in participative atmosphere, as it induces free flow of information among the participating members which is essential for fast and effective decision making. The free flow of information has led to the creation of a borderless world in a big way. The business is being globalized as a consequence of the creation of a borderless world. Japanese work atmosphere is very much participative in nature and so is the principal reason of success of JIT. Participative decision-making at different level of management is helpful in JIT implementation. Organization continues to grow, when it encourages participation and empowerment at every level. Increased participation and empowerment energize greater performance, produce better solutions to problems, and greatly enhance acceptance of decisions. It has been found that group dynamics work to overcome resistance to change, increase commitment to organization, reduce stress levels, and generally make people feel better about themselves and their worlds [27]. Higher level of participation results in increased motivation among the employees. If individuals within the organization see their ideas and efforts contributing to the performance of the business, they will be encouraged still further. On the other hand, if seemingly good ideas are constantly overlooked, this will lead to increased frustration. The Japanese management stresses upon the interaction between management and employee. William Ouchi [28] has focused on the characteristics of an organization. He listed the distinguishing features of Japanese organizations such as lifetime employment, collective decision making, collective responsibility and holistic concern for employees.

JIT is an innovative approach and it is people oriented. Rubenstein [29] has stated that innovation process is essentially a people process and that organizational structure, formal decision-making processes, delegation of authority and other formal aspects of a so called well-run company are not necessary conditions for successful technological innovation.

World class manufacturers put great stress on team work and people involvement at every stage of operation and activity.

An organization must aspire to move along a path from closed system to open system. While secrecy breeds gossip, mistrust, feelings of being alienated and devalued, organizational transparency ensures the trust and support of all concerned. In view of the complexity of tasks, managers are expected to be open to multiple routes of solving problems. Freedom at the workplace is the independence employees need in order to be motivated and perform to the best of their abilities. Freedom encompasses flexibility on the opportunity to voice their opinions freely and the freedom to exercise their creativity to achieve organizational goals. When people have freedom at work, they ought to give their best. They become emotionally committed to the organization, as opposed to become merely rationally committed. Emotionally committed employees go the extra mile in any assignment, actively seek new challenges and remain engaged with the organization through good times and bad. Freedom at workplace makes employees feel empowered, with a strong sense of ownership and contribution, a freedom to make mistake and to have the power to innovate. It is therefore evident that a democratic organization is a 'progressive' organization and employees who are allowed to follow democracy in the truest sense are happy, engaged and most importantly, productive. Harber [30] has stressed on the need for open management and an ability to accept comments and criticisms from employees, as well as, a need to move away from adversarial roles to a sharing of information and goals for successful implementation of JIT. Decision made with an open mind without any presumptions or constraints eliminate many problems of the organization. Shingo [31], when discussing 'Toyota Production System', also balanced JIT techniques with equal emphasis on respect for humanity to generate sense of ownership and pride of work. One of the important factors which Monden [32] considered essential for effective implementation of JIT included respect for humanity that emphasizes employment involvement, cross training, job design, empowerment and communication.

IV. Manufacturing Environment and JIT

Productivity of a manufacturing unit is linked to the optimum utilization of its resources-materials, capital, energy, labour, equipment and technology. Manufacturing environment helps in achieving this goal by making the related process smoother and easier. Good manufacturing environment facilitates in the production of customized products offering many advantages including total customer satisfaction. Manufacturing environment plays a very important role in the successful implementation of JIT. It offers right kind of production atmosphere needed to produce right product at right time and in right quantity. As a result, wastes are eliminated and production cost is optimized. JIT aims rationalization of the production system, which can be achieved through elimination of waste, reduction in defects, increase in machine's utility, improvement in manpower efficiency and reduction in other non-productive works. Hence, it is one of the effective means to control inventory flow, prevent its storage and manage it effectively. JIT is a technique in which stock held by the company is measured in terms of hours of production rather than in days or months [33, 34]. It eliminates waste through simplification of manufacturing processes [6, 7], eliminates excess inventory in order to reduce related production cost and emphasizes on the use of small lot size so as to meet quick customer requirements. Inventory managed on JIT basis removes many types of uncertainties in a production system. It ensures timely delivery of customized products to the customers and thus helping the organization in the long run to acquire its brand status. Manufacturing environments such as preventive maintenance and product flexibility help in reducing inventory. Preventive maintenance reduce the untimely breakdown or failure of machine or its components, which may cause frequent interruption in the operation of a production system, leading to inventory pile-up, which is against the spirit of JIT. Regular maintenance measures ensure continuity in operations, helping the organization running smoothly, without thinking about in-process inventory.

Flexibility in manufacturing system is an effective tool for surviving in the new manufacturing environment involving extreme uncertainties, keeping in mind the unpredictable behaviour of the customer and dynamic nature of market. The success of JIT implementation depends to a great extent on how the organization responds to make atmosphere conducive for innovative developments. The reduction of set up time is crucial for reaching high levels of product flexibility [35, 36]. Reduction in set up times allows increased frequency of set up as well as reducing internal lead times, thereby increasing capacity utilization. The shorter lead time enhances customer response. Also, due to shorter queues in different phases of the processes, results in reduced inventory level. The importance of innovation and organizational theory in implementing a radical innovation such as JIT was stressed by many [37, 38, and 39].

The recent trend toward JIT management system and the ever increasing pressure to reduce work-in-process (WIP) inventories while simultaneously increasing quality has forced companies to install highly integrated, computerized manufacturing system, such as flexible manufacturing system (FMS). A Cellular based flexible manufacturing system is an important tool to produce manufacturing flexibility. The multi cell FMS is suitable for produce to order environment, leading to increased flexibility in final products. Cellular manufacturing uses the principle of group technology (GT), where families of parts with similar manufacturing processes are grouped together, greatly helps in inventory management. It is an innovative approach to ensure variety in the production with additional benefits of reduced material handling, reduced work-in-process (WIP) inventory, reduced setup time and manufacturing lead time, and simplified planning, routing and scheduling activities [40]. Increased global competition, demand for an increased variety of products, reduced product life-cycles and time-to-market are forcing new strategy to adopt. The mass production is being replaced by mass customization of goods and services [41].

V. Shorter Lead Time And JIT

In a dynamic market, where everything is uncertain and unpredictable, it becomes vital for an organization to acquire the ability to fulfill customer's specific demands in very short time. For this to become reality, orders consisting of only a few

items are required to be transferred directly from vendors to shops and need to be supplied within short lead times. The shorter lead time enhances customer response. In a conventional manufacturing system, material handling equipments and setup have their own problems and require delicate handling. It takes some reasonable time to equipment or product changeover, which makes lead time longer. A flexible manufacturing system (FMS), on the other hand, eliminates or reduces majority of shortcomings of conventional system and thus has the ability to reduce the manufacturing lead time drastically. Reduced lead time can help fulfill customer's demand on time, and can produce goodwill for the company. In other words, it increases the life of the business, which has strategic importance.

VI. Supply Chain Management And JIT

The success of a company depends to a great extent on how well it manages its supply chain relationships. Inventory management is closely linked to supply chain management. A supply chain is defined as a network of facilities and distribution options between start and end points that include the functions of procurement of raw materials, transformation of these materials into intermediate and finished products, and the distribution of the finished products to the end users [42].

Supply chain management (SCM) effectively integrates the information and materials flow within the supply chain network starting from product design to delivery [43]. Integration of related activities of a production system facilitates smooth flow of materials within the system, thereby cutting the level of in-process inventory drastically. As a result of effective supply chain management, right product is made available at right time to the customer, which is mainly due to reduced cycle times because of simplified and accelerated operations [44, 45]. This is in tune with the working with JIT. Organizations are realizing the importance of information technology in the success of supply chain management. The use of information technology has not only provided global markets for a company, but also has eliminated many associated problems. It has resulted in reduced lead time, making on-time delivery more reliable and predictable; and thus paving the way for effective implementation of JIT.

VII. Information Technology (It) Based Inventory Management And Jit

Information system is a system of sharing information, and consists of computer hardware, communication technology and software designed to handle information related to business functions [46]. It serves to smooth many organizational functions. An effective information management system coupled with proper manufacturing planning will significantly reduce piling of stocks and lead time and ensure timely delivery of quality products to the customer, endorsing the very basic concept of JIT system. An SCM information system is designed to provide information and information processing capability to support the strategy, operations, management analysis, and decision-making functions in an organization's supply network. It provides high quality, relevant and timely information flow that effectively supports decision-making for inventory replenishment, capacity activation, and for synchronizing material flows at all tiers within the supply chain [47]. The use of telecommunication based networks such as Internet, Intranet, Extranet and EDI helps to gain competitive advantage for the organization. It has made sharing of information easier and faster and organizations using Internet have grown faster in a very short interval of time.

Since suppliers are scattered and sometimes far apart, it is essential to integrate their activities both inside and outside of an organization. This requires an integrated information system for sharing information on various value-adding activities along the supply chain. Information technology is like a nerve system for supply chain management [48]. Hence development and use of effective information system for supply chain management is of utmost importance. A supply chain network can fail in the absence of effective information system. The "Bullwhip Effect" is the most important effect caused due to inefficient supply chain network. It describes the propagation and amplification of orders from one reordering system to another upstream in a supply chain. This effect causes uncertainty in the supply chain management leading to increased on-costs as organizations in the supply pipeline mitigate against the potential risks in customer service levels by, say, increasing available capacity or increasing stock holding [49].

VIII. Supplier-Manufacturer Relationship

The supplier's relationship with manufacturer is important in the context of quality of raw materials being supplied. JIT emphasizes on strong supplier relationship as it makes the system more dependable and eliminates any uncertainty regarding manufacturing schedule, which strongly influences lead time. Burt [50] has thrown light on supplier dependency and its selection and management in respect of a modern manufacturing plant. The manufacturer can work with suppliers to improve overall quality, and to ensure that its supply needs are met. In this way, the manufacturer can eliminate many of its own inspection and control functions. The continuous improvement in this relationship is beneficial in the interest of both parties. A partnership type relationship can prove to be extremely useful and can go a long way in maintaining good relationship between the two. Benefits may be shared proportionately and supplier should be rewarded for on-time delivery of supply materials to the manufacturer. The partnership relation helps them to know each other's requirement more precisely, and makes them answerable for everything, whether good or bad. The result visible in terms of increased product quality, higher productivity and increased benefits.

References

[1]. Singh, D. K (2006). An Exploration of the Components of Customer Satisfaction Affecting JIT Implementation, Prestige Journal of Management and Research, Vol.10 (1&2), pp. 87-95.
[2]. Singh, D.K (2009). Just in Time: Concept and Practices, Ane Books Pvt. Ltd, New Delhi.
[3]. Flynn, B.B; Sakakibara, S and Schroeder, R.G (1995). Relationship between JIT and TQM: Practices and Performance, Academy of Management Journal, Vol. 38, pp. 1325- 1360.
[4]. Lau, R.S.M and Anderson, C.A (1998). A Three-Dimensional Perspective of Total Quality Management, International Journal of Quality and Reliability Management, Vol. 5, pp. 85-98.
[5]. Lau, R.S.M (2000). A Synergistic Analysis of joint JIT-TQM Implementation, International Journal of Production Research, Vol. 38(9), pp. 2037-2049.
[6]. Schonberger, R.J (1986). World Class Manufacturing: The Lessons of Simplicity Applied, Free Press, New York.
[7]. Harmon, R.L and Peterson, L.D (1990). Reinventing the Factory: Productivity Breakthroughs in Manufacturing Today, Free Press, New York.
[8]. Wilson, T.G (1985). Kanban Scheduling - Boon or Bane, Production and Inventory Management, Vol. 26(3), pp. 134-143.
[9]. O'Neal, C (1985). Customer- Supplier Relationships for Just-in-time, CIV Review, Vol. 2(3), pp. 33-40.
[10]. Barnard, C.I (1948). The Functions of the Executive, Harvard university Press, Cambridge, Mass.
[11]. Etziomi, A (1964), Modern Organizations, Prentice Hall, Englewood Cliffs, N.J.
[12]. Shadur, K and Kienzle N.A (December 1999). The Relationship between Organizational Climate and Employee Perceptions of Involvement, Group and Organization Management, pp. 479- 503.
[13]. Hatch, M.J (October 1993). The Dynamics of Organizational Culture, Academy of Management Review, pp. 657-693.
[14]. Smircich, L (September 1983). Concepts of Culture and Organizational Analysis, Administrative Science Quarterly, p.339.
[15]. Spencer, M.S and Guide, V.D (1995). An Exploration of the components of JIT: Case Study and Survey results, International Journal of Operations and Production Management, Vol. 15, pp. 72-83.
[16]. White, R.E; Pearson, J.N and Wilson, J.R (1999). JIT Manufacturing: A survey of Implementation in Small and Large U.S. Manufacturers, Management Science, Vol. 45, pp. 1-15.
[17]. Bright, J and Cooper, C.L (1993). Organizational Culture and the Management of Quality, Journal of Managerial Psychology, Vol. 8, pp. 21-27.
[18]. Emery, C.R; Summers, T.P and Surak, J.G (1996). The role of Organizational Climate in The implementation of Total Quality Management, Journal of Managerial Issues, Vol. 8, pp. 484-496.
[19]. Glover, J (1993). Achieving the Organizational Change necessary for Successful TQM, International Journal of Quality and Reliability Management, Vol. 10, pp. 47-64.
[20]. Morris, L (1994). Organizational Culture and TQM implementation, Training and Development, Vol. 48, pp. 69-71.
[21]. Manoochehri, G.H (1988). JIT for Small Manufacturers, Journal of Small Business Management, Vol. 26, pp. 22-30.
[22]. Mussel White, W.C (1987). The Just-in-time Production Challenge, Training and Development Journal, Vol. 41, pp. 27-29.
[23]. Gettel-Riehl, K and Kleiner, B.H (1987). Lesson from the Japanese Automotive Industry, Industrial Management and Data Systems, U.K; pp. 3-6.
[24]. Koufteros, X.A; Vonderembse, M.A and Doll, W.J (1998). Developing measures of time- based Manufacturing, Journal of Operations Management, Vol. 16, pp. 21-41.
[25]. Sakurai, M and Huang, P.Y (1984). Japan's Productivity Growth: A Managerial and Accounting Analysis, Industrial Management, Vol. 26, pp. 11-18
[26]. Suzuki, K (1985). Work-in-process Management: an illustrated guide to ProductivityImprovement, Industrial Management, Vol. 26, pp. 101-110.
[27]. McGrath, J.E (1984). Groups; Interaction and Performance, Prentice Hall, Englewood Cliffs, NJ.
[28]. William C, Ouchi (1981). Theory Z: How American Business can meet the Japanese Challenge, Reading, Addison Wesley, Mass.
[29]. Rubenstein, A. H (1976). Factors influencing Success at the Project Level, Research Management, Vol. 19(3), pp. 15-20.
[30]. Harber, D ; Samson, D. A; Sohal, A. S and Wirth, A (1989). Just-in- time: the issue of implementation, International Journal of Operations and Production Management, Vol. 9, pp. 13-22.
[31]. Shingo, S (1981). Study of the Toyota Production System from Industrial Engineering point of view, Japan Management Association, Tokyo.
[32]. Monden, Y (1983). Toyota Production System, Institute of Industrial Engineers, Atlanta, GA.
[33]. Karmarkar, U (Sept.-Oct.1989). Getting control of Just-in-time, Harvard Business Review, pp. 122-131.
[34]. Ward, P (May 1994). Logistics: a simple guide, Professional Manager, pp. 10-11.
[35]. Gerwin, D (March-April 1982). Do's and Don'ts of Computerized Manufacture, Harvard Business Review.
[36]. Browne, J ; Dubois, D ; Rathmil, K ; Sethi, S and Steckes, K. E (1984). Classification of Manufacturing Systems, The FMS Magazine.
[37]. Duncan, R (1979). What is the right Structure ? Decision tree analysis provides the answer. Organizational Dynamics, Vol. 7, pp. 59-80.
[38]. Ettlie, J. E ; Bridges, W.P and O'Keefe, R. D (1984). Organizational Strategy and Structural Differences for Radical versus Incremental Innovation, Management Science, Vol. 30, pp. 682-695.
[39]. Damanpour, F (1991). Organizational Innovation: A Meta Analysis of effects of Determinants and Moderators, Academy of Management Journal, Vol. 34, pp. 555-590.
[40]. Akturk, M. S and Turkcan, A (2000). Cellular Manufacturing System design using a holonistic approach, International Journal of Production Research, Vol. 38(10), pp. 2327-2347.
[41]. Pine, B.J (1993). Mass Customization- The New Frontier in Business Competition, Harvard Business School Press.
[42]. Kaihara, T (2003). Multi-agent based Supply Chain Modeling with Dynamic Environment, International Journal of Production Economics, Vol. 85(2), pp. 263-269.
[43]. Verwijmeren, M (2004). Software Component Architecture in Supply Chain Management, Computers in Industry, Vol. 53(2), pp. 165-178.
[44]. O'Brien, James. A (2003). Management Information Systems, Fourth Edition, Galgotia Publications, New Delhi.
[45]. Oz Effy (1999). Management Information Systems, Galgotia Publications, New Delhi.
[46]. Flowers, S (1996). Software Failure: Management failure, John Wiley, U.K.47. Soroor, Tavad; Tarokh, M.J and Keshtgary, M (2009). Preventing failure in IT-enabled systems for Supply Management, International Journal of Production Research, Vol. 47(23), pp. 6543-6557.
[47]. Yamaya, E; Wendy, C and Seltsikas, P (2002). Delivering Enterprise Resource Planning systems through Application Service Providers, Logistics Information Management, Vol. 15(3), pp. 192-203.
[48]. Metters, R (1997). Quantifying the "Bullwhip Effect" in Supply Chains, Journal of Operations Management, Vol. 15(2), pp. 89-100.
[49]. Burt, D.N (July-August 1989). Managing Suppliers up to Speed, Harvard Business Review, pp. 127-135.

International Journal of Modern Engineering Research (IJMER)
www.ijmer.com Vol. 3, Issue. 3, May - June 2013 pp-1587-1592 ISSN: 2249-6645

A Parallel Multiplier - Accumulator Based On Radix – 4 Modified Booth Algorithms by Using Spurious Power Suppression Technique

S. Tabasum, M. P. Chennaiah
M.Tech (VLSI), SSITS, Rayachoty, Kadapa dist India,
Associate prof, SSITS, Rayachoty,Kadapa dist India

Abstract: *In this paper, we proposed a new architecture of multiplier-and-accumulator (MAC) for high-speed arithmetic. This can be implement by using radix-2 booth encoder .By combining multiplication with accumulation and devising a hybrid type of carry save adder (CSA), the performance was improved. This includes the design exploration and applications of a spurious-power suppression technique (SPST) which can dramatically reduce the power dissipation of combinational VLSI designs. Power dissipation is recognized as a critical parameter in modern VLSI field. In Very Large Scale Integration, Low power VLSI design is necessary to meet MOORE'S law and to produce consumer electronics with more back up and less processing systems. The proposed MAC accumulates the intermediate results in the type of sum and carry bits instead of the output of the final adder, which made it possible to optimize the pipeline scheme to improve the performance. The objective of a good multiplier is to provide a physically compact, good speed and low power consuming chip. To save significant power consumption of a VLSI design, it is a good direction to reduce its dynamic power that is the major part of power dissipation.*

Keywords: *low-power design, array multiplier, booth encoder, carries save adder, accumulation, SPST adder, multiplier and accumulator (MAC).*

I. Introduction

In present most digital signal processing methods use nonlinear *functions* such as discrete cosine transform (DCT) or *discrete* wavelet transform (DWT). Because they are basically accomplished by repetitive application of multiplication and addition, the speed of the multiplication *and* addition arithmetic's determines the execution speed and performance of the entire calculation and yield. **O**ne of the accompanying challenges in designing ICs for portable electrical devices is lowering down the power consumption to prolong the operating time on the basis of given limited energy supply from batteries. Therefore, dedicated low- power techniques are not important for high speed multiplication .

The design in proposes a concept called partially guarded computation(PGC), which divides the arithmetic units, e.g., adders and multipliers, into two parts and turns off the unused part to minimize the power consumption. In general, a multiplier uses Booth's algorithm and array of full adders (FAs), or Wallace tree instead of the array of FAs., i.e., this multiplier mainly consists of the three parts: i.Booth encoder, ii.a tree to compress the partial products such as Wallace tree, and iii. adder. Because Wallace tree is to add the partial products from encoder as parallel as possible. The most effective way to increase the speed of a multiplier is to reduce the number of the partial products because multiplication proceeds a series of additions for the partial products. To reduce the number of calculation steps for the partial products, MBA algorithm has been applied mostly where Wallace tree has taken the role of increasing the speed to add the partial products. By using g Booth encoder we can reduce te number partial products it dependence radix. in place of booth encoder we can replace this with spst adder/sub it gives better result.

This paper is organized as follows. In Section II, a simple introduction of a general MAC will be given, and the architecture for the proposed SPST will be described in Section V. In Section III, the BOOTH encoder is described. Finally, the conclusion will be given in Section VI.

II. Overview of Mac

In this section, basic MAC operation is introduced. A multiplier can be divided into three operational teps.

i. The first is radix-2 encoding in which a partial product is generated from the multiplicand (X) and the multiplier(Y).
ii. The second is adder array or partial product compression to add all partial products and convert them into the form of sum and carry.
iii. The last is the final addition in which the final multiplication result is produced by adding the sum and the carry.

If the process to accumulate the multiplied results is included, a MAC consists of four steps, as shown

Fig. 1 which shows the operational steps explicitly
Step1. Booth encoding
Step2. Partial product summation and accumulation,
step3. Final addition

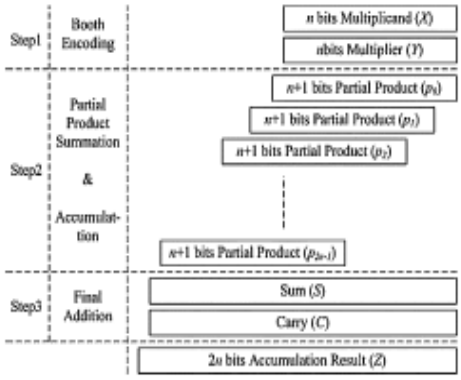

Fig. 1 steps for multiplication and accumulation.

A general hardware architecture of this MAC is shown in Fig. 2. It executes the multiplication operation by multiplying the input multiplier X and the multiplicand Y.

The N -bit 2's complement binary number X can be expressed as

XxY = —$2^{N-1}x_{N-1}+\sum_{i=0}^{N-2}2^i$ (1)

If (1) is expressed in base-4 type redundant sign digit form in order to apply the radix-2 Booth's algorithm.

$X=\sum_{i=0}^{\frac{N}{2}-1} d_i 4_i$ (2)

d_i =—$2x_{2i+1}+x_{2i}+x_{2i-1}$ (3)

If (2) is used, multiplication can be expressed as

XxY=$\sum_{I=0}^{\frac{N}{2}-1} 2^{2i}\,Y$ (4)

If eq used after multiplication and accumulation

P=X+Y+Z=$\sum_{i=0}^{\frac{N}{2}-1} d_i\,2^i$Y+$\sum_{J=0}^{2N-1} z_i\,2^i$ (5)

Each of the two terms on the right-hand side of eq(5) is calculated independently and the final result is produced by adding the two results. The MAC architecture implemented by eq(5) is called the standard design [6]. If N-bit data are multiplied, the number of the generated partial products is proportional to N. In order to add them serially, the execution time is also proportional to the architecture of a multiplier, which is fatest,uses fastest, uses radix-2 Booth encoding that generates partial products and a Wallace tree based on CSA as the adder array to add the partial products. If radix-2 Booth encoding is used, the number partial products, i.e., the inputs to the Wallace tree, is reduced to half, resulting in the decrease in CSA tree step. Each block is decoded to generate the correct partial product. The encoding of the multiplier Y, using the modified booth algorithm, generates the following five signed digits, -2, -1, 0, +1, +2. Each encoded digit in the multiplier performs a certain operation on the multiplicand, X, as illustrated in Table 1.

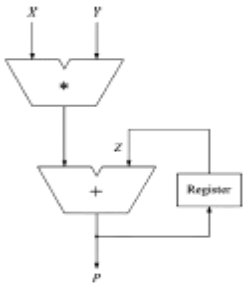

Fig. 2.MAC hardware architecture

III. Modified Booth Encoder

To Booth recode the multiplier term, consider the bits in blocks of three, such that each block overlaps the previous block by one bit. Grouping starts from the LSB, and the first block only uses two bits of the multiplier. Figure 3 the grouping of bits from the multiplier term for use in modified booth encoding. sum and carry.

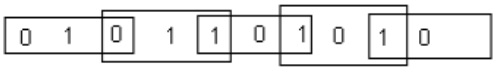

Fig.3. Grouping of bits from the multiplier term

Table.1.Recoding of bits

Block	Re - coded digit	Operation on X
000	0	0 X
001	+1	+1 X
010	+1	+1 X
011	+2	+2 X
100	-2	-2 X
101	-1	-1 X
110	-1	-1 X
111	0	0 X

IV. Proposed Mac Architecture

In this section, the expression for the new arithmetic will be derived from equations of the standard design. From this result, VLSI architecture for the new MAC will be proposed. In addition, a hybrid-typed CSA architecture that can satisfy the operation of the proposed MAC will be proposed

A. Derivation of MAC Arithmetic

1) Basic Concept: If an operation to multiply two -bit numbers and accumulate into a 2-bit number is considered, the critical path is determined by the 2 -bit accumulation operation. If a pipeline scheme is applied for each step in the standard design of Fig. 1, the delay of the last accumulator must be reduced in order to improve the performance of the MAC. The overall performance of the proposed MAC is improved by eliminating the accumulator itself by combining it with the CSA function. If the accumulator has been eliminated, the critical path is then determined by the final adder in the multiplier. The basic method to improve the performance of the final adder is to decrease the number of input bits. In order to reduce this number of input bits, the multiple partial products are compressed into a sum and a carry by CSA. The number of bits of sums and carries to be transferred to the final adder is reduced by adding the lower bits of sums and carries in advance within the range in which the overall performance will not be degraded. A 2-bit CLA is used to add the lower bits in the CSA. In addition, to increase the output rate when pipelining is applied, the sums and carrys from the CSA are accumulated instead of the outputs from the final adder in the manner that the sum and carry from the CSA in the previous cycle are inputted to CSA. Due to this feedback of both sum and carry, the number of inputs to CSA increases, compared to the standard design and [17].

2) Equation Derivation: The aforementioned concept is applied to (5) to express the proposed MAC arithmetic. Then, the multiplication would be transferred to a hardware architecture that complies with the proposed concept, in which the feedback value for accumulation will be modified
and expanded for the new MAC. First, if the multiplication in (4) is decomposed and rearranged, it becomes

$$\text{XxY}=d_0 2Y + d_1 2^2 Y + d_2 2^4 \text{Y} + \ldots\ldots d_{\frac{N}{2}-1} 2^{N-2} \qquad (6)$$

If (6) is divided into the first partial product, sum of the middle partial products, and the final partial product, it can be expressed as eq(7). The reason for separating the partial X product addition as eq(7) is that three types of data are fed

$$XxY=d_0 2Y + \sum_{i=0}^{\frac{N}{2}-2} d_i 2^{2i} Y + d_{\frac{N}{2}-1} 2^{N-2} Y \qquad (7)$$

Now, the proposed concept is applied to Z in (5). If Z is first divided into upper and lower bits and rearranged, (8) will be derived. The first term of the right-hand side in (8) corresponds to the upper bits. It is the value that is fed back as the sum and the carry. The second term corresponds to the lower bits and is the value that is fed back as the addition result for the sum and carry .

$$\text{Z}=\sum_{i=0}^{N-1} z_i 2^i + \sum_{i=N}^{2N-1} z_i 2^i \qquad (8)$$

The second term can be separated further into the carry term and sum term as

$$\sum_{i=N}^{2N-1} z_i 2^i = \sum_{i=0}^{N-1} z_{N+i} 2^{i+N} = \sum_{i=0}^{N-2} (c_i + s_i) 2^{i+N} \qquad (9)$$

Thus, (8) is finally separated into three terms as

$$\text{Z}=\sum_{i=0}^{N-1} z_i 2^i + \sum_{i=0}^{N-2} c_i 2^i 2^N + \sum_{l=0}^{N-2} s_i 2^i 2^N \qquad (10)$$

If (7) and (10) are used, the MAC arithmetic in (5) can be expressed as

$$\text{P}=d_0 2Y + \sum_{i=1}^{\frac{N}{2}-2} d_i 2^{2i} Y + d_{\frac{N}{2}-1} 2^{N-2} Y + \sum_{i=0}^{N-1} z_i 2^i 2^N + \sum_{i=0}^{N-2} c_i 2^i 2^N + \sum_{i=0}^{N-2} s_i 2^i 2^N \qquad (11)$$

If each term of (11) is matched to the bit position and rearranged, it can be expressed as (12), which is the final equation for the proposed MAC. The first parenthesis on the right is the operation to accumulate the first partial product with the added result of the sum and the carry.The second parenthesis is the one to accumulate the middle partial products with the sum of the CSA that was fed back. Finally, the third parenthesis expresses the operation to accumulate the last partial product with the carry

$$P=d_0 2Y + \sum_{i=0}^{N-1} z_i 2^i) + \sum_{i=1}^{\frac{N}{2}-1} d_i 2^{2i} Y + \sum_{i=0}^{N-2} c_i 2^i 2^N) + (d_{\frac{N}{2}-1} 2^{N-2} Y + \sum_{i=0}^{N-2} s_i 2^i 2^N \quad (12)$$

B. Proposed MAC Architecture

If the MAC process which the MAC is organized into three steps. When shown in Fig. 1, it is easy to identify the difference that the accumulation has been merged into the process of adding the partial products. Another big difference from Fig. 1 is that the final addition process in step 3 is not always run even though it does not appear explicitly in Fig. 3. Since accumulation is carried out using the result from step 2 instead of that from step 3, step 3 does not have to be run until the point at which the result for the final accumulation is needed.

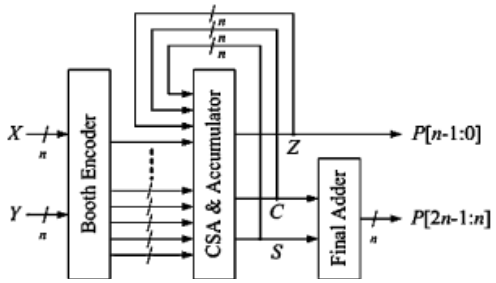

Fig. 4 . Hardware architecture of the proposed MAC

The n -bit MAC inputs, X and Y, are converted into an (n+1)-bit partial product by passing through the Booth encoder. In the CSA and accumulator, accumulation is carried out along with the addition of the partial products. As a result, n -bit S ,C and Z (the result from adding the lower bits of the sum and carry) are generated. These three values are fed back and used for the next accumulation. If the final result for the MAC is needed, P[2n-1:n] is generated by adding and C in the final adder and combined with P[n-1:0] that was already generated.

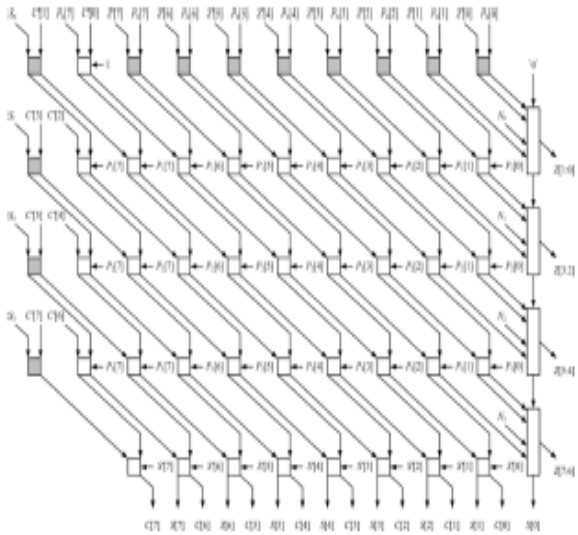

Fig.5 proposed MAC architecture

C. Proposed CSA Architecture

The architecture of the hybrid-type CSA that complies with the operation of the proposed MAC is shown in Fig. 5, which performs 8X 8-bit operation. It was formed based on (12). In Fig. 6, Si is to simplify the sign expansion and Ni is to compensate 1's complement number into 2's complement number. S[i] and C[i] correspond to the i th bit of the feedback sum and carry. Z[i] is the i th bit of the sum of the lower bits for each partial product that were added in advance and is the previous result. In addition, Pj[i] corresponds to the i th bit of the j th partial product. Since the multiplier is for 8 bits, totally four partial products (P0[7:0] ~P3[7:0]) are generated from the Booth encoder. In (11), d0Y and d N/2-1 2^(N-2)Y correspond toP0[7:0] andP3[7:0] respectively.

This CSA requires at least four rows of FAs for the four partial products. Thus, totally five FA rows are necessary since one more level of rows are needed for accumulation. For an n x n -bit MAC operation, the level of CSA is (n/2+1) The white square in Fig. 5 represents an FA and the gray square is a half adder (HA). The rectangular symbol with five inputs is a 2-bit CLA with a carry input.

V. Simulation Results

Csa output:

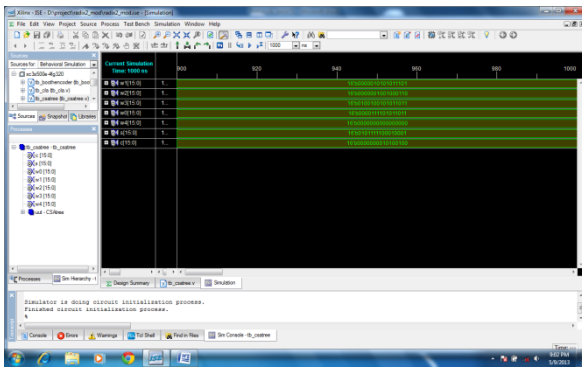

Fig.6. Csa outputs

Mac output:

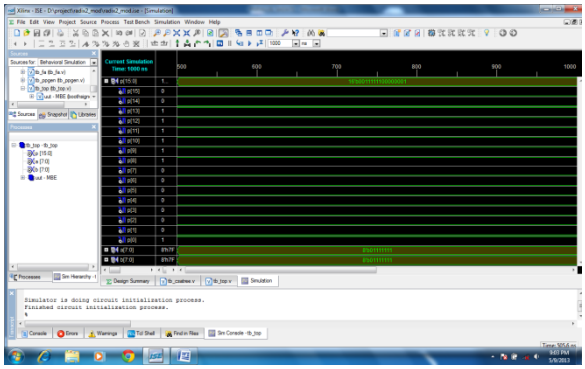

Fig.7.mac outputs

VI. Future Scope of Project

SPST technique:

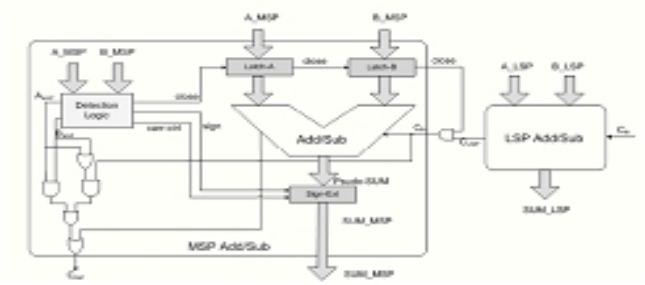

Fig.8 Low-power adder/subtractor design example adopting the proposed SPST

Moreover, we propose the novel glitch-diminishing technique by adding three 1-bit registers to control the assertion of the *close*, *sign*, and *carr-ctrl* signals to further decrease the transient signals occurred in the cascaded circuits which are usually adopted in VLSI architectures designed for multimedia/DSP applications. Hence, the transients of the detection-logic unit can be filtered out; thus, the data latches can prevent the glitch signals from flowing into the MSP with tiny cost..

1) ***When the detection-logic unit turns off the MSP:*** At this moment, the outputs of the MSP are directly compensated by the SE unit; therefore, the time saved from skipping the computations in the MSP circuits shall cancel out the delay caused by the detection-logic unit.

2) ***When the detection-logic unit turns on the*** MSP circuits must wait for the notification of the detection- logic unit to turn on the data latches to let the data in. Hence, the delay caused by the detection-logic unit will contribute to the delay of the whole combinational circuitry, the 16-bit adder/subtractor in this design example.

3) ***When the detection-logic unit remains its decision:*** No matter whether the last decision is turning on or turning off the MSP, the delay of the detection logic is negligible because the path of the combinational circuitry (i.e., the 16- bit adder/subtractor in this design example) remains the same.

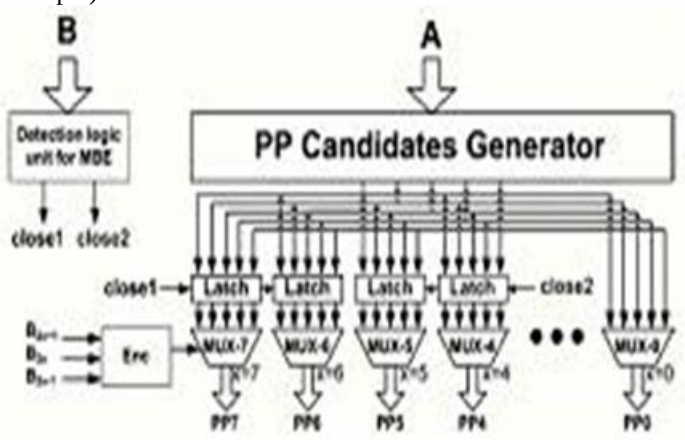

Fig.9 Illustration of multiplication using modified Booth encoding.

From the analysis earlier, we can know that the total delay is affected only when the detection-logic unit turns on the MSP. However, the detection-logic unit should be a speed- oriented design. When the SPST is applied on combinational circuitries, we should first determine the longest transitions of the interested cross sections of each combinational circuitry, which is timing characteristic and is also related to the adopted technology.

The longest transitions can be obtained from analyzing the timing differences between the earliest arrival and the latest arrival signals of the cross sections of a combinational circuitry. Then, a delay generator similar to the delay line used in the DLL designs [16], [17],comprising several invertors and some capacitors, can be used to generate a proper delay to control the "*close*," "*sign*," and "*carr-ctrl*" signals.

VII. Conclusion

In this paper, a new MAC architecture to execute the multiplication- accumulation operation, which is the key operation, for digital signal processing and multimedia information processing efficiently, was proposed.By removing the independent accumulation process that has the largest delay and merging it to the compression process of the partial products, the overall MAC performance has been improved almost twice as much as in the previous work. The proposed SPST can obviously decrease the switching (or dynamic) power dissipation, which comprises a significant portion of the whole power dissipation in integrated circuits. The performance comparisons also illustrate that the SPST-equipped designs are very competitive with the existing designs. Furthermore, the proposed SPST is a fully static CMOS circuit technique which does not aggravate the problems of leakage power, signal racing, and voltage dropping. While the delay has been increased slightly compared to the previous research, actual performance has been increased to about twice if the pipeline is incorporated. Consequently, we can expect that the proposed architecture can be used effectively in the area requiring high throughput such as a real-time digital signal processing.

Reference

[1] O. L. MacSorley, "High speed arithmetic in binary computers," Proc. IRE, vol. 49, pp. 67-91, Jan. 1961.
[2] A D. Booth, "A signed binary multiplication technique," Quart. J. Math., vol. IV, pp. 236-240, 1952.
[3] C. S. Wallace, "A suggestion for a fast multiplier," IEEE Trans. Electron Comput., vol. EC-13, no. 1, pp. 14-17, Feb. 1964.
[4] A. R. Cooper, "Parallel architecture modified Booth multiplier," Proc. Inst. Electr. Eng. G, vol. 135, pp. 125- 128, 1988.
[5] N.R.Shanbag and P. Juneja, "Parallel implementation of a 4x4-bit multiplier using modified Booth's algorithm," IEEE J. Solid-State Circuits, vol. 23, no. 4, pp. 1010-1013, Aug. 1988.
[6] G Goto,T. Sato, M. Nakajima, and T. Sukemura, "A 54x54 regular structured tree multiplier," IEEE J. Solid- State Circuits, vol. 27, no. 9, pp. 1229-1236, Sep. 1992.
[7] J.Fadavi-Ardekani, "MN Booth encoded multiplier generator using optimizedWallace trees," IEEE Trans. Very Large Scale Integr. (VLSI) Syst., vol. 1, no. 2, pp. 120-125, Jun. 1993.
[8] N. Ohkubo, M. Suzuki, T. Shinbo, T. Yamanaka,A. Shimizu,K. Sasaki,and Y. Nakagome, "A 4.4 ns CMOS 54x54 multiplier using pass-transistor multiplexer, IEEE J. Solid-State Circuits, vol. 30, no. 3, pp. 251-257, Mar. 1995.
[9] A.Tawfik, F. Elguibaly, and P. Agathoklis, "New realization and implementation of fixed-point IIR digital filters," J. Circuits, Syst., Comput., vol. 7, no. 3, pp. 191- 209, 1997.

International Journal of Modern Engineering Research (IJMER)
www.ijmer.com Vol. 3, Issue. 3, May.-June. 2013 pp-1593-1596 ISSN: 2249-6645

Iterative Non-Parametric Method for Manipulating Missing Values of Heterogeneous Datasets by Clustering

Sujatha R.[1], Marimuthu M.[2], Sumathi R.[3]
[1]*Assistant Professor, Department of CSE, Shivani Engineering College, Trichy-9,*
[2]*Assistant Professor, Department of CSE, Shivani College of Engineering & Technology,Trichy-9*
[3]*Professor, Department of CSE (P.G), J.J College of Engineering @ Technology, Trichy-9*

Abstract:-*Machine learning and data mining retort heavily on a large amount of data to build learning models and make predictions. There is a need for quality of data, thus the quality of data is ultimately important. Many of the industrial and research databases are plagued by the problem of missing values. A variety of methods have been developed with great success on dealing with missing values in data sets with uniform attributes. But in real life dataset contains heterogeneous attributes. In this paper, apart from the overview of imputation, then discussing about the proposed work i .e a new setting of handling missing data imputation (that is imputing missing data in data sets with mixed attributes and also in clustered data sets) in non parametric mixture kernel based.*

Keywords:-*Data mining, Missing values, Mixed attributes, Imputation, Regression*

I. INTRODUCTION

Data mining, the extraction of hidden predictive information from large databases, is a powerful new technology with great potential to help companies focus on the most important information in their data warehouses. A common problem in data mining is that of automatically finding outliers or anomalies in a database. Outliers are an observation that is numerically distant from the rest of the data. Since outliers and anomalies are highly unlikely, they can be indicative of bad data or malicious behaviour. Bad data interns produce falls outcome. Examples of bad data include skewed data values resulting from measurement error, or erroneous values resulting from data entry mistakes, missing values, missing data. Missing data, or Missing values, occur when no data value is stored for the variable in the current observation. Common solution is either ignore the missing data is called as marginalization or fill in the missing values is called as imputation. Imputed values are treated as just as reliable as the truly observed data, but they are only as good as the assumptions used to create them.

Techniques of dealing with missing values can be classified into three categories [7], [12]. 1) Deletion, 2) Learning without handling of missing values, and 3) Missing value imputation The first technique is to simply omit those cases with missing values and only to use the remaining instances to finish the learning assignments [13].The deletion is classified in two categories they are, i) List wise or Case deletion ii) Pair wise deletion. The second approach is to learn without handling of missing data, such as Bayesian Networks method, Artificial Neural Networks method 15, the methods in [10]. Missing data imputation is a procedure that replaces the missing values with some possible values, such as [11], [12]. A variety of methods have been developed with great success on dealing with missing values in data sets with uniform attributes.(their independent attributes are all either continuous or discrete).

However, these imputation algorithms cannot be applied to many real data sets, such as equipment maintenance databases, industrial data sets, and medical databases, because these data sets are often with continuous, discrete and categorical independent attributes. These heterogeneous data sets are referred to as mixed-attribute data sets and their independent attributes are called as mixed independent attributes. It advocates that a missing datum is imputed if and only if there are some complete instances in a small neighbourhood of the missing datum, otherwise, it should not be imputed. Further, a Non parametric iterative estimator is proposed to utilize all the available observed information, including observed information in incomplete instances with missing values.

In this paper, we present an imputation overview in that we discuss the problem of imputing the mixed attribute datasets and then we see how this problem can be solved by implementing the nonparametric iterative imputation method for estimating missing values in mixed-attribute data sets and also in clustered data sets.

II. IMPUTATION OVERVIEW

Missing data imputation is a procedure that replaces the missing values with some possible values. Imputed values are treated as just as reliable as the truly observed data, but they are only as good as the assumptions used to create them. The imputation consists of many types. In that some types of imputations are, (i) Single Imputation, (ii) Partial Imputation and (iii) Multiple Imputation, (iv) Iterative Imputation. According to our paper, previous work has been handling the missing values in heterogeneous data sets using semi parametric way of iterative imputation method [15].

Normally this method is inconsistent in some datasets. To avoid this problem, and also to improving the efficiency, the non parametric way is possible. So the proposed work based on handling the missing values in heterogeneous datasets and also in clustered data sets (only continuous attributes) using non parametric way of iterative imputation.

III. OBJECTIVE OF OUR WORK

The proposed work bring out the new setting of missing data imputation, i.e., imputing missing data in data sets with mixed attributes (their independent attributes are of different types i.e. the datasets consists of both discrete and continuous attributes), referred to as imputing mixed-attribute data sets in [13]. Although many real applications are in this setting, there is no estimator designed for imputing data sets with heterogeneous attributes. It first proposes two reliable estimators for discrete and continuous missing target values, respectively. Imputing mixed-attribute data sets can be taken as a new problem in missing data imputation because there is no estimator designed for imputing missing data in mixed attribute data sets.

IV. PROPOSED WORK

The challenging issues include, such as how measuring the relationship between instances (transactions) in a mixed-attribute data set, and how to construct hybrid estimators using the observed data in the data set. To address the issue, this research proposes a nonparametric iterative imputation method based on a mixture kernel for estimating missing values in mixed-attribute data sets. A mixture of kernel functions (a linear combination of two single kernel functions, called mixture kernel) is designed for the estimator in which the mixture kernel is used to replace the single kernel function in traditional kernel estimators. These estimators are referred to as mixture kernel estimators.

Based on this, two consistent kernel estimators are constructed for discrete and continuous missing target values, respectively, for mixed-attribute data sets. Further, a mixture-kernel-based iterative estimator is proposed to utilizes all available observed information, including observed information in incomplete instances (with missing values), to impute missing values, whereas existing imputation methods use only the observed information in complete instances (without missing values).To improve the accuracy cluster based non-parametric iterative imputation is proposed. Fig 1 shows that proposed system architecture. It initially considers the database with missing values, and then identifies the attribute type by using appropriate techniques to find attributes of either continuous or discrete attribute. If it is a continuous attribute Mean Pre-Imputation is applied otherwise Mode Pre-Imputation is applied. This is the basic step of imputation techniques. Then by using the pre imputed data sets kernel function is applied separately to both the attributes.

This imputation is said to be single imputation. Mixture kernel function is obtained by integrating both the discrete and continuous kernel function. Estimated value is calculated by the standard formulas. Finally Iterative kernel estimator is applied separately for continuous as well as discrete attributes to get final value for imputation. This data will be imputed in the missing data set to make it as a complete dataset. Further to improve the accuracy clustering algorithm is applied. This clustered data set considered as a first step of the framework.

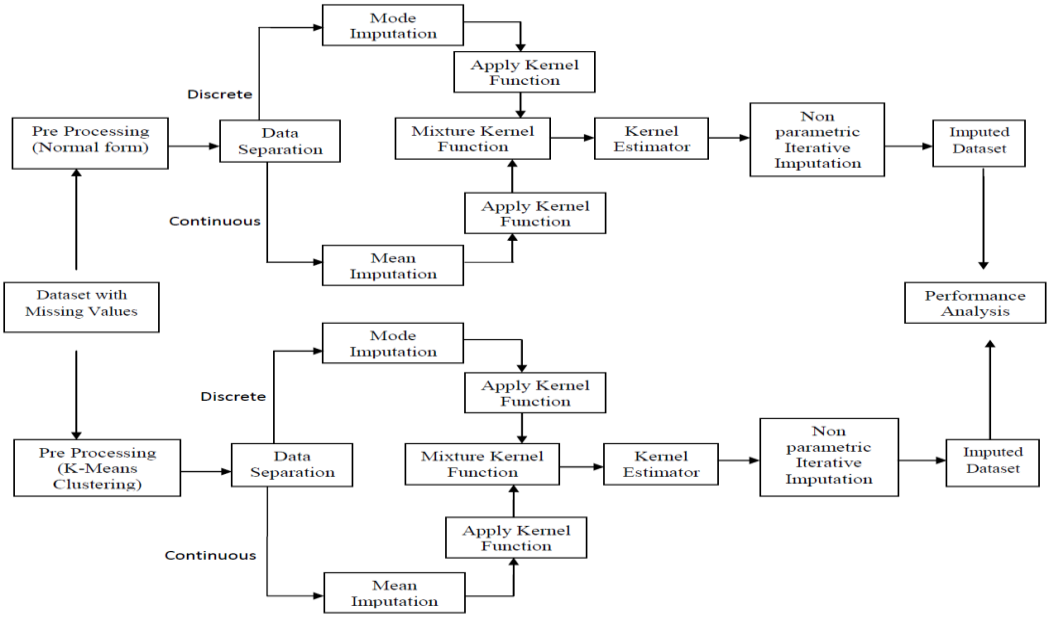

Fig. 1.System Architecture for Proposed System

There are five steps in our proposed system. They are (i) Data Preparation (ii) Single Imputation Using Kernel Function (iii) Constructing the Estimator and Iterative Imputation (iv) Pre-Processing dataset Using Clustering Algorithm (v) Performance Analysis.

4.1 Data Preparation

In this module, from the input heterogeneous data set the records with missing values will be identified and categorized based on attribute type of missing values, attributes are grouped. Mean and mode value for continuous and discrete category is calculated separately. Basic imputation has been done with this calculated value.

4.2 Single Imputation Using Kernel Function

This module shows about the kernel function. After getting the basic imputation, then apply the kernel function separately for both the discrete and continuous attributes. Then integrate both the discrete and kernel function to get the mixture kernel function

4.2.1 Discrete Kernel Function

$$L\left(X_{t,i}^{d}, x_t^{d}\right)=\begin{cases}1 \text{if } X_{t,i}^{d} = x_t^{d} \\ \lambda \text{if } X_{t,i}^{d} \neq x_t^{d}\end{cases} \quad \text{---------- (1)}$$

Where,

X_i^d -- Discrete Variable or attributes

λ -- Smoothing Parameter

Normally discrete attributes are contains a binary format values example is either it will be 0 or 1.so for this step ,the output will shows about the similar values as the imputation for the missing values by taking one attribute as a relation**.**

4.2.2 Continuous Kernel Function

$K(x - X_i /h)$ ---------- (2)

K(.) is a mercer kernel, i.e., positive definite kernel.

4.2.3 Mixture Kernel Function

$K_{h,\lambda,ix} = K(x-X_i/h)\, L(X_i^d, x_i^d, \lambda)$ ---------- (3)

Where,

h->0 and λ->0 (λ, h is the smoothing parameter for the discrete and continuous kernel function , respectively),

$K_{h,\lambda,ix}$ -- symmetric probability density function.

$K(x-X_i/h)$ -- Continuous Kernel Function

$L(X_i^d, x_i^d, \lambda)$ -- Discrete Kernel Function

4.3 Constructing the Estimator and Iterative Imputation

Construct the estimator, separately for both attributes. Estimator is nothing but, it attempts to approximate the unknown parameter using the measurements. Then by the idea of the estimator calculate the iterative value for each attributes by using the formula. The iterative method explains that all the imputed values are used to impute subsequent missing values, i.e., the (t+1)th (t≥1) iteration imputation is carried out based on the imputed results of the t th imputation, until the filled-in values converge or begin to cycle or satisfy the demands of the users.

Normally first imputation is single imputation. It cannot provide valid standard confidence intervals. Therefore running extra (imputation) iterative imputation based on the first imputation is reasonable and necessary for better dealing with the missing values. Since the second iteration imputation is carried out based on the former imputed results. Here, a stopping criterion is designed for nonparametric iterations. With t imputation times, there will be (t-1) chains of iterations. Note that the first imputation won't b considered when talking about the convergence because the final results will be decided mainly by imputation from the second imputation. Of course, the result in the first imputation always generates, to some extent, effects for the final results

4.3.1 Kernel estimator for Continuous Missing attributes

$$\hat{m}(x) = \frac{n^{-1}\sum_{i=1}^{n} Y_i K_{h,\lambda,ix}}{n^{-2}\sum_{i=1}^{n} K_{h,\lambda,ix} + n} \quad \text{---------- (4)}$$

where ,

item n^{-2} m(x) -- only used for avoiding the denominator to be 0.

Y_i -- Denoting the ith Missing Value.

4.3.2 Kernel estimator for Discrete Missing attributes

When the missing value m(X) is in a discrete attribute, the estimator is, let $D_{m(x)} = (0,1,.....,c_u-1)$ denote the range of m(x).One could estimate m(x) by,

$$\hat{m}(x) = \frac{n^{-1}\sum_{i=1}^{n} Y_i K_{h,\lambda,ix}}{n^{-2}\sum_{i=1}^{n} K_{h,\lambda,ix} + n^{-2}} + \frac{\lambda n^{-1}\sum_{i=1}^{n}\sum_{Y\in Dy, y\neq Y_i} K_{h,\lambda,ix}}{n^{-2}\sum_{i=1}^{n} K_{h,\lambda,ix} + n} \quad \text{---------- (5)}$$

Where $l(Y_i, y, \lambda)=1$ if $y= Y_i$ and λ if $y\neq Y_i$.

4.3.3 Iterative Kernel Estimator for continuous Missing attributes

$$\hat{m}(x) = \frac{n^{-1}\sum_{i=1}^{n} Y_i^{\,t}\, K_{h,\lambda,ix}}{n^{-2}\sum_{i=1}^{n} K_{h,\lambda,ix} + n} \qquad \text{---------- (6)}$$

Where,

Y^t_i -- tth imputation of the ith Missing Value

4.3.4 Iterative Kernel Estimator for discrete Missing attributes

$$\hat{m}(x) = \frac{\sum_{i=1}^{n} \sum_{y \in Dy, y \neq Y_i} I(Y_i, y, \lambda) y_t K_{h,\lambda}}{\sum_{i=1}^{n} K_{h,\lambda}} \qquad \text{---------- (7)}$$

Where,

Y^t_i if $\delta_i = 1$ or i=r+1,.....,n

In particular, Y^t_i is the best common class in the discrete target variable, and

$Y^i_t = 0$, i = r+1,...., n.

4.4 Pre-Processing Data set using cluster Algorithm

Before sending data to the data preparation module, clustering take place to group similar data object. By applying the formula mentioned below, the data sets are grouped in two sets with respect to every attribute.

4.5 Performance Analysis

Imputed values without using clustering and using k-means clustering are compared. The performance analysis takes place by using both the method

V. CONCLUSION AND FUTURE WORK

Imputation is the best solution for handling the Missing values. Missing data imputation is a procedure that replaces the missing values with some possible values. But this is not appropriate solution for discrete and categorical missing values. A consistent kernel regression has been proposed for imputing missing values in a mixed-attribute data set and uses the techniques of data driven method for bandwidth selection.

The data-driven (i.e., automatic) bandwidth selection procedures are not guaranteed always to produce good results due to perhaps the presence of outliers or the rounding/discretization of continuous data, among others. The nonparametric estimators are proposed against the case that data sets have both continuous and discrete independent attributes and also in clustered data sets. It utilizes all available observed information, including observed information in incomplete instances (with missing values), to impute missing values, whereas existing imputation methods use only the observed information in complete instances (without missing values).That is the work includes exploring a framework for non parametric iterative imputation based on mixture kernel estimation in both mixture data sets and also in clustered data sets (only continuous attributes).In future work furthermore, this paper could be extended to handle this imputation process in more than one missing value in a single attribute.

REFERENCE

[1]. A. Dempster, N.M. Laird, and D. Rubin, "Maximum Likelihood from Incomplete Data via the EM Algorithm," J. Royal Statistical Soc., vol. 39, pp. 1-38, 1977.
[2]. D. Rubin, Multiple Imputation for Nonresponse in Surveys. Wiley, 1987.
[3]. H. Bierens, "Uniform Consistency of Kernel Estimators of a Regression Function under Generalized Conditions," J. Am. Statistical Assoc., vol. 78, pp. 699-707, 1983.
[4]. J. Han and M. Kamber, Data Mining Concepts and Techniques, second ed. Morgan Kaufmann Publishers, 2006
[5]. J. Racine and Q. Li, "Nonparametric Estimation of Regression Functions with Both Categorical and Continuous Data," J. Econometrics, vol. 119, no. 1, pp. 99-130, 2004.
[6]. J.R. Quinlan, "Unknown Attribute values in Induction," Proc. Sixth Int'l Workshop Machine Learning, pp. 164-168, 1989.
[7]. Y.S. Qin et al., "Semi-Parametric Optimization for Missing DataImputation," Applied Intelligence, vol. 21, no. 1, pp. 79-88, 2007.
[8]. M. Alirera, "A Novel Framework for Imputations of Missing Values in Databases," IEEE Transactions Vol 37,No. 5, 2007.
[9]. Q.H. Wang and R. Rao, "Empirical Likelihood-Based Inference under Imputation for Missing Response Data," Annals of Statistics, vol. 30, pp. 896-924, 2002.
[10]. R. Caruana, "A Non-Parametric EM-Style Algorithm for Imputing Missing Value," Artificial Intelligence and Statistics, Jan. 2001.
[11]. R. Little and D. Rubin, Statistical Analysis with Missing Data, second ed. John Wiley and Sons, 2002.
[12]. S.C. Zhang, "Par imputation: From Imputation and Null-Imputation to Partially Imputation," IEEE Intelligent Informatics Bull., vol. 9, no. 1, pp. 32-38, Nov. 2008.
[13]. Xiaofeng Zhu, Shichao Zhang Senior Member, IEEE,(2011)"Missing Value Estimation for Mixed Attribute Data Sets" , IEEE Transactions on Knowledge and Data Engineering, vol.23,No.1.2011
[14]. Y.S. Qin et al., "POP Algorithm: Kernel-Based Imputation to Treat Missing Values in Knowledge Discovery from Databases," Expert Systems with Applications, vol. 36, pp. 2794-2804, 2009.
[15]. Zhang.S.C, "Estimating Semi-Parametric Missing Values with Iterative Imputation," International Journal of Data Warehousing and Mining, pp. 1-10.2010.

International Journal of Modern Engineering Research (IJMER)
www.ijmer.com Vol. 3, Issue. 3, May.-June. 2013 pp-1597-1601 ISSN: 2249-6645

Improvement in Image Reconstruction of Biological Object by EXACT SIRT cell Scanning Technique from Two Opposite sides of the Target

Kabita Purkait[1], Sanjib Sarkar[2], Kalyan Adhikary[3]

[1](*Associate Professor, Electronics & Communication Engineering, Kalyani Govt. Engineering College, West Bengal, India)*
[2](*M. Tech, Electronics & Communication Engineering, Kalyani Govt Engineering College, Kalyani, West Bengal, India)*
[3](*Asstt. Professor, Electronics & Communication Engineering,* Modern Institute of Engineering *and* Technology,*West Bengal, India)*

Abstract: *In this paper a cell scanning technique from two opposite sides of the target is proposed to reconstruct the complex permittivity of the biological body using Exact Simultaneous Iterative Reconstruction Algorithm. The biological body is illuminated by an array antenna consists of 15x15 half wave dipoles separated by quarter wave spacing from each other with a beam width of 6^0 operating at 1 GHz. The fields are measured by 20 half wave dipoles placed one side of the biological model for 24 transmitter positions on other side of it. The positions of transmitters and receivers are interchanged and views are taken from two opposite sides of the target which improves the quality of the reconstructed image. The accuracy to discriminate the diseased portion from the normal one increases by 5%-10% when reconstruction of complex permittivity of the cells has been done from two opposite sides than that obtained from one single side of the target. Reconstruction of complex permittivity is simulated using FORCE 209 and results are presented using color gradation scale.*

Keywords: *SIRT, double sided scanning, complex permittivity, exact algorithm.*

I. Introduction

Tomography is the pictorial representation of unknown cross section of an object. By this process visualization of the internal structures of an object without the superposition of over- and under-lying structures is possible. Low frequency microwave (about 1 GHz) can be used for this purpose and that's why it is called a non-invasive imaging technique.

Each organ of a biological system has a unique complex permittivity. It consists of a real part called dielectric constant and imaginary part called loss factor or dielectric conductivity. Complex permittivity depends on the tissue type and its condition. When microwave energy is passed through a biological body incident fields at the cells vary with their complex permittivity. Again, complex permittivity in a cell increases with the increase of water content in it. As water content in a cancerous cell increases, complex permittivity also increases in it compared to its normal state. Hence reconstructed complex permittivity can be used to detect cancerous cell in early stage.

Among different reconstruction techniques employed to reconstruct the complex permittivity of the biological target, Simultaneous iterative reconstruction technique shows positive results. In the past few years, iteration reconstruction techniques have been increasingly popular. According to Richmond's moment method dielectric medium is divided into large no. of square cell each of which has constant electric field intensity and complex permittivity. A system of linear equations can be achieved by taking into account that at the centre of each cell total field is equal to incident field and scattered field. Using perturbation technique [3-4] the received field can be used to obtain tomographic image. Subsequent modifications are made in first order and second order algorithm [5].

It has been observed that the above algorithm fails to reconstruct larger model with large number of higher order terms (greater than two) and also fails in case of smaller model with large perturbation.

Considering the limitations of above algorithm, a new exact algorithm [6] has been developed. This algorithm is applied on normal model as well as an diseased model and reconstructed complex permittivity is observed from single side and two opposite sides of the target.

II. An Exact Algorithm For Large Perturbation

The field distribution in unperturbed homogeneous medium is expressed by the following equation:-

$$[C].[E_i]=[E^i] \quad (1)$$

Where E^i is represented as the incident field at i^{th} cell in the free space and E_i represents the internal field at the same i^{th} cell when the medium is assumed to be a homogeneous one having known permittivity distribution and [c] represents the coefficient matrix of homogenous medium.

When the homogeneous biological target is replaced by the inhomogeneous one, the permittivity values of the cell are perturbed simultaneously by small amounts $\Delta\epsilon_i(i=1,2,3..n)$ and if the corresponding changes in the internal field are ΔE_i then

$$[C^{'}].[E_i+\Delta E_i]=[E^i] \quad (2)$$

Where $[C^{'}]$ is the coefficient matrix of the inhomogeneous medium

Subtracting eq 1 from 2 the change in the electric field can be given by

$$\Delta E_i = -x_i E_i^{'} + \sum_{j=1}^{n} x_j E_j \frac{M_{ji(0)}}{\Delta(0)} \quad (3)$$

Where $E_i^{'}$ is the modified field in the i[th] cell under perturbed condition, $\Delta(0)$ and $M_{ji(0)}$ are the determinant and cofactor of (j , i) th element of unperturbed coefficient matrix [C] respectively. x_i is the requisite fractional change in the complex permittivity of the cell with respect to saline water i.e $x_i = (\varepsilon^{'} - \varepsilon_w)/(\varepsilon_w - 1)$ €',€w are the complex permittivity of saline water(74-j40) and model cell respectively. There will be a resultant change in the scattered field at a particular receiver location owing to the change of internal fields at the different cells of the medium caused by perturbation of complex permittivity distribution. The net change in the scattered field, ΔE_R^s (k) at the R[th] receiver location corresponding to the k[th] beam can be determined from the equation

$$\Delta E_R^s = \sum_{j=1}^{n} x_j E_j^{'} \frac{M_{j,R(0)}}{\Delta(0)} \quad (4)$$

Since x_i=0 for all receiver cell as they are located in saleline water.

If E_{Rml} (k) denotes the scattered field intensity at the R[th] receiver location for the kth beam in the inhomogeneous numerical model and E_{Rol}(k) denotes the calculated scattered field intensity at the same receiver location for the same k th beam for the assumed known homogeneous permittivity_ distribution for the object, then the resultant change in scattered field intensity, $\Delta E_k^s(k)$ at a particular receiver location is expressed in terms of the unknown variables xj 's (i.e. the requisite fractional change of unknown permittivity from the assumed initial trial solution of permittivity), relevant cofactors and determinant of coefficient matrix corresponding to the homogeneous medium and perturbed internal fields corresponding to the inhomogeneous model. Therefore, solving previous equation the total change in the scattered field at +

$$\Delta E_R^s(k) = E_{Rml}(k) - E_{Rol}(k) = \sum_{j=1}^{m} x_j E_j^{'} \frac{M_{j,R(0)}}{\Delta(0)} \quad (5).$$

III. Comparative Study between Single Sided Scanning and Multiple Sided Scanning

3.1 Numerical model

The numerical model under study is a biological object, rectangular in shape. The model contains 360 cell of size 1 sq.cm and consists of different human organs viz. liver (46-j10), muscle (50-j23), muscle type material (40-j23) and fat (25-j5). It is surrounded by 340 cells of saline water. It is illuminated by 24 transmitters antenna which is designed with (each of 15x15 dipole array antenna) of beam width 6^0 and the radiation is received by 20 half wave dipoles acting as receiver. The distance between the transmitter and the receiver is 50cm. The total arrangement is immersed in water to get better impedance matching and small antenna size.[5].

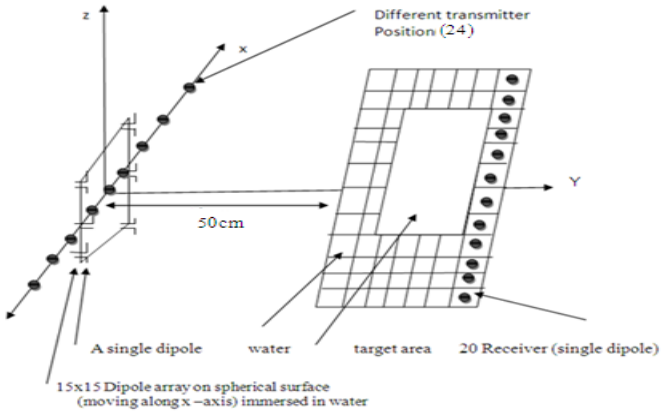

Fig 1 Block diagram of the proposed experimental set up

3.2 Two Opposite Sided scanning of the Biological Target

The quality of the reconstructed image is improved further by incorporating two opposite sided scanning technique which is discussed below in brief:For the different positions of transmitter and receiver complex permittivity is calculated and average is done. A modified cell scanning technique is adopted [7-8] where the beam width of the transmitting antenna is taken as 6^0. Thus the number of cells where change in internal field takes place due to change of complex permittivity in a particular cell is reduced and thereby reduces the error caused by the process of SIRT algorithm itself [3,4,5,6].

.Next, the position of the transmitters and receivers are interchanged and reconstructed complex permittivity of each cell is calculated again by using equation(5). The image of the biological target is reconstructed by using the average value of the complex permittivity in each cell obtained by cell scanning technique from two opposite side of numerical biological object. Employing this, different values of reconstructed complex permittivity are found for the two different positions of transmitters and receivers. Then the average value is calculated.

4.2 Figures and Tables

Using the reconstructed algorithm for all above cases, the experimental data are simulated [9] and corresponding images are shown below:

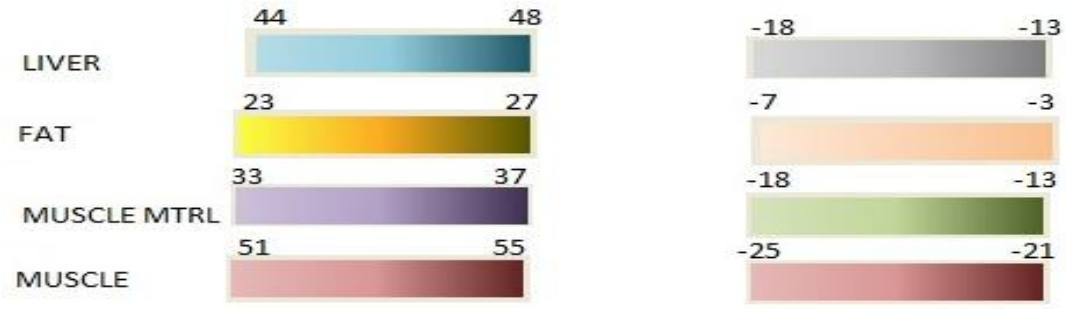

Fig 2 color gradation for real and imaginary parameter respectively

IV. Reconstruction of normal model

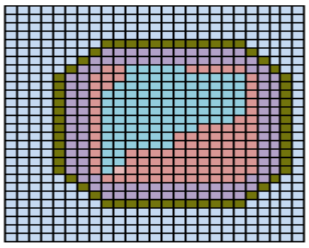

Fig 3.1

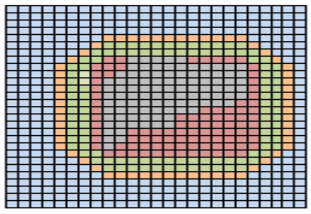

Fig 3.2

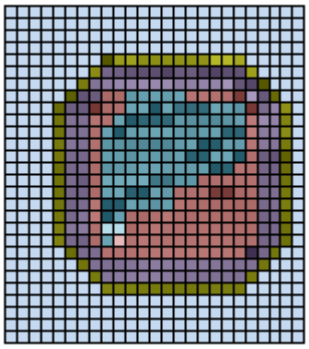

Fig 3.3

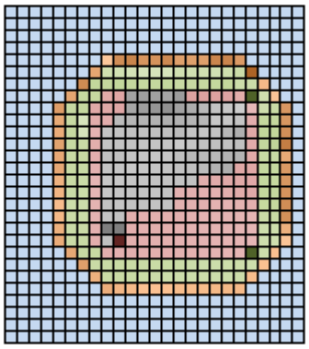

Fig 3.4

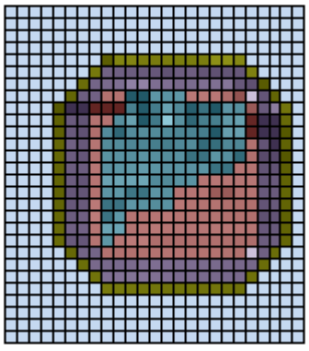

Fig 3.5

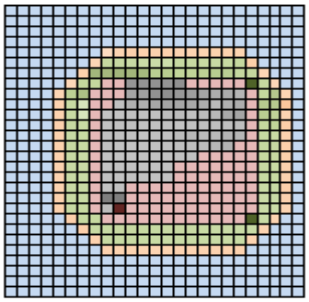

Fig 3.6

Fig 3.1 &3.2: Real and imaginary values of complex permittivity of normal model; Fig 3.3 & 3.4: Reconstructed real and imaginary values of complex permittivity of normal model using single sided view; Fig 3.5 & 3.6 Reconstructed real and imaginary values of complex permittivity normal model using two opposite side views;

V. Reconstruction of Diseased model

The model under study is the same as that considered in earlier case, except its liver region is assumed to be affected and hence characterized by a different value of complex permittivity (48-j12) [1] where as for normal liver it is assumed to the (46-j10).

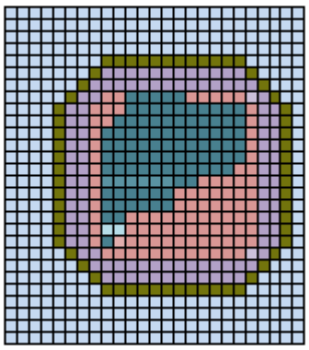

Fig 4.1

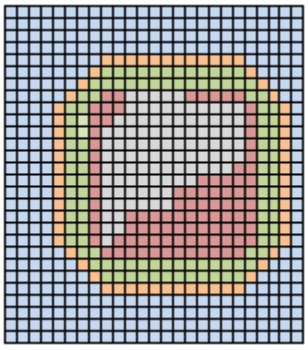

Fig 4.2

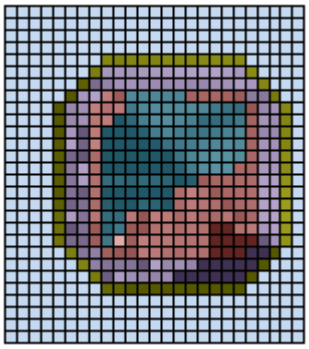

Fig 4.3

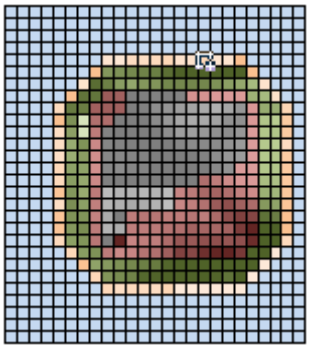

Fig 4.4

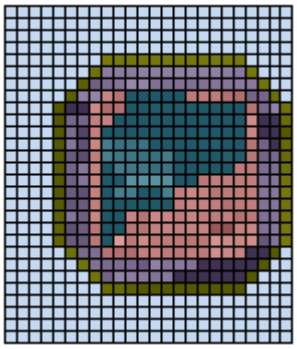

Fig 4.5

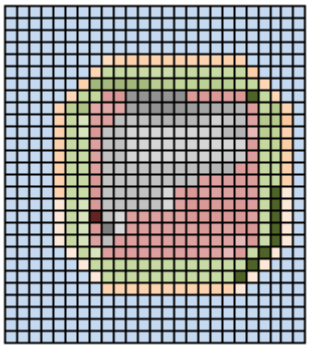

Fig 4.6

Fig 4.1 &4.2: Real and imaginary values of complex permittivity of diseased model; Fig 4.3 & 4.4: Reconstructed real and imaginary values of complex permittivity of diseased model using single sided view; Fig 4.5 & 4.6 Reconstructed real and imaginary values of complex permittivity diseased model using two opposite side views;

Table 1

Average value of permittivity in different organs of the normal model for different cases

Different organs of models	**Average values of complex permittivity of different organs**		
	Normal model	**Reconstructed normal model**	
		Using single side scanning	**Using two opposite side scanning**
Fat	25-j5	24.63-j-4.38	24.70-j4.56
Muscle	53-j27	51.81-j25.12	51.90 -j25.62
Muscle Material	35-j15	33.64-j13.57	34.51-j13.92
Liver	46-j10	44.62-j9.62	45.41-j9.71
Water	76-j40	76-j10	76-j10

Table 2
Average value of permittivity in different organs of the diseased model for different cases

Different organs of models	**Average values of complex permittivity of different organs**		
	Diseased model	**Reconstructed normal model**	
		Using single side scanning	**Using two opposite side scanning**
Fat	25-j5	26.22-j5.96	25.32-j4.56
Muscle	53-j27	51.28 -j22.00	51.91-j29.07
Muscle Material	35-j15	36.33 -j12.93	36.06-j15.43
Liver	48-j12	48.58 -j8.40	48.34-j11.13
Water	76-j40	76-j10	76-j10

VI. CONCLUSION

In this paper an overall improvement in reconstructed image of the biological object has been obtained when Exact SIRT cell scanning technique is applied from two opposite sides of the target.From normal model, the accuracy in reconstructed image of the real part of complex permittivity is increased from (80.4-98.75%) to (92.59%-99.31%) when views are taken from two opposite sides. In case of diseased model the reconstructed image of the imaginary part of the complex permittivity for liver region is far better in double sided cell scanning technique (99.13%) than obtained from single side (70%). The improvement shows that the image quality will be more accurate it will be taken from all sides.

REFERENCES

[1] Susan R Smith & Kenneth R Foster, "Dielectric properties of low-water-content tissues", Phys. Med. Biol., Vol. 30, No. 9, pp.965-973,1985.
[2] H.Richmond, IEEE Trans.Antennas Prop. Vol. AP-B,pp 334-341,1965.
[3] A N Dana & B. Bondopadhyay. Proc. of IEEE; Vol. 74, pp.604-606. 1986.
[4] A N Datta & B. Bondopadhyay.Innov Tech Biol. Med, Vol. 8. pp.409-416. 1987.
[5] K.Purkait. A.N.Datta,"An Improved form of Iterative Reconstruction Algorithm for First Order and Second Order Microwave Image Reconstruction". Indian Journal of Pure & Applied Physics, CSIR, Vol.34.pp.-120-424.
[6] K.Purkait & A.N.Datta, "An Exact Algorithm for Microwave Tomography", presented at symposium HOT-2003,1NRAPHEL.C.U.3rd-5th Feb.2003.
[7] Kabita Purkait and Kalyan Adhikary "Application of Modified Cell Scanning Technique in Exact Algorithm for Medical Diagnosis", IJTS Vol-21,pp.115-127,October 2012.
[8] Kabita Purkait and Kalyan Adhikary," Modification in field measurement applied on exact algorithm for biomedical imaging", IJMER, Vol. 2, Issue-3, pp. 1157-1161, May 2012.
[9] Force 209 FORTRAN Compiler, www.lepsch.com.

International Journal of Modern Engineering Research (IJMER)
www.ijmer.com Vol. 3, Issue. 3, May - June 2013 pp-1602-1605 ISSN: 2249-6645

Applying Second life in New 3DMetaverse Culture to Build Effective positioning Learning Platform for Arabic Language principles

Ahmed Dheyaa Basha[1], Ahmed Isam khaleel[2], Satar Habib Mnaathr[3], Rozinah Jamaludin[4]

*(Center for Instructional Technology and Multimedia (CITM) **Universiti** Sains Malaysia, Penang, 11800, Malaysia)

***Abstract**: This paper aims at investigation an effective e-learning platform where Arabic students from overseas can help and learn others in Malaysia the Arabic Language Principles (ALP) and the new culture of reading Quran by use 3D Metaverse. First, we present the outcomes of preliminary survey to international Muslims students regarding their study interests related to Arabic Language principles (ALP) and Quran culture. Second, we summarize the design and application of our learning platform in Second Life (SL) based on the concept of effective positioning learning that confirms materialized interaction with the external objects/ environment in high process of learning. The platform comprised traditional Arabic architecture for Mosques, such as congregational prayer, Quran recitation, and supplication, use a compass to determine the direction of Kaaba, etc... . The students can also reconnaissance those architectures in virtual space and embodiment with their avatars. Third, we explain the outcome of the analysis of our learning experience in second life (SL) among international and Arabic student based on a lot of interaction between students and with objects in the virtual space. Eventually, We will explicitly and discuss many advantages and constraints of learning process in our study via Metaverse platform in terms effective learning of ALP and Quran culture*.

***Keywords:** Effective positioning Learning, 3DMetaverse, Second life (SL), Engagement of learning .E- learning.*

I. INTRODUCTION

Of late the biggest great interests in applying 3D Metaverse have been growing increasingly and rapidly not just as a collaboration and communication platform or a basic infrastructure of online commerce , but also suitable an infrastructure for immersive and materialized e-learning. Nowadays the second life (SL), is a very popular Metaverse service by private internet Laboratory like an American' Linden Lab (ALL) mimic the many software as a good virtual environment for SL such as phoenix -viewer program which provide a lot of features for SL environment and its applications [1, 5, 6], Moreover (ALL) equips the very effective ambience for building online universities virtual classroom, mosque or place for staff conferences on the internet. Avatar, which materialized a user agent in the three dimension space, can roam around the virtual environment arranged by electronically built objects, interact and collaborate with many of the other materialized 'ideas (avatars). These aspects of the Metaverse have the high great possibility as a platform for effective positioning learning and collaborative and engaged learning among a big number of users that has been some difficulties and obstacles to running on the web based e-learning environment [7, 13]

II. PURPOSE OF STUDY

In this study we have been highly focused on establishing the learning environment for Arabic language principles related teaching and learning the Quran such as congregational prayer , interpretation or Quran recitation, and supplication, use a compass to determine the direction of Kaaba, how the worship in the mosque and some Arabic' culture in 3D Metaverse. Also one of important aims is to provide the international students in Malaysia with their peers from Arabic' countries to learn and study APL and Arabic' culture. The second major goal is to absorb and understand the benefits and disbenefits of 3D Metaverse from the approaches and perspectives of supporting platform for foster the effective positioning learning of ALP and concept of Arabic' culture through to read the Quran and assets of worship in the mosque which materialized in the 3D Metaverse.

III. Terms Used In The Study

1. E-Learning

E-learning is a learning program that makes use of an information network, such as the Internet and multimedia , for course delivery, interaction, and/or facilitating the learning process in different virtual learning environments (VLE) such as MOODLE, blogging tools, social networks, etc.. . Web-based learning is a subset of e-learning and refers to learning using an Internet browser, such as Internet Explorer .In this paper e-learning point to collaboration' station and engagement between participants via suitable electronic means to use 3Dmetaverse [3,8,11].

2. Linden Research

This term derived from Linden Lab, is a privately held American internet company that is best known interesting as the great creator of second life (SL), the major aim is to communicate and collaborate on a lot of projects and applications using (SL) technology around the world[4,12].

3. Metaverse

The term coined in1992 of science fiction novels, where use humans as avatars, through a collective online shared space, to interact with each other and use some software agents in 3D space that uses the metaphor of the real word, in which a lot of collaboration, engagement, and share one of its applications is (SL) created by the gathering of virtually enhanced physically persistent 3D virtual space linked into perceived virtual universe via internet [9, 14].

IV. Methods

1. Introductory survey

Primarily, we managed our survey on students' needs on the topics regarding (ALP) and their culture to about 46 international students from USM university and UUM university in Malaysia from (CITM) faculty and computer sciences from (IT and ICT) apartment for postgraduate students . The participants from this survey were solicited to give answers by free description in Malaysia' universities which mentioned former regarding their needs as well as demographic data related gender, nationality, age, and the length of studying Arabic .As an outcome of the content analysis based on demographic and data, found differences concerning gender. Strongly the female students were more interested in the scarf, meeting in the mosque, and seminar for reading the Quran, while the male students were more interested in terms of congregational prayer especially Friday' day, bowing and prostrating , teach the Quran' principles , and use a compass to determine the direction of Kaaba. Public topics for both genders were traditional structured such as fasting, Eid prayers, Hajj, Umrah and other festivals for Muslims. In addition a lot of them were very interested in the Arabic traditional habits; the "Fig.1" displays some of the effective learning environment for second life (SL).

Fig.1 Displays effective learning environment for second life (SL)

2. Building suitable e-learning environment

In this respect we conducted our survey on the public topics triggered by international students. In addition our specially selected the traditional structuring like prayer and use a compass to determine the direction of Kaaba. All these aspects built in SL for learning APL manner and habits while visiting many of the mosques. Figure 1 displays the snapshots chosen from the ambience of SL in effective learning environment which we have contributed builds in SL.

3. Experiences of Learning

There are two experiences; we conducted in the 3DMetaverse environment, in which we adopted two suitable theoretical framework of learning science, first is effective positioning learning which confirms the interaction and collaboration of learners in contexts of social and cultural. Second is the paradigm of learning by teaching which consider as a key element of concept of collaborative learning. Figure 2 displays the some of the scenes of the experiences of learning.

3.1First experience

Three groups of an international student and Arabic student were partnered in the first experience. All participants or majority of them had little experience using SL. Each group chose one personal computer connected to SL. Hold one avatar, and explored for the learning environment for about one or two hours. Arabic students in Malaysia clarified to the international students about the many Arabs' traditions and habits of prayer such as congregational prayer, Quran recitation, supplication and teach the Quran' principles. The international students keep on experienced those usages while engaging their avatar. In addition they studied by number of questioning on the reason to do this experience, and swapping their suggestions and opinions. Each group had avatar operations and conversations, as well as video were recorded during the experience. Moreover the chat information in second life was conducted and stored also in the log file .After the test; all participants from students had a discussion and collaboration as a group to review their new experience and impression about this culture.

3.2Second experience

Also same three groups of international students from first experience had partnered in the second experience. Three groups of Arabic students were different last time .In addition they made a group of international and Arabic students. Also all participants of students had little experience of using SL .The time was one or two hour o of the experience reversed in

last time, international students had the syllabus related to explain and learning environment ALP with details which mentioned previously .Arabian students questioned once students had a different understanding. They test syllabus together, once their suggestion and opinion didn't match on the habits of visiting a mosque. Moreover the avatar operations, Chat data, and conversation in second life was conducted also and stored into the log file .After the test; all participants from students had a discussion and collaboration as a group to review their new experience and impression about this culture.

V. Results

1. First experience

Finally and after the first experience, the conversation log, Chat data, a record of all avatar operation, and the cloned data of review session was obtained. Concerning to the data collected, the majority of international students referred that the avatar operation in a 3D virtual environment gave them clear comprehension of Arabic' habits and their manner of teaching and learning the Quran and prayer robustly than just the textbook or receiving an explanation in a traditional classroom. Moreover some of Arabic students mentioned were also a very good chance for them to increase their experience to teach another student the detail way of praying in the mosque. Meanwhile, some learners described the sense of mismatch when they learned something different from the actual world. Such as the difficult motion of avatar or some unnatural activity of cited physical objects in the virtual environment, "Fig.2" Displays Scenes of effective learning experiences.

Fig.2 Displays Scenes of effective learning experiences

2. Second experience*:*

As an outcome of the second experience, the all international students debriefed that using an avatar to materialize in the virtual environment to clarify Arabic' habits of Arabic ' students to outstanding their comprehension. Meanwhile Arabic' students had a suggestion and opinion that receive the clarification from international students were very interesting and useful experiencing to reverse their own culture .Moreover, few of them mentioned that was not easy to update their response to international students particularly, once they denied international student's clarification.

VI. Concllsion

This study explained and suggested 3D Metaverse- based learning it can be very effective for the learning of Arabic' habits, principles of Arabic language , and culture compared with the traditional way to learning students with textbook through traditional classroom . Moreover this study suggested process of learning by teaching 3D Metaverse is very useful to foster the consciousness of Arabic culture for both the international and Arab students. In addition this study finds out that the unnatural cloning of the physical space in environment of second life has a big effect on learner's admission of the case and context. This study is very important for collaboration and interaction between learners to exchange the knowledge and skills between them. Current time we plans for the future to include enhancing these problems related this

field as well as expanding into this platform and its possibilities of the 3D Metaverse for effective positioning learning for many languages and different cultures like Arabic language principles(ALP) and culture.

REFERENCES

[1] Bailey, K. M. (1983). Competitiveness and anxiety in adult second language learning: Looking at and through the diary studies.
[2] Brown, J. S., & Adler, R. P. (2008). Open education, the long tail, and learning 2.0. Educause review, 43(1), 16-20.
[3] Bruns, A. (2008). Blogs, Wikipedia, Second Life, and beyond: From production to produsage (Vol. 45). Peter Lang.
[4] Carstensen, L. L., Pasupathi, M., Mayr, U., & Nesselroade, J. R. (2000). Emotional experience in everyday life across the adult life span. Journal of personality and social psychology, 79 (4), 644.
[5] Carter, B. E., & McGoldrick, M. E. (1988). The changing family life cycle: A framework for family therapy . Gardner Press.
[6] Cocciolo, A., & Holbrook, M. (2007). Marketing in the Virtual World: Understanding Consumer Behavior in Second Life. Unpublished essay. http://www. Thinking projects. Org/WP-content/cocciolo_sl_cr. Pdf.
[7] Flintoff, K. (2009). Second Life/simulation: Online sites for generative play. Teaching drama with digital technologies: Applying theatre, drama, and technology to learning, 202-21.
[8] GOKSEL-CANBEK, N., MAKRIDOU-BOUSIOU, D., & DEMIRAY, U. (2009). Lifelong learning through Second Life: Current trends, potentials and limitations. Ανακτηθηκε από: http://academia. Edu. Documents. s3. Amazons. Come/847924/Lifelong_learning_through_Sec ond_Life. Pdf, προσπελάστηκε, 7 (7), 2010.
[9] Kaplan, A. M., & Haenlein, M. (2010). Users of the world, unite! The challenges and opportunities of Social Media. Business horizons, 53 (1), 59-68.
[10] Martin, R. M., & Consalvo, M. Through the looking-glass self: Group identity and avatar design in Second Life. An Online Video Game: New Space of Socialization conference, Montreal, QC. Université de Québec a Montréal. Retrieved from http://lamar. Colostate. Edu/~ rmikealm/docs/costumes. Pdf.
[11] PHOLKE, A. (2007). Second Life as an emerging platform for intercultural education. Unpublished. Masters Dissertation. Berlin: Freie Universität.
[12] Sookhanaphibarn, K., Thawonmas, R., & Rinaldo, F. A MODEL FOR VISITOR CIRCULATION SIMULATION IN SECOND LIFE.
[13] Suler, J. (2004). The online disinhibition effect. Cyberpsychology & behavior, 7 (3), 321-326.
[14] Yee, N. (2006). Motivations for play in online games. CyberPsychology & Behavior, 9(6), 772-77

International Journal of Modern Engineering Research (IJMER)
www.ijmer.com Vol. 3, Issue. 3, May - June 2013 pp-1606-1609 ISSN: 2249-6645

Predicting Total Solar Heat Gain of the Building Using Artificial Neural Network

Rajesh Kumar[1], R. K. Aggarwal[2], Dhirender Gupta[3], Jyoti Dhar Sharma[1]
([1]Deptt. of Physics, Shoolini University, India),
([2]Deptt. of Environmental Science, University of Horticulture & Forestry, India),
([3]Deptt. of Physics, Govt P. G. College, India)

Abstract: *This paper explores total solar heat gain of a six storey building by using neural fitting tool (nftool) of neural network of MATLAB Version 7.11.0.584 (R2010b) with 32-bit (win 32). The calculated total solar heat gain was 199080 kW per year. ANN application showed that data was best fit for the regression coefficient of 0.99794 with best validation performance of 48.9906 during winter.*

Key Words: *Artificial neural network, energy requirement, solar heat gain, regression coefficient*

I. Introduction

Himachal Pradesh is located in north India with Latitude 30° 22' 40" N to 33° 12' 40" N, Longitude 75° 45' 55" E to 79° 04' 20" E, height (from mean sea level) 350 m to 6975 m and average rainfall 1469 mm. For our study we have taken a building in Solan district which is located between the longitudes 76.42 and 77.20 degree east and latitudes 30.05 and 31.15 degree north the elevation of the district ranges from 300 to 3,000 m above sea level. The winter during six months (October to March) are severe and people use electricity (provided on subsidized rates) and conventional fuels (wood, LPG and coal). The summer during six months (April to September) people use electricity (provided on subsidized rates) to lower down the temperature. These results are burden on already depleting conventional fuels and same time causing emission of CO_2 and global warming. The other option to meet out energy requirement is solar passive technologies. This requires measured data of solar radiation which is not available in the state. This can be estimated by using various models on the basis of sunshine hour or temperature data. The mean hourly values of such data for various places in India are available in the handbook by [1]. As in statistical methods we have to deal with higher level of mathematics. Due to tough calculations, the probability of error is more. Evaluation, estimation and prediction are often done using statistical packages such as SAS, SPSS, GENSTAT etc. Most of these packages are based on conventional algorithms such as the least square method, moving average, time series, curve fitting etc. The performances of these algorithms are not robust enough when the data set becomes very large. This approach is very much time as well as mind consuming. Therefore ANN is much better than these methods. Neural networks have the potential for making better, quicker and more practical predictions than any of the traditional methods. They can be used to predict energy consumption more reliably than traditional simulation models and regression techniques. Artificial Neural Networks are nowadays accepted as an alternative technology offering a way to tackle complex and ill-defined problems. They are not programmed in the traditional way but they are trained using past history data representing the behavior of a system.

ANNs are the most widely used artificial intelligence models in the application of building energy prediction. In the past twenty years, researchers have applied ANNs to analyze various types of building energy consumption in a variety of conditions, such as heating/cooling load, electricity consumption, sub-level components operation and optimization, estimation of usage parameters. In 2006, [2] did a brief review of the ANNs in energy applications in buildings, including solar water heating systems, solar radiation, wind speed, air flow distribution inside a room, pre-diction of energy consumption, indoor air temperature, and HVAC system analysis. Olofsson developed a neural network which makes long-term energy demand (the annual heating demand) predictions based on short-term (typically 2–5 weeks) measured data with a high prediction rate for single family buildings [3]. Kreider reported results of a recurrent neural network on hourly energy consumption data to predict building heating and cooling energy needs in the future, knowing only the weather and time stamp [4]. Kalogirou used neural networks for the prediction of the energy consumption of a passive solar building where mechanical and electrical heating devices are not used [5]. Wong used a neural network to predict energy consumption for office buildings with day-lighting controls in subtropical climates [6]. Aydinalp showed that the neural network can be used to estimate appliance, lighting and space cooling energy consumption and it is also a good model to estimate the effects of the socio-economic factors on this consumption in the Canadian residential sector [7]. Sheikh did Short Term Load Forecasting using ANN Technique [8]. Karatasou studied how statistical procedures can improve neural network models in the prediction of hourly energy loads [9].

II. Methods And Material

The six storey administrative block of Shoolini University building at Bajhol-Solan (HP) "Fig 1" has been taken for the study, which worked for seven hours during a day time. The dimensions were length 45 m, 15 m wide and 18 m in height. The neural fitting tool (nftool) of neural network of MATLAB Version 7.11.0.584 (R2010b) with 32-bit (win 32) had been used. The temperature and humidity of the building had been measured by using 'Thermo Hygrometer'. The other required data had been taken from NASA website.

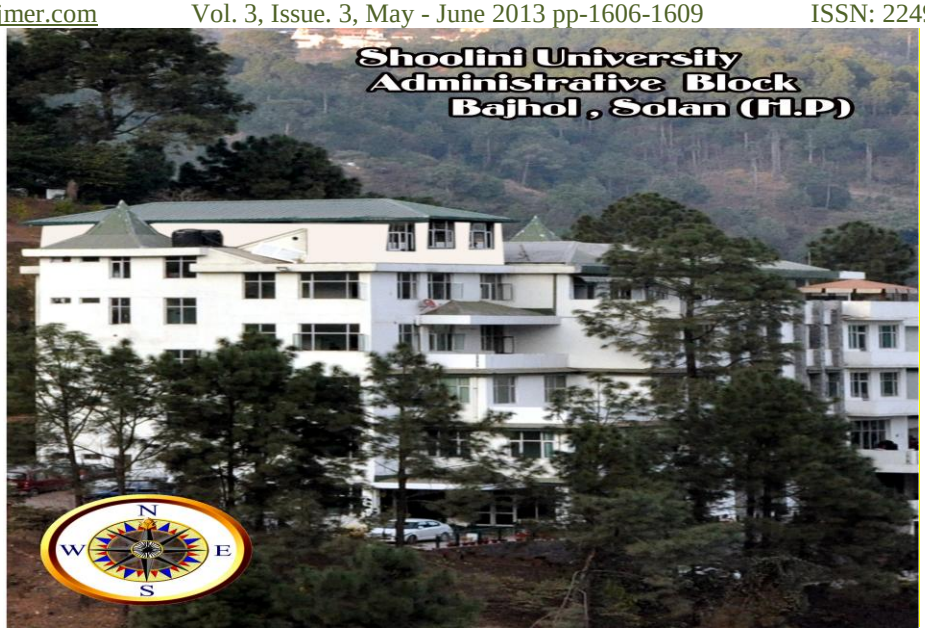

Fig 1. Shoolini University administrative block at Bajhol-Solan (HP)

The solar gain through transparent elements can be written as:

$$Q_s = \alpha_s \Sigma A_i S_{gi} \tau_i \quad (1)$$

where

α_s = mean absorptivity of the space, A_i = area of the ith transparent element (m^2), S_{gi} = daily average value of solar radiation (including the effect of shading) on the ith transparent element (W/m^2), τ_i = transmissivity of the ith transparent element.

Irrespective of developing a new model the neural fitting tool (nftool) of neural network of MATLAB Version 7.11.0.584 (R2010b) with 32-bit (win 32) had been used. Out of six samples four had been used for training, one sample each had been used for validation and testing. The architecture of the artificial neural network used in the study is shown in "Fig 2".

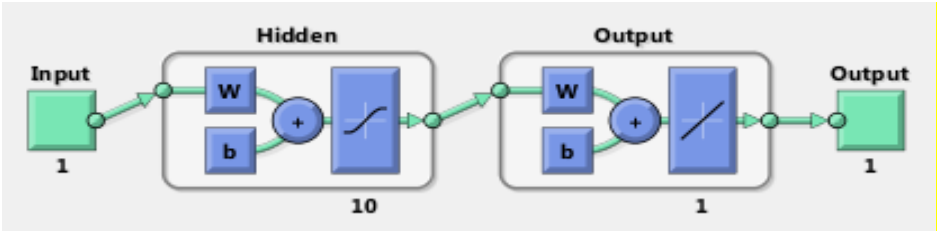

Fig.2 Architecture of neural network

III. RESULTS

The total solar gain in a building during winter is calculated as "Table 1".

Table 1. Solar Heat Gain During Winter

Wall Exposed to Sun	A (In m)	S_g (W/m^2)	Q_s (In kW)
South wall	206.0	202.4	20
North wall	89.7	0	0
West wall	54.4	109.7	2.9
East wall	36.4	107.2	1.9
Roof	518	264.8	65.8
		Total heat gain per annum	114156

Q_s = 90.6 kW = 114156 kW per annum whose ANN graphs are shown in "Fig 3" & "Fig 4"

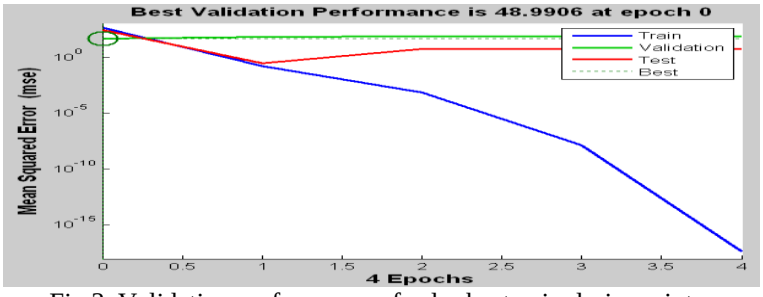

Fig 3. Validation performance of solar heat gain during winter

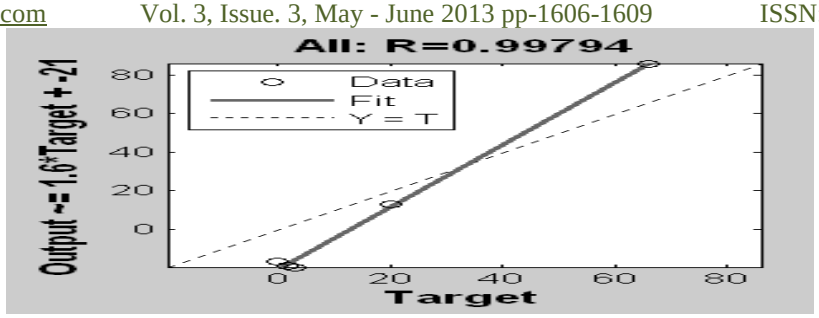

Fig 4. Regression analysis of solar heat gain during winter

The total solar gain in a building during summer is calculated as "Table 2".

Table 2. Solar Heat Gain During Summer

Wall Exposed to Sun	A (In m)	S_g (W/m^2)	Q_s (In kW)
South wall	206.0	202.4	12.5
North wall	89.7	0	0
West wall	54.4	109.7	3.1
East wall	36.4	107.2	1.8
Roof	518	264.8	50.0
		Total heat gain per annum	84924

Q_s = 67.4 kW = 84924 kW per annum whose ANN graphs are shown in "Fig 5" & "Fig 6"

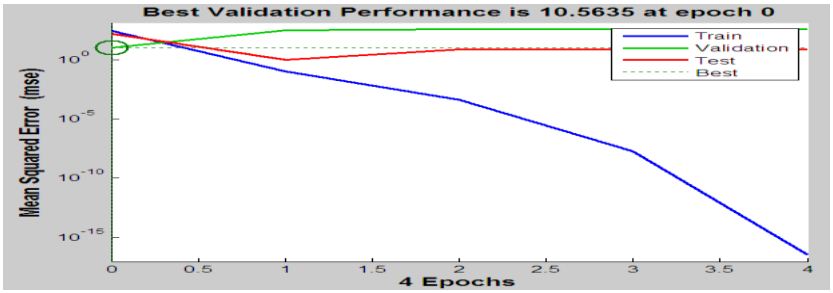

Fig.5. Validation performance of solar heat gain during summer

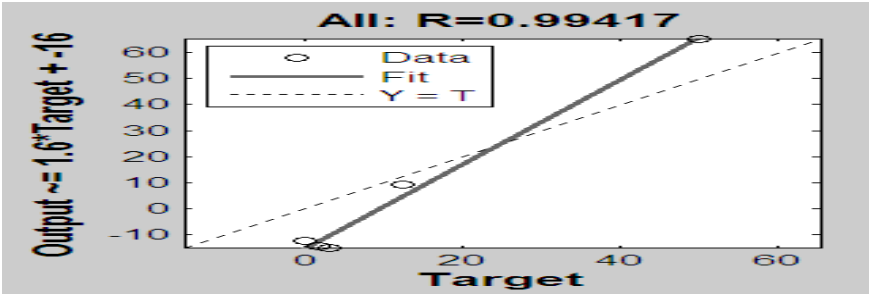

Fig.6. Regression analysis of solar heat gain during summer

Total Load = 1211228 +874668 kW,
Total Load = 2085896 kW

IV. DISCUSSION

In most residential buildings, optimization of thermal comfort and energy consumption is not achieved. From the above system descriptions one can see that ANNs have been applied in a wide range of fields for modelling, prediction and control of building energy systems. What is required for setting up such systems is data that represents the past history and performance of the real system and a suitable selection of ANN models. The accuracy of the selected models is tested with the data of the past history and performance of the real system. The neural network model was used with 10 hidden neurons which didn't indicate any major problem with the training. The validation and test curves were very similar. The next step in validating the network was to create a regression plot, which showed the relationship between the outputs of the network and the targets. If the training were perfect, the network outputs and the targets would be exactly equal, but the relationship was rarely perfect in practice. The three axes represented the training, validation and testing data. The R value was an indication of the relationship between the outputs and targets. If R = 1, this indicated that there was an exact linear relationship between outputs and targets. If R was close to zero, then there was no linear relationship between outputs and targets.

V. CONCLUSION

The study revealed that the total solar heat gain of a six storey building by using neural fitting tool (nftool) of neural network of MATLAB Version 7.11.0.584 (R2010b) with 32-bit (win 32) was 199080 kW per year. ANN application showed that data was best fit for the regression coefficient of 0.99794 with best validation performance of 48.9906 during winter. These results necessitate the use of solar passive technologies to meet out this energy requirement during winters and summers. Increasing awareness of environmental issues has led to development of a large number of energy conservation technologies for buildings, especially in more developed countries [10]. Energy savings potential (ESP) is a very important indicator for developing these technologies.

VI. Limitations

ANN models like all other approximation techniques have relative advantages and disadvantages. There are no rules as to when this particular technique is more or less suitable for an application. Result of ANN depends upon number of hidden layer neurons. In order to get optimize result we should select optimize number of hidden layer neurons. One way of selecting hidden layer neuron using optimize algorithm technique and other way is hit and trial method. In existing proposed model hit and trial method has been used but it is never easy to comment that the used number of hidden neurons is perfect.

References

[1]. A. Man, and S. Rangarajan, *Solar radiation over India* (Allied Publishers, New Delhi, 1982).
[2]. S.A. Kalogirou, Artificial neural networks in energy applications in buildings, *International Journal of Low-Carbon Technologies, 1(3),* 2006, 201–16.
[3]. T. Olofsson and S. Andersson, Long-term energy demand predictions based on short-term measured data, *Energy and Buildings, 33(2),* 2001, 85–91.
[4]. J.K. Kreider, D.E. Claridge, P. Curtiss, R. Dodier, J.S. Haberl and M. Krarti, Building energy use prediction and system identification using recurrent neural networks, *Journal of Solar Energy Engineering, 117(3),* 1995, 161–6.
[5]. S.A. Kalogirou and M. Bojic, Artificial neural networks for the prediction of the energy consumption of a passive solar building, *Energy, 25(5),* 2000, 479–91.
[6]. S.L. Wong, K.K.W. Wan and T.N.T. Lam, Artificial neural networks for energy analysis of office buildings with day lighting, *Applied Energy, 87(2),* 2010, 551–7.
[7]. M. Aydinalp, V.I. Ugursal and A.S. Fung, Modeling of the appliance, lighting, and space cooling energy consumptions in the residential sector using neural networks, *Applied Energy, 71(2),* 2002, 87–110.
[8]. S.K. Sheikh and M.G. Unde, Short Term Load Forecasting using ANN Technique, *International Journal of Engineering Sciences & Emerging Technologies, 1(2),* 2012, 27-107.
[9]. S. Karatasou, M. Santamouris and V. Geros, Modeling and predicting building's energy use with artificial neural networks: methods and results, *Energy and Buildings, 38(8),* 2006, 949–58.
[10]. M. Chikada, T. Inoue et al., Evaluation of Energy Saving Methods in a Research Institute Building, *CCRH. PLEA2001-The 18th Conference on Passive and Low Energy Architecture, Florianopolis-BRAZIL,* 2001, 883–888.

International Journal of Modern Engineering Research (IJMER)
www.ijmer.com Vol. 3, Issue. 3, May - June 2013 pp-1610-1616 ISSN: 2249-6645

A Novel Approach to Ontology Based Hybrid Intelligent Data Mining Assistance (HIDMA)

Syed Abusali.V[1], Syed Ali.A[2]
[1]*Lecturer, Department of Computer Science & Engineering, TJ Institute of Technology, Chennai, India*
[2]*Assistant Professor, Department of Computer Science & Engineering, TJ Institute of Technology, Chennai India*

Abstract : *An efficient application of a data mining process is littered with many difficult and technical decisions such as data refining, feature transformations, algorithms, parameters, evaluation. Subsequently most data mining products provide a large number of models and tools but few provide intelligent assistance for addressing the above mentioned challenges that face the non specialist data miner. In this paper, we propose the realization of a hybrid intelligent data mining assistant(HIDMA) based on the synergistic combination of both declarative and procedural ontology knowledge in order to empower the non specialist data miner throughout the key phases of the Cross Industry Standard Process for Data Mining (CRISP-DM) process.*

Keywords: *Knowledge Acquisition, Knowledge Representation, Ontologies, Case based Reasoning, Data Mining, Declarative and Procedural knowledge.*

I. INTRODUCTION

In order to remain competitive in the business world, decision makers have begun to turn to data mining (DM) technology to cope with the information deluge and meet their informational needs. Although data mining does promise to uncover potentially valuable, useful and implicit knowledge from one's abundant data repositories, the effective application of data mining still faces some very serious challenges:

- Data mining research seems to be based on specialized techniques (statistics, machine learning, information theory, database technology etc.) whereas research on and even epistemological aspects of DM are rare [1].
- Current DM processes make very little use of already existing corporate knowledge. Consequently, DM is more tedious than is necessary and can tend to produce already known information.
- Existing DM methodologies only provide general directives, however what a non specialist really needs are explanations, heuristics and recommendations on how to effectively carry out the particular steps of the methodology.

In this paper, Section 2 presents some key challenges with providing intelligent DM assistance. Section 3 summarizes related work both in the fields of data mining and ontologies, and the use of CBR (Case Based Reasoning) and ontologies. In Sections 4 and 5 respectively, we provide a system overview and design details of our proposed intelligent DM assistant. Section 6 provides a brief discussion and Section 7 presents the conclusions and future work.

II. THE REAL CHALLENGES OF DATA MINING PROCESS IN HIDMA

2.1 Supports for the Non Expert Data Miner

Most Commercial data mining products either do not offer any intelligent assistance (decision support) or tend do so in the form of rudimentary "wizards like" interfaces. These wizards like interfaces make hard assumptions about the level of background knowledge required by a user in order to effectively use the system (i.e. Oracle Data Miner, SAS Enterprise Miner, etc.). This fact has been further supported by [2]. For instance, the following is a concise list of important decisions that must be considered during a DM process:

- How to effectively perform data quality verification?
- How to efficiently perform the data preparation phase (i.e. sampling, missing values, discretization)?
- Which statistical or machine learning algorithm is most appropriate?
- Which training parameters are most appropriate?
- How to deal with a potential class imbalance problem?
- How to avoid model over fitting?
- How to improve the accuracy rate (i.e. error rate)?
- Which evaluation method is most appropriate?

Over the past several decades the fields of statistics and machine learning have produced a myriad of models/algorithms that can be readily exploited by data miners. Consequently this profusion of algorithms has dramatically burdened the data miner with difficult decisions that must be addressed in order to effectively apply DM to produce useful and meaningful results.

2.2 Fostering Knowledge Reuse

With respect to the overall data mining process, most enterprises do not directly manage tacit knowledge (i.e. useful generalizations for answering above questions) in a form that can be effectively stored, refined and reused. Most products simply archive DM activities, but leave it up to the user to intelligently manage this knowledge. An intelligent DM assistant should possess the necessary characteristics that allow it to learn from past experience and empower the user of the system to avoid the repetition of mistakes.

2.3 Beyond Model Selection Support

Previous research efforts into intelligent DM assistants have focused on providing a user with model selection support ([3], [4], [5], [6]). The selection of an appropriate algorithm for a given data mining task may be considered necessary, but is definitely not sufficient for ensuring the successful outcome of a DM project. Our appeal to an intelligent DM assistant implies the realization of a system that is capable of aiding a user throughout the key phases of the data mining process. To complicate matters, and add to the requirements for an intelligent assistant, it must be emphasized that these phases tend to be strongly inter dependent. For instance the choice of a given DM algorithm (data modeling phase) is dependent on the inherent characteristics of the data being mined (data understanding phase), while the activities carried out during the data preparation phase depend both on data quality (data understanding phase) and the chosen DM algorithm (data modeling phase).

2.4 A Need for Detailed Knowledge

DM processes adequately specify the phases, tasks and activities that need to be carried out during a DM project but provide very little detailed knowledge for the novice miner on how to actually carry out a given step. For example, the proper application of a simple linear regression model requires that the user possess some detailed knowledge (or basic heuristics) for effectively carrying out the model evaluation phase for a given DM task (i.e. significance testing, residue normality and model variance).

III. RELATED WORK

Several previous research efforts have demonstrated the effectiveness of using ontologies for supporting the knowledge discovery process. Bernstein et al. have proposed an intelligent data mining assistant based on the use of ontology [8]. Their ontology contains constraints and performance knowledge that is eventually searched for in order to find a ranking of possible satisfactory DM processes (based on user input). As shall be elaborated upon our aim is to provide a hybrid data mining assistant that leverages the synergy between the CBR paradigm and ontology based DM knowledge. Phillips and Buchanan have used ontologies to guide the feature selection step of the knowledge discovery process [7]. Bauer and Baldes have used an ontology based interface to aid non expert users of machine learning (ML) better understand and influence an ML system from a semantic perspective [9]. Canataro and Camito have demonstrated the use of DM ontology to simplify the developmentof distributed knowledge discovery applications in the area of grid computing [10]. Although our DM ontology has similar high level concepts, we have significantly extended our ontology to provide detailed knowledge (i.e. data quality verification, data preparation and model evaluation) using a rule base and associated rule based reasoner. In addition, we have also based our DM ontology model explicitly on the structured approach used by the CRISP DM methodology (industry recognized and virtually the de facto DM process) [11]. Moreover, a number of previous research efforts have demonstrated the effectiveness of combining ontologies with the CBR paradigm. Aamodt et al. have developed a KI CBR framework (CREEK) based on the use of ontologies [12]. Bello Thomas et al. have developed a framework for building CBR systems that use task/method ontology for promoting problem solving methods reuse [13]. Bichindaritz has demonstrated the use of ontologies for facilitating case structuring and acquisition [14].

IV. SYSTEM OVERVIEW

The following is a continuation from previous work where a strong case has been established for exploiting the synergistic combination of DM ontology and the case based reasoning paradigm [15]. This section briefly introduces the key features of both our CBR system and DM ontology implementations. As illustrated in Figure 1, our hybrid DM assistant consists primarily of six major components: a DM Case Base, a DM Ontology, a Case Reasoner, Rule Reasoner, a DL Reasoner (Description Logic), and a DM Assistant Interface. For the DM Case Base, we chose to use the CRISP DM data mining process as a basis for eliciting a set of representative features for our case representation. CRISP DM efficiently captures “knowledge” (in the form of a series of well defined phases, tasks and activities) of the entire data mining effort. From this, we were able to define a DM case representation consisting of 53 features. The majority of our indexes were derived from measures used in the area of data characterization (i.e. general, statistical and information theoretic) [16]. For the reasoning component of our CBR system, we implemented a feature weighted, instance based learning algorithm (IBL) [17].

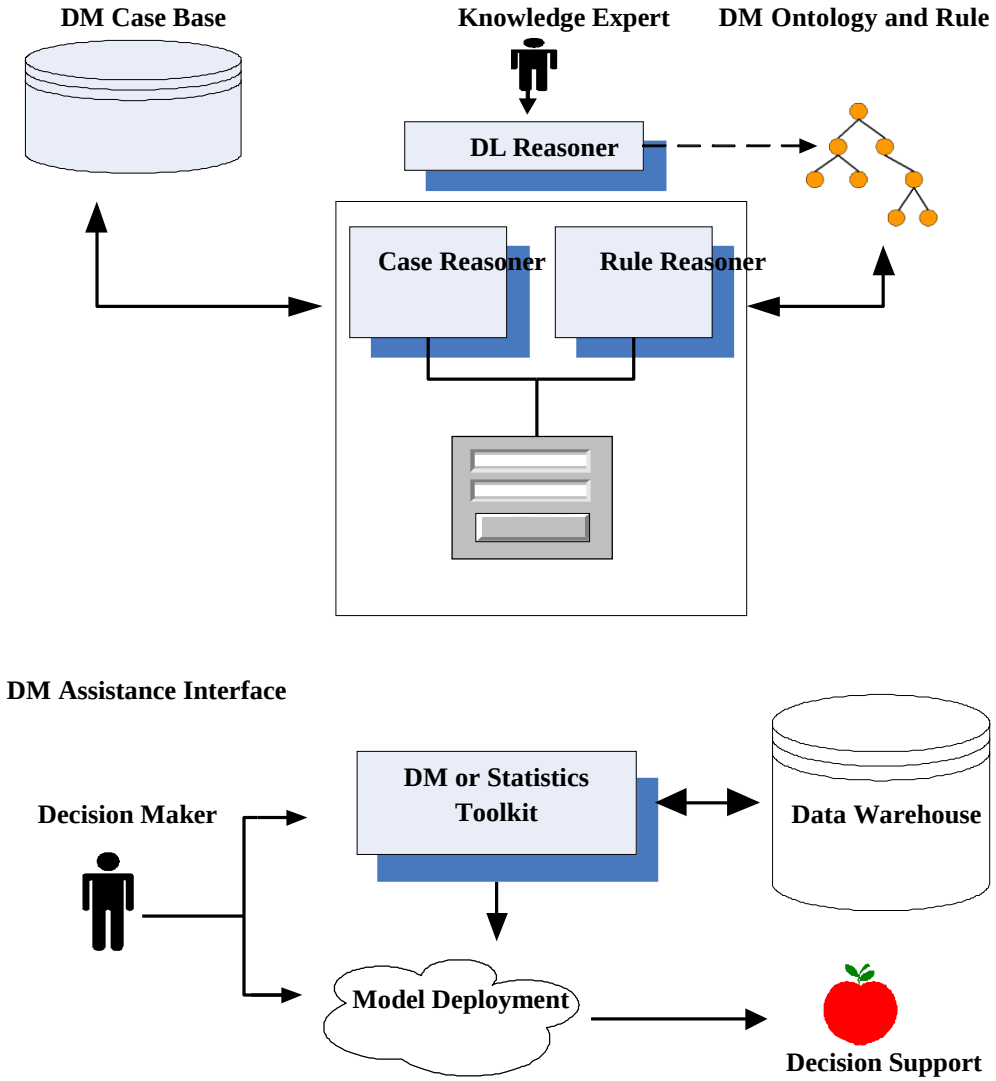

Figure1. System Architecture of Intelligent DM Assistant

Our preliminary CBR evaluation has yielded some promising DM assistant results. Although through its use, the CBR system is capable of learning useful "business problem to DM case" knowledge, it fails to provide the "deeper" knowledge that is essential for supporting a non specialist data miner (i.e. for case adaptation). As such our DM ontology (by formally capturing concepts, relationships, constraints and rules) is capable of complementing the CBR system and addressing this need by assisting the non expert data miner by means of recommendations and heuristics during the course of a DM task. The implementation of our ontology has consisted of two separate phases: (1) the high level knowledge representation of the CRISP DM methodology and (2) the representation of detailed DM knowledge in the form of concepts and rules.

During the early stages of our investigations on the nature of detailed DM knowledge (i.e. how to deal with the class imbalance problem), we concluded that such knowledge tends to most appropriately take a procedural or rule like form. Hence, we have elicited a preliminary set of rules for providing intelligent DM assistance (i.e. heuristics, recommendations, automatic responses) during the key phases of the DM process (Data Understanding, Data Preparation, Data Modeling, Evaluation). These rules are implemented using a proposed rule language standard for the semantic web (SWRL [18]). More specifically, these were implemented using the Protégé SWRL Tab plug in [19]. Subsequently during operation of our DM assistant, a rule based reasoner (JESS [20]) operates on a set of "facts". The facts consist of both automatically supplied and user supplied case attributes. When appropriate the rule based reasoner "fires" rules which then provide heuristics and recommendations to a user or automatically.

We shall be using the general term "advice" to represent any assistance provided by the system (i.e. text message or automated fact response), we do make a clear distinction between a recommendation and a heuristic (both are sub types of the term advice). A recommendation is a more formal type of advice (assertion) while a heuristic should be interpreted less formally by a user (i.e. rule of thumb). The CBR and DM ontology subsystems have well defined knowledge representation roles. The DM ontology defines and manages high level concepts (i.e. tasks, activity types, algorithms, etc.) while the CBR holds detailed case information (i.e. data preparation steps, model parameters, etc.). From another perspective the CBR learns problem (i.e. business and data characteristics) to solution (i.e. data preparation, modeling and evaluation) mappings while DM ontology provides additional assistance (complements where the CBR lacks knowledge) to a user during the

various phases of the DM process. Although not the focus of this paper, the DM ontology also provides the user with basic definitions for all the vocabulary terms used within the DM Assistant Interface. For the moment we are mostly making use of a DL reasoner for the purposes of assuring the consistent evolution of our ontology (consistency checking).

V. ONTOLOGY BASED HYBRID INTELLIGENCE DM ASSISTANCE

This section shall be addressing how the above mentioned system components are synergistically combined to provide a novice data miner with ontology guided DM assistance. In order to facilitate the discussion that follows Figure 2 essentially provides a abstract view of the principle components, some important DM case attributes are represented by the DM Assistance Information Grid, an ontology segment represents some detailed knowledge and several SWRL rules are given. In addition, for the moment ontology guided DM assistance is primarily restricted to the three most important phases of the CRISP DM methodology (i.e. Data Understanding, Data Preparation and Data Modeling). Although the CBR paradigm provides the benefit of retrieving similar cases, the required solution part is rarely an exact match to the current DM problem being attempted.

Hence after the retrieval and reuse CBR phases are completed, the user is faced with the grand challenge of examining the chosen cases' contents and revising certain attributes (i.e. data quality verification, data preparation or data modeling values) in order to retrofit the case to reflect the state of the current DM problem. As a result we have attempted to enrich our DM assistant with complementary knowledge (OWL ontology concepts, individuals and rules) in order to provide the user with adaptation or validation knowledge to complete her DM task.

5.1 Case Facts

Our system is essentially data driven and employs a forward chaining rule based inference engine (JESS). A user basically interacts with the DM Assistant Interface (the DM Assistant Information Grid in Figure 2) by entering or modifying a series of DM case attribute values. The abbreviated DM Assistant Information Grid represents the state of the "working memory" of the system. As the user changes the state of the working memory, the SWRL rules come into play to provide automatic responses (modifying facts) and advice in the form textual messages. The main purpose of the textual messages is to actively assist and empower the user to provide acceptable fact values. Typically having chosen a basis case to work with for a given DM task, a user progresses through the CRISP DM methodology by answering facts.

5.2 Initial Bootstrap Advice

Under ideal circumstances, the state of the initial working memory should be adequately specified from automatically provided facts (i.e. "Ratio of missing values", etc.) to allow the firing of certain rules (and subsequent automatic responses and/or advice) to move the DM process forward. Nevertheless, there are circumstances when user input is required (i.e. identification of incomplete or erroneous values, table joins performed on the data). When such facts are required directly from the user, initial textual messages (bootstrap advice) are given to the user, explaining how to acquire the missing information. This approach is analogous to traditional AI interview or conversational techniques used for soliciting tacit information from the user.

5.3 Detailed Ontology Knowledge

We have currently implemented an OWL DL ontology (using the Protégé editor) of approximately 200 data mining concepts comprising of methodology knowledge (CRISP-DM) and detailed DM knowledge (Data Preparation Advice, Data Modeling advice, DM algorithms, etc.). The concepts illustrated in the ontology segment of Figure 2 (starting from the root Data Prep Advice concept), represent important potential data mining problems that can have a significant impact on the final quality of a generated model. For instance, some algorithms can perform poorly if the quantity of examples becomes large while other machine learning algorithms can be Fairly easily mitigate these problems significantly affected by the curse of dimensionality (too many attributes). An experienced data miner can by applying a supplementary procedure (i.e. aggregation, a cost sensitive learning method, etc.). Specific advice for a given problem is represented by ontology individuals (as indicated by dashed ovals). Complemented with the rule based reasoning approach discussed above, the advice can contain specific textual attributes or associations to more specialized individuals that provide further advice as order to target varying levels of ontology knowledge detail depending on the user's level of DM expertise. For instance, an expert DM user may be satisfied with getting general advice such as "Apply a Dimensionality Reduction technique", while a less experienced user may wish a specific recommendation for using a particular technique such PCA (Principal Component Analysis). The detailed DM knowledge (in the form of SWRL rules) was mainly elicited from introductory data mining texts ([21], [22]), the Weka mailing list [23], scientific articles (too numerous to mention in this paper) and our own DM experiences.

DM Assistant Information Grid

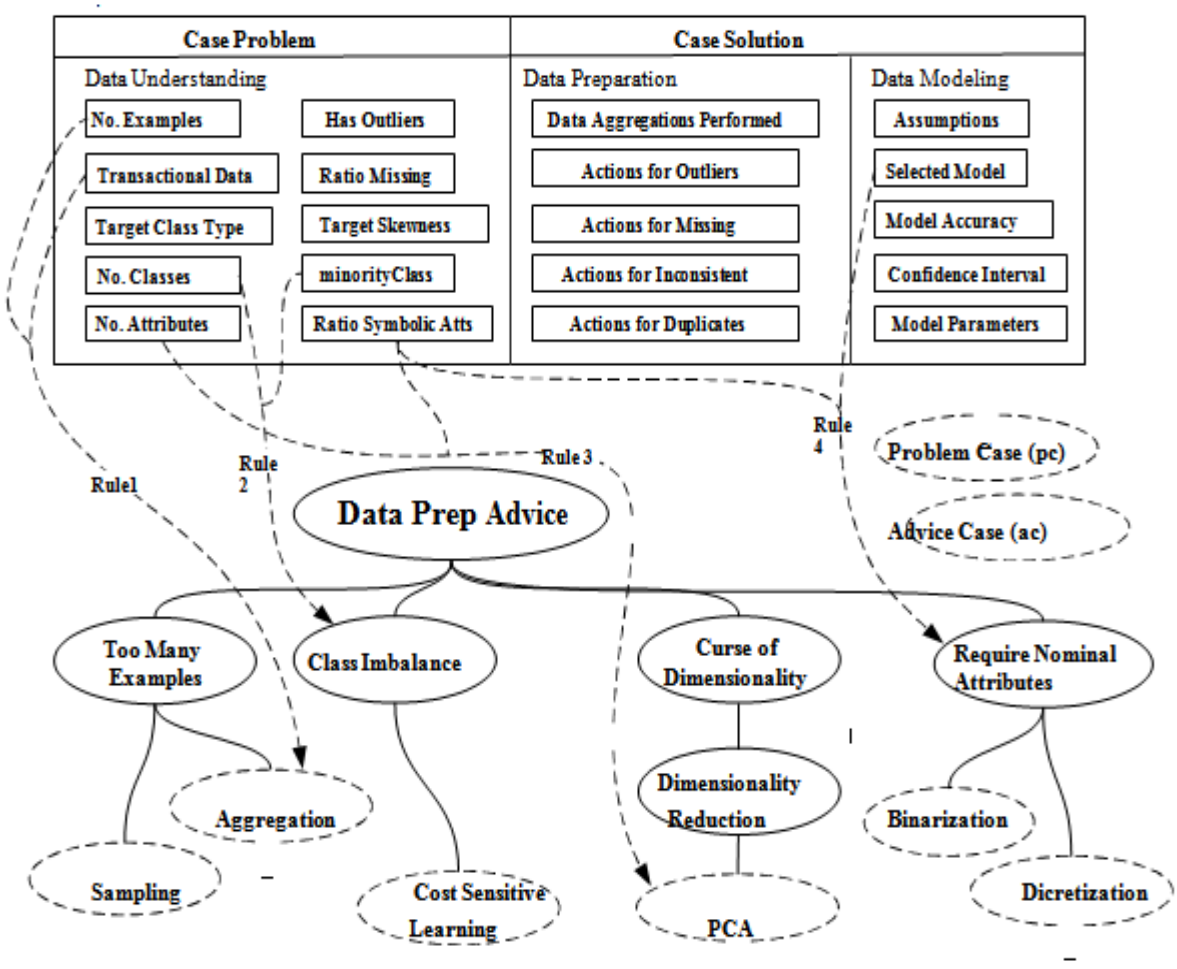

Figure 2. Abstract View of the CBR (case facts), Ontology Knowledge and SWRL Rules

5.4 The Synergistic SWRL Rule Set

The SWRL rules provide two important benefits for the realization of our system, (1) a convenient method for expressing domain knowledge as a set of antecedent consequent pairs and (2) provide an integration mechanism for bridging knowledge from two disparate knowledge bases (CBR and ontology). We have currently defined a preliminary rule set of approximately 50 SWRL rules that span the three main phases of the CRISP-DM methodology. Due to space limitations the examples herein shall only be limited to the Data Preparation phase (some rules are illustrated as dashed lines in Figure 2. For instance, the following rule represents detailed knowledge that may be required for successfully performing the data preparation phase:

Rule1 := NoExamples (pc, ?x1) ^ swrlb:greaterThan(?x1, 30000) ^ transactionData(pc, True) => advice(ac, aggregation)

The above SWRL rule asserts that if the problem case (pc) has an "example count" greater than 30000 and the dataset is of a "transactional type", the user should consider performing an aggregation operation over the dataset. An arbitrary "adaptation case" (ac) individual is used for holding advice values. Furthermore, Rule2 below essentially expresses that if a binary class problem has its minority class represented by less than 15%, a class imbalance problem may be eminent:

Rule2 := numOfClasses(pc, 2) ^ minorityClass(pc, ?x1) ^ swrlb:lessThan(?x1, 0.15) => advice(ac, classImbalance)

Hence, the class Imbalance individual provides advice by offering a cost sensitive learning algorithm (to attempt to improve overall model performance). In addition, the following rule asserts that if the quantity of attributes is greater than 20 (but less than 50 as PCA can be computationally prohibitive) and the "symbolic attributes ratio" is zero(only numerical values)then the system would recommend specifically using the PCA dimensionality reduction technique:

Rule3 := noAttributes(pc, ?x1) ^ swrlb:greaterThan(?x1, 20) ^ swrlb:lessThan(?x1, 50) ^ ratioSymbAttributes(pc, 0) => advice(ac, PCA)

5.5 Current Focus and Limitations

Since the area of data mining is a highly knowledge rich environment (i.e. data refining, feature transformation, algorithms, parameters, evaluation, etc.) it is impossible to foresee capturing all the DM knowledge that is required to support users under all conceivable circumstances. Hence our current prototype detailed ontology knowledge is currently constrained to the following:

(1) Support the data preparation phase for handling common data quality and model input requirements.

(2) Support for common classification models (i.e. linear/logistic regression, naïve bayes, most decision trees, support vector machines.

(3) Common data modeling issues (i.e. class imbalance, curse of dimensionality, basic model over fitting avoidance)

(4) General knowledge for model evaluation (i.e. P-values, cross validation, ROC curves).

(5) Specific tool dependent knowledge is only available for the Weka environment.

Hence more advanced topics such as Meta learning, feature selection, massive datasets, model comparison methods and intricate classifier parameter details are not yet covered. Realistically, our objective has been to elicit a "first pass" to capture common DM knowledge (as is pertinent to our application domain - see Section 6) and subsequently evolve our ontology as the needs arise (i.e. to handle specialized and exceptional DM process conditions).

VI. DISCUSSION

A prototype version of our DM assistant has recently been deployed to support a strategic decision support department. The business objectives consist of analyzing large amounts of student academic details and deriving various predictive and explanatory models using a range of data mining tools (i.e. Oracle Data Miner, SAS Data Miner and Weka). During our early attempts at soliciting detailed DM knowledge using our OWL DL based ontology, we quickly encountered several problems when attempting toimplementproceduralor rule like knowledge,

(1) DL based ontologies are declarative in nature.

(2) Attempting to use existing ontology query languages (i.e. SPARQL, RDQL) for emulating reasoning mechanisms was deemed unmanageable. Hence, this problem was resolved by making use of SWRL rules and an external rule based inference engine (JESS). Several recent research activities in the area of the semantic web have demonstrated a similar need for integrating a rule base and associated reasoner with ontologies ([24], [19]).

In addition, it is worth noting that the SWRL rules could have been implemented purely using propositional rules (without using ontology concepts and individuals). Nevertheless, we believe that the formal capture and representation of detailed DM knowledge within ontology provides some important benefits,

(1) It provides a more explicit form of knowledge representation that is more amenable to human interpretation.

(2) It may provide a knowledge representation format that can be readily exploited by other reasoner (i.e. DL reasoner).

(3) Unlike traditional rule bases where the relationships between the rules tend to be "opaque", the explicit representation of linguistic variables as formal ontology concepts facilitates rule set maintenance.

Overall the proposed approach provides an additional benefit in that knowledge management efforts can be performed in several independent stages. For instance, declarative DM knowledge can first be elicited, and subsequently another domain expert can make use of this knowledge to craft a set of SWRL rules for expressing procedural DM knowledge.

VII. CONCLUSIONS AND FUTURE WORK

Although much work remains to be done, we have presented hybrid architecture for an intelligent data mining assistant. The following are some of the novelty features that our intelligent DM assistant attempts to provide. First by combining both declarative and procedural ontology knowledge, the system addresses the need for supporting the non expert data miner throughout the key phases of the DM process. In addition, the evolution of both knowledge based components (CBR and ontology) provides an effective means to foster knowledge reuse.

Furthermore the use of the DM ontology provides a natural extension to our existing CBR for addressing the need for "deeper" knowledge to empower the data miner. Though our prototype currently only supports classification and regression activities, plans for future research are underway to include the support for clustering and association mining. The next steps will lie in conducting more DM activities in order to increase the size of our case base and elicit more relevant detailed DM knowledge. We are highly optimistic that this synergistic combination of DM ontology knowledge (both declarative and procedural) and the case based reasoning paradigm can significantly empower a non expert data miner for effectively carrying out data mining activities.

References

[1] S. Delisle, Integrating Data Mining and Decision Support via Computational Intelligence, PMKD-DEXA Workshop. Copenhagen, Denmark, 2005
[2] C. Giraud-Carrier, Reporting on the Data Mining Advisor. Proceedings of 10th ACM SIGKDD International Conference on Knowledge Discovery and Data Mining,2005.
[3] A. Kalousis and M. Theoharis, NOEMON: Design, Implementation and Performance Results of an intelligent Assistant for Classification Selection. Intelligent Data Analysis, Elsevier, 1999
[4] MetaL, A Meta Learning Assistant for Providing Data Mining Support, www.metal-kdd.org.
[5] G. Linder and R. Studer, AST: Support for Algorithm Selection with a CBR Approach. Recent Advances in Meta Learning and Future Work, 1999, 38-47
[6] A. Suyama, N. Negishi, and T. Yamaguchi,CAMLET: A Platform for Automatic Composition of Inductive Applications Using Ontologies.Progress in Discovery Science, 2002
[7] J.Phillips and B. Buchanan, Ontology-Guided Knowledge Discovery in Databases, International Conference on Knowledge Capture. Victoria, Canada, 2001
[8] A. Bernstein, F. Provost, and S. Hill, Intelligent Assistance for the Data Mining Process: An Ontology based Approach, IEEE Transactions on Knowledge and Data Engineering, 2005.
[9] M. Bauer and S. Baldes, An Ontology Based interface for Machine Learning, Intelligent User Interfaces. San Diego, California, 2005
[10] M. Cannataro and C. Comito, A Data Mining Ontology for Grid Programming, 1st Int. Workshop on Semantics in Peer to Peer and Grid Computing 2003
[11] CRISP-DM1.0, A Step by step Data Mining Guide, www.crisp-dm.org, 2000
[12] A. Aamodt, Knowledge-Intensive Case Based Reasoning in CREEK, Advancesin Case Based Reasoning, 7th European Conference. Madrid, Spain, Springer, 2004
[13] J. Bello-Thomas, P. Gonzalez Calero, and B. Diaz-Agundo, JColibri: An Object-Oriented Framework for Building CBR Systems, Advances in CBR,7th European Conference. Madrid, Spain, Springer, 2004
[14] I. Bichindaritz, Mémoire: Case Based Reasoning Meets the Semantic Web in Biology and Medecine. Advances in Case based Reasoning,7th European Conference, LNAI, Spain, 2004
[15] M .Charest, S. Delisle, O. Cervantes,and Y. Shen, Intelligent Data Mining Assistance via CBR and Ontologies, to appear in DEXA-PMKD Workshop. Poland, 2006
[16] C. Castliello, G. Castellano, and A. Fanelli, Meta Data: Characterization of Input Features for Meta Learning. Modeling Decisions for Artificial Intelligence, LNAI, 2005, 457-468
[17] D. Aha, D. Kibler, and M. Albert, Instance Based Learning Algorithms. Kluwer Academic Publishers, 1991. 6, 37-66
[18] SWRL SemanticWebRule Language, http://www.w3.org/Submission/SWRL/
[19] M. O'Connor, H. Knublauch, S. Tu, B. Grosol, M. Dean, W. Grosso, nd M. Musen, Supporting Rule System Interoperability on the Semantic Web with SWRL, ISWC, LNCS 3729. Berlin, 2005
[20] JESS,Java Expert System Shell, http://herzberg.ca.sandia.gov/jess/
[21] P. Tan, M. Steinbach, and V. Kumar, Introduction to Data Mining (Boston, MA: Addison-Wesley, 2005).
[22] T. Hastie, R. Tibshirani, and J. Friedman, The Element of Statistical Learning, Data Mining, Inference and Prediction (Berlin, GmbH: Springer, 2001).
[23] I. Witten and E. Frank, Data Mining: Practical Machine Learning Tools and Techniques with Java Implementations. 2 ed (San Francisco, CA: Morgan Kaufman, 2005).
[24] C. Golbreich, Combining Rule and Ontology Reasoners for the Semantic Web, Rules and Rule Markup Languages for the Semantic Web Springer, 2004.

International Journal of Modern Engineering Research (IJMER)
www.ijmer.com Vol. 3, Issue. 3, May - June 2013 pp-1617-1622 ISSN: 2249-6645

Validation of Performance Measures for Green Supplier Selection in Indian Industries

Samadhan P. Deshmukh[1], Vivek K. Sunnapwar[2]
Department of Humanities and Applied Science, Watumull Institute, Worli, Mumbai, India
Department of Mechanical Engineering, Lokmanya Tilak College of Engineering, Navi Mumbai, India

Abstract: *An environmentally conscious supply chain, also called a green supply chain, is a new concept appearing in recent literatures. The purpose of this study is to identify the critical green manufacturing factors considered during supplier selection in the Indian manufacturing sector. The relationship between green supplier selection management practices and environmental performance is studied. The criteria are differentiated for evaluating traditional suppliers and green suppliers. The major activities of the green supply chain; namely green procurement, green manufacturing, green costs, quality, green packaging, customer co-operation are being covered throughout the research. From these above factors best factors for green supplier selection are selected and which can be implemented in any individual manufacturing industry. In this study, factor analysis is done using Statistical Package for the Social Sciences (SPSS) software to help decision makers understand the important environmental dimensions. The study demonstrates use of factor analysis to evaluate the relative importance of various environmental performance measures. This study also aims to develop a decision support tool which should help companies to integrate environmental criteria into their green supplier selection process.*

Keywords: *Green manufacturing; green supplier selection, environmental performance, factor analysis*

I. INTRODUCTION

The Green Supplier selection process is one of the key operational tasks for sustainable supply chain partnership. The powerful supplier should enhance the performance of the supply chain with environmental, social and economical aspects [1]. Due to the current awareness in the environmental aspects, the assortment of the supplier has turned their way and made focus on the green criteria base more than a habitual way [2]. With increasing government regulation and stronger public awareness in environmental protection, firms today simply cannot ignore environmental issues if they want to survive in global market. In addition to complying with the environmental regulations for selling products in certain countries, firms need to implement strategies to voluntarily reduce the environmental impacts of their products. The integration of environmental, economic and social performances to achieve sustainable development is a major business challenge for the new century. Environmental management is becoming more and more important for corporations as the emphasis on the environmental protection by organizational stakeholders, including stockholders, governments, customers, employees, competitors and communities, keeps increasing. Programs such as design for the environment, life cycle analysis, total quality environmental management, green supply chain management and ISO 14000 standards are popular for environmentally conscious practices. A green supplier evaluation system is necessary for a firm in determining the suitability of a supplier as a partner in the green supply chain [3].

This study explains the practices and implementation of green supply chain and environmental performance among various manufacturing industries located in India. Total 7 practices namely green design, green logistic design, green manufacturing, green costs, quality, environment performance assessment, and customer co-operation are considered with 47 sub factors. The study consists of five sections. After this introduction, in section II, review of the relevant literature is given. It helps in establishing a link between green supply chain management and environmental performance measures. Section III contains research methodology. The result and comparative analysis of various factors of green supply chain management by calculating 'mean score' are presented in section IV. Finally, the conclusion is presented in section V.

II. LITERATURE REVIEW

In this work, the articles were studied keeping in mind multi criteria green supplier evaluation and selection approaches ranging from year 2006 to 2012. Based on number of articles studied the following issues were examined - (i) Application of Multi Criteria Decision Making (MCDM) tool (ii) evaluation of green supplier selection criteria.

A literature review of Green Supply Chain Management (GSCM) yielded studies linking green, environmental, or sustainable concepts. Most studies emphasized reduction, re-manufacturing, recycling product design, process design, manufacturing practices, procurement, and some mixture of items across managerial levels. Integrating environmental concepts into these business functions ameliorated environmental pollution. However, a more elaborate and organized analysis will allow efficient implementation of GSCM strategy. Bhateja *et al.* [4] conducted study of various activities of the supply chain processes of various Indian Manufacturing Industries. The six major activities of the supply chain; namely green sourcing & procurement, green manufacturing, green warehousing, green distribution, green packaging, green transportation were covered throughout the research. Deif [5] presented a system model for the new green manufacturing paradigm. An open mixed architecture for the design, planning and control of green manufacturing activities was developed. The model captured various planning activities to migrate from a less green into a greener and more eco-efficient manufacturing.

Agarwal *et al*. [6] presented a methodology to evaluate suppliers using portfolio analysis based on the analytic network process (ANP) and environmental factors. The study introduced green criteria into the framework of supplier selection criteria. A set of criteria covering a wide range of parameters was submitted in the form of table and opinion of expert was taken to select pertinent criteria for vendor selection. The study consisted of four main criteria clusters or dimensions as operational life, environmental friendly, overall performance, and process management. There were 21 sub criteria under the main four dimensions. Buyukozkan and Cifci [7] examined GSCM and GSCM capability dimensions to propose an evaluation framework for green suppliers. The identified components were integrated into a novel hybrid fuzzy multiple criteria decision making (MCDM) model combining the fuzzy Decision Making Trial and Evaluation Laboratory Model (DEMATEL), the Analytic Network Process (ANP), and Technique for Order Performance by Similarity to Ideal Solution (TOPSIS) in a fuzzy context. The combined fuzzy ANP and fuzzy DEMATEL approaches used in the study offered a more precise and accurate analysis by integrating interdependent relationships within and among a set of criteria.

Kumar *et al*. [8] investigated the green supply chain management practices likely to be adopted by the manufacturing industry of electrical and electronics products in India. The relationship between green supply chain management practices and environmental performance was studied. The data were analyzed using "mean score". The results indicated the performance of eco procurement, eco accounting, eco logistics design, eco product design, eco manufacturing, and economic performance, its practices in response to the current wave of national & international green issues. Kuo *et al*. [9] developed a green supplier selection model which integrated artificial neural network (ANN) and two multi-attribute decision analysis (MADA) methods: data envelopment analysis (DEA) and analytic network process (ANP). It also discovered that ANN – MADA had better power of discrimination and noise- insensitivity in evaluating green suppliers' performances. The final green supplier selection had six dimensions including quality, cost, delivery, service, environment and corporate social responsibility. Toke *et al*. [10] gave details on the investigation, practice and evaluation of green supply chain management. The research included various functions like purchasing and inbound logistics, production, distribution and out-bound logistics, and reverse logistics. A number of integration issues potentially affecting each of these functional areas were then presented.

Wu *et al*. [11] used the fuzzy Decision Making Trial and Evaluation Laboratory (DEMATEL) method to find influential factors in selecting GSCM criteria. Awasthi *et al*. [12] presented a fuzzy multi criteria approach for evaluating environmental performance of suppliers. The proposed approach consisted of 12 criteria. Hua *et al*. [13] developed a fuzzy multiple attribute decision-making (FMADM) method with a three-level hierarchical decision-making model to evaluate the aggregate risk for green manufacturing projects. Humphreys *et al*. [14] presented a framework for integrating environmental factors into the supplier selection process. Subsequently, a framework of the supplier selection process which incorporated environmental performance was developed. Chen *et al*. [15] proposed a network to clarify managerial levels and firm-related content. It derived four business functions from product lifecycle management: design, purchasing, manufacturing, and marketing and service. It also associated their related activities with ''greenness''.

Yeh and Chuang [16] developed an optimal mathematical planning model for green partner selection which involved different objectives. Lin *et al*. [17] modelled a green purchasing system by applying the analytic network process (ANP) and linear programming (LP) methods. The ANP provided the solution for green supplier selection. It consisted of criteria like energy saving, pollution reduction, social responsibility etc. Lee *et al.* [2] proposed a model for evaluating green suppliers. The Delphi method was applied first to differentiate the criteria for evaluating traditional suppliers and green suppliers. The major four activities of the green supply chain management; namely green purchasing, green manufacturing, green marketing and reverse logistics were covered throughout the study by Nimawat and Namdev [3]. Sarkis [18] discussed components and elements of green supply chain management. The decision framework was modelled and solved as an analytical network process (ANP).

III. OBJECTIVES OF STUDY

The objective of this study is to investigate the practices and implementation of green supplier selection in Indian industries. The objective is to select best factors for supplier selection with the green manufacturing approach, which can be implemented in individual manufacturing industry. The task of designing the questionnaire was carried out after reviewing a variety of literature. Based on the literature reviewed, a tentative list of the criteria for green supplier selection was developed. In the pre-testing phase of the questionnaire, practicing industry representatives were consulted for their view on the criteria selected and whether all the relevant criteria were covered in the questionnaire. Based on their feedback, the criteria list was modified and put into a structured form, with each sub-criteria falling under their respective criteria/major criteria. At the end of the pre - testing stage, 47 sub-criteria under the heading of 7 major criteria were finalized. Each criterion in the questionnaire was judged on a 5 point Likert Scale, where, 1 = very low, 2 = low, 3 = moderate, 4 = high and 5 = very high. Likert scale is a tried and tested scale has been successfully used in many cases, including supplier selection. Pallant J. [19] stated that the reliability of a scale indicates how free it is from random error. It indicated the extent to which an experiment, test or any other measuring procedure yields the same results. The reliability assessment was conducted on Statistical Package for the Social Sciences (SPSS) software. The methodology adopted is similar to the one described by Pallant J. in her book on SPSS. The responses were obtained from various manufacturing firms, chemical industries, pharmaceutical Industries, automobile industries, small workshops, and chemical laboratories. Managers/ higher level authority in different level of organizations were interviewed. This was made to obtain accurate information and data to help in the formulation of the important green evaluation measures.

Pallant J. stated in her book that reliability can be measured in various ways [19]. The most common method to measure reliability is by using Cronbach's alpha, which was carried out using SPSS. This statistic indicated the correlation of the items that make up the scale. The values ranged from 0 to 1, with higher values indicating greater reliability. Nunnally (1978) recommended a minimum value of 0.7. Cronbach's alpha values are dependent on the number of items on the scale. If the number of items in the scale is less than 10 (as in this study, where each criteria has 10 or less sub-criteria under it) then Cronbach's alpha values can be quite small. Here, the mean inter-item correlations were calculated. J. Pallant recommended their optimum value to be above 0.3.

IV. COMPARATIVE FACTOR ANALYSIS

4.1 RELIABILITY ANALYSIS

Reliability indicates the extent to which an experiment, test or any other measuring procedure yields the same results. Reliability analysis was carried out using total 47 criteria using SPSS software. The final Cronbach's values and the range of correlation coefficients will give an idea about the scale chosen, which should be free from random error. It will also help to find that the sub-criteria have been properly assigned to their respective criteria or not. The final Cronbach's Alpha values should be more than 0.7.

TABLE I. *RELIABILITY ANALYSIS*

Criteria	Total number of Items	Final Cronbach's Alpha	Range of correlation coefficients
Green Design	9	0.859	0.303-0.748
Green Logistics Design	5	0.749	0.370-0.737
Green Manufacturing	7	0.738	0.158-0.688
Green Costs	5	0.861	0.568-0.998
Quality	8	0.774	0.336-0.599
Environment performance assessment	4	0.847	0.529-0.717
Customer Co-operation	6	0.728	0.207-0.587

A visual inspection of the range of correlation coefficients column in Table I reveal that a majority of the correlations are greater than 0.3. Also Cronbach's alpha values are more than a minimum required value of 0.7. The final Cronbach's values and the range of correlation coefficients prove that the scale chosen is free from random error and that the sub-criteria have been properly assigned to their respective criteria. This indicates that the sub-criteria have common factors (Digalwar and Sangwan, 2007).

4.2 KMO AND BARTLETT'S TEST OF SPHERICITY

The next appropriateness for factor analysis was determined by examining the strength of relationships among the sub-criteria. This was conducted by three measures, the coefficients in the correlation matrix, the Kaiser-Meyer-Olkin (KMO) measure of sampling adequacy and Bartlett's test of sphericity. Tabachnick and Fidell recommended an inspection of the correlation matrix for evidence of coefficients greater than 0.3. He stated that if only a few correlations above this level are found, then factor analysis may not be appropriate. The Bartlett's test of sphericity should be significant ($p < 0.05$) in the factor analysis to be considered appropriate. The KMO index ranges from 0 to 1 with 0.6 recommended as the minimum value [19]. Meanwhile Digalwar and Sangwan, (2007) recommended KMO value more than 0.5 as optimal. Final Cronbach's Alpha value and range of correlation coefficients is calculated using reliability analysis. Table I shows the reliability analysis of the major criteria selected for the study.

TABLE II. *KMO AND BARTLETT'S TEST OF SPHERICITY*

Criteria	KMO	Bartlett's significance value (p)
Green Design	0.685	0.000
Green Logistics Design	0.622	0.000
Green Manufacturing	0.654	0.000
Green Costs	0.761	0.000
Quality	0.604	0.000
Environment performance assessment	0.759	0.000
Customer Co-operation	0.604	0.000

Analysis of the KMO measure using SPSS in Table II reveals that all the measures meet the required standard. The Bartlett's test indicates that all the criteria are significant i.e., $p < 0.05$.

4.3 FACTOR ANALYSIS

Factor analysis was conducted on each criterion. The components were extracted in SPSS using principal component analysis with varimax rotation. Initially, factors with an Eigen value over 1 were extracted and the scree plot along with the unrotated factor solution analyzed. Those factors with a significant slope above the bend in the scree plot were extracted. A sample scree plot for green design criteria is shown in Fig.1 and sample component plot for green design is shown in Fig.2.

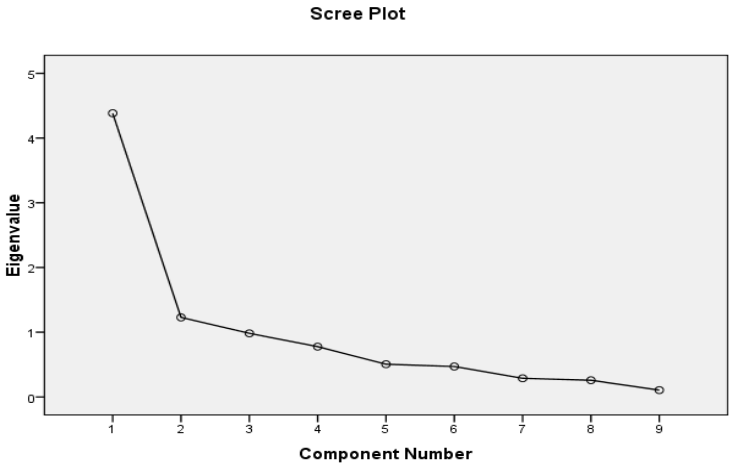

Fig.1 Sample Scree plot for green design

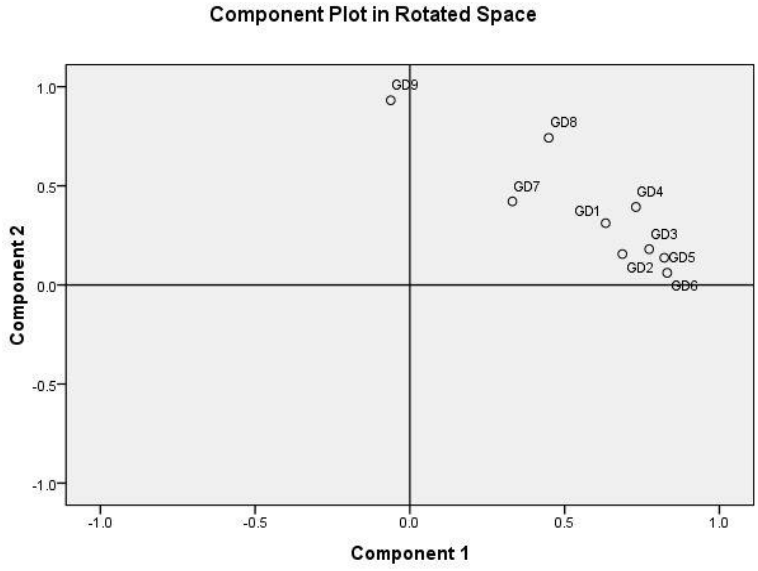

Fig.2 Sample Component plot for green design

The results of the factor analysis are shown in Table III.

TABLE III. *FACTOR ANALYSIS*

Criteria	Eigen value	% variance	Factors extracted
Green Design	4.383 1.229	48.698 62.353	2
Green Logistics Design	2.624 1.286	52.472 78.184	2
Green Manufacturing	2.999 1.196 1.071	37.485 52.441 65.831	3
Green Costs	3.354	67.089	1
Quality	2.647 1.220	52.945 77.350	2
Environment performance assessment	2.768	69.190	1
Customer Co-operation	2.497 1.173	41.615 61.158	2

4.4 IMPORTANCE OF MAIN CRITERIA FROM MEAN VALUE

In order to find out which criteria were considered important by the Indian manufacturing sector an analysis of the mean values was carried out using SPSS. Table IV shows the mean values (M) and standard deviation (S.D) of the criteria and sub-criteria respectively obtained from various respondents. The table shows the important criteria in the descending order of their means. Higher mean values indicate more important criteria. Higher mean values indicate more important criteria.

TABLE IV. *IMPORTANCE OF THE MAJOR CRITERIA*

Criteria	Mean	Std. Deviation
Quality	4.035	0.879
Environment Performance Assessment	3.984	0.825
Green Manufacturing	3.927	0.728
Customer Co-operation	3.863	0.727
Green Costs	3.794	0.799
Green Design	3.692	0.876
Green Logistics Design	3.561	0.863

Fig.3 shows importance of the major criteria in Indian Industries. Mean value gives an indication of the important criteria to be considered in supplier selection using green manufacturing approach.

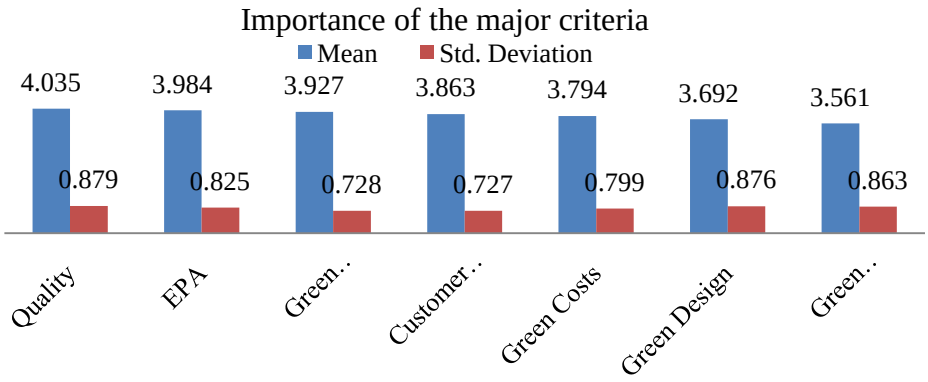

Fig.3 Importance of the major criteria in Indian Industries

V. CONCLUSION

This research presents practitioners with a 1 to 5 item measurement scale for evaluating the different facets of their green supply chain practices implementation. Green supply chain management (GSCM) is a relatively new green issue for the majority of Indian industries. The present empirical study investigated the GSCM practices adopted by different industries in Maharashtra, India. An analysis of the results indicated that quality is the most important criteria for the manufacturing industry in India. Quality was followed by environment performance assessment, green manufacturing, and customer co-operation. Surprisingly green cost, which is generally, regarded the only parameter considered for supplier selection occupies fifth place. This showed that Indian manufacturing companies compromise on cost in order to procure and thus produce products of better quality and environmentally friendly. Supplier providing better service and delivery reliability is chosen over a cheaper supplier who is weaker in these parameters.

REFERENCES

[1] Kannan G., Sarkis J., Sivakumar R., Palaniappan M., Multi Criteria Decision Making approaches for Green supplier evaluation and selection: A literature review, *Conference on the Greening of Industry Network, GIN 2012*, Linkoping – Sweden, October 22–24, 2012.
[2] Lee A.H.I., Kang H-Y, Hsu C-F, Hung H-C., A green supplier selection model for high-tech industry, *Expert Systems with Applications, 36*, 2009, 7917–7927
[3] Nimawat D. and Namdev V., An Overview of Green Supply Chain Management in India, *Research Journal of Recent Sciences, 16*, 2012, 77–82
[4] Bhateja A. K., Babbar R., Singh S., Sachdeva A. , Study of Green Supply Chain Management in the Indian Manufacturing Industries: A Literature Review cum an Analytical Approach for the measurement of performance, *International Journal of Computational Engineering & Management, 13*, 2011, 84–99
[5] Deif A. M., A system model for green manufacturing, *Journal of Cleaner Production, 19*, 2011, 1553–1559

[6] Agarwal G. And Vijayvargy L., Green Supplier Assessment in Environmentally Responsive Supply Chains through Analytical Network Process, *Proceedings of the 2010 Int. Multi Conference of Engineers and computer scientists*, Vol II, Hong Kong
[7] Buyukozkan G., Cifci G., A novel hybrid MCDM approach based on fuzzy DEMATEL, fuzzy ANP and fuzzy TOPSIS to evaluate green suppliers, *Expert Systems with Applications, 39,* 2012, 3000–3011
[8] Kumar S., Chattopadhyaya S., Sharma V., Green Supply Chain Management: A Case Study from Indian Electrical and Electronics Industry, *International Journal of Soft Computing and Engineering,* 1, 2012, 275–281
[9] Kuo R.J., Wang Y.C., Tien F.C., Integration of artificial neural network and MADA methods for green supplier selection, *Journal of Cleaner Production, 18,* 2010, 1161–1170
[10] Toke L. K., Gupta R. C., Dandekar M., Green Supply Chain Management; Critical Research and Practices, *Proceedings of the 2010 Int. Conference on Industrial Engineering and Operations Management*, Dhaka, Bangladesh, 2010
[11] Wu K-J, Tseng M-L, Vy T., Evaluation the drivers of green supply chain management practices in uncertainty, *Procedia - Social and Behavioral Sciences, 25,* 2011, 384 –397
[12] Awasthi A., Chauhan S. S., Goyal S. K. , A fuzzy multicriteria approach for evaluating environmental performance of suppliers, *Int. J. Production Economics, 126*, 2010, 370–378
[13] Hua L., Weiping C., Zhixin K., Tungwa N., Yuanyuan L., Fuzzy Multiple Attribute Decision Making for Evaluating Aggregate Risk in Green Manufacturing, *Tsinghua Science and technology, ISSN 1007-0214, 19/20,* 2005, 627–632
[14] Humphreys P.K., Wong Y.K., Chan F.T.S., Integrating environmental criteria into the supplier selection process, *Journal of Materials Processing Technology, 138,* 2003, 349–356
[15] Chen C-C, Shyur H-J, Shih H-S, Wu K-S., A business strategy selection of green supply chain management via an analytic network process, *Computers and Mathematics with Applications, 64,* 2012, 2544–2557
[16] Yeh W-C, Chuang M-C., Using multi-objective genetic algorithm for partner selection in green supply chain problems, *Expert Systems with Applications, 38,* 2011, 4244–4253
[17] Lin C-T, Chen C-B, Ting Y-C., A Green Purchasing Model by Using ANP and LP Methods, *Journal of Testing and Evaluation, 40, No. 2,*2012
[18] Sarkis J., A strategic decision framework for green supply chain management, *Journal of Cleaner Production, 11,* 2003, 397–409
[19] Pallant J., *SPSS Survival manual* (Open University press, 2001).

International Journal of Modern Engineering Research (IJMER)
www.ijmer.com Vol. 3, Issue. 3, May - June 2013 pp-1623-1629 ISSN: 2249-6645

Performance Comparison of H-infinity and LQR Controllers for the Pressure Regulation of a Hypersonic Wind Tunnel

Rajani S. H[1], Usha Nair[2]
*(Research Scholar, Division of Electrical Engineering, School of Engineering, Cochin university of science and technology, Kerala, India)
** (Head of the Department, Division of Electrical Engineering, School of Engineering, Cochin university of science and technology, Kerala, India)

Abstract : *Hypersonic wind tunnels are used to study the effect of air moving past the fighter planes, space vehicles and similar specimens under test. This paper aims to compare the performance of a h-infinity controller with that of a linear quadratic regulator (LQR) controller for regulating the pressure inside the settling chamber of a hypersonic wind tunnel. The linear model for both the controllers is one and the same and it is state controllable and observable. The h-infinity controller design is based on the selection of weighing function whereas the design of the LQR controller depends on the selection of optimal state feedback controller gain matrix. Performance comparison of both the controllers is carried out based on the settling time, peak overshoot and rise time. Simulation results show that h-infinity controller has better settling time compared to LQR controller.*

Keywords: *H-infinity controller, Hypersonic wind tunnel, Linear quadratic regulator, Settling chamber pressure, Weighting function.*

I. Introduction

Hypersonic wind tunnels are used in aircrafts and space vehicles to investigate the aerodynamic properties of the specimen in hypersonic flow regime. The speed of wind tunnel is indicated by Mach number which is defined as the ratio of speed of aircraft to speed of sound in gas. Hypersonic wind tunnel has a mach number greater than 5. The block diagram representation of the hypersonic wind tunnel is shown in Fig.1. The main parts of a hypersonic wind tunnel are high pressure system, pressure regulating valve, heater, settling chamber, nozzle and test section [1], [2]. Compressed air from the air storage tank is released through a pressure valve to the heater where it is heated to the required temperature and is straightened in the settling chamber and passed to the test section through the nozzle. Settling chamber pressure is controlled by designing a suitable controller for the effective operation of the pressure valve. Here the effectiveness of two controllers with different design strategy in controlling the settling chamber pressure of the hypersonic wind tunnel in terms of their settling time, peak overshoot and rise time is carried out.

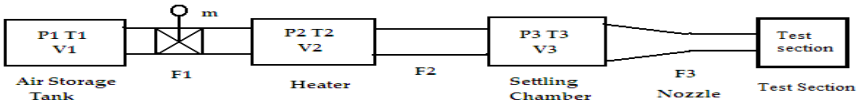

Fig.1: Block diagram of hypersonic wind tunnel

H-infinity methods are used to synthesis controllers that minimize the closed loop impact of a perturbations. H-infinity controllers are designed by properly selecting weighing function [3]-[5]. LQR controller is an optimization-based synthesis problem used to track the output and follow the changes in set point. Based on the performance requirements, the optimal state feedback controller gain matrix is designed for the controller [6]-[9].

II. Model and Analysis of The System

The system performance is decided by the speed of settling chamber pressure and it is accurately controlled by two controllers viz h- infinity and LQR. For modelling the wind tunnel system, the continuity equations and parameter values are selected for the pressure vessels [10] - [12]. The state space model of the system is given in (1) & (2).

$$\begin{bmatrix}\dot{P_1}\\ \dot{P_2}\\ \dot{P_3}\end{bmatrix} = \begin{bmatrix}-K_1/C_1 & 0 & 0\\ K_1/C_1 & -K_3/C_2 & -K_4/C_2\\ 0 & K_3/C_3 & K_4 - K_n/C_3\end{bmatrix}\begin{bmatrix}P_1\\ P_2\\ P_3\end{bmatrix} + \begin{bmatrix}-K_2/C_1\\ K_2/C_2\\ 0\end{bmatrix} m. \quad (1)$$

$$Y_1 = \begin{bmatrix}0 & 0 & 1\end{bmatrix}\begin{bmatrix}P_1\\ P_2\\ P_3\end{bmatrix}. \quad (2)$$

where P_1, P_2 are the upstream and downstream pressures, P_3 is the settling chamber pressure, m is the stem movement of pressure valve, K_1, K_2, K_3 and K_4 are constants, K_n is the nozzle flow constant and, C_1, C_2, C_3 represents the capacitance of the three pressure vessels respectively.

The system is linearized and the transfer function [10] is given in (3).

$$G_p(s) = \frac{-2.369e006s^2 + 7.897e007s + 4.21e005}{0.015s^5 + 0.7802s^4 + 9.89s^3 + 18.46s^2 + 3.377s + 0.01937} \quad . \qquad (3)$$

1.1. Stability Analysis

Stability analysis is carried out on the system model before considering the implementation of h-infinity and LQR controller. By substituting the values of the parameters K_1, K_2, K_3, K_4, Kn, C_1, C_2 and C_3 from [10] in (1) and (2), the state model is obtained with

$$[A] = \begin{bmatrix} -0.0045 & 0 & 0 \\ 0.0045 & 2.51 & 2.51 \\ 0 & 12.85 & -14.14 \end{bmatrix}$$

$$[B] = \begin{bmatrix} 617679.68 \\ 6133259.91 \\ 0 \end{bmatrix}$$

$$[C] = [0 \ 0 \ 1]$$

Controllability and observability tests [13] are carried out on the model using Kalmans test with (4) and (5) respectively.

$$Q_C = [B \ \ AB \ \ A^2B] \ \neq \ 0 \qquad (4)$$

$$Q_O = \left[C^T \ \ A^T C^T \ A^{T^2} C^T\right] \ \neq 0 \qquad (5)$$

It is found that $Q_C \neq 0$ and $Q_O \neq 0$ and rank of the matrix is 3, which is equal to the dimension of the system and hence the system is completely state controllable and observable[13].

1.2. Open Loop Response of the System

The system in (1)-(3) is simulated in Matlab and the open loop response for the settling chamber pressure is obtained in Fig.2. From the figure, it is observed that the peak value of settling chamber pressure is 130 * 10^5 Pa and settling time is 450 secs which is very high for the short duration test.

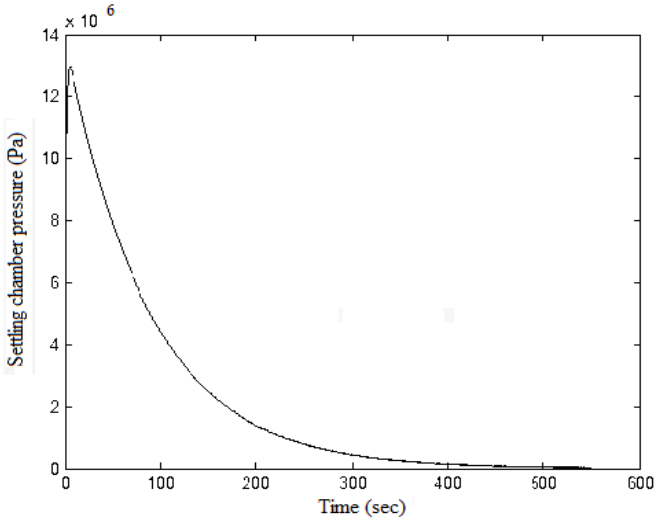

Fig.2. Open loop response of the settling chamber pressure

III. Performance of H-infinity Controller

The main objective of h-infinity controller is to minimize the h-infinity norm which is the energy gain of the system. Standard feedback configuration with weights [3], [14] is given in Fig.3. The controller is designed by properly selecting the weighing functions [14]. Here G is the plant transfer function, G_d the transfer function corresponding to input disturbance, r the set point, u the actuator, v the sensor measurement, K the controller, d the disturbance, n is measurement noise, Z_1 is the settling chamber pressure, Z_2 is control output, weight W_p is the second order transfer function and is selected such that $|S(j\omega)| < 1/ (W_p(j\omega))$, where S is the sensitivity function. Weight W_u indicates control input weight and sensor noise effects are W_n [14].

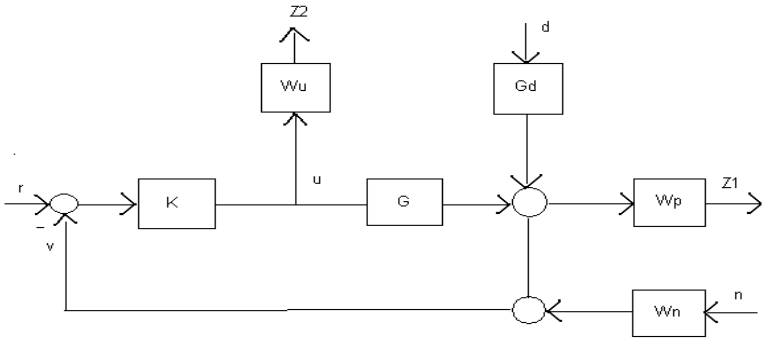

Fig.3. Standard feedback configuration with weights

The multiplicative uncertainty weight W_u is selected [4], [15], [16] by satisfying the stability conditions,

$$|W_u(j\omega)| \geq l_u(\omega), \quad \forall\omega \ . \qquad (6)$$

where l_u is the relative error of the plant transfer function and W_u is selected as

$$W_u = \frac{600s + 210}{20s + 0.0001} \ . \qquad (7)$$

The sensitivity function S(s) [4], [15], [16] is

$$S(s) = (1 + K(s)H(s))^{-1} \ . \qquad (8)$$

The performance requirement is guaranteed if and only if the condition $|S(j\omega)| < \frac{1}{W_p(j\omega)}$, $\forall\omega$ is satisfied.

The nominal performance criterion [17] is given in (9).

$$|W_p(j\omega)| < |1 + G_m(j\omega)|, \quad \forall\omega \ . \qquad (9)$$

The robust performance [5] is defined by criterion

$$|W_p(j\omega)S_p(j\omega)| < 1, \quad \forall\ S_p\ ,\ \omega \qquad (10)$$

Using the performance criterion in (9) and (10), the weighing function W_p is selected [5] as

$$w_p = \frac{30S+20}{20S+1} \qquad (11)$$

The weighing function W_n is chosen by trial and error method [5] as

$$W_n = \frac{1}{10} \ . \qquad (12)$$

After selecting the three weights W_u, W_p, W_n, the h-infinity controller is simulated in Matlab, with the input disturbance transfer function G_d = 1 (with minimum disturbance) and the set points equal to 100*10^5, 80 *10^5, and 50 *10^5 Pa is shown in Fig. 4, 5, and 6 respectively.

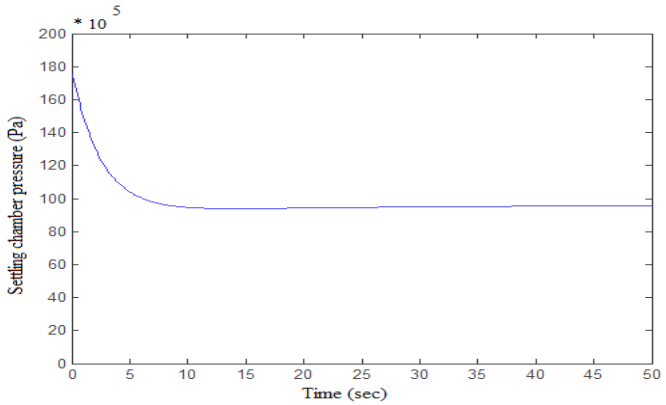

Fig.4. Settling Chamber Pressure with H-infinity Controller for Set point 100 * 10^5 Pa

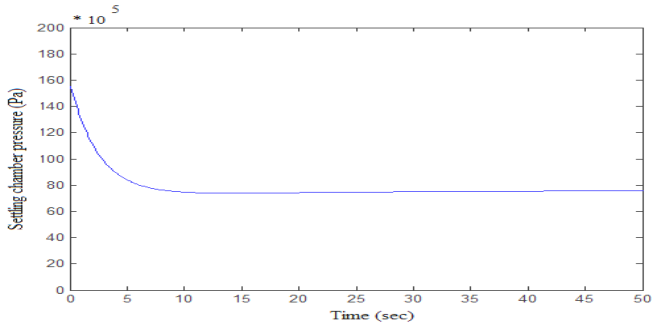

Fig.5. Settling Chamber Pressure with H-infinity Controller for Set point 80 * 10^5 Pa

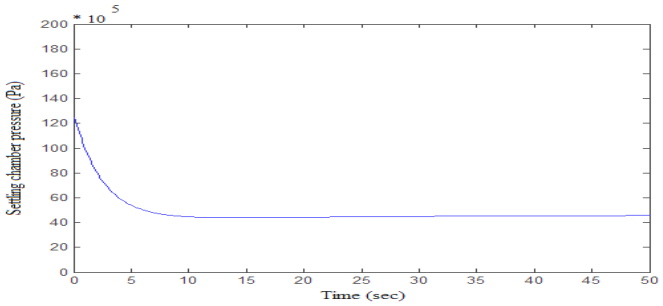

Fig.6. Settling Chamber Pressure with H-infinity Controller for Set point 50 * 10^5 Pa

From the simulation, the h-infinity controller matrix, K is obtained as

$$K = (1.0e+005) *$$

$$\begin{bmatrix} -2.0733 & 1.6054 & 1.1876 & 0.2099 & -0.168 & -0.0007 & 0 & 0 & 0.0001 \\ -1.8229 & 1.4115 & 1.0442 & 0.1845 & -0.1291 & -0.0006 & 0 & 0 & 0 \\ -1.3565 & 1.0503 & 0.7770 & 0.1373 & -0.0960 & -0.0004 & 0 & 0 & 0 \\ 0.9738 & -0.7540 & -0.5578 & -0.0987 & 0.0689 & 0.0003 & -0 & 0 & 0 \\ -0.2895 & 0.2241 & 0.1658 & 0.0294 & -0.0209 & 0.0003 & 0 & 0 & 0 \\ 0.0008 & -0.0007 & -0.0005 & -0.0004 & -0.0001 & -0.000 & 0 & -0.0001 & 0 \\ -0.0035 & 0.0027 & 0.0020 & 0.0004 & -0.0003 & -0.000 & 0 & 0 & 0 \\ -0.0001 & 0.0001 & 0.0000 & 0.0000 & -0.0000 & -0.0000 & 0 & 0 & 0 \\ 0 & 0 & 0 & 0 & 0 & 0 & 0 & 0 & -\infty \end{bmatrix}$$

With set point 100*10^5Pa, the settling time of settling chamber pressure is 12 sec and peak overshoot is 70%. When the set point is changed to 80*10^5Pa, the settling time remains 12 sec whereas peak overshoot is increased to 90% and when the set point is further reduced to 50*10^5Pa, the settling time is 11 sec and the peak overshoot is drastically increased and is >90%. The rise time for the three set points is 1sec. From this it is clear that a change in set point does not effect the settling time whereas there is a drastic increase in peak overshoot with decrease in set point and the rise time remains constant.

IV. Performance of LQR Controller

LQR controller design problem deals with optimizing an energy function, J by designing the state feedback controller, K. A system in state variable form is

$$\dot{x} = Ax + Bu$$
$$y = Cx$$

with x(t) ε R^n and u(t) ε R^m . x is the state of the system and u is the control input. The initial condition is x(0) and states are measurable. The state-variable feedback (SVFB) control law is

u = -Kx

where K is the linear optimal feedback control gain matrix [9], [18]. The closed-loop system using this control becomes

$$\dot{x} = (A - BK)x$$

where v is the new command input. The objective of the controller design is to find the optimal control law that minimizes the following performance index. The performance index (PI) [8], [9], [18] is

$$J = \frac{1}{2}\int_0^\infty (x^T Q X + u^T R u)\, dt \qquad (13)$$

where *J* is the energy function which keeps the total energy of the closed-loop system small. The two matrices Q and R are selected such that Q is positive semi-definite and R is positive definite [6], [9], [18]. The control value u is called optimal control [18] which is given by,

$$u(t) = -R^{-1}B^T P x = -Kx \qquad (14)$$

where P(t) is the solution of Riccati equation and is a real symmetric matrix. Solving the above (14),

$$PA + A^T P - PBR^{-1}BP + Q = 0 \qquad (15)$$

where Q and R are the optimal controller weight matrices and K is obtained as,

$$K = R^{-1}B^T P$$

The plant with LQR controller is shown in Fig.7.

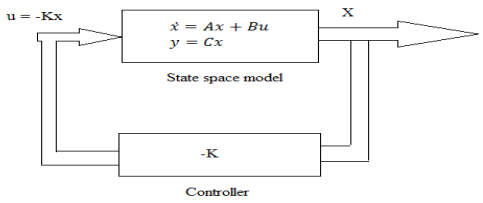

Fig.7. State Feedback Representation of the System with Feedback Gain

Matrices Q and R are selected by trial and error method to find optimal gain matrix, K. Q and R are given by

$$Q = \begin{bmatrix} 1 & 0 & 0 \\ 0 & 1 & 0 \\ 0 & 0 & 1 \end{bmatrix}$$

R = 1,

The optimal gain matrix K is obtained.
K = [-0.9839 1.1041 0.3943].

With these values of gain, the system is simulated to get the response of settling chamber pressure with three different values of set points. Fig. 8, 9, and 10 shows the variation of settling chamber pressure with LQR controller with set points $50 * 10^5$ Pa, $80 * 10^5$ Pa, $100 * 10^5$ Pa respectively.

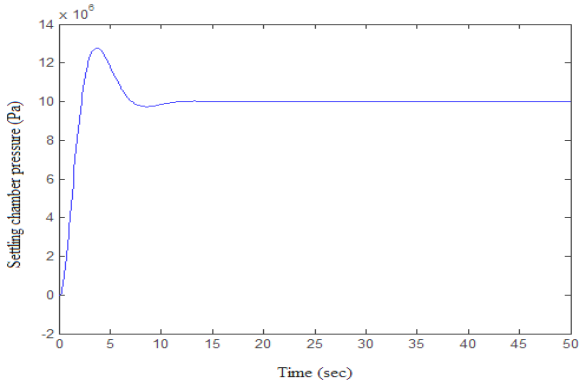

Fig.8. Settling chamber pressure with LQR controller with set point $100*10^5$ Pa .

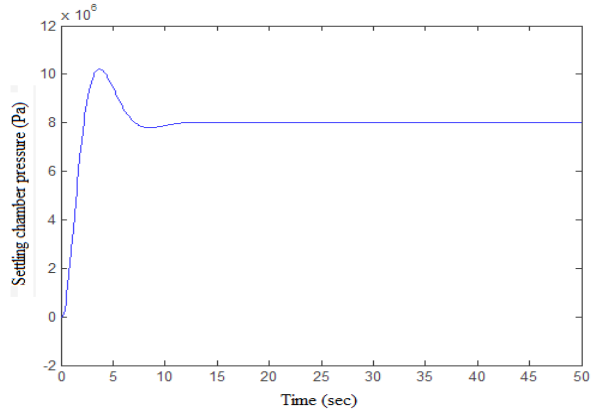

Fig.9. Settling chamber pressure with LQR controller with set point $80*10^5$ Pa

From the responses, it is observed that with set point $100*10^5$Pa, the settling time of settling chamber pressure is 18 sec, peak overshoot is 30% and rise time is 2 sec. When the set point is changed to $80*10^5$Pa, the settling time is 19 sec,

peak overshoot is increased to 31.25% and rise time is 2 sec and when the set point is further reduced to $50*10^5$Pa, the settling time is 18 sec, the peak overshoot is 30% and the rise time remains 2 sec. From this it is clear that a change in set point does not have much effect on the settling time, peak overshoot and the rise time in the case of a LQR controller .

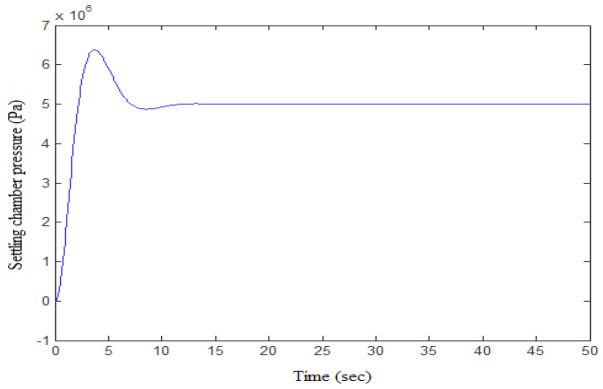

Fig.10. Settling chamber pressure with LQR controller with set point $50*10^5$ Pa.

V. Result and Discussion

Stability analysis is carried out on the hypersonic wind tunnel system model and its open loop response is plotted. From the response, it is clear that the settling time is 450 secs which is further to be improved using a suitable controller. Here the effectiveness of an h-infinity controller and an LQR controller in regulating the settling chamber pressure is studied for different set points. The performance comparison of these two controllers in terms of settling time, peak overshoot and rise time is evaluated and is tabulated in table.1.

Table 1: Performance Comparison Table

	Settling Time(sec)		Peak overshoot(%)		Rise Time(sec)	
Set point	H-infinity	LQR	H-infinity	LQR	H-infinity	LQR
$100*10^5$Pa	12	18	70	30	1	2
$80*10^5$Pa	12	19	90	31.25	1	2
$50*10^5$Pa	11	18	> 90	30	1	2

From the table, it is observed that for an h-infinity controller, the settling time is much lesser than that of an LQR controller. In both the cases settling time does not vary much with change in set points, however the peak overshoot is much higher in the case of an h-infinity controller and the variation with set point is also drastic. The peak overshoot with smaller set point is very high in case of h-infinity controller whereas there is no drastic variation in the case of an LQR controller. The values of peak overshoot with set point $100*10^5$Pa are tolerable for both the controllers whereas with reduction of set point, the peak overshoot is very high for h-infinity controller. The rise time in the case of h-infinity controller is lesser than that of LQR controller. With change in set point, there is no variation in rise time for both the controllers. In case of a hypersonic wind tunnel system, the settling time is more important than that of peak overshoot as the test duration is very short. Hence from these results, it is clear that an h-infinity controller with a set point of $100*10^5$Pa would be a better choice for regulating the settling chamber pressure of a hypersonic wind tunnel.

VI. Conclusion

The performance of two controllers viz h-infinity and LQR for regulating the settling chamber pressure of a hypersonic wind tunnel is compared. The settling time of h-infinity controller is lesser than that of LQR controller and hence it is found to be more applicable in the present study. However the peak overshoot is slightly higher for the h-infinity controller with the same set point as that of LQR controller. As the test duration is very short, lower value of settling time makes h-infinity controller more suitable when compared to LQR controller. The set point of settling chamber pressure while using h-infinity controller cannot be decreased to a very low value as it effects the peak overshoot, however the results can be improved by considering higher values of set points and its effects on the performance characteristics. The results can further be improved by considering nonlinear models of the same system.

References

[1] Yinsheng Luo, Shaobang Xing, Wei Song, Taihong Chen, Qian Gao, Fuzzy and PID compound control of mach number for 0.6 meters supersonic wind tunnel, *Proc. 2nd IEEE Conf. on Artificial Intelligence, Management Science and Electronic Commerce (AIMSEC)*, 2011, 3992-3995.

[2] Cooksey, J. M, A Mach Number and Dynamic Pressure Computer for Analog Reduction of Wind Tunnel Data, *IEEE Transl. J. Aerospace, AS-3(2),* 1965, 47-52.

[3] A.Megretski, *Multivariable Control Systems*, Department Of Electrical Engineering and Computer Science., Massachusetts Institute of Technology, Cambridge, 2004.

[4] Huibert Kwakernaak, Robust Control and Hinfinity Optimization, *International Journal on Automatica, 29(2),* 1993

[5] Rajani. S. H, Binu. L. S, H-infinity control technique for regulating pressure inside a hypersonic wind tunnel, IJCA, *Proc. On International conference on VLSI, communications and instrumentation(ICVCI)*,14(2), 2011, 10-13.

[6] Sandeep Kumar Yadav, Sachin Sharma, Narinder Singh, Optimal Control of double inverted pendulum using LQR controller, *International J. of advanced Research in computer science and software engineering, 2(2),2012*, 189-192.
[7] Y-Z.Yin, H-S Zhang, Linear Quadratic Regulation for discreate-time systems with single input delay, *Proc. of the china control conference, Harbin, china*, 2006, 672-677.
[8] Dan Huang, Shaowu Zhou, Inverted Pendulum Control system based on LQR optimal regulator, *International Journal of Micro Computer Information, 20(2),2004*, 37-39.
[9] Rajani S.H., Bindu M.Krishna, Usha Nair, Regulation of Settling Chamber Pressure in a Hypersonic Wind Tunnel using LQR Controller, *International Journal of Electronics Communication and Computer Engineering, 4(2),* 2013, 466-469.
[10] V. Jacob and L.S Binu,, Adaptive Fuzzy PI controller forHypersonic Wind Tunnel Pressure Regulation, *Proc. 10th National Conference On Technological Trends, NCTT , Trivandrum, India,*, 2009, 184-187.
[11] B.G.Liptak, *Instrument Engineers handbook: Process Control, Elsevier.,* (1995) 587-612.
[12] D. P. Echman, *Automatic Process Control*, (Wiley Eastern Limited, New Delhi, 1958) 21-23.
[13] M.C.Delfour, S.K.Mitter, Controllability and Observability for infinite-Dimentional systems, *International Journal of control, 10(2),* 1972, 329-333.
[14] D-W.Gu,P.Hr.Petkov. M.M.Konstantinov.:, *Robust control Design with Matlab. Library* (Publication, 2005).
[15] Yinsheng Sh.Yasini , A.Karimpour, M.B.Naghibi-Sistani, S.Gharsh., An Automatic Insulin Infusion System Based On H-infinity Control Technique, *Proc. of IEEE, CIBEC*, 2008.
[16] Doyle.J.C., Glover.K,Khargonekar.P.P.and Francis. B.A, State Space Solutions to Standard H2 and H-infinity Control Problems, . *IEEE Transactions on Automatic Control, 34(2),* 1989, 831-847.
[17] P.Dorato, *Robust Control. New York* (IEEE Press, 1987).
[18] Katsuhiko Ogata, *Modern Control Engineering*, (PHI learning Private Limited, New Delhi, 2002) 897-909.

International Journal of Modern Engineering Research (IJMER)
www.ijmer.com Vol. 3, Issue. 3, May-June 2013 Pp-1630-1635 ISSN: 2249-6645

Influence of the Speed of Charging and Discharging of the Test Machine in the Determining of the Compressive Strength of the Concrete

Suélio da Silva Araújo[1], Gilson Natal Guimarães[2] and André Luiz Bortolacci Geyer[3]

[1]*Masters Degree in Civil Engineering from the Federal University of Goiás, Brazil (2011), School of Civil Engineering, Research Assistanship from CNPq - National Council of Scientific and Technological Development.*

[2]*PhD., University of Texas at Austin, USA (1988). Full Professor at the Federal University of Goiás, Brazil.*

[3]*Doctorate in Civil Engineering from the Federal University of Rio Grande do Sul, Brazil (2001). Associate Professor II at the Federal University of Goiás.*

Abstract: *This paper presents a comparative analysis of the results obtained for the test of compressive strength, through a program of interlaboratory tests on hardened concrete, the Company developed Carlos Campos Consultoria e Construções Ltda., in the School of Civil Engineering Federal University of Goiás and in the Department of Technical Support and Control of Furnas Centrais Elétricas S.A., located in Goiânia-Goiás, to identify and evaluate the influence of some factors involved in test compressive strength. For this, we sought to verify the result of compressive strength, the influence of the type of processor (A and B) and upload speed (0.3 and 0.6 MPa/s) body-of-proof cylindrical size 150 mm x 300 mm in the concrete class C30. It was concluded that the type of laboratory significantly affect the results of compressive strength. Furthermore, it is noteworthy that the body-of-evidence dimension 150 mm x 300 mm concrete class C30, tested with a loading speed of the testing machine of 0.3 MPa/s presented the results to the larger dispersions.*

Keyword: *Interlaboratory; Concrete; basic dimension, speed of loading and unloading; Compressive Strength; Dispersion.*

I. Introduction

The research aims to study and evaluate the influence of variables: influence of laboratory and loading speed (0.3 and 0.6 MPa/s) in bodies of the cylindrical specimens of size 150 mm x 300 mm Class C30, in particular, in the result of the compressive strength in hardened concrete and to check the variability of the experimental results.

II. Experimental Program

The experimental program was developed from an interlaboratory evaluation of compressive strength of concrete, the Company developed Carlos Campos Consultoria and Construções Ltda., in the School of Civil Engineering Federal University of Goiás and in the Department of Technical Support and Control of Furnas Centrais Elétricas S.A., located in Goiânia-Goiás.Considering the characteristics of interlaboratory program where it is not possible to fix all the independent variables, so we decided to study the following situation:

- type of concrete (in a level: class C30);
- size of the body-of-proof to a level: 150 mm x 300 mm;
- load speed (in two levels: 0.3 MPa/s and 0.6 MPa/s) body-of-proof cylindrical dimension 150 mm x 300 mm in the concrete class C30.

The body-of-proof standard used in Brazil follows the model of the body-of-proof standard of the United States which is a cylinder of 150 mm x 300 mm (Figures 2.1 and 2.2).

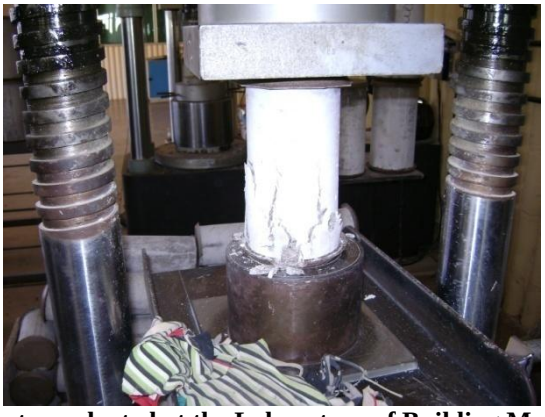

Fig. 2.1 Compressive Strength Test, conducted at the Laboratory of Building Materials Company Carlos Campos Consultoria and Construções Ltda. in Goiânia-GOIÁS

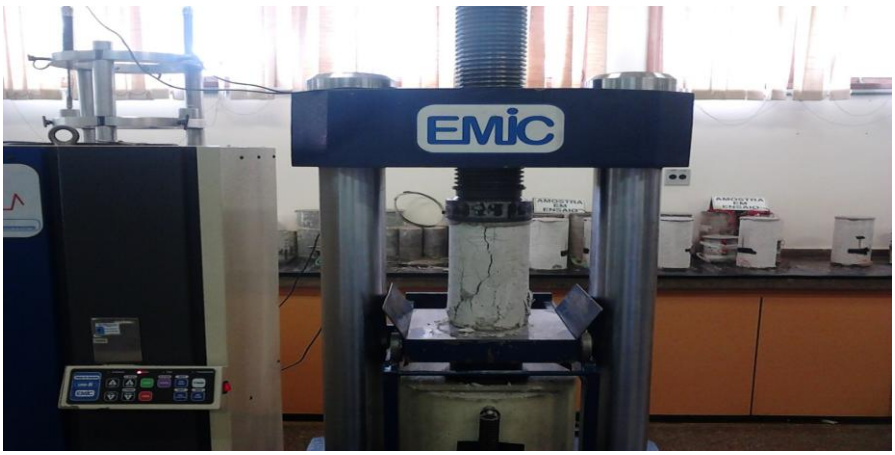

Fig. 2.2 Compressive Strength Test, conducted at the Laboratory of Concrete Department of Technical Support and Control of Furnas Centrais Elétricas S.A. in Goiânia-GOIÁS

As limitations of the study have been:

- Kept all the bodies of the race in the same moisture condition;
- Testing machine with load control with load speed (in two levels: 0.3 MPa/s and 0.6 MPa/s) in bodies of the cylindrical specimens of size 150 mm x 300 mm in the concrete class C30, during the study;
- Materials used in the manufacture of concrete: CP V ARI Portland cement (high early strength), lithology and size of coarse aggregate (granite maximum dimension of 19 mm) and sand type (artificial sand);
- Compressive strength fc (28days) of 30 MPa;
- Type of finishing top of the body-of-evidence (capping with sulfur).

To reduce the influence of the humidity of the body-of-evidence, they were demolded 24 hours after mixed, identified and stored in storage tanks for 28 days, with controlled humidity and temperature as specified by ABNT NBR 5738:2008. Once this term storage, the body-of-evidence were taken from the storage tank and stored in a dry environment at room temperature.

The dosage concrete set concrete class for the sample C30 was obtained by adjustments of concrete mixtures resistance (fc) of about 30 MPa.

Through the graphical behavior of concrete was obtained dash for concrete strength estimated at 28 days at 30 MPa. This trait is presented in Table 2.1.

Table 2.1 - Concrete mix for fc = 30 MPa
Material Proportioning by m³ of concrete Mix design (1 : 3.78 : 4.23)W/C ratio = 0.73

Materials	Conventionally Vibrated Concrete
	Quantity per m³
Cement CP V ARI	236 kg
Artificial sand	891 kg
Gravel size 1 (19 mm)	999 kg
Water	172 kg
Polyfuncitonal Additive	1.65 kg (0.7% of cement)
Superplasticizer	0.94 kg (0.4% of cement)
Silica Fume	18.9 kg (as replacement for 8% of cement in weight)
Fresh Concrete Properties:	
Consistency	130 mm
Air	2 %

Were molded nine (9) body-of-proof for the property compressive strength for each laboratory to meet the test methods ABNT NBR 5739:2007.

2.1 TECHNICAL EVALUATION

Was applied to the statistical analysis technique of variance (ANOVA) contained in Statistica Statsoft Software 7® to the results found in individual laboratories for the concrete samples Class C30 separately and together. The test methodology consists of the application of the Fisher test (F).

III. Presentation And Discussion Of Results

As for the main analysis of this study, it is emphasized that the bodies of the test piece were tested in randomized replicas, before running the test for resistance to compression. This randomization minimizes the effects of

variables that were not or could not be considered in the experiment, as the molding process of the body-of-evidence, distribution of aggregates in concrete, installation of the measuring instrument, among others.
In addition, if any dependency mechanism between the results of subsequent experiments, the randomization of the execution of experiments allows this dependency is diluted among all study situations and thus not favoring either situation.

In Table 3.1 presents the means, standard deviations and coefficients of variation of the results for all study situations obtained for the sample with molded concrete class C30, with a confidence interval of the mean (for 95% confidence) and a level of 5% significance for the property compressive strength.

Table 3.1 - Statistical analysis of the test results - Compressive Strength.

Situation of Study				N°. of Specimen	Compressive Strength (MPa)		
Size (mm)	Type of Laboratory	Type of Concrete	Speed of the Testing Machine (MPa/s)		Average (MPa)	Standard Deviation (MPa)	Coefficient of Variation (%)
———	———	———	———	18	30,9	2,3	7,3
———	———	———	0,3	8	30,1	2,8	9,4
———	———	———	0,6	10	31,5	1,6	5,0
———	A	———	———	9	32,3	0,81	2,5
———	B	———	———	9	29,5	2,4	8,1
150X300	A	C30	0,3	4	31,9	0,82	2,6
	A		0,6	5	32,7	0,66	2,0
	B		0,3	4	28,3	3,1	10,8
	B		0,6	5	30,4	1,4	4,6

OBS.: - Concrete types: concrete class C30 for dimensions 150 mm x 300 mm.
- None of the individual results were considered as spurious values.

We performed a statistical analysis of variance (ANOVA) of individual results of compressive strength to determine the factors statistically significant with a confidence level of 95%.

In Table 3.2 is the analysis of the significance of factors studied for the compression resistance property.

Table 3.2 - ANOVA - Analysis of the Global Experiment - Compressive Strength

Factors Studied	SQ	F	p	Resultado
Model Study	47,90	5,64	0,010	significant
Error (residual)	39,63	———	———	———
Total	87,53	———	———	———
Coefficient of Determination Model (R^2) = 0,55				
Speed of the Testing Machine	———	3,38	0,087	not significant
Laboratory	———	13,36	0,003	significant
Speed x Laboratory	———	0,68	0,424	not significative

Where: SQ = sum of squares; F = parameter of Fischer to the test of significance of the effects; p = probability of error involved in accepting the observed result as valid, this is, as representative of the sample; Result = result of the analysis, indicating that the effect is significant or not, $R^2 = (1 - SQerro/SQtotal)$.

The analysis of variance showed compression strength of the resulting value of the coefficient of determination adopted (R^2) was 0.55, which means that 55% of the total variance of the data of the second stage of compressive strength can be explained by the variables adopted. Therefore, uncontrolled factors accounted for approximately 45% of the variations observed in the study.

With respect to the influence of intensity, taking as a basis the magnitude of F values, it can be seen great influence on the results of the laboratory compressive strength.

The interaction effects were not statistically significant, that is, for each type of laboratory used, depending on the speed of loading and unloading of the machine test, the compressive strength of the concrete shows no difference result (similar behavior).

In column F values of Table 3.2, the interactions involving the effect of speed of loading and unloading the machine test lab x had the lowest values, indicating less influence of this variable on the results of compressive strength. It should be noted, also, that the individual effect of the variable speed loading and unloading of the testing machine is not significant, ie the charging and discharging speeds of the testing machine studied (0.3 MPa/s and 0.6 MPa/s), alone and interacted with the laboratory did not influence the results of compressive strength, but it is noteworthy that the analyzed sample is composed of only 18 body-of-evidence, is necessary to perform further testing on a larger sample of bodies-of-

proof to confirm if this situation repeats.

As a result of ANOVA - Compressive Strength (Table 3.2) have revealed the statistically significant effects of variable laboratory held the grouping of homogeneous medium by the method of Duncan, in order to observe the similarities and differences of the results obtained.

In this method, it was shown that laboratories show similar results, as the average overall compressive strength of the laboratory was 32.3 MPa and average overall compressive strength of laboratory B was 29.5 MPa, that is, the lab had overall average compressive strength 9% higher than the laboratory B. Thus, depending on the laboratory used for the test of compressive strength value approaches.

After making the grouping of mean speed factor loading and unloading of the machine tested by the method of Duncan, was demonstrated for the two types of speed of loading and unloading of the testing machine studied, that they do not influence the strength values compression, as the overall average compressive strength of the body of the test piece size 150 mm x 300 mm tested with the test machine speed of 0.3 MPa/s was 30.1 MPa and average overall resistance compressing the body of the test piece size 150 mm x 300 mm tested with the test machine speed of 0.6 MPa/s was 31.5 MPa/s, that is, the body of the test piece 150 mm in size x 300 mm tested with the test machine speed of 0.6 MPa/s differ only 5% of the general average compressive strength compared to the body of the test piece size 150 mm x 300 mm tested with the test machine speed 0.3 MPa/s.

Figure 3.1 shows the graphical analysis of the study, showing the results for each variable.

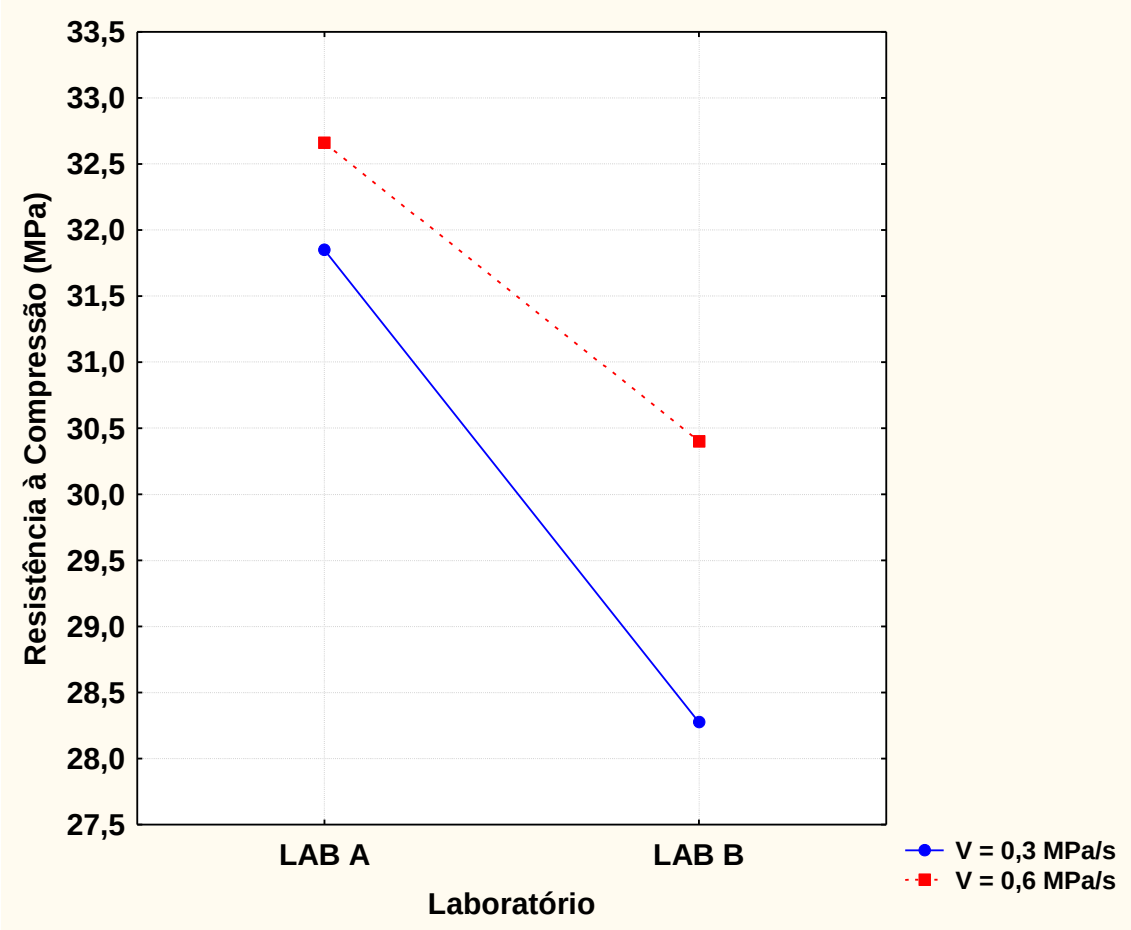

Figure 3.1 - Graphical presentation of study situations, divided by speed of loading and unloading of the testing machine and laboratory.

Figure 3.1 shows the values of compressive strength are shown apart, exhibiting behavior upward between laboratories A and B.

As the bodies of the test piece size 150 mm x 300 mm, tested speeds of loading and unloading of the testing machine of 0.3 MPa/s and 0.6 MPa/s, the results of compressive strength in the laboratory, shown in Figure 3.1, showed averages of 31.9 MPa and 32.7 MPa, and the coefficients of variation were 2.6% and 2.0%. As for the bodies of the test piece size 150 mm x 300 mm tested with the test machine speed of 0.3 MPa/s and 0.6 MPa/s in laboratory B the results showed average compressive strength of 28.3 MPa to 30.4 MPa and their coefficients of variation were 10.8% and 4.6%. As regards the size 150 mm x 300 mm, it was found that the body of the test piece tested with loading and unloading speed of the testing machine of 0.3 MPa/s was dispersed in laboratory B, ie, the body-the proof-tested with the test machine speed of 0.3 MPa/s was 8.2% higher coefficient of variation B in the laboratory with the laboratory A. But the body-of-proof 150 mm x 300 mm tested with speed loading and unloading of the testing machine of 0.6 MPa/s showed greater dispersion in

laboratory B, ie, the body-of-proof tested with speed testing machine of 0.6 MPa/s was 2.6% higher coefficient of variation B in the laboratory compared with the laboratory A.

It was found that the lab B used had the greatest resistance to compression dispersions for changing the speed of loading and unloading of the testing machine.

IV. Conclusion

The true scope of a search is to provide data capable of supporting answers and solutions for the unknowns in the different fields of human knowledge.

Thus, the final considerations aimed at compiling the most important information, cast off the results and settle the practical aspects of the study, facilitating access through technical scientific discoveries.

The final considerations drawn from the presentation and analysis of results presented earlier considered: the influence of laboratory and speed of loading and unloading of the testing machine, and the comparison between these variables obtained in the study and their applicability in the analysis and inspection of structures concrete.

The knowledge of the compressive strength of the concrete is a matter of fundamental importance both in the stages of design and implementation, as in any assessments about the quality of the structures in use. It is necessary to understand the concepts of the test requirements and the variables that influence, to interpret the results and to rule out possible discrepancies caused by deficiencies of the test equipment or operator.

1. After taking the average of the grouping factor loading and unloading speed of the testing machine by the method of Duncan, it was shown for the two types of loading and unloading speed of the testing machine studied that they have little influence values compressive strength, because the overall average compressive strength of the body of the test piece size 150 mm x 300 mm tested with the test machine speed of 0.3 MPa/s was 30.1 MPa and average overall resistance compression of the body of the test piece size 150 mm x 300 mm tested with the test machine speed of 0.6 MPa/s was 31.5 MPa/s.
2. It was found that the body of the test piece tested with loading and unloading speed of the testing machine of 0.3 MPa/s was dispersed in laboratory B because it had more than 8.2% coefficient of variation B in the laboratory with the laboratory A. The body-of-proof tested to speed loading and unloading of the testing machine of 0.6 MPa/s showed greater dispersion in laboratory B because it had more than 2.6% coefficient of variation in laboratory B compared with the laboratory A. It was found that the lab B used had the greatest resistance to compression dispersions for changing the speed of loading and unloading of the testing machine.

In general, the steps inspection of concrete structures involve a series of activities ranging from the collection and analysis of designs and specifications, to the planning and development of research methodology. Furthermore, the effectiveness of the evaluation depends on the knowledge and experience on the part of the researcher. The successful application of the correlations obtained in this study is deeply associated with the professional expertise and prior knowledge about the method of determining the compressive strength of concrete.

It is noted that the results obtained here are valid for materials and test conditions adopted, so you should consider this limit the search.

Acknowledgements

To all of the Master Course in Civil Engineering, School of Civil Engineering, Federal University of Goiás. To all Company Carlos Campos Consultoria e Construções Ltda., The unconditional support and assistance in the execution of the experimental program. To all the staff of Furnas, the suggestions, availability, willingness and readiness to always demonstrated. To all of Realmix and all the Quarry Anhanguera, for providing access aggregates and cement, that every question or request, were always ready to help. The tutor Gilson Natal Guimarães and co-supervisor Professor André Luiz Bortolacci Geyer, the teachings transmitted.

And the teachers of the Master Course in Civil Engineering, School of Civil Engineering, Federal University of Goiás (CMEC - EEC - UFG), the valuable information provided.

This study was conducted with the support of the Federal University of Goiás and the National Council for Scientific and Technological Development - CNPq - Brazil.

In Brazilian society, which, by the Federal University of Goiás, CNPq and Procad / Capes have provided my scholarship and funded the materials needed for research.

References

[1]. ASSOCIAÇÃO BRASILEIRA DE NORMAS TÉCNICAS – ABNT. **NBR 5738:** Concreto – Procedimento para moldagem e cura de corpos-de-prova. Rio de Janeiro: ABNT, 2008.
[2]. _____. **NBR 5739:** Concreto – Ensaio de compressão de corpos-de-prova cilíndricos. Rio de Janeiro: ABNT, 2007.
[3]. _____. **NBR 8953:** Concreto para fins estruturais – Classificação por grupos de resistência. Rio de Janeiro, 2009.
[4]. BEER, F. P.; JOHNSTON Jr, E. R. J. **Resistência dos Materiais**. 3. ed. São Paulo: MAKRON Books do Brasil Editora Ltda., 1995. 1255 p.
[5]. CRESPO, A. A. **Estatística fácil.** 18ª ed. São Paulo: Editora Saraiva, 2002, 224P.
[6]. CUPERTINO, A. L. L., CASTRO, A., INÁCIO, J. J., ANDRADE, M. A. S. **Avaliação de fatores de ensaio que interferem na resistência à compressão e na resistência à tração simples do concreto.** In: CONGRESSO BRASILEIRO DO CONCRETO, 49º., 2007a, Bento Gonçalves - RJ. Anais. São Paulo: Instituto Brasileiro do Concreto, 2007a. CD-ROM.
[7]. JACINTHO, A.E.P.G. de Ávila; GIONGO, J.S. **Resistência Mecânica do Concreto.** In: IBRACON, Concreto: Ensino, Pesquisa e Realizações. Editor: ISAIA, G. S. IBRACON, São Paulo, 2005. cap. 20, p. 605-632. ISBN 85-98576-03-4.

[8]. MARTINS, DANILO GOMES. **Influência do tamanho do corpo de prova nos resultados de ensaios de módulo de deformação e resistência à compressão e suas correlações para concretos produzidos em Goiânia-GO** [manuscrito] / Danilo Gomes Martins. – 2008. Dissertação (Mestrado) – Universidade Federal de Goiás, Escola de Engenharia Civil, 2008.

[9]. METHA, P. K.; MONTEIRO, Paulo J. M. **"Concreto-Microestrutura, Propriedades e Materiais."** 1ª Ed. Português, IBRACON, São Paulo, 2008.

[10]. NEVILLE, A. M. **Propriedades do concreto.** Adam M. Neville; tradução Salvador E. Giammusso. - 2. ed. rev. atual. - São Paulo: Pini, 1997-b. 182.

[11]. SHEHATA, L. D. Deformações Instantâneas do Concreto. In: IBRACON, **Concreto: Ensino, Pesquisa e Realizações**. Editor: ISAIA, G. S. IBRACON, São Paulo, 2005. cap. 21, p. 633-654. ISBN 85-98576-03-4.

International Journal of Modern Engineering Research (IJMER)
www.ijmer.com Vol. 3, Issue. 3, May.-June. 2013 pp-1636-1640 ISSN: 2249-6645

Data Routing in In-network Aggregation in WSN: a Cluster Based approach

Preethi Y. R.[1], Manjunath C. R.[2], Manohar M.[3],
[1, 2] *Department of ISE, SET,. Jain University*
[3]*Nagaraj G S* [4]*, Department of CSE, RVCE, VTU*

Abstract: *Large scale wireless sensor networks (WSNs) consists of many sensor nodes & these networks are deployed in different classes of applications for accurate monitoring, health, environment etc. The sensor nodes equipped with limited power sources. Therefore, efficiently utilizing sensor nodes energy can maintain a prolonged network lifetime. One of the major issues in sensor networks is developing an energy-efficient routing protocol to improve the lifetime of the networks. The proposed approach is a Cluster Based Data Routing for In-Network Aggregation that has some key aspects such as a reduced number of messages for setting up a routing tree, maximized number of overlapping routes, high aggregation rate, and reliable data aggregation and transmission & provides the best aggregation quality when compared to other existing algorithms.*

Keywords: *cluster, data aggregation, energy efficient, Information fusion, In-Network Aggregation, Routing Protocol.*

I. Introduction

A Wireless Sensor Network (WSN) consists of several spatially distributed autonomous devices (sensor nodes) with sensing and communication capabilities that cooperatively sense physical or environmental conditions, such as temperature, sound, vibration, pressure, motion or pollutants at different locations & used in applications such as environmental monitoring, homeland security, critical infrastructure systems, communications, manufacturing etc.WSNs are data-driven networks that usually produce a large amount of information that needs to be routed across the networks. As sensor nodes are energy-constrained devices and the energy consumption is generally associated with the amount of gathered data. Since energy conservation is a key issue in WSNs, Data fusion and Data aggregation is exploited in order to save energy[1][2]. A strategy to optimize the routing task for the available processing capacity can be provided by the intermediate sensor nodes along the routing paths.Data aggregation is defined as the process of aggregating the data from multiple sensors to eliminate redundant transmission and provide fused information to the base station. The main goal of data aggregation algorithms is to gather and aggregate data in an efficient manner so that lifetime of the network increases by decreasing the number of packets to be sent to sink or base station[3], intern reduces the communication costs and energy consumption.

The routing protocol of sensor networks is typically partitioned into two sub routings: (1) flat routing protocol and (2) hierarchical (tree-based or cluster-based) routing protocol [2][3]. In flat routing protocols, data aggregation is accomplished by data centric routing where the sink usually transmits a query message to the sensors, via flooding whereas in the Hierarchical routing protocol data aggregation and data fusion is performed in order to decrease the number of transmitted messages to the sink node. Numbers of algorithms have been proposed to provide data aggregation during the routing in WSNs, majority of them falls in either tree-based or cluster-based algorithms [3][4].Cluster-based algorithms with data aggregation and In-network processing can achieve significant energy savings in WSNs & will be effective in prolonging the network Lifetime[5] , can be either static clustering or dynamic clustering type. Static clustered type networks divide the network proactively into many clusters where as dynamic clustered type networks create a cluster reactively in the vicinity of the event sensing nodes. All the data are collected and aggregated by the cluster head (CH), and then sent to the sink. The main advantage of dynamic type over static type that only the necessary nodes, will participate in the data aggregation, preserving energy of the other sensor nodes. Hence, aggregation rate for dynamic clustered data aggregation is very high [6][11].

II. Hierarchical Cluster Based Approach

In clustered based approaches, each cluster has a cluster-head which is selected among cluster node (members). Cluster-heads plays the role of aggregator which aggregate data received from cluster members locally & then transmits the result to base station (sink)[6].Cluster formation in WSN, nodes in a sensor networks often need to organize themselves to form a cluster, one of the nodes in cluster will be cluster head (CH). Clustering allows hierarchical structures to be built on the nodes and enables more efficient use of resources, such as frequency spectrum, bandwidth, and power. To ensure fair distribution of the workload, the cluster leader is selected randomly at each round of aggregation. The clustering scheme [18] consists of:

Sensor Node: A sensor node of a WSN, a core component, can take on multiple roles in a network, such as simple sensing, data processing, data storage and routing,

Clusters: Clusters for WSNs, is an organizational unit, the dense nature of these networks needed to be broken down into clusters to simplify tasks such a communication.
Cluster-heads: Cluster-heads of a cluster, are the organization leader, often organize the various activities in the cluster such as data-aggregation and organizing the communication schedule of a cluster so on.
Base Station: The base station of the hierarchical WSN, acts as communication link between the sensor network and the end-user.
End User: who generates the query for sensor network, which depend on the application.
Some of cluster based algorithms which are energy constraint protocols are: TEEN [7], APTEEN [8], PEGASIS [9], LEACH [13], InFRA[21] etc. In the Low-Energy Adaptive Clustering Hierarchy (LEACH) [13] algorithm, clustered structures are exploited to perform data aggregation. Cluster-heads (CHs) can act as aggregation points and will communicate directly to the sink node. LEACH-based algorithms assume that the sink can be reached by any node in only one hop, which limits the size of the network for which such protocols can be used. In the Information Fusion-based Role Assignment (InFRA) [21], the algorithm which aims at building the shortest path tree to maximizes information fusion.

III. In-Network Data Aggregation

In data gathering based applications, a considerable number of communication packets can be reduced by in-network aggregation, resulting in a longer network lifetime. In-network aggregation refers to the different ways intermediate nodes forward data packets toward the sink node while combining the data gathered from different source nodes.[2][3] In-network data aggregation is the synchronization of data transmission among the nodes, design of routing protocol is the key component for data aggregation. In-network algorithms, in which a node usually does not send data as soon as it is available since waiting for data from neighboring nodes may lead to better data aggregation opportunities, in turn, will improve the performance of the algorithm and save energy[10].There are two approaches for in-network aggregation with *size reduction* and *without size reduction*. In with size reduction, the size reduction refers to the process of combining & compressing the data packets received by the node & from its neighbors in order to reduce the packet length to be transmitted or forwarded towards sink. In without size reduction, the without size reduction refers to the merging data packets received from the different neighbors in to a single data packets but without processing the value of data [12].

IV. Proposed Approach

In the proposed approach first a routing tree constructed with the shortest paths that connect all source nodes to the sink, maximizing data aggregation. The approach is divided into four phases: setup phase, cluster setup phase, inter cluster routing phase and route repair mechanism.

1. Setup phase

In the setup phase, the base station (BS) transmits a level-1 message with the minimum power. All nodes which receive the message set their level as 1. After that the base station increases its power to attain the next level and transmit a level-2 message. This procedure continuous until the base station transmits corresponding messages to all level [10]. BS broadcast a hello message, figure (1). This message contains the information of upper limit and lower limit of each level and each node calculates the distance from the BS based on received signal strength [13].

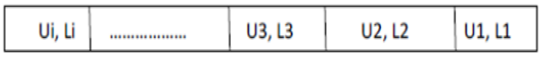

Figure 1.Structure of hello message

Where
Ui: Upper limits of level i
Li: Lower limit of level i

Algorithm 1. Setup phase
#No. of nodes N
BS can transmit i levels; i _1
1. For each level i, message transmitted by BS
2. If(Nodes does not assign previous level and receive new message or BS transmit level i=1)
3. Assign level i
4. End if
5. End for
6. BS broadcast hello message, which contains the information of upper limit and lower limit of each level.
7. Each node calculates the distance from the BS based on received signal strength

2. Cluster setup phase

In this phase each level is divided into clusters. For each level i, each node decide the cluster head for the current round by choosing a nodes randomly. The node which has the higher energy level will be considered as cluster head(CH)[14] .The cluster head for the current round, broadcast the message for the rest of the nodes with the same energy. Each node must inform to the cluster head that it will be a cluster member. Once the clusters are created and TDMA schedule is fixed for all nodes in cluster by CH & data transmission can begin. Each node sends data to its cluster heads with minimal transmission power. This power is estimated by received signal strength of the message. So that data transmission uses a minimal amount of energy [19].When all the data has been received from the cluster members, then the cluster head performs data aggregation function to compress the data into a single signal & process repeats for the next rounds.

Algorithm 2. Cluster setup phase

1. for each (node N)
2. if node N has highest energy level
3. N becomes CH.
4. N broadcasts an message for its cluster nodes.
5. Else
6. N becomes a NCH node.
7. N informs the selected CH and become a member of its cluster.
8. End if.
9. for each (CH)
10. CH creates TDMA schedule for each cluster member.
11. Each cluster member communicates to the CH in its time slot.
12. End for

3. Inter cluster routing

After the cluster formation, the cluster heads broadcast the aggregate data to the next level. At the next level, the nodes aggregate the data received and sends to their cluster heads. In this manner the cluster heads at the last level transmit the final aggregated data to the BS[15].

Algorithm 3.Inter cluster routing

1. For each (level i)
2. for each CH
3. CH receives the data from the cluster member
4. Aggregate the data.
5. If (i ==1)
6. CH transmits data to the BS.
7. Else
8. CH broadcasts data in the next level.
9. End if
10. End for
11. End for

4. Data Transmission Phase

The nodes are divided into different subnets including an cluster head and other nodes after cluster set-up phase. The cluster head may include all nodes of its subnet. The Shortest path from nodes to CH in subnet is calculated by Dijkstra algorithm with the product of the maximum energy consumption of the two nodes and the energy required for sending the data package as a weight. Then CH sends the shortest path tree structure to all sensors in the subnet. Every sensor can transmit data along the path of the shortest path tree in its subnet. The operation is divided into rounds. In each round, SPTs are configured and aggregated data is transmitted from sensors to the cluster-head & the process is repeated. The subnet lifetime is expired if the residual energy of a sensor in the subnet is exhausted [14][15].

Algorithm 4:Data Transmission Phase

```
1.      for each round do
2.          for each subnet do
Weight(I,j)=Esend(I,j)*max{Econsume(i),Econsume(j)}
3.              SPT=Dijkstra{Weight(i,j)}
4.              if Eresidual(k)<=0 then
5.                 break
6.              Ni->Aj::{aggregated data}
7.              end if
8.          end for
9.      end for
```

5. Route Repair Mechanism

The route created to send the data towards the sink node is unique and efficient since it maximizes the points of aggregation. Any failure in one of the node will cause disruption, preventing the delivery of aggregated data [16]. Possible causes of failure include low energy, physical destruction, and communication blockage. In the proposed work a piggybacked, ACK-based route repair mechanism is used, which consists of two parts: detection of failure node and selection of a new Node. When a node needs to forward data to the sink, it simply sends the data packet, sets a timeout, and waits for the ACK message. If the sender node receives ACK from the node within the pre-determined timeout, it will assume that the node is alive .If not, it considers the node as offline and another New node selected. For this, the sender chooses the neighbour with the lowest hop-to-tree level to be its new node; in case of a tie, it chooses the neighbour with the highest energy level. After this repair mechanism, a newly reconstructed path is created & proceeding with forwarding aggregated data towards sink [2][17].This mechanism also provides secured data aggregation[20].

V. Conclusion

Aggregation aware routing algorithms play an important role in event based WSN. The cluster-based algorithm along with data aggregation and in-network processing can achieve significant energy savings. The proposed approach, a cluster based routing protocol will consider the residual energy of nodes to extend the lifetime of sensor networks. These effects on prolonging the network lifetime while incurring acceptable levels of latency and without sacrificing quality. The approach can attain the energy and latency efficiency needed for wireless sensor networks. Furthermore new strategies can be added to control the waiting time for aggregator nodes based on two criteria: average distance of the cluster heads and spatial & semantics of event correlation.

References

[1] Vaibhav Pandey, Amarjeet kaur & Narottam Chand, "A review on data aggregation techniques in wireless sensor network", in Journal of Electronics & Electrical Engineering, ISSN:0976-8106 vol.1 issue 2010,pp 01-08.

[2] Leandro Villas, Azzedine Boukerche, Heitor S. Ramos, " A Lightweight and Reliable Routing Approach for in-Network aggregation in WSN", in Jounal of IEEE Tranactions on computer networks ,vol 38,Mar 2011,pp 393-422.

[3] Rajagopalan, Ramesh and Varshney, Pramod K., "Data aggregation techniques in sensor networks: A survey", (2006), Electrical Engineering and Computer Science. Paper22.

[4] Jamal N. Al-KarakiRazaUl-Mustafa Ahmed E. Kamal , "Data Aggregation and Routing In wireless sensor networks: optimal and heuristic algorithms" ,A survey IEEE wireless communications,vol 11,Dec 2004,pp 6-28.

[5] Woo-Sung Jung, Keun-Woo Lim, Young-BaeKo, "A Hybrid Approach for Clustering-based Data Aggregation in Wireless Sensor Networks", in IEEE transactions on networking,vol 11,pp2-16,Feb 1999.

[6] Sonam Palden Barfunga, PrativaRai, "Energy Efficient Cluster Based Routing Protocol for Wireless Sensor Networks", in International Conference on Computer and Communication Engineering (ICCCE 2012), 3-5 July 2012, Kuala Lumpur, Malaysia

[7] Arati Manjeshwar and Dharma P. Agrawal , **"**TEEN: A Routing Protocol for Enhanced Efficiency in Wireless Sensor Networks", Center for Distributed and Mobile Computing, ECECS Department, University of Cincinnati, Cincinnati, OH 45221-0030,2001.

[8] Manjeshwar and D.P. Agarwal, "APTEEN: A Hybrid Protocol for Efficient Routing and Comprehensive Information Retrieval in Wireless Sensor Networks", in proceedings of Int'l. Parallel and Distributed Processing Symposium (IPDPS), Fort Lauderdale, USA, 2002, pp 195-202.

[9] S. Lindsey and C.S .Raghavendra ,"PEGASIS: Power- Efficient Gathering in Sensor Information Systems",in proceedings of IEEE ICC 2001, vol. 3, Jun 2001, pp.1125-1130

[10] Meenakshi Diwakar and Sushil Kumar ,"An Energy Efficient Level Based Clustering Routing Protocol for Wireless Sensor Networks", in International Journal Of Advanced Smart Sensor Network System, Vol 2, No.2, April 2012.

[11] P. Krishna N. H. Vaidya, M. Chatterjee, "Cluster-based Approach for Routing in Dynamic Networks", Department of Computer Science & Digital Equipment Corporation Texas A&M University,May 2004

[12] Mohammad Mostafizur Rahman Mozumdar, Nan Guofang, Francesco Gregoretti, "An Efficient Data Aggregation Algorithm for Cluster-based Sensor Network", Department of Electronics, Politecnico di Torino, Italy.Journal of Networks, Vol. 4, no. 7, September 2009.

[13] Uk-Pyo Han, Sang-Eon Park, Seung-Nam Kim, "An Enhanced Cluster Based Routing Algorithm for Wireless Sensor Networks" ,Computer Science Department, Kangwon National University, Chunchon, Korea, Vol. 40, Issue 8,pp. 102-114, Aug. 2002
[14] V. Akila, Dr. T. Sheela, Computer Science and Engineering, Bharath University, Chennai , "Overview of Data Aggregation Based Routing Protocols in Wireless Sensor Networks", in International Conference on Information Systems and Computing, Volume 3, Special Issue 1, January 2013
[15] Zhicheng Dai,Bingwen Wang ,Zhi Li,"An Energy Aware & Cluster Based Data Routing Algorithm for Wireless Sensor & Actor Network", in Information Technology Journal 8,1044-1048,2009
[16] Chris Karlof, David Wagner "Secure routing in wireless sensor networks: attacks and counter measures" ,University of California, Berkeley, CA 94720, USA, (2003) ,pp293–315
[17] B. Kumar, N. Vikram and M. Malla Reddy, "Secure Data Collection in Wireless Sensor Networks Using Random Routing Algorithms", in International Journal of Computer Science and Telecommunications ,Volume 2, Issue 4, July 2011.
[18] Harneet Kour,Baba Ghulam Shah Badshah University, Rajouri, "Hierarchical Routing Protocols In Wireless Sensor Networks", in International Journal of Information Technology and Knowledge ManagementDecember 2012, Volume 6, No. 1, pp. 47-52.
[19] Jin Wang, Jianwei Zhang, Jeong-Uk Kim ,**"**An Energy-based Clustering Algorithm for Wireless Sensor Networks", in Computer Networks, vol.38, no.4, pp.393-422, 2002.
[20] Sanjeev SETIA ,Sankardas ROY, "Secure Data Aggregation in Wireless Sensor Networks ",in Computer Science Department, George Mason University, USA,pp1361-1364, 2004.
[21] Eduardo F. Nakamura, Horacio A.B.F. de Oliveira, "On Demand Role Assignment for Event-Detection in Sensor Networks",Department of Computer Science, Federal University of Minas Gerais in 11th IEEE Symposium on Computers and Communications, 2006.

International Journal of Modern Engineering Research (IJMER)
www.ijmer.com Vol. 3, Issue. 3, May - June 2013 pp-1641-1644 ISSN: 2249-6645

Development of Mathematical Models for Determination of Failure Loads of Glass Epoxy Composite Plates

K. Sridevi
Department of Mechanical Engineering, Faculty of Technology and Engineering, The M.S. University of Baroda, India

***ABSTRACT**: This paper deals with the mathematical study of failure loads of glass epoxy composite plates with two serial holes subjected to traction force by two serial rigid pins. To evaluate the effect of joint geometry on the failure loads the geometrical parameters such as the edge distance of first hole-to-hole diameter (E/D), the width of the specimen-to-hole diameter (W/D), and the distance between center of two holes-to-hole diameter (K/D) were varied from 1-4, 2-4, and 3-4 respectively. Mathematical models have been developed for both wet and dry specimens to determine the failure loads of different geometry plates. Wet specimens are specimens immersed in seawater for 24 hours. The unimmersed specimens are called dry specimens. Here Full Cubic models have proved to be very efficient. A comparison of the results from mathematical models with the experimental results from existing literature shows high values of correlation co-efficient, Root Mean Square Error and Maximum Absolute Error. For estimation of the failure loads within the range of E/D, W/D and K/D considered for the study, the mathematical models developed are found to be efficient.*

***Keywords:** composite plates, pin joint, failure load.*

I. INTRODUCTION

Composite materials have a wide range of applications because of their light weight, high strength to weight ratio, good fatigue resistance, corrosion resistance etc. compared to metals. The applicability of composite materials has increased the demand for high reliability materials in various industries like aerospace, aircraft, and automobile. In building complex structures several parts must be joined together. Most of these joints are formed by using mechanical fasteners such as pins because of their low cost, simplicity and easy assembly and disassembly. Also, multiple fasteners can be used in many applications. The difficulty with this method is that the presence of a hole in a laminated plate subjected to external loading introduces a disturbance in the stress field. Stress concentrations are generated in the vicinity of the hole making the joint a weak one. The knowledge of failure strength of a joint helps in selecting the appropriate joint size in a given application. The capability of a composite structure to withstand any physical load can be evaluated either by physical testing or any advanced computational method. Performing physical tests on composites is destructive and costly. So, implementing advanced computational techniques to determine the failure loads are preferred after some experiments are done.

Owing to the significance of the problem, several investigators have developed procedures to determine the strength of pin joints in composite materials. Chang et al. (1982) developed a computer code to find the failure loads and failure mode of composite joints with different ply orientations, different material properties and geometries. Vyasaraj and Kakhandki (2005) obtained analytical solutions for an irregular shaped hole in an orthotropic laminate. Karakuzu et al. (2006) predicted the failure loads experimentally and numerically on glass vinylester composite plates subjected to pin loading. In the numerical analysis, they used the Hashin failure criterion in order to determine failure loads and failure modes. LUSAS commercial finite element software was utilized during their analysis. Whitworth et al. (2008) investigated the characteristic dimensions in tension and compression using point stress failure criteria and Yamada-Sun failure criteria. Murat Pakdil (2009) has studied the failure analysis of composite single bolted joint subjected to pretension on the bolt. The composite laminated plates are stacked with different ply orientations. It was observed that the failure modes and the bearing strength depend on the stacking sequence, geometrical parameters and bolt pretension. Aktas (2011) performed experimental and numerical study to determine the failure behaviour of glass epoxy composite plates with single and two holes. The numerical study was performed by using ANSYS and Yamada-Sun failure criteria. Ozen and Sayman (2011) investigated experimentally and numerically the first failure load and the bearing strength behaviour of pinned joints of glass fibre reinforced woven epoxy composite prepregs with two serial holes subjected to traction forces by two serial rigid pins. The effect of seawater on the bearing strength of the joints was studied by immersing the specimens for 24hours in seawater. It was observed that immersion in seawater reduces the failure load of the specimens. Ondurucu (2012) has studied the effects of joint geometry and stacking sequence on the bearing strength and damage mode experimentally. Damage progression was later examined by using scanning electron microscopy on specimens loaded up to ultimate failure. Khashaba et al. (2013) has dealt with the failure and reliability analysis of composite pinned-joints using theoretical models based on Weibull distribution function with experimental results for a guideline of safe design strength. Soykok et al. (2013) have carried experiments to understand the effect of thermal condition and tightening torque on the failure load and failure behavior of glass epoxy composite joints. It was observed that the load carrying capacity of the joint decreased by increasing the temperature level. The tightening torque was observed to increase the joint strength.

In the present work, mathematical models have been developed to predict the failure loads of composite pin joints under both dry and wet conditions. The results obtained from the mathematical models are compared with the experimental results of Ozen and Sayman (2011).

II. PROBLEM DEFINITION

To evaluate the effects of joint geometry, the ratio of edge distance to the hole diameter (E/D), the ratio of width of the specimen to the hole diameter (W/D) and the ratio of distance between center of two holes to the hole diameter (K/D) were varied from 1-4, 2-4 and 3-4 respectively. Here specimens are considered dry and wet i.e. specimen held in sea water for 24 hours.

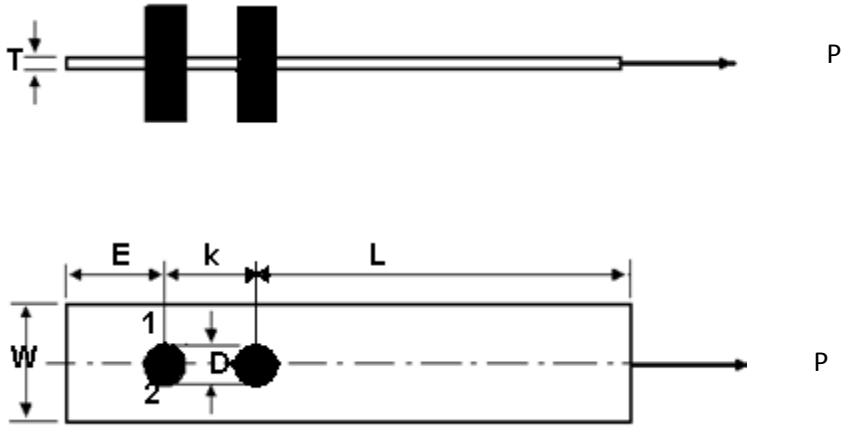

Fig. 1. Geometry of the specimen

The geometry of the composite specimen is shown in Fig. 1. Here W represents the width of the plate, E the edge distance of the first hole from one end of the plate, K is the distance between the two holes and T is the thickness of the plate. The diameter of the holes is shown as D. The total length of the plate is L+K+E. The diameter of the holes, thickness of the plate and the total length of the plate are taken constant as 5mm, 0.8mm and 80mm respectively. A load P is applied to the plate along the longitudinal axis. The plate is symmetric with respect to the longitudinal axis.

The material properties considered, that are given by Ozen and Sayman (2011), are shown in Table 1. Different models are obtained by varying E/D, W/D and K/D but keeping the parameters D, T and total length as constant. Mathematical models are developed to obtain the failure loads of different specimens. A comparison with experimental results is made and correlations are observed.

Table 1: Material properties of the composite plate

E_1 (GPa)	G_{12}(GPa)	μ_{12}	X_t (MPa)	X_C (MPa)	S(MPa)	V_f(%)
22.3	7.5	0.14	295.6	143.9	83.9	57

III. MATHEMATICAL MODELLING

Mathematical models have been developed to predict the failure loads of specimens with different geometries using curve expert. The models are built with the available experimental results. The equation has two independent variables in W/D ratio as x_1 and E/D ratio as x_2. The dependent variable considered here is the failure load P. The thickness of the specimen and the diameter of the hole are constant for all the specimens. Full Cubic model is found to be best suited to determine the failure loads for the existing problem. Equations are developed for dry and wet specimens with K/D ratios equal to 3 and 4 wherein each case W/D varies from 2-4 and E/D varies from 1-4.

These equations can be used to predict the failure load of specimens with other geometric parameters within the given range i.e. for E/D and W/D ratios for which experiments have not been done. It thereby saves the cost and time in carrying out the tests. Hence, the mathematical models are best suited to obtain the results for failure loads. The Full-cubic equation developed is found to be

$$P = a + b*x_1 + c*x_2 + d*x_1^2 + e*x_2^2 + f*x_1^3 + g*x_2^3 + h*x_1*x_2 + i*x_1^2*x_2 + j*x_1*x_2^2$$

Wherein the value of the co-efficients a, b, c, d, e, f, g, h, i and j are given in Table 2. Here model 1 represents dry specimens with K/D=3, model 2 for wet specimens with K/D=3, model 3 for dry specimens with K/D=4 and model 4 for wet specimens with K/D=4.

Table 2: Co-efficients of the full cubic model developed

Model	a	b	c	d	e	f	g	h	i	j
1	-6181	8230	-1440	-2886	248	329	-42	798	-125	-1.5
2	1083	261	-890	-196	1.8	26.8	9.5	706	-72.1	-42
3	1018	-483	-490	451	-6.02	-79.9	18	334	1.15	-52.9
4	6473	-4582	-2921	1317	321	-124	-12	1626	-191	-91.6

IV. RESULTS AND DISCUSSION

Composite specimens with two serial pin holes subjected to traction forces by rigid pins are studied. The specimens are considered both dry and wet i.e. soaked for 24hours in seawater. Mathematical models have been separately developed for both dry and wet specimens. Fig. 2 represents the graphs showing the comparison between the results obtained from the mathematical models with the existing experimental results for different E/D, W/D and K/D ratios. Mathematical models follow the same trend as that of experimental results.

- For a constant W/D ratio, the failure load P increases with increase in E/D ratio and when E/D ratio is maintained constant, the failure load P increases with increase in W/D ratio. This is because when the width of the specimen is increased keeping the edge distance constant the normal and bearing strength increases. Similarly when the edge distance of the hole is increased keeping the width of the specimen constant, the shear strength of the specimen increases.
- With the increase in K/D, for constant W/D and E/D ratios the value of failure load P increases as the distance between the holes increases.
- The failure loads of wet specimens have been observed to be low when compared to the failure loads of dry specimens. So, seawater has a negative effect on the joint strength.

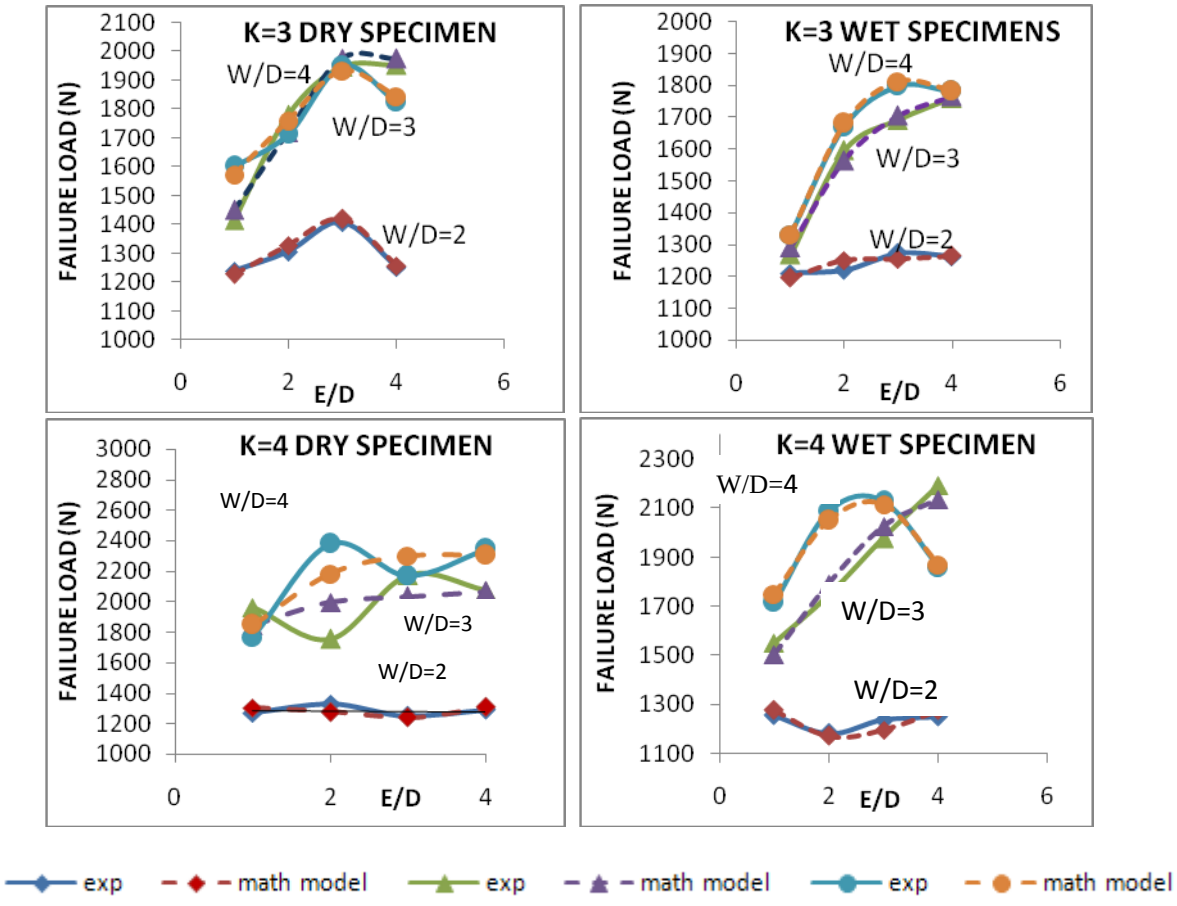

Fig.2 Comparison of Experimental and Mathematical Model Results

- The correlation between the mathematical models and experimental results is found to be high. Table 3 shows the correlation coefficient, Root Mean Square error and maximum absolute error.

Table 3: Correlation coefficient, Root Mean Square error and maximum absolute error

MODEL	Maximum absolute error	Root mean square error	Correlation coeffecient
1	60	30	0.994
2	31	16.96	0.997
3	198	116	0.960
4	58	36.56	0.995

V. CONCLUSIONS

In this paper, mathematical models have been developed to predict the failure loads of glass epoxy composite plates with two serial holes subjected to traction force by two serial rigid pins.

- When W/D=2, the increase in failure load with increase in E/D is relatively less compared to when W/D=3 and 4. This is because as the width of the specimen increases, the bearing strength of the specimen increases. So the specimen tends to fail at higher loads. But the margin in the failure loads for W/D = 2, 3 and 4 show that the specimen is weak for W/D=2.
- At constant E/D ratio, as the W/D ratio increases the failure loads increase. The margin in the failure loads for W/D=2, 3, 4 is observed to increase as the E/D ratio increases from 1 to 4. But the maximum failure load in most of the cases is observed to be at E/D=3. Later with increase in E/D, the failure load is found to decrease.
- When the specimens were soaked for 24hours in seawater, then they are found to fail at lower loads compared to the dry specimens. So, seawater was observed to have a negative effect on the failure loads of the specimens.
- Mathematical models show the same trend in the failure loads of specimens, when compared with the experimental models. So, for estimation of the failure loads within the range considered for the study, the mathematical models developed, i.e., Full Cubic Models proves to be efficient with the given values of Correlation Co-efficient, Maximum Absolute Error and Root Mean Square Error.

REFERENCES

[1] Chang., F.K., Scott, R.A., Springer, G.S., 1982, Strength of mechanically fastened composite joints, Journal of Composite Materials, 16:470-494

[2] Vyasaraj and Kakhandki, 2005, Stress analysis of an orthotropic plate with an irregular shaped hole for different in-plane loading conditions-Part 1, Composite Structures, 70, 255-274

[3] Karakuzu, R., Gulem, T., and Icten, B.M., 2006, Failure analysis of woven laminated glass- vinylester composites with pin loaded hole, Composite Structures, 72 (1), 27-32

[4] Whitworth, H.A., Aluko, O., Tomlinson, N.A., 2008, Application of point stress criterion to the failure of composite pinned joints, Engineering Fracture Mechanics, 75, 1829-1839

[5] Murat Pakdil, 2009, Failure analysis of composite single bolted-joints subjected to bolt pretension, Indian Journal of Engineering and Materials Sciences, 16, 79-85

[6] Aktas, A., 2011, Failure analysis of serial pinned joints in composite plates, Indian Journal of Engineering and Material Sciences, Vol 18, 102-110

[7] Ozen, M., Sayman, O. 2011, Failure loads of mechanical fastened pinned and bolted composite joints with two serial holes, Composites: Part B 42, 264–274

[8] Ondurucu, A., 2012, Progressive failure analysis of glass–epoxy laminated composite pinned-joints, Materials and Design 36, 617–625

[9] Khashaba, U.A., Sebaey, T.A., Alnefaie, K.A., 2013, Failure and reliability analysis of pinned-joints composite laminates: Effects of stacking sequences, Composites: Part B, 45 (2013) 1694–1703

[10] Soykok, I.F., Sayman, O., Ozen, M., Korkmaz, B., 2013, Failure analysis of mechanically fastened glass fiber/epoxy composite joints under thermal effects, Composites: Part B 45, 192-199.

International Journal of Modern Engineering Research (IJMER)
www.ijmer.com Vol. 3, Issue. 3, May.-June. 2013 pp-1645-1648 ISSN: 2249-6645

Modeling and Optimization of Wire EDM Process

K. Kumar[a], R. Ravikumar[b]

[a] *Department of Mechanical Engineering, Arasu Engineering College, Kumbakonam, Tamilnadu, 612501, India*
[b] *Department of Mechanical Engineering, PGP College of Engineering & Technology Namakkal, Tamilnadu, 637001, India.*

Abstract: *The present work is aimed to optimize the parameters of (WEDM) process by considering the effect of input parameters viz. Time On, Time Off, Wire Speed & Wire Feed. Experiments have been conducted with these parameters in three different levels data related to process responses viz. Metal removal rate, surface roughness (Ra) have been measured for each of the experimental run. These data have been utilized to fit a quadratic mathematical model (RSM) for each of the responses, which can be represented as a function of the process parameters. Predicted data have been utilized for identification of the parametric influence in the form of graphical representation for showing influence of the parameters on selected responses. Predicted data given by the models (as per Taguchi's L_{27} OA) design have been used in search of an optimal parametric combination to achieve desired yield of the process. Taguchi techniques have been used for optimization of minimizing the surface roughness. The optimal value has been verified to the predicted value.*

Key words*: Wire EDM, Surface roughness, RSM, DOE, Al-SIC (20%)*

I. INTRODUCTION

WEDM process involves the complex erosion effect by rapid repetitive and discrete spark discharges between the wire tool electrode and work piece immersed in a liquid dielectric medium. WEDM is used in the area of production of aerospace parts micro gas turbine blades and electronic components. As research work even in WEDM much standard references are not available for the selection of the parameters and the level for optimizing the performance characteristics. Hence it is necessary to conduct an extensive experimental investigation to study the effect of different process parameters for the accuracy and surface finish of WEDM machined components an attempt is also made to obtain machinery performance with the RSM. The electrical discharge energy affected by the spark plasma intensity and the discharging time will determine the crater size, which in turn will influence the machining efficiency and surface quality [1]. For determining the optimal parametric settings, lot of work has been done in the engineering design. But mostly all of them concentrated on a single response problem. However, the WEDM processes are having several important performance characteristics like MRR, SR, etc. The optimal parametric settings with to different performance characteristics are different. Scott et al [2] have presented a formulation and solution of a multi objective optimization problem for the selection of the best parameter settings on a WEDM machine. The measures of performance for the model were MRR and surface quality. In that study, a factorial design model has been used to predict the measures of performance as a function of a variety of machining parameters. Lin [3] presented the use of grey relational grade to the machining parameter optimization of the EDM process. Optimal machining parameters setting for WEDM still has some difficulty. It may be noted that most of the prevailing approaches have used complex mathematical or statistical methods such as ANN, dual response approach, genetic algorithm, simulated annealing, linear or non linear or dynamic programming. These approaches are difficult to implement by individuals with little background in mathematics/statistics and so are of little practical use. Ramakrishnan et al [4] also lacks the way to convert multiple objectives into a single objective format though the method is relatively simple. Tanimura et al [5] projected new EDM process using water mist, which requires no tank for the working fluid. They also pointed out that the mist-EDM/WEDM enables non-electrolytic machining even, when electrically conductive water is used as the working liquid. Fu-chen Chen et al [6] Research is based on fuzzy logic analysis coupled with taguchi methods to optimize the precision and accuracy of the high-speed electrical discharge machining (EDM) process, pulse time, duty cycle, peak value of discharge current as the most important parameters, powder concentration, powder size are found to have relatively weaker impacts on the process design of the high speed EDM. H.Singh et al [7] analyze the effects of various input process parameters like pulse on time, pulse off time, gap voltage, peak current , wire feed and wire tension have been investigated and impact on MRR is obtained. Finally they reported MRR increase with increase in pulse on time and peak current. MRR decrease with increase in pulse off time and servo voltage. Wire feed and wire tension has no effect on MRR. A.K.M. Nurul Amin et al [8] Conducting experiments on cutting of tungsten carbide ceramic using electro-discharge machining (EDM) with a graphite electrode by using taguchi methodology. The taguchi method is used to formulate the experimental layout, to analyze the effect of each parameter on the machining characteristics, and to predict the optimal choice for each EDM parameter such as peak current, voltage, pulse duration and interval time. It is found that these parameters have a significant influence on machining characteristic, such as metal removal rate (MRR), electrode wear rate (EWR) and surface roughness (SR). Kuo-Wei Lin et al [9] conduct test Wire Electrical Discharge Machining (WEDM) of magnesium alloyparts via the taguchi method-based gray analysis was conducted; they considered multiple quality characteristics required include material removal rate and surface roughness following WEDM. Kamal Jangra et al [10] Investigated on Influence of taper angle, peak current, pulse-on time, pulse-off time, wire tension and dielectric flow rate are investigated for material removal rate (MRR) and surface roughness (SR) during intricate machining of a carbide block. In order to optimize MRR and SR simultaneously, grey relational analysis (GRA) is employed along with taguchi method. WC-Co composite is studied, grey relational analysis

(GRA) is employed along with taguchi method, the percentage error between experimental values and predicted results are less than 4% for both machining characteristics.

The highlights of this paper is to significance the process parameters and different machining condition on MRR and surface roughness of the Al-sic(20%) mathematical models are developed to correlate the process parameters and performance measures. The objective of the study is to minimize the surface roughness.

II. EXPERIMENTAL WORK

Experiments are conducted in series with three level three full factorial experimentation is developed using DOE with input parameters shown in table 1. Holes of 5mm diameter are drilled on 10mm thick Al-sic(20%) plate WEDM using molybdenum wire of diameter 0.18mm. The influence of process parameters on the machining of drilled hole is also analyzed. The average surface roughness (Ra) value of drilled hole is determined using surface roughness tester.

Table1. L27 orthogonal array with Wire EDM process parameters

Exp No	Speed	Feed	Time ON	Time OFF
1	500	0.5	100	40
2	500	0.5	100	40
3	500	0.5	100	40
4	500	0.7	102	42
5	500	0.7	102	42
6	500	0.7	102	42
7	500	0.9	104	44
8	500	0.9	104	44
9	500	0.9	104	44
10	1000	0.5	102	44
11	1000	0.5	102	44
12	1000	0.5	102	44
13	1000	0.7	104	40
14	1000	0.7	104	40
15	1000	0.7	104	40
16	1000	0.9	100	42
17	1000	0.9	100	42
18	1000	0.9	100	42
19	1500	0.5	104	42
20	1500	0.5	104	42
21	1500	0.5	104	42
22	1500	0.7	100	44
23	1500	0.7	100	44
24	1500	0.7	100	44
25	1500	0.9	102	40
26	1500	0.9	102	40
27	1500	0.9	102	40

The experiments were performed on SPRINT CUT 734 DI WATER CUT WEDM and the experimental setup is shown in figure 1.

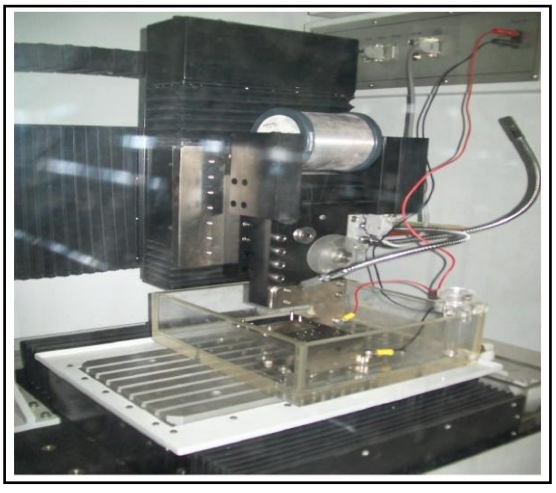

Figure1. WEDM experimental set up

The molybdenum wire as tool electrode with flushed type dielectric fluid pressure 0.2 kgf/cm^2 (distilled water) bath between work piece and electrode. Electrical power and controlling system is controlled with servo controlled resistance capacitance (Rc) circuit which ensures low discharge current with high frequency to control input process parameters.

The analysis is done to study the main effects and their interactions to explore the effect of the influence of parameters on the performances.

In this study, Taguchi method, a powerful tool for parameter design of the performance characteristics has been used to determine optimal machining parameters for maximization of MRR and minimization of SF in wire EDM.

Experiments have been carried out using Taguchi's L27 Orthogonal Array (OA) experimental design which consists of 27 combinations of four process parameters. According to the design prepared by Taguchi, L27 Orthogonal Array design of

experiment has been found suitable in the present work. It considers four process parameters (without interaction) to be varied in three discrete levels. Based on Taguchi's L27 Orthogonal Array design (Table 3), the predicted data provided by the mathematical models can be transformed into a signal-to-noise (S/N) ratio; based on three criteria. The characteristic that higher value represents better machining performance, such as MRR, 'higher-the-better, HB; and inversely, the characteristic that lower value represents better machining performance, such as surface roughness is called 'lower-the-better', LB. Therefore, HB for the MRR, LB for the SF has been selected for obtaining optimum machining performance characteristics.

Table 2. Surface roughness predicted for 27 experiments

Exp No	Ra	Exp No	Ra	Exp No	Ra
1	2.35	10	1.45	19	1.257
2	2.402	11	1.526	20	1.283
3	2.37	12	1.582	21	1.265
4	2.645	13	1.752	22	1.468
5	2.721	14	1.79	23	1.457
6	2.82	15	1.808	24	1.365
7	3.094	16	3.203	25	2.308
8	3.265	17	3.012	26	2.45
9	3.354	18	3.208	27	2.22

From the predicted surface roughness values, the S/N ratios and their corresponding mean of means plots are shown in figure 2 and 3 respectively. Analysis of the result leads to the conclusion that factors at level A3, B3, C1, D3 gives maximum surface roughness. Although factors A factor is not show significant effect on surface roughness, it is recommended to use the factors at level A2, B3, C2, D3 for minimization of Ra as shown in Fig. 2 and 3. Factors A have least contribution for maximization of surface roughness. Figure 4 represents the closeness between the predicted and the observed reading of surface roughness (Ra).

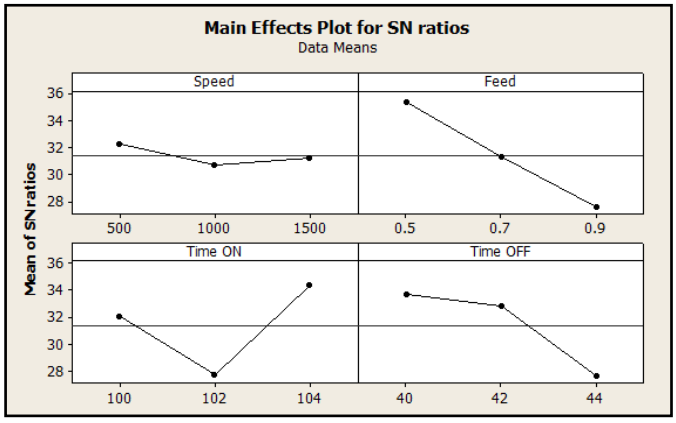

Figure 2. Main effect plot for S/N ratio

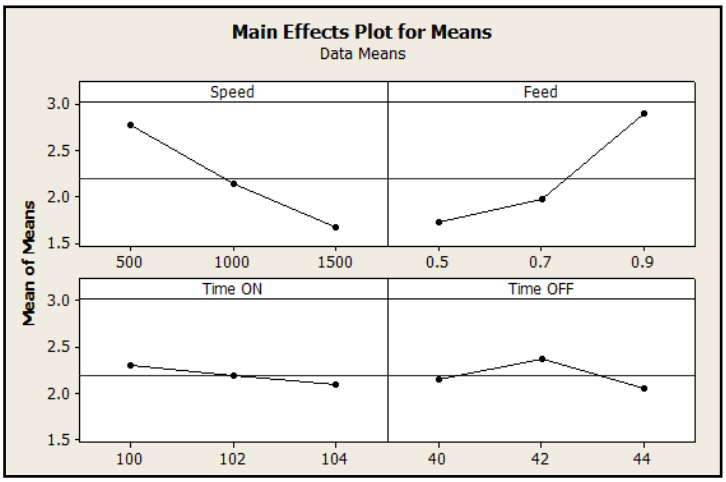

Figure 3. Main effect plot for Means

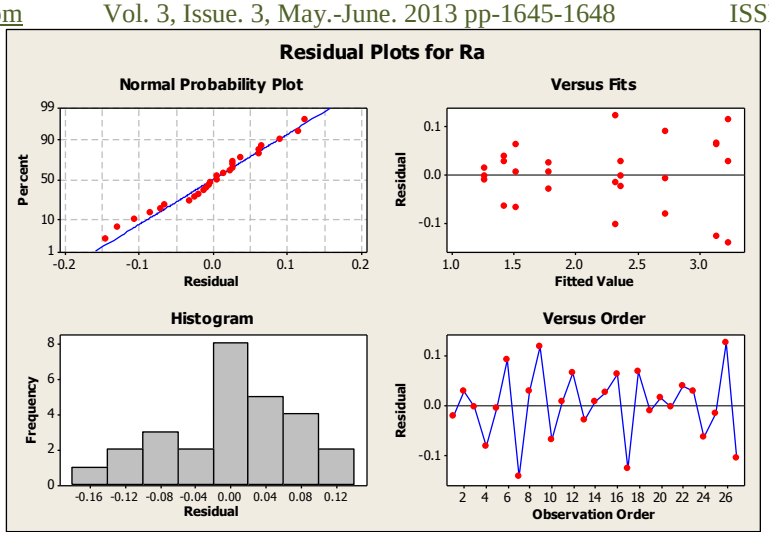

Figure 4. Residual plot for WEDM process parameters

III. CONCLUSION

In this article, an attempt was made to determine the significant machining parameters for performance measures surface roughness in the WEDM process. Factors like speed, feed, Time on and Time off have been found to play a significant role for MRR and surface roughness. Taguchi's method is used to obtain optimum parameters combination for maximization of surface roughness. The conformation experiments were conducted to evaluate the result predicted from Taguchi Optimization.

References

[1] Ho.K.H .Newman S.T..Rahimiford S,.Allen R.D (2004) State of the art in wire electrical discharge machining. Int J Mach Tool Manuf 44 : 1247-1254.

[2] Scott D, Boniya S, Rajurkar KR, (1991) Analysis and optimization of parameter combination in wire electrical discharge machining. Int J Prod research 29 (11) :2189-2207.

[3] Lin JL, Wang KS, Yan BH, Tarang YS (1998) Optimization of the multi-response process by the Taguchi method with grey relational analysis. J Grey syst 10 (4) :355-370.

[4] Ramakrishnan R, Karunamoorthy L (2006) Multi response optimization of wire EDM operations using robust design of experiments. Int J Adv Manuf Technol 29 :105-112.

[5] Tanimura (2006) Taguchi and Gauss elimination method. A dual response approach for parametric optimization of CNC wire cut EDM of PRAlSiCMMC, A. International Journal of Advanced Manufacturing Technology (2006) 28: 67–75

[6] Yih-fong Tzeng, Fu-chen Chen (2007). Multi-objective optimisation of high-speed electrical discharge machining process using a Taguchi fuzzy-based approach, Materials and Design 28 (2007) 1159–1168

[7] H. Singh, R. Garg (2009) Effects of process parameters on material removal rate in WEDM, Journal of achievements in material and manufacturing engineering, Volume 32, Issue.

[8] Mohd Amri Lajis, H.C.D. Mohd Radzi, A.K.M. Nurul Amin (2009) The Implementation of Taguchi Method on EDM Process of Tungsten Carbide. European Journal of Scientific Research, ISSN 1450-216X Vol.26 No.4 (2009), pp.609-617

[9] Kuo-Wei Lin, Che-Chung Wang (2010), Optimizing Multiple Quality Characteristics of Wire Electrical Discharge Machining via Taguchi method-based Gray analysis for Magnesium Alloy. Journal of C.C.I.T., VOL.39, NO.1, May 2010

[10] Kamal Jangra, Sandeep Grover and Aman Aggarwal (2011) Simultaneous optimization of material removal rate and surface roughness for WEDM of WCCo composite using grey relational analysis along with Taguchi method, International Journal of Industrial Engineering Computations 2 (2011) 479–490.

International Journal of Modern Engineering Research (IJMER)
www.ijmer.com Vol. 3, Issue. 3, May - June 2013 pp-1649-1653 ISSN: 2249-6645

An Efficient Deduction Of Data Loss Rate In Wireless Sensor Network

K. Aarthi Priyamvadha, R. Mohanasundaram
Department Of ECE-KSRCE, Tiruchengode

Abstract: *The emerging achievements in the field of wireless sensor networks in communication and information technology has largesse its presence in automation trait with its unique characteristics of reliability and flexibility. The peculiar feature of WSN spins the entire world in soft keys. The key challenge in WSN design is the efficient data transmission with minimum power consumption and prolonged network lifetime. The data transmission in existing active measurement mainly feigns on the collection of energy reports and reduction of network overhead which proceeds in the languishment of scalability and data loss. This has been overcome with the passive measurement of data monitoring that provides the efficiency of data transmission in distributed network environment. This further achieves the power conservation for the entire network. Thereby, it saves the time in transmitting and receiving the data and further allows the consistent data flow in the shortest path provided from source to destination.*

Keywords: *Data aggregation, multicast, WSN, power.*

I. INTRODUCTION

The data communication network has its physical connection in two different way as point to point and multipoint. While many sensors connect to controllers and processing stations directly to a centralized processing station. The emerging trends use multipoint for its data transmission to other networks. Since multipoint environment shares the capacity of the channel either spatially and temporally. With these enhancements, a sensor node is often not only responsible for data collection, but also for in-network analysis, correlation, and fusion of its own sensor data and data from other sensor nodes. When many sensors cooperatively monitor large physical environments, they form a wireless sensor network (WSN). Sensor nodes communicate not only with each other. The primary equipment sensor plays a major role in sensing, processing and transmitting the data from source to destination which also aids in forming the wireless sensor networks. However, the WSN gives the key challenge in various factors include reliable transmission, power management [12] data accuracy in the end to end performance.

The WSN also enhance the communication by finding the shortest distance between the sensor nodes. This can be achieved through algorithms available in the multicast routing protocol. When data being collected from multiple source, there exists the property of redundancy which results in the reduction of efficiency in WSN. Hence, to avoid this bogus message, the wireless communication network introduces the data aggregation.

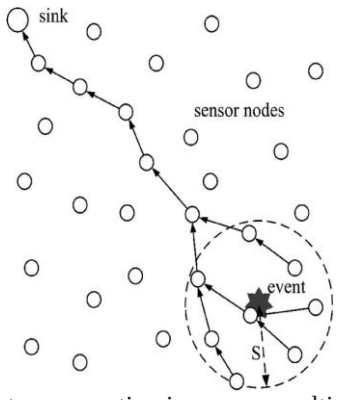

Fig.1 Data aggregation in reverse multicast tree

In the process of data aggregation, a subset of nodes in the network attempts to forward the sensing data they have collected back to the sink via a reverse multicast tree. When an intermediate node in the reverse multicast tree receives data from multiple source nodes, it checks the contents of incoming data, combines them by eliminating redundant information and then forwards the aggregated packet to its parent. The data can be transmitted in reverse multicast routing to the sink through constrained path and data aggregation aids in achieving the end to end performance. A tree structure is commonly used for data aggregation [13]. The inherent data transmission in the multicasting gives the delay.

II. RELATED WORKS

WSN elevates in providing reliable communication but finds it difficult to overcome the latency which is the major hindrance to achieve the accuracy in multicasting. The latency is mainly due to data aggregation[23] in the cluster head. The attacks against the data aggregation in results in faking the sensed data or duplicate the original message without any information in it. As the data aggregating took place with the fake or malicious code, the energy consumption and transmission load increases in wireless sensor network environment. Nodes in the network transmit measurements to parents subject to the interference constraints which is node exclusive. Parents fuse information and transmit it to their parents. Then the Sink computes the sum which it got from its leaf nodes. This allows significant savings but the interference increases the delay. The Aggregated event data needs to reach sink within a deadline, which is specified by each sensor node. It has arbitrary set of source nodes. The sink requires aggregated form of data. This has the main drawback of unreliable links which need to retransmit the data multiple times to achieve success.

III. SYSTEM MODEL

Consider a sensor nodes in which source node has a data packets to send .All these packets are send periodically. The nodes must travel in the shortest path so that it reduces the inherent time delay of the data transfer from source to destination it should also noted that the data should be in consistent flow.
Now consider a sample network where nodes 1,2,3,4, an7 are the sources.

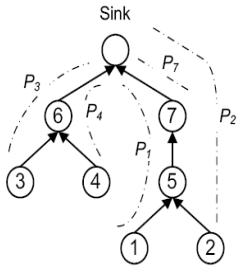

Fig 2.network includes multiple source and single destination

Also, $p_{1,}\ p_{2,}\ p_{3,}\ p_{4,}$ and p_7 represents the path from source to destination. The path from different sources to destination not only involves in the correct delivery of data but also the accuracy and efficiency of data should show it improving the network performance to find shortest path and to save the power. This can be achieved only through the passive measurement of WSN. It passively monitors the traffic in the network and it includes the algorithms to infer the loss rates of packet. The data can be collected by a single node to avoid excess of data and it get incremented to reach the destination. The power should be calculated in order to find the capability of the node to receive and transmit the given data to the respective destination.

IV. PROBLEM FORMULATION

Consider a set of nodes (V) and set of links (L) in a tree (T) represented as , T=(V,L) in a multicast tree. In this, directed graph, the non-negative weight function w and source s terminates with d[U]=δ(U,V) for all vertices Uϵ V. This tree also includes the sub-tree with its leaf nodes. Let α_k be the probability the sink receives data without any loss. So, the loss rate can be calculated accordingly as, $\bar{\alpha}_k = 1 - \alpha_k$ and β_k be the probability in which sink receives data at least from one node. Such that the loss rate can be deduced in WSN by finding the shortest path to reach the destination. This could be achieved in calculating the power consumption of each node and in the process of reducing it. The process can be done by calculating the total power consumption of node and by finding the shortest path to reach the destination.

V. PERFORMANCE EVALUATION

The performance can be evaluated using algorithms and is simulated using NS-2 simulator. In the simulations, the network consisting of random numbers of nodes are generated.

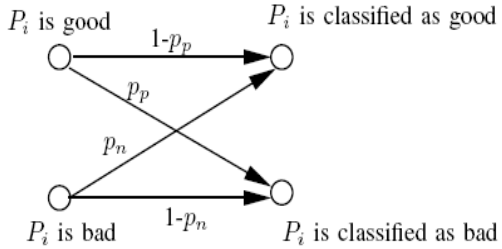

Fig.3 False negative and false positive path generated.

Accordingly, the length of the path can be calculated in which a path is called path positive if the path is good actually and the path is called false negative if it is bad and it is shown in Fig.3.An event is scheduled to drop a packet and in the quick retransmission of lost data to reach the destination provided in the shortest path from source to destination.
It is necessary to evaluate the power consumption of each node and steps must be taken to reduce the maximum power consumption of the node.

ESTIMATION OF SHORTEST PATH: The algorithm used states that heuristic function h is optimal in a closed set such that the length of edge between adjacent nodes x & y in the closed set S.

It must have its heuristic function as,

$$h(x) \leq d(x,y)+h(y)$$

Also, the initial node x to any path X is given by,

$$L(X)+h(x) \leq L(X)+d(x,y)+h(y)=L(Y)+h(y)$$

In whish Y can be defined as the extension path X to include y.

ESTIMATION OF POWER CONSUMPTION: The power consumption and minimization can be achieved in any networks.

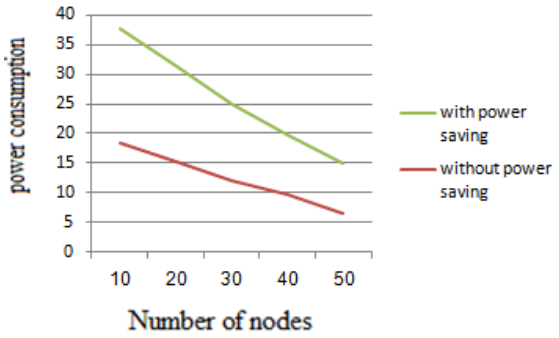

Fig.4 comparing the nodes with power saving and without power saving mechanisms

Consider T=(V,E') for G=(V, E, w). the positive edge function is represented as w and s in v such that power P(V) is assigned to every node v, which gives,

$$P(V)= \max u:(v,u) \in Ew(v,u).$$

The power minimization mechanism mainly deals in putting the system to sleep mode when it is not receiving the data. We have to consider feasible scheduling for minimum power consumption. The power consumption in any network can be minimized in network with different states include sleep, idle and awake which reduce the power to some extent.

VI. RESULTS AND DISCUSSION

Thus, the algorithm results in achieving the shortest path in multicast tree. The algorithm is first evaluated with that of existing algorithms[13]-[16] where we could achieve in finding the shortest path with small number of nodes and the simulation result with less execution represented in the fig.5.

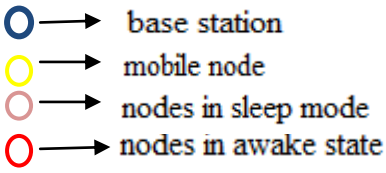

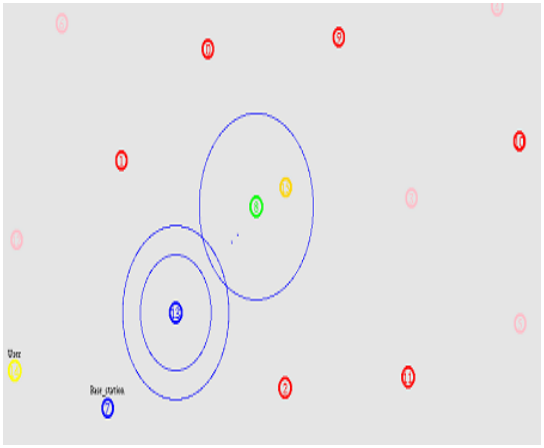

Fig.5. The simulation result shows the data transmission from source to destination in the intermediate nodes in sleep and awake mode.

In this section we compare our proposed algorithm with the event of monitoring the energy consumped per nodes.The link loss rate are selected randomly. The results are averaged over several simulation runs. We notice that the number of links which takes part in data communication in each simulation run depends on the topology of the network and the routing tree. The results shows an improved efficiency in consuming less energy while transmitting the data from the source node to the sink. This also gives the qualified link to transmit the data in the reverse multicast routing. The bad links are identified which results if it does not have the sufficient energy to forward the packet and hence it takes another shortest path to reach the destination. The reasons for path loss includes various factors.

VII. SIMULATION REPORT

M 0.00000 15 (62.00, 145.32, 0.00), (4.95, 196.42), 1300.00
M 0.00000 15 (62.00, 145.32, 0.00), (83.68, 476.63), 1300.00
s -t 0.002983000 -Hs 8 -Hd -2 -Ni 8 -Nx 282.27 -Ny 260.38 -Nz 0.00 -Ne -1.000000 -Nl AGT -Nw --- -Ma 0 -Md 0 -Ms 0 -Mt 0 -Is 8.42 -Id 13.42 -It message -Il 84 -If 0 -Ii 0 -Iv 32
r -t 0.002983000 -Hs 8 -Hd -2 -Ni 8 -Nx 282.27 -Ny 260.38 -Nz 0.00 -Ne -1.000000 -Nl RTR -Nw --- -Ma 0 -Md 0 -Ms 0 -Mt 0 -Is 8.42 -Id 13.42 -It message -Il 84 -If 0 -Ii 0 -Iv 32
s -t 0.002983000 -Hs 8 -Hd -2 -Ni 8 -Nx 282.27 -Ny 260.38 -Nz 0.00 -Ne -1.000000 -Nl RTR -Nw --- -Ma 0 -Md 0 -Ms 0 -Mt 0 -Is 8.255 -Id -1.255 -It AODV -Il 48 -If 0 -Ii 0 -Iv 30 -P aodv -Pt 0x2 -Ph 1 -Pb 1 -Pd 13 -Pds 0 -Ps 8 -Pss 4 -Pc REQUEST
s -t 0.003518000 -Hs 8 -Hd -2 -Ni 8 -Nx 282.27 -Ny 260.38 -Nz 0.00 -Ne -1.000000 -Nl MAC -Nw --- -Ma 0 -Md ffffffff -Ms 8 -Mt 800 -Is 8.255 -Id -1.255 -It AODV -Il 100 -If 0 -Ii 0 -Iv 30 -P aodv -Pt 0x2 -Ph 1 -Pb 1 -Pd 13 -Pds 0 -Ps 8 -Pss 4 -Pc REQUEST
r -t 0.004318640 -Hs 13 -Hd -2 -Ni 13 -Nx 132.57 -Ny 140.15 -Nz 0.00 -Ne -1.000000 -Nl MAC -Nw --- -Ma 0 -Md ffffffff -Ms 8 -Mt 800 -Is 8.255 -Id -1.255 -It AODV -Il 48 -If 0 -Ii 0 -Iv 30 -P aodv -Pt 0x2 -Ph 1 -Pb 1 -Pd 13 -Pds 0 -Ps 8 -Pss 4 -Pc REQUEST
r -t 0.004318666 -Hs 0 -Hd -2 -Ni 0 -Nx 191.67 -Ny 438.49 -Nz 0.00 -Ne -1.000000 -Nl MAC -Nw --- -Ma 0 -Md ffffffff -Ms 8 -Mt 800 -Is 8.255 -Id -1.255 -It AODV -Il 48 -If 0 -Ii 0 -Iv 30 -P aodv -Pt 0x2 -Ph 1 -Pb 1 -Pd 13 -Pds 0 -Ps 8 -Pss 4 -Pc REQUEST
r -t 0.004318707 -Hs 2 -Hd -2 -Ni 2 -Nx 335.70 -Ny 55.04 -Nz 0.00 -Ne -1.000000 -Nl MAC -Nw --- -Ma 0 -Md ffffffff -Ms 8 -Mt 800 -Is 8.255 -Id -1.255 -It AODV -Il 48 -If 0 -Ii 0 -Iv 30 -P aodv -Pt 0x2 -Ph 1 -Pb 1 -Pd 13 -Pds 0 -Ps 8 -Pss 4 -Pc REQUEST
r -t 0.004318816 -Hs 9 -Hd -2 -Ni 9 -Nx 434.75 -Ny 451.83 -Nz 0.00 -Ne -1.000000 -Nl MAC -Nw --- -Ma 0 -Md ffffffff -Ms 8 -Mt 800 -Is 8.255 -Id -1.255 -It AODV -Il 48 -If 0 -Ii 0 -Iv 30 -P aodv -Pt 0x2 -Ph 1 -Pb 1 -Pd 13 -Pds 0 -Ps 8 -Pss 4 -Pc REQUEST
r -t 0.004318821 -Hs 15 -Hd -2 -Ni 15 -Nx 62.37 -Ny 150.92 -Nz 0.00 -Ne -1.000000 -Nl MAC -Nw --- -Ma 0 -Md ffffffff -Ms 8 -Mt 800 -Is 8.255 -Id -1.255 -It AODV -Il 48 -If 0 -Ii 0 -Iv 30 -P aodv -Pt 0x2 -Ph 1 -Pb 1 -Pd 13 -Pds 0 -Ps 8 -Pss 4 -Pc REQUEST
r -t 0.004343640 -Hs 13 -Hd -2 -Ni 13 -Nx 132.57 -Ny 140.15 -Nz 0.00 -Ne -1.000000 -Nl RTR -Nw --- -Ma 0 -Md ffffffff -Ms 8 -Mt 800 -Is 8.255 -Id -1.255 -It AODV -Il 48 -If 0 -Ii 0 -Iv 30 -P aodv -Pt 0x2 -Ph 1 -Pb 1 -Pd 13 -Pds 0 -Ps 8 -Pss 4 -Pc REQUEST
s -t 0.004343640 -Hs 13 -Hd 8 -Ni 13 -Nx 132.57 -Ny 140.15 -Nz 0.00 -Ne -1.000000 -Nl RTR -Nw --- -Ma 0 -Md 0 -Ms 0 -Mt 0 -Is 13.255 -Id 8.255 -It AODV -Il 44 -If 0 -Ii 0 -Iv 30 -P aodv -Pt 0x4 -Ph 1 -Pd 13 -Pds 4 -Pl 10.000000 -Pc REPLY

r -t 0.004343666 -Hs 0 -Hd -2 -Ni 0 -Nx 191.67 -Ny 438.49 -Nz 0.00 -Ne -1.000000 -Nl RTR -Nw --- -Ma 0 -Md ffffffff -Ms 8 -Mt 800 -Is 8.255 -Id -1.255 -It AODV -Il 48 -If 0 -Ii 0 -Iv 30 -P aodv -Pt 0x2 -Ph 1 -Pb 1 -Pd 13 -Pds 0 -Ps 8 -Pss 4 -Pc REQUEST
r -t 0.004343707 -Hs 2 -Hd -2 -Ni 2 -Nx 335.70 -Ny 55.04 -Nz 0.00 -Ne -1.000000 -Nl RTR -Nw --- -Ma 0 -Md ffffffff -Ms 8 -Mt 800 -Is 8.255 -Id -1.255 -It AODV -Il 48 -If 0 -Ii 0 -Iv 30 -P aodv -Pt 0x2 -Ph 1 -Pb 1 -Pd 13 -Pds 0 -Ps 8 -Pss 4 -Pc REQUEST
r -t 0.004343816 -Hs 9 -Hd -2 -Ni 9 -Nx 434.75 -Ny 451.83 -Nz 0.00 -Ne -1.000000 -Nl RTR -Nw --- -Ma 0 -Md ffffffff -Ms 8 -Mt 800 -Is 8.255 -Id -1.255 -It AODV -Il 48 -If 0 -Ii 0 -Iv 30 -P aodv -Pt 0x2 -Ph 1 -Pb 1 -Pd 13 -Pds 0 -Ps 8 -Pss 4 -Pc REQUEST

VIII. CONCLUSION

In this paper, we studied the loss inference problem in wireless sensor networks while the nodes perform data aggregation. This also aids in providing a shortest path and also the correct path to reach the destination. We characterize the condition to achieve this consistent flow of data in the multicast routing and thus achieving the efficient path. By calculating the power consumed per node we can know power consumed for the entire network which proves the reduction in power and energy consumed per node and in the entire network. This gives the reduction in another factor,time. Further, the simulation results showed that our proposed algorithm is accurate in achieving the above mentioned factors.

REFERENCES

[1] Yu yang and Yongjun Xu, "A loss inference algorithm for wireless sensor networks to improve data reliability of digital ecosystems", IEEE transactions on industrial electronics, vol.58, no.6,june 2011.
[2] M. Ulieru, "e-networks in an increasingly volatile world: Design for resilience of networked critical infrastructures," in Proc. Inaugural IEEE Int. Conf. Digital Ecosyst. Technol., Feb. 21–23, 2007, pp. 540–545.
[3] M. Sohail and M. Ulieru, "Opportunistic communication for eNetworks cyberengineering,"in Proc. 33rd Annu. Conf. IEEE Ind. Electron. Soc.,Nov. 5–8, 2007, pp. 950–955.
[4] I. F. Akyildiz, T. Melodia, and K. Chowdhury, "A survey on wireless multimedia sensor networks," Comput. Netw., vol. 51, no. 4, pp. 921–960, Mar. 2007.
[5] J. A. Stankovic, I. Lee, A. Mok, and R. Rajkumar, "Opportunities and obligations for physical computing systems," Computer, vol. 38, no. 11, pp. 23–31, Nov. 2005.
[6] J. A. Stankovic, "When sensor and actuator networks cover the world," ETRI J., vol. 30, no. 5, pp. 627–633, Oct. 2008.
[7] V. C. Gungor, B. Lu, and G. P. Hancke, "Opportunities and challenges of wireless sensor networks in smart grid," IEEE Trans. Ind. Electron, vol. 57, no. 10, pp. 3557–3564, Oct. 2010.
[8] S. Yoo, P. K. Chong, D. Kim, Y. Doh, M. L. Pham, E. Choi, and J. Huh, "Guaranteeing real-time services for industrial wireless sensor networks with IEEE 802.15.4," IEEE Trans. Ind. Electron., vol. 57, no. 11, pp. 3868–3876, Nov. 2010.
[9] B. Lu and V. C. Gungor, "Online and remote motor energy monitoring and fault diagnostics using wireless sensor networks," IEEE Trans. Ind. Electron., vol. 56, no. 11, pp. 4651–4659, Nov. 2009.
[10] R. Caceres, N. G. Duffield, J. Horowitz, and D. Towsley, "Multicast based inference of network internal loss characteristics," IEEE Trans. Inf.Theory, vol. 45, no. 7, pp. 2462–2480, Nov. 1999.
[11] N. G. Duffield, J. Horowitz, F. L. Presti, and D. Towsley, "Multicast topology inference from measured end-to-end loss," IEEE Trans. Inf. Theory, vol. 48, no. 1, pp. 26–45, Jan. 2002.
[12] V. C. Gungor, "A forecasting-based monitoring and tomography frameworkfor wireless sensor networks," in Proc. IEEE Int. Conf. Commun.,
[13] X. Meng, T. Nandagopalz, L. Li, and S. Lu, "Contour maps: Monitoring and diagnosis in sensor networks," Comput. Netw., vol. 50, no. 15,pp. 2820–2838, Oct. 2006.
[14] Y. Li and M. Li, "Iso-Map: Energy-efficient contour mapping in wireless sensor networks," in Proc. Int. Conf. Distrib. Comput. Syst., Jun. 25–27, 2007, pp. 36–43.
[15] G. Hartl and B. Li, "Loss inference in wireless sensor networks based on data aggregation," in Proc. Int. Symp. Inf. Process. Sensor Netw., Apr. 26/27, 2004, pp. 396–404.
[16] Y. Mao, F. R. Kschischang, B. Li, and S. Pasupathy, "A factor graph approach to link loss monitoring in wireless sensor networks," IEEE J. Sel. Areas Commun., vol. 23, no. 4, pp. 820–829,Apr 2005.

International Journal of Modern Engineering Research (IJMER)
www.ijmer.com Vol. 3, Issue. 3, May - June 2013 pp-1654-1660 ISSN: 2249-6645

Performance Improvement through 5S in Small Scale Industry: A case study

P. M. Rojasra[1], M. N. Qureshi[2]
[1]*M.E.Mech. (Student), Mechanical Engineering Department, Faculty of Technology and Engineering, The M.S.University of Baroda, Gujarat (India)*
[2]*Asso.Professor, Mechanical Engineering Department, Faculty of Technology and Engineering, The M.S.University of Baroda, Gujarat (India)*

ABSTRACT: *Small scale industries plays an important role in Indian economy.It has emerged as powerful tool in providing relatively larger employment next to agriculture. Itcontributes more than 50% of the industrial production in value addition terms and generate one third of the export revenue.Global markets are continuously changing and demanding product of high quality and low cost. Such products can be produced using lean manufacturing, a management philosophy that aimed to reduce all types of wastes at all levels of product manufacturing so as to reduce product cost.5S is a basic lean manufacturing tool for cleaning, sorting, organizing and providing necessary groundwork for work place improvement. This paper deals with the implementation of 5S methodology in the Krishna Plastic Company, Udhyognagar, Amreli, Gujarat. Out of the available various lean manufacturing techniques, 5S offers good potential for required improvement.Ten week study is carried out inthe case company. The results after the 5S implementations states that production system efficiencyis improved from 67% to 88.8% in the successive week.*

Keywords:*Analytic Hierarchy Process (AHP), Lean Manufacturing, 5S*

I. INTRODUCTION

To remain in business arena it is of upmost important to win hearts of customer though quality and cost of the product or service. It is also crucial to have sustainable production with continuous improvement. The present need of the organization is to deliver high quality product through continuous improvement [1].However, manufacturing organization throughout the world is under great pressure to reduce the cost and meet the challenge of maintaining global quality standards [2]. Lean Manufacturing is the hymn of survival and success of any organization through minimizing the wastage (Muda) of resources and moving towards implementation of lean manufacturing has become one of the key strategies to achieve cost cutting. The goal of lean manufacturing is to minimize all types of waste or non value added activity through incorporating less human effort, less inventory, less time to develop product and less space to become highly responsive to customer demand, while at the same time producing good quality products in the most efficient and economical manner.

The aim of this paper is to implement 5S methodology and measure the performance improvement in Krishna Plastic Company, a small scale industry situated at Amreli, Gujarat. 5S is Lean manufacturing tool for cleaning, sorting, organizing and providing necessary ground work for work place improvement. 5S is already selected using Analytic Hierarchy Process (AHP), a Multi Criteria Decision Making (MCDM) tool by considering different criteria for case company. AHP is a problem solving framework based on the innate human ability to make sound judgment about small problem. It is a quantitative technique use to facilitate decision that involves multiple competing criteria (Saaty T.L., 1990).

II. PROBLEM STATEMENT

The small scale industries occupy a prominent position of unique importance in economy of India [3]. It has emerged as powerful tool in providing relatively larger employment next to agriculture. Global Markets are continuously changing and demanding product of high quality and low cost. In India, the survival and growth of small scale industry largely depends on its ability to innovate, improve operational efficiency and increase productivity [3]. Many businesses have been trying to adopt new business initiative in order to stay alive in the new competitive market place. Lean Manufacturing is one these initiatives that focus on the cost reduction by eliminating wastes (non value added activities).

Research at Lean Enterprise Research centre (LERC) U.K. indicated that for a typical manufacturing company the ratio of activity could be broken down as, Value added activity – 5%, non-value added activity (waste) – 60% and necessary non-value added activity – 35%.

This implies that up to 60% of the activity at a typical manufacturing company could potentially be eliminated. All Lean manufacturing tools are not possible to implement in small scale industry because of limited resources, i.e. finance, infrastructure, work force etc. The 5S, potential Lean manufacturing tool selected through AHP considering different criteria is to be applying for performance improvement of case company.

III. LITERATURE REVIEW

(1) Chakraborty et al. (2011) studied the critical problems facing by small scale industries while selling their product. SSE (Small Scale Enterprise) is not having huge financial backup and therefore they are depending upon the revenue eared after selling their product. The product sales can only be increased by reducing the cost of the product.(2) Upadhye et al. (2010)

studied the importance of small and medium scale industries in Indian context. Medium size manufacturing industry plays an important role in Indian economy. Their contribution to the economic development of the nation is indeed significant. But the productivity level of these industries is quite low as compared to other country.(3) Palaniappan (2010) described the performance and benefits of small scale manufacturing industry in India. Small scale industries form an important sector constituting 40% of the total output to the privet sector and much more significant is the employment generation capacity of small scale sector.(4) Chauhan et al. (2010) shows the problem to sustain in global market for an organization. Lean manufacturing is hymn of survival and success of any organization. The goal of lean manufacturing is to minimize all types of waste so cost of the product can be reduced.(5) Hudli and Inamdar (2010) described the development of key areas which could be used to assess the adoption and implementation of lean manufacturing practice also presented some of the key areas developed to evaluate and reduce the most optimal project so as to enhance their production efficiency. (6) Lucas et al. (2010) focused on implementation of lean on small manufacturer of all 4-wheel drive vehicles, through implementation of basic lean tool, the small manufacture rapidly increase output and reduce quality defects by 80%. (7) Dalgobind and Anjani (2009) presented methodology for determining the real problem associated with industries in implementation of lean. They also presented selection of required lean tools in the light of company's long term vision. (8) Kumar and Kumar (2010) described the steps undertaken for the implementation of 5S emphasizing on the benefit of an organization. Also described the initiation and benefit of implementing the 5S. (9) Gheorghe (2008) presents a continuous improvement strategy aiming to improve manufacturing at Auto car Exhaust. The implementation of 5S has immediate and significant effect on the sequence of activities in the work post, thus influencing the performance of process in the analyzed company. (10) Khedkar et al. (2012) worked on implementation of 5S on plastic moulding industry. 5S is used in small industry and also showed the advantages and benefits of 5S implementation. (11) Prashant koli (2012) presented the methodology for calculation of each S in 5S system.

IV. RESEARCH METHODOLOGY

Poor workplace conditions may lead to rising of wastes such as time spent in searching for needed items or motion to avoid obstacles. It may also lead to raising an accident. Implementation can be started by establishing good workplace and housekeeping conditions. 5S is lean manufacturing tool for work place organization and it is fundamental to the implementation of lean strategies. 5S is a reference to five Japanese works which described standardized clean up. The 5S are: (ReVelle 2002).

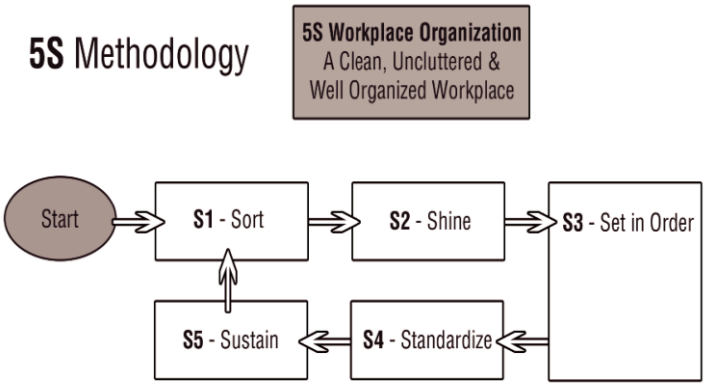

Fig.1 The 5S system

In this paper I focused on 5S rating system, which make us able to understand the improvement criteria for particular S of 5S system. Here we give total rating of 25 score, which is divided in five equal parts for each S of 5S system. We give highest 5 marks to each S. After that we will make a graph which will make us able to understand the efficiency and make able to do better improvement. The detail and calculation of each S is given bellow.

S1 Seiri (Sort):

Seiri is the first S in 5S system, which is basically deal with the availability of materials and process of product manufacturing. For calculation of Seiri rating, we allot 5 criterion regions for seiri arrangement, and decide that the sub system should achieve minimum 3 marks out of 5 because it tends us to define that the system will be in issue when it is above 50% active. Following are the Seiri rating criterion.

(1) Material availability

Give 1 mark if material is fully available or give 0 marks if material is not fully available.

(2) Defective goods

If there are X items which contains Y items as defective

Then the marks will be

Fraction of fine goods = [1- {Y/X}]

(3) Operating condition

Operating condition is an important aspect for the arrangement of material and tools, because without the comfort of operator the best process arrangement also has zero value. Give 1 mark if operating condition is under control and give 0 marks if operating condition is not under control.

(4) Relative information

Relative information about working condition, process guidelines, tools information, material information etc., is also important for Seiri rating. Give 1 mark for full information and give 0 marks for partial information.

(5) Elimination of waste

Elimination of waste is also an important aspect for Seiri rating. Let total N no of wast are listed but only M were eliminated the marks of elimination process will be

Fraction of waste elimination = [1- {M/N}]

Now add all five marks and get total rating of Seiri out of 5. If the Seiri system will get less than 3 marks then do the arrangement again because if it is got below 3 marks it means it has very poor condition of analysis.

S2 Seiton (straighten / set in order)

Seiton is second S of 5S system which deals with the proper arrangement of equipment and tools on the shop floor. The main objectives of Seiton are forming a regular workplace, avoiding time loss while searching the material and mistake proofing work. Following are the Seiton rating criterion.

(1) Sequence rating

Let there are A no. of tools are in proper sequence and B no of tools are not in proper sequence. Then sequence rating will be

Fraction of proper sequence = [1- {B/A}]

(2) Material arrangement rating

This criterion basically deals with the providing of raw material and accessories for the particular operation. Let D be the lack of material and C be the total material required, then

Fraction of material available = [1-{D/C}]

(3) Tool arrangement rating: This criteria shows the consistency if the system about providing service for proper fulfilment of tooling requirement. Let P be the no. of irregular process and Q be the total no. of process.

Fraction of consistency to tool arrangement: [1-{P/Q}]

(4) Material arrangement consistency: The aim of this consistency is “every time perfect arrangement”. Let U be the fail arrangement and V be the total no. of arrangement.

Fraction of consistency: [1-{U/V}]

(5) Working efficiency of Seiton system:

Working efficiency = working time for process / Total time allotted for process

Now do sum of all the above five criteria and note it as the rate of the Seiton system. This rate should have minimum value of 3 points, if not then system will set again or need analysis again.

S3 Seiso (Shine / Clean)

In order to realize effective tasks, it is essential to create a clean and regular working and living environment. This is because dust, dirt and wastes are the source of untidiness, indiscipline, inefficiency, faulty production and work accidents. We can handle cleaning practices by two approaches: “general cleaning of workplace” and “machine, hardware and tool cleanliness”. Seiso process indicates the “Renovation of the work place”.

Seiso system contents the following criteria:

(1) Is the machine clean or not : If the machine is clean then give 1 point and if not then give 0 point

(2) Process path clean: If the path of process is clean then allot 1 point and if not give 0 point.

(3) Proper environment for working condition:

Working environment include the ergonomics of the worker like proper souse of light and air, which makes the worker continuously fresh and energetic and make him stay away from errors during operation. Working condition rating will be

Let J will be total aspect for favourable condition and I be the no. of fail arrangement.

Fraction of environment: [1-{I/J}].

(4) Cleaning consistency:

Let E be the total no. of cleaning required and F be the cleaning not done say inconsistency. So consistency rate will be

Fraction of consistency = [1-{F/E}].

(5) Safety from accident:

Let K be the total no. of accident chances and L be the total no for accidents occurs. Then safety rate will be

Fraction of safety: [1-{L/K}].

After adding all the above five criteria the rate of Seiso system can be recorded. This rate should have minimum value of 3 points, if not then system will set again or need analysis again.

S4 Seiketsu (Standardize):

Seiketsu is generally means for make a peak standard which should be achieve by the manufacturing process practice. Standard should be communicative and easy to understand. Seiketsu rating will be found by calculating the average of previous three S, because standard of any system will rise and fall by mean rate depending factors.

$$Seiketsu(Standarize)rating = \frac{Sierirating + Seiatonrating + Seisorating}{3}$$

S5 Shitsuke (Sustain):

Shitsuke (Sustain) is the last S of the 5S system which is deal with the regularity of maintaining the standard of the organization for the particular process, which is only done by regular practices and by following the proper instruction of machine operating. By doing regular following of accurate of instruction we can maintain the machine condition at its peak level, which may help for better production and stay away from breakdown.

(1) Removing small faults through the aid of cleaning.
(2) Providing the execution of visual control.
(3) Providing the performance of protective activities.
(4) Granting the responsibility of the machine to the operator.
(5) Formation of a disciplined company.

Shitsuke rating will be depending on the previous four S because without that the regularity will not maintain. Therefore Shitsuke rate will be the average of previous four S ratings.

$$Shitsuke(Sustain)rating = \frac{Sierirating + Seiatonrating + Seoso\ rating + Seisukerating}{4}$$

After the calculation of this rating of 5S, efficiency is calculated at the end of every week and will so the performance improvement at the end of four week. The overall efficiency of the 5S system for the permitted or approved period will be average of the particular efficiencies for required week. Also we will make a graph which will show the real condition of the system and can find the improvement required region.

V. CASE STUDY

A Plastic injection molding is a manufacturing process for producing thermoplastic and thermosetting polymer materials. Plastic product produced by injection molding process is widely used in today's world because of high cost of metallic materials and their lack of availability. The industry considered for case study is Krishna Plastic a small scale plastic component manufacturing through Injection Molding. Summary of case organization is given bellow.

TABLE I1
CASE ORGANIZATION'S SUMMARY

Industry characteristics	Detail about case organization
Industry type	Discrete
Industry sector	Manufacturing
Product	Different type of plastic component through plastic injection molding machines
Product type	Non critical components
Product volume & variety	High volume low variety
Company vision	To be a star performer and market leader
Company mission	Continuous improvement of product, process and people.

Each of S is in 5S is implemented in case organization step by step for tem weeks and performance is measure which is given in following table.

TABLE II
S1 SEIRI RATING

Week No.	Duration	Material Availability Rating	Defective goods Rating	Operating Condition Rating	Relative Information Rating	Elimination of Waste Rating	Total Rating
		0 or 1	[1-{Y/X}]	0 or 1	0 or 1	[1-{M/N}]	
Week 1	March 04-09, 2013.	1	0.20	1	1	0.2	3.4
Week 2	March 11-16, 2013.	1	0.40	1	1	0.2	3.6

Week 3	March 18-23, 2013.	1.00	0.40	1	1	0.4	3.8
Week 4	March 25-30, 2013.	1	0.40	1	1	0.4	3.8
week 5	April 01-06, 2013	1	0.60	1	1	0.4	4
week6	April 08-13, 2013	1	0.60	1	1	0.4	4
week7	April 15-20, 2013	1	0.60	1	1	0.6	4.2
week8	April 29-May-04, 2013	1	0.60	1	1	0.6	4.2
week9	May06-11, 2013.	1	0.80	1	1	0.6	4.4
week10	May13-18, 2013.	1	0.8	1	1	0.8	4.6

TABLE III
S2SEITON RATING

Week No.	Duration	Sequence Rating	Material Arrangement Rating	Tool Arrangement Rating	Material Arrangement Consistency Rating	Working Efficiency Rating	Total Rating
		[1-{B/A}]	[1-{D/C}]	[1-{P/Q}]	[1-{U/V}]	w.t./ t.a.t.	
Week 1	March 04-09, 2013.	0.4	0.60	0.6	0.4	1.25	3.25
Week 2	March 11-16, 2013.	0.4	0.60	0.6	0.6	1.21	3.41
Week 3	March 18-23, 2013.	0.40	0.60	0.8	0.6	1.17	3.57
Week 4	March 25-30, 2013.	0.6	0.60	0.6	0.6	1.13	3.53
week5	April 01-06, 2013	0.6	0.80	0.6	0.6	1.11	3.71
week6	April 08-13, 2013	0.8	0.80	0.6	0.6	1.09	3.89
week7	April 15-20, 2013	0.8	0.80	0.6	0.8	1.06	4.06
week8	April 29-May-04, 2013	0.8	0.80	0.8	0.8	1.04	4.24
week9	May06-11, 2013.	1	0.80	0.8	0.8	1.03	4.43
week10	May13-18, 2013.	1	0.8	0.8	0.8	1	4.4

TABLE IV
S3 SEISORATING

Week No.	Duration	Machine Cleanliness Rating	Process Path Cleanliness Rating	Working Environment Rating	Cleaning Consistency Rating	Safety Rating	Total Rating
		0 or 1	0 or 1	[1-{I/J}]	[1-{F/E}]	[1-{L/K}]	
Week 1	March 04-09, 2013.	1	1.00	0.4	0.4	0.6	3.4
Week 2	March 11-16, 2013.	1	1.00	0.4	0.6	0.6	3.6
Week 3	March 18-23, 2013.	1.00	1.00	0.6	0.6	0.6	3.8
Week 4	March 25-30, 2013.	1	1.00	0.6	0.6	0.6	3.8
week5	April 01-06, 2013	1	1.00	0.8	0.6	0.6	4
week6	April 08-13, 2013	1	1.00	0.8	0.6	0.6	4
week7	April 15-20, 2013	1	1.00	0.8	0.8	0.6	4.2
week8	April 29-May-04, 2013	1	1.00	0.8	0.8	0.6	4.2
week9	May06-11, 2013.	1	1.00	0.8	0.8	0.8	4.4
week10	May13-18, 2013.	1	1	0.8	0.8	0.8	4.4

TABLE V
S4SEIKETSU RATING

Week No.	Duration	Total Rating = (S1+S2+S3) /3
Week 1	March 04-09, 2013.	3.35
Week 2	March 11-16, 2013.	3.53
Week 3	March 18-23, 2013.	3.72
Week 4	March 25-30, 2013.	3.71
week5	April 01-06, 2013	3.9
week6	April 08-13, 2013	3.96
week7	April 15-20, 2013	4.15
week8	April 29-May-04, 2013	4.21
week9	May06-11, 2013.	4.41
week10	May13-18, 2013.	4.4

TABLE VI
S5SHITSUKE RATING

Week No.	Duration	Total Rating = (S1+S2+S3+S4) /4
Week 1	March 04-09, 2013.	3.35
Week 2	March 11-16, 2013.	3.53
Week 3	March 18-23, 2013.	3.72
Week 4	March 25-30, 2013.	3.71
week5	April 01-06, 2013	3.9
week6	April 08-13, 2013	3.96
week7	April 15-20, 2013	4.15
week8	April 29-May-04, 2013	4.21
week9	May06-11, 2013.	4.41
week10	May13-18, 2013.	4.4

TABLE VII
EFFICIENCY OF 5S SYSTEM

Week No.	Duration	(S1+S2+S3+S4)*100 / 25	Efficiency
Week 1	March 04-09, 2013.	(3.4+3.25+3.4+3.35+3.35)*100 / 25	67.00%
Week 2	March 11-16, 2013.	(3.6+3.41+3.6+3.53+3.53)*100 / 25	70.68%
Week 3	March 18-23, 2013.	(3.8+3.57+3.8+3.72+3.72)*100 / 24	74.44%
Week 4	March 25-30, 2013.	(3.8+3.53+3.8+3.71+3.71)*100 /25	74.20%
week 5	April 01-06, 2013	(4.0+3.71+4.0+3.9+3.9)*100 / 25	74.04%
week6	April 08-13, 2013	(4.0+3.89+4.0+3.96+3.96)*100 / 25	79.24%
week7	April 15-20, 2013	(4.2+4.06+4.2+4.15+4.15)* / 25	83.04%
week8	April 29-May-04, 2013	(4.2+4.24+4.2+4.21+4.24)*100 / 25	84.24%
week9	May06-11, 2013.	(4.4+4.43+4.4+4.41+4.41)*100 / 25	88.16%
week10	May13-18, 2013.	(4.6+4.4+4.4+4.4+4.4)*100 / 25	88.80%

V. CONCLUSION

The present paper demonstrates the implementation of 5S a lean manufacturing techniques in small scale industry. Lean manufacturing is one of the options to reduce non value-added activity (wastes) and improve operational efficiency of the organization. The efficient implementation of 5S technique leads to subsequent improvement in productivity of the manufacturing plant. The 5S improves environmental performance and thus relate primarily in reduction of wastes in manufacturing. It promotes neatness in storage of raw material and finished products.The 5S implementation leads to the improvement of the case company organization in many ways for instance.(1) Better usage of working area, (2) Work environment improvement (3) Prevention of tools losing. (4) Reduction in accidents. (5) Reduction in accidents. (6) Reduction in pollution. (7) Discipline in the employee. (8) Increasing of awareness and moral of employee. (9) Improvement in the internal communication. (10) Improvement in the internal human relation. (11) Decreasing of mistakes through error proofing. Table no. VI shows efficiency improvement from 67% to 88.8% through successive week.

ACKNOWLEDGEMENTS

The support for this work provided by Shri Sanjay M. Parikh and Prakash M. Parikh owners of the company and all technical and non-technical staff of Shri Krishna Plastic, G.I.D.C. Estate, Amreli, Gujarat (India) is gratefully acknowledged.

REFERENCES

Journal Papers:

[1] Chauhan et al., "Measuring the status of Lean manufacturing using AHP" International journal of Emerging technology vol.1 no.2, pp.115-120. 2010.
[2] Miller et al., "A case study of Lean, sustainable Manufacturing" journal of Industrial Engineering and Management, vol.3 no.1, pp.11-32. 2010.
[3] Girish Sethi and Prosanto Pal, "Energy Efficiency in Small Scale Industries – An Indian Perspective"Tata Energy research Institute.
[4] Chakraborty et al. "Internal obstacles to quality for small scale enterprises"', International Journal of Exclusive management research, vol. 1, no. 1, pp. 1-9, 2011.
[5] Upadhye et al. "Lean manufacturing system for medium size manufacturing enterprise: An Indian case"International journal of management science and engineering management. Vol.5, no. 5 pp. 362-375, 2010.
[6] Hudli and Imandar, "Areas of Lean manufacturing for productivity improvement in a manufacturing unity", world academy of science, engineering and technology vol. 69, 2010
[7] Lukas et al. "Lean implementation in a low volume manufacturing environment: A case study" Proceedings Industrial Engineering Research Conference (2010)
[8] Kumar and Kumar. "Steps for Implementation of 5S", International Journal of management. IT and Engineering. vol. 2, no.6, pp. 402-416, 2012.
[9] Gheorghe Dulhai. "The 5S strategy for continuous improvement of the manufacturing process in auto car exhausts", Management and marketing vol. 3, no. 4, pp. 115-120, 2008.
[10] Khedkar at el. "Study of implementing 5S techniques in Plastic Moulding" International Journal of modern engineering research. vol. 2, no 5, pp. 3653-3656, 2012.
[11] Prashant Koli." General Implementation and Calculation of 5S Activity in any Organization" International journal of Science and Research vol.1 no.3pp.229-232,2012.

International Journal of Modern Engineering Research (IJMER)
www.ijmer.com Vol. 3, Issue. 3, May - June 2013 pp-1661-1665 ISSN: 2249-6645

Reversible Data Hiding VIA Optimal Code for Image

Senthil Rani D.[#], Gnana Kumari R.[*]
[#]*PG-Scholar, M.E-CSE, Coimbatore Institute of Engineering and Technology*
[*]Assistant *Professor, CSE Department, Coimbatore Institute of Engineering and Technology*

Abstract: *Digital watermarking often referred to as data hiding for assuring the information. Data hiding in image processing may occur the permanent distortion and hence the original cover medium may not be able to be reversed exactly, after the hidden data have been extracted out. In our previous work, generalize the method of decompression algorithm as the coding scheme for embedding data and prove the codes can reach the rate–distortion bound as long as the compression algorithm reaches entropy and uses a binary covers for embedding messages. A code construction for recursive reversible data-hiding established a rate–distortion model. In our work presents a novel lossless data-embedding technique, which enables the exact recovery of the original image upon the extraction of the embedded information. After the Decompression, the original message will retrieved. The marked cover is reconstructed and extracting the original message from the cover. In our research work, improve the histogram shifting of compressing features and to construct the recursive code for gray scale covers.*

Keywords: *Difference expansion, Evenodd method, Datahiding, Watermarking, Histogramshifting, Reversible*

I. INTRODUCTION

Data hiding is the general term for embedding message into the covers such as image,audio and video files. The term hiding means making the information imperceptible or keeping the existence of the information secret which is used fot integrity, authentication, media notation, etc. The image that will be embedded the secret data is called the cover image or otherwise called as the stego image. The first stage extracting the portion from the original cover. The second stage is to compressing the features of the original cover and that saves the space for the payloads. The third stage embeds the messages into the feature sequence and called as the marked cover or stego image. The embedding process may introduce the some permanent distortion to the cover, that is the original image cannot reconstructed from the original cover. In this case we need a special kind of data hiding method, which is referred as reversible data hiding. A higher hiding capacity means use more secret data can embedded into the cover. A reversible data hiding, which is also called a distortion-free or lossless data hiding, is a technique that not only embeds the secret data into cover images, but also used for restoring the original images from the stego images after the embedded data have been extracted.

In our previous work, many reversible data hiding schemes were proposed, and most of them use the following techniques: lossless compression technique, difference expansion technique (DE), histogram shifting technique (HS), Interpolation technique. These schemes are either high hiding capacity and poor stego image quality or good stego image quality and low hiding capacity. The distortion are introduced in the original cover. In this paper, a novel reversible data hiding scheme is proposed. The proposed scheme uses an Even-Odd embedding method to reconstruct the image without distortion.

II. RELATED WORK

2.1 Lossless Compression Technique

The reversible data hiding schemes based on lossless compression were proposed The key point of these schemes is to find a subset B in the original. The first methodology is based on lossless compression of subsets or features of the samples comprising the digital object X. If the object X contains a subset B, or a set of features B from X Such that B can be losslessly compressed and be randomized without causing perceptible quality of or object X. The extraction of the hidden message proceeds by extracting the subset B and joining with the bit stream consisting of the compressed bit stream and the message. Replace the set B with its compressed form C(B) and the secret data M , showed in Figure 1. X and X′ indicate the cover image and stego image, respectively.

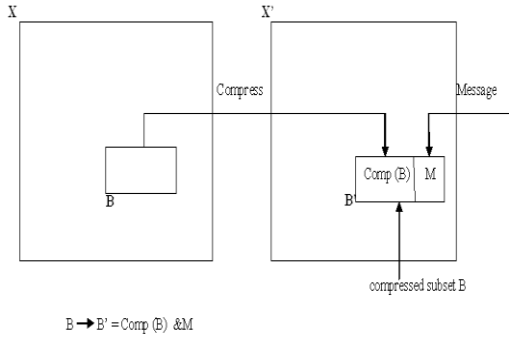

Fig. 1. A data hiding using the lossless compression technique

2.2 Histogram Shifting Technique

The reversible data hiding schemes based on histogram shifting were proposed. In these schemes, peak point in the histogram of the cover image is used to select the embedding area for the secret data, then the part [Peak point +1, Zero point] is shifted to get the embedding area. These schemes were improved by using the histogram of the difference image or predict error image instead of the original image to get a higher peak point. If the peak point is high, the hiding capacity will be large.

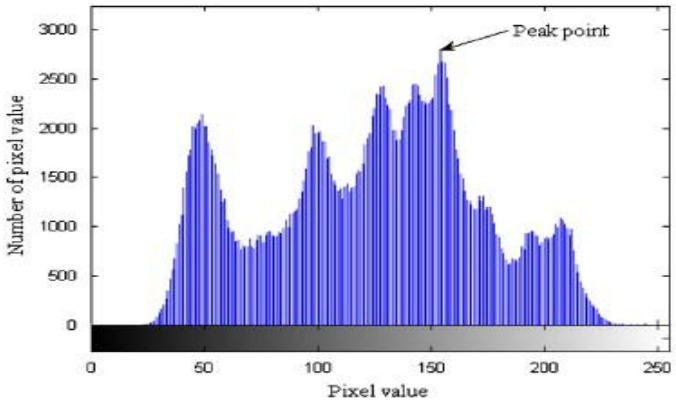

Fig. 2. Histogram of image "Lena"

III. REVERSIBLE DATA HIDING

It introduces a generalization of the well-known LSB (least significant bit) modification method as the underlying irreversible (lossy) embedding technique. This technique modifies the lowest levels- instead of bit planes- of the host signal to accommodate the payload information. In the second part, a lossless data embedding algorithm for continuous-tone images is built on the generalized LSB modification method. This spatial domain algorithm modifies the lowest levels of the raw pixel values as signal features. As in all Type-II algorithms, recovery of the original image is enabled by compressing, transmitting, and recovering these features. This property of the proposed method provides excellent compression of relatively simple image features. Earlier algorithms in the literature tend to select more complex features to improve the compression performance- thus the lossless embedding capacity.

(a) The data hiding where the cover image is subdivided into blocks, and one bit is inserted in each block by flipping the pixel with the lowest visibility. The blocks with even (odd) number of black pixels has bit zero (one) embedded. In this technique, the original image cannot be recovered even if the original parities of black pixels are known, because the precise flipped pixel inside each block cannot be localized.

(b) The second is an efficient compression of the portion to be overwritten by the hidden data.

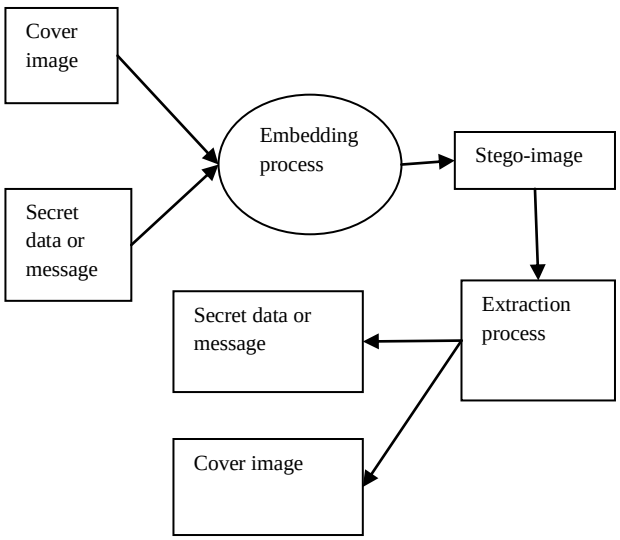

Fig 3. A system architecture of reversible data hiding

3.1. Preprocessing

In this module the preprocessing of database is done. Generally representation of images uses too many features, but only a few of them may be related to the target image. Data hiding method is not easy way to implement the image into the message without storing the images in the database .In this preprocessing module stores the number of the images in

the database .In this preprocessing stage feature extraction is performed for image stored in the database. The cover image or original image extracted the feature, removal of the noisy data in the image.

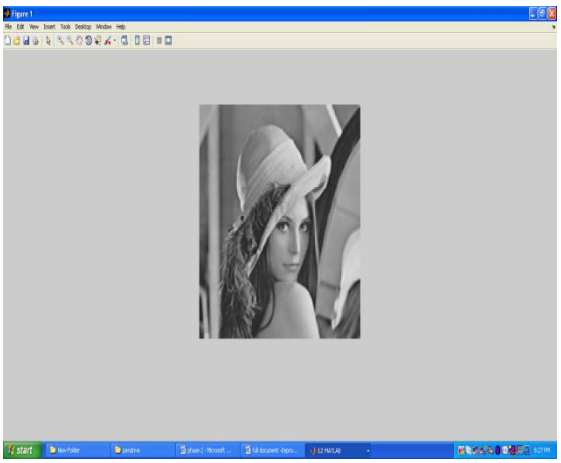

Fig 5. Input image "lena"

3.2. Implement of DE algorithm

In this module reversible data hiding based on difference expansion require location maps to recover cover images, larger embedding capacity can be achieved by constructing a longer feature sequence that can be perfectly compressed. One of such constructions is difference expansion in which the features are the differences between two neighboring pixels. The features are compressed by expansion, i.e., the differences are multiplied by 2, and thus, the LSBs of the differences can be used for embedding messages.DE the features (differences) are compressed by expansion operation**.**

The integer average is

$$L=((x+y))/2 \quad (1)$$

The difference value is

$$h=x-y \quad (2)$$

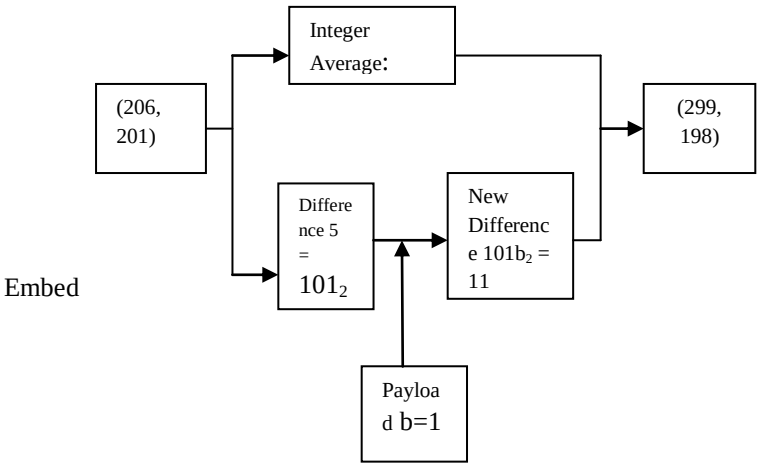

Fig 4.difference expansion algoriothm

3.3 Data embedding

Adaptive arithmetic coder (AAC) as the embedding code, the proposed codes realize continuous embedding rates and reach the maximum embedding rate at the least admissible distortion. Set a proper length for the last block Denote the estimated length of the last block by K_{last}.After compression, the left room in the last block is about $K_{last}(1-H_2(p_0))$bits, in which we will embed not only the information for reconstructing the second last block but also some overhead information. On one hand, to reconstruct the second last block, we need, at most k/2 , bits because the number of "1's" in is not more than $y_{last\ -1}$.On the other hand, the overhead consists of some parameters necessary to the recipient, the length of which is denoted by L_{over} . Thus, the estimated length of the last block is enough, if

$$K_{last}(1 - H_2(p_0)) \geq k/2 + L_{over} \quad (3)$$

The proposed scheme gains from embedding capacity by taking full advantage of the large quantities of smaller difference values where secret data can be embedded. The proposed scheme offers several advantages, namely, the location map is required, the embedding capacity can be adjusted depending on the practical applications, and the high embedding capacity with minimal visual distortion can be achieved.

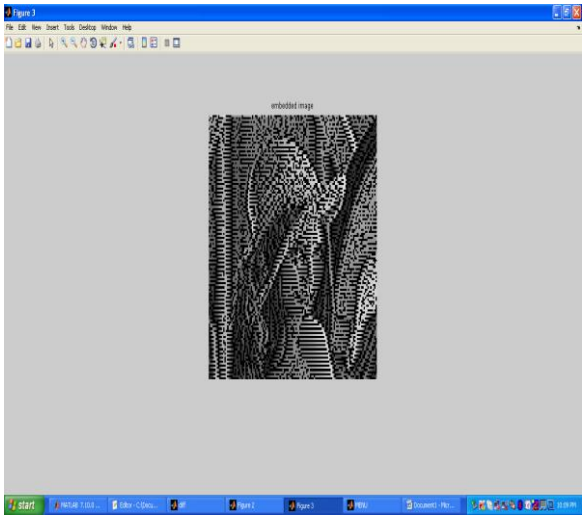

Fig 6. Embedding message into the image

3.4. Generating marked cover

In this module after embedding the message into the feature sequence ,then generate the marked cover .One direct reversible embedding method is to compress the feature sequence and append messages after it to form a modified feature sequence, by which replace the original features to generate the marked cover. Therefore, after extracting the message, the receiver can restore the original cover by decompressing the features. Receiver could extract messages from the marked cover with the help of the reconstructed cover because of reversibility. To extract the message and reconstruct the cover, the extraction process must be performed in a backward manner. To extract messages from the ith block, To reconstruct the cover block and extract messages from the y_1 marked block , we first count the number of "1's" in , that is, equal to 3. Second, we extract messages from the second marked block and decompress the extracted messages successively until we get a 3-bit decompressed sequence.

3.5. Even-Odd Embedding Method

Reversible data hiding is very useful for some extremely image such like medical images and military images. In the reversible data hiding schemes, some schemes are good performance at hiding capacity but have a bad stego image quality, some schemes are good stego image quality but have a low hiding capacity. It is difficult to find the trade-off between the hiding capacity and stego image quality. In this paper, a novel reversible data hiding scheme is proposed. The proposed scheme uses a new embedding method, which is called Even-Odd embedding method, to keep the stego image quality in an acceptable level, and uses the multi-layer embedding to increase the hiding capacity.

IV. PERFORMANCE EVALUATION

In this module we compare the performance of the existing and the proposed system shows embedding rate and retrieval accuracy of the image and messages.

PSNR is most easily defined via the mean squared error (*MSE*). Given a noise-free *m*×*n* monochrome image *I* and its noisy approximation *K*, *MSE* is defined as:

$$MSE = \frac{1}{mn}\sum_{i=0}^{m-1}\sum_{j=0}^{n-1}[I(i,j) - K(i,j)]^2$$

The PSNR is defined as:

$$PSNR = 10.log_{10}\left(\frac{MAX_I^2}{MSE}\right)$$

V. RESULTS AND DISCUSSIONS

Figure 4 shows the hiding capacity and PSNR value of the even and odd embedding method. It is found that accuracy of data hiding capacity and PSNR is higher than existing system.

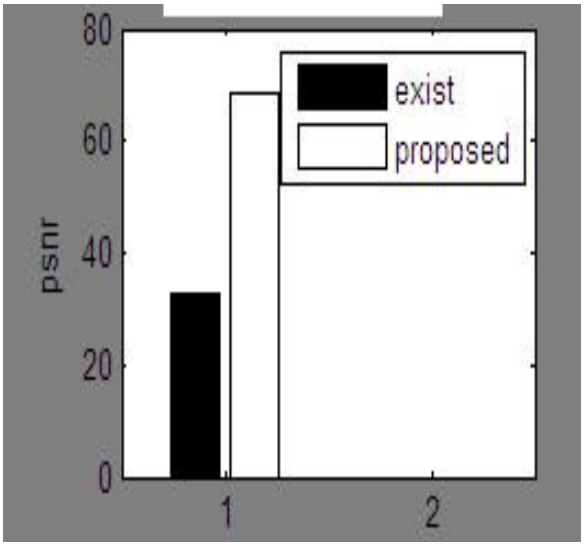

VI. CONCLUSION

In this paper the image is taken from database and hiding the information or message are stored in that image for security purpose. After that it sends to the receiver. The receiver extracted that original message from stego image.(i.e) the image with hiding data called as stego image. The proposed system increased the hiding capacity and PSNR value.

REFERENCES

[1] Biao Chen, Nenghali Yu and Weiming Zhang (2012) 'Improving Various Reversible Data Hiding Schemes Via Optimal Codes for Binary Covers' IEEE Trans. on Image Processing, vol.21,no.6.
[2] J. Fridrich and M. Goljan, "Lossless data embedding for all image formats," in Proc. EI SPIE, Security Watermarking Multimedia Contents IV, San Jose, CA, 2002, vol. 4675, pp. 572–583.
[3] M. U. Celik, G. Sharma, A. M. Tekalp, and E. Saber, "Lossless generalized- LSB data embedding," IEEE Trans. Image Process., vol. 14, no. 2, pp. 253–266, Feb. 2005.
[4] A. M. Alattar, "Reversible watermark using difference expansion of a generalized integer transform," IEEE Trans. Image Process., vol. 13, no. 8, pp. 1147–1156, Aug. 2004.
[5] H.-J. Kim, V. Sachnev, Y. Q. Shi, J. Nam, and H.-G. Choo, "A novel difference expansion transform for reversible data embedding," IEEE Trans. Inf. Forensic Security, vol. 3, no. 3, pp. 456–465, Sep. 2008.
[6] Tian J. (2003) 'Reversible data embedding using a difference expansion' IEEE Trans. Circuits Syst. Video Technol., vol. 13, no. 8, pp. 890–896.
[7] Miscellaneous gray level images [Online]. Available: http://decsai. ugr.es/cvg/dbimagenes/g512.php.

International Journal of Modern Engineering Research (IJMER)
www.ijmer.com Vol. 3, Issue. 3, May - June 2013 pp-1666-1671 ISSN: 2249-6645

Finite Element Analysis & Thickness Optimization of Vacuum Chamber for Electron Microscopy Applications

Mr. Abdul Sayeed AW Shaikh[1], Prof. P.T.Nitnaware[2]
[1, 2] *D. Y. Patil college of Engineering Akurdi, Pune,India*

ABSTRACT: *This paper shows the Finite Element analysis of vacuum chamber. The analysis is done for electron microscopy applications, for scanning electron microscope it require vacuum atmosphere for viewing of the specimen. The specimen is to be viewed in vacuum. The vacuum level required for that is in the range of 93324 Pa, which is less than atmospheric pressure which lead to the compressive forces acting inside the chamber The vacuum chamber is modeled in Catia and Simulation is done in Ansys. Also theoretical calculation is done for safety of vacuum chamber against buckling failure. Also, shell analysis is done for considering the thickness of the vacuum chamber which is done by using Hypermesh.*

Keywords: *FEA, Electron Microscope, Buckling Propagation, ANSYS, Vacuum Chamber*

I. INTRODUCTION

An Electron Microscope uses particle beam of electrons to illuminate the specimen and produce a magnified image. Scanning electron microscope (SEM) and Transmission electron microscope (TEM) are types of its applications. Both these applications requires an vacuum atmosphere to operate. Also the level of vacuum requirement is same for both the applications. The electron gun without vacuum will experience constant interference from air particles in the atmosphere. The distraction would lead to block the path of electron beam and also they would be knocked out of the air and onto the specimen which ultimately distort the surface of the specimen. The vacuum level required for that is in the range of 91991 to 95990 Pa, which is less than that of atmospheric pressure which lead to compressive forces on chamber which causes buckling.

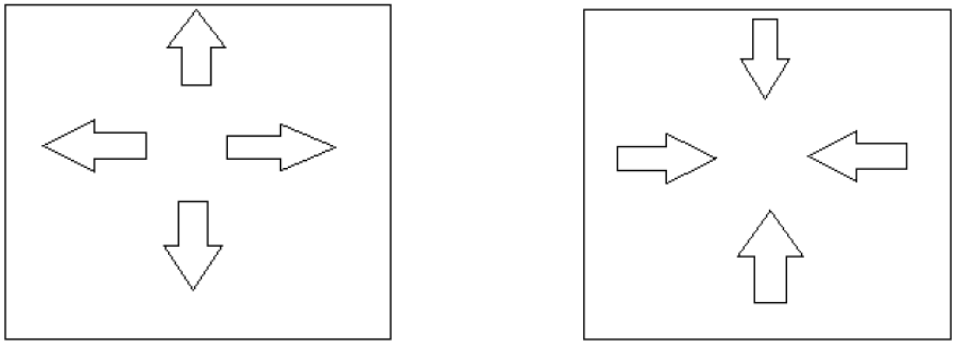

Typical vessel Vacuum vessel

Fig 1.1: Direction of Internal Pressure

II. FINITE ELEMENT METHOD

The finite element method (FEM), sometimes referred to as finite element analysis (FEA), is a computational technique used to obtain approximate solutions of boundary value problems in engineering. Simply stated, a boundary value problem is a mathematical problem in which one or more dependent variables must satisfy a differential equation everywhere within a known domain of independent variables and satisfy specific conditions on the boundary of the domain. Boundary value problems are also sometimes called field problems. The field is the domain of interest and most often represents a physical structure. The field variables are the dependent variables of interest governed by the differential equation. The boundary conditions are the specified values of the field variables (or related variables such as derivatives) on the boundaries of the field. Depending on the type of physical problem being analyzed, the field variables may include physical displacement, temperature, heat flux, and fluid velocity to name only a few. A finite element analysis has been done to the model for the expected stresses for 93324 Pa.

1.1 General Dimension of vacuum chamber

Table No.2.1: Dimensions of vacuum chamber

Description	Value (m)
Vessel Inner Diameter	1.070
Vessel Thickness	0.007
Length of Cylindrical Portion	1.330
Cover inner diameter	0.950
Cover Thickness	0.007
Cover Height	0.250
Base Plate Thickness	0.023
Vessel Flange Thickness	0.035
Cover Flange Thickness	0.035

Table No.2.2: Dimensions of Flanges

Valves	Value (m)	Thickness (m)	Flange Thickness (m)
1	0.205	0.0045	0.023
2	0.154	0.0045	0.023
3	0.120	0.0034	0.023

2.2 Critical Buckling Pressure

Buckling is a failure mode characterized by a sudden failure of a structural member subjected to high compressive stress. Cylindrical vacuum vessels subject to external pressure are subject to compressive hoop stresses. Consider a length L of the vessel,

The total force acting = Intensity of pressure × area

$$= p \times D \times L$$

The total resisting force acting on the vessel walls

$$= \sigma_h \times 2t \times L$$

From above two equation's,

$$\sigma_h \times 2t \times L = p \times D \times L$$

$$\sigma_h = \frac{p \times D}{2t}$$

The compressive hoop force,

$$W_h = \sigma_h \times L \times t$$

$$W_h = \frac{\nabla p_{buckle} \times D \times L \times t}{2t} \quad \ldots\ldots\ldots\ldots (1)$$

Buckling will occur when compressive hoop force will equal to buckle force, W

$$W = \frac{4\pi^2 EI}{(\pi D)^2}$$

$$\text{Since, } I = \frac{L \times t^3}{12}$$

$$W = \frac{4\pi^2 E \times (\frac{Lt^3}{12})}{(\pi D)^2}$$

$$W = \frac{ELt^3}{3D^2} \quad \ldots\ldots\ldots\ldots\ldots\ldots\ldots\ldots\ldots\ldots\ldots\ldots (2)$$

Equating eq^n (1) and (2)

$$\frac{\nabla p_{buckle} \times D \times L}{2} = \frac{ELt^3}{3D^2}$$

$$\nabla p_{buckle} = \frac{2E}{3}(\frac{t}{D})^3$$

$$\nabla p_{buckle} = \frac{2 \times 2 \times 10^{11}}{3} \times (\frac{0.007}{1.056})^3$$

$$\nabla p_{buckle} = 38836.59 \text{ Pa}$$

We have applied approximately p = 7999.2 Pa for 700 torr (10 to 15) % of max buckling pressure as per requirement, the impact will be very small. So it is safe from buckling failure.

Thickness of the vacuum chamber,

$$t = \frac{pDo}{(2 \times f \times J + p)}$$

The design pressure is taken as 1.1 times of the pressure,

$$t = \frac{0.1026 \times 957}{(2 \times 205 \times 0.85 + 0.1026)}$$

$$t = 0.3 \times 10^{-3} \text{ m}$$

In reality the vacuum chamber consist of nozzles and flanges and the above thickness is considered as the vessel is plane without any nozzles and flanges. Due to the nozzles and flanges which create abrupt changes in the cross-section gives rise to stress concentration and reduces the strength of the material. To overcome this problem and to be on the safer side we have taken the thickness of the vacuum chamber as 7 mm.

III. MODELLING

The vacuum chamber comprises of cylindrical vessel with hemi spherical elliptical cover on one side and base plate on other side. The vessel and end cover is modeled in Catia part body workbench separately and fixed together in Catia assembly workbench. The assembly model is then save in stp format so it can be imported to Ansys workbench. The model is split by YZ plane as it is symmetric about it, and giving translation constrain in X-axis. A face to face contact is defined between cover flange and vessel flange

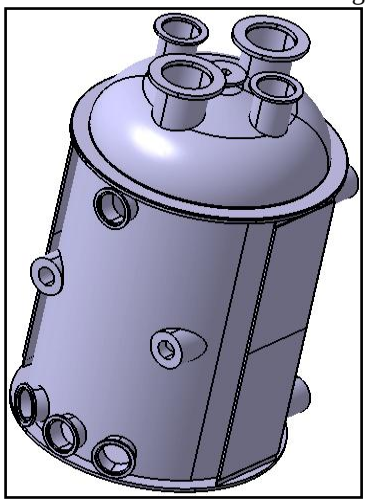

Fig. 3.1 Solid Model

IV. MESHING

Meshing has been done by using the method of Tetrahedron . In Tetrahedron method the component is been divided into small triangle on its surface which gives no of nodes and elements of that component and. The meshing has been done by changing the mesh size of the various component of the vacuum chamber. Due to change in the density of the meshing, it results in the variation of the no of nodes and elements of the meshed parts

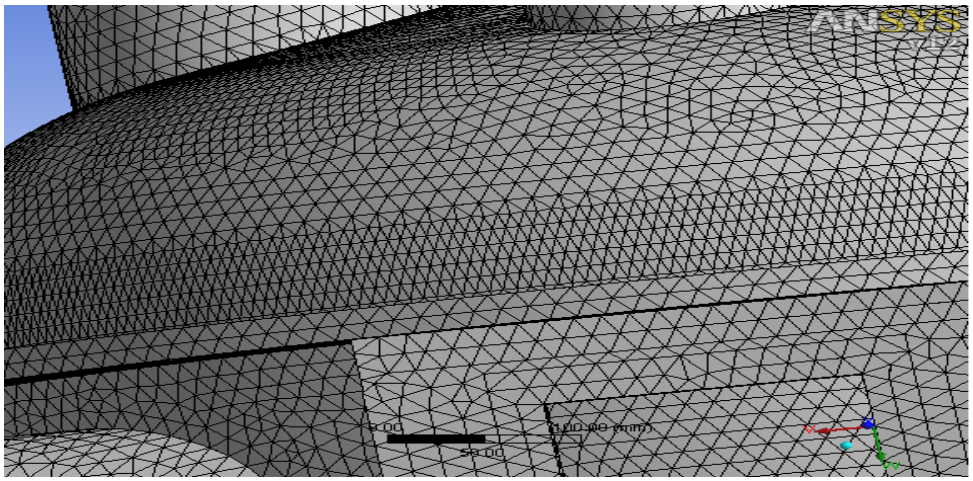

Fig 4.1 Tetradreon Meshing

V. BOUNDARY CONDITIONS

The simulation is done for internal pressure 700 torr which is less than of atmospheric pressure 760 torr that leads to compressive pressure on chamber. One atmospheric pressure equals to 760 torr (mm of Hg). (700 -760) torr = -60 torr = -7999.342 Pa.Thus 7999.342 pa pressures is applied on vacuum chamber walls. Due to negative sign, the direction of pressure is inwards. The faces of valve flanges and side base plate are fixed .

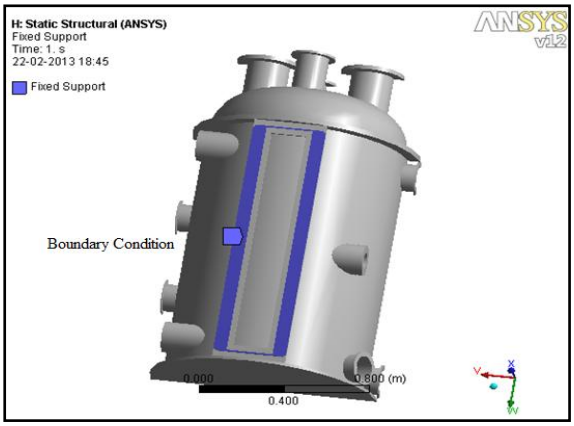

Fig. 5.1 Fix Support

Fig. 5.2 Pressure Applied

5.1 Material Properties

Material: Structural Steel
Young's Mod. of Elasticity, E = 2e11 pa
Poisson's ratio, μ = 0.3
Density, ρ = 7850 kg / m3
Compressive yield strength = 205e6 pa

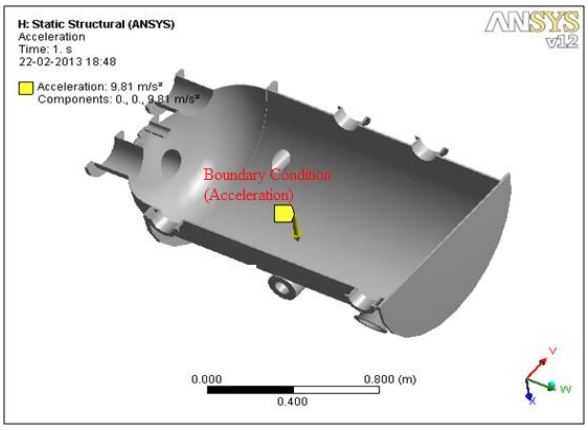

Fig. 5.3 Acceleration

VI. FINITE ELEMENT ANALYSIS

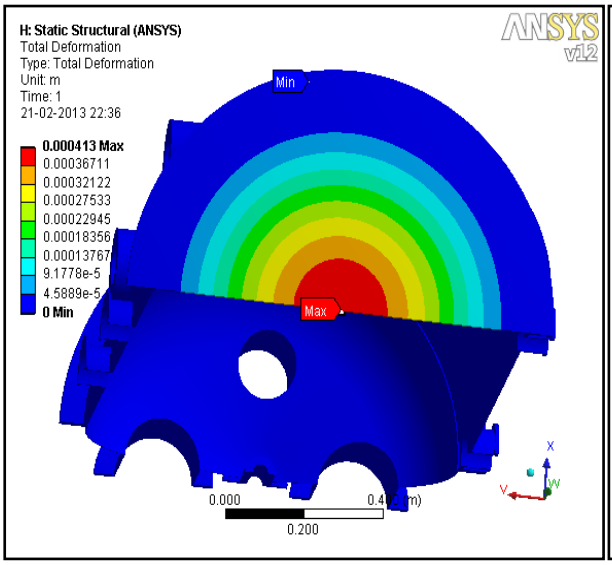

Fig 6.1 Max Deformation for the full body

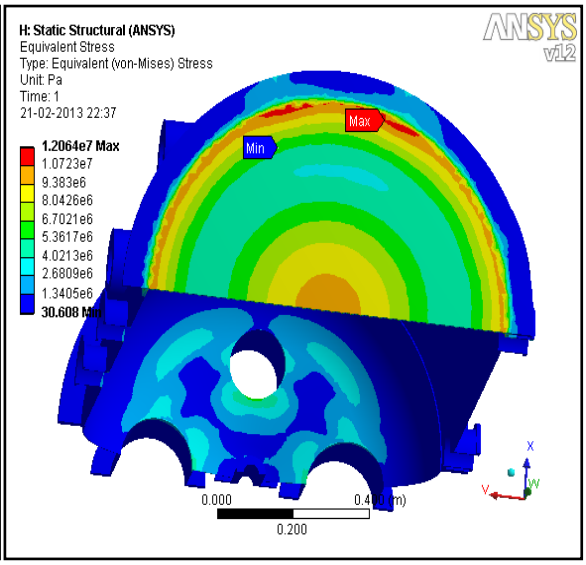

Fig 6.2 Max Von Mises Stress for the full body

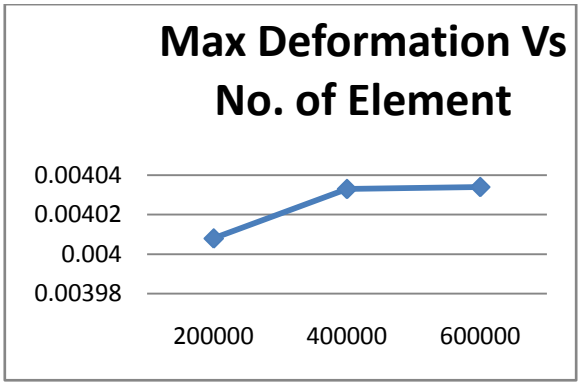

Fig. 6.3

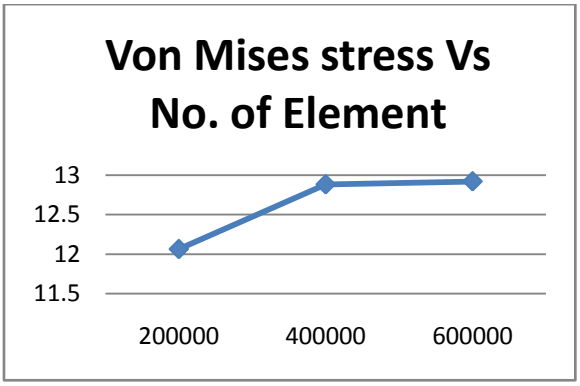

Fig 6.4

VII. RESULTS

Deformation and Von Mises Stress at different regions has been calculated using post processor. VON Mises Criterion also known as the maximum distortion energy criterion, octahedral, is often used to estimate the yield of ductile materials. The Von Mises criterion states that failure occurs when the energy of distortion reaches the same energy for yield/failure in uniaxial compression/tension. Max Von Mises stress calculated

from the analysis is 1.4e7 Pa on the vessel between valve and base plate as shown in Fig 6.8 which is very less than compressive yield strength 205e6 Pa. So it is safe from this criterion.

VIII. SHELL ANALYSIS

To verify the results of solid structural analysis, shell structural analysis for internal pressure 700 torr is done. The difference is that, here middle surface of the solid body is modeled and thickness is given in Hypermesh. It includes similar steps as that of solid structural analysis. Here middle surface of body is to be modeled which go inside and outside the half of thickness and turns into solid body in Ansys workbench. There are six degree of freedom, three for translation and three for rotation. Vacuum chamber middle surface is modeled in Catia surfacing workbench by making all components individually and assembled in Catia assembly workbench. And save in igs format so it can be imported in Ansys workbench. In Ansys workbench, for every part thickness is defined. Symmetry is applied normal to X- axis. i.e. about YZ plane, the vacuum chamber is constrained to translate and rotate in X direction . Each part of vacuum chamber is connected to each other defining line contact b/w valve to flange and valve to vessel and face to face contact between cover flange to vessel flange and side base plate to vessel.

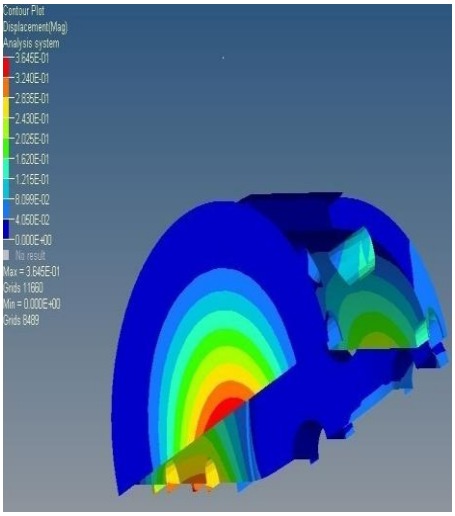

Fig.8.1 Surface Model 8.2 Line contact between valve & flange 8.3 Deformation

Max Deformation = 3.16 E-4 m. The max deformation in both analysis is on the base plate also their difference 1.2 E-5 m is very small. So the result given by solid structural analysis is correct.

IX. CONCLUSION

- The Vacuum chamber is safe from buckling failure as applied p is very small in comparison to max theoretical buckling pressure.
- Compressive yield strength of structural steel is greater than Von Mises stress is calculated by solid structural analysis so it is safe from this criterion.
- A linear graph comes out for max deformation and max Von Mises stress with internal pressure so for different value of internal pressure theoretically they can be calculated

REFERENCES

[1] WANG Wenlong, CAI Guobiao, ZHOU Jianping " Large-Scale Vacuum Vessel Design and Finite Element Analysis" Chinese Journal of Aeronautics 25(2012) 189-197.
[2] M. J. Kraan, Buskop, M. Doets, C. Snippe on "Structral analysis of the vacuum vessel for Lhcb Vertax locator."
[3] J.N.Reddy , An introduction to the Finite Element Method 3rd edn. McGraw-Hill, New Delhi, 2009.
[4] K. Ioki, P. Barabaschi, V. Barabash, S. Chiocchio,W. Daenner,F. Elio, et al., Design improvements and R&D achievements for vacuum vessel and in-vessel components towards ITER construction, Nucl. Fusion 43, 268–273.

International Journal of Modern Engineering Research (IJMER)
www.ijmer.com Vol. 3, Issue. 3, May - June 2013 pp-1672-1680 ISSN: 2249-6645

Modeling the Train Accidents at Railroad Crossings in East Java

Nyono[1], Harnen Sulistio[2], Achmad Wicaksono[3], Ludfi Djakfar[3]

[1]*Student at Doctoral Program, Departement of Civil Engineering, Faculty of Engineering, University of Brawijaya,* [2]*Professor at Doctoral Program, Departement of Civil Engineering, Faculty of Engineering, University of Brawijaya,*[3]*Lecture at Doctoral Program, Departement of Civil Engineering, Faculty of Engineering, University of Brawijaya (Indonesia)*

ABSTRACT: *The growing train movement and people activities around the railroad will increase the frequency of traffic in railroad crossing. This potentially results in the increase in traffic accidents. The prediction of the number of such accidents is influenced by some factors dealing with variables on sensory psychological behaviors and the perception of the drivers passing the crossings. Observations were made at 33 points railroad crossing with not guardrail in East Surabaya DAOP VIII. The responsive variables are determined by the explaining variables namely the number of train accidents in railroad crossing. The explaining variables are those determining the value of responsive variables, consisting of three factors namely train engineering features, road engineering features and environment. The last Poisson regression model possesses four determining variables significant with the number of accidents that is the train speed, the distance of signs and the railroad crossing, flashing lamps and the average daily traffic. The train speed seems to be a primary factor contributing to the high level of accidents. The results of sensivity analysis show that if the train speed increases of 50%, the number of accidents will increase 40%. Facilities that should be quickly provided are among others: provision and installation of flashing lamps and Early Warning System (EWS).*

Key word: *railroad crossing, train engineering features, road engineering features, environment factor, Poisson regression*

I. INTRODUCTION

The System of railway affairs in East Java has been established since the Dutch collonialism era. The lines of train in East Java consist of North Line (Surabaya Pasar Turi – Semarang – Jakarta), Central Line (Surabaya Gubeng – Yogyakarta – Jakarta), South Ring Line (Surabaya Gubeng - Malang – Blitar – Kertosono – Surabaya) and East Line (Surabaya Gubeng – Jember – Banyuwangi). This province also possesses a transportation system of commuter trains with a route of Surabaya – Sidoarjo – Porong, Surabaya – Lamongan – Babat, Surabaya – Mojokerto, and Malang – Kepanjen. The train movement in each operation area (herein called DAOP), each DAOP VII Madiun, Daop VIII Surabaya and DAOP IX Jember is high enough, which result in a complicated problem and one of its negative effects in the increasing number of train movement in east Java is accidents. In East Java, there are 1441 railroad crossings consisting of 1103 crossings without guards, 338 with guards and also gate and 96 illegal crossings (PT.Kereta Api Indonesia, 2010), and the potency to open or to add new railroad crossings is very great, especially the opening of illegal crossings due to the growth of hinterland in either the right or left side railroad because of the growing land use in each railroad areas. The growing train movement and people activities around the railroad will increase the frequency of traffic in railroad crossing. This potentially results in the increase in traffic accidents.

Train accidents in railroad crossing often happen in line with the time development. The prediction of the number of such accidents is influenced by some factors dealing with variables on sensory psychological behaviors and the perception of the drivers passing the crossings (Raslear, 1996); categories of warning equiptments, volume of road traffics, volume of train traffic, visibility of the condition in the crossings (Gitelman and Hakkert 1996); types of warning equiptments, crossing geometric, railroad geometric, volume of rtaffic (Saccomanno, Liping Fu and Moreno 2001); the number of the passing train, active equiptment, road safety, rescuing operation, warning sign of flickering lamps, (Mok and Savage 2003); width of crossing geometric, traffic control equipment, flickering lamp time, speed in heaping land, size of crossing, warning signs, stop sign, number of railroad, number of tract, diameter of road separator, audit of safety, AADT, warnign equiptment, control management, barrier control, status of class of road, types of area aroung the crossing (business, residence, agriculture, etc)(Kang Lee and Ren Hu 2007); number of train identification, levels of service, types of vehicles involved, number of damage of vehicles, number of the people injure or die (Collister and Flaum 2007); factors of engineering in the crossings, of human beings, of environment (Zaharah Ishak 2007); traffic separator, behavior or drivers' responses factors to the equipments in railroad crossings (Ko, Washbum, Courage dan Dowell 2007); volume of traffic and trains per hour, speed of vehicles approaching the crossings, percentage of heavy vehicles, levels of service (LOS), speed of the train approacing the crossings (Zaharah Ishak,Yue and Somenahalli 2010); features of trains, roads, railroad crossings and of traffic (RenHu,ShangLi and KangLee 2011). The above variables really influence the prediction of accidents in railroad crossings, therefore some of the variables that influence one another may be simulated intro a model of prediction of accidents in railroad crossings.

Various models of prediction of train accidents in railroad crossing have been developed. Federal Railroad Adminstration (FRA) of America has studied accidents in railroad crossings by accomodating variables among others multiplication of the average daily traffic factor in roads and traffic of the trains that passed, the number of the passing trains per day, the speed of the trains, the number of tracts, the number of lanes in roads and types of road hardening prove to influence the number of accidents in railroad crossings. Empirical results show that the Poisson regresion is appropriate

for estimaing the possibility of accidents; and the negative binominal regression is good for predicting accident risks and effects (Kang Lee dan Ren Hu 2007). The model was developed using a Petri Nets approach by taking into account components of basic concepts of safety, infrastructure engineering techniques, levels of surrounding enviroment and all factors in human beings (Zaharah Ishak,Yue dan Somenahalli 2010). The zero Possion regression model has also been developed to delienate the relationship between the number of zero death or injury, and additional data and explaining variables were collected in 592 locations of Railroad Grade Crossing (RGC) in Taiwan (RenHu,ShangLi dan KangLee 2011).

Up to now, no research has been made to make a model of prediction of train accidents in railroad crossing with no gate by accomodating and combining and developing all explaining variables that have once been studied by previous researchers with different analyses. The resulted model would be built to predict train accidents in legal railroad crossings without gate when a train is moving in a single track which generally happens in developing countries with the minimal level of the society on the safety of trains – this makes them easy to open ilegal railroad crossings. The results of this present study was expected to be useful for making any action programs to reduce the number of train accidents.

II. THEORIES AND METHOD

The variables of this present research consist of explaining and responsive variables. The responsive variables are determined by the explaining variables namely the number of train accidents in railroad crossing. The explaining variables are those determining the value of responsive variables, consisting of three factors namely train engineering features, road engineering features and environment. The train engineering features factor contains variables of the width of crosing, number of tract, speed of train, volume of passing train, free vision of the engineer of locomotive, guardril in the crossing , the existence of flashing lamp and siren. The road engineering features factors consist of agricultural areas, business, residence, industrial and road lights. In the modelling of the number of accidents, a Poisson regresion analysis calculated using a statistical software GenStat Discovery Edition 3 is employed. The stages of the data analyses are as follows:

1. Testing the distribution in the response variable (*Y*) using the Kolmogorov-Smirnov test of the data on the number of accidents. In this test, the data of the number of accidents are expected to follow the that of Poisson.
2. Establishing the model of the Poisson regression with a general model of $\mu = \exp(\beta_0 + \beta_1 X_1 + ... + \beta_k X_k)$, making the following steps:
   a. Modelling the Poisson regression analysis in each explaining variables (independent variables). Estimating parameters for each combination of the Poisson regession model, with a general model $\mu(x_i, \beta) = \exp(\beta_0 + \beta 1X1i + ... + \beta kXki)$, dengan i = 1, 2, 3, 4, 5.
   b. Testing the parameters in each combination using Chi-Square, in GenStat Software this value are transformed to F dan t statistics.
   c. Testing the model for each combinations simultanesously with deviance criteria.
   d. Determining the best model with the smalles deviance from each combination of variables.
   e. Making an interpretation of the best model.

III. RESEARCH RESULTS

The data distribution following the Poisson distribuition shows specific characteristics among others it is discrite and limited in time or certain areas. The accident posisbility is very small, meaning the any vehicles passing railroad crossings have a very small possibility to get accidents. The average number of accidents is 1, 45, meaning that in the last three years the number of accidents is about 1 -2 times in one point. From the results of the Kolmogorov Smirnov test, the obtained value of the *Kolmogorov-Smirnov Z* is 1.341 with *asymp.Sig. (2-tailed)* or *p-value* of 0,055. It may be concluded that the data on the number of train accidents followed the Poisson distribution. The modelling showing the relationship among the numbers of train accidents in railroad crossings would be made by using the Poisson regression analysis. The analysis consists of three stages, first making a model for each explaining variables, second, modelling a combination of variables that prove to have a significant influence from the results in the first stage, and three, selecting the determining variables in the second stage which are really significant as a whole.

In a model with single determining factor, an analysis for significant 15 explaining variables from the results of a descriptive analysis on the number of accidents is made. In the analysis, an emphasis is given on the results of the regression coefficient test. If the result is significant (probability value < 0,05), this variable will be included in the establishment of the simultaneous model. The analysis of each variable is presented in Table 1 :

Tabel 1. A Poisson Regression Analysis of the Influence of the Train Speed

Variable	estimate	s.e.	t(*)	p-value.	Test results
Train speed	0.0311	0.0115	2.69	0.007	Significant
Train Volume	0.0558	0.0255	2.19	0.029	Significant
Signs	0.223	0.436	0.51	0.609	Not Significant
Distance of signs	-0.0248	0.0126	-1.96	0.049	Significant
Free view	-0.00118	0.000592	-2.00	0.046	Significant

Guardrail	0.182	0.298	0.61	0.541	Not Significant
Flashing Lamp	-0.598	0.29	-2.06	0.039	Significant
Road width	0.362	0.182	2.00	0.046	Significant
Number of lane	0.171	0.472	0.36	0.718	Not Significant
the average daily traffic	0.001436	0.000577	2.49	0.013	Significant
Road flatness	0.223	0.436	0.51	0.609	Not Significant
Types of construction	0.633	0.306	2.07	0.039	Significant
Road marks	0.27	0.295	0.92	0.360	Not Significant
Environment	0.598	0.29	2.06	0.039	Significant
Lighting	0.266	0.333	0.80	0.425	Not Significant

From the result of modelling with a single determining factor of 15 explaining variables, there are 9 (nine) variables with significant influence, mean while the rest (6 variables) do not give any significant influence. Then a simultaneous model involving 9 the (nine) significant variables are analysed. The results of the Poisson regression analysis enclosing the 9 determining factors filtered in the first phase are shown in Table 2.

Table 2. An Analysis of the Poisson Regression of the 9 Chosen Variables

Variable	estimate	s.e.	t(*)	p-value	Test results
Constant	-0.79200	0.52400	-1.510	0.145	-
Train speed	0.01117	0.00647	1.730	0.098	Not Significant
Train Volume	0.00969	0.00882	1.100	0.283	Not Significant
Distance of signs	-0.01170	0.00532	-2.200	0.038	Significant
Free view	-0.00042	0.00023	-1.850	0.078	Not Significant
Flashing lamps	-0.14700	0.13300	-1.110	0.280	Not Significant
Width of road	0.11570	0.08140	1.420	0.168	Not Significant
the average daily traffic	0.00065	0.00037	1.760	0.092	Not Significant
Types of construction	0.04500	0.14300	0.310	0.757	Not Significant
Environment	0.03600	0.13900	0.260	0.800	Not Significant

The last stage is intended to establish a regression model significant to the level of accidents simultaneously or partially. The selection of such a model is made by excluding variables one by one that partially does not influence the level of the accidents. From the results of the selection, there are four variables with significance of 0.05 namely: the train speed (X3), the distance of signs and the railroad crossing (X7), flashing lamps (X10) and the average daily traffic (X14), that significantly influence the level of accidents.

Table 3. A Final Model of the Results of the Poisson Regression Analysis

Variable	estimate	s.e.	t(*)	t pr.	Test results
Constant	-0.5910	0.3670	-1.610	0.118	-
Train speed	0.0130	0.0044	2.960	0.006	Significant
Distance of signs	-0.0125	0.0047	-2.640	0.013	Significant
Flashing lamp	-0.2575	0.0953	-2.700	0.012	Significant
the average daily traffic	0.0011	0.0002	5.680	0.001	Significant

The results of the analysis of the four chosen variables show the p-values of less than 0.005. therefore, the best model has been obtained. The following is the results of the analysis using the Poisson regression equation:
Y = exp(- 0,591 + 0,01302 Train speed – 0,01253 Distance Of Signs – 0,2575 Flashing lamp + 0,001122 Average daily traffic)

The validation of the model will measure the level of appropriatennes of the model with the results of real observation. The results of such validation may be considered through the results of analysis of deviation between the

estimated value and the real value, the correlation value and the deviation test between the results of prediction and real values. From the results of validation and the prediction value and the number of real accidents, it seems that they seem not too different. The following is presented the results of the deviation analysis from the last model and the picture of accidents prediction and the number of real accidents in each point.

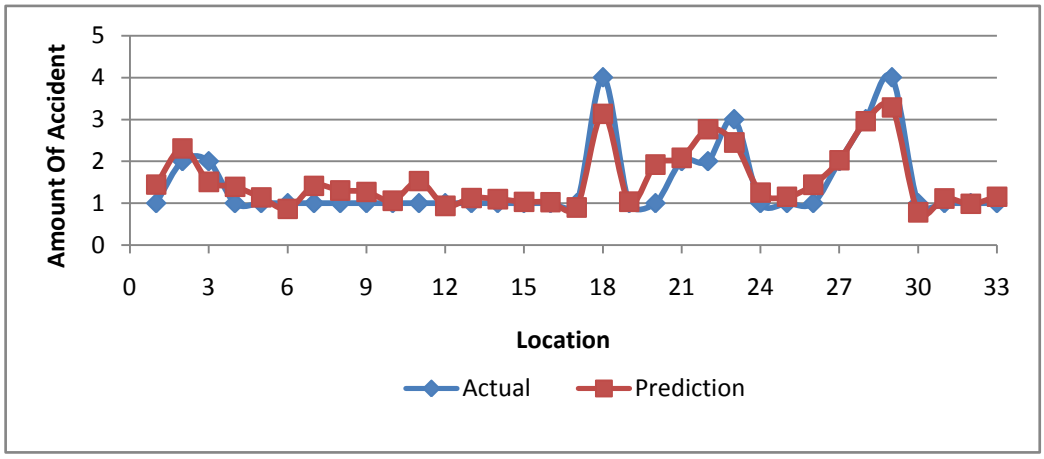

Picture 1. Values of Prediction of the Number of Accidents Based on the Poisson Regression Model

Picture 1 shows that the results of the prediction of the number of accidents reach the actual value. If the prediction value of the number of accident is rounded, there are 27 points (81.8%) posessing the same value between the prediction and the actual ones and 6 other points show differences. The different points are among others the sample points no. 11, 18, 20, 22, 23 and 29. The validation of other models was made by calculating the results of the deviation test of the number of accidents between the prediction and actual values. The test was made using the paired- t-test. As in the Table 5.34, the average difference between the prediction and actual values are -0.0303 with the p-value of 0.662 (higher than 0.05). It can be concluded that there is no significant difference between the prediction value (from the Poisson regression model) and the actual value..

The last Poisson regression model possesses four determining variables significant with the number of accidents. On the basis of the obtained model, decreasing the number of accidents can be reached with the following ways:

- Reducing the train speed when passing railroad crossings.
- Putting in signs in a greater distance before the point of crossing
- Maintaining and keeping flashsing lamps to make them function well
- Giving special attention at morning and afternoon peak hour daily traffic with guard in the railroad crossing with not guardrail.

In this part, an analysis of the level of sensitivity of a determining variable is made with the assumption that the condition of other variables are unchanged. The analysis of sensitivity will be graphically shown by splitting the data into two conditions: availability and unavailability of flashing lamps. The trains speed is around 65 – 90 kms/h, the distance between the sign and the crossing is about 3 – 40 meters, meanwhile the value of the average daily traffic is from 33.8 – 919.6 smp. The level of accidents is too low if in the crossing flashing lamp is available, the train moves in low speed, yje distance between the sign and the crossing is far enough from the crossing point and the daily traffic is not intense.

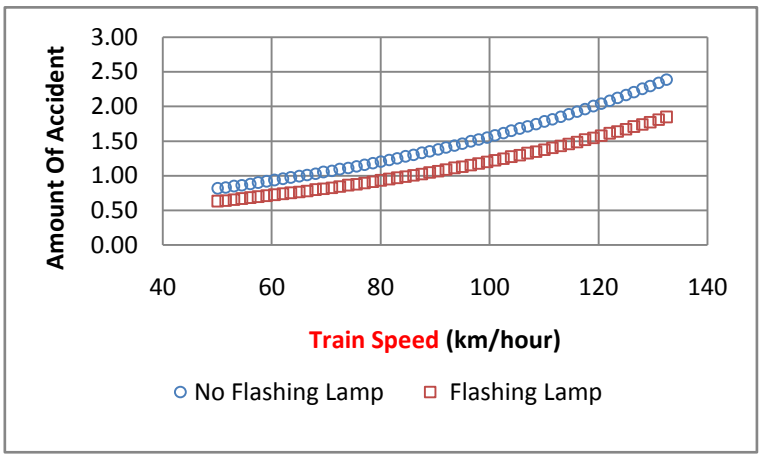

Picture 2. Amount Accident Prediction at few of Velocity

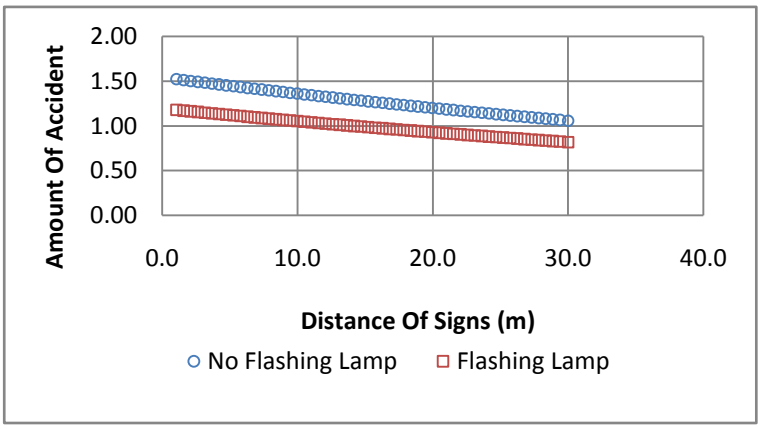

Picture 3. Amount Accident Prediction at few distance of Sign.

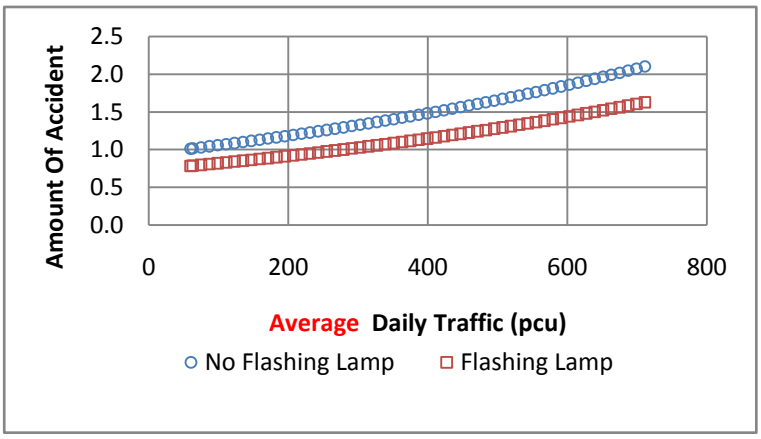

Picture 4. Amount Accident Prediction at few of the average daily traffic

From the results of the sensitivity analysis on the basis of the changes in the train speed and in the number of accidents, it is known that if the increase in the train speed reaches 50%, the number of accidents is predicted to increase around 40%. If the increase is 100%, the number of accidents is predicted to be about 90%. And in the results of the analysis of sensivity of the changes in the distance of the signs and the crossing and in the number of accidents, it is shown that the decrease in the distance of the sign and the crossing point to 50% is predicted to be able to increase the number of accidents up to 20%. If the distance is reduced up to 75%, the number of accidents is predicted to increase about 35%. From the results of the analysis of sensitivity to the changes of the average daily traffic up to 100%, it is predicted to increase the number of accidents of about 8%. If the value of the average daily traffic increases up to 200%, the number of accidents is predicted to increase of 17%.

IV. DISCUSSION

From the results of modelling with the Poisson regression analysis, there are four independent variables found to be significant in the model. The variables are the train speed, flashing lamps, the distance between the signs and the crossing, and the average number of daily traffic. The application of the model of the Poisson regression has a high validation, which is in line with a research Chi-Lee and Ren-Hu (2007) made that the Poisson regression is good for predicting the possibility of accidents; and the negative binomial regression is good for predicting the risks and effects of accidents.

Average daily vehicles passing railroad crossing has a correlation with the number of traffic accidents. The higher the average vehicle crossing the railroad in a year, the higher the number of accidents in raildroad crossings. This also applies to the train speed and the possibility of accidents. Although human factors play a big role in accidents, but this shows that the train, roads and environment features give a big contribution to accidents in railroad crossings.

In the last model, it can be explained that the train features factor is important since from the four determining variables in the number of accidents, three of which are train features such as train speed, flashing lamps, and the distance between the signs and the railroad crossings. Road feature factors are representend by the average daily number of traffics. While the environment factors condsisting of crossing areas (agriculture, housing and industry) are included into the last model. In the process of modelling, from the results of analysis in the first pat, it is evaluated that in the single determining model, the following variables give significant influence on the number of accidents in railroad crossing, namely:

- Train speed
- Train Volume

- The distance between the signs and the railroad crossings
- Free view
- flashing Lamp
- Width of road
- the average daily traffic
- Types of construction
- Environment

But in the advanced model combining all single determining variables, there are merely four variables that prove to have significant influence on the number of accidents. There are five variables considered as variables with strong potentials as the causes of accidents namely:

- Train volume
- Free view
- Width of road
- The average daily traffic
- Types of construction
- Environment

A train feature important to hamper accidents is flashing lamp. This tool contained in the siren, both of which function together. In the whole data, the number of railroad crossings with flashing lamps is 14 points (42,4%) while the rest, 19 points (57.6%) without flashing lamps. The importance of the control equiptment is in line with a research Coleman (1997) made. The control equipment of trafic provides passive-static warning, guidance and in some cases, obligatory action for drivers. Trafic control equipments are assets that give warning that the train is approaching. They are activated by a train in the circuit of tract/rail detection. This active control equiptments are prodived with the same signs of crossings to give a passive control.

The railroad crossings provided with flashing lamps are 14 points, 13 of which (92.9%) became places for accidents once in three years, meanwhile in one other point, 3 times accidents happened. Different from points of observation without flashing lamps amounting 19 points, there are 2 points (10.5%) with a high level of accidents namely 4 incidents during 3 years. This automatic instalation will help reduce the number of accidents. The research results support the research made by Mok and Savage (2003). From the analysis, it can be concluded that the instalation in the Guardrail or flashing lamps contributed about the fifth of reducing the number of accidents. The development from a campaign "safey operation" intended to inform the public about proper attitudes in railroad crossings has long been made. In the 1970s and early 1980s, an instalation of "ditch lamp" in the locomotive has been known.

At present there is a wireless technology of early warning tool in railroad crossings. Due to the development of transportation technology and provision of supporting facilities and infrastructures, a system of transportation arrangement will be needed to improve pleasure and safety of the users of transportation facilities, especially in railroad crossings which are not provided with guardrails. The tool of early warning in railroad crossings has made use of a wireless system, so no cable is needed. This tool may turn on after the sensor works when the traiin will pass the point in one km before it and it will transmit a sign to the warning tool to turn on. This system also uses electric power from solar cells so that it will not depend on the electric supply from the state electricity enterprise. Therefore it may be used in most railroad crossings located in a tract with no electric network.

The train speed seems to be a primary factor contributing to the high level of accidents. The results of sensivity analysis show that if the train speed increases of 50%, the number of accidents will increase 40%. The level of sensitivity of this train speed is far superior than the distance between the signs and the crossings namely 20% and the average daily traffic which is merely of 6%. This result is in line with that of Coofster and Pflaum (2007) stating that the explaining variables significantly influencing the possibility of accidents are the train speed, the number of trains passing the crossings each day, the percentage of heavy vehicles (trucks), the number of vehicle traffic (number of lanes), signs on the roads, flashing lamps, railcrossing angle, the surface of road and railroad crossings, trade, housing and industrial areas. The problem of train speed in Indonesia is dilemmatic. Reducing the train speed will result in the addition of movement time, whereas without reducing the speed, the train often comes late in its destination. It seems in contradiction with the development of railway affairs in other countries, where the train speed has always been added. In Indonesia, it it PT KAI that operates the trains. While the facilities and infrastructure are handled by the government.. Reducing train speed should be made due to bad condition of the track, and this condition happens because fund allocation from the government to maintain the track is very small compared with what actually needs. As a result, from year to year, the condition of the track will be worse. As an operator, reducing the speed is an appropriate choice since if an accident happens, it is the operator (PT KAI) that will be responsible for it. Up to now, the maintenance of the tracks are still held by PT KAI as an operator.

The results of modelling using the Poisson regression will be used to predict the point at which a railroad crossing should be paid attention. A "blackspot" status for a railroad crossing with high level of accidents will be able to help reduce accidents. A blackspot is a crossing with high risk of collision. It is suggested that one of the way is to allocate fund for all fields of problems. A random incident of collision is very various in space and time. A high risk in a certain crossing in a year does not always show high risk in the next year. A risk of collision needed to express any risk may be anticipated in a certain period. This estimation may be obtained using a model to rpedict a frequency of collission and therefore it is accurate and reliable. The identification of a blackspot merely based on the number of collission will not give

any complete picture of the risk in each crossing. The risk of collission consists of two components: frequency and consequence (level o severity). Ignoring such a consequency may result in less intervention in any railroad crossing with the severe level of collission and riska -based model is needed to identify any spots where collissions often happen.

The results of prediction of the number of accidents in each spot may be used to attribute certain characteristics ot the spot. Another indicator to choose the best criteria is comparing the number of expected accidents and that of observed accodents (Rakhmat *et al.,* 2012). The results of the comparison may be in the form of

a. Location which is predictied to be dangerous is actually harmful (*correct positive)*
b. Location which is predictied not to be dangerous is actually not harmful (*correct negative)*
c. Location which is predictied to be dangerous is actually not harmful (*false positive)*
d. Location which is predicted not to be dangerous is actually harmful (*false negative)*

In this case, if the observed number of accidents is higher than the expected one, it can be categorised into *correct positive (CP).* If the observed number of accidents is lower than the expected one, it is categorized as *false positive (FP).* In Table 5.40, it is shown that the criteria excessive number of accidents using the prediction model resilts a number of segment classified as the biggest *correct positive (CP) as* compared with the other three criteria, namely 7 segments (from 10 mist dangerous segments) and 14 segments (from twenty most dangerous segments).

Table 4. A Comparison of Actual and Predicted Values from the Poisson Model

Spot	Actual	Predicted	Information	Spot	Actual	Predicted	Information
1	1	1.45	False Positive	18	4	3.13	Correct Positive
2	2	2.31	False Positive	19	1	1.04	False Positive
3	2	1.51	Correct Positive	20	1	1.92	False Positive
4	1	1.39	False Positive	21	2	2.08	False Positive
5	1	1.14	False Positive	22	2	2.77	False Positive
6	1	0.86	Correct Positive	23	3	2.45	Correct Positive
7	1	1.41	False Positive	24	1	1.25	False Positive
8	1	1.30	False Positive	25	1	1.16	False Positive
9	1	1.27	False Positive	26	1	1.44	False Positive
10	1	1.06	False Positive	27	2	2.03	False Positive
11	1	1.53	False Positive	28	3	2.96	Correct Positive
12	1	0.94	Correct Positive	29	4	3.29	Correct Positive
13	1	1.12	False Positive	30	1	0.78	Correct Positive
14	1	1.10	False Positive	31	1	1.11	False Positive
15	1	1.03	False Positive	32	1	0.99	Correct Positive
16	1	1.02	False Positive	33	1	1.15	False Positive
17	1	0.90	Correct Positive				

In Table 5.40, it is shown that there are 10 spots which are really dangerous namely spot 3 (Bojonegoro regency ; 140+135, SRJ-BWO), spot 6 (Lamongan regency; 162+681, BBT-GEB), spot 12 (Lamongan regency; 179+735, SLR-LMG), spot 17 (Gresik regency; 199+790, LMG-DD), spot 18 (Surabaya city; 222+603, KDA-TES), spot 23 (Sidoarjo regency; 26+121, SPJ-BH), spot 28 (Pasuruan regency; 43+629,, PR-BG), spot 29 (Pasuruan regency, 44+610, PR-BG), spot 30 (Malang regency; 29+128, SN-LW) and spot 32 (Blitar regency; 76+158, NB-SBP).

In this research fangerous segments are determined by comparing three criterias with the data of train accidents from 2010-2012 and applying the resulted model to get the expectation of average number of accidents on the referred population. The criteria to determine the dangerous segments that will be used are among others:

a. The excess of the number of accidents using the model of traffic prediction is made by determining the difference of number of accidents from the prediction model and the results of the observation.
b. The level of accident is mad by comparing the real number of accidents and the daily crossing of a segment,
c. The frequency of accidents is made by ordering the data on traffic accidents from the highes to the lowest.
d. The results of identification of all examined spots using the criteria of the excess number of accidents create a rating of dangerous segments based on the difference between the observede number of accidents and the expexted results of the prediction model. The result of discussion on the basis of the final model of the Poisson regression analysis will results in some implications intended to reduce the level of accdients.

To avoid any collision between the train and general transportation in railroad crossings is made by applying a technology to improve the reliability of the signals, either those in any crossing with/without guard. The available and proper technology for the purpose is installing the AWS (Automatics early Warning System). Since there are thousands of railroad crossings with no automatic gate, it is proper to apply the AOCL (Automatic Open Crossing, Locally monitored)

since it is cost effective. Besides the application of the technologies, other efforts which should be simultaneously applied are as follows:

a. Completing traffic signs on the roads that will cross the railroad crossings.
b. Controlling any railroad crossing by closing or combining two or more crossing into one.
c. Reducing railroad crossing using flyover or underpass

An alarm system in railroad crossing is used by providing flashing lamps and sirens. In each railroad crossing with or without gate, signs and alam/sirens should be provided, since the most effective sense is ears (earing), and ears can respond information without being able to be caught by sense of sight, especially in any crossing surrounded by high buildings. Psychologically, if alarm (siren) is heard, there is tendency for one sense to be more alert than others. For example, for the sense of sight (eyes) although they have seen any written warning, but there is a tendency that the influence of impatience is still higher. Alarm or siren should be placed in each crossing especially those with no gate. It is better any censor or switch alarm/indicator lamp are put 500 mt from the crossing, so that drivers may quickly know the position of the train to take any step to avoid accidents.

V. CONCLUSION

From the discussion above, some conclusions can be made. The train accidents happening in railroad crossings without guardrails in the operational area of DAOP VIII Surabaya for the last 3 (three) years, from 2010 to 2012, are 149 incidents with the following characteristics: hit by persons, by motor cycle (R2) and by personal vehicles or truck (R4) with the death of 30 persons, injuries, 107 persons and no victims of 12 persons. From the results of modelling the Poisson regresion, there are four determining factors of accidents namely train speed, the distance of the signs and the railroad crossing, flashing lamps and the average daily traffic. The train speed possesses the highest sensitivity to the number of accidents.

From the results of modelling to the number of accidents, some reccomendations are offered. Installing flashing lamps in each railroad crossing with not guardrail proves to contribute to the decrease in the number of accidents. So it is recommended that in each railroad crossing without guardrail be put in flashing lamps. It should optimize the participation of the people living around railroad crossings to maintain the warning signs or other safety facilities in railroad crossing with no gate. Any activity of socialization to people living around the crossings should be made in roder to improve their participation in keeping the security and safety in the crossings.

Technical guidance to the people should also be given to improve the participation of the people living around railroad crossings with not guardrail. The operator should make a stronger coordinating with the concerned institutions to improve safety and security in the railroad crossing with no guardrails because of limited budget from the operator to providing the safety facilities. Facilities that should be quickly provided are among others: provision and installation of flashing lamps and Early Warning System (EWS), signs in certain distances (not too near or too far), signs of speed limit and of signal 35 for each railroad crossing with no gate and inspection and control are made in cooperation with concerned institutions to close any illegal railroad with no gate.

REFERENCES

[1] Arikunto, S. 2010, *"Prosedur Penelitian Suatu Pendekatan Praktek"* Gramedia Pustaka Utama Jakarta.
[2] Coleman, Eck and Russell 1997, "Railroad-Highway Grade Crossings A Look Forward" Committee on Railroad-Highway Grade Crossings;
[3] Collister and Pflaum 2007, "A model to predict the probability of highway rail crossing accidents", Overland Kansas USA;
[4] Direktorat Jenderal Perhubungan Darat (2005), "*Pedoman Teknis Perlintasan Sebidang antara Jalan dengan Jalur Kereta Api*" Jakarta.
[5] Farr 1987, "Summary Of The DOT Rail—Highway Crossing" resource allocation procedure-revisited. Report no. DOT/FRA/OS-87/05, Office of Safety Federal Railroad Administration.
[6] Federal Railroad Administration (2001), " Office of Policy and Program Development Grade " Dec 2000 user manual, version 2.0.
[7] Federal Railroad Administration (2002), Office of Policy and Program Development. Grade Dec 2000, Reference manual version 2.0, January 2002.
[8] Federal Highway Administration (2000), " Statistical Models of At – Grade Intersection Accidents – Addendum" March 2000 Publication No. FHWA - RD - 99 -094.
[9] Gitelman And Hakkert 1997, " The Evaluation Of Road-Rail Crossing Safety With Limited Accident Statistics" Transportation Research Institute, Technion-Israel Institute Of Technology, Haifa 32000, Israel.
[10] Hogg, and craig. 1978. *Introduction to Mathematical Statistic*. Fourth Edition. USA: Macmillan Publishing co, Inc.
[11] Hauer 1985, "On The Estimation Of The Expected Number Of Accidents" Transport Safety Studies Group, Department Of Civil Engineering, University Of Toronto, Toronto, Ont., M5s La4, Canada.
[12] Hensher and Button 2000, "Hand Book Of Transport Modelling" , Netherlands;
[13] Hanseon Cho and Rilett 2007, "Improved Transition Preemption Strategy for Signalized Intersections near At-Grade Railway Grade Crossing" DOI: 10.1061/ (ASCE)0733-947X (2007)133:8 (443);
[14] Hair,Black, Babin dan Anderson 2010, *Multivariate Data Analysis*, Seventh Edition copy right 2010 by Pearsion Prentice Hall.
[15] Hermanto Dwiatmoko (2011) "*Program Strategis Peningkatan Keselamatan Perkeretaapian"*, Direktorat Jenderal Perkeretaapian Kementrian Perhubungan Jakarta;
[16] Kleinbaum, R.H.1988. *Applied Regression Analysis and Other Multivariable Method*. Boston: PWS-KENT Publishing Company.
[17] Ko, Washburn, Courage and Dowell 2007, "Evaluation of Flexible Traffic Separators at Highway–Railroad Grade Crossings" DOI: 10.1061/(ASCE)0733-947X (2007);

[18] Lee, Nam, and Park 2005, "Analyzing The Relationship Between Grade Crossing Elements And Accidents", *'Journal of the Eastern Asia Society for Transportation Studies*, Vol. 6, pp. 3658 - 3668, 2005
[19] Lee and Ren Hu 2007, "Accident Risk At A Railway Level Crossing"; *Journal of The Eastern Asia Society for Transportation Studies*;
[20] McCullagh, P, and J.A. Nelder. 1989. *Generalized Linier Model*. Second Edition. London: Champman and Hall.
[21] Myers, R.H. 1990. *Classical and Modern Regression with Applications*. Edisi Keempat. USA: PWS-KENT Publishing Company.
[22] Mok and Savage 2007, "Why has Safety Improved at Rail – Highway Grade Crossing";Risk Analysis;
[23] Nawari 2010, *"Analisis Regresi"* Alex Komputindo Kompas Gramedia Jakarta.
[24] Peterman 2007, "Selected Issue in Proposed Reauthorization Legislation";Federal Railroad Administration Programs;
[25] PT. Kereta Api Indonesia 2010, *Data Base Perkeretaapian*, Surabaya.
[26] Raslear1996, "Driver Behavior At Rail-Highway Grade Crossings: A Signal Detection Theory Analysis"; Washington, DC:U.S. Department of Transportation.
[27] Ren Hu, Shang Li and Kang Lee 2011, "Assessing Casualty Risk of Railroad-Grade Crossing Crashes Using Zero-Inflated Poisson Models" DOI: 10.106 1/(ASCE) TE.1943-543 6.0000243.© 2011 American Society of Civil Engineers ;
[28] Rangkuti, F. (2004) "*Analisis SWOT Teknik Membedah Kasus Bisnis*" Gramedia Pustaka Utama Jakarta.
[29] Saccomanno, Liping Fu, and Moreno 2001, "Risk-Based Model for Identifying Highway – Rail Grade Crossing Blackspots" Transportation Research Record,' *Journal of the Transportation Research Board*, No. 1862, TRB, National Research Council, Washington, D.C.
[30] Sian Tey and Ferreira 2010, "Driver compliance at railway level crossings" Faculty of Engineering, Architecture and Information Technology, The University of Queensland, AND Brisbane St Lucia, QLD 4072, Australia;
[31] Singarimbun, M & Effendi, S. (1995) " *Metode Penelitian Survey*" Jakarta LP3ES.
[32] Yayasan Bhakti Ganesha (2005), Kecelakaan Kereta Api di Indonesia (Permasalahan dan Alternatif Solusi); ITB Bandung.
[33] Zaharah Ishak 2007, " The Development Of Railway Level Crossing Safety Assessment Model" Conference of Australian Institutes of Transport Research (CAITR);
[34] Zaharah Ishak, Yue and Somenahalli 2010, "Level Crossing Modelling Using Petri Nets Approach and Π–Tool" Asian Transport Studies, Volume 1, Issue 2 (2010), 107-121 © 2010 ATS All rights reserved;

International Journal of Modern Engineering Research (IJMER)
www.ijmer.com Vol. 3, Issue. 3, May.-June. 2013 pp-1681-1689 ISSN: 2249-6645

Minimization of Congestion using Backpressure Routing Algorithm in Wireless Networks

A. Priyadharsini, Mr. S. Mohanarangan, Dr. D. Sivakumar
M.E. M.Tech.,(Ph.D).,Computer Science and Engineering
Arunai College of Engineering Tiruvannamalai-606603

Abstract: *Back-pressure-type algorithms have recently received much attention for jointly routing and scheduling over multi-hop wireless networks. However, this approach has a significant weakness in routing because it explores and exploits all feasible paths between each source and destination. While this extensive exploration is essential in order to maintain stability when the network is heavily loaded, under light or moderate loads, packets may be sent over unnecessarily long routes, and the algorithm could be very inefficient in terms of end-to-end delay and routing convergence times. We develop a improvised backpressure routing algorithm that maximizes network throughput and expends an average power that can be pushed arbitrarily close to the minimum average power required for network stability, with a corresponding tradeoff in network delay .This paper proposes a new routing/scheduling back-pressure algorithm that not only guarantees network stability, but also adaptively selects a set of optimal routes based on shortest-path information in order to minimize average path lengths between each source and destination pair . On the other-hand, the proposed algorithm adaptively selects a set of routes according to the traffic load so that long paths are used only when necessary, thus resulting in much smaller end-to-end packet delays as compared to the traditional back-pressure algorithm.*

Index Terms: *Back-pressure routing, shortest path routing, throughput-optimal*

I. INTRODUCTION

Due to the scarcity of wireless bandwidth resources, it is important to efficiently utilize resources to support high throughput, high-quality communications over multi-hop wireless networks. In this context, good routing and scheduling algorithms are needed to dynamically allocate wireless resources to maximize the network throughput region. To address this, throughput - optimal1 routing and scheduling, first developed in the seminal work of [2], has for a comprehensive survey. While these algorithms be extensively studied [3]–[14].We refer to [15] and [16] maximize the network throughput region, additional issues need to be considered for practical deployment. With the significant increase of real-time traffic, end-to-end delay becomes very important in network algorithm design. The traditional back-pressure algorithm stabilizes the network by exploiting all possible paths between source–destination pairs (thus load balancing over the entire network). While this might be needed in a heavily loaded network, this seems unnecessary in a light or moderate load regime. Exploring all paths is in fact detrimental—it leads to packets traversing excessively long paths between sources and destinations, leading to large end-to-end packet delays.This paper proposes a new routing/scheduling back-pressure algorithm that minimizes the path lengths between sources and destinations while simultaneously being overall throughput-optimal. The proposed algorithm results in much smaller end-to-end packet delay as compared to the traditional back-pressure algorithm.

We define a flow using its source and destination. Let f denote a flow in network, denote the set of all flows in the network, F and $A_f[t]$ denote the number of packets generated by flow at time . We first consider the case where each flow associates with a hop constraint H_f . The routing and scheduling algorithm needs to guarantee that the packets from flow f are delivered in no more than H_f hops. Note that this hop constraint is closely related to the end-to-end propagation delay. For this problem, we propose a shortest-path-aided back-pressure algorithm that exploits the shortest-path information to guarantee the hop constraint and is throughput-optimal; i.e., if there exists a routing/scheduling algorithm that can support the traffic with the given hop constraints, then the shortest-path-aided back-pressure can support the traffic as well.

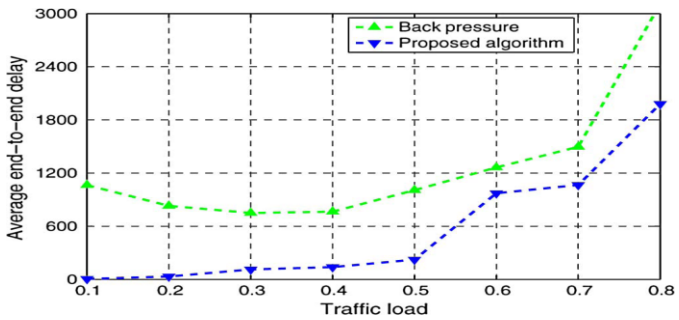

Fig.1. Back pressure via our joint traffic splitting and shortest-path-aided back pressure

Fig.1 illustrates the average end-to-end delays under the back-pressure algorithm and the proposed algorithm under different traffic loads. The network used in the simulation is a grid-like network with 64 nodes and 8 data flows .We have two observations.

1) Under the back-pressure algorithm, surprisingly, the delay first decreases and then increases as the traffic load increases. The second part is easy to understand: The queues build up when the traffic load increases, which increases the queuing delays. The first part is because the back-pressure algorithm uses all paths even when the traffic load is light. For example, in a light traffic regime, using shortest paths is sufficient to support the traffic flows. However, under the back-pressure algorithm, long paths and paths with loops are also used. Furthermore, the lighter the traffic load, the more loops are involved in the route. Hence, the end-to-end delay is large.
2) In the proposed algorithm, the set of routes used is intelligently selected according to the traffic load so that long paths are used only when necessary .We can see that under the proposed algorithm, not only is the delay significantly reduced, but also the delay monotonically increases with the traffic load.

We would like to emphasize that under the proposed algorithm, the delay improvement is achieved without losing the throughput-optimality. The proposed algorithm is still throughput-optimal, but yields much smaller end-to-end delays as compared to the traditional back-pressure algorithm.

II. MATHEMATICAL MODELS

We describe in this section mathematical models, which were built to represent a task allocation framework, parallel applications with security constraints.

A. Network Model: Consider a network represented by a graph $\mathcal{G} = (\mathcal{N}, \mathcal{L})$, where N is the set of nodes and L is the set of directed links. We assume that $|\mathcal{N}| = N$ and $|\mathcal{L}| = L$. Denote by (m ,n) the link from node m to node n . Furthermore, let $\mu = \{\mu_{(m,n)}\}$ denote a link-rate vector such that $\mu_{(m,n)}$ is the transmission rate over link (m ,n). A link-rate vector μ is said to be admissible if the link-rates specified by μ can be achieved simultaneously. Define Γ to be the set of all admissible link-rate vectors. It is easy to see that Γ depends on the choice of interference model and might not be a convex set. Furthermore, Γ is time-varying if link-rates are time-varying. To simplify our notations ,we assume time-invariant link-rates in this paper. However ,our results can be extended to time-varying link-rates in a straightforward manner. Furthermore, we assume that there exist $\mu_{\min}$ and $\mu_{\max}$ such that $\mu_{\min} \leq \mu_{(m,n)} \leq \mu_{\max}$ for all $(m, n) \in \mathcal{L}$ and all admissible μ .

Next, we define a link vector μ to be obtainable if $\mu \in \mathcal{CH}(\Gamma)$, where $\mathcal{CH}(\Gamma)$ denotes the convex hull of Γ .Note that an admissible rate-vector is a set of rates at which the links can transmit simultaneously, while an obtainable rate-vector is a set of rates that can be achieved including using time sharing. As a simple example, consider a network with two nodes {1, 2} and two links {(1, 2),(2, 1)}. Assume the link capacity is one packet per time slot for both links, and half-duplex constraint so that only one link can transmit at one time. Then, $\mu = \{0.5, 0.5\}$ is not an admissible rate-vector since two links cannot transmit at the same time. However, it is obtainable by time sharing.

B. Traffic Model: For network traffic, we let f denote a flow, s(f) denote the source of the flow, and d(f) the destination of the flow. We use to F denote the set of all flows in the network. Assume that time is discredited, and let $A_f[t] (f \in \mathcal{F})$ denote the number of packets injected by flow at time . In this paper, we assume $A_f[t]$ is random and independent and identically distributed across time slots, $A_f[t] = 0$.

III. THROUGHPUT-OPTIMAL ROUTING/SCHEDULING WITH HOP CONSTRAINTS

In this section, we consider the case where each flow is associated with a hop constraint H_f . Packets of flow f need to be delivered within H_f hops. We propose a shortest-path-aided back-pressure algorithm, which is throughput-optimal under hop-constraints. The algorithm is also a building block for the algorithm to be proposed in Section V, which seamlessly integrates the back-pressure and the shortest-path routing. Next, we characterize the network throughput region under hop constraints.

A. Network Throughput Region Under Hop Constraints: We denote by 1_Φ the indicator function with condition Φ, i.e., $1_\Phi = 1$ if condition holds, and $1_\Phi = 0$ otherwise. Given traffic $\mathbf{A} = \{A_f\}_{f \in \mathcal{F}}$ and hop constraint $\mathbf{H} = \{H_f\}_{f \in \mathcal{F}}$, we define $\Lambda_\mathcal{G}$ by saying that $(\mathbf{A}, \mathbf{H}) \in \Lambda_\mathcal{G}$ if there exists such that the following conditions hold.

(i) For any three-tuple $\{n, d, h\}$ such that $n \neq d$ and $N-1 \geq h > 0$, we have

$$A_f 1_{\substack{s(f)=n, d(f)=d \\ H_f=h}} + \sum_{m:(m,n)\in\mathcal{L}} \hat{\mu}^{\{n,d,h\}}_{\{m,d,h+1\}} = \sum_{i:(n,i)\in\mathcal{L}} \hat{\mu}^{\{i,d,h-1\}}_{\{n,d,h\}}. \quad (1)$$

(ii) If $h < H^{\min}_{n\to d}$, then

$$\hat{\mu}^{\{n,d,h\}}_{\{m,d,h+1\}} = 0 \quad (2)$$

where $H^{\min}_{n\to d}$ is the minimum number of hops from node n to node d.

(iii)

$$\left\{\hat{\mu}_{(m,n)}\right\}_{(m,n)\in\mathcal{L}} \in \mathcal{CH}(\Gamma) \quad (3)$$

where

$$\hat{\mu}_{(m,n)} = \sum_{\substack{d:d\in\mathcal{D} \\ h:N-1\geq h>0}} \hat{\mu}^{\{n,d,h\}}_{\{m,d,h+1\}}$$

and D is the set of all destinations.

a) Condition (i) is the flow-conservation constraint, which states that the number of incoming packets to node n with hop constraint h is equal to the number of outgoing packets from node n with hop constraint h-1. Note that the hop constraint reduces by one after a packet is sent out by node n because it takes one hop to transmit the packet from node n to one of its neighbours .We only consider hop constraints up to N-1 because the longest loop-free path has no more than N-1 hops, and considering only loop-free routes does not change the network throughput region.

b) Condition (ii) states that a packet should not be transmitted from node m to node n if node n cannot deliver the packet within the required number of hops.

c) Condition (iii) is the capacity constraint, which states that the rate-vector $\hat{\boldsymbol{\mu}}$ should be obtainable.

B. Queue Management: We introduce our queue management scheme .Recall $H^{\min}_{m\to d}$ is the minimum number of hops from node m to node d (or the length of the shortest path from node to node).Note that $H^{\min}_{m\to d}$ can be computed in a distributed fashion using algorithms such as the Bellman–Ford algorithm. Thus, we assume that node m knows $H^{\min}_{m\to d}$ for all destinations $d \in \mathcal{D}$, and $H^{\min}_{n\to d}$ for n such that $(m, n) \in \mathcal{L}$.

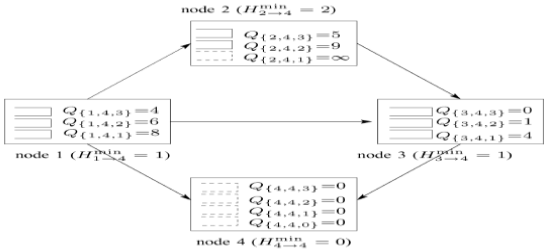

Fig.2.Illustration of queue management and computation of back pressure

We assume node m maintains a separate queue, named queue {m ,d ,h}, for those packets required to be delivered to node d within h hops. For destination d , node m maintains queues for $h = H^{\min}_{m\to d}, \ldots, N-1$, where N-1 is a universal upper bound on the number of hops along loop-free paths. As an example, consider the directed network shown in Fig. 2, and assume that D={4} (i.e., there is only one destination).Each non destination node maintains up to three queues (because for this topology, there are no loop-free paths longer than three hops). Node 1 has queues corresponding to h=1,2,3, respectively. Node 2 does not have a direct path to node 4, hence it maintains only two queues corresponding to h=2,3. Node 3 maintains three separate queues corresponding to h=1, 2, 3, in spite of the observation that there is only one feasible route from node 3 to node 4.We maintain these additional queues because the global network topology is not known by individual nodes. Finally, all queues at the destination for packets meant to itself are set to zero .In Fig. 2, queues into which packets potentially arrive are marked in solid lines, and the "virtual"queues .

C. Queue Dynamics: Let $Q_{\{n,d,h\}}[t]$ denote the queue length at time slot t , and $\mu_{\{m,d,k\}}^{\{n,d,h\}}[t]$ denote the service rate allocated to transmit packets from queue {m ,d, k} to queue{n ,d ,h} over link (m, n) at time t . Since the packets in queue {m ,d ,k} need to be delivered within k hops, they can be only deposited to queues {n ,d, h}. For example, packets from queue {2, 4, 3} can be transferred to queue {3, 4, 2} or queue {3, 4, 1}. Thus, we impose the following constraint on routing: The packets in queue {m ,d, k} can be only transferred to queues {n, d ,h} for $h \leq k-1$, i.e., $\mu_{\{m,d,k\}}^{\{n,d,h\}}[t] = 0 \; for \; all \; h \geq k.$

The dynamics of queue{ n ,d. h} (h≠ d) is as follows:

$$Q_{\{n,d,h\}}[t+1] = Q_{\{n,d,h\}}[t] + A_f[t]1_{s(f)=n,d(f)=d,H_f=h} + \sum_{\substack{k:k-1\geq h \\ m:(m,n)\in\mathcal{L}}} \nu_{\{m,d,k\}}^{\{n,d,h\}}[t] - \sum_{\substack{l:h-1\geq l \\ i:(n,i)\in\mathcal{L}}} \nu_{\{n,d,h\}}^{\{i,d,l\}}[t]$$

Where $\nu_{\{n,d,h\}}^{\{i,d,l\}}[t]$ is the actual number of packets transferred from queue {n ,d ,h} to queue {i ,d, l} and is smaller than $\mu_{\{n,d,h\}}^{\{i,d,l\}}[t]$ when there are not enough packets in queue {n ,d ,h}. Define $u_{\{n,d,h\}}^{\{i,d,l\}}[t]$ to be the unused service. We have

$$\nu_{\{n,d,h\}}^{\{i,d,l\}}[t] = \mu_{\{n,d,h\}}^{\{i,d,l\}}[t] - u_{\{n,d,h\}}^{\{i,d,l\}}[t].$$

We also define $Q_{\{n,n,h\}} = 0$ for all h, i.e., packets delivered are removed from the network immediately.

D. Shortest-Path-Aided Back-Pressure Algorithm: Recall that we have per-hop queues for each destination, which is different from the back-pressure algorithm in [2]. Thus, we first define the back pressure of link (m ,n) under our queue management scheme. We define $P_{\{m,d,k\}}^{\{n,d,h\}}[t]$, the back pressure between queue {m, d, k}and queue {n, d, h} over link (m ,n) , as follows:

- $P_{\{m,d,k\}}^{\{n,a,n\}}[t] = Q_{\{m,d,k\}}[t] - Q_{\{n,d,h\}}[t]$ if $h \leq k-1$ and $h \geq H_{n\to d}^{\min}$;
- $P_{\{m,d,k\}}^{\{n,d,h\}}[t] = -\infty$ otherwise (note that queue $\{n,d,h\}$ does not exist if $H_{n\to d}^{\min} > h$).

The back pressure of link (m ,n) is defined to be

$$P_{(m,n)}[t] = \max\left\{\max_{d\in\mathcal{D},k,h} P_{\{m,d,k\}}^{\{n,d,h\}}[t], 0\right\}$$

that $P_{(1,2)} = 0$, $P_{(1,3)} = Q_{\{1,4,3\}} - Q_{\{3,4,2\}} = 3$, $P_{(1,4)} = Q_{\{1,4,1\}} - Q_{\{4,4,0\}} = 8$, $P_{(2,3)} = Q_{\{2,4,2\}} - Q_{\{3,4,1\}} = 5$, and $P_{(3,4)} = Q_{\{3,4,1\}} - Q_{\{4,4,0\}} = 4$.

Considering the example shown in Fig. 1, it can be verified
Shortest-Path-Aided Back-Pressure Algorithm2
Consider time slot.

Step 0: The packets injected by flow f are deposited into queue $\{s(f), d(f), H_f\}$ maintained at node s(f) .
Step 1: The network first computes $\mu^*[t]$ that solves the following optimization problem:

$$\mu^*[t] = \arg\max_{\mu\in\Gamma} \sum_{(m,n)\in\mathcal{L}} \mu_{(m,n)} P_{(m,n)}[t] \qquad (4)$$

In this algorithm, we allow the packets in queue {m, d ,k} to be transferred to queues {n, d, h} for any h such that h≤ k-1, which is more general than the algorithm proposed in [1], where the packets in queue {m, d, k}can be transmitted only to queue {n , d, k-1] . Where μ is an admissible link-rate vector and $\mu_{(m,n)}$ is the rate over link (m ,n) .

Step 2: Consider link(m, n) . If $\mu^*_{(m,n)}[t] > 0$ and $P_{(m,n)} > 0$, node m selects a pair of queues, say {m, d, k} and {n, d, h}, such that

$$Q_{\{m,d,k\}}[t] - Q_{\{n,d,h\}}[t] = P_{(m,n)}[t]$$

and transfers packets from queue {m, d, k} to queue {n ,d ,h} at rate $\mu^*_{(m,n)}[t]$.

The next theorem shows that the shortest-path-aided backpressure algorithm is throughput-optimal under per-flow hop constraints, and the proof is presented in Appendix A.

Theorem 1: Given traffic A and hop constraint H such that $((1+\epsilon)\mathbf{A}, \mathbf{H}) \in \Lambda_{\mathcal{G}}$ for some $\epsilon > 0$,the network can be stabilized under the shortest-path-aided back-pressure algorithm, and packets delivered are routed over paths that satisfy corresponding hop constraints .

IV. THROUGHPUT-OPTIMAL AND HOP-OPTIMAL ROUTING/SCHEDULING

In Section III, we proposed the shortest-path-aided back-pressure algorithm that is throughput-optimal and supports per-flow hop constraint .In this section, we consider the scenario where no hop constraint is imposed. Recall that N-1 is an upper bound on the number of hops of loop-free paths. Define ℍ such that ℍ[f]=N-1for all f ∈ F . Then, we can assume that a flow is always associated with hop constraint ℍ, i.e., all loop-free paths are allowed. Note that considering only loop-free paths does not change the network throughput region. Thus, we say A is within the network throughput region if $(\mathbf{A}, \bar{\mathbf{H}}) \in \Lambda_{\mathcal{G}}$, which is also written as $\mathbf{A} \in \Lambda_{\mathcal{G}}$.

In this section, we propose an algorithm that is both throughput-optimal and hop-count optimal, i.e., minimizing the average path lengths. Recall that the motivation to develop a hop-optimal algorithm is that such an algorithm will not only minimize the number of transmissions required to support the traffic, but also reduce the average end-to-end transmission delay. (As we will later see from simulations, minimizing hop count does seem to result in smaller end-to-end delays.)

A. Hop Minimization: Given traffic $\mathbf{A} \in \Lambda_{\mathcal{G}}$, we let $\mathcal{S}_{\mathbf{A}}$ denote the set of routing/scheduling policies that stabilize the network .We further define $A_{f,h,\mathcal{P}}[\infty]$ to be the rate at which flow f delivers packets over paths with exactly h hops under policy P , which is well defined when the network can be stabilized. Our objective is to find a policy $\mathcal{P}^*$ such that

$$\mathcal{P}^* = \arg\min_{\mathcal{P}\in\mathcal{S}_{\mathbf{A}}} \sum_{f\in\mathcal{F}} \sum_{N-1\geq h>0} hA_{f,h,\mathcal{P}}[\infty]. \qquad (5)$$

B. Dual Decomposition: To solve optimization problem, we define $\beta_{n,d,h}$ to be the Lagrange multiplier associated with . Then, we can obtain a partial Lagrange dual function as follows:

$$L(\boldsymbol{\beta}) = \min_{\{A_{f,h}\},\hat{\boldsymbol{\mu}}\in\mathcal{CH}(\Gamma)} \Bigg(\sum_{f\in\mathcal{F}, N\geq h>0} hA_{f,h} + \sum_{\{n,d,h\}} \beta_{\{n,d,h\}} \times \left(A_{\text{in}(\{n,d,h\})} + \hat{\mu}_{\text{in}(\{n,d,h\})} - \hat{\mu}_{\text{out}(\{n,d,h\})}\right) \Bigg)$$

where

$$\hat{\mu}_{\text{out}(\{n,d,h\})} = \sum_{i:(n,i)\in\mathcal{L}} \hat{\mu}^{\{i,d,h-1\}}_{\{n,d,h\}}$$

$$\hat{\mu}_{\text{in}(\{n,d,h\})} = \sum_{m:(m,n)\in\mathcal{L}} \hat{\mu}^{\{n,d,h\}}_{\{m,d,h+1\}}$$

and

$$A_{\text{in}(\{n,d,h\})} = \sum_{f\in\mathcal{F}} A_{f,h} 1_{s(f)=n, d(f)=d}.$$

A. Joint Traffic-Splitting and Shortest-Path-Aided Back-Pressure Algorithm: We propose a joint traffic splitting and shortest-path-aided back-pressure algorithm. First, note that

$$\sum_{n,d,h} \beta^*_{n,d,h} \left(\hat{\mu}_{\text{in}(\{n,d,h\})} - \hat{\mu}_{\text{out}(\{n,d,h\})}\right)$$

is linear in terms of $\hat{\boldsymbol{\mu}}$. Thus, we have

$$\max_{\hat{\boldsymbol{\mu}} \in \mathcal{CH}(\Gamma)} \sum_{n,d,h} \beta^*_{n,d,h} \left(\hat{\mu}_{\text{in}(\{n,d,h\})} - \hat{\mu}_{\text{out}(\{n,d,h\})}\right)$$
$$= \max_{\boldsymbol{\mu} \in \Gamma} \sum_{n,d,h} \beta^*_{n,d,h} \left(\mu_{\text{in}(\{n,d,h\})} - \mu_{\text{out}(\{n,d,h\})}\right)$$

Note that the Lagrange multiplier $\beta_{(n,d,h)}$ is related to queue length $Q_{\{n,d,h\}}$, and (7)–(10) are the same as conditions (i)-(iii) defined in Section IV-A, so equality (14) motivates us to use the shortest-path-aided back pressure defined by (4).

V. SIMULATIONS

In this section, we use simulations to study the performance of the proposed joint traffic-splitting and shortest-path-aided back-pressure algorithm .We use the term *the joint algorithm* to refer to the joint traffic-splitting and shortest-path-aided backpressure algorithm. The simulations were implemented using OMNeT++.

A. Simulation Setup: We consider a network with 64 nodes as shown in Fig. 3.The network consists of four clusters, and each cluster is a 4*4 regular grid with two randomly added links .Two neighboring clusters are connected by two links. Here, only two links are used to connect two clusters instead of four or

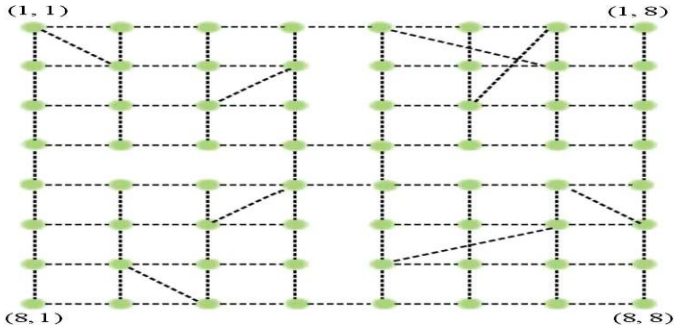

Fig.3. Topology of the network used in the simulations.

more. This is to "force" inter cluster flows to be routed over long paths when the traffic load is high so that the traffic-splitting behavior of the joint algorithm can be easily observed. All links are bidirectional links with capacity one packet/time slot for both directions. All links are assumed to be orthogonalized so they can transmit simultaneously. The propagation delay of a link is assumed to be zero.

TABLE I
FLOWS IN THE NETWORK

Flow ID	(Source, Destination)
1	((1,3), (2,5))
2	((2,3), (2,7))
3	((2,2), (1,6))
4	((3,4), (2,7))
5	((1,1), (1,7))
6	((4,3), (5,4))
7	((4,6), (6,6))
8	((5,3), (5,6))

Eight traffic flows were created in the network, as listed in Table I. Flows 1–5 are inter-cluster flows, and the rest are intra-cluster flows. The packet arrivals of all flows follow Poisson processes. We fixed the arrival rates of intra-cluster flows to be0.2 packets/time slot. All inter-cluster flows have the same arrival rate, denoted by λ (packets/time slot).

B. End-to-End Packet Delays: We also computed the average end-to-end packet delay, averaging over all successfully delivered packets. Similar to the hop count, in Fig.4, we observe that the back pressure performs very poorly when λ is small. This can be attributed to the excessive looping in the route of each packet and can roughly be interpreted as a random walk on the two-dimensional network.

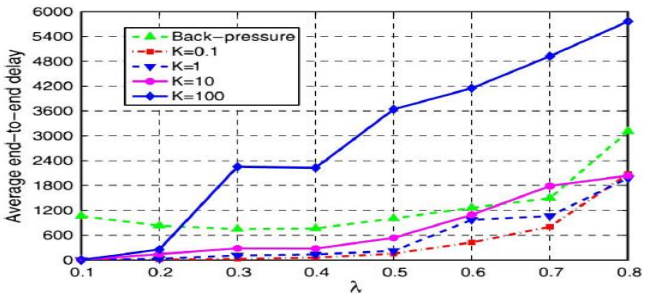

Fig.4. Average end-to-end packet delays under the back-pressure algorithm and the joint algorithm with different K's.

When λ is large, we also observe some improvement of the joint algorithm, with K=0,1,1and10, over the back pressure algorithm. The improvement decreases because the joint algorithm has to exploit long paths in a heavy traffic regime. We further note that the joint algorithm with K=100 performs very poorly in terms of end-to-end packet delay while it has the smallest average hop count. As we have seen in the analysis of Theorem 3, $K \to \infty$ minimizes the average hop count, but results in large queues, hence large end-to-end packet delays.

C .Queue Lengths: Here, we study the total queue length at each node. The average queue length was obtained by averaging over the 100 000 iterations and over all nodes in the network. Fig.5 illustrates the average queue lengths under the joint algorithm with different K's .We observe that the average queue length increases as K increases.

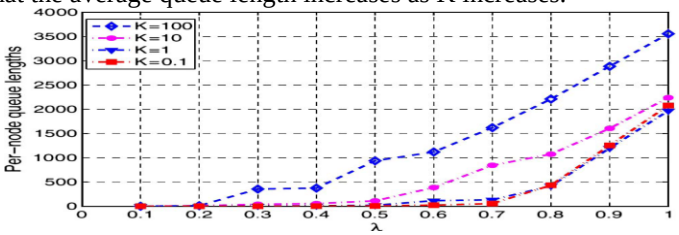

Fig.5. Performance of the joint algorithm with different values of K.

In the simulations, we varied to observe the performance of the back-pressure algorithm and the joint algorithms under different traffic loads. For each, the simulation is executed for 100 000 iterations. When ties occurred in deciding the traffic split or computing the back pressure of a link, we selected the first obtained solution.

D. File Transfer Delay: We also investigated file transfer delays (the duration from the time a file enters the network until it is received at the destination). We compared the back-pressure algorithm with the joint algorithm with K=1. In this simulation, files belonging to the same flow are injected into the source of the flow one by one, and the second file arrives after all packets of the first file are sent out from the source. After a file arrives, the packets of the file are injected into the source node with a constant rate until the complete file is injected.

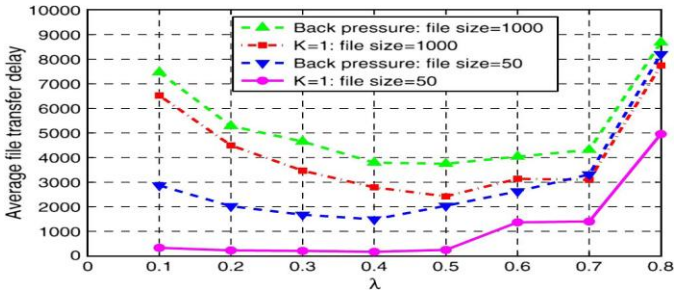

Fig.6. Back-pressure versus the joint algorithm with K=1

Under back-pressure algorithm and the joint algorithm, some packets may be queued in the network for a very long time .We therefore assume the packets of a file are coded using rate less codes so that a file can be completely recovered when 90% of the coded packets are received. Fig. 6 illustrates the file transfer delays of the joint algorithm with K=1 and the back-pressure algorithm. As we can see, when the mean file size is 50, the joint algorithm performs significantly better than the back-pressure algorithm in both light or medium traffic regimes ,but performs similarly to the back-pressure algorithm in the heavy traffic regime. This is because in the heavy traffic regime, the end-to-end packet delays of the two algorithms are similar. When file sizes are large, the two algorithms perform similarly regardless of the traffic load. This is because, for a large-size file, the

dominant component of the file transfer delay is the transmission delay, the number of time slots required to inject all the packets of a file into the network, which is independent of the routing algorithm.

V. CONCLUSION

In this paper, we have proposed new routing/scheduling algorithms that integrate the back-pressure algorithm and shortest path routing. Using simulations, we have demonstrated a significant end-to-end delay performance improvement using the proposed algorithm.

REFERENCES

[1]. L. Ying, S. Shakkottai, and A. Reddy, "On combining shortest-path and back-pressure routing over multihop wireless networks," in *Proc.IEEE INFOCOM*, Rio de Janeiro, Brazil, 2009, pp. 1674–1682.
[2]. L. Tassiulas and A. Ephremides, "Stability properties of constrained queueing systems and scheduling policies for maximum throughput in multihop radio networks," *IEEE Trans. Autom. Control*, vol. 37, no. 12, pp. 1936–1948, Dec. 1992.
[3]. L. Tassiulas and A. Ephremides, "Dynamic server allocation to parallel queues with randomly varying connectivity," *IEEE Trans. Inf. Theory*, vol. 39, no. 2, pp. 466–478, Mar. 1993.
[4]. X. Lin and N. Shroff, "Joint rate control and scheduling in multihop wireless networks," in *Proc. IEEE CDC*, Paradise Island, Bahamas, Dec. 2004, vol. 2, pp. 1484–1489.
[5]. Eryilmaz and R. Srikant, "Fair resource allocation in wireless networks using queue-length-based scheduling and congestion control," in *Proc. IEEE INFOCOM*, 2005, vol. 3, pp. 1794–1803.
[6]. Stolyar, "Maximizing queueing network utility subject to stability: Greedy primal-dual algorithm," *Queue. Syst.*, vol. 50, no. 4, pp. 401–457, Aug. 2005.
[7]. M. Neely, E.Modiano, and C. Li, "Fairness and optimal stochastic control for heterogeneous networks," in *Proc. IEEE INFOCOM*, Miami, FL, Mar. 2005, vol. 3, pp. 1723–1734.
[8]. M. J. Neely, "Optimal backpressure routing for wireless networks with multi-receiver diversity," in *Proc. CISS*, 2006, pp. 18–25.
[9]. Eryilmaz and R. Srikant, "Joint congestion control, routing and MAC for stability and fairness in wireless networks," *IEEE J. Sel. Areas Commun.*, vol. 24, no. 8, pp. 1514–1524, Aug. 2006.
[10]. M. Neely, "Energy optimal control for time-varying wireless networks,"*IEEE Trans. Inf. Theory*, vol. 52, no. 7, pp. 2915–2934, Jul. 2006.
[11]. Yeh and R. Berry, "Throughput optimal control of wireless networks with two-hop cooperative relaying," in *Proc. IEEE ISIT*, Jun. 2007, pp. 351–355.
[12]. Yeh and R. Berry, "Throughput optimal control of cooperative relay networks," *IEEE Trans. Inf. Theory*, vol. 53, no. 10, pp. 3827–3833,Oct. 2007.
[13]. K. Jung and D. Shah, "Low delay scheduling in wireless network," in *Proc. IEEE ISIT*, 2007, pp. 1396–1400.
[14]. L. Ying, R. Srikant, and D. Towsley, "Cluster-based back-pressure routing algorithm," in *Proc. IEEE INFOCOM*, 2008, pp. 484–492.
[15]. X. Lin, N. Shroff, and R. Srikant, "A tutorial on cross-layer optimization in wireless networks," *IEEE J. Sel. Areas Commun.*, vol. 24, no. 8, pp. 1452–1463, Aug. 2006.
[16]. L. Georgiadis, M. J. Neely, and L. Tassiulas, *Resource Allocation and Cross-Layer Control in Wireless Networks*. Hanover, MA: NOW, 2006, Foundations and Trends in Networking.
[17]. M. Andrews, K. Kumaran, K. Ramanan, A. Stolyar, R. Vijayakumar, and P. Whiting, "CDMA data QoS scheduling on the forward link with variable channel conditions," Bell Labs, Tech. Memo, Apr. 2000.
[18]. X. Lin and S. Rasool, "Constant-time distributed scheduling policies for ad hoc wireless networks," in *Proc. IEEE CDC*, 2006, pp. 1258–1263.
[19]. X. Wu and R. Srikant, "Scheduling efficiency of distributed greedy scheduling algorithms in wireless networks," in *Proc. IEEE INFOCOM*, 2006, pp. 1–12.
[20]. Dimakis and J. Walrand, "Sufficient conditions for stability of longest queue first scheduling," *Adv. Appl. Prob.*, pp. 505–521, 2006.
[21]. Eryilmaz, A. Ozdaglar, and E. Modiano, "Polynomial complexity algorithms for full utilization of multi-hop wireless networks," in *Proc. IEEE INFOCOM*, 2007, pp. 499–507.
[22]. Gupta, X. Lin, and R. Srikant, "Low-complexity distributed scheduling algorithms for wireless networks," in *Proc. IEEE INFOCOM*, 2007, pp. 1631–1639.
[23]. S. Sanghavi, L. Bui, and R. Srikant, "Distributed link scheduling with constant overhead," in *Proc. ACM SIGMETRICS*, San Diego, CA, Jun. 2007, pp. 313–324.
[24]. L. Lin, X. Lin, and N. Shroff, "Low-complexity and distributed energy minimization in multi-hop wireless networks," in *Proc. IEEE INFOCOM*, 2007, pp. 1685–1693.
[25]. Joo, X. Lin, and N. B. Shroff, "Understanding the capacity region of the greedy maximal scheduling algorithm in multi-hop wireless networks," in *Proc. IEEE INFOCOM*, Phoenix, AZ, Apr. 2008, pp. 1103–1111.

BIOGRAPHIES

A. Priyadharsini received her B.E degree in Computer Science & Engineering at Sri Lakshmi Ammal Engineering College, Chennai, Tamilnadu, in 2011. Currently, she is studying M.E. Computer Science and Engineering at Arunai College of Engineering, Tiruvannamalai, Tamilnadu. Her project and research area includes networking, wireless communication.
S.Mohanarangan, obtained his M.Tech from Sathyabama university, chennai, Tamilnadu. Currently he is doing his Ph.D in Anna university, chennai, Tamilnadu. He is working as an Associate Professor and Head of the Department of Computer Science and Engineering in Arunai College of Engineering, Tiruvannamalai, Tamilnadu .He is having 14 years of experience in teaching . His research area is networking and communication.

Dr. D. Sivakumar B.E., M.E., Ph.D., M.I.S.T.E., F.I.E.T.E., S.I.A.C.S.I.T completed his under graduation in Electronics and Communication from Madras University and Post graduation in Instrumentation from Annamalai University. He was awarded doctorate under the faculty of information and Communication through Anna University, Chennai.With 17 years of teaching and research experiences in various reputed engineering colleges in and around Chennai in Tamil Nadu, he is presently associated with Arunai College of Engineering, Tiruvannamalai as DEAN (Planning & Execution) and Professor in the Department of ECE. He has guided more than 25 projects for UG and PG students.

International Journal of Modern Engineering Research (IJMER)
www.ijmer.com Vol.3, Issue.3, May-June. 2013 pp-1690-1696 ISSN: 2249-6645

Optimization of Submerged Arc Welding Process Using Six Sigma Tools

Shashank Soni [1]* Ravindra Mohan [2] Dr. Lokesh Bajpai [3] Dr. S. K. Katare [4]
[3] Professor & Head, [4] Professor, [2] Asst. Professor, [1] Student of M-Tech, CIM
Department of Mechanical Engineering, Samrat Ashok Technological Institute Vidisha (M.P)
India. 464001

Abstract: *Many researchers and project managers have attempted to improve project performance by applying new philosophies such as lean principle, just-in-time, pull scheduling, and last planner. However, very little research has been conducted on setting definite quantitative goals for performance improvement while considering the defect rate involved in the submerged arc Welding operations. This research explores practical solutions for welding operations performance improvement by applying the six sigma principle. This principle provides the metrics required to establish performance improvement goals and a methodology for measuring and evaluating improvement. The proposed approach is expected to achieve more reliable workflows by reducing process variability to fit in a desirable range—thereby improving the overall performance through the evaluation of the quality level in current welding operations. To verify the suggested methodology, this case study has been presented and process analyses are performed to observe the performance changes based on the six sigma principle. Critical total quality control, as the sigma level rises, is also discussed.*

Index Terms: *- Total quality management, Six Sigma, DMAIC tool, SPC, Critical total quality.*

I. Introduction

In today's global competition and economic liberalization, quality has become one of the important factors for achieving competitive advantage. A good quality product or service enables an organization to add and retain customers. Poor quality leads to discontented customers, so the costs of poor quality are not just those of immediate waste or rectification but also the loss of future sales. Technological innovations have diffused geographical boundaries resulting in more informed customers. The business environment has become increasingly complex and the marketplace has changed from local to global. Constant pressure is applied on the management to improve competitiveness by lowering operating cost and improving logistic. Customers are becoming increasingly aware of rising standards, having access to wide range of products and services to choose from. There is an ever-increasing demand for quality product and/or services and this global revolution had forced organizations to invest substantial resources in adopting and implementing total quality management strategies. [1]

Total Quality management

TQM is a systems approach to management that aims to enhance value to customer by designing and continually improving organizational processes and systems. It provides a new vision for management leadership. It places customers as principal focal point and redefines quality as customer satisfaction. TQM relies on fact-based decision-making. TQM is a broad-based approach used by world class companies to achieve organizational excellence, the highest weighted category of all the quality and excellence awards. Most of the researchers agree that TQM is a useful philosophy for management if properly planned and. It has been proposed that if TQM is used properly and fully integrated into the business, this approach will help any organization deliver its goals, targets and strategy. [2]

TQM implementation is based on three core elements:

- The TQM philosophy that comprises a set of TQM principles;
- The organizational culture – the present and desired state of culture that will be reached when the TQM philosophy is realized; and
- The implementation strategy – the approach to realizing the philosophy that will specifically include the activities to identify and offset TQM implementation barriers. [2]

Six sigma

Six Sigma is considered as a methodology of implementing TQM. Six Sigma is an innovative approach to continuous process improvement and a TQM methodology. Since quality improvement is the prime ingredient of TQM, adding a Six Sigma program to the company's current business system covers almost all the elements of TQM. Six Sigma has become a much broader umbrella compared to TQM [3].

Six Sigma is new, emerging, approach to quality assurance and quality management with emphasis on continuous quality improvements. The main goal of this approach is reaching level of quality and reliability that will satisfy and even exceed demands and expectations of today's demanding customer [4].

A term Sigma Quality Level is used as an indicator of a process goodness. Lower Sigma quality level means greater possibility of defective products, while, higher Sigma quality level means smaller possibility of defective products within process. Achieving Six Sigma quality level involves leadership, infrastructure, appropriate tools and methods, while quality have to become a part of corporate business plan [4].

The main objective of Six Sigma initiative is to aggressively attack costs of a quality. Overall costs of quality are, usually, divided in tangible and intangible part. The tangible or visible part
of costs of quality, e.g. inspection and warranty costs, scrap, rework and reject, can be approximated with only 10–15 % of overall costs of quality. Remaining 85-90 % of quality costs is usually intangible and, therefore, overlooked and neglected in companies' quality costs analyses.

Tools and methodology within Six Sigma deal with overall costs of quality, both tangible and intangible parts, trying to minimize it, while, in the same time, increasing overall quality level contribute to company business success and profitability [4].

Submerged Arc Welding process

- The Submerged arc welding process (which may be done manually or automatically) creates an arc column between a base metallic electrode and the workpiece.
- The arc, the end of the electrode, and molten weld pool are submerged in a finely divided granulated power that contains appropriate deoxidizers, cleansers and any other fluxing elements.
- The fluxing power is fed from a hopper that is carried on the welding head. The tube from the hopper spreads the power in continue mount in the electrode along the line of weld.
- This flux mound is sufficient depths to submerge completely that are column so that there is no splatter or smoke, and the weld is shielded from all effects at atmospheric gases. As a result of this unique protection, the weld beads are exceptionally smooth.
- The flux adjacent to the arc column melts and floats to the surface of the molten pool; then it solidified to from a slag on the top of the welded metal. The rest of the flux is simply an insulator that can be reclaimed easily.
- The slag that is formed by the molten flux solidifies; the slag will crack off by itself as it cools.
- The unused flux is removed and placed back into the original hopper for use for the next time.
- Granulated flux is a complex, metallic for silicate that can be used over a wide range of metals.

Welds made by the submerged arc welding process have high strength and ductility with low hydrogen or nitrogen content [5].

II. Problem Definition & Methodology

The contact /jaw welding are a continuous production process and during normal production the operators of the welding equipment faced problems with the problems with welded component. The operators experienced lots of scrap page due to variability in the welding strength and requested an immediate attention from the management, initiating the quality study.

This research paper identifies the root causes of failure for a welding process at a manufacturing plants, and purpose to use Operational six sigma methodology to eliminate the problem. In contrast to other methods which measure and identify the non-conformance through destructive testing, a technique is proposed to use a mathematical model, which is later charted using SPC technique. The control chart for mathematical model will identify the failure of the process in real time and will reduced/ eliminate the testing process. The proposed Six Sigma methodology can be applied to eliminate non-conformance in other similar processes.

Operational Six Sigma methodology which is widely used in industries to eradicate these types of problem. Operational Six Sigma was successfully implemented in both the manufacturing and services industries. Many companies in both industries have deployed the process in various activities throughout their organizations. Six sigma is a term used to describe a measure of quality control that is higher than what is provided to be normal. Sigma is a statistical metric that measure variation from an expected outcome. Essentially, the Six means that the process has no more than 3.4 defects per million opportunities.

Six Sigma is a methodology that is intended to reduce process variation to within some specified limit. State that sigma refers to the ability of a process to perform defect-free work. The increase in numerical value that accompanies six sigma suggests that the process is performing better and thus defects are less probable to occur. Consequently, six sigma strives to be a near measure of quality in a process.

Six Sigma aims to reduce variability in a process. Operational Six Sigma follows the DMAIC principle which is the acronym for Define. Measure, Analyze, Improve and Control. The following subsections describe the tasks performed at each step of the welding improvement process, under study.

III. Six Sigma Dmaic Methodology

Dmaic is a closed-loop process that eliminates unproductive steps, often focuses on new measurements, and applied technology for continuous improvement. Implementation of DMAIC Methodology took place in five phases as outlined earlier and established at Motorola. Problem identification and definition takes place in define phase. After identifying main processes, their performance is calculated in measure phase with the help of data collection. Root causes of the problem are found out in analysis phase. Solutions to solve problem and implementing them are in improve phase. Improvement is maintained in control phase.

ROADMAP TO SIX SIGMA

- ***DEFINE****- Set project goals and objectives.*
- ***MEASURE*** *- Measure the defects where they occur.*
- ***ANALYZE*** *- Evaluate data/information for trends, pattern and root causes.*
- ***IMPROVE*** *- Develop, implement and evaluate solution targeted at identified root causes.*
- ***CONTROL*** *- Make sure that almost the problems have cleared, and method is improving.*

I. Section ;Define Phase:-

This phase determines the objectives & the scope of the project, collect information on the process and the customers, and specify the deliverables to customers (internal & external).

Project Title	Optimization of SAW welding process.
Project Start	April to May 2012
Project Location	A large scale manufacturing unit, Surat, Gujarat, India.
Business Case	• Quality control. • Production cost increases. • Reduce the profit margin.
Team Member	Project student- ***Shashank Soni*** & Company employees.
Expert	G. Manager & Sr. Manager. Quality & Industrial Engg. Deptt.

Table (1):- Project Team Charter

Project Plan

- ***Define Phase:-*** 01 April to 10 April-2012
- ***Measure Phase: -*** 11 April to 20 April-2012.
- ***Analyze Phase: -*** 21 April to 30 April-2012.
- ***Improve Phase: -*** 01 May to 10 May-2012.
- ***Control Phase: -*** 11 May to 20 May-2012.

In this phase, the equipment that performs welding also performs several other manufacturing processes. Figure 1 shows the sequences of the manufacturing processes that are performed on welding equipment. A continuous coated strip is stamped, formed; the contacts are welded and trimmed to make the component. The contacts are made of brass. The above sequences of processes are carried out using two sets of assembly; one is located at the front of the equipment and other at the back. Therefore, the corresponding welds are called front and back weld, respectively. The objective of the Six Sigma study is to control and reduce the variability in the welding strength,

Define	*What problem needs to be solved?*
Measure	*What is the capability of the process?*
Analyze	*When and where defects do occurs?*
Improve	*How can process capability be Six Sigma?* *What are the vital factors?*
Control	*What control can be put in place to sustain the again?*

Table (2):- DMAIC Process

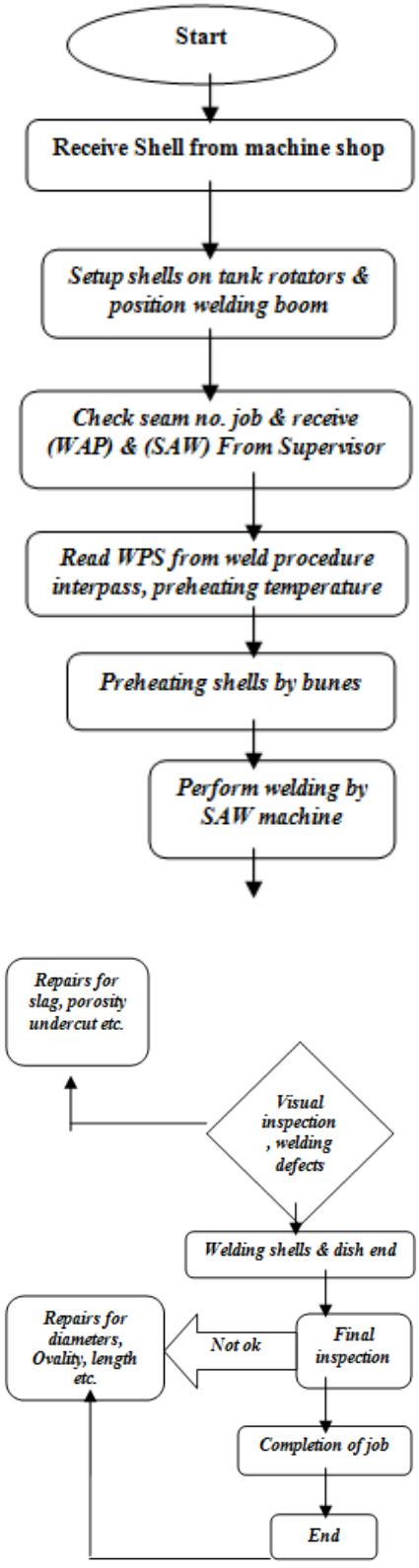

Figure (1):- Sequences of SAW welding process

II. Section; Measure Phase

This phase presents the detailed process mapping, operational definition, data collection chart, evaluation of the existing system, assessment of the current level of process performance etc.

The measure phase actually welding strength is measured in terms of the resistance the joints provide against the shear force. The existing SPC process recommends picking 10 out of 5000 random components that are tested using shear tester. The parts are destroyed using shear force and the destroyed sing shear force and the destruction- point values are plotted on a control chart. Figure 2 illustrates the existing inspection system.

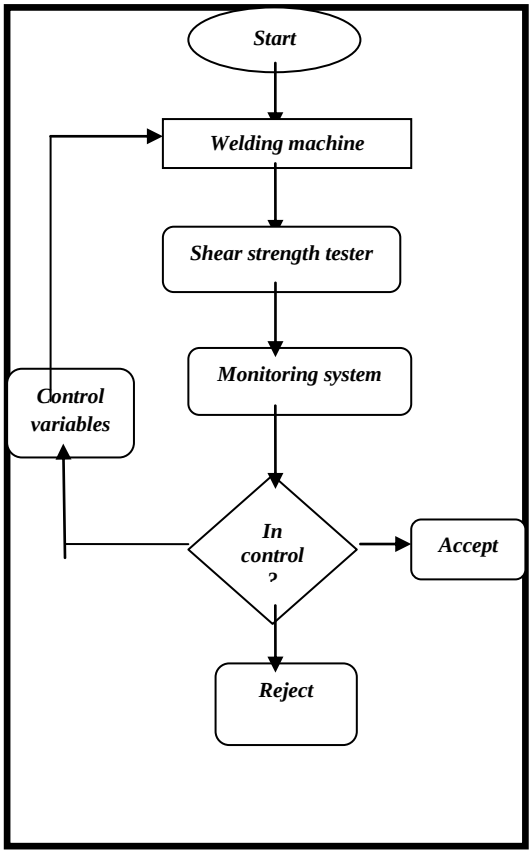

Figure (2):- Exiting testing & inspection system

III. Section (3) Analysis phase:-

The analyze phase is the third step in the DMAIC improvement cycle. The data collected are analyzed and X-bar charts are plotted. The front and back weld are controlled by separate processors; therefore the control charts were plotted separately for the two welds. From the control charts figure 3 & 4, it can be clearly seen that few data points were out of the control limits and the process is out of control.

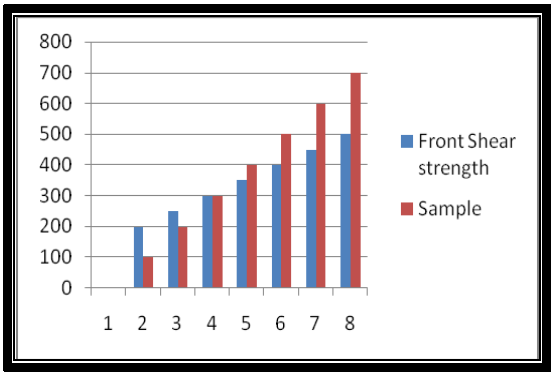

Figure (3):- Front weld X-bar chart

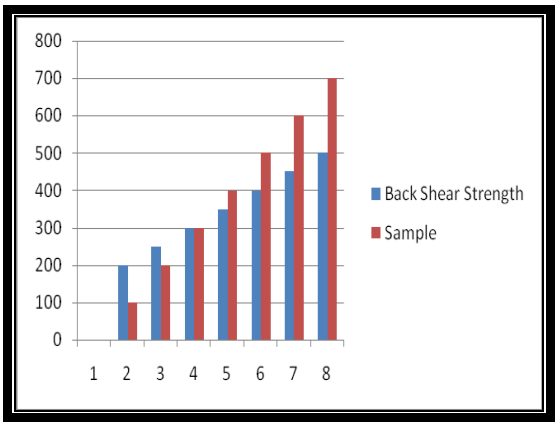

Figure (4):- Back weld X-bar chart

IV. Section: Improve Phase:-

The Improve phase is the fourth step in DMAIC improvement cycle and its aim is to find and implement measures that would solve the problem.

In the improving stage, a new SPC system was proposed to improve the existing system. The disadvantages of the existing system were:

- The occurrence of a defective part lead to scraping the whole batch.
- There was no standard procedure to rectify the problem when it occurs.
- The sample testing procedure is destructive in nature and tested components cannot be used further.

The purpose SPC system uses a real time regression chart instead of an X-bar chart that will resolve the above problem in the existing system. To develop the regression chart a mathematical relationship needs to be established between the welding strength and the parameters influencing it.

As a first step the parameters that influence the welding strength that are shown in the fishbone diagram as shown in figure no.5.

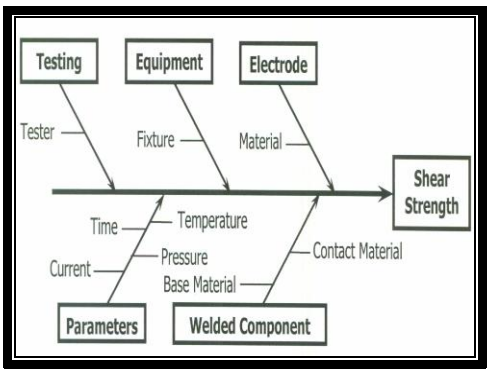

Figure(5) fishbone diagram

In the above fishbone diagram most of the parameters can be assumed to be constant because they experience variation only due to the change causes. Therefore heating time, current and pressure are the only variables that have effect on the shear strength. These three variables with three levels each are in a statistically designed experiment. Table no 3 shows the treatment variables and their levels.

The experiment run will include a full factorial design that is all possible combination of the factors with 4 replicates each.

Table(3) :-variables and levels

	Heating time (Cycles)	Current (k. Amps)	Pressure (PSI)
Low	*120*	*9.6*	*2500*
Mid	*140*	*10.6*	*3000*
High	*160*	*11.0*	*3500*

V. Section: Control Phase:-

The last phase of DMAIC is control, which is the phase in which we ensure that the processes continue to work well, produce desired output results, and maintain quality levels.

The regression function obtained from the experiment runs will yield an equation as follows:

(SS)=A+B*+C*+D*

Where: SS- Shear strength of the welds, A+B*-Heating Time, C*-Current, D*-pressure.

Where A, B, C and D are fitted constants. Using an online data collection system real time monitoring run charts will be plotted for heating time, current, & pressure, individually to monitor the variation in the values. A regression chart will be plotted using the developed mathematical relationship and the shear strength of the welded components can be tweak the controllers with the help of the mathematical relationship during the occurrence of a defective component.

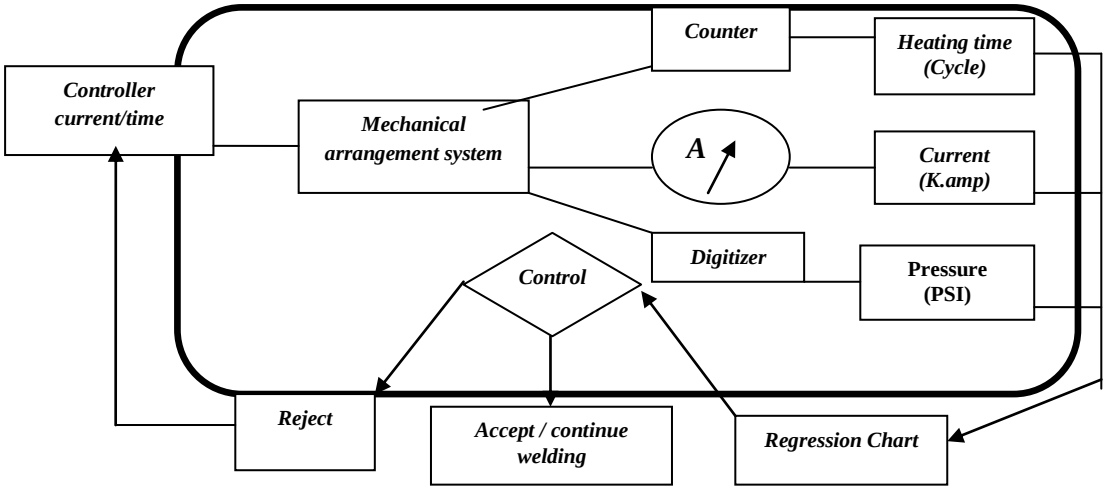

Figure (6):- Real time monitoring system

IV. Result & Conclusion

Operational Six Sigma methodology was selected to solve the variation problem in welding process; the study purposed a real time monitoring system by which the shear strength of the weld can be estimated without destructive testing. Due to 100% inspection, errors made by the selective sampling can be eliminated, reducing the scrapped cost. The implementation of this system will pay for itself in a long run.

Six Sigma was found to be the greatest motivator behind moving everyone in the organization and bringing radical transformation. People in the workplace have developed the required statistical thinking with their involvement in this particular study. Benefits of implementation have been found to be enormous in this case study. However further research is possible in the direction of what the people and organization has to sacrifice for getting this breakthrough in their process. As no gains possible without companying improvement in work habit Six Sigma is continues improvement process involving all operations in the work place and more such opportunities are potentially available in the workplace.

Refrences

[1] Vidhu Shekhar Jha & Himanshu Joshi. "Relevance of Total Quality Management (TQM) or Business Excellence Strategy Implementation for Enterprise Resource Planning (ERP) – A Conceptual Study," international Journal of manufacturing & Industrial Management (2003)1301-1310.
[2] Rallabandi Srinivasu G. Satyanarayana Reddy. "The Contributions of TQM and Six SIGMA in the Organizations to Achieve the Success in Terms of Quality," International Journal of Computer Applications (0975 – 8887) Volume 8– No.4, October 2010.
[3] Anup A.Junankar & P.N Shende(2011). Minimization Of Rework In Belt Industry Using Dmaic; International Journal of Applied Research in Mechanical Engineering, Volume-1, Issue-1, 2011.
[4] M. Soković , D. Pavletić & E. Krulcc.(2006). Six Sigma process improvements in automotive parts production; Journal of Achievements in Materials and Manufacturing Engineering, Vol.19 Issue 1 November2006.
[5] R.K Rajput. "A text book of Manufacturing Technology," Laxmi Publication (p) Ltd, First Edition: 2007, India.
[6] H. Wang, "A Review of Six Sigma Approach: Methodology, Implementation and Future Research", Zhejiang Normal University, Jinhua City, China, pp.1-4
[7] M. Hekmatpanah, M. Sadroddin, S. Shahbaz, "Six Sigma Process and its Impact on the Organizational Productivity", World Academy of Science, Engineering and Technology-43, pp. 365-369, 2008.
[8] Sung H. Park, "Six Sigma for Quality and Productivity Promotion", Published by The Asian Productivity Organization, Hirakawacho, Tokyo, Japan.
[9] M.S. Raisinghani, H. Ette, R. Pierce, G.Cannon, P. Daripaly, "Six Sigma : Concept, Tools and Applications", Industrial Management & Data Systems, Vol. 105, No.4, pp.491-505, 2005
[10] P. Tanuska and T. Skripcak, "Data Driven Scenario Test Generation for Information Systems," International Journal of Computer Theory and Engineering, vol. 3, No. 4, pp. 565-570.
[11] R. Halenar, "Loading data into data warehouse and their testing," Journal of Information Technologies, vol. 2, pp. 7-14, 1999.
[12] Ropp, T. D., Dubikovsky, S., Johnson, M. E., "Using Peer And Team Performance Assessments As Learning Tools On Collaborative Student Projects," *Journal of Aviation/Aerospace Education and Research*, in press.

International Journal of Modern Engineering Research (IJMER)
www.ijmer.com Vol.3, Issue.3, May-June. 2013 pp-1697-1701 ISSN: 2249-6645

Invention of the Plane Geometrical Formulae - Part II

Mr. Satish M. Kaple
Asst. Teacher Mahatma Phule High School, Kherda, Jalgaon (Jamod) - 443402 Dist- Buldana, Maharashtra (India)

Abstract: *In this paper, I have invented the formulae for finding the area of an Isosceles triangle. My finding is based on Pythagoras theorem.*

I. Introduction

A mathematician called Heron invented the formula for finding the area of a triangle, when all the three sides are known. Similarly, when the base and the height are given, then we can find out the area of a triangle. When one angle of a triangle is a right angle, then we can also find out the area of a right angled triangle. Hence forth, We can find out the area of an equilateral triangle by using the formula of an equilateral triangle. These some formulae for finding the areas of a triangles are not exist only but including in educational curriculum also.

But, In educational curriculum. I don't appeared the formula for finding the area of an isosceles triangle with doing teaching – learning process . Hence, I have invented the new formula for finding the area of an isosceles triangle by using Pythagoras theorem.

I used pythagoras theorem with geometrical figures and algebric equations for the invention of the new formula of the area of an isosceles triangle. I Proved it by using geometrical formulae & figures, 20 examples and 20 verifications (proofs).

Here myself is giving you the summary of the research of the plane geometrical formulae- Part II

II. Method

First taking an isosceles triangle ABC

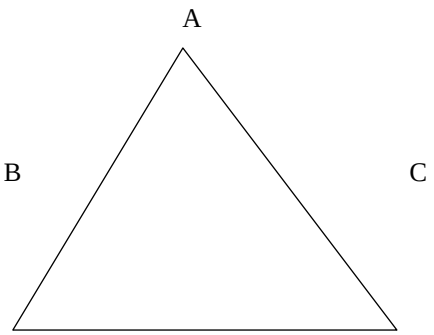

Now taking a, a & b for the lengths of three sides of △ ABC

Draw perpendicular AD on BC.

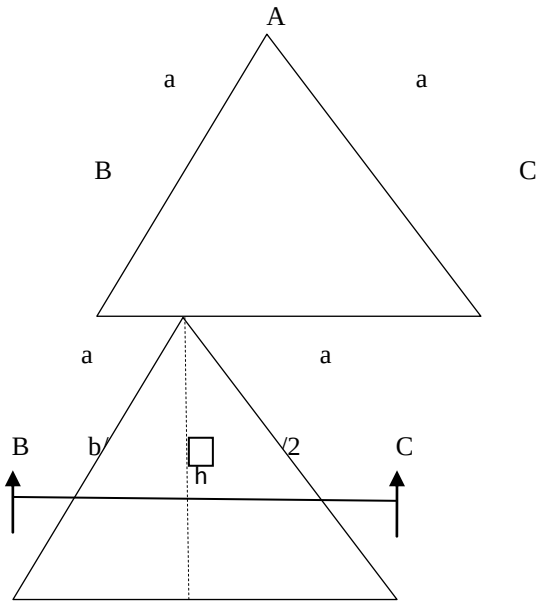

△ABC is an isosceles triangle and it is an acute angle also.

In △ABC,

Let us represent the lengths of the sides of a triangle with the letters a,a,b. Side AB and side AC are congruent side. Third side BC is the base. AD is perpendicular to BC.
Hence, BC is the base and AD is the height.
Here, taking AB=AC = a
Base , BC = b Height, AD = h
In △ ABC, two congruent right angled triangle are also formed by the length of perpendicular AD drawn on the side BC from the vertex A. By the length of perpendicular AD drawn on the side BC, Side BC is divided into two equal parts of segment. Therefore, these two equal segments are seg DB and seg DC. Similarly, two a right angled triangles are also formed, namely, △ ADB and △ADC which are congruent.
Thus,

DB = DC = 1/2 × BC
DB = DC = 1/2 × b = b/2
△ ADB and △ ADC are two congruent right angled triangle.

Taking first right angled △ADC,
In △ADC, Seg AD and Seg DC are both sides forming the right angle. Seg AC is the hypotenuse.

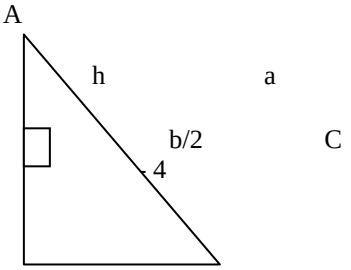

Here, AC =a
Height , AD = h
DC = b/2 and m ∠ ADC = 90^0

According to Pythagoras Theorem,
(hypotenuse) ^{2} = (one side forming the right angle) ^{2} + (second side forming the right angle) ^{2}
In short,
(Hypotenuse) ^{2} = (one side) ^{2} + (second side) ^{2}

$AC^2 = AD^2 + DC^2$
$AD^2 + DC^2 = AC^2$
$h^2 + (b/2)^2 = a^2$
$h^2 = a^2 – (b/2)^2$
$h^2 = a^2 – b^2$
4

$h^2 = a^2 \times 4 – b^2$
4 4
$h^2 = 4a^2 – b^2$
4 4
$h^2 = 4a^2 – b^2$
4

Taking the square root on both side,

$\sqrt{h^2} = \sqrt{\frac{4a^2 – b^2}{4}}$

$\sqrt{h^2} = \sqrt{\frac{1}{4} \times (4a^2 – b^2)}$

$\sqrt{h^2} = \sqrt{\frac{1}{4}} \times \sqrt{4a^2 - b^2}$

The square root of h^2 is h and the square root of ¼ is ½
∴. $h = ½ \times \sqrt{4a^2 – b^2}$
∴. Height, $h = ½ \sqrt{4a^2 – b^2}$
∴. AD =$h = ½ \sqrt{4a^2 – b^2}$
Thus,
Area of △ABC = ½ × Base × Height
= ½ × BC × AD
=½ × b × h
But Height, $h = ½ \sqrt{4a^2 – b^2}$

∴. Area of △ABC = $½ \times b \times ½ \sqrt{4a^2 – b^2}$

$\therefore$ Area of $\triangle ABC = \frac{b}{2} \times \frac{1}{2} \sqrt{4a^2 - b^2}$

$= \frac{b \times 1}{2 \times 2} \times \sqrt{4a^2 - b^2}$

$= \frac{b}{4} \sqrt{4a^2 - b^2}$

$\therefore$ Area of an isosceles $\triangle ABC = \frac{b}{4} \sqrt{4a^2 - b^2}$

For example- Now consider the following examples:-

Ex. (1) If the sides of an isosceles triangle are 10 cm, 10 cm and 16 cm.
Find it's area

$\triangle DEF$ is an isosceles triangle.

In $\triangle DEF$ given alongside,

l (DE) = 10 cm.

l l (DF) = 10 cm. l (EF) = 16 cm

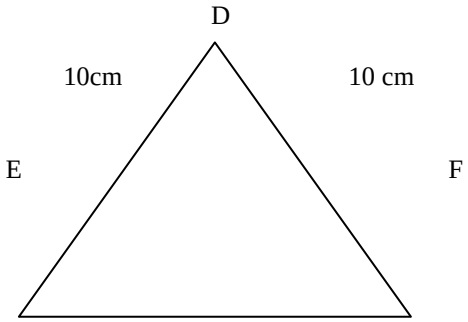

Let,
a = 10 cm
Base, b = 16 cm.
By using The New Formula of an isosceles triangle,
$\therefore$ Area of an isosceles $\triangle DEF$ = A ($\triangle DEF$)

$= \frac{b}{4} \sqrt{4a^2 - b^2}$

$= \frac{16}{4} \times \sqrt{4(10)^2 - (16)^2}$

$= 4 \times \sqrt{4 \times 100 - 256}$

$= 4 \times \sqrt{400 - 256}$

$= 4 \times \sqrt{144}$

The square root of 144 is 12

$= 4 \times 12 = 48$ sq.cm.

$\therefore$ Area of an isosceles $\triangle DEF$ = 48 sq.cm.

Verification :-

☞ Here,

l (DE) = a = 10 cm.

l (EF) = b = 16 cm.

l (DF) = c = 10 cm.

By using the formula of Heron's

Perimeter of $\triangle DEF$ = a + b + c

= 10 + 16 + 10 = 36 cm

Semiperimeter of $\triangle DEF$,

$S = \frac{a + b + c}{2}$

$S = \frac{36}{2}$

S = 18 cm.

$\therefore$Area of an isosceles $\triangle$ DEF $= \sqrt{s(s-a)(s-b)(s-c)}$

$= \sqrt{18 \times (18 - 10) \times (18 - 16) \times (18 - 10)}$

$= \sqrt{18 \times 8 \times 2 \times 8}$

$= \sqrt{(18 \times 2) \times (8 \times 8)}$

$= \sqrt{36 \times 64}$

$= \sqrt{36} \times \sqrt{64}$

The square root of 36 is 6 and the square root of 64 is 8

= 6 × 8 = 48 sq.cm

$\therefore$ Area of $\triangle DEF$ = 48 sq.cm

Ex. (2) In $\triangle GHI$, l (GH) = 5 cm, l (HI) = 6 cm and l (GI) = 5 cm.

Find the area of △ GHI.

☞

△GHI is an isosceles triangle.

In △GHI given alongside,

l (GH) = 5 cm.

l (HI) = 6 cm.

l (GI) = 5 cm

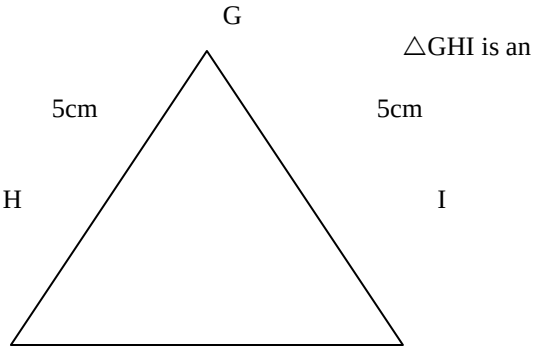

Let,

a = 5 cm

Base, b = 6 cm.

By using The New Formula of area of an isosceles triangle,

∴ Area of an isosceles △GHI = $\frac{b}{4}\sqrt{4a^2 - b^2}$

$= \frac{6}{4} \times \sqrt{4 \times (5)^2 - (6)^2}$

The simplest form of $\frac{6}{4}$ is $\frac{3}{2}$

$= \frac{3}{2} \times \sqrt{(4 \times 25) - 36}$

$= \frac{3}{2} \times \sqrt{100 - 36}$

$= \frac{3}{2} \times \sqrt{64}$

The square root of 64 is 8

$= \frac{3}{2} \times 8 = \frac{3 \times 8}{2} = \frac{24}{2}$

= 12 sq.cm.

∴ Area of an isosceles △GHI = 12 sq.cm.

Verification :-

Here,

l (GH) = a = 5 cm.

l (HI) = b = 6 cm.

l (GI) = c = 5 cm.

By using the formula of Heron's

Perimeter of △GHI = a + b + c

= 5 + 6 + 5

= 16 cm

Semiperimeter of △GHI,

$S = \frac{a + b + c}{2}$

$S = \frac{16}{2}$

S = 8 cm.

∴Area of an isosceles △ GHI = $\sqrt{s(s-a)(s-b)(s-c)}$

$= \sqrt{8 \times (8-5) \times (8-6) \times (8-5)}$

$= \sqrt{8 \times 3 \times 2 \times 3}$

$= \sqrt{(8 \times 2) \times (3 \times 3)}$

$= \sqrt{16 \times 9}$

$= \sqrt{144}$

The square root of 144 is 12

= 12 sq.cm

∴ Area of an isosceles △GHI = 12 sq.cm.

III. Explanation:-

We observe the above solved examples and their verifications, it is seen that the values of solved examples by using the new formula of an isosceles triangle and the values of their verifications are equal.

Hence, The new formula of the area of an isosceles triangle is proved.

Conclusions:-

Area of an isosceles triangle = $\frac{b}{4} \times \sqrt{4a^2 - b^2}$

From the above new formula , we can find out the area of an isosceles triangle. This new formula is useful in educational curriculum, building and bridge construction and department of land records. This new formula is also useful to find the area of an isosceles triangular plots of lands, fields, farms, forests, etc. by drawing their maps.

References:-

[1] Geometry concepts and Pythagoras theorem.

International Journal of Modern Engineering Research (IJMER)
www.ijmer.com Vol. 3, Issue.3, May.-June. 2012 pp-1702-1706 ISSN: 2249-6645

Image Enhancement Using Guided Image Filter and Wavelet Based Edge Detection

DEVI.S[*],JINI CHERIYAN[**]

***Department of electronics and communication engineering,TKM Institute of technology,Karuvelil, Kollam, India.Tel: +919496106841**

**** Department of electronics and communication engineering TKM institute of technology , Karuvelil, Kollam, India. Tel: +919961806239**

Abstract - *This paper proposes a new method for image enhancement by incorporating the concept of guided image filter and wavelet based edge detection. Guided image filter is a spatial domain filter performs the filtering by considering the content of the guidance image, which can be the input image itself or another different image. Guided image filter has no gradient distortion and better performance near the edges. Wavelet based edge detection which is a frequency domain approach is used here for edge detection. It has better performance than any other edge detection methods such as Roberts, sobel operators. This method helps to suppress the noise while preserving the edges. The experimental results prove that the proposed image enhancement method outperforms other methods in both subjective and objective quality, peak-signal-to-noise ratio(PSNR).*

Keywords - *Image enhancement, guided image filter, discrete wavelet transform, wavelet based edge detection, peak signal to noise ratio.*

I. INTRODUCTION

An image [Jonathan Sachs 1996-1999] is synonymous to digital image and is very much essential for daily life applications such as satellite television, medical imaging (magnetic resonance imaging, ultrasound imaging, x-ray imaging), computer tomography etc. It is also essential for the researches in the areas of Science and Technology such as geographical information systems and astronomy. The images collected by different type of sensors are generally contaminated by different types of noises.

Digital images may be contaminated by different sources of noise. Noise may be generated due to imperfect instruments used in image processing, problems with the data acquisition process, and interference, all of which can degrade the data of interest. Furthermore, noise can be introduced by transmission errors and compression also. So image enhancement is a necessary task in image processing.

Image enhancement improves the quality (clarity) [Adithya Goyal et.al. 2012] of images for human viewing. It basically improves the interpretability or perception of information in images for human viewers and providing `better' input for other automated image processing techniques. The principal objective of image enhancement is to modify attributes of an image to make it more suitable for a given task and a specific observer.

During this process, one or more attributes of the image are modified. The choice of attributes and the way they are modified are specific to a given task. Removing blurring and noise, increasing contrast, and revealing details are examples of enhancement operations. For example, an image might be taken of an endothelial cell, which might be of low contrast and somewhat blurred. Reducing the noise and blurring and increasing the contrast range could enhance the image. The original image might, have areas of very high and very low intensity, which mask details. An adaptive enhancement algorithm reveals these details. Adaptive algorithms adjust their operation based on the image information (pixels) being processed. In this case the mean intensity, Contrast and sharpness (amount of blur removal) could be adjusted based on the pixel intensity statistics in various areas of the image. There exist many techniques that can enhance a digital image without spoiling it.

The image enhancement methods can broadly be divided in to the following two categories:

1. Spatial Domain Methods
2. Frequency Domain Method

In spatial domain techniques, we directly deal with the image pixels. The pixel values are manipulated to achieve desired enhancement. In frequency domain methods, the image is first transferred in to frequency domain. It means that, the Fourier Transform of the image is computed first. All the enhancement operations are performed on the Fourier transform of the image and then the Inverse Fourier transform is performed to get the

resultant image. These enhancement operations are performed in order to modify the image brightness, contrast or the distribution of the grey levels. As a consequence the pixel value (intensities) of the output image will be modified according to the transformation function applied on the input values.

This paper proposes a new method which combines the spatial and wavelet domain method for image enhancement. The spatial method used is guided image filter and the wavelet domain method is wavelet based edge detection. Many spatial domain methods include bilateral filter, which having the disadvantage of yielding blurring effect, gradient distortion etc. Guided image filtering performs filtering operation based on the guidance image content. This is a edge preserving, gradient distortion less filter. Wavelet based edge detection method has good visual quality than the conventional edge detectors such as canny, sobel etc.

This paper is organized as follows. In section II, proposed method is discussed. Section III introduces guided image filter. Section IV describes wavelet transform. Section V explains the wavelet based edge detection method. Section V presents the experimental results and discussion while concluding remarks are given in section VI.

II. PROPOSED METHOD

The proposed method is a combination of spatial domain method and wavelet domain method. In this proposed method, the noisy image is passed through guided image filter and some amount of noise gets reduced and the image become blur. Next the edge detection is performed. For that, the guided filter undergoes discrete wavelet transform. Form these coefficients, the edges are detected. Finally, the spatial domain and wavelet domain methods are combined together to form the final denoised output.

III. GUIDED IMAGE FILTER

Guided image filter [Kaiming He et.al.] is an explicit image filter, derived from a local linear model; it generates the filtering output by considering the content of a guidance image, which can be the input image itself or another different image. Guided image filter has a fast and non-approximate linear-time algorithm, whose computational complexity is independent of the filtering kernel size. The guided filter output is locally a linear transform of the guidance image. This filter has the edge-preserving

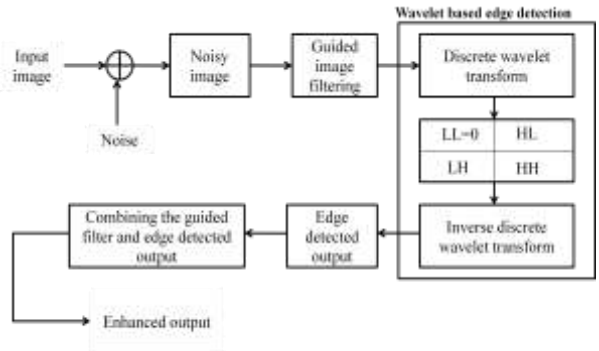

Fig.1. proposed method for image enhancement

smoothing property like the bilateral filter, but does not suffer from the gradient reversal artifacts. Moreover, the guided filter has an O(N) time (in the number of pixels N) exact algorithm for both gray-scale and color images. The guided filter performs very well in terms of both quality and efficiency in a great variety of applications, such as noise reduction, detail smoothing/enhancement, HDR detail smoothing/ enhancement, HDR compression, image matting/feathering and haze removal.

A. Guided filter kernel: We first define a general linear translation- variant filtering process, which involves a guidance image I, an input image p, and output image q. Both I and p are given beforehand according to the application, and they can be identical. The filtering output at a pixel I is expressed as a weighted average:-

$$q_i = \sum_j w_{ij}(p) p_j \qquad (1)$$

Where i and j are pixel indexes. The filter kernel Wij is a function of the guidance image I and independent of p. This filter is linear with respect to p.

The guided filtering kernel W_{ij} is given by:-

$$w_{ij}(p) = \frac{1}{|w|^2} \sum_{k:(ij)\in w_k} (1 + \frac{(I_i - \mu_k)(I_j - \mu_k)}{{\sigma_k}^2 + \varepsilon} \qquad (2)$$

Where I is the guidance image, p is the input image, w_{ij} is the filter kernel is the variance, k_i is the normalizing parameter, w_k is the window centered pixel at pixel k and μ_k is mean of I.

B. Guided filter algorithm: 1. Read the image say I (gray scale image), it acts as a guidance image.
2. Make p=I, where p acts as our filtering image (gray scale image).
3. Enter the values assumed for r and ε, where r is the local window radius and ε is the regularization parameter.
4. Compute the mean of I, p, I*p.
5.The compute the covariance of (I,p) using the formula:-
cov_Ip=mean_Ip -mean_I.*mean_p;
6. Then compute the mean of (I*I) and use it to compute the variance using the formula:-
var_I = mean_II - mean_I .* mean_I
7. Then compute the value of a, b. where a,b are the linear coefficents.
8. Then compute mean of both a and b.
9. Finally obtain the filtered output image q by using the mean of a and b in the formula
q = mean_a .* I + mean_b;

IV. WAVELET TRANSFORM

The wavelet transform [M. Vijay et.al 2012, Amardeep Kaur and Rakesh Singh 2010] always offering great design flexibility while trying to replace standard image processing techniques, wavelet transforms provides an efficient representation of the image by finely tuned to its intrinsic properties. By combining such representations with simple processing techniques in the transform domain, multiresolution analysis can accomplish remarkable performance and efficiency for many image processing problems. Discrete non redundant wavelet analysis techniques. But after the transform plays a major role in image decomposition stage it introduces some artifacts.

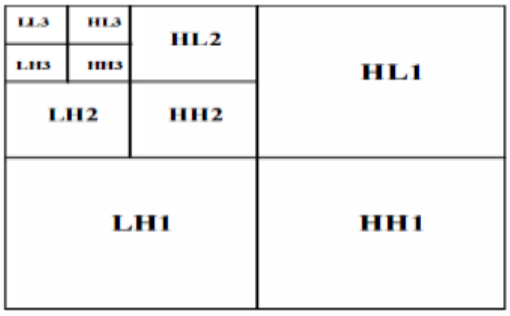

Fig. 2. Image Decomposition (level 3) Using Discrete Wavelet Transform

V. WAVELET BASED EDGE DETECTION

After wavelet decomposition, [D. Sripathi 2003] the horizondal edges of the images are present subband HL subbandof the upper right quadrant. The vertical edges of the image can be similarly identified in the LH subband of the lower left quadrant. To combain this information into a single edge image, simply zero the LL subband of the transform. Then compute the inverse transform and take the absolute value.

VI. RESULTS AND DISCUSSION

Experiments using guided image filter and wavelet based edge detection are conducted on a set of images such as cameraman, peppers, coins, moon, pout, lena and barbara. The images are added with additive white gaussian noise with standard deviation 0.05. The original image is shown in figure 3. Different mages are of different size. So the original image is first resize to [256 256]. Then the original image is added with additive white gaussian noise inorder to generate the noisy image. It is given in figure 4. After the noisy image generation, guided image filter is performed. Figure 5 shows theguided filter output. in guided image filtering, the blurring of the image increases with increase in window size. Next step is wavelet based edge detection. First find the discrete wavelet transform of the image.Then make the lower frequency component as zero. Finally take the inverse wavelet transsform. This is shown in figure 6.Edge detection is also performed using

conventional edge detectores.Unwanted edges are detected using this conventional edge detectors is shown in figure 7. Also it has poor visual quality when it is combined with background information.Finally combines the guided filter and edge detected output. It is shown in figure 8.The proposed algorithm helps to preserve the edges in the images.

Fig. 3. Original image

Fig. 4. Noisy image

Fig. 5. Guided filter output

Fig. 6. Wavelet based edge detected output

Fig. 7. Conventional edge detected output

Fig. 8. Proposed method output

VII. CONCLUSION

In the proposed method, it combines both the spatial domain and wavelet domain method. So the output image is a high quality image. The quality analysis of different images is given in the table 1. From the table, it is clear that the PSNR value of original and noisy image is less than the PSNR value of original enhanced output.

Table 1. Quality analysis of different image

Original image	PSNR of Original and Noisy image	PSNR of Original and enhanced image
Cameraman	19.2021	22.8307
Moon	19.6921	23.2099
Pout	18.9984	23.3161
Peppers	19.1492	23.7844
Lena	19.0770	22.9281
barbara	19.1027	21.5345

REFERENCES

[1]. Adithya Goyal,Akhilesh Bijalwan, Pradeep

[2]. kumar,KUntal, Chowdhury, "Image Enhancement Using Guided Image Filter Technique" International Journal of Engineering and Advanced Technology (IJEAT) ISSN : 2249 – 8958, Volume-1, Issue-5, June 2012.

[3]. Amandeep kaur and Rakesh Singh " Wavelets for Edge Detection in Noisy Images" , National Conference on Computational Instrumentation CSIO Chandigrah, INDIA, 19-20 March 2010.

[4]. D.Sripathi "Discrete Wavelet Transform" , 2003

[5]. Jonathan Sachs "Digital Image Basics" Copyright © Digital Light & Color 1996-1999.

[6]. Kaiming He, Jain Sun and Xiaoou Tang "Guided Image Filtering" Department of Information Engineering, The Chinese University of Hong Kong, Microsoft Research Asia, Shenzhen Institute of Advanced Technology, Chinese Academy of sciences, China.

[7]. Kaiming He, Jain Sun and Xiaoou Tang "Guided Image Filtering" *Journal of Latex Class Files, Vol.X, XXX XXXX.*

[8]. M.Vijay, L.Saranya Devi and M,santhanamari "Image Denoising Based On Adaptive Spatial andWavelet Thresholding Methods" *IEEE international conference on advances in Engineering and Management (ICAESM-2012)* March 30,31.

International Journal of Modern Engineering Research (IJMER)
www.ijmer.com Vol.3, Issue.3, May-June. 2013 pp-1707-1711 ISSN: 2249-6645

Challenges of Wet Briquetting from Locally Available Biomass

Bichitra Bikash[1], Rajib Bhowmik[2], Madhurjya Saikia[3]
[1]*Mehanical Deptt., Assam Down-Town University, Ghy, Assam*
[2]*Mechanical Deptt., Girijananda Chowdhury Inst. Of Management and Technology, Ghy, Assam*
[3]*Mechanical Deptt., Dibrugarh University Inst. Of Engineering and Technolog, Dibrugarh, assam*

ABSTRACT*: This study aims at solving energy crisis in rural area via fuel briquettes from locally available biomasses by a well proven technique called wet briquetting. This technique has different operational stages of briquette production. The challenges faced during each operational stage of briquette production are discussed and solutions of the respective problems are tried to be found as well in order to perfect the method. An economic analysis of this method is also done to show profitability margin.*

Keywords: *Wet briquetting, biomass, briquetting, economic analysis, durability*

I. Introduction

With growing development of Indian economy, energy consumption is increasing day by day. Energy consumption in household shares 40% of total energy consumption all over India. Moreover about 30% of total population resides in the villages which consider a good sum of 0.36 billion of total population. In the domestic household sector cooking is the largest end user accounting for almost 90 percent of the total domestic energy use. The rural masses mostly depend on biomass or kerosene for their energy needs. Gradual price hike in crude oil in international market has greatly affected the rural India. In order to cushion fuel price hike, the rural masses are shifting more to biomass. Deforestation for fuel wood has graven the problem of climate change and global warming. The seriousness of the problem can be sensed by seeing depleting forest reserves. This trend needs to be checked from environment point of view. Development of renewable energy sources helps to reduce the degree of dependence on energy imports as well as it can be a tool for curbing carbon emission. So, emphasis is given to the renewable energy program.

The energy requirement in rural household is mainly for cooking and sometimes heating in colder regions. So there is enormous demand for fuel wood. The one option could be the densification or briquetting to counter this problem. It has a great scope in rural India as India produces large amounts of bio waste material every year. This includes rice straw, wheat straw, coconut shells and fibers, rice husks, stalks of legumes and sawdust. Some of this biomass is just burnt in air; some like rice husk are mostly dumped into huge mountains of waste. Open-field burning has been used traditionally to dispose of crop residues and sanitize agricultural fields against pests and diseases. Instead of burning down these wastes or letting to decompose in open air which raises the problem of GHG production, it can be converted to bio fuels to produce power either by direct combustion or transforming these loose biomass to solid fuels [1, 2]. So these processes become automatic candidates for financing under CDM mode [3].

Biomass briquetting is the densification of loose biomass material to produce compact solid composites of different sizes with the application of pressure [4]. Three different types of densification technologies are currently in use. The first, called pyrolizing technology relies on partial pyrolysis of biomass, which is mixed with binder and then made into briquettes by casting and pressing. The second technology is direct extrusion type, where the biomass is dried and directly compacted with high heat and pressure. The last type is called wet briquetting in which decomposition is used in order to breakdown the fibers. On pressing and drying, briquettes are ready for direct burning or gasification. Some of the advantages of briquettes are given below

1. This is one of the alternative methods to save the consumption and dependency on fuel wood.
2. Densities fuels are easy to handle, transport and store.
3. They are uniform in size and quality.
4. The process helps to solve the residual disposal problem.
5. The process assists the reduction of fuel wood and deforestation.
6. Indoor air pollution is minimized.
7. Briquettes are cheaper than COAL, OIL or LIGNITE
8. There is no sulfur in briquettes.
9. There is no fly ash when burning briquettes.
10. Briquettes have a consistent quality, have high burning efficiency, and are ideally sized for complete combustion.
11. Combustion is more uniform compared to coal.
12. Unlike coal, lignite or oil, briquettes are produced from renewable source of energy, biomass.
13. Loading/unloading and transportation costs are much less and storage requirement is drastically reduced.
14. Briquettes are clean to handle & can be packed in bags for ease of handling & storage.

15. Briquettes are usually produced near the consumption centers and supplies do not depend on erratic transport from long distances.
16. The technology is pollution free and Eco-friendly.
17. The briquette is easy to ignite.
18. Continuous burning and long burning duration.

II. CHALLENGES IN WET BRIQUETTING TECHNOLOGY

The conventional briquetting technologies are capital intensive and unfriendly for smaller scale production. There is a technique called wet briquetting which involves less capital and very low technical machinery which can suit the rural environment for production of briquettes. It is possible to form briquettes from waste crop residues, using a wet process with a hand operated press [5, 6]. First of all suitable biomass is selected. The biomass is decomposed under control environment which is later on pressurized to briquettes. The steps are given below

1) Selection of suitable biomass
2) Decompose biomass
3) Pressurization to form wet briquettes
4) Sun dry wet briquettes

A. Parameters of Selection of biomass

While selecting biomass for wet briquetting, emphasis is given on the local availability of certain type of biomass with lower lignin and ash content. Rice straw, wheat stalks, maize stalks, cotton stalks and barley stalks are some locally available loose biomass or agro residue in rural India. But, the entire available agro residue is not suitable for wet briquetting. For wet briquetting, biomass material is needed to be decomposed before compaction to briquettes. The decomposition period of lignocellulosic biomass depends largely on their lignin content. High lignin containing biomass takes longer time for decomposition. Similarly, biomass having higher ash content is not acceptable for conversion to solid fuel as ash forms clinkers and chances of buildup on the burn pot surfaces, restricting air flow and influencing the removal of ash from the . High ash content also means more frequent dumping of the ash pan. Table 1 shows lignin and ash contents of some locally available agro residues.

Table 1

Lignin and ash contents of some locally available biomasses [7, 8, 9]

Fiber source	Rice straw	Banana fronds	Wheat straw	Barley straw	Maize stalks	Cotton stalks
Lignin (wt %)	9.9	8.0	8.9	13.8	41.0	21.5
Ash (wt %)	17.5	4.7	5.5	10.3	10.2	3.7

B. Parameters governing decomposition of biomass:

Though for other purposes, information on decomposition of lignocellulosic biomass like rice straw is available. Studies on decomposition of brittle rice straw having lower cellulose content revealed that rice straw decomposes fast by anaerobic mechanism when it is incorporated to soil under continuously flooded condition [10]. It is found that at 25ºC under non-flooded conditions, the equivalent of 55% of the rice straw added was mineralized compared to 27% at 58ºC, after 160 days of incubation in soil. Under flooded conditions, the equivalent of 47% of the straw C added was mineralized at 25ºC compared to 19% at 58ºC [11]. The temperature range for optimal decomposition of organic matter is between 52ºC and 60ºCfor aerobic condition [12, 13]. On other hand Acharya et. al., 1935 [14] found that aerobic decomposition of rice straw at about 30ºC is more than that of anaerobic decomposition. He conducted tests in aerobic, anaerobic and water logged condition on rice straw at 30ºC. Among all condition, decomposition was highest in aerobic condition within a period of 6 months. But lignin decomposition was found in higher amount in water logged condition in which biomass specimen was kept one inch below water level. The tests show same trend on use of ammonia.

Decomposition of biomass feedstock can also be enhanced by application of some fungi or bacteria. Hesham et al. 2006 [15] performed tests on rice straw with actinomycetes and observed a weight loss of 61% within a period of 2months.

The high carbon content, high solid content and the low nitrogen content of rice straw require the use of other sources of nitrogen and water to get the proper substrate for the anaerobic digestion process. Nitrogen can be added in inorganic form (ammonia) or in organic form (urea, animal manure or food wastes). Addition of chopped rice straw to dairy manure enhanced the anaerobic digestion process and increased the methane production rate (Hills & Roberts 1981) i.e. more methane means higher carbon mineralization. Somayaji & Khanna et al., 1994 [16] confirmed that addition of chopped rice straw to cattle dung enhanced the organic matter degradation to a high extent (35–51%).

Apart from other biomass, lignocellulosic biomass like rice straw needs some pre-treatment to enhance its degradation. Zhang& Zhang et al., 2006 [17] showed that without thermal pre-treatment, grinding resulted in a significant improvement in terms of solid reduction. Jagdish et al. [18] in his study on wheat straw found that straw size should not increase 1cm. Lower size residue becomes more accessible for the initial microbial attack and led to an enhanced stabilization of microbial biomass.

The impact of temperature is immense and it is widely accepted environmental variable. Finstein and Morris, 1975; Finstein et al., 1986 [19] found that minimum temperature level is necessary for high rates of decomposition. MacGregor et al. (1981) [12] found that optimum composting temperatures, based on maximizing decomposition, were in the range of 52–60ºC for aerobic condition. This evidence has supported by their findings (Bach et al., 1984; McKinley and Vestal, 1984) [13]. On the other hand maximum yield in case of anaerobic condition was found at 25ºC.

Moisture as variable impacts metabolic and physiological activities of micro organism as it serves as medium for transport of dissolved nutrients [20]. Too much moisture is not desirable as it inhibits the decomposition by making the process anaerobic due to water logging (Schulze et al., 1962; Tiquia et al., 1996).Many investigators have found that 50–60% moisture content is suitable for efficient composting[13,19] . Liang et al.2002 [21] found in his study that 50% is the minimal moisture requirement and even higher decomposing rate can be obtained by having 60-70% moisture. By increasing the moisture content higher temperature requirement can be offset.

C. Factors influencing the final briquette quality during pressurization

It is important to understand the factors that govern compacting. Chaney et. al., 2005,[22] said that some principle factors are the design of die, the method of load application, loading rate , maximum pressure applied, the time for which that pressure is maintained and material characteristics, for example particle size and moisture content.

Usually briquetting needs higher amount of pressure for compression. But natural decomposition process can be used to break fibers down and it facilitates bonding [22]. The minimum pressure requirement is about 1Mpa or less.

After compression in a die of a hand press, the briquettes relax and try to come to its original shape. It decides the stability and durability. The stable briquettes have less post die expansion [23] found that the relaxation behavior of briquettes mostly depend on the type of residue. For most types of biomass, maximum rate of relaxation occurred after 10 minutes of removal from die followed by a decreasing relaxation for next 2 hours. Chin et al. [23] propose the following relationship between the relaxed densities and applied die pressure:

$$\rho = a \ln P + b$$

where ρ is the relaxed density, P is the compaction pressure and a, b are empirical constants.

Dwell time during compression is decisive for stability of product. Chin et al., 2004 found that with increase in dwell time, maximum length reduction can be obtained as well as smaller post die relaxation. According to Chaney et al. [22], a hold time greater than 40 seconds does not require rigorous control of this variable can yield briquettes of repeating density.

Particle size of biomass feedstock is crucial for briquetting. Kaliyan and Morey (2006) [24]indicated that generally, the finer the grind, the higher the quality of compact in case of dry briquetting.

Moisture content plays an important role in briquetting of biomass materials. If the moisture content is too high there is a decrease in density and stability. On the other hand, Bellinger et al. [26] showed that energy required to form briquettes is less when there is higher moisture content in the feed stock. Higher moisture in biomass feedstock is desirable for wet briquetting.

Particle size of biomass feedstock is crucial for briquetting. Kaliyan and Morey (2006) [24]indicated that generally, the finer the grind, the higher the quality of compact in case of dry briquetting. In wet briquetting too same trend is followed.

Density of briquettes influences its durability which in turn represents handling characteristics. Durability represents the handling characteristics. Durability for briquettes is measured by following ASAE S269.2 method [25].

According to Saptoadi et al., 2008, briquettes should not be more than 100 g for proper burning [27]. Moreover, a centre hole in briquettes facilitates easier burning of briquettes. Particle size also plays important role in combustion as the voids between particles will be less and less space is available for mass diffusion e.g. water, volatile matter etc [27].

D. Parameters influencing drying of wet briquettes

After the decomposed biomass material are given suitable cylindrical shape with centre hole by a piston press, it should be removed carefully from die and moved aside to dry with minimum handling[25, 28]. It should be ensured that these are placed at a windy place so that briquettes could get even air flow across their whole surface. Fuel briquettes generally take three to six days to dry direct sunlight and in cloudy condition it may increase up to eight to then days.

III. Economic Viability of Wet Briquetting

Before setting up any enterprise, the cost benefit analysis is a must. Then we can forecast the profitability of the enterprise. Sometimes a project even if it looks good may turn out to be fruitless in terms of economic analysis. To be a successful project, it must overcome economic barrier. Therefore, to understand fully the financial feasibility of briquette production, we need to do some preliminary feasibility exercise. The main objective of economic analysis is to compare the cost of briquette production per day per family to cost f fuel wood usage per day per family [28].

Table 1: Parameters for economic analysis

Parameters	Values
Daily wood requirement for a family of 4 members	7
Cost of wood per kg(Taking average), Rs	5
Worker cost per day ,Rs	150
Requirement of worker for the project	6
Maintenance and equipment cost added to worker cost,%	15
Briquettes used per family at an average	12-15

Daily fuel wood cost for the family= Rs 35 per day
Labour cost per day per person=Rs 150
Total labour cost for 6 labors = Rs 900 which will be producing briquettes between 750-1000 briquettes.
Adding 15% for other minor costs, such as equipment and maintenance = Rs 1035.
This is then divided by the 50 families who would be served by this production to arrive at a daily cost of fuel briquettes of Rs 20.7 per day per family.
Therefore, in comparison to the Rs 35 a day for fuel wood, the cost of making fuel briquettes at Rs 20.7 provides a feasible margin for the group to begin briquette production.

Moreover, the cost of production of each briquette can be determined by

$$\text{Cost of briquette} = \frac{6 \times \text{Average Daily Labour cost}}{\text{Average daily Production of 1000 briquettes}}$$

So, in this case the cost of each briquette comes around Rs 0.9. Also it has been noticed from extensive studies an ideal family having 4 to 5 members uses 12-15 briquettes per day. So, total fuel cost of a family is around Rs 18 which is about Rs 17 cheap than that of wood.

IV. Results and Discussions

Wet briquetting depends on the decomposition of biomass materials such as various crop residues. From the above studies we come to opinion that decomposition of finely chopped biomass at anaerobic condition is faster. Moreover, by keeping biomass materials in heap condition at sun will enhance decomposition. However, during compaction of briquettes, wet biomasses need to be kept on pressing at least for 40 seconds and compaction pressure should not be less than 1 Mpa for the purpose to yield good quality briquette. During drying of briquettes, wet briquettes should be placed at windy places so that air circulates around its surfaces. The studies also indicate that briquette should be dried up to 8% moisture content otherwise it will cause severe smoke formation during burning. It has also come to notice that briquettes weighing above 100 gm shows problem during burning and handling. Therefore optimum weight should be less or equal to 100 gm. A cylindrical shaped briquette with a central hole burns at ease .

References

[1.] Campbell C A; Zentner R P; Gameda S; Blomert B; Wall D D (2002). Production of annual crops on the Canadian prairies: trends during 1976–1998. Canadian Journal of Soil Science, 82, pg 45–57.
[2.] Mania S., Tabil L.G. and Sokhansanj S. (2006). Effects of compressive force, particle size and moisture content on mechanical properties of biomass pellets from grasses, Biomass and Bioenergy, Vol 30, pg 648–654. [3] Kishore et al., 2004). Biomass energy technologies for rural infrastructure and village power-opportunities and challenges in the context of global climate change concerns, Energy Policy, Vol 32, pg 801-810.
[3.] Grover P.D. and Mishra S.K. (1994). Development of an appropriate biomass briquetting technology suitable for production and use in developing countries Energy for Sustainable Development, Vol 1.
[4.] Chaney J. O., Clifford M. J., Wilson R. An experimental study of the combustion characteristics of low-density biomass briquettes. Biomass magazine 2010, Vol 1.
[5.] Stanley, R. Fuel Briquettes-Theory and applications from around the world, Legacy Foundation, (2003).
[6.] Stanley, R. Fuel Briquettes-Theory and applications from around the world, Legacy Foundation, (2003).
[7.] Zohar k. And Hadar Y. (1995).Effect of Manganese on Preferential Degradation of Lignin by *Pleurotus ostreatus* during Solid-State Fermentation, Applied And Environmental Microbiology, Vol 65, pg 3057–3062.
[8.] Han Y. W. and Lee J.S. (1975).Chemical Composition and Digestibility of Ryegrass Straw, J. Agric. Food Chem., Vol. 23, pg 931.
[9.] Johnson Sarah, Brar D.S. and Buresh R.J. (2006). Faster anaerobic decomposition of a brittle straw rice mutant: Implications for residue management, Soil Biology & Biochemistry, vol 38, pg 1880–1892.

[10.] Oliver et al., 2000. MNRAS, 316, 749.
[11.] MacGregor, S.T., Miller, F.C., Psarianos, K.M., Finstein, M.S., (1981). Composting process control based on interaction between microbial heat output and temperature. Appl. Environ. Microbiol. 41, 1321-1330.
[12.] McKinley, V.L., Vestal, J.R., Eralp, A.E. 1986. Microbial activity in composting. In: The biocycle guide to in-vessel composting. JG Press Inc., Emmaus, Pennsylvania, pp. 171–181
[13.] Acharya C.N (1933). Studies on the anaerobic decomposition of plant materials, Biochem.J, Vol 29, pg528.
[14.] Hesham et al. 2006. Investigation of optimum conditions of co-composting process by using of sewage sludge and municipally waste, The 1th International and the 4th National Congress on Recycling of Organic Waste in Agriculture, Iran.
[15.] Somayaji, D. & Khanna, S. 1994. Biomethanation of rice and wheat straw. W. J.Microbiol. Biotechnol. 10: 521–523.
[16.] Zhang& Zhang et al., 2006. Efficient conversion of wheat straw wastes into bio hydrogen gas by cow dung compost, Bioresource Technology, Volume 97, Issue 3 Pages 500–505.
[17.] Gabhane, Jagdish., William, S.P.M. Prince., Vaidya, Atul Narayan., Mahapatra, Kalyani.,& Chakrabarti, Tapan., Influence of heating source on the efficacy of lignocellulosic pretreatment – A cellulosic ethanol perspective, Biomass and Bioenergy, 35 (1), 96-102, 2011.
[18.] Finstein M.S., Morris M.L. (1975). Microbiology of municipal solid waste composting. Adv. Appl. Microbiol., 19: 113-151.
[19.] McCartney, D., Tingley, J. (1998). "Development of a rapid moisture content method for compost materials". Compost Sci. 6, 14-25.
[20.] Liang C and McClendon R. W. (2003).The influence of temperature and moisture contents regimes on the aerobic microbial activity of a bio solids composting blend, Bio resource Technology, vol 86, pg 131–137.
[21.] Chaney J. O., Clifford M. J., Wilson R. An experimental study of the combustion characteristics of low-density biomass briquettes. Biomass magazine 2010, Vol 1.
[22.] Chin Ooi and Siddiqui K.M. (2000). Characteristics of some biomass briquettes prepared under modest appliied die pressures, Biomass and Bioenergy, Vol 18, pg 223 to 228.
[23.] Kaliyan N. and Morey R.V. (2008). Factors affecting strength and durability of densified of biomass products, Biomass and Bioenergy, Vol 33, pg 337-359.
[24.] Saikia M and Baruah D. (2013). Analysis of Physical Properties of Biomass Briquettes Prepared by Wet Briquetting Method, International Journal of Engineering Research and Development, Volume 6, Issue 5 (March 2013), PP. 12-14.
[25.] Bellinger, P.L. and H.H.McColly, Energy requirements for forming hay pellets, Journal of Agricultural Engineering, 42, 1961, 244-247.
[26.] Saptoadi, H., 2008. The best biobriquette dimension and its particle size. Asian J. Energy Environ., 9: 161-175.
[27.] Stanley R. (2003).Fuel Briquette making, Legacy Foundation.
[28.] Saikia M, Bhowmik R, Baruah D, Dutta B and Baruah D.C. (2013). Prospect of bioenergy substitution in tea industries of North East India**,** International Journal of Modern Engineering Research (IJMER) Vol.3, Issue.3, May-June. 2013 pp-1272-1278.

International Journal of Modern Engineering Research (IJMER)

www.ijmer.com Vol. 3, Issue. 3, May.-June. 2013 pp-1712-1722 ISSN: 2249-6645

Developing A Die/Mold Through The Phases Of Process Engineering Using Computer Aided Process Planning (Capp)

Mr. Deepak B.Pawar[1], Prof. G.S. Joshi [2], Mr. Swapnil S. Kulkarni [3]

1(M.E. Mech-PDD appearing, D.K.T.E .Ichalkaranji Department of Mechanical, Shivaji University, India)
2(Department of Mechanical engineering, D.K.T.E./Shivaji University, India)
3 (Director, Able Technologies India Pvt. Ltd., Pune, India)

Abstract: *The Die itself needs a well-defined process while being transformed from a stock of material or while it is being assembled with the help of standard components. The varied elements of a die ranging from the standard Die set, the die-block, the punch plate with the punch holder, compression springs and the other elements necessary for assembling the die calls for a make-or-buy decision. While standard parts are preferred to be bought out, the components to be manufactured in-house necessitates an elaborate `Process Plan' for yielding the most economic die with the prescribed specs for quality*
Sheet-metal die is an inseparable constituent of the development process of any given automotive or consumer appliance. In most of the cases, this accounts for a high proportion in the tooling needs of the large size and structural member in any automotive like the chassis and the BIW. Many other brackets and gussets along with peripheral clips etc are invariably made of Sheet-metal due to the strength characteristics complimented by this material and the process of stamping.

Process planning is responsible for the conversion of design data to work instructions through the specification of the process parameters to be used as well as those machines capable of performing these processes in order to convert the piece part from its initial state to final form. The output of the planning includes the specification of machine and tooling to be used, the sequence of operations, machining parameters, and time estimates. Doing all this with computer-aided assistance is called computer-aided process planning (CAPP).CAPP uses computer software to determine how a part is to be made.

Keywords: *Process Plan, Operation Sheet, CAPP, Sheet-metal Die,*

I. Introduction

In general, it is found that the Die (or a Mold) goes through a series of processes which are generally recommended and sequenced at random depending on the availability of the material, machine or the resource. This poses a problem for sequential and timely processing of the Die/ Mold coupled with quality issues. Most of the machining operations are Computerized control including Wire-cut, EDM, VMC machining followed by CMM inspection and so on which has a huge influence over the cost of the Die. As a result, the overall cost of the Die is high

The point to consider here is that even the Die itself needs a well-defined process while being transformed from a stock of material or while it is being assembled with the help of standard components. The varied elements of a die ranging from the standard Die set, the die-block, the punch plate with the punch holder, compression springs and the other elements necessary for assembling the die calls for a make-or-buy decision. While standard parts are preferred to be bought out, the components to be manufactured in-house necessitates an elaborate `Process Plan' for yielding the most economic die with the prescribed specs for quality.

Process planning is responsible for the conversion of design data to work instructions through the specification of the process parameters to be used as well as those machines capable of performing these processes in order to convert the piece part from its initial state to final form. Doing all this with computer-aided assistance is called computer-aided process planning (CAPP).

II. Developing Die through Capp

1.1 Process and Process Engineering- A process is no more than the steps and decisions involved in the way work is accomplished. A process is any orchestrated sequence of activities and associated tasks required to meet goals or objectives. Inputs to the process become outputs. Simply put ,Process engineering is the bridge between Design and manufacturing and it can be brought out by computer aided process planning (CAPP).

1.2 Introduction to CAPP- is a systematic approach to identifying and eliminating time and cost in operations through Process Engineering .During the last several decades, there has been considerable interest in automating the `Process Planning' function by computer systems. An alternative approach to process planning is needed, and Computer Aided Process Planning (CAPP) systems provide this alternative. CAPP plays a bridge between design and manufacturing by translating design specification into manufacturing process detail. Hence, the main focus of this paper is to interpret the basic study of CAPP system for die making process. The output of the planning includes the specification of machine and tooling to be used, the sequence of operations, machining parameters, and time estimates. (CAPP).CAPP uses computer software to determine how a part is to be made. If group technology is used, parts are grouped into part families according to how they

www.ijmer.com Vol. 3, Issue. 3, May.-June. 2013 pp-1712-1722 ISSN: 2249-6645

are to be manufactured. For each part family, a standard process plan is established. Products and their components are designed to perform certain specific functions. Each product has some design specifications which ensure its functionality aspects. The task of manufacturing is to produce components such that they get together the design specifications. The process planning acts as a bridge between design and manufacturing by translating design specifications into manufacturing process in detail. During the various process planning steps in Shape Depositiom Manufacturing[1], the CAD model undergoes a series of geometric operations. In order to withstand the complex geometric operations, a powerful geometric engine should serve as a backbone for the process planner. The process starts with the selection of raw material and ends with the completion of part. Synergy results in when CAM is integrated with CAD to form CAD/CAM systems than a stand alone CAD or CAM systems. In such a system CAPP becomes a direct connection between design and manufacturing.

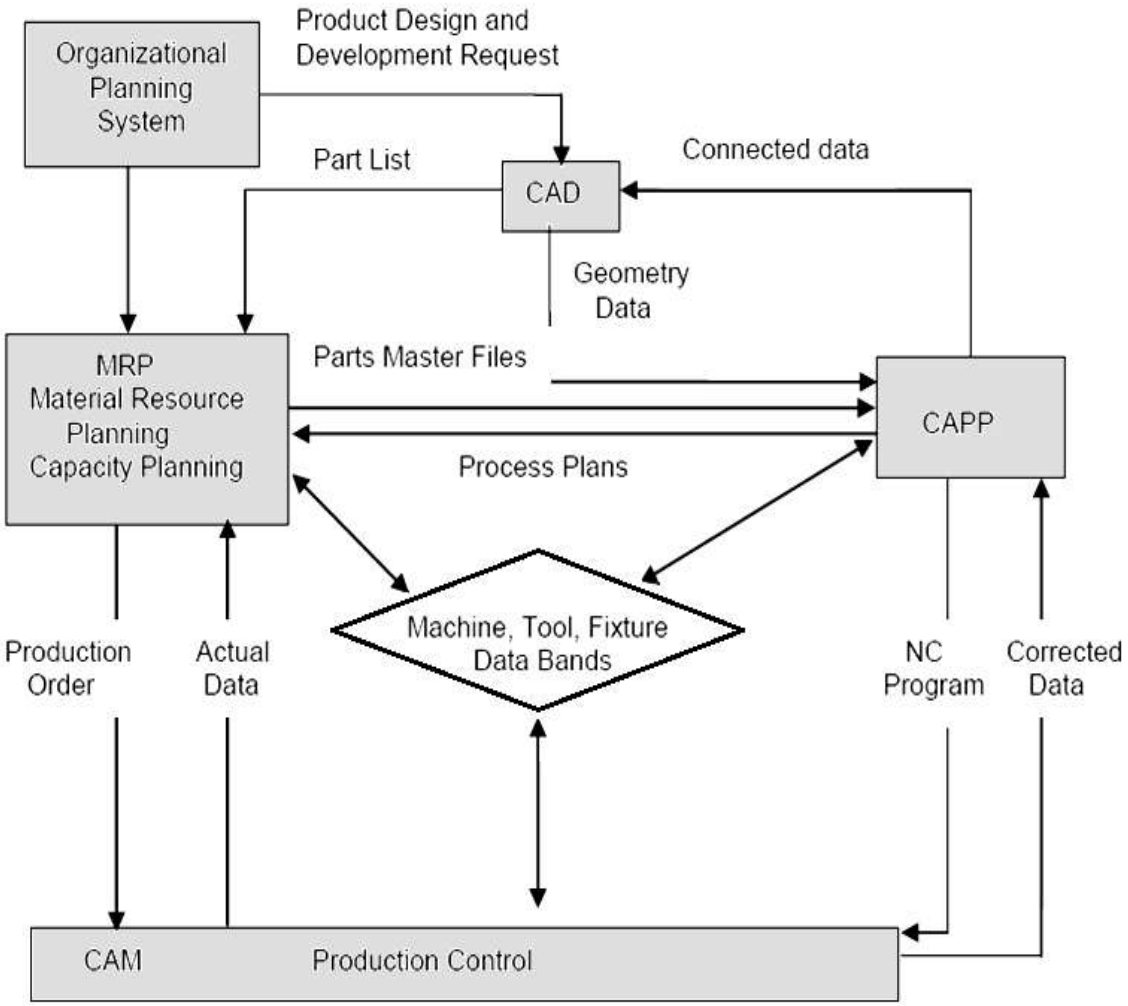

Fig.1- Frame Work Of Process Planning

1.3 CAPP SYSTEMS:

Computer-aided process planning systems are designed around either of two approaches:

1) Retrieval systems and
2) Generative systems

Retrieval CAPP Systems - Also known as variant CAPP systems, based on GT and parts classification and coding, a standard process plan is stored in computer files for each part code number, The standard plans are based on current part routings in use in the factory on an ideal plan prepared for each family. For each new part, the standard plan is edited if modifications are needed

Generative CAPP Systems - Rather than retrieving and editing existing plans from a data base, the process plan is created using systematic procedures that might be applied by a human planner, In a fully generative CAPP system, the process sequence is planned without human assistance and without predefined standard plans, designing a generative CAPP system

www.ijmer.com Vol. 3, Issue. 3, May.-June. 2013 pp-1712-1722 ISSN: 2249-6645

is a problem in expert systems - computer programs capable of solving complex problems that normally require a human with years of education and experience

1.4 IMPORTANT CHARACTERISTICS OF CAPP:

CAPP systems usually serve as link in integrating the CAD and CAM. Though, it is only the partial link due to lack of part feature information provided by existing CAD or drafting system. Part feature information is an essential data for CAPP. In other words, it is a tedious job for CAPP to understand the three dimensional geometry of the designed part from CAD system in terms of their engineering meaning related to assembly and manufacturing. in general, all CAPP planning method and systems suffered from such type of problem and is referred as feature identification in CAPP. Therefore, the main objective feature credit is to bridge the space between the database and automated process planning systems by automatically distinguishing the feature of a part from the geometry and topological data stored in the CAD system. Hence, the features play a vital role in CAPP. In order to identify features and to solve CAD or CAPP interface problem, feature recognition is one of the most efficient technique. Feature recognition transforms a general CAD model into an application specific feature model. evaluated based on the objective functions. The objective of the CAPP problem is to obtain an optimal operation sequence that results in optimizing resources and minimizing production costs as well as processing time.[5]

1.5 BENEFITS OF CAPP:

The use of CAPP systems has the following potential advantages

- Process rationalization and standardization –CAPP leads to more logical and consistent process plans than when traditional process planning is used
- Increased productivity of process planners
- Reduced lead time to prepare process plans
- Improved legibility over manually written route sheets
- CAPP programs can be interfaced with other application programs, such as cost estimating, work standards, and others

1.6 RECENT TRENDS IN CAPP: -

In the global competitive market, various areas such as design process planning, manufacturing and inspection plays a vital role in reducing cost and lead time [14] **.**In the various areas, different kind of interference mechanism has been developed. A lot of difficulty arises while integrating the goal in CIM environment. A CAPP system, depending on the level of sophistication of its capability, may involve automating the interface between design and process planning as well as various process planning tasks.[6] Process Planning tasks such as process sselection, machine tool and cutting tools election, set-up planning, fixture selection, machining parameter selection and so on.

Hence, it is not only desirable but also inevitable to develop a single database technology to address these problems. The major challenges of and research areas are to make CAPP system affordable to the medium and small scale manufacturing industries. Hence a recent trend in CAPP systems includes;

1) Automated translation of the design dimensions.
2) Tolerances into manufacturing dimensions.
3) Tolerances considering process capabilities.
4) Dimensional chains.

1.7 APPROACHES TO PROCESS PLANNING:-

There are basically two approaches to process planning which are as follows :
(i) Manual experience-based process planning, and
(ii) Computer-aided process planning method.
Following difficulties are associated with annual experienced based process planning method:

- It is time consuming and over a period of time, plan developed are not consistent.
- Feasibility of process planning is dependent on many upstream factors (design and availability of machine tools).
- Downstream manufacturing activities such as scheduling and machine tool allocation are also influenced by such process plan [14]..

  Therefore, in order to generate a proper process plan, the process planner must have sufficient knowledge and experience. Hence, it is very difficult to develop the skill of the successful process planner and also a time consuming issue.

1.8 STEPS FOR DEVELOPMENT :-

The following are the activities for this exercise enumerated as steps:

1. Study the complete drawing of the Die and its elements including the material specifications and surface treatment, if any
2. Identify each element as per the bill-of-material (BOM) and assign a make or buy tag

www.ijmer.com Vol. 3, Issue. 3, May.-June. 2013 pp-1712-1722 ISSN: 2249-6645

3. While the materials with the `buy' tag could be procured from competent sources, the materials with the `make' tag should be listed out separately for including in the Process Engineering plan
4. Study the design intent of each element or part and assign appropriate tooling faces for resting, location, orientation and clamping
5. If additional fixtures or non-standard gauges are required, make a list of the same along with a Picture sheet for the operation
6. Allocate the appropriate machine/s for each element during its machining cycle
7. Specify the process of sub-assembly followed by the main assembly
8. Identify critical dimensions/ specs to be measured at each stage for ensuring functionality and smooth assembly
9. Discuss the inspection dimensions for the completed Die in conjunction with the Die Designer
10. Organize the trials and document the results for further improvement in the Die

1.9 CAPP SYSTEM FOR DIE DEVELOPMENT:-

This system was constructed on the basis of the know-how of industrial field engineers. By interviewing them, the production rules of the CAPP system are generated and developed. The cross-section of the product body, drawing coefficient, punch radius (Rp), and die radius (Rd) are considered as the main design parameters. The input data of the system is only the final product geometry of which modeling is performed on AutoCAD software along the major and minor axes of the product. The system is typically composed of recognition of shape, 3-D modeling to calculate the surface area, blank design and process planning modules. It means that we have to return first to rework the die construction by changing the critical die parameters (e.g. die radii, drawing gap, etc.). If it does not solve the problem, a new die design, or a new process planning is required. [2].The scope for this project work, although, is limited to generation of Process Plan aligning with its cross-functional departments.

III. INDENTATIONS AND EQUATIONS

Cutting speed (also called surface speed or simply speed) is the speed difference (relative velocity) between the cutting tool and the surface of the workpiece it is operating on. It is expressed in units of distance along the workpiece surface per unit of time, typically surface feet per minute (sfm) or meters perminute (m/min). Feed rate is the relative velocity at which the cutter is advanced along the workpiece; its vector is perpendicular to the vector of cutting speed. Feed rate units depend on the motion of the tool and workpiece; when the workpiece rotates (*e.g.*, in turning and boring), the units are almost always distance per spindle revolution (inches per revolution [in/rev or ipr] or millimeters per revolution [mm/rev]). When the workpiece does not rotate (*e.g.*, in milling), the units are typically distance per time (inches per minute [in/min or ipm] or millimeters per minute [mm/min]), although distance per revolution or per cutter tooth are also sometimes used.

Cutting Speeds For Various Materials Using A Plain High Speed Steel Cutter

Material Type	Meters Per Min (MPM)	Surface Feet Per Min (SFM)
Steel (Tough)	15–18	50–60
Mild Steel	30–38	100–125
Cast Iron (Medium)	18–24	60–80
Alloy Steels (1320–9262)	20-37	65–120
Carbon Steels (C1008-C1095)	21-40	70–130
Free Cutting Steels (B1111-B1113 & C1108-C1213)	35-69	115–225
Stainless Steels (300 & 400 Series)	23-40	75–130
Bronzes	24–45	80–150
Leaded Steel (Leadloy 12L14)	91	300
Aluminium	75–105	250–350
Brass	90-210	300-700 (Max. Spindle Speed)

Table No.1- Cutting Speeds For High Speed Steel

Approximate Material Cutting Speeds and Lathe Feed Per Revolution
Calculating RPM and Feed Rates

Sr. No.	Material	Ballpark CS with HSS Tool	Cutting Speed HSS Tool	Cutting Speed Carbide Tool	Feed/Rev HSS Tool Lathe	Feed/Rev Carbide Tool Lathe
1	SAE 1020-Low Carbon Steel	100	80-120	300-40	0.002-0.020	0.006-0.035
2	SAE 1050-Ligh	60	60-100	200	0.002-0.005	0.006-0.030

www.ijmer.com Vol. 3, Issue. 3, May.-June. 2013 pp-1712-1722 ISSN: 2249-6645

	Carbon Steel					
3	Stainless Steel Aluminum	100	100-120	240-300	0.002-0.005	0.003-0.006
4	Brass And Bronze	200	110-300	600-1000	0.003-0.025	0.008-0.040
5	Plastic	500	500	1000	0.005-0.50	0.005-0.05

Table No.2- Approximate Material Cutting Speeds and Lathe Feed Per Revolution Calculating RPM and Feed Rates

*Variation in Cutting-Speed & Feed-per-Revolution will exist with different alloys, procedures, tools & desired finishes. Feed-Per-Revolution is also affected by the size of the lathe-tool, as well as the depth of cut. The cutting speed and speed of plastics will vary greatly depending upon the type of plastic.

Table No.2 Approximate Material Cutting Speeds and Lathe Feed Per Revolution Calculating RPM and Feed Rates

Accuracy

However, for more accurate calculations, and at the expense of simplicity, this formula can be used:

$$RPM = \frac{Speed}{Circumference} = \frac{Speed}{\pi \times Diameter}.$$

$$= \frac{1000X20(mm/min)}{\pi X100mm}$$

RPM = 200

*Variation in Cutting-Speed & Feed-per-Revolution will exist with different alloys, procedures, tools & desired finishes. Feed-Per-Revolution is also affected by the size of the lathe-tool, as well as the depth of cut. The cutting speed and speed of plastics will vary greatly depending upon the type of plastic.

Calculations:-

Feed Rate = fm (mm/min)
m = f × n
m = feed rate (mm/min) or MPM
f = feed (mm/rev)
n = rpm
the rate of tool travel through the work piece per unit of time, generally expressed in mm per revolution (turning)
f = 0.010 (mm/rev)
n = 200 rpm
m=0.010X200
m=2 (mm/min)

Drilling Speeds and Feeds :-

The speed of a drill is usually measured in terms of the rate at which the outside or periphery of the tool moves in relation to the work being drilled. The common term for this velocity is surface feet per minute", abbreviated as sfm. Every tool manufacturer has a recommended table of sfm values for their tools. General sfm guidelines are commonly found in resources such as the Machinery Handbook (see Table 1 in this document).

The peripheral and rotational velocities of the tool are related as shown in the following equation:

$$V = \pi * D * N \quad \text{(Eq. 1)}$$

where ,
V is the recommended peripheral velocity for the tool being used
D is the diameter of the tool
N is the rotational velocity of the tool
Since the peripheral velocity is commonly expressed in units of feet/min and tool diameter is typically measured in units of inches, Equation 1 can be solved for the spindle or tool velocity, N in the following manner:

$$N\ [rpm] = 12\ [in/ft] * V\ [sfm] / (\pi * D\ [in/rev]) \quad \text{(Eq. 2)}$$

Equation 2 will provide a guideline as to the maximum speed when drilling standard materials. The optimum speed for a particular setup is affected by many factors, including the following:

- Composition, hardness & thermal conductivity (k) of material
- Depth of hole
- Efficiency of cutting fluid

www.ijmer.com Vol. 3, Issue. 3, May.-June. 2013 pp-1712-1722 ISSN: 2249-6645

• Type, condition and stiffness of drilling machine
• Stiffness of workpiece, fixture and tooling (shorter is better)
• Quality of holes desired
• Life of tool before regrind or replacement

Table 2 contains recommended feeds for various drill diameters. For each diameter range there is a corresponding feed range. Use the smaller values for stiffer/harder/stronger materials and the larger values for softer materials. To calculate the feed rate, use the following formula:

f = N * fr

where
f = feed rate [mm/min]
N = spindle speed [rpm]
fr = feed per revolution [mm/rev]

SR .No.	Material	Recommended Speed(Surface ft/min)
1	Aluminum And Its alloys	250
2	Bronze(High Tensile)	100
3	Cast Iron(Soft)	100
4	Cast Iron(Medium Hard)	80
5	Cast Iron(Hard chilled)	20
6	Hastelloy	20
7	Inconel	25
8	Magnesium and its alloys	300
9	Monel	25
10	High nickel steel	50
11	Mild Steel(.2-.3 C)	100
12	Steel (.4-.5C)	60
13	Tool Steel	40
14	Forgings	40
15	Steel alloys(300-400 Brinell)	30
16	Heated Steels 35-40Rockwell	
	35-40 Rockwell C	20
	40-45 Rockwell C	20
	45-50 Rockwell C	15
	50-55 Rockwell C	15
17	Stainless Steel free machining	40
18	Stainless work hardened	20
19	Titanium alloys	20

Table No.3-HSS speeds for common materials [13]

Sr.No.	Drill Diameter [in]	Recommended Feed,fr [in/rev]
1	under 1/8 "	up to 0.002
2	1/8" to 1/4"	0.002 to 0.004
3	1/4" to 1/2"	0.004 to 0.008
4	1/2" to 1"	0.008 to 0.012
5	1" and over	0.012 to 0.020

Table No.4 HSS feed [13]

Drilling Uddeholm Corrax

Drilling		Drill diameter (mm)				
		1 - 5	5 - 10	10 - 20	20 - 30	30 - 40
Uncoated HSS [1-2]	Cutting speed, v_c (m/min)	13-15				
	Feed, f (mm/rev)	0,05-0,10	0,10-0,20	0,20-0,30	0,30-0,35	0,35-0,40
Coated HSS [1-2]	Cutting speed, v_c (m/min)	13-15				
	Feed, f (mm/rev)	0,05-0,10	0,10-0,20	0,20-0,30	0,30-0,35	0,35-0,40
Indexable insert [3-4]	Cutting speed, v_c (m/min)				180-200	
(cem. carbide inserts)	Feed, f (mm/rev)				0,03-0,08	0,08-0,12
Solid cemented	Cutting speed, v_c (m/min)		100-130			
carbide [5-7]	Feed, f (mm/rev)		0,08-0,10	0,10-0,20	0,20-0,30	0,30-0,35
Brazed cemented	Cutting speed, v_c (m/min)			50-70		
carbide [5-7]	Feed, f (mm/rev)			0,15-0,25	0,25-0,35	0,35-0,40

Table No.5- Cutting Parameters for HSS drill [13]

www.ijmer.com Vol. 3, Issue. 3, May.-June. 2013 pp-1712-1722 ISSN: 2249-6645

Calculations:-

$V = \pi * D * N/1000$

$N = V *1000/\pi * D$

$= 13000/ \pi * 9$

N = 460(RPM)

Also,

f (mm/min) = N * fr (mm/rev)

= 460*0.10

f = 46(mm/min)

Surface Grinding:-

Grinding is a material removal process in which abrasive particles are contained in a bonded grinding wheel that operates at very high surface speeds. The grinding wheel is usually disk shaped and is precisely balanced for high roational speeds. Cutting conditions in grinding The geometry of grinding is shown in the figure:

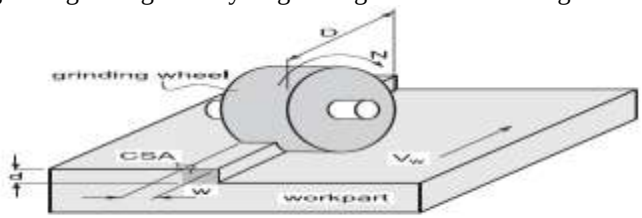

Fig.2 -The Geometry Of Surface Grinding Showing The Cutting Conditions

The geometry of surface grinding showing the cutting conditions.The cutting velocity V in grinding is very high. It is related to the rotational speed of the wheel by

$V = \pi DN$

where D is the wheel diameter, and N is the rotational speed of the grinding wheel.Depth of cut d is called infeed and is defined as the distance between the machined and work surfaces. As the operation proceeds, the grinding wheel is fed laterally across the work surface on each pass by the workpart. The distance at which the wheel is fed is z.

V. FIGURES AND TABLES

WITH THE INPUTS GATHERED DURING COLLECTION PHASE, THE ANALYSIS IS DOCUMENTED AS PER THE PROCESS SHEET BELOW.

PROCESS SHEET

Name of tool-Form /Deep Die
Name of the component -Die Block
Drawing No - ***AT0101***
Material - 20MnCr5 (Case-hardness HRC 58-62)
Qty - 1***no***

Op^{n} No.	Operation Name	Machine Name/ No.	Instrument/ Fixture/ Gauge	Description of operation	Estimated time for setting and machining
10	Milling Rough & Finishing	milling machine	Vernier Caliper - upto 200mm	Hold the blank in vice Clean out the face Finish Face (Name) to size(....+0.5)	8hrs.(Each for 6 faces)
20	Drilling Tapping	Radial Drilling machine	Drill bit(HSS or Carbide) Tap -size M8	Drill hole size ϕ6.8 thru's on P.C.D.Equispaced Tap to depth 15mm	Drilling -1 hr Tapping -1.5hr
30	Surface Grinding Top Face Bottom Face	 Surface grinding m/c cylindrical grinding m/c	 micrometer-50-100 micrometer-50-100	Rest face F,Grind G for clean finish Hold ϕ A and Finish B/C to Size Set speed for grinding = 2300 (rpm) Set depth of cut = 0.003 to 0.005 mm	 1 hr 1.5 hr
40	Heat Treatment	Induction Furnace	Hardness Tester (HRC)	Pack carburize using carbon rich material at about 800°C Case Harden in the furnace at a temperature of 580 to 920°C Make identation using approprite steel ball (indenter) to confirm	4 hr 16 hr 0.5 hr
50	VMC Machining center	V.M.C.(BFW-60)	Bull-nose Cutter Size-10mm Side Face Cutter Size-6mm CMM/Robo-Arm	Run the machining program no - CAM021 Run The CMM Programe No-CMM021	3 hr 1hr

Table No.6 - Process sheet for Die Block

Table No 7- Process sheet for Punch

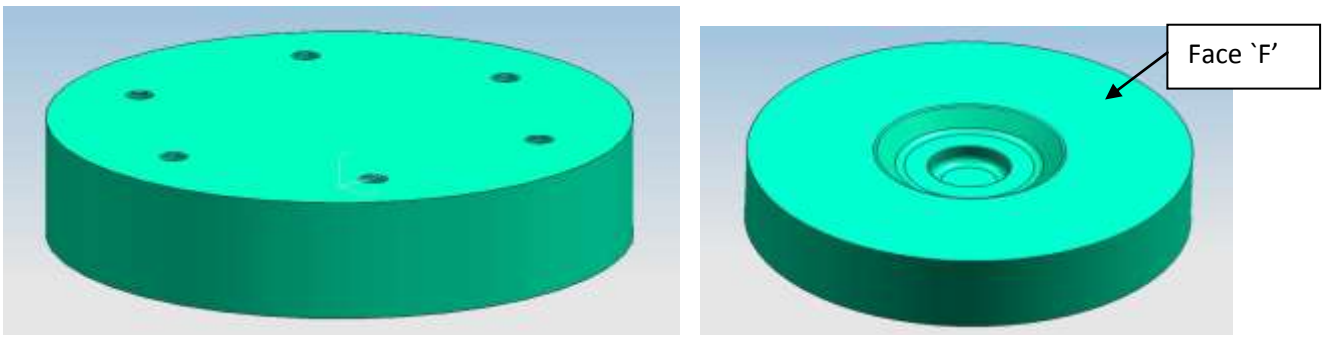

DIE BLOCK (TWO VIEWS)

DIE BLOCK (2D DRAWING)

Fig.3- 2D drawing and 3D representation for Die Block

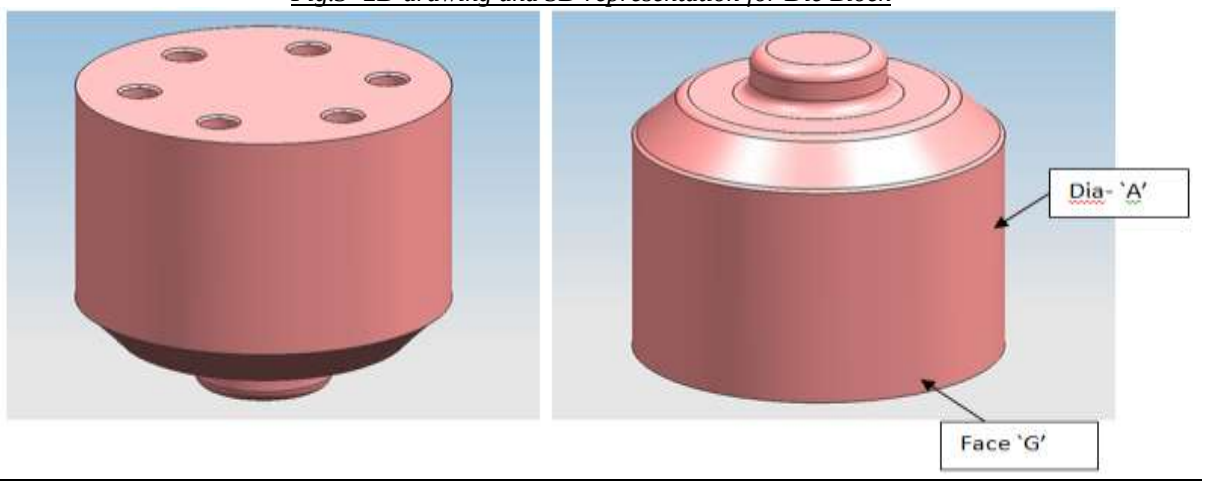

www.ijmer.com Vol. 3, Issue. 3, May.-June. 2013 pp-1712-1722 ISSN: 2249-6645

PUNCH (TWO VIEWS OF THE 3D MODEL)

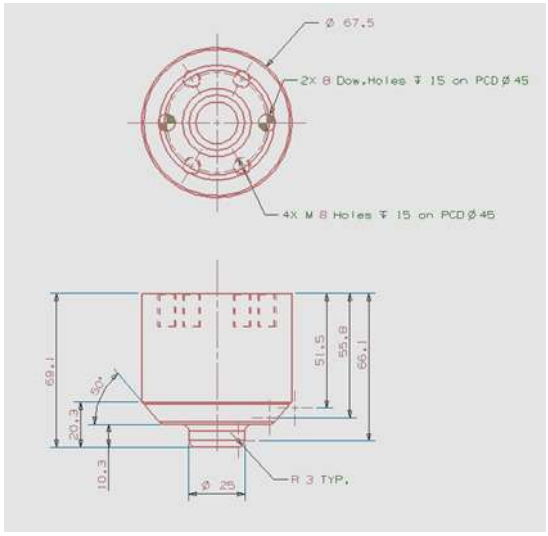

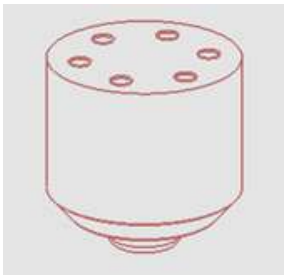

Dimn- `D'

PUNCH (2D DRAWING)

Fig.4- 2D drawing and 3D representation for Punch

Time required for release of the Die

Type of Die → / Type of Process to be used ↓	Type A	Type B	Type C	Type D
Current process (hrs)	80-120	50-80	25-50	Upto 25
(Average)	100	65	37.5	12.5
Proposed process (hrs)	60-95	40-65	20-40	Upto 20
(Average)	72.5	52.5	30	10

Time saved with the implementation of the new process = 23.25%

Table No 8: Results (1): % Time Saved

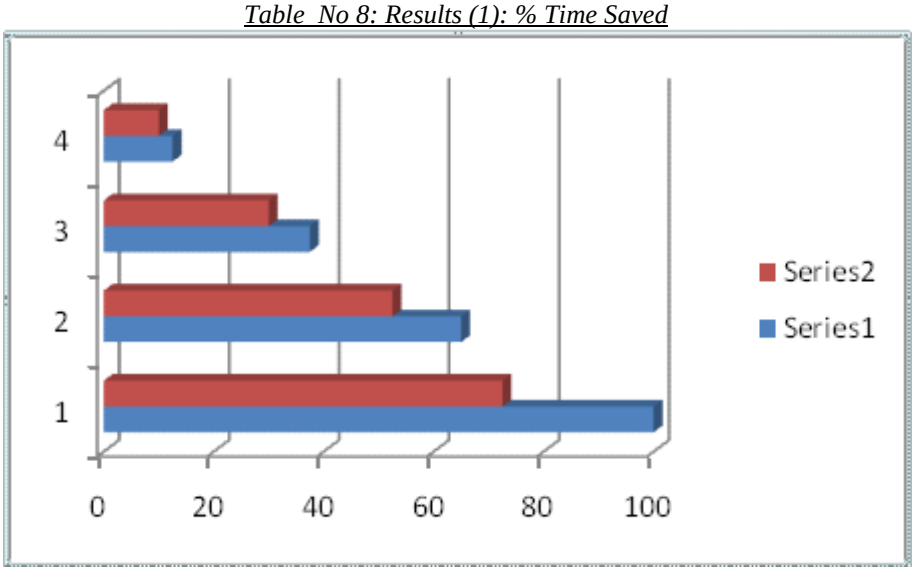

GraphNo.1- Graph of Comparison between CSM and FSM for average of Current process (hrs)Vs. Proposed process (hrs)

www.ijmer.com Vol. 3, Issue. 3, May.-June. 2013 pp-1712-1722 ISSN: 2249-6645

Number of Errors identified during development phase

Type of Die → / Type of Process to be used ↓	Type A	Type B	Type C	Type D
Current process (no. of errors)	15-20	10-12	7-10	2-5
(Average)	17.5	11	8.5	3.5
Proposed process (no. of errors)	10-12	6-8	3-4	1-2
(Average)	11	7	3.5	1.5

Percentage reduction in the number of errors = 43.21%

Table No. 9 - Results (2): % Reduction in Errors

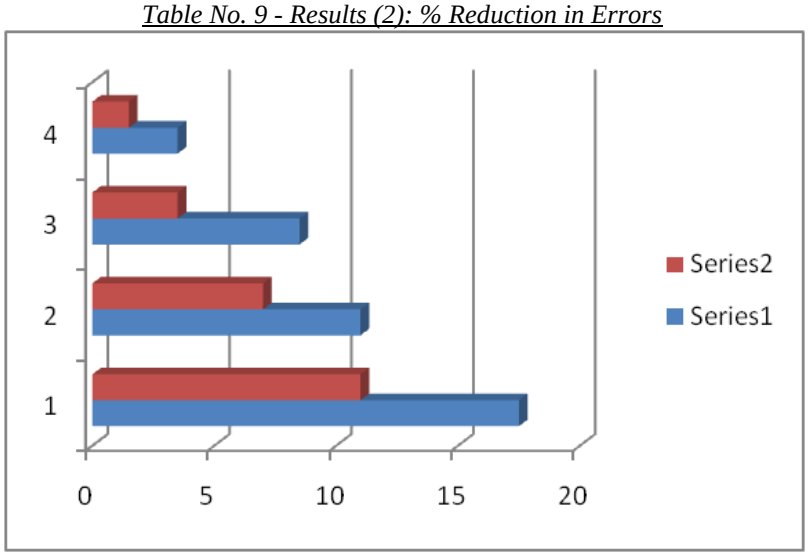

Graph No. 2- Graph of Comparison between CSM and FSM for average of Current process Vs. Proposed process for `number of Errors' identified during development phase

V. CONCLUSION

The objective of this exercise was to administer the use of Process Plan for planning principles as a way to logically and sequentially plan process, to reduce time and errors and improve the process during developing a Die. This study carries evidence of genuine advantages of applying computer aided process plan in a small scale industry. By applying computer aided process planning tool in a die manufacturing industry, a current state map is developed. A future state value stream map is created by eliminating time and errors during developing die. The future state map shows marked improvement in the process planning.

A case study discussed outlines importance of Computer Aided Process Planning tool to achieve effectiveness by using efficiently the process planning. Strategy to shorten proposed process time required for release of the Die and Proposed process for number of Errors identified during development phase. The benefits realized through the pursuit of the Case Study are:-

1. The future state map shows marked improvement in the process and Time saved with the implementation of the new process = 23.25%.
2. Percentage reduction in the number of errors for the new process = 43.21%

For planning the implementation of the CAPP system, it is recommended that the Company should develop 5 to 10nos case studies. This can provide as an input to developing the 'Retrieval Method' which can be maintained for the first 100nos of Dies. Later, upon maturity, this system can be marked for transition to `Generative Method' or `Feature based Method' of Process Planning.

VI. ACKNOWLEDGEMENTS

.The author gratefully acknowledges the support received from Mr.S.S.Kulkarni, Director- Able Technologies (India) Pvt. Ltd. Pune, for his technical and administrative support from conceptual stage to the final stage for execution of this work. The author also would like to thank Dr.V.R.Naik, Head of Department of Mechanical Engineering, Prof. G.S. Joshi, Prof.A.R.Balwan, P.G.Coordinator, at D.K.T.E. Ichalkaranji, for guidance and crucial inputs over the project work.

www.ijmer.com Vol. 3, Issue. 3, May.-June. 2013 pp-1712-1722 ISSN: 2249-6645

REFERENCES

[1] Krishnan Ramaswami, *International Journal of, process planning for shape deposition manufacturing, January 1997*

[2] S.K. Gupta, D.A. Bourne, K.H. Kim, and S.S. Krishna, Rapid Manufacturing Laboratory, Robotics Institute, Carnegie Mellon University, Pittsburgh,. *International Journal of, Automated process planning for sheet metal bending operations, PA 1521.*

[3] Dr.Thomas R. KramerGuest Worker, National Bureau of Standards, & Research Associate, Catholic University, *International Journal of, process planning for a milling machine from a feature-based design*

[4] M. Tisza Department of Manufacturing Technologies, Research Group of Hungarian Academy of Sciences, University of Miskolc, 3515 Miskolc-Egyetemváros, Hungary* Corresponding author: E-mail address: tisza.miklos@uni-miskolc.hu, Received 30.03.2007; published in revised form 01.09.2007, *International Journal of, recent achievements in computer aided process planning and numerical modelling of sheet metal forming processes*

[5] By T.N. Wong, LecturerDepartment of Industrial & Manufacturing Systems EngineeringUniversity of Hong Kong, *International Journal of, development of a knowledge-based automated process planning system*

[6] Sankha Deb, Department of Mechanical Engineering, Indian Institute of Technology Kharagpur, Kharagpur-721302, India. E-mail: sankha.deb@mech.iitkgp.ernet.in J. Raul Parra-Castillo Department of Mechanical Engineering, Escuelas Profesionales de la grada Familia, Cadiz, Spain. E-Mail: raul.parra@polymtl.ca Kalyan Ghosh Department of Maths. & Industrial Engineering, École Polytechnique, Université de Montréal, Montréal, Québec H3C 3A7, Canada. Email: kalyan.ghosh@polymtl.ca *International Journal of ,an integrated and intelligent computer-aided process planning methodology for machined rotationally symmetrical parts Volume 13 Issue 1 ©2011 ijams*

[7] By Ramy F. Harik1, William J. E. Derigent2 and Gabriel Ris2, 1Lebanese American University, ramy.harik@lau.edu.lb,2Université Henri Poincaré - Nancy I, william.derigent@cran.uhp-nancy.fr,Computer-Aided Design & Applications, 5(6), 2008, 953-962953,Computer-Aided Design and Applications© 2008 CAD Solutions, LLC,http://www.cadanda.com, DOI**:** 10.3722/cadaps.2008.953-962, *International Journal of, computer aided process planning in aircraft manufacturing,DOI: 10.3722/cadaps.2008.953-9628*

[8] David J. Cooper Jr.Genworks International 5777 West Maple, Suite 130 West Bloom_eld, MI 48325.http://www.genworks.com david.cooper@genworks.com ,August 21, 1998 (updated August 13, 2002), *International Journal of, understanding multi-state generative process planning, August 21, 1998(updated August 13, 2002*

[9] Dietmar Winkler Stefan Biffl Thomas Östreicher, Vienna University of Technology, Favoritenstrasse 9/188, 1040 Vienna, Austria,{dietmar.winkler, stefan.biffl, thomas.oestreicher}@qse.ifs.tuwien.ac.at, *test-driven automation: adopting test-first development to improve automation systems engineering processes.*

[10] Dhiman Johns, Thapar University, Patiala, *International Journal of Computer Aided Process Planning(CAPP)*\

[11] V. Naranje, S. Kumar, American Journal of Intelligent Systems , *International Journal of,*A Knowledge Based System for Selection of Components of Deep Drawing Die, 2(2): 1-11, (2012)

[12] John Wiley and Sons, M. P. Groover, *International Journal of , Fundamentals of Modern Manufacturing* 2/e,2002

[13] http://www.zianet.com/ebear/metal/heattreat3.html

[14] http://www.ignou.ac.in/upload/Unit-9-CRC.pdf

International Journal of Modern Engineering Research (IJMER)
www.ijmer.com Vol. 3, Issue. 3, May.-June. 2013 pp-1723-1726 ISSN: 2249-6645

Fusion Of HWD And Non Negative Matrix Factorization For Video Watermarking

Gopika V Mane[1], G. G. Chiddarwar[2]
* (Department of Computer Engineering, Sinhgad College of Engineering, University of Pune, India
** (Department of Computer Engineering, Sinhgad College of Engineering, University of Pune, India

ABSTRACT : *In the era of high speed network and World Wide Web, data can be easily accessed in a number of ways to share among each other. This data can be manipulated without any quality loss. Threat of intellectual property rights becomes a crucial issue due to this. The security of these online assets can be obtained using different techniques like encryption, fingerprinting, watermarking. In this paper we propose watermarking algorithms for protecting digital contents like images,audio,video. This algorithm uses a new family of perfect reconstruction, non-redundant, and multiresolution geometrical transforms using the wavelet transform in conjunction with modified versions of directional filter banks (DFB) for decomposition of video frames into frequency bands. Low frequency band is factored using Nonnegative matrix factorization for dimension reduction. This hybrid algorithm proposes a more robust technique for video watermarking with no perceptual quality loss of video.*

Keywords : *Content protection, Digital properties, Directional filter banks (DFB), Security, SVD, Wavelet Based Contourlet transform (WBCT), Watermarking techniques.*

I. INTRODUCTION

With the rapid development of digital multimedia technique and the spread of the internet, digital productions are easily copied and manipulated, so there exists a strong demand to protect the ownership and the copyright of this digital production. Digital watermarking is an excellent tool of copyright protection by embedding some information into the digital production.Copyright protection inserts authentication data such as ownership information and logo in the digital media without affecting its perceptual quality. In recent years, digital watermarking is one of the best potential tools for multimedia authentication by embedding some information into the digital production.

A watermarking algorithm consists of watermark structure, an embedding algorithm and extraction or detection algorithm. In multimedia applications, embedded watermark should be invisible, robust and have a high capacity. Robustness is the resistance of an embedded watermark against intentional attack and normal signal processing operations such as noise, filtering, rotation, scaling, cropping and lossy compression etc. Watermarking techniques may be classified in different ways. The classification may be based on the type of watermark being used, i.e., the watermark may be a visually recognizable logo or sequence of random numbers. A second classification is based on whether the watermark is applied in the spatial domain or the transform domain.

In literature many techniques were proposed for digital watermarking. In the spatial domain, Least significant bit (LSB) substitution is used to embed watermark. In transform domain DFT, DCT, DWT are techniques to embed watermark. Wavelets have been successfully applied to many image processing tasks such as low bit-rate compression and denoising [8]. However, they lack the important feature of directionality and hence, they are not efficient in retaining textures and fine details in these applications [3][4]. There have been several efforts towards developing geometrical image transforms. Directional wavelet transforms [1], complex wavelets [6], curvelets [2] and contourlets [3] are a few examples where all of them are redundant.

In Wavelet-Based Contourlet Transform (WBCT) [4], where DFB is applied to all the detail subbands of wavelets in a similar way that one constructs contourlets. The main difference is that we used wavelets instead of the Laplacian pyramids employed in contourlets. Therefore, the WBCT is non-redundant and can be adapted for some efficient wavelet-based image coding methods [4].

The main disadvantage of the WBCT (and other contourlet-based transforms) is the occurrence of artifacts that are caused by setting some transform coefficients to zero for nonlinear approximation and also due to quantizing the coefficients for coding. In this paper, we introduce Hybrid Wavelets and Directional filter banks (HWD) as a solution for this problem. Here we employ wavelets as the subband multiresolution decomposition. Then we apply the DFB and modified versions of the DFB to some of the wavelet subbands.

This paper is organized into six sections. The second section discusses basic concepts of directional filter bank used in Hybrid Wavelets and Directional filter banks. In third section types of Hybrid Wavelets and Directional filter banks are discussed. Fourth section explains Nonnegative matrix factorization for image dimension reduction. The fifth section illustrates a method for color space separation. Final section states algorithm for video watermarking.

II. HORIZONTAL AND VERTICAL DIRECTIONAL FILTER BANK

Directional filter banks (DFB) [7] decompose the frequency space into wedge-shaped partitions as illustrated in Fig. 1. In this example, eight directions are used, where directional subbands of 1, 2, 3, and 4 represent *horizontal* directions (directions between -45° and +45°) and the rest stand for the *vertical* directions (directions between 45° and 135°). The DFB is realized using an iterated quincunx filter banks.

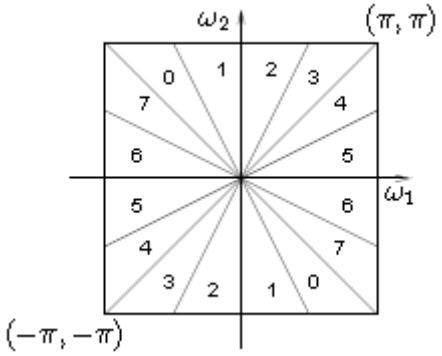

Fig 1. Diretional filter bank frequency partitioning using 8 directions

For the proposed HWD family, we are required to decompose the input into either horizontal directions or vertical directions or both. Hence, we propose Vertical DFB (VDFB) and Horizontal DFB (HDFB), where one can achieve either vertical or horizontal directional decompositions, respectively. Fig. 2 shows the frequency space partitioned by the VDFB and HDFB.

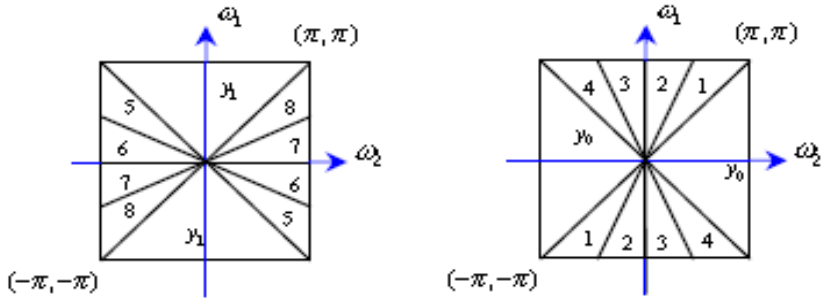

Fig 2. (a) An example of the *vertical* directional filter banks.
(b) An example of the *horizontal* directional filter banks.

III. HYBRID WAVELETS AND DIRECTIONAL FILTER BANKS (HWD)

Here we develop the image transform family of Hybrid Wavelets and Directional filter banks (HWD). For HWD, similar to the WBCT, we consider the wavelet transform as the multiresolution subband decomposition. Wavelets have already shown their good nonlinear approximation property for piece-wise smooth signals [6]; thus, we expect that by adding the feature of directionality in an appropriate manner we could improve the nonlinear approximation results yielded from wavelets. There are efficient algorithms developed for image processing applications such as image coding; therefore, one could properly adapt these algorithm to HWD, Similar adaptive schemes such as those used for wavelet packets can be developed for this new family.

For the WBCT scheme, we apply the DFB to all wavelet detail subbands in such a way to comply the anisotropy scaling law [4]. Because the WBCT coding scheme introduces visible artifacts in the smooth regions of images. These artifacts are mainly introduced by the DFB when we set some transform coefficients to zero. Regarding the human visual system, eyes are more sensitive to low-frequency portions of an image. To reduce artifacts, therefore, we just apply the (modified) DFB to m_α , ($m_\alpha < L$, L is the number of wavelet levels) finest scales of the wavelet subbands. We propose the following two types of the HWD family basis functions:

1. HWD type 1
   a. apply the DFB to the m_α finest diagonal wavelet subbands (HH_i , ($1 \le i \le m_\alpha$)),
   b. apply the VDFB to the m_α finest vertical wavelet subbands (HL_i , ($1 \le i \le m_\alpha$)),
   c. apply the HDFB to the m_α finest horizontal wavelet subbands (LH_i , ($1 \le i \le m_\alpha$)).

2. HWD type 2
   a. apply the DFB to the m_α finest diagonal wavelet subbands (HH_i , ($1 \le i \le m_\alpha$)),
   b. apply the VDFB to the m_α finest horizontal wavelet subbands (LH_i , ($1 \le i \le m_\alpha$)),
   c. apply the HDFB to the m_α finest vertical wavelet subbands (HL_i , ($1 \le i \le m_\alpha$)).

In HWD1, we further directionally decompose the vertical and horizontal coefficients already obtained through wavelet filtering. We use the proposed modified versions of the DFB to lower the complexity and to further reduce the artifacts. In HWD2, however, we decompose the horizontal subbands vertically and the vertical subbands horizontally.

Fig. 3 shows some basis functions of the HWD family as well as the wavelet transform and the WBCT. As seen, the wavelet basis functions are point-wise while those of the HWD family are both directional and point-wise. Note that the nondirectional basis functions of HWD2 are more similar to those of wavelets when compared with the HWD1. In the WBCT all basis functions are directional. The center basis function in these schemes is an instance from coarser scales, which is the same for wavelets and also HWD type 1 and 2. In contrast, for the WBCT it appears as a scattered directional basis function, which is a source of artifacts in this type.

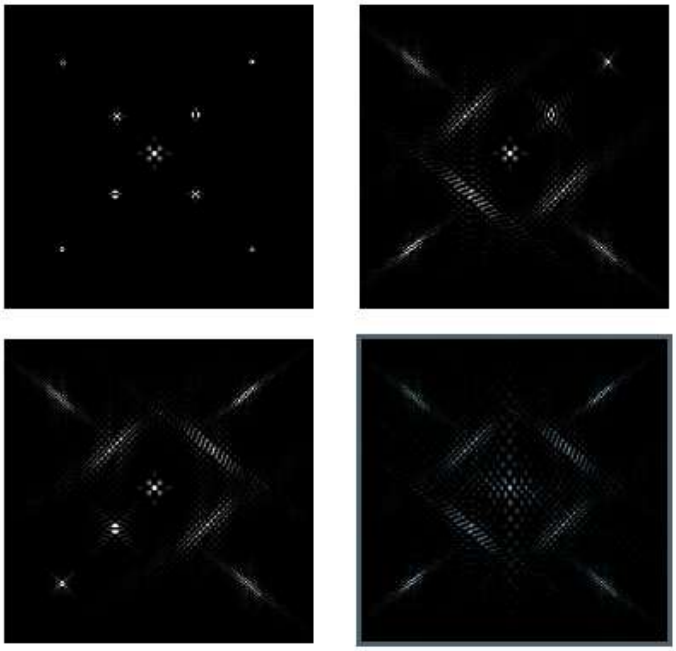

Fig 3. Some basis functions of the wavelets and HWD family.
From left to right, top to bottom: Wavelets, HWD1, HWD2, and WBCT.

IV. NON NEGATIVE MATRIX FACTORIZATION (NMF)

One major drawback of SVD is that the basis vectors may have both positive and negative components, and the data are represented as linear combinations of these vectors with positive and negative coefficients. In many applications, the negative components contradict physical realities. To address this problem, the NMF approach was proposed to search for a representative basis with only nonnegative vectors.

Given a cover image C of size $m \times m$, we can approximately factorize C into the product of two nonnegative matrices B and H with sizes $m \times r$ and $r \times m$ respectively, that is *the* $C = BH$; where $r \leq m$. The nonnegative matrix B contains the NMF basis vectors, and the nonnegative weight matrix H contains the associated coefficients (nonnegative weights). To measure the quality of the approximation factorization $C = BH$, a cost function between C and BH needs to be optimized subject to non-negativity constraints on B and H. This is done by minimizing the I-information divergence which is given by

$$\mathrm{I}\,(\mathrm{C} \,\|\, \mathrm{BH}) = \sum_{ij} \left(Cij \log \frac{Cij}{(BH)ij} - Cij + (BH)ij\right) \qquad (1)$$

which yields the following multiplicative update rules

$$H_{kj} \leftarrow H_{kj} \frac{\sum_i B_{ik} Ci_j / (BH)i_j}{\sum_i B_{ik}} \qquad (2)$$

$$B_{ik} \leftarrow B_{ik} \frac{\sum_i H_{kj} C_{ij} / (BH)_{ij}}{\sum_i H_{kj}} \qquad (3)$$

V. YUV COLOR COMPONENT

Since Pixel values in RGB color space are highly correlated, RGB color space is converted into YUV color space. RGB color space is used for many watermarking algorithms, but RGB color space is complex in describing the color pattern and has redundant information between each component [2]. Also, embedding watermark in RGB color space is less robust than YUV color space. Hence, RGB color space is converted into YUV Color space and then Watermark is embedded. Initially color image is read and R, G, B components of the original Cover Image are separated. Then they are converted into YUV color Space using following equations.

$$Y = 0.299 * R + 0.587 * G + 0.114 * B; \quad (4)$$

$$U = - 0.147 * R - 0.289 * G + 0.436 * B; \quad (5)$$

$$V = 0.615 * R - 0.515 * G - 0.100 * B; \quad (6)$$

VI. PROPOSED ALGORITHM

In proposed algorithm Y component is given to HWD which is used for extracting low frequency component from video frames. These components are pasteurized using NMF where we get two nonnegative matrices.Following are steps for embedding watermark in video frames.

1. Input color video which is divided into number of frames.
2. Extract Y component from video frames.
3. Apply HWD to frame for identifying low frequency part.
4. Input low frequency part for factorization into W1 & H1.
5. Factorize watermark image also using NMF into W2 & H2.
6. The W1 is normalized in between 0 and 1 and is termed as M1.
   M1[i]=(W1[i]-maximum(W1))/(minimum(W1))-(maximum(W1))
7. The weight matrix is obtained by Alpha=0.05*M1[i]
8. The embedding is performed as
   W_{new}=W1+Alpha $\otimes$ W2 $\otimes$ --indicates element wise product.
9. After getting W_{new},using H1 the INMF results the watermarked coefficients of Y component.
10. Inverse HWD is applied to get back the watermarked Y component and these will combined with other color channels of Original video to get back the Watermarked video.

VII. CONCLUSION

This study represents drawbacks of Wavelet based Contourlet transform and give solution using Hybrid Wavelet Directional filter banks. The algorithm proposed used luminance part of video frames to insert watermark and low frequency part of frame results from HWD. Non negative matrix factorization avoid presence of negative entities involved in image which contradicts physical realities. This algorithm proposes new technique for video watermarking with the use of new & robust algorithms.

ACKNOWLEDGEMENTS

We are thankful to staff members and students of ME-II of Sinhgad College of Engineering, Vadgaon, Pune. Maharashtra for their support during preparation of this paper.

REFERENCES

Journal Papers:

[1] T. Jayamalar, Dr. V. Radha, Survey on Digital Video Watermarking Techniques and Attacks on Watermarks, *International Journal of Engineering Science and Technology*, vol. 12, 6963- 6967, 2010.

[2] K.Kishore Kumar, Movva Pavani, V.Seshu Babu, Adaptive Hybrid Video Watermarking using WBCT and NMF,International *Journal of Computer Applications*, Volume 56– No.16, October 2012.

[3] Mr Ming Tong, Tao Chen, Wei Zhang, Linna Dong, New Video Watermark Scheme Resistant to Super Strong Cropping Attacks, *Journal of Information Security*,2012

[4] T. Khatib, A. Haj, L. Rajab, H. Mohammed, A Robust Video Watermarking Algorithm, Journal of Computer.science vol. 4,pp. 910-915, 2008

Theses:

[5] M. N. Do, *Directional multiresolution image representations*. Ph.D. thesis, EPFL, Lausanne, Switzerland, Dec. 2001.

Proceedings Papers:

[6] Pik Wah Chan,Michael R. Lyu,Roland T. Chin, A Novel Scheme for Hybrid Digital Video Watermarking: Approach, Evaluation and Experimentation, *IEEE Transactions On Circuits And Syatems For Video Technology*, VOL. 15, NO. 12, December 2005

[7] R. Eslami and H. Radha, Wavelet-based contourlet transform and its application to image coding, in *proc. of IEEE International Conference on Image Processing*, Oct. 2004.

[8] S. Park, M. J. T. Smith, and R. M. Mersereau, Improved structures of maximally decimated directional filter banks for spatial image analysis, *IEEE Trans. Image Processing*, vol. 13, no. 11, pp. 1424-1431, Nov. 2004.

[9] N. Kingsbury, Image processing with complex wavelets, *Phil. Trans*. R. Soc. London, Sep. 1999.

[10] P. Antoine, P. Carrette, R. Murenzi and B. Piette, Image analysis with two-dimensional continuous wavelet transform, *Signal Processing*, Vol. 31, pp. 241-272, 1993.

International Journal of Modern Engineering Research (IJMER)
www.ijmer.com Vol. 3, Issue. 3, May.-June. 2013 pp-1727-1730 ISSN: 2249-6645

Comparative Study of RCC and Prestressed Concrete Flat Slabs

Vakas K. Rahman[1], Prof. A. R. Mundhada[2]
[1]PG Student, Department of Civil Engineering, P.R.M.I.T. & R, Badnera, Amravati, India-444701
[2]Professor, Department of Civil Engineering, P.R.M.I.T. & R, Badnera, Amravati, India-444701

Abstract—*This paper presents the comparison of R.C.C. and Prestressed Concrete Flat Slab. This work includes the design and estimates for R.C.C. and Prestressed Concrete flat slabs of various spans. The aim of this work is to design R.C.C. as well as prestressed concrete flat slabs for various spans and then compare the results. Programming in MS EXCEL is done to design both types of flat slabs. The idea is to reach a definite conclusion regarding the superiority of the two techniques over one another. Results reveal that a R.C.C. flat slab is cheaper than pre-stressed concrete flat slab for smaller spans but vice versa is true for larger spans.*

Index Terms: *Flat Slab, Prestressed Concrete, R.C.C., Column Strip, Middle Strip, Strand.*

I. Introduction

1.1 Importance & Necessity

Without any semblance of doubt, reinforced cement concrete construction has been the most revolutionary construction technique of modern times. Combining the high compressive strength of concrete with high tensile strength and elasticity of steel has resulted in a composite material that is strong, durable and economical. Moreover, it is time tested.

One of the greatest assets of "homo-sapiens" is the quest for excellence. The human being has constantly refused to sit over his laurels and become complacent. This has often resulted in new invention and improved products and techniques. Very week tensile strength of concrete lead to discovery of R.C.C. Bulkiness of R.C.C resulted in the invention of shells. The problem of serviceability associated with the R.C.C. structures sent the human mind working over-time. The solution was found in prestressing. Like ordinary reinforced concrete, prestressed concrete consists of concrete resisting compression and reinforcement carrying tension. Prestressing became essential in many applications in order to fully utilize the compressive strength of reinforced concrete and to eliminate or control cracking and deflection.

The aim of this work is to design Flat Slab of R.C.C. as well as prestressed concrete variety and then compare the results. The idea is to reach a definite conclusion regarding the Superiority of the two techniques over each other.

1.2 Scope

This work includes the design and estimate for Flat Slabs of various spans, ranging from 6.0 M to 12.0 M, by R.C.C. and Prestressed Concrete techniques. For smaller spans, associated with normal building works, prestressed concrete construction becomes too cumbersome, irrespective of the economics involved. Intensity of assumed loading is kept sufficient enough, so that the factored bending moment will be comparable to that developing in cases of commercial buildings. Post-tensioning is preferred as it is in vogue, in construction of large span slabs.

II. Methodology

To begin with, an R.C.C. FLAT SLAB was manually designed by using the limit state method based on IS: 456-2000. Based on the steps & formulas involved, a design program was prepared in MS EXCEL. The veracity of the program was checked by first designing the manually designed SLAB by using the program & comparing the results. Since in field, a mix richer than M 30 is seldom used for R.C.C., the grade of concrete was maintained at M 30 for R.C.C.

An identical procedure was followed for PRESTRESSED CONCRETE FLAT SLAB. The manual design was based on the working stress method given in the book Prestressed Concrete by N Krishna Raju and checked by limit state method suggested by the IS: 1343-1980. The program for designing the same was developed by using MS EXCEL & its fidelity was checked by first solving the manual problem & comparing the results. Since the onus was on prestressing, the slabs were designed for various concrete grades between M 30 to M 50, Table 11 in IS: 1343 was incorporated into the program as a link so as to directly calculate the prestressing steel index. Design was carried out for parabolic strand profile only, which is the most popular one. Prestressed concrete flat slab of all concrete grades were designed for TYPE 2.

Programs were also prepared for estimating & costing. Rates are based on the latest CSR in Maharashtra. In case of prestressed concrete, some of the rates were obtained from a well-known private Infrastructure company such as IRB and LT.

III. Results And Discusion

Table 1 below gives the cost in rupees for various spans for both R.C.C. Flat Slabs in M: 30 grade concrete & Prestressed Concrete Flat Slabs in M: 30 & higher grade concretes. Figure 1 below depicts the same statistics with the help of bar charts.

Figure 2 below is a short form of Figure 1 where R.C.C. Flat slabs are compared with prestressed concrete flat slabs of different grades of concrete. Figure 3 below give percent saving in cost of construction with respect to higher values.

The cost of prestressed concrete flat slabs includes the cost of accessories like split cones, bearing plates, sheathing tubes, grouting etc.

In our country, concrete grade higher than M 30 is generally not used in case of R.C.C. construction. But in prestressed concrete construction concrete grades such as M 40 and M 50 are used.

Traditionally, column spacing and floor spans in these buildings such as commercial complex, shopping mall and ware house etc has been in the range of 6 to 9 metres, to both contain costs and simplify construction. However, recently there is an increasing preference by building owners and tenants for large floor areas with column-free space and spans from 9 to 16 meters. This has focused the interest of designers and builders on methods of reducing costs and speeding construction of long-span floors.

From the statistics, it is cleared that up to 9 m, Reinforced Cement Concrete flat slabs are economical as compared to Prestressed Concrete Flat Slabs .Therefore in practice for spans up to 9 m, RCC flat slab dominates the Prestressed Concrete flat slab.

Form spans 9m to 12 m, Prestressed Concrete flat slab becomes economical and as the span increases its economical efficiency increases. This may not appeal much especially if we consider the hassles associated with prestressing like skilled workmanship & need for superior quality control. But we must not forget that along with these minor inconveniences prestressing delivers a structure that is better from limit state of serviceability & durability point of view.

Prestressed concrete flat slab were simultaneously designed in different grades for identical spans. The results show gradual increased in cost of flat slab with higher grades of concrete which differs in case of RCC. This is because of the large difference in cost of higher grades as compared to lower grades of concrete irrespective of the saving of concrete due to smaller depth of slab for higher concrete grades.

Span (m)	**Concrete Grade**	**Estimated Cost of Prestressed Concrete Flat Slab (Rupees)**	**Estimated Cost Of RCC Flat Slab For M30 Grade Only(Rupees)**	**% Difference on the basis of Higher Value (%)**
6	M_{30} M_{40} M_{50}	10,41,832.55 11,49,725.88 12,93,028.59	7,97,417.39	23.43
7	M_{30} M_{40} M_{50}	15,47,927.56 14,89,880.00 16,76,070.00	12,75,258.64	17.58
8	M_{30} M_{40} M_{50}	20,05,632.48 21,57,895.70 21,76,305.96	19,34,492.04	3.49
9	M_{30} M_{40} M_{50}	27,28,601.36 29,64,421.83 30,26,162.00	26,87,130.5	≈ 0
10	M_{30} M_{40} M_{50}	37,36,.27.85 40,66,529.37 42,92,180.92	39,76,100.49	-6.04
11	M_{30} M_{40} M_{50}	43,88,401.82 44,99,976.70 48,48,999.00	52,58,044.6	-16.54
12	M_{30} M_{40} M_{50}	56,04,387.18 57,64,089.07 60,83,029.00	76,17,202.13	-26.42

Table.1:"Cost Comparison of R.C.C. And Prestressed Concrete Flat Slab"
(+ve sign showing RCC Flat Slab is economical & -ve sign showing Prestressed Concrete Flat Slab is economical)

Figure 1: Variation of Cost with Span of Slab

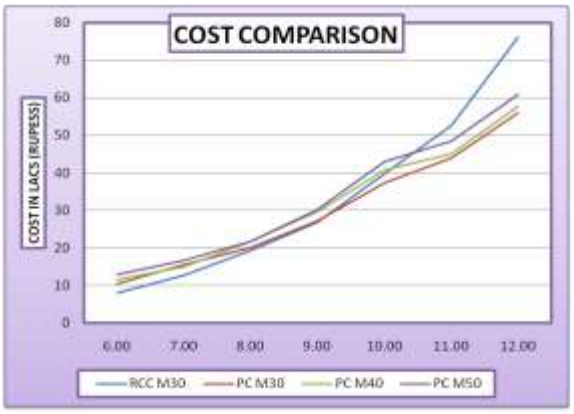

Figure 2: Variation of Cost with Span of Slab

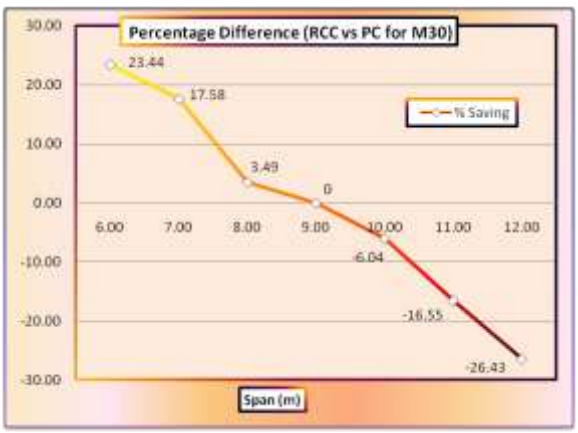

Figure 3: % difference on the basis of Higher value (RCC vs. PC for M30)

IV. Conclusions

Based on the study conducted, it could be concluded that RCC flat slabs are economical up to 9m span but beyond that pre-stressed concrete flat slabs become a better choice. The cost advantage in percentage terms goes on increasing in favour of prestressed concrete with increasing span. Besides, pre-stressed concrete flat slabs being thinner provide greater headroom & result in lesser seismic forces. Better durability of prestressed concrete structures is already a well established fact.

V. Future Scope

Cost comparison of RCC and prestressed concrete waffle slabs for spans above 10m.

References

[1.] DESIGN OF PRESTRESSED CONCRETE FLAT SLAB" The South African Institution of Civil Engineering, South Africa, 1991.
[2.] Guide to Long-Span Concrete Floors, Cement and Concrete Association of Australia, August 2003.
[3.] "Analysis And Design Flat Slab Using Various Codes", M.Anitha, B.Q.Rahman, J. J .Vijay, International Institute of Information Technology Hyderabad, April 2007.
[4.] "Analysis And Design of Flat Slab And Grid Slab And Their Cost Comparison" Amit A. Sathawane & R.S. Deotale, Department of Civil Engineering, Yeshwantrao Chavhan College of Engineering Nagpur.
[5.] "Reynolds Reinforced Concrete Designer's Hand Book".
[6.] IS: 456-2000. Indian Standard Code of Practice for Reinforced Concrete.
[7.] IS: 1343- 1980. Indian Standard Code of Practice for Prestressed Concrete (First Revision).
[8.] N. Krishna Raju, 2007. "Prestressed Concrete", Fourth Edition, Tata McGraw- Hill Company Ltd., New Delhi.
[9.] Dr. S.R. Karve & Dr.V.L. Shah, "Limit State Theory & Design Of Reinforced Concrete".
[10.] B.N Dutta, 2009 "Estimating and Costing In Civil Engineering", Twenty- Sixth Revised Edition UBS Publishers' Distributors Pvt. Ltd. New Delhi.
[11.] Current Schedule of Rates (CSR), 2012-2013, for Public Works Region, Amravati.

International Journal of Modern Engineering Research (IJMER)
www.ijmer.com Vol. 3, Issue. 3, May.-June. 2013 pp-1731-1738 ISSN: 2249-6645

Power Quality Improvement Of Grid Interconnected 3-Phase 4-Wire System Of Distribution Generation

A.Sumalatha[1], K.Ravi Sankar[2]
Department of Electrical and Electronics Engineering, JNTUA College of Engineering And Technology Pulivendula, Kadapa dist. , Andhra Pradesh, INDIA
Academic Assistant Professor of Department of Electrical and Electronics Engineering JNTUA College of Engineering And Technology Pulivendula, Kadapa dist. , Andhra Pradesh, INDIA

Abstract *: Small distributed generation (DG) systems provide standby service during utility outages and, when operated during peak load hours, potentially reduce energy costs. Renewable energy sources (RES) are being increasingly connected in distribution system utilizing power electronic converters. This paper presents a novel control strategy for achieving maximum benefits from this grid -interfacing inverters when installed in 3-phase 4- wire distribution systems. The inverter is controlled to perform as multi-function device by incorporating active power filter functionality. The inverter can thus be utilized as:1)power converter to inject power generated from RES to the grid, and 2)shunt APF to compensate current unbalance, load current harmonics, load reactive power demand and load neutral current. All of these functions may be accomplished either individually or simultaneously. With such a control, the combination of grid- interfacing inverter and the 3-phase 4wire linear/non –linear unbalanced load at the point of common coupling appears as balanced linear load to the grid. This new control concept is demonstrated with extensive MATLAB/ Simulink simulation studies.*

Keywords: *Active power filter (APF), distributed generation (DG), distribution system, grid interconnection, power quality (PQ), renewable energy.*

I. Introduction

ELECTRIC utilities and end users of electric power are becoming increasingly concerned about meeting the growing energy demand. Seventy five percent of total global energy demand is supplied by the burning of fossil fuels. But increasing air pollution, global warming concerns, diminishing fossil fuels and their increasing cost have made it necessary to look towards renewable sources as a future energy solution. Since the past decade, there has been an enormous interest in many countries on renewable energy for power generation. The market liberalization and government's incentives have further accelerated the renewable energy sector growth. Distributed generation (DG) systems are presented as a suitable form to offer high reliable electrical power supply [1]. The concept is particularly interesting when different kinds of energy resources are available, such as photovoltaic panels, fuel cells, or speed wind turbines [2], [3]. Most part of these resources need power electronic interfaces to make up local ac grids [4], [5]. This way, inverters or ac-to-ac converters are connected to an ac common bus with the aim to share properly the disperse loads connected to the local grid [6].

Most sustainable energy sources supply energy in the form of electrical power. Distributed generation (DG) systems are often connected to the utility grid through power electronic converters. A grid-connected inverter provides the necessary interface of the DG to the phase, frequency and amplitude of the grid voltage, and disconnects the system from the grid when islanding. Such a DG system can be designed to operate in both stand-alone and grid-connected modes flexibly according to grid conditions [1], [2]. When the utility grid is not available or the utility power is accidentally lost, the DG is used as an on-site power or standby emergency power service, effectively being an extended uninterruptible power supply (UPS) that is capable of providing long-term energy supply.

The non-linear load current harmonics may result in voltage harmonics and can create a serious PQ problem in the power system network. Active power filters (APF) are extensively used to compensate the load current harmonics and load unbalance at distribution level. This results in an additional hardware cost. However, in this paper authors have incorporated the features of APF in the, conventional inverter interfacing renewable with the grid, without any additional hardware cost. Here, the main idea is the maximum utilization of inverter rating which is most of the time underutilized due to intermittent nature of RES. It is shown in this paper that the grid-interfacing inverter can effectively be utilized to perform following important functions: 1) transfer of active power harvested from the renewable resources (wind, solar, etc.); 2) load reactive power demand support; 3) current harmonics compensation at PCC; and 4) current unbalance and neutral current compensation in case of 3-phase 4-wire system. Moreover, with adequate control of grid-interfacing inverter, all the four objectives can be accomplished either individually or simultaneously. The PQ constraints at the PCC can therefore be strictly maintained within the utility standards without additional hardware cost.

The paper is arranged as follows: Section II describes the system under consideration Section III describes the controller for grid-interfacing inverter. A digital simulation study is presented in Section IV and, finally, Section V concludes the paper.

II. System Descrption

The proposed system consists of RES connected to the Dc-link of a grid-interfacing inverter as shown in Fig. 1.and the simulink design of distribution system is shown in Fig. 2. The voltage source inverter is a key element of a DG system as it interfaces the renewable energy source to the grid and delivers the generated power. The RES may be a DC source or an

AC source with rectifier coupled to dc-link. Usually, the fuel cell and photovoltaic energy sources generate power at variable low dc voltage, while the variable speed wind turbines generate power at variable ac voltage. Thus, the power generated from these renewable sources needs power conditioning (i.e., dc/dc or ac/dc) before connecting on dc-link [6]–[8]. The dc-capacitor decouples the RES from grid and also allows independent control of converters on either side of dc-link. Simulink design of wind energy is shown in Fig. 3.

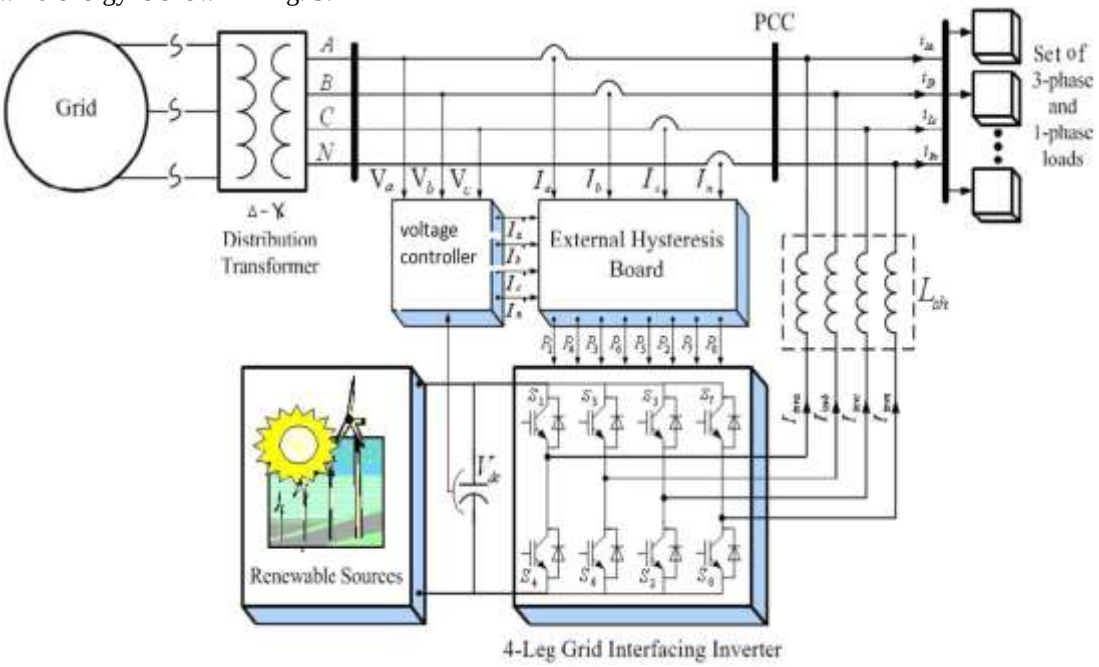

Fig. 1. Schematic of proposed renewable based distribution generation system.

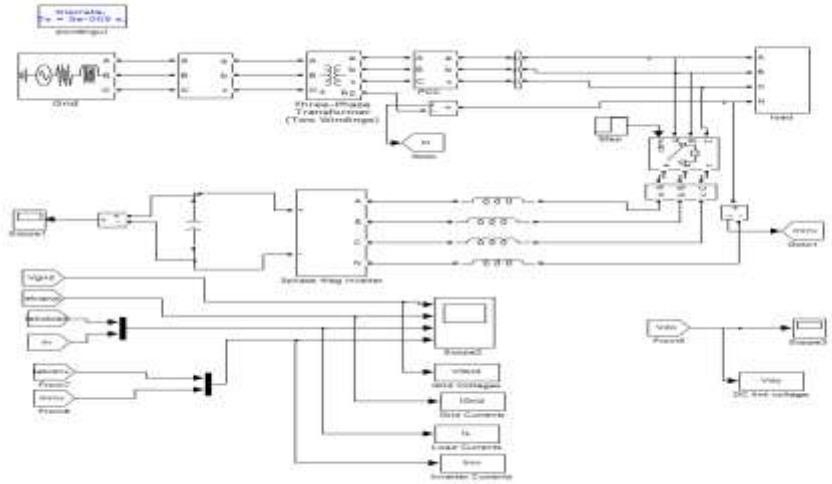

Fig. 2. Simulink Design of Distributed system.

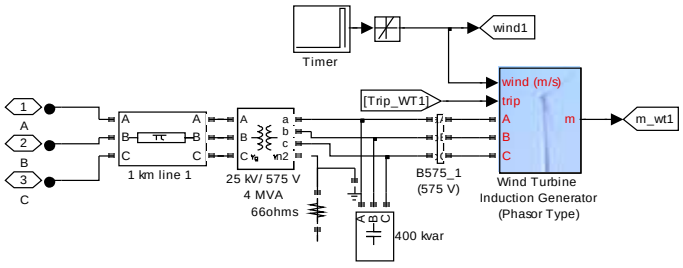

Fig. 3. Simulink Design of Wind Energy system.

III. Proposed Control Strategies

A. ***DC- Link voltage and Power Control Operation*** **:** Due to the intermittent nature of RES, the generated power is of variable nature. The dc-link plays an important role in transferring this variable power from renewable energy source to the grid. RES are represented as current sources connected to the dc-link of a grid-interfacing inverter. Fig. 4 shows the systematic representation of power transfer from the renewable energy resources to the grid via the dc-link. The current injected by renewable into dc-link at voltage level V_{dc} can be given as

$$\mathbf{I_{dc1} = P_{res} / V_{dc}} \quad \mathbf{(1)}$$

where P_{res} is the power generated from RES. The current flow on the other side of dc-link can be represented as,

$$\mathbf{I_{dc2} = P_{inv} / V_{dc} = P_G + P_{Loss} / V_{dc}} \quad \mathbf{(2)}$$

where P_{inv}, P_G and P_{Loss} are total power available at grid-interfacing inverter side, active power supplied to the grid and inverter losses, respectively. If inverter losses are negligible then

$$P_{res} = P_G$$

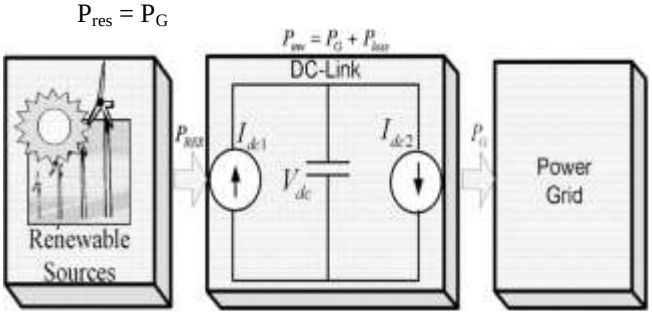

Fig. 4. DC- Link equivalent diagram.

B. ***Control of Grid Interfacing Inverter***

The control diagram of grid- interfacing inverter for a 3-phase 4-wire system is shown in Fig. 5. The fourth leg of inverter is used to compensate the neutral current of load. The main aim of proposed approach is to regulate the power at PCC during: 1) Pres=0; 2) Pres < total load power (P_L); 3) Pres > total load power. While performing the power management operation, the inverter is actively controlled in such a way that it always draws/ supplies fundamental active power from/ to the grid. If the load connected to the PCC is non-linear or unbalanced or the combination of both, the given control approach also compensates the harmonics, unbalance, and neutral current. The duty ratio of inverter switches are varied in a power cycle such that the combination of load and inverter injected power appears as balanced resistive load to the grid.

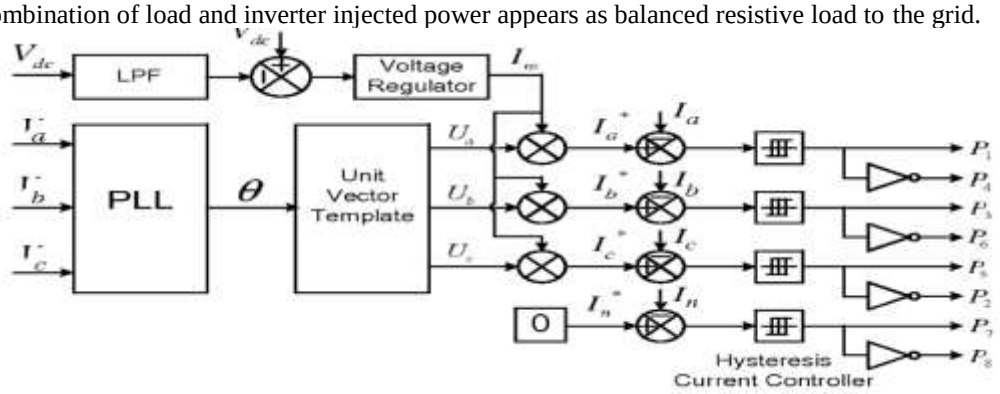

Fig. 5. Block diagram representation of grid-interfacing inverter control.

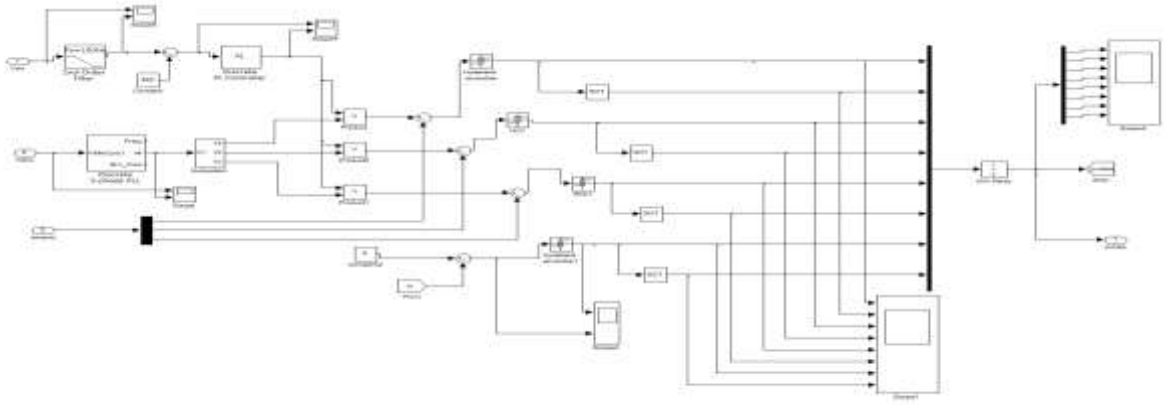

Fig.6. Simulink Design of Grid Interfacing Inverter Control.

The regulation of dc-link voltage carries the information regarding the exchange of active power in between renewable source and grid. Thus the output of dc-link voltage regulator results in an active current (I_m). The multiplication of active

current component (I_m) with unity grid voltage vector templates (U_a, U_b, and U_c) generates the reference grid currents (I_a^*, I_b^*,and I_c^*). The reference grid neutral current (I_n^*) is set to zero, being the instantaneous sum of balanced grid currents. The grid synchronizing angle (θ) obtained from phase locked loop (PLL) is used to generate unity vector template as [9]–[11]

$$\mathbf{U_a = Sin(\theta)} \quad \mathbf{(3)}$$

$$\mathbf{U_b = Sin(\theta - 2\Pi/3)} \quad \mathbf{(4)}$$

$$\mathbf{U_c = Sin(\theta + 2\Pi/3).} \quad \mathbf{(5)}$$

The actual dc-link voltage is sensed and passed through a first-order low pass filter (LPF) to eliminate the presence of switching ripples on the dc-link voltage and in the generated reference current signals. The difference of this filtered dc-link voltage and reference dc-link voltage (V_{dc}^*) is given to a discrete-PI regulator to maintain a constant dc-link voltage under varying generation and load conditions. The dc-link voltage error $V_{dcerr(n)}$ at nth sampling instant is given as:

$$\mathbf{V_{dcerr\,(n)} = V_{dc(n)}^* - V_{dc(n)}.} \quad \mathbf{(6)}$$

The output of discrete-PI regulator at nth sampling instant is expressed as

$$\mathbf{I_{m(n)} = I_{m(n-1)} + K_{PVdc}(V_{dcerr\,(n)} - V_{dcerr\,(n-1)}) + K_{IVdc}\,V_{dcerr(n)}} \quad \mathbf{(7)}$$

where K_{PVdc} = 10 and K_{IVdc}= 0.05 are proportional and integral gains of dc-voltage regulator. The simulink design of grid interfacing inverter using PI controller is shown in Fig. 6. The instantaneous values of reference three phase grid currents are computed as

$$\mathbf{I_a^* = I_m.U_a} \quad \mathbf{(8)}$$

$$\mathbf{I_b^* = I_m.U_b} \quad \mathbf{(9)}$$

$$\mathbf{I_c^* = I_m.U_c.} \quad \mathbf{(10)}$$

The neutral current, present if any, due to the loads connected to the neutral conductor should be compensated by forth leg of grid-interfacing inverter and thus should not be drawn from the grid. In other words, the reference current for the grid neutral current is considered as zero and can be expressed as

$$\mathbf{I_n^* = 0.} \quad \mathbf{(11)}$$

The reference grid currents (I_a^*, I_b^*, I_c^*, and I_n^*) are compared with actual grid currents (I_a, I_b, I_c and I_n) to compute the current errors as

$$\mathbf{I_{aerr} = I_a^* - I_a} \quad \mathbf{(12)}$$

$$\mathbf{I_{berr} = I_b^* - I_b} \quad \mathbf{(13)}$$

$$\mathbf{I_{cerr} = I_c^* - I_c} \quad \mathbf{(14)}$$

$$\mathbf{I_{nerr} = I_n^* - I_n.} \quad \mathbf{(15)}$$

These current errors are given to hysteresis current controller. The hysteresis controller then generates the switching pulses (P_1 *to* P_8) for the gate drives of grid-interfacing inverter. The average model of 4-leg inverter can be obtained by the following state space equations

$$\mathbf{dI_{Inva}/dt = (V_{Inva} - V_a) / L_{sh}} \quad \mathbf{(16)}$$

$$\mathbf{dI_{Invb}/dt = (V_{Invb} - V_b) / L_{sh}} \quad \mathbf{(17)}$$

$$\mathbf{dI_{Invc}/dt = (V_{Invc} - V_c) / L_{sh}} \quad \mathbf{(18)}$$

$$\mathbf{dI_{Invn}/dt = (V_{Invn} - V_n) / L_{sh}} \quad \mathbf{(19)}$$

$$\mathbf{dV_{dc}/dt = (I_{Invad} + I_{Invbd} + I_{Invcd} + I_{Invnd})/C_{dc}} \quad \mathbf{(20)}$$

Where V_{Inva}, V_{Invb}, V_{Invc}, and V_{Invn} are the three-phase ac switching voltages generated on the output terminal of inverter. These inverter output voltages can be modeled in terms of instantaneous dc bus voltage and switching pulses of the inverter as

$$\mathbf{V_{Inva} = (P_1 - P_4)V_{dc}/2} \quad \mathbf{(21)}$$

$$\mathbf{V_{Invb} = (P_3 - P_6)V_{dc}/2} \quad \mathbf{(22)}$$

$$\mathbf{V_{Invc} = (P_5 - P_2)V_{dc}/2} \quad \mathbf{(23)}$$

$$\mathbf{V_{Invn} = (P_7 - P_8)V_{dc}/2} \quad \mathbf{(24)}$$

Similarly the charging currents I_{Invad}, I_{Invbd}, I_{Invcd} and I_{Invnd} on dc bus due to the each leg of inverter can be expressed as

$$\mathbf{I_{Invad} = I_{Inva}(P_1 - P_4)} \quad \mathbf{(25)}$$

$$\mathbf{I_{Invbd} = I_{Invb}(P_3 - P_6)} \quad \mathbf{(26)}$$

$$\mathbf{I_{Invcd} = I_{Invc}(P_5 - P_2)} \quad \mathbf{(27)}$$

$$\mathbf{I_{Invnd} = I_{Invn}(P_7 - P_8)} \quad \mathbf{(25)}$$

C. Switching Control Of IGBTs

The switching pattern of each IGBT inside inverter can be formulated on the basis of error between actual and reference current of inverter, which can be explained as:

If $\mathbf{I_{Inva} < (I_{Inva}^* - h_b)}$, then upper switch S_1 will be OFF (P_1=0) and lower switch S_4 will be ON (P_4=1) in the phase "a" leg of inverter.

If $\mathbf{I_{Inva} > (I_{Inva}^* - h_b)}$, then upper switch S_1 will be OFF (P_1=0) and lower switch S_4 will be ON (P_4=1) in the phase "a" leg of inverter.

where h_b is the width of hysteresis band. On the same principle, the switching pulses for the other remaining three legs can be derived.

IV. Simulation Results

In order to verify the proposed control approach to achieve multi-objectives for grid interfaced DG systems connected to a 3-phase 4-wire network, an extensive simulation study is carried out using MATLAB/Simulink. A 4-leg

current controlled voltage source inverter is actively controlled to achieve balanced sinusoidal grid currents at unity power factor (UPF) despite of highly unbalanced nonlinear load at PCC under varying renewable generating conditions. A RES with variable output power is connected on the dc-link of grid-interfacing inverter. An unbalanced 3-phase 4-wire nonlinear load, whose unbalance, harmonics, and reactive power need to be compensated, is connected on PCC. The system parameter is given in Table I shown.

TABLE I
SYSTEM PARAMETER

3-phase Supply (r.m.s.)	:	V_g=30 V, 60 Hz
3-phase Non-linear Load	:	R=26.66Ω, L=10 mH
1-phase Linear Load (A-N)	:	R=36.66Ω, L=10 mH
1-phase Non-Linear Load (C-N)	:	R=26.66Ω, L=10 mH
DC-Link Capacitance & Voltage:		C_{dc}=3000 μF, V_{dc}=90 V
Coupling Inductance	:	L_{sh}=2.0 mH

Initially, the grid-interfacing inverter is not connected to the network (i.e., the load power demand is totally supplied by the grid alone). Therefore, before time t=0.72s, the grid current profile in Fig. 7(b) is identical to the load current profile of Fig. 7(c). At t=0.72s, the grid-interfacing inverter is connected to the network. At this instant the inverter starts injecting the current in such a way that the profile of grid current starts changing from unbalanced non- linear to balanced sinusoidal current as shown in Fig. 7(b). Fig. 14. shows the simulation results for load and inverter. It can be noticed that as the inverter also supplies the load neutral current demand, the grid neutral current (In) becomes zero after t=0.72 s. The load neutral current due to single phase loads is effectively compensated by the fourth leg of the inverter such that the current in the grid side neutral conductor is reduced to zero. At t=0.72 s, the inverter starts injecting active power generated from RES (P_{res}=P_{inv}). Since the generated power is more than the load power demand the additional power is fed back to the grid. The negative sign of P_{grid}, after time 0.72 s suggests that the grid is now receiving power from RES. Moreover, the grid-interfacing inverter also supplies the load reactive power demand locally. Thus, once the inverter is in operation the grid only supplies/receives fundamental active power which is shown in Fig. 9.

At t=0.82 s, the active power from RES is increased to evaluate the performance of system under variable power generation from RES. This results in increased magnitude of inverter current. As the load power demand is considered as constant, this additional power generated from RES flows towards grid, which can be noticed from the increased magnitude of grid current as indicated by its profile. At t=0.92s, the power available from RES is reduced. The corresponding change in the inverter and grid currents can be seen from Fig. 7. The active and reactive power flows between the inverter, load and grid during increase and decrease of energy generation from RES can be noticed from Fig. 8. The dc-link voltage across the grid- interfacing inverter (Fig. 8(d)) during different operating condition is maintained at constant level in order to facilitate the active and reactive power flow. Thus from the simulation results, it is evident that the grid-interfacing inverter can be effectively used to compensate the load reactive power, current unbalance and current harmonics in addition to active power injection from RES. This enables the grid to supply/ receive sinusoidal and balanced power at UPF.

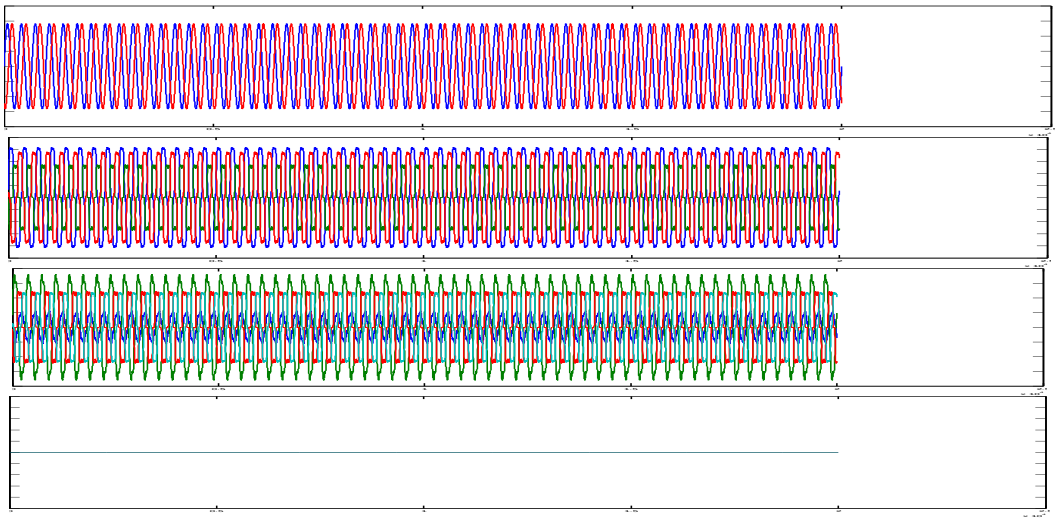

Fig. 7. Simulation results: (a) Grid voltages, (b) Grid currents, (c) Unbalanced load currents, (d) Inverter currents under absence of inverter.

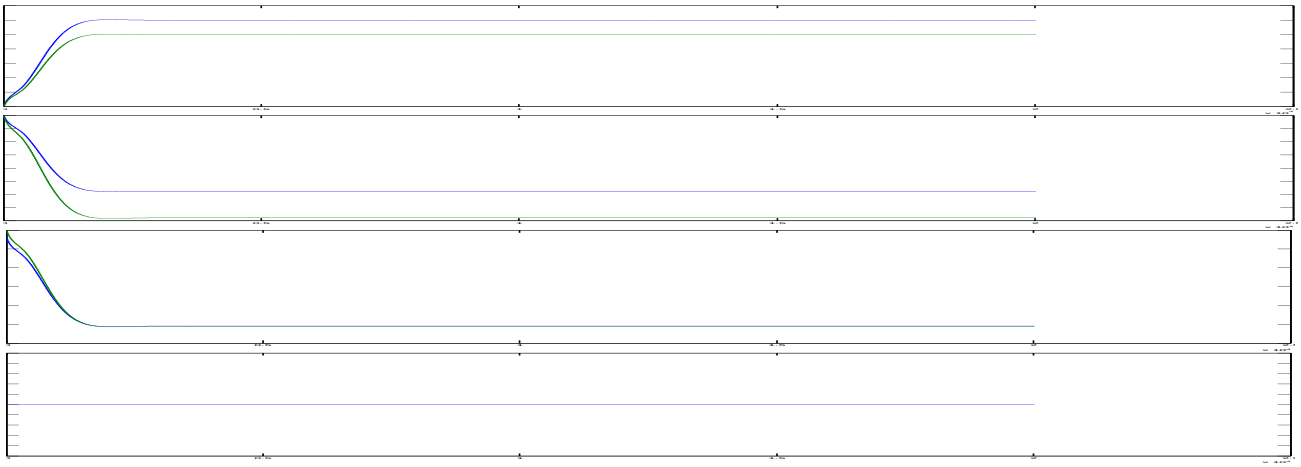

Fig. 8. Simulation results: (a) PQ- Grid, (b) PQ- Load, (c) PQ- Inverter, (d) dc- link voltage under the absence of inverter.

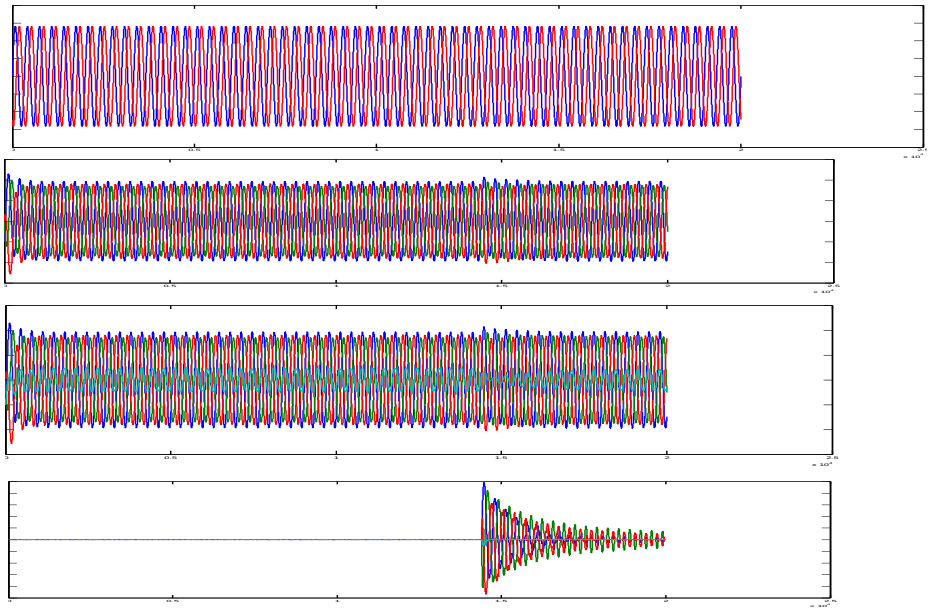

Fig. 9. Simulation results for the active power filtering mode (P_{res}=0) (a) Grid voltages, (b) Grid currents, (c) Load currents, (d) Inverter currents.

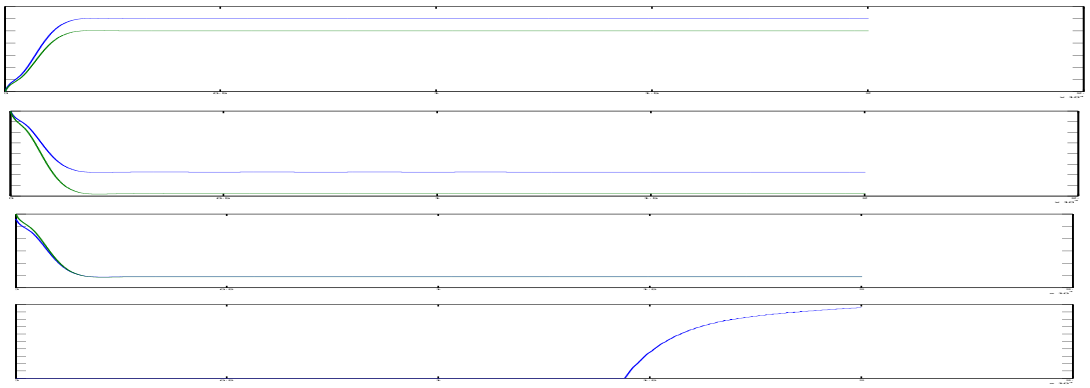

Fig. 10. Simulation results: (a) PQ- Grid, (b) PQ- Load, (c) PQ- Inverter (d) dc- link voltage when there is no power generation from RES

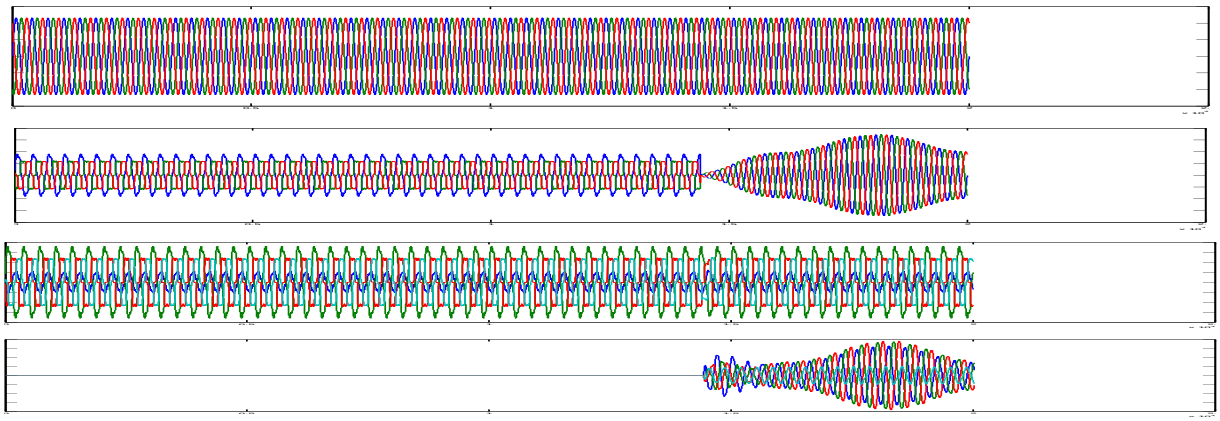

Fig. 11. Simulation results for the active power filtering and renewable power injection mode: (a) Grid voltages, (b) Grid currents, (c) load currents, (d) Inverter currents.

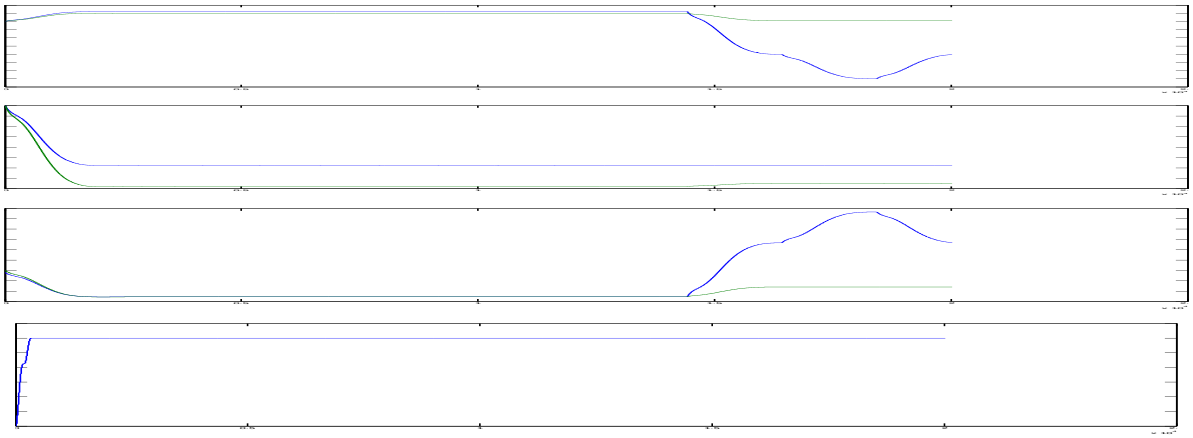

Fig. 12. Simulation results for the active power filtering and renewable power injection mode: (a) PQ- Grid, (b) PQ-Load, (c) PQ- Inverter, (d) dc- link voltage.

V. Conclusion

This paper has presented a novel control of an existing grid interfacing inverter to improve the quality of power at PCC for a 3-phase 4-wireDGsystem. It has been shown that the grid-interfacing inverter can be effectively utilized for power conditioning without affecting its normal operation of real power transfer. The grid-interfacing inverter with the proposed approach can be utilized to:

i) inject real power generated from RES to the grid, and/or,
ii) operate as a shunt Active Power Filter (APF).

This approach thus eliminates the need for additional power conditioning equipment to improve the quality of power at PCC. Extensive MATLAB/Simulink simulation approach and have shown that the grid-interfacing inverter can be utilized as a multi-function device.

It is further demonstrated that the PQ enhancement can be achieved under three different scenarios: 1)P_{res}=0 , 2)P_{res}< P_{Load} , and 3) P_{res} > P_{Load}. The current unbalance, current harmonics and load reactive power, due to unbalanced and non-linear load connected to the PCC, are compensated effectively such that the grid side currents are always maintained as balanced and sinusoidal at unity power factor. Moreover, the load neutral current is prevented from flowing into the grid side by compensating it locally from the fourth leg of inverter. When the power generated from RES is more than the total load power demand, the grid-interfacing inverter with the proposed control approach not only fulfills the total load active and reactive power demand (with harmonic compensation) but also delivers the excess generated sinusoidal active power to the grid at unity power factor.

REFERENCES:

[1] R. H. Lasseter *et al.*, "White paper on integration of distributed energy resources. The CERTS microgrid concept," in *Consort. Electric Reliability Technology Solutions*, 2002, pp. 1–27.
[2] K. Ro and S. Rahman, "Two-loop controller for maximizing performance of a grid-connected photovoltaic-fuel cell hybrid power plant,"*IEEE Trans. Energy Conv.*, vol. EC-13, pp. 276–281, Sept. 1998.
[3] H. Tao, J. L. Duarte, and M. A. M. Hendrix, "A distributed fuel cell based generation and compensation system to improve power quality," in *Proc. IEEE International Power Electronics and Motion Control Conference (IPEMC'06)*, Shanghai, China, Aug. 2006, pp. 1–5.
[4] R. Teodorescu and F. Blaabjerg, "Flexible control of small wind turbines with grid failure detection operating in stand-alone and grid-connected mode," *IEEE Trans. Power Electron.*, vol. 19, no. 5, pp. 1323–1332, Sep. 2004.

[5] R. H. Lasseter and P. Piagi, "Providing premium power through distributed resources," in *Proc. IEEE 33rd Hawaii Int. Conf. System Sciences (HICSS'00)*, 2000, pp. 1–9.
[6] S. R. Wall, "Performance of inverter interfaced distributed generation," in *Proc. IEEE/PES-Transmission and Distribution Conf. Expo.*, 2001, pp. 945–950.
[7] C. Wekesa and T. Ohnishi, "Utility interactive AC module photovoltaic system with frequency tracking and active power filter capabilities," in *Proc. IEEE-PCC'02 Conf.*, 2002, pp. 316–321.
[8] J. Liang, T. C. Green, G. Weiss, and Q.-C. Zhong, "Evaluation of repetitive control for power quality improvement of distributed generation," in *Proc. IEEE-PESC'02 Conf.*, 2002, pp. 1803–1808.
[9] F. Blaabjerg, R. Teodorescu, M. Liserre, and A. V. Timbus, "Overview of control and grid synchronization for distributed power generation systems," *IEEE Trans. Ind. Electron.*, vol. 53, no. 5, pp. 1398–1409, Oct. 2006.
[10] J. M. Carrasco, L. G. Franquelo, J. T. Bialasiewicz, E. Galván, R. C. P. Guisado, M. Á. M. Prats, J. I. León, and N. M. Alfonso, "Powerelectronic systems for the grid integration of renewable energy sources: A survey," *IEEE Trans. Ind. Electron.*, vol. 53, no. 4, pp. 1002–1016, Aug. 2006.
[11] V. Khadkikar, A. Chandra, A. O. Barry, and T. D. Nguyen, "Application of UPQC to protect a sensitive load on a polluted distribution network," in *Proc. Annu. Conf. IEEE Power Eng. Soc. Gen. Meeting*, 2006, pp. 867–872.
[12] M. Singh and A. Chandra, "Power maximization and voltage sag/swell ride-through capability of PMSG based variable speed wind energy conversion system," in *Proc. IEEE 34th Annu. Conf. Indus. Electron. Soc.*, 2008, pp. 2206–2211.
[13] P. Rodríguez, J. Pou, J. Bergas, J. I. Candela, R. P. Burgos, and D. Boroyevich, "Decoupled double synchronous reference frame PLL for power converters control," *IEEE Trans. Power Electron*, vol. 22, no. 2, pp. 584–592, Mar. 2007.
[14] J. M. Guerrero, L. G. de Vicuna, J. Matas, M. Castilla, and J. Miret, "A wireless controller to enhance dynamic performance of parallel inverters in distributed generation systems," *IEEE Trans. Power Electron.*, vol. 19, no. 5, pp. 1205–1213, Sep. 2004.

AUTHORS

A. Sumalatha born in India. She recevied B.tech degree in Electrical and Electronics Engineering from G.Pullaiah College of Engineering and Technology ,Kurnool, A.P. India in 2011. Doing M.tech in Electrical Power Systems at JNTUA College of Engineering and Technology Pulivendula, Kadapa dist., A.P.India.

K. Ravi Sankar born in India. He is working as a Academic Assistant Professor in JNTUA College of Engineering and Technology Pulivendula, Kadapa dist. , A.P. India. He completed his M.tech in Electrical Power Systems.

International Journal of Modern Engineering Research (IJMER)
www.ijmer.com Vol. 3, Issue. 3, May.-June. 2013 pp-1739-1747 ISSN: 2249-6645

Quasi Active Power Factor Correction Scheme for High Efficiency Ac/Dc

Vaddi Ramesh*,P Lakshmi pathi,P Anjappa*****

*(Department of EEE ,Assistant professor in Golden valley integrated campus Madanapalli in India)
(Department of EEE ,Assistant professor in Golden valley integrated campus Madanapalli in India)*(Department of EEE, HOD & Associate professor in Golden valley integrated campus Madanapalli in India)

ABSTRACT: *Harmonic pollution and low power factor in power systems caused by power converters have been of great concern. To overcome these problems several converter topologies using advanced semiconductor devices and control schemes have been proposed. This investigation is to identify a low cost, small size, efficient and reliable ac to dc converter to meet the input performance index of UPS. The performance of single phase and three phase ac to dc converter along with various control techniques are studied and compared. This project presents a novel ac/dc converter based on a quasi-active power factor correction (PFC) scheme. In the proposed circuit, the power factor is improved by using an auxiliary winding coupled to the transformer of a cascade dc/dc fly back converter. The auxiliary winding is placed between the input rectifier and the low-frequency filter capacitor to serve as a magnetic switch to drive an input inductor. Since the dc/dc converter is operated at high-switching frequency, the auxiliary windings produce a high frequency pulsating source such that the input current conduction angle is significantly lengthened and the input current harmonics is reduced. Since the use of a single inductor, the cost z reduced a lot and the efficiency of the system is improved. The power factor is maintained constant by using a buffer capacitor in parallel to the system for compensating the inductive components. It eliminates the use of active switch and control circuit for PFC, which results in lower cost and higher efficiency. Finally an R- load is applied and simulation results are presented*

I. INTRODUCTION

Conventional offline power converters with diode capacitor rectifiers have resulted in distorted input current waveforms with high harmonic contents. To solve these problems, so as to comply with the harmonic standards such as IEC 61000-3-2, several techniques have been proposed to shape the input current waveform of the power converter. A common approach to improving the power factor is a two-stage power conversion approach .The two-stage scheme results in high power factor and fast response output voltage by using two independent controllers and optimized power stages. The main drawbacks of this scheme are its relatively higher cost and larger size resulted from its complicated power stage topology and control circuits, particularly in low power applications. In order to reduce the cost, the single-stage approach, which integrates the PFC stage with a dc/dc converter into one stage, is developed .These integrated single-stage power factor correction (PFC) converters usually use a boost converter to achieve PFC with discontinuous current mode (DCM) operation. Usually, the DCM operation gives a lower total harmonic distortion (THD) of the input current compared to the continuous current mode (CCM). However, the CCM operation yields slightly higher efficiency compared to the DCM operation. A detailed review of the single stage PFC converters is presented.

Generally, single-stage PFC converters meet the regulatory requirements regarding the input current harmonics, but they do not improve the power factor and reduce the THD as much as their conventional two-stage counterpart. The power factor could be as low as 0.8, however, they still meet the regulation. In addition, although the single-stage scheme is especially attractive in low cost and low power applications due to its simplified power stage and control circuit, major issues still exist, such as low efficiency and high as well as wide-range intermediate dc bus voltage stress. To overcome the disadvantages of the single-stage scheme, many converters with input current shaping have been presented in which a high frequency ac voltage source (dither signal) is connected in series with the rectified input voltage in order to shape the input current (Fig.1.1). The auxiliary winding is placed between the input rectifier and the low-frequency filter capacitor to serve as a magnetic switch to drive an input inductor. Since the dc/dc converter is operated at high-switching frequency, the auxiliary windings produce a high frequency pulsating source.

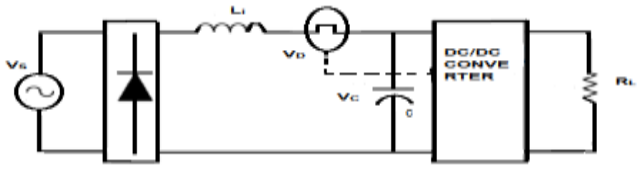

Fig.1.1 General Circuit diagram of dither rectifier with PFC cell.

Another technique based on parallel connection of this dither signal is presented however; the harmonic content can meet the regulatory standard by a small margin. A new concept of quasi-active PFC is proposed to improve the efficiency of a single-stage converter by preventing the input current or voltage stress due the PFC cell from being added to the active switch. In this circuit, the dc/dc cell operates in DCM so that a series of discontinuous pulses is used to shape the input inductor current and the PFC is achieved. As the circuit uses resonance of circuit parameters to achieve PFC, the control of the power factor will be very sensitive to the variation of components values.

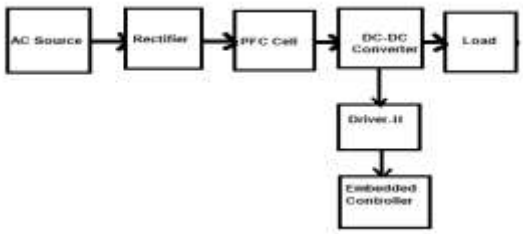

BASIC CONCEPTS OF PROPOSED CIRCUIT

Fig Block diagram of proposed circuit

AC source: It is the first stage of this project. So it is give the AC supply to rectifier. The input side having one inductive filter. It is used to improve the input power factor.

Inverter: It is used to convert dc to ac voltage.the phase shift pulse methosd is used to control the inverter as a result to achieve the ZVS

High Frequency Transformer: It is used for step down purpose. It is also used for isolation purpose. The transformer size should be small due to high frequency.

Rectifier: It converts AC supply to DC supply. DC supply having some ripples. It is filtered with the help of capacitor filter.

Filter: Rectifier converts AC to DC. This output has ripples.It is filtered with a help of Capacitor filters.

Dc Load: The output has DC output votlage. It is used to run the motor, battery charging, and telecommunication applications.

AC Load: Multi level inverter is generate ac output voltage . it is used to run single phase ac motor and any appliance required for ac voltage.

Driver 1 & 2: It is also called as power amplifier because it is used to amplify the pulse output from micro controller. It is also called as opto coupler IC. It provides isolation between microcontroller and power circuits.

Regulated Power supply (RPS): RPS give 5V supply for micro controller and 12V supply for driver. It is converted from AC supply. AC supply is step down using step down transformer

II. PROPOSED QUASI-ACTIVE PFC CIRCUIT

In this project, a new technique of quasi-active PFC is proposed. The PFC cell is formed by connecting the energy buffer (L_B) and an auxiliary winding (L_a) coupled to the transformer of the dc/dc cell, between the input rectifier and the low-frequency filter capacitor used in conventional power converter. Since the dc/dc cell is operated at high frequency, the auxiliary winding produces a high frequency pulsating source such that the input current conduction angle is significantly lengthened and the input current harmonics is reduced. The input inductor L_B operates in DCM such that a lower THD of the input current can be achieved.

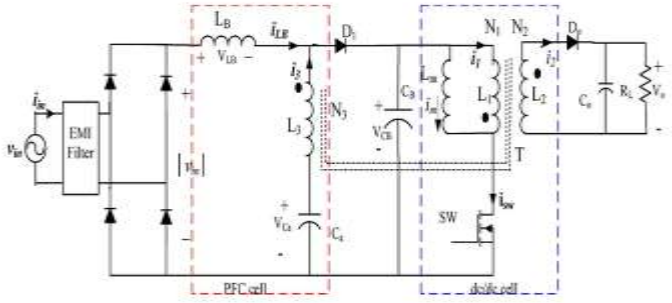

Fig. Proposed quasi-active PFC circuit diagram.

The proposed quasi-active PFC circuit is analyzed in this section. As shown in Fig. 2.2, the circuit comprised of a bridge rectifier, a boost inductor L_B , a bulk capacitor *Ca* in series with the auxiliary windings L_3 , an intermediate dc-bus voltage capacitor C_B ,and a discontinuous input current power load, such as fly back converter. The fly back transformer (*T*) has three windings N_1, N_2 , and N_3 . The secondary winding $N_2 = 1$ is assumed. In the proposed PFC scheme, the dc/dc converter section offers a driving power with high-frequency pulsating source. The quasi active PFC cell can be considered one power stage but without an active switch.

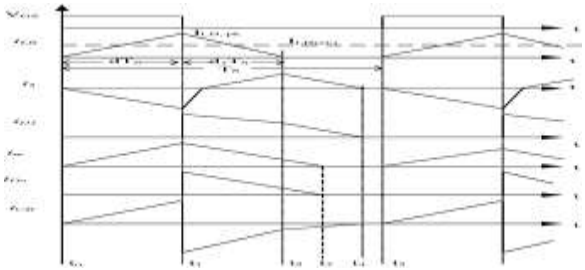

Fig key switching waveforms of the PFC circuit.

To simplify the analysis, the following assumptions have been made.

1.All semiconductors components are ideal. According to this assumption, the primary switch and the rectifiers do not have parasitic capacitances and represent ideal short and open circuits in their ON and OFF states, respectively.

2.The power transformer does not have the leakage inductances because of the ideal coupling.

3.All the capacitors are high enough so that the voltage across them is considered constant.

4.Finally, the input voltage of the converter is considered constant during a switching cycle because the switching frequency is much higher than the line frequency.

Conventional circuit Drawbacks

Low output power

Low efficiency

Poor power factor

More input current harmonics

Advantages of Conventional Circuit

Less voltage spike

High output power

High efficiency

Improve the input power factor

Reduce the input current harmonics

Applications of Conventional Circuit

Battery charging

Battery operated Electric vehicle

Telecom applications

Power supply for DC motor

III. POWER FACTOR AND CONVERTERS

DEFINITION OF POWER FACTOR : Power Factor is a measure of how efficiently electrical power is consumed. In the ideal world Power Factor would be unity (or 1). Unfortunately in the real world Power Factor is reduced by highly inductive loads to 0.7 or less. This induction is caused b The power factor of an *AC* electric power system is defined as the ratio of the real power flowing to the load to the apparent power in the circuit,and is a dimensionless number between 0 and 1 (frequently expressed as a percentage, e.g. 0.5 pf = 50% pf). Real power is the capacity of the circuit for performing work in a particular time. Apparent power is the product of the current and voltage of the circuit. Due to energy stored in the load and returned to the source, or due to a non-linear load that distorts the wave shape of the current drawn from the source, the apparent power will be greater than the real power.

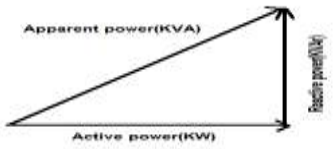

Fig. power factor Triangle

In above figure Active Power is the base line and is the real usable power measured in kW. Reactive power is the vertical or that part of the supply which causes the inductive load. There active power in is measured in kVAr (kilo volt-amperes reactive) Apparent Power is the hypotenuse. This is the resultant of the other two components and is measured in kVA

In an electric power system, a load with a low power factor draws more current than a load with a high power factor for the same amount of useful power transferred. The higher currents increase the energy lost in the distribution system, and require larger wires and other equipment. Because of the costs of larger equipment and wasted energy, electrical utilities will usually charge a higher cost to industrial or commercial customers where there is a low power factor.

Linear loads with low power factor (such as induction motors) can be corrected with a passive network of capacitors or inductors. Non-linear loads, such as rectifiers, distort the current drawn from the system. In such cases, active or passive power factor correction may be used to counteract the distortion and raise the power factor. The devices for correction of the power factor may be at a central substation, spread out over a distribution system, or built into power-consuming equipment.

IV. POWER FACTOR CORRECTION

In general, the term Power Factor represents the ratio of power actually used to the power actually supplied and varies with the losses encountered in a particular system. What are the causes of a low power factor? All inductive circuits within a distribution system require current for the purpose of the excitation of magnetic fields. This applies to:

- Induction motors
- Transformers
- Induction furnaces
- Welding plant
- Induction regulators
- Fluorescent lighting
- High Bay Discharge lighting
- Solenoids
- Electric Clocks

All require excitation currents to establish the magnetic field necessary for the function of each item of plant. Magnetic fields are a fact of electrical life and must be lived with.

Disadvantages without power factor Correction

The following are some of the disadvantages that occur because of the presence of inductive circuits. First of all, the calculation for energy required at the load is:

Watts (W) = Volts (V) x Amps (A) x Power Factor

Initially, as the power factor falls below unity the current in the system increases and in so doing causes the system.voltage decreases with the following effects:

1.Lower voltage on lighting will result in reduced lumen output.

2.Induction motors will run at reduced speeds (increased slip) which will necessitate increased currents to meet the required loads.

3.Because of the increased currents the I2R power loss increases in cables and windings leading to overheating and consequent reduction in equipment life.
4.Capacities of contacts, switches, circuit breakers and fuses may be exceeded with reduction in working life.
5.Efficiency as a whole suffers because more of the input is absorbed in meeting losses.

Advantages of Improved Power Factor

Having looked at the disadvantages let us now consider the advantages of an improved power factor.
1.Ensures that the rated voltage is applied to motors, lamps etc. to obtain optimum performance.
2.Decreased losses in circuits and cables.
3.Decreased losses in distribution transformers.
4.Ensure maximum power output of transformers is utilized and not used in making-up losses.
5.Enables existing transformers to carry additional load without overloading or the necessity of capital cost of new transformers to obtain the financial benefits which will result from lower maximum demand charges?

Simplified Graphical Presentation

Power factor is defined as the Cosine of the angle between W and VA shown above i.e. Cos (W/VA). Thus using trigonometry, for any two given figures, the rest can be worked out. So, if we know the consumption (kWh) and the reactive power (kVArh) we can calculate the Power Factor.

HOW TO IMPROVE POWER FACTOR

How do we approach the problem of improving the power factor? The usual method of making a system capacitive is achieved by introducing static capacitors which consist of chlorinated biphenyl impregnated paper dielectric elements in a sealed case, into the circuits either in the load-source (i.e. in a Sub-Station) or adjacent to the inductive plant.

Due to the fact that these electrostatic capacitors take a leading current they can be used to compensate for the lagging currents of the inductive circuits. When connected in circuit the capacitors act as a reservoir for energy which can be interchanged between the dielectric field of the capacitor and the magnetizing needs of the inductive plant.

Other methods of power factor correction include synchronous motors and synchronous condensers. Synchronous motors are excited by direct current and do not therefore impose a lagging current for magnetizing purposes on the system. These machines are intended primarily for situations where constant speeds are necessary over a wide range of loads, but in addition are able to operate at power factors between unity and 0.8 leading. This feature enables the system generally to benefit and an improved power factor results. However, unless the speed control properties are essential, the high cost of these machines would, for power factor correction purposes only, be quite uneconomic. Synchronous condensers are used purely for situations where larger amounts of corrective kVAr are required and carry no mechanical load. These are not usually considered for normal industrial purposes.

Example: If the consumption was 100,000 kWh and reactive consumption 65,000 kVArh, then, using the methodology earlier, the power factor will be 0.838. If we need to get this above 0.95 to prevent penalty charges, capacitance should be installed. This can be calculated by the installer.

Control of Capacitors : Control of static capacitor banks is carried out by means of contractor equipment which in turn is controlled by a sensing relay. Basically a single phase current and voltage supply is applied to the relay such that at unity power factor the current and voltage vectors are displaced by 90 degrees.
Changes in this angular displacement either lagging or leading are sensed by the relay which then switches the contractors which connect the reactive kVAr required for correction of the power factor, in or out of the system. Control relays can be single or multi-stage depending on the extent of the capacitor equipment in use.

In a smaller installation the capacitor bank would probably be located adjacent to the incoming supply. In progressively larger installations the capacitors would be positioned at different load centres i.e. adjacent to distribution boards. In practice however, it is more economical to group capacitor banks together, using multi-stage control, possibly in a sub-station (which also reduces the possibility of interference to relays).Individual correction should then be limited for example to motors of 37 kW and above. In this case control relays would not be required as capacitors would be switched in and out with the operation of the motor. Individual correction can also be an advantage with welding plant.

V. LEVEL OF CORRECTION

Having established that a need for power factor correction exists, what level of correction should be applied? This depends to a large extent on the geographical location of the plant in question. While improvements in plant efficiency are desirable it is the savings that accrue from lower tariff/contract charges that invariably dictate whether or not an installation shall be carried out. The power factor below which penalty

charges are applied varies according to the grid charging zone and is between 0.85 and 0.98. In general the considered optimum lies between 0.95 and 0.98 lagging. At this level both factors of tariff and efficiency are covered.

VI. PARACETIC CAPACITANCE

The parasitic capacitance was reduced using various methods like increasing the width of the kapton layer, placing an air layer between the windings and shifting the windings. This paper presents the method of EPC cancellation with an embedded ground layer placed so that the electric field energy will be shifted from the unwanted space to ground. The aim of this study, besides eliminating parasitic capacitance, is to maintain the self-capacitances of the windings as close as possible to their original values. Considering the other studies and their results, two different methods of parasitic capacitance reduction are combined to determine if it is possible to have an even lower EPC.The influence of the embedded ground layer on the whole structure is analyzed, considering the shape, position and thickness of the copper layer and modeling a multitude of structures with varying parameters. The obtained results are compared to ones determined with an energetic parameter method in order to evaluate their accuracy.

VII. DC-DC CONVERTERS

DC to DC converters are extremely important in battery-powered electronic devices, such as MP3 players and laptop computers. Those electronic devices often contain several sub circuits, each requiring a voltage level different than that supplied by the battery. Even worse, the voltage of a battery declines as its stored power is drained, so it does not output a constant voltage level. DC to DC converters offer a method of generating multiple controlled voltages from a single battery voltage, thereby saving space instead of using multiple batteries to supply different parts of the device. A boost converter is simply is a particular type of power converter with an output DC voltage greater than the input DC voltage. This type of circuit is used to 'step-up' a source voltage to a higher, regulated voltage, allowing one power supply to provide different driving voltages.(OR) Dc-dc power converters are employed in a variety of applications, including power supplies for personal computers, office equipment, spacecraft power systems, laptop computers, and telecommunications equipment, as well as dc motor drives. The input to a dc-dc converter is an unregulated dc voltage Vg. The converter produces a regulated output voltage V, having a magnitude (and possibly polarity) that differs from Vg. For example, in a computer off-line power supply, the 120 V or 240 V ac utility voltages is rectified, producing a dc voltage of approximately 170 V or 340 V, respectively. A dc-dc converter then reduces the voltage to the regulated 5 V or 3.3 V required by the processor ICs. Required , since cooling of inefficient power converters is difficult and expensive. The ideal dc-dc converter exhibits 100% efficiency; in practice, efficiencies of 70% to 95% are typically obtained. This is achieved using switched-mode, or chopper, circuits whose elements dissipate negligible power. Pulse-width modulation (PWM) allows control and regulation of the total output voltage. This approach is also employed in applications involving alternating current, including high-efficiency dc-ac power converters (inverters and power amplifiers), ac-ac power converters, and some ac-dc power converters (low-harmonic rectifiers).

FLY BACK CONVERTER : Fly-back converter is the most commonly used SMPS circuit for low output power applications where the output voltage needs to be isolated from the input main supply. The output power of fly-back type SMPS circuits may vary from few watts to less than 100 watts. The overall circuit topology of this converter is considerably simpler than other SMPS circuits. Input to the circuit is generally unregulated dc voltage obtained by rectifying the utility ac voltage followed by a simple capacitor filter. The circuit can offer single or multiple isolated output voltages and can operate over wide range of input voltage variation. In respect of energy-efficiency, fly-back power supplies are inferior to many other SMPS circuits but its simple topology and low cost makes it popular in low output power range. The commonly used fly-back converter requires a single controllable switch like, MOSFET and the usual switching frequency is in the range of 100 kHz. A two switch topology exists that offers better energy efficiency and less voltage stress across the switches but costs more and the circuit complexity also increases slightly. The present lesson is limited to the study of fly-back circuit of single switch topology.

VIII. SIMULATION RESULTS

VIII.1 SIMULATION RESULTS FOR PROPOSED PFC CIRCUIT

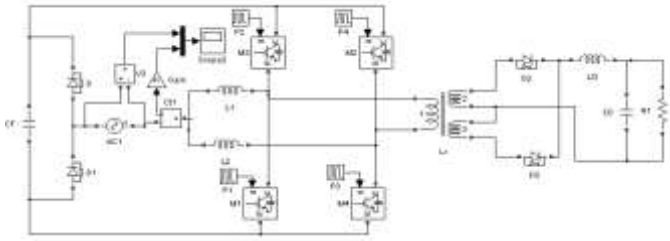

Fig : Simulation circuit diagram for proposed PFC circuit

VIII.2 WAVE FORMS FOR PROPOSED PFC CIRCUIT

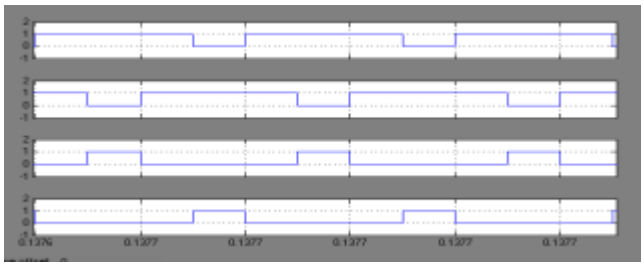

g Transformer input

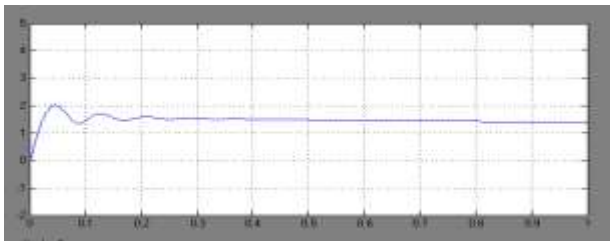

Time (t)

Fig: Output Current

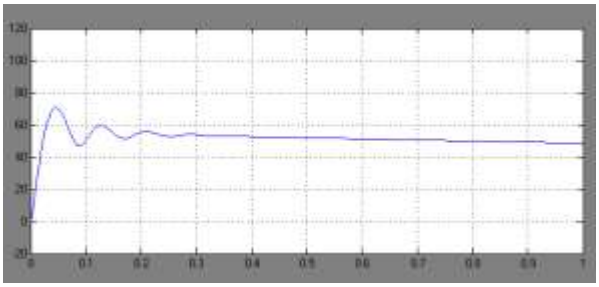

Fig Output Voltage

Time (t)

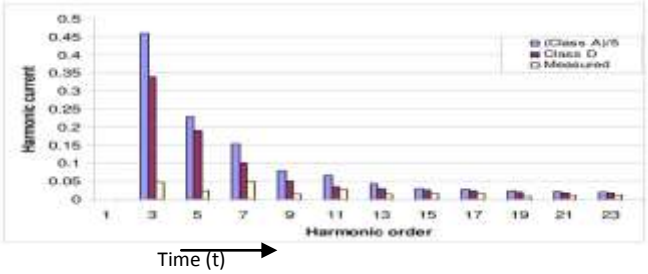

Time (t)

Fig Measured harmonics content o f the input current.

VIII.3 SIMULATION DIAGRAM FOR EMI AND PFC CONVERTER

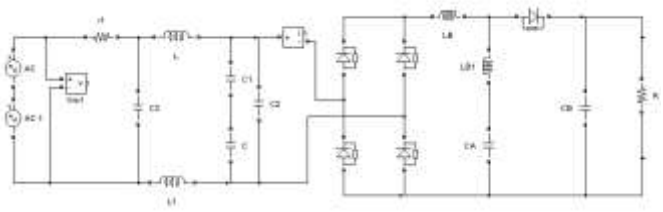

FigCircuit Diagram With Emi And PFC Converter

VIII.4 WAVE FORMS FOR EMI FILTER AND PFC CONVERTER

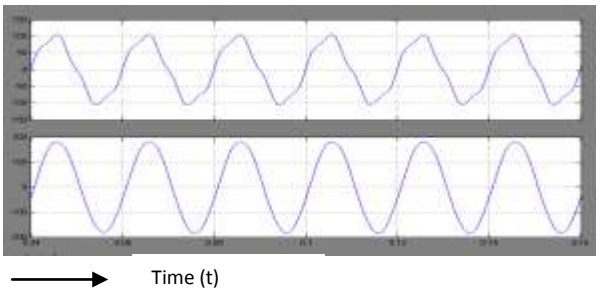

Input Voltage with noice and without noice

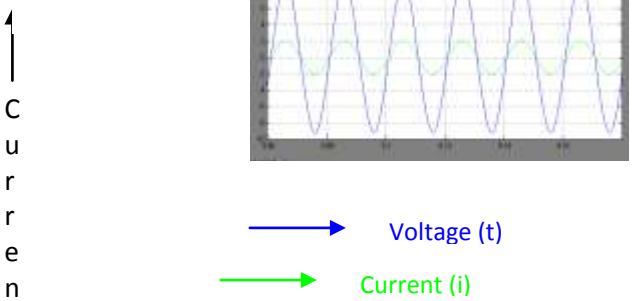

Fig Input Voltage and Current

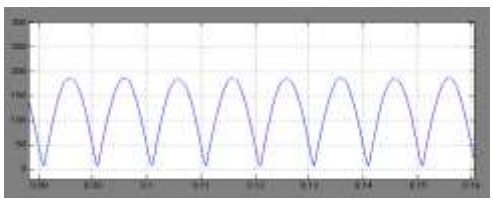

Fig Rectifier Output Voltage

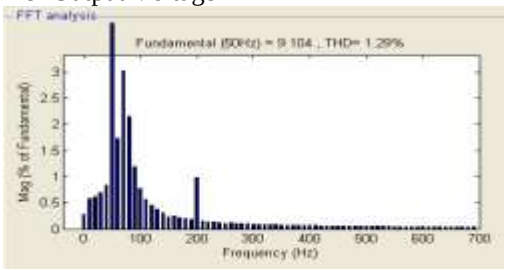

Fig FFT Analysis for Voltage

IX. APPLICATIONS OF PROPOSED CIRCUIT:

1) Power supply regulator

2) Digital logic inputs

3) Microprocessor inputs

X. CONCLUSION

Summary of the Work Done: The proposed method shapes the input current based on a quasi-active power factor correction (PFC) scheme. In this method, high power factor and low harmonic content are achieved by providing an auxiliary PFC circuit with a driving voltage which is derived from a third winding of the transformer of a cascaded dc/dc flyback converter. It eliminates the use of active switch and control circuit for PFC. The auxiliary winding provides a controlled voltage-boost function for bulk capacitor without inducing a dead angle in the line current. The input inductor can operates in DCM to achieve lower THD and high power factor. By properly designing the converter components, a tradeoff between efficiency and harmonic content can be established to obtain compliance with the regulation and efficiency as high as possible.

Scope Of Future Work

- Implementation of transformer less boost ac/dc converter with power factor correction.
- Battery charging load.
- X-Ray unit .
- Electrolyer plant.

BIBLIOGRAPHY

1. Hussain S. Athab "Power Factor Correction by using AC/DC Converter with Quasi-Active scheme" IEEE transactions on power electronics, vol. 25, no. 5, may2010.

2. Garcia, O. Cobos, J.A. Prieto, R. Alou, P. Uceda, J. Div. de Ingenieria "Single phase power factor correction: a survey", IEEE Trans. Power Electronics, Vol. 18, No. 3, May 2003.

3. C. Qian and K. Smedley, "A topology survey of single-stage power factor with a boost type input-current-shaper,"IEEE Trans. Power Electron.,vol. 16, no. 3, pp. 360–368, May 2001.

TEXT BOOKS:

[1]. C. Qian and K. Smedley, "A topology survey of single-stage power factor with a boost type input-current-shaper,"IEEE Trans. Power Electron.,vol. 16, no. 3, pp. 360–368, May 2001.

[2]. "Dr.Muhmmad H.Rashid", Power Electronics circuits, devises, and applications, "Dorling Kindersley publications",Third Edition.

[3]. M.S.Jamil Azgar, "power electronics" new age publications.

[4]. Dr.P.S.Bimbhra, "Power Electronics", khanna publications,2010,Fourth Edition .

International Journal of Modern Engineering Research (IJMER)

www.ijmer.com Vol. 3, Issue. 3, May.-June. 2013 pp-1748-1755 ISSN: 2249-6645

Low Bit Rate Design and Implementation of BPSK Demodulation on FPGA

Nehal.A.Ranabhatt[1], Sudhir Agarwal[2]

**(EC Department, L.C.Institute of Technology,Bhandu, India)*
*** (DCTD Department, Space Application center ,ISRO,Ahmedabad, India*

***ABSTRACT**: This paper présents extended Works on BPSK Modulation at Low Bit Rate and also presents Simulation results and FPGA implementation of BPSK demodulation at Low Bit Rate 1200 bits/second on Altera Stratix III Development Board. Here Binary Sequence ,Carrier Frequency and sampling frequency are user controllable in BPSK modulation that was designed already. So this paper present Design of BPSK Demodulation which demodulate pattern comes at output of BPSK modulation at 1200 bits/second. BPSK demodulation technique was analyzed using QuartusII 9.1 Complier. Design of BPSK Demodulation is completed using VHSIC (Very High Speed Integrated Circuit) Hardware Description Language (VHDL). In BPSK Design one Mega Function ROM is used .BPSK Demodulation was done in Continuous mode. Here system Performance is measured in Noise by measuring BER of system and comparing BER performance to Ideal Theoretical performance.*

***Keywords:** BPSK Demodulation, BPSK Modulation, Bits Per Second, Low Bit rate, FPGA, Bit Error Rate*

I. INTRODUCTION

The aim of the paper is to create a BPSK (Binary Phase Shift Keying) Demodulator which demodulates the Modulated signal comes from Modulator which has Bit rate 1200 bps. First we give Introduction about coherent BPSK Demodulation and then BPSK Demodulation is designed and Implemented on StratixIII FPGA. This paper presents extended work of RTL Design and Implementation of BPSK Modulation at Low Bit Rate .In this BPSK Modulation is Design and Implement at low Bit Rate 1200 bps[1].

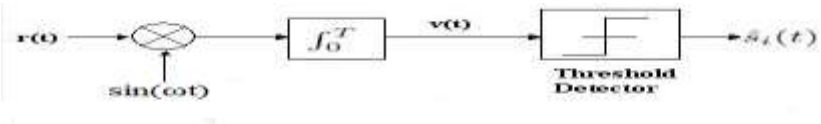

Fig.1 Coherent BPSK Demodulation[2]

In coherent detection technique the knowledge of the carrier frequency and phase must be known to the receiver. This can be achieved by using a PLL (phase lock loop) at the receiver. A PLL essentially locks to the incoming carrier frequency and tracks the variations in frequency and phase. For demonstration purposes we simply assume that the carrier phase recovery is done and simply use the generated reference frequency at the receiver (sin(ωt)).In the demodulator the received signal is multiplied by a reference frequency generator. The multiplied output is integrated over one bit period using an integrator. A threshold detector makes a decision on each integrated bit based on a threshold. Since an NRZ signaling format is used with equal amplitudes in positive and negative direction, the threshold for this case would be "0".[2] Simulation Results for BPSK Demodulation are carried out using ModelSim-Altera 6.5b (Quartus II 9.1).BPSK demodulation is designed for Altera Stratix III FPGA development Board and the device used is EP3SL150F1152c2.

II. CONCEPT OF BPSK DEMODULATION

In BPSK demodulator design modulated bit pattern is given as Input. Samples per bits are fetched in sequence. Then samples of one bit is fetched from Modulated Pattern, are multiplied with Positive and Negative carrier samples. Sum of multiplication output will store in two different arrays. Subtraction block will perform subtraction of two different array in which sum of multiplication output is stored. Comparison block do the comparison based on output of subtraction block.

www.ijmer.com Vol. 3, Issue. 3, May.-June. 2013 pp-1748-1755 ISSN: 2249-6645

Fig.2. Principal of BPSK Demodulation[2]

If subtraction of samples is grater then zero then bit"1" is detected and if subtraction of samples is less then zero then bit "0" is detected at output of demodulator.[2]

III. BPSK DEMODULATION DESIGN ON FPGA

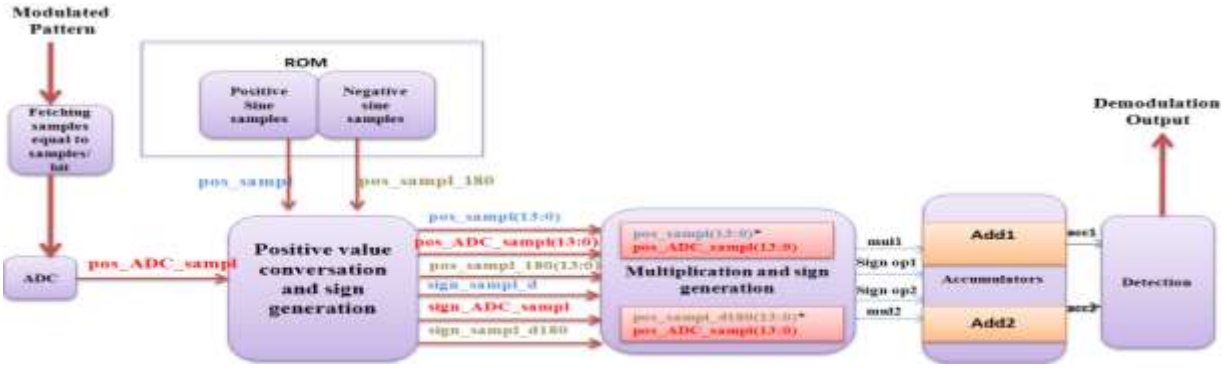

Fig.3.Principal of BPSK Demodulation FPGA

Fig.2 shows basic concept of BPSK demodulation on FPGA. First BPSK modulated output works as input of BPSK demodulation. Then Modulated output passed through analog to digital converter. Then samples per bit and samples of ROM are converted in Positive to Negative range. After this ADC samples are multiply with Positive and Negative samples of sine wave and Added in two different accumulator. Output of accumulators are compared with each other means if value of accumulator1 is grater then accumulator 2 then output is 1 else output is 0.

In this design we have used one Altera MegaFuctions of single port ROM used to store the 10,000 sine wave samples. Incoming clock from ADC is of 120 MHz and entire demodulation design operates on it.1 bit prevails for 1 lakh counter at 120 MHz so we have a counter that counts up to 1 lakh and rollovers. This counter used for generating the demod bit every 1 lakh count. Sine wave address generation logic generates the address for the sine wave samples ROM depending on the carrier frequency constant and sampling frequency constant and counter_10.

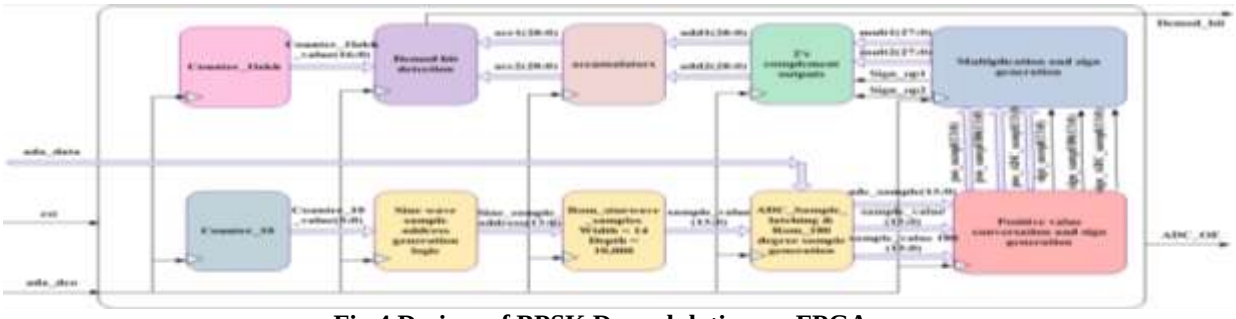

Fig.4.Design of BPSK Demodulation on FPGA

ADC samples are latched and sine wave sample fetched from ROM are latched. Also 180 degree phase shifted sample value is found by subtracting the sample from 3ffe and it is also latched. All the above 3 samples are in range 0 to x"3fffe" and binary offset format, where 0 is equal to x"1fff", positive numbers are in between x"2000 " to x"3ffe" and negative numbers are in between 0 to x"1fffe". For demodulation we bring them in range – x"1fff" to + x"1fff". This we do by converting the numbers in range 0 to x"1fff" and generating the sign bit equal to 1 if negative. Thus for numbers x"1fff" to x"3fffe" we subtract x"1fff" and generate sign bit 0 while for nos 0 to x"1ffe" we subtract them from x"1fff" and generate sign bit 1, indicating negative.Positive value

www.ijmer.com Vol. 3, Issue. 3, May.-June. 2013 pp-1748-1755 ISSN: 2249-6645

conversion and sign bit generation does the above process for all the 3 values.Multiplication and sign generation logic multiplies the positive ADC sample with positive sample and positive sample 180 degree shifted of the ROM. Sign of the two multiplication operations is generated depending on the sign of the samples determined in the previous process.For accumulation purpose we convert the two multiplied values in 2's complement form using the sign bit of each values.Then both the values are added to their respective accumulators. On every 1 lakh count the two accumulator values are compared, if accumulator 1 is greater than accumulator 2 then the bit is decoded as 1 else 0.

IV. SIMULATION RESULTS FOR BPSK DEMODULATION

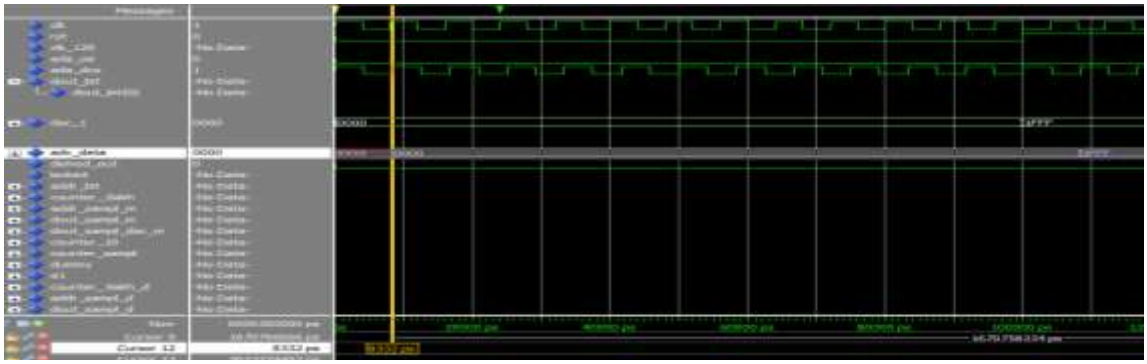

Fig. 5. Reason for getting 1 Bit Delay in Demodulation Output

Fig .5 shows that when Demodulation will start up to one bit ADC data will remain undefined so up 1 bit Demodulation operation can not be started.so we get 1 Bit Delay at output of BPSK Demodulation.

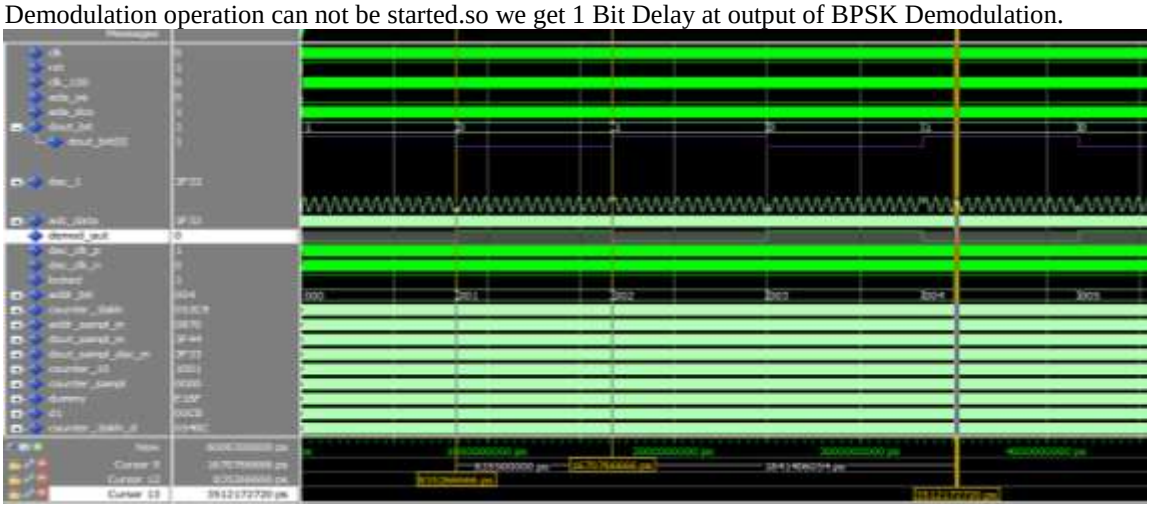

Fig 6. BPSK Demodulation output when fs=12MHz, fc=18K,br=1200

Fig .6 shows BPSK demodulation when fs=12MHz,fc=18KHz and Br=1200 bps.

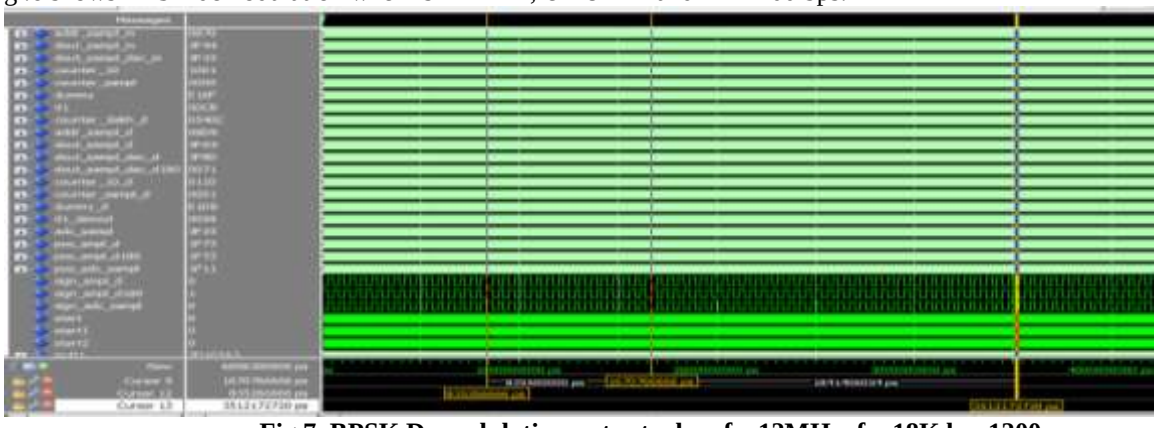

Fig 7. BPSK Demodulation output when fs=12MHz, fc=18K,br=1200

Fig .7 shows remaining signal at output of BPSK Demodulation as shown in Fig.6.

www.ijmer.com Vol. 3, Issue. 3, May.-June. 2013 pp-1748-1755 ISSN: 2249-6645

Fig 8. BPSK Demodulation output when fs=12MHz, fc=18K,br=1200

Fig .8 shows Debugging at one sample. Here after all calculation according to program acc1>acc2 so demod_bit will 0 that can be proved from simulation results.

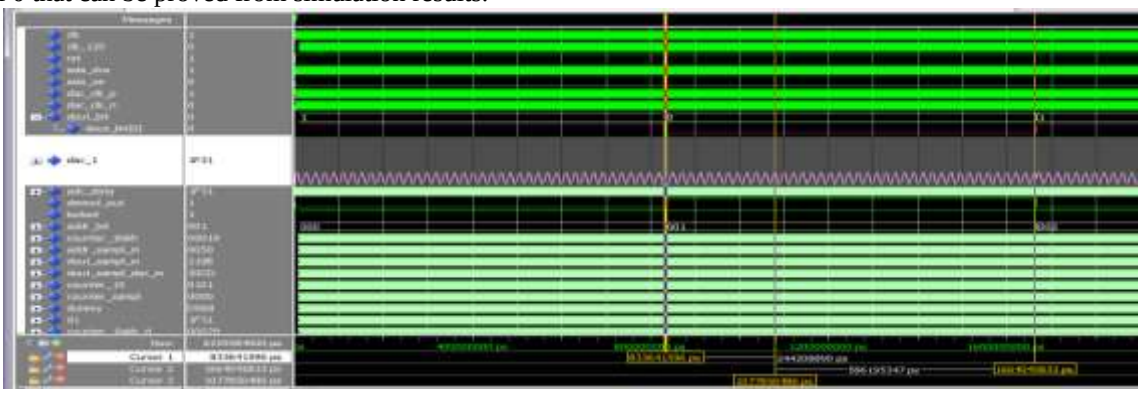

Fig 9. BPSK Demodulation output when fs=12MHz, fc=48K,br=1200

Fig 9. shows BPSK demodulation when fs=12MHz,fc=48KHz and Br=1200 bps.

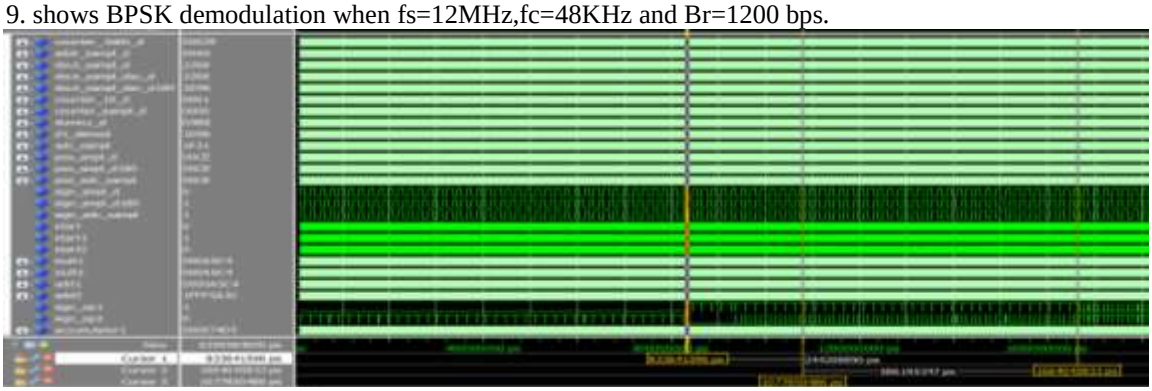

Fig 10. BPSK Demodulation output when fs=12MHz, fc=48K,br=1200

Fig.10 shows remaining signal at output of BPSK Demodulation as shown in Fig.9.

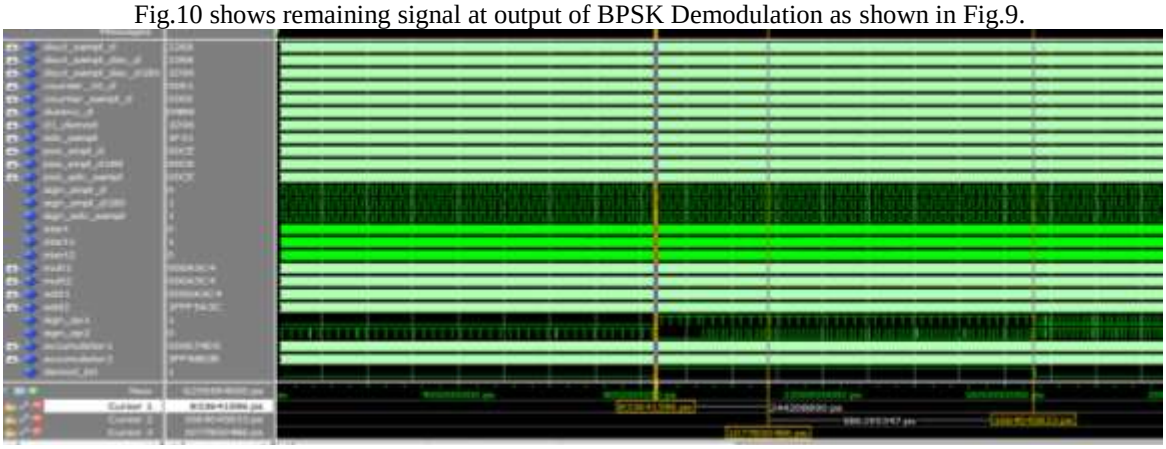

www.ijmer.com Vol. 3, Issue. 3, May.-June. 2013 pp-1748-1755 ISSN: 2249-6645

Fig 11. BPSK Demodulation output when fs=12MHz, fc=18K,br=1200

Fig .11 shows Debugging at one sample. Here after all calculation according to program acc1<acc2 so demod_bit will 0 that can be proved from simulation results.

V. REAL TIME RESULTS FOR BPSK DEMODULATION

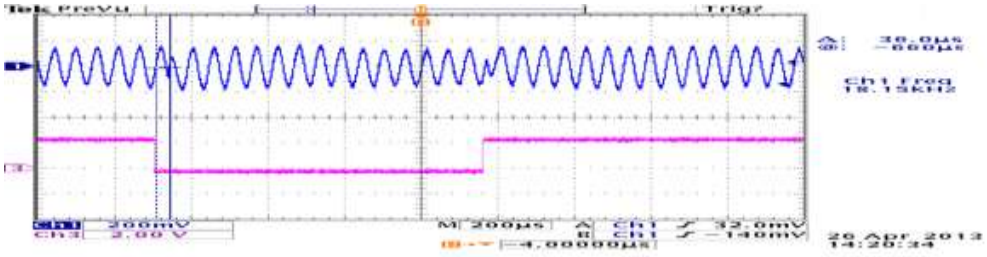

Fig.12 BPSK Demodulation Output On Oscilloscope When fs=12MHz fc=18KHz

Fig13 Experimental set up for BPSK Demodulation When fs=12MHz fc=18KHz

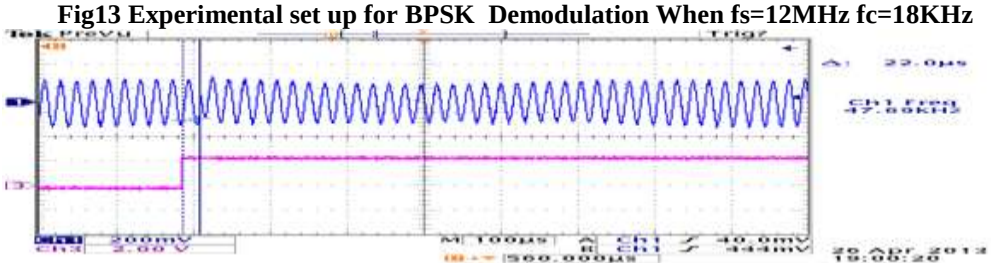

Fig.14 BPSK Demodulation oscilloscope When fs=12MHz fc=18KHz

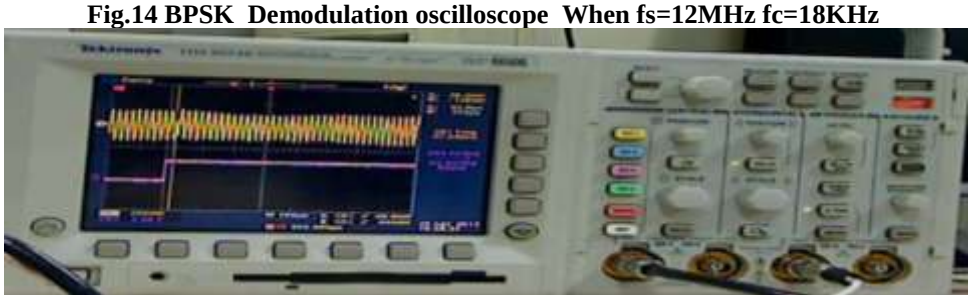

Fig.15 Experimental set up for BPSK Demodulation When fs=12MHz fc=48KHz

Fig 12,14, shows real time results on Oscilloscope for different carrier frequency 18k,48k respectively.Fig13,15 shows experimental set uo for BPSK Demodulation at low Bit Rate 1200bps with carrier frequency 18k,48k respectively.

VI. CALCULATION OF BIT ERROR RATE

To calculate Bit error rate of BPSK system first we add 20MHZ noise in BPSK Modulation spectrum. Then take fc+fm component that is 20.048MHz as center frequency. After that we take plain carrier and measure C/N0 for diffent level. After getting different C/N0 fom this value we can obtain value of Eb/N0 and then we can plot BER versus Eb/No curve which will show the performance of system. Here we compare system performance with standard theoretical value BER curve. C/N0 can be measured in dbc/Hz means it will measure carrier power in 1Hz noise bandwidth and here we take -20dbm reference level for C/N0 calculation. Resolution bandwidth is 500Hz.Eb/N0 can obtain from following formula.

Eb/N0(db)=10 log(C/N0)-10 log(1200)

Spectrum Results for Calculation of Different C/N0

www.ijmer.com Vol. 3, Issue. 3, May.-June. 2013 pp-1748-1755 ISSN: 2249-6645

Fig.16 Spectrum when value of C/N0=36.71dBc/Hz

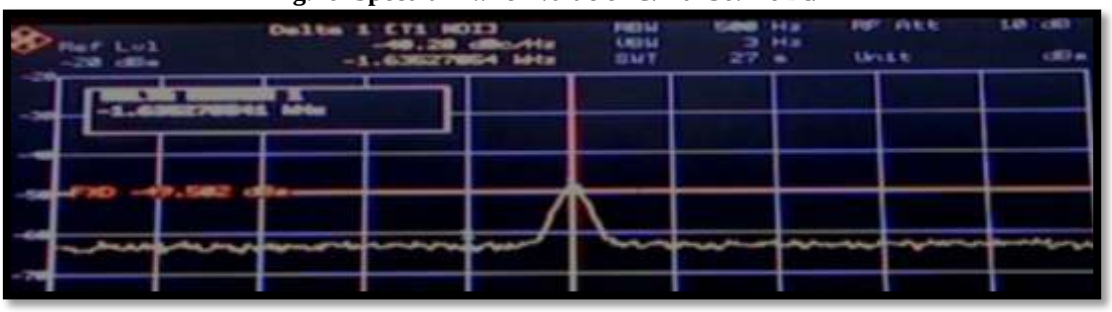

Fig. 17 Spectrum when value of C/N0=36.71dBc/Hz

Fig. 18 Spectrum when value of C/N0=36.71dBc/Hz

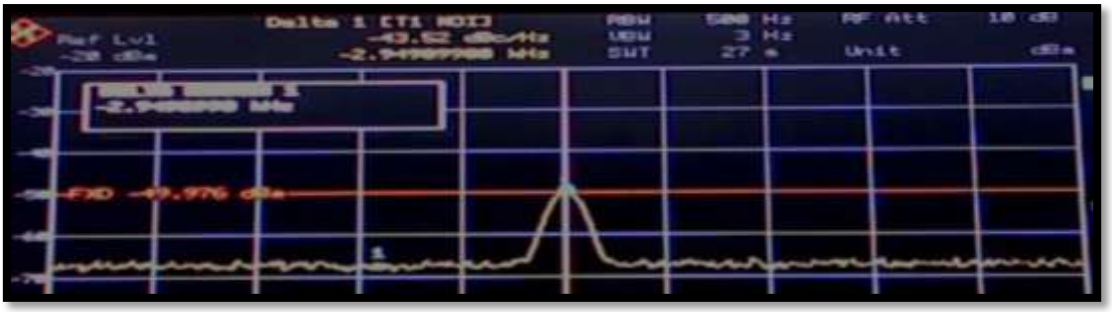

Fig. 19 Spectrum when value of C/N0=36.71dBc/Hz

Fig 16,17,18,19 shows practically measured C/N0 for different Bit Error Rate and then we compare these Results with Theoretical BER Value to Measure System Performance.

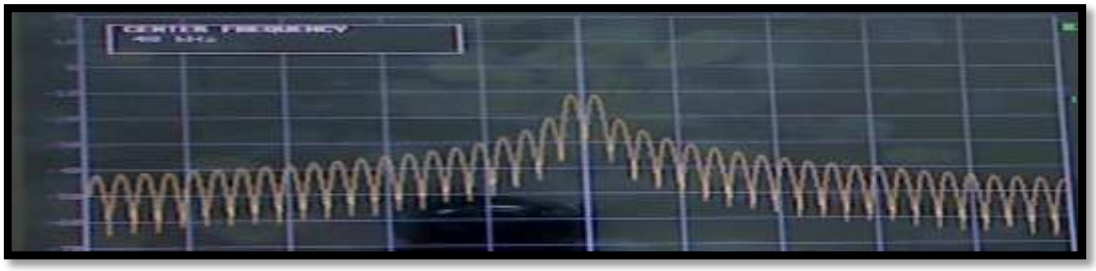

Fig. 20 BPSK Modulation Spectrum

www.ijmer.com Vol. 3, Issue. 3, May.-June. 2013 pp-1748-1755 ISSN: 2249-6645

Above Fig shows BPSK spectrum on spectrum Analyzer with center frequency 48KHz

Table 5.3.1. Calculation on Bit Error Rate

	Theoretical value		Practical value	
BER	**Eb/No**	**C/No(dBc/Hz)**	**Eb/No**	**C/No(dBc/Hz)**
10^{-8}	12	42.7	12.73	43.52
10^{-6}	10.2	41.1	11.6	42.39
10^{-4}	8.2	38.9	9.41	40.20
10^{-2}	4	34.7	5.92	36.71

BER versus Eb/No Curve

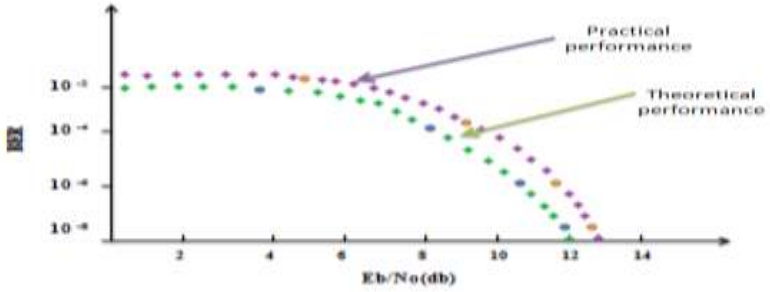

Fig. 21. BER vs Eb/No curve

Fig.21 shows BER for BPSK system.so form above graph we can conclude that system performance is approximately 1dB poor then theoretical value and we ger BER curve higher then theoretical value.

VII. BPSK MODEM IN NOISY ENVIRONMENT

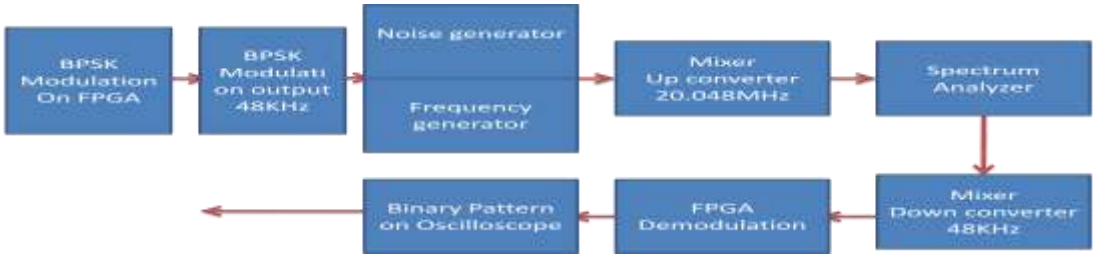

Fig. 22. Block Diagram for BPSK MODEM setup in Noisy Environmen Fig. Block Diagram for BPSK MODEM setup in Noisy Environment

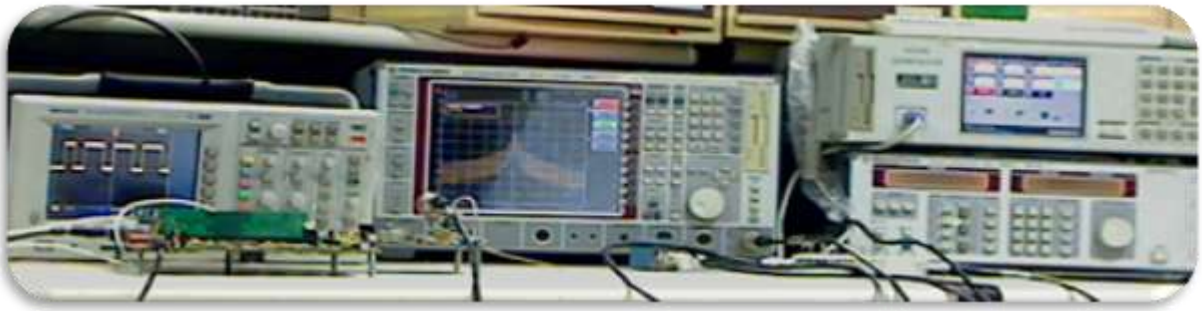

Fig. 23 Experimental setup for BPSK MODEM setup in Noisy Environment Fig. Block Diagram for BPSK MODEM setup in Noisy Environment

Fig 23 shows set up of BPSK Modem in Noisy Environment in which First at output of BPSK Modulation we add Noise and up covert carrier frequency to 20.048MHz .After we calculate BER in Noise environment and to Know system performance. Then carrier frequency down converted using Mixture and output of Mixer givern to FPGA for Demodulation and Output of Demodulation is shown in Oscilloscope with Binary Pattern 101010

VIII. CONCLUSION

In this paper BPSK Demodulation is Implemented on StratixIII FPGA with low Bit rate 1200 bps. In BPSK Modulation carrier frequency, sampling frequency and Input data Pattern are user variable. On Demodulation side Coherent Demodulation is implemented. In which center frequency will not suppressed

www.ijmer.com Vol. 3, Issue. 3, May.-June. 2013 pp-1748-1755 ISSN: 2249-6645

during transmission and phase value of carrier are known so there is no need to recover carrier at Demodulation side. Outputs of BPSK MODEM are shown in Oscilloscope. After Designing BPSK Modem Noise added in BPSK Modulation Output from Noise generator to check system performance in Noisy channel and measure Bit error Rate so that system performance can be Measure in Noisy environment. After observing BER calculation table we can observe that Comparing practical system performance to theoretical value system performance is approximately 1dB down then theoretical standard value. BPSK Modem Design Checked in Noisy Environment and It works.

REFERENCES

[1]. Nehal.A.Ranabhatt, Sudhir Agarwal,RaghunadhBhattar , Priyesh.P.Gandhi,"Design and Implementation of Numerically Controlled Oscillator on FPGA", IEEE xplore

[2]. Nehal.A.Ranabhatt, SudhirAgarwal, Priyesh.P.Gandhi,"RTL Design and Implementation of BPSK Modulation at Low Bit Rate", International Journal of Engineering Research & Technology,ISSN:2278-0181, Vol.2, Issue 28, Feb 2012.

[3]. Nehal.A.Ranabhatt, SudhirAgarwal, Priyesh.P.Gandhi," Design and Simulation of BPSK Demodulation at Low Bit Rate", International Journal of Engineering Research and Development, e-ISSN: 2278-067X, p-ISSN: 2278-800X,Volume 6, Issue 7 (April 2013), PP. 28-31

[4]. Mehmet Sonmez and Ayhan Akbal "FPGA-Based BASK and BPSK Modulators Using VHDL: Design, Applications and Performance Comparison for Different Modulator Algorithms" In March 2012, International Journal of Computer Applications (0975 – 8887) Volume 42– No.13, March 2012.

[5]. S.O.Popescu and A.S. Gontean "Performance comparison of the BPSK and QPSK Modulation Techniques on FPGA" 17th International Symposium for Design and Technology in Electronic Packaging (SIITME) 2011 IEEE .

[6].] S.O. Popescu, A.S.Gontean and G.Budura "BPSK System on Spartan 3E FPGA" SAMI 2012 • 10th IEEE Jubilee International Symposium on Applied Machine Intelligence and Informatics • January 26-28, 2012.

[7]. Michal Kováč "BPSK, QPSK MODULATOR Simulation Model"VUT Faculty of electrical engineering and communication, 2006. 82 s.

International Journal of Modern Engineering Research (IJMER)
www.ijmer.com Vol. 3, Issue. 3, May.-June. 2013 pp-1756-1762 ISSN: 2249-6645

Improving the implementation of new approach for Data Privacy Preserving in Data Mining using slicing

Ravindra S. Wanjari Prof. Devi Kalpana

P.G. Scholar Vivekanand Institute of Technology and Science , Karimnagar , Andhra Pradesh

Assistant Professor, Computer Science and Engineering Department

ABSTRACT: *Some different anonymization techniques, such as generalization and bucketization, have been designed for privacy preserving micro data publishing. Recent work has shown that generalization loses considerable amount of information, especially for high dimensional data. Bucketization, on the other hand, does not prevent membership disclosure and does not apply for data that do not have a clear separation between quasi-identifying attributes and sensitive attributes. In this paper, we present a novel technique called slicing, which partitions the data both horizontally and vertically. We show that slicing preserves better data utility than generalization and can be used for membership disclosure protection. Another important advantage of slicing is that it can handle high-dimensional data.*

*We show how slicing can be used for attribute disclosure protection and develop an efficient algorithm (**An algorithm is a procedure or formula for solving a problem.**) for computing the sliced data that obey the diversity requirement.*

*We show how slicing can be used for attribute disclosure (**uncover**) protection and develop an efficient algorithm for computing the sliced data that obey the '-diversity requirement. Our workload experiments confirm that slicing preserves better utility than generalization and is more effective than bucketization in workloads involving the sensitive attribute. Our experiments also demonstrate that slicing can be used to prevent membership disclosure. Slicing gives us a higher security as well as open source environment. i.e. on integration of project.*

Keywords :—*Privacy preservation, data anonymization, data publishing, data security*

I. INTRODUCTION

Privacy Preserving publishing of microdata has been studied extensively in recent years. Microdata contains records each of which contains information about an individual entity, such as a person, a household, or an organization. Several microdata anonymization techniques have been proposed. The most popular ones are generalization for k-anonymity and bucketization [17] for 'ℓ-diversity [25].

In both approaches, attributes are partitioned into three categories:

1) Some attributes are identifiers that can uniquely identify an individual, such as Name or Social Security Number

2) Some attributes are Quasi Identifiers (QI), which the adversary may already know (possibly from other publicly available databases) and which, when taken together, can potentially identify an individual, e.g., Birthdate, Sex, and Zipcode;

3) some attributes are Sensitive Attributes (SAs), which are unknown to the adversary and are considered sensitive, such as Disease and Salary.

In both generalization and bucketization, one first removes identifiers from the data and then partitions tuples into buckets. The two techniques differ in the next step. Generalization transforms the QI-values in each bucket into "less specific but semantically consistent" values so that tuples in the same bucket cannot be distinguished by their QI values. In bucketization, one separates the SAs from the QIs by randomly permuting the SA values in each bucket. It has been shown [1], [16], that generalization for k anonymity losses considerable amount of information, especially for high-dimensional data. This is due to the following three reasons. First, generalization for k-anonymity suffers from the curse of dimensionality.

In order for generalization to be effective, records in the same bucket must be close to each other so that generalizing the records would not lose too much information. However, in high dimensional data, most data points have similar distances with each other, forcing a great amount of generalization to satisfy k-anonymity even for relatively small k's. Second, in order to perform data analysis or data mining tasks on the generalized table, the data analyst has to make the uniform distribution assumption that every value in a

generalized interval/set is equally possible, as no other distribution assumption can be justified. This significantly reduces the data utility of the generalized data. Third, because each attribute is generalized separately, correlations between different attributes are lost. In order to study attribute correlations on the generalized table, the data analyst has to assume that every possible combination of attribute values is equally possible. This is an inherent problem of generalization that prevents effective analysis of attribute correlations. While bucketization [26], [17] has better data utility than generalization, it has several limitations. First, bucketization does not prevent membership disclosure . Because bucketization publishes the QI values in their original forms, an adversary can find out whether an individual has a record in the published data or not.

II. Privacy Requirements

Several types of information disclosure in microdata publishing have been identified in the literature [6, 16]. An important type of information disclosure is *attribute disclosure*. Attribute disclosure occurs when a sensitive attribute value is associated with an individual. This is different from both *identity disclosure* (i.e., linking an individual to a record in the database) and membership *disclosure* [7, 23] (i.e., learning whether an individual is included in the database). As in [5], this paper considers *attribute disclosure*. *k*-Anonymity [25 , 26] (requiring each equivalence class contains at least *k* records) aims at preventing identity disclosure. Because identity disclosure leads to attribute disclosure (once the record is identified, its sensitive value is immediately revealed), *k*-anonymity can partly prevent attribute disclosure. But because attribute disclosure can occur without identity disclosure [21, 29] (for example, when all records in the equivalence class have the same sensitive value) , *k*-anonymity does not prevent attribute disclosure. Diversity [21] remedies the above limitations of *k*-anonymity by requiring that in any equivalence class, each sensitive value can occur with a frequency of at most 1/_. While there are several other definitions of _-diversity such as recursive (*c*, _) –diversity , the above probabilistic interpretation is the most widely used one in the literature.

A similar privacy requirement is the (*α, k*) - anonymity [29]. _-Diversity ensures that the probability of inferring the sensitive value is bounded by 1/_. However, this confidence bound may be too strong for some sensitive values (e.g., a common form of disease) and too weak for some other sensitive values (e.g., a rare form of cancer). *t*-Closeness [19] remedies the limitations of _-diversity , by requiring the sensitive attribute distribution in each equivalence class to be close to that in the overall data. A closely-related privacy requirement is the template - based privacy [27] where the probability of each sensitive value is bounded separately. Similar to *t*-closeness, semantic privacy [5] also tries to bound the difference between the baseline belief (i.e., the distribution in the overall population) and the posterior belief (i.e., the distribution in each equivalence class). Unlike *t*-closeness that uses Earth Mover's Distance (EMD) (which is an *additive* measure), semantic privacy uses a *multiplicative* measure which bounds the ratio of the probability of each sensitive value in each equivalence class and that in the overall distribution. One advantage of semantic privacy is that it gives a bound on the adversary's knowledge gain: classification accuracy is bounded when semantic privacy is satisfied. Semantic privacy is quite strong and it does not capture semantic meanings of sensitive values as EMD.

III. Utility Measures

It is important that the anonymized data can be used for data analysis or data mining tasks. Otherwise, one can simply remove all quasi-identifiers and output the trivially-anonymized data, which provides maximum privacy. Also, it is unclear what kinds of data mining tasks will be performed on the anonymized data. Otherwise, instead of publishing the anonymized data, one can simply perform the data mining tasks and output their results. Because of this, most utility measures are workload-independent, i.e., they do not consider any particular data mining workload. For example, the utility of the anonymized data has been measured by the number of generalization steps, the average size of the equivalence classes [21] , the discernibility metric (DM) [4] which sums up the squares of equivalence class sizes, and the KL-divergence between the reconstructed distribution and the true distribution for all possible quasi-identifier values [13]. Several researchers have proposed to evaluate the utility of the anonymized data in terms of data mining workloads , such as classification and aggregate query answering (A comprehensive discussion on the privacy-preserving data publishing is given in [9]). Classification accuracy on the anonymized data has been evaluated in [18, 28, 10, 27, 5]. The main results from these studies are : (1) anonymization algorithms can be tailored to optimize the performance of specific data mining workloads and (2) utility from classification is bounded when attributed disclosure is prevented. Aggregate query answering has also been used for evaluating data utility [30, 14, 24].

IV. Proposed Method

In this paper, we present a novel technique called slicing for privacy-preserving data publishing. Our contributions include the following. First, we introduce slicing as a new technique for privacy preserving data publishing. Slicing has several advantages when compared with generalization and bucketization. It preserves better data utility than generalization. It preserves more attribute correlations with the SAs than bucketization. It can also handle high-dimensional data and data without a clear separation of QIs and SAs.

Second, we show that slicing can be effectively used for preventing attribute disclosure, based on the privacy requirement of ℓ -diversity. We introduce a notion called ℓ- diverse slicing, which ensures that the adversary cannot learn the sensitive value of any individual with a probability greater than 1/ℓ, We develop an efficient algorithm for computing the sliced table that satisfies ℓ-diversity. Our algorithm partitions attributes into columns, applies column generalization, and partitions tuples into buckets. Attributes that are highly correlated are in the same column; this preserves the correlations between such attributes. The associations between uncorrelated attributes are broken; this provides better privacy as the associations between such attributes are lessfrequent and potentially identifying.Fourth, we describe the intuition behind membership disclosure and explain how slicing prevents membership disclosure. A bucket of size k can potentially match k^C tuples where c is the number of columns. Because only K of the k^C tuples are actually in the original data, the existence of the other k^C - k tuples hides the membership information of tuples in the original data. Finally, we conduct extensive workload experiments. Our results confirm that slicing preserves much better data utility than generalization. In workloads involving the sensitive attribute, slicing is also more effective than bucketization. Our experiments also show the limitations of bucketization in membership disclosure protection and slicing remedies these limitations. We also evaluated the performance of slicing in anonymizing the Netflix Prize data set.

V. Proposed techniques used

In the proposed work we have used slicing technique and compared it to generalization and bucketization

V.1 Slicing : Slicing first partitions attributes into columns. Each column contains a subset of attributes. This vertically partitions the table. For example, the sliced table in Table 6 contains two columns: the first column contains { Age; Sex} and the second column contains {Zipcode; Disease}. The sliced table shown in Table 5 contains four columns, where each column contains exactly one attribute. Slicing also partition tuples into buckets. Each bucket contains a subset of tuples. This horizontally partitions the table. For example, both sliced tables in Tables 5 and 6 contain two buckets, each containing four tuples. Within each bucket, values in each column are randomly permutated to break the linking between different columns. For example, in the first bucket of the sliced table shown in Table 6, the values {(22,M) , (22,F) (33,F) , (52,F)} are randomly permutated and the values{(47906, dyspepsia),(47906,flu) , (47905, flu), (47905, bronchitis)} are randomly permutated so that the linking between the two columns within one bucket is hidden.

V.1.1 Results:

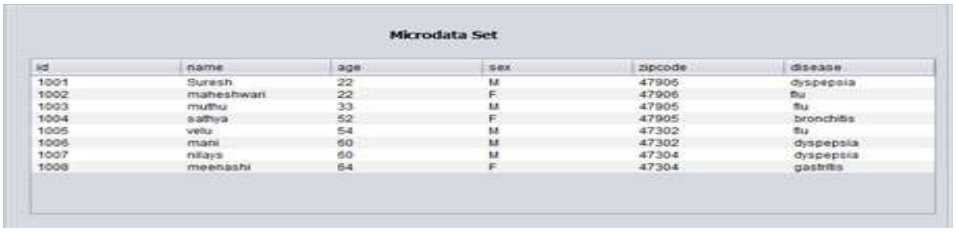

Fig 1 Original Microdata Table

Fig 2 The Generalized Table

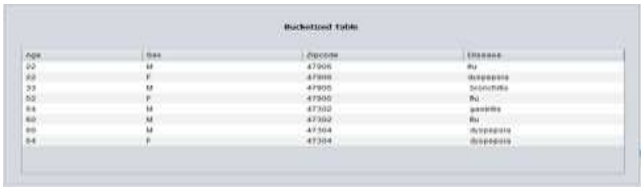

Fig 3 The Bucketized Table

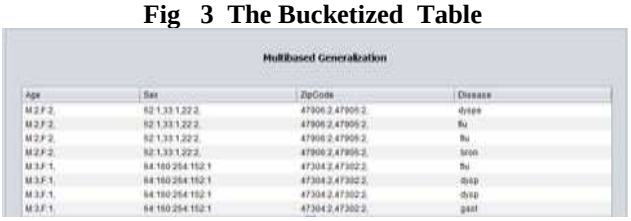

Fig 4 Multiset based generalization

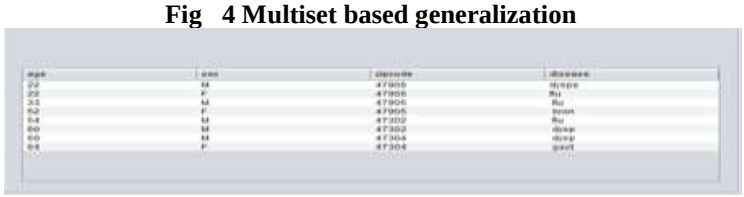

Fig 5 One attribute per column slicing

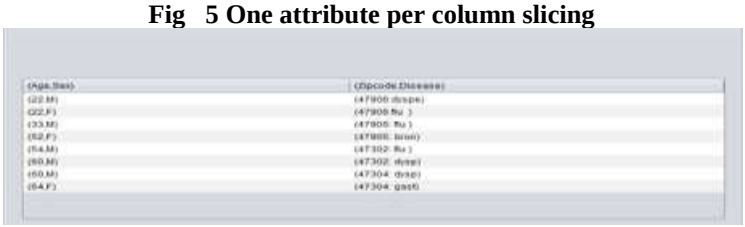

Fig 6 The sliced Table

VI. COMPARITATIVE RESULTS

Two popular anonymization techniques are generalization and bucketization. Generalization replaces a value with a "less-specific but semantically consistent" value. The main problems with generalization are: 1) it fails on high-dimensional data due to the curse of dimensionality and it causes too much information loss due to the uniform-distribution assumption .Bucketization first partitions tuples in the table into buckets and then separates the quasi identifiers with the sensitive attribute by randomly permuting the sensitive attribute values in each bucket. The anonymized data consist of a set of buckets with permuted sensitive attribute values. In particular, bucketization has been used for anonymizing high-dimensional data [. However, their approach assumes a clear separation between QIs and SAs. In addition, because the exact values of all QIs are released, membership information is disclosed.

VII. MEMBERSHIP DISCLOSURE PROTECTION

In this section, we analyze how slicing can provide membership disclosure protection. Bucketization. Let us first examine how an adversary can infer membership information from bucketization. Because bucketization releases each tuple's combination of QI values in their original form and most individuals can be uniquely identified using the QI values, the adversary can determine the membership of an individual in the original data by examining whether the individual's combination of QI values occurs in the released data. Slicing. Slicing offers protection against membership disclosure because QI attributes are partitioned into different columns and correlations among different columns within each bucket are broken. Consider the sliced table in Table 1f. The table has two columns. The first bucket is resulted from four tuples; we call them the originaltuples. The bucket matches altogether 42 ¼ 16 tuples, 4 original tuples and 12 that do not appear in the original table. We call these 12 tuples fake tuples. Given any tuple, if it has no matching bucket in the sliced table, then we know for sure that the tuple is not in the original table. However, even if a tuple has one or more matching bucket, one cannot tell whether the tuple is in the original table, because it could be a fake tuple. We propose two quantitative measures for the degree of membership protection offered by slicing.

The first is the fake-original ratio (FOR), which is defined as the number of fake tuples divided by the number of original tuples. Intuitively, the larger the FOR, the more membership protection is provided. A sliced bucket of size k can potentially match kc tuples, including k original tuples and kc _ k fake tuples; hence, the FOR is kc_1 _ 1. When one has chosen a minimal threshold for the FOR, one can choose k and c appropriately to satisfy the threshold. The second measure is to consider the number of matching buckets for original tuples and that for fake tuples. If they are similar enough, membership information is protected because the adversary cannot distinguish original tuples from fake tuples. Since the main focus of this paper is attribute disclosure, we do not intend to propose a comprehensive analysis for membership disclosure protection. In our experiments (Section 6), we empirically compare bucketization and slicing in terms of the number of matching buckets for tuples that are in or not in the original data. Our experimental results show that slicing introduces a large number of tuples in D and can be used to protect membership information. Generalization. By generalizing attribute values into "less-specific but semantically consistent values," generalization offers some protection against membership disclosure. It was shown in [27] that generalization alone (e.g., used with k-anonymity) may leak membership information if the target individual is the only possible match for a generalized record. The intuition is similar to our rationale of fake tuple. If a generalized tuple does not introduce fake tuples (i.e., none of the other combinations of values are reasonable), there will be only one original tuple that matches with the generalized tuple and the membership information can still be inferred. Nergiz et al. [27] defined a large background table as the set of all "possible" tuples in order to estimate the probability whether a tuple is in the data or not (_-presence). The major problem with [27] is that it can be difficult to define the background table and in some cases the data publisher may not have such a background table. Also, the protection against membership disclosure depends on the choice of the background table. Therefore, with careful anonymization, generalization can offer some level of membership disclosure protection.

VIII. RELATED WORK

Two popular anonymization techniques are generalization and bucketization. Generalization [28], [30], [29] replaces a value with a "less-specific but semantically consistent" value. Three types of encoding schemes have been proposed for generalization: global recoding, regional recoding, and local recoding. Global recoding [18] has the property that multiple occurrences of the same value are always replaced by the same generalized value. Regional record [19] is also called multidimensional recoding (the Mondrian algorithm) which partitions the domain space into nonintersect regions and data points in the same region are represented by the region they are in. Local recoding [36] does not have the above constraints and allows different occurrences of the same value to be generalized differently. The main problems with generalization are: 1) it fails on high-dimensional data due to the curse of dimensionality [1] and 2) it causes too much information loss due to the uniform-distribution assumption [34]. Bucketization [34], [26], [17] first partitions tuples in the table into buckets and then separates the quasi identifiers with the sensitive attribute by randomly permuting the sensitive attribute values in each bucket. The anonymized data consist of a set of buckets with permuted sensitive attribute values. In particular, bucketization has been used for anonymizing high-dimensional data [12]. However, their approach assumes a clear separation between QIs and SAs. In addition, because the exact values of all QIs are released, membership information is disclosed. A detailed comparison of slicing with generalization and bucketization is in Sections 2.2 and 2.3, respectively. Slicing has some connections to marginal publication [16]; both of them release correlations among a subset of attributes. Slicing is quite different from marginal publication in a number of aspects. First, marginal publication can be viewed as a special case of slicing which does not have horizontal partitioning. Therefore, correlations among attributes in different columns are lost in marginal publication. By horizontal partitioning, attribute correlations between different columns (at the bucket level) are preserved. Marginal publication is similar to overlapping vertical partitioning, which is left as our future work . Second, the key idea of slicing is to preserve correlations between highly correlated attributes and to break correlations between uncorrelated attributes thus achieving both better utility and better privacy. Third, existing data analysis (e.g., query answering) methods can be easily used on the sliced data. Recently, several approaches have been proposed to anonymize transactional databases. Terrovitis et al. [31] proposed the km-anonymity model which requires that, for any set of m or less items, the published database contains at least k transactions containing this set of items. This model aims at protecting the database against an adversary who has knowledge of at most m items in a specific transaction. There are several problems with the kmanonymity model: 1) it cannot prevent an adversary from learning additional items because all k records may have some other items in common; 2) the adversary may know the absence of an item and can potentially identify a particular transaction; and 3) it is difficult to set an appropriate m value. He and Naughton [13] used kanonymity as the privacy model and developed a local recoding method for anonymizing transactional databases. The k-anonymity model also suffers from the first two problems above. Xu et al. [35] proposed an approach that combines k-anonymity and '-diversity but their approach considers a clear separation of the quasi identifiers and the sensitive attribute. On

the contrary, slicing can be applied without such a separation. Existing privacy measures for membership disclosure protection include differential privacy [6], [7], [9] and _- presence [27]. Differential privacy [6], [7], [9] has recently received much attention in data privacy. Most results on differential privacy are about answering statistical queries, rather than publishing microdata. A survey on these results can be found in [8]. On the other hand, _-presence [27] assumes that the published database is a sample of a large public database and the adversary has knowledge of this large database. The calculation of disclosure risk depends on the choice of this large database. Finally, on attribute disclosure protection, a number of privacy models have been proposed, including '-diversity [25], ð_; kÞ-anonymity [33], and t-closeness [21]. A few others consider the adversary's background knowledge [26], [4], [22], [24]. Wong et al. [32] considered adversaries who have knowledge of the anonymization method.

IX. Conclusions And Future Work

This paper presents a new approach called slicing to privacy preserving microdata publishing. Slicing overcomes the limitations of generalization and bucketization and preserves better utility while protecting against privacy threats. We illustrate how to use slicing to prevent attribute disclosure and membership disclosure. Our experiments show that slicing preserves better data utility than generalization and is more effective than bucketization in workloads involving the sensitive attribute. The general methodology proposed by this work is that before anonymizing the data, one can analyze the data characteristics and use these characteristics in data anonymization. The rationale is that one can design better data anonymization techniques when we know the data better. In [22], [24], we show that attribute correlations can be used for privacy attacks. While a number of anonymization techniques have been designed, it remains an open problem on how to use the anonymized data. In our experiments, we randomly generate the associations between column values of a bucket. This may lose data utility. Another direction is to design data mining tasks using the anonymized data [14] computed by various anonymization techniques

X. REFERENCES

[1]. C. Aggarwal, "On k-Anonymity and the Curse of Dimensionality," Proc. Int'l Conf. Very Large Data Bases (VLDB), pp. 901-909, 2005.
[2]. Blum, C. Dwork, F. McSherry, and K. Nissim, "Practical Privacy: The SULQ Framework," Proc. ACM Symp. Principles of Database Systems (PODS), pp. 128-138, 2005.
[3]. J. Brickell and V. Shmatikov, "The Cost of Privacy: Destruction of Data-Mining Utility in Anonymized Data Publishing," Proc. ACM SIGKDD Int'l Conf. Knowledge Discovery and Data Mining (KDD), pp. 70-78, 2008.
[4]. B.-C. Chen, K. LeFevre, and R. Ramakrishnan, "Privacy Skyline: Privacy with Multidimensional Adversarial Knowledge," Proc. Int'l Conf. Very Large Data Bases (VLDB), pp. 770-781, 2007.
[5]. H. Cramt'er, Mathematical Methods of Statistics. Princeton Univ. Press, 1948.
[6]. Dinur and K. Nissim, "Revealing Information while Preserving Privacy," Proc. ACM Symp. Principles of Database Systems (PODS), pp. 202-210, 2003.
[7]. C. Dwork, "Differential Privacy," Proc. Int'l Colloquium Automata, Languages and Programming (ICALP), pp. 1-12, 2006.
[8]. C. Dwork, "Differential Privacy: A Survey of Results," Proc. Fifth Int'l Conf. Theory and Applications of Models of Computation (TAMC), pp. 1-19, 2008.
[9]. C. Dwork, F. McSherry, K. Nissim, and A. Smith, "Calibrating Noise to Sensitivity in Private Data Analysis," Proc. Theory of Cryptography Conf. (TCC), pp. 265-284, 2006.
[10]. J.H. Friedman, J.L. Bentley, and R.A. Finkel, "An Algorithm forFinding Best Matches in Logarithmic Expected Time," ACM Trans. Math. Software, vol. 3, no. 3, pp. 209-226, 1977.
[11]. B.C.M. Fung, K. Wang, and P.S. Yu, "Top-Down Specialization for Information and Privacy Preservation," Proc. Int'l Conf. Data Eng. (ICDE), pp. 205-216, 2005.
[12]. G. Ghinita, Y. Tao, and P. Kalnis, "On the Anonymization of Sparse High-Dimensional Data," Proc. IEEE 24th Int'l Conf. Data Eng. (ICDE), pp. 715-724, 2008.
[13]. Y. He and J. Naughton, "Anonymization of Set-Valued Data via Top-Down, Local Generalization," Proc. Int'l Conf. Very Large Data Bases (VLDB), pp. 934-945, 2009.
A. Inan, M. Kantarcioglu, and E. Bertino, "Using Anonymized Data for Classification," Proc. IEEE 25th Int'l Conf. Data Eng. (ICDE), pp. 429-440, 2009.
[14]. L. Kaufman and P. Rousueeuw, "Finding Groups in Data: An Introduction to Cluster Analysis," John Wiley & Sons, 1990.
[15]. D. Kifer and J. Gehrke, "Injecting Utility into Anonymized Data Sets," Proc. ACM SIGMOD Int'l Conf. Management of Data (SIGMOD), pp. 217-228, 2006.
[16]. N. Koudas, D. Srivastava, T. Yu, and Q. Zhang, "Aggregate Query Answering on Anonymized Tables," Proc. IEEE 23rd Int'l Conf. Data Eng. (ICDE), pp. 116-125, 2007.
[17]. K. LeFevre, D. DeWitt, and R. Ramakrishnan, "Incognito: Efficient Full-Domain k-Anonymity," Proc. ACM SIGMOD Int'l Conf. Management of Data (SIGMOD), pp. 49-60, 2005.
[18]. K. LeFevre, D. DeWitt, and R. Ramakrishnan, "Mondrian Multidimensional k-Anonymity," Proc. Int'l Conf. Data Eng. (ICDE), p. 25, 2006.
[19]. K. LeFevre, D. DeWitt, and R. Ramakrishnan, "Workload-Aware Anonymization," Proc. ACM SIGKDD Int'l Conf. Knowledge Discovery and Data Mining (KDD), pp. 277-286, 2006.
[20]. N. Li, T. Li, and S. Venkatasubramanian, "t-Closeness: Privacy Beyond k-Anonymity and '-Diversity," Proc. IEEE 23rd Int'l Conf. Data Eng. (ICDE), pp. 106-115, 2007

[21]. T. Li and N. Li, "Injector: Mining Background Knowledge for Data Anonymization," Proc. IEEE 24th Int'l Conf. Data Eng. (ICDE), pp. 446-455, 2008.
[22]. T. Li and N. Li, "On the Tradeoff between Privacy and Utility in Data Publishing," Proc. ACM SIGKDD Int'l Conf. Knowledge Discovery and Data Mining (KDD), pp. 517-526, 2009.
[23]. T. Li, N. Li, and J. Zhang, "Modeling and Integrating Background Knowledge in Data Anonymization," Proc. IEEE 25th Int'l Conf. Data Eng. (ICDE), pp. 6-17, 2009.
A. Machanavajjhala, J. Gehrke, D. Kifer, and M. Venkitasubramaniam, "'-Diversity: Privacy Beyond k-Anonymity," Proc. Int'l Conf. Data Eng. (ICDE), p. 24, 2006.
[24]. D.J. Martin, D. Kifer, A. Machanavajjhala, J. Gehrke, and J.Y. Halpern, "Worst-Case Background Knowledge for Privacy-Preserving Data Publishing," Proc. IEEE 23rd Int'l Conf. Data Eng. (ICDE), pp. 126-135, 2007
[25]. M.E. Nergiz, M. Atzori, and C. Clifton, "Hiding the Presence of Individuals from Shared Databases," Proc. ACM SIGMOD Int'l Conf. Management of Data (SIGMOD), pp. 665-676, 2007.
[26]. P. Samarati, "Protecting Respondent's Privacy in Microdata Release," IEEE Trans. Knowledge and Data Eng., vol. 13, no. 6, pp. 1010-1027, Nov./Dec. 2001
[27]. L. Sweeney, "Achieving k-Anonymity Privacy Protection Using Generalization and Suppression," Int'l J. Uncertainty Fuzziness and Knowledge-Based Systems, vol. 10, no. 6, pp. 571-588, 2002.
[28]. [30] L. Sweeney, "k-Anonymity: A Model for Protecting Privacy," Int'l J. Uncertainty Fuzziness and Knowledge-Based Systems, vol. 10, no. 5, pp. 557-570, 2002.
[29]. M. Terrovitis, N. Mamoulis, and P. Kalnis, "Privacy-Preserving Anonymization of Set-Valued Data," Proc. Int'l Conf. Very Large Data Bases (VLDB), pp. 115-125, 2008. [32] R.C.-W. Wong, A.W.-C. Fu, K. Wang, and J. Pei, "Minimality Attack in Privacy Preserving Data Publishing," Proc. Int'l Conf. Very Large Data Bases (VLDB), pp. 543-554, 2007.

www.ijmer.com Vol. 3, Issue. 3, May.-June. 2013 pp-1763-1767 ISSN: 2249-6645

DISCLOSURE PREVENTION IN PRIVACY-PRESERVING DATA PUBLISHING

V.Kavitha[1] , M.Poornima[2]

**(Department of Information Technology, Paavai College of Engineering, Anna University, India)*
*** (Department of Computer Sciences and Engineering ,Anna University, India)*

ABSTRACT: *The advancement of information technologies has enabled various organizations (e.g., census agencies, hospitals) to collect large volumes of sensitive personal data (e.g., census data, medical records. Data in its original form, however, typically contains sensitive information about individuals, and publishing such data will violate individual privacy. The current practice in data publishing relies mainly on policies and guidelines as to what types of data can be published and on agreements on the use of published data. In order to protect sensitive information, the simplest solution is not to disclose the information. However, this would be overkill since it will hinder the process of data analysis over the data from which we can find interesting patterns. Moreover, in some applications, the data must be disclosed under the government regulations. Alternatively, the data owner can first modify the data such that the modified data can guarantee privacy and, at the same time, the modified data retains sufficient utility and can be released to other parties safely. This process is usually called as privacy-preserving data publishing. This thesis identifies a collection of privacy threats in real life data publishing, and presents a unified solution to address these threats.*

KEYWORDS: *Privacy, Sensitive data, Data Publishing, Information security.*

I. INTRODUCTION

In recent years, advances in hardware technology have lead to an increase in the capability to store and record personal data about consumers and individuals. This has lead to concerns that the personal data may be misused for a variety of purposes. In order to alleviate these concerns, a number of techniques have recently been proposed in order to perform the data publishing tasks in a privacy-preserving way. A task of the utmost importance is to develop methods and tools for publishing data in a more hostile environment, so that the published data remains practically useful while individual privacy is preserved. This undertaking is called *privacy-preserving data publishing* (PPDP).In the past few years, research communities have responded to this challenge and proposed many approaches.

This paper is organized as follows, section 2 deals with the analysis of data .Section 3 discusses about various protection methods.

Section 4 deals with the various limitations of the privacy models, while section 5 deals with enhancing the anonymization methods. Section 6 concludes the featured description of various protection methods.

II. PRIVATE DATA ANALYSIS

Data analysis is the process of extracting hidden predictive information from large amount of datasets. This analysis can be performed by the data owner or the data owner can outsource the data analysis to other parties. In any case, the privacy concerns of the involved individuals should be addressed and considered at all times. According to Michal Sramka [2010], private data analysis is achievable in the following ways:

II.1 PRIVATE DATA ANALYSIS OVER ORIGINAL DATA

In this scenario, computations are performed over the original private or even confidential data.

- Data analysis is performed by the data owner. No other party will learn the data, and the results of the analysis will stay "in house".
- Data mining is performed over the original data and then the obtained knowledge is published. The published knowledge is protected against privacy leaks in a way that it does not reveal sensitive information about the underlying data. This is achievable by sanitizing the learned knowledge and referred to as the privacy-preserving knowledge publishing as stated by Atzori et al [2008].
- One or several parties own confidential data and another party perform a computation over them. According to Lindell [2002] Secure multiparty computation over distributed data sets are fields that study cryptographic tools that allow to compute a function over confidential data without learning anything else than what can be learned from the output of the function.

II.2 DATA ANALYSIS OVER SANITIZED DATA

In this scenario, data is sanitized and then shared or published for analysis. This is referred to as privacy preserving data publishing (PPDP). Sanitization is usually achieved as a transformation of the data that

www.ijmer.com Vol. 3, Issue. 3, May.-June. 2013 pp-1763-1767 ISSN: 2249-6645

provides pseudonymity, anonymity, or privacy risk reduction by generalizing, masking, randomizing, or even suppressing some data.

III. CLASSIFICATION OF MICRO DATA PROTECTION METHODS

A microdata set can be viewed as a file with *n* records, where each record contains *m* attributes on an individual respondent. The attributes can be classified in four categories which are not necessarily disjoint:

- *Identifiers*. These are attributes that *unambiguously* identify the respondent. Examples are the passport number, social security number, name, surname, etc.
- *Quasi-identifiers or key attributes*. These are attributes which identify the respondent with some degree of ambiguity. (Nonetheless, a combination of quasi-identifiers may provide unambiguous identification.) Examples are address, gender, age, telephone number, etc.
- *Confidential outcome attributes*. These are attributes which contain sensitive information on the respondent. Examples are salary, religion, political affiliation, health condition, etc.
- *Non-confidential outcome attributes*. Those attribute which do not fall in any of the categories above.

In recent years, numerous algorithms have been proposed for implementing *k*-anonymity via generalization and suppression. Samarati [2001] presents an algorithm that exploits a binary search on the domain generalization hierarchy to ¯find minimal *k*-anonymous table. Sun *et al.* [2008] recently improve Samarati's algorithm by integrating the hash-based technique. Bayardo and Agrawal [2005] present an optimal algorithm that starts from a fully generalized table and specializes the dataset in a minimal *k*-anonymous table, exploiting ad hoc pruning techniques. LeFevre *et al*. [2005] describe an algorithm that uses a bottom-up technique and a priori computation. Fung *et al*. present a top-down heuristic to make a table to be released *k*-anonymous. As to theoretical results, Meyerson and Williams [2004] and Aggarwal *et al*
prove that optimal *k*-anonymity is NP-hard (based on the number of cells and number of attributes that are generalized and suppressed) and describe approximation algorithms for optimal *k*-anonymity. Sun *et al*. [2008] prove that *k*-anonymity problem is also NP-hard even in the restricted cases. While focusing on identity disclosure, *k*-anonymity model fails to protect attribute disclosure. Several

Gender	Age	Zip Code	Diseases
Male	25	4370	Hypertension
Male	25	4370	Hypertension
Male	22	4352	Depression
Female	28	4373	Chest Pain
Female	28	4373	Obesity
Female	34	4350	Flu

Table 1: The microdata

Gender	Age	Zip Code	Diseases
Male	22-25	43**	Hypertension
Male	22-25	43**	Hypertension
Male	22-25	43**	Depression
Female	28-34	43**	Chest Pain
Female	28-34	43**	Obesity
Female	28-34	43**	Flu

Table 2: A 3-anonymous table

models such as *p*-sensitive *k*- anonymity, *l*-diversity, (α *k*)-anonymity and *t*-closeness are proposed in the literature in order to deal with the problem of *k*-anonymity. Although these models can achieve privacy properties to some extent, they are not enough for privacy protection.

A key difficulty of data anonymization comes from the fact that data utility (i.e., data quality) and data privacy are conflicting goals. Intuitively, data privacy can be enhanced by hiding more data values, but it decreases data utility; on the other hand, revealing more data values increases data utility, but it may decrease data privacy. Thus, it is necessary to devise solutions that best address both the utility and the privacy of data.

Publishing high dimensional data is part of daily operations in commercial activities and public services. A classic example of high dimensional data is transaction databases. Examples of transactions are web queries, click streams, emails, market baskets, and medical notes. Such data often contain rich information and are excellent sources for data mining. Narayanan and Shmatikov showed that an attacker only needs a little bit information of an individual to identify the anonymized movie rating transaction of the individual in the data set. Such breach occurs when an attacker only needs a little bit information of an individual to re-identify the anonymized rating transaction of the individual in the data set. Existing research on privacy-preserving data publishing focuses on relational data and the objective is to enforce privacy-preserving paradigms (e.g., *k*-anonymity, *l*-diversity, etc) while minimizing the information loss incurred in the anonymizing process. However, methods developed on low dimensional relational data are very inefficient on high dimensional and sparse transactional data.

www.ijmer.com Vol. 3, Issue. 3, May.-June. 2013 pp-1763-1767 ISSN: 2249-6645

III.1 K-ANONYMITY: An anonymization algorithm finds a release candidate that is both useful and safe (according to privacy criterion) from this space of search. K-anonymity is defined as:

Each release of the data must be such that every combination of values of quasi-identifiers can be indistinguishably matched to at least k respondents.

The approach uses domain generalization hierarchies of the quasi-identifiers in order to build k-anonymous tables. The concept of k-minimal generalization has been proposed by Samarati .P [2001] in order to limit the level of generalization for maintaining as much data precision as possible for a given level of anonymity. Subsequently, the topic of k-anonymity has been widely researched.

- K-anonymity having several techniques are P-Sensitive k-anonymity, p+-sensitive k-anonymity, (p,α) sensitive k-anonymity.
- P-sensitive k-anonymity: The modified micro data table T' satisfies p-sensitive k-anonymity property if it satisfies k-anonymity, and for each QI-group in T' , the number of distinct values for each sensitive attribute is at least p within the same QI group.
- P+-sensitive k-anonymity: The modified Micro data table T' satisfies p+-sensitive k-anonymity property if it satisfies k-anonymity, and for each QI-group in T' , the number of distinct categories for each sensitive attribute is at least p within the same QI-group.
- (P,α)-sensitive k-anonymity:The modified microdata table T' satisfies (P,α)-sensitive k-anonymity property if it satisfies k-anonymity, and each QI-group has at least p distinct sensitive attribute values with its total weight at least α.

III.2 *l* -DIVERSITY METHOD

Clearly, while k-anonymity is effective in preventing identification of a record, it may not always be effective in preventing inference of the sensitive values of the attributes of that record. Therefore, the technique of l-diversity was proposed which not only maintains the minimum group size of k, but also focuses on maintaining the diversity of the sensitive attributes. Therefore, the l-diversity model for privacy is defined as follows: *Let a $q*$-block be a set of tuples such that its non-sensitive values generalize to $q*$. A $q*$-block is l-diverse if it contains l "well represented" values for the sensitive attribute S. A table is l-diverse, if every $q*$-block in it is l-diverse.*

A number of different instantiations for the l-diversity definition is available. When there are multiple sensitive attributes, then the l-diversity problem becomes especially challenging because of the curse of dimensionality, methods have been proposed in for constructing l-diverse tables from the data set, though the technique remains susceptible to the curse of dimensionality. Other methods for creating l-diverse tables are discussed in, in which a simple and efficient method for constructing the l-diverse representation is proposed.

III.3 t-CLOSENESS MODEL

The t-closeness model is a further enhancement on the concept of l-diversity. One characteristic of the l-diversity model is that it treats all values of a given attribute in a similar way irrespective of its distribution in the data. This is rarely the case for real data sets, since the attribute values may be very skewed. This may make it more difficult to create feasible l-diverse representations.

Often, an adversary may use background knowledge of the global distribution in order to make inferences about sensitive values in the data. Furthermore, not all values of an attribute are equally sensitive. For example, an attribute corresponding to a disease may be more sensitive when the value is positive, rather than when it is negative. According to Venkatasubramanian.S [2007], a t-closeness model was proposed which uses the property that the distance between the distribution of the sensitive attribute within an anonymized group should not be different from the global distribution by more than a threshold t. The Earth Mover distance metric is used in order to quantify the distance between the two distributions. Furthermore, the t-closeness approach tends to be more effective than many other privacy-preserving data mining methods for the case of numeric attributes.

IV. LIMITATIONS OF CURRENT PRIVACY PRINCIPLES

Initially anonymization was the first technique to prevent disclosure. Since k-anonymity model is not enough to protect sensitive information, several models such as *p*-sensitive *k*-anonymity, *l*-diversity, (*α k*)-anonymity and *t*-closeness have been proposed.

IV.1 LIMITATION OF P-SENSITIVE K-ANONYMITY:

The purpose of *p*-sensitive *k*-anonymity is to protect against attribute disclosure by requiring that there be at least *p* different values for each sensitive attribute within the records sharing a combination of quasi-identifier. This approach has the limitation of implicitly assuming that each sensitive attribute takes values

www.ijmer.com Vol. 3, Issue. 3, May.-June. 2013 pp-1763-1767 ISSN: 2249-6645

uniformly over its domain; that is, that the frequencies of the various values of a confidential attribute are similar. When this is not the case, achieving the required level of privacy may cause a huge data utility loss.

IV.2 LIMITATION OF L-DIVERSITY

The *l*-diversity model protects against sensitive attribute disclosure by considering the distribution of the attributes. The approach requires *l* "well-represented" values in each combination of quasi-identifiers. This may be difficult to achieve and, like *p*-sensitive *k*-anonymity, may result in a large data utility loss. Further, as previously identified, *l*-diversity is insufficient to prevent similarity attack.

IV.3 LIMITATION OF t-CLOSENESS:

The *t*-closeness model protects against sensitive attributes disclosure by defining semantic distance among sensitive attributes. The approach requires the distance between the distribution of the sensitive attribute in the group and the distribution of the attribute in the whole data set to be no more than a threshold *t*. Whereas Li et al. [2007] elaborate on several ways to check *t*-closeness, no computational procedure to enforce this property is given. If such a procedure was available, it would
greatly damage the utility of data because enforcing *t*-closeness destroys the correlations between quasi-identifier attributes and sensitive attributes.

V. DEVELOPING *K*-ANONYMITY ALGORITHMS

***Hash-based Technique*:** *k*-anonymity is a technique that prevents "linking" attacks by generalizing and/or suppressing portions of the released microdata so that no individual can be uniquely distinguished from a group of size *k*. A practical model of *k* anonymity, called full-domain generalization describes, a Hash-based technique previously used in mining associate rules and present an efficient hash-based algorithm to find the minimal *k*-anonymous table, which improves the previous binary search algorithm first proposed by Samarati.

Restricted K-Anonymity:

There are two new variants of the k-anonymity problem, namely, the Restricted k-anonymity problem and Restricted k- anonymity problem on attribute and discuss the connection between the Restricted k-anonymity and the general k-anonymity problems which stresses the significance of investigating this new class of anonymity problem. The theoretical results for restricted k-anonymity problem also provide an alternative NP-hardness proof of general k- anonymity problem.

V.1 ENHANCING K-ANONYMITY MODEL

k-anonymity alone is not enough to protect privacy in data. There are more stronger
algorithms than the k-anonymity model and that protect both sensitive facts and private knowledge in data. The (p+, α)-sensitive k-anonymity model requires that in each combination of quasi-identifiers, there are at least p different sensitive values and the total weight in each combination of quasi-identifiers is at least α. The motivation for this model is the fact that although k-anonymity is effective in protecting identity disclosure, to some extent, it fails to protect sensitive attribute disclosure. (p+, α)-sensitive k-anonymity model, provides an ordinal distance system to evaluate the degree that the sensitive attribute contributes to the database.

VI. CONCLUSION

In an increasingly data-driven society, personal information is often collected and distributed with ease. In this survey, we have presented an overview of recent technological advances in defining and protecting individual privacy and confidentiality in data publishing. In particular, such as hospitals and government agencies, that compiles large data sets, and must balance the privacy of individual participants with the greater good for which the aggregate data can be used.

While technology plays a critical role in privacy protection for personal data, it does not solve the problem in its entirety. In the future, technological advances must combine with public policy, government regulations, and developing social norms.

Due to the wide use of the Internet and the trends of enterprise integration,, simultaneous cooperation and competition, and outsourcing in both public and private sectors, data publishing has become a daily and routine activity of individuals, companies, organizations, government agencies. Privacy-preserving data publishing is a promising approach for data publishing without compromising individual privacy or disclosing sensitive information.

In this thesis, we studied different types of linking attacks in the data publishing scenarios, analysis of data, sequential release, secure data integration and various limitations of the privacy models

www.ijmer.com Vol. 3, Issue. 3, May.-June. 2013 pp-1763-1767 ISSN: 2249-6645

REFERENCES

[1]. *X. Jin, N. Zhang, G. Das, Algorithm-safe privacy preserving data publishing, in: EDBT, 2010.*

[2]. ℓ-diversity: Privacy Beyond k-Anonymity, Ashwin Machanavajjhala Daniel Kifer Johannes Gehrke.

[3].]Protecting Respondents' Identities in Microdata Release, Pierangela Samarati.

[4]. X. Jin, M. Zhang, N. Zhang, G. Das, Versatile publishing for privacy preservation, in: KDD, 2010.

[5]. P.Samarati. Protecting respondent's identities in micro-data release. IEEE Transactions on Knowledge and Data Engineering, 13(6):1010-1027. 2001

[6]. *Bayardo R. J., Agrawal R.: DataPrivacythrough Optimal k*-Anonymization. *Proceedings of the ICDE Conference*, pp. 217–228, 2005.

[7]. ASAP: Eliminating algorithm-based disclosure in privacy-preserving data publishing Xin Jin, NanZhang , GautamDas , 2011

[8]. P.Samarati, L.Sweeney, Protecting privacy when disclosing information: k-anonymity and its enforcement through generalization and suppression,Technical Report, CMU, SRI, 1998.

[9]. K.LeFevre, D.J.DeWitt, R.Ramakrishnan, Mondrian multi-dimensional k-anonymity, in: ICDE, 2006, pp.25–35.

[10]. R.C. Wong, A.W. Fu, K. Wang, J. Pei, Minimality attack in privacy- preserving data publishing, in: VLDB, 2007,543–554.

[11]. N. Koudas, D. Srivastava, T. Yu, Q. Zhang, Distribution-based microdata anonymization, in: VLDB, 2009.

[12]. Machanavajjhala, J. Gehrke, M. Goetz, Data publishing against realistic adversaries, in: VLDB, 2009.

[13]. A.Meyerson, R.Williams, On the complexity of optimal k-anonymity, in: PODS, 2004, pp.223–228.

[14]. X. Jin, N. Zhang, G. Das, Algorithm-safe privacy preserving data publishing, in: EDBT, 2010.

[15]. N.Koudas, D.Srivastava, T. Yu, Q. Zhang, Distribution-based microdata anonymization, in: VLDB, 2009.

[16]. L. Sweeney. K-anonymity: a model for protecting privacy. International Journal on Uncertainty, Fuzziness andKnowledge-based Systems, 10 (5), 2002; 557-570.

[17]. R. Bayardo and R. Agrawal. Data privacy through optimal *k*-anonymity. *In Proceedings of the 21st International Conference on Data Engineering (ICDE)*, 2005.

[18]. G. Aggarwal, T. Feder, K. Kenthapadi, R. Motwani, R. Panigrahy, D. Thomas and A. Zhu. Approximation algorithms for *k*-anonymity. *Journal of Privacy Technology*, paper number 20051120001.

[19]. G. Aggarwal, T. Feder, K. Kenthapadi, S. Khuller, R. Panigrahy, D. Thomas, A. Zhu, Achieving anonymity via clustering, in: PODS, 2006, pp. 153-162.

[20]. H. Park, K. Shim, Approximate algorithms for k-anonymity, in: SIGMOD, 2007, pp. 67-78.

International Journal of Modern Engineering Research (IJMER)
www.ijmer.com Vol. 3, Issue. 3, May.-June. 2013 pp-1768-1773 ISSN: 2249-6645

Color Image Encryption Based on Symmetric and Asymmetric Cryptosystems and Transcendental Numbers

C. A. Jiménez-Vázquez[1], R. Flores-Carapia[2], V. M. Silva-García[3], B. Luna-Benoso[4]
[123]*Instituto Politécnico Nacional, CIDETEC, México.*
[4]*Instituto Politécnico Nacional, ESCOM, México.*

ABSTRACT:*This work presents an algorithm to cipher color images using a hybrid cryptosystem, one which is symmetric FIPS-197 and the other an asymmetric elliptic curve being a nonsingular* $y^2 \equiv x^3 + Ax + B(mod p)$ *over* $Z_p(ECC)$*. The construction of the hybrid cryptosystem proposed, has two important aspects; the first is the generation of a random number, which we will call* γ*, of the same prime length finite field* Z_p*. The issuer figures* γ *ECC with point compression technique, in such a way that the result is a string encryption twice the length of the string representing* p *plus an extra byte called* γ^**. The second aspect is to multiply a* γ^* *by the transcendental number* π *and the resulting product is taken right of the decimal point for the length of the image in bytes. Subsequently, it performs the XOR operation of this with the image bytes generating* I^**.* I^**divides into sections of length equal to* γ^* *and each section is applied to the XOR operation with* γ^* *thus resulting in an encrypted image. The issuer encrypts* γ^* *with AES with the key* K^1 *resulting* γ^{**}*, turns the transmitter key* K^1*, encrypts with our private key by generating ECC* K^**. Consequently, the issuer sends the receiver the encrypted image and the ordered pair* (γ^{**}, K^1)*; this with their private key to perform the reverse process to obtain the original image. The security of this cryptosystem is in the size* γ^* *as this can have a size of over 225 bytes (if taken top* $\geq 10^{270}$*) and would have to prove more than* $2^{225\times 8} - 1$ *possible blocks depending on the size of* p*.*

KEYWORDS: *Encryption, images cipher, transcendental numbers, AES, elliptic curve.*

I. INTRODUCTION

The proliferation of computers and the Internet boom that has happened in recent years has made it possible for anyone to distribute any type and amount of information easily. There are many numbers of applications that make use of the latest exchange systems information across Wifi networks, fiber optic networks, satellites, etc. In the exchange of information and thanks to the popular use of mobile computers, now sharing images is a very important part in our daily lives.However, the importance of images exchange not only applies to our everyday life, such as military class databases which have images of maps with locations of secret facilities, or in the banking industry where millions of dollars are invested daily in the exchange of images containing highly sensitive information. Therefore, much research has been developedon ciphering and deciphering images in which one of the main objectives is to recover the original image from the cipher image without some data loss. To achieve this, it is necessary to ensure the confidentiality, integrity and authenticity of the transmitted image.

In literature different proposals can be found such as the development of a cryptosystem whichcan cipher images using chaotic logistic maps [1].These have an advantage over traditional algorithms such as high security, speed, etc. Another example of this type of cryptosystem is the one in which the encryption is based on DNA sequences [2]. The main characteristic of this algorithm is to reduce the cipher time of a very large image (such as FullHD). There are cryptosystems where a change has been made to the algorithms that are within the international standard as DES [3]. In this proposal the Triple-DES algorithm has been modified, based on the initial permutation that begins the algorithm's rounds [4].This permits each data ciphered generates a different dynamic permutation. There is another work in which image encryption is based on how the Rubik cube rotation generating its sequence to be sorted [5]. This article intends to use Elliptic Curve Cryptography. The ECC has been researched very much over the past 30 years and importantly has been used to solve Fermat's Last Theorem [6].

Elliptic curves were introduced by Neal Koblitz [7] and Victor S. Miller in 1985 [8] independently, and since then, this has been a vast research area in which mathematical work has been developed with this tool. One application is where the ECC has been a digital signature algorithm [9-12] which can be used to replace existing algorithms with equal or greater security. ECC also has been applied in security systems based on radio frequency [13]. Regarding the image encryption with this mathematical tool, there is a paper that makes the image encryption based on a mapping from a point on the curve for each image pixel [14, 15].Based on a point table associated with each point of the curve, each pixel is transformed into its corresponding encrypted pixel. Although this sounds feasible, the problem with this is to know the order of the field that generates the curve. A system with a similar target develops random sequences generated by the cyclic group of the elliptic curve [16]. A crypto system is proposed that generates a random number known as NONCE which transforms the message akin to a point on the elliptic curve [17]. There are many hybrid cryptosystems (such as this article) as shown in [18], which combines chaotic maps with ECC and there is another which is based on using ElGamal homomorphism for ECC [19].

Another feature of this work is the ability to cipher an image (say FullHD) in a fast enough time and achieve good encryption information thanks to the method proposed. To achieve this, we have applied the use of transcendental numbers (in this case π) [20, 21] to achieve this goal, which also created a hybrid cryptosystem which uses ECC and AES encryption to ensure the strengthening of the image.

II. PRELIMINARIES

A nonsingular elliptic curve is the solution set of the equation $y^2 \equiv x^3 + Ax + B \pmod{p}$ and must satisfy $4A^3 + 27B^2 \neq 0 \pmod{p}$. Therefore; the equation condition ensures that there are 3 different solutions. Elliptic curve points form an additive abelian group with $\mathcal{O}$ as the identifying element that satisfies the properties: commutatively, existence of identity and associativity [22].

Let Ebe an elliptic curve and $P_1 = (x_1, y_1),\ P_2 = (x_2, y_2)$ two points over $E$with $P\_1, P_2 \neq \mathcal{O}$. We define $P_1 + P_2 = P_3 = (x_3, y_3)$ as follows:

1. If$x_1 \neq x_2$, then$x_3 = m^2 - x_1 - x_2, y_3 = m(x_1 - x_3) - y_1$, where $m = \frac{y_2 - y_1}{x_2 - x_1}$
2. If $x_1 = x_2$ but$y_1 \neq y_2$, then $P_1 + P_2 = \mathcal{O}$
3. If $P_1 = P_2$ and$y \neq 0$, then$x_3 = m^2 - 2x_1, y_3 = m(x_1 - x_3) - y_1$, where $m = \frac{3x_1^2 + A}{2y_1}$
4. If $P\_1 = P\_2$ and$y_1 = 0$, then$P_1 + P_2 = \mathcal{O}$. We define $P + \mathcal{O} = P$ for all points P over$E$.

The curve's cardinality Eon F_q, corresponds to the point number that is generated in the field. It is a very important issue in safety cryptosystems since it depends on the cryptosystembeing sufficiently robust.The Hasse-Weil theorem relates the point number ofthe field size and for counting the pointgroupSchoof's algorithm can be used. For calculating a root and finding the generator for an elliptic curve E, we $Z^{\frac{p-1}{2}} \equiv 1 \bmod p$, if $p \equiv 3 \bmod 4$, it is given by $\pm Z^{\frac{p+1}{4}} \equiv 1 \bmod p$, this will help us in order to find the field generator which solves the equation $y^2 \equiv x^3 + Ax + B \pmod{p}$ [22-26].
The compression point operation can be expressed as**:**

Compression_Point::$E \backslash \mathcal{O} \rightarrow Z_p \times Z_2$

And is defined as:

Compression_Point$(P) = P = (x, y \bmod 2)$, where $P = (x, y) \in E$

Algorithm 1 shows the inverse operation (**Descompression_Point)** to recover the elliptic curve point $P = (x, y)$ of $(x, y \bmod 2)$. This algorithm computes $\sqrt{z} \bmod p$.

Algorithm 1: Function for recovering the compression point
Require:axis x, byte i
Ensure: Point P.
1: **procedure**Descompression_Point(x, i)
2: $z \leftarrow x^3 + Ax + B$
3: **if**z is not quadratic module remainder p **then**
4: **return** "(fail)"
5: **else**
6: $y \leftarrow \sqrt{z} \bmod p$
7: **if**$y \equiv i \pmod 2$ then
8: **return**(x, y)
9: **else**
10: **return**$(x, p - y)$
11: **end if**
12: **end if**
13: **end procedure**

III. PROPOSED MODEL

The proposed hybrid cryptosystem is the combination of AES symmetric system and the elliptic curve as the asymmetric encryption, but to generate a good disordering of the image, the decimal numbers of π are used.

1. This cryptosystem has two important aspects: The random number generation. In this step we proceed to generate a random number η where $1 \leq \eta \leq \#E(fp) - 1$. This number is encrypted with the point compression technique described above. The data encryption Ψ of length $2l + l$ where$l = \frac{t}{8}, t = \log_2(p)$, will be used as a private random key cryptosystem.
2. Secret number. WhereΨ will serve to multiply by π since π is a transcendental number. All decimals of this number are not periodical, the multiplication by Ψ with the other number would generate another transcendental number. This result, called$F$, will be used to clutter an image.

Definition 3.1 Ψ is the result of encrypting the random number $\eta$where $1 \leq \eta \leq \#E(fp) - 1$, the compression point scheme is used and $\phi = (\Psi)(\pi)$.

Since $\Psi$and ϕ are very large numbers, these are stored in strings of bytes depending on the size of each, i.e., these numbers are arrays of bytes which are treated as large integers.

Let's suppose that we have two entities $A$and B. Entity A sends an encrypted image to entity B, therefore:$A$and$B$ agree with each other to use an elliptic curve cryptosystem and follow the entire procedure described in [27].

- $A$and$B$ have already chosen their private keys for ECC, but A needs to choose a key for the AES asymmetric system which we will call ρ.

To encrypt an image $I_{m \times n}$ of size$m \times n$, where $m$is the rows and n the columns, A must follow these steps:

1. Read the image $I_{m\times n}$ and generate a string of bytes $buffImage$ of size $m \times n \times 3$ for color images of 24 bits of resolution.
2. Read π of a file previously generated. Ashould read $\pi$the same size of the image $I_{m\times n}$in a string of bytes. Only the numbers are taken after the decimal point, the integer number of π is not taken.
3. Generate random number Ψaccording to Definition 3.1 with its private keyσ, for the data format follows the procedure used in [27].
4. Generate random number ϕ according to Definition 3.1 using the string π in numerical representation.
5. Amust encrypt a Ψ by AES through its key ρm this generate Ψ'.
6. Aencryptsits private key ρ ECC and formatting data using [27], this will generate an encrypted key ρ'.
7. ρshould perform the operation $buffCipherImage = \phi \oplus buffImage$, the result will scramble the image the first time.
8. Amust divide $buffCipherImage$ in blocks of $2l + 1$ bytes and each block $buffBlock_i$, where $i = 0, 1, 2, \ldots, \frac{m\times n}{2l+1} - 1$ and A must perform $buffBlock_i = buffBlock_i \oplus \Psi$ by each block. With this A has encrypted all the image information.
9. Now A saves the image and proceeds to save the i-blocks, then A can send to $B\Psi'$ and ρ' which are used for obtainingthe original image.

Therefore A has already encrypted the image and sends the encrypted key ρ' by using ECC and Ψ' that was encrypted with AES.

B In turn, upon receipt of the encrypted image, should do the reverse process as follows:

1. B gets ρ' and Ψ':

a. The key ρ' which must decode ECC through its private key k, obtaining the key ρ.

b. The block Ψ' that is encrypted with AES is decrypted with the key $\rho$to obtainΨ, recalling that this block is used to operate with the image as a random number.

2. Bshould read π according to the image size.
3. Bproceeds in reverse, i.e. operates as in step 8 and then operates according to step 7. Bobtains the original image.

IV. EXPERIMENTAL RESULTS

The experiment that was carried out to test this algorithm was performed on a 2.4 Ghz core i7 with 8 Gb Ram. The way quality encryption is determined is with the proposal made in [4], usingχ^2. With this procedure and plotting the frequency histogram we can determine if the procedure performed was successful. Table 1 and figure 1 show different picture sizes over time encryption of this hybrid cryptosystem for the procedure used in [4] and the value of χ^2. For obtaining these results the curve called P-521was used [28], and also the number prime which is given there.

The security offered by this hybrid cryptosystem, lies in the generation of a random numberthat is obtained by the process of the elliptic curve encryption. This number according tothe prime number that was used to build the field Z_p is about 10^{150}, which is generated by a string byte with a length of 66 bytes having a length of 133 bytes (This size can vary accordingto the size of the prime number that generates Z_p).

Table1: Comparison between our hybrid cryptosystem and Triple DES 96.

Size	Hibrid		Triple DES 96	
	Time$(seg.)$	χ^2	Time$(seg.)$	χ^2
320×200	0.279	755.2238	1.890	750.1360
320×240	0.161	741.2381	2.609	722.5999
640×480	0.269	793.3555	9.101	810.5983
800×600	0.270	734.9383	14.860	761.9178
1024×768	0.292	761.0994	24.203	807.7024
1280×768	0.335	741.3931	28.532	715.9650
1280×1024	0.439	742.6301	35.953	715.0464
1440×900	0.411	802.7540	36.365	798.0950
1600×1024	0.436	747.6839	49.703	761.0825
1600×1200	0.591	827.8274	54.125	773.3616
1920×1080	0.469	716.1687	58.250	760.9197
4096×3112	2.146	798.2641	384.422	886.2007

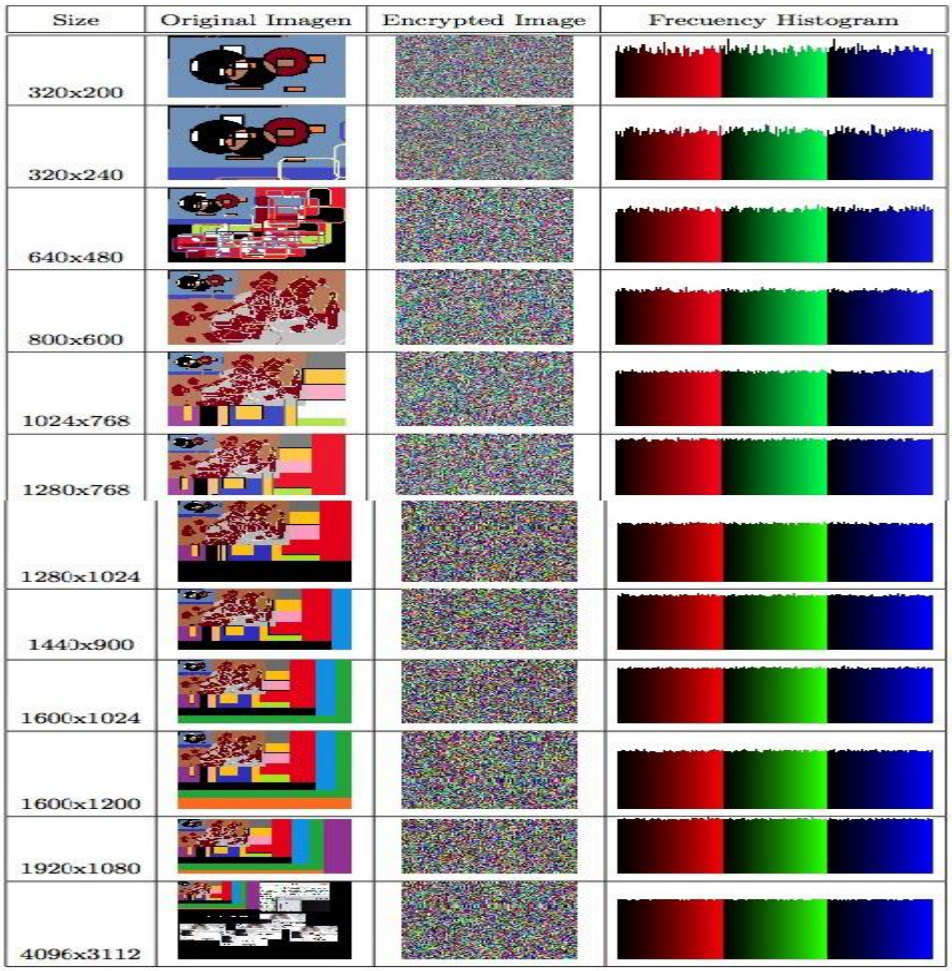

Figure 1: Original images, encrypted images and histograms for different image sizes.

For attacking this cryptosystem, we should know the random number and we should know the private key that uses ECC. ECC's strength lies in solving the discrete logarithm problem for elliptic curves [9, 22] and also the private keys of the sender and receiver being 256 bits. The random number to be sent to the receiver is encrypted using AES with a 128-bit key and this key is encrypted with ECC using the sender's private key. In order to know the random number, we should break both, ECC and AES to obtain it. Yet another way to obtain it would be to try all possibilities to generate the number and validate with multiplication times π. In this example, the number is 133 bytes so we should prove $2^{133\times 8}-1$ operations, but this computationally is very expensive.

Table 2 shows that the security of this cryptosystem increases if we use a prime number to generateZ_p.

Table 2: Security of our cryptosystem

Prime number's order	Operations
10^{150}	$2^{1064}-1$
10^{270}	$2^{2040}-1$
10^{512}	$2^{3400}-1$
10^{1024}	$2^{6808}-1$

V. CONCLUSIONS

The result obtained by χ^2 is quite close to that shown in [4]. However, the time required to obtain the encrypted image increases significantly as we increase the image size. This also presents a hybrid cryptosystem, but the time required for the encryption is significantly much smaller. Although all articles are based on the image histogram, it is sufficiently linear to determine if encryption is good enough. The images used for encryption are small compared with the image presented in this paper which shows the strength of this hybrid cryptosystem.

We must also consider safety presented by the use of random number generation which would be very hard to find because all the combinations would have to be proved.

However, the hybrid cryptosystem's time encryption can still be improved optimizing the operation $Q=kP$ as is proposed in [29, 30, 31].

VI. ACKNOWLEDGEMENT

The authors would like to thank the InstitutoPolitécnicoNacional (SecretaríaAcadémica, COFAA, SIP, Proyecto SIP-20130156, CIDETEC and ESCOM) and the CONACyT for their economic support to develop this work.

REFERENCES

[1]. Ismail Amr Ismail. A digital image encryption algorithm based a composition of two chaotic logistic maps. *International Journal of Network Security, 11(2)*, 2010, 1–10.
[2]. Xiaopeng Wei Shihua Zhou, Qiang Zhang. Image encryption algorithm based on DNA sequences for the big image. *IEEE Computer Society, editor, International Conference on Multimedia Information Networking and Security, 978-0-7695-4258-4/10*, 2010, 884–888.
[3]. Federal Information Processing Standards Publication, editor. *Data Encryption Standard (DES)* U.S. Department of Commerce/National Institute of Standards and Technology, 1999.
[4]. M. Silva-García, R. Flores-Carapia, I. López-Yáñez and C. Rentería-Márquez. Image encryption based on the modified triple-des cryptosystem. *International Mathematical Forum vol. 7, no. 59* 2012, 2929-2942.
[5]. Shaowei XIA Li Zhang, Xiaolin TIAN. *A scrambling algorithm of image encryption based on rubik's cube rotation and logistic sequence*. IEEE Computer Society, editor, nternational Conference on Multimedia and Signal Processing, 2011.
[6]. Andrew Wiles. Modular elliptic curves and fermat's last theorem. *Annals Of Mathematics 142*, 1995, 443–551.
[7]. Neal Koblitz. Elliptic curve cryptosystems. *Mathematics of Computation, 48(177)*, 1987, 203–209.
[8]. Victor S. Miller. Use of elliptic curves in crypyography. *Lecture notes in computer sciences; 218 on Advances in cryptology—CRYPTO 85*, 1985, 417–426.
[9]. *The Elliptic Curve Digital Signature Algorithm (ECDSA)*. American National Standards Institute, 2005.
[10]. *Suite B Implementer's Guide to FIPS 186-3* (ECDSA), 2010.
[11]. Scott Vanstone Don Johnson, Alfred Menezes. *The elliptic curve digital signature algorithm (ecdsa)*. Certicom Office Locations 25801 Industrial Blvd. Hayward, 2001.
[12]. Amar SiadMoncef Amara. *Elliptic curve cryptography and its applications*. IEEE Computer Society, editor, 7th International Workshop on Systems, Signal Processing and their Applications (WOSSPA), 978-1-4577-0690-5/11, 2011.
[13]. Yong Ki Lee. Elliptic-curve-based security processor for rfid. *IEEE Transactions On Computers, 57(11)*, 2008, 1514–1527.
[14]. Kamlesh Gupta. *An ethical way for image encryption using ecc*. IEEE Computer Society, editor, First International Conference on Computational Intelligence, Communication Systems and Networks, 978-0-7695-3743-6/09, 2009,342–345.
[15]. Anita JadhavMeghaKolhekar. Implementation of elliptic curve cryptography on text and image. *International Journal of Enterprise Computing and Business Systems, 1(2)*, 2011.
[16]. S. Sathyanarayana. Symmetric key image encryption scheme with key sequences derived from random sequence of cyclic elliptic curve points. *International Journal of Network Security, 12(3)*, 2011, 137–150.
[17]. K. MuneeswaranMariaCelestin Vigila. Nonce based elliptic curve cryptosystem for text and image applications. *International Journal of Network Security, 14(4)*, 2012, 236–242.
[18]. Sanjay SilakariKamlesh Gupta. Efficient hybrid image cryptosystem using ecc and chaotic map. *International Journal of Computer Applications, 29(3)*, 2011.
[19]. XiamuNiu Li Li, Ahmed A. Abd El-Latif. *Elliptic curve elgamal based homomorphic image encryption scheme for sharing secret images*. ElSevierSignalProcessing(92), 2012, 1069–1078.
[20]. Antonio Rosales G. Números trascendentes: Desarrollo histórico. *Revista digital Matemática, Educación e Internet , 10(2)*, 2010.
[21]. Anita JadhavMeghaKolhekar. Implementation of elliptic curve cryptography on text and image. *International Journal of Enterprise Computing and Business Systems, 1(2)*, 2011.
[22]. Lawrence C.Washington. *Elliptic Curves Number Theory and Cryptography*. Discrete Mathematics and its Applications. Chapman and Hall/CRC, University of Maryland College Park, Maryland, U.S.A., 2 edition, 2008.
[23]. René Schoof. Elliptic curves over finite fields and the computation of square roots mod p. *Mathematics of Computation, 44(170)*, 1985, 483–494.
[24]. Victor Shoup. *A Computational Introduction to Number Theory and Algebra*. Cambridge UniversityPress., 2 edition, 2008.
[25]. Jos'e de Jesús Angel. *Criptografía y curvas elípticas*. Master'sthesis, Universidad Autonoma Metropolitana, 1998.
[26]. William Steain. *An Explicit Approach To Elementary Number Theory (With An Emphasis On Elliptic Curves)*. Math 124. 2001.
[27]. M. Qu-S. Vanstone J. Koeller, A. Menezes. *Elliptic curve systems*. Draft 8. IEEE P1363 Standard for RSA, Diffie-Hellman and Related Public-Key Cryptography, 1996.
[28]. *Recommended Elliptic Curves for Federal Government Use*, 1999.
[29]. M. Anwar HasanBijan Ansari. High-performance architecture of elliptic curve scalar multiplication. *IEEE Transactions On Computers, 57(11)*, 2008, 1443–1453.
[30]. N. Saqib Francisco Rodríguez Henríquez. *Cryptographic Algorithms on Reconfigurable Hardware*. Springer Series on Signals and Communication Tecnology. 2006.
[31]. Ding Yong. Speeding scalar multiplication of elliptic curve over gf(2mn). *InternationalJournal of Network Security, 11(2)*, 2010, 70–77.

International Journal of Modern Engineering Research (IJMER)
www.ijmer.com Vol. 3, Issue. 3, May - June 2013 pp-1774-1782 ISSN: 2249-6645

Gully Erosion Control along NWORIE River in Owerri, Imo State-A Deterministic Model Approach

Okoro, B. C.[1], Ibearugbulem, O. H.[2], Agunwamba, J. C.[3]
[1.] Department of Civil Engineering, Federal University of Technology, Owerri Imo State. Nigeria.
[2.] Department of Civil Engineering, Federal Polytechnic Nekede, Owerri Imo State Nigeria.
[3.] Department of Civil Engineering, University of Nigeria, Nsukka, Nigeria

The study developed a model for gully erosion control. The model, helped to predict total soil loss per annum particularly in the catchment area of Nworie river. Other theoretical models were used to compare results obtained for soil prediction in gully erosion. A Deterministic Model was developed for the study which is called "Project Model" was formulated as for soil loss prediction in the catchment area. The model (formulated as an algorithm for optimizing the amount of soil loss). Soil loss value for Project model in the month of highest annual rainfall was 76.15 metric ton and while that of Universal Soil Loss Equation for the same month was 78.86 metric ton. The study also showed that rainfall depth contributed to soil loss in gully erosion. Test of confidence was carried out with Student t-test and Fisher's test at 5% level of significance and found adequate of the deterministic model. It was recommended that for any known soil value, the project model can be adopted in calculating confidently the amount of soil loss in the area that may precipitate gully erosion.

Key words: *Critical Depth, Erodibility, Gully Erosion, Determinstic Model, Shear Stress, Soil Loss,*

I. INTRODUCTION

Taking steps to preserve the quality and quantity of global soil resources should require no justification. Our future ability to feed ourselves and to live in an unpolluted environment depends on our ability to understand and to reduce the rates at which our soils are currently eroding. Over the last decades, most research on soil erosion by water has concentrated on interrill (sheet) and rill erosion processes operating at the runoff plot scale. Relatively few studies have been conducted on gully erosion operating at larger spatial scales. Recent studies like, Water Erosion Prediction Project (WEPP) Flanagan, (2001), Precision Agricultural-Landscape Modeling System (PALMS) etc. indicate that soil losses by gully erosion are far from negligible in a range of environmental problems. Consequently, there is a particular need for monitoring (through experimental and modeling studies of gully erosion) as basis for predicting the effects of global changes (landuse and climate changes) on gully erosion rates as well as on the contribution of this soil degradation process to overall land degradation Todd, (2010).

For some years recently, channels in some parts along Nworie River were noticed to have entrenched into valleys. These channels generally eroded into red-earth and unconsolidated geologic materials establishing prominent gullies with near vertical slopes.

Increased erosion activities in the vicinity of the early gullies have continued to expand these gullies into a complex system. Most of the gullies especially those with high discharge value are now of canyon proportion, and constitute the most threatening environmental hazard in parts of Nworie River which runs along the Metropolis of Owerri, Imo State (Acholonu, 2008).

The control measures so far adopted in the affected areas have been concentrated on control of surface waters runoff (their volume and velocity), by the construction of some hydraulic structures and planting of trees to strengthen the soil. These measures appear to have given some success in the shallow (4 - 15m deep) gullies which cut mainly into red clayey earth; they have however failed in deep gullies which cut into very permeable and cohesionless sand where the gully walls are indented with spring sand seepages at various horizons.

II. METHODOLOGY

The study focused on development of a model for determining the erosion occurring along the waterside area of Nworie River of Imo State Nigeria.

2.1 LOCATION OF STUDY AREA

Figure 1: Location of the Study Area.

Nworie River catchment basin area was used as the study. The river originates from Mbaitolu LGA of Imo State and passes though Owerri Municipal LGA of Imo State and then empties into the Otamiri River at Nekede, Owerri West LGA, Imo State. The measured length of the river is approximately 9 kilometers and the area of the catchment is approximately, 30 square kilometers.

2.2 RAINFALL DATA IN OWERRI

Rainfall distribution in Owerri, with peaks in July and September and a two-week break in August. The rainy season begins in March and lasts till October or early November. See Table 1. Rainfall is often at its maximum at night and during the early morning hours. However, variations occur in rainfall amount from year to year.

Table 1: Average rainfall from 1979 to 2010

	[mm]
Jan	20.9
Feb	31.8
Mar	155.6
Apr	186.1
May	278.1
Jun	290.1
Jul	312.6
Aug	375.5
Sep	429.9
Oct	313.4
Nov	103.4
Dec	9.8
Ann.	2507.0

Source: AIRBDA Weather Report 2010.

The result of temperature measured in degree centigrade is based on average monthly temperature of the study area, see Table 2.

Table 2: The Average Temperature of the Catchment

	Mean temp. [deg C] 1985-1990	Mean Temp [deg C] 2007	Mean temp. [deg C] 2008
Jan	26.50	26.00	26.25
Feb	28.50	27.00	27.75
Mar	28.00	27.00	27.50
Apr	28.00	27.00	27.50
May	27.00	27.00	27.00
Jun	26.50	25.00	25.75
Jul	25.00	25.00	25.00
Aug	25.30	25.00	25.15
Sep	25.50	25.00	25.25
Oct	26.00	26.00	26.00
Nov	27.00	26.00	26.50
Dec	26.50	26.00	26.25
Ann.	26.65	26.00	26.33

Source: AIRBDA Weather Report (2010)

2.3 MODEL DEVELOPMENT FOR SOIL LOSS

The model was based on the governing sediment continuity equation. The governing sediment continuity equation as stated by Nearing et al. (1989) as:

$$\frac{dq_{sb}}{dx} = q_{ie} + q_{re} \quad (1)$$

where

x (m) = distance downslope.
q_{sb} (kg s^{-1} m^{-1}) = sediment load.
q_{ie} (kg s^{-1} m^{-2}) = interrill erosion rate.
q_{re} (kg s^{-1} m^{-2}) = rill erosion rate.

Integrating equation (1), with respect to independent variable x, the sediment load becomes the model transport capacity and we have the equation as follow;

$$ASL = q_{ie}x + q_{re}x + C \quad (2)$$

where

C = constant of integration (kg/km^2)
q_{re} = rill erosion rate (kg $s^{-1}km^{-2}$)
q_{ie} = interrill erosion rate (kg $s^{-1}km^{-2}$)
x = integration independent value (s)

C is taken as amount of soil loss due to gully erosion, measured in kg/km^2 and is denoted as q_g. in the same way $q_{re}x$ is soil loss due to rill erosion, measured in kg/km^2 is denoted as q_r, while $q_{ie}x$ is amount of soil loss due to interrill erosion, measured in kg/km^2 is denoted as q_i. Substituting these terms into equation (2) gives the project model equation as shown in equation (3).

$$ASL = q_g + q_i + q_r \quad (3)$$

where

ASL = Amount of soil loss in the catchment, measured in kg/km^2.
q_g = Amount of soil loss due to gully erosion
q_i = Amount of soil loss due to interrill erosion
q_r = Amount of soil loss due to rill erosion

2.4 DETERMINATION OF SOIL LOSS DUE TO GULLY EROSION, q_g

In the determination of soil loss due to gully erosion, Agunwamba (2001) gave the equation from soil loss due to gully erosion as:

$$q_g = K_t \tau_f V_c \quad (4)$$

where

K_t = Erodibility of the transport,

The value of K_t depends on density of the soil. This value ranges from 0.077 to 0.11(Gilley, 1990). It is measured in $s^2m^{0.5}kg^{-0.5}$.

τ_f = Shear stress of the soil,

Shear stress of soil, τ_f is the ability of the soil to resist cutting effect from cutting loads. It is measured in N/mm^2. Gilley, (1990) gave the equation of shear stress of soil as:

$$\tau_f = \gamma_w S_f R \left(\frac{f_s}{f_t}\right) \quad (5)$$

For wide channels, f_s/f_t is taken as 0.7. R means the hydraulic radius and it is equal to the critical depth of flow, y_c for wide channels. It is measured in meters (m). The equation of critical depth of flow Henderson, (1966) is:

$$d_c = \sqrt[3]{\frac{q^2}{g}} \quad (6)$$

where q = discharge per ft. (m) of width $m^3/s/m$ (cfs/ft.).
Thus for rill erosion purpose, the hydraulic radius can be taken as y_c:

$$R = y_c = \sqrt[3]{\frac{Q^2}{g}} \quad (6a)$$

S_f means slope along the wide channel. It is a dimensionless parameter.
(Ken, 2004) it is given as:

$$S_f = 1.3 * S \quad (7)$$

where S is the normal slope of the land near the river.

γ_w means the unit weight of the water. It is measured in N/m^3. In most cases, it is taken as 9.8 KN/m^3

V_c = Critical velocity,

Critical velocity means the velocity of water at the critical depth of flow. It is measured in m/s. The equation for critical velocity Agunwamba, (2001) is given as:

$$V_c = \sqrt{g y_C} \quad (8)$$

where g means acceleration due to gravity taken as 9.81m/s^2,

2.5 DETERMINATION OF SOIL LOSS DUE TO RILL EROSION, q_r

The equation for the rate of soil loss (Flanagan, 1995) is given as:

$$q_{re} = q_c\left[1 - \frac{qsb}{q_g}\right] \quad 9$$

Rill detachment capacity for clean water, q_c

q_c means rill detachment capacity for clean water. It is measured in kg/m^2/s. the equation for calculating q_c Elliot, (1988), is given as:

$$q_c = k_r(\tau_f - \tau_c) \quad 10$$

K_r is rill erodibility (sm^{-1}) factor, and it can be calculated using the equation Kr = 0.00197+0.03 vfs + 0.03863e$^{-184orgmat}$.

τ_f is the soil shear stress as defined in equation 5.

τ_c is the soil critical shear stress, it can be calculated using the equation $\tau_c = \gamma RS$ and is measured in MPA or N/mm^2 Carlos, (2007).

Volumetric unit bed sediment transport rate, q_{sb}

q_{sb} means Volumetric unit bed sediment transport rate. It is measured in m^3/s. the equation for q_{sb} Howard, (1994):

$$q_{sb} = \Phi * \omega * d(1 - \mu) \quad 11$$

q_g means the soil loss due to gully erosion as we have it on equation (4).

Φ is a dimensional parameter in the equation and can be calculated with this equation Hood, (2002) as;

$$\Phi = k_e\left\{\frac{1}{\Psi} - \frac{1}{\Psi_c}\right\}^p$$

where ke is effective saturated conductivity (mm/h) from Table A5.

Ψ is taken from Table A1 as 110mm or 0.11m and ψ_c is negligible, it takes value of zero while p is the power of the equation and is 3.

ω is the fall velocit y of the sediment grains, measured in m/s.

d is the sediment grain size, measured in mm.

μ is alluvium porosity

2.6 DETERMINATION OF SOIL LOSS DUE TO INTERRILL EROSION, q_i

The equation for interrill erosion rate, q_{ie} Nearing et al. (1989) is given as:

$$q_{ie} = k_i I_e^2 C_e G_e\left(\frac{R_s}{w}\right) \quad 12$$

where

K_i means, baseline interrill erodibility and it is measured in kgs/m. the equation to calculate K_i is given by Flanagan and Nearing (1995) as:

$$K_i = 2728000 + 19210000\, vfs \quad 13$$

Where, vfs = very fine sand fraction.

I_e means effective rainfall intensity. It is measured in mm/s. The value is the rainfall intensity collected from metrological station of the catchment for the period in question.

C_e means the effect of canopy on interrill erosion. This is the way catchment surface is being covered. This cover can come from leaves and branches of trees, grasses and other man made canopies. It can be estimated with the equation by Nearing et al. (1989) as:

$$C_e = 1 - F_c\, e^{-0.34H_c} \quad 14$$

Laflen et al. (1985), F_c means portion of the soil the canopy covered. This is estimated from site observation to know the percentage of the catchment that is being covered by the canopy and the ones uncovered, the fraction being covered is the F_c. The height of this canopy is denoted as H_c. It is measured in meters.

G_e means the effect of ground cover on interril erosion. Ground cover in this case means humus and dead grasses and leaves, which cover the surface of soil and thus protect it from direct attack of rain drops. It is being estimated (Nearing et al., 1989) as:

$$G_e = e^{-2.5\, g_i} \quad 15$$

g_i is the fraction the catchment covered by the humus.

R_s means the average spacing between one rill and the other. It is measured in meters and got from site observation and measurement.

W means the average width of the rill in the catchment. It is measured in meters and got from site observation and measurement.

2.7 DATA REQUIREMENTS

The parameters used in the study included:

- Rainfall data
- Slope of the land
- Drainage of the catchment area
- Soil characteristics
- Watershed length

- Runoff (discharge) measured in cubic meters

Then from the point where the slope starts to increase to the stream was about 250m and the slope increases to 30% which is $130/100 * 0.39 = 0.507$.

For Nworie Catchment area, Area = 30km^2 (Ministry of Lands, Survey and Urban Planning (2010)) and in circular manner its radius is 3.0902km and diameter is 6.1804km, so L = 9km, Lc = 3.0902km, C_t = 1.7, C_p = 0.8. Considering the exit point along Nworie River, the area of interest is about 2km^2 and the L = 500m and Lc = 230m, all other constants remain the same.

2.8 DISCHARGE FROM THE CATCHMENT

SCS Dimensionless Unit Hydrograph

The Soil Conservation Society Method (SCS) dimensionless hydrograph is a synthetic hydrograph in which the discharge is expressed by the ratio of discharge q to peak discharge q_p and the time t to the time of rise of unit hydrograph, T_p. Given the peak discharge and lag time for the duration of excess rainfall, the unit hydrograph can be estimated from the synthetic dimensionless hydrograph for a given basin. It can be shown that:

$$q_p = \frac{CA}{T_p} \qquad 16$$

where: C = 2.08 and A = drainage area 30 km^2, Tp = Time of rise or Time to peak.

Example of Peak Discharge on September rainfall

$$Q_P = \frac{2.78 C_p A}{T_P} = \frac{2.78 * 1 * 0.4 * 2}{0.407107} = 5.462937262\ m^3/s$$

2.9 UNIVERSAL SOIL LOSS EQUATION (USLE) MODEL:

This is a well recognized model for soil loss prediction from raindrop splash, which loses and raises particles of soil that are then transported by overland flow to reach the hydrographic network. Control measures applied against surface erosion are derived from Universal Soil Loss Equation (U. S. L. E.). According to Bauman, (2002). U. S. L. E., the quantity of soil, A (in ton /acre) removed by sheet erosion on a slope as a consequence of rainstorm occurring over a defined period usually one year is given by the product of six factors:

A = R*K*(LS)*C*P

where R = Rainfall (and runoff) factor, or erosivity factor
K = soil erodibility factor
L = Slope length factor
S = The slope steepness factor
C = The lower and management factor
P = The soil conservation practices factor.

Soil loss in crop land is reduced by adopting appropriate conservation practices. The expected reduction due to P cannot be more than 0.25 as in contouring.

It has been proved from erosion studies that the only factors which obviously could radically be modified by possible interventions are vegetation cover (C) and the topography of slope.

There are various methods of sheet erosion control. The North American green method of erosion control offers a very effective and advanced method of sheet erosion control. The system offers a variety of Erosion Control blankets to suit a variety of situations. It controls erosion in heavy rains and conserves moisture when there is no rain. The erosion control blankets create an ideal environment for seeds to germinate. Because the blankets are so well constructed and porous, the ground accepts additional moisture through rainfall.

Example; R = Rainfall (and runoff) factor, or erosivity factor = 2638.2/26.375 = 100

K = soil erodibility factor 0.36

L = Slope length factor 375

S = The slope steepness factor 60

} 16.82

$$LS = (\lambda / 72.6)m\ (65.41 \sin 2\theta + 4.65 \sin \theta + 0.065)$$

C = The lower and management factor 0.85

P = The soil conservation practices factor. 0.9

A = R *K *(LS) *C *P

$$A = 100 * 0.36 * 16.82 * 0.85 * 0.9 = 463.2228\ ton/km^2/year$$

Plate 1: Erosion at Discharge Point

III. RESULTS AND DISCUSSIONS

The summary results of soil samples obtained in the study area are shown in Table 3. Percentage of clay fraction varied between 10% - 18% in the increasing order. However, cohesion of soil from the study area varied between 18KN/ m^2 -23KN/m^2. There is no much variation in the soil cohesion of the study area.

Table 3: Soil Sample Result of the Study Area

i.	Soil	~~Average of~~ Parameters	Ave. values
	Dark brown organic	% organic content :	45%
	Silty sand	% clay fraction :	10%
		Friction (ϕ) :	10^0
		Cohesion(C) :	22kN/m^2
ii.	Soil	Average of Parameters	
	Light brown silty	% organic content	23%
	Sand	% clay fraction	12%
		Friction	30^0
		Cohesion	18kN/m^2
iii.	Dark red clayey	% Clay fraction	14%
	Sand	Friction	29^0
		Cohesion	21kN/m^2
		Density	19.8kN/m^3
iv.	Reddish Sandy	% Clay fraction	18%
	Clay	Plasticity index	17%
		Friction	27^0
		Cohesion	23kN/m^2

Table 4: Discharge of Flood at Point of Interest of the Study Area (at high depth of rain in each month) (m^3/sec)

	Discharge based on 1 cm drop of water multiply by monthly rain depth in cm		
Month	Area 2km^2 (m^3/sec)	Area 26km^2 (m^3/sec)	Total (m^3/sec)
Jan	11.25	36.13	47.38
Feb	17.15	55.08	72.23
Mar	83.92	269.45	353.37
Apr	100.36	322.26	422.62
May	149.97	481.54	631.51
Jun	156.44	502.32	658.76
Jul	168.59	541.33	709.92
Aug	202.50	650.21	852.72
Sep	231.84	744.41	976.25
Oct	169.02	542.71	711.74
Nov	55.78	179.10	234.88

Dec	5.29	16.97	22.26
Ann.	1352.11	4341.52	

Table 5: Relation Of Climatic Factors to Discharge

Climate factor	Maximum value	Minimum value	Average value
Temperature (^{0}C)	27.75	25.00	26.375
Precipitation [mm/month]	429.9	9.8	219.85
Discharge (m^3/sec/month) one point	231.84	5.29	118.565
Discharge (m^3/sec/month) all points	744.41	16.97	380.69

Universal Soil Loss Equation (USLE Model) Foster, (2003) is computed undergoing the necessary parameter of the equation the annual amount of soil loss is obtained on tonnes per square kilometer (ton/Km^2) and after discretization based on monthly period then the soil loss is summed up to 447.9982ton/km^2 and is presented on Table 4.

Table 6: Monthly Erosion Amount based on Universal Soil Loss Equation (USLE) A = RKLSCP

Month	R	K	LS	C	P	A
Jan	0.794762	0.36	16.82	0.85	0.9	3.681518
Feb	1.146096	0.36	16.82	0.85	0.9	5.308978
Mar	5.657879	0.36	16.82	0.85	0.9	26.20858
Apr	6.766667	0.36	16.82	0.85	0.9	31.34474
May	10.29846	0.36	16.82	0.85	0.9	47.7048
Jun	11.2644	0.36	16.82	0.85	0.9	52.17928
Jul	12.50333	0.36	16.82	0.85	0.9	57.91829
Aug	14.92876	0.36	16.82	0.85	0.9	69.15342
Sep	17.02376	0.36	16.82	0.85	0.9	78.85795
Oct	12.05321	0.36	16.82	0.85	0.9	55.83319
Nov	3.902673	0.36	16.82	0.85	0.9	18.07807
Dec	0.373333	0.36	16.82	0.85	0.9	1.729365
Annual Soil Loss.						447.9982

The Project Model of this study was used in calculating the soil loss caused by Gully, Rill and Interrill erosion in the catchment area and the total is also computed as the Amount of the soil loss under the discretization of monthly period of time and summed up to get that of annual to be 474.92ton/km^2 shown on Table 6 and the significance will publicized on the analysis of hypothesis.

Table 7: Monthly Erosion Amount based Project Model

Month	Mean temp. [deg C]	mm	Discharge in 1cm 2Km^2 m^3/sec	Discharge in 1cm 26Km^2 m^3/sec	Interrill Erosion ton/km^2	Rill Erosion ton/km^2	Gully Erosion ton/km^2	Amount of Soil loss ton/km^2
Jan	26.25	20.86	11.25	36.13	0.0068	-0.0170	3.66	3.65
Feb	27.75	31.80	17.15	55.08	0.0054	0.0371	6.38	6.43
Mar	27.50	155.59	83.92	269.45	0.0023	0.2798	27.32	27.60
Apr	27.50	186.08	100.36	322.26	0.0021	0.3955	37.35	37.74
May	27.00	278.06	149.97	481.54	0.0017	0.4699	48.83	49.30
Jun	25.75	290.06	156.44	502.32	0.0017	0.5738	58.21	58.79
Jul	25.00	312.58	168.59	541.33	0.0016	0.5180	54.89	55.41
Aug	25.15	375.46	202.50	650.21	0.0015	0.7045	75.35	76.06
Sep	25.25	429.85	231.84	744.41	0.0014	0.6695	75.48	76.15
Oct	26.00	313.38	169.02	542.71	0.0016	0.6107	62.89	63.51
Nov	26.50	103.42	55.78	179.10	0.0029	0.1839	18.16	18.35
Dec	26.25	9.80	5.29	16.97	0.0101	-0.0496	1.97	1.93
Ann.	26.33	2506.95	1352.11	4341.52	-	-	470.50	474.92

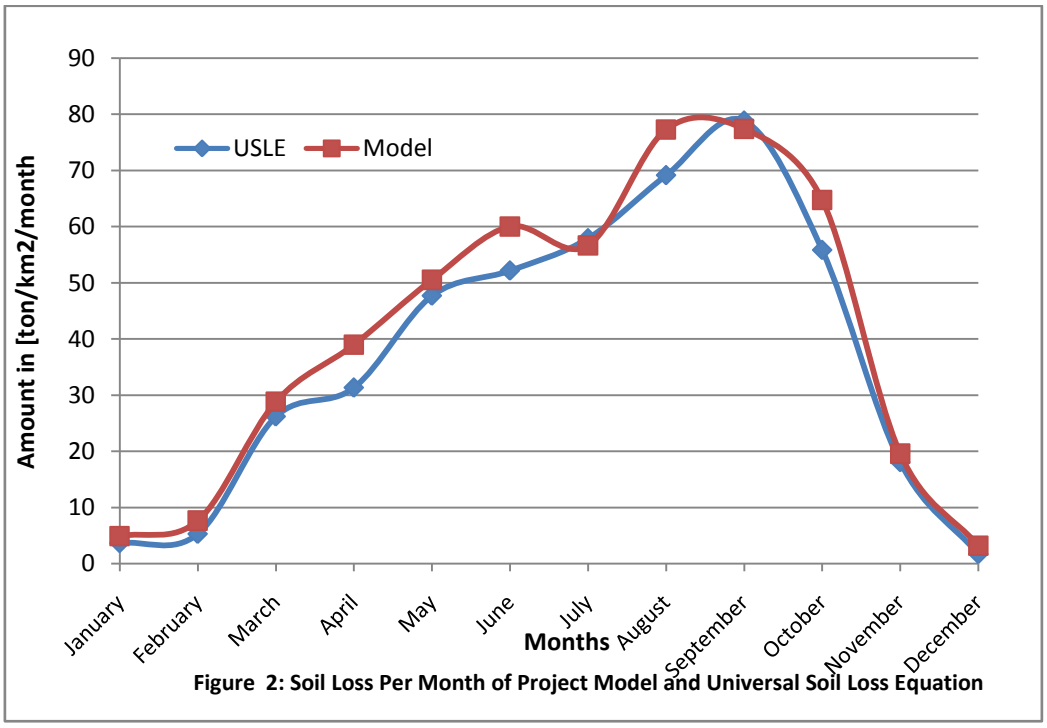

Figure 2: Soil Loss Per Month of Project Model and Universal Soil Loss Equation

Table 8: Monthly Erosion Amount of Project Developed Model and Universal Soil Loss Equation

	Project Developed Model PDM	A USLE	Percentage difference
Month	$Y_{(model)}$	$Y_{(USLE)}$	Δ%
Jan	3.65	3.68	0.815217
Feb	6.43	5.31	21.09228
Mar	27.60	26.21	5.303319
Apr	37.74	31.34	20.42119
May	49.30	47.70	3.354298
Jun	58.79	52.18	12.66769
Jul	55.41	57.92	4.333564
Aug	76.06	69.15	9.992769
Sep	76.15	78.86	3.43647
Oct	63.51	55.83	13.75605
Nov	18.35	18.08	1.493363
Dec	1.93	1.73	11.56069
Ann.	474.92	448.00	6.008929

IV. CONCLUSIONS

The project succeeded in providing information on the type of soil, exposure and soil practices use that play important roles in erosion control. In the study, Interrill(sheet), Rill and Gully erosion have been shown to be significant factors that contributed to the total amount of soil loss. Besides, the project mathematical model that was formulated for optimizing the amount of soil loss was significant in determining control approach for gully erosion.

In addition, the project model results were compared with that of Universal Soil Loss Equation result using Student T-test and Fisher's test and found to be adequate. The results for the T-test and that of the Model were found to be significant at 5% level; the Fisher's test result was significant at 5% level which is adequate, and null hypothesis was rejected.

It could therefore be concluded that for any known soil value, the project model can be adopted in calculating the amount of soil loss in the region confidently without running into difficulties.

REFERENCES

[1] Acholonu, A. D. W. (2008). "Water ` Quality Studies Of Nworie River In Owerri, Nigeria". Mississippi Academy of Sciences.
[2] Agunwamba, J. C. (2001). Waste Engineering And Management Tools. Immaculate Publication Ltd. #2 Aku Street, Ogui N/Layout, Enugu.
[3] AIRBDA Weather Report (2009). Imo State Weather Report. Department of Researcher and Weather Report, Anambra Imo River Basin Metrological Station km 8 Agbala Owerri, Aba Road.
[4] Baumann, J.; Arellano-Monterrosas, J.L. and Borgman, J. (2002). Adaptation Of The Universal Soil Loss Equation To The Tropical Pacific Coastal Region Of The Chiapas State, Mexico. 12th ISCO Conference, Beijing, China, pp. 518–523.
[5] Carlos, A.V.; Bennett, S.J.; Casali, J.; Römkens, M.J.M. and Prasad, S.N. (2007). Self-Similarity And Headcut Dynamics: Basic hypotheses and analysis. USDA-ARS, National Sedimentation Laboratory, P.O. Box 1157, Oxford, MS 38655, USA.
[6] Elliot, W. J.; Robichaud, P. R. and Wagenbrenner, J. W. (1988), Forestry Sciences Laboratory, Rocky Mountain Research Station, Forest Service, U.S. Department of Agriculture, 1221 South Main St., Moscow, ID 83843, USA. (probichaud@fs.fed.us)
[7] Flanagan, D. C. and Nearing, M. A. (1995). USDA-Water Erosion Prediction Project: Hillslope profile and watershed model documentation. NSERL Rep. 10. Natl. Soil Erosion Res. Lab., West Lafayette, IN.
[8] Flanagan, D. C.; Ascough II, J. C.; Nearing, M. A. and Laflen, J. M. (2001). The Water Erosion Prediction Project (WEPP) Model. p. 145–199. In R.S. Harmon and W.W. Doe III (ed.) Landscape erosion and evolution modeling. Kluwer Acad. Publ., New York.
[9] Foster, G. R.; Toy, T. E. and Renard, K. G. (2003). Comparison Of The USLE, RUSLE1.06c, and RUSLE2 for application to highly disturbed lands. p. 154–160. In K.G. Renard et al. (ed.) Proc. Interagency Conf. on Research in the Watersheds, 1st, Benson, AZ. 27–30 Oct. 2003. USDA-ARS, Tucson, AZ.
[10] Foster, S. S. D. (1987) Fundamental Concepts In Aquifer Vulnerability Pollution Risk Protection Strategy. In: Vulnerabiliiv of Soil and Groundwater to Pollutants (ed. by W. Van Duijrenbooden & FI. G. Van Waegeningh), 69-86. TNO Committee on Hydrological Research, Proc. and Info. no. 38. The Hague, The Netherlands.
[11] Gilley, J.E.; Kottwitz, E.R. and Simanton, J.R. (1990). Hydraulic Characteristics Of Rills. Trans. ASAE 33:1900–1906.
[12] Henderson, F. M. (1966). Open Channel Flow. Macmillan Publishing Co., Inc. 866 Third Avenue, New York, 10022.
[13] Hood, S.M.; Zedaker, S.M.; Aust, W.M. and Smith, D.W. (2002). Universal Soil Loss Equation.(USLE)Predicted Soil Loss for Harvesting Regimes in Appalachian Hardwoods. North. J. Appl. For. 19(2):53–58.
[14] Howard, A. D. (1994). A detachment-Limited Model of drainage basin evolution. Water Resources Research, Vol. 30, No. 7. Page 2261-2285.
[15] Howard, A. D. (1994a). 'Badlands', in Abrahams, A. D. and Parsons, A. J. (Eds), Geomorphology Of Desert Environments, Chapman & Hall, London, 21 3–242.
[16] Ken-Bohuslav, P. E. (2004). Hydraulic Design Manual. Texas Department of Transportation (TxDOT) Published by the Design Division (DES) (512) 416-2055.
[17] Laflen, J. M. (1985). Effect Of Tillage Systems On Concentrated Flow Erosion. In: Pla, I.S. (Ed.), Soil Conservation and Productivity, vol. 2. Universidad Central de Venezuela, Maracay, pp. 798–809.
[18] Ministry of Lands, Survey and Urban Planning, (2010): Nworie River Data. Office of Honorable Commissioner Ministry of Lands, Survey and Urban Planning, Owerri Imo State, Nigeria.
[19] Nearing, M. A.; Foster, G. R.; Lane, L. J. and Finkner, S. C. (1989). A Process Based Soil Erosion Model For Usda Water Erosion Prediction Project Technology. Trans. ASAE 32:1587–1593.
[20] Todd, M. (2010). Advisory & Regulatory Services Natural Resource Management. Balancing Conservation and Development Alice Springs, NT 0870 http://www.nreta.nt.gov.au/advis/

International Journal of Modern Engineering Research (IJMER)
www.ijmer.com Vol. 3, Issue. 3, May.-June. 2013 pp-1783-1786 ISSN: 2249-6645

Determination of the Binding Constant of Tris-3, 4, 7, 8-Tetramethyl - (1, 10-Phenanthroline) Iron (II) Sulphate with Sodium Dodecyl Sulphate

[1]Latona D. F., [2]Soriyan O. O. & [3]Ige W. J.
[1]*Osun State Polytechnic, Department of Applied Science, PMB 301, Iree, Nigeria*
[2, 3] *Obafemi Awolowo University, Department of Chemistry, Ile-Ife, Nigeria*

Abstract: *The binding of tris- 3,4,7,8 – tetramethyl- 1,10- phenanthroline)iron(II) sulphate with sodium dodecyl sulphate was done using a unicam UV-Visible spectrophotometer at 25°C and the analyses were done by employing double reciprocal plots. Absorbance were taken at fixed concentration of the metal complex (1.45 x 10^{-5} mol dm^{-3}) and the concentration range of sodium dodecyl sulphate was far below the critical micelle concentration of the surfactant (2.00 x 10^{-5} - 3.50 x 10^{-4} mol dm^{-3}). The binding study was done as a function of alkaline, acidic, benzoate ion and urea concentration at fixed concentration range of 0.50 x 10^{-5} – 3.00 X 10^{-5} mol dm^{-3}. Binding increased at low [H+] to reach a maximum at [H^+] = 2.00 x 10^{-4} mol dm^{-3} after which there was a decrease in binding. The binding reaction was retarded in the presence of OH^- and urea and enhanced in benzoate ion.*

I. INTRODUCTION

Binding constant otherwise known as equilibrium constant is a ratio of rate constant of association and dissociation in binding studies. Over the years a lot of researches have been reported on binding constant determination using various techniques. The equilibrium binding constants of Group I metal cations with gramicidin A in aqueous dispersion of lyso-pc have been determined employing a combination of competitive binding with the Tl+ ion and Tl- 205 NMR spectroscopy (Hinton et al., 1986). The binding constants at 34°C of the Group I metals were reported as Li (32.2 M^{-1}), Na (36.9 M^{-1}), K (52.6 M^{-1}), Rb (55.9 M^{-1}) and Cs (54.0 M^{-1}). While the equilibrium binding constant for the Tl + ion at this temperature was reported as 582 M^{-1}. The relationship between the binding constants, free energy of the binding process, and the cation selectivity of the gramicidin A channel were discussed.

Furthermore, on Alkali metal ions, the binding constants between polymer-supported azacrown ether ion exchanger, { (4,5) : (13,14) – dibenzo- 6,9,12 – trioxa – 3,15, 21- triazazabicyclo[15.3.1] heneicosa – 1(21),17,19 - triene-2,16-dione:DBPDA ion exchanger} with alkali metal ions (Li^+, Na^+, K^+) picrates were studied by spectrophotometry. The binding constants of alkali metal ions were in the order Li < Na < K and that the alkaline metal ions formed 1:1 complexes with ligands of DBPDA ion exchanger. The enthalpy and entropy changes were found in the ranges of -2.71 – 3.79 kcal/mol and -16.52- 20.57eu, respectively (Choi et al., 1993). Binding constants between Indomethacin Ester to Human serium Albumin were calculated by Scatchard model. It was reported that the binding to human serium albumin was 14 x 10^{-5} mol/l (Trnavska and Verner, 1983).

Moreover, the kinetics and equilibrium binding of dyes, 2 – (p- Toluidino)naphthalene-6-sulfonate (TNS) and N-(4 – sulfobutyl)- 4- [4 – [p- (dipentylamino) phenyl] butadienyl} pyridinium inert salt (RH421) to ribulose 1,5 – bisphosphate carboxylase/ oxygenase (RUBISCO) was investigated. The investigation revealed that TNS binds in a reversible bimolecular reaction non – covalently to RUBISCO, the water – soluble enzyme for carbon dioxide fixation and that TNS dose not change the substrate activity at the active site of RUBISCO. The rate constants for the association and dissociation were given as (1.2 ± 0.2) x 10^7 dm^3 mol^{-1} s^{-1} and 1020 ± 300 s^{-1}, respectively. While the binding of RH421 to RUBISCO was reported to be a diffusion – controlled reversible bimolecular reaction with an association rate constant of (7 ± 0.6) x 10^9 dm^3 mol^{-1} s^{-1} and dissociation rate constant of (1.8 ± 0.2) x 10^4 s^{-1}. The dissociation constants obtained from kinetically determined rate constants were in good agreement with those measured by equilibrium techniques (Frank et al., 1997).

The association of Rose Bengal (RB) with bovine serium albumin (BSA) was investigated by absorption spectroscopy and the binding constant was determined from the effect observed in the absorbance at 548nm upon addition of the protein according to the Benesi – Hildebrand treatment. It was concluded that the RB to BSA interaction was dominated by hydrophobic effects (Abuin et al., 2007).

II. MATERIALS AND METHODS

Tris-(3,4,7,8-tetramethyl-l,10-phenanthroline)iron(II) sulphate,$Fe(Me_4phen)_3]SO_4$ was synthesized and purified according to the literature method (Shakhashuri, and Gordon, 1964). The complex was characterized by its UV-visible spectra. The maximum absorption peaks (λmax) determined was 500nm . These are in excellent agreement with the literature values (Shakhashuri and Gordon , 1964)

Purified sodium dodecyl sulphate (99%) was used without further recrystallisation. The purity was ascertained by determination of the critical micelle concentration in aqueous solution at 25°C. The value of 8.20 x 10^{-3} mol dm^{-3} obtained is in good agreement with the literature value (Williams et al, 1985). Analar grade (BDH) sodium hydroxide (NaOH), sodium benzoate (C_6H_5COONa), sulphuric acid (H_2SO_4) ,and urea were used.

Synthesis of Tris - (3,4,7,8-tetramethyl-l, 10-phenanthroline) iron (II) sulphate: Tris- (3, 4, 7, 8 – tetramethyl -l, 10 - phenanthroline) iron (II) sulphate was synthesized by dissolving a mixture of 0.3985 g (≈ 1.686 x 10^{-3} mole) of 3, 4, 7,8 tetramethyl (1, 10-phenanthroline) ligand and 0.2204 g (≈ 5.621 x 10^{-4} mole) of ferrous ammonium sulphate ($FeSO_4$ $(NH_4)_2$ SO_4. $6H_2O$) in 5 ml of distilled water in a beaker. The resulting dark red solution was heated . Then the solution was stirred briefly and allowed to cool at room temperature.It was later left to dry in a dessicator.

Investigation of Binding of Iron(II) complexes with sodium dodecyl sulphate (SDS): The investigation of binding of Iron(II) complexes with sodium dodecyl sulphate (SDS) was done using a Unicam UV-Visible spectrophotometer and the analysis were done using double reciprocal plot. The absorbance was taken at maximum absorption peak (λmax) and the concentration range of sodium dodecyl sulphate was (2.00xl0^{-5} - 3.50 xl0^{-4} mol dm^{-3}). The fraction of Iron(II) complex ion bound (α) to the SDS was calculated from:

$$\alpha = \frac{A - A_O}{A_\infty - A_O}$$

Where Ao =absorbance of the complex when no SDS was added

A∞ = absorbance when the Iron(II) complex solution was saturated with SDS.

A = absorbance when known amounts of SDS were added.

Concentration of total Iron (II) complex ion was obtained by using the molar extinction coefficient at λ_{max}. The concentration of the free Iron (II) complex ion $[Fe^{2+}]_f$ was obtained from

$$[Fe^{2+}]_f = [Fe^{2+}]_T - \alpha [Fe^{2+}]_T$$

Where $[Fe^{2+}]_T$ is the total concentration of Iron (II) complex. The average number of molecules of iron (II) complex combined with each SDS (υ) was obtained from:

$$\upsilon = \frac{\left[Fe^{2+}\right]_{bound}}{\left[SDS\right]_{Total}}$$

The plot of l/υ against 1 / $[Fe^{2+}]_f$ was made and the binding constants. were calculated from the slope and intercept using the below equation:

$$\frac{1}{\upsilon} = \frac{1}{n_s} + \frac{1}{n_s K\left[Fe^{2+}\right]_f}$$

III. RESULTS AND DISCUSSION

The binding constants were obtained from double reciprocal plot as shown in Fig. I. The binding constant of tris-3,4,7,8- tetramethyl- (1,10- phenanthroline)iron(II) sulphate, $Fe(Me_4phen)_3^{2+}$ with sodium dodecyl sulphate, SDS in neutral medium was 3.94 x 10^5. At fixed concentration range of acid, binding increased to a maximum value and later decreased with increase in $[H^+]$. Maximum was at $[H^+]$ = 2.00 x 10^{-4} mol dm^{-3}. Table I shows the binding constants (K) as a function of $[H^+]$ in $Fe(Me_4phen)_3^{2+}$. Increase in binding constant with increase in $[H^+]$ was due to the dominance of hydrophobic interaction at low acid concentrations which allows rapid attraction of the complex to the pre micellar surface due to higher negative charge density on SDS. However, as protonation of SDS increases there was consequent decrease in the negative charge density on the pre micelles thereby leading to a decrease in binding. This is in consonance with the kinetic data.

The effect of added sodium benzoate on the binding constant revealed general increase in binding constants with increase in benzoate ion concentrations (Table II). The reason for the increase is due to the orientation of the phenyl group on the benzoate ion which aligns itself below the headgroups of SDS monomers via hydrophobic interaction causing an increase in the negative charge density in the region of the head group and therefore leading to increased coulombic attraction between the metal complex and the monomers.

Furthermore, at fixed concentration range of hydroxyl ion (5.00 x 10^{-6} – 3.00 x 10^{-5} mol dm^{-3}). Binding constant as a function of OH^- showed that binding constant decreased with increase in $[OH^-]$ as shown in Fig. III. The reason is that OH^- increases the dielectric constant of the medium of the reaction, hence leading to a decrease in the hydrophobicity of the medium. Therefore, hydrophobic interaction between the metal chelate complex and SDS was reduced. Binding constant decreased with increased in [urea] as evident in Table IV. This is attributed to the fact that urea reduces the negative charge density on SDS which consequently led to a decrease in electrostatic attraction between the metal center of the metal complex and SDS.

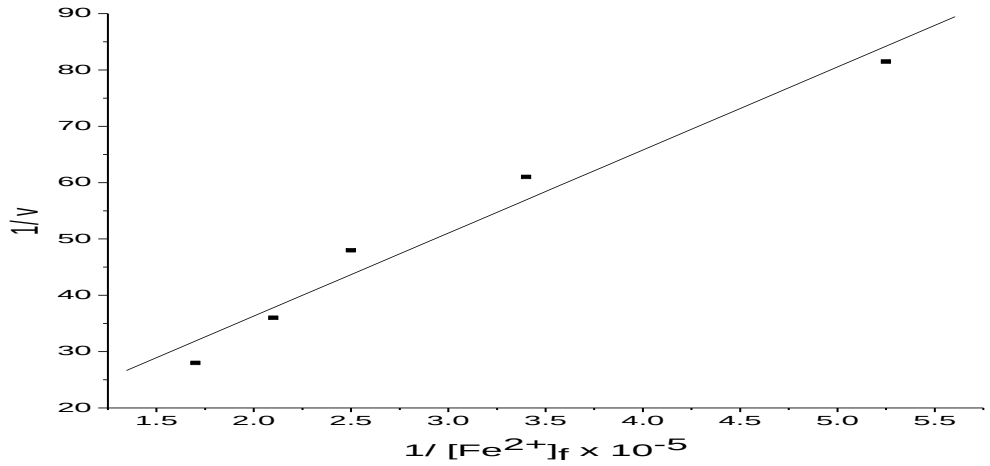

Figure I: Plot of 1/v versus $1/[Fe^{2+}]_f$ as a function of 0.50 x 10^{-4}mol dm^{-3} H^+ of binding between $Fe(Me_4phen)_3^{2+}$ and SDS.

Table I: Binding constant (K) as a function of $[H^+]$

	$[Fe(Me_4phen)_3^{2+}]$= 1.45 x 10^{-5} mol dm^{-3}
$[H^+]$ mol dm^{-3}	**K ± 1.35 x 10^4**
0.50 x 10^{-4}	2.58 x 10^4
1.00 x 10^{-4}	2.99 x 10^4
1.50 x 10^{-4}	5.21 x 10^4
2.00 x 10^{-4}	6.16 x 10^4
2.50 x 10^{-4}	5.39 x 10^4
3.00 x 10^{-4}	5.28 x 10^4

Table II: Binding constant (K) as a function of $[C_6H_5COONa]$

	$[Fe(Me_4phen)_3^{2+}]$=1.45 x10^{-5} mol dm^{-3}
$[C_6H_5COONa]$ mol dm^{-3}	**K ± 1.02 x 10^5**
0.50 x 10^{-5}	1.54 x 10^5
1.00 x 10^{-5}	1.74 x 10^5
1.50 x 10^{-5}	1.77 x 10^5
2.00 x 10^{-5}	2.01 x 10^5
2.50 x 10^{-5}	2.08 x 10^5
3.00 x 10^{-5}	4.27 x 10^5

Table III: Binding constant (K) as a function of $[OH^-]$

	$[Fe(Me_4phen)_3^{2+}]$=1.45 x 10^{-5} mol dm^{-3}
$[OH^-]$ mol dm^{-3}	**K ± 0.16 x 10^5**
0.50 x 10^{-5}	1.54 x 10^5
1.00 x 10^{-5}	1.36 x 10^5
1.50 x 10^{-5}	1.34 x 10^5
2.00 x 10^{-5}	1.21 x 10^5
2.50 x 10^{-5}	1.15 x 10^5
3.00 x 10^{-5}	1.10 x 10^5

Table IV: Binding constant (K) as a function of [urea]

	$[Fe(Me_4phen)_3^{2+}]$=1.45 x 10^{-5} mol dm^{-3}
[urea] mol dm^{-3}	**K ± 0.14 x 10^5**
0.50 x 10^{-5}	1.56 x 10^5
1.00 x 10^{-5}	1.39 x 10^5
1.50 x 10^{-5}	1.28 x 10^5
2.00 x 10^{-5}	1.25 x 10^5
2.50 x 10^{-5}	1.20 x 10^5
3.00 x 10^{-5}	1.18 x 10^5

IV. CONCLUSION

The binding constant is majorly dependent on the rate constant of association than rate constant of dissociation. Results obtained from earlier work on the kinetics of binding of association reaction followed the same trend with the binding constant determination for the same reaction. Generally, rate constants of association is far greater than that of dissociation. The greater the binding constant the lower the rate of dissociation and vice – versa or the more stabilized the complex is with respect to dissociation. The binding process is best explained by both hydrophobic/electrostatic attraction between the metal complex and the surfactant as both phenomenon was used to explain the results obtained. However, in the absence of the substrates, hydrophobic effect took precedence over electrostatic attraction. Conversely, in the presence of substrates like H^+, OH^-, $C_6H_5COO^-$ and urea, electrostatic effect best explain the binding reaction.

REFERENCES

[1]. Abuin A, Aspee A, Lissi E, Leon L. (2007). Binding of rose bengal to bovine serium albumin. J. Chil. Chem.Soc. 52, No2, 1196 – 1197.

[2]. Choi Y.K, Kim D.W, Kim C.S and Jeon Y.S. (1993). Binding properties of Alkali Metal ions with DBPDA ion exchanger. Journal of the Korean chemical society, Vol. 37, No. 5, 12 – 16.

[3]. Frank J, Holzwarth J.F, VanHoek A, Vissei J.W.G and Vater J. (1997). Kinetics and equilibrium binding of the dyes TNSand RH421 to ribulose 1,5 –bisphosphate carboxylase/oxygenase(RUBISCO). J. Chem. Soc., Faraday Trans., 2379 – 2385.

[4]. Hinton J.F, Whaley W.L, Shungu D, Koeppe R.E and Millett F.S (1986). Equilibrium binding constants for the group I metal with gramicidine – A determined by competition studies Tl+ 205 nuclear magnetic resonance spectroscopy. Biophys. J; 50(3); 539 – 544.

[5]. Trnavska Z, Verner P (1983). Binding of Indomethacin Ester with Tropic Acid to Human Serum Albumin. Pharmacology Vol. 26, No. 5, 270 – 273.

[6]. Shakhashuri B.Z and Gordon G.(1964). The oxidation of tris-(1,10- phenanthroline)iron(II) by aqueous chloride. Inorg. Chem.7, 2454 – 2456.

[7]. Williams R.J, Phillips J.W and Mysel K.J.(1985). Critical micelle concentration of sodium dodecyl sulphate at 25oC. Trans. Faraday Soc. 51, 728- 737.

International Journal of Modern Engineering Research (IJMER)
www.ijmer.com Vol. 3, Issue. 3, May.-June. 2013 pp-1787-1791 ISSN: 2249-6645

Development of a Sheet-Metal Component with a Forming Die Using CAE Software Tools (Hyper form) For Design Validation and Improvement

Mr. Amit D. Madake[1], Dr. Vinayak R. Naik[2], Mr. Swapnil S. Kulkarni[3]
1(M.E. Mech-PDD appearing, Student of D.K.T.E.Ichalkaranji Department of Mechanical, Shivaji University, India)
2 (Head of Department of Mechanical, D.K.T.E.Ichalkaranji, Shivaji University, India)
3 (Director, Able Technologies India Pvt. Ltd., Pune, India)

ABSTRACT: *Sheet-metal die is an inseparable constituent of the development process of any given automotive or consumer appliance. In most of the cases, this accounts for a high proportion in the tooling needs of the large size and structural member in any automotive like the chassis and the BIW. Many other brackets and gussets along with peripheral clips etc are invariably made of Sheet-metal due to the strength characteristics complimented by this material and the process of stamping.*

Keywords: *Blank holding Force, Die block, Forming Die Design, HYPERFORM, Punch.*

I. INTRODUCTION

Sheet metal forming is one of the most commonly used processes in industry. Throughout the years, the sheet metal forming industry experienced technological advances that allowed the production of complex parts. However, the advances in die design progressed at a much slower rate, and they still depend heavily on trial-and-error and the experiences of skilled workers. During the development of the Die, a reduction in the number of trials would directly influence the cycle time for development. A shorter cycle time can be planned with due utilization of software tools that would predict the trial results without actually conducting the same. The simulation offered by the software during the process of stamping lends important insights into the modifications needed in the die and/or the component to effect a simplified and productive die. Normally, a Forming die (including Draw die) calls for refined design parameters for ensuring a smooth passage through the trial phase of the developed Die normally accompanied by crucial review inputs over the design of the component too. The study of the papers offers enough inputs to take up the project work in identifying a `process-oriented' solution that could be used as a reference for academicians and the corporate entities while faced with the challenges associated with the elusive process of `Forming'

II. Sheet Metal Forming Process

Sheet metal forming processes are the complex interaction between specimen (geometry, tolerance, surface topology, etc.), the forming process (tooling, forming machine, force, lubrication, etc.) and the material (ductility, material parameters, microstructure, corrosion resistance, residual stress, etc.) which exist in forming processes. Most problems in sheet metal forming come from a bad control of holding, restraining and spring back.

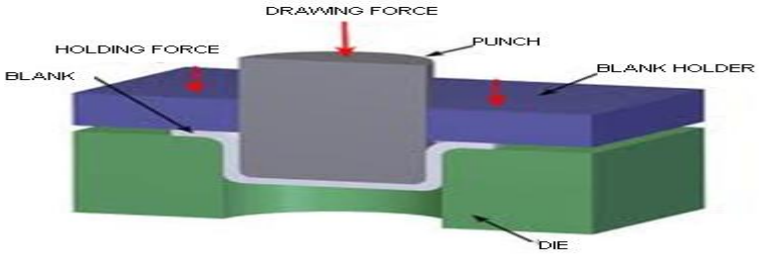

Figure 1.1: Schematic Diagram of Forming With Punch and Die

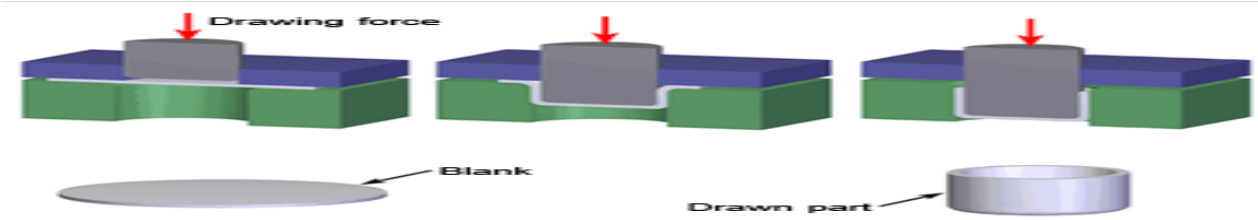

Figure 1.2: Schematic Diagram for the stages of `Forming' process

Geometrical defects in sheet metal forming: The Forming or deep drawing process allows the production of large quantities of sheet metal parts of various complexities. During the process a piece of sheet metal is clamped between the die and the blankholder. A force is applied to the blankholder to prevent wrinkling of the sheet and to control the material flow during the deformation. When the punch is pushed into the die cavity the sheet deforms plastically and thereby it takes the

specific shape of the tools The quality of the final product shape is determined by the tools design, process parameters, shape and material of the blank. It is important to carefully consider all these factors prior to manufacturing; otherwise a defective product could result. Typical defects which are observed in sheet metal forming practice are wrinkling, necking and subsequent fracture, drawing grooves. In addition to these defects, there is also always geometrical distortion caused by elastic springback. Right after forming, the shape of the deformed product closely conforms to the geometry of tools. However, as soon as the tools are retracted, an elastically-driven change of the product shape takes place.
The attempt of this work would also be to minimize the defects evident during the development phase of the component.

III. Die Design Calculations

The component chosen for this dissertation would is derived from the projects being undertaken by the sponsoring company- Able Technologies (India) Pvt. Ltd., Pune. The case study shall incorporate the design and development of the component named - `Cup' that is used over the subassembly of a popular two wheeler mounting bracket.

III.1 The specs along with the drawing for this component are given below:

Component Name –Cup
Material – CRCA Steel EDD Grade as per IS513-1994
Thickness – 1.00 +/- 0.03 mm

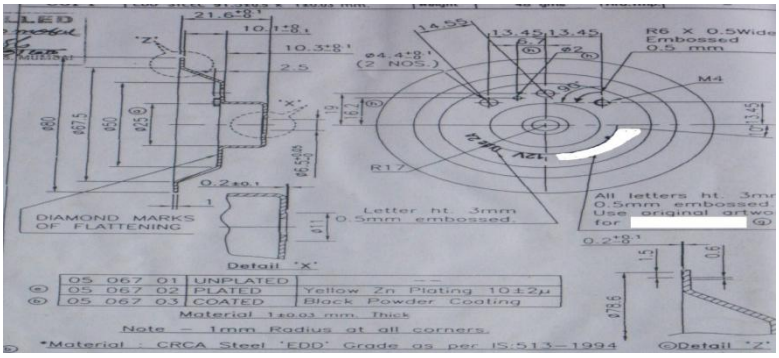

Figure 2: Extract from the part drawing for the component

III.2. Developed Blank Diameter = 112 mm. (radius at each step ignored for sake of simplicity since the component is not required to mate in the assembly and the function does not call for precise control over the flange diameter)

III.3. Draw Ratio – At this component, the Draw = H/d = 20.6/67.5 = 0.31 which indicates the draw is simple & may require only one stage for completion.

III.4. Draw Force – Draw Force can be calculated by empirical relation,
P = . d. t. s. ((D/d) – C)
Where, P = Draw Force in Tons
D = Blank Diameter in mm = 112 mm
d = Punch Diameter in mm = 25 mm
t = Thickness of Metal in mm = 1.00 mm
S = Yield strength of Metal in Kg/mm^2 = 40 Kg/mm^2
C = Constant (Take 0.6 to 0.7)
We know that,
P = . d. t. s. ((D/d) – C)
P = π x 25 x 1 x 40 x ((112/25)-0.6)
P =12183.2 Kg
P =12 Ton
Factor of safety should be taken 1.25,
Therefore, Draw Force (P) = 12 x 1.25 = 16.25 ≈ 17 Ton

III.5. Die Block Dimension –
Diameter = ø165 mm
Material for Die block should be use HCHCr & OHNS
Hardness – Die Block should be harden upto 60 to 62 HRC

III.6. Top Plate – Top Plate Dimension = 320 mm x 250 mm
Thickness for Top Plate should be 32 to 35 mm (Take 35 mm)
III.7. Bottom Plate – Bottom Plate Dimension = 400 mm x 250 mm
Thickness for Bottom Plate should be 22 to 25 mm (Take 25 mm)

III.8. Punch Height – Height for Punch should be 69.1 mm

III.9. Draw & Punch radius – The Draw radius usually ranges from 4 to 10 times the Blank thickness,
Therefore, Radius of Draw Die = Rd =4.5 x 1 = 4.5 mm
The Punch radius usually ranges from 3 to 4 times the Blank thickness,
Therefore, Radius of Punch = Rp =3 x 1 = 3.0 mm

III.10. Shut Height – The Shut Height of the unit shall be,
H = Die thickness + Lower shoe thickness + Punch Height + Punch Plate thickness + Upper shoe thickness – Penetration of Punch in Die = 45 + 25 + 69.1 + 29 + 35 – 3.1 = 200 mm.

III.11. Blank Holding Force – Blank Holding Force (B.H.F.) is always 30 % of Draw Force, therefore B.H.F. can be calculated as, Blank Holding Force (B.H.F.) = 30 % of Draw Force
= 30 % x 17 = 5.1 Ton ≈ 5.0 Ton
Material for Blank Holder should be use EN-353 or 20MnCr5
Hardness – Blank Holder should be harden upto 30 to 35 HRC

III.12. Press Tonnage or Press capacity –Press Tonnage can be calculated by using following formula,
Press Tonnage = Draw Force + Blank Holding Force (B.H.F.)
= 17 + 5 = 22 ≈ 25 Ton
Therefore, Press Capacity of 25 Ton shall be suitable.

IV. FIGURES AND TABLES

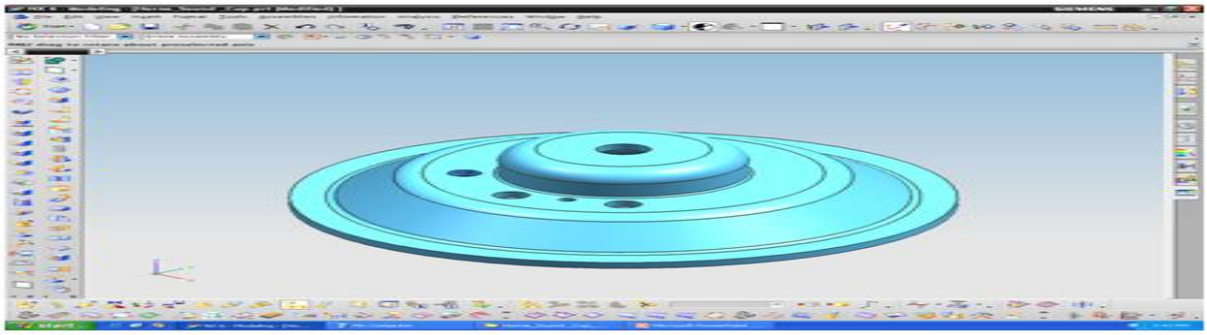

Figure 3: Solid model of the component (Cup) using CAD software `Unigraphics NX-6'

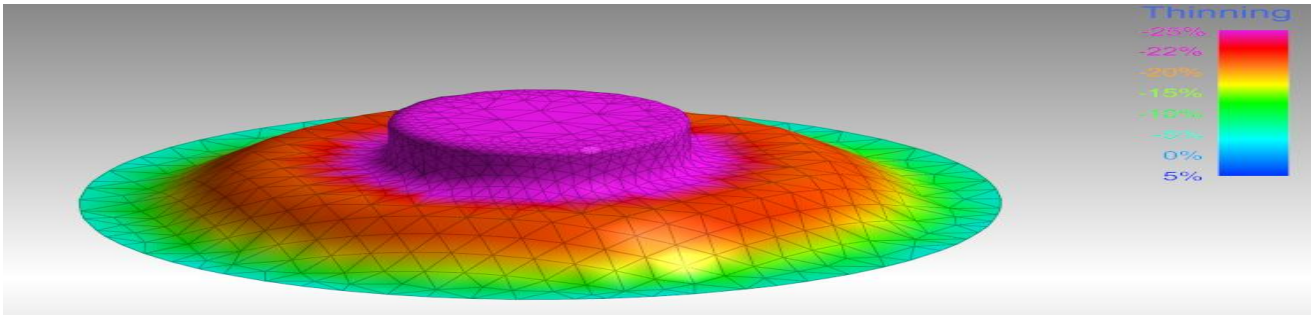

Analysis of component (Cup) using CAE/Simulation software `HYPERFORM'
Figure 4.1: Result of Analysis for Blank holding force at 5 Ton
Observation: Maximum thinning recorded – 25% of the thickness of the component (acceptable part quality)

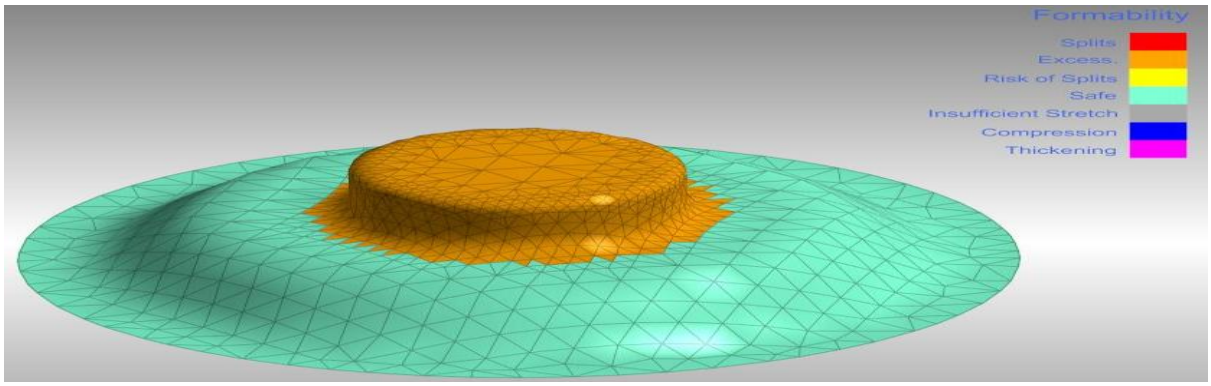

Figure 4.2: Result of Analysis for `Blank holding force' at 5 Ton
Observation: No splits or any major defects observed (acceptable part quality)

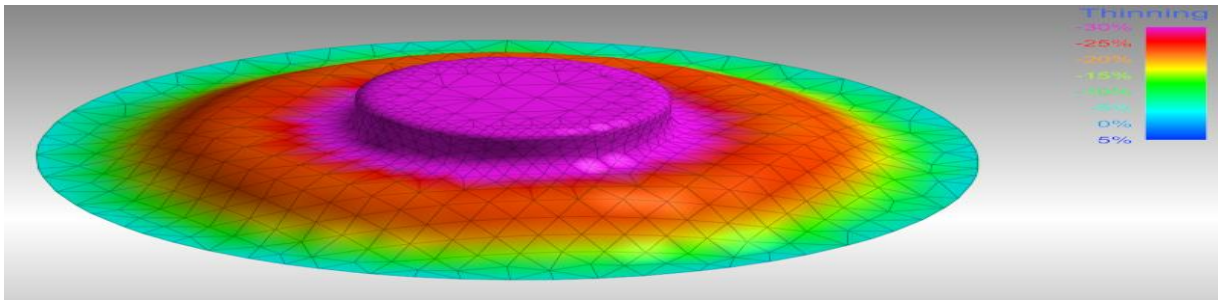

Figure 4.3: Result of Analysis for Blank holding force at 10 Ton

Observation: Maximum thinning recorded – 30% of the thickness of the component (unacceptable part quality)

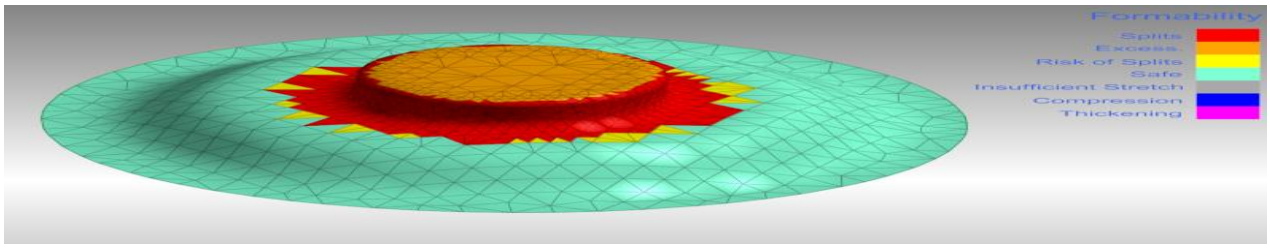

Figure 4.4: Result of Analysis for Blank holding force at 10 Ton

Observation: Large region exposed to the tendency for splits (unacceptable part quality)

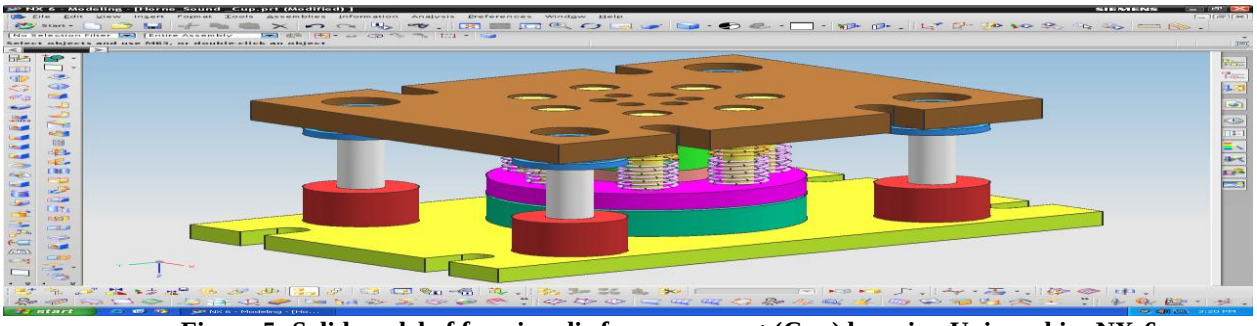

Figure 5: Solid model of forming die for component (Cup) by using Unigraphics NX-6

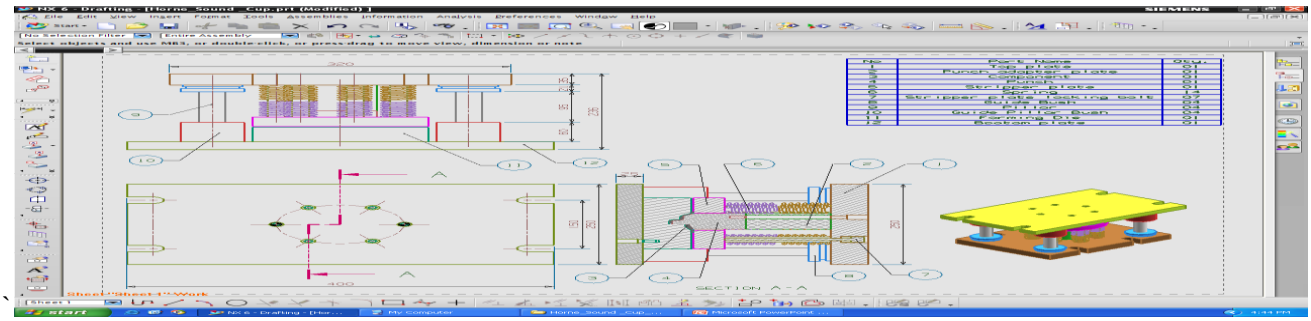

Figure 6: Schematic sketch of forming die for component (Cup) by using Unigraphics NX-6

V. CONCLUSION

Sufficient research and deliberation using the proven QC tools backed up with CAE software support (HYPERFORM) has offered a feasible solution to the problem at hand. Steel material like HCHCr (High carbon High Chromium) & OHNS (Oil Hardening non Shrinkage) grade for both punch and die block to suit the components having EDD (Extra Deep Draw) is recommended per the practices found in the industries. The operating condition involving the magnitude of blank holding pressure is varied and the results analyzed. Thinning and Formability are ascertained in this study. For finding the range of load at which the thinning or formability is unacceptable, the iteration for analysis with a blank holding force of 10Ton was applied and the results recorded as per figure 4.3 & 4.4. Suitable blank holding pressure (5Ton) is recommended for a defect-free component as per figure 4.1 & 4.2. The results obtained by mathematical treatment and the results obtained through the use of software (analytical) agree reasonably well. These results also establish generic guidelines for forming die design for Extra Deep Draw (EDD) materials. In order to expand the range of application of the developed method, parts with more complex geometries can be considered as future scope of work.

ACKNOWLEDGEMENTS

The author gratefully acknowledges the support received from Mr.S.S.Kulkarni, Director- Able Technologies (India) Pvt. Ltd.Pune, for his technical and administrative support from conceptual stage to the final stage for execution of this work. The author also would like to thanks Dr.V.R.Naik, Head of Department of Mechanical Engineering, Prof.A.R.Balwan, P.G.Coordinator, at D.K.T.E.Ichalkaranji, for guidance and crucial inputs over the project work.

REFERENCES

[1] Arash Behrouzi, Bijan Molaee Dariani, Mahmood Shakeri Department Of Mechanical Engineering, Amirkabir University Of Technology,Tehran, Iran,Majlesi Journal Of Mechanical Engineering, Die Shape Design In Channel Forming Process By Compensation Of Springback Error Vol.3/No.2/Winter 2010 Page No.17-26.

[2] Juraj HUDAK,Miroslav TOMAS, Department Of Technologies & Materials, Technical University Of Kosics, Annals Of Faculty Engg.Hunedoara-International Journal Of Engineering, Analysis Of Forces In Deep Drawing Process, TOM IX (Year 2011) Fascicule 1.(ISSN-1584-2665) Page No.219-221.

[3] Hakim S. Sultan Aljibori Mechanical Engineering Department, Faculty Of Engineering University Malaya, 50603, Kuala Lumpur, Malaysia, Abdel Magid Hamouda Mechanical And Industrial Engineering Department,Faculty Of Engineering, Qatar University, Doha, Qatar,European Journal Of Scientific Reasearch, Finite Element Analysis Of Sheet Metal Forming Process,ISSN 1450-216X Vol.33 No.1 (2009),PP.57-69.

[4] Y. Park1 J. S. Colton Professor, Fellow ASME The George W. Woodruff School Of Mechanical Engineering, Georgia Institute Of Technology, Atlanta, GA 30332-0405,Failure Analysis Of Rapid Prototyped Tooling In Sheet Metal Forming -Cylindrical Cup Drawing, Vol.127,Feb 2005, Page No.126-137.

[5] A.Wifi, A.Mosallam Department Of Mechanical Design & Production, Faculty Of Engg, Cariro University, Giza12316, Egypt, Some Aspects Of Blank-Holder Force Schemes In Deep Drawing Process, Vol.24 Issue 1 Sept.2007, Page No.315-321.

[6] Se-Ho Kim, Seung-Ho Kim, Hoon Huh,Department Of Mechanical Engineering, Korea Advanced Institute Of Science And Technology, Science Town, Taejon, 305-701 South Korea,Tool Design In A Multi-Stage Drawing And Ironing Process Of A Rectangular Cup With A Large Aspect Ratio Using Finite Element Analysis, Received 16 October 2001; Accepted 3 January 2002, Page No.863-875.

[7] Peter Kostka,Peter Cekan,Slovak University Of Technology In Bratislava, Faculty Of Mechanical Engineering, Department Of Materials & Technologies, Computer Simulated And Experimental Verification Of Tooling For Progressive Deep Drawing,8th International LS- DYNA Users Conference Metal Forming (1),Page No.9-59 To 9-65.

[8] Fuh-Kuo Chen, And Yeu-Ching Liao,Department Of Mechanical Engineering National Taiwan University, Finite Element Analysis Of Draw-Wall Wrinkling In A Stamping Die Design, VIII International Conference On Computational Plasticity COMPLAS VIII.E.Onate And D.R.J.Owen,2005.Page No.1-4.

[9] Z. Marciniak The Technical University Of Warsaw,Poland J.L. Duncan The University Of Auckland, New Zealand, S.J. Hu The University Of Michigan, USA. Mechanics Of Sheet Metal Forming, ISBN 0 7506 5300 0, Page No.1-163.

[10] Simtech Simulation Technologies Simtech 37 Rue Des Acacias, Introduction To Sheet Metal Forming Processs, 75017 Paris

[11] France.Smith & Associates,530 Hollywood Drive, Monroe, Michigan 48162- 2943 © 1993, 2001,Forming Flanges And Process Limitations,C041 REV June 23, 2005.

[12] I.A. Burchitz Project Number: MC1.02121 I.A. Burchitz, Rotterdam, Netherlands, Improvement Of Springback Prediction In Sheet Metal Forming,Page No.5-134.

Amit Dattatray Madake
***(M.E. Mech-PDD appearing, Student of D.K.T.E.Ichalkaranji Department of Mechanical, Shivaji University, India*)**

M. E. (Mech.) Product design and development student department of mechanical engineering Textile and Engg. Institute, Ichalkaranji, Kolhapur. Has four years of academic experience and six years of industrial experience. To his credit there is one paper at international journal.

Prof. (Dr.) V. R. Naik

Working presently as professor and HOD (Mech.) has 17 years of academic experience and six years of industrial experience. He has around in various reputed organisations in the areas of Design and Development. To his credit there are twenty two papers at national and international conferences and five papers in the various journals of national and international repute. He is also principal investigation to various funded project.

Mr. Swapnil Shashikant Kulkarni

Director at AbleTech/ Mentor at IdeaMaps has been associated with the function of R&D over his career of 18 years in the industry. While addressing his role, he has dealt with the techno-commercial aspects in `Product' and `Tool Design' assignments for OEM's. Besides, he has had been applying the learning in the Mechanical Engineering domain with the Electronics and IT segment for evolving innovative products in the `Renewable Energy' sector as also the `Consumer products'.

International Journal of Modern Engineering Research (IJMER)
www.ijmer.com Vol. 3, Issue. 3, May.-June. 2013 pp-1792-1795 ISSN: 2249-6645

The Kinetics of Binding of Tris-(3, 4, 7, 8-Tetramethyl-1, 10-Phenanthroline) Iron (II) Sulphate with Sodium DODECYL Sulphate

Latona D. F.[1], Ige W. J.[2] and Soriyan O. O.[3]
1Osun State Polytechnic, Department of Applied Science, PMB 301, Iree, Nigeria.
2&3 Obafemi Awolowo University, Department of Chemistry, Ile-Ife, Nigeria.

ABSTRACT : *The kinetics and effects of substrates on the binding of an anionic surfactant, sodium dodecyl sulphate (SDS) to tris-(3,4,7,8-tetramethyl-1,10-phenanthroline)iron(II)sulphate ($Fe(Me_4phen)_3^{2+}$ was investigated in this study. The kinetics of the reaction was studied by ultraviolet–visible (UV–VIS) spectrophotometry and the activation energy, Ea, free energy of activation, $\Delta G^{\ddagger}$, entropy of activation , $\Delta S^{\ddagger}$ and enthalpy of activation, $\Delta H^{\ddagger}$ were obtained from the temperature dependence study of the rate of binding using Eyring's equations.*

The results showed that the reaction was invariant with Iron(II) complex concentration and that the rate of binding is inhibited by sodium dodecyl sulphate . The rate of binding was enhanced by H^+ at low $[H^+]$ and a maximum was reached at $[H^+]$ of 2.00 x 10^{-4}M. Beyond these concentrations of H^+ , the reaction was inhibited by H^+. The results further showed that hydroxyl ion and urea inhibited the binding of SDS to $Fe(Me_4phen)_3^{2+}$. The rate of binding was accelerated in the presence of benzoate ion. The effect of substrates on the activation energy were in the order: benzoate ion > H^+ > urea > OH^- > Neutral. While negative values of $\Delta S^{\ddagger}$ in indicated that the formation of the activated complex from the reactants was accompanied by a large decrease in entropy. Approximately the same values of $\Delta G^{\ddagger}$ were obtained suggesting a common *mechanism for the binding process.*

I. INTRODUCTION

1,10- phenanthroline ligand has wide application in Co-ordinate chemistry because of its ability to form stable chelates with transition metal. This ligand like other complexes of aromatic diimines has been greatly employed for the quantitative determination of metals (Alexiev et al., 1994). A study of DNA binding of Iron(II) complexes with 1,10-phenanthroline by spectrophotometric titration showed salt concentration dependence of the binding constant (Mudasir et al., 2003). Investigation on the catalysis of aquation of Iron(II) penanthroline complexes showed that the micellar inhibition was due to favourable thermodynamic/hydrophobic/electrostatic binding between the Fe(II) and sodium dodecyl sulphate monomer aggregates (Ige and Soriyan, 1986). Reports on the kinetic studies of racemisation and dissociation of Iron(II) phenanthroline complexes with sodium dodecyl sulphate revealed that racemisation and dissociation rates of the complexes increased with increase in sodium dodecyl sulphate concentration to reach limiting values at concentrations above the critical micelle concentration (Tachiyashiki and Yamatera, 1986). However, this work shall investigate the rate of binding of tris-(3,4,7,8-tetramethyl- 1,10-phenanthroline)iron(II) sulphate with sodium dodecyl sulphate in its monomeric form with the view to establishing quantitative insight into the extent of electrostatic and hydrophobic interaction between the complex and the anionic surfactant.

II. EXPERIMENTAL

The complex $Fe(Me_4phen)_3SO_4$ was synthesized and purified according to the literature method (Shakhashuri and Gordon, 1964). The complex was characterized by its UV- visible spectra. The maximum absorption peak (λ_{max}) determined was 500nm, which was in aggrement with the literature values (Shakhashuri and Gordon, 1964). Purified sodium dodecyl sulphate (99%) was used with further recrystallisation. The purity was ascertained by the determination of the critical micelle concentration (CMC) in aqueous solution at 25°C. The value of 8.20 x 10^{-3} mol dm^{-3} obtained was in good aggrement with the literature value (Williams et al., 1985). Analar grade (BDH), sodium hydroxide (NaOH), sodium benzoate (C_6H_5COONa), sulphuric acid (H_2SO_4) and urea were used.

II.1 Kinetics: Kinetic data were established by monitoring change in absorbance of ferrous complex at absorption maximum (λmax) as a function of time using unicam UV- visible spectrophotometer. The concentration of the complex was 1.45 x 10^{-5} mol dm^{-3}. The concentration of sodium dodecyl sulphate ranged within (2.00 x 10^{-4} – 8.00 x 10^{-4} mol dm^{-3}). The kinetic runs were performed under pseudo – first order kinetics and rates constants were obtained from the slope of $In(A_\infty - A_t)$ versus time. The effect of H^+, OH^-, C_6H_5COONa and urea on binding were investigated. Activation parameters were determined within the temperature range, 25°C – 70°C at fixed concentration values of the complex as stated above, at fixed [SDS] = 2.00 x 10^{-4} mol dm^{-3}. Activation energies were obtained from Arrhenius equation from the slope of a plot of In k_{obs} vs 1/T (K^{-1}) and the activation parameters were obtained from Erying's equation (Svirberly and Kundel, 1967).

III. RESULTS AND DISCUSSION

The observed rate constant of binding, k_{obs} was invariant with $Fe(Me_4phen)_3^{2+}$ at fixed SDS concentrations in neutral aqueous medium. This simply shows that the complex is located in the same region of the stern layer and that previous work by Ige and Soriyan, 1986 showed that the Iron(II) complex is stabilized with respect to dissociation in the micellar phase. The overall data of the rate of binding of the complex by SDS in neutral medium showed inhibition on

addition of the sodium dodecyl sulphate approaching saturation at higher [SDS] as shown in figure I. The reason is because as [SDS] increases the number of oligomers increases with the bulky complex experiencing steric hinderance not expected for monomeric SDS. Hence , this steric consideration predominates over hydrophobic character of the aggregates.

Moreover, rate of binding increased with increase in hydrogen ion concentration until k_{obs} attained a maximum at $[H^+]$ 2.00 x 10^{-4} mol dm^{-3} after which $[H^+]$ inhibites rate of binding as shown in figure II. Increase in rate of binding was attributed to the fact that as H^+ was added, the $–OSO3^-$ head group of the surfactant was readily protonated. The lauryl sulphonic acid is more hydrophobic than SDS, therefore rate of binding increases because of the enhanced hydrophobic interaction between the lauryl sulphonic acid and the Iron(II) complex however, k_{obs} increased until all the SDS was protonated. Beyond this saturation point, added protons remained in solution and increases the dielectric constant of the solution. This led to a decrease in the rate of binding and it is also significant to note that further increase in $[H^+]$ beyond saturation point led to repulsion between the incoming positively charged Iron(II) complex and the protons in the diffuse guoy-chapman layer, hence the rate of binding decreased.

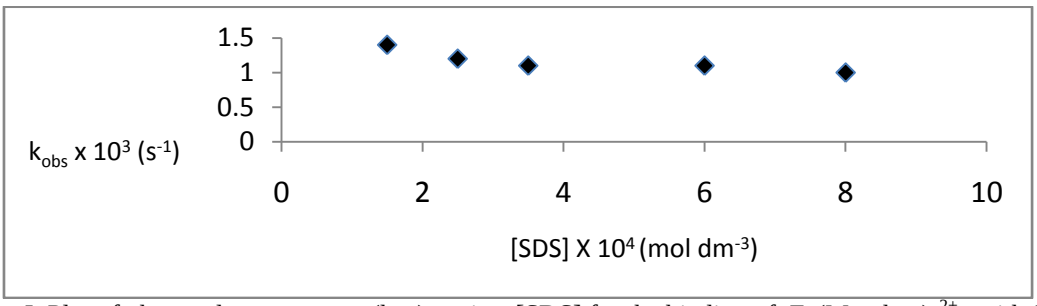

Figure I: Plot of observed rate constant (k_{obs}) against [SDS] for the binding of $Fe(Me_4phen)_3^{2+}$ with SDS, Temperature = 25°C.

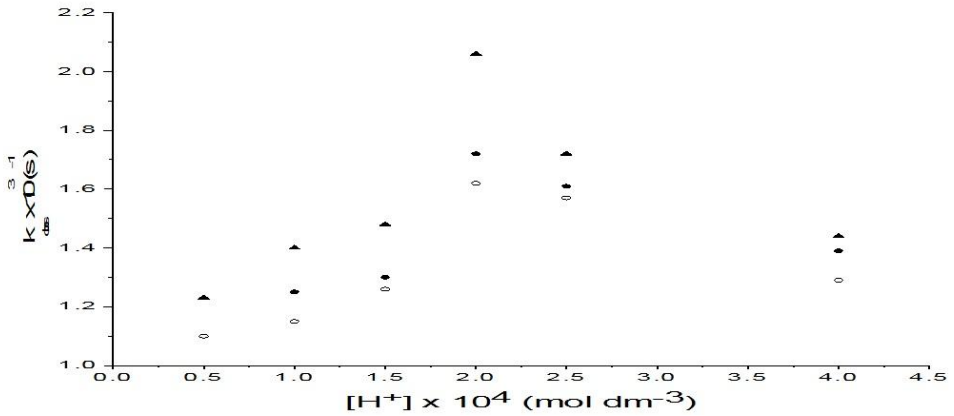

Figure II**:** Plots of k_{obs} versus $[H^+]$ for binding between $Fe(Me_4phen)_3^{2+}$ and SDS (▲ [SDS] 1.50 x 10^{-4} mol dm^{-3}, ● [SDS] 2.50 x 10^{-4} mol dm^{-3}, and ○ SDS] 3.50 x 10^{-4} mol dm^{-3})

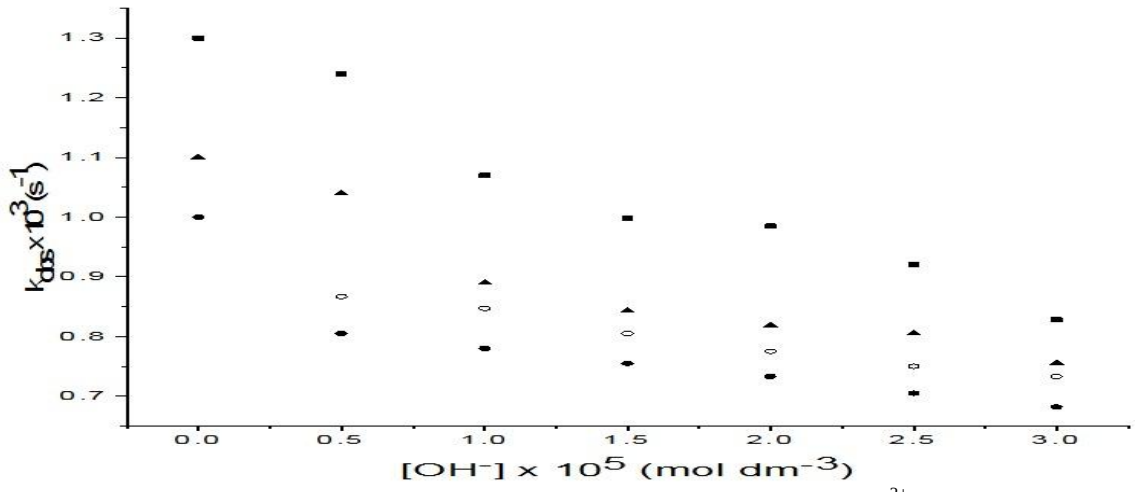

Figure III: Plots of k_{obs} versus $[OH^-]$ for binding between Fe $(Me_4phen)_3^{2+}$ and SDS. ■ [SDS] 2.00 x 10^{-4} mol dm^{-3}, ▲ [SDS] 4.00 x 10^{-4} mol dm^{-3}, ○ [SDS] 6.00 x 10^{-4} mol dm^{-3} and ● [SDS] 8.00 x 10^{-4} mol dm^{-3})

Furthermore, hydroxyl inhibited the rate of binding as shown in figure III. Inhibition is due to increase in the dielectric constant of the medium as $[OH^-]$ increases which consequently led to decrease in the hydrophobicity of the medium (Menger and Portony, 1969). Hence hydrophobic interaction between the metal complex and SDS was significantly reduced as $[OH^-]$ increases. The rate of binding was catalysed in the presence of sodium benzoate (figure IV). The observed 83% increase in k_{obs} at the fixed lowest concentration of SDS and 14% increase at the highest fixed concentration of SDS within the same benzoate concentration range for the complex and general increase in the rate of binding is due to the orientation of the benzoate ion as suggested by previous kinetic data (Burrows et al., 1982) and confirmed by NMR data (Tachiyashiki and Yamatera, 1986). This unique orientation shows that phenyl group of the benzoate ion aligns below the head group of the SDS monomers due to its hydrophobic nature as shown in figure V. This orientation causes an increase in the negative charge on the pre-micelle resulting to increase in coulombic or electrostatic attraction between the positively charged metal complex and the micellar surface, leading to increase in the rate of binding. Furthermore, rate of binding was inhibited in urea dependent study as shown in figure VI. The decrease in rate of binding in the presence of urea can be attributed to the fact that urea reduces the negative charge density on SDS by interaction through hydrogen bonding between its protons and SDS head group. Increase in urea concentration decreases the negative charge density on SDS which results to a decrease in the electrostatic attraction between the Iron(II) complex and the surfactant thereby leading to a

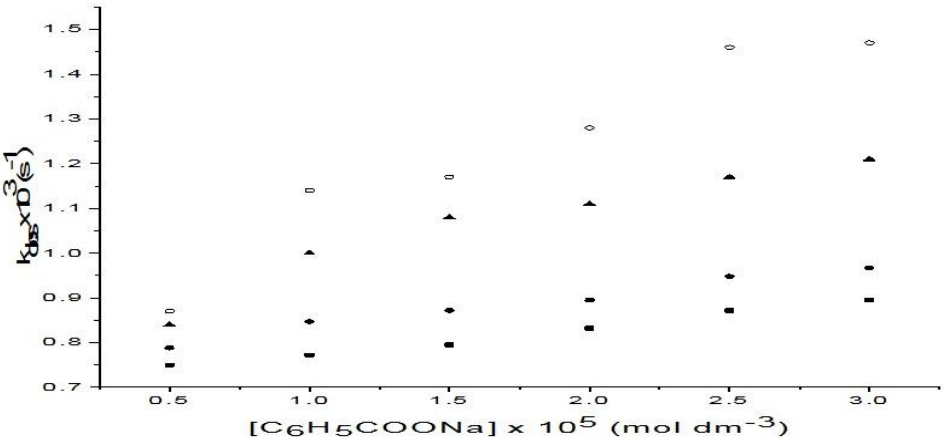

Figure IV: Plots of k_{obs} versus $[C_6H_5COONa]$ for binding between $Fe(Me_4phen)_3^{2+}$ and SDS. ○ [SDS] 2.00 x 10^{-4} mol dm^{-3}, ▲ [SDS] 3.00 x 10^{-4} mol dm^{-3}, ● [SDS] 5.00 x 10^{-4} mol dm^{-3} and ■ [SDS] 7.00 x 10^{-4} mol dm^{-3})

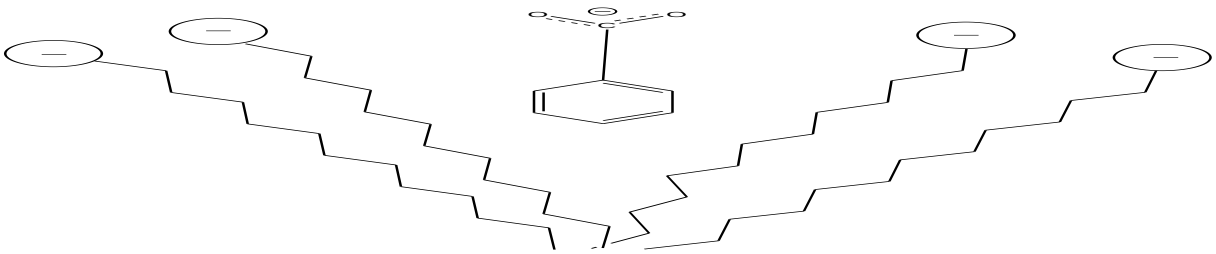

Figure V: Benzoate ion – SDS molecule interaction

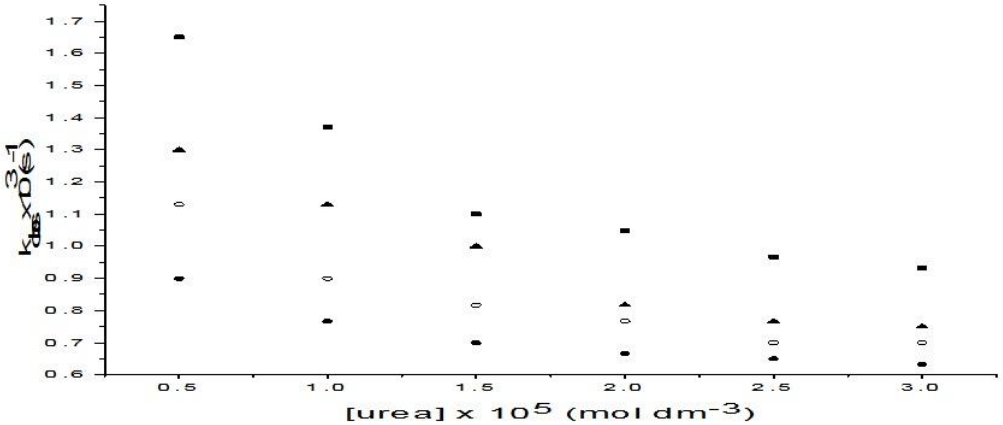

Figure VI : Plots of k_{obs} versus [urea] for binding between $Fe(Me_4phen)_3^{2+}$ and SDS. ■ [SDS] 2.00 x 10^{-4} mol dm^{-3}, ▲ [SDS] 4.00 x 10^{-4} mol dm^{-3}, ○ [SDS] 6.00 x 10^{-4} mol dm^{-3} and ● [SDS] 8.00 x 10^{-4} mol dm^{-3}).

decrease in rate of binding. However, partial neutralization of the negative charge density on SDS by the protons on urea should in turn increase the hydrophobicity of the medium. Obviously in this case decrease in electrostatic attraction predominates over increase in hydrophobicity.

Moreso, presence of urea would enhance steric hinderance and this added steric consideration has the additional effect of inhibiting the rate of binding with increase in urea concentration.

Furthermore, temperature dependent study as shown in Table I revealed the activation parameters.

Table I. Activation parameters of binding of the complex with SDS

Substrate	Ea(kJmol^{-1})	$\Delta H^{\ddagger}$ (kJmol^{-1})	$\Delta S^{\ddagger}$ (kJK^{-1}mol^{-1})	$\Delta G^{\ddagger}$ (kJmol^{-1})
_	39.96	37.48	-9.69	58.23
Urea	30.28	27.80	-10.02	58.77
Benzoate ion	16.46	13.98	-10.13	57.29
OH^-	33.69	31.21	-9.91	58.94
H^+	26.82	24.34	-10.11	57.43

IV. CONCLUSION

It was shown that both electrostatic and hydrophobic interactions played significant role in the binding of metal chelate complexes with surfactants. The binding of the complex was inhibited by SDS concentration and independent of complex concentration. H^+, OH^-, C_6H_5COONa and urea greatly affects the binding process either by electrostatic or hydrophobic interaction. The mechanism of binding is the same in all the systems due to the approximate invariance in the free energies of activation. The negative values of entropy of activation shows entropy decrease upon achieving the transition state, which often indicates an association mechanism.

REFERENCES

[1]. Alexiev A , Rubio S , Deyanova M , Stoyanova A , Sicilia D, and Perez Bendito D (1994) Improved catalytic photometric determination of iron(III) in cetylpyridinium premicellar aggregates. Anal. Chim. Acta, 295, 211- 219 .

[2]. Burrows H.D, Ige J, and Umoh S.A (1982) DodecylPyrazinium halides. Their synthesis ,characterisation and use in the micellar catalysis of the aquation of tris(1,10 – phenanthroline)iron(II) perchlorate in aqueous perchloric acid medium. J. Chem. Soc. Faraday Trans. 1, 78,917 - 955.

[3]. Ige J , and Soriyan O (1986) Micellar inhibition of aquation of tris – (3,4,7,8 – tetramethyl -1 ,10 phananthroline)iron(II) by sodium dodecyl sulphate in aqueous acid medium .J. Chem . Soc. Faraday Trans I, 82, 2011 – 2023.

[4]. Menger F.M, and Portnoy C.E (1969) The chemistry of reactions proceeding inside molecular aggregates. J. Am. Chem. Soc, 89, 4698 – 4703.

[5]. Mudasir K , Wijaya K ,Yoshioka N,and Inoue H (2003) DNA binding of iron(II) complexes with 1,10 – phenanthroline and 4,7 – diphenyl 1,10 – phenanthroline. J. Inorg. Biochem. 94(3), 263 – 271.

[6]. Shakhashuri B.Z ,and Gordon G (1964) The oxidation of tris(1,10 – phenanthroline)iron(II) by aqueous chloride. Inorg. Chem. 7, 2454 – 2456.

[7]. Svirbely W.J , and Kundell A.K (1967) The Kinetics of competitive – consecutive second – order reactions involving difunctional unsymmetrical molecules. The kinetics of the alkaline hydrolysis of diethyl malate. Journal of the American Chemical Society 89;21,5354 – 5359.

[8]. Tachiyashiki S and Yamatera H (1986) Micellar effect on the kinetics of the aquation and base hydrolysis of tris(1, 10 phenanthroline)iron(II) and chloropentaamine cobalt(III) ions. Inorg. Chem. 25, 3043 – 3047.

[9]. Williams R.J, Phillips J.W, and Mysel K.J (1985) Critical micelle concentration of sodium dodecyl sulphate at 25^{O}c. Trans. Faraday Soc. 51,728 – 737.

International Journal of Modern Engineering Research (IJMER)
www.ijmer.com Vol. 3, Issue. 3, May.-June. 2013 pp-1796-1800 ISSN: 2249-6645

Theoretical and Computational Studies of Nano-Structured Materials and its Commercial Prospects in India

Basanta Pathak
Assistant Professor in Physics Haflong Govt. College, Haflong, Assam, India

ABSTRACT: *Theoretical analysis and Computer simulations have proven to be cost-effective and powerful tools in scientific studies of materials, particularly at nano-scale where synthesis of nano-structures, interpretation of their observed character and exploration of new structures are not always straight forward. We present here fundamental principles of techniques used today for computational simulations of materials, their capabilities and limitations.*

We then illustrate efficacy of such studies through review of their applications to nano-structures of oxide materials and mechanical behaviour of nano-structured materials. The area of nano-science and technology is growing rapidly around the world and nano-materials based products, especially in the consumer sector, are coming into market very rapidly. India is competing with great difficulty, with other developed countries to make its position strong in this field. In other respect, several challenges have to be overcome in terms of production of nano-materials at commercial scale, their processing, applications and commercialization.

I. INTRODUCTION

Nanotechnology, defined as the application of nano-science in technological devices/processes/products, is fast emerging as an important enabling technology capable of impacting almost all the sectors of industries and consumer products. Therefore, not surprisingly, all governments and industries the world over are investing heavily in the development of nano-technology based processes, products and systems. Nano-technology represents a very broad area and is composed of three main fields, i.e., nano-materials, nano-tools and nano-devices. Of these, both research and commercialization have occurred to a significant level only in the area of nano-materials. In India also much of the research and technology development work has taken place in the arena of nano-materials. Thus, this paper will concentrate on highlighting the status of nano-materials research and commercialization in India. Nano-materials represent a class of materials characterized by a feature size of less than 100nm. In the case of nano-particles, the feature size is the particle diameter while in carbon nano-tubes; it is the nano-tube diameter. At the other extreme, in the case of bulk materials, either the grain size in homogeneous materials or the reinforcing particle size and spacing in the case of composites represent the feature size. Thin films having thickness less than 100nm or multi-layer coatings with the thickness of each layer less than 100nm also qualify as nano-materials. Therefore, it is important to note that while nano devices will certainly have to be made from nano-materials, nano-materials itself impacts areas beyond nano-technology. For example, the recently developed nano-steel by a Japanese company [13] is a nano-material which will impact the automobile and infrastructure industry by providing high strength, high toughness steel sheets with superior formability and corrosion resistance. It is also important to understand that merely bringing the feature size to below 100nm is not enough; more importantly, such a decrease in feature size should result in significant enhancement of strength, toughness or electrical, electronic, optical and magnetic properties.

With about a hundred elements in the periodic table as building blocks, there exist a very large number of materials that can be synthesized with different combination of these elements in different proportions. Interestingly, the structure of a material may not be unique, as different physical conditions or growth routes can trap a material in different meta-stable states. Properties of a material, which are completely determined by the chemistry and its structure exhibit tremendous diversity. While it is fundamentally interesting how some of the properties can be classified into different universality classes, it is intriguing how the properties can change drastically with a slight change in chemistry or structure. A simple and commonly known example is of silicon verses carbon. While they belong to the same group of the periodic table and exit similar chemical boding when in the same structure, the known ground state structures of silicon and carbon are diamond and graphite.

At the nano-scale; there are at least two fundamental ways in which the diversity in the properties of materials becomes richer and interesting----------

(a) Structure of a bulk-material can be altered at nano-scale[5] length-scale greater than the crystalline unit cells) and result in different properties (for example, mechanical behaviour of nano-structures or nano-grained metal) and

(b) A Nano-structure has a large fraction of atoms at the surface (or interface) whose chemistry can be different from the atoms belonging to the bulk, hence possesses very different properties. [6]

Experimental control and investigating of the structure and properties of nano-structures can be quite different and expensive. Measured properties of a nano-structure sensitively depend on how the experimental probe interfaces with the nano-structure mechanically, electrically or chemically. This necessitates use of tools that are complementary in their capabilities.

Nano-structures are also known as low dimensional systems: dimensionality d of a nanostructure is the number of directions in which the size of a structure is greater than about 100nm (along the remaining 3-d directions, the system is spatially confined). Due to confinement of quantum electronic states and deviation in the local co-ordination of atoms from that in the bulk, interesting quantum effects and chemistry [6] emerge at nano-scale. Small changes in their structure can be introduced through doping or the strain constraints (as present in epitaxial films) at their interface with surrounding, which

result in large and often qualitative changes in their properties. In spite of availability of very large and powerful computers, many important problems in materials science are too large to be solved through simulations. Secondly, a large amount of data generated in large scale simulations can be quite hard to learn fundamentals from. Modelling plays an important role in such problems which enables efficient solution of a problem and extraction of its essential mechanisms. Modelling typically makes use of symmetries in integrating out irrelevant high energy degrees of freedom of a system. In any case, a computer based solution of a challenging problem in materials usually involves a judicious choice of numerical accuracy and computational costs: higher the accuracy, greater is the cost.

II. APPLICATIONS TO NANO-STRUCTURES AND NANO-MATERIALS

While the structure of a system can be theoretically determined through minimization of the total energy function, it is often a very hard task. The cause of this difficulty lies in the fact the total energy function can be a highly nonlinear function of atomic positions with several possible local minima. Most methods of minimization of a function typically start with an initial guess for a minimizing vector (structure) and iteratively determine the minimum of the function in the same basin. The phase space of structures grows exponentially and search through all possible basins of energy function to determine its global minimum is a task that cannot be solved using the known computing concepts in time that scales as a polynomial of the system size. Genetic algorithm provides a popular option to try to find a global minimum. In the context of structural optimization of nano-clusters, we presented an algorithm that was based on physical intuition and symmetry [12]. The level of difficulty in determination of structures reduces as one goes to structures with higher dimensionality (clusters are zero dimensional nano-objects) and regularity/periodicity along the extended dimension. For example, the structure of a nano-wire or a nao-tube is determined with fewer parameters even though number of atoms in it can be large. We review here now computational studies of nano-structures in 2 and 1 dimensions, whose structure is relatively simpler to determine and properties can be quite interesting.

III. TWO DIMENSIONAL NANO-STRUCTURES OF FERRO-ELECTRIC OXIDES

Miniaturization of devices and development of chips with a very high density of devices have been central to technological evolution over the last several decades. Ferro-electric or piezo-electric oxides, also known as smart and functional materials, are essential to the Micro-Electro-Mechanical systems (MEMS), which are used in a very wide range of applications ranging from ultra sound detectors in a hospital to the ones on submarine.

Ferro-electric oxides possess spontaneous (in the absence of field) electric dipole or polarization that couples strongly with strain, which allows them to be used as sensors as well as actuators of mechanical strain. Since this spontaneous polarization can be switched to other directions with applied electric field, they can also be used in non volatile memories (known as FeRAMs). Scaling down of MEMS or FeRAMs to nano-scale (NEMS) depend crucially on how properties of a ferro-electric films change when the film thickness shrinks to less than nano-meter. Fundamentally, the question of existence of polarization in nano-thin films of ferro-electrics is also related to probing how the ferro-electric phase transitions occur when a material is confined to less than 100nm along one of the directions. In our work, we have combined investigation of this with the search for lead free ferroelectrics. While the development of lead free ferroelectrics is essential to environment friendly technologies, it is also chemically interesting and challenging to find alternative routes to develop better ferro-electrics without the stereo-chemically active lone pair chemistry of lead. Here, we review our work that tries to make use of tenability at nano-scale of two types:

(a) Strain engineering of epitaxial films of $BaTiO_3$ [8] and

(b) Artificial super lattices of $BaTiO_3/SrTiO_3$ (BTO/STO) [10].

IV. MECHANICAL BEHAVIOUR OF NANO-STRUCTURED MG-ZN-Y ALLOYS

Bulk materials with nano-scale structure for example consisting of nano-sized (<100nm) grains, often exhibit a very high mechanical strength. [7] Such materials have a large fraction of atoms at the interfaces between grains. Due to different structural geometry and chemistry, this can qualitatively change their properties at different scales. Recently, addition of small amount of Y and Zn was report to have improved strength of Mg and also incorporate creep resistance at high temperatures [2]. The origin of these interesting properties was linked with nano-scale structure of these alloys long periodic structures. While mechanical behaviour of a material involves processes at different, particularly longer length scales, direct understanding of such phenomena from first principles is really ambitious. While classical MD simulations [7] have proven to be very effective in assessing role of different mechanisms responsible for unique mechanical behaviour of nano-structured materials, such methods fail to capture the effects of detailed chemistry. We used first principles calculations to confirm the stability of long-periodic structures and evaluate their implications to mechanical behaviour through phenomenological concepts such as stacking faults.

Outcome of first principles calculations can be connected to mechanical behaviour, even to brittleness versus ductility through the concepts of ----------

(a) Cleavage (or surface) energy, which is the energy required to separate away its two halves separated by a crystallographic plane or a grain boundary, and

(b) Generalized stacking fault energy surface, which is the energy required to slide a half of a crystal with respect to another.

While the former relates to energy release rate required for crack propagation during brittle failure(Griffith Criterion), the minima and maxima of the latter relate to intrinsic and unstable stacking fault energies(Rice theory).

Our simulations [1] of different polytypes of Mg revealed that the 6-layer structures of Mg are remarkably stable, and only about 50 mev/atom higher in energy than the hcp structure. Origin of this could be traced through topological analysis of electron density to the similarity in bending of 2-layer and 6-laye structures and finally to the close-packed nature of the two. Addition of small amount (2%) Y to Mg results in the 1-layer structure lower in energy then the hcp structure. Through extensive stacking fault in the basal plane reduces dramatically with addition of Zn, and showed that 6-layer structure should exhibit activation of the slip on prismatic plane. These findings should be useful in understanding deformation mechanisms in these nano-structured alloys of Mg.

V. INDIAN SCENARIO

(a) Government Support: Compared to developed countries, India has initiated a focused effort on nano-technology only in 2001, i.e. 5-7 years after countries like USA, EU, Japan, Korea and Tiwan started their own programmes. In October 2001, India launch a major programme in nano-technology when Development of science and technology(DST) launched the nano-science and technology Initiative(NSTI) and operated it for 5 years during the period 2001-02 to 2006-07. During this phase, the emphasis was on creating centres of Excellence in various aspects of nano-technology in the various universities and R & D laboratories in India. Bulk of the funding was utilized to procure specialized equipment required for nano-science like AFM, SEM, TEM, Nanoindentor etc. In all, about 100 projects were funded under NSTI.

Enthused by the over whelming response to the NSTI programme, DST has now initiated the Nano-Mission programme with a funding of Rs.1,000 crores over the period 2007-08 to 2001-12[16]. However, unlike NSTI, Nano Mission has created three full fledged institutions of Nano-science and Nano-technology in Bangalore,Kolkata and Mohali respectively. Further, the Nano-Mission will not only support high quality research in nano-science(as NSTI did earlier) but also fund projects focussing on application and product development with the active participation of Indian industries. It should also be pointed out that other governmental agencies like CSIR, DBT, DRDO, DAE and ISRO are also undertaking major projects in the area of nano-science and nano-technology.

(b) Industrial Support to Nanomaterials: Unlike in USA, Europe and Japan, the Indian industries have started looking at nano-technology as a solution for their problems only recently. Among the bigger companies, Reliance Industries, Tata Chemicals, Mahindra and Mahindra, Ashoke Leyland, Asian Paints, Crompton Greaves have initiated programmes in the area of nano-materials on their own or in collaboration with academic/R & D institutions. In addition, industry associations like Confederation of Indian Industry (CII), Federation of Indian Chambers of Commerce and Industry (FICCI), Society for Indian automobile Manufacturers (SIAM), Automotive Component Manufacturers Association (ACMA) have realized the importance of nanomaterials and nanotechnology and have started arranging get together among the industry representatives and experts in nano-materials/nanotechnology to evaluate the possibilities with respect to nano-materials in the industry.

(c) Nanomaterials: Commercialisation: The migration of the technology developed at the laboratory to the market place is more challenging than the development of the technology itself. Apart from the scalability and cost-effectiveness of the process/technology to enable large-scale production, it is important to ensure that sufficient market (new or replacement) is available for the product produced using the process/technology. Even if sufficient market is waiting to be tapped, marketing skill largely determines the actual market size for the product.

The ARCI technology for nanosilver based candle filter has been transferred to SBP Aquatech Pvt. Ltd., a Hyderabad company, which will have an initial capacity to product 500 candles a day [18]. The product, already in the market (fig1) is now undergoing initial marketing trials.

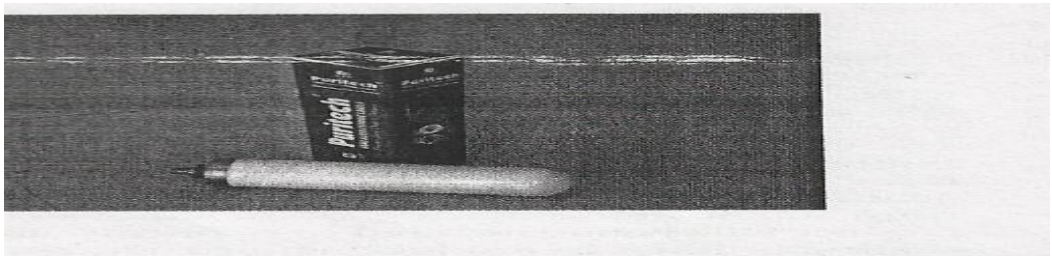

Fig1: Commercial nanosilver-coated ceramic candle filters for drinking water. (technology developed and transferred by ARCI)

Like the Hyderabad Company marketing nanosilver candle filters, there are a few more companies operating in the area of nano-materials and all of them are operating at small scales. For example, United Nanotechnology products, Kolkata has set up a pilot scale production facility for nanocrystalline Lithium iron phosphate required for making the electrode for Li-ion batteries [19]. However, the above product is largely meant for export. Similarly, Monad Nanotech Ltd. And Innovation Unifed Technologies, both from Mumbai, are selling carbon nanotubes and carbon nanofibres, but in small quantities.

(d) Safety, Health and Environmental (SHE) Issues: It is increasingly becoming apparent that nanotechnology, though touted as the future solution for almost all our technological requirements, has to be assessed carefully and now with regard to safety, health and environmental (SHE) issues so that we do not repeat the mistakes made in the past with regard to

asbestos, chlorofluorocarbons etc. The technology community should evaluate the SHE issues with an open mind, on the basis of scientific data, and voluntarily embark on regulatory measures and create specific standards for nanotechnology products. In extreme cases, wherein the health, safety or environmental concerns are sufficiently high, the concerned product/technology should be abandoned or temporarily suspended till specific evaluation studies are carried out to resolve the issue.

VI. NANOMATERIALS: APPLICATION DEVELOPMENT

As India is already behind the developed countries in both nano research and application development by 5-10 years, it is important that India chooses the application areas for nano-materials wherein either the Indian market is very large in the world context or which are unique/specific to India. Examples of the former include two and three wheelers, auto component and textiles markets while the health, drinking water are examples of the latter. The application-oriented research in India in the last few years has focused primarily on energy, environment and health related areas. For example, the invention of flow induced electrical response in carbon nano-tubes has direct relevance in biological and biomedical applications [14]. Indian Institute of Science has transferred the exclusive rights of this technology to an American start-up to commercialize the gas-flow sensors. Nanocrystalline gold triangles developed by a group at National Chemical Laboratory (NLC) have been shown to be useful for cancer treatment by hyperthermia, where the irradiation of the cancer cells is carried out by infra-red radiation [15].

Name	Type	Country	Products
Bayer	Big Chemical	Germany	Bulk production of Baytube carbon nanotubes
BASF	Big Chemical	Germany	Bulk production of various nanomaterials (Uses include food additives and sunscreen)
Degussa	Big Chemical	Germany	Bulk production of a range of ultrafine and nanomaterials
ICI/Uniquema	Big Chemical	UK	Bulk production of nanomaterials (including nano titanium dioxide for sunscreens)
Mitsubshi Chemical	Big Chemical	Japan	Bulk production of carbon nanotubes
Advanced Nanomaterials	Nano Specialist	Australia	Bulk production of a range of nanomaterials (Uses include sunscreens,catalysts, cosmetics and coatings)
Nanophase	Nano Specialist	USA	Bulk production of a range of nanomaterials
Hyperion Catalysis	Nano Specialist	USA	Nanotubes for incorporation into plastics
Carbon Nanotechnologies Inc	Nano Specialist	USA	Bulk production of carbon nanotubes
Umicore	Specialty Chemical	Belgium	Bulk production of nanomaterials (including nano titanium dioxide for sunscreens)
Elementis	Specialty Chemical	UK	Bulk production of nanomaterials (including nanoparticles ZnO sunscreens)
Nanogist	Nano Specialist	South Korea	Bulk production of nanomaterials (anti microbial silver nanoparticles)
Qinetiq Nanomaterials	Nano Specialist	UK	Bulk production of a range of nano- materials

Table1: Major global manufacturers of engineered nano materials

These materials have also found their use in insulin delivery for advanced diabetics. NCL has already applied for an American patent for this breakthrough. The achievements of a research group at University of Delhi on drug delivery are highly commendable. This group has developed 11 patentable technologies for improved drug delivery systems using nanoparticles. One of the important achievements of this research is the development of a reverse micelles based process for the synthesis of hydrogel nanoparticles for encapsulating water-soluble drugs. This technology has been sold to Dabur research foundation in India. They are also co-developing nano-polymer and liposome based drug delivery systems. A research group at Banaras Hindu University has developed a novel method to produce a membrane out of carbon nanotubes for treating contaminated drinking water [3]. Eureka Forbes, in collaboration with IIT Madras, has come out with a nanosilver-based water filter for the removal of dissolved pesticides in drinking water [4]. Among the Indian research laboratories, ARCI is one of the fast growing research centres with a unique mandate to develop and demonstrate technology and transfer the same to industries. ARCI has set up the Centre for Nanomaterials with a view to develop nanomaterial synthesis and application technologies which are scalable and economical in comparison to existing technologies.

VII. CONCLUSIONS

After a brief presentation of basic principles of the computational methods in materials science, we reviewed computational modelling and prediction of temperature strain phase diagram of ultra thin epitaxial films of $BaTiO_3$ that would help in design of devices based on epitaxial films of oxides.

Secondly, we showed how these calculations can be used within simple phenomenological theories to connect with complex materials properties relevant to mechanical behaviour, through an example of nano-structured Mg alloys. There are certain limitations of the current methods in computational materials science particularly in view of their applications to nano-scale materials. Another limitation of the existing methods lies in applications to dynamical quantum phenomena including transport of electrons through nano-structures. Finally, multi-scale simulation methods (which employ different methodologies for different scales in the same simulation) are expected to have a great impact in biological as well s materials sciences at all scales.

The awareness about nano-materials and nano-technology and its benefits to society has continuously increased among the Indian Scientific and Industrial Community over the last decade. The intensity of scientific research in the area has also increased considerably over the years; though in terms of number of quality publications in technical journals, we still lag behind countries like Korea, China and Taiwan leave alone the leading countries like USA, Japan and Europe. However, in the areas of application development and commercialization of nano-materials based technologies, India is far behind even compared to countries like Singapore.

REFERENCES

[1]. Datta, U V Waghmare, U Ramamurty, Actu Mat 56, 2531 (2008).
[2]. Abe E, Kawamura Y, Hayashi K, Inoue A, Actu Mater. 50, 3854 (2002).
[3]. Srivastava, O.N.Srivastava, S.Talapatra, R.Vajtai, P.M.Ajayan, Nature Materias, 3(2004)610.
[4]. S. Nair, T.T.Renjis and T.Pradeep, J.Environ.Monit, 5(2003)363.
[5]. Carl C. Koch, Nanostructured Materials: Processing, Properties and Applications, William Andrew Publishing; Enlarged 2nd edition (2006).
[6]. C.N.R.Rao, Achim Mullar, Anthony K. Chutham, Nanomaterials chemistry: Recent Developments and New Directions, Wiley-VCH; 1 edition (2007).
[7]. H.Van Saygenhoven, Materials science and Engineering A 483, 33(2008).
[8]. Jaita Paul, T.Nishimatsu, Y.Kawazoe and U.V.Waghmare, Phys.Rev.Lett.99, 077601(2007).
[9]. K.J.Choi et. al, Science 306, 1005 (2004).
[10]. L.Kim, J.Kim, D.Jung, J.C.Lee and U.V.Waghmare, Appl. Phys. Lett. 87, 052903(2005).
[11]. Michael Plischke and Birger Bergersen, Equilibrium Statistical Mechanics, World Scientific, 3rd Edition (2006).
[12]. R. Pushpa, S.Narasimhan and U.V.Waghmare, J.Chem.Phys.121, 5211(2004).
[13]. S.Tetsuo, F.Yoshimasa, K.Shinjiro, JEE Technical report No.4, November 2004(originally published in JFE GIHO No.4)
[14]. S.Ghosh, A.K.Sood, N.Kumar, Science, 299(2003) 1042
[15]. S.Sankar, A.Rai, B.Ankamwar, A.Singh, A.Ahmed, M.Sastry, Nature Materials, 3(2004)487.
[16]. http.//nanomission.gov.in/.
[17]. www.nanotechproject.org.
[18]. www.Sbptechnology.com
[19]. www.unitednanotechnologies.com

International Journal of Modern Engineering Research (IJMER)
www.ijmer.com Vol. 3, Issue. 3, May - June 2013 pp-1801-1804 ISSN: 2249-6645

The Effect of Varying the Composition of Phosphorus on the Microstructure and Mechanical Properties of Tin-Bronze Alloys

Durowoju M. O. and Babatunde I. A.
Department of Mechanical Engineering, Ladoke Akintola University of Technology, Ogbomoso, Nigeria

ABSTRACT: *An investigation was carried out to assess the effect of phosphorus addition on copper- tin alloys. However, the effect of an increase in phosphorus above 0.25% has received little or no attention. Much effort has been expended only to study the effect of phosphorus as a deoxidizing agent on copper and its alloys. In this study, a new approach of casting phosphorus tin-bronze using an improvised vacuum crucible pots, made of clay mould was adopted. This method offers low cost and consumes less energy. The various microstructures that result from the slow cooling rate during the casting process enhance mechanical properties and were carefully examined. It was observed that the hardness and tensile strength increases as phosphorous content is increased from 0.1% to 1.0%. An optimum value of 0.9% phosphorus was obtained with corresponding hardness and tensile strength of 140HB and 912.26MPa respectively.*

KEYWORDS: *Deoxidizing, microstructure, tin-bronze.*

I. INTRODUCTION

Phosphor bronze is characterized by high tensile strength, good corrosion and resistance to wear, high mechanical load and excellent elastic properties. It also possesses good castability and machinability. Phosphorus improves soundness and cleanliness of casting, which causes improvement in strength and ductility [6, 4, 2]. During the last two decades, many materials have been cast successfully using various methods including horizontal continuous casting, vacuum casting and strip casting techniques; for stainless steel, high silicon-steel, as well as copper and copper alloys. It is believed that these casting processes are suitable for producing bronze and phosphorus bronze plate without experiencing low productivity [5, 2]. Thus, the retention of as little as 0.1% phosphorus further increases the strength and hardness of the alloy [4, 1, 7].

Due to these advantages, phosphorus bronze is widely used for high-load, high speed, spring, condenser tube, gears, marine fitting, diaphragms, bellows, lock-washers and cotter pins applications, as well as poorly lubricated bearings in corrosive environments. The structure and proprieties of alloy depend on melting and casting conditions, which influences the alloy crystallization [3, 5].

Many types of castings can be used for copper and its alloys, such as sand, shell, investment, permanent mold, chemical sand, centrifugal and die casting. The technological specifications for casting processes are the most important factors to obtain good results [3, 6, 4, 9]. In this study, the effect on microstructure and mechanical properties by increasing phosphorus content in as-cast tin-bronze alloys using an improvised vacuum crucible pots is presented.

II. MATERIALS AND METHOD

II.1 Materials: Tin bronzes may conveniently be divided into two groups: low-tin bronzes and high-tin bronzes. Low-tin bronzes are those in which the tin content is less than 17%. This is the maximum theoretical limit of the solubility of tin in the copper-rich solid solution. In practice, the usual limit of solid solution is nearer to 14%, although it is rare to find a bronze with this tin content in a homogeneous single phase [3, 9]. In this study, a low tin-bronze was selected as the experimental alloy and Table 1 shows its chemical composition.

Table 1.0: Composition of the investigated phosphorus-bronze alloy

Samples (%wt)	Cu	Sn	P
A	95	5.0	0.0
B	95	4.9	0.1
C	95	4.8	0.2
D	95	4.7	0.3
E	95	4.6	0.4
F	95	4.5	0.5
G	95	4.4	0.6
H	95	4.3	0.7
I	95	4.2	0.8
J	95	4.1	0.9
K	95	4.0	1.0
L	92	6.5	1.5
M	92	6.0	2.0
N	92	5.5	2.5
O	92	5.0	3.0
P	92	4.5	3.5
Q	92	4.0	4.0
R	92	3.5	4.5
S	92	3.0	5.0

II.2 Casting Technique : Clay is one of the most widely used ceramic raw materials which are found naturally in great abundance, often used as mined without any further processing. When mixed in the appropriate proportions, clay and water form a plastic mass that is very amenable to shaping [6]. The formed piece is dried to remove some of the moisture and fired at an elevated temperature to improve its mechanical strength.

In this study, an improvised clay molded vacuum crucible pots of 5mm thickness was employed. The crucible pots consist of the melting and the casting sections. Each sample was charged in each of the crucible pots and sun-dried for 72hours. The preliminary study performed revealed that the crucible pot attains a temperature of 1850°C before adequate heat can be transferred to melt the sample. With this knowledge, each sample in the crucible pot was heated to a temperature of 1850°C, after which the cast alloys in rod forms were obtained.

II.3 Etching and Surface preparation : Micro-structural analysis is used in research studies to determine the micro-structural changes that occur as a result of varying parameters such as composition, heat treatment or processing steps [8, 7]. An optical metallurgical microscope was employed to carry out the metallographic analyses on the selected specimens. The analyses capture a square shape of approximately 3mm x 3mm of the specimen. All samples were prepared by grinding and polished with silicon carbide gel in the order 220, 320, 400 and 600 grit sizes. Optical examination was performed prior to etching with 2% alcoholic ferric chloride solution, to identify inclusions, porosity, and other casting defects.

III. EXPERIMENTAL STUDY

III.1 Brinell Hardness measurement : In order to determine the variation of hardness based on casting technique, *Leitz 8299 micro-hardness tester* was used to perform the micro-hardness tests of the cast samples. A load 250Kg was used for indentation on the polished samples for 15 seconds. The indentation was square shaped. Diagonal length of square was measured by a scale attached on the microscope.

III.2 Tensile Strength Measurement : The tensile tests were performed using a *Monsanto Tensometer* tensile testing machine, equipped with a data acquisition system for recording the strain and load. The strain was measured with a strain gauge and extensometer attached at the center of each specimen (giving a very precise measurement but limited to the elastic region of the cast specimens).

IV. RESULTS AND DISCUSSIONS

IV.1 Microstructure Analysis : Fig 1.0 below shows the variation of microstructure as phosphorus content increases. The residual phosphorus may be sufficient to be present as copper-phosphide which appears dark-blue in the microstructures at the initial stage. It may easily be distinguished from cuprous oxide by the fact that the latter is translucent with a copper reflection in the centre. There are no traces of porosity and the grain structure is lightly delineated (as the percentage of phosphorus increases up 0.9%) by the use of alcoholic ferric chloride etchant. These microstructures consist of regularly shaped primary grains of eutectic. The eutectoid constituent is made up of two phases, alpha (the copper-rich solid solution of tin in copper) and delta (an intermetallic compound of fixed composition). The constituent of the eutectic has become absorbed by the primary grains and is not visible as separate particles up to 0.7% phosphorus. A blue-grey colour began to set in as the percentage of phosphorus increases from 0.1% to about 0.7% and later appeared bright-red.

In addition, the vacuum casting employed enabled the phosphorus to be evenly dispersed, thus producing fine grains which appear within the region of the cast samples and improve the mechanical properties of alloys. As the percentage of phosphorus increases from 1.0 to 2.5%, the secondary phases (intermetallics boundaries) exist, indicates the coarse dendrite structure of the matrix compound (Fe-P) having bright-red contrast and precipitated at the grain boundaries.

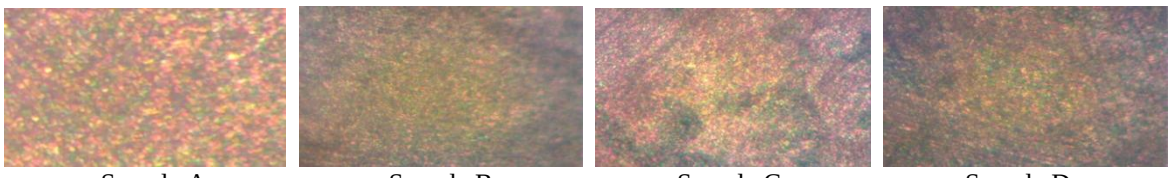
Sample A Sample B Sample C Sample D

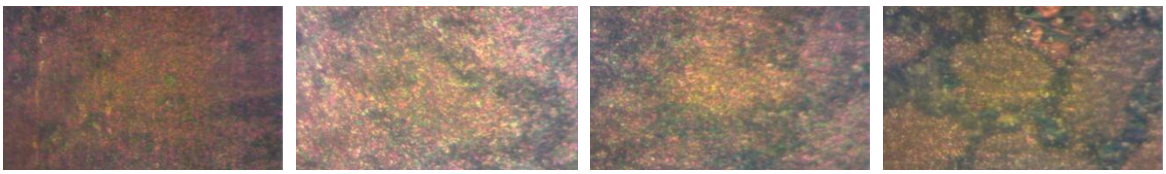
Sample E Sample F Sample G Sample H

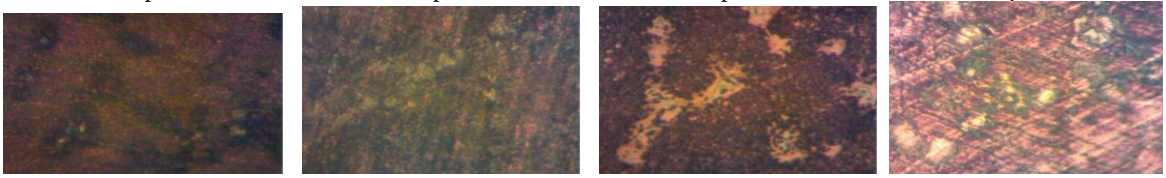
Sample I Sample J Sample K Sample L

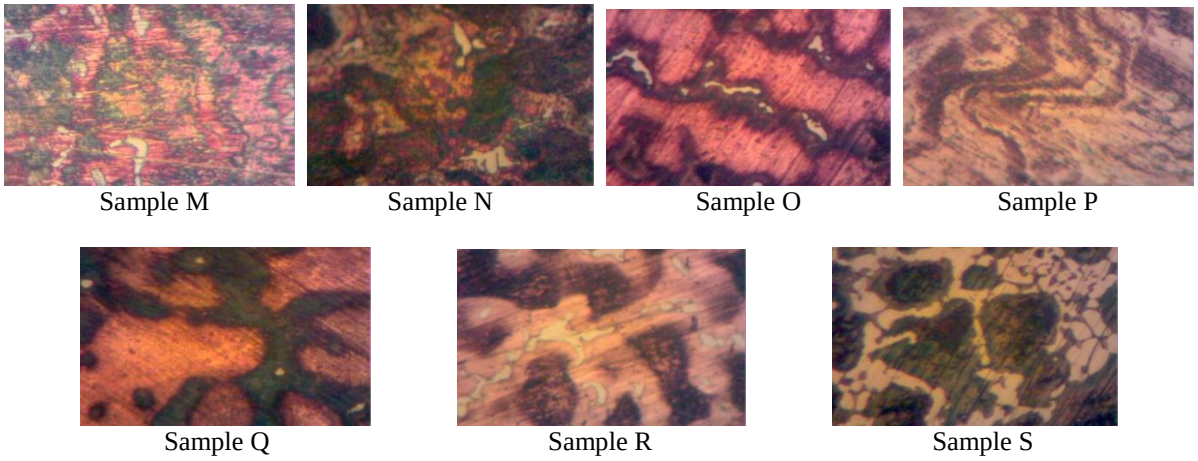

Fig 1.0: The microstructure of the as-cast phosphorus bronze

IV.2 Results of Mechanical Testing: In this study, it was observed that at 0.1-0.2%P, the material is very hard and strong with low level of ductility. As the percentage of phosphorus increases from 0.3-1.5%, the materials become harder and tough due to the formation of grain boundary edges, thus experiences high level of ductility (long plastic deformation before fracture). Table 2 below shows the variation in the considered mechanical properties in the samples

Table 2.0: Variation in the mechanical properties of the samples

Samples (wt %)	Hardness (HB)	Tensile Strength (MPa)	Elongation (%)
95Cu-5Sn	107	520.18	12.00
95Cu-4.9Sn-0.1P	112	542.05	18.00
95Cu-4.8Sn-0.2P	121	565.38	25.00
95Cu-4.7Sn-0.3P	128	590.22	38.80
95Cu-4.6Sn-0.4P	133	616.75	38.40
95Cu-4.5Sn-0.5P	138	631.39	49.16
95Cu-4.4Sn-0.6P	140	707.98	46.18
95Cu-4.3Sn-0.7P	140	780.55	24.00
95Cu-4.2Sn-0.8P	140	821.13	33.87
95Cu-4.1Sn-0.9P	140	912.26	12.70
95Cu-4.0Sn-1.0P	136	864.88	27.31
92Cu-6.5Sn-1.5P	112	761.39	20.80
92Cu-6.0Sn-2.0P	101	691.42	27.60
92Cu-5.5Sn-2.5P	90.7	592.79	5.75
92Cu-5.0Sn-3.0P	81.3	577.59	22.92
92Cu-4.5Sn-3.5P	72.4	561.78	25.00
92Cu-4.0Sn-4.0P	65.5	530.93	26.42
92Cu-3.5Sn-4.5P	59.5	509.69	17.69
92Cu-3.0Sn-5.0P	51.9	499.55	12.40

This tendency can be identified in the microstructure as an indication of small grain sizes results in the improvement of hardness and tensile strength. At about 2.0-5.0%P, the materials experiences little plastic deformation due to a few reductions in cross-section (necking), reduces the hardness of the materials further. It is observed from the plot that the peak hardness increases with phosphorus content. Also it is to be noted that the magnitude of the peak hardness observed is marginally different, due to varying phosphorus content.

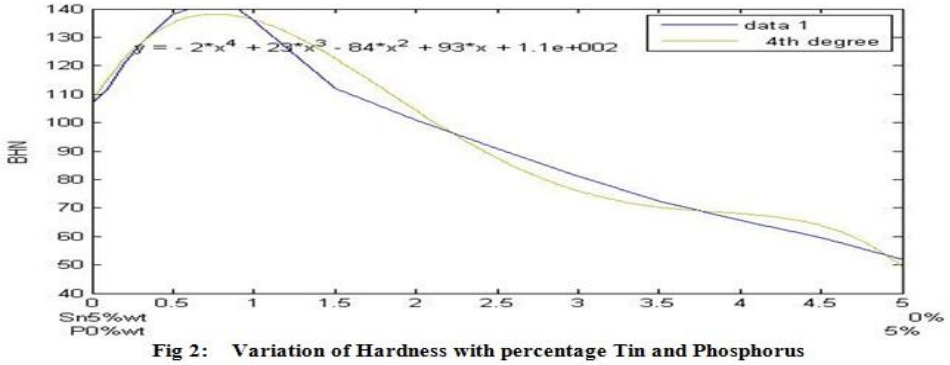

Fig 2: Variation of Hardness with percentage Tin and Phosphorus

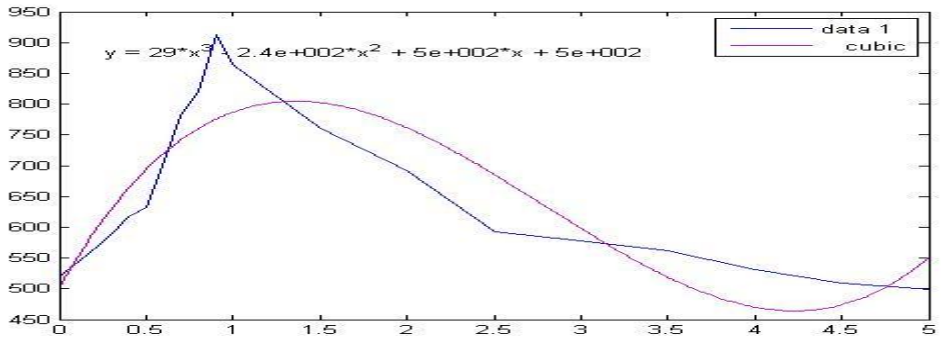

Fig 3: Variation of Tensile strength with percentage Phosphorus

V. CONCLUSIONS

In this study, microstructural characterization of phosphorus tin-copper alloys was carried out and the results obtained are given as follows:

(i) The microstructure of sample J, with composition 95Cu4.1Sn0.9P (%wt) revealed a complete homogenous eutectic structure and the grains are evenly distributed.

(ii) Similarly, sample J also gives an optimum hardness and tensile strength of 140HB and 912.26MPa.

REFERENCES

[1] Aksoy, M., Kuzucu, V., Turhan, H., 2002; "A note on the effect of phosphorus on the microstructure and mechanical properties of leaded-tin bronze", Journal of Material Processing Technology, Vol. 124, pp. 113 – 119.

[2] Caron, R. N, and Shapiro, S, (1977); "Mechanism of Yield Strength Enhancement in Heavily Cold Rolled Phosphorus Bronze", Metallurgical Transactions (A), Vol. 8, pp 111-117.

[3] Copper Development Assocaition (CDA), 1991; Copper and Copper Alloy Castings, Properties and Applications.

[4] Glazowska, I., Romankiewics, F., Krasicka, E. C., Michalski, M., 2005; "Structure of Phosphorus Tin Bronze CuSn10P Modified with Mixture of Microadditives", Archices of Foundary, Vol. 5, No. 15, pp. 94 – 100.

[5] Hwang, J. D., Li, B. J., Hwang, W. S., and Hu, C. T., 1998; "Comparison of Phosphorus Bronze Metal Sheet Produced by Twin Roll Casting and Horizontal Continuous Casting", Journal of Materials Engineering and Performance, Vol. 7, pp 495-503.

[6] Kutz, M. 2002; Handbook of Materials Selection, John Wiley & Sons, Inc., New York.

[7] Mairb R. H., 2011; "Microstructure and Hardness Effects on Behavior of Copper Alloy under Creep – Fatigue Interaction", Eng. And Tech. Journal, Vol. 29, pp. 1641 – 1640.

[8] Silva, R.J.C., Figueiredo, E., Araújo, M.F., Pereira, F.,Fernandes, F.M.B.,2008; "Microstructure Interpretation of Copper and Bronze Archaeological Artefacts from Portugal", Materials Science Forum, Vols. 587-588, pp 365-369.

[9] Taşliçukur, Z., Altuğ, G. S., Polat, S., Atapek, S. H., and Türedi, E., 2012; "A Microstructural Study on CuSn10 Bronze Produced By Sand And Investment Casting Techniques", Brno, Czech Republic, EU.

International Journal of Modern Engineering Research (IJMER)
www.ijmer.com Vol. 3, Issue. 3, May - June 2013 pp-1805-1810 ISSN: 2249-6645

Seismic Analysis of RCC Building with and Without Shear Wall

P. P. Chandurkar[1], Dr. P. S. Pajgade[2],
[1]*Post graduate student in structural engineering,* [2]*Department of Civil engineering, Prof. Ram Meghe Institute of Technology and Research Badnera, Sant Gadge Baba Amravati University, Amravati, Maharashtra 444602 India*

ABSTRACT: *In the seismic design of buildings, reinforced concrete structural walls, or shear walls, act as major earthquake resisting members. Structural walls provide an efficient bracing system and offer great potential for lateral load resistance. The properties of these seismic shear walls dominate the response of the buildings, and therefore, it is important to evaluate the seismic response of the walls appropriately. In this present study, main focus is to determine the solution for shear wall location in multi-storey building. Effectiveness of shear wall has been studied with the help of four different models. Model one is bare frame structural system and other three models are dual type structural system. An earthquake load is applied to a building of ten stories located in zone II, zone III, zone IV and zone V. Parameters like Lateral displacement, story drift and total cost required for ground floor are calculated in both the cases replacing column with shear wall.*

KEYWORDS: *ETAB v 9.5.0, framed structure, Seismic analysis, Shear wall,*

I. INTRODUCTION

Shear wall are one of the excellent means of providing earthquake resistance to multistoried reinforced concrete building**.** The structure is still damaged due to some or the other reason during earthquakes. Behavior of structure during earthquake motion depends on distribution of weight, stiffness and strength in both horizontal and planes of building. To reduce the effect of earthquake reinforced concrete shear walls are used in the building. These can be used for improving seismic response of buildings. Structural design of buildings for seismic loading is primarily concerned with structural safety during major Earthquakes, in tall buildings, it is very important to ensure adequate lateral stiffness to resist lateral load. The provision of shear wall in building to achieve rigidity has been found effective and economical. When buildings are tall, beam, column sizes are quite heavy and steel required is large. So there is lot of congestion at these joint and it is difficult to place and vibrate concrete at these place and displacement is quite heavy. Shear walls are usually used in tall building to avoid collapse of buildings. When shear wall are situated in advantageous positions in the building, they can form an efficient lateral force resisting system. In this present paper one model for bare frame type residential building and three models for dual type structural system are generated with the help of ETAB and effectiveness has been checked.

II. BUILDING MODELING

For this study, a 10-story building with a 3-meters height for each story, regular in plan is modeled. These buildings were designed in compliance to the Indian Code of Practice for Seismic Resistant Design of Buildings .The buildings are assumed to be fixed at the base and the floors acts as rigid diaphragms. The sections of structural elements are square and rectangular and their dimensions are changed for different building. Storey heights of buildings are assumed to be constant including the ground storey. The buildings are modeled using software ETAB Nonlinear v 9.5.0.Four different models were studied with different positioning of shear wall in building. Models are studied in all four zones comparing lateral displacement, story drift, % Ast in column, concrete quantity required, steel and total cost required in all zones for all models.

The plan of the building model are given below

Model 1 – Floor plan of the bare framed structure.
Model 2 – Floor plan of the dual system with shear wall one on each side.
Model 3 - Floor plan of the dual system with shear wall on corner with L = 4.5m
Model 4 – Floor plan of the dual system with shear wall on corner with L = 2m.
All calculations are carried out at ground floor.
All diamensions are in mm.

TABLE 1: Preliminary data

	For ten story
No. of stories	TEN (G+9)
Floor to Floor Height	3.0 m
Beam size longitudinal and transverse direction	230x500 mm^2
Column size	300x600 mm^2
Thickness of slab	150 mm
Thickness External Wall	230 mm
Thickness of Internal wall	115 mm
Grade of Concrete and steel	M20 and Fe415

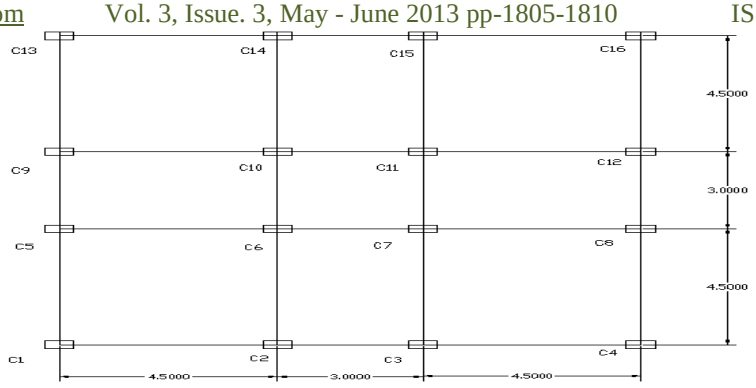

Figure 1: model 1

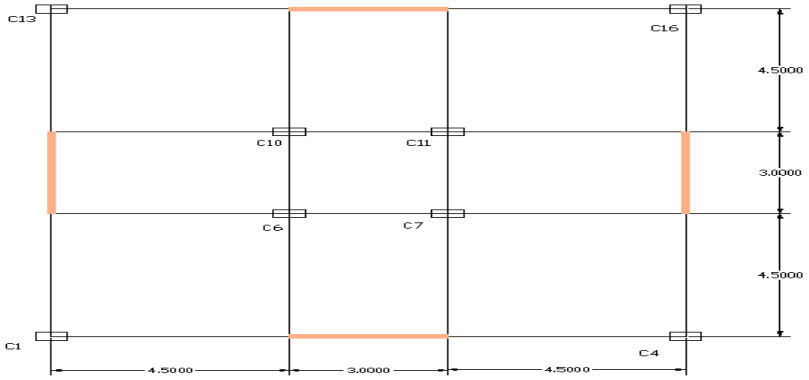

Figure 2: model 2

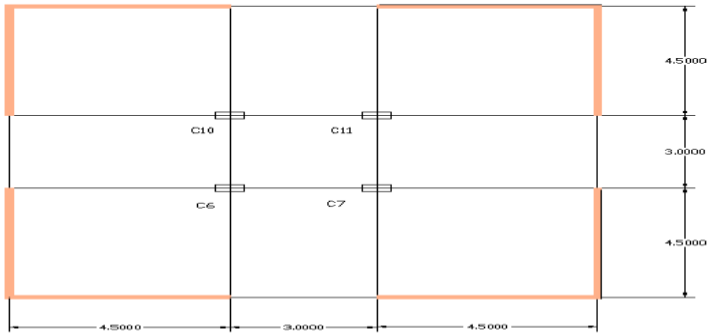

Figure 3: model 3

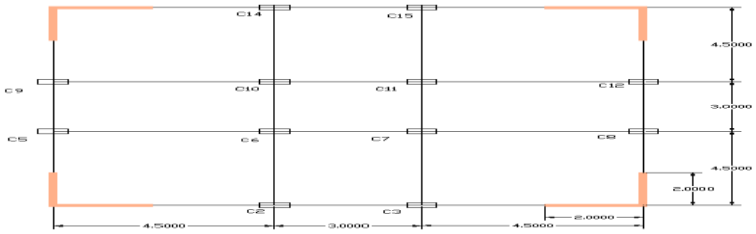

Figure 4: model 4

III. RESULT AND DISCUSSION

III.1 LATERAL DISPLACEMENT

Lateral displacement for all model in all four zones are as shown in fig.

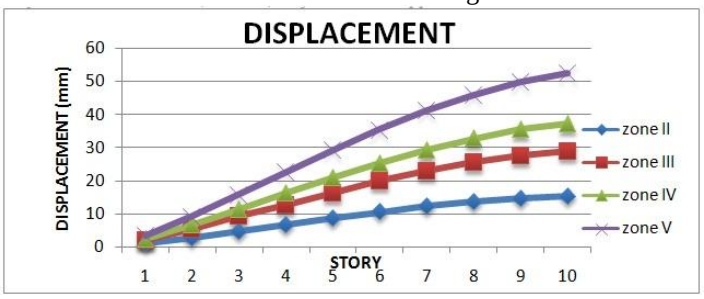

Figure 5: displacement of model 1

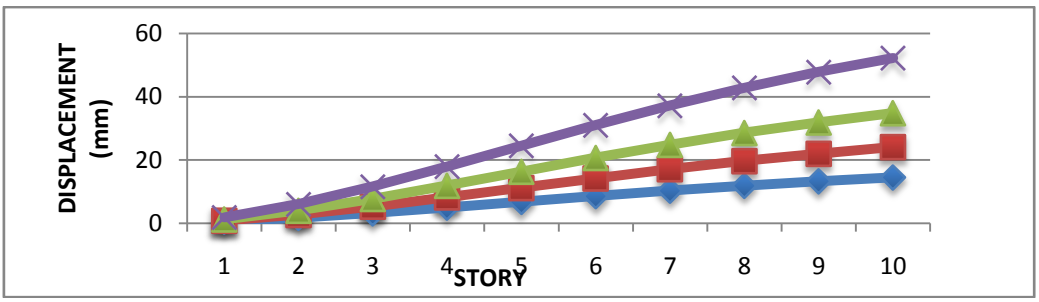

Figure 6: displacement of model 2

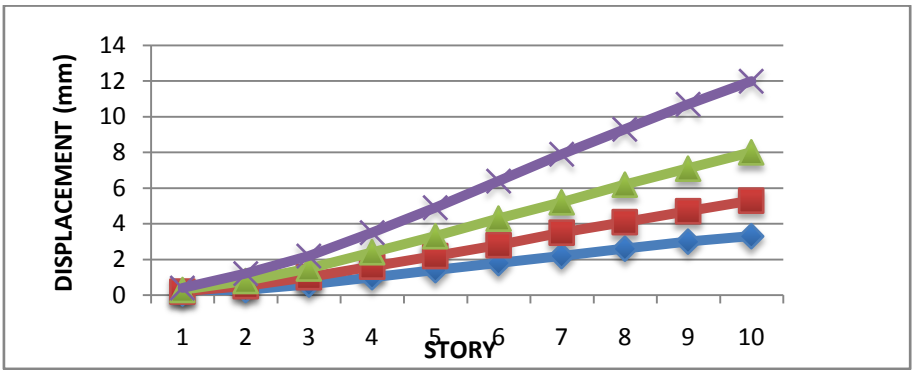

Figure 7: displacement of model 3

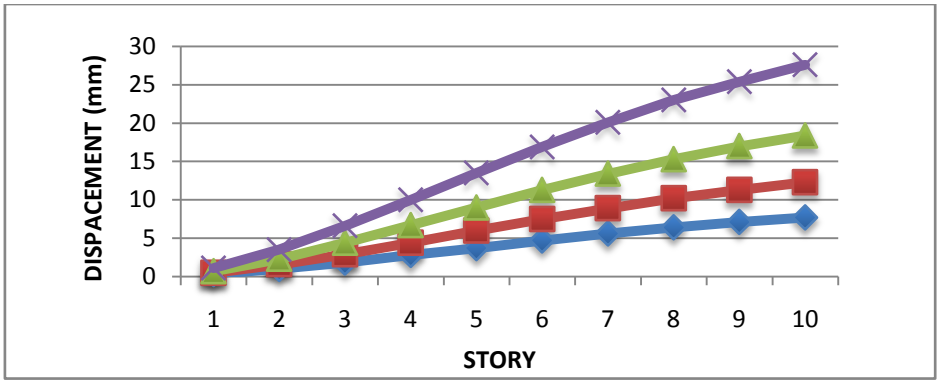

Figure 8: displacement of model 4

From results it is observed that the displacement of all models in zone II, III, IV is reduced upto 40% as compared with zone V.

3.2 STORY DRIFT RATIO

Story drift is the displacement of one level relative to the other level above or below. Story drift ratio according to the zones of each model is shown in fig. In Software value of story drift is given in ratio.

$$\text{Story drift ratio} = \frac{\text{difference between displacement of two stories}}{\text{height of one story}}$$

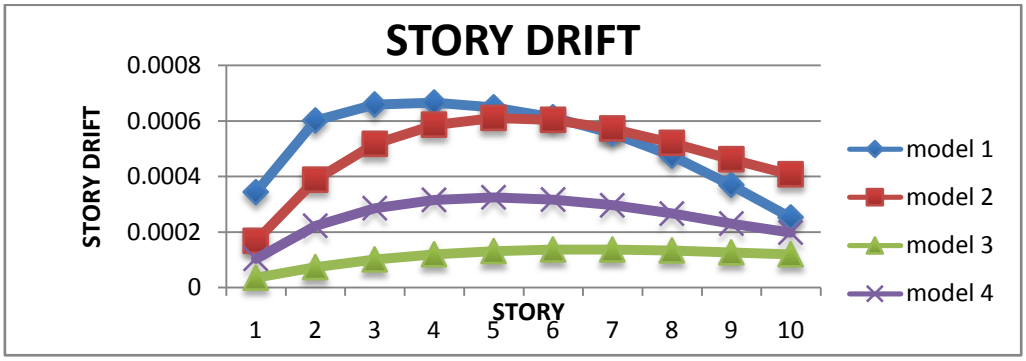

Figure 9: story drift for zone II

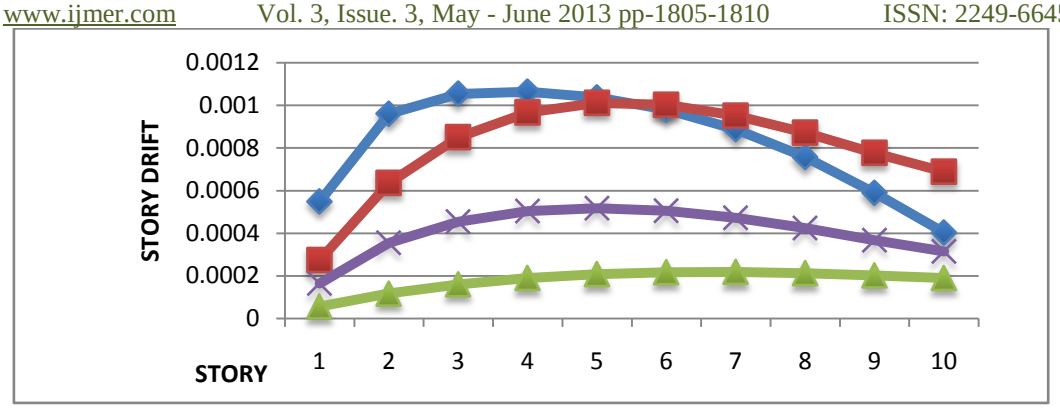

Figure 10: story drift for zone III

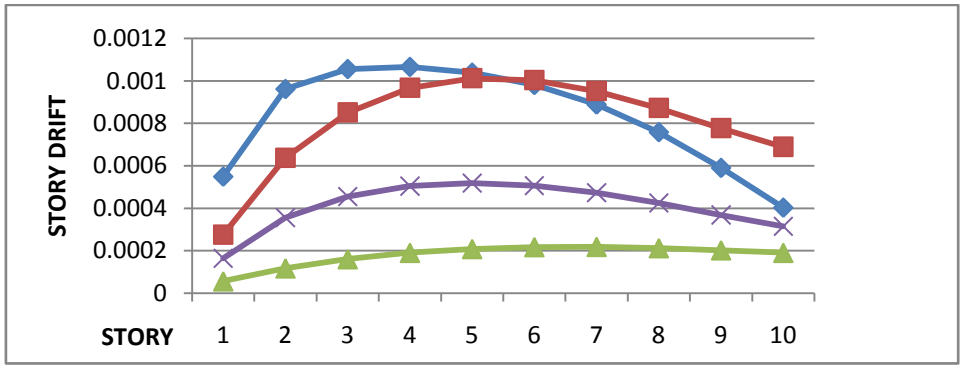

Figure 11: story drift for zone IV

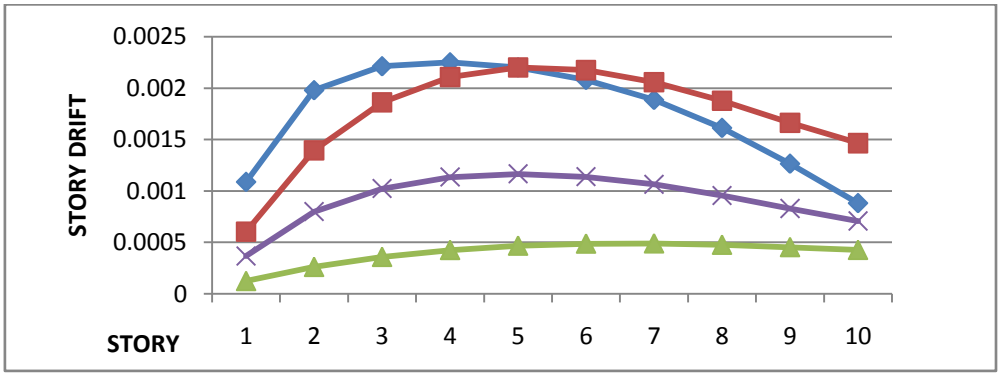

Figure 12: story drift for zone V

From the result observed that the story drift is maximum for model 1 i.e. bare frame without shear wall as compared with other model in all zones. While compared with zone story drift is maximum in zone V and minimum in zone II. Model 3 has the minimum value of story drift in all zones as compared with other models.

3.3 Concrete quantity in mm^3

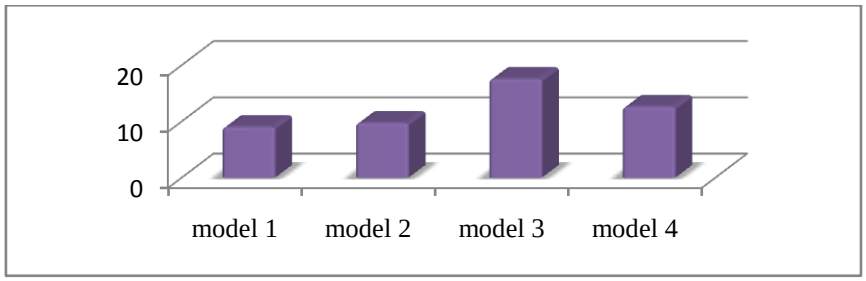

Figure 13: chart of concrete quantity in mm^3models

As the shear wall in model 3 are large (4500x3000 mm), the quantity of concrete require for that model is more as compared with other models.

3.4 Concrete Cost in Rs

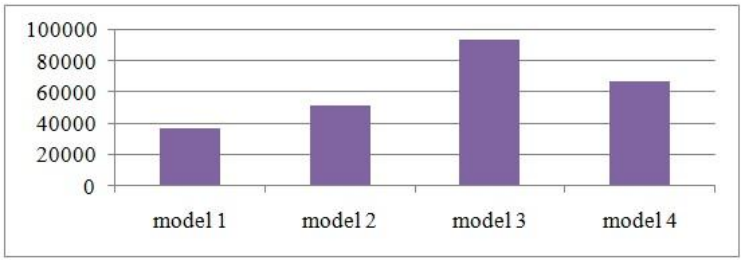

Figure 14: chart for concrete cost in rs

3.5 STEEL COMPARISION

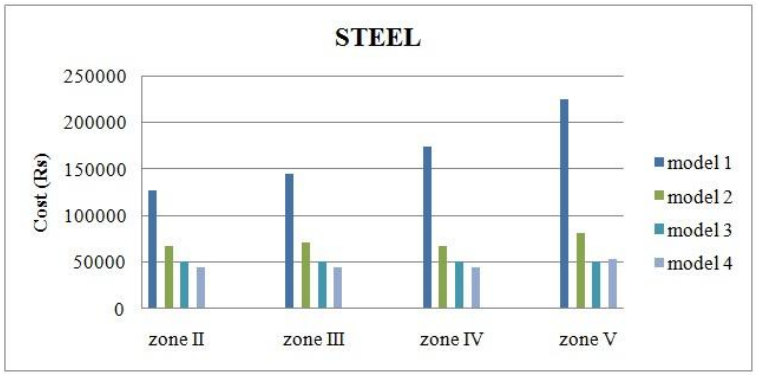

Figure 15: chart of required steel in all zones

From the above graph, it is observed that model 1 require more steel in all zone as compared with other zones. In zone V, steel required is much higher in all models except that in model 3.

3.6 TOTAL COST

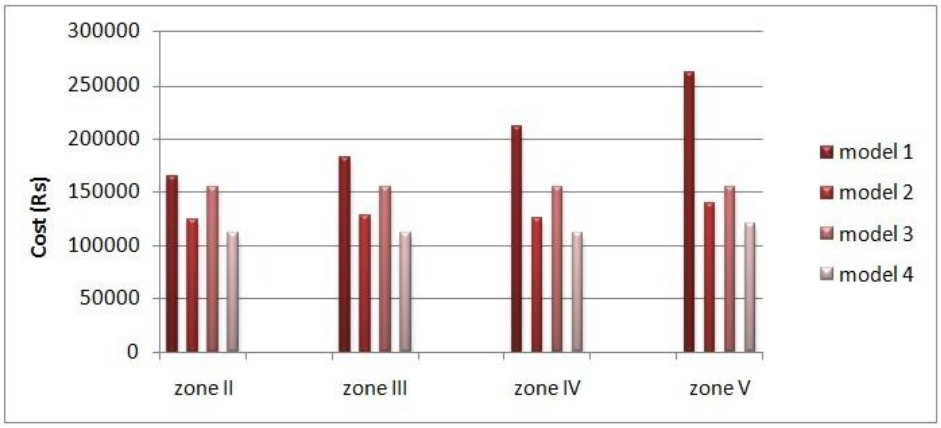

Figure 16: chart showing total cost

Comparing the total cost i.e. concrete and steel cost of structure, model 1 required more cost in all zones while model 3 require same cost in all zones. The corner shear wall in 2m length (model 4) is economical to provide as it require less cost comparing with other models.

3.7 % Ast IN COLUMN

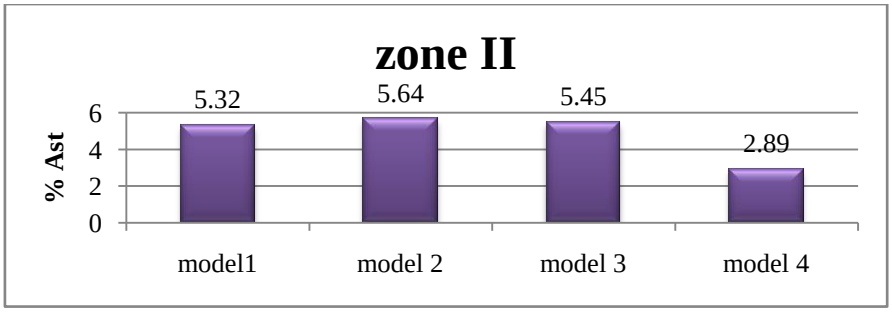

Figure 17: % ast in column c6

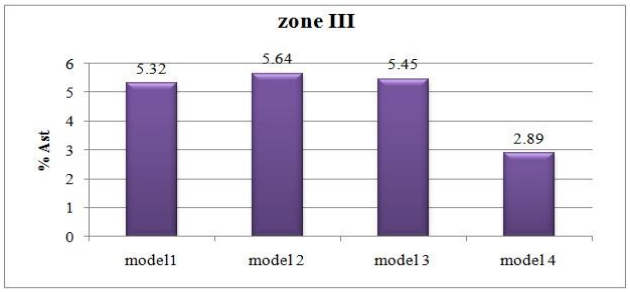

Figure 18: % ast in column c6

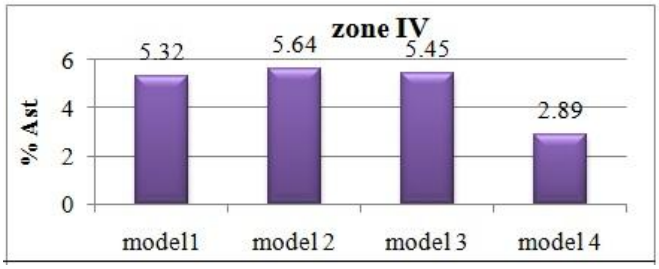

Figure 19: % ast in column c6

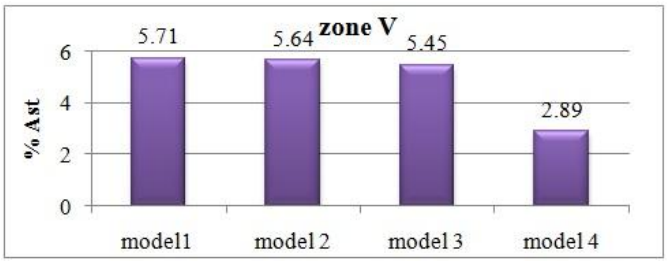

Figure 17: % ast in column c6

From the above result it is seen that, there is no increase in % Ast of central column in dual system where as %Ast of same column in frame structure increases and maximum in zone V.

IV. CONCLUSION

From all the above analysis, it is observed that in 10 story building, constructing building with shear wall in short span at corner (model 4) is economical as compared with other models. From this it can be concluded that large dimension of shear wall is not effective in 10 stories or below 10 stories buildings. It is observed that the shear wall is economical and effective in high rise building.

Also observed that

1. Changing the position of shear wall will affect the attraction of forces, so that wall must be in proper position.
2. If the dimensions of shear wall are large then major amount of horizontal forces are taken by shear wall.
3. Providing shear walls at adequate locations substantially reduces the displacements due to earthquake.

REFERANCES

[1]. Anshumn. S, Dipendu Bhunia, Bhavin Rmjiyani (2011), "Solution of shear wall location in Multi-storey building." International Journal of Civil Engineering Vol. 9, No.2Pages 493-506.
[2]. M. Asharaf, Z. A. Siddiqi, M. A. Javed, "Configuration of Multi-storey building subjected to lateral forces". Asian Journal of Civil Engineering (Building & Housing), Vol. 9, No. 5 Pages 525-537.
[3]. H.-S. Kim, D.-G. Lee"Analysis of shear wall with openings using super elements" Engineering Structures 25 (2003) 981–991
[4]. M. Shariq, H. Abbas, H. Irtaza, M. Qamaruddin "Influence of openings on seismic performance of masonry building walls" Building and Environment 43 (2008) 1232–1240
[5]. Sid Ahmed Meftah, Abdelouahed Tounsi, Adda Bedia El Abbas "A simplified approach for seismic calculation of a tall building braced by shear walls and thin-walled open section structures" Engineering Structures 29 (2007) 2576–2585
[6]. Quanfeng Wang , Lingyun Wang, Qiangsheng Liu "Effect of shear wall height on earthquake response" Engineering Structures 23 (2001) 376–384P.A. Hidalgo, R.M. Jordan, M.P.
[7]. Martinez "An analytical model to predict the inelastic seismic behavior of Shear-wall, reinforced concrete structures" Engineering Structures 24 (2002) 85–98Duggal S. K.(2010), " Earthquake Resistant Design Structues". Oxfored University press YMCA library building, Jai Singh road, New Delhi. Bureau of India Standard, Is-1893, Part 1 (2002), "Criteria for earthquake resistant design of structures." Part 1
[8]. General Provision and building, New Delhi, India.
[9]. Bureau of Indian Standard, IS-456(2000), "Plain and Reinforced Concrete Code of Practice".

International Journal of Modern Engineering Research (IJMER)
www.ijmer.com Vol. 3, Issue. 3, May - June 2013 pp-1811-1814 ISSN: 2249-6645

Security Enhancement of Single Sign on Mechanism for Distributed Computer Networks

Jean Jacob[1], Mary John[2]
[1](Information Technology, Rajagiri School of Engineering & Technology, India)
[2](Department of Information Technology, Rajagiri School of Engineering and Technology, Rajagiri Valley, Cochin, India

ABSTRACT: *Single sign-on mechanisms allow users to sign on only once and have their identities automatically verified by each application or service they want to access afterwards. There are few practical and secure single sign-on models, even though it is of great importance to current distributed application environments. Most of current application architectures require the user to memorize and utilize a different set of credentials (eg, username/password or tokens) for each application he/she wants to access. However, this approach is inefficient and insecure with the exponential growth in the number of applications and services a user has to access both inside corporative environments and at the Internet. Single sign-on (SSO) is a new authentication mechanism that enables a legal user with a single credential to be authenticated by multiple service providers in distributed computer networks. Recently, Chang and Lee proposed a new SSO scheme and claimed its security by providing well-organized security arguments. In this paper, however, it is shown that their scheme is actually insecure as it fails to meet security during communication. This paper shows the Chang & Lee scheme and it aims to enhance security using AES encryption and decryption. Implementation is done using socket programming in Java.*

KEYWORDS: *Authentication, Attacks, Decryption, Encryption, Single Sign on*

I. INTRODUCTION

Identification of user is an important access control mechanism for client–server networking architectures. The goal of a single sign on platform is to eliminate individual sign on procedures by centralizing user authentication and identity management at a central identity provider. In a single sign-on solution, the user should seamlessly authenticated to his multiple user accounts (across different systems) once he proves his identity to the identity provider. Nevertheless, in many current solutions, the user is required to repeat sign on for each service using the same set of credentials, which are validated at the identity provider by each service.

User authentication [3], [4] plays a crucial role in distributed computer networks to verify the legacy of a user and then can be granted to access the services requested. To prevent bogus servers, users usually need to authenticate service providers. After mutual authentication, a session key may be negotiated to keep the confidentiality of data exchanged between a user and a provider [4], [5], [6]. In many scenarios, the anonymity of legal users should be protected as well [4], [7], [6]. These protocols offer varying degrees of efficiency. This paper aims to ensure more security to the existing Chang Lee SSO scheme. It also aims to add additional security during data transfer between user and provider. It also proposes further research into more efficient enhancements to the current work. The main objective of this paper is to enhance security for single sign-on solutions and eliminate the need for users to repeatedly prove their identities to different applications and hold different credentials for each application.

II. RELATED WORKS

In 2000, Lee and Chang [4] proposed a user identification and key distribution scheme to maintain user anonymity in distributed computer networks. Later, Wu and Hsu [8] pointed out that Lee-Chang scheme is insecure against both impersonation attack and identity disclosure attack. Meanwhile, Yang et al. [9] identified a weakness in Wu-Hsu scheme and proposed an improvement. In 2006, however, Mangipudi and Katti [10] pointed out that Yang et al.'s scheme suffers from DoS (Deniable of Service) attack and presented a new scheme. In 2009, Hsu and Chuang [11] showed that both Yang et al. and Mangipudi-Katti schemes were insecure under identity disclosure attack, and proposed an RSA-based user identification scheme to overcome the drawbacks.

On the other hand, it is usually not practical by asking one user to maintain different pairs of identity and passwords for different service providers, since this could increase the workload of both users and service providers as well as the communication overhead of networks. To tackle this problem, single sign-on (SSO) mechanism [12] has been introduced so that after obtaining a credential from a trusted authority, each legal user can use this single credential to authenticate itself and then access multiple service providers. Intuitively, an SSO scheme should meet at least two basic security requirements, i.e., soundness and credential privacy. Soundness means that an unregistered user without a credential should not be able to access the services offered by service providers. Credential privacy guarantees that colluded dishonest service providers should not be able to fully recover a user's credential and then impersonate the user to log in other service providers. Formal security definitions of SSO schemes were given in [13]. Chang and Lee made a careful study of SSO mechanism. Firstly, they argued that Hsu-Chuang user identification scheme, actually an SSO scheme, has two weaknesses: (a) An outsider can forge a valid credential by mounting a credential forging attack since Hsu-Chang scheme employed naive RSA signature without any hash function to issue a credential for any random identity selected by a user ; and (b) Hsu-Chuang scheme requires clock synchronization since timestamp is used in their scheme. Then, Chang and Lee presented an interesting RSA based SSO scheme, which is highly efficient in computation and communication (So it is suitable for mobile devices), and does not rely on clock synchronization by using nonce instead of timestamp. Finally, they presented well-organized security

analysis to show that their SSO scheme supports secure mutual authentication, session key agreement, and user anonymity. In [13], Han et al. proposed a generic SSO construction which relies on broadcast encryption plus zero knowledge (ZK) proof showing that the prover knows the corresponding private key of a given public key. So, implicitly each user is assumed to have been issued a public key in a public key infrastructure (PKI). In the setting of RSA cryptosystem, such a ZK proof is very inefficient due to the complexity of interactive communications between the prover (a user) and the verifier (a service provider). Therefore, compared with Han et al.'s generic scheme, Chang-Lee scheme has several attracting features: less underlying primitives without using broadcast encryption, high efficiency without resort to ZK proof, and no requirement of PKI for users.

Table I: Notations used in the algorithm

Notations	Descriptions
SCPC	A trusted authority
U_i, P_j	The user and the service provider, respectively
ID_X	The identity of the entity X
S_X	The secret token of the entity X
e_X	The public key of the entity X
d_X	The private key of entity X
$E_K(M)$	A symmetric encryption of plaintext M using a key K
$D_K(C)$	A symmetric decryption of ciphertext C using a key K
$h(\cdot)$	The one-way hash function
$\|\|$	The concatenation operator

III. PROPOSED SCHEME

The notations used in the algorithm are explained in Table I. The scheme consists of three phases:

A. *System Initialization Phase*

SCPC does the following

1. selects large two primes p, q and computes p*q.
2. determines the key pair (e,d) such that e *d ≡ 1mod φ(N),where φ(N)=(p − 1)*(q − 1).
3. chooses a generator g over the finite field Z∗n, where n is a large odd prime number.
4. SCPC protects the secrecy of d and publishes (e,g,n,N).

B. *Registration Phase*

1. Each user U_i registers a unique identity $ID_i$with a fixed bit length.

2. Obtain a secret token $S_i=(ID_i||h(ID_i))^d$ mod N, from the SCPC through a secure channel where h(·) is a cryptographic one-way hash function.

C. User Identification Phase

U_i submits the request with a random nonce n1, m1 to P_j . On receiving m1, P_j chooses a random number k and then generates a random nonce n2. P_j calculates $Z = g^k$ mod n, u = h(Z||ID_j ||n1), and the signature $v = (u||h(u))^{dj}$ mod N_j .Next, P_j sends the message m2 = {Z,v,n2} back to U_i.. After receiving m2 from P_j, U_i computes u =h (Z||ID_j ||n1) and performs the next step. U_i verifies the signature v by checking the equivalency of v^e_j mod N?=(u||h(u))mod N_j . Otherwise, U_i informs P_j that someone has tampered with Z and aborts the protocol. Otherwise, U_i chooses a random number t to be his short-term private key and computes $w = g^t$ mod n. U_i calculates the parameter k_{ij} as $k_{ij} = Z^t$ mod n. U_i generates a random nonce n3 and calculates three parameters K_{ij}, x and y in accordance with the following equations: K_{ij} = h(ID_j ||k i_j), the session key, x = $S_i^{h(Kij\ ||w||n2)}$ mod N, y = E_{Kij} (IDi||n3||n2), where E(·) is a symmetric crypto system such as DES or AES. U_i sends m3 = {w,x,y} to P_j After receiving m3, P_j computes k_{ij} as $k_{ij} = w^k$ mod n. P_j can obtain the session key K_{ij} by computing K_{ij} =h(ID_j || k_{ij}). P_j uses K_{ij} to decrypt cipher text y and retrieves IDi, n3, and n2. If n2 is valid, Pj computes SIDi = (IDi||h(IDi)). P_j verifies the validity of the identity IDi by checking $SID_i^{h\ (Kij\ ||w||n2)}$ mod N ? = x^e mod N. If the equation holds, P_j trusts that U_i is a legal user. P_j computes V = h(n3) and sends m4 = {V } to Ui. After receiving m4 from P_j, U_i computes V ||= h(n3) and confirms that V? = V '. When both the equations are same, U_i trusts that P_j is an authorized service provider and P_j has really calculated the common session key K_{ij}.

C. ***Encryption and Decryption Phase:*** Encryption and Decryption between user and provider is ensured using AES algorithm which is more secure than DES and there are currently no known non-brute-force attacks against AES. Data which is send from each provider to user is encrypted and send to the user, then the user decrypts it and the original data is retrieved. All these encryption and decryption are done using the more secure Advanced Encryption Algorithm (AES). The implementation is done using socket programming in Java and it uses server programs and client programs. To run in different machines, programming is based on IP address of the systems. Using the multithreading features of Java, all the providers can be run in parallel. The overall checking of authentication of user and provider are explained in fig.1.

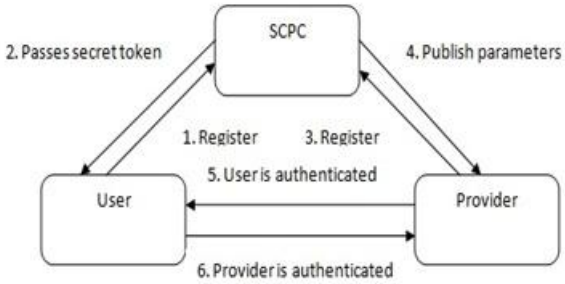

Figure 1: Checking authentication of user and provider

III.1. ADVANTAGES OF SSO

- Users need only one password for access to all applications and systems.
- Users can access the corporate network at the start of their workday.
- Users have immediately have access to all necessary password-protected applications.
- Users don't need to remember multiple passwords.
- Users don’t have to write down their passwords.
- Users don't have to guess passwords, which potentially expose applications to unauthorized users.

For example, Google Accounts allows a user to sign on to different services provided by Google using the same username/password pair. Another famous example is RSA SecurID [14], which a two factor authentication solution based on a OTP token and classical username/password credentials, allowing a user to sign on to several SecurID enabled services using the same token. However, a recent attack to EMC facilities exposed the overall fragility of this heuristic system. Even though their security was unaffected by current attacks, both solutions still require the user to repeatedly perform the sign on procedure. In most of current transparent single sign-on architectures, the user receives some kind of "authentication ticket" after he successfully signs on to the identity provider. When the user desires to sign on, he sends this ticket to the intended service provider or application, which then verifies it's validity by direct communication with the identity provider. This approach has several drawbacks, such as complex management and the requirement of secure online communication between applications and identity providers, which increases network traffic and processing loads.

IV. METHODOLOGY

In the existing system, different security schemes are proposed by many researchers. In the proposed system, various Client-Server programs are written to implement the project using socket programming in Java. This work uses the multithreading features of Java to run in parallel for different providers. Chang-Lee algorithm is used for user identification phase. But, it is using a less secure DES algorithm. This paper user a more secure AES algorithm to enhance the security features. So, this scheme is more secure than Chang-Lee scheme.

V. CONCLUSION

This paper proposes a secure single sign-on mechanism based on one-way hash functions and random nonces to solve the weaknesses described above and to decrease the overhead of the system. Encryption and Decryption of data sent between user and provider can improve security of communication. Encryption and Decryption process can be done using a more secure algorithm, ie, AES Encryption. AES is strong enough to be certified for use by the US govt. for top secret information. AES is federal information processing standard and there are currently no known non-brute-force attacks against AES. Thus AES is given priority than other standards when security is taken into consideration. By using this sso scheme, users need only one password for secure access to all applications and systems and would lock out the hackers entering into the system. But there are some vulnerability problems and there should be a good password, one that is very hard to crack.

This paper proposes further research into more efficient enhancements for security of single sign on for distributed computer networks. For third-party sites, credential generation and synced, cloud-based storage can be provided. Auto login, Smart cards, Biometrics are other methods to enhance security for single sign on mechanism for distributed computer networks.

REFERENCES

[1]. Weaver and M. W. Condtry, "*Distributing Internet services to the network's edge*", *IEEE Trans. Ind. Electron.*, 50(3): 404-411, Jun. 2003.
[2]. L. Barolli and F. Xhafa, "*JXTA-OVERLAY: A P2P platform for distributed, collaborative and ubiquitous computing*", *IEEE Trans. Ind.Electron*., *58(6):* 2163-2172, Oct. 2010.
[3]. L. Lamport, "*Password authentication with insecure communication"*,*Commun. ACM, 24(11*): 770-772, Nov. 1981.
[4]. Chin-Chen Chang, "*A secure single mechanism for distributed computer networks*," *IEEE Trans. On Industrial Electronics* ,*vol. 59, no. 1,* Jan 2012.
[5]. W. B. Lee and C. C. Chang, "*User identification and key distribution maintaining anonymity for distributed computer networks*," Computer Systems Science and Engineering, *15(4*): 113-116, 2000.
[6]. W. Juang, S. Chen, and H. Liaw, *Robust and efficient password authenticated key agreement using smart cards*, *IEEE Trans. Ind. Electron*.,*15(6):* 2551-2556, Jun. 2008.
[7]. X. Li, W. Qiu, D. Zheng, K. Chen, and J. Li, "*Anonymity enhancement on robust and efficient password-authenticated key agreement using smart cards*," *IEEE Trans. Ind. Electron., 57(2):* 793-800, Feb. 2010.
[8]. T.-S. Wu and C.-L. Hsu, "*Efficient user identification scheme with key distribution preserving anonymity for distributed computer networks,"* Computers and Security, *23(2*): 120-125, 2004.
[9]. Y. Yang, S. Wang, F. Bao, J. Wang, and R. H. Deng, *"New efficient user identification and key distribution scheme providing enhanced security,"* Computers and Security, *23(8):* 697-704, 2004.
[10]. K. V. Mangipudi and R. S. Katti, "*A secure identification and key agreement protocol with user anonymity (sika),"* Computers and Security, *25(6):* 420-425, 2006.
[11]. C.-L. Hsu and Y.-H. Chuang, *"A novel user identification scheme with key distribution preserving user anonymity for distributed computer networks*," Inf. Sci., *179(4):* 422-429, 2009.
[12]. Data Encryption Standard, NIST Std. FIPS PUB 46-2, 1988.
[13]. Advanced Encryption Standard, NIST Std. FIPS PUB 197, 2001.
[14]. W. Stallings, *Cryptography and Network Security*, 4th ed. Upper Saddle River, NJ: Pearson, Nov. 2005, pp. 334–340.

International Journal of Modern Engineering Research (IJMER)
www.ijmer.com Vol. 3, Issue. 3, May - June 2013 pp-1815-1816 ISSN: 2249-6645

Nucleus Equals Center in Assosymmetric Rings

K. Jayalakshmi[1], K. Madhavi Devi[2]
Sr. Asst. Prof in Mathematics, J. N. T. University, Anantapur College of Engg, J.N.T.University. Anantapur, Anantapur. (A.P.) INDIA.

ABSTRACT: *Suppose R is a prime assosymmetric not associative ring with idempotent e and [R, R] ⊆ N then either R is associative or N = Z and e is the identity element of R if and only if e ∈ N = Z. 2010 MATHEMATICS SUBJECT CLASSIFICATION: 17A99*

KEYWORDS: *Prime ring, assosymetric ring, nucleus, center.*

I. INTRODUCTION

Kleinfeld [2] defined a class of nonassociative ring in which the associative law of multiplication has been weaked to the condition that $(P(x), P(y), P(z)) = (x, y, z)$ … (1)
for every permutation P of x, y and z. These rings are neither flexible nor power associative. But the associator and the commutator are in the nucleus of the ring. Suvarna and Jayalakshmi [3] have proved that prime assosymmetric ring is either associative or nucleus equals center. Using the results of Kleinfeld, Suvarna and Jayalakshmi we investigate the properties and the structures of prime assosymmetric rings and show that if R is prime and not assocative with an idemponent e and commutator contained in the nucleus than e is the identity element of R if and only if $e \in N = Z$. Throughout this section R represents a nonassociative assosymmetric ring. We have nucleus $N = \{n \in R / (n, R, R) = 0 = (R, n, R) = (R, R, n)\}$ and the center $C = \{c \in R / [c, R] = 0\}$. A ring is said to be prime if for any two ideals A, B such that $AB = 0$ implies either $A = 0$ or $B = 0$.

II. MAIN SECTION

Lemma 1: Suppose R has a peirce decomposition with respect to an idempotent e. Then the submodules R_{ij}, $i, j = 0, 1$ satisfy the following
(i) $R_{ii} R_{ii} \subseteq R_{ii} + R_{ji}$ $i \neq j$.
(ii) $R_{ij} R_{ji} \subseteq R_{ii} + R_{ij} + R_{ji}$, $i \neq j$.
(iii) $R_{ij} R_{ij} \subseteq R_{ij}$, $i \neq j$.
(iv) $R_{ii} R_{jj} \subseteq R_{ii} + R_{jj}$, $i \neq j$.
Proof: To prove (i) let $x_{11}, y_{11} \in R_{11}$ then using $(ex_{11} = x_{11}e = x_{11})$ we have $e(x_{11} y_{11}) = -(e, x_{11}y_{11}) + (e\, x_{11})y_{11} = -(y_{11}, x_{11}, e) + x_{11}y_{11} = -(y_{11}\, x_{11})e + y_{11}\, x_{11} + x_{11}\, y_{11}$.
Thus $e(x_{11}\, y_{11}) + (\, y_{11}\, x_{11})e = x_{11}\, y_{11} + y_{11}\, x_{11}$. … (2)
Assume that $x_{11}\, y_{11} = r_{11} + r_{10} + r_{01} + r_{00}$, $y_{11}\, x_{11} = s_{11} + s_{10} + s_{01} + s_{00}$ for $r_{ij}, s_{ij} \in R_{ij}$, then the identity (2) given $r_{11} + r_{10} + s_{11} + s_{10} = r_{11} + r_{10} + r_{01} + r_{00} + s_{11} + s_{10} + s_{01} + s_{00}$. Therefore $r_{00} = -s_{00}$, $r_{01} = 0 = s_{10}$ ($R_{ij} = 0 = R_{ji}$).Similarly by symmetry we obtain $r_{10} = 0 = s_{01}$ that is $x_{11}\, y_{11} = r_{11} + r_{00}, y_{11}\, x_{11} = s_{11} - r_{00}$. Hence $r_{11}r_{11} \subseteq r_{11} + r_{00}$.We see that $r_{10} + r_{01} \subseteq r_{11} + r_{10} + r_{01}$ if $x_{10} \in r_{10}, y_{01} \in r_{01}$.
To prove (ii) and hence $e(x_{10}\, y_{01}) = -(e, x_{10}, y_{01}) + (e, x_{10})\, y_{01} = -(y_{01}, x_{10}, e) + x_{10}y_{01} = -(y_{01}x_{10})e + y_{01}x_{10} + x_{10}y_{01}$.Thus $e(x_{10}y_{01}) + (\, y_{01}x_{10})e = y_{01}x_{10} + x_{10}y_{01}$.That is $e(x_{10}y_{01}) + (\, y_{01}x_{10})e = x_{10}y_{01} + y_{01}x_{10}$.Thus $x_{10}y_{01} = r_{11} + r_{10} + r_{01} + r_{00}$ we have $y_{01}x_{10} = s_{11} + s_{10} + s_{01} + s_{00}$ for $R_{ij}, s_{ij}, \in R_{ij}$. Hence again from (2) we get $r_{11} + r_{10} + s_{11} + s_{10} = r_{11} + r_{10} + r_{01} + r_{00} + s_{11} + s_{10} + s_{01} + s_{00}$. Therefore $r_{11} = -s_{11}$, $r_{00} = 0 = s_{00}$. Now consider $x_{10}\, y_{01} = r_{11} + r_{10} + r_{01}$ and $y_{01}x_{10} = -r_{11} + s_{10} + s_{01}$.We see that $R_{10}R_{01} \subseteq R_{11} + R_{10} + R_{01}$.
Consider $x_{10} \in R_{10,}\, y_{10} \in R_{10}$. Then $e(x_{10}\, y_{10}) = -(e, x_{10}, y_{10}) + (ex_{10})y_{10} = -(y_{10}, x_{10}, e) + x_{10}y_{10} = -(y_{10}x_{10})e + y_{10}x_{10} + x_{10}y_{10}$. Also $e(x_{10}y_{01}) + (y_{10}x_{10})e = y_{10}x_{10} + x_{10}y_{10}$, $e(x_{10}y_{10}) + (y_{10}x_{10})e = x_{10}y_{10} + y_{10}x_{10}$. We see that$x_{10}y_{10} = r_{11} + r_{10} + r_{01} + r_{00}$ and $y_{10}x_{10} = s_{11} + s_{10} + s_{01} + s_{00}$ for $r_{ij}, s_{ij} \in R_{ij}$. Hence from (2) $r_{11} + r_{10} + s_{11} + s_{01} = r_{11} + r_{10} + r_{01} + r_{00} + s_{11} + s_{10} + s_{01} + s_{00}$ and $r_{10} = -s_{01}, r_{11} = 0 = s_{11}$, $r_{00} = 0 = s_{00}$. But $x_{10}y_{10} = r_{01} + r_{00}y_{10}\, x_{10} = s_{01} - r_{10}$. Hence obtain $R_{10}R_{10} \subseteq R_{10} + R_{01}$ i.e, $R_{ij}R_{ij} \subseteq R_{ij} + R_{ji}$.
To prove (iv) considering $R_{11}R_{00} = R_{00}R_{11} \subseteq R_{11} + R_{00}$ and $x_{11} \in R_{11}, y_{00} \in R_{00}$ we have
$e(x_{11}y_{00}) = -(e, x_{11}, y_{00}) + (ex_{11})y_{00} = -(y_{00}, x_{11}, e) + x_{11}y_{00} = -(y_{00}x_{11})e + y_{00}x_{11} + x_{11}y_{00}$. Hence $e(x_{11}y_{00}) + (\, y_{00}x_{11})e = y_{00}x_{11} + x_{11}y_{00}$. That is $e(x_{11}y_{00}) + (\, y_{00}x_{11})e = x_{11}y_{00} + y_{00}x_{11}$. So $x_{11}y_{00} = r_{11} + r_{10} + r_{01} + r_{00}$ and $y_{00}x_{11} = s_{11} + s_{10} + s_{01} + s_{00}$ for $r_{ij}, s_{ij}, \in R_{ij}$. Also from (2) we see that $r_{11} + r_{10} + s_{11} + s_{01} = r_{11} + r_{10} + r_{01} + r_{00} + s_{11} + s_{10} + s_{01} + s_{00}$. Therefore $r_{00} = -s_{00}$, $r_{01} = 0 = s_{10}$, $r_{10} = 0 = s_{01}$. Thus $x_{11}y_{00} = r_{11} + r_{00}$ and $y_{10}x_{11} = s_{00} - r_{00}$. Hence we have $R_{11}R_{00} \subseteq R_{11} + R_{00.}$ ♦
Lemma 2: Suppose R has an idempotent e such that $(e, e, R) = (0) = (e, R, e)$. If R has the property $[R, R] \subseteq N$ then R has a peirce decomposition and R_{ij} satisfy
(i) $R_{ij} R_{ij} \subseteq R_{ii} + R_{jj}$ $i \neq j$
(ii) $R_{ii} R_{ji} = (0) = R_{ij}R_{ii}$ $i \neq j$
(iii) $R_{ij} R_{ij} \subseteq R_{ij}$ $i \neq j$
(iv) $R_{ij} R_{jj} \subseteq R_{ii} + R_{jj}$ $i \neq j$
Proof: To prove (i) let $x_{11} \in R_{11}, x_{00} \in R_{00}$

Since $x_{11} = [e, x_{11}] \in N$ and $x_{00} = [x_{00}, e] \in N$ we have $0 = (x_{11}, y_{00}, e) = (x_{11}y_{00})e - x_{11}y_{00}$ and $0 = (e, y_{00}, x_{11}) = -e(y_{00}x_{11})$. Or $(x_{11}y_{00})e = x_{11}y_{00}$ and $e(y_{00}x_{11}) = 0$. Similarly $e(x_{11}y_{00}) = x_{11}y_{00}$ and $(y_{00}x_{11})e = 0$. But $e(x_{11}y_{00}) = -(e, x_{11}, y_{00}) + (ex_{11})y_{00} = -(y_{00}, x_{11}e) + x_{11}y_{00} = -(y_{00}x_{11})e + y_{00}x_{11} + x_{11}y_{00}$. Hence $e(x_{11}y_{00}) + (y_{00}x_{11})e = y_{00}x_{11} + x_{11}y_{00}$. That is $x_{11}y_{00} + 0 = x_{11}y_{00} + y_{00}x_{11}$. There fore we obtain $y_{00}x_{11} = 0$. Hence we see that $R_{11}R_{11} \subseteq R_{11} + R_{00}$

To prove (ii) consider $R_{11}R_{01} = (0) = R_{10}R_{11}$. Let $x_{11} \in R_{11}$ and $x_{01} \in R_{01}$. Now $x_{11} = [e, x_{11}] \in N$ and $x_{01} = [x_{01}, e] \in N$. Thus $0 = (x_{11}, y_{01}, e) = (x_{11}y_{01})e - x_{11}y_{01}$ and $0 = (e, y_{01}, x_{11}) = -e(y_{01}x_{11})$. Or $(x_{11}y_{01})e = x_{11}y_{01}$ and $e(y_{01}x_{11}) = 0$. Similarly $e(x_{11}y_{01}) = x_{11}y_{01}$ and $(y_{01}x_{11})e = 0$. That is $e(x_{11}y_{01}) = -(e, x_{11}, y_{01}) + (ex_{11})y_{01} = -(y_{01}, x_{11}e) + x_{11}y_{01} = -(y_{01}x_{11})e + y_{01}x_{11} + x_{11}y_{01}$. Thus $e(x_{11}y_{01}) = 0 + y_{01}x_{11} + x_{11}y_{01}$ which is nothing but $x_{11}y_{01} = y_{01}x_{11} + x_{11}y_{01}$

$x_{11}y_{01} = 0$. That is $R_{11}R_{01} = 0$. ...(3)

Now let $x_{10} \in R_{10}$, $x_{11} \in R_{11}$ and $x_{10} = [e, x_{10}] \in N$ and $x_{11} = [x_{11}, e] \in N$. Then we have $0 = (x_{10}, y_{11}, e) = (x_{10}y_{11})e - x_{10}y_{11} = (e, y_{11}, x_{10}) = -e(y_{11}x_{10})$. Or $(x_{10}y_{11})e = x_{10}y_{11}$ and $e(y_{11}x_{10}) = 0$. Similarly $e(x_{10}y_{11}) = x_{10}y_{11}$ and $(y_{11}x_{10})e = 0$.That is $e(x_{10}y_{11}) = -(e, x_{10}, y_{11}) + (ex_{10})y_{11} = -(y_{11}, x_{10}, e) + x_{10}y_{11} = -(y_{11}x_{10})e + y_{11}x_{10} + x_{10}y_{11}$. Hence $x_{10}y_{11} = -0 + y_{11}x_{10} + x_{10}y_{11}$ that is $y_{11}x_{10} = 0$ which is nothing but $R_{11}R_{10} = (0)$ … (4)

From (3) & (4) $R_{11}R_{01} = (0) = R_{11}R_{10}$. That is $R_{ii}R_{ji} = (0) = R_{ii}R_{ij}$.

To prove (iii) consider $R_{10}R_{10} \subseteq R_{10}$ and let $x_{10} \in R_{10}$, $x_{10} \in R_{10}$, $x_{10} = [e, x_{10}] \in N$ and $x_{10} = [x_{10}, e] \in N$. Then we have $0 = (x_{10}, y_{10}, e) = (x_{10}y_{10})e - x_{10}y_{10}$ and $0 = (e, y_{10}, x_{10}) = -e(y_{10}x_{10})$. Or $(x_{10}y_{10})e = x_{10}y_{10}$ and $e(y_{10}x_{10}) = 0$. Similarly $e(x_{10}y_{10}) = x_{10}y_{10}$ and $(y_{10}x_{10})e = 0$. So $e(x_{10}y_{11}) = -(y_{10}x_{10})e + y_{10}x_{10} + x_{10}y_{10}$.That is $x_{10}y_{10} = -0 + y_{10}x_{10} + x_{10}y_{10}$. Hence $y_{10}x_{10} = 0$. That is $R_{10}R_{10} \subseteq R_{10}$ which shows that $R_{ij} \subseteq R_{ij}$.

Now to prove (iv) we shall consider $R_{11}R_{00} \subseteq R_{11} + R_{00}$ and $x_{11} \in R_{11}$, $x_{00} \in R_{00}$.

Since $x_{11} = [ex_{11}] \in N$ and $x_{00} = [x_{00}e] \in N$ we have $0 = (x_{11}, y_{00}e) = (x_{11}y_{00})e - x_{11}y_{00}$ and $0 = (ey_{00}, x_{11}) = -e(y_{00}x_{11})$. Or $(x_{11}y_{00})e = x_{11}y_{00}$ and $(y_{00}x_{11})e = 0$. Similarly $e(x_{11}y_{00}) = x_{11}y_{00}$ and $(y_{00}x_{11})e = 0$. $e(x_{11}y_{00}) = -(y_{00}x_{11})e + y_{00}x_{11} + x_{11}y_{00}$. That is $x_{11}y_{00} = 0 + y_{00}x_{11} + x_{11}y_{00}$. Hence $x_{11}y_{00} = 0$ which is nothing but $R_{ii}R_{jj} \subseteq R_{ii} + R_{jj}$. ♦

Theorem 1: Let R be a prime ring with an idempotent e. If R is not associative then e is the identity element of R if and only if $e \in N$.

Proof: Assume that $e \in N$ so $e \in Z$. Consider the peirce decomposition $R = R11 + R10 + R01 + R00$ of R with respect to e. Since $R10 = eR_{10} = R_{10}e = (0)$. We have $R = R_{01}e = eR_{01}$ (0) and $R = R_{11} + R_{00}$. Also $e \in N$ implies that R_{11} and R_{00} are ideals of R. And also since R is prime, $e \in R_{11}$ implies that $R_{00} = (0)$. Thus $R = R_{11}$ and e is the identity element of R. Conversely, let e be the idempotent element, then $ex = xe = x$ and see we have $(e, x, y) = (ex)y - e(xy) = xy - xy = 0$. That is $(e, x, y) = 0$ implies $e \in N$. ♦

A careful inspection of the Lemma 2 and Theorem 1 in [3] shows that $[R, N]$ can be replaced to by the weak condition $[R, R]$ contained in the nucleus thus we have the following theorem

Theorem 2: Let R be a prime ring such that $[R, R] \subseteq N$ Then either R is associative or $N = Z$. ♦

From Lemma 1 and Lemma 2, Theorem 1 and Theorem 2 we obtain the mainTheorem

Main Theorem 3: If R is prime not associative with an idempotent e and $[R, R] \subseteq N$ then e is the identity element of R if and only if $e \in N = Z$.

REFERENCES

[1]. Boers.A.H, "On assosymmetric rings" Indag, Maths N.S. vol – 5 No. 1 (1994) pp. 9–27.
[2]. Kleinfeld.E, "Assosymmetric rings", proc. Amer maths soc; vol – 8 (1957) pp 983 – 986.
[3]. Suvarna.K & Jayalakshmi.K, "On the nucleus of prime assosymmetric ring" J. Pure & Appl.phys, vol – 22, No – 1 Jan – Mar 2010, pp 81–83.

International Journal of Modern Engineering Research (IJMER)
www.ijmer.com Vol. 3, Issue. 3, May - June 2013 pp-1817-1824 ISSN: 2249-6645

Study of Floating Body Effect in SOI Technology

Vandana B.
(M.Tech, Member IEEE), Electronic Engineering, Citd, Hyderabad, India

ABSTRACT: *The paper presents the floating body effects of PD/FD of SOI technology and also discusses the issues behind the effects, gives the clear description of factors effecting floating body such as threshold voltage, drain current, gate-to-body tunneling kink effect. And also shows the merits/demerits of PDSOI/FDSOI.*
KEY WORDS: *FDSOI, PDSOI, Floating body effect, Kink effect*

I. INTRODUCTION

Silicon on Insulator is a semiconductor electronic device which is now used as an integrated chip in almost all highly reliable/efficient in digital/analog electronic devices. Before the use of SOI in market BULK technology was leading technology in electronic industry, due to following reasons such as latch up, parasitic capacitance and leakage currents in bulk technology fail to continue in developing highly effective devices. The design rules which help in developing SOI technology was extracted from bulk technology by incorporating oxide layer over the silicon substrate, 50% of the problem was solved such as leakage currents, eliminating wells, scaling of the device effect threshold voltage is reduced and latch up problem. SOI, new device architectures allow optimum electrical properties to be obtained for low power and high performance circuits. In SOI an interesting observation is that the body terminal is either tied to gate or left free for floating called as "floating body" as when the floating body is considered it has some important features in reducing power consumption and improving the device efficiency, about these features an important description is shown in upcoming sections and the reasons for the body tied are also shown.

II. ADVANTAGES OF SOI OVER BULK TECHNOLOGY

The description of SOI technology is described briefly in [1]. SOI advantages is given below, according to these advantages it has been given clearly that what factors are superior to bulk technology and is described for each and every advantage.

2.1 SOI Advantages:

The SOI wafer structure has several important advantages over CZ bulk or epitaxial starting wafer architectures. SOI wafers potentially offer "perfect" transistor isolation (lower leakage), tighter transistor packing density (higher transistor count/higher IC function at the same lithographic resolution), reduced parasitic drain capacitance (faster circuit performance and lower power consumption), and simplified processing relative to bulk or epitaxial silicon wafers. Due to these advantages, SOI wafers appear ideal for leading edge integrated circuits with high speed, high transistor count, low voltage/low power operation, and battery operated systems requirements, such as portable logic or microprocessor ICs.
Silicon-on-insulator (SOI) wafers have traditionally been used for extreme environmental applications, such as high temperature and severe environments (e.g., outer space). However, they are expected to expand into mainstream CMOS applications due to these advantages:

- Excellent lateral and vertical isolation of active devices from substrate:

1. Elimination of inter-device leakage and latch-up in CMOS structures
2. Effective reduction of substrate coupling in RF circuits (allows higher quality inductors with increased Q factor)
3. Effective reduction of interference and cross-talk between devices in mixed-signal ICs
4. Reduced soft errors (e.g., in SRAM) from radiation effects (electron hole pair generation)
5. Different voltages may be used on different devices without the added processing steps required for triple wells.

- Faster device operation (speed/power product) due to reduction of parasitic capacitance (primarily due to reduced source-drain junction capacitance, but also from gate-to-substrate capacitance and metal-to-substrate capacitance):

1. IBM reported a 20% to 35% increase in chip speed for their PowerPC chips [2, 3]

- Lower power consumption (speed/power product) due to lower operating voltages on devices and lower parasitic capacitance:

1. IBM reported a 35% to 70% reduction in power consumption for their PowerPC chips
2. More functions per die area or reduced die area per function; SOI allows tighter layout design rules (higher integration density), mainly due to reduced STI layout area required for lateral junction isolation (resulting from the absence of wells and the possibility of direct contact of the source-drain diodes in the NMOS and PMOS transistors) [2, 3, 4]
3. Performance improvement equivalent to next technology node without scaling (e.g., performance of 0.25 micron devices on SOI wafers equivalent to performance of 0.18 micron devices on bulk wafers)
4. Potential to simplify device fabrication steps:
5. Fewer masks and ion implantation steps, made possible by the elimination of well and field isolation implants
6. Less complex (costly) lithography and etching required to achieve next-generation performance
7. As noted above, SOI wafers offer the potential to simplify the process presently used for CMOS devices fabricated in bulk wafers. The process used for deep submicron

- CMOS on bulk wafers may be described in the following (highly simplified) way:

1. Formation of shallow trench isolation (STI) regions, which surround and define the active areas where transistors will be fabricated
2. Formation of deep n-type and p-type wells in the active areas, using high energy ion implantation; these wells are vertically "profiled" using multiple ion implantation steps to achieve:

2a) A deep doping peak (the "deep well"), which suppresses latch-up, reduces soft errors (caused by charge pairs generated from radiation effects), and which provides part of the ESD protection path NOTE: if a deeper "triple well" (which is typically a deep n-well structure beneath and around a shallower p-well) is used for voltage isolation from substrate, it is formed just prior to formation of these n-type and p-type "twin wells"
2b) A shallower doping peak (the "field channel stop"), located just below the STI trench bottom, which suppresses lateral leakage between adjacent transistors within the wells (intra-well) and between adjacent transistors at the well boundaries (inter-well)
2c) A very shallow doping peak at the silicon surface (the "$V_t$adjust"), which sets the threshold voltage of the transistors

3. Formation of the gate stack, including the gate oxide insulator and the Poly silicon gate on top of it (the poly silicon gate is highly doped, n-type for the n-channel transistors and p-type for the p-channel transistor); the gate electrode is subsequently defined by lithography and anisotropic etching.
4. Formation of the transistor body and contacts, including:

4a) Formation of source-drain extensions using ultra-low energy ion implantation (which is self aligned to the gate electrode) and rapid thermal annealing (RTA)
4b) Formation of halo (punch-through stop) regions by self-aligned, high tilt implantation (and RTA)
4c) Following the formation of a sidewall space on the gate, formation of source-drain contact regions by high dose, low energy implantation (and RTA)
4d) Formation of salicide (Self-Aligned siLICIDE) contact metal on the top of the gate and source-drain regions. [8]

The opportunity for fabrication process simplification mainly occurs in step 2 (specifically 2a and 2b), above. The use of SOI wafers eliminates the need for the high-energy ion implantation processes that form the deep n-type and p-type "twin" wells (step 2a) and field channel stop isolation regions (step 2b), which are presently required in leading edge bulk CMOS IC fabrication. Also, the formation of deep "triple well" structures using high energy ion implantation processes (see note in step 2a, above) is unnecessary with SOI wafers to achieve voltage (electrical) isolation from the substrate. Note that the ion implantation and RTA processes for the formation of transistors, e.g., extension and contact source/drain formation (steps 4a and 4c), poly-silicon gate doping (in step 3), and threshold voltage adjustment (step 2c) are still required with SOI wafers.

III. FD/PD SOI

SOI (silicon on insulator) which means silicon device is fabricated on insulator using silicon dioxide, it is fabricated as three layered device such as the bottom most layer is the substrate which is lightly doped. The insulating layer is created by flowing oxygen onto a plain silicon wafer and then heating the wafer to oxidize the silicon, thereby creating a uniform buried layer of silicon dioxide which is called as buried oxide layer (BOX). The insulating layer increases device performance by reducing junction capacitance as the junction is isolated from bulk silicon. The decrease in junction capacitance also reduces overall power consumption. And the top most layer is same as bulk CMOS which help in channel creation. SOI is also a 4 terminal device source, drain, gate and the body; here source and drain terminals are interchange. The width of the silicon film decides whether the SOI is fully depleted or partially depleted fig 1(b). If the width of silicon film laid over the buried oxide is thin then the device is said to be fully depleted and if the width of the silicon film is thick then it is said to be partially depleted fig 1(a). Silicon on Insulator fabrication process helps in achieving greater performance and offers less power consumption as compared to bulk CMOS process.

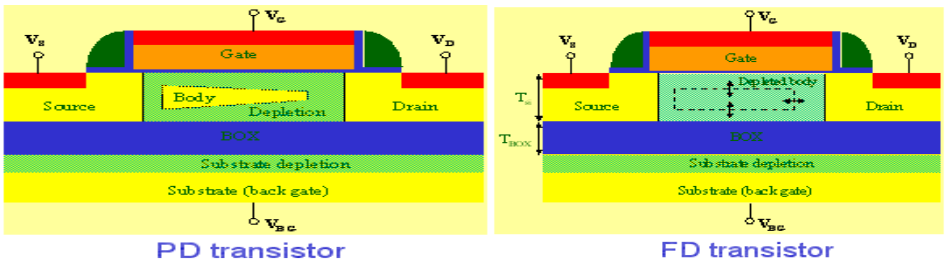

(a) (b)

Figure 1 1(a) PD SOI, 1(b) FD SOI transistor

The FD devices have several advantages compared to the PD devices; however, there are some drawbacks also. These are some of the tradeoffs in use of the FD versus PD SOI
MOSFETs:

- Fully-depleted SOI devices are naturally free from kink effect, because the majority carriers can penetrate more easily into the source; thus, preventing the excess carriers accumulation [7].

- FD SOI has an enhanced sub-threshold swing, S (see Figure 4). For the bulk and PD devices, 1/S = 85 to 90 mV/decade, and for FD SOI, 1/S = 65 to 70 mV/decade, which is close to an ideal characteristic of a MOS transistor at room temperature (1/S = 60 mV/decade) [10].
- Fully-depleted SOI devices have the highest gains in circuit speed, reduced power requirements and highest level of soft-error immunity [9]. FD devices operate faster because of a sharper sub-threshold slope, and a reduced threshold voltage that allows for faster switching of the MOS transistors. These transistors also have increased drive currents at relatively low voltages.
- Several drawbacks of the FD SOI design and process come along with their benefits:
- Although FD MOSFETS are naturally free from the kink effect, the interface coupling effect affects their operation [7, 5]. The interface coupling is inherent to fully depleted SOI devices, where all parameters (threshold voltage, trans-conductance, interface-trap response etc.) of one channel are insidiously affected by the opposite gate voltage (at the buried oxide).

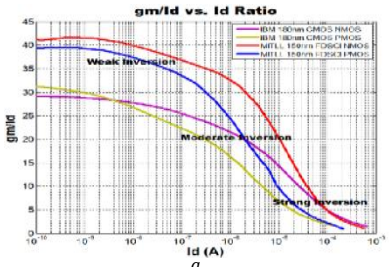

Figure 2 $\frac{g_m}{I_d}$vs$I_d$ratio

- While FD SOI MOSFETs offer a reduced body effect and a nearly ideal gm/Id ratio when biased in the weak or moderate inversion region, a weak (not fully eliminated) current voltage kink still exists in the strong inversion region. Therefore, additional technology optimization is required to use these transistors for baseband analog applications [12]. Besides, accumulation at the back interface can lower the breakdown voltage and introduce the kink effect.
- The threshold voltage fluctuation due to SOI thickness variation is one of the most serious problems in FD SOI MOSFETs. In comparison, partially depleted SOI devices are built on a thicker silicon layer and are simpler to manufacture.
- Most design features for developing PD devices can be imported from the bulk silicon devices and used in the SOI environment with only modest changes. This makes circuit redesign for the PD devices simpler than for the FD microcircuits.

IV. SOI MOSFET TRANSISTORS

The major difference between a bulk-Si MOS transistor and a SOI MOS transistor from the circuit designer point of view is that the later has smaller junction capacitance and has a floating body [16]. These effects include parasitic bipolar current, self-heating and body contact resistance, some other effects and characteristics associated with SOI MOSFETs:

IV.1 Threshold Voltage: For a thick-film SOI device, which essentially behaves like a bulk device due to absence of interaction between the front and back depletion regions, the threshold voltage is same as in a bulk device and is given as:

$$V_{th} = V_{FB} + 2\varphi_F + \frac{qN_a x_{dmax}}{C_{ox}} \quad (1)$$

For a thin-film SOI device, the expressions for threshold voltage as a function of the different possible steady-state charge conditions at the back interface are given as [16]: the below equations shows the threshold voltage equation in three operating regions

$$V_{th1,inv2} = \phi_{ms} - \frac{Q_{ox1}}{C_{ox1}} + 2\phi_F - \frac{Q_{depl}}{2Cox_1} \quad (2)$$

$$V_{th1,depl} = V_{th1,acc2} - \frac{C_{si}C_{ox2}}{C_{ox1}(C_{si}+C_{ox2})}(V_{G2} - V_{G2,acc} \quad (3)$$

$$V_{th1,acc2} = \phi_{MS1} - \frac{Q_{ox1}}{C_{ox1}} + \left(1 + \frac{C_{si}}{C_{ox1}}\right)2\phi_F - \frac{Q_{depl}}{2_{cox1}} \quad (4)$$

IV.2 Body Effect: In a bulk device, the body effect is defined as the dependence of the threshold voltage on the substrate bias. In an SOI transistor, it's similarly defined as the dependence of the threshold voltage on the back-gate bias. In a thick film device, the body effect (or, more aptly back-gate effect) is negligible due to absence of coupling between the front and back gate. In a thin-film fully depleted device, the body effect parameter, is obtained from eqn. (3),

$$\gamma \equiv \frac{\partial V_{th1}}{\partial V_{G2}} = -\frac{C_{si}C_{ox2}}{C_{ox1}(C_{si}+C_{ox2})} \quad (5)$$

It can be seen from eqn. (5) that the threshold voltage dependence on back-gate bias is linear in case of thin-film SOI transistors.

IV.3 Floating-Body Effects: Floating body effect (FBE) is the major parasitic effect in SOI-MOSFETs and is a consequence of the complete isolation of the transistor from the substrate. The effect is related to the built-up of a positive charge in the silicon body of the transistor, originating from the holes created by impact ionization. This charge cannot be removed rapidly enough, primarily because no contact with the Si film (body) is available.

When the drain voltage is large enough, the channel electrons can obtain sufficient energy in the high electric field near the drain and to generate electron hole pairs via the impact ionization mechanism. The generated electrons rapidly flow into the drain, and the holes migrate toward the lowest potential region, i.e., the p-type floating body. Then the holes caused at the lowest potential region will be swept into the source since the source/body diode is forward biased

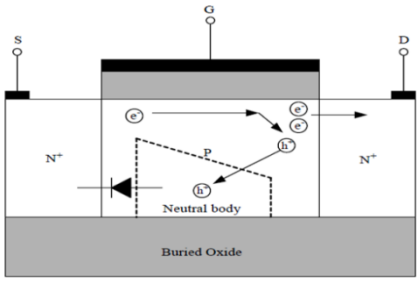

Figure 3 Representing FLOATING body effect in PD SOI

There are various consequences of this built up charge, which are generally referred to as the floating-body effects, such as [5]: kink-effect; negative conductance and trans-conductance; hysteresis and instabilities, single transistor latch (the transistor cannot be turned off by reducing gate voltage), bipolar transistor action, and premature breakdown. The FBE can lead to circuit instabilities, frequency-dependent delay time, and pulse stretching. Many of the negative consequences of the FBE could be eliminated by using a body contact for every MOSFET, but this is generally not an optimum solution. It should be noted that these typical SOI effects can be observed even in the bulk-Si MOSFETs at low temperatures when the substrate becomes semi-insulating and if the substrate contact is left floating.

Considering the MOS portion of the partially-depleted SOI NMOS device, the threshold voltage is subject to the floating body effect. The accumulated holes near the body-emitter junction in the thin-film due to the parasitic bipolar device caused by the floating body increase the body-emitter voltage (V_{BE}). As a result, the threshold voltage is lowered. Considering this effect, the threshold voltage model (V_T) and the conducting current through the front channel (I_{CH}) under the front gate oxide have been reported in [5]. In this subsection, the current conduction mechanisms for the MOS portion and the parasitic bipolar portion of the partially-depleted SOI NMOS device have been explained. In the next subsection, the temperature-dependent kink effect model is derived for the device biased in the triode region ($V_{DS}\_V_{DSAT}$) and the saturation region
($V_{DS} > V_{DSAT}$)

1) Triode Region $\boldsymbol{V_{DS}\_V_{DSAT}}$***:*** Fig. (4,6) shows the current conduction mechanism of the partially-depleted SOI NMOS device biased in the triode region. In the front channel region near the drain, there is no impact ionization. Therefore, no holes are injected into the floating body. As a result, the body-emitter voltage (V_{BE}) is small.
Consequently, the parasitic bipolar device does not turn on. Under this situation, the floating body can be regarded as two diodes connected back to back. At the body-emitter junction, which is forward biased, the conducting current isI_F. At the body-collector junction, which is reverse biased, the conducting current isI_R. Considering the impact ionization effect at the body-collector junction, the conducting current mis magnified by a factor of MB—the conducting current becomes MBIR. Considering the current conduction of the parasitic bipolar device (I_F = MBIR), from [5-7], the body-emitter voltage can be obtained

$$V_{BE} = \frac{2kT}{q}\ln\left[\frac{-I_{reco} + \sqrt{I_{reco}^2 + 4I_{ES}M_B(I_{gen} + I_{diff})}}{2I_{ES}}\right] \qquad (6)$$

2) Saturation Region $\boldsymbol{V_{DS>}V_{DSAT}}$***:*** For the partially-depleted SOI NMOS device biased in the saturation region, the current conduction mechanism is shown in Fig. (6,4). In this region, due to$V_{DS>}V_{DSAT}$, the impact ionization in the front channel region near the drain is important. As a result, a large amount of holes due to the front channel impact ionization are injected into the floating body.[11,13,14]
Consequently, the accumulated holes near the body-emitter junction turn on the bottom parasitic bipolar device since the body-emitter voltage V_{BE} becomes large. From [5], in the saturation region, V_{BE} can be expressed as

$$V_{BE} = V_{BE1} + V_{BE2} - (V_{BE1} + V_{BE2})^{1/m} \qquad (7)$$

Where V_{BE1} is the V_{BE} when recombination current dominates the parasitic bipolar device; V_{BE2} is the V_{BE} when diffusion current dominates the parasitic bipolar device. Based on the above analysis as shown in Fig. 1(a) and (b), the drain current of the partially depleted, SOI NMOS device is composed of the front channel current in the front MOS portion and the collector current in the bottom parasitic bipolar device. The above formulas are the closed-form analytical temperature-dependent kink effect model for the partially-depleted SOI NMOS device.

(In order to estimate the Floating body voltage, especially its transient characteristics in PD-SOI circuits, we consider physics-based models consisting of the body capacitance associated with the body region and various current components. The equivalent circuit representation of the PD-SOI NMOSFET is shown in Fig. 1. The transient Floating body (node \B") potential V_B(t) can be determined from the net current and the time-varying body capacitance as follows:

$$\frac{dQ_B(t)}{dt} - I_{ii}(t) - I_{diode}(t) + I_h(t) = 0, C_B(t) = C_{of} \| C_{ch}(t) + C_{js}(t) + C_{jd}(t) + C_{ob}, \qquad (8)$$

where I_{ii}(t), I_{diode} (t), and I_h(t) represent the impact ionization current in the body-drain junction, the net electron current component (i_B(t) and i_C(t)) into floating body region which is the base region of the parasitic npn bipolar transistor, and the out-going hole current from the body-source junction, respectively [15]

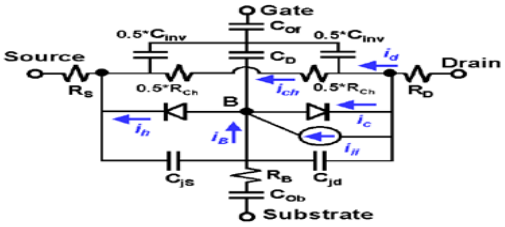

Figure 4 Equivalent circuit and floating body current components for the PD-SOI NMOSFET model.

IV.4 Self Heating Effects: Due to thermal isolation of substrate by the buried insulator in an SOI transistor, removal of excess heat generated by the Joule effect within the device is less efficient than in bulk, which leads to substantial elevation of device temperature. The excess heat mainly diffuses vertically through the buried oxide and laterally through the silicon island into the contacts and metallization. Due to the relatively low thermal conductivity of the buried oxide, the device heats up to 50 to 150C. This increase in device temperature leads to a reduction in mobility and current drive, thus degrading the device performance over a period of time.[5,7]

IV.5 Impact Ionization: The semi-conductor equations that we have used to derive our approximate formulae have explicitly excluded the physical phenomena that lead to the kink effect. To account for the rise in the drain-source current we introduce a simple conceptual model to justify a phenomenological correction term. If we attribute the kink effect entirely to impact ionization effects then we can write $I_{ds} = I_{dso} + I_{Kink}$ with $I_{kink} = MI_{dso}$ whete I_{dso} is the current that would be obtained if impact ionization effects were absent. When impact ionization is present it provides a source of current and the electron current equation has the modified form $\nabla J_n = G_{I-I}$

Where the impact ionization source is usually modeled by $G_{I-I} = -\alpha_n J_n$ with $\alpha n = A_n \exp(-\beta n / F)$ with n α strongly dependent on the electric field strength F [24]. Adopting the assumptions of Jacunski *et al.* [25], but introducing a more accurate approximation, leads to the fitting function.

IV.6 Floating Body and Parasitic Bipolar Effects:

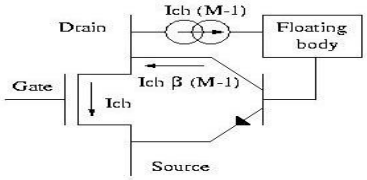

Figure 5: Parasitic bipolar transistor of the SOI MOSFET

The presence of a floating volume of silicon beneath the gate is at the origin of several effects unique to SOI, generically referred to as floating body effects [21]. There exists a parasitic bipolar transistor in the MOS structure. If we consider an n-channel device, the N+ source, the P-type body and the N+ drain indeed form the emitter, the base, and the collector of an NPN bipolar transistor, respectively. In a bulk device, the base of the bipolar transistor is usually grounded by means of a substrate contact. But, due to the floating body in an SOI transistor, the base of the bipolar transistors is electrically floating. This parasitic bipolar transistor (fig.5) is origin of several undesirable effects in SOI devices.
Next, we discuss some important floating body and parasitic bipolar effects in SOI devices.

IV.7 Kink Effect: The kink effect consists into the appearance of a *kink* in the output characteristics of an SOI MOSFET working in strong inversion, as shown in. The kink is very strong in n channel transistors but, is usually absent from p-channel devices.

Let us consider a thick-film, partially depleted SOI n-channel transistor. When the drain voltage is high enough, the channel electrons can acquire sufficient energy in the high electric field zone near the drain to create electron-hole pairs, due to an impact ionization mechanism. The generated electrons move into the channel and the drain, whereas the holes, which are majority carriers in the p-type body, migrate towards the place of lowest potential *i.e.*, the floating body.
The injection of holes into the floating body forward biases the source-body diode. The floating body reaches a positive potential, as given by the following equation [8]:

$$I_{holes,gen} = I_{so}\left[\exp\left[\frac{qV_{BS}}{nKT}\right] - 1\right] \qquad (8)$$

The increase of body potential gives rise to lowering of threshold voltage and source-body potential barrier. More minority carriers are able to flow from source to the channel, thereby causing an excess drain current and producing many more pairs through the avalanche process. This positive feedback results in a sudden increase in I_D or "kink" in output characteristics. If the minority carrier lifetime in the silicon film is high enough, the kink effect can be reinforced by the NPN

bipolar transistor (fig. 5). The "base" hole current is amplified by the bipolar gain, which gives rise to an increased net drain current, sometimes referred to as *second kink* [22].

Now, let us consider the case of a thin-film, fully depleted SOI n-channel MOSFET. It has been shown [23] that the electric field near the drain is lower in the fully depleted device than in partially depleted one. As a result, less electron-hole pair generation takes place in the fully depleted device. Also, contrary to the case of a partially depleted transistor, the source-to-body diode is "already forward biased" due to the full depletion of the film, and therefore, holes can readily combine in the source without having to raise the body potential there. This explains why thin film fully depleted n-channel MOSFETs are free of kink effect. [16, 22, 23]

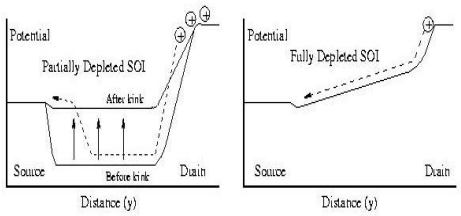

Figure 6: Potential in neutral region from source to drain in PD and FD SOI Devices

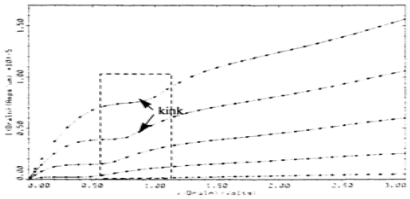

Figure 7 kink effect

The p-channel devices are free of kink effect because coefficient of electron-hole pair generation by energetic holes is much lower than that by energetic electrons. The kink effect is not observed in bulk devices as the majority carriers generated by impact ionization can escape into the substrate or to a well contact. The kink effect can be eliminated from the partially depleted SOI MOSFETs if a body contact is provided for removal of excess majority carriers from the device body. Self heating, bipolar currents and kink effect are said to be the major disadvantages of SOI technology when the body is left floating.

IV.8 Effect of Changes in Back Oxide Thickness on Kink Voltage: The kink voltage is found to have a significant dependence on the thickness of the back oxide in a SELBOX structure. The dependence of kink voltage, on back oxide thickness for a fixed gap length is 0.03 μm. Keeping the gap length constant, if we vary the back oxide thickness we can expect a change in the gap resistance. For the estimation of gap resistance, back oxide thickness is the length of the resistance and the gap length is the width of the gap resistance. As we increase the back oxide thickness keeping the gap length constant, the effective gap resistance increases. This will lead to an increase in the body potential. Consequently, the body potential at which kink occurs will be reached at a lower drain voltage. With reduced oxide thickness, the back oxide gap resistance also reduces and the rise in the body voltage will be reduced. In this case, the body voltage needed to cause the kink will occur at a higher drain voltage and hence the kink voltage will be higher. Therefore, a device with thinner back oxide is more bulk-like and will be less susceptible to kink phenomenon. Even though a very small gap length is required to virtually eliminate kink phenomenon from the device characteristics, producing a small gap length can be technologically challenging [18]. Fabrication of devices with large gap length is likely to be easier. But, with increase in the gap length, the device tends to become more bulk-like and thus lose the associated advantages of SOI such as reduced source-body and drain-body capacitances.

IV.9 Output Characteristics: The expression of the current characteristics I_D (V_{G1} , V_{G2} , V_{DS}) of a thick-film SOI MOS transistor is identical to that of a bulk MOSFET, with some modifications due to the parasitic bipolar effects coming up due to the presence of an electrically floating body.

The derivation of the current characteristics of a thin film, fully depleted SOI device can be done [4] using assumptions of the classical gradual channel approximation [17]. The saturation current in an SOI MOSFET is given as:

$$I_{Dsat} \cong \frac{1}{2}\frac{W}{L}\frac{\mu_n C_{ox\,1}}{(1+\alpha)}(V_{G1} - V_{th})^2 \qquad (9)$$

Where

$\alpha = \frac{C_{si}}{C_{ox\,1}}$ FD device with back interface in accumulation

$\alpha = \frac{C_{si}C_{ox\,2}}{C_{ox\,1}(C_{si}+C_{ox\,2})}$ FD device with back interface in depletion

$\alpha = \frac{\epsilon_{si}}{x_{dmax}\ C_{ox}}$ For bulk and partially depleted devices

Since, a fully depleted SOI < a bulk < a back accumulation SOI, the drain saturation current is highest in the fully depleted device, lower in the bulk device, and even lower in the device with back accumulation. This high saturation current

in a thin-film, fully depleted SOI MOSFETs brings about an increase in current drive, which contributes to excellent speed of fully depleted SOI CMOS circuits

IV.10 Edge Effects : The lateral edges of the SOI MOSFETs represent a parasitic conduction path between the source and the drain. This sidewall transistor operates in parallel with the main transistor, and strong coupling and charge sharing between the front, back, and the edge channels dictate its threshold voltage. Special edgeless devices (e.g. H-gate transistor, which has two p+ body contacts that inhibit any conduction path along the sidewalls may be designed, but this is a space-consuming alternative [7,8].

V. METHODS FOR REDUCING FLOATING BODY EFFECTS

In order to achieve the full potential of SOI technology. it is increasingly important to reduce the floating body effects. Many different schemes have been proposed in the past [19]

V.1 Body contact: Contacting silicon underneath the gate region to the ground effectively suppresses the kink effect as well as the parasitic lateral bipolar effects. Several schemes exist to provide the transistor with body contact. Figure 7a shows the normal body contact. It consists of a *P+* region which is in contact with the P-type silicon underneath the gate. However, in transistors with a large gate width, the presence of single body contact at one end of the channel may not be sufficient to suppress the kink and BJT effects, especially when considering the high resistance of the weakly doped channel region.

The H gate MOSFET design, shown in Figure 7b. Helps to solve this problem, since body contacts are presented at both ends of the channel [19]. However, the efficiency of such a contact scheme depends on channel resistance, which is usually very high in modem processes. In addition, such body contacts occupy a lot of area

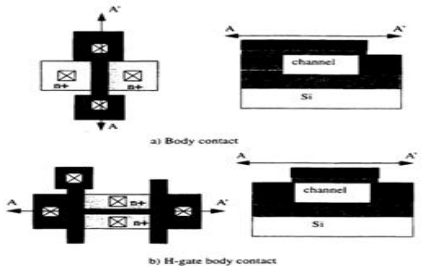

Figure 7 NMOS transistor with body contact

V.2 Source Body Tie Structure: A more compact method, source body tie structure, has been proposed by Omura and Izumi [20]. As illustrated in Figure 1. lOa, the P+ body ties are created on the side of the N+ source diffusion. If the device width is large, additional P+ regions can be formed in the source (such that a P+ N+ P+ N+ structure is introduced). Such a device has the main drawbacks of being asymmetrical (source and drain cannot be switched), and the effective channel width is smaller than the width of the active area. An alternative method involving Schottky contact in source drain region has been proposed by Sleight and Mistry [21] as shown in Figure 8. It provides symmetrical operation. However, increased leakage current associated with Schottky contact degrades device performance.

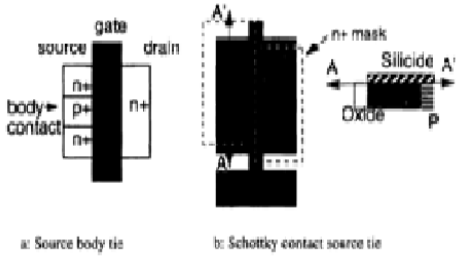

Figure 8 source body tie body contact in SOI structure

The methods discussed above are effective in reducing the floating body effects but have either a limited area of applications or they cannot fully fulfill the advantages of the SOI structure.

VI. CONCLUSION

Finally the paper conclude by presenting brief description about the floating body and the factors that effecting floating body in both partially and fully depleted SOI technology. In FDSOI n-MOSFET has lower leakage current than PDSOI n-MOSFET. The leakage current is inversely proportional to the threshold voltage, channel length and gate oxide thickness. The threshold voltage in PD SOI n-MOSFET is more than that of FDSOI n-MOSFET.

The main drawback in PDSOI n-MOSFET is kink effect, which is eliminated in FDSOI n-MOSFET. A careful trade-off between these two effects must be achieved in order to optimize the circuit performance. The Silicon-On-Insulator (SOI) fabrication process is quickly becoming the answer to the technical challenges facing the integrated circuits (IC) industry.

REFERENCES

[1]. SILICON ON INSULATOR TECHNOLOGY REVIEW Rahul Kr. Singh, Amit Saxena, Mayur Rastogi International Journal Of Engineering Sciences & Emerging Technologies May 2011. ISSN: 2231 – 6604 Volume 1, Issue 1, Pp: 1-16 ©IJESET
[2]. SPECIAL REPORT SOI Wafer Technology For CMOS Ics Robert Simonton President, Simonton Associates
[3]. Www.Chips.Ibm.Com/Bluelogic
[4]. J.P. Colinge, "SILICON-ON-INSULATOR TECHNOLOGY: Materials To VLSI, Second Edition", Kluwer Academic Publishers, 1997, Chapters 4 & 5.
[5]. TEMPERATURE-DEPENDENT KINK EFFECT MODEL FOR PARTIALLY-DEPLETED SOI NMOS DEVICES S. C. Lin And J. B. Kuo
[6]. RELIABILITY EVALUATION OF FULLY DEPLETED SOI (FDSOI) TECHNOLOGY FOR SPACE APPLICATIONS. Ashok K. Sharma NASA/GSFC, Greenbelt, MD Alexander Teverovsky QSS Group,
[7]. S.Crisoloveanu, "ELECTRICAL CHARACTERIZATION OF SOI MATERIALS AND DEVICES", Kluwer Academic Publishers, 1995.
[8]. S.Crisoloveanu, "SOI TECHNOLOGIES, MATERIALS AND DEVICES," 1996 IEEE International SOI Conference, 1996, Pp. 3-12.
[9]. M.I. Current, S.W. Bedell, I.J. Malik, L.M. Feng, F.J. Henley, "WHAT IS THE FUTURE OF SUB-100NM CMOS: ULTRA SHALLOW JUNCTIONS OR ULTRATHIN SOI?", Solid State Technology, V.43, N9, September, 2000
[10]. R. Berger, J. Burns, C-L Chen, C. Chen, M. Fritze, P. Gouker, J. Knecht, A. Soares, V. Suntharalingam, P. Wyatt, D-R Yost, Craig L. Keast, "LOW POWER, HIGH PERFORMANCE, FULLY DEPLETED SOI CMOS TECHNOLOGY", DARPAJMTO AME Review, 31 August, 1999.
[11]. S.Crisoloveanu, "Architecture Of SOI Transistors: What's Next?", 2000 IEEE International SOI Conference, 2000, Pp. 1-2.
[12]. Ying-Che Tseng; W. Margaret Huang, David J. Monk, P. Welch, J. M. Ford, J.S. Woo, "AC Floating Body Effects And The Resultant Analog Circuit Issues In Submicron Floating Body And Body- Grounded SOI MOSFET's," IEEE Transactions On ED, V.46, N 8, August 1999
[13]. 0.5 Mw Sub-Threshold Operational Transconductance Amplifiers Using 0.15 Mm Fully Depleted Silicon-On-Insulator (FDSOI) Process Piotr Olejarz 1, Kyoungchul Park 2, Samuel Macnaughton 2, Mehmet R. Dokmeci 3 And Sameer Sonkusale 2,*
[14]. Chi-Hon Ho, Jun-Yi Pon, And Yao-Tsung Tsai* "THE BRANCH-CUT METHOD AND ITS APPLICATION TO PARTIALLY DEPLETED SOI MOSFET SIMULATION FOR KINK EFFECT DEFINITION" *Journal Of The Chinese Institute Of Engineers, Vol. 31, No. 7, Pp. 1219-1224 (2008)* 1219
[15]. Jeong-Hyong Yi,_ Young-June Park And Hong Shick Min "ANALYTICAL MODEL FOR AND SCALE-DOWN EFFECT OF A FLOATING BODY VOLTAGE IN SOI MOSFETS"Journal Of The Korean Physical Society, Vol. 40, No. 4, April 2002, Pp. 668_671
[16]. B. Cheng, V. Ramgopal Rao, And J.C.S. Woo, "Sub 0.18 Um SOI Mosfets Using Lateral Asymmetric Channel Profile And Ge Pre-Amorphization Salicide Technology," *Proceedings Of The IEEE SOI Conference*, October 5-8, Stuart, Florida, USA, 1998.
[17]. S.M. Sze, "*Physics Of Semiconductor Devices*," 2nd Ed., New York, J. Wiley & Sons,
[18]. 1981 M. Y. Hammad, "Analytical Modeling Of The Partially-Depleted SOI MOSFET," IEEE Transactions On Electron Devices, Vol. 48, No. 2, Pp. 252–258, 2001. View At Publisher · View At Google Scholar· View At Scopus
[19]. N. Annamalai And M. Biwer, "Leakage Current In SOI Mosfets", IEEE Trans. On Nuclear Science, Vol. 35, Pp. 1372 - 1378, 1988
[20]. Y Omura And K. Izumi, "Simplified Analysis Of Body-Contact Effect For MOSFETISOI", EEE Trans. On Electron Devices, Vol. 35, Pp. 1391 - 1393, 1988.
[21]. J. Sleight And K. Mistry, "A Compact Schottky Body Contact Technology For SOI Transistors" International Electron Devices Meeting, (IEDM) Digest, Pp. 4 19 - 422. 1997.
[22]. S. Cristoloveanu, And S.S. Li, "*Electrical Characterization Of Silicon-On-Insulator Materials And Devices*," Kluwer Academic Publishers, 1995.
[23]. C.E.D. Chen, M. Matloubian, R. Sundaresan, B.Y. Mao, C.C. Wei, And G.P. Pollack, "Single Transistor Latch In SOI MOSFET's," *IEEE Electron Device Lett*., Vol. 9, P. 636, 1988.
[24]. H. C. De Graaff And F. M. Klaassen, "*Compact Transistor Modelling For Circuit Design*," Springer-Verlag, 1990.
[25]. M. D. Jacunski, M. S. Shur, A. A. Owusu, T. Ytterdal, M. Hack And B. Iniguez, "A Short Channel DC SPICE Model For

International Journal of Modern Engineering Research (IJMER)
www.ijmer.com Vol. 3, Issue. 3, May - June 2013 pp-1825-1827 ISSN: 2249-6645

A Novel Method for Collaborative Spam E- Mails

Sayyed Saissen[1], Sayeed Yasin[2]
[1]*M.Tech, Nimra College of Engineering & Technology, Vijayawada, A.P., India*
[2]*Asst.Professor, Dept.of CSE, Nimra College of Engineering & Technology, Vijayawada, A.P., India*

***ABSTRACT*:** With the increasing popularity of electronic mail (E-mail), several people and companies found it an easy way to distribute a massive amount of unsolicited messages to a tremendous number of users at a very low cost. These unwanted bulk messages or junk emails are called spam E- mails. The majority of spam mails that has been reported recently are unsolicited commercials promoting services and products including sexual enhancers, cheap drugs and herbal supplements, health insurance, travel tickets, hotel reservations, and software products. Spam E- mails has become an epidemic problem that can negatively affect the usability of electronic mail as a communication means. Besides wasting users time and effort to scan and delete these spam messages received; it consumes network bandwidth and storage space, slows down e-mail servers, and provides a medium to distribute harmful and/or offensive content. This paper presents a novel method for collaborative spam messages.

***KEYWORDS*:** COSDES, E- Mail, HTML, Spam.

I. INTRODUCTION

Internet is the most widely used area all over the world. In internet most widely used are Electronic mails (E-mails). E-mails play a major role for the communication between the users .The people who are using E- mails cannot verify the duplicate and near duplicate web documents creating the more problems on the web search engines. These documents will increase the space required to store the index, slow down the search results and the annoy users. According to the data availability on the internet, the huge data are shorts texts such that mobile phone short messages (SMS), instant messages, chat log, BBS titles etc.

The statistical information is given by the Information Industry Ministry of china that more than one billion mobile phone short messages are sent each day in Mainland China. You already know how much of email is spam, but here are a bunch of other factoids as per [1] you may not be aware of:

- Ninety percent of spam is in English. A year ago it was ninety six, so spam is getting more "international."
- Eighty eight percent of all spam is sent from bot nets (networks of compromised PCs).
- Ninety one of spam contains some form of link.
- Unsolicited newsletters are increasing and are now the second most common spam type.
- Spam from webmail services like Gmail and Hotmail is not as common as you might think. Only **0.7%** of spam is sent from the webmail accounts.
- One in 284 emails contain malware.
- One in 445 emails are phishing emails.
- As many as ninety five billion phishing emails were in circulation in 2010.
- Unfortunately, the status of duplicate and the near duplicate messages is very complex. Among these especially the near duplicates and spam mails.

These differences may result from various causes, such as:

1. Same contents appearing on various different sites are all crawled, processed and indexed.
2. Mistake introduced while parsing these noisy and loosely structured and noisy text (HTML page may contain ads., and it is known as shorting of semantics useful for parsing).
3. Manual typos (all information on Internet are created by people originally) and manual revising while being referred as well as reused.
4. Explicit modification to make the short messages suitable for difference usage.

Checking may be applicable manually when the scale of the repository is small. e.g. hundreds or hundreds or thousands of instances. When the amount of instances increases to millions and more, obviously, it becomes impossible for the human beings to check them one by one, which is tedious, costly and prone to error. Resorting to computers for such kind of repeatable job is desired, of which the core is an algorithm to measure the difference between any pair of the short messages, including duplicated and near duplicated ones.

II. RELATED WORK

Spam, or unwanted commercial email, has become an increasing problem in the recent years. Estimates suggest that perhaps seventy percent of all email traffic is spam. As spam clutters inboxes, time and effort must be devoted to either deleting it after it is received, or preventing it from even reaching the users [2]. In [3], the authors presented the results of combining classifier outputs for improving both accuracy and reducing false positives for the problem of spam detection. In [4], the authors specified that a set of independently developed spam filters may be combined in simple ways to provide substantially better filtering than any of the individual filters. In [5], the authors introduced a novel hybrid model, Partitioned Logistic Regression, which has several advantages over both naive Bayes and logistic regression. This model separates the original feature space into various disjoint feature groups.

In [6], the authors proposed a decentralized privacy preserving approach to spam filtering. The solution exploits robust digests to identify the messages that are a slight variation of one another and a structured peer-to-peer architecture between mail servers to collaboratively share knowledge about spam. In [7], the authors specified that the algorithm aims to detect spam web pages. In this algorithm, the web page gains the spam rank value through forward links, which are the links of reverse direction used in the traditional link-based algorithm. In [8], the authors have analyzed the TF-IDF algorithm to first find the relevancy of the comments with respect to the subject and further checking for repetition of the words in the comments. In [9], the authors have worked with Bayesian algorithm to filter e-mail spams. The major goal is to propose a model for an incremental spam filtering and test the model using the three training schemes.

The problem of unsolicited bulk email or spam is today well-known to every user of the Internet. Spam messages not only causes misuse of time and computational resources, thus leading to financial losses, but it is also often used to advertise illegal goods and services or to promote online frauds. To evaluate the performance of the highest probability SVM nearest neighbor classifier, this is an improvement over the SVM nearest neighbor classifier, on the task of the spam filtering. SVM nearest neighbor (SVM-NN) is the combination of the SVM and k-NN classifiers. Highest probability SVM nearest neighbor (HP-SVM-NN) classifier applied to the task of the spam filtering with variable relative error cost. The major strengths of the SVM are the training is relatively easy. No local optimal, unlike in the neural networks. It scales relatively well to high dimensional data and the tradeoff between the classifier complexity and error can be controlled explicitly.

III. PROPOSED WORK

In the proposed work, a complete collaborative spam detection system (COSDES) is introduced. The algorithm model of Cosdes is illustrated in Figure 1. Initially, three parameters- Tm (the maximum time span for reported spams being retained in the system), Td (the time span for triggering Deletion Handler), and Sth (the score threshold for determining spams) should be given for Cosdes. Before starting to do the spam detection, Cosdes collects feedback spams for the time Tm in advance to construct an initial database. Three major modules are included in Cosdes:

- Abstraction Generation Module
- Database Maintenance Module
- Spam Detection Module

With regard to the Abstraction Generation Module, each e-mail is converted to an e-mail abstraction by Structure Abstraction Generator with procedure SAG. Three types of action handlers- Deletion Handler, Insertion Handler, and Error Report Handler; are involved in Database Maintenance Module. Note that although the term "database" is used, the collection of the reported spams can be essentially stored in main memory to facilitate the process of matching. In addition, Matching Handler in the Spam Detection Module takes charge of determining results.

```
System Cosdes
Input: T_m: the maximum time span for reported spams being retained in
           the system,
       T_d: the time span for triggering Deletion Handler,
       S_th: the score threshold for determining spams
1   switch (circumstance)
2   case: when receiving a reported spam
3     if (EA.reporter.S_R > S_initial);
4       Trigger Insertion Handler(EA);
5       Increase S_R of the reporter in RepTable; // Rep: Reputation
6     break;
7   case: when receiving a testing email
8     Trigger Matching Handler(EA, S_th);
9     if (the testing email is classified as a spam);
10      Trigger Insertion Handler(EA);
11    break;
12  case: when receiving a misclassified ham
13    Trigger Error Report Handler(EA);
14    break;
15  case: for every T_d
16    Trigger Deletion Handler(T_m);
17    break;
End
```

Figure 1: Algorithm for COSDES

Cosdes deals with four circumstances by the handlers, and the detailed procedure flow will be explained as follows: For Insertion Handler, initially, the corresponding SpTree is found in the SpTable according to the tag length of the inserted spam, and nowNode is assigned as the root of this SpTree. In lines 3 to 8, we iteratively insert the subsequences of the e-mail abstraction along the path from root to leaf. If nowNode is an internal node, the subsequence with 2i tags is inserted into the level i. Meanwhile, the hash value of this subsequence is then computed. Then, "nowNode" is assigned as the corresponding child node based on the type of the next tag. If the next tag is a start (or end) tag, nowNode is assigned as the left (or right) child node. Finally, when nowNode is processed to a leaf node, the subsequence with the remaining tags is stored.

The principal concept of collaborative spam detection is to collect the human judgment to block subsequent near-duplicate spam. To ensure the truthfulness of the spam reports and to prevent malicious attacks, we propose the reputation mechanism to evaluate the credit of each reporter. The fundamental idea of the reputation mechanism is to utilize the reputation table to maintain a reputation score "SR' of each reporter according to the previous reliability record. Each inserted spam is given a suspicion score equal to "SR" of the reporter. In such a context, when doing near-duplicate detection, if the sum of the suspicion scores of matched spams exceeds a predefined threshold, the testing e-mail will be classified as a spam.

IV. CONCLUSION

Collaborative Spam Detection System (COSDES) possesses an efficient near duplicate matching scheme and a progressive update scheme. The progressive update scheme not only adds in the new reported spams, but also removes obsolete ones in the database. With Cosdes maintaining an up-to-date spam database, the detection result of each incoming E-mail can be determined by the near duplicate similarity matching process. In addition, to withstand the intentional attacks, a reputation mechanism is also provided in Cosdes to ensure the truthfulness of user feedback.

REFERENCES

[1]. http://royal.pingdom.com/2011/01/19/ email-spamstatistics/
[2]. Message Labs Spam Intercepts data, 2006, http://www.messagelabs.com/publishedcontent/publish/threat_watch_d otcom_ en / threat_statistics/spam_intercepts/DA_114633.chp. html
[3]. Gray and M. Haahr, "Personalised, Collaborative Spam Filtering," Proc. First Conf. Email and Anti-Spam (CEAS), 2004.
[4]. Androutsopoulos, J. Koutsias, K. V. Chandrinos, and C. D. Spyropoulos, "An experimental comparison of Naive Bayesian and keyword-based anti-spam Filtering with personal e-mail messages", In Proc. Of SIGIR-2000, ACM, 2000.
[5]. M.-T. Chang, W.-T. Yih, and C. Meek, "Partitioned Logistic Regression for Spam Filtering," Proc. 14th ACM SIGKDD Int'l Conf. Knowledge Discovery and Data mining (KDD), pp. 97-105, 2008.
[6]. E. Damiani, S.D.C. di Vimercati, S. Paraboschi, and P. Samarati, "P2PBased Collaborative Spam Detection and Filtering," Proc. Fourth IEEE Int'l Conf. Peer-to-Peer Computing, pp. 176-183, 2004.
[7]. Chenmin Liang, Liyun Ru, Xiaoyan Zhu. R-SpamRank: "A Spam Detection Algorithm Based on Link Analysis", State Key Laboratory of Intelligent Technology and Systems (LITS), Department of Computer Science and Technology Department, Tsinghua University, Beijing, 100084, China
[8]. H. Drucker, D. Wu, and V.N. Vapnik, "Support Vector Machines for Spam Categorization," Proc. IEEE Trans. Neural Networks, pp. 1048- 1054, 1999.
[9]. Lixin Fu and Geetha Gali, "Classification Algorithm for Filtering Email spam", Recent Progress in Data Engineering and Internet Technology, 2012, Volume 157, 149-154, DOI: 10.1007/978-3-642- 28798-5_21

International Journal of Modern Engineering Research (IJMER)
www.ijmer.com Vol. 3, Issue. 3, May - June 2013 pp-1828-1831 ISSN: 2249-6645

Design and Implementation of an Encryption and Decryption Using Non-Linear RM-PRNG

M. Venkatananda Reddy[1], M. Mohan Reddy[2]
Department of ECE, Santhiram Engineering College, Nandyal[1],
Assistant professor, Santhiram Engineering College, Nandyal[2]

ABSTRACT: *Pseudo Random Number Generator (PRNG) is an algorithm for generating a sequence of numbers. Due to speed in number generation pseudorandom numbers are very important. The increasing application of cryptographic algorithms to ensure secure communications is widely used. So, Here we propose a new reseeding mixing method to extend the system period length and to enhance the statistical properties of pseudo random number generator (PRNG). The reseeding method removes the short periods which are occurred by CB-PRNG and the mixing method extends the system period length by Xoring with ALG. The output sequence of RM-PRNG is used as a key to the encryption and decryption modules. The simulation results are obtained by using Modelsim and Synthesis is observed by Xilinx ISE 10.1*

Keywords: *Encryption, Decryption, Reseeding, Mixing, PRNG, Peroid Extension*

I. INTRODUCTION

It is hard to imagine a well-designed cryptographic application that doesn't use random numbers. Session keys, initialization vectors, salts to be hashed with passwords, unique parameters in digital signature operations, and nonces in protocols are all assumed to be random by system designers. . Unfortunately, many cryptographic applications don't have a reliable source of real random bits, such as thermal noise in electrical circuits or precise timing of Geiger counter click [Agn88, Ric92]. Instead, they use a cryptographic mechanism, called a Pseudo-Random Number Generator (PRNG) to generate these values. The PRNG collects randomness from various low-entropy input streams, and tries to generate outputs that are in practice indistinguishable from truly random streams. Typical PRNG consists of unpredictable input called "seed" value and a secret state "S". Software approaches use machine state information like movement of the mouse, keystrokes, contents of memory registers, and hardware latency to create a seed value. Prngs operate by repeatedly scrambling the seed to generate random output. Typically, the seed is a short, random number that the PRNG expands into a longer, random-looking bitstream.

A PRNG often starts in a random state and must process many seeds to reach a secure state **S**. Upon request, it must generate outputs that are indistinguishable from random numbers to an attacker who doesn't know and cannot guess **S**. In this, it is very similar to a stream cipher. Additionally, however, a PRNG must be able to alter its secret state by repeatedly processing input values (seed). See Figure 1 for a high-level view of a PRNG.

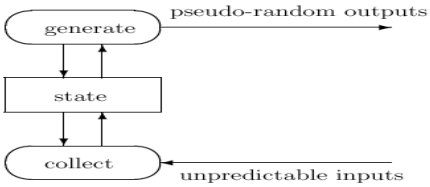

Fig 1. Model of PRNGs

Prngs are produce long period random number sequence linear prngs are very useful, some of the linear prngs are linear feedback shift registers (lfsrs), linear congruential generators (lcgs), and multiple recursive generators (mrgs).These linear prngs are good in hardware cost and throughput rate. But due to their linear structure output random numbers of these generators are easily predictable. To overcome the predictability problem nonlinear chaos-based prngs (CB-prngs) [8] were proposed, it is efficient in hardware cost, but due to quantization error there exists short periods in such nonlinear prngs. They produce only one bit per iteration hence throughput rate is low. And then to produce long periods and high throughput rate reseeding-mixing PRNG (RM-PRNG) were proposed. The RM-PRNG consists of a CB-PRNG and MRG [1], [8]. The reseeding method removes the short periods in the CB-PRNG and by mixing MRG with CB-PRNG the overall system period length increases.

In this paper, we propose a encryption and decryption technology; in this technology has an encryption scheme the message or information is encrypted by using an encryption method, the plain text is converted into unreadable cipher text. An adversary that can see the cipher text should not able to determined anything about the original message. However the cipher text is converted to plain text (original message) by using decryption method. In this encryption and decryption methods are implementing an operation of the plain text and RM-PRNG key with "**Xoring"** operation.

II. RM-PRNG

Fig. 2 shows the schematic diagram of the RM-PRNG, which is composed of three modules: Nonlinear Module, Reseeding Module, and Vector Mixing Module. In a 32-b implementation, the Nonlinear Module has a controlled 32-b state register and a Next-State construction circuitry. The state register stores the state value (Xt) which is set to seed1 by using the start command. The next state construction is used to produce the next state value (X_{t+1}) by using recursive formula $X_{t+1}=F(X_t)$ [1].

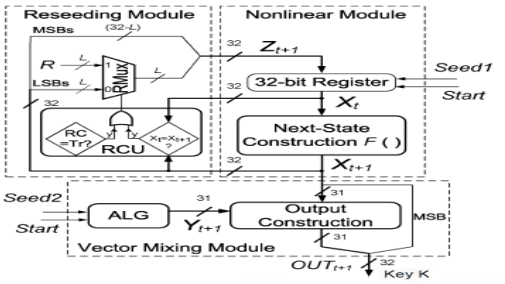

Figure 2. Structure of RM-PRNG

For each generated state value, the reseeding control unit (RCU) in the Reseeding Module compares the values for checking the fixed point condition,and increases the reseeding counter (RC) at the same time. The RC will be reset and the reseeding operation will be activated when either the fixed point condition is detected or the RC reaches the reseeding period. When RC reaches the reseeding period T_r or the fixed point condition is detected then RC will be reset and the reseeding operation will be activated. The sate register will be loaded through the rmux, when reseeding is activated [1]. The value of X_{t+1} is directly loaded into the state register if the reseeding is not activated. Vector Mixing Module is implemented by an auxiliary linear generator (ALG) and output construction. By mixing X_{t+1} with the output Y_{t+1} from ALG in Vector Mixing Module, we obtain the output of the RM-PRNG (32-bit implementation).

A. Nonlinear Module: We use the LGM as the next-state construction function in the Nonlinear Module so that
$X_{t+1} = F(X_t) = \gamma x_t (1- X_t)$, $t \geq 0$..... (1)
Choosing a value 4 for not only makes the LGM Chaotic but also simplifies the implementation of (1) to merely left-shifting the product by 2 b. However, the state size decreases from 32 to 31 b, because the dynamics (1) are the same. This is equivalent to a degradation of resolution by 1 b. In addition, fixed as well as short periods exist when the LGM is digitized. From exhaustive runs for all of the seeds, we obtain all other periods for the 32-b LGM without reseeding. They are given in Table I with the longest period (18 675) and the set of short listed separately along with their total occurrences. Clearly, the performance of a CB-PRNG using only the Nonlinear Module is unsatisfactory. To solve the fixed points and short-period problem, a Reseeding Module is in order.

B. Reseeding Module: *The* removal of the fixed points by the reseeding mechanism is obvious. When the fixed point condition is detected or the reseeding period is reached, the value loaded to the state register will be perturbed away from in the RCU by the fixed pattern according to the formula

$$Z_{t+1} = \begin{cases} X_{t+1}[j], & 1 \leq j \leq 32 - L; \\ R[i], & 33 - L \leq j \leq 32, \ i = j + L - 32 \end{cases}$$

Where subscripts ,i ,j are the bit-index, L is integer. In order to minimize the degradation of the statistical properties of chaos dynamics, the magnitude of the perturbation of the fixed pattern should be small compared Here, we set L=5 so that the maximum relative perturbation is only $(2^5-1)/232$ and the degradation can be ignored [15]. Clearly, the effectiveness of removing short-periods depends on the reseeding period as well as the reseeding pattern. However, choosing the optimal reseeding period and the reseeding pattern is nontrivial. Nevertheless, several guidelines to choose a suitable combination had been proposed and discussed in our previous work . First, the reseeding period should avoid being the values or the multiples of the short periods of the unperturbed digitized LGM. Otherwise, if the 5 lsbs of equal to when the reseeding procedure is activated. Then no effective reseeding will be realized and the system will be trapped in the short-period cycle. Hence, prime numbers should be used as the reseeding period candidates. Although the average period of the reseeded PRNG has increased more than 100 times relative to that of the non reseeded counterpart, the period can in fact be extended tremendously in the Vector Mixing Module described below.

C. Vector Mixing Module: The Vector Mixing Module is constructed by using ALG and output construction. In this module an efficient MRG which is called as DX generator acts as the ALG. By using the following recurrence formula

$$Y_{t+1} = Y_t + B_{DX} . Y_{t-1} \ mod \ M, t \geq 7$$

In output construction unit, to obtain the lsbs of the output
The lsbs of Y_{t+1} and that of X_{t+1} are mixed by using XOR operation according to the following equation

$$OUT_{t+1}[1 : 31] = X_{t+1}[1:31] \oplus Y_{t+1}[1:31]$$

To form the full 32-b output vector out_{t+1} the MSB of X_{t+1} is added to $out_{t+1}[1:31]$.
The DX generatator is implemented described below the implementation [of the DX generator is (the ALG) done by using

8-word registers, circular-left-shift (CLS), circular 3-2 counter and End Around Carry- carry look ahead adder (EAC-CLA). By using flip-flops the eight-word register was implemented. For generating two partial products signal Y_{t-7} is circular-left-shifted 28 and 8 b using the modules CLS-28 and CLS-8 respectively. To combine these three 31-b operands into two 31-b operands a circular 3-2 counter is used, which Consumes 247 gates. To evaluate Y_{t+1} 31-b EAC-CLA is used with 348 gates. The schematic design of the 31-b EAC-CLA [4], [9] is shown in Figure 2(b). The schematic design of the 31-b EAC-CLA includes four modules they are propagation and generation (PG) generators, end-around-carry (EAC) generator, internal carry (IC) generator, and clas [5]. When EAC is generated by group of pgs, EAC is then fed to the IC generator and then to least-significant 8-b CLA. On clas, the final addition was performed.

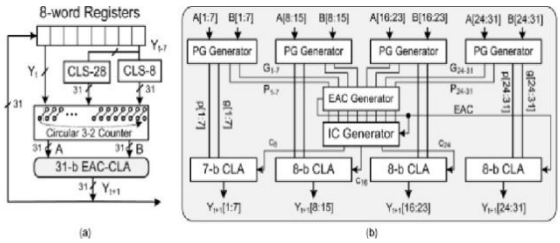

Figure 3. (a) Structure of the DX generator.
(b) Structure of the 31-b EAC-CLA.

III. PROPOSED ENCRYPTION AND DECRYPTION

In this proposed Encryption and decryption technlogy is where security engineering meets mathematics. It provides us with the tools that underlie most modern security protocols. It is probably the key enabling technology for protecting distributed systems, yet it is surprisingly hard to do right. Encryption and decryption technlogy is the practice and study of techniques for secure INFORMATION SHARING in the presence of ADVERSARYIES. In encryption and decryption technlogy, encryption is the process of encoding messages or information in such a way that hackers cannot read it. Encryption and decryption technology is designed around computational hardness assumptions, making such algorithms hard to break in practice by any adversary. Encryption is the process of converting plain text or information into unintelligible cipher text. Any adversary that can see the cipher text should not know anything about the original message. Decryption is the reverse, in other words, moving from the unintelligible cipher text back to plaintext. The statistical properties of cryptographic methods are the reason for the excellent pseudorandom testability of encryption and decryption technlogy processor cores. and finally the RM-PRNG key using an Encryption and decryption in as shown fig4.

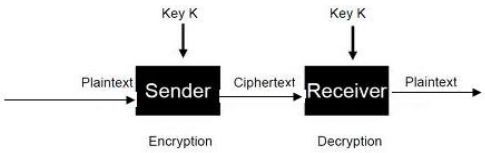

Figure 4. Encryption and decryption technology

IV. RESULTS AND SIMULATION

Pseudo Random Number Generator, Encryption and Decryption were designed using Verilog language in modelsim 6.4. All the simulations are performed using modelsim 6.4 simulator. The simulated output of Pseudo Random Number Generator, Encryption and Decryption are shown in Figure 5&6 And also FPGA implementation of synthesis using Xilinx10.1 in fig7 and also FPGA result in fig8.

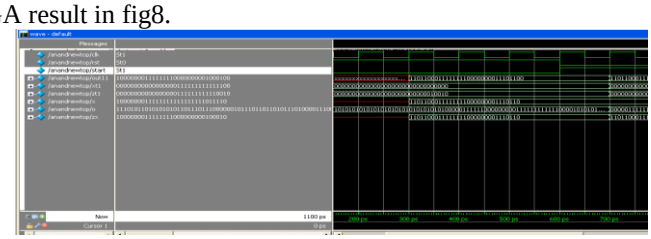
Figure 5. Simulation results for RM-PRNG key


Figure 6. Simulation results of encryption and decryption

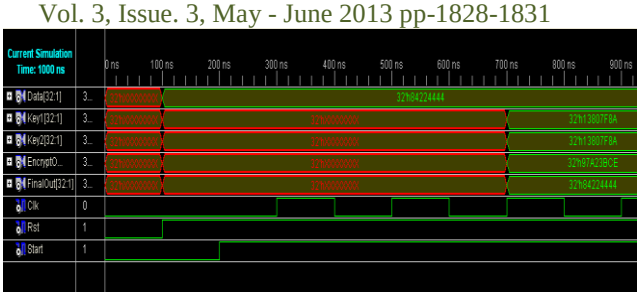

Figure 7: synthsis result.

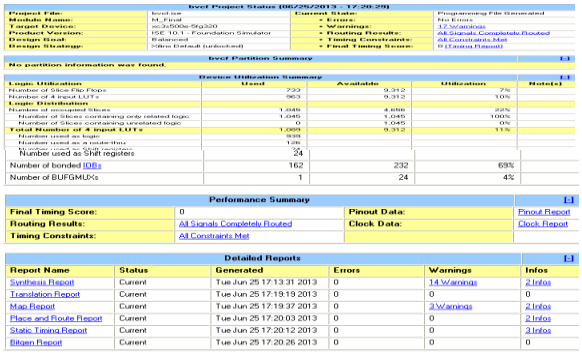

Figure 8.FPGA result

V. CONCLUSION

We proposed a Encryption and decryption using RM-PRNG to ensure secure communication. A hardware implementation of RM-PRNG is to offer long periods and high throughput rate to established statistical standards for PRNGs.

The reseeding mechanism solves the short-period problem, while mixing a CB-PRNG with a long-period DX generator extends the period length.Hence,Simulation and Synthesis is observed by ModelSim 6. 4b and Xilinx ISE 10.1

REFERENCES

[1]. Chung-Yi Li, Yuan-Ho Chen, Tsin-Yuan Chang, Lih-Yuan Deng and Kiwing To, "Period Extension and Randomness Enhancement Using High-Throughput Reseeding-Mixing PRNG" transactions on (vlsi) systems, vol. 20, no. 2, february 2
[2]. T. Sang, R. Wang, and Y. Yan, "Clock-controlled chaotic keystream generators," Electron. Lett., vol. 34, no. 20, pp. 1932–1934, Oct. 1998.
[3]. D. Mukhopadhyay, "Group properties of non-linear cellular automata," J. Cellular Autom., vol. 5, no. 1, pp. 139–155, Oct. 2009.
[4]. D. Mukhopadhyay,D. R. Chowdhury, and C. Rebeiro, "Theory of composing non-linear machines with predictable cyclic structures," in Proc. 8th Int. Conf. Cellular Autom. Res. Ind., 2008, pp. 210–219, Springer.
[5]. J. E. Gentle, Random Number Generation and Monte Carlo Methods,2nd ed. New York: Springer-Verlag, 2003.
[6]. D. Knuth, The Art of Computer Programming, 2nd ed. Reading, MA: Addison-Wesley, 1981.
[7]. Klapper and M. Goresky, "Feedback shift registers, 2-adic span, and combiners with memory," J. Cryptology, vol. 10, pp. 111–147, 1997.
[8]. D. H. Lehmer, "Mathematical methods in large-scale computing units," in Proc. 2nd Symp. Large Scale Digital Comput. Machinery, Cambridge, MA, 1951, pp. 141–146, Harvard Univ. Press.
[9]. S. Li, X. Mou, and Y. Cai, "Pseudo-random bit generator based on couple chaotic systems and its application in stream-ciphers cryptography," in Progr. Cryptol.-INDOCRYPT, 2001, vol. 2247, pp. 316–329, Lecture Notes Comput. Sci.
[10]. L. Y. Deng and H. Xu, "A system of high-dimensional, efficient, long cycle and portable uniform random number generators," ACM Trans. Model Comput. Simul., vol. 13, no. 4, pp. 299–309, Oct. 1, 2003.
[11]. J. Cermak, "Digital generators of chaos," Phys Lett. A, vol. 214, no.3–4, pp. 151–160, 1996.
[12]. T. Sang, R.Wang, and Y.Yan, "Perturbance-based algorithm to expand cycle length of chaotic key stream," Electron. Lett., vol. 34, no. 9, pp. 873–874, Apr. 1998. \
[13]. L. Blum, M. Blum, and M. Shub, "A simple unpredictable pseudorandom number generator," SIAM J. Comput., vol. 15, pp. 364–383, 1986.
[14]. N. Masuda and K. Aihara, "Cryptosystems with discrete chaotic map," IEEE Trans. Circuits Syst.-I 29, pp. 28-40, 2002.
[15]. J. Fridrich, "Image encryption based on chaotic maps," IEEE Int. Conf. Systems, Man and Cybernetics, vol. 2, pp. 1105-1110, 1997.
A. Dornbusch, and J. P. Gyvez, "Chaotic generation of PN sequences: AVLSI implementation," IEEE ISCAS 5, pp. 454-457, 1999.
[16]. H. Niederreiter, Random Number Generation and Quasi-Monte Carlo Methods. Philadelphia, PA: SIAM, 1992.
[17]. S. M. Mathyas and C. H. Meyer, "Generation, distribution and installation of cryptographic keys," IBM Syst. J., vol. 17, no. 2, pp. 126–137,1978.
[18]. T.Kuusela, "Random number generation using a chaotic circuit," J. NonlinearSci., vol. 3, no. 4,pp. 445–458, 1993.
[19]. A statistical test suite for random and pseudorandom number generators for cryptographic applications, http://csrc.nist.gov/rng

International Journal of Modern Engineering Research (IJMER)
www.ijmer.com Vol. 3, Issue. 3, May.-June. 2013 pp-1832-1836 ISSN: 2249-6645

EZR: Enhanced Zone Based Routing In Manet

Bency Wilson[1], Geethu Bastian[2], Vinitha Ann Regi[3], Arun Soman[4]
Department of Information Technology, Rajagiri School of Engineering and Technology, Rajagiri Valley, Cochin, India

ABSTRACT: *Proposed system makes use of both proactive and reactive mechanisms. The core idea behind the topic deals with an efficient routing mechanism in MANET. It uses a hybrid scheme that combines the advantages of both proactive and reactive schemes. By dividing the entire network into different zones, we implement the idea of keeping data in source trees in each node and by making use of GPS mechanism we can parallely monitor the speed and co-ordinates of all nodes in the network. Within a zone we are making use of proactive routing mechanism and outside the zone we are implementing a dynamic routing mechanism. The main benefits of this routing mechanism include bandwidth efficiency, less control messages, saving of battery power etc.*

KEYWORDS: *GPS, hybrid, MANET, routing, zone*

I. INTRODUCTION

MANET (MOBILE AD-HOC NETWORK) is a collection of mobile nodes that communicates wirelessly with each other or by relaying other nodes as routers. It doesn't rely on any base station and don't have a fixed infrastructure of their own. Routing in MANET is made possible by hop by hop forwarding. There exists various metrics like number of hops, traffic density for effectively selecting the route to forward the packet. The MANET environment is highly dynamic. So a good routing protocol for MANET was designed by considering the dynamic nature and battery constraint. So a good routing protocol should minimize the computing load on the host and traffic load in the network. There exist several routing protocols in MANET. The most prominent among them are reactive, proactive and hybrid protocols.

In proactive scheme each node maintains complete routing information of the network in routing tables. If there exist any possible change in network topology it broadcasts network status information in the entire network and the routing tables are updated periodically. To maintain up to date status of the network it needs a lot of network resources including memory. It's not suited when the network mobility is high. Examples include Global state routing (GSR), hierarchical state routing (HSR), destination sequenced distance vector routing (DSDV).

In reactive routing protocol each node maintains only information about the active routes in the network. In order to find a new route to destination it need to issue a route request which reduces the communication overhead in proactive scheme. But there exists sufficient delay in route discovery and forwarding of data packet. Examples of reactive protocol are ad-hoc on demand distance vector routing (AODV), Dynamic source routing (DSR), temporally ordered routing algorithm (TORA).Hybrid routing protocols offer an efficient framework that contains the strengths of proactive and reactive routing protocols. Zone routing protocol (ZRP) comes under this category.

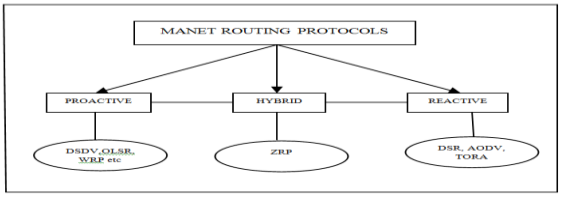

Fig 1: MANET routing protocols

II. RELATED WORK

II.1 STAR: Source Tree Adaptive Routing: THE STAR PROTOCOL COMES UNDER THE CLASSIFICATION OF PROACTIVE ROUTING. PROACTIVE ROUTING PROTOCOLS MAINTAIN THEIR INFORMATION CONTINUOUSLY. A NODE WHICH IS USING PROACTIVE OR TABLE DRIVEN PROTOCOL HAS A TABLE WHICH CONTAINS INFORMATION ON HOW TO REACH OTHER NODES IN THE NETWORK. CHANGES IN THE TOPOLOGY ARE REGULARLY PROPAGATED IN THE NETWORK, THEREBY KEEPING THE TABLE UP-TO-DATE. SINCE STAR USES TABLE DRIVEN APPROACH, ALL ROUTES ARE ALREADY PRESENT IN ROUTING TABLE. THEREFORE THE LATENCY IN FINDING NEW ROUTES IS LOW. BUT THE ROUTING OVERHEAD IS RATHER HIGH IN TERMS OF CONTROL MESSAGES. THE STAR PROTOCOL IS BASED ON LINK STATE ALGORITHM. BUT THE DIFFERENCE IS IN PERIODIC UPDATING PROCEDURE. THE CORE IDEA BEHIND THE STAR PROTOCOL IS TO MAINTAIN A SOURCE TREE AT EACH NODE IN THE TOPOLOGY. A SOURCE TREE IS NOTHING BUT CONNECTS A NODE TO ALL THE DESTINATIONS THROUGH LOOP FREE TREE BRANCHES. OR SOURCE TREE CAN BE VIEWED AS A SET OF LINKS CONTAINING PREFERRED PATHS TO DIFFERENT DESTINATIONS. ALSO, A SOURCE TREE IS MUCH LIGHTER COMPARED TO A ROUTING TABLE.

The STAR protocol can be run by 2 approaches. It is done either by LORA or by ORA approach. The aim of the LORA approach is not to find a shortest path, but instead find paths which are reasonable with respect to some metric. LORA can keep the overhead of routing messages to minimum. STAR also supports ORA approach if required. ORA approach implies that the source trees will be exchanged by the nodes which are the routers only when the router detects a change in the source tree rather than the periodic updating scheme with link state routing. For the purpose of saving transmission bandwidth and energy, only when a router detects changes like possibility of looping, node failure, network partitions etc. It will report changes to the source tree. The deletion of a link to reach at a destination is evident with the

addition of a new link to the same destination. So link deletions need not be communicated by the router. Only in case of loss of path to one or more destinations by a router, there is the need of communicating its neighbors. In the STAR protocol, the topology of a network is modelled as a directed graph G=(V,E), where V is the set of nodes and E is the set of edges connecting the nodes. Consider a link between a router u and a destination router v. For this, router u is called the head node of the link in the direction from u to v. By way of exchange of hello messages, link level protocol is assumed that keeps track of neighbourhood information. Each and every node in the network maintains a source tree connecting the router to all destinations in the network that are known to the router. Thereby the router can know about all its neighbours. Through the exchange of source trees with the neighbouring routers, routers can also know about their source trees. The basic update unit used to communicate changes to source trees is the link state update (LSU). An update message will contain one LSU which is used to report the characteristics of a link. An LSU for a link i -> j can be represented as $LSU_{i,j}$ =(i, j, l, t), where i and j are the source and destination routers also l, which denotes link cost and t, the timestamp or sequence number of the last update. To keep track of latest routes, STAR make use of sequence numbers as we already said. Validation of LSU is done with the help of these sequence number. So when a router receives an Link State Update, it can check whether it contain more recent information. This is done by comparing sequence number of the new with that of the link stored locally. Like that a router keeps their own source tree and the source tree reported by its neighbours. This forms a partial topology graph for a router. This partial topology graph is maintained for each and every node in network, thereby STAR protocol need significant memory. Also the processing overhead will be very large when considering a large mobile network.

II.2 DREAM-Distance Routing Effective Algorithm For Mobility : DREAM protocol belongs to the category of proactive routing protocol. It makes use of a GPS system through which it gets an idea of its geographical coordinates. It stores a routing table called location table which is exchanged between the nodes which significantly reduces the bandwidth. But reactive protocol makes use of less bandwidth. So it is better idea to make use of both the ideas and implement a protocol. The control messages which are used in reactive protocols are shorter than the control messages used in proactive protocols. But since the route has to be discovered before sending the data, a delay may also be incurred. Here the mobility of nodes also imposes a big problem .The speed of the nodes also may vary.

The DREAM protocol is a combination of both proactive and reactive protocol. Here the concept is based on zones. There are inter zones and intra zones discovery. If the receiver is within the zone at a distance <=k from the sender, then an intra-zone discovery is done which is based on proactive way. If it locates in another zone different from that of the sender, then it uses a reactive way. The choice of the zone is static which is based on node movement. When a source node S wants to send information packets to a destination node D, it retrieves the location information of D stored within it location tables. Using this location information as a reference, S determines those nodes amongst its neighbours who are "in the direction" of D, and forwards the message packet to them. On receipt of this information packet, the intermediate neighbouring nodes in turn perform a lookup into their location tables to retrieve the location entry for the destination D. The intermediate nodes in turn forward the message packet to those nodes, amongst it neighbours who are in the direction of D, similar to S. This process continues until the destination D is eventually reached. This effectively results in using a reactive approach, as individual nodes in the path determine the next hop in an on-demand manner. In the DREAM algorithm, each node participates in the transmission of control messages containing the current location of a particular node to all other nodes within the network, in the form of Location Update messages. The frequency of such updates is determined by the distance factor and mobility rate of each node.

The advantages of the DREAM protocol are as follows:

1) It efficiently uses the bandwidth and the energy since the control message carries only the coordinates and the identifier of a node.
2) It is inherently loop-free, as each data message propagates away from its source in a specific direction.
3) It is robust as the messages reach the destination by following specific paths.
4) It is adaptive to mobility.

II.3 LAR-Location Aided Routing: Reactive protocols are better preferred compared to proactive since it maintains the active routes and a new route is discovered only on demand. Reactive protocols are divided into two categories: source routing and hop-by-hop routing Source routing maintains a route to forward the packet to destination which is a major drawback in large network. On the other hand the hop-by-hop routing depends on the routing table in each node to forward the message. Here the header contains the destination and next hop address only.

LAR mainly based on the concept of flooding and location awareness node knows its position by means of a GPS. Here the sender forwards a message to destination containing its id and id of destination by means of flooding algorithm. The neighbour node on receiving it forwards the message to its neighbour and so on. If a node receives duplicate message (recognized by checking the sequence number) it discards any one of them to save the bandwidth. Each neighbour node appends its own ID to the message header and forwards it further to destination through the active routes. Destination on receiving it resends a Route reply along the route in the message header or piggybacks it with another route request to the source. In LAR the source node calculates the expected zone to flood the packet. If the source node knows more mobility information of the destination node the size of the expected zone can be reduced which helps to increase the performance. Each node defines a request zone to forward the route request. All the nodes in that region receive the route request packet. The request zone includes the expected zone and possible surroundings around it. A time-out period is set by each node in the network. If the route is not discovered before time-out, the source node will consider expanded request zone and forwards route request again. To optimize the route discovery process collects information from an intermediate node which

contains best location information to the destination node (assuming that source information is out of date compared to intermediate node).

LAR mainly focuses on reducing the control message overhead of Ad-hoc on-demand distance vector (AODV) routing protocol. It floods only the portion of the message that contains the route to destination. So the bandwidth of the network can be saved by using this approach. The main drawback of this approach is that every node should know the speed and location of the destination node and it can't dynamically learn about the neighbour nodes in the network.

III. PROPOSED SYSTEM

PROPOSED SYSTEM MAKES USE OF BOTH PROACTIVE AND REACTIVE MECHANISMS. WHEN A NETWORK IS NEWLY INITIALIZED, BY THE USE OF HELLO MESSAGES A NODE COMES TO KNOW ABOUT ITS NEIGHBOURS. EACH NODE KNOWS ABOUT THE NODES IN THE NETWORK BY MEANS OF GPS, THEREBY IT CAN MONITOR BOTH ITS SPEED AND COORDINATES. THE COLLECTED INFORMATION IS THEN STORED IN A TREE CALLED SOURCE TREE. A SOURCE TREE IS MAINTAINED FOR EACH AND EVERY NODE IN A NETWORK. SOURCE TREES ARE EXCHANGED ONLY WHEN THE ROUTER DETECTS A CHANGE IN THE NETWORK.

THE BASIC UPDATE UNIT USED TO COMMUNICATE CHANGES TO SOURCE TREES IS THE LINK STATE UPDATE (LSU). AN UPDATE MESSAGE WILL CONTAIN ONE LSU WHICH IS USED TO REPORT THE CHARACTERISTICS OF A LINK. AN LSU FOR A LINK I -> J CAN BE REPRESENTED AS $LSU_{I,J}$ =(I, J, L, T), WHERE I AND J ARE THE SOURCE AND DESTINATION ROUTERS ALSO L, WHICH DENOTES LINK COST AND T, THE TIMESTAMP OR SEQUENCE NUMBER OF THE LAST UPDATE. VALIDATION OF LSU IS DONE WITH THE HELP OF THESE SEQUENCE NUMBER. SO WHEN A ROUTER RECEIVES AN LINK STATE UPDATE, IT CAN CHECK WHETHER IT CONTAIN MORE RECENT INFORMATION. THIS IS DONE BY COMPARING SEQUENCE NUMBER OF THE NEW WITH THAT OF THE LINK STORED LOCALLY. A SOURCE TREE IS MUCH LIGHTER WHEN COMPARED TO A ROUTING TABLE. WE CAN MAKE USE OF DIJIKSRA'S ALGORITHM IN SOURCE TREE TO FIND SHORTEST PATH BETWEEN NODES.

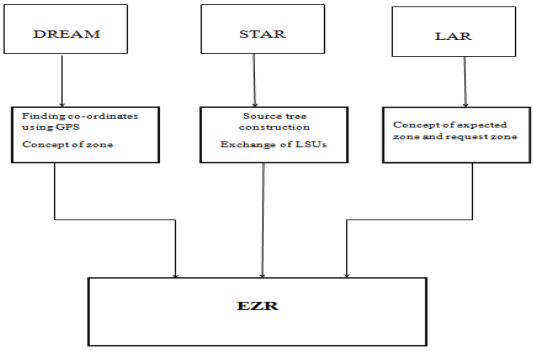

Fig 2: The EZR protocol

When a source node wants to transmit data to destination, first of all source node needs to define a zone. Zone is defined with a radius which can be calculated with the formula Displacement=Speed * Time. That is R=speed*(t1-t0), where speed is the average speed of the destination, t0 is the time in which speed is calculated and t1 is the time in which source node is trying to send the data.

Proposed system makes use of request zone and expected zone to forward the data from source to destination. The zone defined by the source is equivalent to its request zone where the expected zone is one in which the destination resides. For this first the source node check whether the destination is in the request zone. If yes, then with the help of immediate neighbours, it will forward data to the destination. If the destination lies outside the zone, then we can expand the request zone in the direction of destination by including the nearest neighbour of the request zone. Then the node in the boundary of a zone forwards the route request to the nearest neighbour. And finally it reaches the destination. So when the destination sent route reply, it also includes the public key of the destination. For security, data is encrypted with that public key and at the destination; it decrypts the data with the private key of destination.

III.1 Algorithm: STEP 1: Initialize Total number of nodes in the network.
STEP 2: Obtain geographical co-ordinates of the node with GPS.
STEP 3: Broadcast hello messages to nodes in zone.
STEP 4: Receive Hello message.
STEP 5: Each node creates source tree.
STEP 6: All nodes initialize sequence number of links to 0.
STEP 7: Stores the co-ordinates, neighbor node id and link state information with sequence number in source tree.
STEP 8: If an event occurs, exchange LSU's.
STEP 8.1: If Sequence number of new LSU > Sequence number of link information, then goto step 8.1.1
STEP 8.1.1: Update source tree.
STEP 8.2: Else, discard LSU.
STEP 9: If Source wants to transmit final destination, then goto step 9.1
STEP 9.1: Define request zone with radius R= Speed*(t1-t0).
STEP 10: If destination is within the request zone, then goto step 10.1
STEP 10.1: Then forward the data directly.

STEP 11: Else, expand request zone in the direction of destination.
STEP 11.1: Define expected zone containing destination node.
STEP 11.2: Forward RREQ to nearest neighbor within the border of request zone.
STEP 12: Destination receives RREQ.
STEP 13: Destination sends RREP with its public key.
STEP 14: Source sends data encrypted with public key of destination.
STEP 15: Stop.

IV. SIMULATION RESULTS

We simulated the protocols DSDV, DSR and EZR using network simulator NS2 for 8 nodes. We analysed the packets dropped in each protocol using AWK script. And the results we obtained are
DSDV: 154222
DSR: 132464
EZR: 101605

The simulation results of 3 protocols are shown in figure 3, 4, 5. And the graphical analysis of packet dropping is plotted in figure 6. When we analysed the graphical result, the EZR which we proposed outperforms the other two.

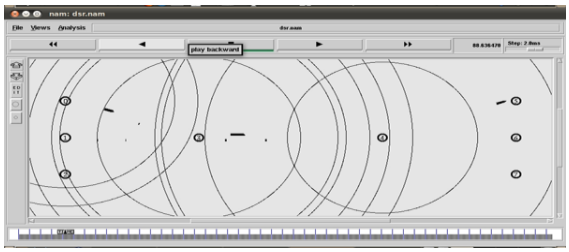

Fig 3: DSDV Protocol

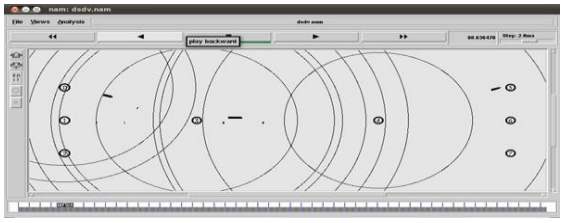

Fig 4: DSR Protocol

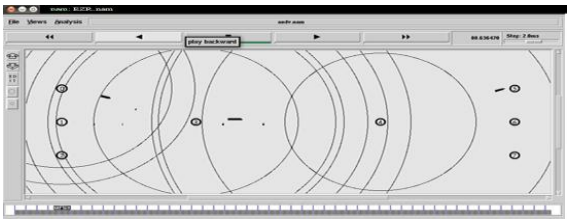

Fig 5: EZR Protocol

Fig 6: Comparison of DSDV, DSR, EZR

V. CONCLUSION

In this paper, 3 routing protocols of MANET are compared. And also by overcoming almost all disadvantages we proposed a new routing scheme. The compared protocols are STAR, DREAM and LAR. The core idea behind the STAR protocol is to maintain a source tree at each node in the topology. A source tree is nothing but connects a node to all the destinations through loop free tree branches. By the proper exchange of source trees, routers can know about their neighbours. The basic update unit used to communicate changes to source trees is the link state update (LSU).

In DREAM, using GPS a node's location co-ordinates are found out. Then through the exchange of these on the basis of expected destination's direction data is sent. This scheme is actually a combination of reactive and proactive routing mechanisms. Here control messages are less. Also this is having high bandwidth efficiency and is also robust. LAR is a reactive scheme, which is on demand. Flooding and Location awareness by GPS are 2 schemes for sending data. This scheme is also bandwidth efficient.

Proposed system makes use of both proactive and reactive mechanisms. When a network is newly initialized, by the use of hello messages a node comes to know about its neighbours. Each node knows about the nodes in the network by means of GPS, thereby it can monitor both its speed and coordinates. The collected information is then stored in a tree called source tree. By dividing the entire network into different zones, we implement the idea of keeping data in source trees in each node and by making use of GPS mechanism we can parallely monitor the speed and co-ordinates of all nodes in the network. Within a zone we are making use of proactive routing mechanism and outside the zone we are implementing a dynamic routing mechanism. The main benefits of this routing mechanism include bandwidth efficiency, less control messages, saving of battery power etc. From simulation results, EZR is having high performance than DSDV and DSR routing protocols.

REFERENCES

[1]. Jan-Erik Ekberg, Ad-Hoc Routing protocols: TheSTAR routing protocol
[2]. Yottttg-BaeKo and Nitin H. Vaidya,Department of Computer Science,Location-Aided Routing (LAR) in Mobile Ad Hoc Networks MOBICOM 9S Dallas Texas USA ACM 1998.
[3]. C.Sommer and F. Dressler,"Progressing Towards Realistic mobility Models in VANET Simulations "IEEECommunications Magazine, , vol. 46 (11), pp. 132-137, November 2008.
[4]. Harish Shakywar, Sanjeev Sharma, Santoh Sahu,' Performance Analysis of DYMO, LANMAR, STAR Routing Protocols for Grid Placement model with varying Network Size', Int. J. Comp. Tech. Appl., Vol 2 (6), 1755-1760
[5]. Mehran Abolhasan a, Tadeusz Wysocki a, Eryk Dutkiewicz,' A review of routing protocols for mobile ad hoc networks', Ad Hoc Networks 2 (2004) 1–22.
[6]. M. S. Corson and A. Ephreruides, "A distribukd routing algorithum for mobfie wireless networks~ACM L ***Wreless Network,vol.*** 1, no. 1, pp. 61+1, 1995.
[7]. S. Corson audJ. Macker, 'Mobde ad hocnetworting(remet]Routing protocol performance issues and evaluation considerations (internet-Draft)V Mar. 1998.
[8]. D. Johnson and D. A. Mrdtz, "Dynamic source routing in ad hoc wireless nehvorks~' in *Mobile Computing(T.imeilenski* and H. Korth, eds.), Huwere Academic Publishers, 1996.

International Journal of Modern Engineering Research (IJMER)
www.ijmer.com Vol. 3, Issue. 3, May - June 2013 pp-1837-1842 ISSN: 2249-6645

Reduction of the losses on the electric distribution network Low tension of the Beninese Company of Electrical energy (SBEE)

Houndedako Sossou[1], Dai Tometin Derrick[1], Chetangny K. Patrice[2], Espanet Christophe[2]

[*]*Laboratoire d'Electrotechnique, de Télécommunication et d'Informatique Appliquée (LETIA)*
Ecole Polytechnique d'Abomey-Calavi, Université d'Abomey-Calavi 01 BP 2009 Cotonou, Bénin.
[**]*FEMTO-ST Département Energie, Université de Franche-Comté, France.*
2, Avenue Jean Moulin 90000 Belfort, France

ABSTRACT: *The authors approached in this article, the problems of the losses on the distribution network of electrical energy of the Beninese Company of Electrical energy more precisely in district NVENOUMEDE and various approaches for their minimization.*

According to the international standards in force, the maximum voltage drop of a network should not exceed 10% of the nominal voltage. At the conclusion of measurements taken by the authors, the voltage drop is about 79,52% between phase and neutral and of 68,42 between phases. Thus, the network causes enormous nuisances to the subscribers and maintains a permanent conflict between supplier and consumers.

The various approaches simulated by the authors made passed the voltage drop fall of phase from 79,52% to 10,75% and the losses active from 243 kW to 33 kW respectively variations of 86,5% and 92,12%.

KEYWORDS: *Dispersed PV Generation, Distribution network, Energy losses, Network reconfiguration, Voltage drop*

I. INTRODUCTION

The voltage drop and the active losses of an electrical distribution network are very important factors of appreciation of the quality of energy provided by a distributer. In the cities of the commune of Abomey Calavi, the quality of distributed energy is strongly threatened. Inadmissible voltage drops are regularly recorded. The measuring devices give 60 V for the measurements taken between phase and neutral instead of 220 V while for measurements between phases, we often read 120 V instead of 380 V.

Taking into account the dearness of electrical energy, the distributer is held to at least limit the losses of energy on its network. According to [1], [2], [3], [4] and [5], the reconfiguration of the network is a good alternative for the distributer, because it makes it possible to reduce the active power, to balance the loads of the system, to improve the profile of voltage in the nodes, to increase the safety and the reliability of the system, just as the improvement of the quality of power. Several forms of reconfiguration can be considered, in particular the displacement of the separation points, the adjustment of the taps.

In this document, the authors proposed the reconfiguration of low voltage (LV) distribution network, mainly by building new high voltage (HV) lines and also identifying the node of the center of gravity of the loads where the transformer must be connected; then, the authors suggested the connection of photovoltaic mini-power stations to the network studied to precise nodes [6].

The undertaken study and the results obtained are based on the real problems encountered on the LV electric line which feeds zone Pk 14 of district NVENOUMEDE of the commune of Abomey-Calavi.

II. Material and methodology

II.1 Characteristics of the studied network: The characteristics of the studied network are summarized in table 1:

Table 1: General characteristics of LV network of Nvènoumèdé and of transformer HV/LV

	Parameters	**Value**
Nodes	Nodes number	132
Line	LV customers number	2632
	Current called at the peak	391 A
	Developed length of feeder	6864 m
	Length of the most distant point	2022 m
	Section of lines	50 mm²
Transformer	Primary voltage (kV)	15
	Secondary voltage (V)	400
	Nominal power (kVA)	400
	Voltage of short-circuit	4%
	No-load Losses (W)	460
	No-load current (nominal In)	2,3%

II.2 Mathematical formulation of the objective to be optimized: The problem of optimization is related to one or more objectives which one tries to minimize (or to maximize). The main objective that the authors considered is: the minimization of the losses Joules. They expressed this objective by mathematical expressions which are integrated in the algorithms of optimization.

II.2.1 The losses Joules: To express this objective in an algorithm of optimization, the authors used the expression:

$$f_{objectif} = \sum_{k} R_k . I_k^2 \quad (1)$$

where: R_k : the resistance of the branch K;

I_k: the module of the complex current in the branch K;

To minimize the expression (1) led to a reduction of one of the costs of exploitation.

II.2.2 Formulation of the constraints of safety: *The constraints of safety* are the constraints related to the voltage on the level of each node of the network and with the currents on each branch of the network.

II.2.3 Amplitude of the voltage: It is necessary thus, when we seek a network configuration, that the voltage in each node lies between $V_{nominal} = \pm 5\,\%$ for HV distribution network and $U_{nominal} = +6 \text{ and } -10\,\%$ for LV distribution network (according to the European and French standard in particular). This constraint is expressed by the expression:

$$\frac{V_{in} - V_i}{V_{in}} < \varepsilon_{i\ max} \quad (2)$$

where : V_{in} : nominal voltage to node i

V_i : module of voltage to node i

$\varepsilon_{i\ max}$: variation of maximum voltage acceptable

II.2.4 Acceptable currents: The constraint of safety is related to the currents on the branches which should not exceed the acceptable maximum currents in permanent mode, guaranteed by the manufacturers. It is expressed by the relation:

$$\frac{|I_j|}{I_{j\max\ adm}} < 1 \quad (3)$$

where I_j: the current on the branch j

$I_{j\max\ adm}$: the acceptable maximum current in the branch j

II.3 Modeling of the network: Fig.1 presents the studied network, which was entirely modeled under NEPLAN. The course of LV network to its various nodes was raised with a GPS. Fig.2, always result obtained under software Neplan shows the level of voltage drop of the network in its actual position. This voltage drop varies from 10,12 to 79,52%. The more we move away from the transformer, the more the value of the voltage drop moves away from the value fixed by the standard.

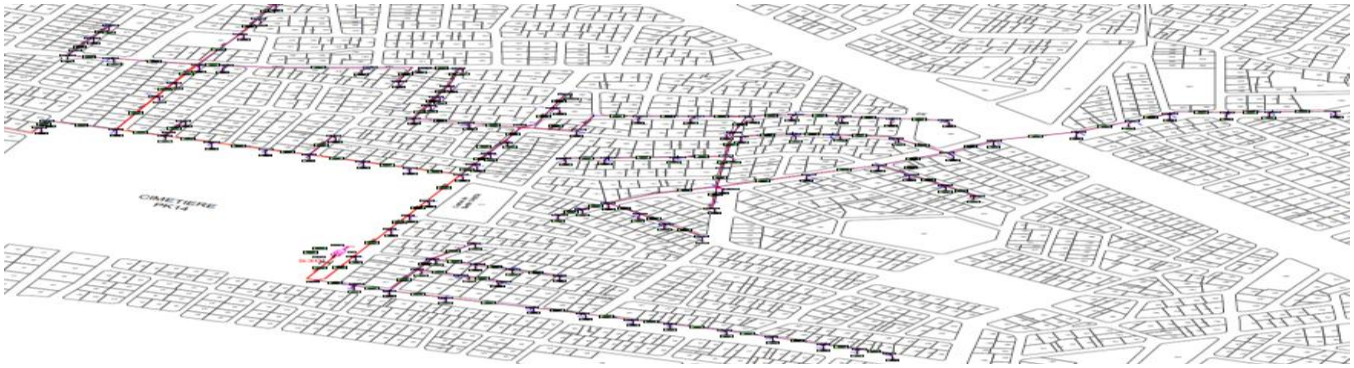

Figure 1: Model of the configuration of LV network of Nvènoumèdé PK 14 obtained under NEPLAN

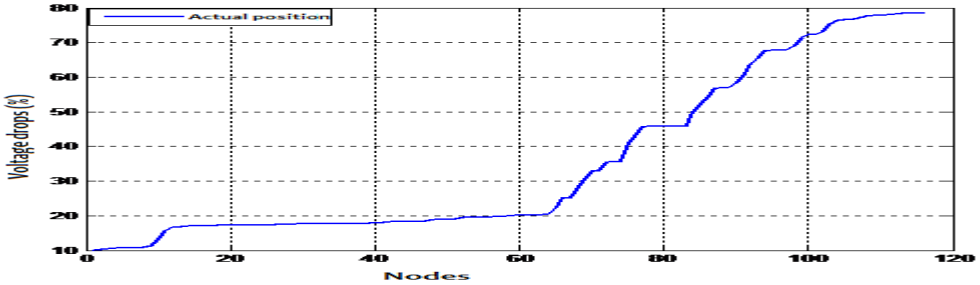

Figure 2: Actual position of LV network in three-phase current

With the analysis of these two figures we note the influence of two factors on the technical performances of the distribution network:

II.3.1 Structural factor: The structure and the characteristics of the low voltage network studied presents an irregular distribution over a length of network of approximately 6 km which outdistance the consumers of more than $2\ km$ of the transformer for wires whose section is of $3 \times 50\ mm^2$. That leads to inadmissible voltage drops.

The voltage drop in a line is evaluated by the vectorial representation of Fig.3.

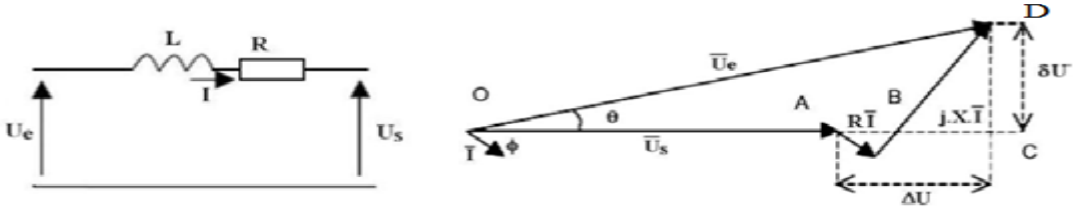

Figure 3: Vectorial representation of the voltage drop

In practice, we can admit that the voltage OC = OD and voltage drop in the wires are represented by AC. Thus, we can write: $AB = RI \times \cos\Phi$ (4)

$$BC = L\omega I \times \sin\Phi \quad (5)$$

$$AC = AB + BC = I \times (R\cos\Phi + L\omega\sin\Phi) \quad (6)$$

Thus, the voltage drop in the wire Δu is expressed by the following equation:

$$\Delta u = I \times (R\cos\Phi + L\omega\sin\Phi) \quad (7)$$

Where, R is the resistance of wire (Ω), $L\omega$ the inductive reactance of the wire (Ω), I the current (A) and Φ dephasing. The relation of the voltage drop depends on type of line to knowing single-phase or three-phase. Then, for a single-phase line, the equation is given by:

$$\Delta u = 2I \times (R\cos\Phi + L\omega\sin\Phi) \quad (8)$$

For a balanced three-phase line, the equation is given by:

$$\Delta u = 3I \times (R\cos\Phi + L\omega\sin\Phi) \quad (9)$$

In these case, the line of distribution is three-phase and the expression of the current can be given by:

$$I = \frac{P}{U\sqrt{3}\cos\emptyset} \quad (10)$$

where, P is the power (W) and U the voltage (V).

Thus, the equation (10) can be represented by the following equation:

$$\Delta u = \frac{P}{U}\sqrt{3}(R + L\omega\tan\emptyset) \quad (11)$$

From this equation, we deduce the following equation:

$$\frac{\Delta u}{u} \times 100 = 100\frac{P}{U^2}\sqrt{3}(R + L\omega\tan\emptyset) \quad (12)$$

However $R = r \times l$ and $L = x \times l$

The expression (12) becomes:

$$\frac{\Delta u}{u} \times 100 = 100\frac{P}{U^2}\sqrt{3}(r + x\omega\tan\emptyset) \times l \quad (13)$$

With, P is the power in Watts, U the voltage in volts, R and $L\omega$ in Ω.

While expressing R and $L\omega$ in Ω/km and the length of the line by l, the preceding equation becomes:

$$\frac{\Delta u}{u} \times 100 = 100\frac{P \times l}{U^2}(R + L\omega\tan\emptyset) \quad (14)$$

II.3.2 Demographic factor : The district Nvènoumèdé PK14, there is still that a few years, was tiny room to a population installed in the perimeters of cemetery PK14 close to the inter-states road Cotonou-Lome. But today it largely extended with a strong population which does not cease increasing. This situation contributes to the continuous degradation of the functional parameters of the network and influences negatively the quality of the electrical energy provided to the consumers exposed thus to frequent disturbances.

II.3.3 Influence of photovoltaic voltage injected on the voltage of the network: The contribution of the voltage provided by the photovoltaic system is the difference between the voltage drop (ΔV) in the line with and without a photovoltaic generator. The relation of the voltage drop at the end of a balanced three-phase line having length l is given as follows:

$$\Delta V = \int_0^x I(l)Z(l)dl \quad (15)$$

with, the current (I) and impedance (Z) function of the length (l) of the line.

A photovoltaic generator reduced the voltage drop by reducing the current which forwards by the line. The contribution of the voltage by the photovoltaic system in a given point, example of the point (B) of Fig.4, is the difference in voltage drop with and without photovoltaic system:

$$\Delta V_B = \int_0^A [I(l) - I_{pv}] Z(l)\, dl + \int_A^B I(l)\, Z(l)\, dl \qquad (16)$$

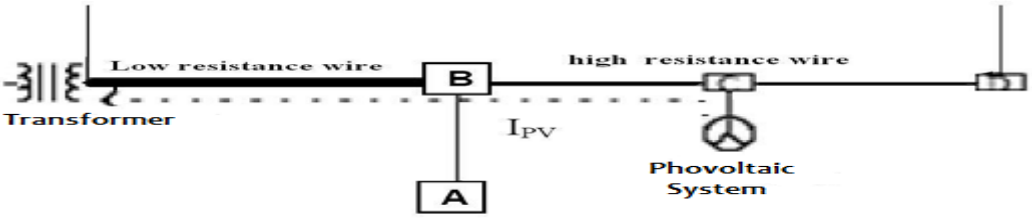

Figure 4: Photovoltaic voltage injected in the electrical line

As the current provided by the photovoltaic generator is constant, the equation (13) can be written as follows:

$$\Delta V_B = \int_0^B I(l)\, Z(l)\, dl - I_{pv} Z_A \qquad (17)$$

where Z_A is the total impedance of the line of transformer up to point A.

The contribution of the voltage of the photovoltaic generator is given by the following relation:

$$VS_B = I_{pv} Z_A \qquad (18)$$

Thus, the contribution of the photovoltaic tension at any point of the line is equal to the product of the photovoltaic current and the impedance of the line between the transformer and the photovoltaic generator.

III. RESULTS

III.1 Simulation with displacement of the transformer: With an aim of reducing the associated costs to the creation of a new transformer we analyzed the option of a simple optimal displacement of the existing transformer named Pk14 and calculated the level of improvement that could bring.

The curve of Fig.5 shows that for this option, the voltage drop expressed in % is reduced meadows of half, but still not meeting the standards in force.

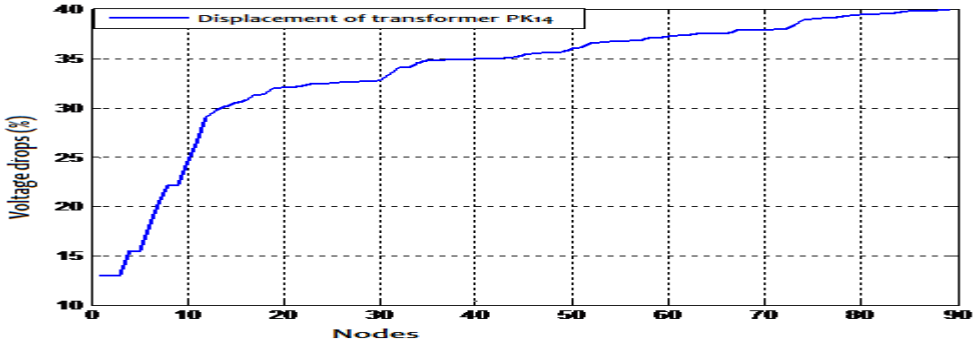

Figure 5: Variation of the voltage drop according to the nodes (case of reconfiguration by displacement of the initial station)

III.2 Simulation with displacement of transformer plus injection of an autonomous source:

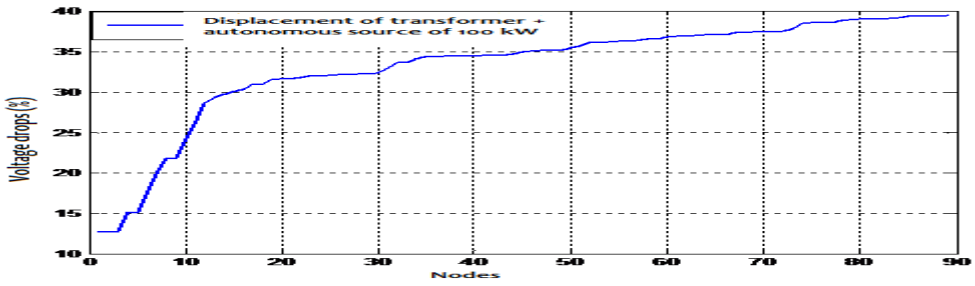

Figure 6: Variation of the voltage drop according to the nodes (case of reconfiguration by displacement of the initial transformer plus injection of an autonomous source)

The shape of the curve of Fig.5 and the level of the voltage drops show that the situation remains unchanged and the voltage drop to the node more degraded remains important, that is to say approximately 40%.

III.3 Simulation of the actual position plus creation of new transformer : While maintaining the initial transformer to its current location, we sought the most optimal position of the new transformer which would improve the tension with all the nodes and which would discharge the current transformer and the derivation low tension lines affected as shown in the Fig.7. The latter indicates the choice of the position of the new transformer.

.

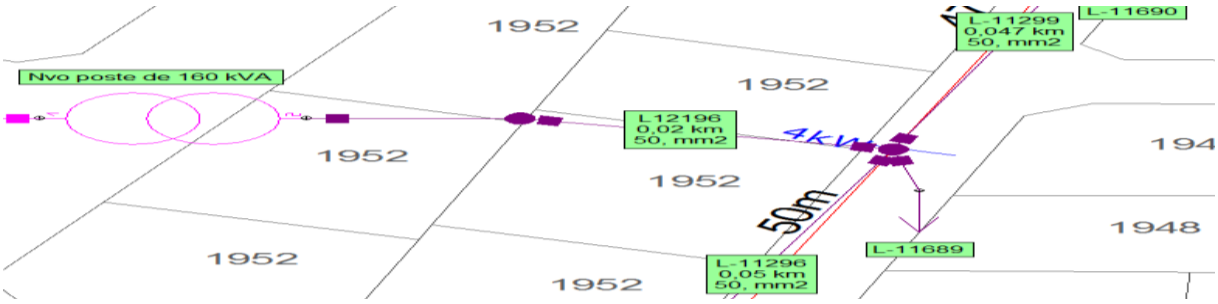

Figure 7: Choice of the position of the new transformer

With this position chosen, we successively connected the transformers of 50 kVA, 100 kVA and of 160 kVA and each time we compared the load circulating with the normal load which the initial transformer of 400 kVA can support. Results obtained, only the transformer of 160 kVA enables us to satisfy this condition and to reduce the voltage drops to the node more degraded to 10.75%. The results obtained of this simulation made it possible to plot the curve of Fig.8 which is variation of the voltage drop according to the nodes (case of reconfiguration with transformer).

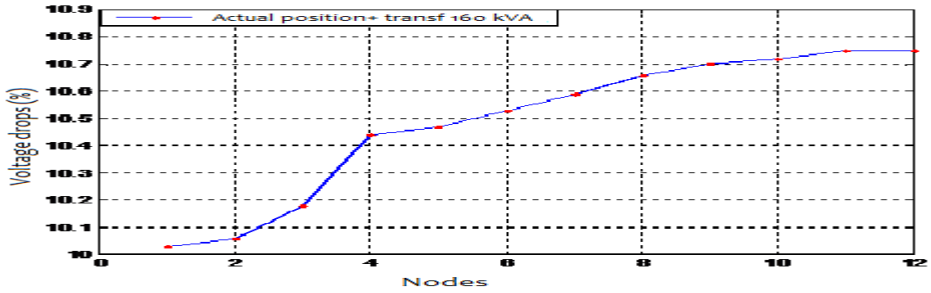

Figure 8: Variation of the voltage drop according to the nodes (case of reconfiguration with transformer)

However this option would suffer in the event of degradation from the voltage source coming from the Electric Community of BENIN (CEB) and which drops sometimes in lower part of 20%. Thus, the authors have proposed the autonomous addition of source for better appreciating the profile of the voltage drop.

III.4 Simulation of the actual position plus an additional autonomous PV source: Consequently we sought to replace the transformer by an autonomous additional source and to carry out a new simulation. This time we successively injected powers of 50.75 and 100 kW. Fig.9 shows the evolution of the voltage drop for these various powers.

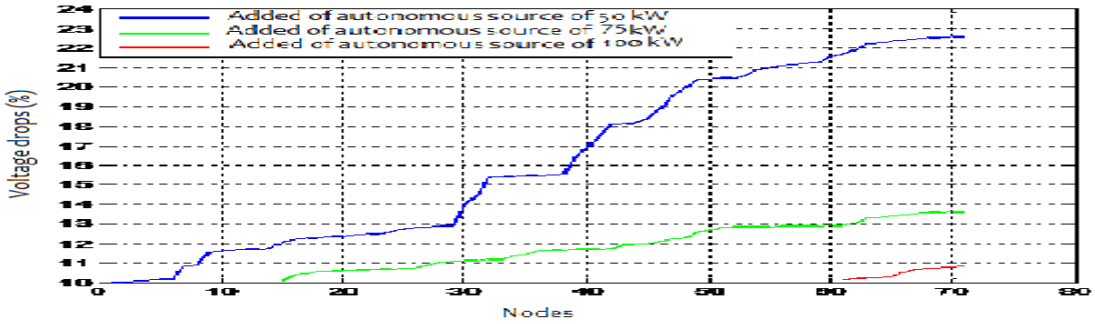

Figure 9: Evolution of the voltage drop with variation of the power of the autonomous source

III.5 Synthesis of the analyzes of simulation: To carry out the best alternative of solution to be applied to give satisfaction to the zone Pk14, we established the layout of Fig.10 which gathers the results of all simulations carried out (variation of the voltage drop according to the nodes) as well as the impact of improvement that they bring.

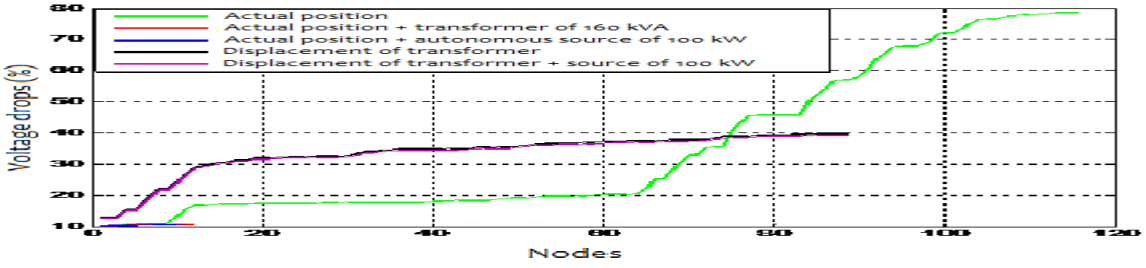

Figure 10: Variation of the voltage drop according to the nodes (case of all simulations carried out**)**

The levels of satisfaction justifying our choice and which also reduces the level of the active losses in the network are consigned in table 2.

Table 2: Important results of various simulations

	Actual position	Actual position + station of 160 kVA	actual position + autonomous source of 100 kW	Displacement of the station	Displacement of the station + autonomous source of 100 kW
Number affected nodes	116	12	11	89	89
Number overloaded elements	32	0	0	12	12
Level of load of the principal station	113 % 485.9 kW	68.37% (294 kW)	86.27% (371 kW)	107.67% (463 kW)	87.9% (378 kW)
Active losses	243 kW	33 kW	37 kW	57 kW	49 kW
Minimal voltage drop	10.01	10.03	10.12	13.01	12.72
Maximum voltage drop	79.52	10.75	10.82	39.04	39.39

IV. DISCUSSION

Analysis of the summary graph of Fig.10, it arises that only the solutions of creation of new transformer of 160 kVA or injection of autonomous additional source of power 100 kW make it possible to improve quality of the voltage and the energy distributed in the zone of Nvènoumèdé Pk14.

Because of quality sometimes degrading (although rare) of source from CEB, the solution which consist to inject additional autonomous source of 100 kW appears the best satisfactory to us.

It appears, when the length l of the dipole or the resistance of cable, or the power called increase, the drop voltage increases proportionally. But it decreases proportionally with the square of the tension. It is what explains the voltage drops on the network studied of Nvènoumèdé and which vary from 10 to 79,56% as we move away from the transformer; this also explains the nuisances related to the bad quality of the power provided to the customers.

V. CONCLUSION

The results obtained for the two types of possible solutions are very satisfactory. The insertion of the photovoltaic systems in the electrical distribution network improves the voltage in end of network and decreases the current forwarded by the line.

Thus, it is shown by various simulations which as well the insertion of the photovoltaic renewable energy sources as the creation of a new station can have the same technical repercussions on BT network.

The choice between the two solutions will take place only after the economic evaluation of the two systems. The economic evaluation will have the aim of determining the costs of each approach.

REFERENCE

[1]. M. E. Baran, and F. F. Wu, Network Reconfiguration in Distribution Systems for Loss Reduction and Load Balancing, IEEE Transaction on Power Delivery, vol. 4(2), 1989, 1401-1407.
[2]. J. S. Savier and D. Das, Impact of Network Reconfiguration on Loss Allocation of Radial Distribution Systems, IEEE Transaction on Power Delivery, vol. 22(4), 2007, 2473 2480.
[3]. M. A. Kashem, V. Ganapathy and G. B. Jasmon, Network Reconfiguration for Load Balancing in Distribution Networks, IEE Proceeding of Generation Transmission and Distribution, vol. 146(6), 1999, 563- 567.
[4]. S. Civanlar, J. J. Grainger, H.Yin, and S. S. H. Lee, Distribution Feeder Reconfiguration for Loss Reduction, IEEE Transaction on Power Delivery, vol. 3(3), 1988, 1217–1223.
[5]. D. Shirmohammadi and H. Wayne Hong, Reconfiguration of Electric Distribution Networks for Resistive Line Losses Reduction, IEEE Transaction on Power Delivery, vol.4(2), 1989, 1492-1498.
[6]. P. Poggi, M. Muselli, N. Stefka and Nedeltcheva, Reducing Voltage Drops at the End of the Feeder by Grid–Connected Rooftop PV Systems for: Case Study in Corsica Island, Energy, Vol. 25(8), 2000, 741 - 756.

International Journal of Modern Engineering Research (IJMER)
www.ijmer.com Vol. 3, Issue. 3, May - June 2013 pp-1843-1846 ISSN: 2249-6645

Human Detection, Tracking and Trajectory Extraction in a Surveillance Camera network

Peyman Babaei
Dep. of Computer, West Tehran Branch, Islamic Azad University, Tehran, Iran

ABSTRACT: *This paper proposes human tracking and recognition method in a camera network. Human matching in a multi-camera surveillance system is a fundamental issue for increasing the accuracy of recognition in multiple views of cameras. In camera network, videos have different characteristics such as pose, scale and illumination. Therefore it is necessary to use a hybrid scheme of scale invariant feature transform to detection and recognition human's behaviors. The main focus of this paper is to analyze activities for tracking and recognition humans to extract trajectories. Extracting the trajectories help to detect abnormal behavior which may be occluded in single- camera surveillance.*

KEYWORDS: *Camera network, Multi-camera surveillance, Human's behavior, Trajectories extraction.*

I. INTRODUCTION

Tracking and behavior recognition are two fundamental tasks in video surveillance systems which are widely employed in commercial applications for purposes of statistics gathering and processing. The number of cameras and complexity of surveillance systems have been continuously increasing to have better coverage and accuracy. Multi-camera systems become increasingly attractive in machine vision. Applications include multi view object tracking, event detection, occlusion handling and etc. In this paper, we develop method for tracking and recognition by a traffic video surveillance system of two cameras with a partially overlapping field of view.

This paper is organized as follows: an overview of the past works in section2. Our proposed architecture and algorithm is presented in section3. Results of subjective evaluations and objective performance measurements with respect to Ground-truth are presented in section4. Section5 contains the conclusion.

II. PAST WORKS ON MULTI-CAMERA SURVEILLANCE

In the last few years, a lot of works in detecting, describing and matching feature points has deployed. In a camera network features' matching between multiple images of a scene is an important component of many computer vision tasks. Although the correspondences can be hand selected, such a procedure is hardly conceivable as the number of cameras increases or when the camera configuration changes frequently, as in a network of pan-tilt-zoom cameras [1]. Other methods for finding correspondences across cameras [2] have been developed through a feature detection method such as the Harris corner detection method [3] or scale invariant feature transform [4]. In [5] shown that corners were efficient for tracking and estimating structure from motion. A corner detector is robust to changes in rotation and intensity but is very sensitive to changes in scale. The Harris detector finds points where the local image geometry has high curvature in the direction of both maximal and minimal curvature, as provided by the eigen-values of the Hessian matrix. They develop an efficient method for determining the relative magnitude of the eigen-values without explicitly computing them. Such color-based matching methods have also been used to track moving objects across cameras [6, 7]. Scale invariant features matching were first proposed in [8] and attracted the attention of the computer vision systems for invariant to scale, rotation, and view-point variations. Also uses a scale-invariant detector in the difference of Gaussian (DOG) scale space. In [4] fits a quadratic to the local scale-space neighborhood to improve accuracy. Then creates a Scale Invariant Feature Transform descriptor to match key-points using a Euclidean distance metric in an efficient best-bin first algorithm where a match is rejected if the ratio of the best and second best matches is greater than a threshold.

A comparative study of many local image descriptors [9] shows the superiority of this method with respect to other feature descriptors for the case of several local transformations. In [10] develop a scale-invariant Harris detector that keeps key points at each scale only if it's a maximum in the Laplacian scale-space [11]. More recently, in [12] integrate edge-based features with local feature-based recognition using a structure similar to shape contexts [13] for general object-class recognition. In [14] propose a matching technique based on the Harris corner detector and a description based on the Fourier transform to achieve invariance to rotation. Harris corners are also used in [15], where rotation invariance is obtained by a hierarchal sampling that starts from the direction of the gradient. In [16] introduce the concept of maximally stable external region to be used for robust matching. These regions are connected components of pixels which are brighter or darker than pixels on the region's contour; they are invariant to affine and perspective transform, and to monotonic transformation of image intensities. Among the many recent works populating the literature on key-point detection, it is worth mentioning the scale and affine invariant interesting points recently proposed in [17], as they appear to be among the most promising key-point detectors to date. The detection algorithm can be sketched as follows: first Harris corners are detected at multiple scales, and then points at which a local measure of variation is maximal over scale are selected. This provides a set of distinctive points at the appropriate scale. Finally, an iterative algorithm modifies location, scale, and neighborhood of each point and converges to affine invariant points. In [18] describe a matching procedure wherein motion trajectories of objects tracked in different cameras are matched so that the overall ground plane can be aligned across cameras following a homograph transformation [19-21].

III. PROPOSED ARCHITECTURE

First, we review the function of a typical single-camera and multi-camera surveillance system as presented in our previous work [22], the function of a typical single-camera surveillance system is illustrated in Fig.1. The first part of the processing flowchart is very general, which is marked "Detecting & Matching Features Extraction Pipeline". This pipeline may produce all target information (pose, scale, illumination, color, shape, etc.), and potentially the description of the scene. The end of the processing pipeline, the human tracking and classification is done.

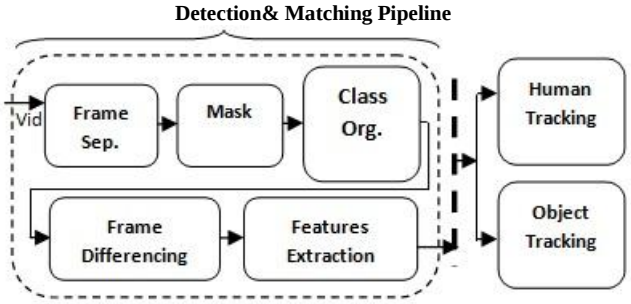

Fig. 1: Single Camera Processing

Only the matching features have to be stored, instead of high quality video suitable for automated processing. This method enables the multi-camera surveillance system. The video surveillance system, as described in the above, cannot provide an adequate solution for many applications [23-27]. A multi-camera surveillance system tracking targets from one camera to the next can overcome all these limitations. A typical multi-camera surveillance network is illustrated in Fig.2. Fusing at the matching features level requires merging all the features from the cameras on to a full representation of the environment. This approach distributes the most time consuming processing between the different cameras, and minimizes communication, since only the extracted features needs to be transmitted, no video or image. Given these advantages, system communicates only the matching features for fusion.

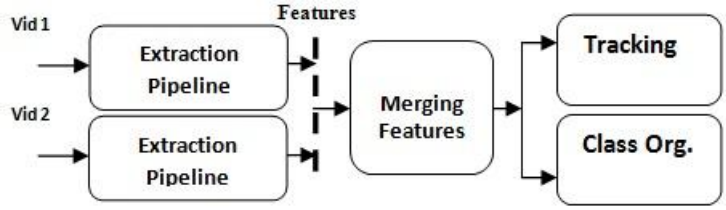

Fig. 2: Multi camera network Processing

The problem of multi-view activity recognition has been addressed in many papers, but almost the information of multiple views is fused centrally. Our proposed framework is decentralized. The pose of cameras at intersection is shown in Fig.3.

Fig 3: Camera setup in a network

In Fig.4, the structure camera network is illustrated. Each of the cameras has processing cores in four levels. The input stream is fed to detection level. At the decision level, control commands are issued to classify the detected human based on extracted description features. Processing cores in three upper levels exchange the requisite information to track and recognition more accurately.

Fig 4 Structure camera network

The Scale Invariant Feature Transform has been shown to perform better than other local descriptors [9]. Given a feature point, the descriptor computes the gradient vector for each pixel in the feature point's neighborhood and builds a normalized histogram of gradient directions. The descriptor creates a neighborhood that is partitioned into sub-regions of 4×4 pixels each. For each pixel within a sub-region and adds the pixel's gradient vector to a histogram of gradient directions by quantizing each orientation to one of 8 directions and weighting the contribution of each vector by its magnitude. Principle features of our scheme are summarized as Communication Efficiency: camera network is particularly well-suited for low bandwidth; and unsupervised: the method does not require the pre-calibration into the scene and, hence, can be used in traffic scenes where the system administrator may not have control over the activities taking place. Fig.5 shows the matching results using descriptor created for a corresponding pair of points.

Fig 5 Matching results using descriptor.

IV. EXPERIMENTAL RESULTS

We have experimented with various feature detectors including the Harris corner detector (HCD), curvilinear structure detector (CSD), and difference of Gaussian (DoG) scale space. In Fig.6, the experimental result contain the comparison of these methods is shown. We showed that suing SIFT point descriptors in a camera network can improves the performance with respect to the other calibration systems. Here it is shown that descriptor lead to excellent performances compared to other existing approaches. As explained, description is computed as follows: once a key-point is located and its scale has been estimated, one or more orientations are assigned to it based on local image gradient direction around the key-point. Then, image gradient magnitude and orientation are sampled around the key-point, using the scale of the key-point to select the level of Gaussian blur. The gradient orientations obtained are rotated with respect to the key-point orientation previously computed. Finally, the area around the key-point is divided in sub-regions, each of which is associated an orientations histogram weighted with the magnitude.

Table1: Number of matching by features descriptors.

True Positive & False Positive					
S1 Results (number of occlusion: 31)			**S2 Results (number of occlusion: 23)**		
t **seconds**	**True Positive**	**False Positive**	***t*** **seconds**	**True Positive**	**False Positive**
120s	8	0	120s	4	0
180s	10	0	180s	12	0
240s	17	0	240s	17	0
300s	22	1	300s	27	1
360s	33	1	360s	31	1
420s	45	2	420s	38	1
480s	52	3	480s	41	2

In table2 counting and classification results are presented. As shown, the overall accuracy is about 90% for using DOG detector in counting cars and about 94% for Bus and Trucks. This system can be as an input to calibration system in multi-camera surveillance system.

Table2. Counting and classification results

Number of object matching by algorithm						
Algorithm	**Objects**			**Human**		
	Count	**Video**	**Acc.**	**Count**	**Video**	**Acc.**
DoG	61	73	83%	53	56	94%
HCD	68	73	93%	55	56	98%
CSD	67	73	91%	54	56	96%

V. CONCLUSION

In this paper we considered the problem of features matching in a camera network with overlapping fields of view. We showed that suing SIFT point descriptors in a camera network can improves the performance with respect to the other calibration systems. In particular it returned good results for scale changes, zoom and image plane rotations, and large view-

point variations. These conclusions are supported by an extensive experimental evaluation, on different scenes. Therefore, tracking and recognition using SIFT becomes feasible. This should result in highly robust trackers.

ACKNOWLEDGEMENTS

This work was supported by Islamic Azad University, West Tehran Branch.

REFERENCES

[1]. Z.Fu, W.Hu and T.Tan, "Similarity Based Vehicle trajectory clustering and Anomaly Detection", In Proc. Intl. Conf. on Image Processing (ICIP'5), Vol 2, pp.602-605, 2005.
[2]. T.V.Mathew and K.V.Krishna Rao, "Introduction to Transportation Engineering." Chapter 39,'Traffic Intersections', NPTEL, 2007.
[3]. P.Babaei and M.Fathy,"Multi-Camera Systems Evaluation in Urban Traffic Surveillance versus Traditional Single-Camera Systems for Vehicles Tracking," 3rd International Conference on Computer and Electrical Engineering (ICCEE 2010), vol.4, pp.438-442, 2010.
[4]. P.Babaei and M.Fathy, "Vehicles tracking and classification using traffic zones in a hybrid scheme for intersection traffic management by smart cameras", In IEEE Conf. on Signal and Image Processing, (ICSIP 2010), pp. 49–53, 2010.
[5]. T.Bouwmans, F.E.Baf and B.Vachon, "Background modeling using mixture of Gaussians for foreground detection: a survey", In proc of Patents on Computer Science 1, pp.219–237, 2008.
[6]. M.A.Najjar, S.Ghosh and M.Bayoumi, " A Hybrid adaptive Scheme based on selective gaussian modeling for real time object detection", In IEEE Symp. Circuit and systems, pp.936-939, 2009.
[7]. S.S.Cheung and C.Kamath, "Robust techniques for background subtraction in urban traffic video," EURASIP J.Applied Signal Processing, vol. 5, pp. 2330-2340, 2005.
[8]. E.B.Ermis, P.Clarot, P.Jodoin, "Activity Based Matching in Distributed Camera Networks," IEEE Transaction on Image Processing, vol. 19, no. 10, OCT. pp.2595–2613, 2010.
[9]. D.Devarajan, Z.Cheng, and R Radke, "Calibrating distributed camera networks," Proc. IEEE, vol. 96, no. 10, pp. 1625–1639, OCT. 2008.
[10]. C.Harris and M.Stephens, "A combined corner and edge detector," in Proc. of 4th Alvey Vision Conf., pp. 147–151, 1988.
[11]. D.Lowe,"Distinctive image features from scale-invariant keypoints,"In Int. J. Comput. Vis., vol.60, no.2, pp. 91–110, 2004.
[12]. B.Song and A.R.Chowdhury,"Stochastic adaptive tracking in a camera network," in Proc.IEEE Int.Conf.Computer Vision, pp.1–8, 2007.
[13]. S.Khan and M.Shah,"Tracking multiple occluding people by localizing on multiple scene planes,"IEEE Trans. Pattern Anal. Mach. Intell.,vol. 31, no. 3 , pp. 505–519, Mar. 2009.
[14]. D.G.Lowe, "Object recognition from local scale-invariant features," in Proc. of ICCV, pp. 1150–1157, 1999.
[15]. K.Mikolajczyk, C.Schmid,"A performance evaluation of local descriptors," in Proc. Of CVPR, 2003, pp. 257–263.
[16]. K.Mikolajczyk and C.Schmid, "Indexing based on scale invariant interest points," in Proc. Of ICCV, pp. 525-531, 2001.
[17]. T.Lindeberg, "Feature detection with automatic scale selection," in Proc. Of IJCV, vol. 30, no.2, pp.79-116, 1998.
[18]. K.Mikolajczyk, A.Zisserman,"Shape recognition with edge-based features," in Proc. of the British conf. Machine Vision 2003.
[19]. S.Belongie, J.Malik and J.Puzicha, "Shape context: A new descriptor for shape matching and object recognition," in Proc. of NIPS, pp. 831-837, 2000.
[20]. A.Baumberg,"Reliable feature matching across widely separated views," in Proc. of CVPR, pp.774– 781, 2000.
[21]. N.Allezard, M.Dhome, F.Jurie,"Recognition of 3D textured objects by mixing view-based and model based representations," in Proc. of ICPR, 2000.
[22]. J.Matas, O.Chum, M.Urban, T.Pajdla,"Robust wide baseline stereo from maximally stable external regions," in Proc. of BMVC, pp. 384–393, 2002.
[23]. K.Mikolajczyk, C.Schmid,"Scale and affine invariant interest point detectors,"In Int. Com. Vis. Vol. 60, no.1, pp. 63–86, 2004.
[24]. L.Lee, R.Romano, and G.Stein,"Monitoring activities from multiple video streams: Establishing a common coordinate frame," IEEE Trans.Pattern Anal.Mach Intell., vol.22, no.8, pp.758–767, Aug. 2000.
[25]. X.Wang, K.Tieu, and E.Grimson,"Correspondence-free activity analysis and scene modeling in multiple camera views," IEEE Trans. Pattern Anal. Mach. Intell., vol.32, no.1, pp.56–71, Jan. 2010.
[26]. D.Makris, T.Ellis, and J.Black, "Bridging the gap between cameras," in Proc. of CVPR, vol. 2, pp. 205–210, 2004.
[27]. T.Chang and S.Gong, "Tracking multiple people with a multi-camera system," in Proc. Of IEEE Multi-Object tracking, pp. 19–26, 2001.

International Journal of Modern Engineering Research (IJMER)
www.ijmer.com Vol. 3, Issue. 3, May - June 2013 pp-1847-1849 ISSN: 2249-6645

Phytochemical Investigation of 9, 10-Dimethoxy-2-Methyl-1, 4-Anthraquinone, A Compound of Tectona Grandis

Manoj Kumar[1], Nempal Singh[2], L.P. Singh[1], Sachin Kumar[2], Nishi[2]
[1]*Dept. of Chemistry, R.B.S. College Agra, U. P.*
[2]*Dept. of Applied Science, Indraprastha Inst. of Technology, Amroha, U. P.*

ABSTRACT: *In this paper we have reported the Phytochemical investigation of 9, 10-Dimethoxy-2-methyl-1,4-anthraquinone which is a secondary compound of Tectona Grandis. The crushed plant material has been extracted with different organic solvents with increasing polarity. The extract then subjected to column chromatography in order to get pure organic constituents. The purity of compounds has been checked by qualitative TLC. The pure compound is then subjected to structural characterization to establish their structures.*
KEYWORDS: *Tectona Grandis, Phytochemical, Verbenaceae*

I. INTRODUCTION

Phytochemistry plays an important role in medicinal chemistry. In India, extreme variations of climate and geographic conditions, provide rich vegetation comprising 1,30,000 species of plants belonging to about 120 families and at least 24,000 of these plants have been used in indigenous Ayurvedic and Unani systems of medicine. Isolation of active principles which possess anti-cancer, anti-inflammation, antileprosy, antifertility and wide range of biological properties from aromatic and medicinal plants and their successful utilization to alleviate human suffering have encouraged research workers to continue investigation of new drugs from the plant kingdom with an ever increasing zeal. As a result, phytochemical research has made tremendous progress in recent times and a very large number of new secondary metabolites viz. alkaloids, terpenoids, steroids, flavonoids and related phenolic compounds, tannins, cumarins, quinones etc. have been discovered. Some of the notable discoveries in medicinal chemistry are : the isolation of the sedative reserpine, antidysentric emetine, antibiotics coumaromycine and novobiocin, antimalarial quinine, antileukemic drug vincristine, pain killer morphine, anticoagulant dicoumarol and tumor-damaging compounds of the podophyllotoxin group. Besides, some of the plant products are readily convertible to valuable drugs e.g. digitalin, a steroidal glyceride of *Digitalis purpurea*, constitutes an important intermediate in the preparation of a number of steroidal hormones. Also well known are number of plant-derived insecticides of the rotanoid group and various plant hormones.

Inspite of all efforts carried out so far, a vast majority of the terrestrial flora remains yet to be explored. More recently, this field has made tremendous progress due to the advent of modern scientific technology which has been revolutionized during last few decades with the introduction of more sophisticated instruments carrying out more precise work. At the central Drug Research Institute at Lucknow, an extensive screening programme of Indian medicinal plants has been in operation for the last several years.

***Tectona grandis* Linn.**

Family	–	Verbenaceae
Genus	–	*Tectona*
Species	–	*grandis*

Tectona grandis Linn. popularly known as teak or 'Sagwan' is a huge tree which occurs throughout the country. It is one of the best timbers valued for high class furniture and is extensively used for the cabinet making. The powder of teak wood is used in skin inflation caused by Melanorrhoea usitatissema. The oily product of wood chips is used for the treatment of eczema and ring worm. Earlier work on this plant led to the isolation of a number of quinones and related compounds. Re-investigation of this plant yielded four known compounds alongwith a new 1,4-antraquinone derivative. The hot petrol-ether (60-80º) extract of the stem heartwood on column chromatography and preparative TLC separation gave following compounds :

1. Lapachol (2-hydroxy-3—[3-methyl-2-butenyl]-1,4-napthoquinone) : $C_{15}H_{14}O_3$
2. Tecomaquinone I : $C_{30}H_{24}O_4$
3. Tectoquinone : $C_{15}H_{10}O_2$
4. Dehydro-α-lapachone : $C_{15}H_{12}O_3$
5. 9, 10-Dimethoxy-2-methyl-1,4-anthraquinone : $C_{17}H_{14}O_4$

In this paper we have limited our study to the Phytochemical investigation of 9, 10-Dimethoxy-2-methyl-1,4-anthraquinone ($C_{17}H_{14}O_4$) only.

II. EXPERIMENTAL DETAILS

II.1. Sample preparation: The air dried coarsely powdered heartwood shavings were extracted with light petrol on steam bath for 3 x 12 hours. The resulting extract was taken in ether and then separated into acidic and neutral fractions by extracting with Na_2CO_3 solution. The acidic and neutral fractions were examined separately and the compound so obtained is 9, 10-Dimethoxy-2-methyl-1,4-anthraquinone-yellow crystals.

II.2. Characterization of 9,10-Dimethoxy-2-methyl-1,4-anthraquinone: It was isolated as yellow crystals from fraction-4. It showed homogeneous behavior on TLC plate. Its molecular formula $C_{17}H_{14}O_4$ was established from high resolution mass spectrometry.

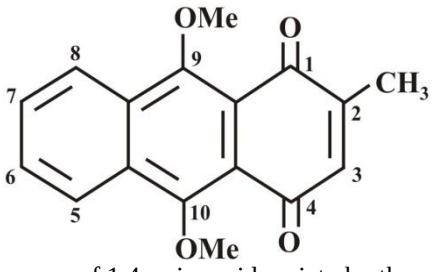

The infrared spectrum showed the presence of 1,4-quinonoid moiety by the appearance of a strong band at 1660 cm^{-1} and UV spectrum displayed absorption maxima at 215, 248, 270, 298 and 400 nm.

The ^1H NMR spectrum, [400 MHz, $CDCl_3$] exhibited the presence of two methoxy groups and a methyl group by the appearance of a pair of singlets at 4.06 and 4.08 and a narrowly split doublet at 2.19 (J = 1.5 Hz) respectively. Quinonoid H-3 proton signal appeared as quartet at 6.80 (J = 1.5 Hz) and showed coupling with C-2 methyl group. Aromatic proton signals for H-5, H-8 appeared as double doublets at 8.38 and 8.40 (J = 7, 1 Hz, each) and H-6, H-7 as triplets at 7.73 and 7.76 (J = 7 Hz, each) respectively. The sequence of the protons was established by spin decoupling experiments. Detailed assignments of signals are given in the following table.

Table – I
1H NMR spectral data of 9, 10-Dimethoxy-2-methyl-1,4-anthra-quinone.

Proton	Chemical shift (ppm and multiplicity	Coupling constant
H–8	8.4dd	J= 7, 1 Hz
H–5	8.38dd	J= 7, 1 Hz
H–7	7.76t	J= 7 Hz
H–6	7.73 t	J= 7 Hz
H–3	6.80 q	J= 1.5 Hz
–OCH3	4.08s	–
–OCH3	4.06s	–
–CH3	2.19d	J= 1.5 Hz

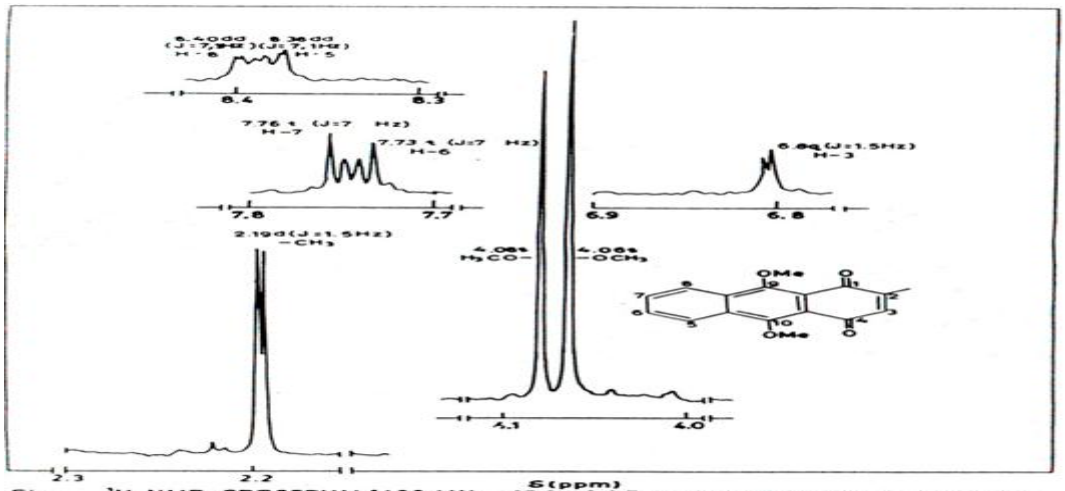

Fig. ^1H NMR SPECTRUM [400 MH_z , $CDCl_3$] OF 9,10-DIMETHOXY-2-METHYL-ANTHRA-1,4-QUINONE

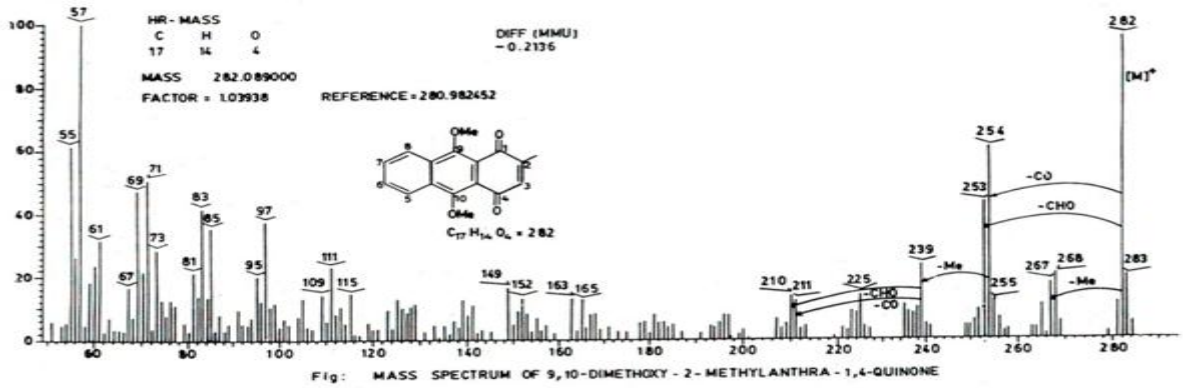

Fig: MASS SPECTRUM OF 9,10-DIMETHOXY-2-METHYLANTHRA-1,4-QUINONE

The peri position of the methoxyl groups was ascertained by NOE difference spectroscopy. There were clear NOE between C-9-OMe and H-8 (5%), C-10-OMe and H-5 (5%), C-2 Me and H-3 (20%).

Mass spectrum showed a molecular ion peak at m/z 282.089 (100%) corresponding to its molecular composition $C_{17}H_{14}O_4$. Other important peaks were at m/z 267 $[M\text{-}Me]^+$, 254 $[M\text{-}CO]^+$, 253 $[M\text{-}CHO]^+$, 239 $[254\text{-}Me]^+$, 211$[239\text{-}CO]^+$ and 210 $[239\text{-}CHO]^+$.

These spectral studies led to the above structure for 9, 10-Dimethoxy-2-methyl-1,4-anthraquinone.

The occurrence of 1,4-anthraquinones is very rare in nature. It is a second report of the isolation of 1,4-anthraquinone derivative from natural products. The first report was the isolation of viocristin (I) and isoviocristin (II) from the mycelium of *Aspergillus cristatus*. However, 9,10- anthraquinones are more prevalent in nature.

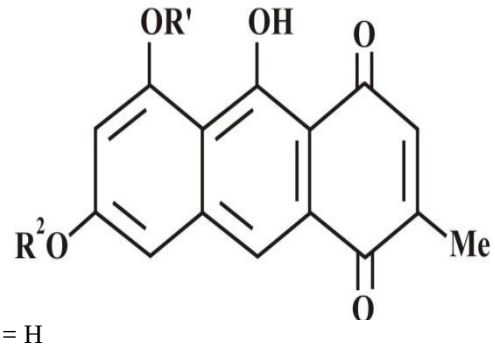

I; R^1 = Me R^2 = H
II; R^1 = H R^2 = Me

Isolation of 9,10-Dimethoxy-2-methyl-1,4-anthraquinone :

It was isolated as yellow crystals from fraction-4, 20mg. It gave single spot on TLC plate.

UV $\lambda_{max}^{(Et_2O)}$: 215, 248, 270, 298 and 400 nm.

IR $\upsilon_{max}^{(CCl_4)}$: 2860 – 2820, 1660 (C═O), 1540, 1320, 1230 cm^{-1}.

^{1}H NMR 90 MHz, $CDCl_3$, □ (ppm) :8.40dd and 8.38dd (J = 7.1 Hz, H-8, H-5), 7.76t and 7.73t (J = 7 Hz, each H–7, H–6), 6.80q (J = 1.5 Hz, H-3), 2.19d (J = 1.5 Hz, ─CH_3), 4.08s (─OCH_3), 4.06s (─OCH_3).

MS (m/z) : 282.089$[M]^+$ (100%) (calculated for $C_{17}H_{14}O_4$), 282.0890, 267 $[M\text{─}Me]^+$, 254 $[M\text{─}CO]^+$, 253 $[M\text{─}CHO]^+$, 239 $[254\text{ ─}Me]^+$, 211 $[239\text{ ─}CO]^+$, 210 $[239\text{ ─}CHO]^+$, 165, 71, 57 etc.

III. RESULTS AND DISCUSSION

The ^{1}H NMR spectrum, [400 MHz, $CDCl_3$] exhibited the presence of two methoxy groups and a methyl group by the appearance of a pair of singlets at 4.06 and 4.08 and a narrowly split doublet at 2.19 (J = 1.5 Hz) respectively. Quinonoid H-3 proton signal appeared as quartet at 6.80 (J = 1.5 Hz) and showed coupling with C-2 methyl group. Aromatic proton signals for H-5, H-8 appeared as double doublets at 8.38 and 8.40 (J = 7, 1 Hz, each) and H-6, H-7 as triplets at 7.73 and 7.76 (J = 7 Hz, each) respectively. Mass spectrum showed a molecular ion peak at m/z 282.089 (100%) corresponding to its molecular composition $C_{17}H_{14}O_4$. Other important peaks were at m/z 267 $[M\text{-}Me]^+$, 254 $[M\text{-}CO]^+$, 253 $[M\text{-}CHO]^+$, 239 $[254\text{-}Me]^+$, 211$[239\text{-}CO]^+$ and 210 $[239\text{-}CHO]^+$.

REFERENCES

[1]. R.N. Khanna, P.K. Sharma and R.H. Thomson, J. Chem. Soc. Perkin Trans. I, 1821 (1987).
[2]. P. Rudman, Chem. & Ind., 1356 (1960).
[3]. R.H. Thomson and A.R. Burnett, J. Chem. Soc. (C), 1261 (1967).
[4]. P. Singh, S. Jain and S. Bhargava, Phytochemistry (in press).
[5]. The Wealth of India : Raw Materials, C.S.I.R., New Delhi, Vol. V, p. 319 (1959).
[6]. Benthall, 347; Bhatia & Manohar Lal, J. Indian Chem. Soc. Industr. Edn., 4, 236 (1941).
[7]. W. Sandermann and H.H. Dietrichs, Holzforschung 13, 137 (1959).
[8]. Wealth of India, Raw Material, C.S.I.R. Publication, New Delhi, Vol. III (1952).
[9]. R.H. Thomson, Naturally Occurring Quinones, Academic Press, London and New York (1971), p. 203.
[10]. K.C. Joshi, P. Singh and R.T. Pardasani, Planta Medica 32, 71 (1977).

International Journal of Modern Engineering Research (IJMER)
www.ijmer.com Vol. 3, Issue. 3, May - June 2013 pp-1850-1853 ISSN: 2249-6645

Secure network monitoring system using mobile agents

Larkins Carvalho[1], Nielet D'mello[2]
[1](Department of Information Technology, Xaviers Institute of Engineering/Mumbai University, India)
[2](Department of Computer Engineering, Fr. Conceicao Rodrigues College of Engineering / Mumbai University, India)

ABSTRACT: *There is a tremendous growth in computer network which demands efficient and secure network monitoring and network management. Mostly SNMP (Simple Network Management Protocol) based client server architecture is used for network management which uses SNMP as a protocol to provide Centralized approach of network management which is quite efficient in terms of performance. Foremost problems related to this architecture are heterogeneity in networks, limited amount of bandwidth, lack of resources, lack of fault tolerance capability and huge amount of traffic generated on central Server which can degrade the performance of network.*

In this paper, we propose a system which follows distributed and decentralized approach for the purpose of network monitoring and management which reduces the traffic over the network. To facilitate distributed and decentralized monitoring, we proposed a secured multi-agent based architecture in which, we created different mobile agents for the purpose of getting network related information. Mobile agents retrieve network related information, which act as an Input for network administrator.It keeps an eye on an activity of each and every registered client using the mobile agent. The proposed application also focuses on reducing the network bandwidth used for monitoring the network by using agent per client architecture (mobile/roaming agent).

KEYWORDS: *controller agent, decentralized approach, mobile agents, snmp, secure network monitoring*

I. INTRODUCTION

The advancements and globalization in the field of computer network have created many tribulations like security and network overhead [1][4]. To avoid these problems, network administrator has to monitor and manage network according to predefined security policy. Since last decade, network monitoring and its management have been the biggest challenges for any distributed network infrastructure. In recent years, mostly organizational network infrastructure used protocols like SNMP for network management and monitoring purpose. These protocols follow centralized approach of client server based architecture. In current communication infrastructure, many organizations follow centralized approach for network monitoring and network management that is all the work of all the clients is been handled through a single server and all the processing is done by server alone which creates extra burden on network and huge amount of traffic at the central server thereby reducing the performance of the network. So it created problems like limitation of bandwidth, high network latency, lack of fault tolerance capability, etc.

To reduce these type of problems we have implemented "SECURE NETWORK MONITORING". The main objective of this system is the implementation of separate monitoring system, implementation of mobile agent[2] at every client in the network. Here in this approach, user of each client machine will know that his machine is being monitored by network administrator or someone else. In order to achieve confidentiality and integrity, multi agent based architecture is developed which has various capabilities such as file monitoring[3], client activities monitoring etc.

This application has two modules, server and client. Server will receive data/reports/logs from client module and will perform the appropriate action. Client module will monitor each & every client pc for any activity like,

1. Internet usage
2. Storage usage
3. File system
4. Media activities
5. Performance related activities (e.g. which process is making excessive use of client processor, resulting in poor performance of client system)
6. Current running & executing processes
7. Information about open ports and target machines to which client is connected.

Based on the info received from client admin can perform various actions like killing the processes on client machine, shut it down, send the message to client etc. While sending data over the network there is possibility that it may get seen by malicious users, to avoid this data send by system is encrypted/decrypted using a basic algorithms.

II. EXISTING SYSTEMS

Over the past few years extensive research work, on mobile agent implementation in network management has been done. Also, due to the increasing requirements in telecommunications, variety of transported flows in network must handle multimedia data traffic reliably with a high quality of service. There are several threads of research that have used mobile agents in a telecommunications network to manage connectivity and load balancing.

Rapid advancement of computer network requires efficient network monitoring and management for better utilization of resources. In current communication infrastructure, many organizations follow centralized approach for network monitoring and network management that is all the work of all the clients is been handled through a single server and all the processing is done by server alone which creates extra burden on network and huge amount of traffic at the central server thereby reducing the performance of the network. So it created problems like limitation of bandwidth, high

network latency, lack of fault tolerance capability, etc. Network monitoring and management followed centralized approach that is all the work of all the clients is been handled through a single server and all the processing was also done by server itself. It results in a huge amount of network traffic at the central server. Due to the huge network traffic performance of network degrades gradually.

The distinction between the existing systems and the proposed system can be enlisted as follows:

Existing System	**Proposed System**
Centralized Approach	Decentralized approach
Most of the processing is done by server itself.	Each client performs his own processing & gives result to the server.
Load balancing problem occurs	Load balancing problem is resolved.

III. MOBILE AGENTS

Mobile agents[2] are programs being sent across the network from the client to the server or vice versa. An agent that can be executed after being transferred over the network will be called an agent host. A software agent is a common name and describes a software entity that computerizes some of the regular or difficult tasks on behalf of human or other agents. Mobile agents can travel in network following their itinerary and carrying logic and data to perform a set of management tasks at each of the visited nodes in order to meet their designed objectives.
Mobile agents allow the transformation of current networks into remotely programmable platforms. Mobile agents are a powerful software interaction model that let a program to be moved between hosts for remote execution. They are solutions for managing distributed networks.

To overcome the serious issue of network traffic and to enhance the performance of network, a mobile agent is used. To control and manage network traffic, network infrastructure requires some intelligent system which should have the ability to give response dynamically and take right decision.
In order to reduce complexity and improve reliablility, we need to follow decentralized approach where mobile agents are the opinion. Mobile agents have the property of load balancing by which they distribute the overall load among different nodes.

Fig 1 shows the client server communication architecture. This architecture consists of one manager who generates no of mobile agents and sends it to the network of managed node. They travel from one node to another autonomously and asynchronously and perform monitoring and management task at each node and collect network related information. After completing monitoring and management task, mobile agents sent back to manager.

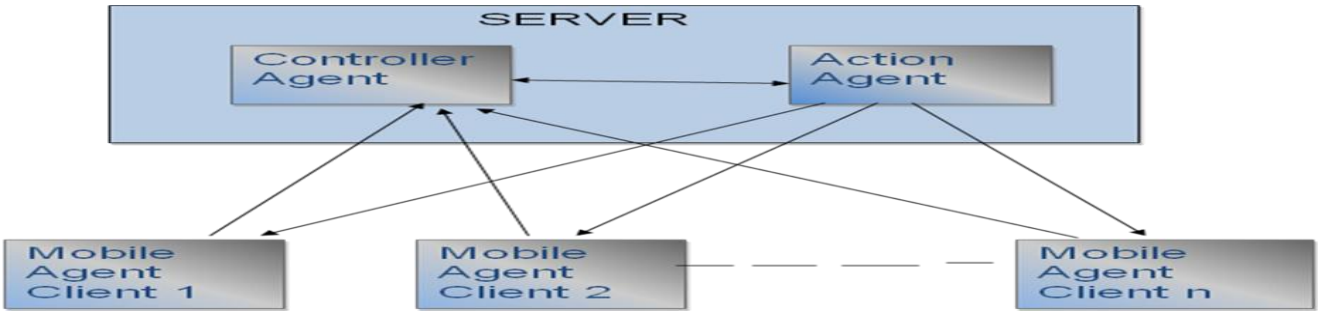

Figure 1. Client server communication

IV. IMPLEMENTATION DETAILS

IV.1 ALGORITHM

For Server:-
Step 1: Start
Step 2: Run the Server.
Step 3: Wait for the Client for Connection.
Step 4: Check for any incoming Connection from Client, if Yes, Register the client and add it in the list of Connected Clients.
Step 5: Wait for the Information From Client.
Step 6: If any incoming information from Client then notifies Admin.
Step 7: Follow Steps 3 to 5 for more clients.
For Client:-
Step 1: Start.
Step 2: Check for the Server.
Step 3: If server is available then Connect and Go to Step 5.
Step 4: If not then Log Error and Go to Step 2.
Step 5: Monitor the client and send the information to server.
Step 6: If any action requested from server then execute that action.

Step 7: After executing the action notify server about it.
Step 8: Go to step 5.

IV.2 ARCHITECTURE

Figure 2. Architecture showing multiple agents

In order to achieve confidentiality [6] and integrity in network monitoring, architecture based on multiple agents have been proposed. It is composed of different types of mobile and static agents which have the capability of resource monitoring, user activities monitoring. The fig 2 shows the architecture consisting of multiple agents[5]. In this architecture, we have one master controller agent (MCA) which is a main server and different Controller agent (CA). Each CA was dispatched from MCA and performed some specific task by dispatching monitor agent and action agent and then sent the response back to the MCA. Monitor Agent travels through a set of nodes and looks for the illegal and unauthorized activity against predefined rules set. After retrieving information regarding user activity and processes, mobile agent sends this information back to Controller agent.

In the same way, Action agent reaches to destination and performs action according to policy like System log off, unwanted process Killing, System shutdown.

IV.3 EXPERIMENTAL RESULTS

The GUI of the system displays multiple client details after the admin logs into the system. Fig 3 shows a general view of multiple client activities that can be monitored by the admin. Fig 4 shows specific details that can be viewed and the actions that can be performed

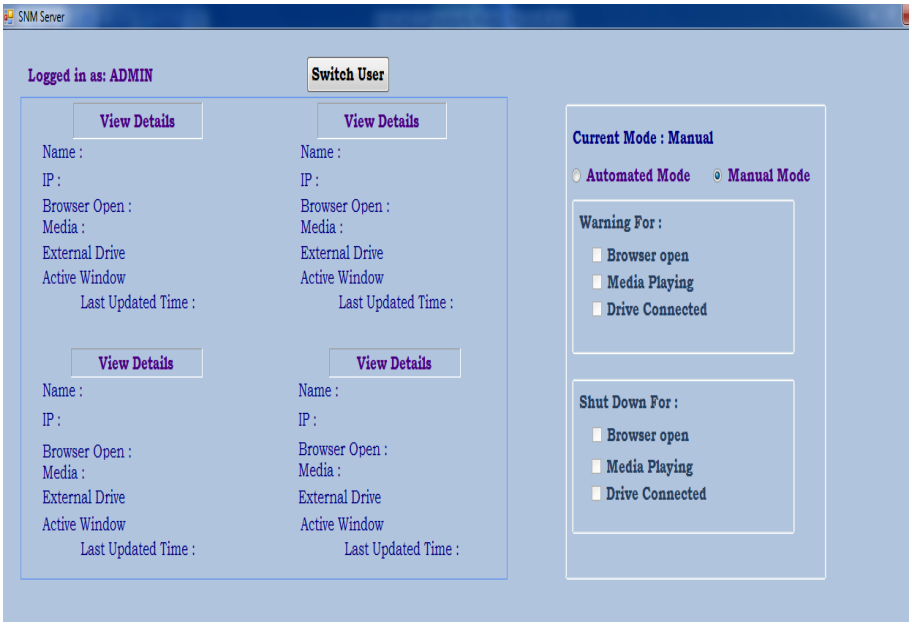

Fig 3. Main screen to monitor multiple clients

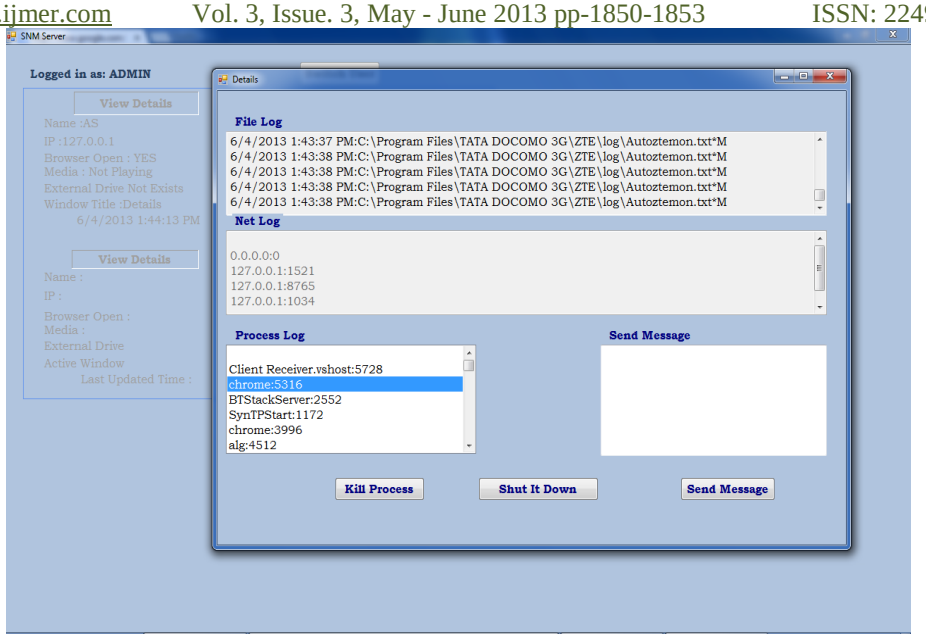

Fig 4. GUI to view multiple logs and perform actions

V. CONCLUSION

In the process of making software application for Network Monitoring and Management using mobile agent which can be used for network monitoring, the various prospects which we have focused for network monitoring are Network Utilization, List processes currently being used, Network services and IP address verification. With this we have provided an authentication to the mobile agents by using simple cryptography algorithm which can stop any unauthorized agent to get executed in the network. With the help of Action agents we can take corrective action on client's suspicious activities.
Furthermore, mobile agent based network monitoring and management can overcome the shortcomings of SNMP and CMIP by decentralizing network monitoring and management.

REFERENCES

Journal Papers:

[1]. *Network Traffic Analysis and Intrusion Detection Using Packet Sniffer*, Second International Conference on Communication Software and Networks, 2010

[2]. *Enhancing the Efficiency of Secure Network Monitoring Through Mobile Agents*, International Conference. on Computer & Communication Technology ICCCT, 2010

[3]. *Network Information Monitoring System in IPV6 Campus*, International Conference on System Science, Engineering Design and Manufacturing Information, 2011

[4]. *Network Sniffer Implement Network Monitoring*, International Conference on Computer Application and System Modeling (ICCASM), 2010

[5]. *A Secure Access Control Scheme Based On Group for Peer To Peer Network*, International Conference on Systems and Informatics (ICSAI), 2012

[6]. *Privacy Preserving and Ownership Authentication in Ubiquitous Computing Devices Using Secure Three Way Authentication*, International Conference on Innovations in Information Technology (IIT), 2012

International Journal of Modern Engineering Research (IJMER)
www.ijmer.com Vol. 3, Issue. 3, May - June 2013 pp-1854-1756 ISSN: 2249-6645

Struts 2- The modern web application framework

Nielet D'mello[1], Larkins Carvalho[2]
1(Department of Computer Engineering, Fr. Conceicao Rodrigues College of Engineering / Mumbai University, India)
2(Department of Information Technology, Xaviers Institute of Engineering/Mumbai University, India)

ABSTRACT: *Information systems are widely used today in every possible field. Traditional web applications respond slowly to the user interface, thus, wasting bandwidth and causing inconvenience to the users. Interactive web applications that present a lot of functionality are increasingly substituting their desktop counterparts. However, the browser and the web itself were originally designed for viewing and exchanging documents and data and not for running applications. Over the years, web pages have slowly been transformed into web applications and as a result, they have been forcefully fit into an unnatural mold for them.Many patterns and frameworks have been used to build web application, yet their efficiency does not match to that of the Struts2 framework. The struts 2 framework is a brand new framework that introduces many architectural refinements over the existing ones to make the web based systems more efficient to use. In this paper we describe and analyze the modern framework-Struts2 for implementing web applications in a way that completes this transition and creates a more natural environment for web applications to live in.*

Keywords: *actions, interceptors, internationalization, struts2 framework, web applications*

I. INTRODUCTION

A web application is simply, or not so simply, an application that runs over the Web. With rapid improvements in Internet speed, connectivity, and client/server technologies, the Web has become an increasingly powerful platform for building all classes of applications, from standard business-oriented enterprise solutions to personal software. The latest iterations of web applications must be as full featured and easy to use as traditional desktop applications. Yet, in spite of the increasing variety in applications built on the web platform, the core workflow of these applications remains markedly consistent, a perfect opportunity for reuse. Frameworks such as Struts 2 strive to release the developer from the mundane concerns of the domain by providing a reusable architectural solution to the core web application workflows. Struts 2 is build from the ground up on best practices and proven community-accepted design patterns.

This paper focuses on emphasizing all the salient features provided by the Struts 2 framework that makes web application development convenient to the developers.

II. SUMMARY OF STRUTS2 FRAMEWORK

A *web application framework* is a piece of structural software that provides automation of common tasks of the domain as well as a built-in architectural solution that can be easily inherited by applications implemented on the framework. Struts2 is popular and mature web application framework based on the MVC[1] design pattern. Struts2 is not just the next version of Struts 1, but it is a complete rewrite of the Struts architecture. The WebWork framework started off with Struts framework as the basis and its goal was to offer an enhanced and improved framework built on Struts to make web development easier for the developers. After some time, the Webwork framework and the Struts community joined hands to create the famous Struts2 framework. The framework is designed to streamline the full development cycle, from building, to deploying, to maintaining applications over time. The figure provides a simple depiction of the context in which Struts 2 is used. As depicted in figure 1, Struts 2 sits on top of two important technologies. At the heart of all Struts 2 applications lie the client/server exchanges of the HTTP protocol. The Java Servlet API exposes these low-level HTTP communications to the Java language.

Figure 1. The technology stack

Struts 2 provides certain strong features that makes it a favourite of the web application developers. Struts2 has improved the form tags and the new tags allow the developers to write less code. Also, Struts2 has recognised the takeover by Web2.0 technologies, and has integrated AJAX[1][2] support into the product by creating AJAX tags, that function very similar to the standard Struts2 tags. Moreover, integration with other frameworks like Spring, Tiles and SiteMesh is now easier with a variety of integration available with Struts2. Tag markups in Struts2 can be tweaked using Freemarker templates. This does not require JSP or java knowledge. Basic HTML, XML and CSS knowledge is enough to modify the tags. Thus, web applications can be easily designed using Struts 2 in a robust way.

III. HOW STRUTS 2 FRAMEWORK WORKS

Struts 2 is a second-generation web application framework that implements the Model-View-Controller (MVC) design pattern. Struts 2 framework can be also called 'MVC from 30,000 feet' or 'pull-MVC' as it provides a cleaner implementation of MVC.. The Model-View-Controller pattern in Struts2 is realized with following five core components: **Actions, Interceptors, Value Stack / OGNL, Results / Result types, View technologies.**

Struts 2 is slightly different from a traditional MVC framework in that the action takes the role of the model rather than the controller, although there is some overlap. The fig. 2 depicts the Model, View and Controller to the Struts2 high level architecture. The controller is implemented with a Struts2 dispatch servlet filter as well as interceptors, the model is implemented with actions, and the view as a combination of result types and results. The value stack and OGNL provide common thread, linking and enabling integration between the other components. The fig 2 describes the Struts 2 request lifecycle.

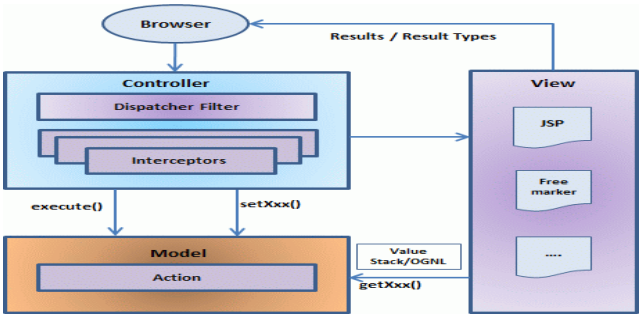

Figure 2. Struts2 request lifecycle

Based on the above diagram, user's request life cycle in Struts 2 as follows:

1. Firstly the user sends a request to the server for requesting for some resource (ex. A web page) through the browser.
2. The FilterDispatcher looks at the request and then determines the appropriate Action.
3. Configured interceptors functionalities are applied such as validation, file upload etc.
4. Selected action is executed to perform the requested operation.
5. Again, configured interceptors are applied to do any post-processing if required.
6. Finally the result is prepared by the view and returns the result to the user.

IV. STRUTS2 CORE COMPONENTS

IV.1 ACTION: Actions are the core of the Struts2 framework, as they are for any MVC (Model View Controller) framework. Each URL is mapped to a specific action, which provides the processing logic necessary to service the request from the user. But the action also serves in two other important capacities. First, the action plays an important role in the transfer of data from the request through to the view, whether it's a JSP or other type of result. Second, the action must assist the framework in determining which result should render the view that will be returned in the response to the request. An example of Struts 2 action mapping is:

```
<action name="locale" class="Locale" method="execute">
<result name="success">/index.jsp</result>
<result name="error">/errorpage.jsp</result>
</action>
```

Here, depending upon the result, the struts2 actions determine the page to be displayed.

IV.2 INTERCEPTORS: Interceptors allow for crosscutting functionality to be implemented separately from the action as well as the framework. Web application developers can achieve the following using interceptors: Providing preprocessing logic before the action is called, providing post processing logic after the action is called and catching exceptions so that alternate processing can be performed. Many of the features provided in the Struts2 framework are implemented using interceptors; examples include exception handling, file uploading, lifecycle callbacks and validation etc.

IV.3 VALUESTACK/OGNL: The ValueStack is a Struts 2 construct that presents an aggregation of the properties of a stack of objects as properties of a single virtual object. If duplicate properties exist—two objects in the stack both have a name property—then the property of the highest object in the stack will be the one exposed on the virtual object represented by the ValueStack. The ValueStack represents the data model exposed to the current request and is the default object against which all OGNL expressions are resolved.

OGNL(*Object-Graph Navigation Language*) is a powerful expression language (and more) that is used to reference and manipulate properties on the ValueStack. The Object-Graph Navigation Language (OGNL) is tightly integrated into Struts 2 to provide support for data transfer and type conversion. OGNL provides an expression language that allows developers to map form fields to Java-side properties, and it also provides type converters that automatically convert from the strings of the request parameters to the Java types of your properties.

V. LOCALISATION USING STRUTS2

Internationalization (i18n) is the process of planning and implementing products and services so that they can easily be adapted to specific local languages and cultures, a process called localization. The internationalization process is sometimes called translation or localization enablement. Internationalization is abbreviated i18n because the word starts with an i and ends with an n, and there are 18 characters between the first i and the last n. Struts2 provides localization i.e. internationalization (i18n) support through resource bundles, interceptors and tag libraries in the following places: The UI tags, messages and errors and within action classes. Struts2 uses resource bundles to provide multiple language and locale options to the users of the web application. The simplest naming format for a resource file is: **bundlename_language_country.properties** (example. es_ES for Spanish locale).

An illustration of localization is as follows:

```
<body>
   <s:property value="getText('global.success')" />
</body>
```

In the code above, the property value will automatically be identified by Struts2 using the locale from the properties file. The English and French locale properties file will be:

global_en.properties:

```
global.success = Successfully authenticated
```

global_fr.properties:

```
global.success = Authentifi é avec success
```

Thus, by using Struts2 framework, localization is easily achieved in the web applications to design multi-lingual applications that can be launched globally.

VI. CONCLUSION

Struts2 framework has proved to be a break through over the traditional frameworks and patterns. Moreover, several refinements introduced by Struts 2 framework makes it more feasible option to be considered when choosing the right framework for a web application. While it is yet to be widely adapted in the WWW arena, this framework will surely go miles ahead to produce simple yet robust web applications.

REFERENCES

Journal Papers:

[1]. Zhou Dongxing , Li Xinke, “Design and application of a web development model based on MVC and AJAX”, JOURNAL OF HEFEI UNIVERSITY OF TECHNOLOGY, Vol . 31 No. 9 Sept. 2008

[2]. [2]Nana Qi, Zhimin Yang “Struts 2 Framework and Web Application based on AJAX”, IEEE,2012, 903-908

[3]. Books:

[4]. Chad Michael Davis, Scott Stanlick, Struts 2 in action

[5]. Rebecca Riordan, Headfirst AJAX.

Website:

I. Struts 2 Documentation – http://struts.apache.org/